



U.S. Department
of Commerce

Volume 105
Number 1
January 2007

Fishery Bulletin



**U.S. Department
of Commerce**

Carlos M. Gutierrez
Secretary

**National Oceanic
and Atmospheric
Administration**

Vice Admiral
Conrad C. Lautenbacher Jr.,
USN (ret.)

Under Secretary for
Oceans and Atmosphere

**National Marine
Fisheries Service**

William T. Hogarth
Assistant Administrator
for Fisheries



The *Fishery Bulletin* (ISSN 0090-0656) is published quarterly by the Scientific Publications Office, National Marine Fisheries Service, NOAA, 7600 Sand Point Way NE, BIN C15700, Seattle, WA 98115-0070. Periodicals postage is paid at Seattle, WA. POSTMASTER: Send address changes for subscriptions to *Fishery Bulletin*, Superintendent of Documents, Attn.: Chief, Mail List Branch, Mail Stop SSOM, Washington, DC 20402-9373.

Although the contents of this publication have not been copyrighted and may be reprinted entirely, reference to source is appreciated.

The Secretary of Commerce has determined that the publication of this periodical is necessary according to law for the transaction of public business of this Department. Use of funds for printing of this periodical has been approved by the Director of the Office of Management and Budget.

For sale by the Superintendent of Documents, U.S. Government Printing Office, Washington, DC 20402. Subscription price per year: \$36.00 domestic and \$50.40 foreign. Cost per single issue: \$28.00 domestic and \$35.00 foreign. See back for order form.

Fishery Bulletin

Scientific Editor

Adam Moles, Ph.D.

Associate Editor

Elizabeth Calvert

National Marine Fisheries Service, NOAA
11305 Glacier Highway
Juneau, Alaska 99801-8626

Managing Editor

Sharyn Matriotti

National Marine Fisheries Service
Scientific Publications Office
7600 Sand Point Way NE, BIN C15700
Seattle, Washington 98115-0070

Editorial Committee

Harlyn O. Halvorson, Ph.D.	University of Massachusetts, Boston
Ronald W. Hardy, Ph.D.	University of Idaho, Hagerman
Richard D. Methot, Ph.D.	National Marine Fisheries Service
Theodore W. Pietsch, Ph.D.	University of Washington, Seattle
Joseph E. Powers, Ph.D.	National Marine Fisheries Service
Harald Rosenthal, Ph.D.	Universität Kiel, Germany
Fredric M. Serchuk, Ph.D.	National Marine Fisheries Service
George Watters, Ph.D.	National Marine Fisheries Service

***Fishery Bulletin* web site: www.fishbull.noaa.gov**

The *Fishery Bulletin* carries original research reports and technical notes on investigations in fishery science, engineering, and economics. It began as the Bulletin of the United States Fish Commission in 1881; it became the Bulletin of the Bureau of Fisheries in 1904 and the *Fishery Bulletin* of the Fish and Wildlife Service in 1941. Separates were issued as documents through volume 46; the last document was No. 1103. Beginning with volume 47 in 1931 and continuing through volume 62 in 1963, each separate appeared as a numbered bulletin. A new system began in 1963 with volume 63 in which papers are bound together in a single issue of the bulletin. Beginning with volume 70, number 1, January 1972, the *Fishery Bulletin* became a periodical, issued quarterly. In this form, it is available by subscription from the Superintendent of Documents, U.S. Government Printing Office, Washington, DC 20402. It is also available free in limited numbers to libraries, research institutions, State and Federal agencies, and in exchange for other scientific publications.

U.S. Department
of Commerce
Seattle, Washington

Volume 105
Number 1
January 2007

Fishery Bulletin

Contents

Articles

- 1–18 Wexler, Jeanne B., Seinen Chow, Toshie Wakabayashi, Kenji Nohara, and Daniel Margulies
Temporal variation in growth of yellowfin tuna (*Thunnus albacares*) larvae in the Panama Bight, 1990–97
- 19–29 McDermott, Susanne F., Katherine P. Maslenikov, and Donald R. Gunderson
Annual fecundity, batch fecundity, and oocyte atresia of Atka mackerel (*Pleurogrammus monopterygius*) in Alaskan waters
- 30–38 Hobbs, James A., William A Bennett, Jessica E Burton, and Bradd Baskerville-Bridges
Modification of the biological intercept model to account for ontogenetic effects in laboratory-reared delta smelt (*Hypomesus transpacificus*)
- 39–48 Laidig, Thomas E., James R. Chess, and Daniel F. Howard
Relationship between abundance of juvenile rockfishes (*Sebastes* spp.) and environmental variables documented off northern California and potential mechanisms for the covariation
- 49–61 Harley, Shelton J., and Jenny M. Suter
The potential use of time-area closures to reduce catches of bigeye tuna (*Thunnus obesus*) in the purse-seine fishery of the eastern Pacific Ocean
- 62–73 Secor, David H., and Philip M. Piccoli
Oceanic migration rates of Upper Chesapeake Bay striped bass (*Morone saxatilis*), determined by otolith microchemical analysis

The conclusions and opinions expressed in *Fishery Bulletin* are solely those of the authors and do not represent the official position of the National Marine Fisheries Service (NOAA) or any other agency or institution.

The National Marine Fisheries Service (NMFS) does not approve, recommend, or endorse any proprietary product or proprietary material mentioned in this publication. No reference shall be made to NMFS, or to this publication furnished by NMFS, in any advertising or sales promotion which would indicate or imply that NMFS approves, recommends, or endorses any proprietary product or proprietary material mentioned herein, or which has as its purpose an intent to cause directly or indirectly the advertised product to be used or purchased because of this NMFS publication.

MBLWHOI Library

MAR 19 2007

WOODS HOLE
Massachusetts 02543

- 74–87 **Matkin, Craig O., Lance G. Barrett-Lennard, Harald Yurk, David Ellifrit, and Andrew W. Trites**
Ecotypic variation and predatory behavior among killer whales (*Orcinus orca*)
off the eastern Aleutian Islands, Alaska
- 88–101 **Stockhausen, William T., and Michael Fogarty**
Removing observational noise from fisheries-independent time series data using ARIMA models
- 102–115 **Pitcher, Kenneth W., Peter F. Olesiuk, Robin F. Brown, Mark S. Lowry, Steven J. Jeffries, John L. Sease, Wayne L. Perryman, Charles E. Stinchcomb, Lloyd F. Lowry**
Abundance and distribution of the eastern North Pacific Steller sea lion (*Eumetopias jubatus*) population
- 116–120 **Gerritsen, Hans D., and David McGrath**
Precision estimates and suggested sample sizes for length-frequency data
- 121–130 **Farley, Edward V. Jr, James M. Murphy, Milo D. Adkison, Lisa B. Eisner, John H. Helle, Jamal H. Moss, and Jennifer Nielsen**
Early marine growth in relation to marine-stage survival rates for
Alaska sockeye salmon (*Oncorhynchus nerka*)
- 131–139 **Ganias, Konstantinos, Cristina Nunes, and Yorgos Stratoudakis**
Degeneration of postovulatory follicles in the Iberian sardine *Sardina pilchardus*: structural changes
and factors affecting resorption

Notes

- 140–146 **Arrizabalaga, Haritz, Victoria López-Rodas, Eduardo Costas, and Alberto González-Garcés**
Use of genetic data to assess the uncertainty in stock assessments due to the assumed stock structure:
the case of albacore (*Thunnus alalunga*) from the Atlantic Ocean
- 147–152 **Cherel, Yves, Richard Sabatié, Michel Potier, Francis Marsac, and Frédéric Ménard**
New information from fish diets on the importance of glassy flying squid (*Hyaloteuthis pelagica*)
(Teuthoidea: Ommastrephidae) in the epipelagic cephalopod community of the tropical Atlantic Ocean
- 153–157 **Conti, Stéphane G., Benjamin D. Maurer, Mark A. Drawbridge, and David A. Demer**
Measurements of total scattering spectra from bocaccio (*Sebastes paucispinis*)
- 158–159 **Guidelines for authors**

Abstract—Tuna larvae (at flexion, postflexion, and transformation stages) were collected by dip net and light traps at night in the northwestern Panama Bight during the season of reduced upwelling (June–September) of 1990, 1991, 1992, and 1997. The larvae were identified as yellowfin tuna (*Thunnus albacares*) by mtDNA analysis. Ichthyoplankton data from bongo and Tucker trawl tows were used to examine the potential prey abundance in relation to the mean size-at-age and growth rates of the yellowfin tuna larvae and their otoliths. The most rapid growth rates occurred during June 1990 when plankton volumes were at their highest levels. The lowest plankton volumes coincided with the lowest growth rates and mean sizes-at-age during the August–September 1991 period. High densities of larval fish were prevalent in the ichthyoplankton tows during the 1991 period; therefore intra- and interspecific competition for limited food resources may have been the cause of slower growth (density-dependent growth) in yellowfin tuna larvae. The highest mean sea-surface temperature and the lowest mean wind stress occurred during an El Niño-Southern Oscillation (ENSO) event during the 1997 period. There appeared to be no clear association between these environmental factors and larval growth rates, but the higher temperatures may have caused an increase in the short-term growth of otoliths in relation to larval fish size.

Temporal variation in growth of yellowfin tuna (*Thunnus albacares*) larvae in the Panama Bight, 1990–97

Jeanne B. Wexler (contact author)¹

Seinen Chow²

Toshie Wakabayashi³

Kenji Nohara³

Daniel Margulies¹

Email address for J. B. Wexler: jwexler@iattc.org

¹ Inter-American Tropical Tuna Commission
8604 La Jolla Shores Drive
La Jolla, California 92037-1508

² National Research Institute of Fisheries Science Nagai
6-31-1 Yokosuka
Kanagawa 283-0316 Japan

³ National Research Institute of Far Seas Fisheries
5-7-1 Shimizu-Orido
Shizuoka 424-8633 Japan

Yellowfin tuna (*Thunnus albacares*) larvae inhabit the mixed layer of all tropical and subtropical oceans of the world (Ueyanagi, 1969; Nishikawa et al., 1985). When recruited to the commercial fishery, yellowfin tuna are one of the most important tuna species worldwide (Collette and Nauen, 1983; FAO, 2004). Near-daily spawning of yellowfin tuna, and the subsequent dispersal of fertilized eggs, appears to be largely dependent on the occurrence of surface water temperatures equal to or greater than 24°C (Schaefer, 1998). In the eastern Pacific Ocean (EPO), yellowfin tuna spawn continuously between 0° and 20°N (Schaefer, 2001). Despite widespread spawning of yellowfin tuna throughout the EPO, the larvae are patchy in distribution (Ahlstrom, 1971), and relatively large numbers have been collected only near islands (Graves et al., 1988; this study) and near shore (González Armas, 2002).

The larvae of *Thunnus* are difficult to identify by meristic, morphological, or pigmentation characteristics (Matsumoto et al., 1972; Potthoff, 1974; Richards et al., 1990; Lang et al., 1994). In the EPO, the late-larval and early-juvenile stages of yellowfin and bigeye (*T. obesus*) tuna co-exist and cannot be differentiated by these con-

ventional methods. However, allozyme (Graves, et al., 1988) and recent molecular (Takeyama et al., 2001; Chow et al., 2003) analyses have made it feasible to identify larvae of these two species that inhabit the EPO.

The growth dynamics of yellowfin tuna during early life stages may have a profound effect on cohort strength (Houde, 1987), but growth rates have not been described for the larvae in the Pacific Ocean. Larval and juvenile stage durations and corresponding growth rates (Houde, 1989), starvation rates (Margulies, 1993), and larval transport and predation (Grimes, 2001) may be strongly influenced by biological and physical processes that would affect prerecruit survival in yellowfin tuna. Standing stocks of phytoplankton and zooplankton in the EPO, where yellowfin tuna larvae are found are seasonally variable (Blackburn et al., 1970; Owen and Zeitschel, 1970; Lauth and Olson, 1996; González Armas, 2002) and influenced by interannual events such as El Niño-Southern Oscillation (ENSO) conditions (Dessier and Donguy, 1987; Fiedler, 1992; Chavez et al., 1999; Strutton and Chavez, 2000). In the northwestern Panama Bight of the EPO, nearshore ichthyoplankton surveys (from 1989 to 1993)

Table 1

Collections of yellowfin tuna larvae by night-lighting (NL) and light traps (LT) near Frailes del Sur in the northwestern Panama Bight, 1990–1997.

Sampling period	Number of sampling dates	Number of larvae collected	Number used for age and growth analyses	Number used for () and identified as <i>T. albacares</i> by PCR-RFLP analysis	Age range (days)	Standard length range (mm)
21–26 June 1990	3	97 (NL)	25	(5) 1	8–18	6.2–19.6
5–25 July 1991	5	13 (NL) 9 (LT)	13	(13) 10	11–15	9.1–12.7
4–7 September 1991	2	126 (NL)	43	(34) 26	12–20	7.1–12.4
24 June–3 July 1992	3	47 (NL)	22	(34) 19	10–14	7.6–12.0
7 August 1997	1	98 (NL)	69	(71) 69	11–18	8.7–14.5

(IATTC¹; IATTC²; Lauth and Olson, 1996; Owen³) and experiments with captured scombrid larvae (from 1986 to 1997) at the Achotines Laboratory of the Inter-American Tropical Tuna Commission (IATTC) (Olson and Scholey, 1990; Margulies, 1993; Scholey, 1993; Wexler, 1993) have provided an opportunity to explore factors controlling prerecruit growth and survival of scombrids. These small- and fine-scale studies may provide some understanding of the recruitment variability of yellowfin tuna in the Panama Bight, considering that yellowfin tuna exhibit limited, small-scale movements within the EPO (Schaefer, 1991; Wild, 1994) and that processes important to recruitment probably occur at small scales (Fortier and Leggett, 1985).

The Panama Bight is characterized by distinct seasonal and interannual variations in atmospheric and oceanic conditions (Wooster, 1959; Smayda, 1963, 1966; Forsbergh, 1963, 1969). The climatological and physical oceanographic properties that occur within the Panama Bight are determined by the north-south seasonal movement of the northeast trade winds of the Atlantic Ocean, the equatorial calm belt (i.e., the doldrums), the southeast trade winds of the Pacific Ocean, and the convergence of these trade wind systems within the doldrums (i.e., the intertropical convergence zone, ITCZ) (Smayda, 1966). From January through April, the ITCZ is displaced to the south and strong northerly trade winds create a dry season and produce local upwelling. From about May through December, the

ITCZ is displaced to the north and the Panama Bight is dominated by southeast trade winds and a rainy season characterized by reduced upwelling, higher sea-surface temperatures (SSTs), lower ocean salinities, and a deeper thermocline and mixed layer (Lauth and Olson, 1996). The growth and subsequent survival of yellowfin tuna larvae that occur during the reduced upwelling season may be regulated more by the spatial patchiness of prey organisms coincident with lower plankton volumes (Owen, 1989). ENSO events could further affect the seasonal availability of nutrients and food organisms during this period (Barber and Chavez, 1986; Dessier and Donguy, 1987; Fiedler, 1992; Chavez et al., 1999). A mild ENSO event occurred during our sampling periods in 1991–92 (Barber et al., 1996) and a strong event occurred in late 1997 (Chavez et al., 1999; Strutton and Chavez, 2000; Glynn et al., 2001).

The objectives of this study were 1) to identify the species of *Thunnus* sampled in the northwestern Panama Bight by molecular analysis, 2) to determine ages and compare the size-at-age data of yellowfin tuna larvae collected during the periods of reduced upwelling of 1990, 1991, 1992, and 1997, and 3) to explore relationships between the temporal variation in growth rates and measured levels of plankton and physical processes in the Panama Bight.

Materials and methods

Larval fish collections

Fish larvae were collected in the northwestern Panama Bight (Fig. 1) during the seasons of reduced upwelling in June 1990, July and September 1991, June and July 1992, and August 1997 (Table 1). Most of the larvae were collected with a dipnet just below the ocean surface after they were attracted with an underwater light at night (night-lighting, NL) (Olson and Scholey, 1990) near Frailes del Sur in the vicinity of the 100- and 200-meter isobaths. Larvae were also collected in this area in July 1991 by a light trap (LT) (design described in Thorrold,

¹ IATTC (Inter-American Tropical Tuna Commission). 1992. Annual report of the Inter-American Tropical Tuna Commission 1990, 261 p. IATTC, 8604 La Jolla Shores Drive, La Jolla, CA 92037.

² IATTC (Inter-American Tropical Tuna Commission). 1992. Annual report of the Inter-American Tropical Tuna Commission 1991, 271 p. IATTC, 8604 La Jolla Shores Drive, La Jolla, CA 92037.

³ Owen, R. W. 1997. Oceanographic atlas of habitats of larval tunas in the Pacific Ocean off the Azuero Peninsula, Panama, 32 p. Inter-American Tropical Tuna Commission Data Report 9. IATTC, 8604 La Jolla Shores Drive, La Jolla, CA 92037.

1993) deployed near the surface. All larvae were fixed in 95% ethyl alcohol shortly after capture, except for some that were caught alive and used in laboratory experiments. Fish used in laboratory experiments were not used for the age and growth analyses. SSTs were recorded with a bucket thermometer, and the salinity of a sample of water taken just below the surface was measured with a handheld salinometer. Visual observations of environmental conditions (e.g., wind, currents, and weather) were recorded at the time of sampling.

Laboratory procedures and analyses

Larvae of the genus *Thunnus* were sorted from other scombrid larvae by the morphological features and meristics described in Nishikawa and Rimmer (1987) and Ambrose (1996). The standard length (SL) of each larva was measured in distilled water before the sagittal otoliths were removed for aging and before the remaining tissue of each individual was placed in 95% ethyl alcohol for species identification. The sagittae were removed, cleaned of tissue with chlorine bleach, rinsed in distilled water, dried, and embedded distal side up with Eukitt (O. Kindler, Freiberg, Germany) mounting medium on a glass slide. The diameter along the longest axis of each sagitta was measured with an ocular micrometer and light microscope. The sagittae were polished at the surface until the increments were clearly visible with transmitted light at a magnification of 480 or 720 \times . Daily increments (previously validated in Wexler et al., 2001) of the left and right sagittae were counted "blindly" (i.e., repeated counts were made without prior knowledge of the previous counts) by the first author until the same number of increments were counted at least three times in one of the sagittae. The number of increments in the sagitta that was more clearly read (which usually resulted in a higher count) was used as a direct estimate of age for that fish.

The temporal variation in growth was examined by comparing the size-at-age data of the larvae and their otoliths among collection periods through analysis of covariance (ANCOVA) and a multiple range comparison test (Tukey HSD) (XLSTAT vers. 7.5.2, Addinsoft USA, New York, NY) ($\alpha=0.05$).

DNA analysis and species identification

The flanking region between ATPase 6 and cytochrome oxidase subunit I (COI) genes of mtDNA was amplified by using the polymerase chain reaction (PCR),

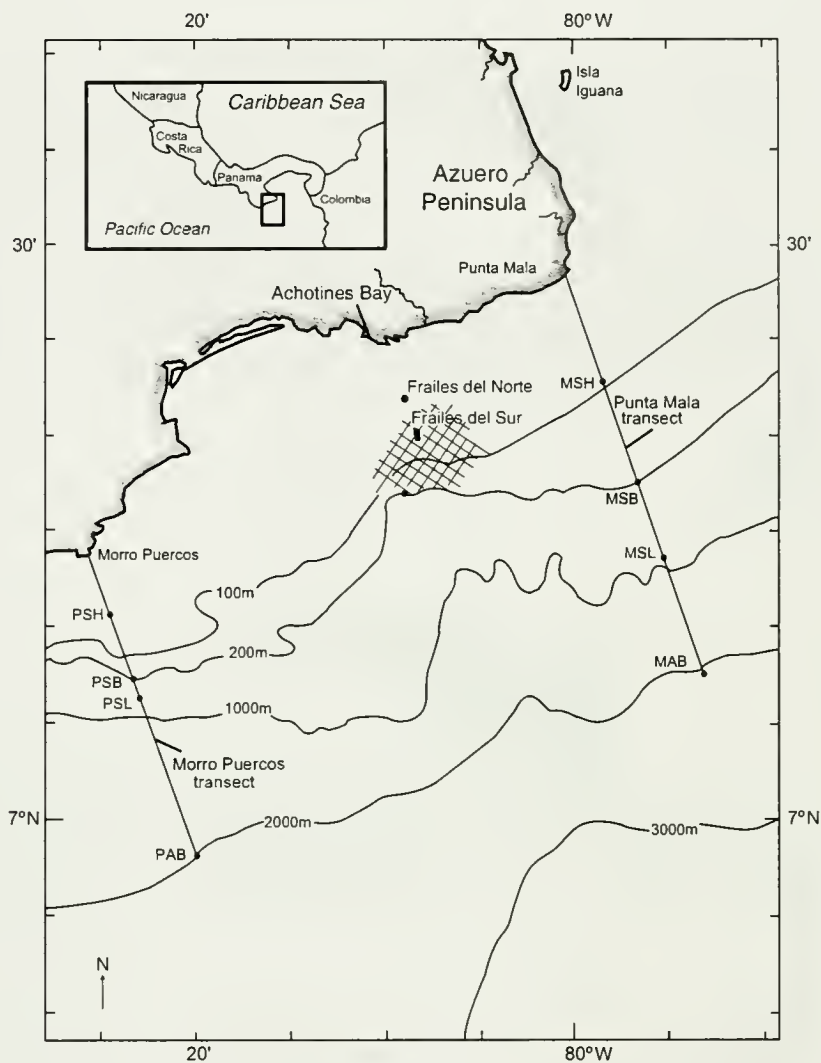


Figure 1

Locations where yellowfin tuna (*Thunnus albacares*) larvae were collected with an underwater light at night (cross hatched; from 1990–92 and 1997) and where ichthyoplankton sampling occurred (during 1990–92) near the Achotines Laboratory, on the Azuero Peninsula of the northwestern Panama Bight. Ichthyoplankton sampling stations along the Punta Mala and Morro Puercos transects are the following: Mala abyss (MAB), Mala slope (MSL), Mala shelf break (MSB), Mala shelf (MSH), Puercos abyss (PAB), Puercos slope (PSL), Puercos shelf break (PSB), Puercos shelf (PSH).

and restriction fragment length polymorphism (RFLP) patterns were used to identify the species of *Thunnus* larvae according to protocols of Takeyama et al. (2001) and Chow et al. (2003). Albacore (*T. alalunga*), yellowfin, and bigeye tunas in the Pacific Ocean can be identified by the diagnostic restriction profile of *Mse* I digestion (Chow and Inoue, 1993), and this enzyme assay was used to identify the species of larvae collected in 1990–92. Chow et al. (2000) found, however, that many specimens of bigeye tuna in the Atlantic Ocean shared the same restriction profile with yellowfin tuna; this also occurred in the Pacific Ocean, but at a much lower frequency (1 out of 144 individuals examined). Takeyama et al.

Table 2

Maximum distances traveled for each collection group of yellowfin tuna larvae recruited to the sampling area based on back-calculated spawning dates, the period of time over which the larvae were exposed to environmental conditions during their life history, and an average, maximum current speed and direction for the Panama Bight region (Fiedler, 2002). The average latitudinal and longitudinal degrees traveled were used to estimate an area occupied by larvae of all collection groups. The mean sea surface temperature (SST) is based on monthly averages within 1- by 1.5-degree ares for each collection group period within the estimated area.

Collection group	First spawn date	Last sample date	Monthly mean SST (SE) and ranges (°C)	Time period exposed to ambient SST (days)	Number of days feeding	Maximum meters traveled @ .25 m/sec	Maximum nautical miles traveled	Degrees
I	6/6/1990	6/26/1990	27.84 (0.090) 26.4–28.7	20	17	432,000	233	3.89
II	6/19/1991	7/25/1991	27.90 (0.063) 26.6–28.7	36	33	777,600	420	7.00
III	8/14/1991	9/7/1991	27.60 (0.059) 26.5–28.4	24	21	518,400	280	4.66
IV	6/9/1992	7/3/1992	28.00 (0.066) 26.4–29.0	24	21	518,400	280	4.66
V	7/19/1997	8/7/1997	29.10 (0.046) 28.3–30.0	19	16	410,400	222	3.69
							mean degrees	4.78

(2001) found another restriction enzyme (*Tsp* 509I) that was diagnostic for bigeye tuna regardless of where the specimens came from. Therefore, in addition to using *Mse* I digestion, *Tsp* 509I was also used for all individuals collected in 1997.

Back-calculated dates

Spawning dates were back-calculated for each larva by subtracting the number of otolith increments counted from the date the larva was collected. An additional day was also subtracted because the first increment in yellowfin tuna is present at hatching approximately 20 hours after fertilization (senior author, personal commun.) and the second increment does not form until the third day after fertilization (approximately two days after hatching); increments are formed daily thereafter (Wexler et al., 2001). During the reduced upwelling season when SSTs are warmer, first feeding of the larvae occurs at first light, approximately three days after hatching (Margulies et al., in press) when, on average, three increments are present in the sagittae. Therefore, three days were subtracted from the estimated spawning date to estimate the time period that the larvae of each collection group were feeding until they were collected (Table 2). "Collection-group period" is defined as the time period from the time of first spawning to the time when larvae were sampled.

Estimated area occupied by larval cohorts

The yellowfin tuna larvae that were collected near the Frailes Islands may be recruited locally from offshore

areas; this conjecture is based on measurements of the mean monthly fields of velocity and direction of the North Equatorial Countercurrent (NECC) (up to 0.25 m/s) (Fiedler, 2002), southerly surface winds (up to 5 m/s) (Fiedler, 2002), and the location and proportion of reproductively active female yellowfin tuna (Schaefer, 1998) that are found during June–September in the Panama Bight area (Fig. 2). The earliest back-calculated spawning date for a larva within each collection group was used to estimate the maximum amount of time the larvae within that group were exposed to environmental and feeding conditions (Table 2). This amount of time and the maximum current speed and direction during this season were used to calculate maximum average distances traveled and the potential area occupied by each collection group until sampled at the Frailes Islands (Table 2, Fig. 2).

Ichthyoplankton and oceanographic surveys

During 1990–92 ichthyoplankton and oceanographic sampling were conducted from a 25-ft Boston whaler along the Morro Puercos (P) and Punta Mala (M) transects (Fig. 1) (IATTC¹; IATTC²; Lauth and Olson, 1996). Data collected from these surveys were used to describe the temporal variation of conditions within the planktonic community that may correspond to that of larval yellowfin tuna growth rates. In 1990, oblique bongo tows were made from the surface to 50 m along both transects with 335- μ m mesh nets (Lauth and Olson, 1996). As a measure of relative abundance, standardized plankton volumes under 10 m² of sea surface were calculated by following procedures of Smith and Richardson (1977), and the estimates for each side of the

bongo were averaged. Beginning in 1991, a 0.6-m² Tucker trawl equipped with a 335-mm mesh net, flow meter, and temperature-depth logger was used to sample ichthyoplankton at discrete depths at only the Punta Mala shelf break (MSB). These surveys were designed to study the vertical distribution and *in situ* growth and starvation rates of tuna larvae and the abundance of their zooplankton prey (IATTC¹; IATTC²). Two replicate tows of 4 to 5 minutes were made at each of three or four depth strata: 0–5 (stratum 1), 5–20 (stratum 2), 20–40 (stratum 3), and 40–60 m (stratum 4). Plankton volumes were standardized (Smith and Richardson, 1977) at each depth stratum and were added together for each sampling day to compare the mean plankton volumes collected by the Tucker trawl with those collected by the bongo tows of the previous year. Mean plankton volumes were compared between collection group periods by using a one-way analysis of variance (ANOVA), the Student-Newman-Keuls multiple range comparison test (SNK test), and a *t*-test for unequal variance ($\alpha=0.05$) when appropriate (Zar, 1984). In 1991, all four depth strata were sampled, but in 1992 only the first three strata were sampled. Additionally, a 73- μ m mesh net with a mouth area of 0.014 m² was nested inside the Tucker trawl in 1992 to collect microzooplankton simultaneously with all other plankters. The displaced volume of the microzooplankton was included in the total standardized plankton volume for each sampling day. Water temperatures, surface wind speeds (m/s), and salinity values (psu) were measured (described in Lauth and Olson, 1996) during each sampling day.

Plankton displacement volumes for all years were also standardized as plankton volume per volume of water filtered (mL/m³) to compare mean values between years and with literature values. The mean of each standardized volume for the 1990 oblique tows (0–50 m) and for discrete depths between 0 and 40 m of the 1991 and 1992 data were compared between collection group periods by using ANOVA, the SNK test, and a *t*-test for unequal variance ($\alpha=0.05$) (Zar, 1984).

Sea-surface temperatures and wind stress climatology

The oceanographic surveys provided physical data within a limited portion of the area where *Thunnus* larvae potentially occurred since hatching. Therefore, area- and time-specific (monthly averages within 1- by 1.5-degree areas) SSTs to 5 m depth and wind stress climatology data (all data sets based on a hindcast ocean analysis system model described by Ji et al. [1995]) for the estimated area of each collection group period (Table 2, Fig. 2) were accessed from the internet (IRI⁴). Wind velocities in m/s were calculated from wind stress values based on a constant drag coefficient of 1.3×10^{-3} (Sverdrup et al., 1942; Large and Pond, 1981; Ji et al.,

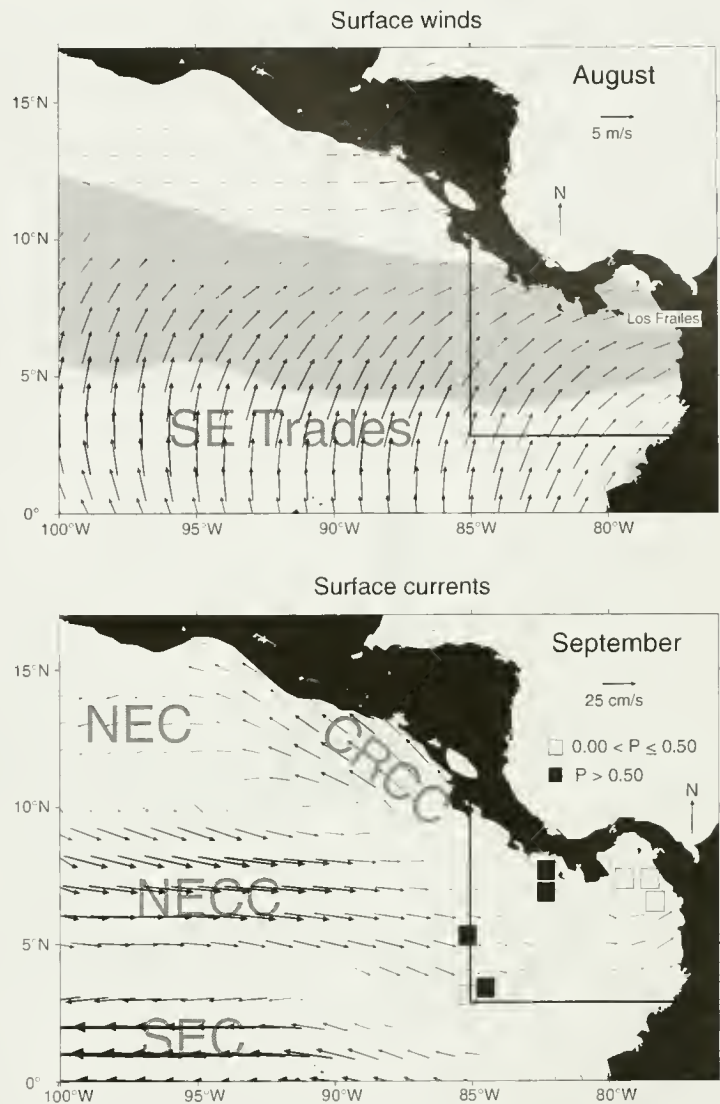
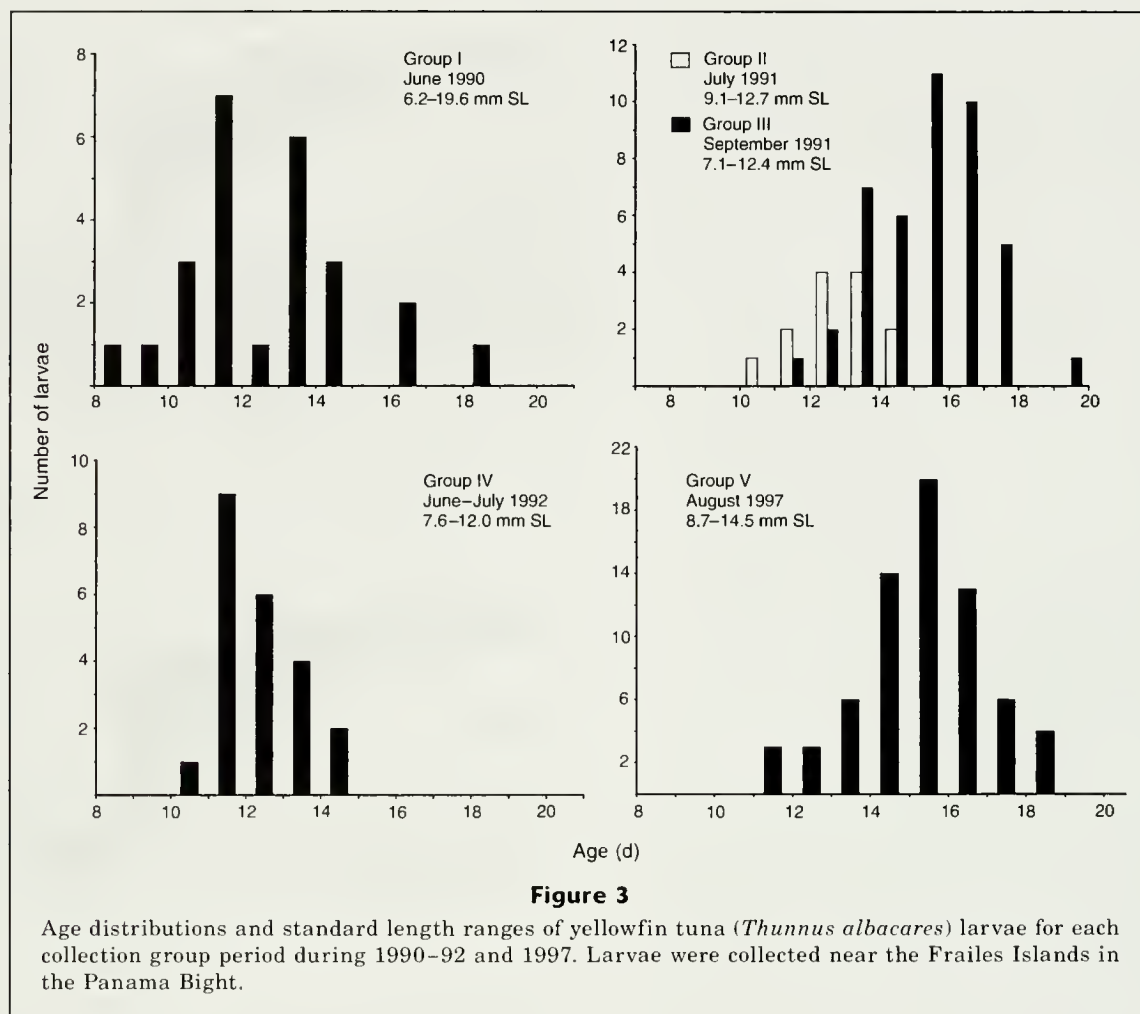


Figure 2

Monthly fields of surface wind velocity (for August) and surface current velocity (for September) representative of the seasonal extremes during the reduced upwelling period in the Panama Bight (after Figure 3 of Fiedler, 2002). Shading indicates surface wind divergence (intertropical convergence zone) during August, NEC = North Equatorial Current, SEC = South Equatorial Current, NECC = North Equatorial Counter Current, and CRCC = Costa Rica Coastal Current. The area between the vertical and horizontal lines and the land mass represents the estimated maximum average area (in degrees) (see Table 2) potentially occupied by each larval yellowfin tuna cohort during its life history. The spawning distribution of yellowfin tuna within the area is presented as the proportions (*P*) of reproductively active females in relation to the total numbers of mature females captured within 1-degree areas during the second and third quarters between 1987 and 1989 (from Schaefer, 1998).

⁴ International Research Institute for Climate Prediction (IRI). 2006. Website: <http://ingrid.ldeo.columbia.edu/SOURCES/.NOAA/.NCEP/.EMC/.CMB/.Pacific/.monthly/> (accessed on 14 October 2005).



1995). Physical data were compared between collection group periods using ANOVA and the SNK test.

Results

Collections and identification

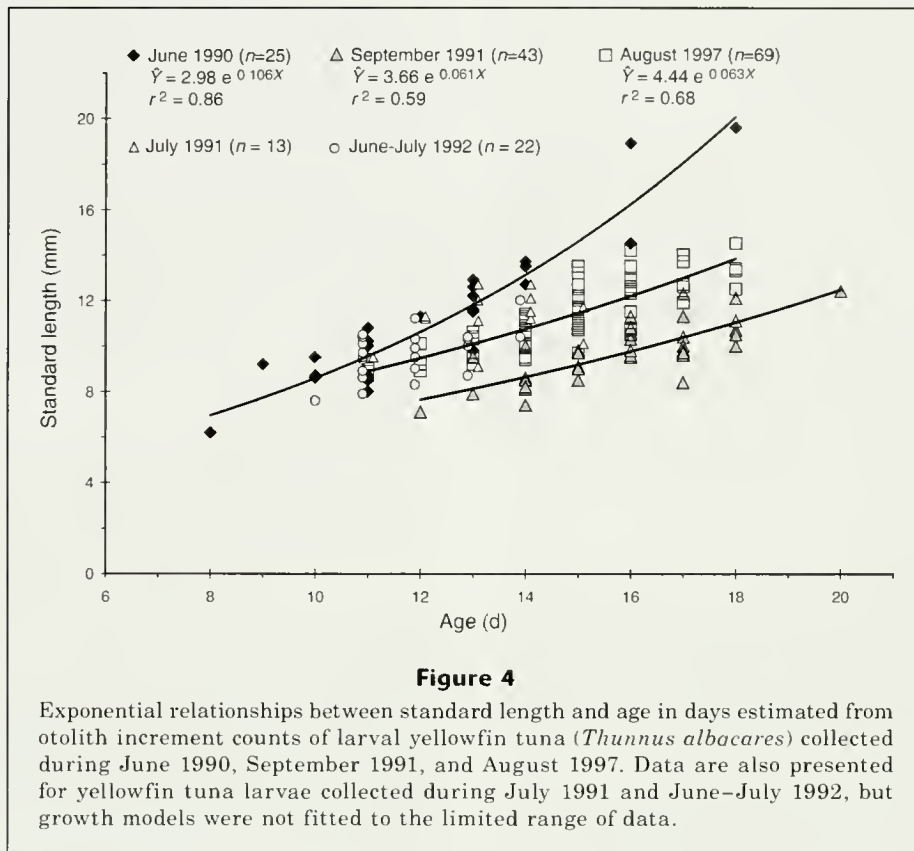
The occurrence of fairly large numbers (approximately 100 or more) of larval and early-stage juvenile *Thunnus* was sporadic, but not uncommon, in night-light collections during certain months of each year of the reduced upwelling season (Table 1). Based on back-calculated spawning dates and the average surface current speed, the collection site within an 8-degree latitude by 8-degree longitude area (between 2-10°N and 77-85°W) was estimated as the average maximum area potentially occupied by yellowfin tuna larvae of each collection group during their early life history (Table 2, Fig. 2). At the time of collection, sizes of larvae ranged from 6.2 to 19.6 mm SL (Table 1), and all were either in the flexion, postflexion, or transformation stages of development (stages described in Ambrose, 1996). Other

scombrid species (i.e., *Auxis* sp., *Euthynnus lineatus*, and *Scomberomorus sierra*) were also found when *Thunnus* larvae were collected, but were not usually predominant in the collections.

Successful PCR amplification occurred in 80% of the larvae analyzed, and subsequent RFLP analysis indicated that the *Thunnus* larvae collected near the Frailes Islands were *T. albacares* (Table 1).

Size-at-age and growth

The ages of yellowfin tuna larvae collected ranged from 8 to 20 days (Table 1, Fig. 3). The age range was mostly limited between 11 and 14 days for the larvae collected in July 1991 (collection group II) and in June-July 1992 (collection group IV); therefore growth models were not fitted to the data (Figs. 3 and 4). However, a comparison of the size-at-age between all five groups within this limited age range indicated that both SLs and otoliths were significantly smaller for larvae collected in September 1991 (collection group III) (ANCOVA and Tukey multiple comparison test, $P < 0.0001$), and that SLs were similar between the larvae of 1990 (collection group I) and July



1991 (collection group II) and between those of 1992 and 1997 (collection groups IV and V).

The length-at-age data were used to examine and compare growth relationships of all yellowfin tuna larvae collected in June 1990, September 1991, and August 1997 (collection groups I, III, and V, respectively). An exponential model provided the best fit to each of the three groups of data (Fig. 4). The variances were homogeneous after log transformation of the length data for each group, and the slopes were compared. The slope and the average growth rate obtained through differentiation of the exponential equation of the 1990 data (1.28 mm/d, SE=0.134) were significantly greater than those of the September 1991 (0.60 mm/d, SE=0.033) and 1997 (0.71 mm/d, SE=0.038) data (ANCOVA, $P < 0.0001$, Tukey multiple comparison test). The elevations (i.e., adjusted means or intercepts) of the 1991 and 1997 data were significantly different ($P < 0.0001$) and indicated that the mean length-at-age was significantly smaller for larvae of the September 1991 collection group (Fig. 4).

Similar results were obtained for otolith growth rates (based on the exponential relationships between otolith diameter and age) for the three years (Fig. 5). The slopes were compared after log transformation of the otolith data for each group. The growth rate of the 1990 data was significantly faster than that of the 1991 and 1997 data (ANCOVA, $P < 0.0001$, Tukey multiple com-

parison test), and the elevations were different between the 1991 and 1997 data, indicating that otoliths were significantly smaller for larvae of the September 1991 collection group (Fig. 5).

A comparison of the linear relationships between otolith diameter and SL (ANCOVA, $P < 0.0001$, Tukey multiple comparison test; Fig. 6) revealed that the otoliths of the 1997 group were larger and grew significantly faster in relation to fish size than those of the 1990 and 1991 groups. Otoliths of the fastest (1990 group) and slowest (1991 group) growth periods were growing at the same rate in relation to fish length, but the slower-growing group had significantly larger otoliths in relation to fish size than those of the faster-growing group ($P < 0.0001$; Fig. 6).

Standing stocks of ichthyoplankton

Ichthyoplankton and physical parameters were measured at four stations along the P and M transects on two sampling days in June 1990 (16 tows total, each to 50 m), at the MSB station on the M transect on six sampling days in June and July 1991 (12 tows each depth strata 1–4), at the MSB station on three sampling days in August 1991 (six tows each strata 1–4 and four tows each strata 1–3), and at the MSB station on two sampling days in June and July 1992 (six tows each strata 1–3) (Table 3, Fig. 1). The sampling days lay within the

period of time when each collection group of larvae could have been feeding in the estimated area of occurrence (Table 2, Fig. 2). Ichthyoplankton tows were not made in the Panama Bight during 1997.

Mean standardized plankton volumes were variable and significantly different (ANOVA, $P < 0.001$) among collection-group periods (Fig. 7). The mean plankton volume (\pm SE) in 1990 (157.3 ± 13.53 mL) when the fastest larval growth rate occurred was greater and different from all other sampling or collection periods (SNK test), and ranged from 106.5 to 310.4 mL under 10 m^2 of sea surface (Table 3, Fig. 7). The mean plankton volumes during June–July 1991 (82.3 ± 3.46 mL) and during August–September 1991 (62.8 ± 5.86 mL), when the slowest growth rate occurred, were similar and less than those for all other periods (SNK test); volumes ranged from 43.7 to 102.4 mL under 10 m^2 of sea surface (Table 3, Fig. 7).

Mean plankton volumes, expressed as the amount filtered per volume of water sampled within the first three depth strata, were also significantly different (ANOVA, $P < 0.001$) among collection group periods. Means were similar between the 1990 and 1992 groups and between the two 1991 groups (SNK test). Volumes ranged from 0.199 to 0.559 mL/m^3 during 1990 and 1992 and from 0.075 to 0.235 mL/m^3 during the two 1991 periods (Table 3).

Plankton volumes included relatively large numbers of fish larvae (predominantly preflexion stages) during the least (August–September 1991) and most (June 1990)

rapid growth periods, and mean values were not significantly different (t -test for unequal variances, $P > 0.20$). Numbers of larvae under 10 m^2 of sea surface ranged from 686.8 to 4786.1 and from 934.5 to 2685.6 in 1990 and 1991, respectively. Few scombrid larvae occurred in the ichthyoplankton samples for each of the two years, but were greatest during the 1991 period. The number of scombrid larvae under 10 m^2 ranged from 0 to 2.7 and from 0 to 12.7 in 1990 and 1991, respectively. *Thunnus* larvae (preflexion stage) were collected only in August 1991, and the numbers ranged from 0.5 to 5.5 larvae under 10 m^2 of sea surface.

Environmental effects

Mean SSTs were significantly different among all collection group periods (ANOVA, $P < 0.0001$). SSTs were similar between the local sampling area (Fig. 1) and the estimated region of each collection group (Fig. 2) in that they were significantly lower for the August–September 1991 period (group III) and higher for the July–August 1997 period (group V) (ANOVA, $P < 0.0001$, SNK test; Table 2, Fig. 7).

The mean wind stress was significantly lower for the 1997 collection-group period (group V) when compared with all other group periods (ANOVA, $P < 0.0001$, SNK test; Fig. 7). The monthly means within each 1- by 1.5-degree area were similar and ranged from 0.084 to 0.517 dynes/cm² for group-collection periods I–IV, and for the 1997 period (group V), they ranged from 0.027 to 0.462 dynes/cm². Wind velocities calculated from the wind stress values were low to moderate, ranging from 1.59 to 3.94 m/s (modes of 2.45 and 2.60 m/s) for groups I–IV and from 0.90 to 3.72 m/s (modes of 1.2 and 1.7 m/s) for group V.

Higher salinity values, ranging from 33 to 34 psu, occurred during July–August 1997 (group V) during an ENSO event, and during the 1990–92 collection-group periods (I–IV) values ranged from 29 to 32 psu, when both the fastest and slowest growth rates of yellowfin tuna larvae occurred.

Discussion

This study describes the first *in situ* growth rates for yellowfin tuna larvae occurring in the Pacific Ocean. Previous efforts to age and describe growth of yellowfin tuna during the early stages of develop-

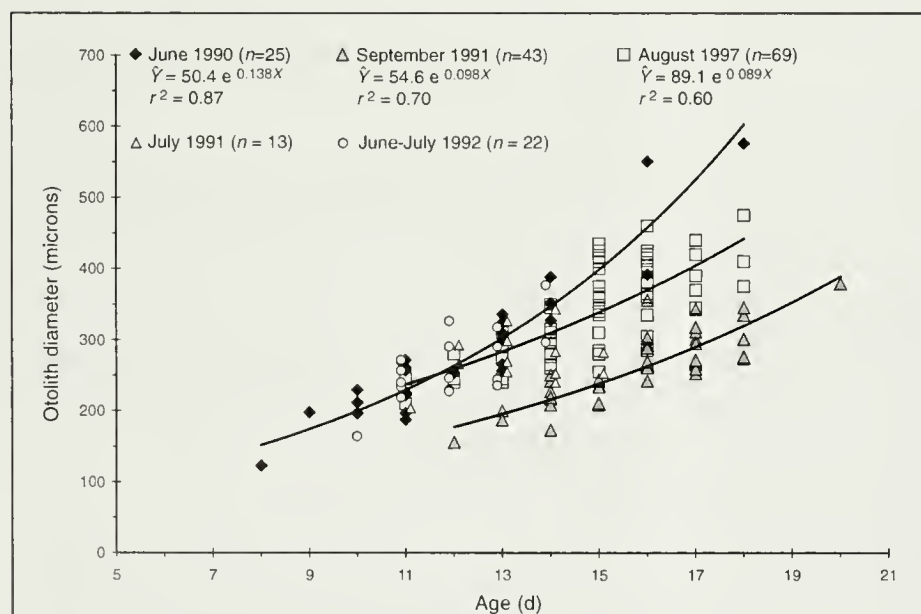


Figure 5

Exponential relationships between sagittal otolith diameter and estimated age in days of larval yellowfin tuna (*Thunnus albacares*) collected during June 1990, September 1991, and August 1997. Data are also presented for yellowfin tuna larvae collected during July 1991 and June–July 1992, but growth models were not fitted to the limited range of data.

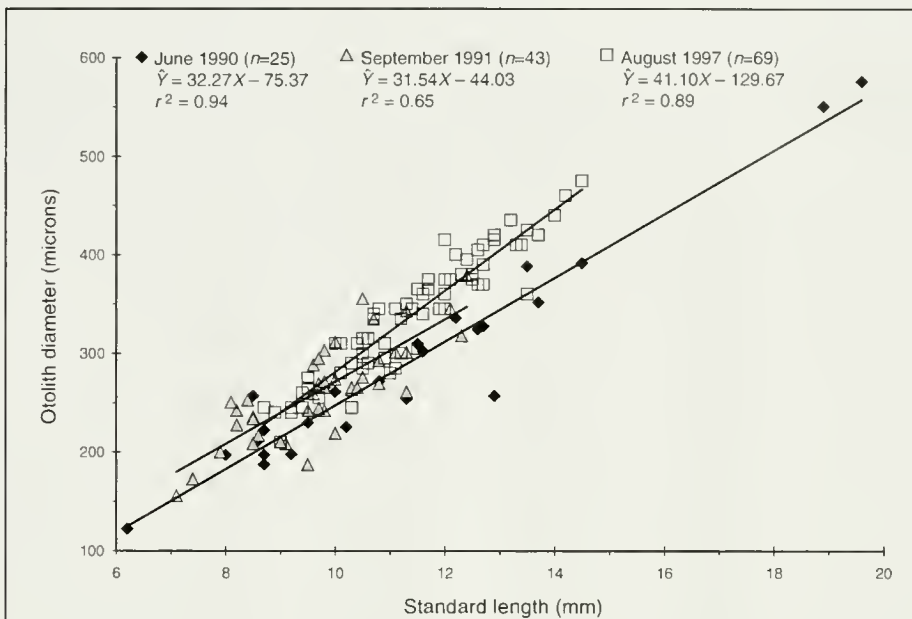


Figure 6

Linear relationships between otolith diameter and standard length for larval yellowfin tuna (*Thunnus albacares*) collected during June 1990, September 1991, and August 1997.

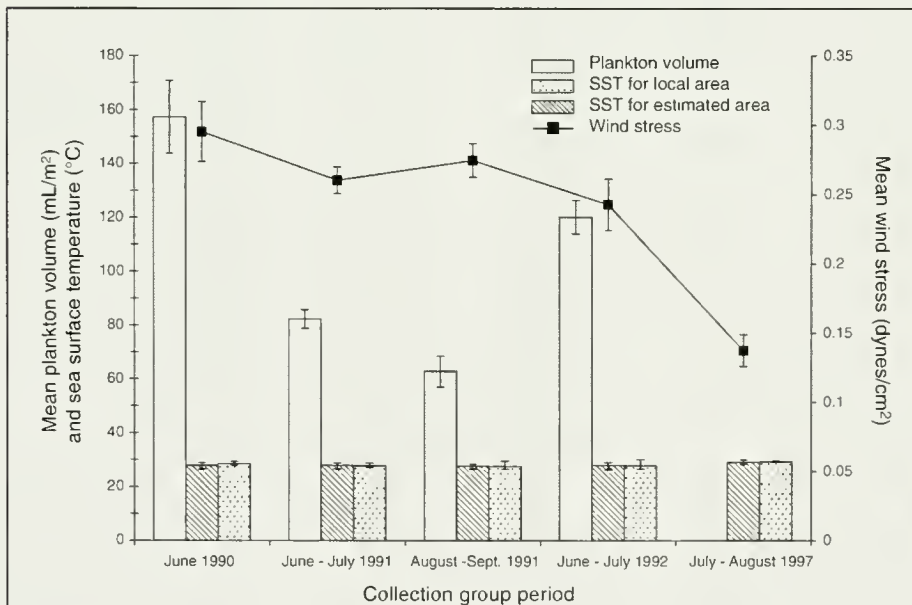


Figure 7

Standardized mean plankton volumes and monthly mean wind stress and sea surface temperature data for the local sampling area (Fig. 1) and the estimated area (Fig. 2) potentially occupied by each larval yellowfin tuna (*Thunnus albacares*) cohort during its life history. The standard errors of the means are indicated for plankton and wind stress, and the ranges for the mean water temperatures are also indicated. Plankton data were collected from ichthyoplankton tows in the vicinity of the Frailes Islands (see Fig. 1) and area- and time-specific physical data were extracted from the internet (IRI⁴).

Table 3

Standardized plankton displacement volumes collected from ichthyoplankton surveys conducted along the Punta Mala (M) and Morro Puercos (P) transects during 1990–1992 in the Panama Bight. Station definitions are described in Figure 1.

Sampling date	Transect	Station	Tow depth (m)	mL plankton volume/10m ² of sea surface	mL/m ³	Sum of depth strata 1–4	Sum of depth strata 1–3	
19 June 1990	M	MAB	0–50	121.3	0.219			
		MAB	0–50	242.3	0.425			
		MSL	0–50	123.9	0.226			
		MSL	0–50	118.5	0.208			
		MSB	0–50	143.0	0.260			
		MSB	0–50	156.0	0.280			
		MSH	0–50	167.6	0.328			
		MSH	0–50	310.4	0.559			
20 June 1990	P	PAB	0–50	140.9	0.252			
		PAB	0–50	129.1	0.264			
		PSL	0–50	205.8	0.393			
		PSL	0–50	163.6	0.301			
		PSB	0–50	113.2	0.199			
		PSB	0–50	125.6	0.240			
20 June 1990	P	PSH	0–40	106.5	0.245			
		PSH	0–40	149.5	0.333			
17 June 1991	M	MSB	0–5.7	6.6	0.117			
			5.3–25.8	21.5	0.105			
			21.2–27.0	39.6	0.147			
			43.1–48.1	2.4	0.049	70.1	67.7	
		MSB	0–5.4	8.4	0.155			
			5.2–21.9	20.9	0.125			
			21.2–48.2	38.2	0.142			
			42.5–67.2	10.2	0.041	77.7	67.5	
			MSB	0–5.7	13.0	0.229		
				5.4–21.9	31.5	0.190		
12 July 1991	M	MSB	22.9–44.5	23.9	0.111			
			43.8–67.2	10.5	0.045	96.9	68.4	
			MSB	0–6.1	14.4	0.235		
				4.9–23.7	32.8	0.175		
		MSB	22.9–48.2	32.0	0.127			
			43.8–67.2	10.5	0.045	89.6	79.1	
			MSB	0–5.7	9.9	0.176		
				4.9–21.9	19.9	0.117		
				21.2–44.5	24.7	0.106		
				40.2–67.2	12.4	0.046	67.0	54.5
16 July 1991	M	MSB	0–5.7	4.6	0.081			
			5.3–23.7	19.7	0.107			
			21.2–44.5	25.9	0.111			
			40.2–67.2	12.5	0.046	62.8	50.3	
		MSB	0–5.4	6.2	0.114			
			5.2–21.9	24.4	0.146			
			20.2–44.5	36.4	0.150			
			40.2–64.0	15.5	0.065	82.5	67.0	
			MSB	0–5.4	5.2	0.096		
				5.3–20.9	31.6	0.203		
19 July 1991	M	MSB	21.2–46.0	31.3	0.126			
			43.1–70.1	13.2	0.049	81.3	68.0	
			MSB	0–5.4	5.2	0.096		
				5.3–20.9	31.6	0.203		
		MSB	21.2–46.0	31.3	0.126			
			43.1–70.1	13.2	0.049	81.3	68.0	

continued

Table 3 (continued)

Sampling date	Transect	Station	Tow depth (m)	mL plankton volume/10m ² of sea surface	mL/m ³	Sum of depth strata 1-4	Sum of depth strata 1-3	
23 July 1991	M	MSB	0-5.4	7.9	0.147	80.6	69.1	
			5.5-20.9	21.0	0.137			
			21.2-46.5	40.2	0.159			
			43.1-61.8	11.4	0.061			
		MSB	0-5.7	9.7	0.171	83.9	68.9	
			5.5-22.9	18.5	0.116			
			21.2-46.5	40.8	0.162			
25 July 1991	M	MSB	0-5.7	9.2	0.163	102.4	84.9	
			5.3-25.8	30.9	0.150			
			22.1-46.5	44.9	0.184			
			43.1-70.1	17.4	0.065			
15 August 1991	M	MSB	0-5.4	9.4	0.174	93.2	67.2	
			5.1-20.9	23.3	0.147			
			21.2-38.9	34.5	0.195			
			43.1-62.3	25.9	0.135			
15 August 1991	M	MSB	0-5.7	5.7	0.101	78.0	53.1	
			5.3-19.2	15.4	0.111			
			21.2-44.5	32.0	0.137			
15 August 1991	M	MSB	0-6.7	8.6	0.129	78.0	62.4	
			5.3-21.9	24.3	0.146			
			21.2-44.5	29.5	0.126			
			36.0-56.5	15.6	0.076			
		MSB	0-5.7	9.3	0.165	66.0	50.6	
			5.3-21.9	18.8	0.113			
			21.2-40.2	22.5	0.119			
			43.8-67.2	15.3	0.066			
			0-5.7	8.6	0.151			
		MSB	5.7-21.9	20.2	0.125	66.0	50.6	
			22.9-43.8	27.7	0.133			
			0-6.1	8.4	0.138			
			5.3-21.9	22.2	0.134			
21 August 1991	M	MSB	21.2-44.5	36.0	0.154	78.0	62.4	
			MSB	0-5.7	12.3			0.217
			6.1-19.2	18.5	0.142			
		MSB	21.2-48.2	53.6	0.199	66.0	50.6	
			0-5.7	6.5	0.115			
			5.3-21.9	12.8	0.077			
			21.2-44.5	19.2	0.082			
23 August 1991	M	MSB	45.0-67.2	7.9	0.035	46.3	38.4	
			MSB	0-6.4	5.4			0.084
			5.5-21.9	12.3	0.075			
		MSB	21.2-44.5	18.5	0.079	43.7	36.2	
			43.8-67.2	7.5	0.032			
			0-5.7	8.1	0.143			
23 August 1991	M	MSB	5.3-21.9	19.7	0.119	43.7	36.2	
			21.2-44.5	32.6	0.140			
			0-5.7	8.1	0.143			

continued

Table 3 (continued)

Sampling date	Transect	Station	Tow depth (m)	mL plankton volume/10m ² of sea surface	mL/m ³	Sum of depth strata 1-4	Sum of depth strata 1-3
23 August 1991 (continued)		MSB	45.9-67.2	9.5	0.044	69.9	60.4
			0-5.7	7.3	0.128		
			5.3-23.7	23.4	0.127		
			21.2-44.5	31.2	0.134		
22 June 1992	M	MSB	43.1-67.2	10.9	0.046	72.9	61.9
			0-5.0	14.6	0.294		
			5.4-20.2	34.6	0.234		
			20.2-40.0	60.0	0.303		
		MSB	0-5.0	11.5	0.233	109.2	
			5.0-20.2	39.3	0.259		
			20.2-40.0	52.4	0.264		
		MSB	0-5.0	16.9	0.342	103.3	
			5.0-20.2	56.3	0.370		
			20.2-40.0	70.9	0.358		
2 July 1992	M	MSB	0-5.0	23.4	0.473	144.1	
			5.0-20.2	54.5	0.359		
			20.2-40.0	54.2	0.274		
		MSB	0-5.0	23.4	0.473	132.1	
			5.0-20.2	54.5	0.359		
			20.2-40.0	54.2	0.274		
2 July 1992	M	MSB	0-5.0	19.7	0.397	118.4	
			4.5-20.2	48.9	0.312		
		MSB	0-5.0	10.7	0.216		
			5.4-18.7	37.5	0.280		
20.2-40.0	65.9	0.333	114.0				

ment may have been precluded by the patchiness in their distribution and the difficulties in species identification. The only other growth study done on yellowfin tuna larvae was conducted in the Gulf of Mexico (Lang et al., 1994), but the species identifications were based on morphology and meristics, and the larvae were younger than those in our study. Results from our mtDNA analysis enabled us to examine species-specific growth rates of older larval stages of yellowfin tuna and associated factors affecting their growth and distribution.

Distribution

Yellowfin tuna larvae have consistently appeared in the night-light collections near the Frailes Islands during the reduced upwelling season, but not during the season when strong upwelling occurs and other species of scombrid larvae and plankton levels are more abundant (Smayda, 1966; Forsbergh, 1969; Lauth and Olson, 1996). The absence of yellowfin tuna larvae from our sampling area during the upwelling season may be associated with a cessation of spawning by yellowfin tuna during this period (Schaefer 1998, 2001; Margulies et al., in press) and with the temperature threshold of their larvae. Lower mean water temperatures typically occur

during the upwelling season (Lauth and Olson, 1996) and have ranged from 17.3° to 25.8°C within the upper 50 m (Owen³). In the laboratory, survival of first-feeding yellowfin tuna larvae is poor at ambient water temperatures of <21°C and at dissolved oxygen levels <2.2 mg/L (<33.0 % of oxygen saturation) (Margulies et al.⁵). These temperature and dissolved oxygen requirements probably determine and limit the distribution of yellowfin tuna larvae within the mixed layer and determine whether or not they can survive during the upwelling season when water temperatures are lower. The distribution of yellowfin tuna larvae during the upwelling season may also be strongly influenced by the occurrence of strong westerly directed currents and northerly winds resulting in larval transport away from the coastal areas of the Panama Bight during this season.

The area of larval distribution since hatching may actually be smaller or larger than what we have estimated, depending on the amount of passive transport and

⁵ Margulies, D., V. P. Scholey, J. B. Wexler, R. J. Olson, J. M. Suter, and S. Hunt. In press. A review of IATTC research on the early life history and reproductive biology of scombrids conducted at the Ashotines Laboratory from 1985 to 2005. Inter-American Tropical Tuna Commission, Special Report 16. IATTC, 8604 La Jolla Shores Drive, La Jolla, CA 92037.

the swimming behavior of the larvae within the mixed layer. Passive transport would probably occur only during the egg, yolk-sac, and first-feeding stages (the first 8–10 days after fertilization) because yellowfin tuna larvae are competent swimmers and can hold their position against strong currents in the laboratory beginning at around 8–10 mm SL (D. Margulies, personal commun.). Although the maximum average area of larval yellowfin tuna distribution from the time of hatching is probably our best estimate, the physical and biological processes that occur in such a large area may not be representative of processes occurring on much smaller scales that may be more specific to conditions affecting larval transport, growth, and survival (Owen, 1989).

Prey abundance

Our ichthyoplankton data were collected within a 0.5-degree area that included the Frailes Islands where larvae were sampled and may provide an index of prey abundance (at least for the first one or two weeks of feeding until piscivory occurs). Although our data were spatially limited, the measured plankton volumes provide the only available estimates of zooplankton levels for the periods of interest.

The use of different gear types (i.e., the bongo and Tucker trawl) for ichthyoplankton collections during 1990–92 may have affected the amount of microzooplankton sampled during the different years. Microzooplankton abundance has not been compared between these two types of sampling nets. However, Shima and Bailey (1994) reported that the bongo and 1-m Tucker nets caught similar numbers and size distribution of larval walleye pollock (*Theragra chalcogramma*). The higher plankton volumes collected by the bongo in 1990 may be an underestimate of plankton abundance compared to the volumes of water being sampled by the Tucker trawl with a larger mouth opening (McGowan and Fraundorf, 1966). Given that plankton volumes were probably under-represented in the bongo tows, the difference in magnitude between the amounts of plankton sampled by each net type may actually be greater.

Another potential bias in comparing plankton volumes among the different years was that more areas (stations) were sampled with the bongo in 1990 than with the Tucker trawl in other years (MSB station only). However, the mean plankton volume would have been similar in 1990 if only the MSB station had been used in the analysis (Table 3).

Growth

Daily growth rates estimated from the exponential models for each of the three years (1990, 1991, and 1997) ranged from 0.46 to 2.06 mm/d and were generally greater than those reported for other congeners (Jenkins and Davis, 1990; Lang et al., 1994). However, the larvae represented in those studies were predominantly younger and in earlier stages of development (and thus would exhibit slower absolute growth) than the flexion

and postflexion larvae and transitional juvenile stages of yellowfin tuna collected in our sampling area. The slower growth rates observed in southern bluefin tuna (*Thunnus maccoyii*) larvae were also associated with density-dependent and oligotrophic conditions in the East Indian Ocean (Rochford, 1962; Jenkins and Davis, 1990; Young and Davis, 1990). Our growth rates, however, were comparable to similar developmental stages of other scombrids that inhabit relatively similar, productive nearshore waters, such as king and Spanish mackerels (*Scomberomorus cavalla* and *S. maculatus*, respectively; DeVries et al., 1990), black skipjack (*Euthynnus lineatus*; Wexler, 1993), and little tunny (*Euthynnus alletteratus*; Allman and Grimes, 1998).

Distinct differences in the average size-at-age and growth rates were very apparent between our 1990 and September 1991 collections of yellowfin tuna larvae. Size-dependent processes (i.e., predation and starvation; Pepin, 1988; Grimes and Isely, 1996) or density-dependent growth and survival (Jenkins et al., 1991) may affect the size-frequency distributions of surviving larvae. A simulation model (Pepin, 1988) demonstrated that with increased food abundance, the mean and variance in larval growth rates increases, but, as predator abundance increases, the variance in growth rates decreases for any given mean. Instantaneous growth rates for yellowfin tuna larvae of a similar age in 1990 were 2 to 3 times higher than those in 1991, and plankton volumes were 2 to 7 times higher than those in 1991. Increases in food availability, such as that during 1990, may also attract predators and result in greater rates of mortality of the slowest-growing individuals, so that they are not represented in the sampled population. Although the larvae in 1991 were growing more slowly than those in 1990, they probably do not represent the slowest-growing larvae of their cohort. Typically, postflexion larval and early-stage juvenile scombrids collected during the reduced upwelling season in our sampling area have exhibited more variable growth (Wexler, 1993), but have been predominantly healthy (Margulies, 1993). Therefore, slower or faster growing survivors at this stage may be independent of their nutritional condition, and larvae collected by the sampling method we used represent the survivors and most competent individuals of their cohort.

Growth may have been slower in 1991 because of higher larval densities, limited food availability, and available prey composition. A strong inverse relationship exists between growth rates and stocking densities of yellowfin tuna larvae and early-stage juveniles (up to 18 days after hatching) fed a constant food supply in the laboratory (IATTC⁶, IATTC⁷; Margulies et al.⁵). The re-

⁶ IATTC (Inter-American Tropical Tuna Commission). 2000. Annual report of the Inter-American Tropical Tuna Commission 1998, 357 p. IATTC, 8604 La Jolla Shores Drive, La Jolla, CA 92037.

⁷ IATTC (Inter-American Tropical Tuna Commission). 2002. Annual report of the Inter-American Tropical Tuna Commission 2001, 148 p. IATTC, 8604 La Jolla Shores Drive, La Jolla, CA 92037.

relationship may be even more pronounced under limited food conditions (Jenkins et al., 1991). Although we have only indirect evidence for density-dependent growth of the 1991 cohorts, the occurrence of more yellowfin tuna larvae sampled at the surface with the night light and the large numbers of other fish larvae collected in the ichthyoplankton tows coincident with the lower plankton volumes may indicate growth-limited conditions during this period. The slower growth of the late-stage larvae in 1991, when plankton abundance was much lower, may also be indicative of the types or species of preferred prey (zooplankters and fish larvae) that were available in the area that the larvae occupied. In the laboratory, yellowfin tuna larvae have predominantly selected all stages of cyclopoids over other types of copepods when offered a mixed assemblage of zooplankton prey (Margulies et al., 2001) and have become piscivorous beginning at approximately 6–7 mm in SL (Margulies et al.⁵). During this transitional stage in their diet, growth becomes much more rapid and variable (Kaji et al., 1999; Margulies et al.⁵), and the availability of specific types of fish larvae may influence their ability to switch to piscivory in the ocean. Yellowfin tuna larvae readily consume other, smaller conspecifics in the laboratory, but it is not known if there is a preference or growth advantage for consuming certain species of fish larvae during the transition to a more piscivorous diet. Although the available prey composition could affect the growth of late-stage yellowfin tuna larvae, intra- and interspecific competition for limited food resources during the 1991 period may have been the principal cause of slower growth.

The temporal variation in size-at-age within the same season and year (1991) may be related to the physical and biological characteristics of the area occupied by each group of larvae since hatching. Larval distribution could be determined by the location and timing of yellowfin tuna spawning and the small- and large-scale dynamics of physical oceanographic processes. Average sizes of the larvae and their otoliths of the 1991 August–September group were distinctly and significantly smaller than those of all other groups. The back-calculated first-feeding dates of this group coincided with the lowest plankton volumes measured in our local sampling area and with the only collection of first-feeding yellowfin tuna larvae from our ichthyoplankton tows. In contrast, the mean sizes of larvae and otoliths of the 1991 July group were similar to those of the fastest-growing group of 1990, despite low plankton volumes similar to those of the September 1991 period. We believe that the September 1991 group may have been spawned nearer to our local sampling area (Fig. 2) and that they were more exposed to feeding conditions in the vicinity of the Frailes Islands than were the faster-growing larvae of the July 1991 group.

Physical effects on growth

The probability of feeding success in marine larvae, and subsequent growth rates and survival, may increase

with moderate levels of wind-induced microscale turbulence in their feeding environment (Rothschild and Osborn, 1988; Cury and Roy, 1989; Ware and Thomson, 1991; MacKenzie et al., 1994; IATTC⁸, IATTC⁹). Preliminary estimates of wind speeds that produce optimal turbulent velocities and maximum survival of first-feeding yellowfin tuna larvae in the laboratory are moderate to high (D. Margulies, personal commun.) compared to wind speeds measured in the Panama Bight during this study. This estimate of optimal wind speeds is based on the assumption that maximum abundances of yellowfin tuna larvae in the EPO occur at depths of 0 to 20 m. However, the data on wind stress and velocities in the estimated area of larval distribution may not represent the frequency of optimal wind speeds associated with areas where first feeding of each cohort occurred. Additionally, wind event durations and frequencies, for which data were not available, may also play a significant role in the optimal survival of marine larvae (Wroblewski et al., 1989). Although moderate to high wind-induced turbulence may enhance early larval survival, growth rates may actually be slower during a portion of the larval phase as a result of higher larval densities and increased competition for limited resources.

Temperature-limited or -enhanced growth was not clear from our analyses of the yellowfin tuna larvae collected. Although a parabolic relationship between growth rates and SSTs was evident, it is unlikely that the two slowest-growing groups represented by the upper (29.1°C; group V) and lower (27.6°C; group III) mean temperatures in our study (Table 2) are approaching thermal tolerance limits for yellowfin tuna larvae. In the laboratory, successful hatching of yellowfin tuna larvae still occurs at upper temperatures of 32–34°C and first-feeding larvae are able to survive and feed between temperatures of 21° and 32°C (Margulies et al.⁵). Lower temperatures during the August–September 1991 (group III) period (Table 2) may have resulted in slower growth than that of the other collection periods, but we have only found significantly slower growth rates and differences in the mean sizes at first feeding when mean temperatures were less than 27°C in the laboratory (senior author, personal commun.). In contrast to the most rapid growth rate in 1990, the larvae in 1997 were growing more slowly when a strong ENSO event and the highest SSTs occurred. The optimum temperature range for growth of yellowfin tuna larvae in the Gulf of Mexico was 29–29.5°C (Lang et al., 1994), which was a similar temperature range for larvae of the 1997 period in our study. We do not, however, have information on relative food abundances during this

⁸ IATTC (Inter-American Tropical Tuna Commission). 2001. Annual report of the Inter-American Tropical Tuna Commission 1999, 183 p. IATTC, 8604 La Jolla Shores Drive, La Jolla, CA 92037.

⁹ IATTC (Inter-American Tropical Tuna Commission). 2002. Annual report of the Inter-American Tropical Tuna Commission 2000, 171 p. IATTC, 8604 La Jolla Shores Drive, La Jolla, CA 92037.

time. Interactive effects of food availability and temperature may have a profound effect on growth, and we would expect that energetic demands become greater at the higher water temperatures, in which case the potential for faster growth would be attained through increased food consumption (Houde, 1989), providing food resources are not limited. Thus, it may be more reasonable to assume that food availability has a more significant impact on growth than SSTs during the reduced upwelling season when temperatures are consistently greater than 27°C.

Although water temperature has been shown to regulate the formation and short-term growth of otoliths in some marine fish species (Barber and Jenkins, 2001), the causal factor affecting otolith growth could also be associated with food availability (Govoni et al., 1985; Johnson et al., 2002) and composition (Woodbury, 1999). Otolith growth appears to be a conservative measure of somatic growth (i.e., otoliths continue to grow even with decreases in somatic growth; Campana and Neilson, 1985); therefore a significant change in otolith growth could signal a dramatic change in the larval feeding environment. We observed significant interannual differences between relationships of otolith size and fish size. Otoliths were disproportionately larger in slower growing groups of larvae, but additionally, during the period of 1997 when SSTs were abnormally high, otoliths were growing at a greater rate in relation to fish size (Fig. 6). Elevated water temperatures have been shown to increase short-term otolith growth (Hoff and Fuiman, 1993; Barber and Jenkins, 2001). Although temperature may have affected otolith growth in 1997, lower food levels may have been the causal factor for a significantly slower otolith growth rate and the smaller mean otolith diameter of the 1991 group.

Recruitment implications

The probability of survival from early stages of development to recruitment in marine fishes is thought to be influenced by prerecruit starvation and predation mortality associated with slower growing and nutritionally weakened individuals (Cushing, 1975; Houde, 1987; Margulies, 2001) and predator-prey interactions and densities (Cowan and Houde, 1992). However, Peterman et al. (1988) have demonstrated that the survival rate of prerecruits older than 19 days of age is more variable than earlier life stages, and it is this stage that determines recruitment strength in northern anchovy (*Engraulis mordax*). Yellowfin tuna in the Pacific Ocean exhibit a pattern of reproduction that has strong potential for regulation of recruitment during prejuvenile stages, when initial numbers in a cohort are quite large and vital rates (e.g., growth, mortality) are high (Houde, 1987; Margulies, 2001). However, the potential for recruitment fluctuations is also high for the relatively long juvenile stage of yellowfin tuna as well (Houde, 1987; Margulies, 2001). In the EPO, yellowfin tuna are recruited to the fishery at a fork length of about

30 cm and at an age of approximately 6 months (Wild, 1994; Maunder and Harley¹⁰). Recruitment estimates calculated at quarterly intervals for yellowfin tuna in the EPO are variable and may be influenced by environmental fluctuations (Maunder and Harley¹⁰). It is not clear what effect slower or faster growing cohorts may have on recruitment, but the growth- and stage-specific mortality rates (Houde, 1987; Pepin, 1991; Comyns et al., 2003) of a cohort may determine whether it survives to recruitment or when it enters the fishery. We were unable to estimate mortality rates for the larvae collected in each of the three years because during some years they were collected on single sampling dates (Essig and Cole, 1986). Nonetheless, the recruitment estimate (ca. 1.44×10^7 individuals) following the period in 1991, when the smallest size-at-age and the slowest-growing larvae were present was approximately half the amount estimated (ca. 3.11×10^7 individuals) following the period in 1990 (Maunder and Harley¹⁰; Maunder¹¹), when larvae were larger and growing more rapidly. The recruitment estimate following the 1997 period (ca. 3.06×10^7 individuals) was slightly less than that following the 1990 period. Larvae of the 1997 group were growing at a rate similar to that of the 1991 group, but the mean size-at-age was significantly greater, which may indicate a size advantage favorable for prerecruit survival (Miller et al., 1988). The growth rates and conditions estimated for yellowfin tuna larvae within the small scale area of our study may apply to localized recruitment estimates within the Panama Bight and not those of the entire EPO, given that restricted movements of yellowfin tuna occur in the EPO (Schaefer, 1991; Wild, 1994). Although these inferences may be applicable only to recruitment within the Panama Bight, they may still indicate that growth rates and the mean size-at-age during the larval and early-juvenile stages are a contributing factor to recruitment variability of yellowfin tuna in the EPO.

Our study provides the first examination of factors affecting larval growth and possibly prerecruit survival of yellowfin tuna in the Pacific Ocean. Future research is necessary to better understand small-scale variability in growth and mortality rates of yellowfin tuna larvae within their feeding environment. To that end, we are conducting further studies at the Achotines Laboratory in Panama to examine vital rates of this species and the interactions of these vital rates with biological and physical processes to complement our field measurements and to gain more insight into prerecruit survival of yellowfin tuna.

¹⁰ Maunder, M. N., and S. J. Harley. 2004. Status of yellowfin tuna in the eastern Pacific Ocean in 2002 and outlook for 2003, p. 5–119. Inter-American Tropical Tuna Commission, stock assessment report 4. IATTC, 8604 La Jolla Shores Drive, La Jolla, CA 92037.

¹¹ Maunder, M. 2004. Personal commun. Inter-American Tropical Tuna Commission, 8604 La Jolla Shores Drive, La Jolla, CA 92037.

Acknowledgments

We are grateful to the entire staff of the IATTC's Achotines Laboratory who made this study possible. We especially thank R. Lauth, D. Soliz, M. Samaniego, A. Cano, J. Stadler, and M. Vergara, the principal crew members of the *Achotines III* during frequently hazardous field sampling. We also thank I. Díaz, D. Domínguez, K. Herrera, and A. García for processing and sorting ichthyoplankton samples. T. Foreman, R. Owen, E. Espinoza, D. Ballesteros, Y. Ballesteros, and P. Vergara also assisted in the field sampling. Logistic and maintenance support was provided by J. Budria, V. Scholey, and E. Espinoza. T. Foreman, R. Olson, R. Lauth, and R. Owen were principally involved in the development of the ichthyoplankton and oceanographic sampling program, and the raw data were processed by R. Lauth, J. Stadler, R. Owen, and R. Olson. We also thank M. Samaniego, E. Espinoza, D. Mancilla, S. Thorrold, R. Jope, C. Vergara, D. Soliz, P. Vergara, B. Ballesteros, Y. Ballesteros, D. Ballesteros, and A. Cano, who assisted with or conducted night-light and light-trap operations. Helpful discussions were appreciated and provided by D. Ambrose, R. Deriso, P. Fiedler, S. Harley, R. Olson, R. Owen, P. Smith, and P. Tomlinson. M. Maunders provided the quarterly recruitment estimates. C. Patnode helped with final preparations of the figures. W. Bayliff, S. Harley, R. Owen, K. Schaefer, and two anonymous reviewers provided helpful review comments. Finally, we thank the former and present directors, J. Joseph and R. Allen, and the chief scientist of the Tuna-Billfish Program, R. Deriso, of the IATTC for their continued support of this research.

Literature cited

- Ahlstrom, E. H.
1971. Kinds and abundance of fish larvae in the eastern tropical Pacific, based on collections made on EAST-ROPAC I. *Fish. Bull.* 69:3-77.
- Allman, R. J., and C. B. Grimes.
1998. Growth and mortality of little tunny (*Euthynnus alletteratus*) larvae off the Mississippi River plume and Panama City, Florida. *Bull. Mar. Sci.* 62:189-197.
- Ambrose, D. A.
1996. Scombridae: Mackerels and tunas. In *Guide to the early stages of fishes in the California Current region* (H. G. Moser, ed.), p. 1270-1285. *Calif. Coop. Ocean. Fish. Inves., CALCOFI Atlas* 33.
- Barber, M. C., and G. P. Jenkins.
2001. Differential effects of food and temperature lead to decoupling of short-term otolith and somatic growth rates in juvenile King George whiting. *J. Fish Biol.* 58:1320-1330.
- Barber, R. T., and F. P. Chavez.
1986. Ocean variability in relation to living resources during the 1982-83 El Niño. *Nature* 319:279-285.
- Barber, R. T., M. P. Sanderson, S. T. Lindley, F. Chai, J. Newton, C. C. Trees, D. G. Foley, and F. P. Chavez.
1996. Primary productivity and its regulation in the equatorial Pacific during and following the 1991-1992 El Niño. *Deep-Sea Res. II* 43:933-969.
- Blackburn, M., R. M. Laurs, R. W. Owen, and B. Zietzschel.
1970. Seasonal and areal changes in standing stocks of phytoplankton, zooplankton and micronekton in the eastern tropical Pacific. *Mar. Biol.* 7:14-31.
- Campana, S. E., and J. D. Neilson.
1985. Microstructure of fish otoliths. *Can. J. Fish. Aquat. Sci.* 42:101-1032.
- Chavez, F. P., P. G. Strutton, G. E. Friederich, R. A. Feely, G. C. Feldman, D. G. Foley, and M. J. McPhaden.
1999. Biological and chemical response of the equatorial Pacific Ocean to the 1997-98 El Niño. *Science* 286:2126-2131.
- Chow, S., and S. Inoue.
1993. Intra- and interspecific restriction fragment length polymorphism in mitochondrial genes of *Thunnus* tuna species. *Bull. Nat. Res. Inst. Far Seas Fish.* 30:207-224.
- Chow, S., H. Okamoto, N. Miyabe, K. Hiramatsu, and N. Barut.
2000. Genetic divergence between Atlantic and Indo-Pacific stocks of bigeye tuna (*Thunnus obesus*) and admixture around South Africa. *Mol. Ecol.* 9:221-227.
- Chow, S., K. Nohara, T. Tanabe, T. Itoh, S. Tsuji, Y. Nishikawa, S. Ueyanagi, and K. Uchikawa.
2003. Genetic and morphological identification of larval and small juvenile tunas (Pisces: Scombridae) caught by a mid-water trawl in the western Pacific. *Bull. Fish. Res. Agency* 8:1-14.
- Collette, B. B., and C. E. Nauen.
1983. FAO species catalogue. Vol. 2, Scombrids of the world. An annotated and illustrated catalogue of tunas, mackerels, bonitos, and related species known to date. *FAO Fish. Synop.* 125, 137 p. FAO, Rome.
- Comyns, B. H., R. F. Shaw, and J. Lyczkowski-Schultz.
2003. Small-scale spatial and temporal variability in growth and mortality of fish larvae in the subtropical northcentral Gulf of Mexico: implications for assessing recruitment success. *Fish. Bull.* 101:10-21.
- Cowan, J. H., Jr., and E. D. Houde.
1992. Size-dependent predation on marine fish larvae by ctenophores, scyphomedusae and planktivorous fish. *Fish. Oceanogr.* 1:113-126.
- Cury, P., and C. Roy.
1989. Optimal environmental window and pelagic fish recruitment success in upwelling areas. *Can. J. Fish. Aquat. Sci.* 46:670-680.
- Cushing, D. H.
1975. *Marine ecology and fisheries*, 278 p. Cambridge Univ. Press, Cambridge, England.
- Dessier, A., and J. R. Donguy.
1987. Response to El Niño signals of the epipelagic copepod populations in the eastern tropical Pacific. *J. Geophys. Res.* 92:14,393-14,403.
- De Vries, D. A., C. B. Grimes, K. L. Lang, and D. B. White.
1990. Age and growth of king and Spanish mackerel larvae and juveniles from the Gulf of Mexico and U.S. South Atlantic Bight. *Envir. Biol. Fish.* 29:135-143.
- Essig, R. J., and C. F. Cole.
1986. Methods of estimating larval fish mortality from daily increments in otoliths. *Trans. Amer. Fish. Soc.* 115:34-40.
- FAO (Food and Agriculture Organization).
2004. *Fishery statistics: capture production, 2002*. FAO Yearbook, *Fish. Stat.* 94/1, 654 p.

- Fiedler, P. C.
1992. Seasonal climatologies and variability of eastern tropical Pacific surface waters. NOAA Tech. Rep. NMFS 109, 65 p.
2002. The annual cycle and biological effects of the Costa Rica Dome. *Deep-Sea Res.* 1, 49:321–338.
- Forsbergh, E. D.
1963. Some relationships of meteorological, hydrographic, and biological variables in the Gulf of Panama. *Inter-Am. Trop. Tuna Comm. Bull.* 7:1–109.
1969. On the climatology, oceanography and fisheries of the Panama Bight. *Inter-Am. Trop. Tuna Comm. Bull.* 14:45–385.
- Fortier, L. and W. C. Leggett.
1985. A drift study of larval fish survival. *Mar. Ecol. Prog. Ser.* 25:245–257.
- Glynn, P. W., J. L. Mate, A. C. Baker, and M. O. Calderon.
2001. Coral bleaching and mortality in Panama and Ecuador during the 1997–1998 El Niño-Southern Oscillation event: Spatial/temporal patterns and comparisons with the 1982–1983 event. *Bull. Mar. Sci.* 69:79–109.
- González Armas, R.
2002. Aggregation of fish larvae in El Bajo Espiritu Santo in the Gulf of California, their changes in the patterns of distribution and the oceanographic processes that influence them. [In Spanish]. Ph.D. diss, 216 p. Centro de Investigaciones del Noroeste S. C. La Paz, Baja California South.
- Govoni, J. J., A. J. Chester, D. E. Hoss, and P. B. Ortner.
1985. An observation of episodic feeding and growth of larval *Leiostomus xanthurus* in the northern Gulf of Mexico. *J. Plankton Res.* 7:137–146.
- Graves, J. E., M. A. Simovich, and K. M. Schaefer.
1988. Electrophoretic identification of early juvenile yellowfin tuna, *Thunnus albacares*. *Fish. Bull.* 86:835–838.
- Grimes, C. B.
2001. Fishery production and the Mississippi River discharge. *Fisheries* 26(8):17–26.
- Grimes, C. B., and J. J. Isely.
1996. Influence of size-selective mortality on growth of gulf menhaden and king mackerel larvae. *Trans. Am. Fish. Soc.* 125:741–752.
- Hoff, G. R., and L. A. Fuiman.
1993. Morphometry and composition of red drum otoliths: changes associated with temperature, somatic growth rate, and age. *Comp. Biochem. Physiol.* 106A:209–219.
- Houde, E. D.
1987. Fish early life dynamics and recruitment variability. *Am. Fish. Soc. Symp.*
1989. Comparative growth, mortality, and energetics of marine fish larvae: temperature and implied latitudinal effects. *Fish. Bull.* 87:471–495.
- Jenkins, G. P., and T. L. O. Davis.
1990. Age, growth rate, and growth trajectory determined from otolith microstructure of southern bluefin tuna *Thunnus maccoyii* larvae. *Mar. Ecol. Prog. Ser.* 63:93–104.
- Jenkins, G. P., J. W. Young, and T. L. O. Davis.
1991. Density dependence of larval growth of a marine fish, the southern bluefin tuna, *Thunnus maccoyii*. *Can. J. Fish. Aquat. Sci.* 48:1358–1363.
- Ji, M., A. Leetmaa, and J. Derber.
1995. An ocean analysis system for seasonal to interannual climate studies. *Mon. Wea. Rev.* 123:460–481.
- Johnson, M. W., J. R. Rooker, D. M. Gatlin III, and G. J. Holt.
2002. Effects of variable ration levels on direct and indirect measures of growth in juvenile red drum (*Sciaenops ocellatus*). *J. Exp. Mar. Biol. Ecol.* 274:141–157.
- Kaji, T., M. Tanaka, M. Oka, H. Takeuchi, S. Ohsumi, K. Teruya, and J. Hirokawa.
1999. Growth and morphological development of laboratory-reared yellowfin tuna *Thunnus albacares* larvae and early juveniles, with special emphasis on the digestive system. *Fish. Sci.* 65:700–707.
- Lang, K. L., C. B. Grimes, and R. F. Shaw.
1994. Variations in the age and growth of yellowfin tuna larvae, *Thunnus albacares*, collected about the Mississippi River plume. *Environ. Biol. Fish.* 39:259–270.
- Large, W. G., and S. Pond.
1981. Open ocean momentum flux measurements in moderate to strong winds. *J. Phys. Oceanogr.* 11:324–336.
- Lauth, R. R., and R. J. Olson.
1996. Distribution and abundance of larval scombridae in relation to the physical environment in the northwestern Panama Bight. *Inter-Am. Trop. Tuna Comm. Bull.* 21:125–167.
- MacKenzie, B. R., T. J. Miller, S. Cyr, and W. C. Leggett.
1994. Evidence for a dome-shaped relationship between turbulence and larval fish ingestion rates. *Limnol. Oceanogr.* 39:1790–1799.
- Margulies, D.
1993. Assessment of the nutritional condition of larval and early juvenile tuna and Spanish mackerel (Pisces: Scombridae) in the Panama Bight. *Mar. Biol.* 115:317–330.
2001. Preface. Early life history studies of yellowfin tuna, *Thunnus albacares*. *Inter-Am. Trop. Tuna Comm. Bull.* 22:5–8.
- Margulies, D., J. M. Suter, S. L. Hunt, R. J. Olson, V. P. Scholey, J. B. Wexler, and A. Nakamura.
In press. Spawning and early development of captive yellowfin tuna, *Thunnus albacares*. *Fish. Bull.*
- Margulies, D., J. B. Wexler, K. T. Bentler, J. M. Suter, S. Masuma, N. Tezuka, K. Teruya, M. Oka, M. Kanematsu, and H. Nikaido.
2001. Food selection of yellowfin tuna, *Thunnus albacares*, larvae reared in the laboratory. *Inter-Am. Trop. Tuna Comm. Bull.* 22:9–51.
- Matsumoto, W. M., E. H. Ahlstrom, S. Jones, W. L. Klawe, W. J. Richards, and S. Ueyanagi.
1972. On the clarification of larval tuna identification particularly in the genus *Thunnus*. *Fish. Bull.* 70:1–12.
- McGowan, J. A., and V. J. Fraundorf.
1966. The relationship between size of net used and estimates of zooplankton diversity. *Limnol. Oceanogr.* 11:456–469.
- Miller, T. J., L. B. Crowder, J. A. Rice, and E. A. Marschall.
1988. Larval size and recruitment mechanisms in fishes: toward a conceptual framework. *Can. J. Fish. Aquat. Sci.* 45:1657–1670.
- Nishikawa, Y., M. Honma, S. Ueyanagi, and S. Kikawa.
1985. Average distribution of larvae of oceanic species of scombroid fishes, 1956–1981. *Far Seas Fish. Res. Lab., S Ser.* 12, 99 p.
- Nishikawa, Y., and D. W. Rimmer.
1987. Identification of larval tunas, billfishes and other scombroid fishes (Suborder Scombroidei): an illustrated guide, 20 p. CSIRO Mar. Lab. Rep. 186, Melbourne, Australia.

- Olson, R. J., and V. P. Scholey.
1990. Captive tunas in a tropical marine research laboratory: growth of late-larval and early-juvenile black skipjack *Euthynnus lineatus*. *Fish. Bull.* 88:821-828.
- Owen, R. W.
1989. Microscale and finescale patchiness of small plankton in coastal and pelagic environments. *J. Mar. Res.* 47:197-240.
- Owen, R. W., and B. Zeitzschel.
1970. Phytoplankton production: seasonal change in the oceanic eastern tropical Pacific. *Mar. Biol.* 7:32-36.
- Pepin, P.
1988. Predation and starvation of larval fish: a numerical experiment of size-and growth-dependent survival. *Biol. Ocean.* 6:23-44.
1991. Effect of temperature and size on development, mortality, and survival rates of the pelagic early life history stages of marine fish. *Can. J. Fish. Aquat. Sci.* 48:503-518.
- Peterman, R. M., M. J. Bradford, N. C. H. Lo, and R. D. Methot.
1988. Contribution of early life stages to interannual variability in recruitment of northern anchovy (*Engraulis mordax*). *Can. J. Fish. Aquat. Sci.* 45:8-16.
- Potthoff, T.
1974. Osteological development and variation in young tunas, genus *Thunnus* (Pisces, Scombridae), from the Atlantic Ocean. *Fish. Bull.* 72:563-588.
- Richards, W. J., T. Potthoff, and J. Kim.
1990. Problems identifying tuna larvae species (Pisces: Scombridae: *Thunnus*) from the Gulf of Mexico. *Fish. Bull.* 88:607-609.
- Rochford, D. J.
1962. Hydrology of the Indian Ocean. Part II: the surface waters of the southeast Indian Ocean and the Arafura Sea in the spring and summer. *Aust. J. Mar. Freshwater Res.* 13:226-251.
- Rothschild, B. J., and T. R. Osborn.
1988. Small scale turbulence and plankton contact rates. *J. Plankton Res.* 10:465-474.
- Schaefer, K. M.
1991. Geographic variation in morphometric characters and gill-raker counts of yellowfin tuna *Thunnus albacares* from the Pacific Ocean. *Fish. Bull.* 89:289-297.
1998. Reproductive biology of yellowfin tuna (*Thunnus albacares*) in the eastern Pacific Ocean. *Inter-Am. Trop. Tuna Comm. Bull.* 21:201-272.
2001. Reproductive biology of tunas. *In* Fish physiology, Vol. 19, Tuna: physiology, ecology, and evolution (B. A. Block, and E. D. Stevens, eds.), p. 225-270. Academic Press, San Diego, CA.
- Scholey, V. P.
1993. Effects of temperature and food concentration on growth and survival of late-larval and early-juvenile black skipjack, *Euthynnus lineatus*. M.Sci. thesis, 56 p. Univ. Washington, Seattle, WA.
- Shima, M., and K. M. Bailey.
1994. Comparative analysis of ichthyoplankton sampling gear for early life stages of walleye pollock (*Theragra chalcogramma*). *Fish. Oceanogr.* 3:50-59.
- Smayda, T. J.
1963. A quantitative analysis of the phytoplankton of the Gulf of Panama I. Results of the regional phytoplankton surveys during July and November, 1957 and March, 1958. *Inter-Am. Trop. Tuna Comm. Bull.* 7:191-253.
1966. A quantitative analysis of the phytoplankton of the Gulf of Panama III. General ecological conditions, and the phytoplankton dynamics at 8°45'N, 79°23'W from November 1954 to May 1957. *Inter-Am. Trop. Tuna Comm. Bull.* 11:353-612.
- Smith, P. E., and S. L. Richardson.
1977. Standard techniques for pelagic fish egg and larva surveys. *FAO Fish. Tech. Paper*, 175, 100 p. FAO, Rome.
- Strutton, P. G., and F. P. Chavez.
2000. Primary productivity in the equatorial Pacific during the 1997-98 El Niño. *J. Geophys. Res.* 105:26,089-26,101.
- Sverdrup, H. U., M. W. Johnson, and R. H. Fleming.
1942. Dynamics of ocean currents. Chapter 13. *In* The oceans their physics, chemistry, and general biology, p. 431-515. Prentice-Hall, Inc., New York, NY.
- Takeyama, H., S. Chow, H. Tsuzuki, and T. Matsunaga.
2001. Mitochondrial DNA sequence variation within and between tuna *Thunnus* species and its application to species identification. *J. Fish Biol.* 58:1646-1657.
- Thorrold, S. R.
1993. Post-larval and juvenile scombrids captured in light traps: preliminary results from the central Great Barrier Reef lagoon. *Bull. Mar. Sci.* 52:631-641.
- Ueyanagi, S.
1969. Observations on the distribution of tuna larvae in the Indo-Pacific Ocean with emphasis on the delineation of the spawning areas of albacore, *Thunnus alalunga*. *Bull. Far Seas Fish. Res. Lab.* 2:177-256.
- Ware, D. M., and R. E. Thomson.
1991. Link between long-term variability in upwelling and fish production in the northeast Pacific Ocean. *Can. J. Fish. Aquat. Sci.* 48:2296-2306.
- Wexler, J. B.
1993. Validation of daily growth increments and estimation of growth rates of larval and early-juvenile black skipjack, *Euthynnus lineatus*, using otoliths. *Inter-Am. Trop. Tuna Comm. Bull.* 20:399-440.
- Wexler, J. B., D. Margulies, S. Masuma, N. Tezuka, K. Teruya, M. Oka, M. Kanematsu, and H. Nikaido.
2001. Age validation and growth of yellowfin tuna, *Thunnus albacares*, larvae reared in the laboratory. *Inter-Am. Trop. Tuna Comm. Bull.* 22:52-91.
- Wild, A.
1994. A review of the biology and fisheries for yellowfin tuna, *Thunnus albacares*, in the eastern Pacific Ocean. *FAO Fish. Tech. Paper* 336:52-107. FAO, Rome.
- Woodbury, D.
1999. Reduction of growth in otoliths of widow and yellowtail rockfish (*Sebastes entomelas* and *S. flavidus*) during the 1983 El Niño. *Fish. Bull.* 97:680-689.
- Wooster, W. S.
1959. Oceanographic observations in the Panama Bight, "Askoy" Expedition, 1941. *Bull. Am. Mus. Nat. Hist.* 118:119-151.
- Wroblewski, J. S., J. G. Richman, and G. L. Mellor.
1989. Optimal wind conditions for the survival of larval northern anchovy, *Engraulis mordax*—a modeling investigation. *Fish. Bull.* 87:387-398.
- Young, J. W., and T. L. O. Davis.
1990. Feeding ecology of larvae of southern bluefin, albacore and skipjack tunas (Pisces: Scombridae) in the eastern Indian Ocean. *Mar. Ecol. Prog. Ser.* 61:17-29.
- Zar, J. H.
1984. *Biostatistical analysis*, 2nd ed., 718 p. Prentice-Hall, Englewood Cliffs, NJ.

Abstract—Annual potential fecundity, batch fecundity, and oocyte atresia were estimated for Atka mackerel (*Pleurogrammus monopterygius*) collected in Alaskan waters during 1993–94. Atka mackerel were assumed to be determinate spawners on the basis of decreasing fecundity after batch spawning events. Histological examination of the ovaries indicated that oocytes in the vitellogenic stage and higher had been spawned in the current spawning season. For an average female of 40 cm, potential annual fecundity was estimated to be 41,994 eggs, average batch size (i.e., batch fecundity) was estimated to be 6689 eggs, and there were 6.13 batches per spawning season. Atresia was estimated by examining postspawning specimens and was found to be substantial. The average amount of atresia for a 40-cm fish was estimated to be 11,329 eggs, resulting in an estimated realized fecundity of only 30,664 eggs and 4.64 batches of eggs per spawning season.

Annual fecundity, batch fecundity, and oocyte atresia of Atka mackerel (*Pleurogrammus monopterygius*) in Alaskan waters

Susanne F. McDermott (contact author)¹

Katherine P. Maslenikov²

Donald R. Gunderson²

Email address for S F. McDermott: Susanne.McDermott@noaa.gov

¹ National Marine Fisheries Service
Alaska Fisheries Science Center
7600 Sand Point Way NE
Seattle, Washington 98115

² University of Washington
School of Aquatic and Fisheries Sciences
Box 355020
Seattle, Washington 98195

The reproductive biology of Atka mackerel (*Pleurogrammus monopterygius*) is characterized by batch spawning by females and nest-guarding by males. This member of the greenling family (Hexagrammidae) is distributed in Russian and Alaskan waters where it is usually found in dense aggregations and associated with areas of fast currents, such as the passes between the Aleutian Islands (Lowe et al., 2002). Peak spawning occurs from July through October in Alaskan waters (McDermott and Lowe, 1997) and from June through September off Kamchatka (Zolotov, 1993). Batches of adhesive eggs are spawned in rock crevices and are guarded by males until they hatch (Gorbunova, 1962; Zolotov, 1993). Studies with archival tags have indicated that males guard nests for 3–4 months (Nichol and Somerton, 2002). Batches of eggs in different phases of development were found within one nest, indicating a promiscuous mating system (Zolotov and Tokranov, 1989; Zolotov, 1993; Lowe et al., 2003).

Atka mackerel females spawn their annual complement of eggs in several batches over the course of the spawning season. Zolotov (1993) reported that females spawn an average of three batches of eggs per season and that there is at least a two-week hiatus between spawnings in Kamchat-

kan waters. To estimate the number of batches spawned by a female, it is necessary to estimate annual fecundity and batch fecundity. Annual fecundity is defined as the total number of eggs spawned by a female in a single year and batch fecundity is defined as the numbers of eggs released at one time (Nichol and Acuna, 2001). Direct estimation of annual fecundity is possible if the number of eggs to be spawned that season is fixed or determinate (Hunter et al., 1985). Fish with determinate fecundity are described as showing a well-defined hiatus (or gap) in oocyte-size distribution between the advanced oocytes that will be spawned that year and the immature oocytes that will not develop until the following spawning seasons (Hunter et al., 1985). Species that are characterized by continuous oocyte development and oocyte-size distributions have often been described as indeterminate spawners (Hunter et al., 1985) that have the ability to develop unyolked oocytes continually and add them to the standing stock of advanced-yolked oocytes even after spawning begins. Hunter and Macewicz (2001) stated that potential fecundity can be estimated if three key requirements are met: 1) one can identify a certain standing stock or size range of

Manuscript submitted 22 April 2004
to the Scientific Editor's Office.

Manuscript approved for publication
15 March 2006 by the Scientific Editor.
Fish. Bull. 105:19–29 (2007).

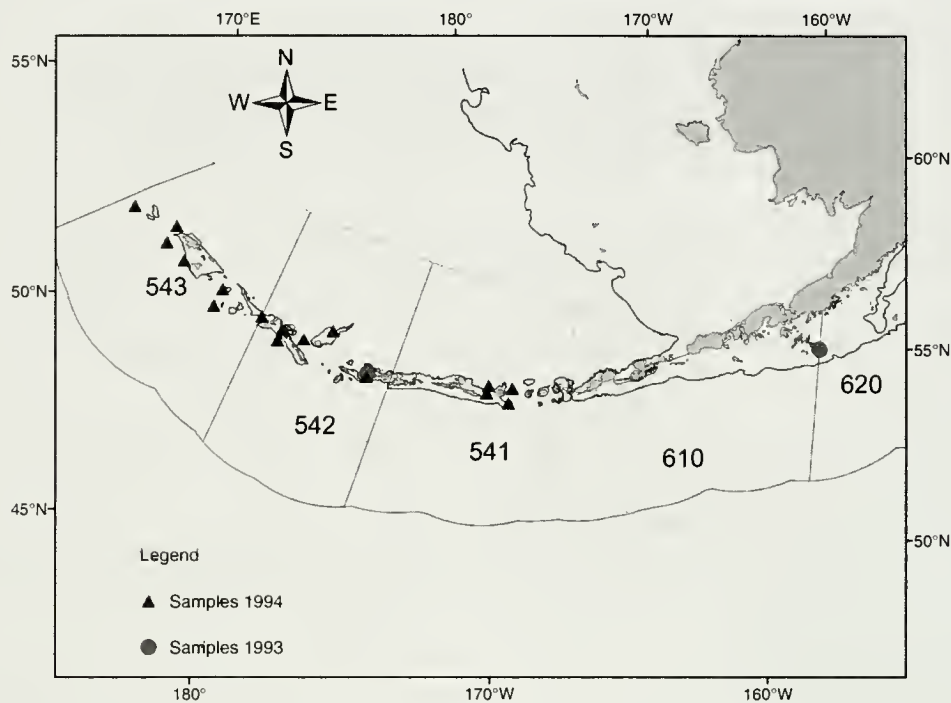


Figure 1

Sampling locations for Atka mackerel (*Pleurogrammus monopterygius*) collected for estimates of annual fecundity and batch fecundity in 1993–94 in the Aleutian Islands, Alaska.

oocytes into which no new oocytes are recruited once spawning begins; 2) females used to estimate potential fecundity have not spawned; and 3) atretic losses are negligible or can be estimated. Recent studies have shown that many fish species reabsorb a substantial number of their oocytes before spawning or at the end of the spawning season—a process known as atresia (Hunter and Macewicz, 1985; Kjesbu et al., 1991; Ma et al., 1998). Atretic losses in Icelandic cod (*Gadus morhua*) and Atlantic herring (*Clupea harengus*) occur mainly during the earlier phase of vitellogenic development, decrease as oocytes mature, and are negligible near the time of spawning (Harðardóttir et al., 2001; Kurita et al., 2003). Scombroid fishes (mackerels and tunas) have been described as having extensive atresia at the end of their spawning season (Hunter and Macewicz, 2001).

Previous studies (Zolotov, 1993) have described Atka mackerel as determinate spawners. However, no study to date has examined the oocyte-size distribution or shown that fecundity decreases after spawning. We examined the oocyte-size distribution for mature oocytes over time. Additionally, all ovaries were examined histologically to identify advanced oocyte stages, presence of postovulatory follicles, and oocyte atresia. We estimated potential annual fecundity and batch fecundity. The number of batches to be spawned was calculated by dividing total fecundity by batch fecundity. Potential fecundity was studied by comparing prespawning individuals with those that had spawned at least one batch of eggs in order to determine if advanced oocytes

are added throughout the spawning season. Atresia of mature oocytes was estimated from ovaries of post-spawning females to calculate realized fecundity as a measure of oocytes actually spawned per year.

Materials and methods

Data collection

All Atka mackerel examined in this study were either collected by the National Marine Fisheries Service (NMFS) fisheries observers aboard commercial fishing vessels during the commercial Atka mackerel fishery in 1993 or by Alaska Fisheries Science Center (AFSC) scientists during the 1994 NMFS bottom trawl survey of the Aleutian Islands (Table 1, Fig. 1).

During both years, Atka mackerel were subsampled from individual trawl tows. Collections were stratified by fish size; no more than five fish per size group were collected in each NMFS statistical area during a sampling year. The fork length of each fish was measured to the nearest centimeter, and each fish was weighed to the nearest 0.1 kg. In most cases, the stomach was emptied before weighing the fish. The ovaries were excised and placed in labeled cloth bags in 10% formalin solution buffered with sodium acetate (20 g per liter solution). In order to determine maturity stage, and presence of atresia, all ovaries were processed histologically. Four ovarian sections (4- μ m thick) were stained

Table 1

Number of fish collected by year, month, and National Marine Fisheries Service (NMFS) statistical area. The number of samples with postovulatory follicles, i.e., in spawning or postspawning condition are shown in parentheses.

Year	Month	NMFS statistical areas				Total
		541	542	543	620	
1993	October		4 (4)		5 (5)	9
1994	June	57				57
	July		49	34 (11)		83
	August			10 (9)		10
Total		57	53	44	5	159

with hematoxylin (Sigma Aldrich, St. Louis, MI) and eosin counterstain (Sigma Aldrich, St. Louis, MI) (H&E). Maturity stages were determined by using categories developed by McDermott and Lowe (1997). Ovaries of prespawning females were defined by the lack of hydrated oocytes in June and the absence of postovulatory follicles once hydrated oocytes were present in July. Presence of atresia was determined according to classifications developed by Hunter and Macewicz (1985).

For the estimation of annual fecundity, only females whose ovaries had not shown any signs of releasing oocytes (i.e., all hydrated oocytes were within their follicles and ovaries contained no postovulatory follicles) were used. Different stages of postovulatory follicles can be distinguished in fish that have spawned multiple batches (McDermott and Lowe, 1997). These different stages indicate that postovulatory follicles persist in ovaries longer than the time period between batch spawning events, minimizing the possibility of incorrectly classifying a partly spent fish as a prespawning fish. Prespawning and partly spent specimens were compared to examine determinate spawning.

Gravimetric method

The gravimetric method was used to count and measure oocytes in weighed samples of Atka mackerel ovarian tissue (Hunter et al., 1985). In our fecundity analysis, small cross-sections were excised from preserved Atka mackerel ovaries. The amount of tissue removed was dependent on the size of eggs present, typically ranging from 0.3 g to 2.5 g. The target sample size was approximately 1000 eggs. The cross-section was divided into wedges in order to ensure a representative sample of ovarian wall tissue in relation to the tissue containing eggs. Ovarian wall tissue weight represents a substantial part of total ovary weight and needed to be represented proportionally in the subsamples. The samples were weighed to the nearest 0.001 g and allowed to sit in water for several hours before han-

dling to reduce exposure to formalin. Ovary tissue was teased apart manually under a dissecting microscope and spread evenly in a 50% solution of glycerol in a dish over a grid partitioned by 1-cm squares. The dissecting microscope was equipped with a Javelin Ultrachip CCTV video camera (model JE-7442, Javelin Electronics, Los Angeles, CA), connected to a computer equipped with BioScan Optimas 4.0 scanning software (Bioscan Inc., Edmonds, WA).

All oocyte stages used in our study were previously described by McDermott and Lowe (1997). It was possible to distinguish the cortical alveoli oocyte stage (stage 3) from the more advanced oocyte stages (stage 4 [oil droplet stage] and stage 5 [vitellogenic stage]) when using the dissecting microscope and camera image to examine whole eggs. Oocytes in stage 4 and above showed a distinct ring around the nucleus, which was attributed to the oil and yolk droplets accumulating in the oocyte. Stage-3 oocytes did not show a distinct ring around the nucleus. However, it was not possible to distinguish oil-droplet oocytes (stage 4) from vitellogenic oocytes or more advanced stages (stage 5+) when examining whole eggs. Because oocyte development is usually attributed to oil-droplet and yolk accumulation, it was initially assumed that oocytes below stage 4 would not be spawned in the current spawning event and therefore would serve as reserve oocytes to be spawned in later spawning seasons. To determine oocyte-size composition, all oocytes stage 4 and above were measured along a vertical axis in each 1-cm square of a grid until 250 eggs had been measured. All eggs in the sample determined to be oocyte stage 4 or above were then counted manually under the dissecting microscope to arrive at an estimate of the number of eggs present per gram of tissue that were oocyte stage 4 and greater.

Location of tissue samples within the ovary

We examined six specimens to determine if location of tissue samples within the ovary affected estimates of fecundity. Two specimens had ovaries in the vitellogenic stage, two had ovaries in the early hydration stage, and two had ovaries in the spawning stage. We took three tissue samples per ovary lobe (six per specimen). The samples were taken from the anterior, center, and posterior location within each lobe of the ovary.

All eggs within the tissue sample that were oocyte stage 4 and above were counted and the first 100 oocytes were measured. Analysis of variance (ANOVA) (S-plus, 7.0 for Windows, Insightful Corp., Seattle, WA) (Venables and Ripley, 2002) was used for this examination with ovary lobe (left or right), position within the ovary, and maturity stage as factors. This analysis was carried out for the mean number of eggs per gram of tissue and mean egg size as response variables. The ANOVA indicated that the tissue sample could be taken from either lobe of the ovaries at any location. All further samples were therefore taken from a central location within either one of the ovary lobes.

Determinate versus indeterminate spawning

Direct estimation of annual fecundity is possible if the number of eggs to be spawned that season is fixed (determinate) and there is a well-defined gap in the oocyte-size distribution between advanced oocytes that will be spawned that year and the immature oocytes. In contrast, indeterminate spawners have the ability to develop unyolked oocytes continually and add them to the standing stock of advanced-yolk oocytes even after spawning begins.

To examine whether Atka mackerel are determinate spawners as previously described (Zolotov, 1993), we measured their oocytes to obtain a size distribution for oocytes over time. Additionally, we compared the potential fecundity of prespawning fish with the potential fecundity of fish that had spawned at least one batch. When all oocytes stage 4 and greater were summed, the tally exceeded the expected number of oocytes to be spawned per year, given the number of eggs in the first batch and the previous estimate of an average of three batches per female (Zolotov, 1993). This total number of oocytes led to the hypothesis that stage-4 oocytes may be developed, but not spawned, in a given year and are

part of the standing stock of oocytes to be spawned in the following year. This hypothesis was supported when we found both oil droplet oocytes and atretic advanced-stage oocytes in the spent ovaries of nine specimens collected in 1993 (Fig. 2A).

The specimens from 1994 were consequently divided into two ovary stages:

- 1 Prespawning-stage ovaries: ovaries with the most advanced oocyte stage of vitellogenic or hydrated oocytes that showed no evidence of having been spawned, i.e., did not have postovulatory follicles (POFs).
- 2 Spawning-stage ovaries: ovaries that had spawned at least one batch of eggs and therefore contained POFs.

Potential annual fecundity was estimated with the gravimetric method and the total number of oocytes were further divided into stage-4 and stage-5+ oocytes by using the methods described below. The data were log-transformed and linear regressions were fitted by using S-plus. Ovaries of prespawning and spawning fish were compared by testing for differences in intercepts and slopes with S-Plus (Venables and Ripley, 2002).

Separation of stage-4 oocytes from more advanced oocytes

To test whether Atka mackerel retain all of their stage-4 oocytes as a standing stock for the next year's fecundity, it became necessary to separate the stage-4 oocytes from the rest of the more developed oocyte stages and then subtract the stage-4 oocytes from the total oocyte count. It was not possible to distinguish the oil-droplet-stage oocytes from oocytes in the vitellogenic stage or migratory nucleus stage when examining whole oocytes with the dissecting microscope image and the Optimas software. Therefore, we examined nine ovaries that were recently spent, which contained only healthy stage-4 oocytes and atretic hydrated oocytes that could be easily distinguished (Fig. 2A). The average size distribution of stage-4 oocytes was estimated by measuring approximately 250 stage-4 oocytes per ovary. This size distribution could then be applied to the prespawning-stage ovaries, assuming that stage-4 oocyte-size distributions in spent ovaries were the same as those in prespawning-stage ovaries. To test this assumption, the size distribution from prespawning-stage ovaries in histological preparations was compared to the size distribution in postspawning fish by using ANOVA.

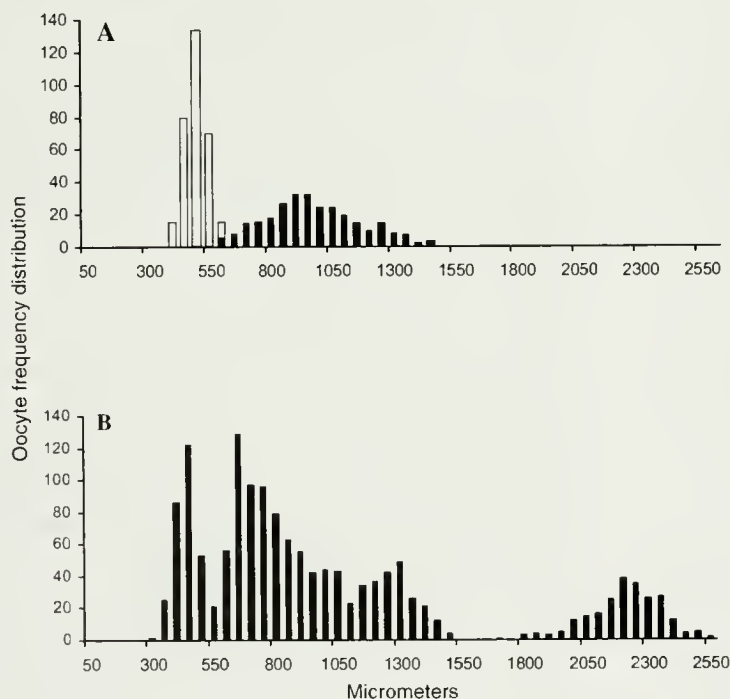


Figure 2

Atka mackerel (*Pleurogrammus monopterygius*) oocyte-size frequency distribution of (A) stage-4 (clear bars) and advanced atretic eggs (black bars) typical of a recently spent ovary, measured from whole oocytes (October 1993); (B) an ovary collected on 2 August 1994, with a hydrated batch of oocytes ready to be spawned (oocytes larger than 1800 μm are hydrated).

In order to deduce the population of stage-4 oocytes from the whole population of stage 5+ oocytes in prespawning-stage ovaries, we determined the size overlap between stage-4 and stage-5 oocytes by examining histological sections from six prespawning-stage ovaries. All oocytes that had been sectioned through the nucleus were measured with a compound microscope and camera system with Optimas software. We determined that all oocytes smaller than 525 μm were stage-4 oocytes and did not overlap in size with stage-5 oocytes in the prespawning-stage ovaries (Fig. 3A). We used the postspawning-stage ovaries that had only stage-4 oocytes and atretic hydrated oocytes to estimate the proportion of stage-4 oocytes that was less than 525 μm . This proportion was then applied to the prespawning-stage ovaries to estimate the number of stage-4 oocytes present.

The total number of stage-4 oocytes in the tissue sample for each prespawning-stage ovary was estimated from

$$\hat{n}_{4i} = \frac{c_i}{\bar{p}} \quad (1)$$

and

$$\bar{p} = \frac{g_i}{m_i}, \quad (2)$$

where \hat{n}_{4i} = estimated total number of stage-4 oocytes in a tissue sample of a prespawning specimen i ;

c_i = total number of stage-4 oocytes <525 μm in a tissue sample for a prespawning specimen i ;

\bar{p} = the estimated proportion of total stage-4 oocytes <525 μm , estimated from ovaries of a postspawning female;

g_i = total number of stage-4 oocytes <525 μm in postspawning-stage ovaries; and

m_i = total number of all stage-4 oocytes in postspawning-stage ovaries.

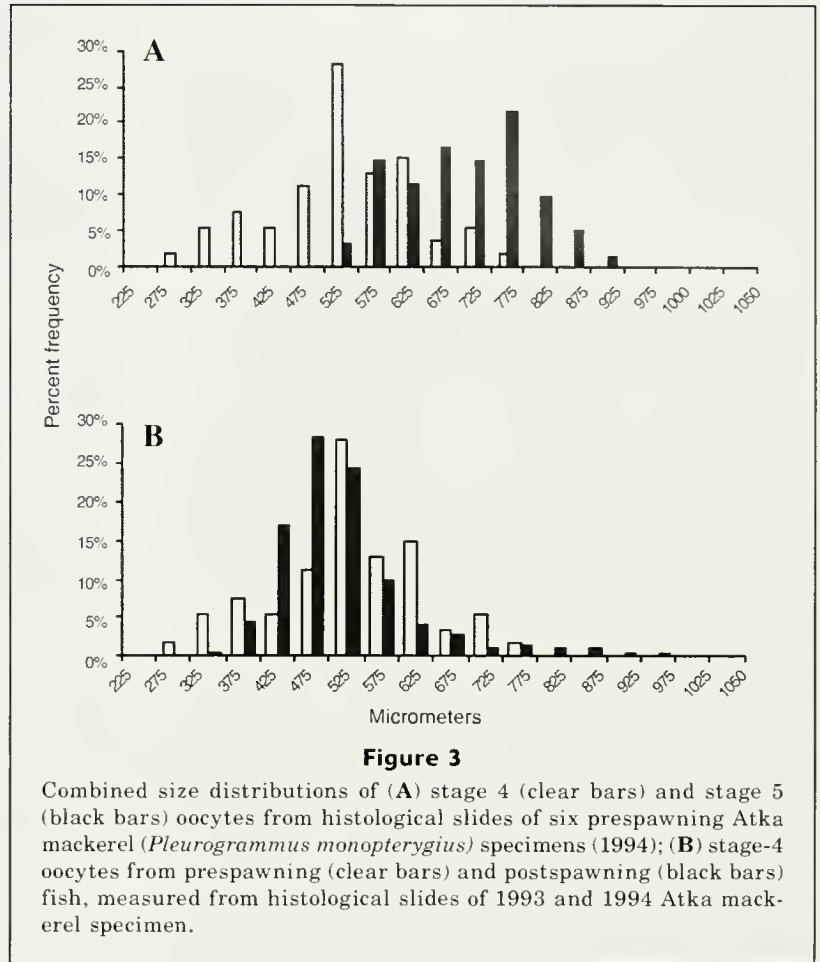
Estimation of potential annual fecundity and batch fecundity

Potential annual fecundity and batch fecundity were calculated by using prespawning specimens. Two scenarios were examined for potential fecundity:

Scenario 1: potential fecundity_{total} (counting oocytes stage 4 and greater); and

Scenario 2: potential fecundity_{stage5+} (counting only oocytes stage 5+).

The following equation was used:



$$\hat{F}_i = \frac{n_i O_i}{W_i}, \quad (3)$$

where \hat{F}_i = estimated potential fecundity or batch fecundity for a prespawning specimen i ;

n_i = number of oocytes in the tissue sample of a prespawning specimen (for potential fecundity_{total}: oocytes of stage 4 and greater; for potential fecundity_{stage5+}: oocytes of stage 5+; for batch fecundity, number of hydrated oocytes);

O_i = total ovary weight (g) for a prespawning specimen i ; and

W_i = weight of tissue sample (g) for a prespawning specimen i .

Prespawning-stage ovaries that contained oocytes in the early hydration stage (stage 7) or greater were examined to estimate batch fecundity. Atka mackerel appear to hydrate one batch of oocytes at a time and the hydrated oocytes can be clearly separated from less developed oocytes by a gap in oocyte-size distribution (Fig. 2B).

Length-fecundity relationships

Length-fecundity relationships and their 95% confidence intervals were computed for potential annual fecundity (\hat{F}_l), batch fecundity (\hat{B}_l), and the number of atretic oocytes (\hat{E}_l) by using nonlinear regression in S-plus (Venables and Ripley, 2002) with the following model:

$$Y = aL^b \quad (4)$$

where $y = \hat{F}_l, \hat{B}_l, \hat{E}_l$;
 a and b = fecundity parameters to be estimated; and
 L = fork length.

Oocyte atresia

Occurrence of atresia was divided into high occurrence (more than 10% of oocytes are atretic) and low occurrence (less than 10% of oocytes are atretic) by examining visually all histological slides. Because incidence of atresia was low in prespawning- and spawning-stage ovaries, it was not quantified further.

The occurrence of oocyte atresia in spent oocytes or oocytes that had been spawned was determined by counting the number of atretic oocytes present in the tissue sample of whole oocytes. Atretic eggs were easily distinguished from nonatretic eggs by their shriveled appearance, dark to almost black coloration, and dense texture. In postspawning fish, it appeared that all oocytes in an advanced stage were atretic and that stage-4 or smaller oocytes were healthy (Fig. 2A). When the histological slides of the same specimen were examined for verification of the oocyte stages, it appeared that all atretic oocytes that were counted corresponded to alpha and beta atresia stages (Hunter and Macewicz, 1985). The total number of atretic oocytes for each specimen (E_l) was calculated by multiplying atretic oocytes per gram of tissue by total weight of both ovaries.

Realized annual fecundity

Realized annual fecundity is defined as the number of oocytes actually spawned per fish in a given year. In order to take the occurrence of atresia into account, a predicted realized fecundity-at-length was calculated by subtracting predicted atresia-at-length from the predicted potential fecundity-at-length, by using

$$\hat{R}_l = \hat{F}_l - \hat{E}_l, \quad (5)$$

where \hat{R}_l = estimated realized annual fecundity at length l ;
 \hat{F}_l = estimated potential annual fecundity at length l ; and
 \hat{E}_l = estimated number of atretic oocytes at length l .

Variance (Var) of the predictions at length was calculated as the sum of the variances (estimated with

S-plus) of the predicted values for potential fecundity-at-length and atresia-at-length:

$$\text{Var}(\hat{R}_l) = \text{Var}(\hat{F}_l) + \text{Var}(\hat{E}_l). \quad (6)$$

Annual number of batches spawned

The potential number of batches spawned for each specimen i was estimated from

$$\hat{D}_i^{pot} = \frac{\hat{F}_i}{\hat{B}_i}, \quad (7)$$

where (\hat{D}_i^{pot}) = the potential number of batches spawned for each specimen i ;

\hat{F}_i = potential fecundity for specimen i , and
 \hat{B}_i = batch fecundity for specimen i .

Batch number for realized fecundity for specimen i was calculated by using the predicted proportion of atretic eggs per length category and applying it to each specimen:

$$\hat{D}_{il}^{real} = \frac{\hat{F}_l(1 - p_l^{atr})}{\hat{B}_l}, \quad (8)$$

where

$$p_l^{atr} = \frac{\hat{E}_l}{\hat{F}_l}, \quad (9)$$

where \hat{D}_{il}^{real} = the batch number per specimen i at length l ;

p_l^{atr} = the predicted proportion atretic at length l ;

\hat{E}_l = the predicted number of atretic eggs at length l ; and

\hat{F}_l = the predicted potential fecundity at length l .

The relationship between batch number and length was examined for both potential and realized fecundity with linear regression (S-plus).

Results

Data collection

Nine samples were collected after spawning events in October 1993 in NMFS statistical areas 542 ($n=4$) and 620 ($n=5$) (Table 1, Fig. 1). One hundred-fifty fish were collected from June through August in 1994 in NMFS statistical areas 541 ($n=57$), 542 ($n=49$), and 543 ($n=44$). Most (130) of these fish were in prespawning condition, i.e., contained no postovulatory follicles, and 20 had spawned at least one batch of eggs. Because the fish were collected during the NMFS Aleutian survey, which systematically moves from east to west along the Aleutian archipelago, all specimens in area 541 (Eastern Aleutian Islands) were considered prespawning fish. Spawning commenced in late July in area 542 and by the middle of August all fish collected showed signs of spawning.

Location of tissue samples in ovaries

The effect of ovary lobe location or position within the ovary was not significant for either average egg size ($P=0.07$, 0.43 , respectively) or mean number of eggs per gram of ovary tissue ($P=0.07$, 0.53 , respectively). Maturity stage of ovary had a significant effect on both eggs per gram ($P<0.0001$) and average egg size ($P<0.0001$).

Separation of oil-droplet–stage oocytes (stage 4) from more advanced oocytes

There was no significant difference in mean egg size for stage-4 oocytes in pre- and postspawning fish ($P=0.59$) (Fig. 3B). We determined that all oocytes smaller than $525\ \mu\text{m}$ that were measured were stage-4 oocytes (Fig. 3A). The proportion of stage-4 oocytes less than $525\ \mu\text{m}$ (\bar{p}) was 0.755 based on samples of postspawning fish in 1993, with $g_i = 1592$ (the number of stage-4 oocytes that measured smaller than $525\ \mu\text{m}$), and $m_i = 2110$ (the total number of stage-4 oocytes measured). This proportion was treated as a constant when estimating the number of oocytes in stage 5 and larger.

Determinate versus indeterminate spawning

With the exception of hydrated eggs, Atka mackerel are characterized by a continuous oocyte-size distribution much like that of an indeterminate spawner (Fig. 4). Atka mackerel ovaries contain several stages of developing oocytes throughout the spawning season.

However, the length-fecundity relationship for the total number of oocytes decreased after the fish had spawned their first batch (Fig. 5A) and there was a significant difference in intercept and slope ($P=0.01$ and 0.001 , respectively). When the length-fecundity relationship for oocytes in stage 5+ was examined, the potential fecundity also decreased after spawning (Fig. 5B), with a significant difference in intercept and slope ($P=0.003$ and $P=0.009$, respectively). The numbers of stage-4 oocytes did not appear to differ substantially before and after spawning for fish of comparable size (Fig. 5C) although the slope of the length-fecundity relationship differed significantly ($P=0.012$). Furthermore, there was no reduction in the number of stage-4 oocytes at comparable fish lengths for the nine spent fish collected late in the spawning season (October) versus prespawning and spawning fish collected in June–August.

Oocyte atresia

Incidence of oocyte atresia in prespawning and spawning fish was found to be low. Only 15 of the 150 ovaries examined showed any signs of atresia. Of these 15 ovaries, high occurrence of atresia (more than 10% of oocytes affected) was found in 3, and low occurrence of

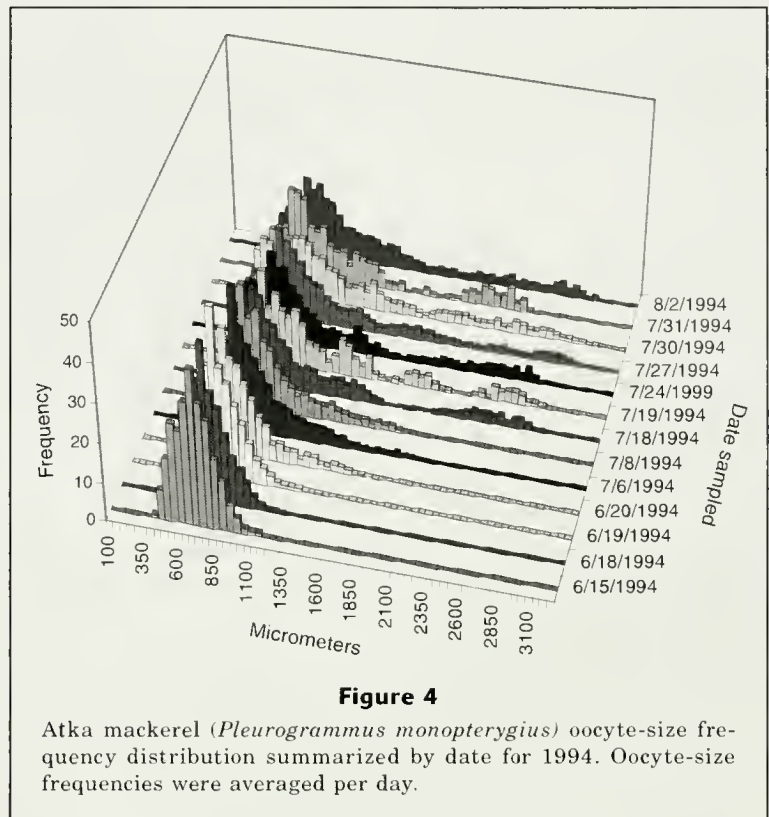


Figure 4
Atka mackerel (*Pleurogrammus monoptyerygius*) oocyte-size frequency distribution summarized by date for 1994. Oocyte-size frequencies were averaged per day.

atresia (less than 10% of oocytes affected) was found in 12. Therefore, atresia in ovaries of pre- and postspawning fish was not quantified further.

Atresia was found to be present in all of the nine ovaries of postspawning fish examined in the study and the number of atretic oocytes corresponded roughly with the number of oocytes spawned in a batch (batch size). This finding indicates that Atka mackerel may use atresia to regulate reproductive output at the end of the spawning season.

Estimates of annual fecundity and batch fecundity

Length-fecundity parameters (a and b) for predicted fecundities for scenario 1 (oocytes \geq stage 4) and scenario 2 (oocytes \geq stage 5), as well as estimates of batch fecundity and atretic eggs are shown in Table 2 with their respective standard errors. Predicted potential fecundity for both scenarios is shown in Figure 6A.

The length-fecundity relationship for oocytes at stage 5+ is the most realistic because it appears that most stage-4 oocytes will not be spawned in the current season. Predicted potential and realized fecundity for stage 5+ oocytes are illustrated in Figure 6A with their respective confidence intervals. Because the estimates of potential fecundity were treated as data in the length-fecundity regressions, the variance estimates and confidence intervals are conservative. Data and model fit for the relationship of batch fecundity to length is shown in Figure 6B, and the data and model fit for the number of

Table 2

Atka mackerel length-fecundity coefficients derived with the equation $F = aL^b$, where F = fecundity and L = fish fork length (cm). SE = standard error of the mean. CI = 95% confidence intervals for predicted values of the mean. n = number of fish in sample.

Fecundity type	Constants				n	Estimate for 40-cm female ($\pm 95\%$ CI)
	a		b			
	Estimate	SE	Estimate	SE		
Potential fecundity _{total}	0.5601	0.5067	3.0865	0.2409	130	49,321 \pm 2535
Potential fecundity _{stage5+}	2.3716	2.0913	2.6517	0.2352	130	41,994 \pm 2061
Number of atretic eggs	0.0013	0.0083	4.3303	1.6502	9	11,329 \pm 8802
Batch fecundity	0.1157	0.1923	2.9726	0.4536	33	6689 \pm 577
Realized fecundity _{total}						37,992 \pm 7873
Realized fecundity _{stage5+}						30,664 \pm 7730
	Mean value		SD			
Batch number potential _{stage5+}	6.13		1.35		33	6.13 \pm 2.64
Batch number potential _{total}	7.04		1.52		33	7.04 \pm 2.98
Batch number realized _{stage5+}	4.64		1.03		33	4.64 \pm 2.01
Batch number realized _{total}	5.6		1.15		33	5.33 \pm 2.25

atretic eggs in the ovary by length category is shown in Figure 6C. Average number of batches corresponding to potential and realized fecundity are shown in Figure 6D.

The average fork length for females during the 1994 NMFS survey was 40 cm (Lowe and Fritz, 1994). Potential fecundity (stage 5+) was estimated to be 41,994 eggs, and realized annual fecundity was estimated to be 30,664 eggs for a 40-cm female (Table 2). Batch fecundity for a 40-cm female was estimated to be 6689 eggs and the number of batches spawned showed no statistically significant relationship with length for both potential ($P=0.35$) and realized ($P=0.75$) fecundity (Fig. 6D). The estimated number of batches produced annually per female was calculated by using the grand mean and standard deviation for all specimens combined. The average number of batches of eggs for potential and realized fecundity was estimated at 6.1 and 4.5 batches per year, respectively, with corresponding 95% confidence intervals of ± 2.64 and ± 2.21 batches. This result would indicate that the average female has the potential to spawn about 6 batches, but may reabsorb 1–2 batches of eggs at the end of the season.

Discussion

The reproductive strategy of Atka mackerel and other hexagrammids has been characterized by low fecundity and large eggs, high parental care, and by larvae hatched at an advanced stage of development (Gorbunova, 1962). Potential fecundity for an average female

Atka mackerel of 40 cm was 41,994 eggs for oocytes at stage 5+ and is higher than the estimates for Kamchatkan waters by Gorbunova (1962), who gave a range between 5000 and 31,000 eggs for a 52-cm female. Zolotov (1993) estimated potential fecundity to be 38,700 eggs (vitelline oocytes plus hydrated oocytes in first batch) off Kamchatka, which is also slightly lower than our estimate. Our batch fecundity estimate of 6689 eggs for an average female of 40 cm is similar to Zolotov's (1993) estimate of 6930 for a fish of the same size.

Atka mackerel are characterized by a continuous size distribution of oocytes much like that of indeterminate spawners. However, Atka mackerel have a distinct spawning season (July–October) during which they spawn batches containing a large number of eggs (Zolotov, 1993; McDermott and Lowe, 1997). This spawning pattern differs from that of typical indeterminate spawners that spawn a small number of eggs (in relation to the total number present) almost continuously for many months, as characterized by the northern anchovy (*Engraulis mordax*) (Hunter et al., 1985). Atka mackerel seem to lie somewhere in the middle of determinate versus indeterminate spawning fish. It appears that there is a potential to develop and spawn up to seven batches if all stage-4 oocytes are developed and spawned. Most of the stage-4 oocytes still remaining in the ovary during the spawning phase probably constitute the pool of oocytes to be spawned in the next season. However, those oocytes could be a reserve to be developed and spawned in highly productive years (i.e., during favorable spawning conditions). Estimates of fecundity based on oocytes at stage 5+ may be conservative if some of the stage-4 oocytes are

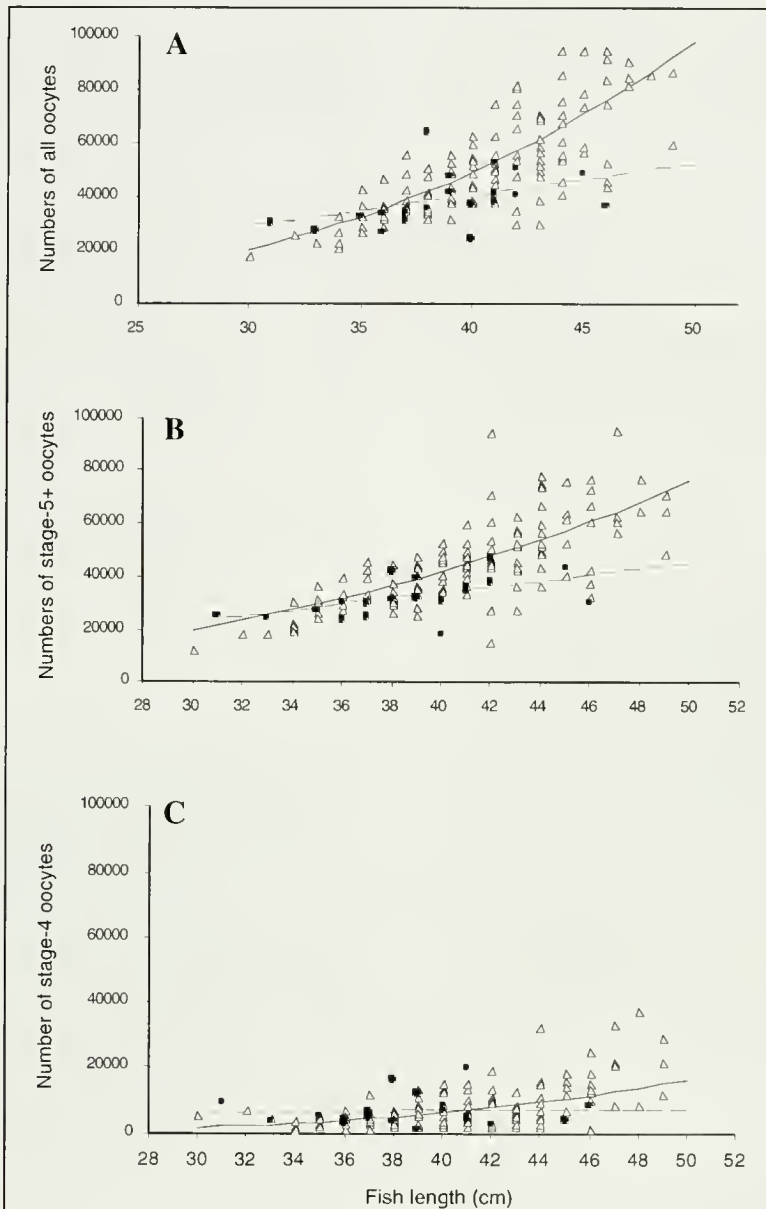


Figure 5

Fecundity of Atka mackerel (*Pleurogrammus monoptyerygius*) at the prespawning (clear triangles) and spawning (solid squares) phase for (A) total number of oocytes at stage 4 and above, (B) oocytes at stage 5+, and (C) for oocytes at stage 4 only. Regression lines for prespawning and spawning fish are indicated by solid and dashed lines, respectively.

developed and spawned late in the spawning season. However, knowledge of batch size, length of spawning season, and the spawning interval between batches (1–2 weeks) (Gorbunova, 1962; Zolotov, 1993; McDermott and Lowe, 1997), gives us confidence that our estimate of fecundity is realistic. Given that there are 14 days between batches, a 75-day incubation period (Lowe et al., 2003; McDermott, 2003), and that 4.6 batches are spawned annually, the spawning season

would be 120 days, which is similar to that observed in the present study.

Conclusions

Prespawning Atka mackerel did not show much atresia during egg development; however high levels of atresia became apparent when ovaries of postspawning fish

were examined. Examination of ovaries of prespawning females alone would lead to the assumption that the potential fecundity is close to the realized fecundity. Atresia in postspawning Atka mackerel has been

described in earlier studies (Gorbunova, 1962; Zolotov, 1993), where 400–500 atretic eggs per ovary and the prolonged presence of atretic eggs in the ovaries before reabsorption have been reported. However, this is the first study where atresia from recently spent ovaries has been included in the fecundity analysis in a quantitative manner. When recently spent ovaries were examined, it appeared that atresia had a major effect on potential fecundity and that an average of 1–2 batches were reabsorbed at the end of the spawning period in the ovaries examined. It should be noted that specimens with ovaries in the prespawning phase and specimens with recently spent ovaries were collected in different years. Atresia is likely to be related to feeding ecology, availability of appropriate substrate and environmental conditions for spawning, and could potentially change from year to year. Interannual variability of atresia should be examined in the future.

Acknowledgments

We thank G. Thompson and J. Ianelli for their statistical advice and F. Morado for his advice and assistance with histological work. We also thank all the observers and scientists who collected specimens and the commercial fishing industry for providing sampling platforms. G. Stauffer, B. Miller, A. Hollowed, S. Lowe, and S. Hinckley helped greatly by critically reviewing drafts of this paper. This research was supported by the Joint Institute for the Study of the Atmosphere and Ocean (JISAO) under NOAA Cooperative Agreement no. NA67RJ0155 (contribution no. 986).

Literature cited

- Gorbunova, N. N.
1962. Spawning and development of greenlings (family Hexagrammidae). In Greenlings: taxonomy, biology, interoceanic transplantation (T. S. Rass, ed.), p. 1–103. Tr. Inst. Okeanol., Akad. Nauk. SSSR 59:118–182. In Russian (translated by Isr. Program. Sci. Trans., 1970). [Available from Natl. Tech. Inf. Serv., Springfield, VA, as TT 69-55097 S.]
- Harðardóttir, K., O. S. Kjesbu, and G. Marteinsdóttir.
2001. Atresia in Icelandic cod (*Gadus morhua* L.) prior to and during spawning. Report of the working group on modern approaches to assess maturity and fecundity of warm- and cold-water fish and squids (O. S. Kjesbu, J. R. Hunter, and P. R. Withames, eds.), 140 p. Institute of Marine Research, Bergen, Norway.

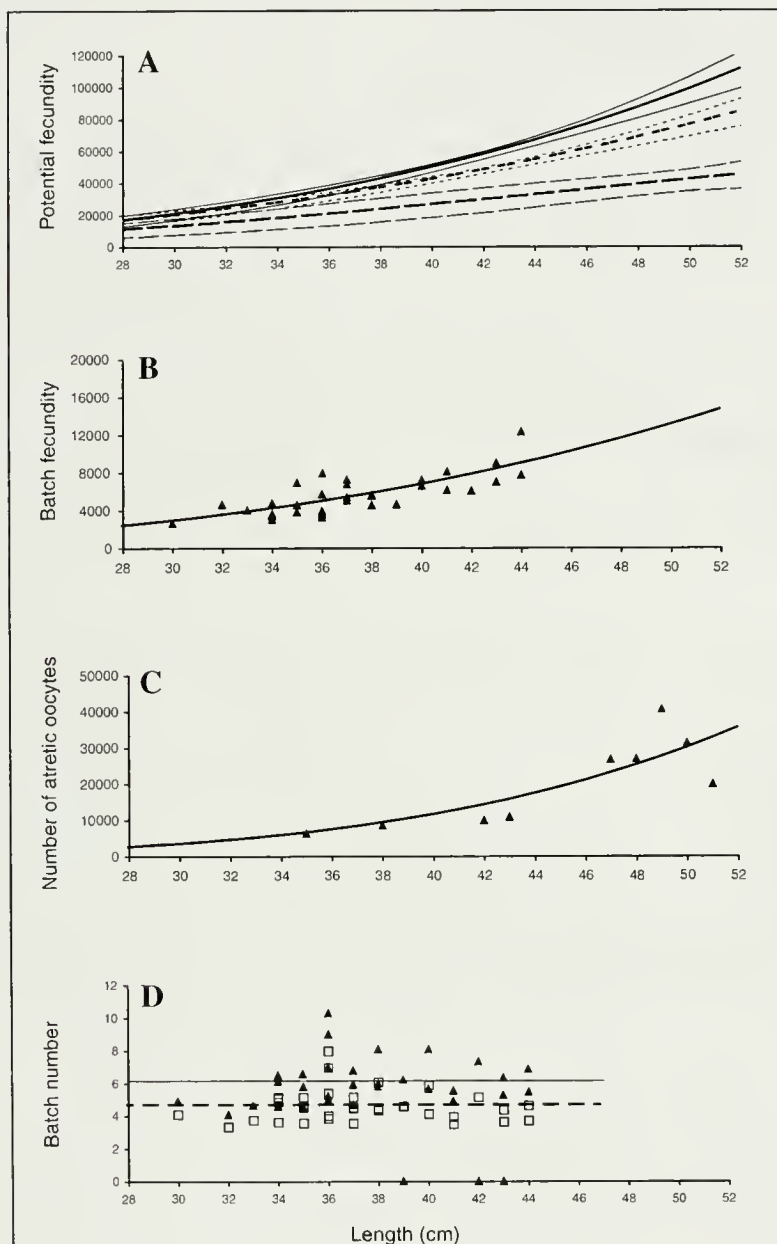


Figure 6

(A) Model fit and 95% confidence intervals for potential fecundity of Atka mackerel (*Pleurogrammus monopterygius*) at length for total number of oocytes (solid lines), stage-5+ oocytes (short dashed lines), and realized fecundity (long dashed lines). (B) Data and model fit (line) for Atka mackerel batch fecundity by length. (C) Data and model fit for number of atretic oocytes in spent ovaries of Atka mackerel by length. (D) Number of batches spawned by length for potential fecundity (solid triangles) and realized fecundity (open squares) and the estimated population means (solid line for potential fecundity and dashed line for realized fecundity) for Atka mackerel.

- Hunter, J. R., N. C. H. Lo, and R. J. H. Leong.
1985. Batch fecundity in multiple spawning fishes. In An egg production method for estimating spawning biomass of pelagic fish: application to the northern anchovy, *Engraulis mordax* (R. Lasker, ed.), p. 67-77. U.S. Dep. Commer., NOAA Tech. Rep. NMFS 36.
- Hunter, J. R., and B. J. Macewicz.
1985. Rates of atresia in the ovary of captive and wild northern anchovy, *Engraulis mordax*. Fish. Bull. 83:119-136.
2001. Improving the accuracy and precision of reproductive information used in fisheries. Report of the working group on modern approaches to assess maturity and fecundity of warm-and cold-water fish and squids (O. S. Kjesbu, J. R. Hunter, and P. R. Withames, eds.), 140 p. Institute of Marine Research, Bergen, Norway.
- Kjesbu, O. S., J. Klungsoyr, H. Kryvi, P. R. Whitthames, and M. Greer Walker.
1991. Fecundity, atresia, and egg size of captive Atlantic cod (*Gadus morhua*) in relation to proximate body composition. Can. J. Fish. Aquat. Sci. 48: 2333-2343.
- Kurita, Y., S. Meier, and O. S. Kjesbu.
2003. Oocyte growth and fecundity regulation by atresia of Atlantic herring (*Clupea harengus*) in relation to body condition throughout the maturation cycle. J. Sea Res. 49:203-219.
- Lowe, S. A., and L. Fritz.
1994. Atka mackerel. In Stock assessment and evaluation report for the groundfish resources of the Bering Sea/Aleutian Islands regions, 11-1-11-43. North Pacific Fisheries Management Council, P.O. Box 103136, Anchorage, Alaska, 99510.
- Lowe, S., J. Ianelli, H. Zenger, and R. Lauth.
2003. Stock assessment of Aleutian Islands Atka mackerel. In Stock assessment and evaluation report for the groundfish resources of the Bering Sea/Aleutian Islands regions, p. 711-776. North Pacific Fisheries Management Council, P.O. Box 103136, Anchorage, Alaska 99510.
- Lowe, S., J. Ianelli, H. Zenger, and R. Reuter.
2002. Atka mackerel. In Stock assessment and evaluation report for the groundfish resources of the Bering Sea/Aleutian Islands regions, p. 609-667. North Pacific Fisheries Management Council, P.O. Box 103136, Anchorage, Alaska 99510.
- Ma, Y., O. S. Kjesbu, and T. Jørgensen.
1998. Effects of ration on the maturation and fecundity in captive Atlantic herring, (*Clupea harengus*). Can. J. Fish. Aquat. Sci. 55:900-908.
- McDermott, S. F.
2003. Estimating abundance of a patchily distributed fish, Atka mackerel, *Pleurogrammus monopterygius*. Ph.D. diss., 149 p. Univ. Washington, Seattle, WA.
- McDermott, S. F., and S. A. Lowe.
1997. The reproductive cycle and sexual maturity of Atka mackerel, *Pleurogrammus monopterygius* in Alaska waters. Fish. Bull. 95:321-333.
- Nichol D. G., and E. I. Acuna.
2001. Annual batch fecundities of yellowfin sole, *Limanda aspera*, in the eastern Bering Sea. Fish. Bull. 99:108-122.
- Nichol, D. G., and D. A. Somerton.
2002. Diurnal vertical migration of the Atka mackerel *Pleurogrammus monopterygius* as shown by archival tags. Mar. Ecol. Prog. Ser. 239:193-207.
- Venables, W. N., and B. D. Ripley.
2002. Modern applied statistics with S-plus, 495 p. Springer-Verlag Inc., New York, NY.
- Zolotov, O. G.
1993. Notes on the reproductive biology of *Pleurogrammus monopterygius* in Kamchatkan waters. J. Ichthyol. 33:(4):25-37.
- Zolotov, O. G., and A. M. Tokranov.
1989. Reproductive ecology of hexagrammidae and cottidae in the Pacific waters of Kamchatka. J. Ichthyol. 3:430-438.

Abstract—We investigated age, growth, and ontogenetic effects on the proportionality of otolith size to fish size in laboratory-reared delta smelt (*Hypomesus transpacificus*) from the San Francisco Bay estuary. Delta smelt larvae were reared from hatching in laboratory mesocosms for 100 days. Otolith increments from known-age fish were enumerated to validate that growth increments were deposited daily and to validate the age of fish at first ring formation. Delta smelt were found to lay down daily ring increments; however, the first increment did not form until six days after hatching. The relationship between otolith size and fish size was not biased by age or growth-rate effects but did exhibit an interruption in linear growth owing to an ontogenetic shift at the postflexion stage. To back-calculate the size-at-age of individual fish, we modified the biological intercept (BI) model to account for ontogenetic changes in the otolith-size–fish-size relationship and compared the results to the time-varying growth model, as well as the modified Fry model. We found the modified BI model estimated more accurately the size-at-age from hatching to 100 days after hatching. Before back-calculating size-at-age with existing models, we recommend a critical evaluation of the effects that age, growth, and ontogeny can have on the otolith-size–fish-size relationship.

Modification of the biological intercept model to account for ontogenetic effects in laboratory-reared delta smelt (*Hypomesus transpacificus*)*

James A. Hobbs (contact author)^{1,2}

William A. Bennett^{1,2}

Jessica E. Burton¹

Bradd Baskerville-Bridges³

Email address for J. A. Hobbs: jahobbs@ucdavis.edu

¹ Bodega Marine Laboratory
2099 Westside Road
Bodega Bay, California 94923-0247

² John Muir Institute for the Environment
University of California, Davis
One Shields Ave.
Davis, California 95616

³ Department of Animal Sciences
University of California, Davis
One Shields Ave.
Davis, California 95616

Otolith-based back-calculation models of size-at-age rely on the assumption that the relationship between otolith and somatic growth is a constant proportion. This has often been examined by simply correlating otolith size with fish size for different aged fish. However, correlations of size among similarly growing body parts over time may not equate to proportional growth among these body parts (Cock, 1966). A comprehensive evaluation of the assumption of proportionality requires examining whether somatic variability is independent of age in the otolith-size–fish-size (OS-FS) relationship (Hare and Cowen, 1995). This requires an assessment of the residual variability between otolith size and fish size-on-age to remove the potential influence of age that can bias the OS-FS relationship (Hare and Cowen, 1995). Furthermore, the “growth effect,” where slow-growing fish have larger otoliths than fast-growing fish for similar-size fish, and the “ontogenetic effect,” where shifts in the OS-FS relationship occur, also need to be addressed before back-calculations. None of these proposed factors necessarily operate in isola-

tion and can occur simultaneously in multiple life stages (Hare and Cowen, 1995; Vigliola et al., 2000; Morita and Matsuishi, 2001). Therefore, before choosing an appropriate model for back-calculating size-at-age, it is necessary to identify the potential mechanisms responsible for variability in the OS-FS relationship.

Back-calculation models differ primarily in their ability to compensate for potential deviations away from a constant proportion between otolith size and fish size. The biological intercept (BI) model (for details on the model see Campana [1990]) compensates for growth effects by incorporating estimates of fish size and otolith size at the origin of the OS-FS proportionality. The time-varying growth (TVG) model adjusts the contribution of small and large increments with regard to body size (see Sirois et al. [1998] for full details), whereas the modified Fry (MF) model directly incorporates the allometric shape of the

Manuscript submitted 24 November 2004
to the Scientific Editor's Office.

Manuscript approved for publication
15 March 2006 by the Scientific Editor.

Fish. Bull. 105:30–38 (2007).

* Contribution number 2313 from the
Bodega Marine Laboratory, Bodega Bay,
California 94923-0247.

relationship into the back-calculation model (for details see Vigliola et al. [2000]). Therefore, although these models can compensate for growth effects when age and ontogenetic effects are linked, they cannot provide accurate estimates when ontogenetic influences act independently of effects caused by growth and age. One means of compensating for ontogenetic shifts in the OS-FS relationship is to use the BI model separately for specific life stages. This model can be useful for providing accurate back-calculations across stage-specific transitions, such as metamorphosis (Jenkins, 1987; Campana, 1990; Otterlei et al., 2002).

We first assess whether the number of ring increments in otoliths accurately reflects absolute age in larvae and juvenile cultured (known-age) delta smelt (*Hypomesus transpacificus*). Second, we evaluate the degree to which age-independent variability occurs in the OS-FS relationship, as well as whether growth rate and ontogenetic effects modify the proportionality of otolith growth to fish growth. Finally, we modify the BI model to account for ontogenetic stage-specific transitions of the OS-FS relationship and compare these results with those from the TVG and MF models to assess the performance of our model for size-at-age back-calculations for delta smelt.

The delta smelt is a small osmerid fish endemic to the San Francisco Bay estuary (McAllister, 1963; Moyle, 2002). Historically one of the most common fishes, it was listed as "threatened" under the Federal and State Endangered Species Acts in 1993 (Moyle et al., 1992; USFWS, 1995; Sweetnam, 1999). Recent precipitous declines in the populations have led to a major investigation regarding the cause of such declines. A few of the potential sources include contaminants and exotic species (Bennett and Moyle, 1996; Bennett et al., 2005), both of which may result in reduced growth rates and poor recruitment. Examination of these hypotheses requires accurate estimates of back-calculated size-at-age for a growth-history assessment of the delta smelt (Fujiwara et al., 2005).

Materials and methods

Larval rearing and otolith examination

All known-age delta smelt larvae were reared at the University of California Davis's delta smelt culturing facility located at the U.S. Bureau of Reclamation John F. Skinner fish facility in Byron, California. Newly hatched larvae were raised in 75-L black tanks at 20 larvae/L. Each tank maintained a flow-through system with filtered water from the Sacramento-San Joaquin delta. Ambient water temperatures during the rearing period ranged from 17° to 20°C and salinities from 0 to 1 ppt. The tanks were held in refrigerated cargo containers under 40-W florescent lights for a 12 h light:12 h dark cycle. Larvae up to 30 days after hatching (dah) were fed *Isochrysis* spp. enriched rotifers. *Nanochloropsis* spp. (green micro-algae) paste was added to create

"green" conditions necessary for larval feeding (Baskerville-Bridges¹; Baskerville-Bridges et al., 2004). Larvae more than 30 dah were fed *Artemia* sp. (brine shrimp) nauplii enriched in Super Selco® (Inve Aquaculture NV, Belgium). Ten larvae up to 10 dah were sacrificed daily with an overdose of MS222 (FINQUEL MS-222 Argent Chemical Laboratories, Inc., Redmond, WA) and fixed in 95% ethanol. Fish from 10 dah to 60 dah were sampled every other day and fish from 60 dah to 100 dah were sampled every 5–7 days (Table 1). Samples were collected from bins representing two spawning pairs of fish.

Sagittal otoliths were dissected from larvae and juveniles with fine forceps and dissecting needles. For larvae, care was taken to photograph and analyze only the sagittal otoliths, which were identified by orientation to the notochord. In delta smelt, the sagittal otoliths are located near the notochord, whereas lapilli are located distally and posteriorly in relation to the sagittae. Otoliths were mounted in Crystal Bond thermoplastic glue (Crystalbond™ 509, Ted Pella Inc. Redding, CA) with the sulcus side down. Otoliths from fish 92 dah and older were sanded with 1200-grit wet and dry sandpaper and polished with 0.3-micron alumina and a polishing cloth. Sagittal otolith radii were measured with a light microscope at 400–100× magnification. All otoliths were analyzed with Image Pro 4.0® (Media Cybernetics, Silver Spring, MD). The first increment was determined as the first ring after the nucleus core. Otolith radius was measured with the aid of image analysis, from the core to the dorsal edge, because this direction was consistently the clearest trajectory. All references to otolith size are radial measurements from the core to the dorsal edge. Sagittae were read by two readers without knowledge of fish age. Two readings were made by each reader and reread if age differences exceeded 10%. If age estimates continued to vary, the otolith was removed from the data set.

Statistical analyses

To determine if increment formation occurred on a daily basis, a Student's *t*-test was used to determine the statistical significance of the slope from a linear regression of increment counts on known age. Under the null hypothesis, the slope of increment counts on known age was equal to one. We rejected the null hypothesis if the slope significantly differed from one.

Statistical analyses, similar to those of Hare and Cowen (1995), were used to evaluate age-independent variability in the OS-FS relationship, as well as growth rate and ontogenetic effects. First, regression models (linear and polynomial) of standard length and otolith

¹ Baskerville-Bridges, B. 2001. Progress and development of delta smelt culture: year-end report 2000. Interagency Ecological Program news letter 14:24–29. Department of Water Resources 827 7th St., Room 301, Sacramento, CA 95814.

Table 1
Summary of sample size, number of increment at designated days after hatching, and mean size-at-age.

Date	No. of Larvae sampled	Days after hatching	Mean no. of increments counted	Difference between days after hatching and mean no. of increments counted	Mean standard length (mm)
March 24	10	0	0	0	5.2
March 25	10	1	0	1	5.2
March 29	10	5	0.4	4.6	5.8
March 31	10	7	1.4	5.6	6.1
April 3	10	10	4.2	5.8	6.6
April 7	5	14	7.8	6.2	7.3
April 11	5	18	12.4	5.6	7.4
April 19	5	26	20	6	8.7
April 25	5	32	25.2	6.8	9.6
May 1	5	38	31.8	6.2	9.9
May 11	5	48	42.8	5.2	12.2
May 21	5	58	52.4	5.6	14.6
May 28	5	65	59.8	5.2	16.5
May 31	5	68	61	7	16.2
June 4	5	72	65.8	6.2	17.1
June 8	5	76	69.8	6.2	17.2
June 12	5	80	73.8	6.2	19.4
June 15	5	84	78.2	5.8	19.6
June 24	5	92	84.4	7.6	20.9
July 2	5	100	94	6	23.5

radius were regressed on age and otolith radius and age on standard length. Second, Pearson correlation coefficients of the otolith radius and standard length-on-age residuals were quantified to estimate the amount of age-independent variability. If no age-independent variability existed in the OS-FS relationship, the residuals of otolith radius-on-age and standard length-on-age should be perfectly correlated. The unexplained variability in the correlation between the residuals of the two models can be considered the degree to which age-independent variability can influence the OS-FS relationship. To account for growth rate effects, Pearson correlation coefficients were quantified for the residuals of age-on-length and otolith radius-on-length. Moreover, significant growth effects were detected with a positive correlation. Lastly, the slopes of the OS-FS relationship for each life stage were compared to account for ontogenetic effects. If otolith growth and fish somatic growth are in constant proportion throughout the life stages in question, the slopes between otolith-fish size should not be significantly different (Cock, 1966). The slope of otolith size to fish size was calculated with an allometric model of the form $y = ax^b$, where log transformation results in the formula $\log(y) = \log(a) + b \times \log(x)$ and the parameter b is equal to the slope (Gould, 1966).

Back-calculations

Size-at-age was back-calculated by using three models (Table 2). First, we examined the TVG model. This model accounts for variability in the underlying assumption of constant proportionality of otolith size to fish size by adjusting the contribution of increment widths by a growth factor. Second, we applied the MF model, which accounts for a nonlinear relationship between otolith size and fish size by directly estimating the shape parameters with a simple allometric model. Finally, a modified stage-specific form of the BI model was applied. Although this model depends on a constant proportion between otolith and fish size, we mediated this effect by applying the model to each specific life stage. To account for our stage-specific differences in the OS-FS relationship, we back-calculated size-at-age for the larval stage (5.4 mm SL to 12 mm SL) and juvenile stage (>12 mm SL) with 12 mm SL as the biological intercept. The mean back-calculated size-at-age trajectory was compared to measured standard lengths at time of sampling. We evaluated the fit of each model to the standard length-at-sampling data by comparing the r^2 values, as well as the minimum and maximum percent deviation of the mean back-calculated size-at-age value from the mean length-at-sampling.

Table 2

Summary of the three back-calculation models examined in this study: the time-varying growth (TVG) model (Sirois et al. 1998), modified Fry (MF) model (Vigliola et al. 2000), and the biological intercept (BI) model (Campana 1990). L =standard length; R =otolith radius; L_{op} =standard length-at-biological intercept; L_i =standard length-at-age i ; L_{cpt} =standard length-at-capture; R_{op} =otolith radius-at-biological intercept; R_i =otolith radius-at-age i ; R_{cpt} =otolith radius-at-capture; W =mean otolith increment width during each life stage; W_i =otolith increment width at i ; G_e =growth effect; and a =allometric shape parameter.

Back-calculation models	Equation	Reference
Time-varying growth (TVG)	$L_i = L_{op} + j(W_i + G_e(W_i - W))(L_{cpt} - L_{op})(R_{cpt} - R_{op})^{-1}$	Sirois et al. (1998)
Modified Fry (MF)	$L_i = a + \exp(\ln(L_{op} - a) + \ln(L_{cpt} - a) - \ln(L_{op} - a))$ $(\ln(R_i) - \ln(R_{op}))(\ln(R_{cpt}) - \ln(R_{op}))^{-1}$	Vigliola et al. (2000)
Biological intercept (BI)	$L_i = L_{cpt} + (R_i - R_{cpt})(L_{cpt} - L_{op})(R_{cpt} - R_{op})^{-1}$	Campana (1990)

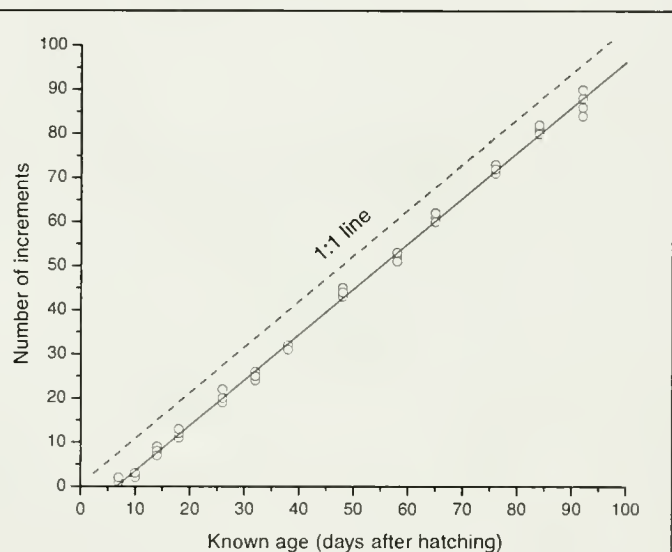
Results

Validation of daily otolith increment formation

The relationship between the number of increments and days after hatching of delta smelt larvae are shown in (Table 1; Fig. 1). The slope of the regression of increment count on known-age was not significantly different from one and thus indicated that increment formation occurred daily. However, the intercept was significantly different from zero ($P < 0.001$), indicating that the first increment was not laid at hatching, rather that ring formation began 6 dah. This observation was confirmed by examination of larvae sampled at one and five dah (Table 1).

Mean somatic and otolith growth

All somatic otolith-growth relationships were best described by life-stage-specific linear regression models, where larval (0–20 dah, 5–12 mm SL) and juvenile (>20 dah, >12 mm SL) life stages were considered separately. Calculated Akaike information criterion (Sokal and Rohlf, 1973) for the linear models were lower than polynomial models ranging from the 2nd to 9th orders. Somatic growth showed variations in growth over time: fast growth occurred from hatching to 40 dah, followed by a period of slowed growth from 40 dah up to 80 dah. After 80 dah, fish experienced a period of rapid somatic growth associated with the juvenile stage (Fig. 2, A and C). Otolith growth showed a different trend. Otolith growth was slow from hatching to 40 dah, which then increased exponentially from 40 dah to 100 dah, indicating that the relationship between otolith growth and fish growth changes abruptly around 40 dah with the completion of caudal flexing (Fig. 2B). Finally, the relationship between otolith size and fish size was best described by a stage-specific linear regression (Fig. 2D), which accounted for the lack of constant linear proportionality of otolith growth to fish growth. It is important to note that some patterns in the residuals were apparent in the early larval stages. However, we do

**Figure 1**

Relationship between the number of increments and the known age for delta smelt (*Hypomesus transpacificus*). Dotted line is the 1:1 ratio line. Solid line is the linear regression line.

not consider these slight deviations to have a significant effect on further residual analyses.

Growth and ontogenetic effects and size back-calculations

Correlations of age-independent effects and growth-rate effects are shown in Figure 3, A and B. The strong correlation between standard length-on-age residuals and otolith radius-on-age residuals may indicate that otolith size is proportional to fish size. The age-independent variability in the OS-FS relationship was accounted for by examining the unexplained variability in the residual analysis of otolith and fish size-on-age. Only 11% of the unexplained variability could be associated with age-independent effects. The Pearson correlation coefficient for the residual of standard length-on-age and otolith

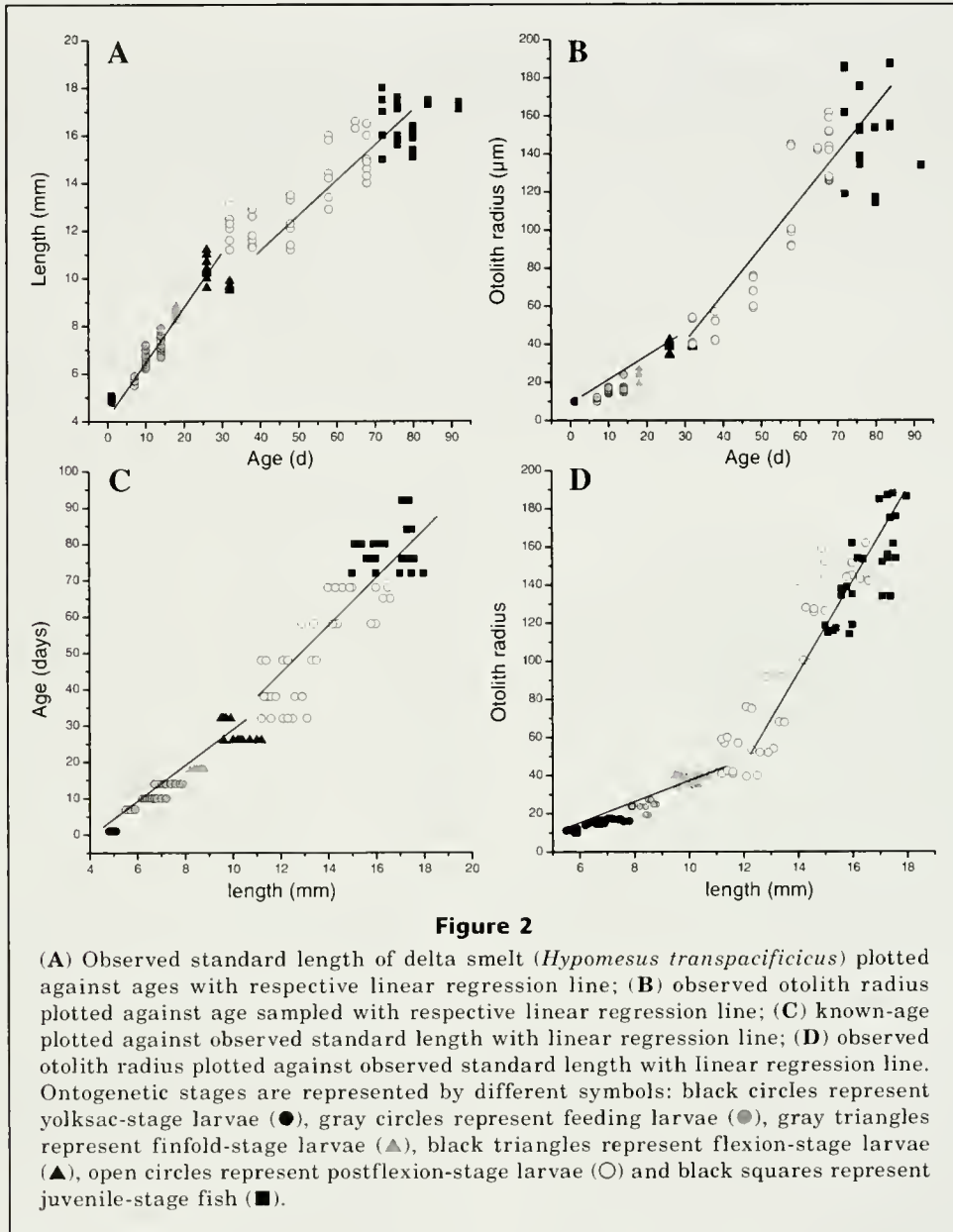


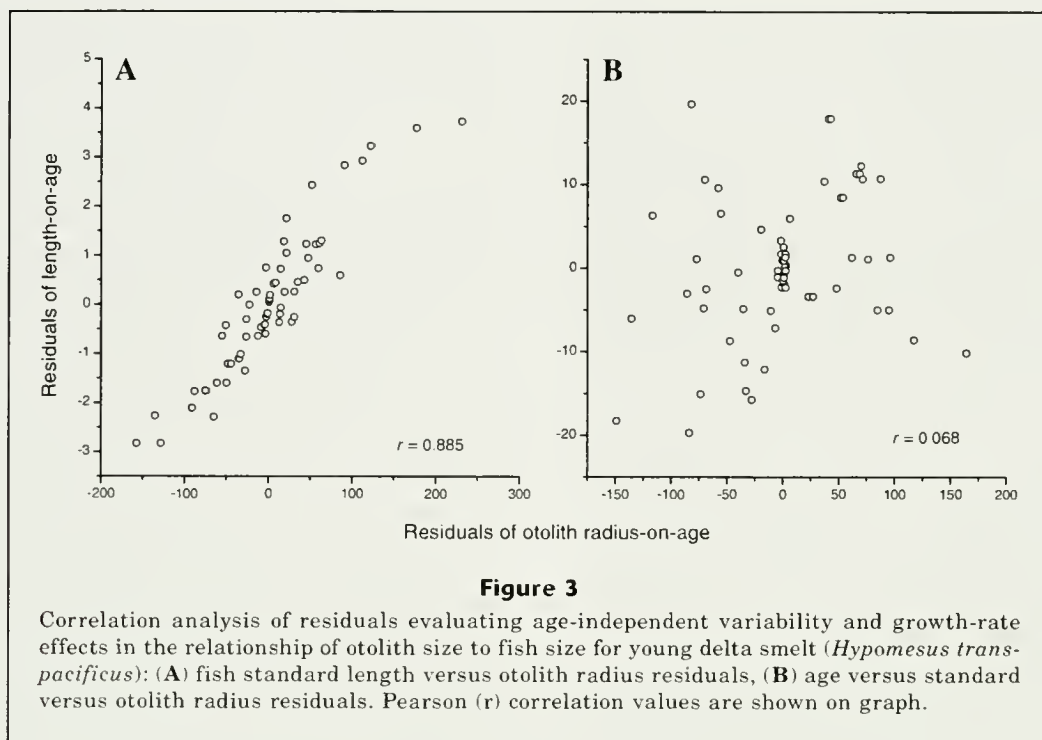
Table 3

Comparison of the allometric slope (*b*) values ($\log(\text{otolith radius}) = b \times \log(\text{standard length})$). *P* values are from Student's *t*-statistic.

Life stage	I	II	III	IV	V	VI
I	—					
II	<0.001	—				
III	<0.001	ns	—			
IV	ns	<0.01	<0.001	—		
V	<0.001	ns	ns	<0.001	—	
VI	<0.001	ns	ns	<0.001	ns	—

radius-on-age was 0.885 ($P=0.001$) (Fig. 3A). Comparison of the residuals of otolith radius-on-length and age-on-length demonstrated that there was no significant growth rate effect on the OS-FS relationship (Fig. 3B). The Pearson correlation coefficient was 0.068 ($P=0.244$).

A simple log transformation of an allometric model demonstrated ontogenetic differences in the slopes of the OS-FS relationship (Fig. 4). Slopes were significantly reduced for the newly hatched yolk-sac stage (I) and the larval flexion stage (IV). However, stage-I larvae were the same age; therefore variability due to ontogeny may be difficult to evaluate. Variability in fish length for stage-IV larvae may reflect subtle ontogenetic differences in caudal fin flexing and thus variation in the OS-FS relationship (Table 3).



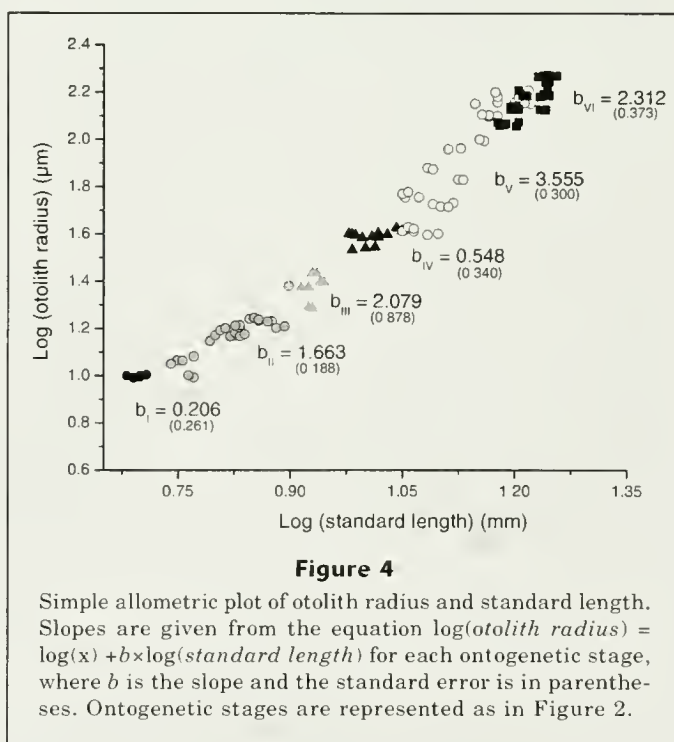
Comparison of the TVG, BI, and MF models

To account for ontogenetic change in the OS-FS relationship, we applied the BI model separately for pre-flexion and postflexion larvae. Mean back-calculated size-at-age for the TVG model varied from -10.3% to $+0.93\%$ of the observed mean-length-at-age and consistently underestimated size from 20 dah to 100 dah. The stage-specific BI model varied from -3.5% to $+6.4\%$, centering closely around zero, and the MF model varied from $+2.4\%$ to $+13.1\%$ and consistently overestimated size from 15 dah to 100 dah (Table 4; Fig. 5). These results indicate that the ontogenetic stage-specific BI model more accurately describes the observed mean size-at-age trajectories for delta smelt. However, the observed size-at-age was variable from 50 dah to 100 dah, resulting in statistically reasonable fits for all the models, with r^2 values ranging from 0.994 to 0.935 (Table 4).

Discussion

Validation of daily otolith increment formation

Accurate size-at-age estimates are important for measuring subtle differences in growth during the early life history of fishes because they are used to examine factors affecting recruitment success for many species (Rice et al., 1987; Sirois and Dodson, 2000). However, variability in age estimates can occur. Much of this variability in age estimates depends largely on when



the first increment is estimated to have formed (Campana and Neilson, 1985; Campana, 2001). In this study, increment formation in laboratory-reared delta smelt began six dah, about the time of first feeding. Numerous studies of other smelt species have also revealed that

daily increments form at first feeding (Sepulveda, 1994; Hirose and Kawaguchi, 2001). However, for some species of smelt, increment formation does occur at hatching (Ohama, 1990). Otterlei et al. (2002) demonstrated that temperature could further increase age variability by altering the timing of the first increment depending upon when, in the season, a fish was born. Delta smelt spawn from late February through June, potentially resulting in cohorts experiencing temperature differences of more than 10°C at birth (Moyle, 2002). This temperature difference could result in up to a two-fold change in the embryonic development and lead to a 2–3 day difference

in the timing of first feeding for delta smelt (first author, unpubl. data).

Otolith-size–fish-size relationship

The results of this study showed that minimal age-independent variability occurred in the OS-FS relationship and that growth rate effects were negligible (Fig. 3, A and B). Removing the effect of age resulted in a strong correlation between otolith growth and fish growth, indicating that at the preflexion stage, otolith growth was proportional to somatic growth. However, the OS-FS relationship showed a significant interruption in linear growth due to an ontogenetic shift at the postflexion stage, thus demonstrating that the assumption of constant proportionality was violated (Fig. 4). Moreover, this change in proportionality corresponded with the transition from preflexion larvae to postflexion-stage juveniles. Several studies, across broad taxonomic orders have demonstrated similar deviations from proportionality in the OS-FS relationship (e.g., flatfish (*Rhombosolea tapirina* and *Ammotretis rostratus*) [Jenkins, 1987], rainbow smelt (*Osmerus mordax*) [Sirois et al., 1998], and Atlantic cod (*Gadus morhua*) [Otterlei et al., 2002]), which were also associated with life-stage transitions.

Measured growth-rate effects were weak for delta smelt (Fig. 3B) and, thus, are not likely to further explain the age-independent variability in the OS-FS relationship. In contrast, Sirois et al. (1998), found significant growth-rate effects in the OS-FS relationship for rainbow smelt. Furthermore, Hare and Cowen (1995) found both growth-rate effects and ontogenetic shifts in the OS-FS relationship for bluefish larvae (*Pomatomus saltatrix*). These studies highlight the different mechanisms responsible for the variability in the otolith and somatic growth relationship, and, thus, potential violations in the constant assumed proportionality for linear back-calculation models.

Other factors that can influence the OS-FS relationship include temperature and salinity. In the field, delta smelt can experience a broad range of temperatures during their larval stage. The effects of differing temperatures at this life stage on the OS-FS relationship and the influence on otolith back-calculations from field-caught fish is unknown. It is assumed that otolith growth is allometric to fish growth during seasonally variable temperatures. For our study, delta smelt were reared in temperature and salinity controlled conditions, and therefore temperature and salinity were considered to have negligible effects and did not influence the variability in the OS-FS relationship. However, temperature variability can result in different

Table 4

Comparison of growth curves generated from otolith size-at-age data. r^2 = coefficient of determination for estimates of size-at-age and known size-at-age for each age group. “% range of mean size-at-capture” represents the variability between estimated size and known mean size at time of sampling.

Model	r^2	% range of mean size at capture
Biological intercept	0.994	–3.5 to +6.4
Modified Fry	0.935	+2.4 to +13.1
Time-varying growth	0.038	–10.3 to +0.90

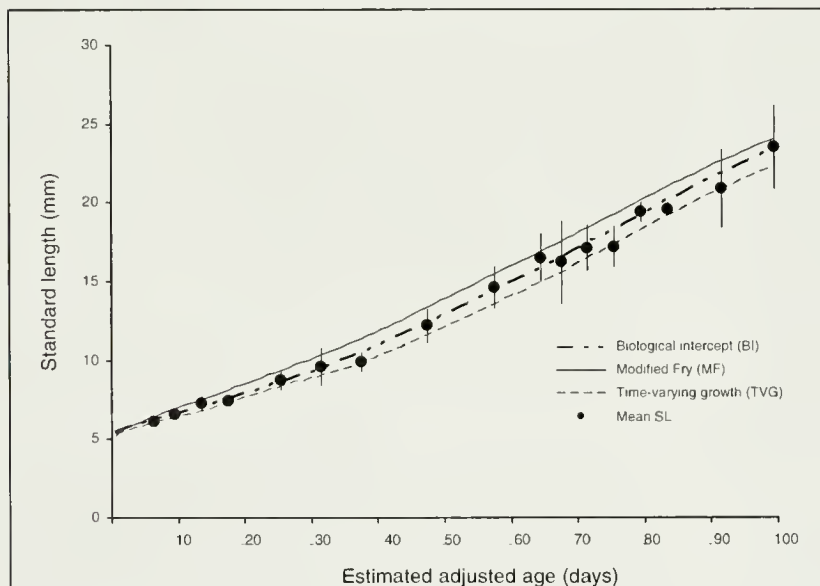


Figure 5

Growth curves back-calculated from delta smelt (*Hypomesus transpacificus*) otoliths. Size-at-age data for laboratory-reared fish are shown as points with ± 1 standard deviation. Three models of back-calculation were used to generate growth curves from otoliths: the modified Fry (MF), the stage-specific biological intercept (BI), and the time-varying growth (TVG) model.

OS-FS relationships and inaccurate size back-calculations. Indeed, Otterlei et al. (2002) found significant differences in the OS-FS relationships for Atlantic cod reared at different temperatures and therefore temperature effects can result in biased back-calculations if not considered in back-calculation procedures.

Despite the strong correlation between otolith and somatic growth during the preflexion stage, a significant shift in this relationship occurred during caudal fin flexing in the juvenile stage. This morphological transition signals a deviation from constant proportionality in the OS-FS relationship for delta smelt. Therefore, the appropriate choice of a back-calculation model will depend on the form of the relationship between otolith size and fish size. Incorrect assumptions regarding the shape of the OS-FS relationship in various back-calculation models may cause errors in back-calculation of size-at-age and the predictability of growth rates (Hare and Cowen, 1995; Otterli et al., 2002). Campana (1990) suggested the use of a stage-specific form of the BI model to account for the ontogenetic shifts in the OS-FS relationship.

Comparison of the TVG and MF model with the stage-specific BI model

The ontogenetic stage-specific BI model used in our study provided the most parsimonious size-at-age estimates. The TVG consistently underestimated size-at-age, whereas the MF model over-estimated size-at-age for fish greater than 30–40 dah (Fig. 5). Estimated mean size-at-age for the stage-specific BI model was most similar to the observed size-at-age with the minimum and maximum percent deviation of individual size-at-age symmetrically distributed about the mean observed size-at-age. In contrast, the minimum and maximum percent deviation was negative for the TVG model and positive for the MF model (Table 4).

Unlike the stage-specific BI model, the TVG and MF models did not accurately estimate size-at-age because of ontogenetic shifts in the OS-FS relationships. The TVG model was developed to compensate for growth-rate effects in the OS-FS relationship (Sirois et al., 1998). However, for reared delta smelt, growth rate effects in the OS-FS relationship were minimal. When growth-rate effects are negligible, the results of the TVG and the nonstage-specific BI model should be identical (Sirois et al., 1998). This study demonstrates that when ontogenetic shifts occur in the OS-FS relationship independent of growth-rate effects, the TVG model may give poor estimates of size-at-age. Moreover, Vigliola et al. (2000) found the MF model accurately estimated size-at-age for three species of *Diplodus* (seabream), because of the allometric OS-FS relationship. However, for delta smelt, the simple allometric relationship of the MF model consistently resulted in an overestimation of size-at-age because of an ontogenetic shift in the OS-FS relationship.

The transition from the preflexion larval stage to the postflexion juvenile stage created difficulties for accurately estimating size-at-age for both the TVG and MF

models. Owing to the unique ontogenetic shift in the OS-FS relationship that delta smelt undergo, the stage-specific BI model more accurately estimated fish size-at-age. However, because of the variability in observed length-at-age, each model described population growth rates with a high degree of certainty (all r^2 values were greater than 0.93). Therefore, we argue that caution should be taken when describing patterns in hatchery-reared growth rates because measured growth rates in our study were significantly reduced in comparison to field growth rates (first author, unpubl. data). Finally, although the intercepts for the stage-specific BI model were derived from the mean population life-stage transition (12 mm SL), the size at life-stage transitions for individuals can be variable, resulting in complex individual biological intercepts that were not taken into consideration.

Conclusions

Criteria for choice of growth back-calculation models

The recent interest in back-calculated size-at-age for individual fish based on otolith increments has resulted in the development of numerous methods to back-calculate size-at-age. The choice of various back-calculation methods can be difficult because assumptions underlying each model may not be evaluated completely. To guide the proper choice of back-calculation models, we recommend a critical examination of the OS-FS relationship. Furthermore, the assessment of ontogenetic variability and growth effects (i.e., Hare and Cowan, 1995) should be evaluated prior to choosing a model. Application of back-calculation techniques requires validation of otolith growth and somatic growth relationships for each species. Therefore, validation may even need to be conducted on a species- or stock-specific basis, and at various levels of environmental variability (see Otterlei et al., 2002). Moreover, accounting for ontogenetic and growth effects on the proportionality of otolith size to fish size will help guide the development and application of appropriate back-calculation models and will lead to accurate estimates of size-at-age for fish recruitment studies. Thus, we conclude that the modified BI model will allow for an accurate estimate of growth histories and reliable information for determining factors influencing delta smelt recruitment.

Acknowledgments

We thank D. Martasian, J. Raum, L. Lewis, and Z. Kane for the work on this project. We also thank the Association of Bay Areas Governments (ABAG), Interagency Ecological Program, and the CALFED Bay-Delta Ecosystem Restoration Program for Funding; the Graduate Group in Ecology at University of California Davis; and S. Morgan and P. Moyle for helpful comments on the manuscript.

Literature cited

- Baskerville-Bridges, B., J. C. Lindberg, and S. I. Dorsoshev.
2004. The effect of light intensity, algal concentration, and prey density on the feeding behavior of delta smelt larvae. *In* Proceedings of the symposium early life history of fishes in the San Francisco estuary and watershed (F. Feyrer, ed.), p. 219–228. Am. Fish. Soc., Santa Cruz, CA.
- Bennett, W. A.
2005. Critical assessment of the delta smelt population in the San Francisco estuary, California. *San Franc. Estuary Watershed Sci.* 3:(2) Article 1.
- Bennett, W. A., and P. B. Moyle.
1996. Where have all the fishes gone? Interactive factors producing fish declines in the Sacramento-San Joaquin estuary. *In* San Francisco Bay: The ecosystem: further investigations into the natural history of San Francisco Bay and Delta with reference to the influence of man (J. T. Hollibaugh, ed.), p. 519–542. Pacific Division of the American Association for the Advancement of Science, San Francisco, CA.
- Campana, S. E.
1990. How reliable are growth back-calculations based on otoliths? *Can. J. Fish. Aquat. Sci.* 47:2219–2227.
2001. Accuracy, precision, and quality control in age determination, including a review of the use and abuse of age validation methods. *J. Fish Biol.* 59:197–242.
- Campana, S. E., and J. D. Neilson.
1985. Microstructure of fish otoliths. *Can. J. Fish. Aquat. Sci.* 42:1014–1032.
- Cock, A. G.
1966. Genetical aspects of metrical growth and form in animals. *Q. Rev. Biol.* 41:131–190.
- Fujiwara, M., B. E., Kendall, R. M., Nisbet, and W. A. Bennett.
2005. Analysis of size trajectory data using an energetic-based growth model. *Ecology* 86:1441–1451.
- Gould, S. J.
1966. Allometry and size in ontogeny and phylogeny. *Biol. Rev.* 41:587–640.
- Hare, J. A., and R. K. Cowen.
1995. Effect of age, growth rate, and ontogeny on the otolith size-fish size relationship in bluefish, *Pomatomus saltatrix*, and the implications for back-calculation of size in fish early life history stages. *Can. J. Fish. Aquat. Sci.* 52:1909–1922.
- Hirose, T., and K. Kawaguchi.
2001. Daily otolith increments and growth of reared chika *Hypomesus japonicus* larvae. *B. Jpn. Natl. Fish. Res. Inst.*:141–144.
- Jenkins, G. P.
1987. Age and growth of co-occurring larvae of two flounder species, *Rhombosolea tapirina* and *Ammotretis rostratus*. *Mar. Biol.* 95:157–165.
- McAllister, D. E.
1963. A revision of the smelt family, Osmeridae. National Museum of Canada. Bulletin no. 191. Biological Series, no. 71, 53 p. Ottawa, Dept. of Northern Affairs and National Resources, Ottawa, Canada.
- Morita, K., and T. Matsuishi.
2001. A new model of growth back-calculation incorporating age effect based on otoliths. *Can. J. Fish. Aquat. Sci.* 58:1805–1811.
- Moyle, P. B.
2002. Inland fishes of California: revised and expanded, 502 p. Univ. California Press, Berkeley, CA.
- Moyle, P. B., B. Herbold, D. E. Stevens, and L. W. Miller.
1992. Life history and status of delta smelt in the Sacramento-San Joaquin estuary, California. *Trans. Am. Fish. Soc.* 121:67–77.
- Ohama, H.
1990. Age determination of Japanese smelt with daily otolith increment. *Nippon Suisan Gakkaishi* 56:1053–1057.
- Otterlei, E., A. Folkvord, and G. Nyhhammer.
2002. Temperature-dependent otolith growth of larval and early juvenile Atlantic cod (*Gadus morhua*). *ICES J. of Mar. Sci.* 59:401–410.
- Rice, J. A., L. B. Crowder, and M. E. Holey.
1987. Exploration of mechanisms regulating larval survival in Lake Michigan [USA] bloater: A recruitment analysis based on characteristics of individual larvae. *Trans. Am. Fish. Soc.* 116:703–718.
- Sepulveda, A.
1994. Daily growth increments in the otoliths of European smelt *Osmerus eperlanus* larvae. *Mar. Ecol. Prog. Ser.* 108:33–42.
- Sirois, P., and J. J. Dodson.
2000. Critical periods and growth-dependent survival of larvae of an estuarine fish, the rainbow smelt *Osmerus mordax*. *Mar. Ecol. Prog. Ser.* 203:233–245.
- Sirois, P., F. Lecomte, and J. J. Dodson.
1998. An otolith-based back-calculation method to account for time-varying growth rate in rainbow smelt (*Osmerus mordax*) larvae. *Can. J. Fish. Aquat. Sci.* 55:2662–2671.
- Sokal, R. R., and J. F. Rohlf.
1973. An introduction to biostatistics, 368 p. W.H. Freeman, San Francisco, CA.
- Sweetnam, D. A.
1999. Status of delta smelt in the Sacramento-San Joaquin estuary. *Cal. Fish Game* 85:22–27.
- USFWS (United States Fish and Wildlife Service).
1995. Sacramento-San Joaquin Delta Native Fishes Recovery Plan, 142 p. United States Fish and Wildlife Service, 911 NE 11th Avenue, Portland, Oregon 97232-4181.
- Vigliola, L., M. Harmelin-Vivien, and M. G. Meekan.
2000. Comparison of techniques of back-calculation of growth and settlement marks from the otoliths of three species of *Diplodus* from the Mediterranean Sea. *Can. J. Fish. Aquat. Sci.* 57:1291–1299.

Abstract—We estimated annual abundance of juvenile blue (*Sebastes mystinus*), yellowtail (*S. flavidus*), and black (*S. melanops*) rockfish off northern California over 21 years and evaluated the relationship of abundance to oceanographic variables (sea level anomaly, nearshore temperature, and offshore Ekman transport). Although mean annual abundance was highly variable (0.01–181 fish/minute), trends were similar for the three species. Sea level anomaly and nearshore temperature had the strongest relationship with interannual variation in rockfish abundance, and offshore Ekman transport did not correlate with abundance. Oceanographic events occurring in February and March (i.e., during the larval stage) had the strongest relationship with juvenile abundance, which indicates that year-class strength is determined during the larval stage. Also of note, the annual abundance of juvenile yellowtail rockfish was positively correlated with year-class strength of adult yellowtail rockfish; this finding would indicate the importance of studying juvenile abundance surveys for management purposes.

Relationship between abundance of juvenile rockfishes (*Sebastes* spp.) and environmental variables documented off northern California and potential mechanisms for the covariation

Thomas E. Laidig (contact author)

James R. Chess

Daniel F. Howard

Email address for T. E. Laidig: tom.laidig@noaa.gov

National Marine Fisheries Service
Southwest Fisheries Science Center
Fisheries Ecology Division
110 Shaffer Road
Santa Cruz, California 95060

Success of annual recruitment of juvenile rockfishes (*Sebastes* spp.) from the pelagic to a demersal phase is highly variable and leads to large fluctuations in year-class strength in the fisheries (Ralston and Howard, 1995). With the abundance of many rockfish stocks at historic low levels, assessment of recruitment is paramount for fishery managers to improve plans for sustainable harvests. Fisheries models (such as the stock synthesis model) often include recruitment data (PFMC¹). In recent years, larval and juvenile rockfish abundance data have been included in stock assessments for bocaccio (*S. paucispinis*) and cowcod (*S. levis*) (MacCall², Butler et al., 2003). If the larval or juvenile abundance data do not accurately reflect the numbers of adults, the models can either over- or underestimate the biomass available to the fishery.

Rockfishes are viviparous, giving birth to larvae that reside in open water for several months before recruiting from the plankton to a more benthic life (Love et al., 2002). The habitat where rockfish initially recruit varies among species and includes floating drift algae (e.g., splitnose rockfish, *S. diploproa* [Shaffer et al., 1995]), soft sediments (e.g., stripetail rockfish, *S. saxicola* [Johnson et al., 2001]), and deeper rocky areas with crevices (e.g., rosy rockfish, *S. rosaceus* [Love et al., 2002]). A major area of recruitment is the nearshore

environment, where numerous species of rockfish recruit in the kelp canopy, sand channels, on rocky outcrops, and in midwater among the kelp stipes (Anderson, 1983).

The factors that influence the magnitude of juvenile recruitment of rockfishes are not well known. VenTresca et al.³ suggested that upwelling was the major factor contributing to the annual variability of juvenile rockfish abundance off Monterey, California. Ralston and Howard (1995) found that the highest survival of blue (*S. mystinus*), and yellowtail rockfish (*S. flavidus*), occurred when sea surface temperature and upwelling were at intermediate levels. Ainley et al.

¹ PFMC (Pacific Fisheries Management Council). 2002. Status of the Pacific Coast groundfish fishery through 2001 and acceptable biological catch for 2002, 26 p. PFMC, 7700 NE Ambassador Place, Suite 200, Portland, Oregon 97220.

² MacCall, A. D. 2002. Status of bocaccio off California in 2002. In Appendix to the status of the Pacific coast groundfish fishery through 2001 and acceptable biological catches for 2002, 58 p. Pacific Fisheries Management Council, 7700 NE Ambassador Place, Suite 200, Portland, Oregon 97220.

³ VenTresca, D. A., J. L. Houk, M. J. Padack, M. L. Gingras, N. L. Crane, and S. D. Short. 1996. Early life-history studies of nearshore rockfishes and lingcod off central California, 1987–92. Cal. Fish Game. Resources Division. Admin. Rep. 96-4, 77 p.

(1993), using seabird diet to assess the abundance of juvenile rockfishes, also reported the greatest abundance of rockfishes in years of intermediate upwelling. Yoklavich et al. (1996) and Johnson et al. (2001) observed that, during years when upwelling was delayed, those rockfishes released later in the year had increased survivorship. In addition, Pastén et al. (2003) observed that monthly tidal cycles were important in estimating the numbers of newly recruited black rockfish (*S. inermis*) in the western Pacific.

In our study, we examined the relationship between the annual abundance of juvenile rockfishes recruiting to the nearshore kelp beds off northern California and three oceanographic variables (sea level anomaly, nearshore temperature, and offshore Ekman transport) over 21 years. Three species of juvenile rockfishes (blue, yellowtail, and black rockfish, [*S. melanops*]) were surveyed. Parturition (the release of larvae from the mother) in these species occurs in the winter and the resulting pelagic larvae and juveniles spend between three to five months in the offshore midwater environment (Love et al., 2002). All juveniles of these species migrate in mid to late spring and early summer from the offshore pelagic environment to nearshore midwater and benthic environments on or next to rocky outcrops, commonly with dense algal growth; this movement we define here as juvenile recruitment (Anderson, 1983).

Materials and methods

Surveys of young-of-the-year (YOY) rockfishes were conducted annually between 1 July and 15 September from 1983 to 2003 within two kelp beds along the northern California coast (Dark Gulch [39°14'N; 123°46'W] and Salmon Point [39°12'N; 123°46'W]) in Mendocino County (Fig. 1). Each kelp bed included high-relief bedrock interspersed with low-relief cobble and sand areas. They were bounded by shoreline on two sides, a sand channel on one side, and deep water on the remaining side, and thus each kelp bed was isolated.

Strip transects were conducted by using SCUBA. Researchers swam in one direction 2 m above the sea floor and counted all juvenile rockfishes within 3 m in any direction for one minute. At the end of each one-minute survey, the numbers of each species were recorded. The researcher would then haphazardly choose another direction to swim and conduct rockfish counts for another minute. Surveys were made throughout the kelp bed at both sites from the surface to 20 m. YOY rockfishes were distinguished from older conspecifics by their size (less than 80 mm standard length in August) and from other rockfish species by body shape and pigment patterns (Anderson, 1983; Love et al., 2002).

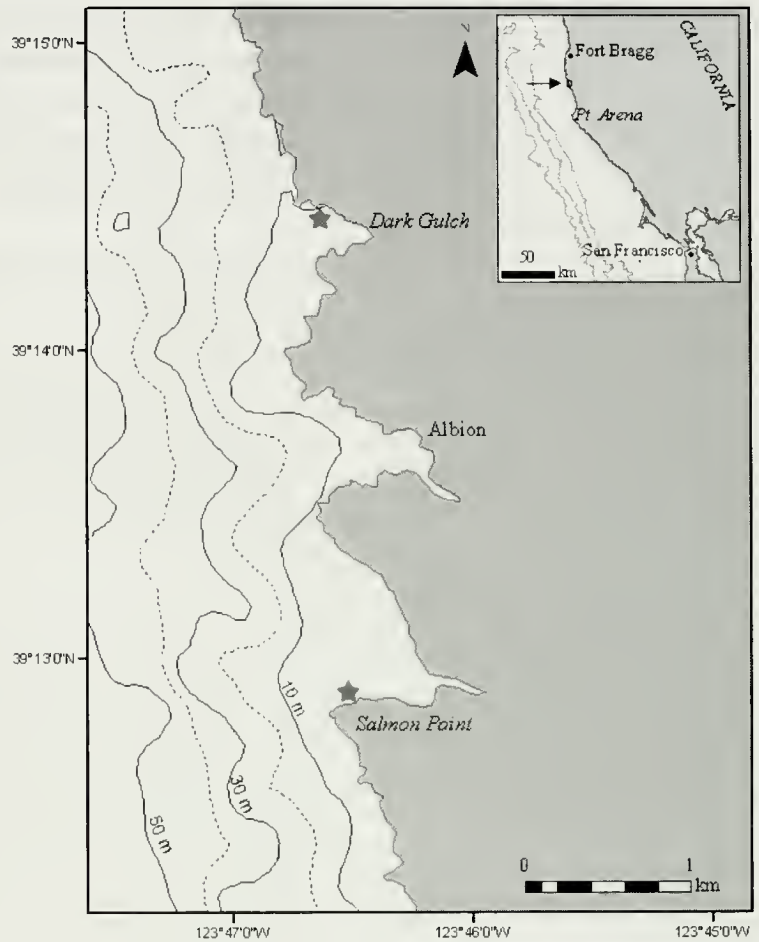


Figure 1

The survey sites in Mendocino County, California. Dark Gulch and Salmon Point kelp beds are represented by the stars.

Surveys were conducted only when appropriate conditions occurred. First, surveys were conducted between the hours of 0900 and 1700 to standardize light conditions. Second, surveys were made only when underwater visibility was greater than 4 m. Underwater visibility was measured by Secchi disk, transect line, and by estimating the distance at which objects (i.e., fishes and rocks) could be seen. Third, swell height had to be less than 2 m for diver safety and to standardize sea conditions.

An index of annual abundance (index) for each species of juvenile rockfish was computed by pooling all one-minute surveys for a year at each study site, and dividing by the total number of one-minute surveys for that year. We used a paired t-test to compare species-specific indices between the two study sites. Data were log-transformed to equalize the variance among years. We used cross-correlation analysis to examine patterns in the index among species. For no time series (either biological or environmental) was there a significant autocorrelation present. Therefore, our observations complied with the assumption of independence.

We related three oceanographic data sets (sea level anomaly, nearshore temperature, and offshore Ekman transport) to abundance data. Sea level anomaly data were collected from a shore station (with an acoustic gauge measuring in mm) at Arena Cove, CA (38°54'N), and monthly means were obtained from the University of Hawaii Sea Level Center. These data represent a measure of change in sea level height over time and were adjusted for local atmospheric conditions. Sea level anomalies reflect water movement—a positive anomaly being associated with poleward flow and a negative anomaly associated with equatorward flow. Nearshore temperature data were continuously collected at the Dark Gulch site throughout the study. Temperature monitors were located in two areas of the kelp bed, one at 8 m and the other at 15 m water depth. Temperature was recorded hourly and these data were averaged daily, monthly, and seasonally. The offshore Ekman transport data were determined from data gathered by a buoy 20 km offshore of 39°N (Albion, CA). Monthly mean offshore Ekman transport was derived from geostrophic wind stress data determined from atmospheric pressure values at mean sea level (at 6-hour intervals) and obtained from Environmental Research Division, Southwest Fisheries Science Center (NOAA⁴). Offshore Ekman transport was used as a measure of cross-shelf water transport. The offshore flow of surface water causes deep, cold, nutrient-rich water to be brought to the surface to replace the displaced surface waters (the process of upwelling). Monthly and seasonal values were determined for all oceanographic data sets and years, and the seasonal values represented the mean from January to June. The months of July to December were not considered in our analysis because this time period was after the time of juvenile rockfish recruitment to the kelp bed.

The comparison of the abundance index for each species and the oceanographic variables involved numerous statistical tests. Cross-correlation coefficients were computed in pairwise comparisons of the index and the oceanographic data. For each year in the time series, we used both seasonal and monthly means of the oceanographic variables and the annual log-transformed index. We also applied principal components analysis (PCA) to evaluate the relationships among monthly oceanographic variables, and also the relationships among the log-transformed index of the three species. We used canonical correlation analysis (CCA) to explicitly examine the correlations between these oceanographic and rockfish PCAs. PCA develops an ordination space constrained to be a linear combination of the variables (i.e., the eigenvectors). CCA does the same, except the ordination space is constrained to be a linear combination of the other set of variables. The fish data, there-

fore, are displayed in a space defined by a combination of the oceanographic data (the canonical scores).

Year-specific catch-at-age data for adult yellowtail rockfish were compared with the juvenile yellowtail rockfish abundance index to evaluate the relationship between juvenile rockfish abundance and subsequent landings of adults in the fishery. No age data were available for the adult blue or black rockfishes. Age and catch data of adult yellowtail rockfish commercially caught in trawls from 1997 to 1999 were retrieved from the CALCOM database⁵ for the three closest ports to our study sites (Bodega Bay, Fort Bragg, and Eureka, CA). We used expanded age compositions by year class, which were determined from a subset of aged fish for that region. For example, in 1997 there were 10 year-classes in a subset of fish that were aged from Bodega Bay, whereas only six year classes existed in the subset of aged fish for 1998 from Bodega Bay. Year-specific catch-at-age data were determined for each year and port and regressed against the log-transformed index. Significance levels were determined for each port-year combination and for all ports combined.

Results

Over 21 years, 172 dives and 3333 one-minute surveys were completed, averaging 8.2 dives/year and 158.7 one-minute surveys/year (Table 1). The average number of one-minute surveys per dive was 19.4 surveys/dive (calculated by dividing the total number of one-minute surveys by the total number of dives). Total number of dives per year varied from 4 in 1993 to 14 in 1983, and the number of one-minute surveys varied from 80 in 1993 to 330 in 1983. The total number of dives at Dark Gulch was 113, whereas only 59 dives were conducted at Salmon Point. Similarly, nearly twice as many one-minute surveys were completed at Dark Gulch (2165) compared to Salmon Point (1168). This difference was mainly due to sea conditions; Salmon Point sometimes experiences larger ocean swells (because it is less protected), making sampling unsafe.

The abundance index for each species varied among years but was not significantly different (t-test; $n=21$; $P>0.05$) between the two study sites. For this reason, the data from both sites were pooled. The index was highly variable for all species (Fig. 2). For blue rockfish, the index varied from 181 fish/min in 1987 to 0.26 fish/min in 1992. For yellowtail rockfish, the index ranged from 162 fish/min in 1985 to 0.03 fish/min in 1994. Abundance of black rockfish peaked in 1999 at 22 fish/min and was lowest in 1998 at 0.01 fish/min.

⁴ NOAA (National Oceanic and Atmospheric Administration). Environmental Research Division. Southwest Fisheries Science Center. NOAA/NMFS/SWFSC, 1352 Lighthouse Ave., Pacific Grove, CA 93950-2097. Website: <http://www.pfeg.noaa.gov> (accessed 15 March 2006).

⁵ CALCOM (California Cooperative Survey). Commercial landings sampling program maintained by California Department of Fish and Game, 350 Harbor Blvd., Belmont, CA 94002; Pacific States Marine Fisheries Commission, 350 Harbor Blvd., Belmont, CA 94002; and Fisheries Ecology Division, SWFSC, NMFS, NOAA, 110 Shaffer Rd., Santa Cruz, CA 95060. Website: 128.114.3.187 (accessed on 15 March 2006).

Table 1

Number of dives and total number of one-minute surveys of juvenile rockfishes by year at each dive site. Data were collected between 1 July and 15 September, 1983–2003.

Year	Number of dives			Number of 1-minute surveys		
	Dark Gulch	Salmon Point	Total	Dark Gulch	Salmon Point	Total
1983	12	2	14	270	60	330
1984	8	3	11	185	99	284
1985	8	4	12	94	35	129
1986	9	2	11	124	30	154
1987	9	3	12	94	18	112
1988	4	3	7	62	38	100
1989	5	3	8	119	68	187
1990	4	2	6	71	33	104
1991	3	3	6	60	60	120
1992	3	3	6	60	60	120
1993	2	2	4	40	40	80
1994	3	3	6	60	60	120
1995	4	3	7	80	40	120
1996	4	1	5	88	22	110
1997	5	3	8	124	71	195
1998	7	2	9	188	40	228
1999	6	5	11	133	89	222
2000	4	3	7	82	84	166
2001	3	3	6	62	63	125
2002	4	4	8	85	87	172
2003	6	2	8	84	41	125
Total	113	59	172	2165	1168	3333
Average	5.4	2.8	dives/year 8.2	103.1	55.6	surveys/year 158.7
Standard deviation	2.6	0.9	2.7	54.7	22.8	63.9

Year-to-year variability was generally synchronous among the three species (Fig. 2). Abundance was below average for the three species in 1983–84, and 1989–98. Above average abundance in all three species occurred in 1985, 1987, 1988, and in 2001. Black rockfish attained relatively greater numbers in 1986, 1999, 2000, and 2003 compared to the other two species. In addition, blue rockfish experienced higher than average abundances in 2001 and 2002 compared to the other species. Generally, the index for black rockfish was lower than for the other two species, but black rockfish abundance was extremely high in 1999, but the abundance of the other two species was below average. Indices for blue and yellowtail rockfish were significantly correlated ($P < 0.001$, $r = 0.91$), and the index for black rockfish was not significantly correlated with either of the other two species. Using the log-transformed index, we found that blue, yellowtail, and black rockfish were all significantly correlated ($P < 0.01$, $r = 0.76$) with each other. We used the log-transformed index for the remaining analyses.

In evaluating seasonal oceanographic variables, sea level anomaly and nearshore temperature were sig-

nificantly and positively correlated ($P < 0.05$, $r = 0.53$), nearshore temperature and offshore Ekman transport were significantly and negatively correlated ($P < 0.05$, $r = -0.69$), and sea level anomaly and offshore Ekman transport were not significantly correlated. There was no significant correlation between the seasonal oceanographic variables and the index for any species.

With PCA, 65% of the variability in the monthly oceanographic (_O) data sets was explained by the first eigenvector ($PC1_O$). $PC1_O$ was characterized by the contrast between Ekman transport and the other two variables (Table 2). The second eigenvector ($PC2_O$) explained 30% of the variability and was associated with high sea level anomaly. For the rockfish abundance (_F) indices, 77% of the variability was explained in the first eigenvector ($PC1_F$), which was associated with the abundance time series of all three species. The second eigenvector ($PC2_F$) explained 15% of the variability and was associated with the contrast between blue rockfish abundance and the other two species, especially late in the time series. Although $PC3_F$ explained only 8% of the variability in these time series, it was associated

Table 2

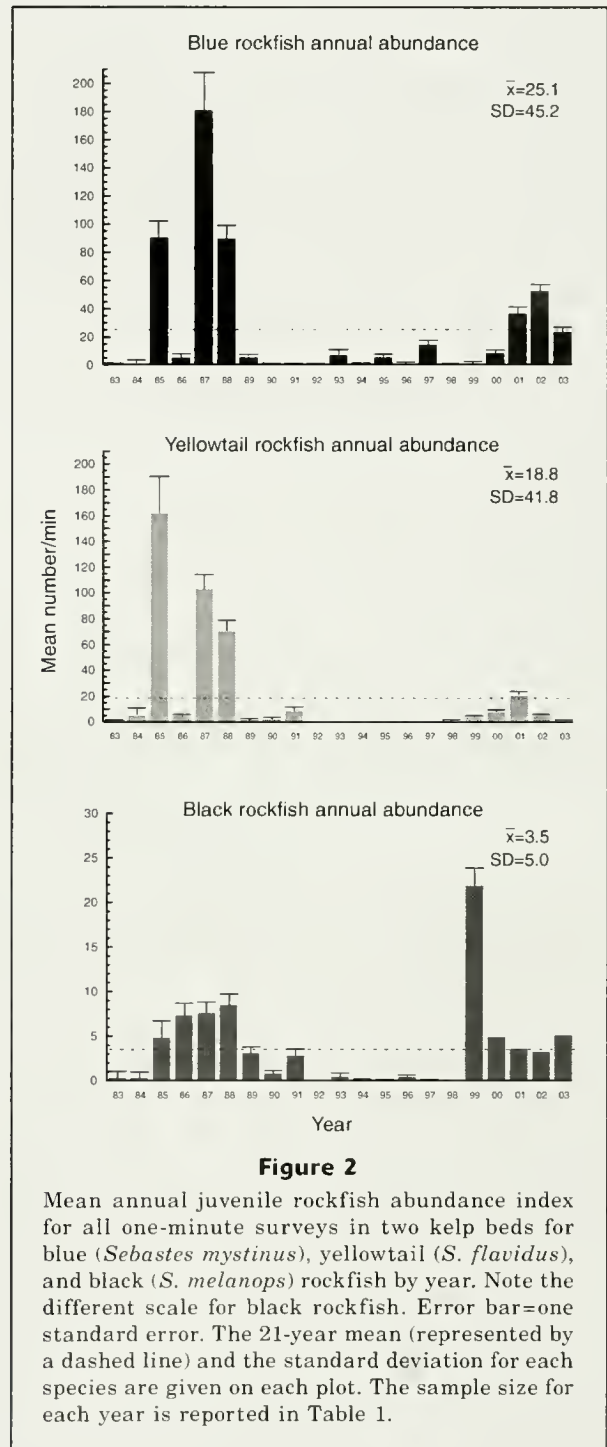
Eigenvectors determined from the principal components analysis (PCA) for the monthly oceanographic variables ($_O$) and log-transformed annual juvenile rockfish abundance ($_F$) index by species

	PC1 _O	PC2 _O	PC3 _O
% variance explained	64.5	29.5	6.0
Nearshore temperature	0.68	-0.04	0.73
Sea level anomaly	0.46	0.80	-0.39
Ekman transport	-0.57	0.40	0.56
	PC1 _F	PC2 _F	PC3 _F
% variance explained	77.1	14.6	8.3
Blue rockfish	0.55	0.83	0.13
Yellowtail rockfish	0.60	-0.28	-0.75
Black rockfish	0.58	-0.49	0.64

with the unique pattern in abundance of black rockfish, especially in contrast to yellowtail rockfish.

Correlations varied between the log-transformed abundance indices and the monthly means of the oceanographic variables (Table 3). All three species were significantly and negatively correlated with sea level anomaly during some of the months from January to June. For nearshore monthly temperature, there was a similar pattern of negative correlation with index for all species during January to June. Only blue rockfish were significantly correlated ($P < 0.001$, $r = 0.58$) with offshore Ekman Transport, and only in February (Table 3). Months of high nearshore temperature or sea level anomaly resulted in low juvenile rockfish abundances. For example, when the abundance index for blue rockfish was compared with sea level anomaly in February (Fig. 3), years of highest abundance of blue rockfish were always years of low sea level anomaly (i.e., 1985, 1987, 1988, 2001, and 2002), but years of low sea level anomaly did not always lead to particularly high rockfish abundance (i.e., 1989). However, years of highest sea level anomaly (e.g., 1983, 1992, and 1998) resulted in the lowest blue rockfish abundance.

The results of the CCA also indicate that low annual abundance was associated with years of high nearshore temperatures and high sea level anomaly. The first canonical correlation was 0.57, which was significantly different from zero ($P < 0.0001$), and explained 97 % of the covariance between the two data sets. The remaining two canonical correlations were not significant and explained little of the variability. Blue, yellowtail, and black rockfish were negatively correlated with the first canonical variable for the oceanographic data set (-0.43, -0.45, and -0.55, respectively; Fig. 4). This indicates that fish abundances were low when temperatures and sea level anomalies were high.



The data for year-class strength of commercially caught adult yellowtail rockfish corresponded with the annual abundance index for juvenile yellowtail rockfish (Table 4), and were significantly correlated for all ports combined for 1997 ($P < 0.01$, $n = 29$, $r = 0.48$) and 1999 ($P < 0.04$, $n = 31$, $r = 0.36$), but not for 1998 ($P < 0.1$, $n = 21$, $r = 0.37$). For 1997, juvenile rockfish abundance was significantly correlated with adult fish numbers at Bodega

Bay ($P < 0.02$, $R = 0.43$, Fig. 5A), Ft. Bragg ($P < 0.001$, $r = 0.62$), and Eureka ($P < 0.01$, $r = 0.78$). In 1998, Bodega Bay was the only port where adult fish numbers were significantly correlated ($P < 0.05$, $r = 0.38$, Fig. 5B) with juvenile abundance. In 1999, Eureka was the only port where adult fish numbers were significantly correlated ($P < 0.05$, $R = 0.35$) with juvenile abundance. From the 1998 adult numbers in Bodega, 1985 was the largest year class of adult yellowtail rockfish, which corre-

sponded to the highest index for juvenile yellowtail rockfish (Fig. 5B).

Discussion

The 21-year time series of juvenile rockfish abundance allowed us to examine long-term change in recruitment of commercially and recreationally important species off the coast of California. The year-to-year variability in recruitment likely relates to variability in year-class strength of the population entering the fisheries. The synchrony in recruitment variability among the three rockfish species indicates that similar environmental processes affect the abundance of all three species. By examining oceanographic variables, we determined that sea level anomaly and nearshore temperatures in February and March were important influences on juvenile rockfish abundance.

Year-to-year variability in young rockfish abundance has been documented in other studies off the west coast of the United States. Yoklavich et al. (1996) found a twenty-fold increase in the abundance of pelagic larval rockfishes off central California in 1993 compared to numbers obtained during a similar time period in 1992. They attributed this difference to increased offshore transport and possibly lower predation rates. Moser et al. (2000) observed large fluctuations in annual larval rockfish abundance off southern California from 1951 to 1998, which was attributed to the reproductive output of each species and oceanographic variables. Mearns et al. (1980) determined that the variability in recruitment of juveniles was the major source of seasonal and annual fluctuations in rockfish catches for strip-tail and calico rockfish (*S. dallii*). Matthews (1989) observed that recruitment levels varied between years for three species of rockfishes recruiting to nearshore habitats. Ainley et al. (1993) discovered a three-fold difference in pelagic juvenile rockfish abundance in seabird diets in central California between similar periods in 1985 and 1986, and they attributed this to cross shelf advection of larvae in January and February. Ralston and Ianelli (1998) reported a large variability in juvenile bocaccio abundance over a 13-year period and attributed some of this variability to El Niño events.

Year-class strength was likely established in the period from February through March during the larval stage of the three

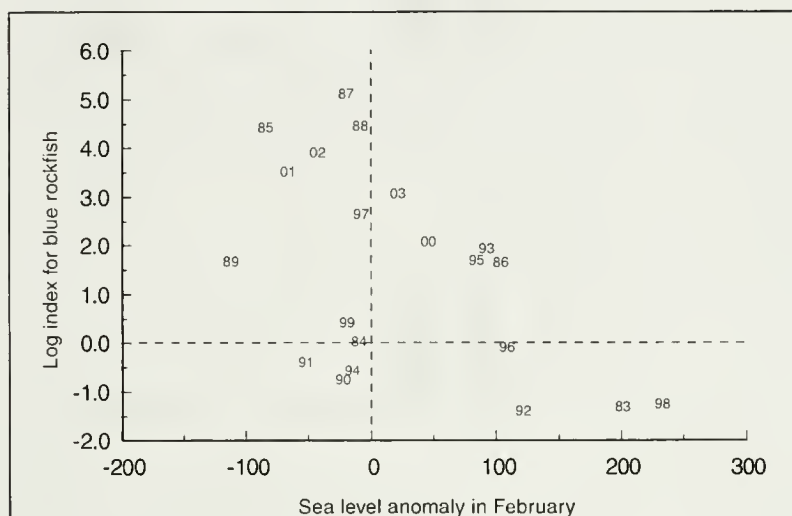


Figure 3

An example of the log-transformed annual abundance index for blue rockfish (*Sebastes mystinus*) and average sea level anomaly in February for each year of the survey (1983–2003). Numbers represent individual years. Dashed lines represent the zero line for both axes.

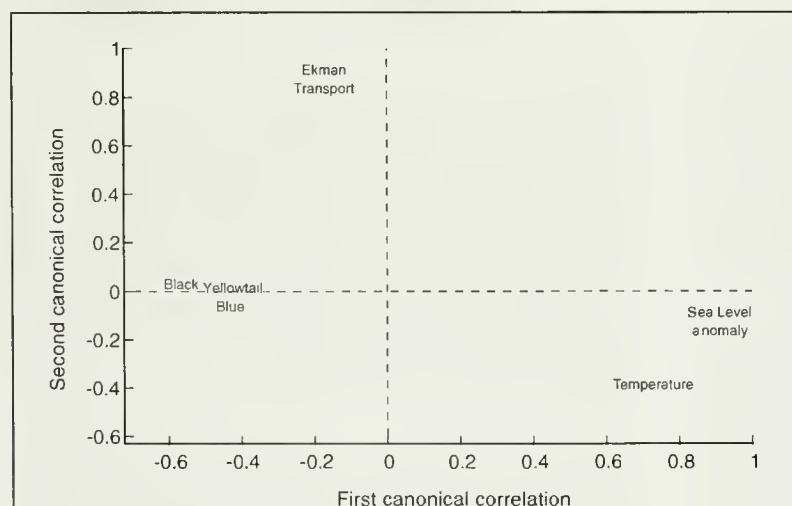


Figure 4

The first and second canonical correlations for the annual abundance index (INDEX) for each rockfish species and the oceanographic factors with the axes defined by the oceanographic data set. Dashed lines represent zero line for both axes.

Table 3

Correlations between the log-transformed annual juvenile rockfish abundance index by species and the oceanographic variables by month. * = $P < 0.05$; ** = $P < 0.01$; + = $P < 0.1$.

	Jan	Feb	Mar	Apr	May	Jun
Sea level anomaly						
Blue rockfish	-0.36	-0.71**	-0.63**	-0.51*	-0.37+	-0.40+
Yellowtail rockfish	-0.48*	-0.53*	-0.57**	-0.55**	-0.55**	-0.35
Black rockfish	-0.64**	-0.53*	-0.52*	-0.42+	-0.65**	-0.55**
Temperature						
Blue rockfish	-0.22	-0.53*	-0.52*	-0.41+	-0.19	-0.21
Yellowtail rockfish	-0.32	-0.54*	-0.53*	-0.48*	-0.46*	-0.32
Black rockfish	-0.54*	-0.62**	-0.55**	-0.47*	-0.65**	-0.48*
Offshore Ekman transport						
Blue rockfish	0.05	0.58**	0.42+	0.01	-0.02	0.03
Yellowtail rockfish	0.27	0.27	0.39+	0.21	0.17	-0.01
Black rockfish	0.29	0.25	0.19	0.29	0.40+	0.01

Table 4

Correlation coefficients between the log-transformed annual juvenile rockfish abundance index and year-specific adult yellowtail rockfish (*Sebastes flavidus*) commercial landings, by year class, at three ports closest to the study area. * = $P < 0.05$; ** = $P < 0.01$; + = $P < 0.1$. Listed in parentheses is the number of year classes determined in each year and the number of adult yellowtail rockfish otoliths that were aged (no. of year classes, number of otoliths aged).

	All ports	Bodega	Bragg	Eureka
1997	0.48 (10, 172)**	0.43 (10, 16)*	0.62 (10, 84)**	0.78 (9, 72)**
1998	0.37 (9, 141)+	0.38 (6, 30)*	0.21 (9, 89)	0.32 (7, 22)+
1999	0.36 (12, 198)*	0.32 (9, 84)+	0.25 (11, 37)	0.35 (12, 77)*

species of rockfishes in our study. The abundance of all three species were significantly and negatively correlated with sea level anomaly and nearshore temperature during this time period. Ralston and Howard (1995) also argued that year-class strength was set in the larval period for rockfishes with winter parturition. They analyzed data from midwater trawls in May and June and compared them with data from nearshore surveys in summer. Because there was a strong correlation between the two data sets, they postulated that the year-class was set earlier in the year than May, probably during the larval stage. VenTresca et al.³ also reported evidence of the establishment of year-class strength in the larval stage. In 1992, they found large concentrations of larval rockfishes in January, but three to four months later very few juveniles appeared in midwater trawls. They surmised that the El Niño conditions of elevated water temperatures and reduced upwelling resulted in poor survival.

Synchrony in juvenile abundance among rockfish species has been observed in other studies. Ralston and Howard (1995) ascertained that trends in abundance for juvenile blue and yellowtail rockfish from midwater trawls were highly correlated over the 10 years of their

study. Ammann (2001) discovered a comparable pattern in recruitment of juvenile yellowtail and black rockfish to the kelp bed environment in 1999 and 2000. Stephens et al. (1984) reported that juvenile abundance of both blue and olive rockfish (*S. serranoides*), dropped to virtually zero during the years 1978–81. In our study, blue, yellowtail, and black rockfish covaried over a period of 21 years.

Although offshore Ekman transport, or upwelling, has been suggested as a predictor of year-class strength, we found it to have little correlation with the abundance of juvenile rockfishes from northern California. Maximum upwelling off the central California coast occurs in late spring and summer (Rosenfeld et al., 1994; Yoklavich et al., 1996). This upwelling occurred after the larval period for winter-spawning *Sebastes* spp., and therefore after the timing of year-class determination. Larson et al. (1994) found that larger pelagic juveniles were often close to shore even when upwelling was strong, indicating that later-stage pelagic juveniles were not directly affected by upwelling. If water movement onshore and offshore influences the population size of juvenile rockfishes, perhaps this effect occurs during the early stages.

Temperature and sea level anomaly proved to be important correlates with year-class strength for juvenile rockfishes. Of the three environmental variables examined, nearshore temperature and sea level anomaly were significantly and negatively correlated with the abundance of all three species. Moser et al. (2000) reported a similar relationship, with reduced abundance of larval bocaccio and cowcod during periods of high temperature off southern California. Ralston and Howard (1995) reported a negative correlation between recruited juvenile blue and yellowtail rockfish year-class strength and sea surface temperature in January through March. Stephens et al. (1984) surmised that warm water was the limiting factor in the low recruitment of juvenile blue and olive rockfish during 1978–81

off southern California. Ainley et al. (1993) determined that sea level during February and sea surface temperature in March were negatively correlated with pelagic rockfish abundance for the period of 1973–90 off central California.

Temperature affects the growth rates of rockfishes, which, in turn, affects species abundance. Johnson et al. (2001) determined that growth rates declined during months of high temperatures for juveniles of three rockfish species. However, Boehlert and Yoklavich (1983) found increased growth rates for juvenile black rockfish with increased temperature in the laboratory, except under starvation conditions. Therefore, reduction in growth rates may be due to lower prey availability during El Niño conditions (Mullin and Conversi, 1989). This lower growth rate of juvenile rockfishes during periods of high temperatures may lead to reduced survival and lower year-class strength.

Although growth can vary directly with temperature, temperature may also have an indirect effect on rockfish abundance. Strong El Niño events, associated with unusually high water temperatures lasting from a few months to over a year, have occurred off California in 1982–83, 1991–92, and 1997–98 (Fedorov and Philander, 2000; Rebstock, 2001). VenTresca et al. (1995) observed reduced condition factor and gonadal indices for blue rockfish during the 1983 and 1992 El Niños off central California when water temperatures were elevated. These reductions could lead to fewer larvae being produced and hence ultimately to a lower abundance of juveniles. El Niño events can also lead to changes in the strength and timing of the annual phytoplankton bloom, both of which can reduce the distribution and abundance of the zooplankton on which the juvenile rockfishes feed (Lenarz et al., 1995). This reduction in food availability could lead to lower growth or survival of the juvenile rockfishes. Keister et al. (2005) found several warm-water species of euphausiids, chaetognaths, and copepods in Oregon waters during the 1997–98 El Niño. Rebstock (2001) observed that during periods of high temperatures in 1983, 1992, and 1998, the species richness of copepods was lower than a 49-year average. Copepods are a preferred prey item for juvenile rockfishes (Reilly et al., 1992). A change in species composition to less desirable food sources (e.g., prey is less nutritious or less available to young rockfishes). Although the exact mechanism is not clear, we observed that the three

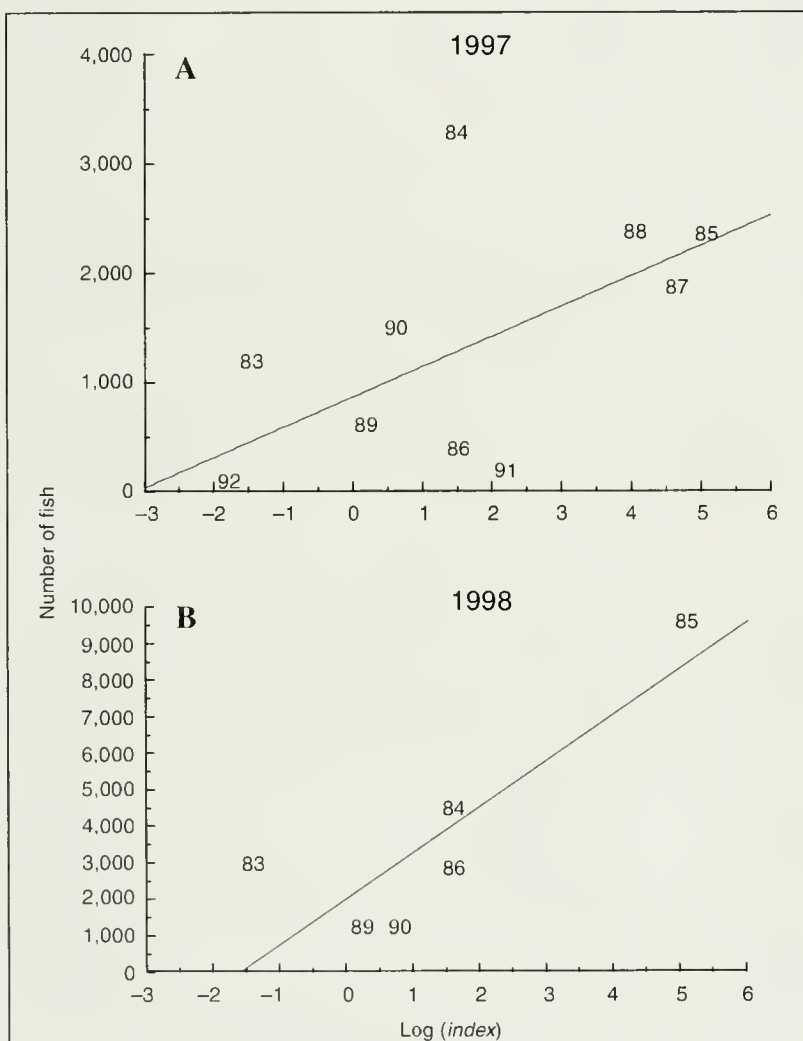


Figure 5

Year-specific catch-at-age data from commercial trawl-caught adult yellowtail rockfish (*Sebastes flavidus*) from Bodega Bay, CA, and the log-transformed annual abundance index for yellowtail rockfish. (A) 1997 landings; (B) 1998 landings. Numbers represent the year class of aged fish. The solid line represents predicted values from the relationship of the catch-at-age data and the log-transformed index.

years of lowest abundance for juvenile rockfishes occurred during El Niño events.

The primary factors that lead to annual fluctuations in abundance were similar for blue, yellowtail, and black rockfish. These three species are found in similar areas at the planktonic stage (Lenarz et al., 1991; Larson et al., 1994). Therefore, it is expected that changes in ocean conditions affect all three species similarly. Nearshore temperature and sea level anomaly had high negative correlations with abundance for all three species, whereas offshore Ekman transport was not correlated with abundance. This finding implies that poor recruitment occurs during years of high temperature and strong, positive sea level anomaly (poleward flow), and vice versa. Our results indicate that recruitment is poor during periods of strong, positive sea level anomaly and that recruitment is strong only during years of negative sea level anomaly (equatorward flow). However, poor recruitment also occurs in some years with negative sea level anomaly. Therefore, other factors are probably involved in the process and can affect year-class strength in rockfishes. Some of the other factors that have been suggested to have at least some influence on rockfish recruitment include adult spawning biomass (Mason, 1998), increased predation by siphonophores and chaetognaths on larval stages during years of high sea temperature (Yoklavich et al., 1996), turbulence (Ainley et al., 1993), and diet of juvenile rockfishes (Reilly et al., 1992).

Large-scale multiyear oceanographic events (e.g., Pacific Decadal Oscillation and the El Niño-Southern Oscillation indices) also appear to affect juvenile rockfish abundance. Large changes in indices reflect regime shifts in ocean conditions, such as those occurring in 1977, 1989, and 1998 (Hare and Mantua, 2000; Benson and Trites, 2002). Although the mechanisms that affect or cause changes in abundance are unclear, our time series of juvenile rockfish abundance reflects these large-scale shifts in ocean conditions by the generally high recruitment prior to 1989, the much reduced recruitment from 1989 to 1998, and the generally higher recruitment after 1998.

We have continued our juvenile rockfish surveys to present, and have had the opportunity to determine the usefulness of our abundance index as a predictor of rockfish year-class strength. In 2005, average monthly temperature was elevated from January to June (as much as two degrees above average as measured by our temperature monitors). Interestingly, the abundance index of all three species of juvenile rockfishes from our surveys in 2005 was very low. Black and yellowtail rockfish abundances, in particular, were at the third lowest level estimated during what is now a 23-year time-series of recruitment. Therefore, our results demonstrate our ability to predict annual levels of abundance for these species of juvenile rockfishes.

Juvenile yellowtail rockfish abundance in our study reflected adult yellowtail rockfish abundance in the fishery. Mearns et al. (1980) also reported a relationship between juvenile abundance and subsequent adult

biomass for stripetail and calico rockfishes by following yearly cohorts from seasonal trawls in southern California over nine years. The high recruitment for bocaccio in 1985 was manifested in the recreational fishery in Monterey Bay, CA in subsequent years (Mason, 1998). Similar trends were observed with large year-classes of chilipepper, *S. goodei*, and yellowtail rockfish (Mason, 1998). Ralston and Ianelli (1998) also found that the abundance of juvenile bocaccio was an indicator of year-class strength in the fishery. Accordingly, the study of juvenile rockfish abundance can help predict good and bad year classes entering a fishery. These data can then be incorporated into fisheries models (see stock assessments for widow rockfish, *S. entomelas*, [He et al.⁶]) to better manage the stocks.

Acknowledgments

We first thank Edmund (Ted) Hobson for his initial conception of this project and his many years of data collection and direction. We also thank all the divers who helped with juvenile rockfish surveys, especially Kelly Silberberg for his many years of dedication to this project. We thank Peter Adams, Steve Ralston, Susan Sogard, Ralph Larson, Mary Yoklavich, and four anonymous reviewers for helpful comments on drafts of this manuscript. Lastly, we thank Craig Syms and Brian Wells for their generous help with statistical matters.

Literature cited

- Ainley, D. G., W. J. Sydeman, R. J. Parrish, and W. H. Lenarz. 1993. Oceanic factors influencing distribution of young rockfish (*Sebastes*) in central California: A predator's perspective. Calif. Coop. Oceanic Fish. Invest. Rep. 34:133-139.
- Ammann, A. 2001. Evaluation of a standard monitoring unit for the recruitment of fish in central California. M.Sci. thesis, 92 p. Univ. California, Santa Cruz, CA.
- Anderson, T. W. 1983. Identification and development of nearshore juvenile rockfishes (genus *Sebastes*) in central California kelp forests. M.Sci. thesis, 216 p. California State Univ., Fresno, CA.
- Benson, A. J., and A. W. Trites. 2002. Ecological effects of regime shifts in the Bering Sea and eastern North Pacific Ocean. Fish and Fisheries 3:95-113.
- Boehlert, G. W., and M. M. Yoklavich. 1983. Effects of temperature, ration, and fish size on growth of juvenile black rockfish, *Sebastes melanops*. Environ. Biol. Fish. 8:17-28.

⁶ He, X., D. E. Pearson, E. J. Dick, J. C. Field, S. Ralston, and A. D. MacCall. 2005. Status of the widow rockfish resource in 2005, 119 p. Pacific Fisheries Management Council, 7700 NE Ambassador Place, Suite 200, Portland, Oregon 97220.

- Butler, J. L., L. D. Jacobson, J. T. Barnes, and H. G. Moser.
2003. Biology and population dynamics of cowcod (*Sebastes levis*) in the southern California Bight. *Fish. Bull.* 101:260–280.
- Fedorov, A. V., and S. G. Philander.
2000. Is El Niño changing? *Science* 288:1997–2002.
- Hare, S. R., and N. J. Mantua.
2000. Empirical evidence for North Pacific regime shifts in 1977 and 1989. *Prog. Oceanogr.* 47:103–145.
- Johnson, K. A., M. M. Yoklavich, and G. M. Cailliet.
2001. Recruitment of three species of juvenile rockfish (*Sebastes* spp.) on soft benthic habitat in Monterey Bay, California. *Calif. Coop. Oceanic Fish. Invest. Rep.* 42:153–166.
- Keister, J. E., T. B. Johnson, C. A. Morgan, and W. T. Peterson.
2005. Biological indicators of the timing and direction of warm-water advection during the 1997/1998 El Niño off the central Oregon coast, USA. *Mar. Ecol. Prog. Ser.* 295:43–48.
- Larson, R. J., W. H. Lenarz, and S. Ralston.
1994. The distribution of pelagic juvenile rockfish of the genus *Sebastes* in the upwelling region off central California. *Calif. Coop. Oceanic Fish. Invest. Rep.* 35:175–221.
- Lenarz, W. H., R. J. Larson, and S. Ralston.
1991. Depth distributions of late larvae and pelagic juveniles of some fishes of the California Current. *Calif. Coop. Oceanic Fish. Invest. Rep.* 32:41–46.
- Lenarz, W. H., F. B. Schwing, D. A. VenTresca, F. Chavez, and W. M. Graham.
1995. Explorations of El Niño events and associated biological population dynamics off central California. *Calif. Coop. Oceanic Fish. Invest. Rep.* 36:106–119.
- Love, M. S., M. Yoklavich, and L. Thorsteinson.
2002. The rockfishes of the northeast Pacific, 405 p. Univ. California Press, Berkeley, CA.
- Mason, J.
1998. Declining rockfish lengths in the Monterey Bay, California, recreational fishery, 1959–94. *Mar. Fish. Rev.* 60:15–28.
- Matthews, K. R.
1989. A comparative study of habitat use by young-of-the-year, subadult, and adult rockfishes on four habitat types in central Puget Sound. *Fish. Bull.* 88:223–239.
- Mearns, A. J., M. J. Allen, M. D. Moore, and M. J. Sherwood.
1980. Distribution, abundance, and recruitment of soft-bottom rockfishes (Scorpaenidae: *Sebastes*) on the southern California mainland shelf. *Calif. Coop. Oceanic Fish. Invest. Rep.* 21:180–190.
- Moser, H. G., R. L. Charter, W. Watson, D. A. Ambrose, J. L. Butler, S. R. Charter, and E. M. Sandknop.
2000. Abundance and distribution of rockfish (*Sebastes*) larvae in the Southern California Bight in relation to environmental conditions and fishery exploitation. *Calif. Coop. Oceanic Fish. Invest. Rep.* 41:132–147.
- Mullin, M. M., and A. Conversi.
1989. Biomasses of euphausiids and smaller zooplankton in the California Current—geographic and interannual comparisons relative to the Pacific whiting, *Merluccius productus*, fishery. *Fish. Bull.* 87:633–644.
- Pastén, G. P., S. Katayama, and M. Omori.
2003. Timing of parturition, planktonic duration, and settlement patterns of the black rockfish, *Sebastes inermis*. *Environ. Biol. Fish.* 68:229–239.
- Ralston, S., and D. F. Howard.
1995. On the development of year-class strength and cohort variability in two northern California rockfishes. *Fish. Bull.* 93:710–720.
- Ralston, S., and J. N. Ianelli.
1998. When lengths are better than ages: the complex case of bocaccio. In *Fishery stock assessment models: proceedings of the international symposium on fishery stock assessment models for the 21st century* (October 8–11, 1997, Anchorage, Alaska) (F. Funk, T. J. Quinn II, J. Heifetz, J. N. Ianelli, J. E. Powers, J. F. Schweigert, P. J. Sullivan, and C.-I. Zhang, eds.), p. 451–468. Lowell Wakefield Fisheries Symposium No. 15. Univ. Alaska Sea Grant College Program AK-SG-98-01, Fairbanks, AK.
- Rebstock, G. A.
2001. Long-term stability of species composition in calanoid copepods off southern California. *Mar. Ecol. Prog. Ser.* 215:213–224.
- Reilly, C. A., T. Wyllie Echeverria, and S. Ralston.
1992. Interannual variation and overlap in the diets of pelagic juvenile rockfish (genus: *Sebastes*) off central California. *Fish. Bull.* 90:505–515.
- Rosenfeld, L. K., F. B. Schwing, N. Garfield, and D. E. Tracy.
1994. Bifurcated flow from an upwelling center: a cold water source for Monterey Bay. *Continental Shelf Res.* 14:931–964.
- Shaffer, J. A., D. C. Doty, R. M. Buckley, and J. E. West.
1995. Crustacean community composition and trophic use of the drift vegetation habitat by juvenile split-nose rockfish, *Sebastes diploproa*. *Mar. Ecol. Prog. Ser.* 123:13–21.
- Stephens, J. S. Jr., P. A. Morris, K. Zerba, and M. Love.
1984. Factors affecting fish diversity on a temperate reef: the fish assemblage of Palos Verde Point, 1974–1981. *Environ. Biol. Fish.* 11:259–275.
- VenTresca, D. A., R. H. Parrish, J. L. Houk, M. L. Gingras, S. D. Short, N. L. Crane.
1995. El Niño effects on the somatic and reproductive condition of blue rockfish, *Sebastes mystinus*. *Calif. Coop. Oceanic Fish. Invest. Rep.* 36:167–174.
- Yoklavich, M. M., V. J. Loeb, M. Nishimoto, and B. Daly.
1996. Nearshore assemblages of larval rockfishes and their physical environment off central California during an extended El Niño event, 1991–1993. *Fish. Bull.* 94: 766–782.

Abstract—Skipjack (*Katsuwonus pelamis*), yellowfin (*Thunnus albacores*), and bigeye (*Thunnus obesus*) tunas are caught by purse-seine vessels in the eastern Pacific Ocean (EPO). Although there is no evidence to indicate that current levels of fishing-induced mortality will affect the sustainability of skipjack or yellowfin tunas, fishing mortality on juvenile (younger than 5 years of age) bigeye tuna has increased, and overall fishing mortality is greater than that necessary to produce the maximum sustainable yield of this species. We investigated whether time-area closures have the potential to reduce purse-seine bigeye catches without significantly reducing skipjack catches. Using catch and effort data for 1995–2002, we identified regions where the ratio of bigeye to skipjack tuna catches was high and applied simple closed-area models to investigate the possible benefits of time-area closures. We estimated that the most optimistic and operationally feasible 3-month closures, covering the equatorial region of the EPO during the third quarter of the year, could reduce bigeye catches by 11.5%, while reducing skipjack tuna catches by 4.3%. Because this level of bigeye tuna catch reduction is insufficient to address sustainability concerns, and larger and longer closures would reduce catches of this species significantly, we recommend that future research be directed toward gear technology solutions because these have been successful in many other fisheries. In particular, because over 50% of purse-seine catches of bigeye tuna are taken in sets in which bigeye tuna are the dominant species, methods to allow the determination of the species composition of aggregations around floating objects may be important.

The potential use of time-area closures to reduce catches of bigeye tuna (*Thunnus obesus*) in the purse-seine fishery of the eastern Pacific Ocean

Shelton J. Harley (contact author)

Jenny M. Suter

Inter-American Tropical Tuna Commission
8604 La Jolla Shores Drive
La Jolla, California, 92037–1508
Present address for S. J. Harley: Ministry of Fisheries
PO Box 1020
Wellington, New Zealand

Email address for S. J. Harley: harleys@fish.govt.nz

The Inter-American Tropical Tuna Commission (IATTC) was established by an international convention in 1950 and is responsible for the conservation of tunas and management of fisheries for tunas and other species taken by tuna-fishing vessels in the eastern Pacific Ocean (EPO). Such conservation and management is accomplished by measures imposed by the nations participating in the fishery in response to recommendations by the scientific staff of the IATTC. Currently, the IATTC has adopted two measures to ensure the conservation of bigeye tuna in the EPO (IATTC¹): catch limits for each longline fleet (based on their 2001 catch levels) and a series of closures for the purse-seine fleet. In this article, we examine the use of the temporary closure of a given area, referred to as a “time-area closure,” for management of the purse-seine fishery.

Since the early 1990s, considerable purse-seine fishing effort in the EPO has been directed at tunas associated with floating objects, including man-made fish-aggregating devices (Lennert-Cody and Hall, 2000). The predominant species captured are skipjack (*Katsuwonus pelamis*), bigeye (*Thunnus obesus*), and yellowfin (*Thunnus albacares*) tunas. The floating-object (FOB) fishery has had no noticeable affect on skipjack tuna abundance (Maunder, 2002a) and little effect on yellowfin tuna because the catches of yellowfin tuna from the floating

object fishery are small compared to the catches from other purse-seine fisheries (Maunder, 2002b). However, the FOB has led to a considerable increase in fishing mortality on juvenile bigeye tuna (Maunder and Harley, 2002; Harley et al., 2005).

The most recent bigeye tuna stock assessment (IATTC, 2004) has indicated that overall fishing effort should be reduced by at least 38% to allow the stock to produce the maximum sustainable yield (MSY). This assessment is based on a single EPO stock with no net migration between the eastern and western Pacific; however, a “Pacific-wide” assessment has provided a very similar picture of low movement rates for bigeye tuna in the EPO (Hampton et al.²).

Since the expansion of the FOB fishery, catches of bigeye tuna from the purse-seine fishery have exceeded those from the longline fishery in some years (Table 1). The bigeye tuna

¹ IATTC (Inter-American Tropical Tuna Commission). 2003. Resolution on the conservation of tuna in the eastern Pacific Ocean, 3 p. Resolution C-03-12, IATTC, 8604 La Jolla Shores Drive, La Jolla, California 92037.

² Hampton, J., P. Kleiber, Y. Takeuchi, H. Kurota, and M. Maunder. 2003. Stock assessment of bigeye tuna in the western and central Pacific Ocean, with comparisons to the entire Pacific Ocean, 81 p. SCTB16 BET-1. Sixteenth meeting of the standing committee on tuna and billfish, Mooloolaba, Queensland, Australia; 9–16 July 2003.

Table 1

Annual catches (metric tons) of bigeye (*Thunnus obesus*) and skipjack (*Katsuwonus pelamis*) tuna from purse-seine (PS) fisheries by set type (FOB=floating object associated school, UNA=tuna school unassociated with dolphins, and DOL=tuna school associated with dolphins) and longline fisheries from the eastern Pacific Ocean, east of 150°W, as used in the stock assessments.

Year	Bigeye tuna						Skipjack tuna					
	FOB	UNA	DOL	PS total	Longline total	Annual total	FOB	UNA	DOL	PS total	Longline total	Annual total
1990	3360	1351	0	4711	98,990	103,700	34,980	35,788	867	71,635	42	71,677
1991	1963	1739	38	3740	104,159	107,874	37,655	22,958	786	61,399	33	61,432
1992	1154	4343	0	5497	84,396	89,893	45,556	35,333	869	81,758	24	81,782
1993	6274	4724	134	11,132	72,351	80,420	48,144	34,865	714	83,723	63	83,786
1994	37,901	2624	0	40,525	71,360	100,734	47,992	22,916	516	71,424	69	71,493
1995	45,204	6291	0	51,495	58,076	95,403	81,253	50,715	1032	133,000	74	133,074
1996	66,568	4280	0	70,848	46,771	98,124	74,260	34,635	729	109,624	40	109,664
1997	69,293	1868	48	71,209	52,078	103,693	123,002	29,510	6004	158,516	94	158,610
1998	43,226	5183	91	48,500	45,632	80,787	115,370	25,108	2879	143,357	65	143,422
1999	49,452	6574	0	56,026	32,565	73,176	178,824	84,036	1214	264,074	94	264,168
2000	83,489	3266	0	86,755	46,424	116,579	116,508	81,551	440	198,499	29	211,049
2001	56,753	1273	14	58,040	60,572	103,421	115,571	20,163	1218	136,952	61	144,949
2002	61,230	1166	0	62,396	68,195	103,394	118,485	32,471	2093	153,048	145	157,593

caught in the longline fishery are larger (110–160 cm) and considerably more valuable than the smaller bigeye tuna (50–80 cm) caught mostly by the purse-seine fishery.

Improving the long-term sustainability of the bigeye tuna fisheries could be achieved by reducing the fishing mortality of the smaller individuals that are caught predominantly in the FOB fishery. Annual catches of skipjack tuna from the purse-seine fishery in the EPO are larger and more economically important than those of bigeye tuna (Table 1). Furthermore, there are no concerns regarding sustainability of the skipjack tuna population in the EPO (Maunder, 2002a). Thus, bigeye tuna caught by the FOB fishery are essentially bycatch of the targeted skipjack tuna fishery; thus determining a mechanism by which the catches of bigeye tuna are reduced while minimizing losses in the catches of skipjack tuna is an important management issue.

Hall (1996) argued that to understand and solve bycatch problems it is important to classify the problem by a number of factors (e.g., time, space, and the level of control that fishermen have). With this information, there are many potential tools that can be used by fisheries managers to reduce fishing mortality, e.g., gear regulations, catch limits, closed seasons, and closed areas (Beverton and Holt, 1957). Time and area closures (time-area closures) are recommended as a means to reduce catches of sharks (Baum et al., 2003), protect billfishes from exploitation by the longline fishery (Goodyear, 1999), and protect biodiversity hotspots (Worm et al., 2003). Although time-area closures are not particularly appropriate for fisheries managed under quota systems, they may be beneficial for effort-managed fisheries (Horwood et al., 1998) or fisheries

targeting multispecies (Hilborn et al., 2004), such as those for tunas in the EPO.

In this study, we investigated the potential of time-area closures to reduce bigeye tuna catches while minimizing impacts on the catches of skipjack tuna. In contrast to common closure-strategy studies, i.e., those studies devoted to fisheries targeting a single species, we investigated the potential impacts of time-area closures on two species: a large and highly productive skipjack tuna stock, and a considerably smaller and less productive bigeye tuna stock.

We used catch and effort data from the purse-seine fishery to search for potential time-area hotspots for bigeye catches and then applied simple “in-sample” closed-area models to predict the potential impact of closures of these areas. We discuss the likely use of such closures in the light of our findings, alternative management actions that could possibly reduce bigeye tuna catches, and finally, the strengths and weaknesses of the approach used for the closed-area models.

Although yellowfin tuna form an important part of the purse-seine fishery in the EPO, where annual catches are greater than those for bigeye and skipjack tuna combined, we did not consider them in our analysis. Within the EPO purse-seine fishery there are essentially two fleets: one targets yellowfin tuna schools associated with dolphins or schools not associated with dolphins and the other targets mainly skipjack tuna associated with floating objects. In our study, we focused on the second fleet and there are many reasons to believe that effort could not be transferred from one fleet to the other, e.g. markets, technological differences (the vessels require different equipment), geographical

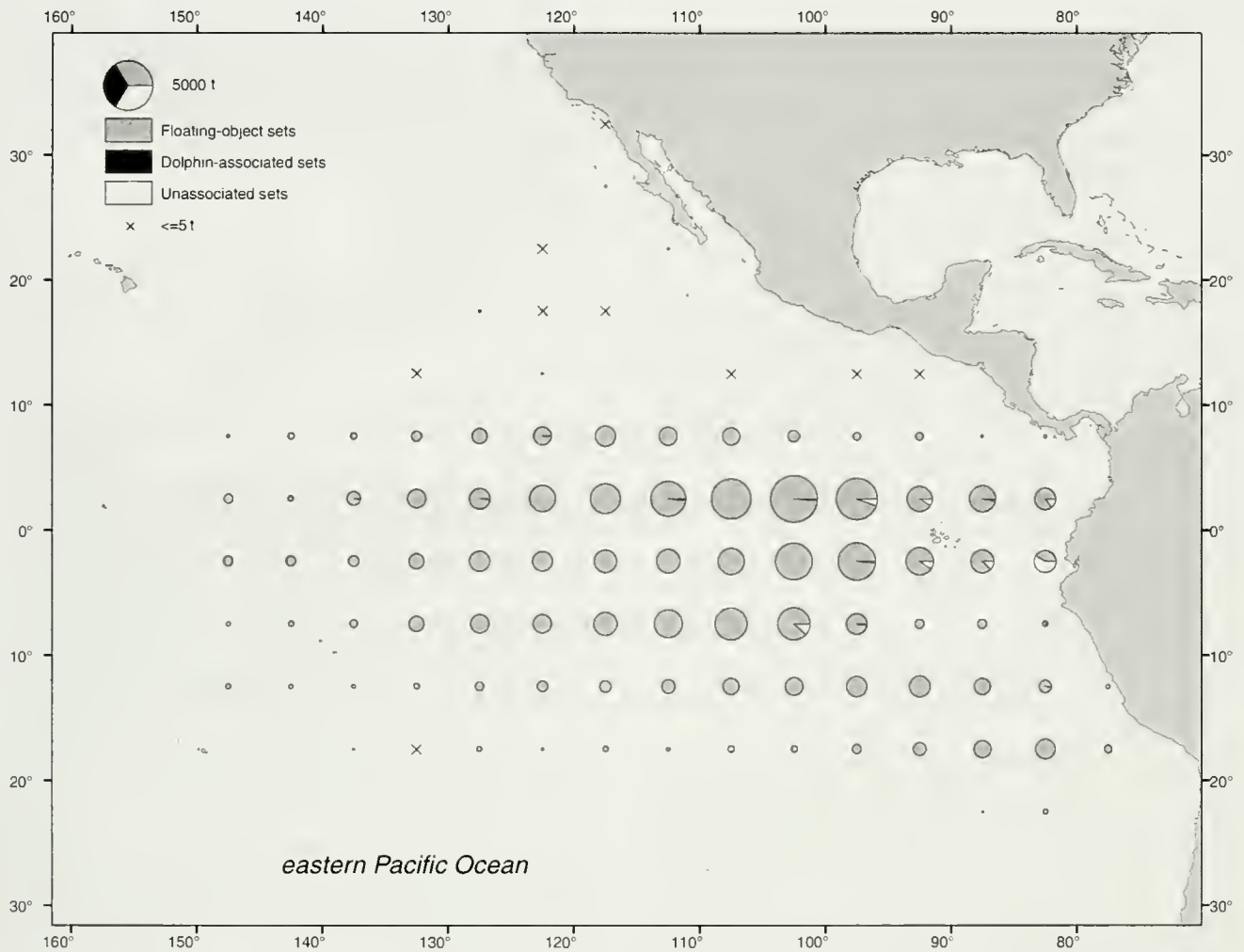


Figure 1

Average annual distribution of the purse-seine catches of bigeye tuna (*Thunnus obesus*), by set type and 5-degree latitude by 5-degree longitude area, in the eastern Pacific Ocean, 1995–2002. The size of the circles is proportional to the catch in each area.

(the fisheries have limited spatial overlap), and restrictions on dolphin mortality limits. In addition, only a small proportion (about 10%) of the purse-seine catches of yellowfin tuna are taken in floating-object sets. Later we discuss extensions to our analysis to include not only yellowfin tuna, but a range of bycatch species taken in the different purse-seine fisheries.

Materials and methods

Data

We used set-by-set catch and effort data from purse-seine vessels that operate in the EPO. The majority of the data was obtained by scientific observers. In the absence of observer data, we used records from the logbooks of the vessels. Data were grouped by 5-degree latitude by 5-degree longitude areas (hereon referred to as 5°×5° areas) by seasonal quarter. The FOB fishery, which is respon-

sible for over 90% of the purse-seine catches of bigeye tuna, was in an expansion phase during 1992–94; therefore we restricted our attention to data for 1995–2002 (Table 1). Because very small amounts of bigeye and skipjack tuna are caught in dolphin-associated (DOL) sets, we excluded these from the analysis and instead focused on sets of tuna associated with floating objects and sets on schools not associated (UNA) with dolphins. For 1995–2002, these two set types were responsible for over 99% of bigeye and skipjack tuna catches from the purse-seine fishery (IATTC, 2004). These two set types were combined in the closed-area model because it was possible to switch effort between those two types of sets. The spatial distribution of catches by set type for bigeye and skipjack tuna are provided in Figures 1 and 2.

Definition of “hotspot”

In defining the spatial and temporal extent of the bigeye catches, we looked for areas where the ratio of bigeye to

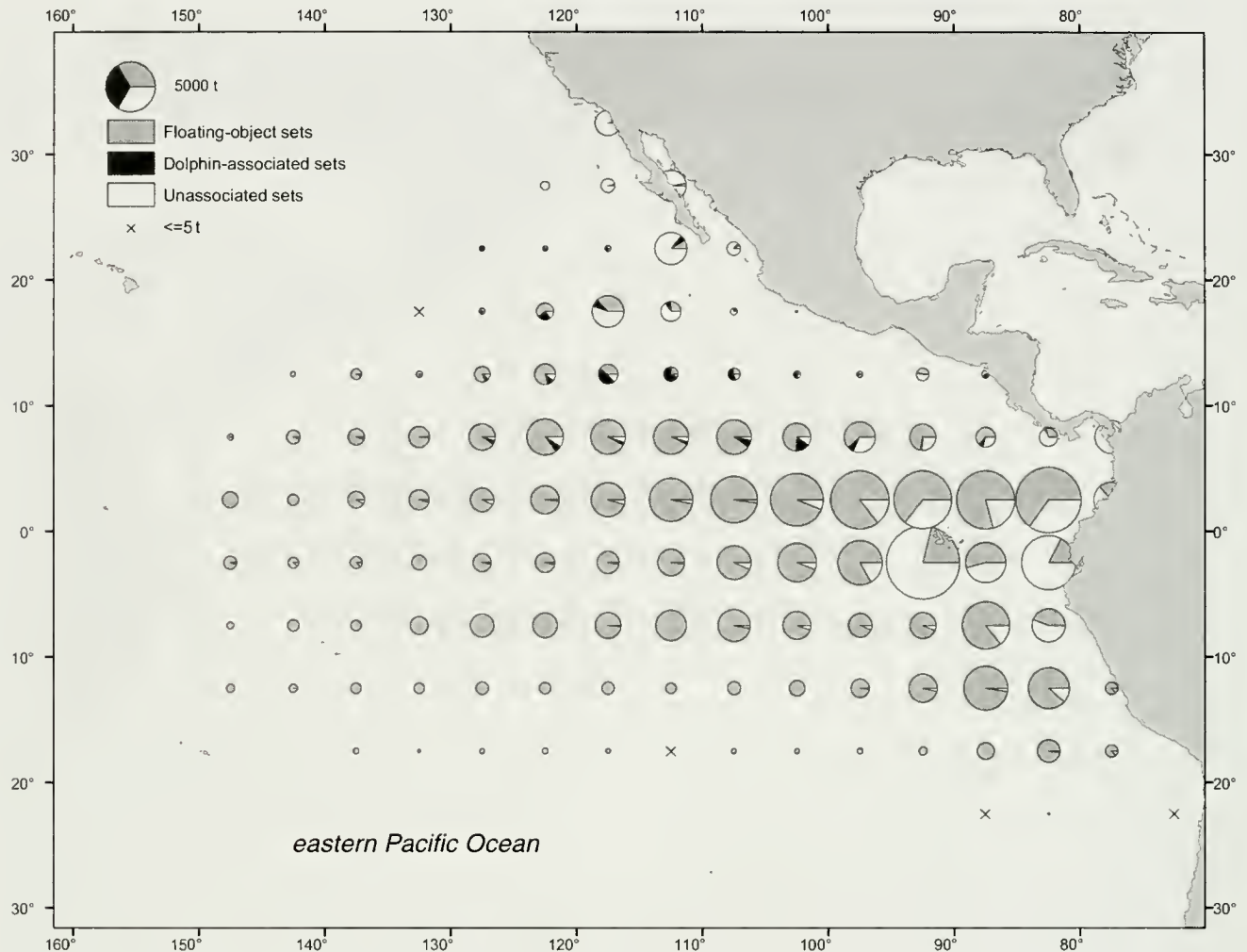


Figure 2

Average annual distribution of the purse-seine catches of skipjack tuna (*Katsuwonus pelamis*), by set type, in the eastern Pacific Ocean, 1995–2002.

skipjack tuna catches was high, rather than just areas of high bigeye tuna catches, because we wanted areas where the losses in skipjack tuna catches would be minimized. We chose $5^\circ \times 5^\circ$ areas by quarter of the year as the scale for the individual hotspots.

We defined an index for each time-area strata for each year. The index was a ratio of bigeye tuna catch to skipjack tuna catch that was robust to annual fluctuations in the abundance of either species. We then summed the annual indices over the time period to find areas that consistently resulted in high bigeye to skipjack tuna ratios. The indices were calculated separately for each year so that they were not dominated by data from years with exceptionally high or low catches of either species.

The data used for this and the closed-area analysis were the following:

$B_{i,j,t}$ = bigeye catch in quarter i in area j in year t ;
 $S_{i,j,t}$ = skipjack catch in quarter i in area j in year t .

We standardized catches within a year on the basis of the median catch of the year.

$$b_{i,j,t} = B_{i,j,t} / \text{median}(B_{\dots,t});$$

$$s_{i,j,t} = S_{i,j,t} / \text{median}(S_{\dots,t}).$$

The location of hotspots did not differ noticeably if we standardized by the mean or total catch for each year, rather than the median.

Using the standardized catches, we defined the annual index for a single $5^\circ \times 5^\circ$ area by quarter, $\theta_{i,j,t}$ as

$$\theta_{i,j,t} = \begin{cases} 0 & \text{where } b_{i,j,t} = 0 \\ 1 & \text{where } s_{i,j,t} = 0 \\ f(b_{i,j,t}, s_{i,j,t}) & \text{otherwise} \end{cases} \quad (1)$$

$$\text{where } f(b_{i,j,t}, s_{i,j,t}) = \frac{b_{i,j,t} / s_{i,j,t} - \min(b_{i,j,t} / s_{i,j,t})}{\max(b_{i,j,t} / s_{i,j,t}) - \min(b_{i,j,t} / s_{i,j,t})}. \quad (2)$$

Note that the index is scaled to be between 0 and 1, and the larger values within this range were associated with greater bigeye-skipjack ratios. To obtain an overview of the hotspots over the 1995–2002 period we summed the annual indices

$$\bar{\theta}_{i,j} = \sum_{t=1995}^{t=2002} \theta_{i,j,t}. \quad (3)$$

We defined hotspots as those time-area regions where the summed index was in the top 20% of the values.

Closed-area model

The basic model is summarized in four steps:

- 1 Choose an area to close in a given time period.
- 2 Re-allocate effort from the chosen area during the period of the closure to other areas in proportion to the effort in each area. Leave the effort outside the closure period unchanged.
- 3 Calculate the new catch of each species expected in each area based on the new effort and catch per unit of effort (CPUE) for each species in each area.
- 4 Compare new annual catches to original catches.

The possible consequences of these assumptions and alternative modeling approaches are detailed in the discussion.

The data used for the closed-area analysis were similar to those used in the hotspot analysis. The definitions of catches remained the same (e.g., $B_{i,j,t}$), although the spatial strata reflected by j differed, depending on the closure considered.

We incorporated effort in terms of the number of sets, $E_{i,j,t}$, and defined the CPUE of bigeye and skipjack tuna in tons per set,

$$U_{i,j,t}^b = \frac{B_{i,j,t}}{E_{i,j,t}} \quad (4)$$

and

$$U_{i,j,t}^s = \frac{S_{i,j,t}}{E_{i,j,t}}. \quad (5)$$

We allocated effort from a time-area closure ($i=x$ and $j=y$) to the remaining areas in that time period on the basis of proportion of effort in each area ($P_{i,j,t}$) (excluding the closed area) e.g.,

$$P_{i,j,t|i=x,j \neq y} = \frac{E_{i,j,t}}{\sum_{i=x,j \neq y} E_{i,j,t}}. \quad (6)$$

For each time-area closure we determined the new effort allocation, $E_{i,j,t|x,y}$, as

$$E_{i,j,t|x,y} = \begin{cases} 0 & \text{where } i=x \text{ and } j=y \\ E_{i,j,t} + E_{x,y,t} \cdot P_{i,j,t|x,y} & \text{where } i=x \text{ and } j \neq y. \\ E_{i,j,t} & \text{where } i \neq x \end{cases} \quad (7)$$

The new catch for each time-area closure was estimated as the new effort multiplied by the original CPUE:

$$B_{i,j,t|x,y} = E_{i,j,t|x,y} \cdot U_{i,j,t}^b \quad (8)$$

and

$$S_{i,j,t|x,y} = E_{i,j,t|x,y} \cdot U_{i,j,t}^s. \quad (9)$$

because it was assumed that CPUE in an area will not change when additional effort is added with closure.

The summary statistic for each simulated closure was the percentage change in bigeye and skipjack tuna catches, compared to the catches observed in the absence of a closure.

$$\Delta B_{x,y,t} = \frac{\sum_{i,j} B_{i,j,t|x,y} - \sum_{i,j} B_{i,j,t}}{\sum_{i,j} B_{i,j,t}} \times 100 \quad (10)$$

and

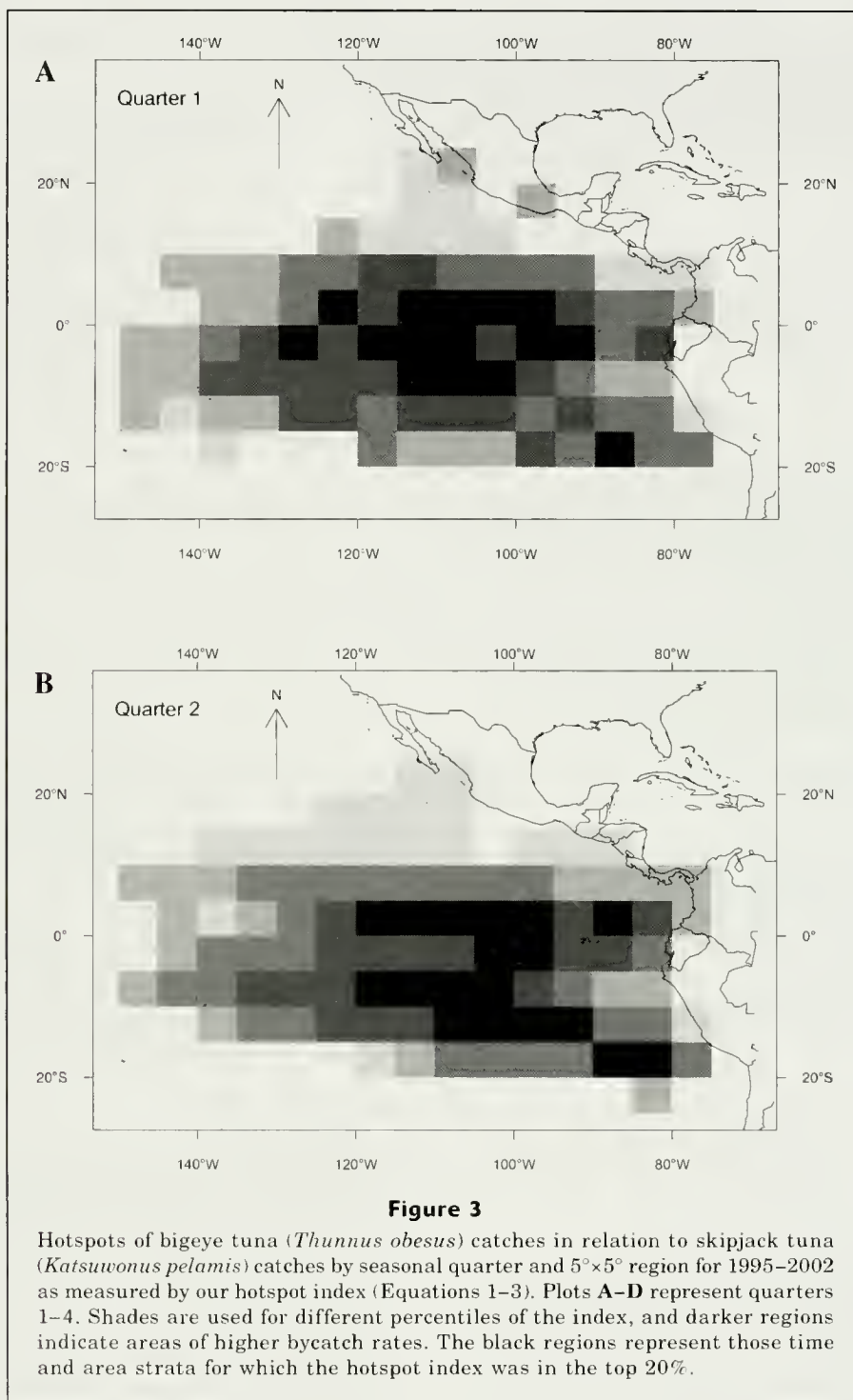
$$\Delta S_{x,y,t} = \frac{\sum_{i,j} S_{i,j,t|x,y} - \sum_{i,j} S_{i,j,t}}{\sum_{i,j} S_{i,j,t}} \times 100. \quad (11)$$

We repeated the calculations for the catch and effort data in each year (1995–2002) to consider the potential variability in the effect of a closure due to interannual variation in the spatial distribution of fish and fishing effort.

In addition to the model described above, we also considered a “two set-type” model in which FOB and UNA sets were redistributed separately (i.e., we did not allow switching between set types). Although this model gave very similar results, it was probably less realistic; therefore the results are not presented here.

Simulated closures

We compared the performance of two closed areas for each quarter and year. The first closed area corresponded to the hotspots (those $5^\circ \times 5^\circ$ areas for a quarter for which $\bar{\theta}_{i,j,t}$ was in the top 20% associated with each quarter). A closure of the hotspots should be optimal in the sense of reducing bigeye tuna catch with minimal impact on skipjack tuna catch but may not be practical from a management perspective because the $5^\circ \times 5^\circ$ areas are not continuous. The second closed area approximated the hotspot closure, but it was a more practical, continuous region. It extended from 5°N – 10°S , to 90° – 120°W . The total area of this closure was the same as the total area of the hotspot regions. We refer to this as the practical closure. In each case, effort during the closure period was redistributed between two areas, one north and one south of the equator, in proportion to the effort in each open area. Summaries of the effort and CPUE data, stratified by the areas that we used in the practical closure analysis, are provided in Table 2.



Results

Hotspots

The hotspots were not evenly spread over the year; the third seasonal quarter contained more 5°×5° hotspots (24) than the other quarters (15–18 each) (Fig. 3). During quarters 1 and 4, most of the hotspots were

located between 5°N and 10°S, whereas during quarters 2 and 3, the hotspots extended south to 15°S. Over all time-area strata, 90% of the hotspots were west of 90°W and east of 135°W, and over 95% were between 5°N and 15°S—indicating that the hotspots are found within a fairly restricted area.

When we compared the hotspots to the practical closure, 75% of the hotspots were found within the prac-

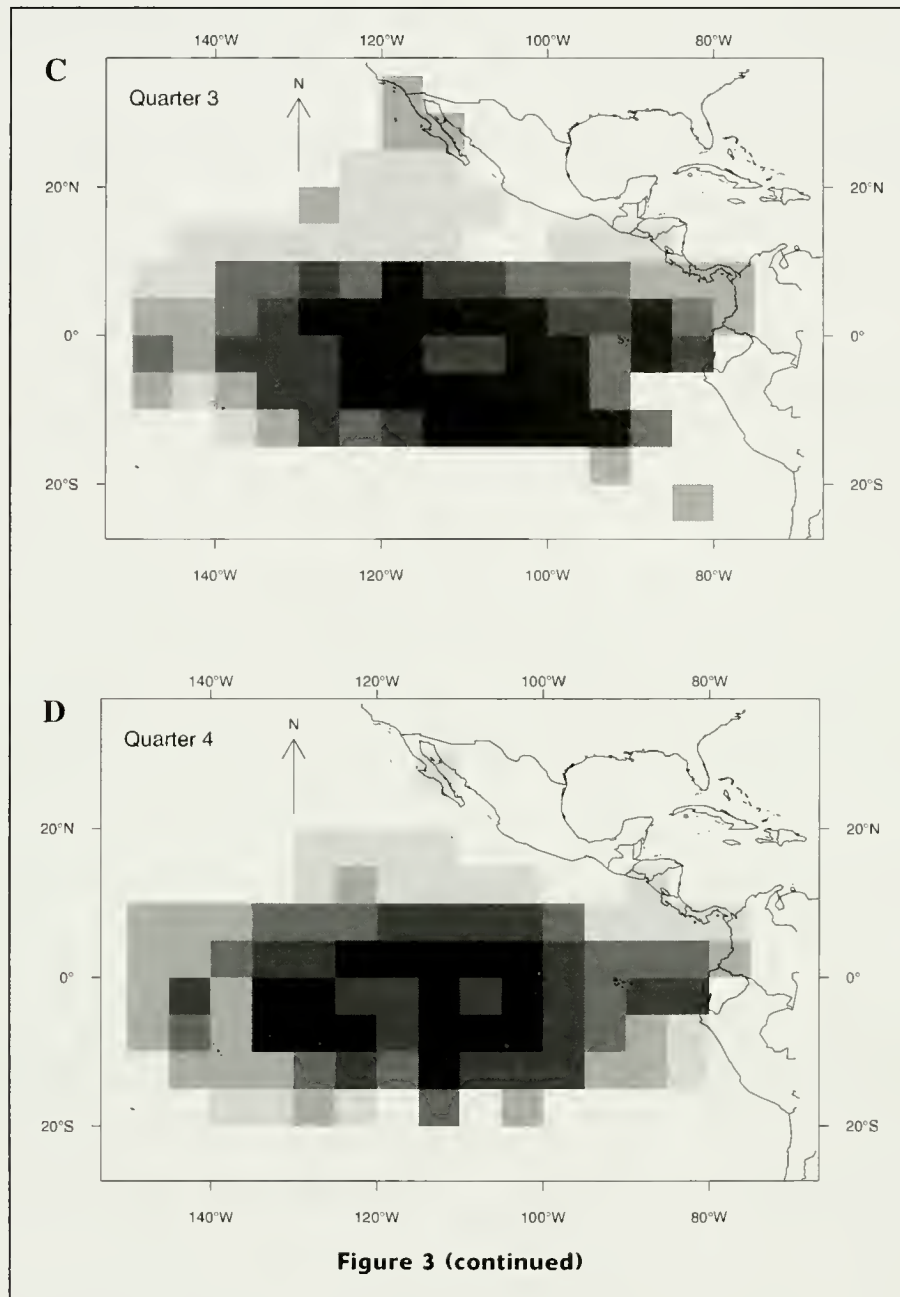


Figure 3 (continued)

tical closure area. Of the remaining 25% of hotspots, most were west of 120°W.

Time-area simulations

Over all years and quarters, the predicted decrease in bigeye tuna catches associated with the hotspot closure ranged from 2.8% to 23.7%, whereas the change in skipjack tuna catches ranged from a 0.9% increase to a 14.1% reduction (Fig. 4). The greatest reductions in bigeye tuna catch were associated with second- and third-quarter closures (mean reduction=14.6%). The mean reductions in skipjack tuna catches did not vary

much across quarters (means ranged from 2.8% to 3.7%). For several years, there was little or no predicted reduction in skipjack tuna catch associated with a hotspot closure. Based on the median of the ratios, the greatest contrast between bigeye and skipjack tuna catch reductions was associated with a third quarter closure; the average percentage reduction in bigeye tuna catch was 14.6%, versus 2.8% for skipjack tuna. The performance of second-quarter closures was similar to that of third-quarter closures, but the former was much more variable across years.

The performance of the practical closure was generally similar to that of the hotspot closure. Over all years and

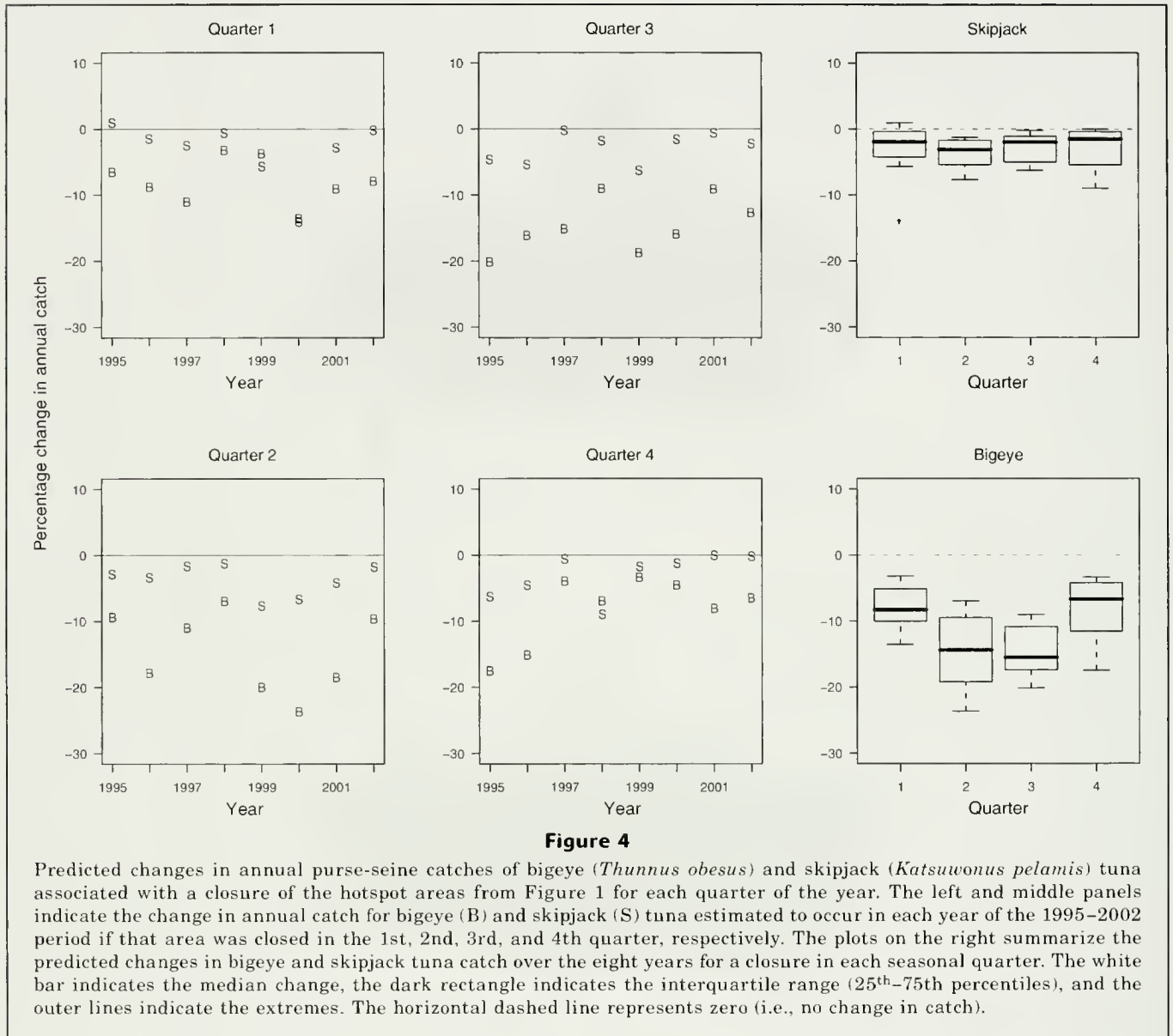


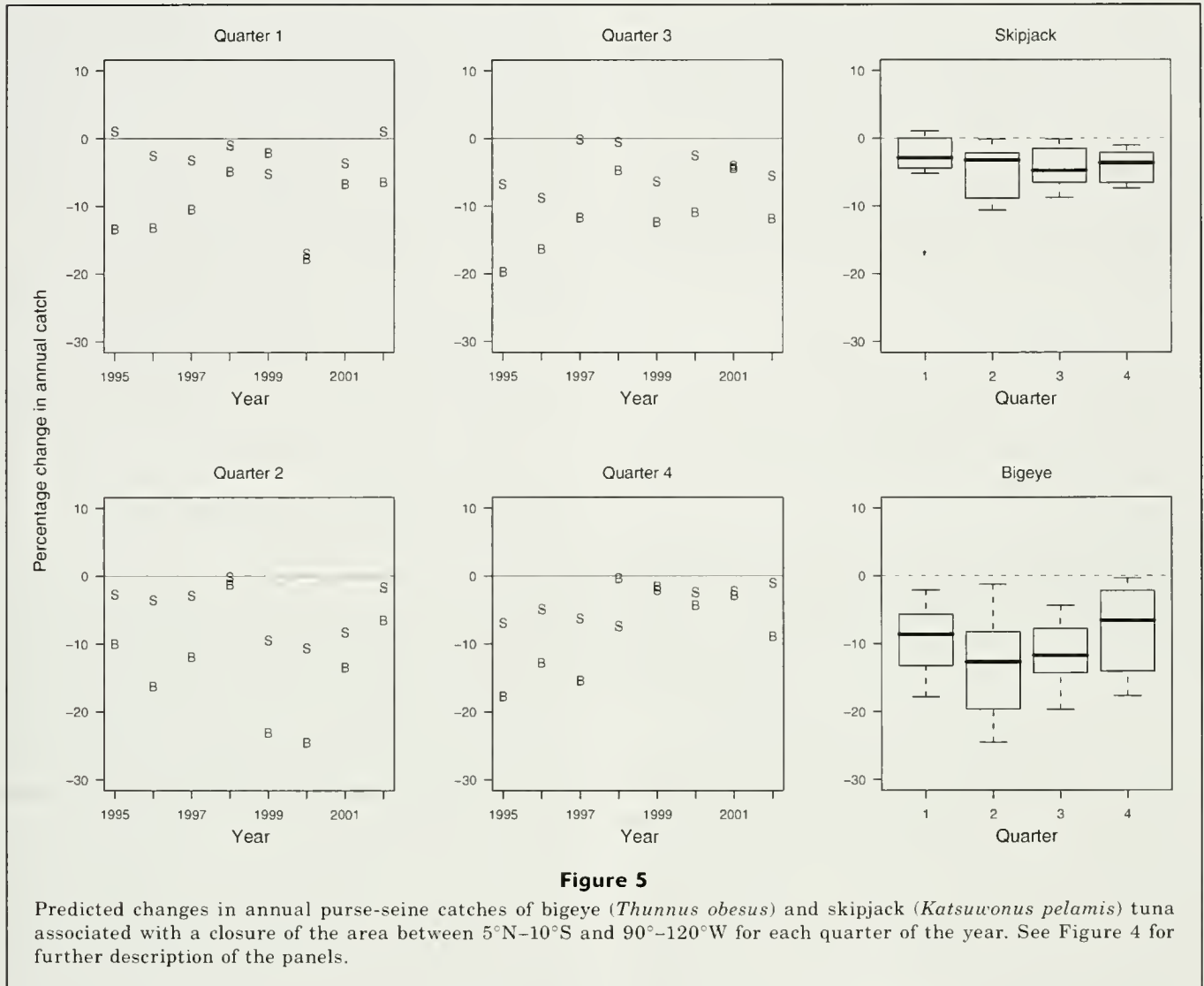
Figure 4

Predicted changes in annual purse-seine catches of bigeye (*Thunnus obesus*) and skipjack (*Katsuwonus pelamis*) tuna associated with a closure of the hotspot areas from Figure 1 for each quarter of the year. The left and middle panels indicate the change in annual catch for bigeye (B) and skipjack (S) tuna estimated to occur in each year of the 1995–2002 period if that area was closed in the 1st, 2nd, 3rd, and 4th quarter, respectively. The plots on the right summarize the predicted changes in bigeye and skipjack tuna catch over the eight years for a closure in each seasonal quarter. The white bar indicates the median change, the dark rectangle indicates the interquartile range (25th–75th percentiles), and the outer lines indicate the extremes. The horizontal dashed line represents zero (i.e., no change in catch).

Table 2

Summary of annual purse-seine effort and catch per unit of effort for bigeye (*Thunnus obesus*) and skipjack (*Katsuwonus pelamis*) tuna by set type (FOB=tuna school associated with floating object(s); UNA=tuna school not unassociated with floating object(s)) for the three areas modeled in the “practical” closure. A “practical” was a more practical, continuous region. It extended from 5°N–10°S, to 90°–120°W. The total area of this closure was the same as the total area of the hotspot regions. The means and standard deviations (SD) were calculated from annual values for 1995–2002.

Area		Number of sets		Bigeye catch per set		Skipjack catch per set	
		FOB	UNA	FOB	UNA	FOB	UNA
Practical closure	Mean	532	229	14.75	0.9	21.64	9.97
	SD	228	295	7	1.27	9.9	8.61
North	Mean	474	882	4.4	0.1	19.42	5.65
	SD	301	517	2.53	0.12	10.19	4.17
South	Mean	404	296	10.43	0.44	17.43	5.48
	SD	377	278	6.35	0.53	7.4	5.14



quarters, the predicted reductions in bigeye tuna catches associated with the practical closure ranged from 0.3% to 24.5% (777 metric tons [t] to 20,206 t), and the change in skipjack tuna catches ranged from a 1.1% increase to a 17.0% reduction (1204 t to 32,773 t) (Fig. 5). The extreme values of skipjack tuna catch were associated with first-quarter closures. As with the hotspot closure, the greatest reductions in bigeye tuna catch were associated with second- and third-quarter closures (average reductions of 13.4% and 11.5%, respectively, across years) and again the mean reduction in skipjack tuna catches did not vary greatly across quarters (mean reductions ranging from 3.8% to 4.9%). Based on the median of the ratios, the greatest contrast between bigeye and skipjack tuna reductions was associated with a second-quarter closure; the average percentage reduction in bigeye tuna catches was 13.4%, versus 4.9% for skipjack tuna catches.

Overall, the hotspot closure predicted slightly greater reductions in bigeye tuna catches and slightly lesser reductions in skipjack tuna catches than did the prac-

tical closure, but the difference in the median of the ratios (5.0 times for the hotspot closure and 3.8 times for the practical closure) is probably not significant. Results for both closures may indicate that a closure during the second or third quarters is optimal. Because the predicted variability in performance was less for a third-quarter closure than a second-quarter closure (in both analyses), the former was preferred as a management tool.

Discussion

Time-area closures are one of a number of fisheries management options (Hilborn et al., 2004). In our study we investigated, using simulations that use historical catch and effort data, whether time-area closures could be a useful tool to reduce bigeye tuna catches in the purse-seine fishery without leading to large reductions in the catches of skipjack tuna.

In the remainder of this article we discuss our findings in terms of the recent stock assessment recommendations for reductions in fishing effort—more specifically whether reductions predicted in our study would be sufficient to reach management objectives. We also discuss alternative measures for reducing bigeye tuna catches in the purse-seine fisheries of the EPO and describe potential improvements for our time-area closure modeling approach that may lead to a more accurate analysis of the likely performance of closures that may be considered in the future.

Predicting performance of time-area closures

Following Hall (1996), we looked for time-area strata in which there were high bigeye tuna to skipjack tuna ratios. These areas were relatively confined geographically and did not vary greatly by quarter. For this reason, the hotspot and practical closures predicted similar results.

Simulation of a practical closure (and one that able to be implemented) indicated that moderate average reductions in bigeye tuna catch (11.5%) could be achieved with lesser average reductions in skipjack tuna catches (4.9%). When we considered these reductions in terms of total catch by weight, the annual bigeye tuna catch reductions ranged up to 20,206 t (average 5722 t) and up to 32,773 t (average 6,807 t) for skipjack tuna.

Based on the current mix of fishing gears in the bigeye tuna fisheries in the EPO, and the estimated maximum sustainable yield (MSY) of about 77,000 t (IATTC, 2004), the purse-seine share of the MSY was around 40,000 t (S. J. Harley, unpubl. data). Considering current purse-seine catches of over 60,000 t, and the 11.5% reduction predicted for the practical closure, we believe that these closures alone are unlikely to yield the required reductions in bigeye tuna catches from the purse-seine fishery.

The closures investigated in our study were based on strata where the ratio of bigeye tuna to skipjack tuna

catches was the greatest. For these closures, the reduction in catches (in metric tons) is about the same for bigeye and skipjack tuna, but if a closure is larger or longer, the losses in skipjack catches would quickly outweigh the reductions in bigeye tuna catches. Therefore, although we did not examine larger or longer closures in our study, it is unlikely that these closures could lead to the necessary reductions in bigeye tuna catches without unacceptable losses in skipjack tuna catches.

The lack of effectiveness of the time-area closures is related to the extent of the interaction between skipjack and bigeye tunas. For the 1995–2002 period, 94% of the bigeye tuna caught by purse-seiners was taken in sets that also caught skipjack tuna (Table 3). This percentage is greater than the proportion of skipjack tuna catch that was taken in association with bigeye tuna (68%). Given this fact, it is not surprising that time-area closures are insufficient.

Management alternatives to reduce catches of bigeye tuna

We have shown that time-area closures alone are unlikely to result in the necessary reductions in fishing mortality for bigeye tuna; therefore alternative or supplementary management actions would be appropriate. In many instances, studies of fish behavior (Wardle, 1983) and gear technology (Larsen and Isaksen, 1993) have led to changes in gear configurations and deployment, resulting in significant reductions of catches of unwanted species. A good example of this type of change is the reduction of dolphin catch from tuna-dolphin aggregations in the EPO (NRC, 1997).

In the 1970s, many thousands of dolphins (mostly *Stenella* sp. and *Delphinus* sp.) were caught and killed by purse-seine vessels that set on dolphins in order to catch the yellowfin tuna that were associated with them (NRC, 1997). Through the introduction of fine-mesh net panels, use of a “back-down” procedure, and the avoidance of areas where oceanographic conditions could lead to net collapse, this mortality was reduced dramatically by the 1990s (NRC, 1997).

It is also possible to exploit behavioral differences among fish species. Through examination of the differential behavior of cod (*Gadus morhua*) and haddock (*Melanogrammus aeglefinus*), it was found that it was possible to configure bottom trawl nets to catch the target species and allow the other species to escape through larger meshes (Cotter et al., 1997). Sorting grids have also been used to allow the escape of unwanted species (Larsen and Isaksen, 1993; Misund and Beltestad³; IATTC⁴). Unless studies of bigeye and skipjack tuna be-

Table 3

Proportion of the annual floating-object fishery catches of bigeye (*Thunnus obesus*) and skipjack (*Katsuwonus pelamis*) tuna that are caught in sets with or without other species.

Year	Bigeye tuna		Skipjack tuna	
	Without	With	Without	With
1995	0.05	0.95	0.31	0.69
1996	0.06	0.94	0.25	0.75
1997	0.05	0.95	0.25	0.75
1998	0.04	0.96	0.27	0.73
1999	0.02	0.98	0.39	0.61
2000	0.08	0.92	0.38	0.62
2001	0.11	0.89	0.44	0.56
2002	0.08	0.92	0.29	0.71
Average	0.06	0.94	0.32	0.68

³ Misund, O. A., and A. K. Beltestad. 1994. Size-selection of mackerel and saithe in purse seine. International Council for the Exploration of the Sea Council Meeting, 1994/B:28.

⁴ IATTC (Inter-American Tropical Tuna Commission). 1999. Report of the bycatch working group, 25 p. 63rd Meeting of the IATTC; June 8–10, 1999. IATTC, 8604 La Jolla Shore Drive, La Jolla, California 92037.

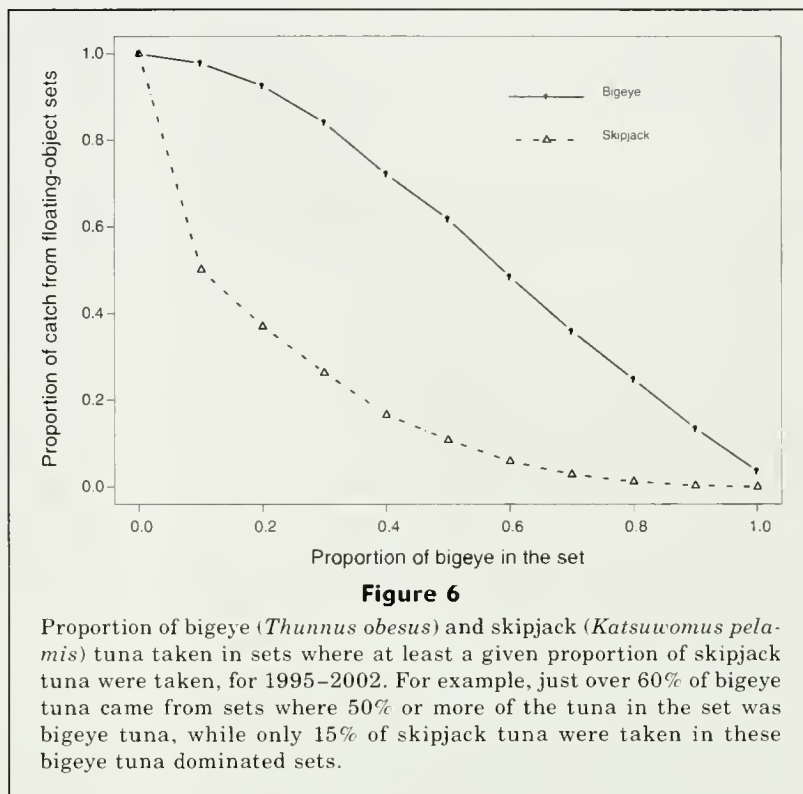
havior determine a mechanism by which bigeye, but not skipjack tuna, can escape through a sorting grid in a purse-seine net, sorting grids are more likely to be useful for overall reductions in catches of small tunas than as a mechanism for reducing bigeye tuna catches without reducing skipjack tuna catches.

Lennert-Cody and Hall (2000) used a range of statistical models to determine factors (e.g., area, season, characteristics of the floating object and the purse-seine net) that were associated with higher catches of bigeye and skipjack tuna. Unfortunately, many factors were confounded because the fishing practices of the fleet often differ in time and space, making it difficult to determine which gear characteristics may be important. Thus, it appears unlikely that analysis of fishery-collected data will lead to technical measures with the potential to reduce catches of bigeye tuna.

Although it may be difficult to determine important factors relating to bigeye tuna catch rates, fisheries data can be used to examine the nature of the catches of this species. For example, we found that 94% of bigeye tuna are caught in sets that also caught skipjack tuna. We were interested in how the bigeye tuna catches were distributed; were they predominantly from a small number of sets with high catches or from a large number of sets with small catches? Our analysis of this question, based on data for 1995–2002, is presented in Figure 6. It shows that only 5% of bigeye tuna were caught in single-species sets, but that about 50% of bigeye tuna came from sets that contained at least 60% of this species. These sets are responsible for only 7% of the skipjack tuna catch from the floating-object fishery and a smaller proportion of the overall skipjack catch given that about 30% of skipjack tuna catch is still taken from schools unassociated with dolphins (IATTC, 2004).

The analysis of the catch composition of purse-seine sets described above indicates that if fishing captains can determine, at least roughly, the species composition of an aggregation prior to setting (i.e., which species is dominant), large reductions in bigeye tuna catches could be achieved by not setting on bigeye-tuna-dominated aggregations. Such a measure would have little impact on overall skipjack tuna catches and would not require the fleet to be restricted in its activity by time-area closures.

Schaefer and Fuller (2005) used a range of electronic tags, supplemented with sonar images of fish aggregations around floating objects, to describe differences in the behavior of skipjack and bigeye tunas around floating objects. Exploitation of these differences, combined with the potential ability of fisherman to identify large aggregations of bigeye tuna around floating objects,



may lead to the development of fishing practices that can reduce bigeye tuna catches with minimal impact on skipjack tuna catches.

Critical to this approach will be the establishment of incentives 1) to encourage both the identification of the schools and 2) not to set on bigeye-tuna-dominated aggregations. Similar to the dolphin mortality limits currently applied by the IATTC, it could also be possible to have individual vessel limits for bigeye tuna and let fishermen determine how best to modify their fishing operations in order to achieve a given limit. Harley et al.⁵ used historical catch-by-vessel data and found that individual vessel limits of about 350 t would be sufficient to reduce purse-seine catches of bigeye tuna in the EPO by 50% in most years. Independent studies of fish behavior, coupled with experimental work investigating modifications in fishing practices and gear, could be fruitful.

Modeling potential effects of time-area closures

We applied simple closed-area models that used historical catch and effort data. Several assumptions are implicit in these models. First, we assumed that the fishing fleet has the flexibility to reallocate effort out-

⁵ Harley, S. J., P. K. Tomlinson, and J. M. Suter. 2004. Possible utility of catch limits for individual purse-seine vessels to reduce fishing mortality on bigeye tuna in the eastern Pacific Ocean, 8 p. Inter-American Tropical Tuna Commission, 5th working group on stock assessments, 11–13 May 2004, Document SAR-5-05 BET A. IATTC, 8604 La Jolla Shore Drive, La Jolla, California 92037.

side the closed area. We redistributed effort during the closure to other areas in proportion to historical effort within the same seasonal quarter. Previous studies have chosen not to redistribute effort (Goodyear, 1999), to redistribute effort in proportion to target catch (Worm et al., 2003), or to redistribute effort with the assumption that catch, rather than effort, is a limiting factor (Baum et al., 2003). A good understanding of fleet dynamics is necessary to determine appropriate models for effort redistribution.

Second, we assumed that redistributed effort would yield the same CPUE as previous effort in the area. Redistributed effort assumes that CPUE will remain unchanged when more fish are removed. It is likely that CPUE would decline with abundance as a result of increased effort, therefore it is possible that our analysis overestimates the catches during the closure. Similarly, our model assumes that CPUE is constant within each area, i.e. regardless of where one fishes within the area, one achieves the same CPUE. In reality, it is possible that fishermen could fish close to the edge of the closed area and potentially undermine the effectiveness of a closure.

Related to these first two points is the case of switching between fishing modes. By grouping FOB and UNA sets in our model, we allowed for switching between set types when fishing outside the closed area. Harley et al.⁴ showed that the purse-seine vessels that catch the majority of the bigeye tuna, fish almost exclusively on floating-objects (over 90% of the sets). Even with this information, we still believe that the implicit assumption of grouping the two set types is acceptable. We did not consider dolphin-associated sets (that catch almost exclusively yellowfin tuna). We consider it much less likely that effort would be shifted towards dolphin-associated schools for several factors, including politics, market pressure, technological and gear differences, and the inexperience that many skippers who participate in the FOB fishery would have with this alternative mode of fishing.

Finally, we implicitly assumed in our model that fish not caught as a result of the closure could not be caught later in the year. This assumption could lead us to underestimate catches outside of the closure. Thus, we have two potential biases in opposite directions that could affect our conclusions. The best way to quantify these biases would involve a model that integrated population and fisheries dynamics.

A dynamic approach to modeling closed areas could take into account the abundance of fish in different areas and the movement of fish between areas during the year. Modeling the relationship between effort and catches in different areas should include accounting for abundance (e.g., through the use of the catch equation).

Tagging data are necessary to estimate stock parameters, such as residence times within a closed area and fish movement rates between the open and closed areas. In addition to conventional tagging data, information from electronic tagging of bigeye tuna (Schaefer and

Fuller, 2002) could provide a basis for describing movement by means of simple movement models (e.g., those of Adam et al. [2003]). Because the vessels catch bigeye and skipjack tunas together, the model must include the movement patterns of both species.

This approach is extremely data demanding, and many of the data for this approach are not yet available. Notwithstanding these problems, future analysis of time-area closures should include consideration of important biological factors such as those described above, as well as socioeconomic data that may be important for predicting fleet dynamics.

Another extension of the modeling approach in our study is to consider additional target and bycatch species. Worm et al. (2003) considered bycatch from the United States swordfish and tuna longline fisheries in the Atlantic when modeling closed areas. With this approach it would be useful to include not only yellowfin tuna and dolphin sets in the model, but also the bycatch species that are taken in the different areas and fisheries.

Conclusions

Time-area closures are one of the many management actions available for the regulation of fisheries. Because of the strong interactions between bigeye and skipjack tunas, we have shown that time-area closures alone are unlikely to be sufficient to address concerns regarding the sustainability of bigeye tuna because it may not be possible to achieve the necessary reductions in bigeye tuna catches without large losses in skipjack tuna catches. We suggest that it will be important to investigate aspects of fish behavior to determine measures that could be used either in conjunction with, or instead of, closures to help reduce mortality on juvenile bigeye tuna while sustaining the important skipjack fishery.

Acknowledgments

We thank R. Allen, W. Bayliff, R. Deriso, and three anonymous reviewers for comments on this manuscript, and M. Hall, C. Lennert-Cody, M. Maunder, and K. Schaefer for useful discussions of closed areas and management options for bigeye tuna.

Literature cited

- Adam, M. S., J. Sibert, and D. Itano.
2003. Dynamics of bigeye (*Thunnus obesus*) and yellowfin (*T. albacares*) tuna in Hawaii's pelagic fisheries: analysis of tagging data with a bulk transfer model incorporating size-specific attrition. *Fish. Bull.* 101: 215–228.
- Baum, J. K., D. Kehler, R. A. Myers, B. Worm, S. J. Harley, and P. A. Doherty.
2003. Collapse and conservation of shark populations in the Northwest Atlantic. *Science* 299:389–392.

- Beverton, R. J., and S. J. Holt.
1957. On the dynamics of exploited fish populations. *Fish. Invest. London* 19:1–533.
- Cotter, A. J. R., T. W. Boon, and C. G. Brown.
1997. Statistical aspects of trials of a separator trawl using a twin rig trawler. *Fish. Res.* 29:25–32.
- Goodyear, C. P.
1999. An analysis of the possible utility of time-area closures to minimize billfish bycatch by U.S. pelagic longlines. *Fish. Bull.* 97:243–255.
- Hall, M. A.
1996. On bycatches. *Rev. Fish Biol. Fisheries* 6:319–352.
- Harley, S. J., M. N. Maunder, and R. B. Deriso.
2005. Assessment of bigeye tuna (*Thunnus obesus*) in the eastern Pacific Ocean. *Col. Vol. Sci. Pap. ICCAT*, 57(2):218–241.
- Hilborn, R., K. Stokes, J. J. Maguire, T. Smith, L. W. Botsford, M. Mangel, J. Orensanz, A. Parma, J. Rice, J. Bell, K. L. Cochrane, S. Garcia, S. J. Hall, G. P. Kirkwood, K. Sainsbury, G. Stefansson, and C. Walters.
2004. When can marine reserves improve fisheries management? *Ocean Coast. Manag.* 47:197–205.
- Horwood, J. W., J. H. Nichols, and S. Milligan.
1998. Evaluation of closed areas for fish stock conservation. *J. Appl. Ecol.* 35:893–903.
- IATTC (Inter-American Tropical Tuna Commission).
2004. Tunas and billfishes in the eastern Pacific Ocean in 2003. *Fishery Status Report* 2, 114 p. IATTC, La Jolla, California.
- Larsen, R. B., and B. Isaksen.
1993. Size selectivity of rigid sorting grids in bottom trawls for Atlantic cod (*Gadus morhua*) and haddock (*Melanogrammus aeglefinus*). *ICES Mar. Sci. Symp.* 196: 178–182.
- Lennert-Cody, C. E., and M. A. Hall.
2000. The development of the purse seine fishery on drifting fish aggregating devices in the eastern Pacific Ocean: 1992–1998. *In Tuna fishing and fish aggregating devices*, p. 78–107. [Title translated into English. The paper is in English, but the book is in French]. IFREMER (French Research Institute for Exploitation of the Sea), Issy-les-Moulineaux Cedex, France.
- Maunder, M. N.
2002a. Status of skipjack tuna in the eastern Pacific Ocean in 2001 and outlook for 2002. *In Stock assessment report 3: status of the tuna and billfish stocks in 2001*, p. 135–200. IATTC, La Jolla, CA.
2002b. Status of yellowfin tuna in the eastern Pacific Ocean in 2001 and outlook for 2002. *In Stock assessment report 3: status of the tuna and billfish stocks in 2001*, p. 47–134. IATTC, La Jolla, CA.
- Maunder, M. N., and S. J. Harley.
2002. Status of bigeye tuna in the eastern Pacific Ocean in 2001 and outlook for 2002. *In Stock assessment report 3: status of the tuna and billfish stocks in 2001*, p. 201–311. IATTC, La Jolla, CA.
- NRC (National Research Council).
1997. Dolphins and the tuna industry, 176 p. National Academy Press, Washington D.C.
- Schaefer, K. M., and D. W. Fuller.
2002. Movements, behavior, and habitat selection of bigeye tuna (*Thunnus obesus*) in the eastern equatorial Pacific, ascertained through archival tags. *Fish. Bull.* 100:765–788.
- Schaefer, K. M., and D. W. Fuller.
2005. Behavior of bigeye (*Thunnus obesus*) and skipjack (*Katsuwonus pelamis*) tunas within aggregations associated with floating objects in the equatorial eastern Pacific. *Mar. Biol.* 146:781–792.
- Wardle, C. S.
1983. Fish reactions to towed fishing gears. *In Experimental biology at sea* (A. MacDonald, and I. G. Friede, eds.), p. 167–195. Academic Press, New York, NY.
- Worm, B., H. K. Lotze, and R. A. Myers.
2003. Predator diversity hotspots in the blue ocean. *Proc. Natl. Acad. Sci. USA* 100:9884–9888.

Abstract—Oceanic incidence and spawning frequency of Chesapeake Bay striped bass (*Morone saxatilis*) were estimated by using microchemical analysis of strontium in otoliths. Otoliths from 40 males and 82 females sampled from Maryland's portion of the Chesapeake Bay were analyzed for seasonal and age-specific patterns in strontium and calcium levels. The proportion of oceanic females increased from 50% to 75% between ages seven to 13; the proportion of oceanic males increased from 20% to ~50% between ages four to 13. Contrary to an earlier model of Chesapeake Bay striped bass migration, results indicated that a substantial number of males undertook oceanic migrations. Further, we observed no mass emigration of females from three to four years of age from the Chesapeake Bay. Seasonal patterns of estuarine habitat use were consistent with annual spawning runs by striped bass of mature age classes, but with noteworthy exceptions for newly mature females. Evidence of an early oceanic presence indicated that Chesapeake Bay yearlings move into coastal regions—a pattern observed also for Hudson River striped bass. Otolith microchemical analyses revealed two types of behaviors (estuarine and oceanic) that confirm migratory behaviors recently determined for other populations of striped bass and diadromous species (e.g., American eels [*Anguilla rostrata*] American shad [*Alosa sapidissima*] and white perch [*Morone americana*]).

Oceanic migration rates of Upper Chesapeake Bay striped bass (*Morone saxatilis*), determined by otolith microchemical analysis*

David H. Secor (contact author)¹

Philip M. Piccoli²

Email for D. H. Secor: secor@cbl.umces.edu

¹ Chesapeake Biological Laboratory
University of Maryland Center for Environmental Science
Solomons, Maryland 20688

² University of Maryland
Department of Geology
College Park, Maryland 20742

As an estuarine-dependent species, striped bass (*Morone saxatilis*) demonstrate large plasticity in migration patterns (Secor and Piccoli, 1996). Striped bass in Chesapeake Bay are partial migrants; only a fraction of individuals will leave estuarine habitats for oceanic waters (Kohlenstein, 1981). Never the less, Chesapeake Bay striped bass are the major contributors to interjurisdictional ocean fisheries (Merriman, 1941; Wirgin et al., 1993). Rates of contributions by Chesapeake Bay striped bass to those fisheries are determined by lifetime patterns of habitat use, ontogenetic rates of egress from Chesapeake Bay, and regional rates of exploitation and natural mortality (Dorazio et al., 1994). Rates of oceanic residence have been shown to vary by sex and increase with age. Analyzing striped bass tagged in the Potomac River, Kohlenstein (1981) advanced the working hypothesis that young striped bass remain in or near the tributary in which they were spawned for two or three years. At this point a substantial proportion of immature females (ca. 50%) emigrate from the Bay, remaining in ocean waters until sexually mature (age 5–7 years). In contrast, males are mature by age 2 but remain in the Bay throughout their lives. This hypothesis remains untested, although substantial deviation from this proposed pattern is indicated by tagging studies and catch records.

From recaptured striped bass tagged on Chesapeake Bay spawning grounds, Dorazio et al. (1994) estimated that by 800 mm total length (TL), approximately half of the population (males and females combined) used ocean habitats. This length would correspond to an age of seven to 10 years (Secor et al., 1995b). Tagging studies comprise quasilongitudinal analyses, which could provide estimates of age-specific egress rates if tagged and recaptured fish are representative of the population. However, striped bass are moderately long lived and show migration behaviors that vary substantially with sex and age. Therefore, tagging studies often do not comprise sufficient spatial and temporal scales to provide the precise information needed to predict how Chesapeake Bay striped bass contribute to coastal fisheries.

Striped bass longevity exceeds 30 years (Merriman, 1941; Secor et al., 1995b). Life table analysis has indicated that maximum reproductive rate occurs relatively late in life (10–12 years) (Secor, 2002) and that accumulation of adult biomass (reproductive potential) represents an important “storage mechanism” (Warner and Chesson, 1995), improving the

Manuscript submitted 23 July 2004
to the Scientific Editor's Office.

Manuscript approved for publication
17 April 2006 by the Scientific Editor.

Fish. Bull. 105:62–73 (2007).

* Contribution 4041 of the University of Maryland Center for Environmental Science, Chesapeake Biological Laboratory, Solomons, Maryland.

odds of recruitment over the lifetime of a fish (Secor, 2000a, 2000b, in press). Life-table-based models (e.g., Goodyear, 1984) depend upon the assumption that annual spawning occurs, which remains unsubstantiated for this species. If spawning frequency declines with age, for instance, then generation time and age-at-maximum reproductive value will be substantially overestimated, which in turn will affect biological reference points (Marshall et al., 2003).

Electron probe micro-analysis (EPMA) of Sr has been developed as a method to reconstruct individual patterns of migration and habitat use by anadromous populations of striped bass (Secor, 1992). In estuarine environments, strontium is often a reliable tracer of salinity; higher marine concentrations (7 ppm) become diluted in estuarine environments by freshwater inputs when freshwater Sr:Ca end-members (where "end-members" are the source of a Sr:Ca ratio) are low (Ingram and Sloan, 1992). Kraus and Secor (2004a) surveyed available data and determined that 83% of estuaries have low freshwater end-members, indicating that the ratio of Sr to Ca should be positively (but not necessarily linearly) related to salinity in most estuaries.

In our study we applied EPMA to examine the fraction of Chesapeake Bay striped bass that migrate to ocean waters and the frequency at which females and males undertake spawning runs. We previously used this method to chart age- and sex-specific patterns of Hudson River striped bass (Secor and Piccoli, 1996; Zlokovitz and Secor, 1999; Secor et al., 2001). Expectations for ontogenetic rates of emigration (i.e., Kohlenstein, 1981) and annual spawning were tested. In addition, we sought evidence for contingent groups (subpopulation groups with similar lifetime migration patterns; Secor, 1999), which we observed previously in Hudson River striped bass.

Material and methods

Samples

Samples collected during spawning runs present the best opportunity to collect a representative sample of mixed age classes, sexes, and migratory behaviors. These samples comprise mostly those ages that have fully recruited to the mature population. We note in our study that this sample incompletely represents migratory behaviors for those females that have not yet become mature and are not participating in the year's spawning run. During the period 15 April–30 May 2000, we obtained samples of 247 male and 122 female striped bass from the upper Chesapeake Bay (N. of 39°00'; $n=27$), mid-Bay (N. of 37°53'W'S. of 39°00'; $n=76$); Choptank River ($n=199$), Patuxent River ($n=33$), and Potomac River ($n=28$). Capture methods were diverse and included the use of gill- and pound-nets (Maryland Department of Natural Resources monitoring), electro-shocking (National Marine Fisheries Service Northeast Center and University of Maryland scientific collections), and

charter boat angling. All fish were measured (fork length [FL] and weight [g]), sex and diet were determined, and otoliths and scales were collected. Fork lengths ranged from 685 to 1110 mm for females and from 320 to 1029 mm for males.

Otolith Sr:Ca measures

To conduct EPMA analyses, otoliths (sagittae) were extracted, soaked in 1% sodium hypochlorite solution, rinsed with deionized water, and embedded within a resin (Secor et al., 1992). Transverse sections, approximately 1 mm thick, were cut through the otolith cores with a metallurgical wafering saw. The sections were mounted on glass slides, polished on wetted 600-grain sandpaper, and polished again on a slurry of 0.3- μm alumina until their surfaces were free of pits and abrasions, which can cause artifacts in microprobe analysis (Kalish, 1990). Annuli were enumerated based upon standard criteria under optical microscopy (Secor et al., 1995b). Before analysis, otoliths were cleaned ultrasonically and carbon-coated in a high-vacuum evaporator.

X-ray intensities for Sr and Ca were quantified by using a JEOL 8900 electron probe microanalyzer (Center for Microscopy and Microanalysis, Univ. Maryland, College Park, MD). Calcite (CaCO_3) and strontianite (SrCO_3) were used as reference standards and the protocol was checked by using secondary standards containing both Ca and Sr. The details of this analysis can be found elsewhere (Secor and Piccoli, 1996). Detection limits for Sr were approximately 230 ppm (± 2 standard errors). Four slides, each containing four otolith sections, were loaded into the specimen chamber of the microanalyzer. After initial calibration to Sr and Ca standards (at programmed settings and intervals), transect assignments were made for up to 16 otolith sections. Transects comprised a series of point measurements from young to old ages across the sectioned otolith. X-ray maps of otolith structure were collected by using wavelength spectrometers.

Sr was expressed as a ratio of Ca (Sr:Ca) because of expected competitive interactions between the isotopic species (Kraus and Secor, 2004a). Further Sr:Ca records were converted to salinity exposure profiles according to the model (Secor et al., 1995a):

$$\text{"Salinity inhabitance" (sic) (psu)} = 40.3 (1 + 56.3 e^{-1523(\text{Sr:Ca})^{-1}})^{-1}; \quad r^2 = 0.94; \quad n = 54$$

where "salinity inhabitance" (sic) is the salinity level (practical salinity units, psu) in the otoliths for the period of time represented for each Sr:Ca datum.

Oceanic incidence of striped bass

For our analysis, a subsample of 122 fish (40 males and 82 females) was drawn from the upper Bay ($n=10$), mid-Bay ($n=46$), and Choptank River ($n=66$). Estimated salinity records for the last year of life (recent

habitat use) were determined from at least five point measurements taken across the last completely-formed annulus (i.e., the last full year of life prior to winter). Opaque zone formation on the otolith occurs just prior to the spawning season (Zlokovitz et al., 2003); therefore measurements were taken between the penultimate and most peripheral (recently formed) opaque zones. We selected the record of maximum salinity, because at least one point in this series can be influenced by the previous year's spawning run, Oceanic habitat use was defined as salinities >29, and individual fish were classified accordingly. Because of unequal sampling among ages, we analyzed four age classes by sex: 4–6, 7–9, 10–12, and 13–18 years of age. Two-way classification tables were constructed to evaluate differences between age classes and sexes in probability of recent oceanic residence.

Life history transects and spawning frequency

Life history transects of salinity exposure, a series of Sr:Ca ratios from the juvenile period to the end of life, were constructed from EPMA measurements from 30 female and 10 male striped bass. This subsample was drawn from the upper Bay ($n=2$), mid-Bay ($n=27$), and Choptank River ($n=11$). To weight seasonal data among ages, time series were selected so that four or five analyzed points were included for each annulus. Data were standardized (Z score = $(\text{transect datum} - \text{transect mean})/\text{transect standard deviation}$) and plotted to examine variations about the transect mean (Sokol and Rohlf, 1981).

Time-series data represented by the life history transects were expected to show autocorrelation across seasonal points and ages. An appropriate method of data analysis that shows interdependence among repeated measures on the same individual is repeated measures multivariate analysis (RM-MANOVA) (Chambers and Miller, 1995). This analysis simultaneously fits several dependent variables to independent factors of interest (SAS, Statistical Analysis System, SAS Institute, Inc., Cary, NC) and evaluates the matrix equation,

$$S_t = \text{Sex}\beta + E,$$

where S_t = salinities at seasonal points; and
 t = relative distance between successive opaque zones.

For each fish, S_t is arrayed in n rows, Sex contains two treatment levels for each factor (male vs. female) arrayed in n rows, and E is the matrix of model residuals. Degrees of freedom in the analysis depend upon n , which represents the number of individual fish. To avoid the problem of interdependence of seasonal data for combined ages, separate MANOVAs were performed for each age class.

To conduct the RM-MANOVA, it was necessary to have equal numbers of seasonal points (S_t) for each age class. Therefore, narrow annuli that had fewer than

three seasonal (interannual) points were omitted from analyses. This excluded analyses of some of the oldest age classes, which typically exhibit narrow annuli (Secor, 1992). For years sampled with more than four or five seasonal points, the extra points were omitted from our analysis. Selection of points to be included was based upon their proximity to the axial distances of the prescribed intervals (either [0, 0.25, 0.5, 0.75] or [0, 0.2, 0.4, 0.6, 0.8]). Individual probe points within transects were separated by 10 to 35 microns.

Results

Demographics

Ages among the sampled Maryland Chesapeake Bay striped bass ranged from three to 18 years and sizes ranged 320 to 1110 mm FL. Females were significantly older and larger than males (ANOVA; $P<0.01$) and grew at a faster rate. Males were more heavily represented by ages <10 years than females in age-frequency distributions, although fish with ages >15 years were observed for both sexes. Relatively strong year class contributions within the sample occurred for 1982, 1989, 1993, and 1996 and coincided with high young-of-the-year juvenile abundances observed in those years (Secor, 2000a).

Oceanic incidence of striped bass

Female fish, more often than male fish, were classified as having a recent period of oceanic residence based upon the analysis of the last fully formed annulus, but this difference was not significant (χ^2 , $P>0.1$). For individual age classes with sample sizes >5, oceanic incidence ranged from 60% to 75% for females and from 17% to 50% for males (Table 1). There was an indication that the proportion of fish of both sexes with oceanic residence increased with age. Oceanic incidence was observed consistently for >50% of the females. For males, oceanic incidence was 8–32% less than for females within each age class. Error bars, based upon a binomial probability distribution, indicated a fairly well-estimated oceanic classification rate for the age class 10–12 years due to a relatively high sample size. For this age class, oceanic incidence was estimated at 59% and 50% for females and males, respectively. Conversely, use of oceanic habitat for males at ages <10 was poorly estimated because of low sampling size. Indeed, estimated ratios for this group could not be statistically resolved from zero. With increased size, oceanic incidence (sexes combined) tended to increase (Table 1), although there was a decline in the proportion of fish with evidence of oceanic residence from 65.8% for the size class 900–999 mm FL to 46.1% for the size class >1000 mm FL.

Life history transects

Life history transects showed considerable variability (Fig. 1). It is noteworthy that some males exhibited

some degree of oceanic incidence (fish identification [ID] number=98, 198, 260) throughout portions of their lives and many females exhibited a pattern of estuarine use (e.g., ID=197, 263, 271, 272, 280, 281). A single instance of freshwater residency was observed for a fairly long-lived female (ID=271; age=11 years; FL=875 mm). Mean lifetime salinity exposure differed significantly between males and females (Kruskal-Wallis ANOVA; $P=0.01$), with females exhibiting an average 10% higher use of high-salinity habitat during the mature portion (age>6) of their lives (Fig. 2).

The male sample, albeit small ($n=10$), did not exhibit age-dependent patterns in salinity exposure (Fig. 2). In part, high variance in older age classes (8–12) obscured any pattern of salinity exposure at ages <6 years. Females showed a strong and nearly linear trend of increased salinity exposure with age (Fig. 2). Modal salinity increased from a range of 20–25 to a range of 25–30 for ages 2 and 7, respectively. Interestingly, both males and females showed that a polyhaline (salinity>18) habitat was used during the period between age 1 and 2 years. Thus, yearlings may be preferentially using polyhaline regions, followed by a return of some individuals to lower salinity regions (because slightly depressed salinities were observed for ages 2 and 3 compared to age 1 yr in Fig. 2). We have observed a similar pattern in Hudson River striped bass (Zlokovitz et al., 2003). The ontogenetic trend of increased salinity exposure with age in females could be related to maturation (ages 6–8 years)—a pattern observed in two-thirds of female fish (Fig. 3). Males also showed a rise in salinity exposure with age, albeit less consistently (Fig. 4).

Spawning frequency

Life history transects for the sample of ten males and thirty females gave evidence of strong intra-annual patterns in the salinity levels of their habitat (Figs. 3 and 4). Intra-annual trends often showed nadirs at or near the opaque zone of the otolith, a pattern occurring in both males (e.g., ID=124, 196, 327) and females (e.g., ID=192, 297, 298). In some instances, seasonal cycles indicated either less than annual (Fig. 3; ID=320; Fig. 4; ID=298, 300) or greater than annual (Fig. 3; ID=99; Fig. 4; ID=295, 300) cycles in patterns of salinity exposure.

Significant seasonal effects on patterns of salinity exposure were observed for ages 6 and 8 and for pooled ages 6–11 (Table 2), indicating that across individuals there was a seasonal pattern in salinity exposure for

Table 1

Degree of oceanic incidence of Chesapeake Bay striped bass collected in 2000. Data is presented for age classes by sex, and for size-class pooled sexes (the latter to permit comparison with results of Dorazio et al., 1994). Lower (LCL) and upper (UCL) confidence limits are presented for oceanic incidence by age class.

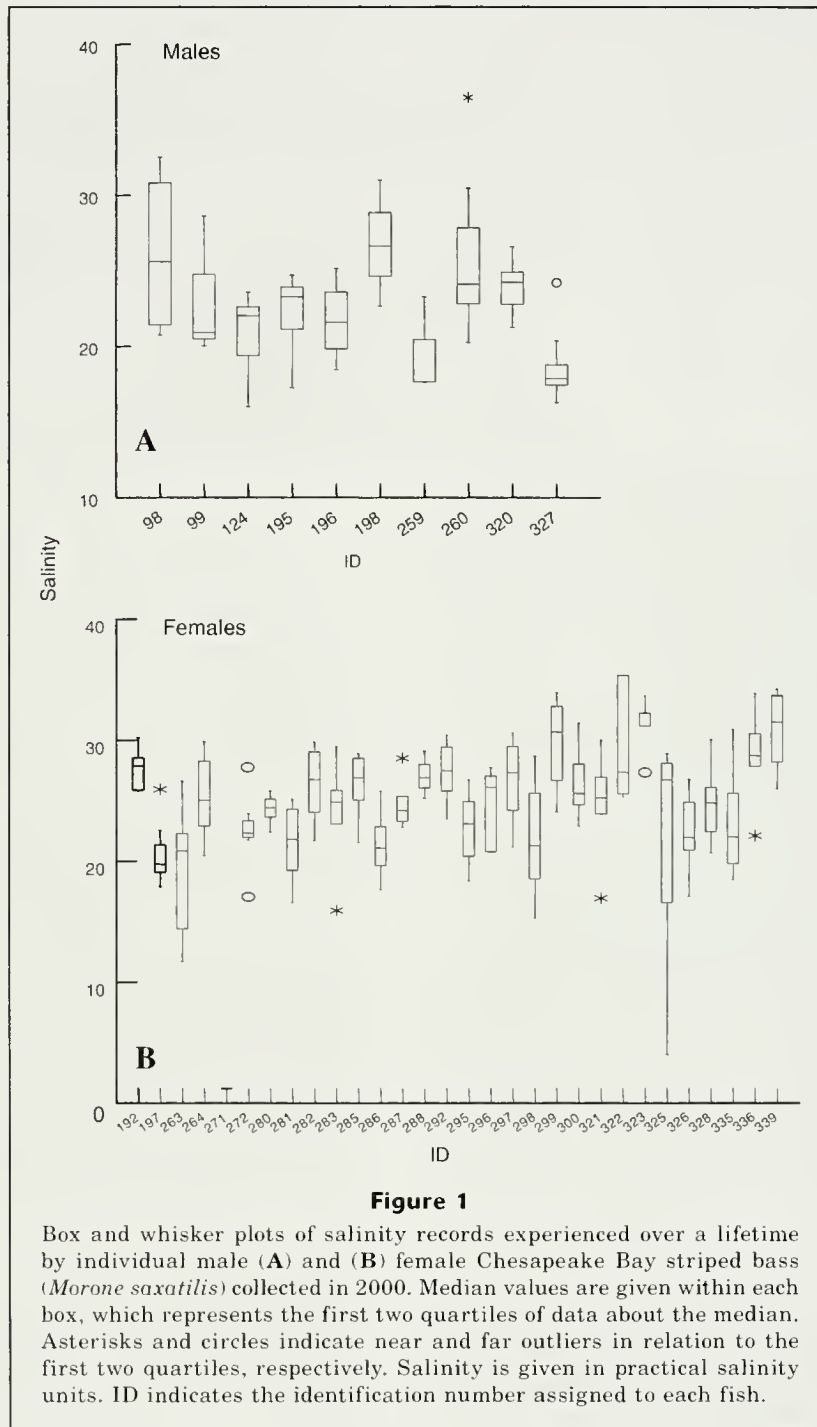
Age class (yr)	Oceanic incidence (%)	
	Males (<i>n</i> ; LCL–UCL)	Females (<i>n</i> ; LCL–UCL)
4–6	20.0 (5; 0–41.3)	—
7–9	25.0 (8; 0–50.2)	55.5 (18; 42.5–68.1)
10–12	50.0 (18; 37.4–62.5)	58.8 (51; 56.8–62.5)
13–18	44.4 (9; 34.0–77.4)	76.9 (13; 60.8–93.6)

FL size class (mm)	Oceanic incidence (%)	
	This study (<i>n</i>)	Dorazio et al. (1994)
300–599	20.0 (8)	<5.0
600–699	—	~8.0
700–799	42.9 (14)	~35.0
800–899	59.0 (44)	~80.0
900–999	65.8 (41)	~90.0
>1000	46.1 (13)	>95.0

mature age classes. The other analysis of five, rather than four, seasonal points of measurement in the otolith did not show strong evidence for seasonality, although pooled age classes 6–11 and 7–11 showed marginal significance at $P=0.06$. In the selection of individuals that contained five seasonal points, sample sizes were substantially reduced. This reduced sample size in turn would have resulted in less statistical sensitivity. Despite high variances among individuals for each seasonal measurement, there was a trend for a seasonal nadir in salinity exposure near the opaque zone on the otolith (seasonal interval=0) (Fig. 5). This trend was especially apparent in males, and in females >6 years.

There was a slight indication of sex-related differences in seasonality of salinity exposure. Significant between-sex differences occurred for S_0 at ages 8 and 11, and all mature age class groupings (Table 2). Significant differences occurred for $S_{0.25}$ at ages 8 and 9 and mature age groupings 7–11 and 8–11; and for $S_{0.5}$ at age 8 and all mature age groupings. Males were found at lower salinities at these seasonal points than were females (Fig. 5).

X-ray maps of Sr within otolith sections showed clear concentric patterns of alternating high and low regions of Sr in association with annuli (Fig. 6). X-ray maps confirmed the cyclical patterns observed in the life history transects (Figs. 3 and 4), but with greater apparent difference between peak and nadir levels of Sr. In one of the X-ray maps (Fig. 6, bottom panel), a high level of Sr occurred within the first annulus).



Discussion

Oceanic incidence of striped bass

Our analysis and that of Dorazio et al. (1994) does not support Kohlenstein's (1981) model of mass egress of female striped bass from Chesapeake Bay after ages two or three. Rather, our life history transects indicated a fairly gradual shift to use of ocean habitats—a

shift associated with maturation at ages five to eight (Table 1; Fig. 2). For mature age classes, evidence of oceanic residence was observed for 50–75% of the female sample. Also, in contrast to previous expectations, otolith microanalysis indicated that a large fraction of males leave Chesapeake Bay, albeit at rates <50%.

Mirroring the results of Dorazio et al.'s (1994) tagging experiment, our results showed a trend of increasing oceanic residence with fish size, but found

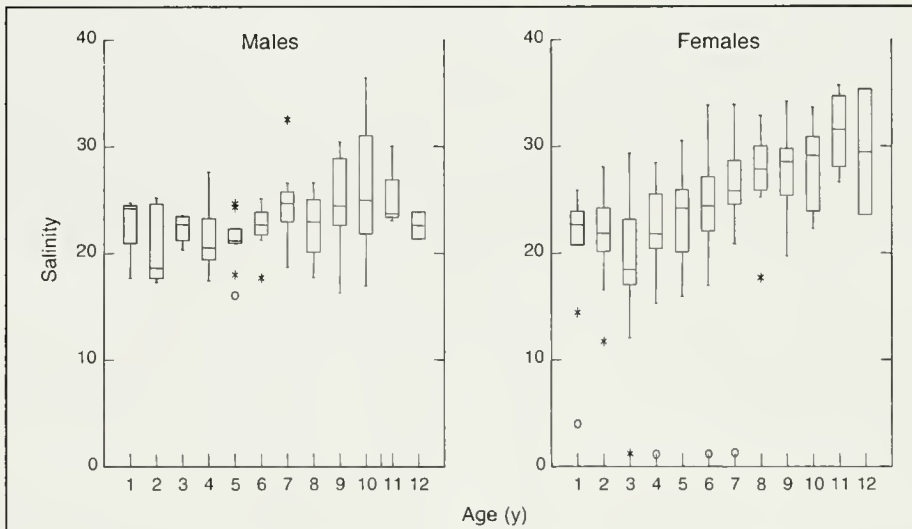


Figure 2

Box whisker plots of age-specific salinities experienced by Chesapeake Bay striped bass (*Morone saxatilis*) collected in 2000. Salinity data for each fish include quarterly seasonal salinity records. Median values are given within each box, which represents the first two quartiles of data about the median. Asterisks and circles indicate near and far outliers in relation to the first two quartiles, respectively. Salinity is given in practical salinity units. ID indicates the identification number assigned to each fish.

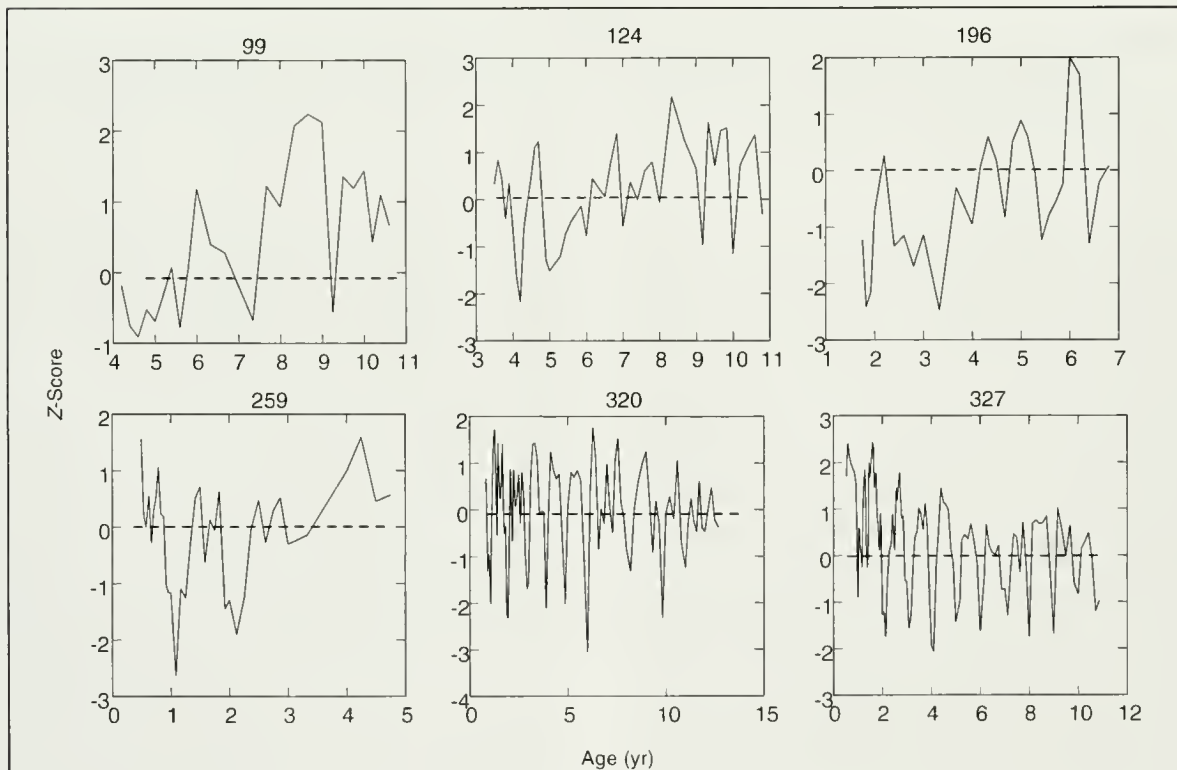
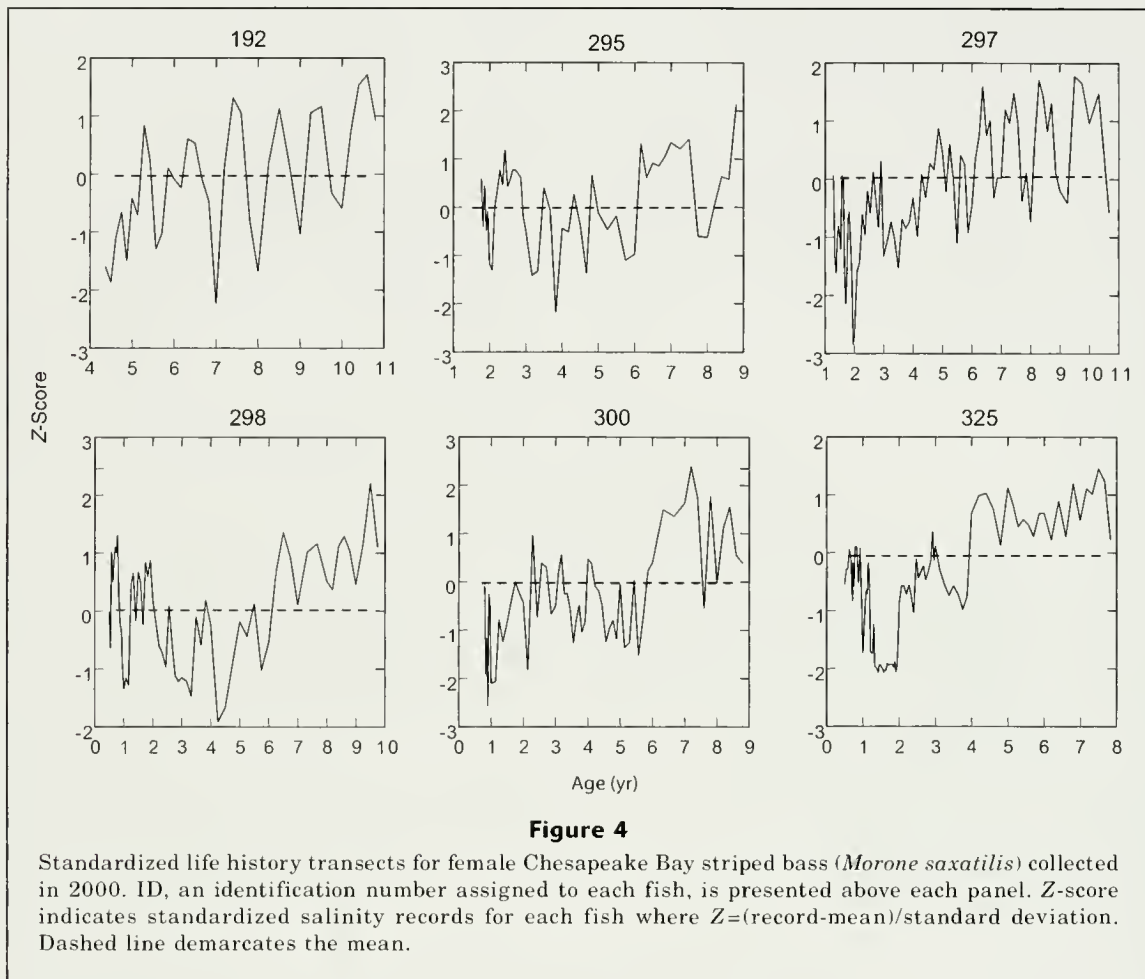


Figure 3

Standardized life history transects for male Chesapeake Bay striped bass (*Morone saxatilis*) collected in 2000. ID, an identification number assigned to each fish, is presented above each panel. Z-score indicates standardized salinity records for each fish where $Z = (\text{record} - \text{mean}) / \text{standard deviation}$. Dashed line demarcates the mean.



two important differences. First, we did not observe >90% oceanic incidence at >900 mm TL (877 mm FL) (Table 1). Rather, a substantial fraction of striped bass remained resident in Chesapeake Bay throughout their lives regardless of age or size. At ages >12 years, 25% of the female sample was estimated to have been resident in Chesapeake Bay. As an extreme example, one individual female resided in freshwater during its entire 11-yr lifespan. Secondly, early rates of oceanic migrations at sizes <700 mm TL (<685 mm FL) were substantially higher than rates indicated in the Dorazio et al. (1994) model, which predicted <5% of individuals migrate to ocean waters. Several factors may have contributed to the different results. Dorazio et al. (1994) predicted the degree to which Chesapeake Bay striped bass migrate to coastal regions north of Cape May New Jersey. Thus, their recapture sample represents only a subset of possible coastal fish. This bias would tend to underestimate oceanic residence; yet the Dorazio et al. (1994) estimates tend to be higher for larger mature striped bass. Recapture and reporting rates probably varied between coastal and Chesapeake regions because of more restrictive fishing regulations in Chesapeake Bay that contributed to an overestimate of migrant fish to northern ocean habitats.

In comparing our results to those of past tagging studies, we must also carefully consider limitations to the otolith microchemistry approach. We have sought to overcome some of the past hurdles regarding low sample size and resolution, yet these remain principal concerns. Despite large improvements in microprobe technology, otolith microchemistry remains a very expensive and time-consuming procedure to evaluate population-specific patterns in fish migration. Sample sizes, while larger than in many past projects, remain modest. Also, ages and sizes were not uniformly distributed in the populations sampled because of strong year classes, and this lack of uniform distribution would curtail generalizations across size and age classes. This strong year class phenomenon is common in striped bass, and it is likely that migration patterns in Chesapeake Bay striped bass typically will be influenced by dominant year classes (Merriman, 1941).

A central assumption in using strontium as a tracer of salinity levels is that the ratio of strontium to calcium (Sr:Ca) in the otolith can accurately distinguish between oceanic (salinity >29) and estuarine (salinity <30) habitat use. First, the designation, between oceanic and estuarine water is somewhat arbitrary, particularly considering that the mouth of Chesapeake

Table 2

Repeated measures MANOVAs for effects of sex on seasonal salinities experienced by Chesapeake Bay striped bass (*Morone saxatilis*). S_t = salinity at seasonal point t , where t = relative distances between successive opaque zones in otoliths. "Season" is defined by two intervals on the otolith as a proportion of otolith increment width. Univariate F tests (P -values reported) for contrasts between males and females are given for each seasonal point. Differences among seasonal salinities ("Seasonality") within each age were evaluated with a Wilk's statistic (Chambers and Miller, 1995). The interaction between season and sex tested whether sex affected patterns of seasonality in salinity levels in otoliths. NS=not significant.

Contrast between males and females							
Age (yr)	n	S_0	$S_{0.25}$	$S_{0.5}$	$S_{0.75}$	Seasonality	Season \times Sex
1	11	NS	NS	NS	NS	NS	NS
2	19	NS	NS	NS	NS	NS	NS
3	21	NS	NS	NS	NS	NS	NS
4	29	NS	NS	NS	NS	NS	NS
5	33	0.09	NS	NS	NS	NS	NS
6	35	NS	NS	NS	NS	0.02	0.04
7	32	NS	NS	NS	NS	NS	NS
8	22	0.02	0.01	0.04	NS	0.04	NS
9	22	NS	0.03	NS	NS	NS	NS
10	20	NS	NS	NS	NS	NS	NS
11	7	0.04	NS	0.07	NS	0.07	NS
6-11	138	0.04	NS	0.02	NS	0.04	NS
7-11	103	0.04	0.01	0.03	NS	0.09	NS
8-11	71	0.03	0.002	0.01	NS	NS	NS

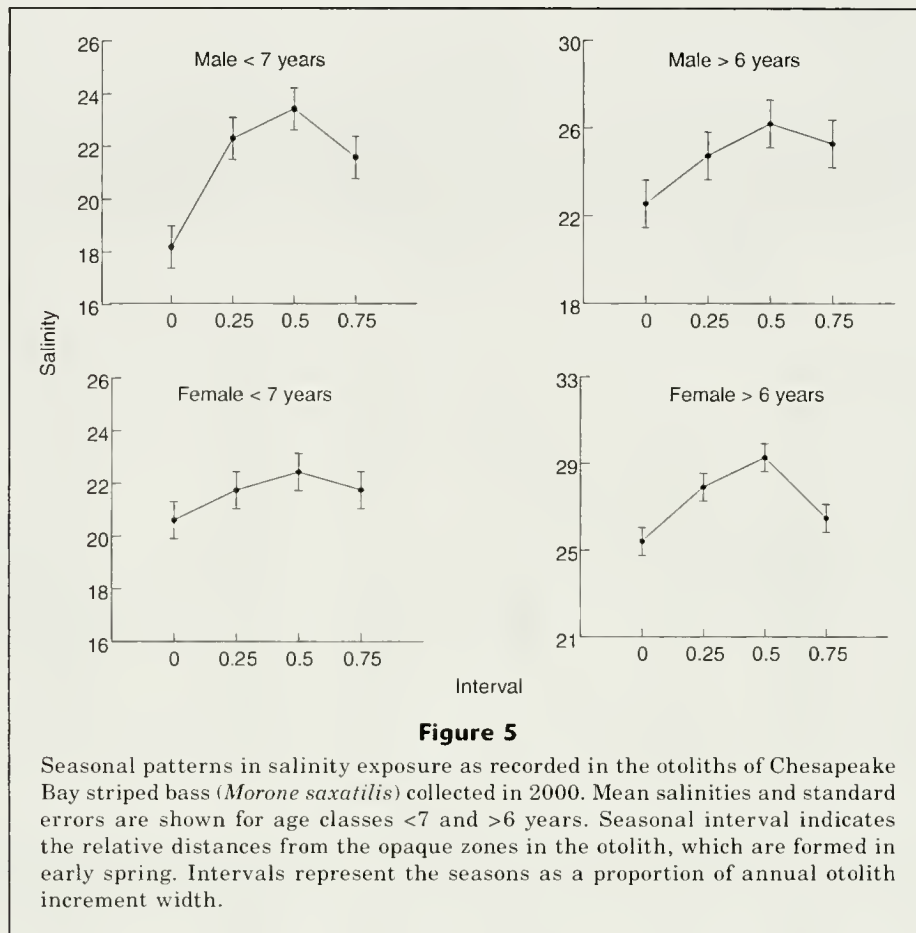
Contrast between males and females								
Age	n	S_0	$S_{0.2}$	$S_{0.4}$	$S_{0.6}$	$S_{0.8}$	Seasonality	Season \times Sex
5	31	0.09	NS	NS	NS	NS	NS	NS
6	31	NS	NS	NS	0.03	NS	NS	NS
7	22	NS	0.003	NS	NS	NS	NS	NS
8	19	0.02	0.07	0.02	NS	NS	NS	NS
9	13	NS	0.01	0.02	NS	NS	NS	NS
10	11	NS	NS	0.02	NS	NS	NS	NS
11	5	NS	NS	NS	NS	NS	NS	NS
6-11	101	0.001	0.007	0.001	0.01	0.05	0.06	NS
7-11	70	0.001	0.001	0.001	NS	NS	0.06	NS
8-11	48	0.005	0.01	0.001	0.08	NS	NS	NS

Bay averages about 25–30 psu during summer and fall months. Still, it was necessary to have a designation for assessing habitat use, and the above designations may have resulted in a liberal estimate of oceanic residence. A second issue is the resolution of the relationship of otolith Sr:Ca ratio to salinity. Resolution level estimated by experimental work of Secor et al. (1995a) was a salinity of 6 psu, which would support the contention that estimates presented here are fairly precise if error is unbiased. Still, the relationship between otolith Sr:Ca and salinity was logistic and very rapid changes in Sr:Ca were predicted to occur with small changes in salinity at salinities between 25 and 35 psu. These rapid changes at high salinities could indicate higher unexplained variability at salinities >24 psu.

Finally, our samples were unequally weighted across subpopulations of striped bass. For instance, no lower Chesapeake Bay subpopulations (those spawning in

the James, York, and Rappahannock systems) were represented in our sample). Recent tagging studies have either focused more narrowly on the Potomac River (Kohlenstein, 1981) or have drawn a larger and more representative sample from the Maryland section of Chesapeake Bay (Dorazio et al., 1994). Studies on Virginia subpopulations of striped bass have historically shown low rates of oceanic residence (<5%; Vladykov and Wallace, 1952; Massman and Pacheco, 1961). Kohlenstein (1981) effectively argued that these and other early tagging studies (i.e., Mansueti, 1961) were not appropriately stratified to provide evidence of an increased likelihood of oceanic residence by larger size fish.

In sum, we believe that our otolith microchemistry results indicate higher rates of early oceanic residency in females and overall higher rates of oceanic migrations by males than were observed in previous tag-



ging studies (Kohlenstein, 1981; Dorazio et al., 1994). Further, increasing trends in oceanic habitat use with age observed in our study are consistent with the two previous tagging studies. The increased incidence of males in ocean environments shown in our study and previous ones could reflect a true increased likelihood of emigration, perhaps driven by increased striped bass density, or by poorer habitat conditions in Chesapeake Bay. This view would be consistent with the near historically high abundances of Chesapeake Bay striped bass and the increased incidence of summertime hypoxia in Chesapeake Bay during the past two decades (Hagy et al., 2004). However, error due to the otolith microchemistry approach in classifying fish to oceanic or estuarine habitat use must be acknowledged and caution should precede application of the estimates of oceanic residence provided in this study.

Spawning frequency

In general, otolith microchemical analyses gave evidence for the view that most mature striped bass undertake annual spawning runs. For females, immature age classes did not show significant seasonality in changes in salinity, but many mature age classes did. Further, cycles in salinity were largely defined by a nadir that

occurs during early spring as evidenced by changes in the chemistry of the opaque zone of the otolith. Thus, evidence of the use of low-salinity habitat was recorded near the opaque zone, consistent with the view of an annual up-estuary migration to low-salinity spawning habitats. Where such nadirs were not observed in the otolith microchemistry, two interpretations are plausible: 1) no spawning migration occurred, or 2) the otolith microchemistry method had insufficient resolution to allow us to detect the spawning migration. The resolution issue relates to two problems. First, the spacing of the microprobe assays could have been such that a spawning run event was missed. Second, spawning-run striped bass occur in low-salinity regions for short periods during which they are not growing and thus incorporating Sr material into their otoliths. In this instance, there would be an insufficient signal for otolith microanalysis of Sr to detect. Despite these likely sources of error, we were still able to detect a dominant annular cycle in otolith Sr for mature age classes of males and females. Therefore, we believe that the otolith microchemistry analysis supports annual spawning for the majority of mature Chesapeake Bay striped bass.

Alternatively, spawning in striped bass may occur less than once a year. Less than an annual spawning, once thought to be specific to relatively few taxa (e.g.,

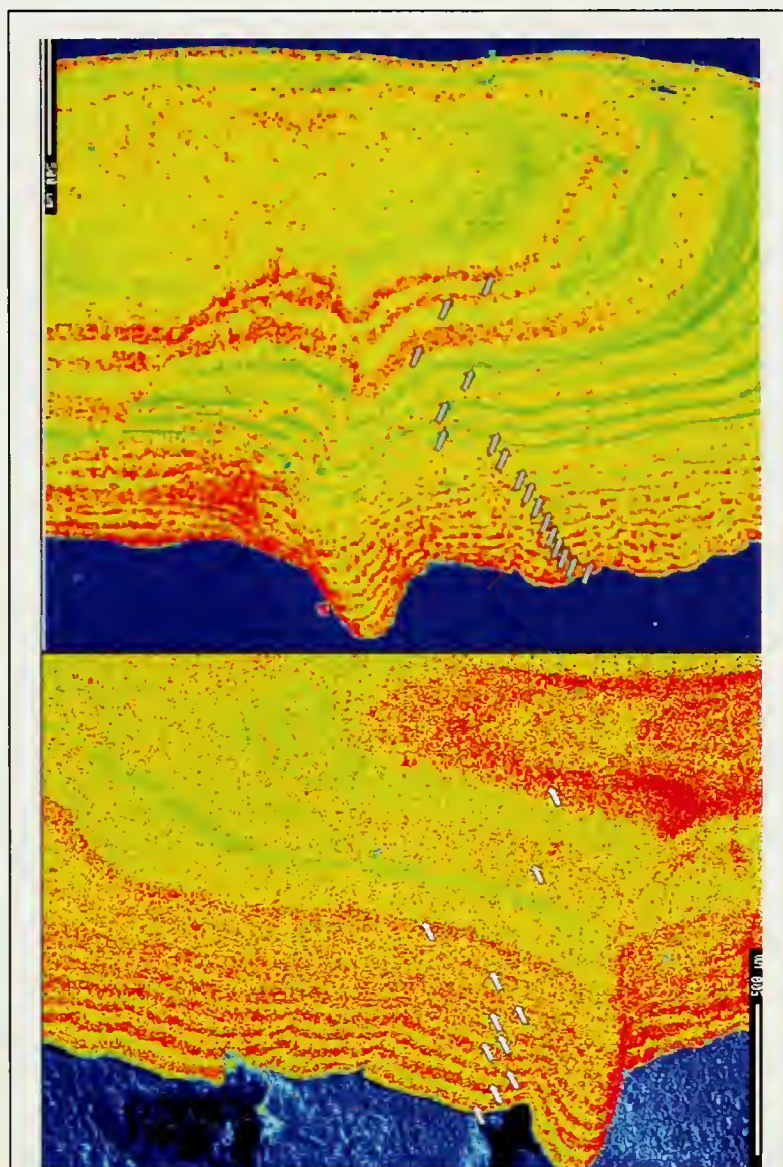


Figure 6

X-ray composition maps of strontium (Sr) seen in otolith for two female striped bass (*Morone saxatilis*) (17 and 11 years old) collected in Chesapeake Bay in 2000. Arrows demarcate annuli. The “warmer” colors (red, orange) represent regions with higher Sr concentrations whereas the “cooler” colors (yellow, green) represent regions with lower Sr concentrations. Composition maps show the coincidence of strontium banding patterns with banding patterns of annuli, indicative of annual anadromous migrations from high to low salinity waters.

sturgeons; Gross et al., 2002) could in fact be common in some longer-lived species (Rideout et al., 2005). For instance, data-archiving electronic tags inserted on Atlantic bluefin tuna (*Thunnus thynnus*) have definitively shown that many adults are found outside spawning habitats for an entire annual spawning season (Block et al., 2005). Further evidence is provided by the reproductive behavior of Atlantic cod (*Gadus morhua*;

Jørgensen et al., 2006), a species that does not always spawn each year because of density dependence or other environmental limits on its ability to provision gonads. Interestingly, evidence for this can be observed in two female life history transects in our study of striped bass (Fig. 4: ID=295, 300), where no nadir was observed at age seven following a clear nadir at age six (female striped bass typically mature between five and seven

years of age). We also should expect that, for similar energetic reasons, not every female, which undertakes a springtime up-estuary migration, will actually spawn. Some mature females in a spawning run will not spawn; rather, they will reabsorb final-stage oocytes (first author, personal observ.). Therefore, accurate measurement of spawning frequency depends on both the probability of successful spawning in the field and the frequency of up-estuary migratory runs.

X-ray maps confirmed an annual cycling in otolith strontium, but also showed cycles during the immature period of females, contrary to patterns observed from life history transects. Further, X-ray mapping and life history transects indicated that many yearlings move into oceanic regions—a pattern observed for Hudson River striped bass (Zlokovitz et al., 2003) but not yet described for Chesapeake Bay striped bass. The possibility that young-of-the-year or yearling striped bass are present in ocean environments deserves additional research in the Chesapeake Bay and elsewhere.

Contingent migration behavior

In past research on Hudson River striped bass, we observed modalities in lifetime migration behaviors (Secor et al., 2001); groups of individuals that share similar migration behaviors with some, but not all, members of their population are termed “contingents” (Hjort, 1914¹; Gilbert 1917²; Secor, 1999). In particular, one contingent comprising a small fraction of the Hudson River springtime sample was resident to freshwater and oligohaline regions and was heavily contaminated by polychlorinated biphenyls—an apparent consequence of this lifetime migration behavior (Zlokovitz and Secor, 1996; Ashley et al., 2000). A similar contingent migration behavior has been reported for the Stewiacke River population of striped bass in Nova Scotia (Morris et al., 2003). In contrast, only a single Chesapeake Bay striped bass (of 40 analyzed) exhibited freshwater resident behavior. Small sample sizes could indicate considerable error in estimates of the frequency of this behavior among populations if these estimates are based on research to date, but the fact that three distinct populations exhibited this behavior in our study indicates that contingent migration structuring is common to Chesapeake Bay striped bass.

Contingent migration structure has been observed across diverse taxa, such as American eels (*Anguilla rostrata*), American shad (*Alosa sapidissima*), white perch (*Morone americana*), bluefish (*Pomatomus salta-*

trix), and Atlantic bluefin tuna (Secor, 1999, in press; Fromentin and Powers, 2005). Here, a nursery or foraging habitat associated with one contingent migration behavior may make a small contribution in a given year, but over a decade may contribute significantly to spawning stock biomass. Thus, over generation-long time scales, we should expect that minority lifetime migration behaviors can contribute significantly to sustained recruitment. Further research is needed to determine the proximate cause of contingent structure, but based upon research on the sympatric white perch, we advance the hypothesis that Chesapeake Bay striped bass contingent migration structuring results from divergent early growth rates and dispersal behaviors associated with early growth (Kraus and Secor, 2004b).

Acknowledgments

We acknowledge NOAA MARFIN (Marine Fisheries Initiative, Northeast Center) support for this research. S. McGuire assisted with otolith preparation and data analyses. Personnel at Maryland Department of Natural Resources, Horn Point Environmental Laboratory, and the U. S. Fish and Wildlife Service assisted in collection of striped bass. The electron probe microanalyzer was purchased, in part, by a grant from the National Science Foundation (EAR 98-1244).

Literature cited

- Ashley, J. T. F., D. H. Secor, E. Zlokovitz, J. E. Baker, and S. Q. Wales.
2000. Linking habitat use of Hudson River striped bass to accumulation of polychlorinated biphenyl congeners. *Environ. Sci. Technol.* 34:1023–1029.
- Block, B. A., L. L. H. Teo, A. Walli, A. Boustany, M. J. W. Sokesbury, C. J. Farwell, K. C. Weng, H. Dewar, and T. D. Williams.
2005. Electronic tagging and population structure of Atlantic bluefin tuna. *Nature* 434:1121–1127.
- Chambers, R. C., and T. J. Miller.
1995. Evaluating fish growth by means of otolith increment analysis: Special properties of individual-level longitudinal data. *In* Recent developments in fish otolith research (D. H. Secor, S. E. Campana, and J. M. Dean, eds.), p. 155–175. Belle W. Baruch Library in Marine Sciences Number 19. Univ. South Carolina Press, Columbia, SC.
- Dorazio, R. M., K. A. Hattala, C. B. McCollough, and J. E. Skjveland.
1994. Tag recovery estimates of migration of striped bass from spawning areas of the Chesapeake Bay. *Trans. Am. Fish. Soc.* 123:950–963.
- Fromentin, J. M., and P. E. Powers.
2005. Atlantic bluefin tuna: population dynamics, ecology, fisheries, and management. *Fish and Fisheries* 6:281–306.
- Goodyear, C. P.
1984. Analysis of potential yield per recruit for striped
- ¹ Hjort, J. 1914. Fluctuations in the great fisheries of northern Europe. *Rapports Conseil Permanent International Pour L'exploration de la Mer*, 20:1–228. Library, Chesapeake Biological Laboratory, P.O. Box 38, Solomons, MD 20688.
- ² Gilbert, C. H. 1917. Contributions to the life-history of the sockeye salmon. Paper No. 4, report to the Commissioner of Fisheries. British Columbia Fisheries Department, 48 p. + plates. Library, Pacific Biological Station, Fisheries and Oceans Canada, 3190 Hammond Bay Road, Nanaimo, V9R 5K6 British Columbia, Canada.

- bass produced in Chesapeake Bay. *N. Am. J. Fish. Manage.* 4:488–496.
- Gross, M. R., J. Repka, C. T. Robertson, D. H. Secor, and W. Van Winkle.
2002. Sturgeon conservation: insights from elasticity analysis. *Am. Fish. Soc. Symp.* 28:3–10.
- Hagy, J. D., W. R. Boynton, C. W. Wood, and K. V. Wood.
2004. Hypoxia in Chesapeake Bay, 1950–2001: long-term changes in relation to nutrient loading and river flow. *Estuaries* 27:634–658.
- Ingram, B. L., and D. Sloan.
1992. Strontium isotopic composition of estuarine sediments as paleosalinity-paleoclimate indicator. *Science*. 255:68–72.
- Jorgensen, C., B. Ernande, O. Fiksen, and U. Dieckmann.
2006. The logic of skipped spawning in fish. *Can. J. Fish. Aquat. Sci.* 63:200–211.
- Kalish, J. M.
1990. Use of otolith microchemistry to distinguish progeny of sympatric anadromous and non-anadromous salmonids. *Fish. Bull.* 88:657–666.
- Kohlenstein, L. C.
1981. On the proportion of the Chesapeake stock of striped bass that migrates into the coastal fishery. *Trans. Am. Fish. Soc.* 110:168–179.
- Kraus, R. T., and D. H. Secor.
2004a. Partitioning of strontium in otoliths of estuarine fishes: experimentation in a model system, white perch *Morone americana* (Gmelin). *J. Exp. Mar. Biol. Ecol.* 302:85–106.
2004b. The dynamics of white perch (*Morone americana* Gmelin) population contingents in the Patuxent River Estuary, Maryland USA. *Mar. Ecol. Prog. Ser.* 279:247–259.
- Mansueti, R. J.
1961. Age, growth, and movements of the striped bass, *Roccus saxatilis*, taken in size selective fishing gear in Maryland. *Chesapeake Sci.* 2:9–36.
- Marshall, C. T., L. O'Brien, J. Tomkiewicz, G. Marteinsdóttir, M. J. Morgan, F. Saborido-Rey, F. Köster, J. L. Blanchard, D. H. Secor, G. Kraus, P. Wright, N. V. Mukhina, and H. Björnsson.
2003. Developing alternative indices of reproductive potential for use in fisheries management: Case studies for stocks spanning an information gradient. *J. Northw. Atl. Fish. Sci.* 33:161–190.
- Massman, W. H., and A. L. Pacheco.
1961. Movements of striped bass tagged in Virginia waters of Chesapeake Bay. *Chesapeake Sci.* 2:37–44.
- Merriman, D.
1941. Studies of the striped bass (*Roccus saxatilis*) of the Atlantic coast. *USFWS Fish. Bull.* 50:1–77.
- Morris, J. A., R. A. Rulifson, and L. H. Toburen.
2003. Life history strategies of striped bass, *Morone saxatilis*, populations inferred from otolith microchemistry. *Fish. Res.* 62:53–63.
- Rideout, R. M., G. A. Rose, and M. P. M. Burton.
2005. Skipped spawning in female iteroparous fishes. *Fish and Fisheries* 6:50–72.
- Secor, D. H.
1992. Application of otolith microchemistry analysis to investigate anadromy in Chesapeake Bay striped bass. *Fish. Bull.* 90:798–806
1999. Specifying divergent migration patterns in the concept of stock: the contingent hypothesis. *Fish. Res.* 43: 13–34.
2000a. Longevity and resilience of Chesapeake Bay striped bass. *ICES J. Mar. Sci.* 57:808–815.
2000b. Spawning in the nick of time? Effect of adult demographics on spawning behavior and recruitment of Chesapeake Bay striped bass. *ICES J. Mar. Sci.* 57:403–411.
2002. Estuarine dependency and life history evolution in temperate sea basses. *Fish. Sci.* 68(suppl. 1): 178–181.
In press. The year-class phenomenon and the storage effect in marine fishes. *J. Sea Res.*
- Secor, D. H., J. M. Dean, and E. H. Laban.
1992. Otolith removal and preparation for microstructural examination. Chapter 3 in *Otolith microstructure examination and analysis* (D. Stephenson and S. Campana, eds.), p. 17–59. Special Publication, *Can. J. Fish. Aquat. Sci.* 117.
- Secor, D. H., A. Henderson-Arzapalo, and P. M. Piccoli.
1995a. Can otolith microchemistry chart patterns of migration and habitat utilization in anadromous fishes? *J. Exp. Mar. Biol. Ecol.* 192:15–33.
- Secor, D. H., and P. M. Piccoli.
1996. Age- and sex-dependent migrations of the Hudson River striped bass population determined from otolith microanalysis. *Estuaries* 19:778–793.
- Secor, D. H., J. R. Rooker, E. Zlokovitz, and V. S. Zdanowicz.
2001. Identification of riverine, estuarine, and coastal contingents of Hudson River striped bass based upon otolith elemental fingerprints. *Mar. Ecol. Prog. Ser.* 211:245–253
- Secor, D. H., T. M. Trice, and H. T. Hornick.
1995b. Validation of otolith-based ageing and a comparison of otolith and scale-based ageing in mark-recaptured Chesapeake Bay striped bass, *Morone saxatilis*. *Fish. Bull.* 93:186–190.
- Sokol, R. R., and F. J. Rohlf.
1981. *Biometry*, 2nd ed., 859 p. W. H. Freeman and Co., New York, NY.
- Vladykov, V. D., and D. H. Wallace.
1952. Studies of the striped bass, *Roccus saxatilis* (Walbaum), with special reference to the Chesapeake Bay region during 1936–1938. *Bull. Bingham Oceanogr. Coll.* 14:132–177.
- Warner R. R., and P. L. Chesson.
1995. Coexistence mediated by recruitment fluctuations—a field guide to the storage effect. *Am. Naturalist* 125:769–787.
- Wirgin, I., L. Maceda, J. R. Waldman, and R. N. Crittenden.
1993. Use of mitochondrial DNA polymorphisms to estimate the relative contributions of the Hudson River and Chesapeake Bay striped bass to the mixed fishery on the Atlantic Coast. *Trans. Am. Fish. Soc.* 122: 669–684.
- Zlokovitz, E. R., and D. H. Secor.
1999. Effect of habitat use on PCB body burden in Hudson River striped bass (*Morone saxatilis*). *Can. J. Fish. Aquat. Sci.* 56 (suppl.1):86–93.
- Zlokovitz, E. R., D. H. Secor, and P. M. Piccoli.
2003. Patterns of migration in Hudson River striped bass as determined by otolith microchemistry. *Fish. Res.* 63:245–259.

Abstract—From 2001 to 2004 in the eastern Aleutian Islands, Alaska, killer whales (*Orcinus orca*) were encountered 250 times during 421 days of surveys that covered a total of 22,491 miles. Three killer whale groups (resident, transient, and offshore) were identified acoustically and genetically. Resident killer whales were found 12 times more frequently than transient killer whales, and offshore killer whales were encountered only once. A minimum of 901 photographically identified resident whales used the region during our study. A total of 165 mammal-eating transient killer whales were identified, and the majority (70%) were encountered during spring (May and June). The diet of transient killer whales in spring was primarily gray whales (*Eschrichtius robustus*), and in summer primarily northern fur seals (*Callorhinus ursinus*). Steller sea lions (*Eumetopias jubatus*) did not appear to be a preferred prey or major prey item during spring and summer. The majority of killer whales in the eastern Aleutian Islands are the resident ecotype, which does not consume marine mammals.

Ecotypic variation and predatory behavior among killer whales (*Orcinus orca*) off the eastern Aleutian Islands, Alaska

Craig O. Matkin (contact author)¹

Lance G. Barrett-Lennard²

Harald Yurk²

David Ellifrit³

Andrew W. Trites⁴

Email address for C. O. Matkin: cmatkin@acsalaska.net

¹ North Gulf Oceanic Society
3430 Main St. B1
Homer, Alaska 99603

² Vancouver Aquarium Marine Science Center
University of British Columbia
845 Avison Way
Vancouver, B.C., Canada V6G 3E2

³ Center for Whale Research
355 Smugglers Cove
Friday Harbor, Washington 98250

⁴ Marine Mammal Research Unit, Fisheries Centre
University of British Columbia
Vancouver, B.C., Canada V6T 1Z4

In 1992, flipper tags from fourteen Steller sea lions (*Eumetopias jubatus*) were found in the stomach of a killer whale (*Orcinus orca*) that had died in Prince William Sound (Heise et al., 2003). This discovery prompted considerable interest and speculation about the role that killer whales may have played in the decline and lack of recovery of Steller sea lions in western Alaska (Barrett-Lennard et al., 1995). Since the late 1970s, Steller sea lions in the Gulf of Alaska and Aleutian Islands have declined by over 80% (Merrick et al., 1987; Trites and Larkin, 1996; Loughlin and York, 2000; Winship and Trites, 2006). Similar sharp declines have also occurred among some populations of harbor seals (*Phoca vitulina*), northern fur seals (*Callorhinus ursinus*), and sea otters (*Enhydra lutris*) (York, 1987; Pitcher, 1990; Trites, 1992; Estes et al., 1998). Whether or not these declines are related to killer whales is currently the subject of considerable scientific debate (Springer et al., 2003; Trites et al.,

2006; DeMaster et al., 2006; Mizroch and Rice, 2006).

Most knowledge about killer whales in the North Pacific has been gathered between California and the northern Gulf of Alaska, where three distinct lineages of killer whales have been identified: fish-eating “resident” killer whales, which appear predictably in large groups from Washington to Alaska; marine mammal-eating “transient” killer whales, which appear infrequently and in smaller groups; and “offshore” killer whales, whose feeding habits are poorly known, but are thought to eat fish, including sharks (Matkin et al., 1999a; Barrett-Lennard, 2000; Ford et al., 2000; Saulitis et al., 2000). These groups are genetically and behaviorally distinct, but have overlapping geographic ranges and are considered as ecotypes because of their differences in diet. However, prior to our study, it was not known whether these lineage and ecotype distinctions extended to the northwestern Gulf of Alaska and the

Aleutian archipelago, nor was much known about the extent to which killer whales prey on Steller sea lions and other species of marine mammals in these regions.

The goals of our study were 1) to determine whether the eastern Aleutian Islands are also home to the three lineages and ecotypes of killer whales that have been identified elsewhere in the northeastern Pacific; 2) to derive estimates of killer whale numbers for this region; and 3) to document the behaviour of killer whales foraging on marine mammals. Obtaining such information about killer whale numbers, diets, and hunting behavior is critical for resolving the role that killer whales may have played in the decline and lack of recovery of Steller sea lions and other species of marine mammals in western Alaska.

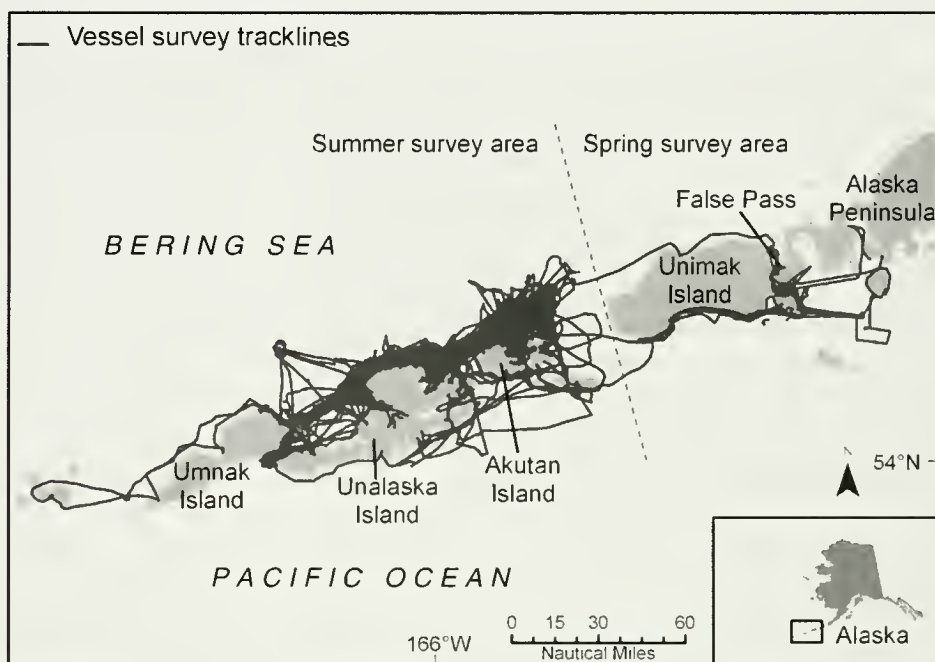


Figure 1

Tracks of the vessels during the surveys for killer whales (*Orcinus orca*) for the years 2001–2004. The vessels tended to return to areas that produced encounters with killer whales. The spring False Pass–Unimak Island surveys are distinguished from the summer Unimak Pass–Umnak Island surveys by the dashed line.

Materials and methods

Following the research method used to collect information on killer whales in other regions (Matkin et al., 1999a; Ford et al., 2000), five types of data were gathered: photo-identification pictures of individuals and groups, acoustic recordings of killer whale calls, skin tissue samples for genetic analysis, prey samples, and accounts of predation. Additionally, we documented the presence of potential marine mammal prey. Analysis of these data allowed the determination of killer whale ecotypes and a description of killer whale feeding habits.

Field methods

Boat-based surveys over a wide geographic range occurred during June–September 2002–2004 from Unimak Pass to Samalga Pass, and surveys over a relatively small range occurred in May and early June 2003–2004 in the False Pass–Unimak Island region. Surveys in the broader region traversed 19,686 nautical miles and were focused in the Bering Sea within twenty miles of the shoreline between Unimak Pass and eastern Umnak Island (Fig. 1). The 2003–2004 False Pass–Unimak surveys traversed 1970 miles in Ikatan Bay and along the Pacific shore of Unimak Island. We operated in areas of suspected high killer whale density according to information provided by local fishermen and researchers from the National Marine Mammal Laboratory (NMML) (Dahlheim, 1997) during previous transect

surveys that covered broader regions. We modified our surveys each season to cover the areas that were most productive in providing killer whale encounters.

The research was conducted from aluminum-hull fishing vessels (powered by diesel inboard engines) ranging from 10 to 14 meters in length. Survey effort varied by year with a total of 372 days from 2001 to 2003 from the Unimak Pass to Samalga Pass in summer and a total of 49 survey days in 2003 and 2004 in the False Pass–Unimak Island region in spring (Table 1). All sightings of marine mammals during vessel surveys were recorded and the number of individuals was estimated to determine the relative abundance of potential prey items.

Photographs of the left side of dorsal fins and saddle patches of killer whales were taken with a Nikon F-100 camera (B and H Photo, New York, NY) equipped with either fixed 300-mm lenses or 100–300 zoom lenses and loaded with Fuji Neopan ASA1600 black and white film (B and H Photo New York, NY). These photographs were checked against existing photo-catalogues of Alaskan killer whales (Dahlheim, 1997; Matkin et al., 1999a) and other unpublished photographs. Tissue samples of at least one whale in each group were collected for genetic analysis and biopsy when weather and behavior of the whales permitted close approach. These samples were collected by using lightweight darts and an air-powered rifle (Barrett-Lennard et al., 1996). The outer skin portion of the samples was used for genetic analysis, and the underlying blubber portion was used for

Table 1

Survey effort (in days) and number of encounters with resident and transient killer whales (*Orcinus orca*) in the eastern Aleutians (2001–2004). "Survey days" are the days spent looking for whales; "Miles" are given in nautical miles.

Year	Dates	False Pass–Unimak Island region (single vessel 2003–2004)				Eastern Aleutians (Single vessel 2001, two vessels 2002–04)				
		Survey days	Miles	Encounters		Survey days	Miles	Encounters		
				Resident	Transient			Resident	Transient	
2001		—	—			19 Jun– 18 Aug	16	835	13	1
2002		—	—	—		17 Jun– 24 Aug	188	6599	57	4
2003	16 May– 3 Jun	18	642	0	13	10 Jun– 31 Aug	108	6321	49	4
2004	4 May– 3 Jun	31	1328	0	32	7 Jun– 9 Sep	130	6766	70	7
Total		49	1970	0	45		372	20,521	189	16

contaminant analysis, lipid and fatty acid, and stable isotope analysis (see Herman et al., 2005). Genetic analysis involved sequencing the entire mitochondrial control region (see Barrett-Lennard [2000] for details). Acoustic recordings were made when whales were vocalizing and ambient noise levels permitted using an Offshore Acoustics™ (Offshore Acoustics, Nanaimo, British Columbia) hydrophone with a built-in preamplifier and a Sony WM-D6C (B and H Photo, New York, NY) cassette recorder. This system had a frequency response of 10 Hz to 8 KHz (± 3 dB).

Single, continuous observation periods with killer whales were termed encounters. During these vessel-based observation periods, the location of the killer whales was plotted at approximately 5-min intervals by using a global positioning system (GPS) linked to a computer with Nobletec™ (Nobletec, Beaverton, OR) navigational software. Time spent in different behavioral states (e.g., feeding, socializing, resting, traveling) was recorded on data sheets. Whales were observed continuously during encounters, and any signs of possible predation were recorded. During behavioral observations, marine mammal kills were confirmed only when marine mammal parts were observed in the mouths of the whales, or when bits of blubber, skin, or viscera, hair were collected, or blood or oil was observed on the surface of the water. Predation on fish was confirmed by observations of fish in the mouths of whales or by collecting and inspecting floating parts. To document the potential marine mammal prey in the region during the period of the study, we recorded the time, location, and number of all marine mammals sighted.

Analytical methods

Photo-identification All photographic negatives were examined over a light table with an 8.0 power Peak™ (B

and H Photo, New York, NY) magnification loop. Identifiable individuals were recorded and assigned a unique alphanumeric name in order to be tracked throughout the study. Whales that could not be positively re-identified were not assigned a name. From this photographic database, the actual number and identity of individual killer whales and groups of whales present for each encounter were determined. Because some of the photographs were of poor quality, these photographs were rejected from further analyses; thus not all the whales encountered were identifiable.

Acoustics We inspected acoustic recordings for the presence of discrete calls by listening to tapes and monitoring real-time spectrograms using Cool Edit 2000™ (Syntrillicum Software Corp., Phoenix, AZ) sound manipulation software. Calls were analyzed following the protocol of Ford (1991) and Yurk (2005). Killer whales produce a variety of different types of vocalizations that can be described as clicks, whistles, and calls (Ford, 1989). Calls are the most common type of vocalization, occurring in over 90% of all encounters with vocalizing killer whales. These pulsed vocalizations occur as either signals of a frequently repeated acoustic pattern or as signals of variable acoustic pattern (Ford, 1991). Discrete calls were chosen for this analysis because they retain their recognizable acoustic structure for many years and likely for many generations (Yurk, 2005). Recognized calls were digitized at a 44.1-kHz sampling rate with a 16-bit sample size and further analysed spectrographically using Canary 1.2.4 sound analysis software (Cornell Laboratory of Ornithology, Ithaca, NY). The spectrographic analysis was done by using fast-Fourier transformations (FFT) of time series of the recorded sound pressure waves with sizes of 1024 points for each analyzed time series. The FFT identifies the composing sine waves in sound pressure waves of

acoustic signals and allows spectrographic representations of the sound frequency versus time and pressure. Spectrograms were produced with an 87.5% overlap of the analyzed time series. Resulting spectrograms had a time resolution of 2.9 milliseconds and a frequency resolution of 43 Hz.

We categorized calls by ear and by visual inspection of distinct upper and lower frequency components of the sound spectrum (UFC and LFC, respectively), as described by Miller and Bain (2000) and Yurk et al. (2002). When categorizing the calls as distinct, particular attention was given to 1) the existence and contour shapes of UFCs; 2) LFC contour shapes; 3) LFC segmentation (elements separated by silent intervals); and 4) the component structure (elements within the LFC arising from abrupt shifts in contour and not separated by silent intervals) of the LFCs (Ford, 1991; Yurk, 2005).

The three known ecotypes of killer whales inhabiting waters off British Columbia and southern Alaska (resident, transient, and offshore) are acoustically distinguishable by 1) vocalization rate; 2) the occurrence of different discrete calls; 3) the syllables used in calls; and 4) the production rate and characteristics of echolocation clicks. Transient killer whales, which appear to rely on passive listening to catch their marine mammal prey, vocalize less frequently than resident killer whales (Deecke et al., 2005). Transients rarely use echolocation clicks, in contrast to resident and offshore killer whales (Deecke et al., 2005). All calls of transient killer whales are distinct from the calls of resident whales by 1) an audible quavering of the fundamental sound frequencies (instead of a crisp appearance of these sound frequencies that is typical of calls from resident killer whales), and 2) a distinctively lower amount of different call syllables and a distinct order of these syllables compared to those in calls of resident killer whales (Yurk, 2005). Transient and resident killer whales are distinguishable from offshore killer whales by their use of unique call types (Yurk, 2005). We determined whether the encountered whales fell into discrete acoustic groups and, if so, whether those acoustic groups were similar to any of the acoustic groups observed in British Columbia and southern Alaska. Analysis was completed by Yurk (2005), independent of knowledge of genetic differences and social associations among groups. Call rates were estimated from field estimates of killer whale group sizes for each encounter.

Genetics DNA was extracted from the skin portion of the biopsies using proteinase K digestion, phenol and chloroform purification, and ethanol precipitation using standard procedures (Sambrook et al., 1989)

We obtained mtDNA sequences using the following procedure: 1) the entire D-loop region was PCR-amplified by using custom-designed primers that annealed to the flanking tRNA-Thr and 12s-rRNA regions (Barrett-Lennard, 2000); 2) the PCR product was purified with QIAQuick® spin columns (Qiagen, Valencia, CA) following protocols supplied by Qiagen, Ltd. (Valencia, CA); 3)

a sequencing reaction was performed with Fs-Taq® (Applied Biosystems, Foster City, CA) system reagents and protocols supplied by Applied Biosystems, Ltd. (Foster City, CA); and 4) the sequence was resolved on an Applied Biosystems 377 (Applied Biosystems, Foster City, CA) automated DNA sequencer. Because the sequence was too long (950 bases) to be entirely resolved in one direction, sequencing reactions were run from each end of the amplified fragment. We visually checked the output graphs from the automated sequencer and corrected the computer-generated sequences accordingly. We also used the approximately 400-base overlap in the sequences of opposite directions to check for errors. As a final check of accuracy, we overlaid each output graph with a reference graph on a transparent sheet, and scanned the two graphs for differences. We then aligned unique sequences using the program CLUSTAL-W (European Bioinformatics, Cambridge, UK) (Thompson et al., 1994).

Results

Summary of survey effort and encounters with killer whales

On 250 occasions, groups of one or more killer whales were encountered during the surveys that covered a total of 22,491 miles in 421 days in the eastern Aleutians and False Pass–Unimak Island area (Table 1). The majority of survey effort and encounters occurred west of Unimak Pass during summer; surveys in False Pass–Unimak Island area were not initiated until 2003. From approximately half of our encounters with groups of killer whales in both regions, we obtained genetic samples or acoustic recordings (Table 1). Killer whales of the offshore ecotype were encountered only once (in 2003) and both acoustic and genetic samples were obtained during this encounter.

Use of acoustic data, genetic analysis, and group association to infer lineage

Genetic and acoustic analyses revealed the presence of three killer whale populations. As described in more detail below, one population clustered genetically and acoustically with resident killer whales ranging from Puget Sound, Washington to Kenai Fjords, Alaska, and a second population clustered with transient killer whales from the same general area. Accordingly, those two groups were provisionally classified as a resident killer whale group and a transient killer whale group, respectively. The third population clustered genetically with offshore killer whales sampled off British Columbia, and were provisionally classified as an offshore killer whale group. Acoustic comparison was not possible in the case of offshore killer whales because of a scarcity of recordings.

Resident, transient, and offshore killer whales have never been observed interacting socially in the ar-

areas where they were previously identified and studied (Puget Sound to Kenai Fjords), and no interaction was observed in our study between the genetically or acoustically distinguished groups. Therefore, it was possible to infer the population status from the group-association patterns of individuals for which there was no genetic or acoustic data. Animals observed in association with whales of known genetic or acoustic type were assumed to be of that same type. We did not use diet as a criterion for classification to avoid circular reasoning (evidence of dietary differences between populations becomes tautological if diet is used to define populations).

Acoustic analysis During 31 of 39 encounters in which we recorded killer whale vocalizations and did not collect genetic samples, the use of distinct calls, use of echolocation clicks, and the call rate were consistent with attributes of resident killer whale vocalizations from other regions of the Northeast Pacific (Table 2) (Yurk, 2005). All encounters had average call rates of three calls or more per minute, and strings of echolocation clicks were abundant across encounters. During these encounters, 23 structurally distinct calls were identified. Seven calls showed no obvious similarities to calls recorded elsewhere in the northeast Pacific and 15 had structural similarities, sharing some call components with calls used by killer whales that regularly occur in the northern Gulf of Alaska. However, no call from these encounters was identical to any call of the known killer whale call repertoires.

The resident-type killer whales encountered in western Alaska possibly belong to groups that are distinct from the groups of resident killer whales in other regions of Alaska because no call syllables or call patterns (sequence of syllables) between groups were found to match. Resident killer whales learn their distinct call structures in their maternal group, in which they remain for life, and call structures remain stable and group-specific for more than one generation (Ford, 1991; Yurk et al., 2002). However, because we do not know the complete call repertoires of killer whales in western

Alaska we cannot be sure that we will not find complete call-type matches in the future.

In eight killer whale encounters that did not yield genetic samples (five from False Pass and three from other areas in the eastern Aleutians), vocal activity or average call rate was considerably lower than the three calls per minute that are typical for residents, and was closer to one or less than one call per minute, which is typical for transient killer whales from other areas of the northeast Pacific (Deecke et al., 2005; Saulitis et al., 2005). Furthermore, all recorded calls showed typical characteristics of transient type calls, such as the quavering of the fundamental sound frequencies and the lower number of call syllables compared to those in calls from resident killer whales.

The three encounters that were not from the False Pass region (Table 2) contained three distinct calls that were structurally similar but did not show identical order of syllables or identical syntax to calls used by members of the AT1 transient community. The AT1 transient community is thought to be limited to the Prince William Sound and Kenai Fjords region and to use a distinct call repertoire (Saulitis et al., 2005).

In the recordings made during five encounters in the False Pass region in 2003 and 2004 (Table 2), 14 distinct calls were identified in more than one of the recording sessions. Thirteen of these 14 distinct calls were identified from recordings made during two encounters in 2003. Ten of these 13 calls were also recorded during 3 encounters with killer whales in May 2004 in the same area. Thus, although the majority of calls recorded in 2004 were already identified in 2003, one new distinct call was found. This high number of same distinct-type calls is typical for transient killer whales (Deecke, 2003). Call repertoires of resident killer whales are generally much larger, and this larger repertoire is likely responsible for the detection of several new calls from newly encountered whales in recordings from consecutive years (Ford, 1991; Yurk, 2005). All call types recorded in the False Pass region appeared to be distinct from calls recorded from transient killer whales in other regions of the North Pacific. However, some structural similarity (in the form of matching call components) was found for some of the 14 calls recorded in our study and for the calls recorded from a transient community that inhabits waters along the west coast of North America. These results may indicate that the transient killer whales we encountered in the eastern Aleutians comprise one or more unique populations or communities that show some acoustic similarity with transient killer whales found in other regions of the Pacific.

Genetic analysis A total of 93 skin samples were collected from 2001 through 2004 by using biopsy darting techniques. Separation of ecotypes based on mtDNA haplotype (Barrett-Lennard, 2000) showed that 47 of the 93 samples were of transient-type lineage, 42 were of the resident-type lineage, and 4 were of the offshore-type lineage. Preliminary classifications of lineages based

Table 2

Location and number of encounters that produced recordings of killer whales (*Orcinus orca*) used in our acoustic analyses from 2001 through 2004 in the Eastern Aleutians and False Pass, Alaska.

Year	Location	Number of encounters
2001	Unalaska	3
2002	Unalaska, Akutan Island, Umnak Island	31
2003	False Pass	2
2004	False Pass	3
Total		39

on morphology and behavior and determined from field observations and photographs were consistent with the genetic analysis. For the 26 encounters that yielded both genetic and acoustic data, the two kinds of data provided identical classifications of lineage.

All 35 killer whales sampled in the False Pass–Unimak Island region had transient haplotypes. Eight of the nine samples collected in the area in 2003 had the GAT1 haplotype, which was first identified in transient killer whales from the northern Gulf of Alaska area in or near Kenai Fjords and Prince William Sound. The remaining sample contained the AT1 haplotype, formerly sequenced only in members of the AT1 transient population of the Prince William Sound area. In 2004, 14 of 26 killer whales sampled in the False Pass–Unimak Island area had the GAT1 haplotype, and the remainder had a GAT2 haplotype, a similar but not identical haplotype known to exist at a low frequency in the Gulf of Alaska transient killer whale population (Barrett-Lennard, 2000). Eleven of the 12 transient whales sampled in the summer months during 2001–2004 in the eastern Aleutians had the GAT1 haplotype, and the remaining one had the GAT2 haplotype.

Ecotypic parameters

Resident killer whales During a majority of our encounters, resident killer whales tended to be found and to travel along or near the 200-meter depth contour (Fig. 2A). This contour corresponds to a steep drop-off from the coastal shelf.

Approximately 92% of the encounters with killer whales during our summer surveys from Unimak Pass to Umnak Island were with whales determined by genetics, acoustics, or group association to be of the resident ecotype; however, this ecotype was not encountered in the spring surveys east of Unimak Pass (Table 1). A minimum of 901 resident whales used the Eastern Aleutians during the study; this count was based on individuals identified from photographs taken from 2001 through 2004. Of these individuals, 143 were seen only once during the study, and the remainder were repeatedly identified. The number of new, previously un-photographed whales observed each year declined from 534 whales in 2002 to 211 whales in 2003, to 156 whales in 2004 (Table 3). The decline in new whale sightings each year may indicate that we have identified the majority of whales that use this area during the summer months; however, there may be hundreds of whales that occasionally use the area but have not been encountered. The study area is likely only a portion of the range of the identified resident whales; several whales were matched with individuals seen in photographs taken in the Pribilof Islands over 200 miles to the west.

The numbers of individuals that could be positively identified in each resident ecotype encounter ranged from 4 to 109. A total of 347 whales were placed in 82 tentative matrilineal groups which consisted of a reproductive female and her offspring of both sexes. These matrilineal

Table 3

Number of sightings of individual resident killer whales (*Orcinus orca*) in the eastern Aleutians from June to September, 2001 through 2004.

Year	Previously identified whales	New whales identified	Total whales identified
2001	0	38	38
2002	38	496	534
2003	268	211	479
2004	334	156	490
Total		901	

were determined from repeated association of individuals in both photographs and field observations. This method of determining matrilineal groups was demonstrated effective in other population studies of resident killer whales (Bigg et al., 1990; Matkin et al., 1999b). Most of the matrilineal groups comprised two generations (mother and offspring), although some included a probable grandmother. All matrilineal groups were of consistent composition and maintained their structure over the course of the study, which has been the case in all other resident populations studied to date (Matkin et al., 1999a; Ford et al., 2000). The structure of the population was inferred from 41 groups of one or more matrilineal groups that appeared to be longer-term associations. These groups could be considered as tentative pods (as defined by Bigg et al., 1990). Twenty-one of these groups, containing 266 whales, were sighted frequently enough that basic age and sex classes could be determined. These groups contained 65 adult males (24.4%), 105 females or immature males (39.5%), and 96 juveniles and calves (36.1%). These proportions of males, females and immature males, and juveniles and calves are comparable to those observed in other resident populations in Alaska and British Columbia (Leatherwood et al., 1990).

There was no evidence that resident killer whales consumed marine mammals. Whales belonging to the resident ecotype were observed consuming fish only during infrequent observations of predation (halibut were identified from samples, and salmon were probable from visual observations only). Much of the predation by resident killer whales was not visible at the surface and therefore prey samples could not be obtained. Resident whales were the only killer whales observed removing fish from the lines of commercial fishermen and observed following and feeding on fish discards from trawlers.

Transient killer whales A total of 165 individual killer whales were determined to be transients from encounters during 2001–2004 (Table 4). A majority of these whales (114) were photographed during the May–June field work in the False Pass–Unimak Island region in

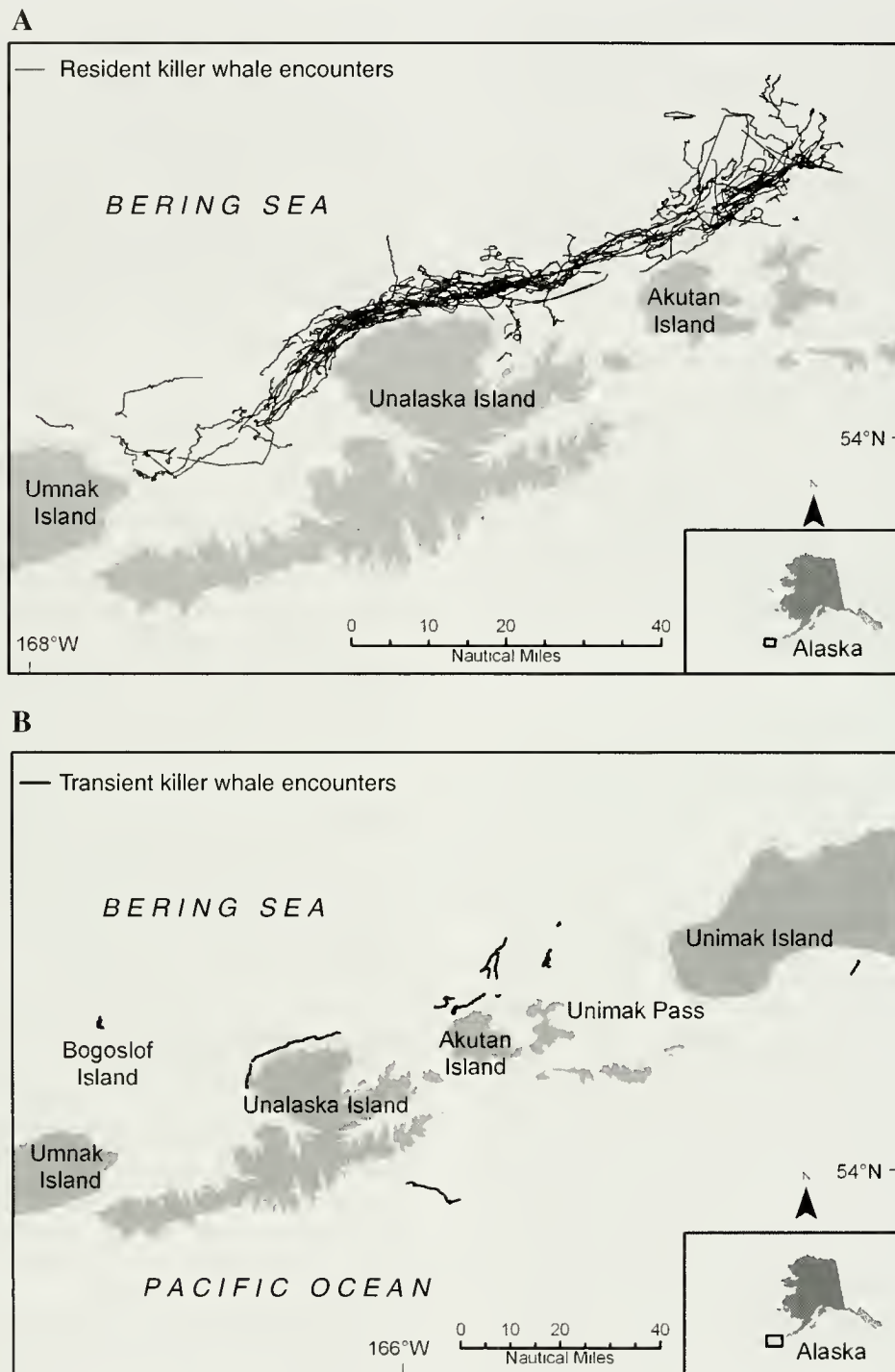


Figure 2

Tracks of the vessels during times that the vessels accompanied groups of killer whales (*Orcinus orca*) 2002–2004. (A) tracks of vessels following resident killer whales in the Eastern Aleutians during summer; (B) tracks of vessels following transient killer whales in the Eastern Aleutians during summer; (C) tracks of transient killer whales near False Pass–Unimak Island during spring.

2003 and 2004 (Fig. 2B). The remaining 51 individuals were photographed during the summer field season when encounters with transient killer whales were relatively

infrequent in the eastern Aleutians from Unimak Pass west to Umnak Island (Fig. 2C). There were only six transient whales (less than 4% of the total identified)

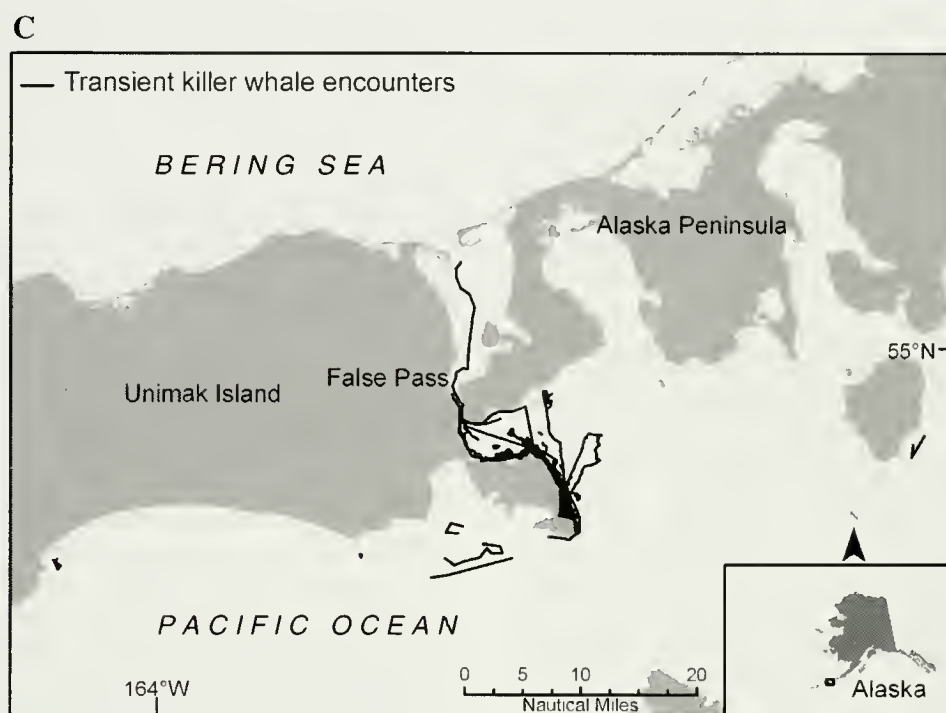


Figure 2 (continued)

Table 4

Number of individual transient killer whales (*Orcinus orca*) identified by region and by year. And the overlap of individuals between regions.

Year	Regions				Overlap of individuals between regions
	False Pass (May–June)		Eastern Aleutians (July–September)		
	Total whales	New whales	Total whales	New whales	
2001	—	—	5	5	—
2002	—	—	18	18	—
2003	84	84	25	18	2
2004	75	30	22	16	4
Total		114		51	6

that were common to both regions and time periods, although the regions are geographically adjacent (Figs. 1 and 2). In the second year, 2004, in False Pass–Unimak Island, 74 whales were identified and 45 (60%) had been photographed the previous year. In the Unimak Pass–Unimak Island surveys in both 2003 and 2004, only about 28% of the whales identified had been previously photographed in the region.

Offshore killer whales Only one encounter, which occurred in the eastern Aleutians (10 July 2003), was with killer whales identified by genetic and acoustic data as the offshore ecotype. We photographed 54 offshore killer whales in this encounter, although not all whales

present were photographed. A total of 44 of these offshore whales had been previously photographed off British Columbia, Washington State, and Kenai Fjords, Alaska, and 10 had not been previously photographed (Ellis¹).

Description of the marine mammal prey base

Although we did not measure the actual abundance of potential marine mammal prey, we recorded sightings of all marine mammals and calculated average group

¹ Ellis, G. 2005. Unpubl. data. Fisheries and Oceans Canada, Pacific Biological Station, 3190 Hammond Bay Road, Nanaimo, British Columbia, Canada V9T 6A7.

Table 5

Number of sightings, harassments, and observed kills of known marine mammal prey species of killer whales (*Orcinus orca*).

Prey species	Prey species				
	Total no. of sightings	Average group size	No. of harassments	No. of observed kills	No. observed to have escaped
Gray whale (May–June only)	18 ¹	1.4	19	18	1
Dall's porpoise	521	3.9	3	0	3
Steller sea lion	153	53.4	1	1	0
Humpback whale	834	4.1	0	1	0
Northern fur seal	388	4.2	5	4	1
Minke whale	42	1.2	2	2	0
Harbor porpoise	18	4.9	0	0	0
Harbor seal	82	9.6	0	0	0
Sea otter	94	3.7	0	0	0
California sea lion	2	1.0	0	0	0
Fin whale	15	2.2	0	0	0
Sperm whale	7	1.6	0	0	0
Baird's beaked whale	10	9.4	0	0	0
Total			31	26	5

¹ This number comprises only live whales; most kills were already dead when observed and were not included in these sightings.

size as an indication of the relative availability of potential prey (Table 5). During the 346 survey days in the eastern Aleutians in June–September 2002–2004, the largest number of pinniped sightings was of northern fur seals (375 sightings), which were frequently encountered as single individuals resting at the surface, or were observed on the rookery at Bogoslof Island. Steller sea lions (124 sightings) were counted during our repeated monitoring of rookeries and haulouts in the region, resulting in a relatively large average group size (53.4 sea lions) but were encountered only occasionally off the rookeries. Other pinnipeds included harbor seals (73 sightings), which were primarily observed hauled out in small groups of less than 30 individuals, and two sightings of individual California sea lions (*Zalophus californianus*). Sea otters were observed on 81 occasions. The most frequently encountered cetacean was the humpback whale (*Megaptera novaeangliae*; 834 sightings), followed by Dall's porpoise (*Phocoenoides dalli*; 521 sightings). Less frequently observed species were minke whales (*Baleanoptera acutorostrata*; 42 sightings), fin whales (*Baleanoptera physalus*; 15 sightings), sperm whales (*Physeter macrocephalus*; 7 sightings), and Baird's beaked whales (*Berardius bairdii*; 10 sightings).

During 49 survey days in the False Pass–Unimak Island region in May and early June 2003–2004, Steller sea lions were the most frequently encountered pinniped (29 sightings), although some fur seals (13 sightings) and harbor seals (9 sightings) were also observed. Sea otters were also present (13 sightings). The most frequently encountered cetaceans were gray whales (18 sightings) and harbor porpoises (*Phocoena phocoena*;

18 sightings). Other cetaceans sighted in this region were minke whales (3 sightings) and humpback whales (1 sighting).

Predation on marine mammals

Predation on or harassment of marine mammals was observed on 31 occasions and was attributed solely to the transient killer whale ecotype. Attacks that did not yield proof of a kill (i.e., tissue, blood, or prey in the mouth) were considered harassments. Gray whales (*Eschrichtius robustus*) were the most frequently taken species (Table 5), with 19 apparent harassments, of which 18 resulted in kills, observed in False Pass in 2003 and 2004 (May to early June). In all but one case, the gray whale was already dead and was being consumed when we found the whale. The only other predatory event during this period was a single harassment of Steller sea lions that were hauled out. During the summer season in the eastern Aleutians (Unimak Pass–Unimak Island), northern fur seals were the most frequently harassed prey; four of the five observed harassments resulted in kills. Other species included Dall's porpoises (harassed on three different occasions), two minke whales (harassed and killed), one Steller sea lion (harassed and killed), and one humpback whale (harassed).

Discussion

Our analysis indicates that the three killer whale ecotypes in the eastern North Pacific also are found in the

eastern Aleutian Islands. All killer whales examined by acoustic or genetic analysis could be placed unequivocally in the resident, transient, or offshore lineage.

Resident killer whales

A vast majority of the whales observed in the eastern Aleutians during summer were determined to be of the resident ecotype. Our minimum estimate of 901 whales is as high as any density of resident killer whales in any region of the eastern North Pacific studied to date (Matkin et al., 1999a; Ford et al., 2000).

Our data indicate that the eastern Aleutian resident killer whales comprise a distinct population, but evidence is equivocal at this time. No repeated associations have been recorded between eastern Aleutian residents and those photographed off Kodiak Island north and eastward, despite extensive field effort and examination of photographic databases for matches. However, at least one group of resident killer whales has been photographed in both regions (Durban²). Acoustic analysis indicates that resident whales sampled in the eastern Aleutians have call repertoires distinct from other well-known resident populations described from Kenai Fjords through Washington State. However, on the basis of structural similarities among calls from these regions, it can not be ruled out that some social contact occurs or that these whales share a recent common ancestry. The structure of some call syllables appears to change quickly in a climate of diminishing social contact (Deecke et al., 2000), whereas the overall syllable type and the syntax of syllables in calls remains stable for a longer period of time (Ford, 1991; Yurk, 2005). Genetic samples taken in the eastern Aleutians revealed only the NR haplotype, whereas those from Kodiak Island waters and in Kenai Fjords yielded a mixture of NR and southern resident haplotypes (SR haplotypes) (Barrett-Lennard, 2000). An examination of nuclear alleles is needed to clarify the relationship between eastern Aleutian residents and other resident killer whales in other regions of the North Pacific.

Offshore killer whales

Only one group of whales was determined to be of the offshore ecotype, with 54 individuals identified in a single encounter. Most (44) of the individuals identified in that encounter had been identified in other regions, including southern British Columbia and Kenai Fjords, Alaska, indicating that there is a single wide-ranging population in the eastern North Pacific. This ecotype is not known to consume marine mammals and the only reported stomach contents are salmonid bones, crab shell, sculpin, and eelgrass (Heise et al., 2003).

Transient killer whales

Transient killer whales, as determined in our analyses, were the only whales observed consuming marine mammals and were not seen feeding on fish or engaging in behaviors associated with fish-feeding in other areas (Ford and Ellis, 1999; Saulitis et al., 2000). This observation supports findings in other regions that indicate transient killer whales are a distinct ecotype specializing in marine mammal prey and comprise a subset of the total whales found in any region (Matkin et al., 1999b; Ford et al., 2000). Most of the 165 transient individuals identified in our study were present only in spring and early summer when gray whales were migrating. We documented only 51 different transient individuals in late summer, at which time their appearance was sporadic and they seemed to leave the region for periods of weeks or longer.

Transient killer whales in the eastern Aleutians display a unique call repertoire that is distinct from the repertoire of transient killer whales in other regions. Therefore, the eastern Aleutian group may represent a separate population. Other than three whales photographed near the Barren Islands by NMML in 2001 (Durban²), and resighted east of Unalaska Island in 2002; no other transient whales from this area have been photographed north and east of the Shumagin Islands. The results of mitochondrial DNA analysis are equivocal because the three haplotypes we identified all occur in waters of the northern Gulf of Alaska. Again, extensive examination of nuclear alleles and comparison with those from other regions will be needed to clarify population structure.

For example, more detailed genetic analysis of eastern Aleutian transient killer whales exhibiting the AT1 haplotype has shown that they have dissimilar nuclear alleles from those of the threatened AT1 population of Prince William Sound and Kenai Fjords (Barrett-Lennard³). This finding indicates that the similarity of their haplotypes reflects historical lineage sorting rather than a recent descent from a common maternal ancestor. Because haplotypes reflect maternal lineages, the co-occurrence of two haplotypes in the transient whale aggregations encountered in the False Pass–Unimak Island area during spring supports the idea that distinct matrilineages that may not associate at other times of year join to form these aggregations.

The small overlap (3.6% of the individuals) between transient killer whales encountered west of Unimak Pass in summer and transient killer whales observed in spring in the False Pass–Unimak Islands area indicates there is further seasonal and spatial structuring in the population. The large percentage of new transient killer whales encountered in each year of summer studies, compared to the lower percentage of resighted individu-

² Durban, J. 2005. Unpubl. data. National Marine Mammal Lab, National Marine Fisheries Service, 7600 Sand Point Way NE, Seattle, WA 98115.

³ Barrett-Lennard L. 2005. Unpubl. data. Vancouver Aquarium, 845 Aviso Rd, Vancouver, BC, Canada. V6G 3E2

als in the spring, indicates that a smaller percentage of the summer whales have been identified. A survey of nearshore waters from the Gulf of Alaska to the Aleutian Islands revealed that the highest densities of transient killer whales were from the Shumagin Islands through the eastern Aleutian Islands, and an estimated abundance of 226 (CV=0.45) transient killer whales were present west of the Shumagin Islands in summer (Zerbini et al., 2006).

Transient killer whales near False Pass in May were concentrated on the Pacific Ocean side of Unimak Island and in Ikatan Bay, where gray whales pass along a shallow shelf and water depth rarely exceeds 70 meters (Fig. 1). Reports from mariners and pilots have indicated that other areas around Unimak Island and along the Bering Sea coast (e.g., Cape Lutke and the coastline near Nelson Lagoon) may also be points of interception of gray whales by killer whales. Our own surveys (Fig. 2B) indicate that transient killer whales inhabit a wide area around Unimak Island and the tip of the Alaska Peninsula, where we recorded kills of gray whales at Deer Island (110 km northeast of False Pass) and Cape Lutke (140 km southwest of False Pass).

Despite uncertainties regarding the range of transient killer whales, it is evident that they are numerous, concentrated, and consistently present in the spring from Unimak Pass eastward. Gray whales have been previously reported as killer whale prey (Matkin and Saulitis, 1994); however, the extent to which transient killer whales were focused on gray whale predation during May–June around Unimak Island has not been previously described. Although subsequent surveys in these areas during summer (C. O. Matkin, unpubl. data; Durban².) have identified some of the same whales as those identified in the spring, most of the whales do not remain in these nearshore waters. It is not known whether these transient whales move offshore and disperse, follow the gray whales into the Bering Sea, or move into other unstudied regions.

The distribution of most, if not all, transient killer whales that we identified undoubtedly extends well beyond our survey area. Technical advances in satellite and radio tagging procedures that could be applied to killer whales would aid considerably in understanding the movements and range of transients in this region. Without a better understanding of the range of these whales, it is impossible to fully assess their impact on prey populations.

Northern fur seals appear to be an important prey for killer whales from late June to September west of Unimak Pass. This finding is based on observed kills compared to kills of other species. A substantial number of the fur seals sighted in summer were likely associated with the recently established and expanding fur seal rookery on Bogoslof Island. This population increased rapidly from 898 pups in 1992 to 5096 pups in 1999 (Angliss and Lodge, 2004). Additionally, peak numbers of migrating fur seals pass through Unimak Pass into the Bering Sea in June on their way to the

Pribilof Islands and then migrate back to the Pacific in peak numbers during October–November (Bigg, 1990).

Northern fur seals have long been indicated as an important prey for killer whales in the Pribilof Region (Hanna, 1923; Zenkovich, 1938; Tomilin, 1957). However, their importance as prey in the eastern Aleutians has not been previously documented and may have developed with the growth of the Bogoslof rookery. This geographic region presents an opportunity to examine the effects of killer whale predation on an apparently stable or increasing population of fur seals—a species that is declining in other areas.

Minke whales made up a substantial proportion of summer predation despite the relative low frequency with which they were sighted, and the apparent difficulty that killer whales have in capturing this fast swimming species in open water (Ford et al., 2005). Minke whales appear to be a minor part of the diet of killer whales from Washington State to northern southeastern Alaska (Ford et al., 2005).

We observed the harassment of a humpback whale by killer whales once; during the attack, other humpback whales rapidly converged on the attackers and appeared to drive the killer whales away. No injuries were apparent. Harassments of humpbacks have been reported in other regions of Alaska (Saulitis et al., 2000), but did not result in a kill or apparent injury. Photographs of scars indicate that most killer whale attacks on baleen whales target young animals, probably calves on their first migration from low-latitude breeding and calving areas to high-latitude feeding grounds (Mehta⁴).

Although none of the attacks that we observed on Dall's porpoises resulted in confirmed kills, Dall's porpoises could be a significant prey as has been indicated in other regions (Ford et al., 1998; Saulitis et al., 2000); however, more observations are needed. Harbor seals were conspicuously absent from our prey observations despite also being an important prey in other regions of Alaska (Saulitis et al., 2000; Matkin et al., in press). Harbor seals are found in relatively low numbers in the eastern Aleutians.

Although Steller sea lions were observed as prey on one occasion and were harassed on another, they did not appear to be a primary target of the transient killer whales we observed during our spring and summer surveys. Whether or not they are an important prey during other seasons (fall and winter) is not known and will require additional study or the application of other methods to be fully assessed.

Although our study was limited by a small sample size in the summer, it provided significant information on the distribution of transient killer whale prey and the importance of fur seals in the killer whale diet during summer west of Unimak Pass and the importance of grey whales in killer whale diet during spring from Unimak Pass east. An increase in sample size of ob-

⁴ Mehta, A. 2005. Unpubl. data. Woods Hole Oceanographic Institute, Woods Hole, MA 02543-1050.

served kills is therefore important to develop greater confidence and detail in estimating the composition of killer whale diets.

Our seasonal bias towards spring and summer leaves uncertainty about killer whale diets during fall and winter. In this regard, analytical techniques that include identification of fatty acids, stable isotopes, and contaminants may prove useful when coupled with field observations to obtain a more complete picture of the feeding habits of killer whales during these seasons (Herman et al., 2005).

Conclusions

Our work underscores the importance of determining lineages and ecotypes of killer whales before making assumptions regarding feeding habits and potential impact of killer whales on prey populations. Although there may be well over 100 marine mammal-eating transient killer whales that aggregate in False Pass–Unimak Island region to feed on gray whales in spring, the majority of the killer whales present in summer are fish-eating residents. In the summer, marine-mammal-eating transients are far less abundant than in spring.

Our study indicates that the diet of transient killer whales off the eastern Aleutian Islands contrasts with the diets of transient killer whales in other parts of the North Pacific. In British Columbia, for example, transient killer whale diet is composed primarily of harbor seals (Ford et al., 1998), whereas both harbor seals and harbor porpoise are the primary prey of killer whales in northern Glacier Bay and Icy Strait region of southeastern Alaska (Matkin et al., 2005). Further north, in Prince William Sound and Kenai Fjords, the dominant prey of the AT1 transient killer whales are harbor seals and Dall's porpoises (Saulitis et al., 2000). Only in the Gulf of Alaska (Kenai Fjords) has predation by some Gulf of Alaska transient killer whales apparently focused on sea lions (Matkin et al., 2005).

Killer whale feeding behavior needs to be examined on a region-by-region basis, as well as seasonally. Experience in other regions of the North Pacific has shown that estimated population sizes, life history parameters, and dietary information can be obtained with a concerted long-term research effort. Our study has demonstrated that the eastern Aleutians also support the presence of three killer whale ecotypes, as has been previously described along the Pacific Coast of North America. It also has developed minimum estimates of the numbers of transient and resident killer whales that use the region and has provided information that may indicate that grey whales and northern fur seals are important prey items in this region at certain times and in certain areas. Steller sea lions were not a primary prey during our spring and summer surveys. Whether or not killer whales are impeding population recovery of Steller sea lions in the eastern Aleutian Islands cannot be answered decisively, nor can the effect that killer whales may be having on other species in this region

as yet be ascertained. Answers to these and other questions are expected to become clearer as the observational database for killer whales is expanded and the data for regions within the North Pacific are compared.

Acknowledgments

Financial support was provided by the Cooperative Institute for Arctic Research (CIFAR), the National Marine Mammal Laboratory, the National Oceanic and Atmospheric Administration, the Steller Sea Lion Research Initiative (SSLRI), the North Pacific Universities Marine Mammal Research Consortium (NPUMMRC), the North Pacific Marine Science Foundation, and the Alaska Sea Life Center (ASLC). Field biologists included P. Nielson, T. Markowitz, D. Power, and L. Mazzuca and vessel operations were directed by M. Brittain. Vessel operators were B. Schauff, P. Thompson, B. Laukitis, D. Graves, T. Peterson, A. Bartlett, and G. Marshall. Assistance in the field was provided by L.A. Holmes, R. Brewer, V. Vergara, T. Ciosek, G. Calef, C. Bianchini, A. G. MacHutchon, K. Leonard, F. Nicklin, K. Walker, D. Masters, and R. Blancato. Office and logistic support were provided by P. Rosenbaum and J. Rose.

Literature cited

- Angliss, R. P., and K. L. Lodge.
2004. Alaska marine mammal stock assessments, 2003. NOAA Technical Memo. NMFS-AFSC-144, 237 p.
- Barrett-Lennard, L. G.
2000. Population structure and mating patterns of killer whales (*Orcinus orca*) as revealed by DNA analysis. Ph.D. diss., 92 p. Univ. British Columbia, Vancouver, B.C., Canada.
- Barrett-Lennard, L. G., K. A. Heise, E. Saulitis, G. Ellis, and C. Matkin
1995. The impact of killer whale predation on Steller sea lion populations in British Columbia and Alaska. Report of the Marine Mammal Research Consortium, Univ. British Columbia, 6248 Biological Sciences Road, Vancouver, BC, V6T-1Z4, Canada.
- Barrett-Lennard, L. G., T. G. Smith, and G. M. Ellis.
1996. A cetacean biopsy system using lightweight pneumatic darts, and its effect on the behavior of killer whales. *Mar. Mamm. Sci.* 12:14–27.
- Bigg, M. A.
1990. Migration of northern fur seals (*Callorhinus ursinus*) off western North America. Canadian Technical Report of Fisheries and Aquatic Sciences no. 1764, 64 p.
- Bigg, M. A., P. F. Olesiuk, G. M. Ellis, J. K. B. Ford, and K. C. Balcomb III.
1990. Social organization and genealogy of resident killer whales (*Orcinus orca*) in the coastal waters of British Columbia and Washington State. Report of the International Whaling Commission. (special issue) 12:386–406.
- Dahlheim, M. E.
1997. A Photographic catalog of killer whales, *Orcinus orca*, from the central Gulf of Alaska to the southeastern Bering Sea. NOAA Tech. Rep. NMFS-131, 54 p.

- Deecke, V. B.
2003. The vocal behaviour of transient killer whales (*Orcinus orca*) communicating with costly calls. Ph.D. diss. 138 p. Univ. St. Andrews, St. Andrews, Scotland.
- Deecke, V. B., J. K. B. Ford, P. J. B. Slater.
2005. The vocal behavior of mammal-eating killer whales: communicating with costly calls. *Anim. Behav.* 69(2):395–405.
- Deecke, V. B., J. K. B. Ford, and P. Spong.
2000. Dialect change in resident killer whales: implications for vocal learning and cultural transmission. *Anim. Behav.* 60(5):629–638.
- DeMaster, D. P., A. W. Trites, P. Clapham, S. Mizroch, P. Wade, R. J. Small, and J. Ver Hoef.
2006. The sequential megafaunal collapse hypothesis: testing with existing data. *Prog. Ocean.* 68:329–342.
- Estes, J. A., M. T. Tinker, T. M. Williams, and D. F. Doak.
1998. Killer whale predation on sea otters links oceanic and nearshore ecosystems. *Science* 282:473–476.
- Ford, J. K. B.
1991. Vocal traditions among resident killer whales (*Orcinus orca*) in coastal waters of British Columbia. *Can. J. Zool.* 69:1454–1483.
1989. Acoustic behaviour of resident killer whales (*Orcinus orca*) off Vancouver Island, British Columbia. *Can. J. Zool.* 67:727–745.
- Ford, J. K. B., G. M. Ellis, D. R. Matkin, K. C. Balcomb, D. Briggs, and A. B. Morton.
2005. Killer whale attacks on minke whales: prey capture and antipredator tactics. *Mar. Mamm. Sci.* 21:603–618.
- Ford, J. K. B., and G. M. Ellis.
1999. Transients: Mammal-hunting killer whales, 96 p. Univ. British Columbia Press, Vancouver, Canada.
- Ford, J. K. B., G. M. Ellis, and K. C. Balcomb.
2000. Killer whales, 2nd ed., 104 p. Univ. British Columbia Press, Vancouver, Canada.
- Ford, J. K. B., G. M. Ellis, L. G. Barrett-Lennard, A. B. Morton, and K. C. Balcomb III.
1998. Dietary specialization in two sympatric populations of killer whales (*Orcinus orca*) in coastal British Columbia and adjacent waters. *Can. J. Zool.* 76:1456–1471.
- Hanna, G. D.
1923. Rare mammals of the Pribilof Islands, Alaska. *J. Mammal.* 4:209–215.
- Heise, K., L. G. Barrett-Lennard, E. Saulitis, C. Matkin, and D. Bain.
2003. Examining the evidence for killer whale predation on Steller sea lions in British Columbia and Alaska. *Aquat. Mamm.* 29:325–334.
- Herman, D. P., D. G. Burrows, P. R. Wade, J. W. Durban, C. O. Matkin, R. G. LeDuc, L. G. Barrett-Lennard, and M. M. Krahn.
2005. Feeding ecology of eastern North Pacific killer whales *Orcinus orca* from fatty acid, stable isotope, and organochlorine analyses of blubber biopsies. *Mar. Ecol. Prog. Ser.* 302:275–291.
- Leatherwood, S., C. O. Matkin, J. D. Hall, and G. M. Ellis.
1990. Killer whales, *Orcinus orca*, photo-identified in Prince William Sound, Alaska, 1976 through 1987. *Can. Field Nat.* 104:362–371.
- Loughlin, T. R., and A. E. York.
2000. An accounting of the sources of Steller sea lion mortality. *Mar. Fish. Rev.* 62(4):40–45.
- Matkin, C. O., G. M. Ellis, P. Olesiuk, and E. L. Saulitis.
1999a. Association patterns and genealogies of resident killer whales (*Orcinus orca*) in Prince William Sound, Alaska. *Fish. Bull.* 97:900–919.
- Matkin, C. O., G. M. Ellis, E. L. Saulitis, L. G. Barrett-Lennard, and D. Matkin.
1999b. Killer whales of southern Alaska. North Gulf Oceanic Society, Homer, AK.
- Matkin, C. O., and E. Saulitis.
1994. Killer whale (*Orcinus orca*): biology and management in Alaska. U.S. Mar. Mamm. Comm., Washington D.C., 80 p. [Contract T75135023.]
- Matkin, C. O., E. Saulitis, D. Maldini, J. Maniscalco, and L. Mazzuca.
2005. Steller sea lion predation by killer whales in Kenai Fjords/Prince William Sound, Alaska. In *Synopsis of research on Steller sea lions: 2001–2005* (T. R. Loughlin, S. K. Atkinson, and D. G. Calkins, eds.), p. 212–226. Alaska Sea Life Center's Steller Sea Lion Research Program, Seward, AK.
- Matkin, D. R., J. M. Straley, and C. M. Gabriele.
In press. Killer whale feeding ecology and non-predatory interactions with other marine mammals. In *Proceedings of the fourth Glacier Bay science symposium, 2004* (J. F. Piatt, and S. M. Gende, eds.). U.S. Geological Survey, Information and Technology Report USGS/BRD/ITR-2005, Washington, D.C.
- Merrick, R. L., T. R. Loughlin, and D. G. Calkins.
1987. Decline in abundance of the northern sea lion, *Eumetopias jubatus*, in 1956–86. *Fish. Bull.* 85:351–365.
- Miller, P. J. O., and D. E. Bain.
2000. Within-pod variation in the sound production of a pod of killer whales, *Orcinus orca*. *Anim. Behav.* 60(5):617–628.
- Mizroch, S. A., and D. W. Rice.
2006. Have North Pacific killer whales switched prey species in response to depletion of the great whale populations? *Mar. Ecol. Prog. Ser.* 310:235–246.
- Pitcher, K. W.
1990. Major decline in number of harbor seals, *Phoca vitulina richardsi*, on Tugidak Island, Gulf of Alaska. *Mar. Mamm. Sci.* 6:121–134.
- Sambrook, J., E. F. Fritsch, and T. Maniatis.
1989. *Molecular cloning: a laboratory manual*. 3rd ed. Cold Spring Harbor, NY.
- Saulitis, E., C. O. Matkin, and F. H. Fay.
2005. Vocal repertoire and acoustic behavior of the isolated ATI killer whale subpopulation in southern Alaska. *Can. J. Zool.* 83:1015–1029.
- Saulitis, E. L., C. O. Matkin, K. Heise, L. Barrett Lennard, and G. M. Ellis.
2000. Foraging strategies of sympatric killer whale (*Orcinus orca*) populations in Prince William Sound, Alaska. *Mar. Mamm. Sci.* 6:94–109.
- Springer, A. M., J. A. Estes, G. B. van Vliet, T. M. Williams, D. F. Doak, E. M. Danner, K. A. Forney, and B. Pfister.
2003. Sequential megafaunal collapse in the North Pacific Ocean: an ongoing legacy of industrial whaling? *Publ. Nat. Acad. Sci.* 100:12,223–12,228.
- Thompson, J. D., D. G. Higgins, and J. Gibson.
1994. Clustal W: improving the sensitivity of progressive multiple sequence alignment through sequence weight-

- ing position specific gap penalties and weight matrix choice. *Nucl. Acids Res.* 22:4673–4680
- Tomilin, A. G.
1957. Cetacea. Vol. 9 of *Mammals of the U.S.S.R. and adjacent countries* (V. G. Heptner, ed.), 756 p. Izd. Akad. Nauk SSSR, Moscow. [Translated from Russian by Israel Prog. Sci Transl., 1967.]
- Trites, A. W.
1992. Northern fur seals: why have they declined? *Aquat. Mamm.* 18:3–18.
- Trites, A. W., V. B. Deecke, E. J. Gregr, J. K. B. Ford, and P. F. Olesiuk.
2006. Killer whales, whaling and sequential megafaunal collapse in the North Pacific: a comparative analysis of the dynamics of marine mammals in Alaska and British Columbia following commercial whaling. *Mar. Mamm. Sci.* 22.
- Trites, A. W., and P. A. Larkin.
1996. Changes in the abundance of Steller sea lions (*Eumetopias jubatus*) in Alaska from 1956 to 1992: How many were there? *Aquat. Mamm.* 153–166.
- Winship, A. J., and A. W. Trites.
2006. Risk of extirpation of Steller sea lions in the Gulf of Alaska and Aleutian Islands: a population viability analysis based on alternative hypotheses for why sea lions declined in western Alaska. *Mar. Mamm. Sci.* 22:124–155
- York, A. E.
1987. Northern fur seal, *Callorhinus ursinus*, eastern Pacific population (Pribilof Islands, Alaska, and San Miguel Island, California). In *Status, biology, and ecology of fur seals* (J. P. Croxall, and R. L. Gentry, eds.), p. 9–21. NOAA Tech. Rept. NMFS 51.
- Yurk, H.
2005. Vocal culture and social stability in resident killer whales (*Orcinus orca*) of the northeastern Pacific. Ph. D. diss., 126 p. Univ. British Columbia, Vancouver, British Columbia, Canada.
- Yurk, H., L. G. Barrett-Lennard, J. K. B. Ford, C. O. Matkin.
2002. Cultural transmission within maternal lineages: vocal clans in resident killer whales in southern Alaska. *Anim. Behav.* 63(6):1103–1119.
- Zenkovich, B. A.
1938. On the grampus or killer whale (*Grampus orca* Lin.). *Priroda* 4:109–112. [Translated from Russian by L. G. Robbins. U.S. Geological Survey S(570).
- Zerbini, A. N., J. M. Waite, J. W. Durban, R. LeDuc, M. E. Dahlheim, and P. R. Wade.
2006. Estimating abundance of killer whales in the nearshore waters of the Gulf of Alaska and Aleutian Islands using line transect sampling. *Mar. Biol.* DOI 10.1007/s0027006-0347-8.

Abstract—Abundance indices derived from fishery-independent surveys typically exhibit much higher interannual variability than is consistent with the within-survey variance or the life history of a species. This extra variability is essentially observation noise (i.e. measurement error); it probably reflects environmentally driven factors that affect catchability over time. Unfortunately, high observation noise reduces the ability to detect important changes in the underlying population abundance. In our study, a noise-reduction technique for uncorrelated observation noise that is based on autoregressive integrated moving average (ARIMA) time series modeling is investigated. The approach is applied to 18 time series of fin-fish abundance, which were derived from trawl survey data from the U.S. northeast continental shelf. Although the *a priori* assumption of a random-walk-plus-uncorrelated-noise model generally yielded a smoothed result that is pleasing to the eye, we recommend that the most appropriate ARIMA model be identified for the observed time series if the smoothed time series will be used for further analysis of the population dynamics of a species.

Removing observational noise from fisheries-independent time series data using ARIMA models

William T. Stockhausen (contact author)

Michael J. Fogarty

Email address for W. T. Stockhausen: William.Stockhausen@noaa.gov

National Ocean and Atmospheric Administration
National Marine Fisheries Service
Northeast Fisheries Science Center
166 Water Street
Woods Hole, MA 02543

Present address for corresponding author: National Marine Fisheries Service
Alaska Fisheries Science Center
7600 Sand Point Way NE
Seattle, Washington 98115

Time series of species abundance from fishery-independent surveys, such as bottom trawl or acoustic surveys, are important in monitoring temporal change in the abundance of marine populations. For commercially important species, catch and effort data from the commercial fishery may be available, allowing estimation of temporal trends of the stock population by means of stock assessment models (e.g., virtual population analysis). However, such records are not available for many species, especially those with little commercial (but perhaps significant ecological) value. Fishery-independent surveys may thus constitute the only source of information for assessing temporal changes in the abundance of these species (Pennington, 1985; Helser and Hayes, 1995).

Annual estimates of abundance derived from fisheries-independent surveys are typically regarded as providing a relative measure of population abundance (i.e., they are indices of abundance, not true estimates of total population size) (Grosslein, 1969; Clark, 1979). Thus, the expected value of the abundance index (e.g., mean catch-per-tow for trawl surveys) is regarded as proportional to the size of the actual population, although the constant of proportionality (the catchability) is unknown. As such, relative changes in an abundance index should reflect similar relative changes in the actual population, and trends

in the time series of such an index should reflect similar trends in the corresponding population.

Unfortunately, abundance indices derived from large-scale fishery-independent surveys typically exhibit interannual variability much higher than one would expect from within-survey variance (Byrne et al., 1981; Pennington, 1985). Part of the variability in such indices is presumably due to the variability in the underlying population—a variability that is caused by population-dynamic processes such as recruitment. However, part of the variability is due to observation noise that arises from both within-survey sampling variability because of the heterogeneous distribution of many fish stocks (Byrne et al., 1981), and because of environmentally driven factors that affect catchability over time (Byrne et al., 1981; Collie and Sissenwine, 1983). Low signal-to-noise ratios in abundance indices that are due to high observation noise reduce chances of detecting important changes or trends in actual population abundance. Variability due to within-survey sampling can be reduced (before the fact) by adding more stations to a survey, but additional stations will not reduce variability caused by changes in catchability.

Time series modeling using autoregressive integrated moving average (ARIMA; Box and Jenkins, 1976) models provides an approach to re-

moving observation noise from abundance estimates. ARIMA models are frequently used in economic forecasting (Enders, 2004) and are becoming more common in fisheries research. Recent applications of ARIMA models to other fisheries problems include forecasting monthly landings in the Mediterranean (Lloret et al., 2000), testing theories of population dynamics (Becerra-Munoz et al., 1999), and modeling nutrient dynamics in an upwelling system (Nogueira et al., 1998).

In the context of reducing the influence of observational noise in time series data, Cleveland and Tiao (1976) first developed a noise-reduction and smoothing algorithm for processes that could be described by an ARIMA time series model. Their approach requires that the ARIMA model for the unobserved, underlying process be known. This known model, in turn, uniquely determines the ARIMA model for the observed time series contaminated by observation noise and allows one to estimate the variance of the observation noise. Unfortunately, although the ARIMA model for an unobserved, underlying process may be known in some instances (from theory, perhaps), in many cases the model for the unobserved process will be unknown.

Box et al. (1978) extended Cleveland and Tiao's (1976) ideas and developed a noise-reduction algorithm based on the ARIMA model for the observed time series. However, the ARIMA model for the observed time series merely constrains, but does not determine, the model for the unobserved, underlying process; it provides only an upper bound for the observation error variance. Consequently, this approach generally requires an external estimate of the observation error variance to determine the appropriate level of noise reduction.

Pennington (1985) first applied these ARIMA-based time series modeling techniques to smoothing abundance indices derived from trawl survey data. He assumed that an observed abundance time series reflected a combination of the underlying population abundance and independent, uncorrelated, and multiplicative observation noise (the latter arising perhaps from environmentally driven changes in catchability). He further assumed that both the (log-transformed) observed time series and unobserved population process could be represented by ARIMA models. Pennington (1985) then developed an alternative algorithm to that of Box et al. (1978); his derivation allowed particular simplification in the case where the underlying population process could be modeled as a random walk. In this simple case, the resulting noise reduction filter is an exponentially-weighted average of the observed time series for the endpoint of the time series (Pennington, 1985). More importantly, the observation error variance can be easily estimated from the ARIMA model parameters and an external estimate is unnecessary. Thus, for the case where a random walk model for the underlying process is valid, the appropriate level of smoothing is objectively determined.

As a demonstration, Pennington (1985) applied his noise reduction algorithm to groundfish trawl survey data for haddock (*Melanogrammus aeglefinus*) from the

northeastern Atlantic coast of the United States. He found that the variances of the smoothed indices were "considerably lower" than those of the originals. However, this demonstration used an ARIMA model derived from a much longer time series that had been generated from a stock assessment based on commercial catch data. Pennington (1985) assumed that this model represented the underlying population and therefore did not develop models based on the observed time series. Although this assumption was perfectly reasonable, given that such alternative data (the stock assessment) were available, it cannot be applied to situations when only survey data are available to fishery analysts.

The ARIMA model Pennington (1985) derived from stock assessment results was a random walk model; therefore the appropriate level of noise reduction for the corresponding survey data could be objectively determined from the model parameters. Pennington's (1985) method was later used to apply random walk models to survey data (Fogarty et al.¹; Pennington, 1986; Anonymous, 1988, 1993). Pennington (1986) found that random walk models were appropriate for the survey time series considered in his study. However, random walk models were assumed *a priori* in the remaining three references (Fogarty et al.¹; Anonymous, 1988, 1993) to generate smoothed abundance trajectories; because less than 25 observations for each time series were considered in these references, reliable identification of the model structure for each time series was considered problematic and random walk models were used as "null" models.

When it is an appropriate description of the underlying process, a random walk model yields an objective determination of the degree of noise reduction appropriate to an observed time series. However, an *a priori* adoption of this model should be viewed with some skepticism. Additionally, if a random walk model is not an appropriate description of the underlying process, the resulting smoothed time series may seem reasonable, but the result no longer has support as the unobserved, underlying process. In this circumstance, we regard the effect of the ARIMA algorithm as merely smoothing, and not necessarily as noise reducing.

As such, we feel that the utility of ARIMA-based approaches to noise reduction for abundance indices derived from survey data has not been adequately explored to date. In addition, substantially longer time series (e.g., 40 observations) are now available with which to test this concept. In our study, we test the utility of the ARIMA time series noise reduction approach propounded by Pennington (1985), using time series of abundance indices from fishery-independent trawl survey data for nine finfish species (Table 1) during two seasons on Georges Bank. We first review the original methods developed by Cleveland and Tiao

¹ Fogarty, M. J., J. S. Idoine, F. P. Almeida, and M. Pennington. 1986. Modeling trends in abundance based on research vessel surveys. ICES CM (council meeting) 1986/G, p. 92. ICES, Copenhagen, Denmark.

Table 1

Time series of abundance indices for the following finfish species on Georges Bank were derived from a fisheries-independent trawl survey and used to test the ARIMA-based smoothing algorithm.

Common name	Scientific name	Type
Winter skate	<i>Leucoraja ocellata</i>	Elasmobranch
Little skate	<i>Leucoraja erinacea</i>	Elasmobranch
Silver hake	<i>Merluccius bilinearis</i>	Groundfish
Atlantic cod	<i>Gadus morhua</i>	Groundfish
Haddock	<i>Melanogrammus aeglefinus</i>	Groundfish
Winter flounder	<i>Pseudopleuronectes americanus</i>	Flatfish
Yellowtail flounder	<i>Limanda ferruginea</i>	Flatfish
Atlantic herring	<i>Clupea harengus</i>	Pelagic schooling fish
Atlantic mackerel	<i>Scomber scombrus</i>	Pelagic schooling fish

(1976) and Box et al. (1978). Framing the problem in terms of power spectra, we also offer some additional new insights into this noise reduction approach. Next, we apply the ARIMA-based noise reduction approach to the time series data and present the results. We have implemented Box et al.'s (1978) algorithm, not Pennington's (1985). Finally, we discuss our perceptions of the utility of this approach in light of our results and overall experience with it.

Materials and methods

General characteristics of ARIMA models

In this section, we first briefly review ARIMA models for stochastic processes. Then we review the approach of Box et al. (1978) for obtaining maximum likelihood estimates for an underlying ARIMA time series from a time series of observations with independent and identically distributed (IID) observation noise.

ARIMA models are parsimonious models that can adequately represent many stochastic time series (Box and Jenkins, 1976). Stochastic time series that can be represented by ARIMA models are essentially the output of a linear filter applied to an input time series of white noise (Box and Jenkins, 1976). We will refer to such time series as ARIMA processes.

For a zero-mean stochastic time series $\{z_t\}$ that can be expressed as an ARIMA model, we denote the model (using the notation of Box and Jenkins, 1976) as

$$\varphi(B)z_t = \alpha(B)a_t, \quad (1)$$

where z_t = the value of the time series at time t ;

$\varphi(B)$ = the generalized autoregressive (AR) operator;

$\alpha(B)$ = the moving average (MA) operator;

B = the backward shift operator; and

a_t = IID normally distributed random variables with mean zero and variance σ_a^2 .

The backward shift operator B has the property that $Bz_t = z_{t-1}$; hence $B^m z_t = z_{t-m}$. The operators $\varphi(B)$ and $\alpha(B)$ are polynomials in B of order $p+d$ and q (respectively) such that

$$\begin{aligned} \varphi(B) &= 1 - \sum_{j=1}^{p+d} \varphi_j B^j \\ \alpha(B) &= 1 - \sum_{j=1}^q \alpha_j B^j. \end{aligned} \quad (2)$$

Furthermore, $\varphi(B)$ can be factored such that $\varphi(B) = \phi(B)(1-B)^d$, where the (ordinary) AR operator $\phi(B)$ has a form similar to $\varphi(B)$ but is of order p . The operator $(1-B)^d$ represents d sequential applications of the backward difference operator $1-B$ such that the original time series $\{z_t\}$ is self-differenced d times before application of the AR operator $\phi(B)$.

As a shorthand, an ARIMA model that consists of an AR operator of order p , d backward difference operations, and a MA operator of order q is abbreviated as (p,d,q) . A $(p,0,0)$ model is referred to as an AR model of order p , or AR(p) in shorthand notation, and a $(0,0,q)$ model is referred to as a MA model of order q (MA(q) in shorthand). A $(p,0,q)$ model is referred to as an autoregressive-moving average model (ARMA(p,q) in shorthand) and a $(0,d,q)$ model is referred to as an integrated moving average model (IMA(d,q) in shorthand). Finally, a random walk model is $(0,1,0)$, while a random-walk-plus-uncorrelated-observation noise (RWPUN) model is $(0,1,1)$.

In general, ARIMA models represent nonstationary time series. However, the time series that results from applying the backward difference operator d times to a (p,d,q) ARIMA process is a stationary ARMA(p,q) process. Typical constraints imposed on ARIMA models are that, when B is regarded as a complex variable, the polynomial in B representing the generalized autoregressive operator has zeros on or outside the unit circle ($|B|=1$), whereas the polynomials representing the ordinary autoregressive operator and the moving

average operator have zeros outside the unit circle. Additionally, the white noise variance, σ_a^2 , must be finite. These constraints ensure that a model is invertible and stationary (or, if not stationary, that at least it is of a suitable form).

One final property of ARIMA models is of interest here. The power spectrum for an ARMA (p,q) process represented by equation 1 is given by

$$p_z(f) = \frac{1}{2} \sigma_a^2 \frac{|\alpha(e^{-i2\pi f})|^2}{|\varphi(e^{-i2\pi f})|^2} = \frac{1}{2} \sigma_a^2 \frac{\alpha(B)\alpha(F)}{\varphi(B)\varphi(F)} \quad (3)$$

$$\text{where } B = e^{-i2\pi f}; 0 \leq f \leq \frac{1}{2},$$

and the forward shift operator, $F=B^{-1}$, has the opposite effect to B (i.e., $F^m z_t = z_{t+m}$).

ARIMA models of time series with observation noise

Suppose, then, that y_1, y_2, \dots, y_T represent a time series of observations at times $t = 1, 2, \dots, T$ such that

$$y_t = z_t + e_t, \quad (4)$$

where the z_t 's represent the unobserved, underlying process and the e_t 's are IID normal variables with variance σ_e^2 (i.e., $e \sim N(0, \sigma_e^2)$) that are also independent of the z_t 's (i.e., $\langle e_j, z_k \rangle = 0$ for all j, k). The goal is to estimate the unobserved time series $\{z_t\}$ by using the observed time series $\{y_t\}$. For the analysis of fishery-independent time series, it seems reasonable to assume that only the ARIMA model for the observed time series $\{y_t\}$ is known (it can be estimated using standard techniques). In particular, this assumption means that the model for $\{z_t\}$ is unknown within constraints implied by the observation equation. However, to develop the approach used here it is helpful to start as though the model for the unobserved process $\{z_t\}$ were known.

Thus, we assume that the time series $\{z_t\}$ can be represented by an ARIMA (p,d,q) process:

$$\varphi(B)z_t = \alpha(B)c_t, \quad (5)$$

where the c_t 's are IID and $c_t \sim N(0, \sigma_c^2)$. Substituting in $y_t - e_t$ for z_t and rearranging, one obtains

$$\varphi(B)y_t = \alpha(B)c_t + \varphi(B)e_t, \quad (6)$$

which can be expressed as an ARIMA model for $\{y_t\}$ of the form

$$\varphi(B)y_t = \eta(B)d_t, \quad (7)$$

where the d_t 's are IID, $d_t \sim N(0, \sigma_d^2)$ and the MA operator is $\eta(B)$. Thus, the generalized AR operator for the observed $\{y_t\}$ is identical to that for the unobserved $\{z_t\}$. Furthermore, because $\alpha(B)$ has order q and $\varphi(B)$

has order $p+d$, $\eta(B)$ must be of order $\max(p+d, q)$. This requirement for $\eta(B)$ constrains the order of potential ARIMA models that could describe the observed process: if $p+d \leq q$ then the observed process is also a (p, d, q) process, otherwise it is a $(p, d, p+d)$ process.

In the more realistic situation where $\{y_t\}$ is observed, we can determine the generalized AR operator $\varphi(B)$ and MA operator $\eta(B)$ for the observed process. Its ARIMA model will be order (P, D, Q) , say, where the minimum possible value for Q is $P+D$. The model for the corresponding unobserved, underlying process $\{z_t\}$ will have order $(p=P, d=D, q \leq \max(P+D, Q))$ and its associated generalized AR operator will also be $\varphi(B)$. Furthermore, recognizing that c_t and e_t are independently distributed, it can be shown that the moving average operator for the unobserved process, $\alpha(B)$, is additionally constrained by the ARIMA model for the observed process such that the following relationship must be satisfied:

$$\sigma_c^2 \alpha(B)\alpha(F) = \sigma_d^2 \eta(B)\eta(F) - \sigma_e^2 \varphi(B)\varphi(F). \quad (8)$$

In this equation, σ_e^2 , $\eta(B)$, and $\varphi(B)$ are known from the ARIMA model for the observed process, whereas σ_c^2 , σ_d^2 , and $\alpha(B)$ are unknown.

In general, many combinations of σ_c^2 , σ_d^2 , and $\alpha(B)$ will satisfy the equality. Defining an "acceptable model" for the unobserved process as one that, given the model for the observed process, $\alpha(B)$ satisfies the previous equation and its zeros are on or outside the unit circle, Box et al. (1978) show that 1) for every given model of an observed process, at least one acceptable model for the unobserved process exists; 2) for a given model of an observed process, the possible values of σ_c^2 are bounded; and 3) for a given model, every σ_c^2 between 0 and the upper bound (K^* , say) determines a unique acceptable model. The upper bound on the observation error variance, K^* , is determined from the constraint that, for a model of the unobserved process to be acceptable, $\sigma_c^2 \alpha(B)\alpha(F) \geq 0$ everywhere on the unit circle (i.e., the power spectrum of the corresponding MA process is non-negative definite). Then, from equation 8, K^* is given by

$$K^* = \min_{|B|=1} \left\{ \frac{\sigma_d^2 \eta(B)\eta(F)}{\varphi(B)\varphi(F)} \right\} \quad (9)$$

and is completely determined by the ARIMA model for the observed process. When $\sigma_e^2 = K^*$, the variance of the added white noise is maximal, as will be the smoothing of the observed time series.

It is instructive to interpret Equations 8 and 9 in terms of constraints on the power spectra of $\{z_t\}$, $\{y_t\}$, and $\{e_t\}$, although this interpretation is strictly correct only when $\{z_t\}$ and $\{y_t\}$ are stationary. Let $p_z(f)$, $p_y(f)$, $p_e(f)$ denote the power spectra for $\{z_t\}$, $\{y_t\}$, and $\{e_t\}$, respectively. Recalling the definition of the power spectrum (Eq. 3), Equation 8 on the unit circle can be easily recast (multiply both sides by $2/(\varphi(B)\varphi(F))$) as

$$p_z(f) = p_y(f) - p_e(f) \tag{10}$$

because the power spectrum for white noise is constant with frequency: $p_e(F) = 2\sigma_e^2$. Because power spectra are nonnegative definite and $p_e(f)$ does not depend on f , the maximum possible observation noise variance K^* corresponds to the minimum of $p_y(f)$ over f (see Fig. 1). Thus, Equation 9 can be recast as

$$K^* = \min_{0 \leq f \leq 1/2} \{p_y(f)\} / 2. \tag{11}$$

Note also that Equation 10 can be recast again as

$$p_z(f) = \left(1 - \frac{p_e(f)}{p_y(f)}\right) p_y(f) = \omega^*(f) p_y(f), \tag{12}$$

where $\omega^*(f)$ represents the term in parentheses. It will be seen below that $\omega^*(f)$ is identical to the polynomial of smoothing weights (Eq. 14) on the unit circle.

Returning to the estimation problem now, knowledge of σ_e^2 , then, together with the ARIMA model for the observed process, is sufficient to estimate $\{z_t\}$ (Box et al., 1978). When t is not close to the endpoints of the time series, the smoothed (maximum likelihood) estimate of

z_t , which we denote as $E(z_t|y)$, is a symmetric moving average filter of $\{y_t\}$ (Cleveland and Tiao, 1976; Box et al., 1978):

$$E(z_t|y) = \omega(B)y_t, \tag{13}$$

such that

$$\omega(B) = \frac{\sigma_a^2}{\sigma_d^2} \frac{\alpha(B)\alpha(F)}{\eta(B)\eta(F)} = \left[1 - \frac{\sigma_e^2}{\sigma_d^2} \frac{\varphi(B)\varphi(F)}{\eta(B)\eta(F)}\right], \tag{14}$$

where the second equality follows from equation 8. Note that $\omega(B)$ is identical to $\omega^*(f)$ (Eq. 12) on the unit circle ($B = e^{-i2\pi f}$), so that Equations 13 and 14 are also interchangeable in terms of relations among power spectra. Equation 13 is equivalent to Equation 2 in Pennington (1985). It turns out (Cleveland and Tiao, 1976) that equation 14 is also valid for t near the endpoints of the time series; thus, one merely uses the ARIMA model for the observed time series to hindcast or forecast additional "observations" as needed. Box et al. (1978) describe a method for calculating the coefficients of $\omega(B)$; because this reference may be difficult to obtain, we repeat their description in the Appendix.

In the case where the model for the underlying process is (0,1,0) (i.e., a random walk model), the model for the observed process is (0,1,1) (i.e., a RWPUN, model). For this case, Pennington (1985) noted that the value of the MA parameter η_1 of the observed process (θ in his notation) is

$$\eta_1 = \frac{\sigma_e^2}{\sigma_d^2}, \tag{15}$$

so that Equation 14 is completely determined by the ARIMA model for the observed process and the observation error variance, σ_e^2 , can be estimated.

Application of the noise reduction algorithm to bottom trawl survey data

We applied Box et al.'s (1978) noise reduction algorithm to 18 time series of abundance indices for finfish (nine species \times two seasons; species are listed in Table 1) on Georges Bank in the northwest Atlantic. Time series for the fall survey spanned 40 years (1963–2002), and the spring time series spanned 36 years (1968–2003).

Stratified random bottom trawl surveys have been conducted annually on the northeastern continental shelf of the United States from Cape Hatteras to the Gulf of Maine in the fall since 1963 and in the spring since 1968 by the National Marine Fisheries Service (NMFS), Northeast Fisheries Science Center (NEFSC) (Azarovitz, 1981; Anonymous, 1988; Reid

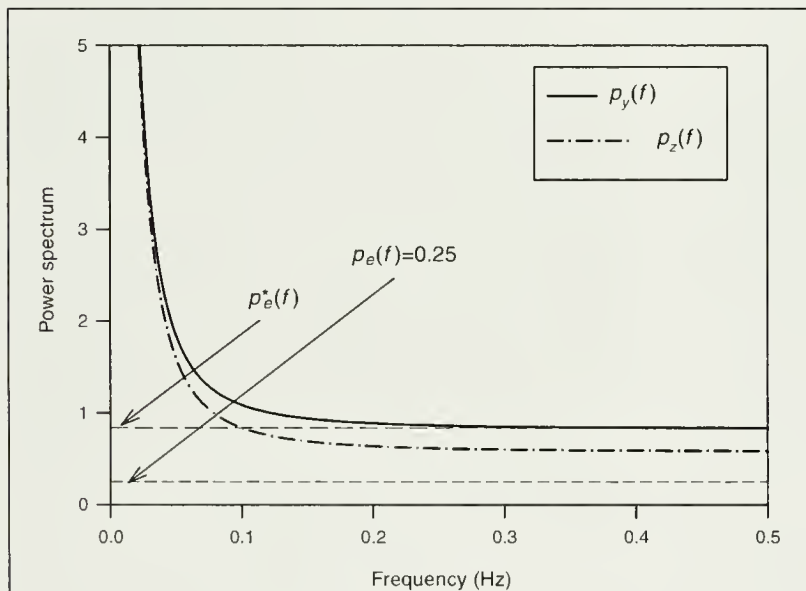


Figure 1

Example power spectra illustrating relationships between $p_y(f)$ (the power spectrum of the observed time series), $p_e(f)$ (the power spectrum of the white observational noise, a constant), and $p_z(f)$ (the power spectrum of the unobserved, underlying time series). In this example, $p_e(f) = 0.25$ so that $p_z(f)$ has the same basic shape as $p_y(f)$, but is shifted downwards at all frequencies by 0.25. $p_e^*(f)$ represents the maximum possible level, consistent with $p_y(f)$ (and the ARIMA model for the observed time series $\{y_t\}$), for the power spectrum of the assumed observational noise. Note that in this case, maximal smoothing (i.e., taking $p_e(f) = p_e^*(f)$) eliminates all high frequency energy and would result in over-smoothing.

et al., 1999). We derived annual time series of estimated total abundance during the spring and fall seasons for nine finfish species from trawl survey catch records for the Georges Bank area. Reported catches (biomass) from strata encompassing Georges Bank were expanded on a per-tow basis by using species and length-specific corrections for catchability and coefficients from Edwards (1968) and Harley and Myers (2001). Annual stratified mean (expanded) catch-per-tow was then calculated for each species for both seasonal surveys. Finally, annual total population abundance was calculated by applying a swept area factor to the stratified mean catch-per-tow. Abundance indices corresponding to fall surveys spanned 1963–2002, and those corresponding to spring surveys spanned 1968–2003. Following Pennington (1985), we assumed that changes in catchability induced a lognormal error structure on the observed time series. However, because some time series (notably those for the schooling pelagic fish herring and mackerel) included zeroes, a $\ln(x)$ transformation was not applicable to all series. Thus, before further analysis, all time series were $\ln(x+1)$ transformed.

For each resulting time series, we used SAS (vers. 8, SAS Institute, Cary, NC) to identify candidate ARIMA models, to estimate parameters for these models, and to extend the time series by using forecasts and hindcasts before applying the smoothing algorithm. Candidate model structures for each time series were based on examination of empirical autocorrelation, partial autocorrelation, and inverse autocorrelation functions for the series (Box and Jenkins, 1976). When these functions indicated that the series was nonstationary, we applied the backward difference operator $(1-B)$ to the series and examined the correlation functions for the new (differenced) series. In addition, because of its special significance in terms of interpretation, we always tried a RWUPN model as a candidate. Once candidate models were identified, we estimated coefficients for each model and calculated the associated Akaike information criterion (AIC; Akaike, 1973). AIC provides an objective criterion based on information theory for selecting the “best” approximating model from among a group of good candidate models (i.e., the criterion selects the model with the minimum AIC).

We examined the residuals and the empirical autocorrelation, inverse autocorrelation, and partial autocorrelation functions of the residual time series for significant deviation from white noise. When significant deviation was indicated, we dropped the model from further consideration. We also dropped models with orders (P,D,Q) that were inconsistent with the assumption of additive (after log transformation) observation noise ($Q \geq P+D$). Following this screening procedure, we were left with a group of “good” alternative models. We then selected the ARIMA model with the smallest AIC from among the remaining candidates as the “best” model to smooth the data.

We developed a MATLAB (vers. 6.5, The Mathworks Inc., Natick, MA) program to perform the noise reduction for each time series based on an extended version

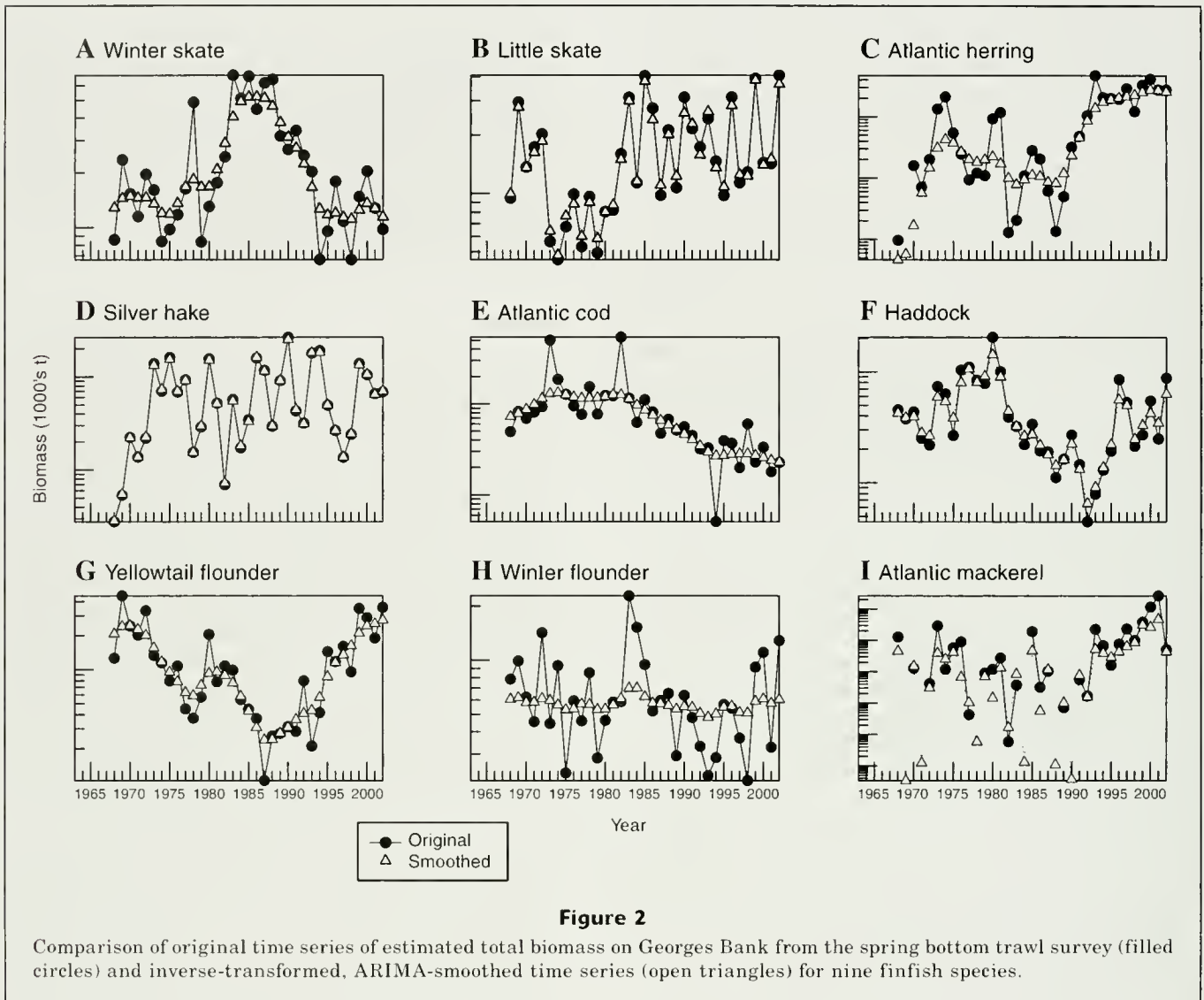
of the series and its associated ARIMA model. To allow smoothed estimates to be calculated near the ends of each time series, we extended each time series before smoothing to 40 years before its start by hindcasting with the selected ARIMA model and to 40 years past its end by forecasting with the model. Using the MATLAB program, we then calculated K^* , the maximal smoothing weights $\omega(B)$ corresponding to $\sigma_e^2 = K^*$, and the smoothed estimates $E(z_t|y)$, following the approach of Box et al. (1978) outlined previously.

Results

The abundance indices we derived from fishery-independent bottom trawl surveys for nine finfish species during two seasons displayed a wide variety of trends, as well as a high degree of apparent interannual variability. This variability may be associated with environmentally driven, high-frequency changes in catchability, but we regarded it here as observation noise (Figs. 2 and 3). For example, springtime winter skate (*Leucoraja ocellata*) biomass appeared to increase by a factor of six during the early 1980s from a lower (but highly variable) mean level of ~140,000 t, to which it subsequently returned in the early 1990s (Fig. 2A). Yellowtail flounder (*Limanda ferruginea*), in contrast, declined by a factor of 10 during the 1970s and early 1980s from a high at the beginning of the time series and then began to rebound in the latter 1980s (Fig. 2G). Most recently, yellowtail flounder appear close to regaining their earlier peak abundance.

The 18 ARIMA models corresponding to the $\ln(x+1)$ -transformed abundance indices formed a diverse set (Tables 2 and 3). Half the time series were found to be nonstationary; however, one application of backward differencing ($d=1$) sufficed to achieve stationarity in all nine instances. Interestingly, the ARIMA models for all nine of these time series were consistent with RWPUN models (i.e., $[0,1,1]$ models). For all the models, autoregressive orders (p) ranged between 0 and 3, and moving average orders (q) ranged from 1 to 5. The spring and fall models for little skate (*L. erinacea*) had the highest AR order, and the spring model for silver hake (*Merluccius bilinearis*) had the highest MA order. Only the models for little skate, Atlantic herring (*Clupea harengus*), and yellowtail flounder exhibited the same ARIMA order for both the spring and fall. And although none of the models reflected pure AR processes ($q=0$, an impossibility given the observation noise assumption), two were found to be pure MA processes (winter flounder and Atlantic mackerel [*Scomber scombrus*], both in spring). All nine IMA processes were RWPUN processes (i.e., $(0,1,1)$).

The effect of ARIMA-based noise reduction on these 18 sets of indices was fairly variable in outcome (Figs. 2 and 3). Little or no smoothing occurred for little skate (spring, Fig. 2B), silver hake (spring, Fig. 2D), and haddock (*Melanogrammus aeglefinus*) (fall, Fig. 3F). Moderate smoothing occurred for winter skate (spring, Fig. 2A; fall, Fig. 3A), little skate (fall, Fig. 3B),



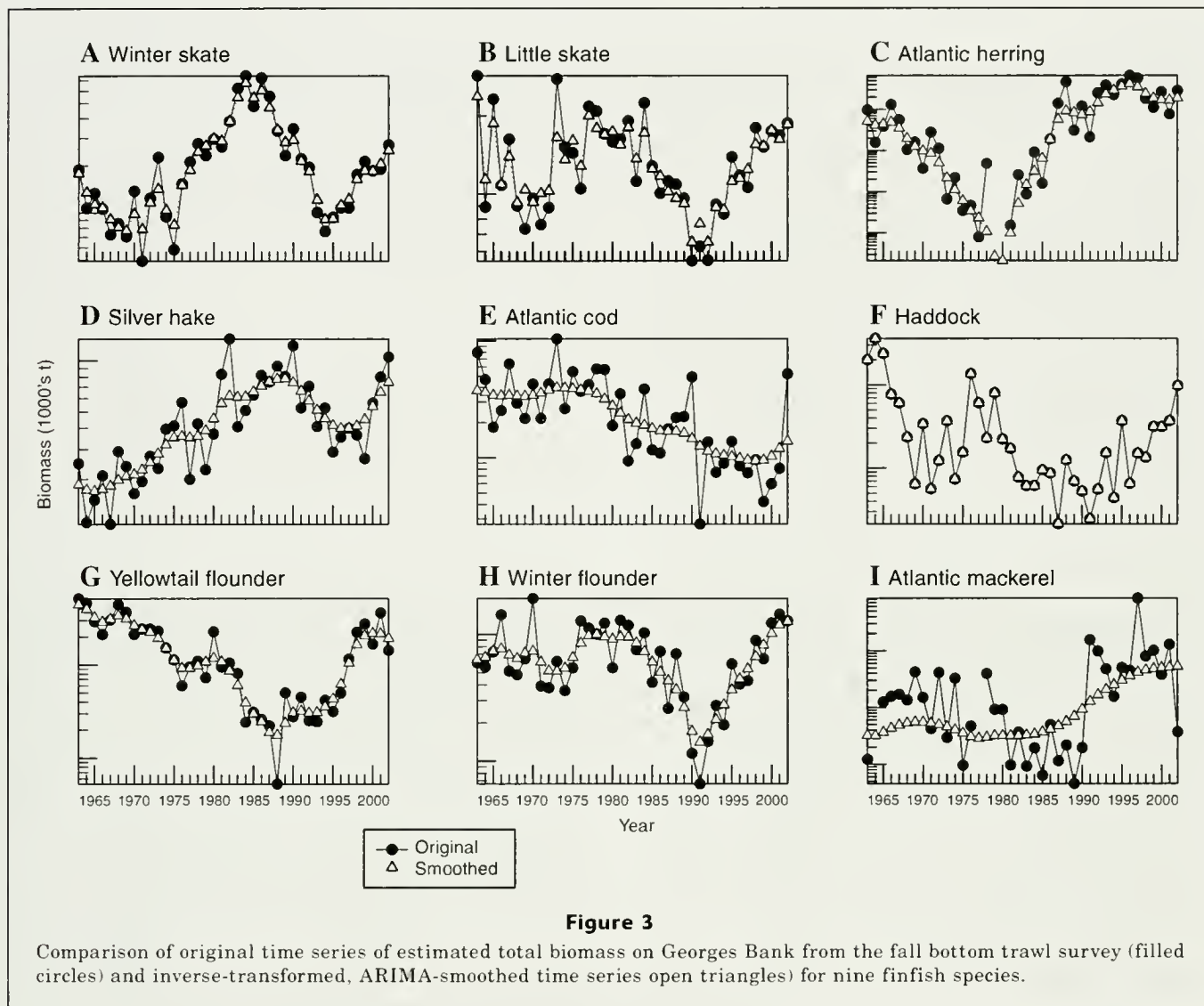
Atlantic herring (fall, Fig. 3C), haddock (spring, Fig. 2F), yellowtail flounder (spring, Fig. 2G; fall, Fig. 3G), winter flounder (*Pseudopleuronectes americanus*) (fall, Fig. 3H), and Atlantic mackerel (spring, Fig. 2I). A high degree of smoothing occurred for Atlantic herring (spring, Fig. 2C), silver hake (fall, Fig. 3D), Atlantic cod (*Gadus morhua*) (spring, Fig. 2E; fall, Fig. 3E), winter flounder (spring, Fig. 2H), and Atlantic mackerel (fall, Fig. 3I).

Impressions obtained from visually comparing the original and smoothed time series were consistent with the fraction of innovation variance (K^*/σ_d^2 , Tables 2 and 3) in the observed time series ascribed to observation error. Recall that we chose to perform the maximal amount of smoothing possible (i.e., taking $\sigma_d^2 = K^*$ in Eq. 13). Our visual classifications fell fairly neatly into the following categories based on K^*/σ_d^2 : 1) a low degree of smoothing corresponded to $K^*/\sigma_d^2 < 0.25$, 2) a moderate degree of smoothing corresponded to $0.25 < K^*/\sigma_d^2 < 0.60$,

and 3) a high degree of smoothing corresponded to $0.60 \geq K^*/\sigma_d^2$.

In addition, it appeared that the degree of smoothing varied inversely with the order of the moving average component of the ARIMA model for the observed time series. When the order of the moving average component was greater than 2, the degree of overall smoothing was typically small. Substantially more smoothing was evident when the order of the moving average component was 1, because of the equivalence with an exponentially weighted smoother.

The nine time series found to be RWPUN processes provided a means to check whether our choice to perform the maximal amount of smoothing was reasonable. For such time series, the value of the moving average coefficient, η_l , is equal to the ratio of the observation noise variance, σ_e^2 , to the innovation variance σ_d^2 . Consequently, $\sigma_d^2 \cdot \eta_l = \sigma_e^2$. For eight of the nine series, the ratio of σ_e^2 to K^* was greater than 80% (Table 4).



Discussion

Abundance indices derived from large-scale fishery-independent surveys typically exhibit interannual variability much higher than one would expect from within-survey variance (Pennington, 1985). Although true variability in the underlying population due to population-dynamic processes is reflected in the variability of an index, so too is observational noise arising both from within-survey sampling variability as well as from environmentally driven factors that affect catchability. Low signal-to-noise ratios in abundance indices due to high observational noise reduce one's ability to detect important changes or trends in actual population abundance.

To reduce the impact of white observation noise on time series data, Cleveland and Tiao (1976) developed an approach to noise reduction and smoothing that was based on their knowledge of the ARIMA model (Box and Jenkins, 1976) for an associated unobserved

but underlying stochastic process. Box et al. (1978) extended this approach to address the situation where the ARIMA model for the underlying process was unknown, relying instead on an ARIMA model associated with the observed time series. In general, and certainly in regard to fishery-independent survey data, a model structure for the unobserved, underlying process will not be available. Hence, Box et al.'s (1978) approach will be the norm.

In the situation where the observed time series is stationary, we found that a frequency domain interpretation of Box et al.'s (1978) algorithm is particularly enlightening. When the time series is stationary, observation noise increases the power spectral density (PSD) of the observed process over that of the unobserved process by a fixed amount at all frequencies (Fig. 1). Consequently, the PSD of the unobserved process has the same shape as the PSD of the observed process, but with a fixed amount removed at

Table 2

ARIMA smoothing results for $\ln(x+1)$ transformed time series based on spring surveys. Here, σ_d^2 is the innovation variance for the transformed time series and κ^* is the maximum consistent observation noise variance, scaled to σ_d^2 (i.e., K^*/σ_d^2). The degree of smoothing is based on a visual comparison of the original and smoothed time series.

Species	ARIMA model (p,d,q)	σ_d^2	κ^*	Degree of smoothing
Winter skate	(0,1,1)	0.33	0.52	medium
Little skate	(3,0,4)	0.30	0.14	low
Atlantic herring	(0,1,1)	4.90	0.59	high
Silver hake	(0,0,5)	0.85	0.02	low
Atlantic cod	(0,1,1)	0.47	0.71	high
Haddock	(1,0,3)	0.42	0.29	medium
Yellowtail flounder	(0,1,1)	0.45	0.49	medium
Winter flounder	(0,0,1)	0.33	0.89	high
Atlantic mackerel	(0,0,2)	16.9	0.34	medium

Table 3

ARIMA smoothing results for $\ln(x+1)$ transformed time series based on fall surveys. Here, σ_d^2 is the innovation variance for the transformed time series and κ^* is the maximum consistent observation noise variance, scaled to σ_d^2 (i.e., K^*/σ_d^2). The degree of smoothing is based on a visual comparison of the original and smoothed time series.

Species	ARIMA model (p,d,q)	σ_d^2	κ^*	Degree of smoothing
Winter skate	(2,0,3)	0.17	0.31	medium
Little skate	(3,0,4)	0.12	0.38	medium
Atlantic herring	(0,1,1)	4.75	0.48	medium
Silver hake	(0,1,1)	0.22	0.61	high
Atlantic cod	(1,0,1)	0.55	0.77	high
Haddock	(2,0,3)	0.75	<0.01	low
Yellowtail flounder	(0,1,1)	0.40	0.45	medium
Winter flounder	(0,1,1)	0.40	0.50	medium
Atlantic mackerel	(0,1,1)	7.00	0.84	high

Table 4

For time series consistent with random-walk-plus-uncorrelated-noise models, the table provides a comparison between the estimated observation noise variance (σ_e^2) and the maximum noise variance (K^*). The latter was used to smooth all time series.

Season	Species	$\eta_1 = \sigma_e^2/\sigma_d^2$	σ_d^2	K^*	σ_e^2/K^*
Fall	Atlantic herring	0.392	4.75	2.28	0.82
	Silver hake	0.566	0.22	0.13	0.93
	Yellowtail flounder	0.342	0.40	0.18	0.76
	Winter flounder	0.420	0.40	0.20	0.84
	Atlantic mackerel	0.832	7.00	5.88	0.99
Spring	Winter skate	0.438	0.33	0.17	0.84
	Atlantic herring	0.541	4.90	2.89	0.92
	Atlantic cod	0.680	0.47	0.33	0.96
	Yellowtail flounder	0.399	0.45	0.22	0.81

all frequencies. Because the unobserved PSD must be nonnegative, the maximum observation noise (and thus the maximum noise reduction and smoothing that may occur) consistent with additive white noise corresponds to the minimum value of the observed process's PSD. Presumed higher values for the observation noise would require that the PSD for the unobserved process be negative over some frequency range. Box et al.'s (1978) algorithm computes the maximum possible observation noise and uses a time domain formula to calculate a smoothed, "unobserved" time series consistent with additive white noise for any noise level up to the maximum.

The ARIMA-based noise reduction approach was first applied to fisheries trawl survey data by Pennington (1985), who developed an alternative algorithm to that of Box et al. (1978) for estimating the smoothed time series. This algorithm was subsequently used in several studies (Pennington, 1985; Fogarty et al.¹; Pennington, 1986; Anonymous, 1988, 1993) to smooth time series of abundance indices derived from trawl survey data for the northeast coast of the United States. Of these studies, perhaps only Pennington (1986) constitutes a convincing demonstration of the utility of the ARIMA-based approach to time series noise reduction when the ARIMA model for the underlying process is unknown. Pennington's (1985) demonstration relied on an ARIMA model developed for the (usually unobserved) underlying population that was based on stock assessment results for the particular species considered. In contrast, RWPUN models were assumed *a priori* in Fogarty et al.¹ and Anonymous (1988, 1993) because the short time series (<25 observations per series) considered made identification of the underlying ARIMA models problematic. Only in Pennington (1986) was a model used that was fitted to trawl survey data and tested for appropriateness.

However, substantially longer time series are now available to test the ARIMA-based noise reduction concept. Consequently, to revisit the utility of the ARIMA-based approach for smoothing time series data derived from fisheries-independent trawl survey data, we applied Box et al.'s (1978) approach to smoothing to time series of annual abundance indices derived from the NMFS/NEFSC fisheries-independent bottom trawl survey of nine finfish species during two seasons on Georges Bank. Time series for the fall spanned 40 years (1963–2002), and the spring time series spanned 36 years (1968–2003). The species, comprising two elasmobranchs, three groundfish, two flatfish, and two pelagic schooling species, presented a broad range of life history characteristics (Table 1).

The noise reduction results we obtained varied among species and between seasons. Despite smoothing at the maximum level of noise reduction consistent with each model, very little smoothing was obtained for haddock (fall), little skate (spring), and silver hake (spring). The models for these time series had among the highest moving average orders (3–5). Examination of the PSD for each model in the frequency domain revealed very

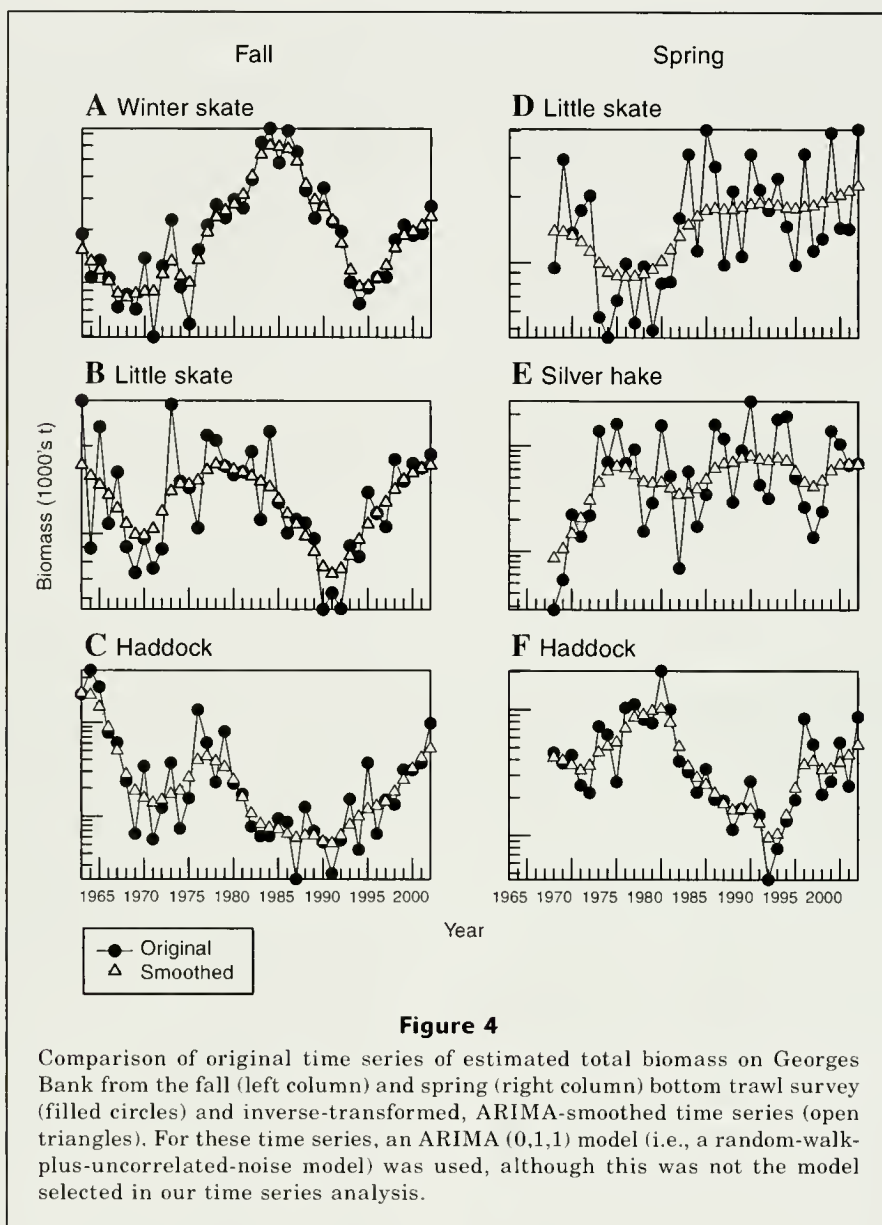
small minima, indicating no scope for noise reduction. Typically, models that had a MA order >2 exhibited substantially less smoothing than models with a MA order ≤ 2 . Models that were of MA order 1 generally resulted in the greatest smoothing. Models that were of MA order 0 did not (and could not) occur.

Of the 18 time series we considered (Tables 2 and 3, Figs. 2 and 3), only half were adequately represented as random-walk-plus-uncorrelated-noise (RWPUN) models. The ARIMA models we developed were varied in structure, ranging from a simple MA(1) model to rather complicated models with multiple parameters. Thus, our results provide evidence against the appropriateness of assuming a particular model structure *a priori* when the objective of the analysis is to identify the underlying dynamic structure of the population. This evidence is further strengthened by the results of Becerra-Munoz et al. (1999), who found only 9 of 52 abundance time series for finfish species from the NMFS/NEFSC bottom trawl survey that corresponded to random walk models.

As an exercise, we also attempted to smooth the nine data sets that were not adequately described as RWPUN models, using this model structure as an *a priori* assumption, even though our analysis indicated that other models were more appropriate. We were not able to estimate convergent models for three species: Atlantic cod (fall), winter flounder (spring), and Atlantic mackerel (spring). For the remaining six time series, the smoothed results appeared to be quite reasonable (Fig. 4), although we obtained little noise reduction when we employed the "correct" ARIMA model. The RWPUN-smoothed time series for haddock (Fig. 4, C and F) were similar to that for spawning biomass derived from virtual population analysis (see Brodziak et al.²), but the smoothed time series for silver hake (Fig. 4E) exhibited higher frequency variability than that found for total biomass with a production model (see Brodziak et al.³). From the standpoint of estimating the unobserved underlying process, these smoothed results should be viewed with some skepticism: the use of the RWPUN model is rather arbitrary in this situation and it may impose artificial structure on the smoothed results. However, it may be that these time series do not meet one of the key assumptions of the noise reduction method: namely that the observation noise is uncorrelated. The ARIMA models for all six time series had MA orders ≥ 3 , and one effect of correlated observation noise could be to increase the MA

² Brodziak, J., M. Traver and L. Col. 2005. Georges Bank haddock. *In* Assessment of 19 northeast groundfish stocks through 2004 (R. K. Mayo, and M. Terceiro, eds.), section 2, p. 30–80. 2005 groundfish assessment review meeting. Northeast Fisheries Science Center, Woods Hole, Massachusetts; 15–19 August 2005. NEFSC Ref. Doc. 05-13. NEFSC, 166 Water Street, Woods Hole, MA 02543.

³ Brodziak, J. K. T., E. M. Holmes, K. A. Sosebee, and R. K. Mayo. 2001. Assessment of the silver hake resource in the Northwest Atlantic in 2000, 134 p. NEFSC Ref. Doc. 01-03. NEFSC, 166 Water Street, Woods Hole, MA 02543.



order of the observed time series beyond that expected for uncorrelated noise.

Of the nine species considered, only three (little skate, Atlantic herring, and flounder) had models that exhibited the same ARIMA order for both the fall and spring surveys. Taken at face value, this would indicate that the other six species exhibited substantially different dynamical processes during the fall and spring that influenced abundance on Georges Bank. One potential mechanism for this could be differential seasonal migration patterns that result in changes in catchability that have different autocorrelation structures. For example, cod are distributed across the bank during the spring survey, but are found only in deeper waters on the periphery of the bank during the fall where they may be less available to the survey. Assuming that all Georges

Bank cod are available to the spring survey, if the fraction of cod available to the survey in the fall is density dependent or is driven by autocorrelated environmental conditions, then the fall survey abundance will exhibit dynamical behavior different from that of the spring survey abundance (note: if this were the case, it would be inappropriate to smooth the fall time series for cod with the ARIMA noise reduction approach applied in our study because, as noted previously, one of the basic assumptions with this approach is that the observation noise is uncorrelated). Other plausible mechanisms can be developed, as well. However, we feel it more likely that the inconsistency in ARIMA order between spring and fall surveys for the same species is an estimation problem and indicates that even a 40-year time series may not be long enough to reduce the variability inher-

ent in ARIMA model estimation to reasonable levels for most species.

Alternative methods, such as locally weighted scatterplot smoothing (LOESS), moving average filters, exponential smoothing filters, Kalman filters, and frequency-domain approaches can be applied to time series to achieve smoother results (e.g., Cleveland and Grosse, 1991; Hamilton, 1994). These approaches typically employ at least one user-determined parameter that can be used to change the amount of smoothing that an algorithm achieves. Generally, one "fiddles" with the adjustable parameters until a "nice," smoothed fit is achieved. However, we think it important to distinguish between these smoothing algorithms and the ARIMA-based noise reduction algorithms. It is quite possible to smooth out real fluctuations in the underlying population process. The principal advantage that we see for the ARIMA-based noise reduction algorithms (used with an appropriate model) over alternative methods is that the former provide a more objective approach to determining an appropriate level of smoothing. As noted previously, Pennington (1985) showed that when a RWPUN model is appropriate, the ARIMA smoothing approach is completely determined by the ARIMA model for the observed time series because it is possible to determine the observation noise variance from the model parameters. In the more general case, Box et al.'s (1978) algorithm at least yields a maximum value for the variance of the observational noise and thus sets an upper limit to the amount of noise reduction and smoothing that can be achieved. For trawl survey data, our results from nine time series where RWPUN models were appropriate (and we can consequently estimate the actual observation noise variance) indicate that smoothing at ~90% of the maximum possible noise reduction level is not an unreasonable default percentage (Table 4).

One drawback to the greater application of ARIMA-based noise reduction methods to time series data is the lack of an integrated software package that allows a user 1) to quickly evaluate an appropriate ARIMA model for a given time series, and 2) to calculate the smoothed time series. We used SAS for the first step and MATLAB for the second, but we found this arrangement rather awkward and burdensome. However, econometrically oriented software packages such as ForecastPro⁴ or AutoBox⁵ that automate model selection may substantially simplify the first step even if they don't address the second step.

On the whole, ARIMA-based time series models appear to provide the basis for a more objective approach to reducing observation noise in time series data, including time series of fishery abundance indices derived from trawl survey data, than do more conventional

smoothing approaches. In the absence of additional information regarding the level of observation noise, we recommend smoothing trawl survey data at 90% of the maximum possible noise reduction level. We also suggest that development of an integrated software package for implementing ARIMA-based noise reduction will facilitate future use of this method.

Finally, if a smoothed time series is desired (e.g., for graphical presentation only), then use of a RWPUN model in lieu of a model-fitting exercise will generally yield a curve pleasing to the eye. Alternatively, other methods such as LOESS could be employed to generate the smoothed results. However, if the resulting time series is to be used for further analysis of the dynamical behavior of the fish stock, we strongly recommend that a model-fitting approach be used to identify the most appropriate ARIMA model for the observed time series, from which the time series for the unobserved, underlying process can be computed. Otherwise, real fluctuations in the underlying process may be over-smoothed, resulting in an apparent dynamical behavior that displays little variability. This oversmoothing, in turn, may lead to erroneous conclusions being drawn regarding, for example, the resiliency of a stock to exploitation or environmental change, and to perhaps concomitant errors being propagated in advice provided to fishery managers.

Acknowledgments

We would like to thank M. Pennington for his insightful comments on an early version of this manuscript. The comments and suggestions from two anonymous reviewers were also very helpful and are much appreciated. This work was supported by the National Research Council, which provided funding support for one of us (Stockhausen) as a postdoctoral fellow at the Northeast Fisheries Science Center.

Literature cited

- Akaike, H.
1973. Information theory as an extension of the maximum likelihood principle. *In* Second international symposium on information theory (B. N. Petrov, and F. Csaki, eds.), 267-281. Akademiai Kiado, Budapest, Hungary.
- Anonymous.
1988. An evaluation of the bottom trawl survey program of the Northeast Fisheries Center. NOAA Tech. Memo. NMFS-F/NEC-52, 83 p. Northeast Fish. Center, 166 Water St., Woods Hole, MA 02543.
1993. Status of fishery resources off the northeastern United States for 1993. NOAA Tech. Memo. NMFS-F/NEC-101, 140 p. Northeast Fish. Center, 166 Water St., Woods Hole, MA 02543.
- Azarovitz, T. R.
1981. A brief historical review of the Woods Hole Laboratory trawl survey time series. *In* Bottom trawl surveys (W. G. Doubleday, and D. Rivard, eds.), 62-67. Can. Spec. Pub. Fish. Aquat. Sci., vol. 58.

⁴ Business Forecast Systems, Inc. 2006. Website: <http://www.forecastpro.com/products/fpfamily/index.html> (accessed on 29 March 2006).

⁵ Automatic Forecasting Systems. 2003. Website: <http://www.autobox.com/autoboxdesc.htm> (accessed on 29 March 2006).

- Becerra-Munoz, S., D. B. Hayes, and W. W. Taylor.
1999. Stationarity and rate of damping of modeled indices of fish abundance in relation to their exploitation status in the Northwest Atlantic Ocean. *Ecol. Mod.* 117:225-238.
- Box, G. E. P., S. C. Hillmer, and G. C. Tiao.
1978. Analysis of seasonal time series. *In* Seasonal analysis of economic time series (A. Zellner, ed.), 309-334. U.S. Dep. Comm., Washington, DC.
- Box, G. E. P., and G. M. Jenkins.
1976. Time series analysis: forecasting and control, 575 p. Holden-Day, Oakland, CA.
- Byrne, C. J., T. R. Azarovitz, and M. P. Sissenwine.
1981. Factors affecting variability of research trawl surveys. *Can. Spec. Pub. Fish. Aquat. Sci.* 58:238-273.
- Clark, S. H.
1979. Application of bottom trawl survey data to fish stock assessment. *Fisheries* 4:9-15.
- Cleveland, W. S., and E. Grosse.
1991. Computational methods for local regression. *Stats. and Comp.* 1:47-62.
- Cleveland, W. P., and G. C. Tiao.
1976. Decomposition of season time series: a model for the Census X-11 program. *J. Am. Stat. Assoc.* 71:581-587.
- Collie, J. S., and M. P. Sissenwine.
1983. Estimating population size from relative abundance data measured with error. *Can. J. Fish. Aquat. Sci.* 40:1971-1983.
- Edwards, R. L.
1968. Fishery resources of the North Atlantic area. *In* The future of the fishing industry in the United States (D. W. Gilbert, ed.), p. 52-60. Univ. Washington, Seattle, WA.
- Enders, W.
2004. Applied econometric time series, 460 p. John Wiley and Sons, Inc., Hoboken, NJ.
- Grosslein, M. D.
1969. Groundfish survey program of BCF Woods Hole. *Comm. Fish. Rev.* 31:22-30.
- Hamilton, J.
1994. Time series analysis, 820 p. Princeton Univ. Press, Princeton, NJ.
- Harley, S. H., and R. A. Myers.
2001. Hierarchical Bayesian models of length-specific catchability of research trawl surveys. *Can. J. Fish. Aquat. Sci.* 58:1569-1584.
- Helser, T. E., and D. B. Hayes.
1995. Providing quantitative management advice from stock abundance indices based on research surveys. *Fish. Bull.* 93:290-298.
- Lloret, J., J. Leonart, and I. Sole.
2000. Time series modeling of landings in northwest Mediterranean Sea. *ICES J. Mar. Sci.* 57:171-184.
- Nogueira, E., F. F. Perez, and A. F. Rios.
1998. Modelling nutrients and chlorophyll a time series in an estuarine upwelling ecosystem (Ria de Vigo: NW Spain) using the Box-Jenkins approach. *Estuar. Coast. Shelf Sci.* 46:267-286.
- Pennington, M.
1985. Estimating the relative abundance of fish from a series of trawl surveys. *Biometrics* 41:197-202.
1986. Some statistical techniques for estimating abundance indices from trawl surveys. *Fish. Bull.* 84: 519-525.
- Reid, R. N., F. P. Almeida, and C. A. Zetlin.
1999. Fishery-independent surveys, data sources, and methods. NOAA Tech. Memo. NMFS-NE-122. Northeast Fish. Sci. Center, 166 Water St., Woods Hole, MA 02543.

Appendix

For the convenience of the reader, we summarize here Box et al.'s (1978) algorithm to calculate the coefficients of the smoothing polynomial $\omega(B)$. Recall from Equation 14 that

$$\omega(B) = \left[1 - \frac{\sigma_e^2}{\sigma_d^2} \frac{\varphi(B)\varphi(F)}{\eta(B)\eta(F)} \right], \quad (\text{A.1})$$

where $\varphi(B)$ is a polynomial of order $P+D$ and $\eta(B)$ is a polynomial of order Q . Because $Q \geq P+D$, one can write

$$\begin{aligned} \varphi(B) &= 1 - \varphi_1 B^1 - \varphi_2 B^2 \dots - \varphi_Q B^Q, \\ \eta(B) &= 1 - \eta_1 B^1 - \eta_2 B^2 \dots - \eta_Q B^Q, \end{aligned} \quad (\text{A.2})$$

where $\varphi_j = 0$ for $j > P+D$.

First, define

$$C(B) \equiv \frac{\varphi(B)}{\eta(B)}; C(B) = 1 + C_1 B^1 + C_2 B^2 + \dots \quad (\text{A.3})$$

One can solve for the coefficients of C using an iterative process by recognizing that the coefficients of each power of B in the following expression must be zero:

$$0 = \varphi(B) - \eta(B)C(B).$$

Consequently, one obtains

$$C_1 = \eta_1 - \varphi_1; C_j = \eta_j - \varphi_j + \sum_{i=1}^{j-1} C_{j-i} \eta_i, j = 2, \dots, Q \quad (\text{A.4})$$

and higher order coefficients of C (i.e., for $j > Q$) can be computed recursively using the relation

$$C_j = \sum_{i=1}^Q C_{j-i} \eta_i. \quad (\text{A.5})$$

Next, define

$$X(B, F) \equiv C(B) \frac{\varphi(F)}{\eta(F)} \quad (\text{A.6})$$

$$\text{where } X(B, F) = X_0 + \sum_{j=1}^{\infty} X_j (B^j + F^j).$$

From this definition, one obtains

$$X(B, F)\eta(F) \equiv C(B)\varphi(F). \quad (\text{A.7})$$

The largest degree of F on the righthand side of this equation is Q . By matching coefficients of F^j on both sides of the equation, Box et al. (1978) found, for $j=0,1,\dots,Q$, that

$$\eta X = C\varphi, \quad (\text{A.8})$$

where \mathbf{X} , φ are $Q+1$ column vectors $\mathbf{X}^T=(X_0, X_1, \dots, X_Q)$, $\varphi^T=(1, -\varphi_1, \dots, -\varphi_Q)$ and η , \mathbf{C} are $(Q+1) \times (Q+1)$ matrices such that

$$\mathbf{C} = \begin{bmatrix} 1 & C_1 & \cdot & \cdot & C_Q \\ & \cdot & \cdot & \cdot & \cdot \\ & & \cdot & \cdot & \cdot \\ & & & \cdot & C_1 \\ \mathbf{0} & & & & 1 \end{bmatrix} \quad (\text{A.9})$$

$$\eta = \begin{bmatrix} 1 & -\eta_1 & \cdot & \cdot & -\eta_Q \\ -\eta_1 & \cdot & \cdot & \cdot & -\eta_Q \\ \cdot & \cdot & \cdot & \cdot & \cdot \\ \cdot & \cdot & \cdot & \cdot & \cdot \\ -\eta_Q & & & & \mathbf{0} \end{bmatrix} + \begin{bmatrix} \mathbf{0} & 0 & & & \mathbf{0} \\ 0 & 1 & & & \\ \cdot & \eta_1 & \cdot & & \\ \cdot & & & & \\ 0 & -\eta_{Q-1} & \cdot & -\eta_1 & 1 \end{bmatrix}.$$

Thus, Equations A.8 and A.9 define a set of $Q+1$ equations in $Q+1$ unknowns (X_0, X_1, \dots, X_Q) which can be solved for by matrix inversion such that

$$\mathbf{X} = \eta^{-1} \mathbf{C}\varphi. \quad (\text{A.10})$$

For $j > Q$, the X_j 's are computed recursively by using the relation

$$X_j = \sum_{i=1}^Q X_{j-1} \eta_i. \quad (\text{A.11})$$

Finally, the coefficients of $\omega(B)$ are given by

$$\omega_0 = 1 - \frac{\sigma_e^2}{\sigma_d^2} X_0; \quad \omega_j = -\frac{\sigma_e^2}{\sigma_d^2} X_j, \quad j=1, \dots. \quad (\text{A.12})$$

Abstract—The eastern Steller sea lion (*Eumetopias jubatus*) population comprises animals that breed along the west coast of North America between California and southeastern Alaska. There are currently 13 major rookeries (>50 pups): five in southeastern Alaska, three in British Columbia, two in Oregon, and three in California. Overall abundance has increased at an average annual rate of 3.1% since the 1970s. These increases can largely be attributed to population recovery from predator-control kills and commercial harvests, and abundance is now probably as high as it has been in the last century. The number of rookeries has remained fairly constant ($n=11$ to 13) over the past 80 years, but there has been a northward shift in distribution of both rookeries and numbers of animals. Based on the number of pups counted in a population-wide survey in 2002, total pup production was estimated to be about 11,000 (82% in southeastern Alaska and British Columbia), representing a total population size as approximately 46,000–58,000 animals.

Abundance and distribution of the eastern North Pacific Steller sea lion (*Eumetopias jubatus*) population

Kenneth W. Pitcher¹

Peter F. Olesiuk²

Robin F. Brown³

Mark S. Lowry⁴

Steven J. Jeffries⁵

John L. Sease⁶

Wayne L. Perryman⁴

Charles E. Stinchcomb⁴

Lloyd F. Lowry⁷

Email address for K. W. Pitcher:
ken_pitcher@fishgame.state.ak.us

¹ Division of Wildlife Conservation
Alaska Department of Fish and Game
525 West 67th Avenue
Anchorage, Alaska 99518

² Pacific Biological Station
Department of Fisheries and Oceans Canada
Nanaimo, BC V9T 6N7, Canada

³ Marine Mammals Research Program
Oregon Department of Fish and Wildlife
7118 NE Vandenberg Avenue
Corvallis, Oregon 97330

⁴ Southwest Fisheries Science Center
National Marine Fisheries Service, NOAA
8604 La Jolla Shores Drive
La Jolla, California 92037

⁵ Marine Mammal Investigations
Washington Department of Fish and Wildlife
7801 Phillips Road SW
Lakewood, Washington 98498

⁶ National Marine Mammal Laboratory
National Marine Fisheries Service, NOAA
7600 Sand Point Way, NE
Seattle, Washington 98115

⁷ 73-4388 Pa'iaha Street
Kailua-Kona, Hawaii 96740

The Steller sea lion (*Eumetopias jubatus*) is the largest of the Otariidae and inhabits the North Pacific Rim from California to Japan. Individuals breeding at rookeries¹ located along the west coast of North America from California northward through southeastern Alaska (Fig. 1) to 144°W longitude form a distinct population segment, generally referred to as the eastern population. Historically, exchange of reproductive females with the Steller sea lion population to the north and west of 144°W longitude has been extremely low as shown by genetic studies (Bickham et al., 1996) and resightings of marked animals (Raum-Suryan et al., 2002). This indicates that population changes have been driven by birth and death rates within each population because immigration and emigration of breeding females among populations were too infrequent to affect population dynamics. More recent genetic analyses have confirmed the ancient divergence of the eastern and western populations. However, two new rookeries (White Sisters and Graves Rocks, Fig. 1) at

the northern end of the range of the eastern population appear to have been colonized by females from both populations (O'Corry-Crowe et al., 2005). The number of western female immigrants to the eastern population has been small (in the 100s) to date, has not had a major impact on the growth dynamics of the overall eastern population and has been limited to the extreme northern range of the eastern population. However, the presence of breeding female immigrants from the western population within the range of the eastern population indicates that our prior assumption that population dynamics of the eastern population was completely driven by internal rates of reproduction and survival was incorrect for the past several years.

¹ For purposes of this paper, rookeries are arbitrarily defined as traditional, terrestrial sites where >50 pups are born annually. Other terrestrial sites used by sea lions are referred to as haulouts. Small numbers of pups are also born on haulouts, but probably constitute <1% of the total <100 in the eastern population.

Manuscript submitted 28 March 2006
to the Scientific Editor.

Manuscript approved for publication
21 June 2006 by the Scientific Editor.
Fish. Bull. 107:102–115 (2007).

In recent years, attention has focused on the western Alaskan population because of a precipitous decline since the 1970s (Loughlin et al., 1992; Trites and Larkin, 1996) resulting in an "endangered" classification under the U.S. Endangered Species Act. The eastern population is currently classified as "threatened." Abundance from southern Oregon through southeastern Alaska has generally shown an increasing trend (Calkins et al., 1999; Brown et al.²; DFO, 2003), whereas numbers in southcentral California have declined substantially (Le Boeuf et al.³; Hastings and Sydeman, 2002). This is the first detailed population-wide status evaluation of abundance, trend, and distribution with a historical perspective for the eastern population. We also present the results of the first population-wide census of pup production conducted in 2002 and apply life-table analysis to estimate total population size.

In our study, we reviewed records of Steller sea lion abundance, with particular emphasis on data collected at rookeries. Some counts date back to the early 1900s, but early surveys were not systematic and methods lacked standardization, and some of the counts may have been affected by culling and hunting activities. Although these earlier survey methods preclude formal statistical analyses, the historical data provide a general sense of gross changes in abundance and distribution. Systematic surveys began in most regions along the west coast in the 1970s, but counting techniques varied among the researchers and agencies conducting the surveys, and surveys were not coordinated between jurisdictions. Nevertheless, these time series indicate changes in relative abundance within each geopolitical region. In recent years, there has been an effort to compare and calibrate counting techniques, especially for pups (Snyder et al., 2001; P. F. Olesiuk, unpubl. data), and to synthesize survey results (Loughlin et al., 1992).

Materials and methods

Count data used to estimate population trends between the late 1970s and 2004 were of two types: 1) counts of pups obtained between late June and early July (at the end of the pupping season) when most pups are <1 month of age, and 2) counts of juveniles and adults ≥ 1 year of

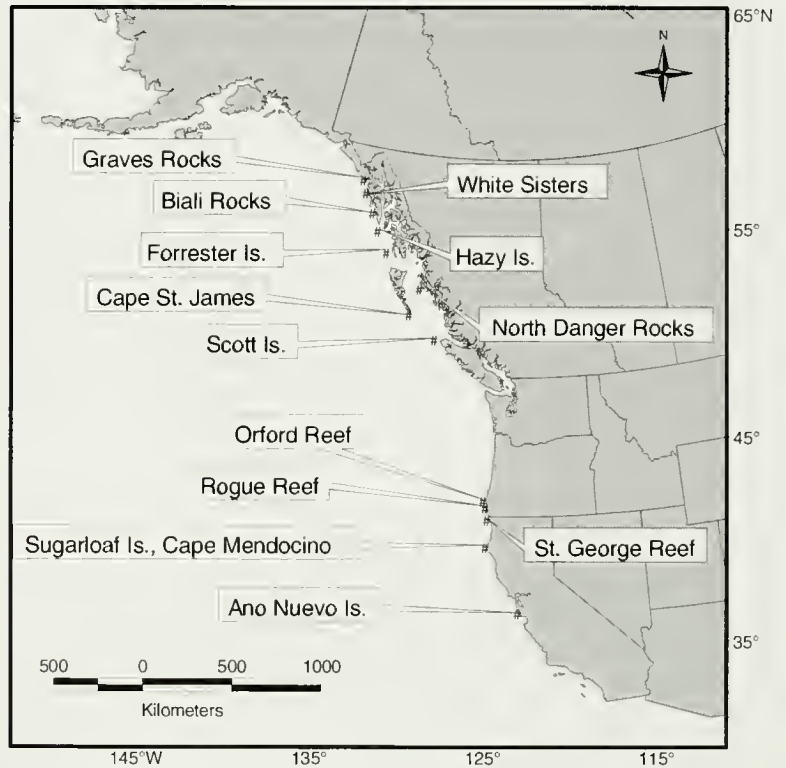


Figure 1

Geographic range of the eastern Steller sea lion (*Eumetopias jubatus*) population showing locations of major (>50 pups born) breeding rookeries.

age (i.e., nonpups) obtained from mid June to early July (mid to late in the breeding season). Steller sea lions normally give birth between late May and early July and breed between late May and mid July, although timing of these events varies somewhat geographically (Pitcher et al., 2001). Counts of pups are the preferred index to population size for many species of pinnipeds (Berkson and DeMaster, 1985). For the Steller sea lion, the vast majority of births occur at traditional rookeries, and because pups are confined to land for the first month of life, surveys of rookeries at the end of the pupping season provide a nearly complete estimate of annual pup production.

Pups are more difficult to count than nonpups because of their small size and dark color. This disadvantage is especially pronounced for counts made at oblique angles from aircraft circling rookeries or from vessels adjacent to the sites. From the mid 1970s to the late 1990s, pups were usually counted by placing people on rookeries, herding nonpups into the water, and tallying the number of pups while walking through the rookery (Calkins and Pitcher, 1982). However, the methods of obtaining such counts are disruptive to sea lions (Lewis, 1987), and counts may not be possible where rookeries are protected in parks or ecological and nature reserves. More recently, vertical 126-mm format aerial photography has been shown to be as accurate and far less disruptive (Snyder et al., 2001) for counting pups. Depending on the physical size,

² Brown, R. F., S. D. Riemer, and B. E. Wright. 2002. Population status and food habits of Steller sea lions in Oregon. Report from Oregon Dept. of Fish and Wildlife to Oregon State Univ. Contract F0225A-01, 17 p. Oregon Department of Fish and Wildlife, Marine Mammal Research Program, 7118 NE Vandenberg Ave., Corvallis, OR 97330.

³ Le Boeuf, B. J., K. Ono, and J. Reiter. 1991. History of the Steller sea lion population at Año Nuevo Island, 1961–1991. NOAA Admin. Report NMFS-SWFSC LJ-91-45C, 9 p.

substrate, and topography of rookeries, high-quality oblique 35-mm photographs can sometimes provide counts of pups with an acceptable accuracy (P. F. Olesiuk, unpubl. data). In 2002, vertical 126-mm format photography was used at all rookeries within the range of the eastern population to obtain the first estimate of total pup production (pup numbers at some rookeries had been reported previously but not for all rookeries in a single year). We have included additional counts of pups made at some sites between 2003 and 2005 for trend analyses within geographic subareas. However, only counts from the complete population-wide survey in 2002 were used to estimate total population abundance in order to provide an estimate for a single point in time.

Few reliable counts of pups were available before the 1970s, but counts of non-pups on rookeries have dated back to the early 1990s. Non-pups are easier to count, and there tends to be a high degree of correlation for counts of non-pups between oblique 35-mm format and vertical 126-mm format images (Fritz and Stincomb, 2005). However, some Steller sea lions, particularly juveniles, range widely (Raum-Suryan et al., 2002); therefore counts at haulouts within a particular geographic area may not necessarily represent the number of animals supported by local rookeries, although breeding animals show a higher degree of site fidelity. The number and proportion of various sex and age classes of non-pups that are hauled out varies with season, time of day, and (in some cases) with tide (Winthrow, 1982; Calkins et al., 1999).

Counts from the 2002 population-wide survey (Table 1) indicated a fairly tight relationship between the number of pups and nonpups counted on rookeries (Fig. 2). A similar pattern was noted for rookeries in British Columbia and the relationship persisted over the three decades concurrent pup and nonpup counts were available (P. F. Olesiuk, unpubl. data). The historical counts of nonpups (or total animals where pups and nonpups were not distinguished) on rookeries thus likely provide a general index of the size of the breeding population associated with each rookery.

Systematic surveys have been conducted to monitor trends of the eastern Steller sea lion population, but methods and schedules have varied depending on the agency conducting the surveys. In southeastern Alaska, the Alaska Department of Fish and Game periodically conducted ground counts of pups on rookeries from 1979 through 1998, and used vertical 126-mm format photography to count pups since 1998. In British Columbia, the Department of Fisheries and Oceans has conducted province-wide aerial surveys of rookeries and haulout sites at 2–5 year intervals since the early 1970s, using oblique 35-mm format photography to count both pups and nonpups. In 1998 and 2002, both pups and nonpups were counted at British Columbia rookeries with the use of vertical 126-mm format photography. There are no Steller sea lion rookeries in Washington, but the Washington

Table 1

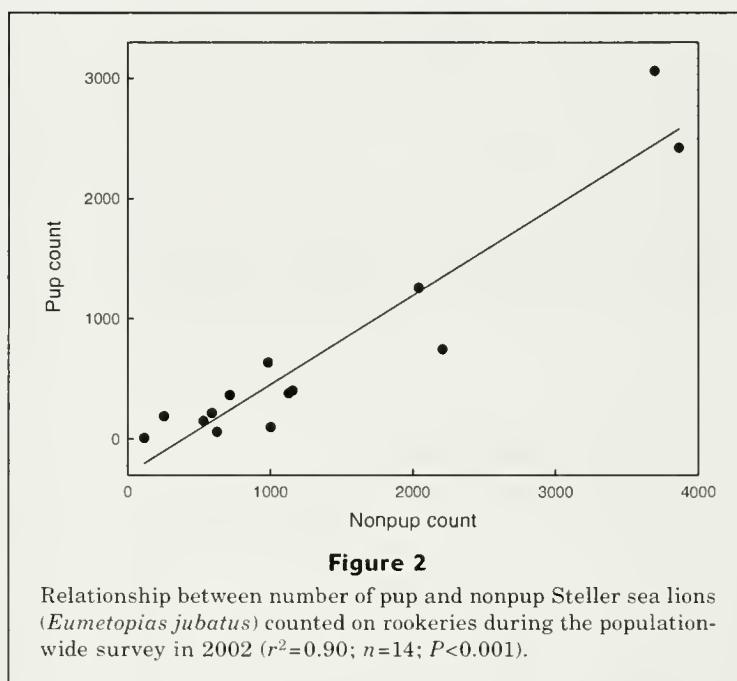
Counts of pups and nonpups for each rookery and for all haulout sites combined by region for the population-wide survey of the eastern Steller sea lion (*Eumetopias jubatus*) population in 2002. Pup counts were made from vertical 126-mm format images, and nonpup counts from either vertical 126-mm format images or oblique 35-mm photographs. Nonpup counts included counts of pups at the indicated number of major sites (used by >50 animals on a regular basis during the breeding season), as well as counts of pups at numerous minor sites and counts of a few scattered animals.

Site	Pups	Nonpups
Southeastern Alaska		
Graves Rocks	98	1001
White Sisters	403	1156
Biali Rocks	59	625
Hazy Islands	1257	2050
Forrester Island	3060	3699
Haulout sites (20 major sites)	9	6752
Southeastern Alaska total	4886 (49%)	15,283 (43%)
British Columbia		
North Danger Rocks	207	592
Cape St. James	655	982
Scott Islands	2451	3865
Haulout sites (24 major sites)	5	6681
British Columbia total	3318 (33%)	12,120 (34%)
Washington		
Haulout sites (2 major sites)	0 (0%)	651 (2%)
Oregon		
Orford Reef	382	1178
Rogue Reef	746	1264
Haulout sites (7 major sites)	8	1727
Oregon total	1136 (11%)	4169 (12%)
California		
Saint George Reef	367	716
Sugarloaf Island-Cape Mendocino	150	588
Año Nuevo Island	189	255
Haulout sites (6 major sites)	7	1543
California total	713 (7%)	3102 (9%)
Eastern population	10,053	35,325

Department of Fish and Wildlife has conducted numerous aerial surveys of haulout sites during the breeding season using oblique 35-mm format photography since 1978. In Oregon, the Oregon Department of Fish and Wildlife has conducted state-wide aerial surveys of nonpups on rookeries and haulouts using oblique 35-mm format photography on a nearly annual basis since the mid-1970s and has periodically obtained ground, or more recently vertical 126-mm format or high-resolution digital 35-mm format, pup counts. In California, the National Marine Fisheries Service, Southwest Fisheries Science Center, conducted statewide surveys during early July beginning in 1996 using vertical 126-mm format photography to count pups and nonpups at all rookeries and haulout sites. Time series of counts that were obtained with assorted methods were also available for some rookeries in California dating back to the 1970s. Although these surveys provide reliable information on changes in relative abundance within each region or at a particular rookery, they are difficult to synthesize into a population-wide assessment because of uncoordinated survey schedules and methods. Given the consistency within, but inconsistency between, these geo-political jurisdictions, we assessed trends in abundance by region (southeastern Alaska, British Columbia, Washington, Oregon, and California). Counts for each region were converted to natural logarithms and then regressed on year to determine average annual population growth rates.

We estimated the total population size in 2002 from the predicted ratio of pups to nonpups in the population (Calkins and Pitcher, 1982; Trites and Larkin, 1996). From life tables for a stable sea lion population in the Gulf of Alaska, Calkins and Pitcher (1982) estimated total population size to be about 4.5 times the number of pups born. In order to apply this approach to the eastern population, which was not stable but increasing (see "Results" section), we conducted sensitivity analyses to determine how this multiplier varies with population growth rate (λ) by incrementally changing each of the life history parameters that affect it, namely juvenile mortality rates, adult mortality rates, age at maturation, and fecundity rates (Lotka, 1907; Cole, 1954).

We also reviewed historical records of Steller sea lion abundance in an attempt to relate current population size with abundance prior to the initiation of standardized surveys. Although these records provide insights into relative population levels, caution must be used because the older counts were obtained by a variety of methods and the seasonal timing of counts was inconsistent. In most cases the counts were made by professional biologists or naturalists hired by government agencies to conduct sea lion investigations, and special trips were made to rookeries to obtain first-hand counts; therefore it is unlikely numbers were grossly in-



accurate. Because of the *ad hoc* nature of these counts, it was difficult to synthesize them into even a regional estimate of abundance, or to conduct statistical analyses; therefore these counts were generally examined on a rookery-by-rookery basis (Appendix).

Results

Southeastern Alaska

Counts of Steller sea lion pups in southeastern Alaska increased from 2219 in 1979 to 5510 in 2005 (Fig. 3A), representing an average annual rate of increase of 3.2% ($r^2=0.91$; $n=10$; $P<0.001$). Prior to the early 1980s, the only rookery in southeastern Alaska was the Forrester Island complex. Only 50–100 animals were recorded when the site was first noted in the 1920s, and 350 animals were recorded when the site was revisited in 1945, and there was no mention of pupping in either case (Rowley, 1929; Imler and Sarber, 1947). Thus, although count data are extremely limited, it appears that Steller sea lion abundance was probably quite low in southeastern Alaska during the first half of the 20th century. Counts are not available, but the Forrester Island rookery must have grown dramatically through the 1950s and 1960s (Fig. 4A). By the time the first aerial survey was conducted in 1961, Forrester Island had grown to about one-third its current size in terms of both the numbers of pups and nonpups (Bigg, 1985). However, increases at Forrester Island appear to have slowed since the late 1970s, showing only a slight increase in pup production (0.6% per year; $r^2=0.40$; $n=13$; $P=0.021$) and no discernible increase in the number of nonpups ($r^2=0.22$; $n=12$; $P=0.125$).

With the slowing of growth on Forrester Island, several new rookeries were established in southeastern Alaska (Calkins et al., 1999) (Appendix I). Hazy Islands were a substantial haulout in the 1950s (Mathisen and Lopp, 1963), but pup counts increased after they were first observed in 1979 (13% per year, $r^2=0.76$; $n=11$; $P<0.001$). White Sisters developed into a rookery in the early 1990s and counts of pups also increased rapidly (16% per year, $r^2=0.87$; $n=10$; $P<0.001$). In recent years, Graves Rocks and Biali Rocks appear to be developing into rookeries; 175 and 100 pups were counted respec-

tively at the two sites in 2005. Growth of these four new rookeries accounted for about 48% of the increase in total pup production in southeastern Alaska during the 1980s, and for about 74% of the total increase since 1990.

In addition to the five rookeries, sea lions use about 20 major haulout sites (>50 animals) and several smaller sites in southeastern Alaska on a regular basis during the breeding season, as well as numerous other sites during the nonbreeding season. During the 2002 survey, a total of 6752 nonpups were counted at haulout sites and another 8531 nonpups were counted at rookeries (Table 1).

British Columbia

There are currently three Steller sea lion rookeries in British Columbia: the Scott Island complex (Triangle, Beresford-Maggot, and Sartine Islands), Cape St. James, and North Danger Rocks. Counts of pups from oblique 35-mm format photographs increased from 941 in 1971 to 3276 in 2002 (Fig. 3B), representing an average annual rate of increase of 3.2% ($r^2=0.71$; $n=9$; $P=0.005$), similar to the overall rate observed in southeastern Alaska. However, piecewise regressions provide a better fit to the time series of pup counts, indicating that most of this increase has occurred since the 1980's ($r^2=0.85$; $n=9$; $P=0.002$). Significant increases in pup production ($P<0.005$) were evident at all three rookeries (Appendix), but mean rates varied among sites (3.7% at Scott Islands, 2.0% at Cape St. James, and 2.7% on North Danger Rocks). Numbers of nonpups on rookeries also increased significantly ($r^2=0.89$; $n=9$; $P<0.001$), paralleling the increases in pup production (Fig. 3B).

Counts on rookeries in British Columbia date back to 1913 (Newcombe and Newcombe, 1914) and indicate breeding populations were historically large (Fig. 4B). Extensive sea lion reduction programs were conducted in British Columbia from 1912 through 1966, and attempts were made to commercially harvest sea lions during the 1960s. One major rookery, the Sea Otter Group, was eradicated by intensive control efforts during the 1920s and 1930s. The site was visited each year toward the end of the pupping season and all pups and as many nonpups as possible were killed, and by about 1940 it was no longer used as a rookery. Predator-control kills and commercial harvests in British Columbia continued into the 1960s and impacted all rookeries, and the breeding population was reduced to about 30% of peak levels by the late 1960s (Bigg, 1985). It appears that numbers at Scott Islands have fully recovered from these kills, but numbers at the two other rookeries are still below historical peak levels (Appendix).

Sea lions also currently use 24 major haulout sites (>50 animals) in British Columbia on a regular basis during the breeding season, up from 18 sites when systematic province-wide surveys were initiated in the early 1970s (Bigg, 1985). Numbers of animals counted on these sites increased at rate of 4.0% since the early 1970s ($r^2=0.82$; $n=9$; $P<0.001$), which is not significantly different from

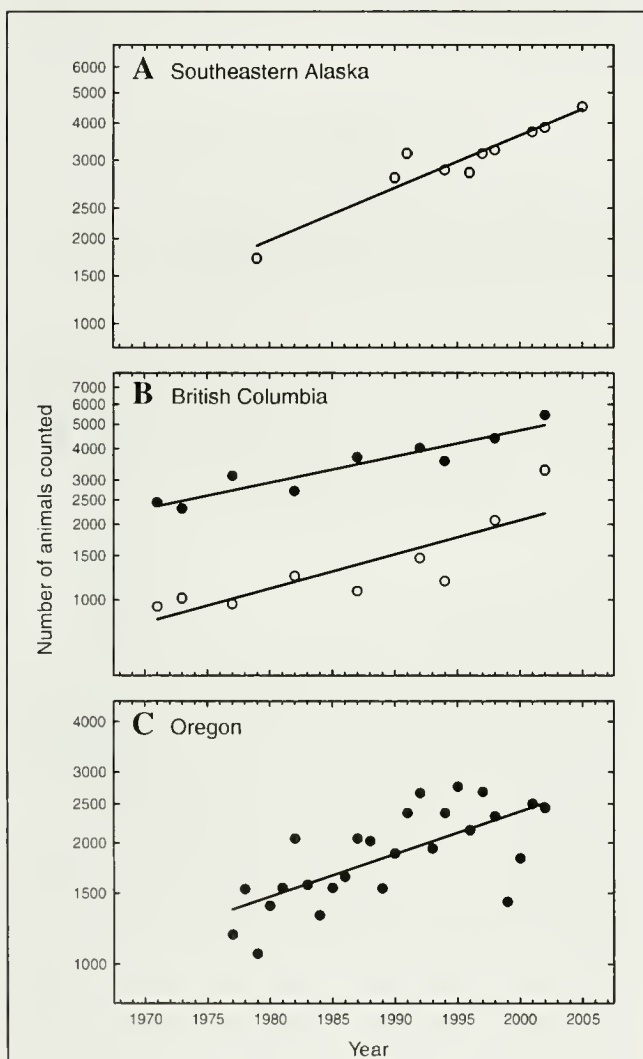


Figure 3

Recent trends in counts of Steller sea lion (*Eumetopias jubatus*) pups (○) and nonpups (●) on rookeries in (A) Southeastern Alaska, (B) British Columbia, and (C) Oregon. These areas combined account for over 90% of pup production in the eastern population. Survey techniques were standardized within each region, but differed among regions. The slopes are all statistically significant ($P<0.001$), and none differed significantly from the overall rate of increase of 3.1%.

the rate of growth observed on rookeries. During the 2002 survey, 6681 nonpups were counted on haulout sites, and another 5439 on rookeries (Table 1).

Washington

There are no rookeries in Washington, but Steller sea lions are found along the coast throughout the year. Four haulouts, including two major sites (>50 animals), are regularly used during the breeding season. Since 1989, surveys have been conducted almost annually, and numbers of sea lions counted have increased at an average annual rate of 9.2% ($r^2=0.38$; $n=37$; $P<0.001$). These animals are assumed to be immature animals and nonbreeding adults associated with rookeries from other areas. Juvenile sea lions branded as pups on Forrester Island in southeastern Alaska (Raum-Suryan et al., 2002) and on Rogue Reef in Oregon (R. F. Brown, unpubl. data) have been observed in Washington.

Older records indicate that current abundance on the Washington coast is reduced from historical levels (Fig. 4C). Between 2000 and 3000 Steller sea lions were reported to be present during August and September of 1914, 1915, and 1916 on Jagged Island (Kenyon and Scheffer, 1959), compared with a maximum statewide breeding season count of 847 during 1978–2001. Washington State Department of Fisheries offered a bounty of \$8.00 for sea lions between 1944–48, but in 1949 this was reduced to \$3.00 and limited to inside waters because aerial patrols indicated that the main coastal haulouts at Jagged Island and Split Rock had been reduced from 600 sea lions in the 1930s to fewer than 100 by 1949 (Scheffer, 1950). Only sporadic counts were available for individual sites during the 1950s and 1960s, but they indicate that few sea lions (<100 animals) were present during the breeding season and that total abundance did not exceed 500 during any season by the 1950s (Scheffer, 1950; Kenyon and Scheffer, 1959).

Oregon

Steller sea lions breed and pup at two rookeries, located at Rogue Reef and Orford Reef, and occupy seven major haulout sites in Oregon during the breeding season. The total number of nonpup sea lions on rookeries increased from 1186 in 1977 to 2442 in 2002 (Fig. 3C), representing an average annual rate of increase of 2.5% ($r^2=0.49$; $n=26$; $P<0.001$). Although not as well documented, pup numbers also appear to have increased. In 1990, 492 and 298 pups were observed during ground counts at Rouge Reef and Orford Reef respectively, compared with 746 and 382 pups on 126 mm format images in 2002 (2.3% average annual rate of increase). During the 2002 population-wide survey, an additional 1727 nonpups were counted at haulout sites in Oregon (Table 2).

Historical data on Steller sea lion abundance in Oregon are few (Fig. 4D). Pearson and Verts (1970) counted 862 animals (including some pups) during a state-wide aerial

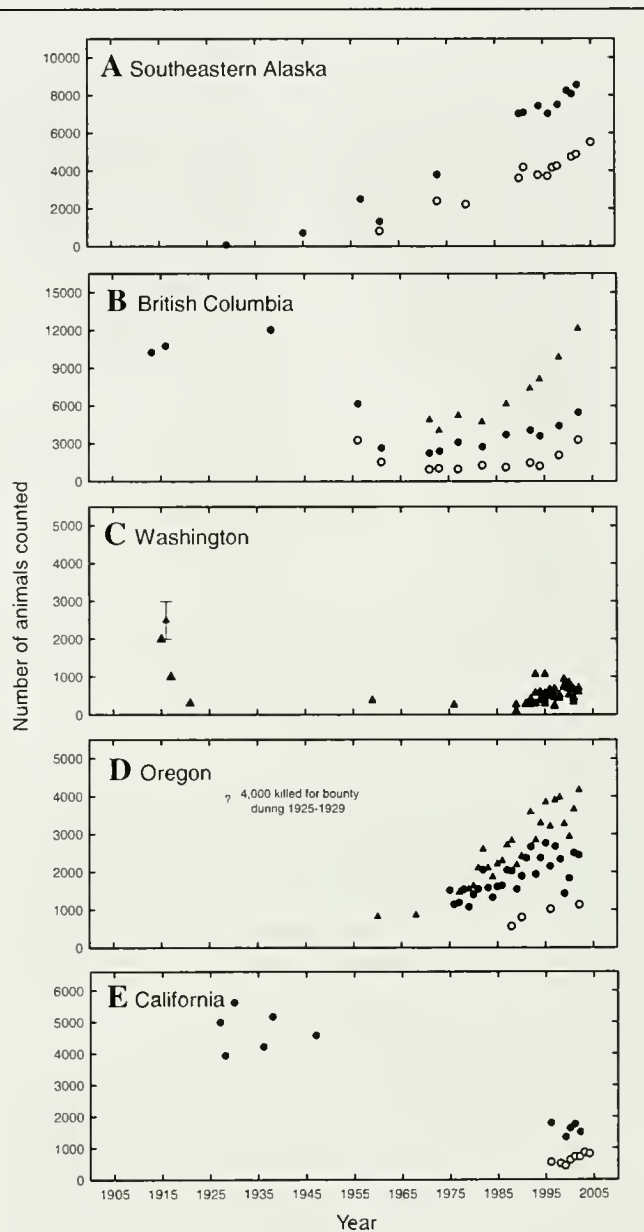


Figure 4

Historical counts over the last century of Steller sea lion (*Eumetopias jubatus*) pups (○), non-pups on rookeries (●), and total nonpups on rookeries and haulouts (▲) for (A) Southeastern Alaska, (B) British Columbia, (C) Washington, (D) Oregon, and (E) California.

survey in June 1968, somewhat lower than the 1977 nonpup count of 1461 animals. The largest rookery was Orford Reef, where 475 animals, including pups, were counted. Interestingly, only 125 animals were reported at Rogue Reef, which is currently the largest rookery in Oregon, and Pearson and Verts (1970) suggested that it was no longer used as a rookery. Earlier counts are lacking, but the population was presumably substantially larger in the 1920s because about 4000 sea lions were

Table 2

Results of life-table sensitivity analyses showing the potential change in ratio of total population size to pups for a population increasing at 3.1% per annum. The vital rates in Calkins and Pitcher's (1982) life tables¹ for a stable population of Steller sea lions (*Eumetopias jubatus*) were incrementally adjusted until a population growth rate, λ , of 3.1% was attained. The corresponding stable sex- and age-distributions were calculated by using Cole's (1954) finite approximations of Lotka's (1907) population equations.

Parameter that changed	Relative change	Population growth rate (λ)	Pup multiplier
Δ Mortality all ages	-15%	3.1%	5.0
Δ Juvenile mortality	-27%	3.1%	5.2
Δ Adult mortality	-33%	3.1%	4.7
Δ Fecundity	+32%	3.1%	4.2
Δ Age at maturation	-1.6 years	3.1%	4.2

¹ Calkins, D. G., and K. W. Pitcher. 1982. Population assessment, ecology and trophic relationships of Steller sea lions in the Gulf of Alaska. In Environmental assessment of the Alaskan continental shelf. p. 447-546. U.S. Department of Commerce and U.S. Department of Interior, Final Report of Principal Investigators 19:1-565.

killed for bounty on the Oregon coast during 1925-29 (Pearson and Verts, 1970), although some of these may have been nonbreeding animals associated with rookeries in California, British Columbia, and Alaska.

California

Steller sea lions historically have used six rookeries in California (San Miguel Island, Año Nuevo Island, the Farallon Islands, Seal Rocks off San Francisco, Sugarloaf Island-Cape Mendocino, and Saint George Reef). San Miguel Island and Seal Rocks are no longer used by Steller sea lions and only a few pups have been born on the Farallon Islands each year since the 1980s. There may have also been several additional small rookeries south of Año Nuevo (Bonnot, 1928; Rowley, 1929).

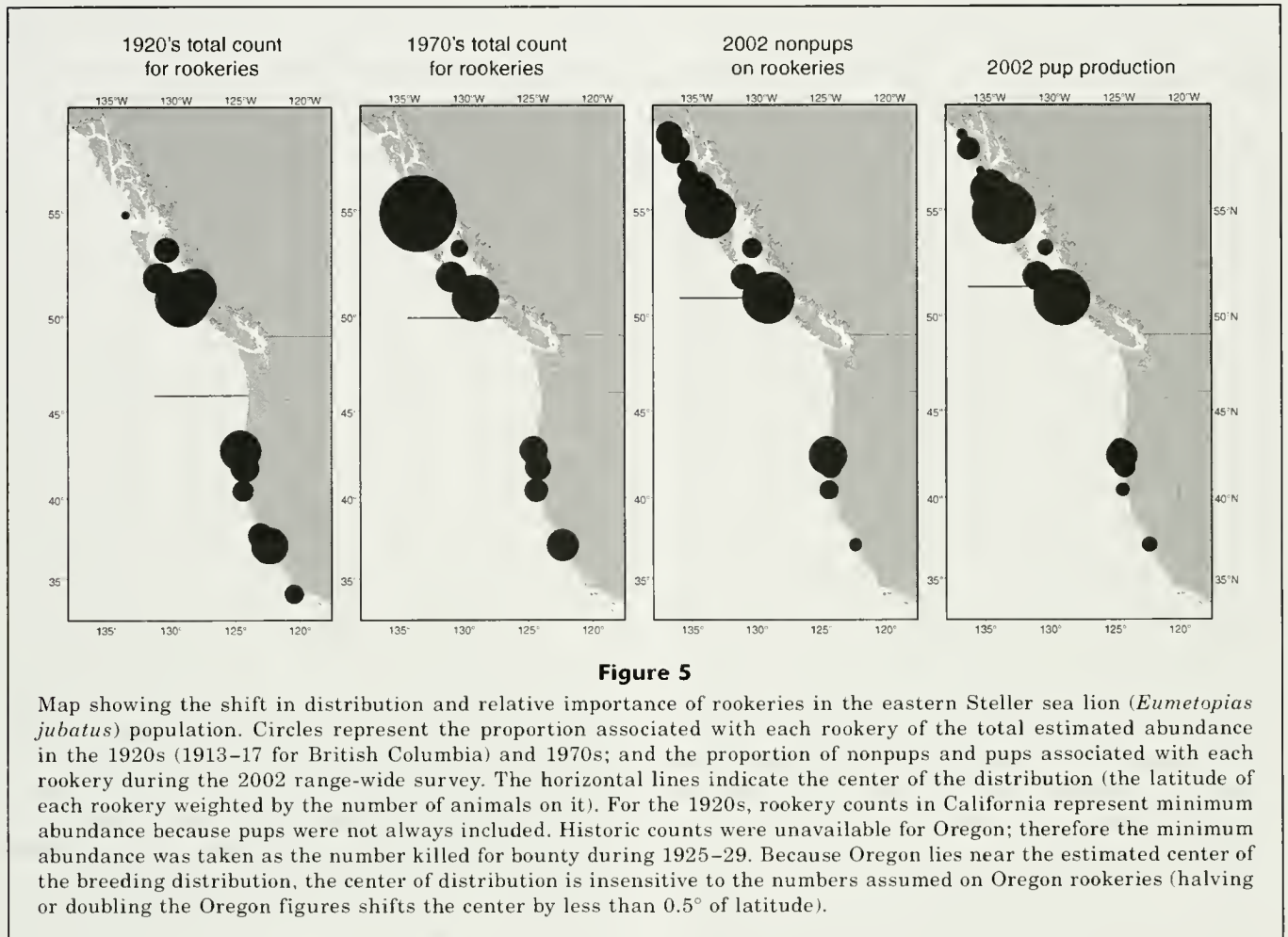
Statewide surveys, with the use of vertical 126-mm format aerial photography, were implemented in California in 1996. From 1996 through 2004 there was no discernible statewide trend for nonpups on rookeries ($r^2=0.408$; $n=7$; $P=0.123$), however, pup production increased at an average annual rate of 8% ($r^2=0.68$; $n=8$; $P=0.012$).

Although there has been a long and intermittent time series of counts for rookeries in California over the last 75 years (Bonnot, 1928, 1929; Bonnot and Ripley, 1948; Bartholomew and Boolootian, 1960; Orr and Poulter, 1967; LeBoeuf et al., 1991; Stewart et al., 1993), caution is warranted when attempting to evaluate population trends from the older data because they are drawn from a variety of sources where different survey methods were used. Statewide, total counts of nonpups at the six rookeries during the first half of the 20th century were on the order of 3900-5600. The 2004 count at these same six sites was 1578 nonpups and 818 pups—indicating that, perhaps, only about a third as many animals are currently present in the state (Fig. 4E). Population trends differed markedly among sites (Appendix).

Historically, Steller sea lions extended south to the Channel Islands in southern California, and San Miguel Island was considered to have been the southernmost

rookery (Bonnot, 1928, 1929). It appears that Steller sea lion were once more abundant than California sea lions (*Zalophus californianus*) in that area (Bartholomew, 1967). Steller sea lions were reported to breed there in small numbers; Bonnot (1929) counted 50 pups in 1928. Abundance of nonpups in the Channel Islands peaked at about 2000 in the late 1930s (Appendix), although hunting and harassment could have resulted in fewer animals being present during the surveys (Bonnot and Ripley, 1948; Stewart et al., 1993). Numbers subsequently declined—the main declines occurring between the late 1930s and 1950s (Bartholomew and Boolootian, 1960; Bartholomew, 1967). No births have been recorded since 1982 and no adults have been seen since 1983 (Stewart et al., 1993).

In central California, Steller sea lion abundance at Año Nuevo and the Farallon Islands is currently only about 20% of the levels reported between the 1920s and 1960s (Appendix). Steller sea lions had deserted the rookery at Seal Rocks near the entrance to San Francisco Bay by the late 1920s, purportedly as a result of persistent harassment by fishermen (Rowley, 1929). During the 1920s, Año Nuevo Island and the Farallon Islands were identified as the most important rookeries in California, with 625 and 400 pups counted at each site, respectively, in 1922 (Bonnot, 1929). On Año Nuevo, numbers remained at high levels until the early 1960s, then declined thru the mid-1990s (Orr and Poulter, 1967; Le Boeuf et al., 1991) (Appendix). Since 1996, both pup production ($r^2=0.035$; $n=8$; $P=0.656$), and nonpup numbers ($r^2=0.018$; $n=8$, $P=0.755$) have been stable. Fewer counts are available for the Farallon Islands, but the pattern appears to be similar (Appendix); abundance was at high levels from the 1920s to early 1960s and then declined sharply during the 1960s or early 1970s (Hastings and Sydeman, 2002). Pup production on the Farallons has been low since at least 1974 (Appendix). An average of only nine pups was counted between 1996 and 2004 and the site presently does not meet our criteria for a rookery (>50 pups). Nonpup numbers were stable ($r^2=0.173$;



$n=15$; $P=0.123$) at low levels (Appendix) between 1974 and 2004.

Steller sea lions have been counted only sporadically at the Sugarloaf-Cape Mendocino and Saint George Reef rookeries in northern California until recent years (Appendix). Numbers of nonpups have been relatively stable since 1996 at both Sugarloaf-Cape Mendocino ($r^2=0.106$; $n=8$; $P=0.431$) and Saint George Reef ($r^2=0.128$; $n=9$; $P=0.345$). A comparison of counts made during the 1927–47 period with recent counts (Appendix) indicates that current abundance is probably only slightly reduced from historical levels. The Sugarloaf-Cape Mendocino rookery is small; counts of pups increased from 62 in 1996 to 131 in 2004, representing an average annual increase of 13% ($r^2=0.725$; $n=8$; $P=0.007$). For the Saint George Reef rookery, located near the California-Oregon border, counts of pups increased from 243 in 1996 to 444 in 2004, representing an average annual rate of 10% ($r^2=0.70$; $n=8$; $P=0.009$). Over the same period, counts of nonpups showed no discernible trend ($r^2=0.11$; $n=12$; $P=0.431$).

Steller sea lions use about six major (>50 animals) haulout sites along the California coast between Saint George Reef and Año Nuevo Island, as well as numer-

ous smaller sites, during the breeding season. In 2002, a total of 1543 nonpups were counted at haulouts, in addition to the 1559 nonpups counted on rookeries. At least 12 former Steller sea lion haulout sites and perhaps a few rookeries between the Channel Islands and Año Nuevo Island (Bartholomew and Boolootian, 1960; Bonnot, 1928; Bonnot and Ripley, 1948; Rowley, 1929) have been abandoned.

Overall trend for the eastern North Pacific Steller sea lion population

The eastern North Pacific Steller sea lion population has exhibited significant and similar annual rates of growth in all three regions that support the largest rookeries: 3.2% in southeastern Alaska, 3.2% in British Columbia, and 2.5% in Oregon (Fig. 3). Combining the trend trajectories for these three regions, which currently account for over 90% of total pup production in the eastern population, overall abundance is estimated to have increased by about 215% over the last 25 years, representing an annual rate of increase of 3.1%. The time series for California is shorter; however pup production increased significantly at 7% per year between 1996 and 2004.

With the exception of the southernmost rookery at Año Nuevo Island and the (former) Farallon Islands rookery, both greatly reduced from historical levels, pup production has increased consistently throughout the range of the eastern population over the past 25+ years.

The total population-wide pup count in 2002 was 10,053 pups, of which 49% were found in southeastern Alaska, 33% in British Columbia, 11% in Oregon, and 7% in California (Table 1). This represents minimum pup production because some pups may have died and disappeared from rookeries prior to the survey, or were born after the census. Following Trites and Larkin (1996), we applied an arbitrary adjustment of 10% to account for pups that had been missed during our survey, giving a pup production estimate of 11,060. Using life tables, Calkins and Pitcher (1982) estimated the ratio of total animals to pups in a stationary population would be about 4.5:1. Our sensitivity analyses indicated that for a population increasing at 3.1%, the ratio could be as low as 4.2:1 if the growth were due to increased fecundity, or as high as 5.2:1 if the growth was due to reduced juvenile mortality (Table 2). The eastern population is thus estimated to have numbered about 46,000–58,000 animals in 2002. During the 2002 survey, we actually counted 45,378 animals (10,053 pups and 35,325 non-pups) on rookeries and at haulouts. This count represents an absolute minimum population size because not every site was surveyed and some animals were absent from rookeries and haulouts during the surveys and therefore were not counted.

The general sparseness and lack of standardization of the pre-1970 counts prevents a rigorous comparison of current and historical population levels; however several clear patterns emerge (Appendix). In southeastern Alaska abundance was apparently quite low during the first half of the 20th century, but numbers have increased consistently since that time. We have no explanation for the low numbers during the early 1900s because we are not aware of large-scale hunting or predator control efforts. Numbers were high in British Columbia in the early 1900s but were then reduced by about 70% by predator control and hunting. They have since recovered to levels approximately two-thirds of those of the early 1900s. Numbers on haulouts in Washington State were severely reduced by bounty hunting in the early to mid-1900s. Although there has been substantial recovery, peak numbers still appear to be only about half of levels of 1915. There are no count data available for Oregon prior to 1968, but the fact that about 4000 sea lions were killed for bounty during 1925–29 would indicate a sizable population at that time. There has been a substantial recovery since the 1968 surveys. The California population was apparently large during the early 1900s. Sites in southern California began declining in the late 1930s and that portion of the range was abandoned by the 1980s. Numbers in central California remained high into the 1960s, then declined to low levels, and stabilized during the 1990s. In northern California numbers were likely reduced during the mid 1900s, but now appear

to be approaching levels of the early 1900s. Overall, the eastern population currently appears to be similar in size to historical levels of the early 1900s; the large population increase in southeastern Alaska balances out the declines in the southern portion of the range.

Although the number of rookeries used by the eastern Steller sea lion population has remained relatively constant (range 10–13), their distribution has shifted (Fig. 5). In the 2002 survey, the breeding population was centered (the latitude of each rookery weighted by the number of animals on it) at about 51.5°N (central British Columbia coast). Just over half of the rookeries (7 of 13) and births (57%) occurred north of that latitude, with the northernmost rookery at 58.2°N. For the 2002 population-wide survey, the pattern was similar for both pups and total numbers (pups and nonpups), suggesting they both provided an index of breeding distribution. In comparison, during the 1970s the breeding population was centered at roughly 49.9°N (central Vancouver Island), with the northernmost rookery at 54.8°N, representing a northward shift of 0.5° of latitude or 65 km per decade. In the 1920s, the breeding population was probably centered somewhere around 46.0°N (Washington-Oregon border); only two small rookeries accounted for about 13% of total abundance situated north of 51.5°N (the current center of pupping). At the southern end of their range, the declines of Steller sea lions appear to have begun in southern California (San Miguel) between the late 1930s and 1950s, and were followed by declines in central California between 1960 and 1990; however the two northernmost sites in California exhibited relative stability. Conversely, at the northern end of their range, Steller sea lions probably began breeding in significant numbers in southern southeastern Alaska (Forrester Island) in the late 1940s or 1950s and extended their breeding range to central southeastern Alaska (Hazy Islands) in the early 1980s, and northern southeastern Alaska (White Sisters) in the 1990s. Overall, the southern end of the breeding range contracted by about 3° latitude (330 km), and the northern limit was extended by about 5° latitude (550 km).

Discussion

The population increases observed in recent years over most of the range of eastern North Pacific Steller sea lion population almost certainly represent recovery from the impacts of prior predator-control programs, harvesting, and indiscriminate killing that took place prior to protection under the Canadian Fisheries Act of 1970 and implementation of the U.S. Marine Mammal Protection Act in 1972. The overall annual rate of increase of 3.1% was widespread (from Oregon to southeastern Alaska) and has been underway for at least 25 years, and there is no evidence of it slowing with increasing sea lion densities. The consistent, long-term observed rate of increase of 3.1% throughout most of the range of the eastern population is well below the theoretical maximum intrinsic rate of increase for pinnipeds

(Wade, 1998; Harkonen et al., 2002). This annual rate of increase indicates that either some factor or factors are still limiting the growth rate of this population or that the growth potential of this otariid is less than the theoretical maximum, which was derived from phocid population growth rates. We have observed Steller sea lions that have been shot or entangled in marine debris, and this undocumented mortality could be preventing the population from increasing at a higher rate. In addition, the Steller sea lion tends to have a longer period of maternal investment and a lower reproductive rate than most phocids (Pitcher et al., 1998), both of which may limit the growth potential of populations.

Although the three geographic regions supporting the largest rookeries all increased at about the same rate, individual rookeries often exhibited different population growth rates or temporal changes in growth rates. At the northern end of the range, Forrester Island accounted for essentially all of the population growth until the 1970s; however the observed rate of change has slowed since the 1980s. At the same time, some of the rookeries to the south of Forrester Island in British Columbia and to the north of it in central-northern southeastern Alaska have exhibited higher-than-average growth rates since the 1980s. The mechanism causing these geographic patterns is unknown, but could involve 1) dispersal of breeding animals between rookeries, 2) differences in local conditions that affect reproduction and survival, or 3) a shift in distribution of prey resources. Some dispersal of breeding females from their natal rookeries has been shown to occur. Six of 31 females that were marked as pups on the Forrester Island rookery were subsequently observed to have given birth on other rookeries (Raum-Suryan et al., 2002). The authors of that study concluded that the Steller sea lion generally conformed to the metapopulation concept as depicted by Hanski and Simberloff (1997), in that local breeding populations (rookeries) and movements among these local populations have the potential of affecting local dynamics.

For our assessment of long-term historic population trends, we relied mainly on counts of non-pups (or occasionally pups and nonpups combined) on rookeries, as few reliable pup counts were available prior to the 1970s. The 2002 population-wide survey (Fig. 2) and the last 30 years of counts in British Columbia indicated there is a relationship between the numbers of nonpups and pups on rookeries. However, departures from this relationship can occur, especially where existing rookeries are being abandoned or new rookeries are being formed. For example, the Farallon Islands, which no longer meet our definition of a rookery, now serves largely as a haulout site (Le Boeuf et al., 1991). The historical rookery on the Sea Otter Group in British Columbia, the only rookery known to have been extirpated by control efforts, is also still used during the breeding season as a haulout by nonbreeding animals. Conversely, in southeastern Alaska, the new rookeries were established at sites previously used as major haulouts by nonbreeding animals. The lack of accurate pup counts may, thus, have influenced our historical interpretation of historical data and our

depiction of the exact breeding range, but there is a general consensus that the breeding range has shifted. Pup production in southern California has disappeared and in central California has dropped to less than one-fifth of what it was in the 1920s. Few, if any, pups were born in southeastern Alaska in the early 1900s, whereas this area now accounts for nearly half of total pup production in the eastern North Pacific population.

Control programs and harvesting clearly depleted the eastern Steller sea lion population and may have contributed to its redistribution, but the kills cannot fully explain the shift in the distribution. For example, while control efforts were underway in British Columbia during the 1950s and 1960s, animals may have taken refuge just north of the British Columbia-Alaska border at Forrester Island, or animals breeding on Forrester Island may have benefited from reduced competition as a result of the reductions on British Columbia rookeries. However, the northward expansion of the breeding range in southeastern Alaska continued through the 1980s and 1990s, even though killing of sea lions in British Columbia ceased in the 1960s. At the southern end of their range, sea lions were apparently very abundant in California before the 1860s, but were depleted during the 1870s because of intense hunts of sea lions for oil and hides (Bonnot, 1929). The last organized kills were made in 1909, although hunting, especially of bulls for trimmings (genitals, lips with whiskers, and gall bladders) continued into the 1930s. Nevertheless, the population declines in southern California began in the late 1930s, and in central California began in the late 1960s and early 1970s, well after major kills by humans had ended (Hastings and Sydeman, 2002).

The reason for the northward shift in the overall breeding distribution is unknown, and different factors may have been in play at the southern and northern ends of the range. In the south, competition with increasing populations of other pinnipeds may have been a factor in range constriction (Stewart et al., 1993). In particular, the number of California sea lions breeding in California increased from at most a few thousand in the 1920s (Bonnot, 1928) to about 240,000 in 2000 (Lowry and Maravilla-Chavez, 2005). It is likely that California sea lions and Steller sea lions compete with each other because 1) their ranges overlap, 2) they share the same haulout sites, and 3) they probably consume many of the same prey species. On San Miguel Island and the Farallon Islands, where Steller sea lions used to predominate (Bartholomew and Boolootian, 1960; Ripley et al., 1962; Stewart et al., 1993), the declines in Steller sea lions coincided with large increases in numbers of California sea lions (Stewart et al., 1993; Hasting and Sydeman, 2002).

For unknown reasons, southeastern Alaska represents the only area throughout the range of the eastern North Pacific population where new Steller sea lion rookeries have been established. Steller sea lion rookeries are normally located on remote, offshore islands or reefs and require adequate areas above high water levels where young pups can survive most weather conditions. There

must also be adequate prey on a consistent basis within the foraging range of lactating females. Perhaps the limited availability of such sites has restricted the establishment of new rookeries at other locations.

Changes in the ocean environment, particularly towards warmer water temperatures (Field et al., 2006), have also been proposed as a factor that has favored the California sea lion and other pinnipeds over the Steller sea lion in the southern part of their range (Bartholomew and Boolootian, 1960). Environmental conditions can affect sea lion populations directly or indirectly. Temperature could directly affect the survival of animals and such effects would be expected to be most evident at the latitudinal extremes of the range. The ocean environment can also act indirectly by affecting marine food webs, and thus the quantity and quality of prey available to sea lions. Unfortunately, with historical survey data being so scant, and with sea lions having been artificially reduced below natural levels, one can only speculate about the long-term effects of environmental conditions on the eastern Steller sea lion population, but conditions currently appear to be favorable through much of their range.

A somewhat similar change in Steller sea lion distribution and the establishment of new rookeries have been noted along the Asian coast. There the southern range limit has moved northward by 500–900 km over the past 50 years and several new rookeries have been established (Burkanov and Loughlin, in press).

Based on the population-wide survey in 2002, pup production for the eastern population is currently estimated to be about 11,000, and total abundance on the order of 46,000–58,000. It should be emphasized that this should be regarded as a “general” estimate because several factors can affect the accuracy of pup counts and correction factors. Following Trites and Larkin (1996), we added 10% to pup counts to estimate pup production (i.e., actual number of births), which seems reasonable, but the adjustment is subjective and arbitrary, and in reality the adjustment probably varies from site-to-site and year-to-year. The sex and age structure of populations, and hence the ratio of pups to nonpups, may differ between populations and change with population status in ways we do not understand. We attempted to delineate the possible range of changes in the correction factors by using sensitivity analyses, which showed the multiplier could either decrease if population productivity is controlled by fecundity or age at maturation, or increase if population productivity is controlled by mortality. Assessments for the western North Pacific population have indicated that the population declines were primarily due to poor juvenile survival (York, 1994), and if this is in fact the main determinant of population growth, the pup multiplier and estimated abundance of the eastern population may lie toward the high end of our range.

During the 2002 population-wide survey, a surprisingly large number of nonpups were observed (75–100% of the number expected based on our life table analysis). Because one would expect appreciable numbers of juveniles and adults to be dispersed at sea and missed during surveys, the actual size of the eastern population

may be near the upper end of our estimated range. On the other hand, 2002 may merely have been an exceptional year for pup production, although the more recent pup counts available for California (2003 and 2004) and southeastern Alaska (2005) indicate that pup numbers have continued to increase. The apparent surplus of nonpups observed during the 2002 survey could also be indicative of the presence of nonbreeding animals associated with the western population in our survey area. Studies (where sea lions have been branded) have shown there is some overlap in the nonbreeding range of the two populations (Raum-Suryan et al., 2002), although there is no reason to expect a higher degree of movement from west to east. Moreover, the observed ratios of total counts to pup counts was uniformly high over the entire range of the eastern population (4.1 in southeastern Alaska, 4.7 in British Columbia, 4.7 in Oregon, and 5.4 in California), and if anything decreased slightly towards the north where one would expect the greatest overlap with the western population. The high nonpup to pup ratios indicate that high survival rather than high fecundity may be the primary mechanism responsible for population growth.

Steller sea lions in the eastern population currently breed at 13 major rookeries (>50 pups born), and the highest concentration of breeding animals is in southeastern Alaska, northern British Columbia, and near the Oregon-California border. Currently there is a large gap (993 km) between the Scott Islands rookery off northwestern Vancouver Island and the Orford and Rogue Reef rookeries in southern Oregon. There are no records of rookeries along this coastline, and natives hunting sea lions along the Washington coast had no knowledge of rookeries in that state (Scheffer, 1950). However, it would not be surprising to see new rookeries founded or re-established at haulout sites along this gap, as has occurred in southeastern Alaska, if the eastern population continues to increase in the northern part of its range. Nonbreeding animals use approximately 59 major haulout sites (>50 animals during) during the breeding season, plus numerous smaller sites and many seasonal haulout sites. The major haulouts are widely distributed from Cape Fairweather (58.8°N, 137.9°W) to Año Nuevo Island (37.1°N, 122.3°W), providing Steller sea lions with access to coastline spanning about 22° of latitude or 2400 km.

During the 1970s the eastern population represented only about 10% of the total number of Steller sea lions along the North American coast. With the large decline in the western population in conjunction with the increase in the east, this percentage has changed dramatically; about 55% of pup production in North America now occurs in the eastern population. We anticipate that continued monitoring and comparisons of the growing eastern population with the western population will provide insight into factors that ultimately regulate Steller sea lion populations, and we hope this synthesis for the eastern population will contribute toward better coordination of surveys and standardization of counting methods over the distribution range of the species.

Acknowledgments

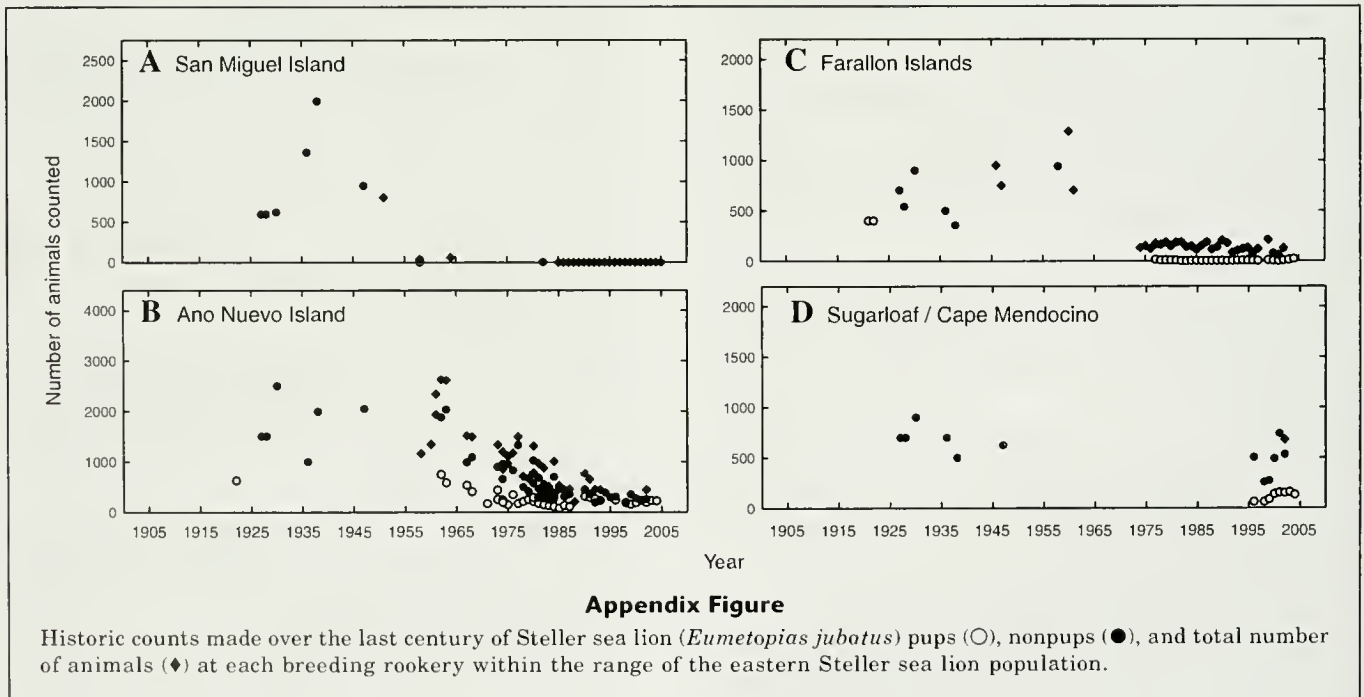
We thank S. Riemer and B. Wright of the Oregon Department of Fish & Wildlife for their extensive contributions to survey work, counting, and database management. D. McAllister of the Alaska Department of Fish and Game conducted many of the surveys in southeastern Alaska. We thank K. Raum-Suryan for drafting Figure 1. R. DeLong and R. Small reviewed and provided useful comments on an earlier draft of this manuscript. We appreciate the timely comments and suggestions provided by three anonymous reviewers and by the editorial staff of Fishery Bulletin. Surveys in the U. S. were conducted under research permits from the Office of Protected Resources of the National Marine Fisheries Service and in Canada with authorization of Fisheries and Oceans Canada. Surveys in Oregon were conducted under special use permits granted by the U.S. Fish & Wildlife Service, Oregon Coastal Refuge Complex, and surveys at protected sites in B.C. were authorized by the Ecological Reserves Unit of B.C. Parks and Parks Canada.

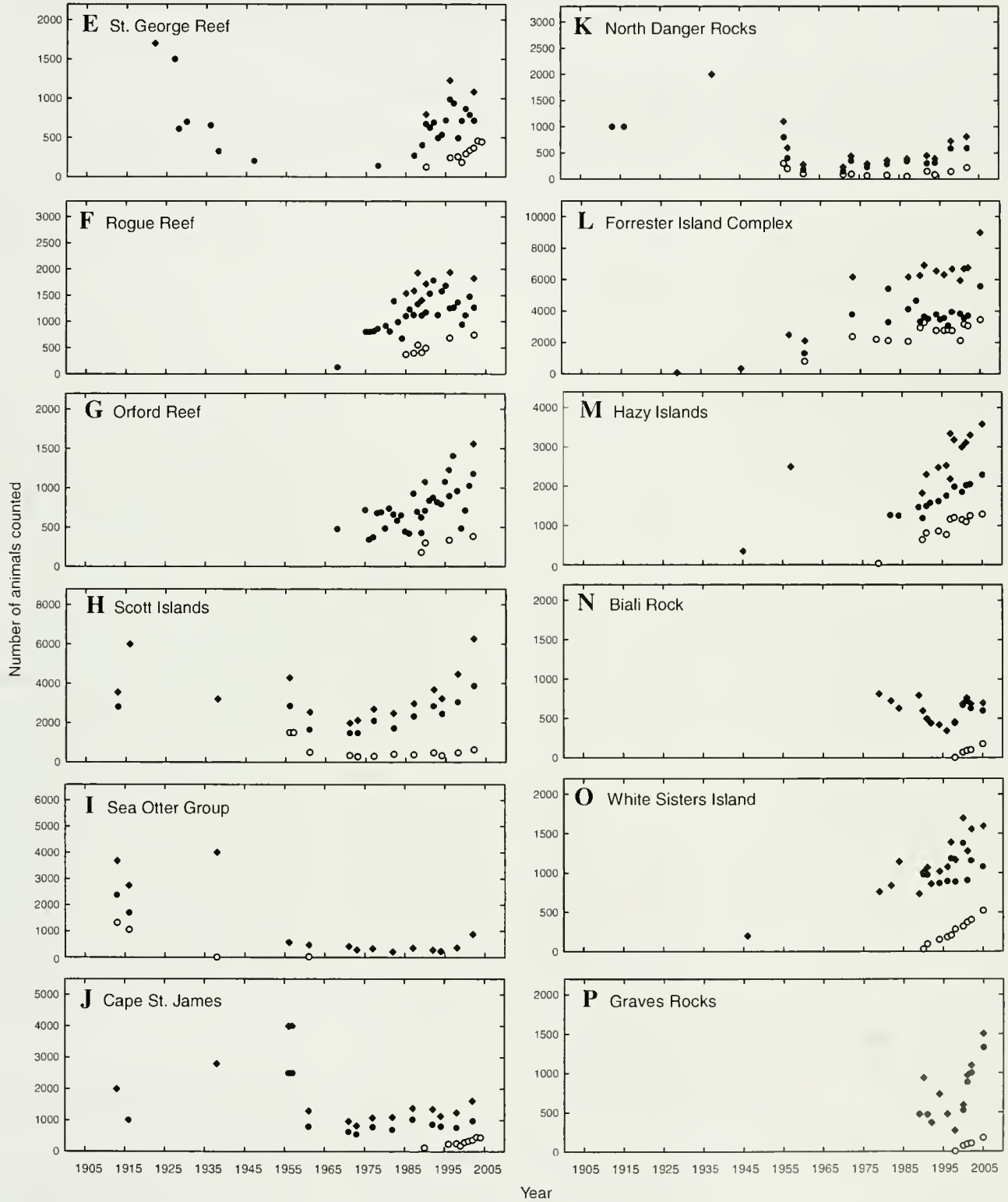
Literature cited

- Bartholomew, G. A.
1967. Seal and sea lion populations of the Channel Islands. *In* Proceedings of the symposium on the biology of the California Channel Islands (R. N. Philbrick, ed.), p. 229–244. Santa Barbara Botanical Garden, Santa Barbara, CA.
- Bartholomew, G. A., and R. A. Booloitian.
1960. Numbers and population structure of pinnipeds on the California Channel Islands. *J. Mammal.* 41:366–375.
- Berkson, J. M., and D. P. DeMaster.
1985. Use of pup counts in indexing population changes in pinnipeds. *Can. J. Fish. Aquat. Sci.* 42: 873–879.
- Bickham, J. W., J. C. Patton, and T. R. Loughlin.
1996. High variability for control-region sequences in a marine mammal: implications for conservation and biogeography of Steller sea lions (*Eumetopias jubatus*). *J. Mammal.* 77:95–108.
- Bigg, M. A.
1985. Status of Steller sea lion (*Eumetopias jubatus*) and California sea lion (*Zalophus californianus*) in British Columbia. *Can. Spec. Pub. Fish. Aquat. Sci.* 77:1–20.
- Bonnot, P.
1928. The sea lions of California. *Calif. Fish and Game.* 14:1–16.
1929. Report on the seals and sea lions of California. California Division of Fish and Game. *Fish. Bull. No.* 14, 61 p.
- Bonnot, P., and W. E. Ripley.
1948. The California sea lion census for 1947. *Calif. Fish and Game* 34:89–92.
- Burkanov, V. N., and T. R. Loughlin.
In press. Distribution and abundance of Steller sea lions on the Asian coast, 1720s–2005. *Mar. Fish. Rev.*
- Calkins, D. G., D. C. McAllister, K. W. Pitcher, and G. W. Pendleton.
1999. Steller sea lion status and trend in Southeast Alaska: 1979–1997. *Mar. Mamm. Sci.* 152:462–477.
- Cole, L. C.
1954. The population consequences of life history phenomena. *Quarterly Rev. Biol.* 29:103–137.
DFO (Department of Fisheries and Oceans, Canada).
2003. Steller sea lion (*Eumetopias jubatus*). DFO, Can. Sci. Advis. Sec. Stock Status Rep. 2003/037, 9 p.
- Field, D. B., T. R. Baumgartner, C. D. Charles, V. Ferreira-Bartina, and M. D. Ohman.
2006. Planktonic foraminifera of the California Current reflect 20th century warming. *Science* 311:63–66.
- Fritz, L. W., and C. Stinchcomb.
2005. Aerial, ship, and land-based surveys of Steller sea lions (*Eumetopias jubatus*) in the western stock in Alaska, June and July 2003 and 2004. NOAA Tech. Memo. NMFS-AFSC-153, 56 p.
- Hanski, I., and D. Simberloff.
1997. The metapopulation approach, its history, conceptual domain and application to conservation. *In* Metapopulation biology: ecology, genetics and evolution (Hanski and M. Gilpin, eds.), p. 5–26. Academic Press, London, England.
- Harkonen, T., K. C. Harding, and M. Heide-Jorgensen.
2002. Rates of increase in age-structured populations: a lesson from the European harbour seal. *Can. J. Zool.* 80:1498–1510.
- Hastings, K. K., and W. J. Sydeman.
2002. Population status, seasonal variation in abundance, and long-term population trends of Steller sea lions (*Eumetopias jubatus*) at the South Farallon Islands, California. *Fish. Bull.* 100:51–62.
- Imler, R. H., and H. R. Sarber.
1947. Harbor seals and sea lions in Alaska. U.S. Fish Wildl. Serv., Spec. Sci. Rep. 28, 23 p.
- Kenyon, K. W., and V. B. Scheffer.
1959. Wildlife surveys along the northwest coast of Washington. *Murrelet* 42:29–37.
- Lewis, J. P.
1987. An evaluation of a census-related disturbance of Steller sea lions. M.S. thesis, 89 p. Univ. Alaska, Fairbanks, Alaska.
- Lotka, A. J.
1907. Relation between birth rates and death rates. *Science* 26: 21–22.
- Loughlin, T. R., A. S. Perlov, and V. A. Vladimirov.
1992. Range-wide survey and estimation of total number of Steller sea lions in 1989. *Mar. Mamm. Sci.* 8:220–239.
- Lowry, M. S., and O. Maravilla-Chavez.
2005. Recent abundance of California sea lions in western Baja California, Mexico and the United States. *In* Proceedings 6th California Islands symposium, Ventura, California, U.S., December 1–3, 2003, p. 485–497. National Park Service Tech Publ. CHIS-05-01, Institute for Wildlife Studies, Arcata, CA.
- Mathisen, O. A., and R. J. Lopp.
1963. Photographic census of the Steller sea lion herds in Alaska, 1956–58. U.S. Fish Wildl. Serv., Spec. Sci. Rep. Fish. No. 424, 20 p.
- Newcombe, C. F., and W. A. Newcombe.
1914. Sea lions on the coast of British Columbia. *Ann. Rep. British Columbia Comm. Fish for 1913, p.* 131–145.
- O’Corry-Crowe, G., T. Gelatt, K. Pitcher, and B. Taylor.
2005. Crossing significant boundaries: evidence of mixed-stock origins of new Steller sea lion, *Eumetopias jubatus*, rookeries in Southeast Alaska (Abstract). *In*

- The 16th biennial conference on the biology of marine mammals (book of abstracts); December 12–16, 2005, San Diego, California, 330 p. Society for Marine Mammology.
- Orr, R. T., and T. C. Poulter.
1967. Some observations on reproduction, growth, and social behavior in the Steller sea lion. *Proc. Calif. Acad. Sci.* 32:377–404.
- Pearson, J. P., and J. P. Verts.
1970. Abundance and distribution of harbor seals and northern sea lions in Oregon. *Murrelet* 51:1–5.
- Pitcher, K. W., V. N. Burkanov, D. G. Calkins, B. J. Le Boeuf, E. G. Mamaev, R. L. Merrick, G. W. Pendleton.
2001. Spatial and temporal variation in the timing of births of Steller sea lions. *J. Mammal.* 82:1047–1053.
- Pitcher, K. W., D. G. Calkins, and G. W. Pendleton.
1998. Reproductive performance of female Steller sea lions: an energetics-based reproductive strategy? *Can. J. Zool.* 76:2075–2083.
- Raum-Suryan, K. L., K. W. Pitcher, D. G. Calkins, J. L. Sease, and T. R. Loughlin.
2002. Dispersal, rookery fidelity, and metapopulation structure of Steller sea lions (*Eumetopias jubatus*) in an increasing and a decreasing population in Alaska. *Mar. Mamm. Sci.* 18:746–764.
- Ripley, W. E., K. W. Cox, and J. L. Baxter.
1962. California sea lion census for 1958, 1960 and 1961. *Calif. Fish. Game* 48:228–231.
- Rowley, J.
1929. Life history of the sea-lions on the California coast. *J. Mammal.* 10:1–39.
- Scheffer, V. B.
1950. Mammals of the Olympic National Park and vicinity. *Northwest Fauna* no. 2, p. 192–225.
- Snyder, G. M., K. W. Pitcher, W. L. Perryman, and M. S. Lynn.
2001. Counting Steller sea lion pups in Alaska: an evaluation of medium-format, color, aerial photography. *Mar. Mamm. Sci.* 17:136–146.
- Stewart, B. S., P. K. Yokum, R. L. DeLong, and G. A. Antonelis.
1993. Trends in abundance and status of pinnipeds on the southern California Channel Islands. *In* Third California Islands symposium: recent advances in research on the California islands (E. Hochberg, ed.), p. 501–516. Santa Barbara Museum of Natural History, Santa Barbara, CA.
- Trites, A. W., and P. A. Larkin.
1996. Changes in the abundance of Steller sea lions (*Eumetopias jubatus*) in Alaska from 1956 to 1992: how many were there? *Aquat. Mamm.* 22:153–166.
- Wade, P. R.
1998. Calculating limits to the allowable human-cause mortality of cetaceans and pinnipeds. *Mar. Mamm. Sci.* 14:1–37.
- Withrow, D. E.
1982. Using aerial surveys, ground truth methodology, and haulout behavior to census Steller sea lions, *Eumetopias jubatus*. M.S. thesis, 102 p. Univ. Washington, Seattle, WA.
- York, A. E.
1994. The population dynamics of northern sea lions, 1975–1985. *Mar. Mamm. Sci.* 10:38–51.

Appendix





Appendix Figure (continued)

Abstract—For most fisheries applications, the shape of a length-frequency distribution is much more important than its mean length or variance. This makes it difficult to evaluate at which point a sample size is adequate. By estimating the coefficient of variation of the counts in each length class and taking a weighted mean of these, a measure of precision was obtained that takes the precision in all length classes into account. The precision estimates were closely associated with the ratio of the sample size to the number of size classes in each sample. As a rule-of-thumb, a minimum sample size of 10 times the number of length classes in the sample is suggested because the precision deteriorates rapidly for smaller sample sizes. In absence of such a rule-of-thumb, samplers have previously under-estimated the required sample size for samples with large fish, while over-sampling small fish of the same species.

Precision estimates and suggested sample sizes for length-frequency data

Hans D. Gerritsen (contact author)¹

David McGrath²

Email address (for H. D. Gerritsen): hans.gerritsen@marine.ie

¹ Fisheries Science Service, Marine Institute
Rinville, Oranmore
County Galway, Ireland

² Commercial Fisheries Research Group
Galway-Mayo Institute of Technology
Dublin Road
Galway, Ireland.

Length measurements are fundamental to many aspects of fisheries science. However, there is little formal guidance on the appropriate size of a length sample. Such guidance is of particular relevance when the number of fish available exceeds the number that can be measured at a reasonable cost, and a subsample needs to be taken. Clearly, the required precision of a length sample depends on the purpose of sampling. In order to identify modes of individual year classes for a length-based assessment, the precision of the sample needs to be quite high. Sample sizes of more than 1000 are necessary to identify more than half the modes in a typical length distribution (Erzini, 1990). A sample size of at least 100 adult fish was recommended for age-based stock assessment purposes (Anderson and Neumann, 1996), although the authors did not mention how they arrived at this number.

Regardless of the type of assessment that is used, the shape of the length-frequency distribution is of interest, rather than simple summary statistics such as the mean or the variance. For this reason, it has proved difficult to quantify what constitutes a representative or adequately precise length distribution. Some studies have attempted to find minimum or optimum sample sizes by comparing samples to an expected distribution (e.g., Muller¹; Gomez-Buckley et al.²; Vokoun et al., 2001). However, the true distribution is usually unknown, and dissimilarity

from the expected distribution does not necessarily indicate an imprecise sample. In addition, these methods provide only indirect measures of precision that are difficult to evaluate objectively.

Thompson (1987) used the precision of a sample explicitly to establish an appropriate sample size. Thompson proved that a sample size of 510 is sufficient to be 95% confident that all estimated proportions in a multinomial distribution are no more than 5% from the true proportion. However, Thompson based this figure ($n=51$) on a worst-case scenario, which, in the present case, is a length-frequency distribution that is evenly apportioned over three size classes. Because this is not the typical shape of a length-frequency distribution used in fisheries science, Thompson's measure of precision is too conservative for the vast majority of cases.

For most fisheries applications, it would be more useful to define the

¹ Müller, H. 1996. Minimum sample sizes for length distributions of the catch estimated by an empirical approach. ICES CM 1996/J12, 18 p.

² Gomez-Buckley, M., L. Conquest, S. Zitzer, and B. Miller. 1999. Use of statistical bootstrapping for sample size determination to estimate length-frequency distributions for pacific albacore tuna (*Thunnus alalunga*). Final report to National Marine Fisheries Services, FRI UW 9902, 7 p. Website: <http://www.fish.washington.edu/research/publications/pdfs/9902.pdf> (accessed 31 March 2006).

precision of a length-frequency sample as the mean precision over the entire size range. However, it appears that this approach has not been used to establish an optimum sample size. Such mean precision estimates over the entire size range might be used to obtain a rule-of-thumb for sample sizes that are required in order to obtain a certain precision level of the catch at each location. In the present study we aim 1) to determine a rule-of-thumb for obtaining an appropriate sample size when the number of fish available in a particular sample exceeds the number that can be measured at a reasonable cost, and 2) to examine the sample sizes that have been taken in the past, in absence of such guidance.

Materials and methods

Data were used from the Irish Groundfish survey, which was carried out on RV *Celtic Explorer* in the waters around Ireland during October and November 2005. The catch was sorted into species and, if appropriate, into size grades, each of which were treated as a separate length sample. Length measurements were taken from all fish and squid species that were caught. If the number of individuals in a sample was large, a subsample was taken by repeatedly transferring the sample from each fish box into two other boxes and discarding one of these. This method ensures that the entire catch is represented uniformly in the subsample. At the time of the survey, the samplers did not have any particular guidance on the appropriate size for a subsample; they used their own judgment to decide on the sample size.

The precision of the number of observations in each length class of a random sample can be estimated by assuming a multinomial distribution (Smith and Maguire, 1983). If the precision in each length class is expressed in the form of a coefficient of variation (CV), an overall measure of precision can be obtained by weighting each CV by the number of fish in each length class. This mean weighted CV (MWCV) provides a description of the precision over the entire range of size classes in a length frequency distribution.

Under the assumption of a multinomial distribution, the standard deviation (σ_i) of the number of fish in a sample that are length category i can be estimated by

$$\sigma_i = \sqrt{np_i(1-p_i)}, \quad (1)$$

where n = the total number of fish in the sample; and p_i = the proportion of the sample that is length i .

The coefficient of variation (CV) of the number of fish at length i , is given by

$$CV_i = \frac{\sigma_i}{np_i} \quad (2)$$

and the mean weighted coefficient of variation (MWCV) is given by

$$MWCV = \sum p_i CV_i = \frac{\sum \sigma_i}{n}. \quad (3)$$

The highest possible value of the MWCV results from a length-frequency distribution that is evenly distributed over a large number of size classes. The number of fish at each length class are then Poisson distributed with a standard deviation that equals the square root of the number at length (Zar, 1999). The theoretical maximum MWCV is therefore given by

$$MWCV = (n/c)^{-0.5}, \quad (4)$$

where c = the number of size classes in the sample.

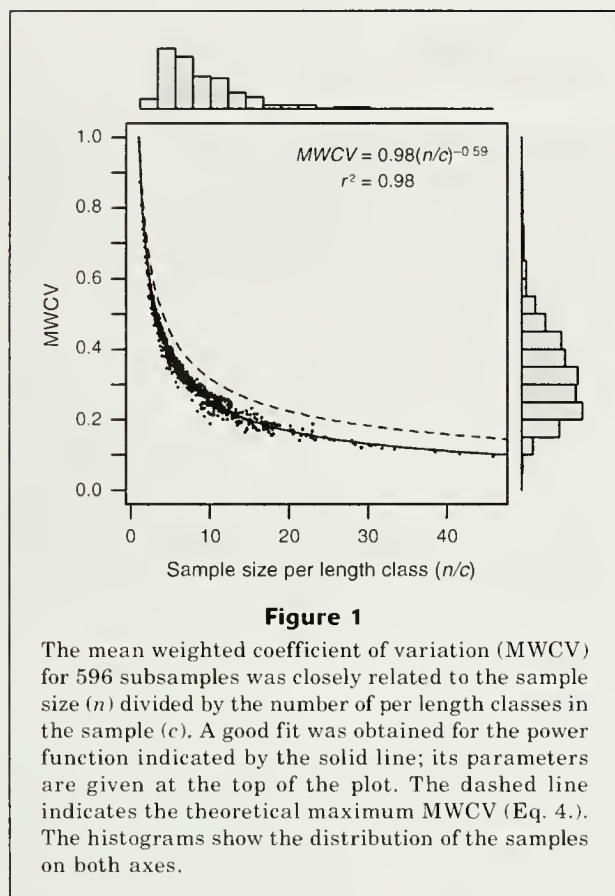
The minimum MWCV is zero and would result from a distribution where all observations fall within a single length category. Therefore, the MWCV estimates will always lie between zero and the curve described by Equation 4.

Results

During the 2005 survey, a total of 2332 length samples were taken for 80 different species of fish and squid. In most cases, the sample size was limited by the number of individuals in the catch. However, 596 samples were deemed too large to measure all individuals and subsamples were taken. The median subsample size was just under a quarter of the total catch (by weight), whereas 90% of the subsamples were smaller than half of the total catch. The four most common species that were subsampled were poor cod (*Trisopterus minutus*), blue whiting (*Micromesistius poutassou*), haddock (*Melanogrammus aeglefinus*), and Norway pout (*Trisopterus esmarkii*).

The estimated MWCV of the subsamples was closely associated with the ratio of the number of individuals measured to the number of length classes in the sample (Fig. 1). The MWCV appeared to follow an exponential curve that was close to the maximum MWCV given by Equation 4. The MWCV decreased very rapidly with increasing sample size up to sample sizes of around 10 times the number of length classes in the sample, after which the sample size would need to be increased considerably for a moderate further improvement in precision. If the sample size is taken as 10 times the number of length classes in the distribution, an MWCV of around 0.25 can be expected; a sample size of 48 times the number of length classes would result in an MWCV of 0.10 and a sample size of 155 times the number of length classes would be necessary to reduce the MWCV to 0.05.

The mean sample size in the subsamples taken on the survey was just under nine times the number of length classes per sample, resulting in a mean MWCV of 0.33. However, there was quite a large spread in the sample sizes (Fig. 1); therefore some samples were measured with very low precision, whereas others had



excessively large sample sizes. The range of sample sizes was between 2.2 and 24.7 times the number of length classes (2.5% and 97.5% quantiles), resulting in a range of MWCVs between 0.14 and 0.61. With a minor increase in effort, the sample size might be increased to 10 per length class for each subsample, resulting in an MWCV of around 0.25 for all samples. Considering that the precision deteriorates very rapidly for sample sizes of less than 10 per length class, a minimum sample size of 10 times the number length classes in the sample is suggested as a rule-of-thumb in the present case.

The previous analysis shows that, in order to obtain the same level of precision for all subsamples, the sample size should be directly proportional to the number of size classes. In absence of specific guidance on the sample size during the 2005 survey, the chosen sample size was only weakly correlated to the number of length classes in the sample of poor cod and haddock, whereas no significant correlation was found for blue whiting and Norway pout (Fig. 2). The same figure also shows that the MWCV in subsamples tended to increase with the mean length of the fish in the sample. This increase indicates that samples with a large mean size tended to be sampled with lower precision than samples of smaller fish of the same species.

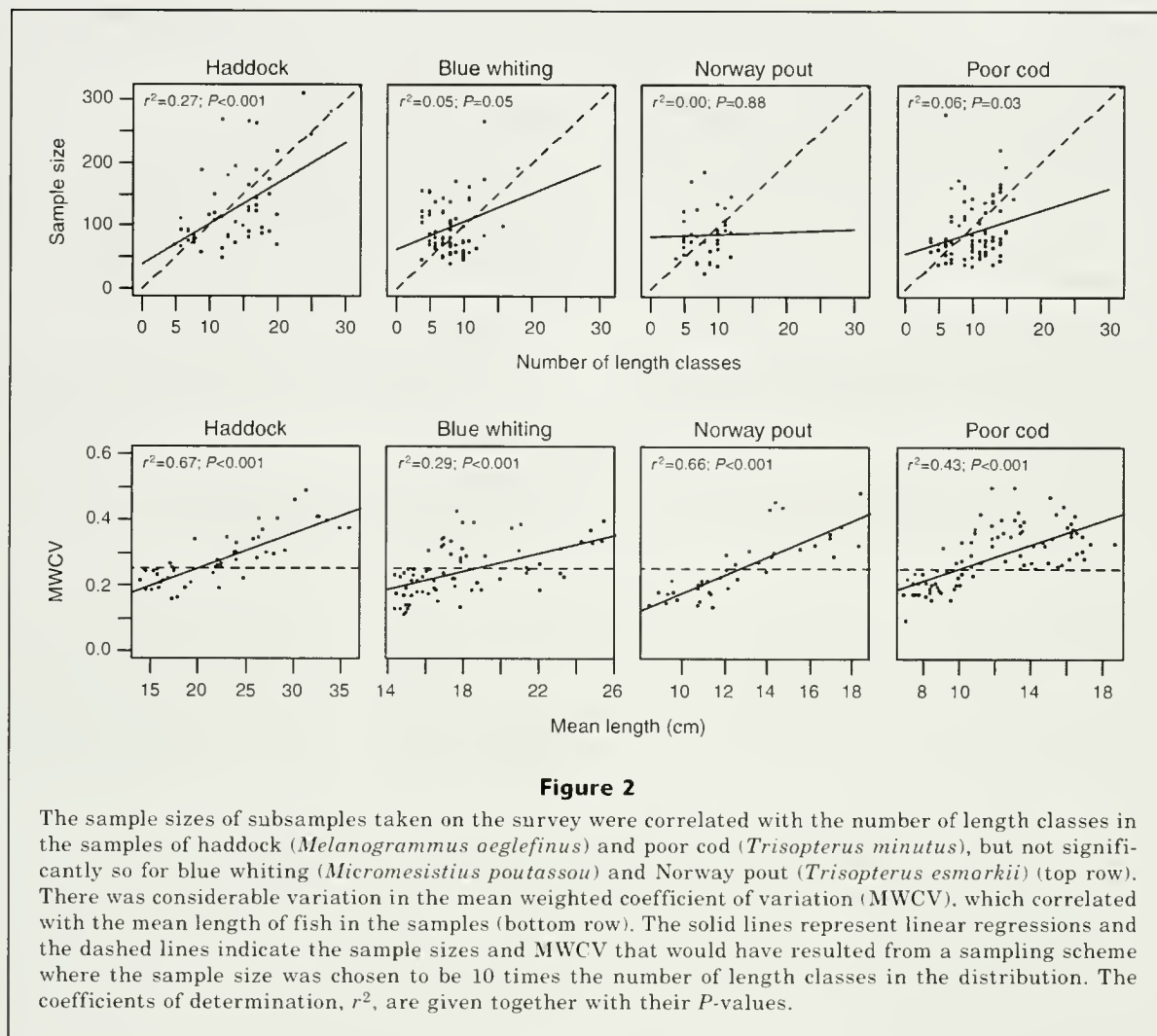
Discussion

Length distributions that result from combining a number of different samples exhibit greater variation than predicted under the multinomial model given in Equation 1 (Smith and Maguire, 1983). Fish populations are usually not uniformly mixed; therefore individual samples are not random samples from the population (Pennington et al., 2002). The simple multinomial model does not take account of the between-sample variability and will therefore underestimate the total variance. However, Equation 1 does provide an unbiased estimate of the variability within each sample, which is the variability that would occur if one could repeatedly take a random sample at the same location and time and measure these without error. This is the variability that is of interest when deciding whether the sample size is large enough to estimate the length distribution from a particular haul with a certain precision. Therefore, the MWCV is a suitable measure for this exercise.

In order to obtain a precise population estimate, it is important to maximize the number of sampling locations because of the considerable between-sample variability that is usually present (Pennington et al., 2002). Pennington et al. (2002) suggested maximizing the number of sampling locations at the expense of the number of fish measured. However, the number of hauls is often limited by practical considerations, and length measurements can be obtained quickly and cheaply. Therefore, it seems prudent to sample enough fish from each haul to obtain a length distribution that is representative of that catch at that particular location. Detailed information on the length distribution at each station can be valuable for exploratory data analysis, such as investigating the spatial structure in the data. Nevertheless, this level of sampling may not be strictly necessary for a precise population estimate of the length-frequency distribution for an age- or length-based assessment.

The samples in Figure 1 included a large range of species and size categories of fish, but the variability in the MWCV was small after taking account the sample sizes. This small amount of variability indicates that the MWCV is not very sensitive to the exact shape of the distribution and can be predicted with high precision, at least within the range of distributions encountered on the survey. A minimum sample size of 10 times the number of length classes in the sample appears to be a reasonable compromise between effort and precision in the present case.

The current analysis has focused on subsampling during surveys; however the same principles can be applied to any process of collecting data for which the shape of the distribution is of interest. The desired precision level for these cases will depend on a number of factors. For certain species that are of little commercial or scientific interest, but which may span across a large number of length classes, the suggested sample size of 10 per length class may be excessive. Likewise, as the MWCV is directly proportional to the number of length



classes in the sample, the choice of the interval of the length classes will determine the precision. Although increasing the size of length intervals will reduce the MWCV, this action will result in a loss of information which is undesirable. The cost of sampling, the detail required, and the purpose of the data collection need to be considered before the required precision level can be determined for applications other than the present example.

Without formal guidance on the appropriate sample size, the sample sizes chosen were, at best, weakly correlated with the number of size classes in the samples. It appears that the samplers under-estimated the required sample size for samples with large fish, whereas samples of smaller fish of the same species were over-sampled. This tendency to under-estimate the sample size may be related to the fact that the volume of a sample increases with the cube of its mean length; therefore a sample size of large fish may appear to be larger than the same number of small fish. In addition, samples with large fish tend to be spread out over a

larger number of size classes, thus requiring higher sample numbers.

In practice, it will be difficult for a sampler to estimate both the number of size classes and the number of fish in a sample. Therefore, the Marine Institute in Ireland is developing a software application that allows samplers to examine the length frequencies of the samples directly after they have been measured. The software estimates the weight of the suggested sample size for each distribution. Because size distributions tend to be similar on consecutive hauls, the sampler can gain an insight into the required weight of an appropriate sample for each species and size category.

The information contained in a length-frequency distribution is largely a function of sample size. The present method allows the amount of information contained in a length-frequency distribution to be quantified in terms of precision, allowing samplers to make informed decisions on the sample size that is required to obtain an adequate estimate of the length-frequency distribution of a particular catch.

Acknowledgments

Free R-software has been used for this work and the authors would like to thank the R development core team and all contributors to the R project (<http://www.R-project.org>). We also thank Colm Lordan and two anonymous reviewers for their valuable comments.

Literature cited

- Anderson, R. O., and R. M. Neumann.
1996. Length, weight, and associated structural indices. *In Fisheries techniques*, 2nd ed. (B. R. Murphy and D. W. Willis, eds.), p. 447-482. Am. Fish. Soc., Bethesda, MD.
- Erzini, K.
1990. Sample size and grouping of data for length-frequency analysis. *Fish. Res.* 9:355-366.
- Pennington, M., L. M. Burmeister, and V. Hjellvik.
2002. Assessing the precision of frequency distributions estimated from trawl-survey samples. *Fish. Bull.* 100:74-80.
- Smith, S. J., and J. J. Maguire.
1983. Estimating the variance of length composition samples. *In Sampling commercial catches of marine fish and invertebrates* (W. G. Doubleday and D. Rivard, eds.), p. 165-170. Can Spec. Pub. Fish. Aquat. Sci. 66, Ottawa, Canada.
- Thompson, S. K.
1987. Sample size for estimating multinomial proportions. *Am. Statist.* 41:42-46.
- Vokoun, J. C., C. F. Rabeni, and J. S. Stanovick.
2001. Sample-size requirements for evaluating population size structure. *N. Am. J. Fish. Manage.* 21:660-665.
- Zar, J. H.
1999. *Biostatistical analysis*, 4th ed., 663 p. Prentice-Hall, Inc., Englewood cliffs, NJ.

Abstract—We tested the hypothesis that larger juvenile sockeye salmon (*Oncorhynchus nerka*) in Bristol Bay, Alaska, have higher marine-stage survival rates than smaller juvenile salmon. We used scales from returning adults (33 years of data) and trawl samples of juveniles ($n=3572$) collected along the eastern Bering Sea shelf during August through September 2000–02. The size of juvenile sockeye salmon mirrored indices of their marine-stage survival rate (e.g., smaller fish had lower indices of marine-stage survival rate). However, there was no relationship between the size of sockeye salmon after their first year at sea, as estimated from archived scales, and brood-year survival size was relatively uniform over the time series, possibly indicating size-selective mortality on smaller individuals during their marine residence. Variation in size, relative abundance, and marine-stage survival rate of juvenile sockeye salmon is likely related to ocean conditions affecting their early marine migratory pathways along the eastern Bering Sea shelf.

Early marine growth in relation to marine-stage survival rates for Alaska sockeye salmon (*Oncorhynchus nerka*)

Edward V. Farley Jr¹

James M. Murphy¹

Milo D. Adkison²

Lisa B. Eisner¹

John H. Helle¹

Jamal H. Moss¹

Jennifer Nielsen³

Email address for E. V. Farley: Ed.Farley@noaa.gov

¹ NOAA, Auke Bay Laboratory
National Marine Fisheries Service, NOAA
11305 Glacier Highway
Juneau, Alaska 99801

² Juneau Center, School of Fisheries and Ocean Sciences,
University of Alaska Fairbanks
11120 Glacier Highway
Juneau, Alaska 99801

³ U.S. Geological Survey, Alaska Science Center
1011 East Tudor Road
Anchorage, Alaska 99503

Pacific salmon (*Oncorhynchus* spp.) experience relatively high mortality rates during the first few months at sea (Hartt, 1980), and it is believed that size plays an important role in survival (Parker, 1968; Pearcy, 1992). Size-dependent mortality of juvenile salmon may be concentrated during two specific life-history stages. The first stage is thought to occur just after juvenile salmon enter the marine environment, where smaller individuals are believed to experience higher size-selective predation (Parker, 1968; Willette et al., 1999). The second stage is thought to occur after the first summer at sea, when smaller individuals may not have sufficient energy reserves to survive late fall and winter (Beamish and Mahnken, 2001). Thus, larger individuals likely have a higher probability of survival during both of these stages, and size and growth while salmon reside in the estuary and during their first summer at sea may be important for survival.

Previous studies indicate that scale radius length is proportional to fish body length (Francis, 1990; Ricker,

1992) and, in particular, incremental increases in sockeye salmon (*O. nerka*) scale radius are strongly correlated with somatic growth (Fukuwaka and Kaeriyama, 1997). In our study, scales from adult Bristol Bay sockeye salmon were examined to determine the relationship between size after their first year at sea and survival to adulthood. We compared the time series (1965–97) of brood-year returns per spawner with scale growth measurements taken from adult sockeye salmon returning to the Egegik and Kvichak River systems in Bristol Bay, Alaska.

Juvenile sockeye salmon enter the marine waters of the eastern Bering Sea during May and June (Burgner, 1991) and migrate through Bristol Bay to the Bering Sea and North Pacific during the summer and early fall months (Straty, 1981; Farley et al., 2005). Two differing models of seaward migration are believed to exist for juvenile Bristol Bay sockeye salmon: in some years juvenile sockeye salmon migrate along the coastal waters of the eastern Bering Sea near the Alaska Peninsula, and in other

Manuscript submitted 27 March 2006
to the Scientific Editor.

Manuscript approved for publication
5 July by the Scientific Editor.

Fish. Bull. 105:121–130 (2007).

years their migration is farther offshore (Farley et al., 2005). We also compared the size of juvenile Bristol Bay sockeye salmon collected during late summer and early fall (2000–02) trawl surveys along the eastern Bering Sea shelf with indices of their abundance, marine stage survival rate after our survey, and returns per spawner from these cohorts. Interannual differences in the size and growth rates of juvenile sockeye salmon were also compared to their early marine distribution and ocean conditions. The specific objectives of this study were to determine whether larger, presumably faster growing, juvenile sockeye salmon in fact had higher survival rates than smaller, presumably slower growing individuals, and what aspects of the marine environment might influence these growth rates.

Materials and methods

Data

Our research focused on Bristol Bay sockeye salmon because this region has the largest returns and commercial harvest of sockeye salmon in the world. Scales from adult sockeye salmon, their fork lengths, and data on brood-year return per spawner for the Egegik and Kvichak Rivers in Bristol Bay, Alaska, as well as annual totals of the number of adult Bristol Bay sockeye salmon returns and spawners, were obtained from the Alaska Department of Fish and Game (ADF&G). Salmon scales are collected annually by ADF&G to estimate the age composition of adult sockeye salmon for fishery management. Age was designated by the European notation, i.e., *a.b*, where *a* = the number of winters spent in freshwater prior to going to sea and *b* = the number of winters spent in the ocean (Koo, 1962a). Salmon scale collections and brood year return per spawner data were available for the dominant freshwater and ocean age groups of sockeye salmon sampled in the Kvichak River (brood year returns for ages 1.2, 1.3, 2.2, 2.3; 1965–97) and the Egegik River (brood year returns for ages 1.3, 2.2, 2.3; 1965–97).

Scales were selected for measurement by following the procedures described in Ruggerone et al. (2005). Briefly, scales were selected when our age determination matched that previously made by ADF&G, the shape of the scale indicated that the scale was from the “preferred area” (below the dorsal fin and above the lateral line—see Koo, 1962b), and the circuli and annuli were clearly defined and not affected by scale regeneration or significant resorption along the measurement axis. The number of scale samples for each river system and age group are provided in Table 1.

Scales from adult sockeye salmon were digitized following procedures described by Hagen et al.¹ and Rug-

Table 1

The total number of scale samples for sockeye salmon (*Oncorhynchus nerka*) for brood years 1965–97 from the Egegik and Kvichak River systems in Bristol Bay, Alaska. Age groups are 1.2, 1.3, 2.2, and 2.3.

River	Age group			
	1.2	1.3	2.2	2.3
Egegik	0	1265	1592	1581
Kvichak	1563	1441	1582	1246

gerone et al. (2005). The scale measurement axis was determined by a perpendicular line drawn from a line intersecting each end of the first saltwater annulus. Distance (mm) between the focus and the outer edge of the scale was designated as the total scale length. The relationship between total scale length and adult fork length was linear for both the Egegik River (*F*-test, $P < 0.001$; $r^2 = 0.41$) and Kvichak River (*F*-test, $P < 0.001$; $r^2 = 0.36$) sockeye salmon samples. For an index of total growth through the first year at sea, we measured the distance from the focus to the outer edge of the first saltwater growth zone for each fish. A time series of annual means of the individual growth during the first year at sea ($MSWI_{i,a,t}$) estimated for each adult freshwater age group (*a* represents 1 or 2) within a river system (*i* represents Egegik, Kvichak) was used as an index of size that sockeye salmon would have attained after their first year (*t*) at sea.

The total number of fish caught and the fork lengths (mm) of juvenile sockeye salmon within each trawl haul were recorded during the Bering-Aleutian Salmon International Survey (BASIS) research cruises along the eastern Bering Sea shelf during fall (August–September) 2000 to 2002 (Fig. 1). The surveys were conducted over a broad area of the shelf and over major oceanographic domains (coastal and middle domains; Kinder and Schumacher, 1981) along the eastern Bering Sea shelf. In addition, the surveys were designed to sample the entire population of juvenile sockeye salmon from Bristol Bay lake systems to reduce the chance of sample variability that could affect one’s ability to interpret results from these samples. Recent descriptions of juvenile salmon migration pathways along the eastern Bering Sea shelf (Farley et al., 2005) and genetic stock composition indicate that juvenile sockeye salmon collected during the surveys were primarily from Bristol Bay.

Fish were collected by using a mid water rope trawl (see Farley et al., 2005 for description) rigged to sample the top 15 m of the water column. We attempted to collect scales from juvenile sockeye salmon during all three years of the survey; however, sample sizes of scales (from the preferred location on fish) were too small for statistical analyses because of descaling of the juvenile salmon by our mid-water rope trawl. Data

¹ Hagen, P. T., D. S. Oxman, and B. A. Agler. 2001. Developing and deploying a high resolution imaging approach for scale analysis. Doc. 567, p. 11. North Pacific Anadromous Fish Commission, 889 Pender Street, Vancouver, Canada.

collected during each trawl included the trawl speed obtained with a global positioning system and the height and width of the net opening obtained with a Simrad FS900 (Simrad, Lynnwood, WA) net sounder. The mean date of collection of juvenile sockeye salmon sampled for length differed slightly between years (i.e., 26 August during 2000; 5 September during 2001; 1 September during 2002); lengths were adjusted to account for these differences.

Survival and early marine-stage growth rates inferred from adult scales

For each freshwater age group, we calculated an index of survival rate that normalized the data and removed possible density-dependent effects (i.e., Peterman et al., 1998; Mueter et al., 2002). Specifically, our index of survival rate was the time series of residuals from a Ricker model defined by

$$\ln\left(\frac{R_{i,a,2,t+2} + R_{i,a,3,t+3}}{S_{i,t-(a+1)}}\right) = \alpha_{i,a} - \beta_{i,a} S_{i,t-(a+1)} + \varepsilon_{i,a,t}, \quad (1)$$

where t = the first ocean year for sockeye salmon;

S = the total number of spawners within river system i (i represents Egegik or Kvichak);

R = the total return (catch+spawners) for each freshwater age group a (a represents freshwater age 1 or 2) within river system i ;

α and β = model parameters representing the number of recruits per spawner at low numbers of spawners and the level of density dependence (Quinn and Deriso, 1999); and

$\varepsilon_{i,a,t}$ = the normally distributed residuals of the model.

For our analysis, partitioning salmon brood-year productivity by freshwater age group was necessary to directly compare our index of survival with our time series of $MSW1_{i,a,t}$ growth.

Analysis of covariance (ANCOVA) was used to examine the effect of $MSW1_{i,a,t}$ on our indices of survival (see Fig. 2, A–D for scatter plots of $\varepsilon_{i,a,t}$ and $MSW1_{i,a,t}$ and the addition of river system, age group and year were used as factors in the model. The results indicated that the year factor was highly significant (F -test, $P < 0.001$) and that $MSW1_{i,a,t}$ was not significant (F -test,

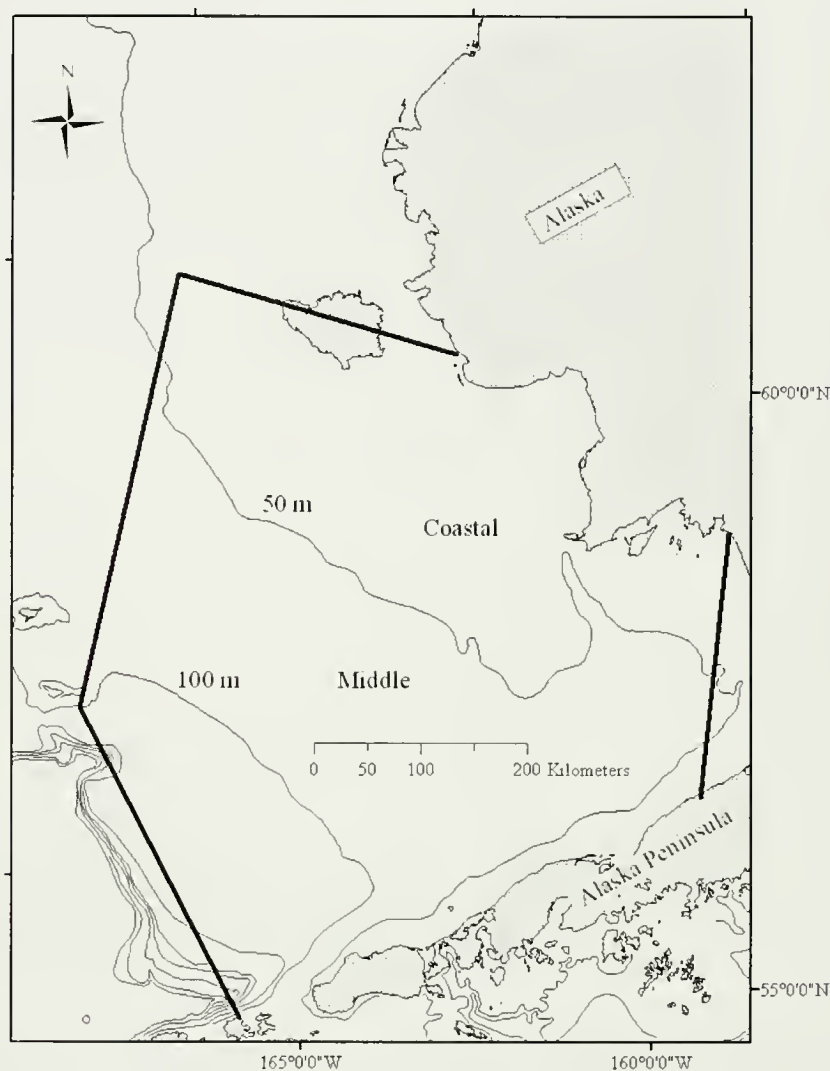
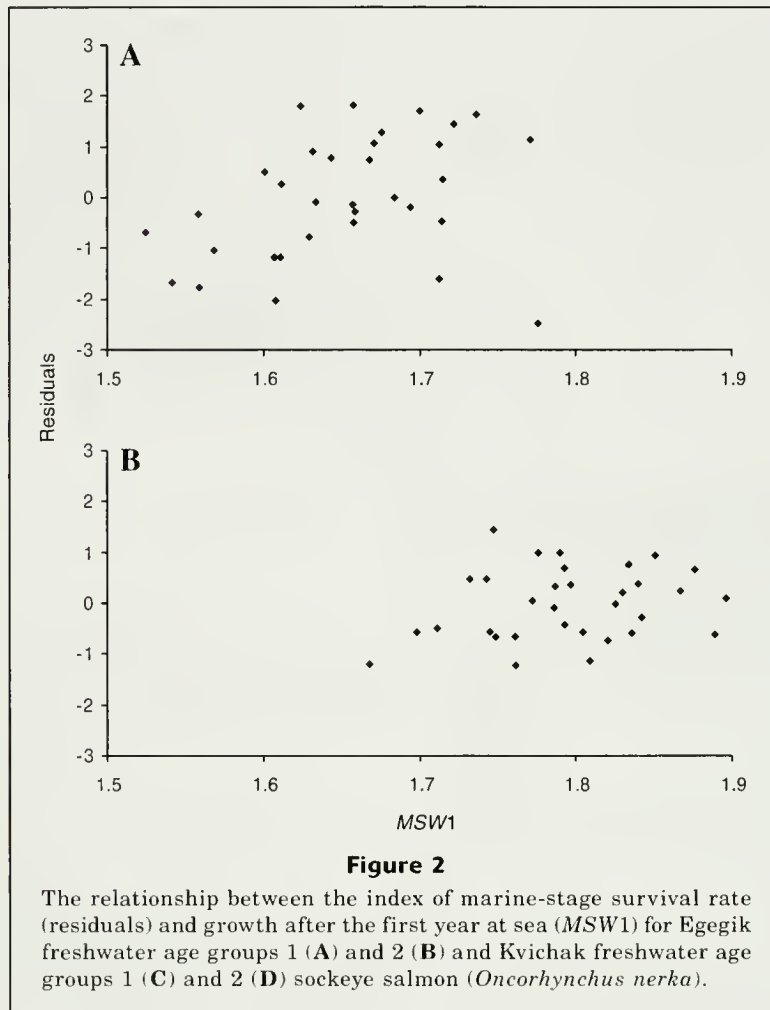


Figure 1

Survey area of the annual August–September (2000–2002) Bering-Aleutian Salmon International Survey (BASIS) within the coastal and middle domains of the eastern Bering Sea.

$P = 0.18$). It was possible that during some years all fish could have had excellent growth and attained a large size, but the ANCOVA model would have attributed the large size to the highly significant year factor. However, when we removed the year factor from the ANCOVA model, $MSW1_{i,a,t}$ was less significant (F -test, $P = 0.27$). In addition, the residuals from these models contained significant positive autocorrelation.

Because our data contained significant autocorrelation and showed a time series character, we created univariate time series models (Wei, 1990) for both $MSW1_{i,a,t}$ and $\varepsilon_{i,a,t}$ to determine whether autoregressive or moving average components were present. The univariate models were developed by examining the sample autocorrelation and partial autocorrelation functions for each time series. Time series data were considered white noise processes, i.e., uncorrelated random variables



with constant mean and variance, when none of the components of the sample autocorrelation and partial autocorrelation functions differed significantly ($P=0.01$) from zero (Wei, 1990).

Multivariate time series models in the form of linear transfer function (LTF) models (Liu and Hudak, 1992) were developed to describe the relationship between $MSW1_{1,a,t}$ and our index of survival rate for each freshwater age group and river system. All the univariate time series of survival rate indices contained significant positive first-order autoregressive parameters (see Table 2). Therefore, we included the first order autoregressive parameter in the LTF models. The models were defined as

$$\epsilon_{i,a,t} = c_{i,a} + \lambda_{i,a} MSW1_{1,a,t} + \frac{1}{(1 - \phi_{1,i,a} B)} N_{i,a,t}, \quad (2)$$

where t, i, a are described in Equation 1;

$MSW1$ = the early marine growth index for sockeye salmon during their first year at sea;

ϕ_1 = the autoregressive lag 1 parameter;

B = the symbol for the backshift operator (i.e., $B \times S_t = S_{t-1}$);

$c_{i,a}$ and $\lambda_{i,a}$ = parameters within the model; and
 $N_{i,a,t}$ = a sequence of random errors that are independently and identically distributed with a normal distribution.

Parameters within the univariate and LTF models were deemed significant when their t -value was greater than 2.0 ($P < 0.05$).

Autocorrelation analysis was used to examine whether the model residuals were white noise. Univariate and LTF models were compared by using Schwartz's Bayesian criterion (SBC; Wei, 1990) to determine if the inclusion of $MSW1$ in Equation 2 improved the model fit.

Analyses of data from juveniles collected by trawling

Next, we developed an index of relative survival rate of adult Bristol Bay sockeye salmon for 2000–02, and indices of abundance and marine-stage survival rate of juvenile sockeye salmon collected during 2000–02 to compare with mean lengths of juvenile sockeye salmon collected during those years. Relative survival was defined as the number of returning adult sockeye salmon from brood-year escapements that contributed to the

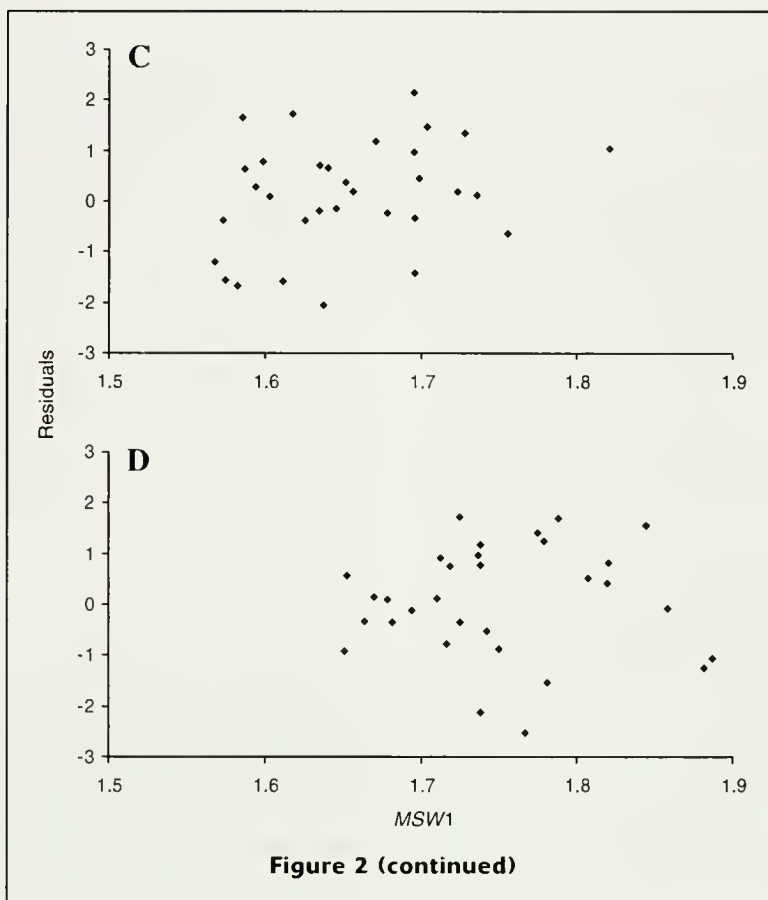


Table 2

Univariate (Univ) and linear transfer function (LTF) models indicating the effect of early marine growth index (*MSW1*) on the index of marine stage survival rates for each freshwater age group of sockeye salmon (*Oncorhynchus nerka*) returning to the Egegik and Kvichak rivers. Other variables include the constant (*Const*) and the autoregressive parameter ϕ_1 . Model statistics included the number of effective observations (*n*), the coefficient of determination (r^2), residual standard error (*RSE*), the number of parameters (*M*), and Schwartz's Bayesian criterion (*SBC*).

River	Age (yr)	Model	<i>n</i>	r^2	<i>RSE</i>	<i>M</i>	<i>SBC</i>	Model coefficients			<i>t</i> -value		
								<i>Const.</i>	<i>MSW1</i>	ϕ_1	<i>Const.</i>	<i>MSW1</i>	ϕ_1
Egegik	1	Univ	32	0.34	0.958	2	4.19	0.13	—	0.48	0.40	—	3.37
		LTF	32	0.41	0.908	3	4.22	-10.38	6.36	0.30	-2.22	2.25	2.07
	2	Univ	32	0.17	0.630	2	-22.64	0.02	—	0.42	0.10	—	2.64
		LTF	32	0.25	0.601	3	-22.19	-6.61	3.69	0.41	-1.74	1.75	2.59
Kvichak	1	Univ	32	0.29	1.075	2	11.56	-0.15	—	0.54	-0.36	—	3.60
		LTF	32	0.29	1.074	3	14.97	1.06	-0.73	0.54	0.21	-0.24	3.62
	2	Univ	32	0.35	0.986	2	6.00	-0.32	—	0.64	-0.64	—	3.99
		LTF	32	0.35	0.985	3	9.43	0.71	-0.59	0.64	0.18	-0.26	3.98

juvenile sockeye salmon in the trawl samples taken during years 2000, 2001, and 2002. For instance, juvenile sockeye salmon contributing to the early marine population during 2000 comprised age-2.0 fish from the

1997 and age-1.0 fish from the 1998 brood-year escape-ments, and these fish would have returned as adults during 2002 and 2003. Relative marine-stage survival rate (RS) was thus calculated as

$$RS_t = \frac{\sum_{a=1}^2 (R_{a,2,t+2} + R_{a,3,t+3})}{(S_{t-2} + S_{t-3})/2}, \quad (3)$$

where t = the year juvenile sockeye salmon were sampled ($t=2000, 2001, 2002$);

a = the freshwater age (1.0 or 2.0);

R = is the total number of returning adult sockeye salmon to Bristol Bay after year t ; and

S = the total number of spawners in Bristol Bay that contributed to the juvenile salmon population during year t .

For instance, freshwater juvenile sockeye salmon (ages 1.0 and 2.0) sampled during 2000 came from cohorts spawning during 1998 (age 1.0) and 1999 (age 2.0) and returned to Bristol Bay during 2002 as adult salmon at age 1.2 and 2.2 in 2002 and at age 1.3 and 2.3 in 2003. The numbers of returning adult and spawning Bristol Bay sockeye salmon were estimated from brood-year return information provided by ADF&G.

Annual indices of juvenile sockeye salmon abundance (IA) were defined as

$$IA_t = (SA/\overline{ma})\overline{C}_t, \quad (4)$$

where SA = the estimated survey area (189,000 km²);

\overline{ma} = the mean area sampled by a trawl haul during the survey (distance traveled during the tow multiplied by the width of the net); and

\overline{C}_t = the mean number of juvenile sockeye salmon caught during year t ($t=2000, 2001, 2002$).

This formula would give the abundance of juvenile sockeye salmon in the survey area if we assumed that catchability with our midwater trawl was 1, (i.e., all fish in front of the net were caught). Because this is unlikely, we treat our estimates as an index rather than as actual abundance. In fact, our juvenile sockeye salmon abundance indices were less than the resultant adult returns in some years, indicating that catchability of the net was much less than 1. One study (Shuntov et al., 1993) where larger surface trawl gear was used to sample juvenile salmon indicated that catchability of juvenile salmon was 0.3. We therefore divided our abundance indices by 0.3, although we still considered these values to be indices.

An index of juvenile sockeye salmon marine-stage survival rate (IMS) was estimated by

$$IMS_t = \frac{\sum_{a=1}^2 (R_{a,2,t+2} + R_{a,3,t+3})}{IA_t} \times 100, \quad (5)$$

where R is defined above in Equation 3, IA_t is defined in Equation 4, t is the year juvenile sockeye salmon were

sampled ($t=2000, 2001, 2002$), and a is freshwater age (age 1.0 or 2.0).

These survival rate indices were correlated with the mean length of juvenile fish collected during the corresponding first year at sea. Because the mean date for juvenile sockeye salmon sampled for length differed among years, we adjusted fish lengths to provide a standardized length using September 1 as the standard date. Adjusted mean fish lengths were calculated by assuming three different daily growth rates: 1) 0 mm/day, representing no daily growth at sea; 2) 0.3 mm/day, the lower end of published growth-rate ranges for juvenile Pacific salmon; and 3) 1.7 mm/day, representing the upper end of the ranges (see Fisher and Percy, 1988, 1990; Fukuwaka and Kaeriyama, 1994; Orsi et al., 2000 for daily growth-rate ranges for juvenile Pacific salmon).

Results

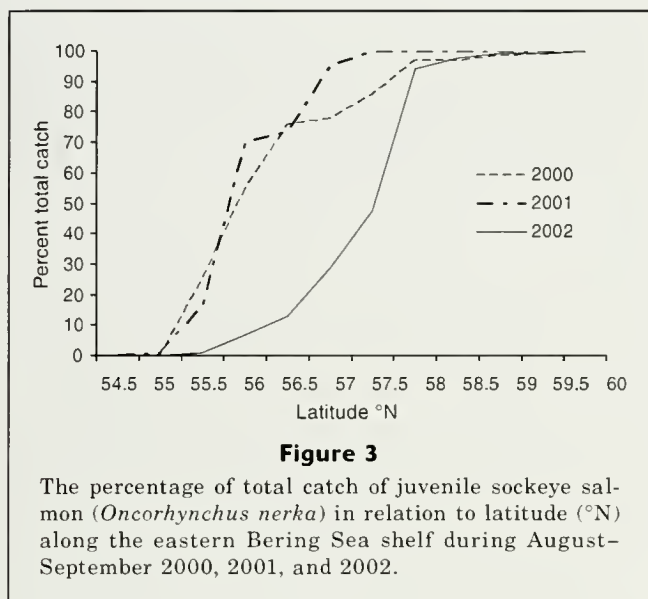
Analyses of adult scale data

Examination of the autocorrelation and partial autocorrelation functions for Kvichak River freshwater age groups 1 and 2 and the Egegik River freshwater age-group-1 MSW1 univariate time series indicated that these time series had a constant mean and variance. For the Egegik River freshwater age-group-2 MSW1 growth index, the sample autocorrelation and partial autocorrelation functions indicated that a lag-1 autoregressive parameter was appropriate and the estimate of the parameter was significant (t -test, $P<0.01$). Coefficients of variation were less than 4% for the MSW1 growth-rate indices for each freshwater age group, and thus confirmed the univariate model results that these time series varied little over time. By comparison, the coefficients of variation for the time series of returns per spawner for each freshwater age group were between 70% and 135%.

The MSW1 growth index was not significantly related to survival in any of the LTF models except for Egegik freshwater age group 1 (Table 2). Parsimonious univariate models were reasonable explanations of survival for both river systems and age groups, having values of SBC nearly as low as the "best" models. The sample autocorrelation and partial autocorrelation functions indicated that a lag-1 autoregressive parameter was appropriate for the all of the univariate survival rate time series models. The estimates of the lag-1 autoregressive parameter were positive for all of the univariate models.

Analyses of data from juveniles collected by trawling

The distribution of juvenile sockeye salmon along the eastern Bering Sea varied among years (Fig. 3). During 2000 and 2001, 75% of the total catch of juvenile sockeye salmon occurred south of 56°N, within the middle domain and south within the stratified waters near the



coastal domain along the Alaska Peninsula. During 2002, 75% of the total catch of juvenile sockeye salmon occurred north of 57°N, with 50% of the total catch occurring north of 58°N within the shallow stratified waters near the northern coastal domain.

Average fork length of juvenile sockeye salmon was significantly smaller during 2001 than during 2000 and 2002 for growth rates greater than 0.3 mm/day (t -test; $P < 0.01$) and not significantly different from 2000 (t -test; $P = 0.05$) for growth rates equal to 0 mm/day (Table 3). The rank order of juvenile sockeye salmon fork lengths was the same for all growth rates, and the largest fish taken in 2002 and the smallest, in 2001. For all three growth rates, average fork length was significantly larger during 2002 than during 2000 and 2001 (t -test; $P < 0.01$).

The marine-stage survival rate and abundance in the indices mirrored the observed variation in fish fork length; they were highest during 2002 and at or near their lowest during 2001 (Table 4). In addition, the nearshore distribution of juvenile sockeye salmon (2001; Fig. 3) appeared to coincide with lower indices of abundance and marine-stage survival rate, whereas fish distributed in the northern area of our survey (2002; Fig. 3) exhibited higher marine-stage survival rate and abundance.

Discussion

Our study indicates that the size of Bristol Bay sockeye salmon after their first year at sea is not directly related to their survival, when size is measured from growth rings on the scales of adults returning to the Egegik and Kvichak rivers. Analyses of the MSW1 growth index indicated that most of the time series had a constant mean and variance. Similar studies where adult scales

Table 3

Average fork length of juvenile sockeye salmon (*Oncorhynchus nerka*) collected along the eastern Bering Sea during 2000, 2001, and 2002. Daily growth rate (mm) was assumed to be 0, 0.30, and 1.7. Statistics include sample size (n), average fork lengths, and standard deviation (SD) of the original length data.

Year	m	Average fork length (mm)			SD
		0	0.3	1.7	
2000	834	174.77	176.53	184.76	19.99
2001	802	171.91	170.61	164.53	35.55
2002	1936	197.96	197.94	197.83	34.74

Table 4

Indices of abundance (IA), marine-stage survival rate (IMS), and relative marine-stage survival rate (RS) for juvenile sockeye salmon (*Oncorhynchus nerka*) collected along the eastern Bering Sea during 2000, 2001, and 2002.

Year	IA	IMS	RS
2000	130	21%	3.8
2001	137	15%	1.9
2002	180	34%	6.0

from Atlantic (*Salmo salar* L.; Crozier and Kennedy, 1999), coho (*O. kisutch*; Briscoe, 2004), and chum (*O. keta*; Helle, 1979) salmon were used to measure growth (size) of salmon during their first year at sea revealed that the survival rate of a cohort was statistically unrelated to variation in growth (size) of the salmon. The relative uniformity in the size of salmon after their first year at sea and the lack of a relationship between size and survival rate is contrary to the prevailing paradigm that the size achieved by fish after their first summer at sea is important to survival (Beamish and Mahnken, 2001). However, these results do not necessarily invalidate this paradigm; the adult scale samples available for analysis may reflect only those juvenile salmon that had attained sufficient size in order to survive to adulthood, and not those that died at sea (Crozier and Kennedy, 1999).

In support of this possibility, when we directly measured the fork length of juvenile sockeye salmon (Tables 3 and 4) during late summer and early fall surveys along the eastern Bering Sea shelf (2000–02), smaller fish had lower indices of marine-stage survival rate. This result is consistent with that from other studies of teleost fish, where larger individuals gained a survival advantage over smaller conspecifics during the juvenile life-history stage (Parker, 1968; Healey, 1982; Holtby et

al., 1990; Pearcy, 1992; Sogard, 1997; Mortensen et al., 2000; Beamish and Mahnken, 2001; Moss et al., 2005). This result is also in accord with the critical-size and critical-period hypothesis in which brood-year survival is determined by the number of juvenile salmon that have reached a critical size by the end of their first marine summer (Beamish and Mahnken, 2001; Beamish et al., 2004). The assumption with this hypothesis is that fish that do not reach a critical size after their first summer at sea will die because they are unable to meet minimum metabolic requirements during late fall and winter (Beamish and Mahnken, 2001). Although our results indicate that larger juvenile sockeye salmon have higher relative marine-stage survival rate after their first year at sea, it is difficult to directly address when the mortality would occur because sockeye salmon can spend an average of 2 to 3 years at sea. However, the overwhelming evidence from field and laboratory studies of juvenile stages of teleost fishes seems to indicate that size-selective mortality occurs during winter because larger members of a cohort are better than smaller members at tolerating physical extremes and enduring longer periods without food (Sogard, 1997).

One other test of the critical-size and critical-period hypothesis is that mortality rates after this period should be large in relation to other sources of early marine mortality (Beamish et al., 2004). To interpret our indices of marine-stage survival rate as the actual post-survey marine survival rate requires making a variety of questionable assumptions (e.g., that the vulnerability of juvenile salmon to our gear is known). However, if our estimates are close to correct, they would indicate that marine-stage mortality rates of juvenile sockeye salmon may be greater than 70% (Table 4) after our late-summer-early-fall surveys. These marine-stage mortality rates are substantial and approach late fall and winter mortality rates of greater than 90% found for other Pacific salmon (Beamish et al., 2004).

Lengths of juvenile sockeye salmon differed significantly among years if we assumed daily growth rates of 0.3 mm and greater. Differences in fork length of juvenile sockeye salmon could reflect annual differences in early marine growth rates or may also reflect annual differences in the size of smolt leaving Bristol Bay lake systems. However, limited surveys of sockeye salmon smolt from the Kvichak and Ugashik Rivers during 2000 through 2002 (Egegik River sampling was not undertaken in 2002) by ADF&G indicate that differences in smolt length among years and within age classes and river systems were less than 9%. In addition, the smallest average smolt size among these three years was seen during 2002, the year with the largest juvenile sockeye salmon size. Thus, it is likely that annual differences in length observed during our survey were due to differences in marine growth rates between years.

The annual variability in juvenile sockeye salmon size and in indices of marine-stage survival rates may be linked to the early marine migration of these salmon along the eastern Bering Sea shelf. Although we had

only three years of data, size and survival indices of Bristol Bay sockeye salmon were lowest when juvenile sockeye salmon were distributed nearshore along the Alaska Peninsula (i.e., the coastal migration pathway) and highest when they were distributed farther north and offshore. In support of this theory, the coastal migration pathway of juvenile Bristol Bay sockeye salmon observed by Straty (1981) during the late 1960s and early 1970s coincided with a significantly lower production of Bristol Bay sockeye salmon that occurred before the mid 1970s (Adkison et al., 1996).

The annual variability in seaward migration pathways is likely related to ocean conditions on the shelf during spring and summer. Recent studies indicate that sea surface temperatures along the eastern Bering Sea in summer, the period when juvenile sockeye salmon are present on the shelf, is positively correlated with Bristol Bay sockeye salmon survival rates (Mueter et al., 2002). It is possible that the effect of sea surface temperatures on survival rates of juvenile Bristol Bay sockeye salmon is a result of its influence on early marine distribution of juvenile sockeye salmon. For example, during the late 1960s and early 1970s, the nearshore migration of juvenile Bristol Bay sockeye salmon was thought to be a result of sockeye salmon using the warmer nearshore waters rather than the colder sea surface temperatures offshore in order to maximize their growth (Straty, 1981). Depth-averaged sea temperatures from an oceanographic mooring along the eastern Bering Sea middle shelf domain from mid-July to mid-September were consistently warmer during 2001 through 2002 than during 1995 through 1997 (Overland and Stabeno, 2004). Presumably, the warmer sea temperatures during 2001 would have been conducive to offshore migration of juvenile sockeye salmon during that year. Although sea temperatures were warmer during 2001 through 2002, sea temperatures along the shelf were 1° to 2°C cooler from late June to September during 2001 than during 2002 (Overland and Stabeno, 2004). Thus, it may be that warmer sea temperatures during the time juvenile sockeye salmon first are present over the eastern Bering Sea shelf (beginning in June) provide a conduit for rapid offshore migration (and possibly higher survival) and that cooler sea temperatures delay offshore migration.

Our results indicate that after the first summer in the Bering Sea, larger juvenile sockeye salmon may gain a survival advantage over smaller individuals. This result, coupled with previous findings of reduced juvenile-to-adult survival for pink (Moss et al., 2005) and coho (Beamish et al., 2004) salmon that spend their first summer in the coastal waters of the Gulf of Alaska and Strait of Georgia, indicates that reduced growth of Pacific salmon during their first year at sea may lead to substantial salmon mortality, presumably during their first winter at sea. This phenomenon may not be seen if size of the salmon after their first year at sea is inferred from the scale growth increments of returning adults, because these individuals could be a biased sample from the faster-growing portion of the

population (Crozier and Kennedy, 1999). We suggest that annual variability in the size of sockeye salmon may be related to summer sea surface temperatures along the eastern Bering Sea shelf temperatures that appear to influence the spatial distribution and early marine migration pathways of this species.

Acknowledgments

P. Hagen, formally with the Alaska Department of Fish and Game in Juneau, Alaska, was instrumental in aging and creating digital pictures of juvenile sockeye salmon scales. We gratefully appreciate the help of the captains (M. Cavanaugh and S. Brandstetter) and the crew of the FV *Sea Storm* and captain C. Bronson and the crew of the FV *Great Pacific* for their fine efforts and technical assistance in all aspects of the field surveys. We thank A. Wertheimer, G. Kruse, and three anonymous reviewers for suggestions during this study and comments on the manuscript.

Literature cited

- Adkison, M. D., R. M. Peterman, M. F. Lapointe, D. M. Gillis, and J. Korman.
1996. Alternative models of climatic effects on sockeye salmon, *Oncorhynchus nerka*, productivity in Bristol Bay, Alaska, and the Fraser River, British Columbia. *Fish. Oceanogr.* 5:137-152.
- Beamish, R. J., and C. Mahnken.
2001. A critical size and period hypothesis to explain natural regulation of salmon abundance and the linkage to climate and climate change. *Prog. Oceanogr.* 49:423-437.
- Beamish, R. J., C. Mahnken, and C. M. Neville.
2004. Evidence that reduced early marine growth is associated with lower marine survival of coho salmon. *Trans. Am. Fish. Soc.* 133:26-33.
- Burgner, R. L.
1991. Life history of sockeye salmon (*Oncorhynchus nerka*). In *Pacific salmon life histories* (C. Groot and L. Margolis, eds.), p. 3-117. Univ. British Columbia Press, Vancouver, Canada.
- Briscoe, R. J.
2004. Factors affecting marine growth and survival of Auke Creek, Alaska coho salmon (*Oncorhynchus kisutch*). M.S. thesis, 57 p. Univ. Alaska Fairbanks, Fairbanks, AK.
- Crozier, W. W., and J. A. Kennedy.
1999. Relationships between marine growth and marine survival of one sea winter Atlantic salmon, *Salmo salar* L., from the River Bush, Northern Ireland. *Fish. Manage. Ecol.* 6:89-96.
- Farley, E. V., Jr., J. M. Murphy, B. W. Wing, J. H. Moss, and A. Middleton.
2005. Distribution, migration pathways, and size of western Alaska juvenile salmon along the eastern Bering Sea shelf. *Alaska Fish. Res. Bull.* 11(1):15-26.
- Fisher, J. P., and W. G. Pearcy.
1988. Growth of juvenile coho salmon (*Oncorhynchus kisutch*) off Oregon and Washington, USA, in years of differing coastal upwelling. *Can. J. Fish. Aquat. Sci.* 45:1036-1044.
1990. Spacing of scale circuli versus growth rate in young coho salmon. *Fish. Bull.* 88:637-643.
- Francis, R. I.
1990. Back-calculation of fish length: a critical review. *J. Fish Biol.* 36:883-902.
- Fukuwaka, M., and M. Kaeriyama.
1994. A back-calculation method for estimating individual growth of juvenile chum salmon by scale analysis. *Scientific Reports of the Hokkaido Salmon Hatchery* 48:1-9.
1997. Scale analyses to estimate somatic growth in sockeye salmon, *Oncorhynchus nerka*. *Can. J. Fish. Aquat. Sci.* 54:631-636.
- Hartt, A. C.
1980. Juvenile salmonids in the oceanic ecosystem: the critical first summer. In *Salmonid ecosystems of the North Pacific* (W. J. McNeil and D. C. Himsworth, eds.), p. 25-57. Oregon State Univ. Press, Corvallis, OR.
- Healey, M. C.
1982. Timing and relative intensity of size-selective mortality of juvenile chum salmon (*Oncorhynchus keta*) during early sea life. *Can. J. Fish. Aquat. Sci.* 39:952-957.
- Helle, J. H.
1979. Influence of marine environment on age and size at maturity, growth, and abundance of chum salmon, (*Oncorhynchus keta*) from Olsen Creek, Prince William Sound, Alaska. Ph.D. diss., 118 p. Oregon State Univ., Corvallis, OR.
- Holtby, L. B., B. C. Andersen, and R. K. Kadowaki.
1990. Importance of smolt size and early ocean growth to interannual variability in marine survival of coho salmon (*Oncorhynchus kisutch*). *Can. J. Fish. Aquat. Sci.* 47:2181-2194.
- Kinder, T. H., and J. D. Schumacher.
1981. Hydrographic structure over the continental shelf of the southeastern Bering Sea. In *The eastern Bering Sea shelf: oceanography and resources*, vol. 1 (D. W. Hood and J. A. Calder, eds.), p. 31-52. Univ. Washington Press, Seattle, WA.
- Koo, T. S. Y.
1962a. Age designation in salmon. In *Studies of Alaska red salmon* (T. S. Y. Koo, ed.), p. 41-48. Publications in Fisheries, New Series 1, Univ. Washington, Seattle, WA.
- 1962b. Age and growth studies of red salmon scales by graphical means. In *Studies of Alaska red salmon* (T. S. Y. Koo, ed.), p. 49-121. Publications in Fisheries, New Series 1, Univ. Washington, Seattle, WA.
- Liu, L., and G. B. Hudak.
1992. Forecasting and time series analysis using the SCA statistical system, 435 p. Scientific Computing Associates Corporation, Oak Brook, IL.
- Mortensen, D., A. Wertheimer, S. Taylor, and J. Landingham.
2000. The relation between early marine growth of pink salmon, *Oncorhynchus gorbuscha*, and marine water temperature, secondary production, and survival to adulthood. *Fish. Bull.* 98:319-335.
- Moss, J. H., D. A. Beauchamp, A. D. Cross, K. Myers, E. V. Farley Jr., J. M. Murphy, and J. H. Helle.
2005. Higher marine survival associated with faster growth for pink salmon (*Oncorhynchus gorbuscha*). *Trans. Am. Fish. Soc.* 134:1313-1322.

- Mueter, F. J., D. M. Ware, and R. M. Peterman.
2002. Spatial correlation patterns in coastal environmental variables and survival rates of salmon in the north-east Pacific Ocean. *Fish. Oceanogr.* 11(4):205–218.
- Orsi, J. A., M. V. Sturdevant, J. M. Murphy, D. G. Mortensen, and B. L. Wing.
2000. Seasonal habitat use and early marine ecology of juvenile Pacific salmon in southeastern Alaska. *N. Pac. Anad. Fish Comm. Bull.* 2:111–122.
- Overland, J. E., and P. J. Stabeno.
2004. Is the climate of the Bering Sea warming and affecting the ecosystem? *EOS, Trans. Am. Geophys. Union.* 85(33):309–312.
- Parker, R. R.
1968. Marine mortality schedules of pink salmon of the Bella Coola River, Central British Columbia. *J. Fish. Res. Board Can.* 25:757–794.
- Pearcy, W. G.
1992. Ocean ecology of the North Pacific salmonids, p. 179. Univ. Washington Press, Seattle, WA.
- Peterman, R. M., B. J. Pyper, M. F. Lapointe, and M. D. Adkison.
1998. Patterns of covariation in survival rates of British Columbian and Alaskan sockeye salmon (*Oncorhynchus nerka*) stocks. *Can. J. Fish. Aquat. Sci.* 55:2503–2517.
- Quinn, T. J., II, and R. B. Deriso.
1999. Quantitative fish dynamics, 542 p. Oxford Univ. Press, New York, NY.
- Ricker, W. E.
1992. Back-calculation of fish lengths based on proportionality between scale and length increments. *Can. J. Fish. Aquat. Sci.* 49:1018–1026.
- Ruggerone, G. T., E. V. Farley Jr., J. Nielsen, and P. Hagen.
2005. Seasonal marine growth of Bristol Bay sockeye salmon (*Oncorhynchus nerka*) in relation to competition with Asian pink salmon (*O. gorbuscha*) and the 1977 ocean regime shift. *Fish. Bull.* 103:355–370.
- Shuntov, V. P., V. I. Radchenko, V. V. Lapko, and Y. N. Poltev.
1993. The distribution of the Pacific salmon in the Sakhalin-Kuril region at a period of anadromous migration (in Russian). *J. Ichthy. Moscow* 33:348–358.
- Sogard, S. M.
1997. Size-selective mortality in the juvenile stage of teleost fishes: a review. *Bull. Mar. Sci.* 60(3):1129–1157.
- Straty, R. R.
1981. Ecology and behavior of juvenile sockeye salmon (*Oncorhynchus nerka*) in Bristol Bay and the eastern Bering Sea. In *The eastern Bering Sea shelf: oceanography and resources*, vol. 2 (D. W. Hood and J. A. Calder, eds.), p. 285–320. Univ. Washington Press, Seattle, WA.
- Wei, W. W. S.
1990. Time series analysis: univariate and multivariate methods, 478 p. Addison-Wesley Publ. Company, Redwood City, CA.
- Willette, T. M., R. T. Cooney, and K. Hyer.
1999. Predator foraging mode shifts affecting mortality of juvenile fishes during the subarctic spring bloom. *Can. J. Fish. Aquat. Sci.* 56:364–376.

Abstract—Inaccuracy in the aging of postovulatory follicles (POFs) and in estimating the effect of temperature on the resorption rate of POFs may introduce bias in the determination of the daily spawning age classes with the daily egg production method (DEPM). To explore the above two bias problems with field-collected European pilchard (*Sardina pilchardus*, known regionally as the Iberian sardine), a method was developed in which the time elapsed from spawning (POF age) was estimated from the size of POFs (i.e., from the cross-sectional area in histological sections). The potential effect of the preservative type and embedding material on POF size and the effect of ambient water temperature on POF resorption rate are taken into account with this method. A highly significant log-linear relationship was found between POF area and age; POF area shrank by approximately 50% per day. POFs were also shown to shrink faster at higher temperatures (approximately 3% per degree), but this temperature effect is unlikely to be an important source of bias in the assignment of females to daily spawning classes. The embedding material was also shown to influence the size of POFs, the latter being significantly larger in resin than in paraffin sections. In conclusion, the size of POFs provides an indirect, reliable estimation of the time elapsed from spawning and may thus be used to test both the validity of POF staging criteria for identifying daily classes of spawners and the effect of other factors (such as temperature and laboratory processing) in applications of the DEPM to *S. pilchardus* and other fish species.

Degeneration of postovulatory follicles in the Iberian sardine *Sardina pilchardus*: structural changes and factors affecting resorption

Konstantinos Ganias^{1,2}

Cristina Nunes²

Yorgos Stratoudakis²

Email for K. Ganias: kganias@bio.auth.gr

¹ School of Biology

Laboratory of Ichthyology

Aristotle University of Thessaloniki

54 124 Thessaloniki, Greece

² Instituto Nacional de Investigação Agrária e das Pescas

Instituto de Investigação das Pescas e do Mar

Avenida de Brasília s/n, 1449-006

Lisbon, Portugal

The postovulatory follicle (POF) consists of the follicular layers that remain in the ovary of fish after the release of the ovum during spawning (Saidapur, 1982). Initially, the POF is a distinct structure, but it rapidly deteriorates and becomes undetectable within a few days (Hunter and Goldberg, 1980). The study of POF degeneration is important in fishery studies because it permits the assignment of spawning females to daily classes to provide estimates of the daily fraction of spawning fish in the population (POF method, Hunter and Goldberg, 1980). The most common application of the POF method is in the daily egg production method (DEPM; Parker, 1980), where spawning fraction, together with other adult parameters, are used to estimate daily specific fecundity (Picquelle and Stauffer, 1985) for the fisheries-independent estimation of spawning biomass. A prerequisite for such applications is the existence of an accurate aging key that describes the time course of POF degeneration (Hunter and Macewicz, 1985).

In most DEPMs, the degeneration of POFs is described by a small number of histomorphological stages (see "Materials and methods" section) that are usually assumed to correspond to distinct daily classes (see review by Stratoudakis et al., 2006). How-

ever, because the process of POF degeneration is continuous and DEPM samples are usually obtained opportunistically throughout the day, the direct assignment of POF stages to daily classes of spawning fish can be imprecise. Also, morphological stages are often attributed to daily classes without prior validation and thus can lead to biased estimates of the spawning fraction. Validation is best performed in the laboratory by sacrificing female spawning fish at known time intervals after ovulation (e.g., Hunter and Goldberg, 1980; Pérez et al., 1992). Alternatively, in fish with daily spawning synchronicity, such as with the Iberian sardine *Sardina pilchardus* (also known as the European pilchard, FAO, 1985) (Bernal et al., 2001; Zwolinski et al., 2001; Ganias et al., 2003), validation can be performed indirectly through the examination of field samples collected at different hours of the day (Goldberg et al., 1984).

Another source of potential bias in the POF method is the duration of follicular degeneration, which may be temperature-dependent (Hunter and Macewicz, 1985), because the metabolic rates of poikilotherms, like fish, may be directly affected by ambient temperature. As a result, POF degeneration may be faster at higher temperatures and may lead to biased

Manuscript submitted 12 May 2006
to the Scientific Editor.

Manuscript approved for publication
5 July 2006 by the Scientific Editor.

Fish. Bull. 105:131–139 (2007).

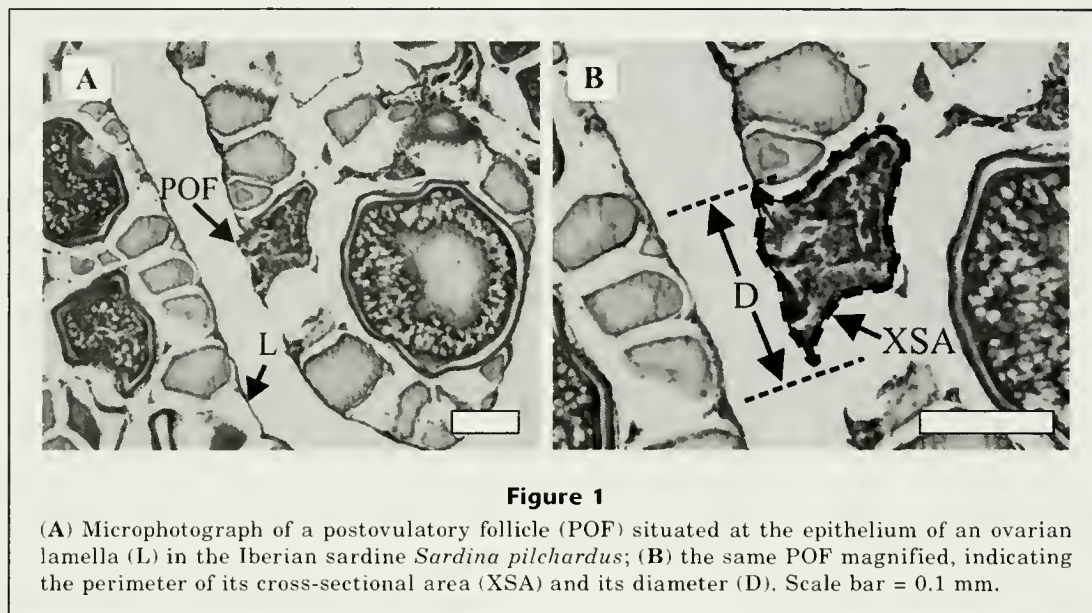


Figure 1
 (A) Microphotograph of a postovulatory follicle (POF) situated at the epithelium of an ovarian lamella (L) in the Iberian sardine *Sardina pilchardus*; (B) the same POF magnified, indicating the perimeter of its cross-sectional area (XSA) and its diameter (D). Scale bar = 0.1 mm.

estimates of the spawning fraction and biomass when spatial variation in ambient water temperature is large within a survey area. This dependence can be assessed under laboratory conditions through inspection of specimens spawning under different temperature regimes (Fitzhugh and Hettler, 1995). Alternatively, the effect of temperature on POF degeneration can be studied in the wild by the examination of individuals caught at variable environmental conditions (Ganias et al., 2003; Roumillat and Brouwer, 2004).

Because of the above unresolved issues of the POF method (that can be species specific), the spawning fraction remains the most poorly estimated DEPM parameter (Hunter and Lo, 1997; Stratoudakis et al., 2006). The main objective of our study was to devise a method whereby one can test indirectly for potential sources of bias in the attribution of stage and age to the POFs of the field-collected sardine *S. pilchardus*. We used the size of POFs (cross-sectional area and diameter) as an index of POF age and, together with other histomorphological characteristics (follicle shape, state of the granulosa layer), we refined existing criteria for determining the stage and age of POFs in sardine. Then, we modeled the size of POFs as a function of POF age, ambient temperature, type of preservative, and type of embedding material. The analysis allowed us to test whether our staging criteria were valid and to examine whether temperature and laboratory processing introduced bias in the process.

Materials and methods

Adult sardines were collected off Portugal and the Gulf of Cadiz in 1997, 1999, and 2005 within the framework of DEPM surveys for the estimation of the spawning biomass of the Atlanto-Iberian sardine stock (ICES,

2004). Sampling was conducted during peak spawning months for sardine (January–March), either on board the RV *Noruega* or from the commercial purse-seine fleet. During the surveys, sea surface temperature (SST) was recorded on an extensive grid representing hydrographic casts that covered the whole sampling area during the ichthyoplankton surveys (ICES, 2004).

Fish gonads were immediately removed after capture and placed in jars either with AFA (65 parts by volume of 50% alcohol, 32 parts formalin, and 13 parts glacial acetic acid) solution [1997, 1999] or with 4% formalin [2005]. In the laboratory, ovaries were embedded either in paraffin (1997, 2005) or in resin (1999), and histological sections (paraffin: 5 μm ; resin: 3 μm) were stained with hematoxylin and eosin. Histological slides were examined and scored for maturity, atresia, and presence of POFs. When POFs were detected, slides were scanned in detail to locate the largest follicle situated along the epithelium of the lamellae. These POFs were photographed with a digital camera attached to the microscope at various magnifications so that the whole follicle would fit into the microphotograph (Fig. 1A). The cross-sectional area of the whole POF (all samples) and the distance between the two extremes of the follicle on the lamella (POF diameter, paraffin samples) were measured with UTHSCSA image analysis software (Univ. Texas Health Science Center, San Antonio, Texas) (Fig. 1B). Differences in the dimensional (size, shape) and fine histological (degeneration of the granulosa layer) characteristics were used, together with existing descriptions for *Sardina* populations (Atlantic: Pérez et al., 1992; Mediterranean: Ganias et al., 2003), to describe the pattern of POF resorption.

The evolution in the shape of POFs was assessed through the allometric relationship between diameter (D) and cross-sectional area (XSA):

$$XSA = a \times D^b, \quad (1)$$

where a and b are parameters.

In case of isometry, (i.e., $b=2$), shrinkage is supposed to occur evenly in all dimensions, and the shape of the regressing POFs does not undergo significant changes. In any other case ($b>2$, or $b<2$), the shape is altered along resorption, and thus its intermediate phases may be used in the staging of POFs.

Existing histological criteria for the staging of sardine POFs were refined and based on two hauls from the 2005 survey that contained more than 90 histological specimens each. Given that individuals in each sample were caught at the same time and temperature, POFs in each daily cohort should have been at the same stage and have had the same age, maximizing the morphological contrast among daily classes. Furthermore, one of these hauls was performed in the evening, just before the average daily spawning hour for the Iberian sardine (20:00; Zwolinski et al., 2001; ICES, 2004) and thus provided information on the final histological state of each daily class of POFs.

After refining the staging criteria and classifying the POFs from all surveys into daily classes, we used the time of capture and daily spawning hour to estimate the exact age of POFs, i.e., the time in hours elapsed between spawning and sampling. The effect of POF age and other factors on POF cross-sectional area were tested with a generalized linear model (GLM) with an overdispersed Poisson distribution and a logarithmic link function. Apart from POF age, the effect of temperature, sampling year, and the one-way interaction of year with age were considered in the model. The significance of the relationship between POF age and size indicated whether our staging and aging criteria were accurate. Furthermore, because the laboratory processing of the ovaries differed from year to year, the year effect and its interaction with age was used to test the effect of preservation medium (AFA, formalin) and embedding material (paraffin, resin) on the size of POFs. Residual inspection plots revealed the adequacy of the fitted model.

Results

A total of 249 ovaries with POFs were detected and used in our analysis (1997: 65, 1999: 104, 2005: 80). The two hauls from the 2005 survey that were used for refining POF staging criteria contained many females with POFs at various stages and sizes, facilitating the distinction between successive daily classes of spawners. The frequency distribution of POF cross-sectional areas in the two hauls displayed three size modes, which were considered to correspond to different age classes (Fig. 2).

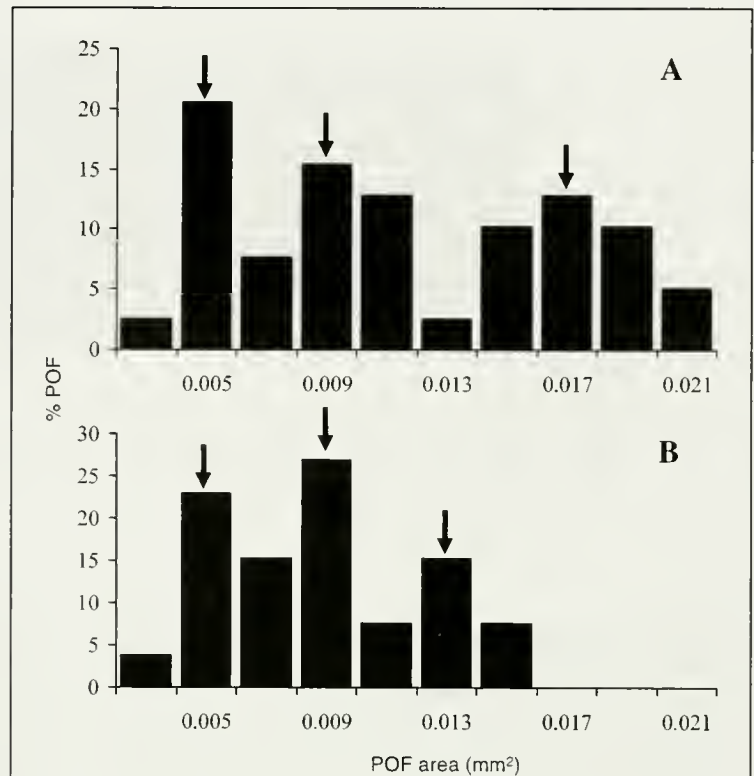


Figure 2

Frequency distribution of postovulatory follicle (POF) cross-sectional areas from two samples of the Iberian sardine *Sardina pilchardus* from the 2005 survey. (A) Sample collected at 12:00, $n=48$; (B) sample collected at 17:30, $n=32$. Arrows indicate POF size modes in each sample.

The most advanced size mode in the sample hauled at 12:00 (Fig. 2A) consisted of larger POFs compared to the POFs in the sample hauled at 17:30 (Fig. 2B). Re-examination and comparison of POF size modes in each sample showed that, apart from size, they differed in shape and in the fine histological characteristics of the follicular layers (Fig. 3). In particular, large POFs had an irregular shape and contained a large, convoluted, and thick granulosa layer (Fig. 3A). In the intermediate size mode, the shape of the follicle changed to semirectangular and the granulosa layer tended to lose its convoluted appearance and to form a single layer (Fig. 3B). Finally, in the smaller size mode, all POFs displayed a triangular shape (Fig. 3, C–E). However, more detailed examination showed that these triangular POFs could be further separated into 1) a group of slightly larger POFs with a thin layer of the granulosa (Fig. 3C), and 2) a group of very small POFs that contained only granulosa remnants in the form of residual vacuoles (Fig. 3, D and E).

POF diameter increased significantly with POF cross-sectional area (Fig. 4) and the relationship was not significantly different between the paraffin samples from 1997 and 2005 ($P>0.05$). The allometric coefficient b of Equation 1 differed significantly from the square

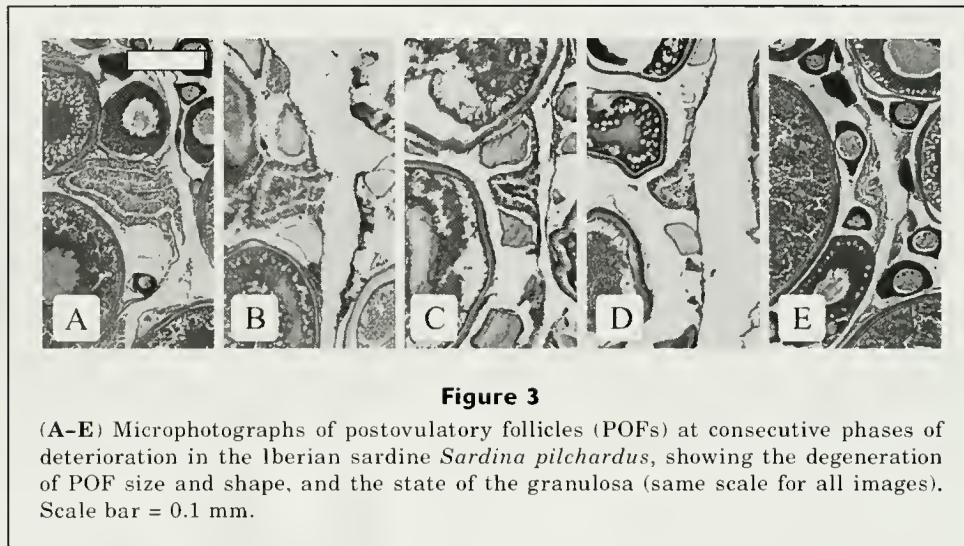


Figure 3

(A-E) Microphotographs of postovulatory follicles (POFs) at consecutive phases of deterioration in the Iberian sardine *Sardina pilchardus*, showing the degeneration of POF size and shape, and the state of the granulosa (same scale for all images). Scale bar = 0.1 mm.

($P < 0.001$), indicating that POF resorption in the Iberian sardine is not isometric, i.e., the shape of POFs changes throughout degeneration. More specifically, b was estimated to be 1.5 (standard error=0.13), indicating that the diameter of POFs along the lamellar epithelium diminishes at a lower rate than that for the overall POF area. This allometric pattern of POF resorption confirms the shape differences along POF degeneration described above and shown in Figure 3.

The differences in the dimensional characteristics and the morphological state of the granulosa (Table 1) were used to assign POFs from all surveys into four daily classes. The reliability of these aging criteria was confirmed by a very good relationship between POF age and POF size in all years of the study (Table 2; Fig. 5A). The rate of resorption, i.e., the relationship of

the slope of the POF cross-sectional area to POF age was not found to differ significantly between the three years, indicating that estimates of resorption rate are not biased either by the preservation medium (AFA or formalin) or by the embedding material (paraffin or resin). In all study years, POFs were shown to shrink exponentially with time in a way that their cross-sectional area decreased daily by almost 50% (Fig. 5A).

The relationship of the intercept of the POF cross-sectional area on POF age in the GLM was similar for the two preservation mediums (no significant difference between 1997 and 2005), but differed significantly between the two embedding materials (significant difference between 1999 and the other two years) (Table 2). POF area at any given time was significantly higher for resin (Fig. 5A), indicating that processing in paraffin wax leads to a higher shrinkage of all cellular structures in the gonad. This higher rate of shrinkage was also evident by differences in the histological appearance of POFs between the two embedding materials, especially at earlier phases of degeneration (Fig. 6). The structure of POFs in resin was more compact and the cellular organization of the granulosa was clearly visible (Fig. 6A). On the other hand, in paraffin sections, the cells of the granulosa layer were hardly detectable and the follicular folds were usually detached from the surrounding theca (Fig. 6B).

During the entire survey period, sea surface temperature ranged between 11.6° and 19.3°C, and there were marked interannual differences (2005 being the coldest [mean SST: 14°C ± 2.1] and 1997 being the warmest year [mean SST: 16.2°C ± 2.2]). The fitted GLM showed that ambient temperature had a significant effect on the rate of POF degradation (Table 2; Fig. 5B). However, this effect appeared to be limited because an increase of 1°C in ambient temperature accelerated the rate of POF resorption by only 3% (compared to the reduction of POF area by almost 50% per day since spawning; Table 2). This finding indicates that the maximum dif-

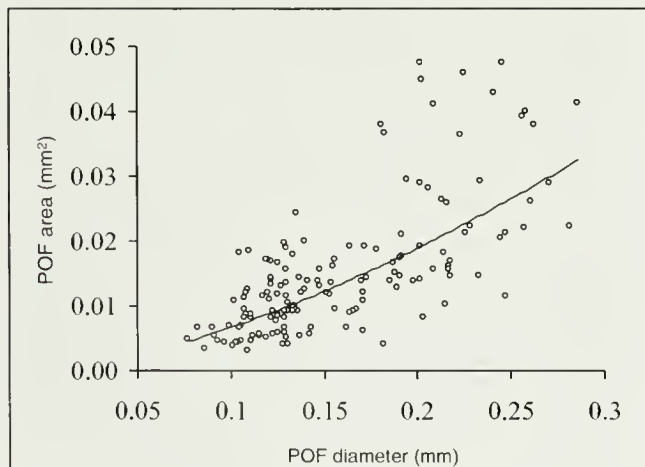


Figure 4

Allometric relationship between postovulatory follicle (POF) diameter and POF cross-sectional area for the Iberian sardine *Sardina pilchardus*.

Table 1

Summary of dimensional (shape, cross-sectional area) and fine histological (state of the granulosa layer) characteristics of different daily classes of postovulatory follicles (POFs) in the two embedding materials (P=paraffin; R=resin) for the Iberian sardine *Sardina pilchardus*.

Daily POF class	Shape	State of granulosa	Cross-sectional area (mm ²)
<1	Irregular	Thick and looped	0.0164 ± 0.0004 (P)
			0.0355 ± 0.0001 (R)
1-2	Rectangular	One well-formulated layer	0.0093 ± 0.0002 (P)
			0.0176 ± 0.0005 (R)
2-3	Triangular	A thin receding layer	0.0059 ± 0.0002 (P)
			0.0126 ± 0.0003 (R)
>3	Triangular	Resorption almost completed, some residual vacuoles	0.0042 ± 0.0002 (P)
			0.0072 ± 0.0004 (R)

ference in POF duration for the Iberian sardine across the study years could never exceed 0.5 days, thus reducing the concerns in relation to the potential bias introduced by varying ambient temperatures in the estimation of the spawning fraction.

Discussion

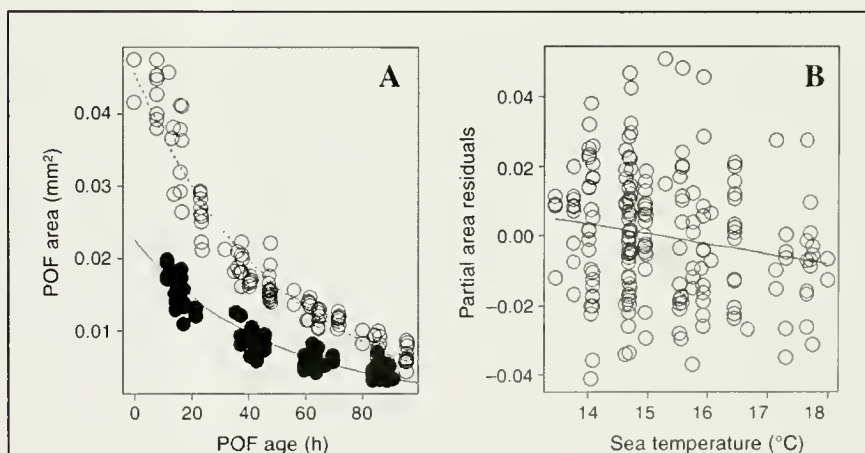
The incorrect attribution of age to POFs and the effect of temperature on POF resorption rate constitute major sources of potential bias in the determination of daily spawning classes in routine applications of the DEPM (Stratoudakis et al., 2006). Our method was devised as an indirect way to test the above issues together with the effect of laboratory processing, i.e., type of preservative and embedding material. The method is based on the assumption that in species with diel spawning synchronicity, such as in *S. pilchardus*, daily classes of spawning fish have, at any given time, POFs of similar size. The first task in our analysis was to refine existing staging criteria for the POFs of *Sardina pilchardus*. This task was mainly attempted through analyzing the frequency distribution of POF cross-sectional areas in females caught simultaneously and by inspecting POFs in each size-age mode for differences in the cytomorphological characteristics.

The main cytomorphological changes during the degeneration of POFs in sardine ovaries are the gradual deterioration of the structure of the follicular layers and alterations in the dimensional characteristics (shape and size), accompanied by a decrease in their overall number in the slide. Histo-

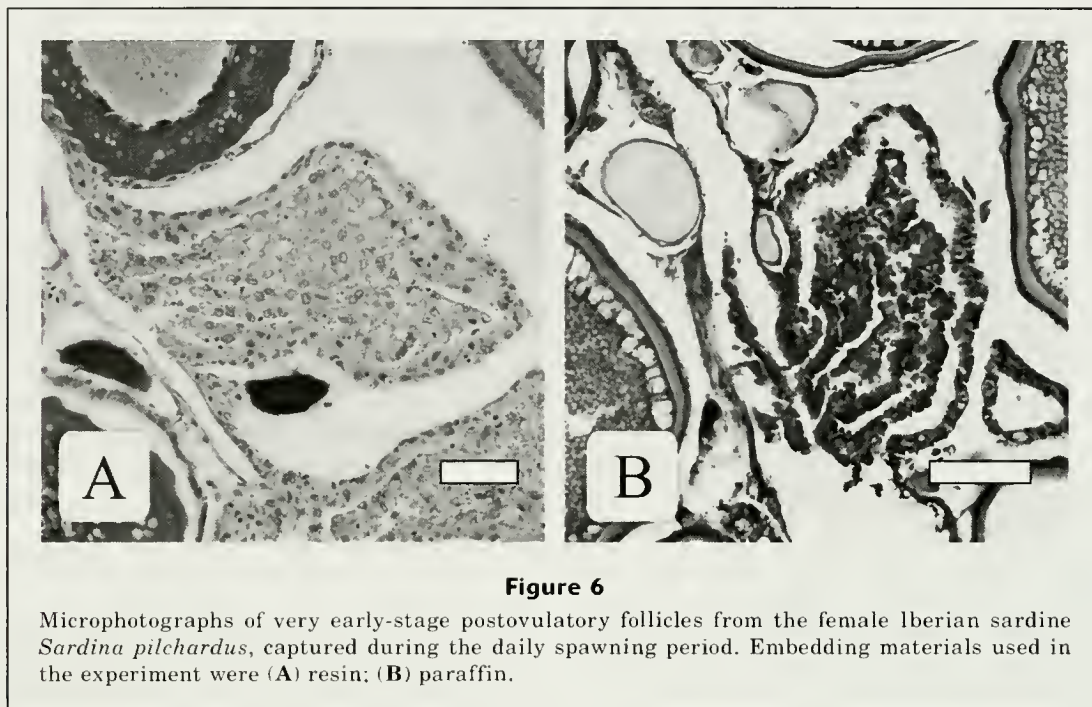
Table 2

Summary statistics of the general linear model fitted to the postovulatory follicle cross-sectional area for the sardine *Sardina pilchardus*. All parameter estimates were tabulated at the scale of the linear predictor (the intercept for resin as an increment). SE = standard error.

Variable	Estimate	SE	<i>t</i> -value	<i>P</i>
Age (hour)	-0.021	0.0004	-46.78	<0.001
Temp (°C)	-0.030	0.012	-2.44	0.016
Intercept (paraffin)	-3.344	0.197	-16.98	<0.001
Intercept (resin)	0.710	0.027	25.90	<0.001

**Figure 5**

(A) Degeneration of the postovulatory follicle (POF) cross-sectional area (POF area) with time elapsed from spawning (POF age) for the Iberian sardine *Sardina pilchardus*; ○=resin ; ●=paraffin. (B) Effect of ambient temperature on the sardine POF cross-sectional area.

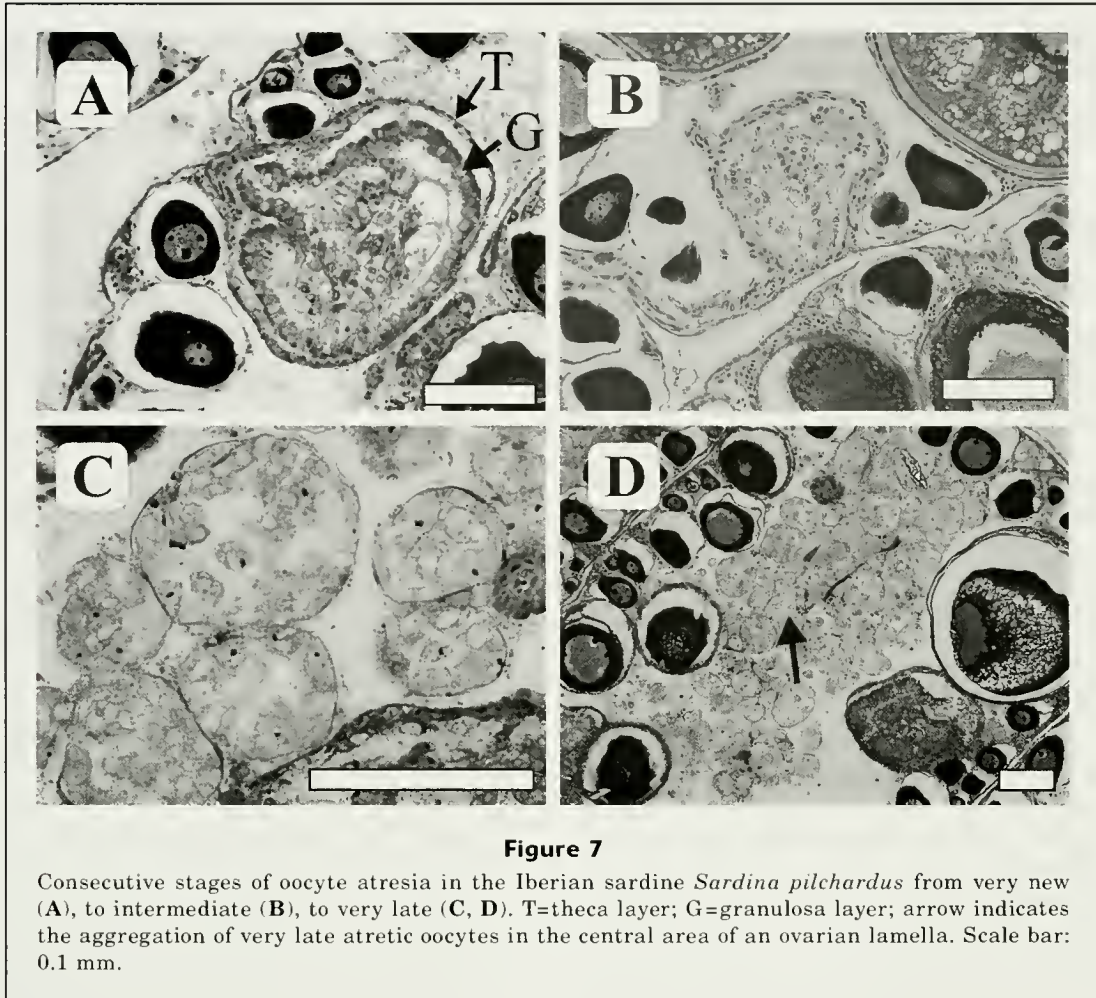


logical changes in the granulosa seem to follow the general pattern of degeneration described for other populations of sardine (Japanese sardine [*Sardinops melanostictus*]: Murayama et al., 1994; Mediterranean sardine [*S. pilchardus*]: Ganas et al., 2003; Pacific sardine [*Sardinops sagax*]: Goldberg et al., 1984; South African sardine [*S. sagax*]: Akkers et al., 1996) and other fish species (see interspecific comparison in Hunter and Macewicz, 1985). The information provided in our study mostly concerns the changes in the dimensional characteristics of POFs and how these may be used in the aging of these POFs.

The evolution in the shape of POFs is allometric because the POF surface along the lamellar epithelium decreases at a lower rate than the overall area of the follicles. As a result, throughout degeneration, POFs passed consecutively from an irregular to a semirectangular and finally a triangular shape, providing a useful additional morphological criterion for determining the stage of the POF. POFs remain for the whole of their "life" on the epithelium of the lamellae, where they occupy approximately the space of an oocyte at the yolk vesicle stage (early POFs) or of a primary oocyte (late POFs). For an indeterminate spawner like sardine, where recruitment of new spawning batches of oocytes occurs continuously and directly from the oogonia, fast resorption is necessary because the aggregation of old POFs would restrict the space available for the development of new oocytes. On the other hand, late atretic pre-ovulatory follicles separate from the epithelium and concentrate medially in the lamellae—a pattern that has also been observed in other fish species such as striped mullet (*Mugil cephalus*) (McDonough et al., 2005). Late atretic follicles remain in fish ovaries for

long periods, which might extend up to the next spawning season (Hunter and Lo, 1997; Miranda et al., 1999). Therefore, their separation from the lamellar epithelium possibly constitutes a mechanism for managing space availability for the newly recruited spawning batches.

The aforementioned morphological phases and the different histological characteristics of the granulosa layer were used, together with follicle size, in the aging of POFs. Four daily classes were identified, implying that full POF resorption in the Iberian sardine exceeded 72 hours. The duration of POF degeneration is variable among fish species, ranging from less than 1 day in the skipjack tuna (*Katsuwonus pelamis*) (Hunter et al., 1986) to more than 7 days in the piau-jejo (*L. taeniatus*) (Santos et al., 2005). However, there are reports of intraspecific variability in the duration of POF resorption, both under laboratory conditions (e.g., Atlantic menhaden, *Brevoortia tyrannus*; Fitzhugh and Hettler, 1995) and in the field (e.g., spotted seatrout [*Cynoscion nebulosus*]: Roumillat and Brouwer, 2004). In some cases the duration of POF resorption is underestimated because late POFs can be confused with late atretic stages (e.g., northern anchovy [*Engraulis mordax*] Hunter and Macewicz, 1980). However, given that surveys for refining the DEPM are undertaken at peak spawning months (Stratoudakis et al., 2006), POFs would so greatly outnumber atretic follicles in fish ovaries that there would be little confusion in distinguishing the two and thus would lead to a very minor bias in the duration of POF resorption. In addition, POFs in *S. pilchardus* are effectively distinguished from all types of atresia, and this distinction has been confirmed by the high degree of consistency in the scoring of post-ovulatory and atretic follicles by different observers. At



all stages, atretic follicles constitute enclosed cellular structures (Fig. 7), whereas POFs always maintain an opening towards the ovarian lumen (Fig. 3). In addition, as previously reported, late atretic oocytes separate from the epithelium of the lamellae (Fig. 7D), whereas POFs remain on the epithelium until full resorption (Fig. 3).

Sardine POFs shrank exponentially with time, reducing to almost half their size daily. Therefore, after the exponential relationship of POF resorption with time is estimated, ages may be estimated by applying the data for the cross-sectional areas of POFs and times of capture to the model. The measurement of POF cross-sectional areas is not very time consuming and could be merged into the routine of histological analysis for DEPM analyses. Finally, the attribution of ages may be finely tuned by inspecting histomorphological characteristics, especially from specimens that lie outside the fitting curve.

Before applying the above aging procedure to fish populations, attention should be drawn to other factors that may affect POF cross-sectional area, such as the laboratory treatment of ovaries and the environmental conditions at sampling, e.g., water tempera-

ture. In our study, the use of different preservation media (AFA solution and formalin) did not appear to affect the size of the POFs. On the other hand, the embedding material significantly affected the follicle's size, for POFs in resin were almost double those in paraffin. Resin is known to maintain cellular organization in tissues slightly affected, whereas paraffin causes significant shrinkage (Casotti, 2001; Dorph-Petersen et al., 2001). Besides size, the morphological characteristics of the follicles also differed between the two materials. Although the whole POF structure remained compact in resin, follicular folds in paraffin had shrunk and were detached from the thecal layer, even in young POFs. These differences, in combination to the thinner slices that are achieved with resin, make resin a much better material for detailed histological observations. However, for accuracy in the staging of POFs, both resin and paraffin seem to provide similar results.

Water temperature may affect the rate of POF resorption in teleosts both in the field (Ganias et al., 2003; Roumillat and Brouwer, 2004) and laboratory studies (Fitzhugh and Hettler, 1995). However, this effect has never been precisely quantified and thus temperature

could never be introduced as an auxiliary factor in the aging of POFs. In the present study, temperature had a significant effect on the rate of POF resorption. This effect appeared to be limited because an increase of 1°C in ambient temperature was estimated to accelerate the rate of POF resorption by almost 3%. Nevertheless, the maximum range of 4–5°C that can be observed during sardine DEPM surveys off the Iberian Peninsula corresponds to a 12–15% maximum difference in the rate of resorption and thus to a maximum of 8 hours lag in the degree of POF degeneration. The results of this analysis imply that in each DEPM survey, temperature differences between the subareas of the survey area are not expected to introduce serious bias in the correct classification of POFs and to subsequently affect estimates of their ages. Finally, given that the late daily classes of POFs are usually excluded from the estimation of spawning fraction, the maximum effect between the most extreme temperatures is even less important (<10%).

Tests, such as described in our study, should be performed at least once for each species or population to assess bias in the criteria used to determine POF stages and ages. Moreover, the test would provide comparative information on POF resorption rates, the impact of embedding material, and the effects of temperature and other environmental parameters on the estimates. In routine DEPM analyses, the measurement of POF cross-sectional areas could increase technical work, but not necessarily the precision in the estimates of the spawning fraction because females are again broken down into spawning nights as they were with the histological staging method. However, in cases where such relationships of POF age on POF size are already available, correspondence of POF sizes to spawning nights would be much more realistic than simple histological staging, which strongly depends on the experience of the observer and the quality of the slides.

Acknowledgments

This work was supported by the program PELAGICOS (PLE/13/00) funded by the Portuguese Ministry of Science and the National Sampling Plan for DEPM surveys funded by the European Union. The contribution of K. Ganas was funded by a postdoctoral scholarship in Portugal (FCT-BPD/17488/2004). We thank four anonymous reviewers for helpful recommendations. In particular, we thank all IPIMAR (Instituto de Investigação das Pescas e do Mar) staff that contributed to the collection of DEPM samples and the histological preparations.

Literature cited

- Akkers, T. R., Y. C. Melo, and W. Veith.
1996. Gonad development and spawning frequency of the South African pilchard *Sardinops sagax* during the 1993–1994 spawning season. *S. Afr. J. Mar. Sci.* 17:183–193.
- Bernal, M., D. Borchers, L. Valdes, A. Lago de Lanzos, and S. T. Buckland.
2001. A new aging method for eggs of fish species with daily spawning synchronicity. *Can. J. Fish. Aquat. Sci.* 58:2330–2340.
- Casotti, G.
2001. Effects of season on kidney morphology in house sparrows. *J. Exp. Biol.* 204:1201–1206.
- Dorph-Petersen, K., J. Nyengaard, and H. Gundersen.
2001. Tissue shrinkage and unbiased stereological estimation of particle number and size. *J. Microsc.* 204:232–246.
- Fitzhugh, R. G., and F. W. Hettler.
1995. Temperature influence on postovulatory follicle degeneration in Atlantic menhaden, *Brevoortia tyrannus*. *Fish. Bull.* 93:568–572.
- Ganas, K., S. Somarakis, A. Machias, and A. Theodorou.
2003. Evaluation of spawning frequency in a Mediterranean sardine population (*Sardina pilchardus sardina*). *Mar. Biol.* 142:1169–1179.
- Goldberg, S. R., V. Alarcon, and J. Alheit.
1984. Postovulatory follicle histology of the Pacific sardine, *Sardinops sagax*, from Peru. *Fish. Bull.* 82:443–445.
- Hunter, J. R., and S. R. Goldberg.
1980. Spawning incidence and batch fecundity in northern anchovy, *Engraulis mordax*. *Fish. Bull.* 77:641–652.
- Hunter, J. R., and N. C. H. Lo.
1997. The daily egg production method of biomass estimation: some problems and potential improvements. *Oceanografika* 2:41–69.
- Hunter, J. R., and B. J. Macewicz.
1980. Sexual maturity, batch fecundity, spawning frequency, and temporal pattern of spawning for the northern anchovy, *Engraulis mordax*, during the 1979 spawning season. *Calif. Coop. Oceanic Fish. Invest. Rep.* 21:139–149.
1985. Measurement of spawning frequency in multiple spawning fishes. In an egg production method for estimating spawning biomass of pelagic fish: application to the northern anchovy, *Engraulis mordax* (R. Lasker, ed.), p. 79–93. NOAA Tech. Rep. NMFS 36.
- Hunter, J. R., B. J. Macewicz, and H. R. Sibert.
1986. The spawning frequency of skipjack tuna, *Katsuwonus pelamis*, from the South Pacific. *Fish. Bull.* 84:895–903.
- ICES (International Council for the Exploration of the Sea).
2004. The DEPM estimation of spawning-stock biomass for sardine and anchovy. *ICES Coop. Res. Rep.*, 91p.
- McDonough, C. J., W. A. Roumillat, and C. A. Wenner.
2005. Sexual differentiation and gonad development in striped mullet (*Mugil cephalus* L.) from South Carolina estuaries. *Fish. Bull.* 103:601–619.
- Miranda, A. C. L., N. Bazzoli, E. Rizzo, and Y. Sato.
1999. Ovarian follicular atresia in two teleost species: a histological and ultrastructural study. *Tissue and Cell* 31:480–488.
- Murayama, T., M. Shirashi, and I. Aoki.
1994. Changes in ovarian development and plasma levels of sex hormones in the wild female Japanese sardine (*Sardinops melanostictus*) during the spawning period. *J. Fish Biol.* 45:235–245.

- Parker, K.
1980. A direct method for estimating northern anchovy, *Engraulis mordax*, spawning biomass. *Fish. Bull.* 78:541-544.
- Pérez, N., I. Figueiredo, and B. J. Macewicz.
1992. The spawning frequency of sardine, *Sardina pilchardus* (Walb.), off the Atlantic Iberian coast. *Bol. Inst. Esp. Oceanogr.* 8:175-189.
- Picquelle, S. J., and G. Stauffer.
1985. Parameter estimation for an egg production method of anchovy biomass assessment. *In* An egg production method for estimating spawning biomass of pelagic fish: application to the northern anchovy, *Engraulis mordax* (R. Lasker, ed.), p. 7-16. NOAA Tech. Rep. NMFS 36.
- Roumillat, W. A., and M. C. Brouwer.
2004. Reproductive dynamics of female spotted seatrout (*Cynoscion nebulosus*) in South Carolina. *Fish. Bull.* 102:473-487.
- Saidapur, K. S.
1982. Structure and function of postovulatory follicles (corpora lutea) in the ovaries of nonmammalian vertebrates. *Int. Rev. Cytol.* 75:243-285.
- Santos, B., E. Rizzo, N. Bazzoli, Y. Sato, and L. Moro.
2005. Ovarian regression and apoptosis in the South American teleost *Leporinus taeniatus* Lutken (Characiformes, Anostomidae) from the Sao Francisco Basin. *J. Fish Biol.* 67:1446-1459.
- Stratoudakis, Y., M. Bernal, K. Ganias, and A. Uriarte.
2006. The daily egg production method (DEPM): recent advances, current applications, and future challenges. *Fish and Fisheries* 7:35-57.
- Whitehead, P. J. P., Wongratana, T., and G. J. Nelson.
1985. Clupeid fishes of the world (Suborder Clupeoidei): an annotated and illustrated catalogue of the herrings, sardines, pilchards, sprats, shads, anchovies, and wolf-herrings. FAO species catalogue, vol. 7, part 1, 303 p. FAO, Rome.
- Zwolinski, J., Y. Stratoudakis, and E. Soares.
2001. Intra-annual variation in the batch fecundity of sardine off Portugal. *J. Fish Biol.* 58:1633-1645.

Use of genetic data to assess the uncertainty in stock assessments due to the assumed stock structure: the case of albacore (*Thunnus alalunga*) from the Atlantic Ocean

Haritz Arrizabalaga¹ (contact author)

Victoria López-Rodas²

Eduardo Costas²

Alberto González-Garcés³

Email address for H. Arrizabalaga: harri@pas.azti.es

¹ AZTI Tecnalia
Herrera Kaia
Portualdea z/g
20110 Pasaia (Gipuzkoa) Spain

² Universidad Complutense
Genética, Facultad de Veterinaria
Avda. Puerta de Hierro s/n
28080 Madrid. Spain

³ IEO
Cabo Estay, Canido
Apdo 1552
Vigo (Pontevedra), Spain

Stock assessments can be problematic because of uncertainties associated with the data or because of simplified assumptions made when modeling biological processes (Rosenberg and Restrepo, 1995). For example, the common assumption in stock assessments that stocks are homogeneous and discrete (i.e., there is no migration between the stocks) is not necessarily true (Kell et al., 2004a, 2004b).

On the other hand, it is essential that the stock structure assumed during the assessment and management process corresponds to the real population structure of the resource. Otherwise, fishery management becomes inefficient (less productive populations may be overfished and collapse, while more productive populations may be underexploited [Allendorf et al., 1987; Begg et al., 1999]) and may affect biological attributes, such as growth, productivity, or genetic diversity (Ricker, 1981). In spite of this problem, current regulations on several fisheries are based on spatial schemes that do not necessarily reflect the real biological structure

of the populations (Pawson and Jennings, 1996; Stephenson, 1999; Ward, 2000). In these cases, the results of stock assessments may be biased and, in general, an important level of uncertainty exists in stock assessments (NRC, 1994; Turner, 1998) due to the assumed stock structure.

An assessment of the magnitude of this uncertainty is important so as to increase confidence in the assessment itself. Moreover, quantifying the uncertainty allows the evaluation of the relative effect of stock structure assumptions with respect to other assumptions about biological, fishery, or modeling parameters in the assessment. Knowing the relative importance of the effect of these underlying assumptions will allow management scientists to prioritize the types of research needed to better ground the stock assessments with real information.

In this note, we suggest a way to assess uncertainty in stock assessments that is due to assumptions of stock structure. The assessment is essentially based on a sensitivity analysis conducted by testing alter-

native stock structure hypotheses derived from available genetic, fishery, and biological information. The method is illustrated with albacore (*Thunnus alalunga*, Bonn. 1788) in the Atlantic Ocean.

Albacore is a highly migratory species distributed between latitudes 45°N and 45°S. Studies of albacore reproduction in the Atlantic Ocean have shown different spawning periods and areas in both hemispheres (Beardsley, 1969; Koto, 1969). Shiohama (1971) and Uozumi (1996), based on Japanese longline distribution studies, described an adult concentration area in each hemisphere. These findings, along with studies of larval concentration areas (Ueyanagi, 1971), support the existence of two separate populations, one in each hemisphere. Based on these studies, it is assumed within the International Commission for the Conservation of Atlantic Tunas (ICCAT) that there are two albacore management units in the Atlantic, separated by parallel 5°N. However, various authors have suggested the possibility that albacore move between the north and south Atlantic (reviewed in González-Garcés, 1997). Moreover, the continuous spatial distribution of catches around the equator also suggests this possibility (Fig. 1).

Recent studies have shown genetic differences between north and south Atlantic albacore (Takagi et al., 2001; Arrizabalaga et al., 2004), but it is still unclear whether the limit between both populations is at latitude 5°N or somewhere else. In fact, results from Arrizabalaga et al. (2004) are not concordant with the limit at latitude 5°N because a sample from the Gulf of Guinea (1°N, 15–16°W) was genetically more like the sample from the north Atlantic than the one from the south Atlantic. This observation may indicate that either the limit between both stocks may be located farther south than that currently assumed or that

Manuscript submitted 15 June 2005
to the Scientific Editor's Office.

Manuscript approved for publication
14 December 2005 by the Scientific Editor.
Fish. 105:140–146 (2007).

there may be some interchange between individuals of both stocks. An earlier statistical comparison of blood group frequencies in albacore found in the Gulf of Guinea (lat. 0°–9°S, long. 0°–8°W), northwest Atlantic (lat. 23°–31°N, long. 60°–70°W) and middle-north Atlantic (lat. 1°–34°N, long. 11°–40°W) in an earlier study (Suzuki, 1962) did not show differences between them, again indicating that the fish present in the Gulf of Guinea may belong to the northern population.

Materials and methods

Taking into account the above findings, we assessed the uncertainty in north and south Atlantic albacore stock assessments by means of a sensitivity analysis. This analysis consisted in assessing both stocks, either under alternative stock boundaries or by assuming certain migration rates between them.

Stock assessment under the assumption of alternative boundaries between stocks

Two alternative boundaries between albacore stocks were considered: at lat. 0°N and lat. 5°S. The catch-at-age within lat. 5°N–0°N and lat. 5°N–5°S was removed from the southern catch-at-age matrix and added to the northern one, by using available catch (ICCAT¹), size, and growth information (Bard, 1981; Sarralde et al., 2002). For each boundary, abundance and fishing mortality rates were estimated separately for each stock by virtual population analysis (VPA) by using the VPA-2box, vers. 3.0 program (Porch et al., 2001). This program assesses the abundance and mortality of one or two intermixing stocks by fitting age-structured population equations to fishery data. All stock assessment options were maintained as in the ICCAT 2001 report (ICCAT²) and variance of estimated parameters was computed by performing 400 nonparametric bootstraps of the abundance indices.

¹ ICCAT (International Commission for the Conservation of Atlantic Tunas). Website: <http://www.iccat.int/> (accessed 31 June 2005).

² ICCAT (International Commission for the Conservation of Atlantic Tunas). 2001. Report of the ICCAT SCRS albacore stock assessment session (Madrid, Spain; October 9 to 15, 2000). Collect. Vol. Sci. Pap. ICCAT, 52, p. 1283–1390. International Commission for the Conservation of Atlantic Tunas, Corazón de María 8, 28002 Madrid, Spain.

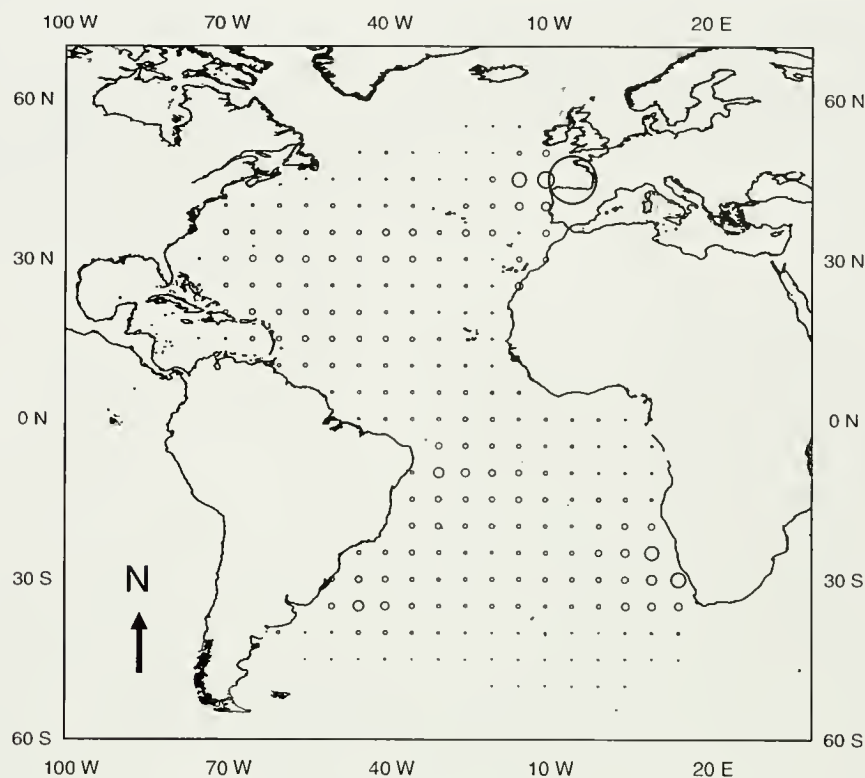


Figure 1

Spatial distribution of Atlantic and Mediterranean albacore (*Thunnus alalunga*) catches (ICCAT, 2001). The size of the circles is proportional to the square root of the total catch at each location.

Stock assessment under the assumption that there is migration between stocks

Blood group frequency data in Arrizabalaga et al. (2004) were used, with the assumption that the sample in the Gulf of Guinea was within the currently accepted range limit for both stocks, and therefore that it may be made up of a mixture of albacore belonging to the northern and southern populations. The proportion that each population would contribute to the mixture was calculated according to Cavalli-Sforza and Bodmer (1981) as

$$x_m = mx_A + (1-m)x_B, \quad (1)$$

where m = the fraction of population A in the mixture; x_m = the allelic frequency in the mixture; and x_A and x_B = the allelic frequencies in populations A and B, respectively.

The variance of m is given by

$$\sigma_m^2 = \frac{1}{(x_A - x_B)^2} \left[\sigma_{x_m}^2 + m^2 \sigma_{x_A}^2 + (1-m)^2 \sigma_{x_B}^2 \right], \quad (2)$$

where, $\sigma_{x_m}^2$, $\sigma_{x_A}^2$ and $\sigma_{x_B}^2$ are the variances of the allelic frequencies in the mixture and populations A and B,

respectively. When several diallelic loci are analyzed, the fraction of population A in the mixture can be computed as a weighted average:

$$\bar{m} = \frac{\sum \frac{m}{\sigma_m^2}}{\sum \frac{1}{\sigma_m^2}} \quad (3)$$

Using three lectins, for which the positive lectin binding proportion in the Gulf of Guinea was intermediate between the proportions for the northern and southern populations as described in Arrizabalaga et al. (2004), we obtained m values shown in Table 1. The weighted mean proportion indicated that 79% of the fish present in the Gulf of Guinea would belong to the northern Atlantic population, and this result was used to formulate plausible migration hypotheses for the two stocks. The mean historical (1975–99) catch around the equator (between lat. 5°N and lat. 5°S) has been 1218 metric tons (t) per year, and therefore 974 t would belong to fish from the North Atlantic population and 244 t to fish from the South Atlantic population. In reference to the average total catch in each stock (38,960 t and 27,111 t in the northern and southern stocks, respectively), these quantities would imply that about 2.5% of the fish from the North Atlantic and 0.9% from the South Atlantic are present in the Gulf of Guinea every year. Assuming that albacore in this area are migrating from one stock to the other, these percentages would, in broad terms, represent the yearly transfer rates between stocks.

Several scenarios were established and tested. Scenario number 1 reflects the above situation (2.5% and 0.9% annual migration rates from north to south and south to north, respectively). However, high variances for mixing proportions were obtained because no diagnostic loci was detected, and those precision estimates could, in fact, be overestimated because not all fish were sampled from different schools in the study of Arrizabalaga et al. (2004). This overestimation may indicate that annual migration rates vary considerably from those in scenario 1. Thus, a range of alternative migration scenarios were explored in which additional biological or fishery aspects were taken into account. Scenarios 2, 3, 7, and 8, reflected the situation in which migration occurs only in one direction (5% yearly from north to south and south to north in scenarios 2 and 3, respectively, and 10% from north to south and south to north in scenarios 7 and 8, respectively). Because no fishing effort targeting albacore exists in the equatorial area, the real migration rate may be higher than the one inferred from catches in that area. Accordingly, in scenario 4, twice the migration rates of scenario 1 (5% from north to south and

Table 1

Proportion of albacore (*Thunnus alalunga*), with a given blood group in the North Atlantic, Gulf of Guinea, and South Atlantic determined with three different lectins (Con A: *Concanavaline A*; WGA: *Triticum vulgare*; ECA: *Eritrina cristagally*; from Arrizabalaga et al., 2004) and estimated mixing proportions in the Gulf of Guinea. m =proportion of northern origin fish in the Gulf of Guinea sample; \bar{m} =weighted average proportion. Standard deviation of m and \bar{m} is given in parentheses.

Lectin	Con A	WGA	ECA
North Atlantic	0.2500	0.4500	0.0500
Gulf of Guinea	0.2174	0.3913	0.0435
South Atlantic	0.0357	0.2857	0
m	0,8478 (0,5553)	0,6427 (0,7794)	0,8695 (1,2006)
\bar{m}		0,7900 (0,4232)	

1.8% from south to north) were adopted. In scenario 5, migration was considered to be limited to the adult fraction of the stock (ages 5–8+), as size distributions in this area indicated, and finally in scenarios 6 and 9, high rates of migration (5% and 10%, respectively) in both directions were chosen. Although these scenarios are believed to be representative of the true nature of mixing between the stocks, it should be stressed that they represent only some of many different possible mixing scenarios.

All scenarios were tested by assuming an overlap migration model (fish return back to the area of origin for spawning) and using the VPA-2box program (Porch et al., 2001). No diffusive migration was considered because it is not consistent with observed genetic differentiation. Results for all scenarios were compared (in terms of spawning stock biomass trends and the small sample bias-adjusted version of the Akaike information criteria ([AICc, Hurvich and Tsai, 1995]) with the base case where no migration was assumed to occur between stocks.

Results

Stock assessment under the assumption of alternative boundaries between stocks

Best fits for northern and southern stocks were obtained by assuming different stock boundaries, at lat. 5°S and lat. 5°N, respectively. However, estimated abundance and fishing mortalities, with the assumption of any of the alternative stock limits, showed minor differences with respect to the base case (Table 2). The effect of considering the limit in lat. 0°N or in lat. 5°S was practically the same because most of the catch in the equatorial area happens in the Northern Hemisphere (between lat. 5°N and lat. 0°N). All coefficients of variation (CV) were below 15%, except for the F_{5+}^{87-99} in the south Atlantic, which were between 15% and 30%.

Table 2

Results of model fits for alternative boundaries between stocks of albacore (*Thunnus albacore*). Instantaneous fishing mortality (F) and abundance (N , in millions of individuals) estimates are averaged by age groups (subscripts) and time periods (superscripts). Corresponding mean coefficients of variation are given within parentheses. n = number of data points; p = number of estimated parameters; AICc = adjusted Akaike information criteria (Hurvich and Tsai, 1995).

Limit	North Atlantic albacore			South Atlantic albacore		
	5°N	0°N	5°S	5°N	0°N	5°S
-logL	66.68	66.74	66.52	80.85	81.98	82.20
Deviance	117.04	117.01	116.92	61.95	61.97	62.02
n	117.00	117.00	117.00	62.00	62.00	62.00
p	14.00	14.00	14.00	12.00	12.00	12.00
AICc	149.15	149.12	149.04	92.31	92.34	92.39
F_1^{75-86}	0.11 (0.2%)	0.11 (0.23%)	0.11 (0.19%)	0.00 (0.75%)	0.00 (0.86%)	0.00 (0.92%)
F_1^{87-96}	0.16 (3.87%)	0.16 (4.27%)	0.16 (3.97%)	0.01 (6.84%)	0.01 (6.87%)	0.01 (6.63%)
F_{2-4}^{75-86}	0.39 (0.19%)	0.37 (0.22%)	0.37 (0.18%)	0.11 (0.8%)	0.11 (1.02%)	0.11 (1.12%)
F_{2-4}^{87-99}	0.44 (10.44%)	0.41 (10.91%)	0.4 (9.9%)	0.2 (8.44%)	0.2 (8.95%)	0.21 (8.46%)
F_{5+}^{75-86}	0.3 (0.21%)	0.3 (0.24%)	0.3 (0.19%)	0.16 (0.86%)	0.15 (1.12%)	0.15 (1.24%)
F_{5+}^{87-99}	0.2 (11.48%)	0.21 (13.97%)	0.22 (11.17%)	0.3 (18.46%)	0.26 (29.39%)	0.25 (22.42%)
N_1^{75-86}	10.37 (0.19%)	10.6 (0.22%)	10.67 (0.18%)	8.23 (0.87%)	8.17 (1.05%)	8.16 (1.14%)
N_1^{87-96}	8.76 (3.94%)	9.02 (4.33%)	9.12 (4.16%)	7.55 (8.6%)	7.37 (8.52%)	7.3 (9%)
N_{2-4}^{75-86}	12.51 (0.15%)	12.87 (0.18%)	12.97 (0.15%)	13.64 (0.78%)	13.68 (0.99%)	13.69 (1.09%)
N_{2-4}^{87-99}	9.07 (7.97%)	9.47 (8.5%)	9.62 (7.99%)	11.96 (7.97%)	11.56 (8.14%)	11.61 (8.33%)
N_{5+}^{75-86}	3.29 (0.17%)	3.35 (0.2%)	3.36 (0.16%)	4.31 (0.83%)	4.37 (1.07%)	4.41 (1.19%)
N_{5+}^{87-99}	1.65 (7.87%)	1.81 (8.4%)	1.85 (7.67%)	3.57 (10.04%)	3.57 (10.19%)	3.59 (10.12%)

Stock assessment under the assumption of migration between stocks

Fits under several migration scenarios were more parsimonious than under the assumption of no migration between stocks (Table 3). Scenarios 1 ($p_{NS}=0.025$, $p_{SN}=0.009$), 2 ($p_{NS}=0.05$, $p_{SN}=0$), 3 ($p_{NS}=0$, $p_{SN}=0.05$), 4 ($p_{NS}=0.05$, $p_{SN}=0.018$), 6 ($p_{NS}=0.05$, $p_{SN}=0.05$), and 7 ($p_{NS}=0.1$, $p_{SN}=0$) showed lower AICc values than in the base case (BC).

Spawning stock biomass (SSB) values and trends under scenarios 1, 2, 3, 4, 5, 6, and 7 were similar to the ones observed in the base case, especially in the second half of the study period (except for the SSB of the southern stock over the last two years, which showed more variability, Fig. 2). In contrast, scenarios 8 and 9 showed a very different pattern in the last half of the series. In the north Atlantic, after the decline of the SSB during the beginning of the 1980s, the recovery was much more effective under these two scenarios, reaching higher values at the end of the 1990s than in the 1970s. Meanwhile, the SSB values for the southern stock were only slightly lower than those under the assumption of no migration, and under scenario 9 they were higher than in the base case over the last two years (Fig. 2).

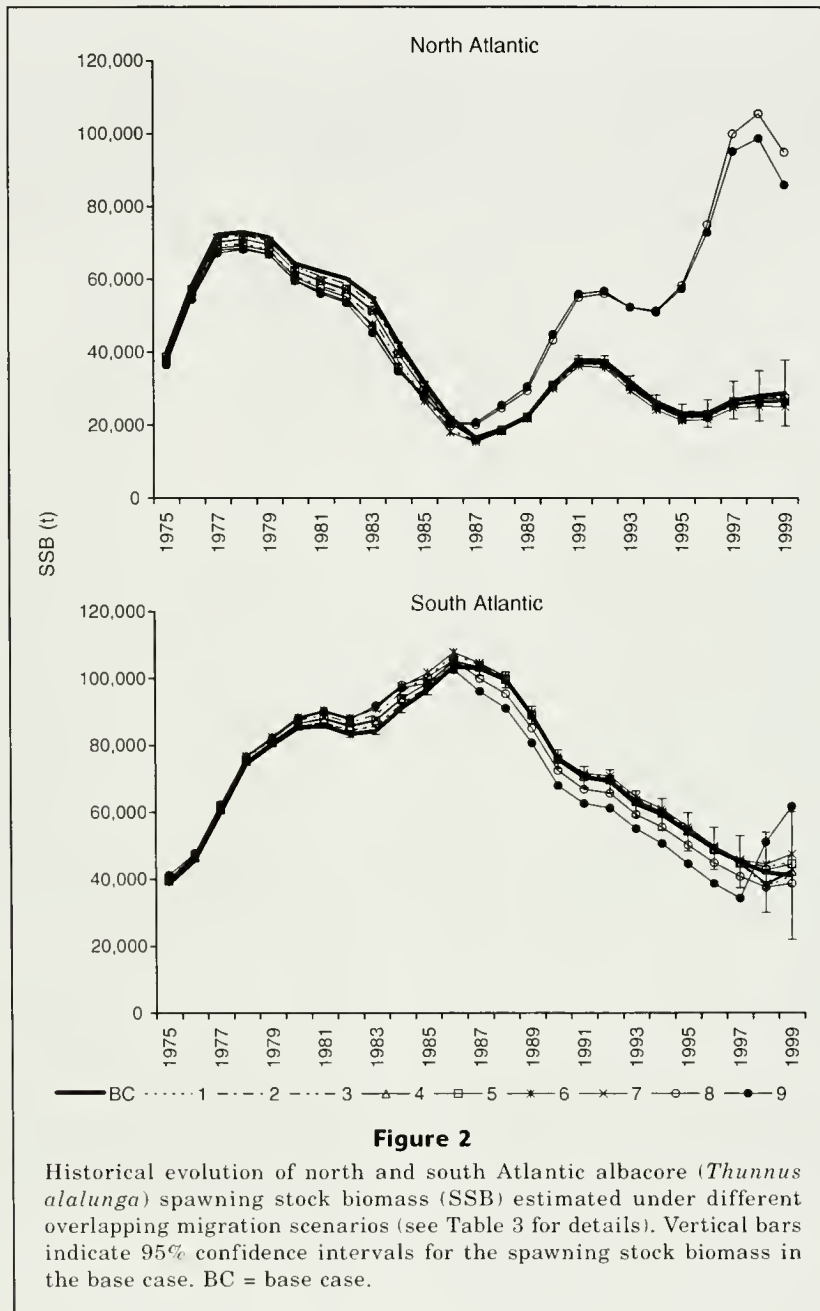
Table 3

Considered overlap migration scenarios and associated results of model fits for albacore (*Thunnus alalunga*). $n = 179$; $p = 25$; AICc = adjusted Akaike information criteria (Hurvich and Tsai, 1995); BC = base case; p_{NS} = annual migration rate from north to south; p_{SN} = annual migration rate from south to north.

Scenario	p_{NS}	p_{SN}	Age range (yr)	AICc
BC	0	0	1-8+	18.76
1	0.025	0.009	1-8+	13.74
2	0.05	0	1-8+	15.12
3	0	0.05	1-8+	18.03
4	0.05	0.018	1-8+	13.10
5	0.05	0.018	5-8+	19.41
6	0.05	0.05	1-8+	17.67
7	0.1	0	1-8+	12.77
8	0	0.1	1-8+	37.58
9	0.1	0.1	1-8+	46.81

Discussion

The method used to assess the uncertainty in the stock assessments that is due to the assumed stock structure



is based on a simple sensitivity analysis conducted by testing alternative stock structure hypotheses. When plausible hypotheses are generated from the cumulated knowledge on the biology and fisheries of the species, the effect of these hypotheses on the assessment results can be studied. However, it is also important to consider a range of alternative hypotheses so that they produce significantly different results in the assessment, in reference to the base case. The wide range of results allows us to discern the level of migration that is of concern for assessment purposes and shows the level of migration that is not likely to be realistic, given the available catch and effort data. However, several other sources of

uncertainty should be taken into account at this stage. The analysis could be extended to future biomass projections under different management strategies in order to indicate those management strategies that are more robust to violation of stock structure assumptions. This kind of study should run parallel to other studies where additional sources of uncertainty (e.g., in biological parameters or fishery data) are quantified because this approach would show their relative importance so that research could be prioritized with the goal of providing improved information on stock status.

In the case of Atlantic albacore, recent genetic studies indicate that, either the limit between both popula-

tions is not at lat. 5°N, but farther south, or that some amount of migration exists between them. Because no diagnostic loci were found by Arrizabalaga et al. (2004), the estimated proportions from each stock in the Gulf of Guinea sample could not be precisely determined and the true nature of mixing between north and south Atlantic albacore has yet to be fully determined. In spite of this uncertainty, the present exercise has made it possible to explore the response of biomass trends in different plausible discrete-stock scenarios and stock-mixing scenarios.

Although it is not possible to determine where the real line lies between populations, we can conclude from our knowledge about the current low level of reported equatorial catch and the size structure of this catch and if we assume a limit of latitude 0° north or latitude 5°S that our current perceptions of the stock structure of this species are probably accurate. On the other hand, several migration scenarios fitted the observed catch-at-age and abundance indices better than the scenario of no migration. In all these scenarios, SSB trends were very similar and values did not differ significantly from the ones in the base case; therefore it can be concluded that, although some rate of migration between stocks likely exists, the perception that we have about stock status, assuming there is no migration, is quite realistic. In other words, uncertainty in northern and southern Atlantic albacore stock assessments associated with the assumed stock structure does not seem to be important, given current biological knowledge and fishery data.

The highest variations in SSB were observed for northern Atlantic albacore in scenarios with high migration rates from south to north, showing high levels of SSB at the end of the study period. However, the observed difference in SSB levels with respect to the base case in the South Atlantic was not that pronounced, showing that northern Atlantic albacore biomass is more sensitive to biomass input from the south than vice versa. This result occurs because the minimum level of SSB in the north Atlantic in 1987 coincides in time with the maximum SSB in the southern stock, which is an order of magnitude higher. In this case, a migration rate of 10% from south to north would imply the input of approximately half the biomass present in the north at that moment, leading to a more rapid recovery of historic levels than under the null migration assumption. However, the existence of such important migration rates from south to north seems unlikely given the observed catch-at-age and abundance indices for both stocks.

The present analysis allows for the increase in confidence levels regarding stock assessment results for northern and southern Atlantic albacore obtained within ICCAT, assuming that stocks are separated at lat. 5°N and that there is no migration between them. This information is essential in order that the catch- and effort-related management measures that are in force for Atlantic albacore remain effective. Nevertheless, additional hypotheses, such as migration between North Atlantic and Mediterranean albacore, or between South

Atlantic and Indian Ocean albacore, should be investigated further as future research findings are made available. Moreover, it should be noted that migration between stocks could vary among years, and a yearly based assessment of genetic mixture, based on DNA analysis, would be more useful for quantitative stock assessments.

Acknowledgments

We are grateful to Clay Porch for his help in the use of VPA-2box and statistical considerations regarding the interpretation of the results. Mauricio Ortiz, Hilario Murua, Dorleta García, two anonymous referees, and the scientific editor also made helpful suggestions. We are also grateful to the Spanish “Comisión de Ciencia y Tecnología” (CICYT) and the “Departamento de Agricultura y Pesca” of the Basque Government for the funding of the MAR98-0233 and RP2002023 research projects, respectively.

Literature cited

- Allendorf, F. W., N. Ryman, and F. M. Utter.
1987. Genetics and fishery management: past, present and future. *In* Population genetics and fishery management (N. Ryman and F. M. Utter, eds.), p. 1–19. Univ. Washington Press, Seattle and London.
- Arrizabalaga, H., E. Costas, J. Juste, A. González-Garcés, B. Nieto, and V. López-Rodas.
2004. Population structure of albacore *Thunnus alalunga* inferred from blood groups and tag-recapture analyses. *Mar. Ecol. Prog. Ser.* 282:245–252.
- Bard, F. X.
1981. Atlantic albacore tuna (*Thunnus alalunga* Bonnatte 1788). From population dynamics to demographic strategy. Ph.D. diss., 333 p. [In French.] Université Pierre et Marie Curie, Paris, France.
- Beardsley, G. L.
1969. Proposed migrations for albacore, *Thunnus alalunga*, in the Atlantic Ocean. *Trans. Am. Fish. Soc.* 98:589–598.
- Begg, G. A., K. D. Friedland, and J. B. Pearce.
1999. Stock identification and its role in stock assessment and fisheries management: an overview. *Fish. Res.* 43:1–8.
- Cavalli-Sforza, L. L., and W. F. Bodmer.
1981. The genetics of human populations, 942 p. Freeman and Com., San Francisco, CA.
- González-Garcés, A.
1997. Contribution to knowledge about north Atlantic albacore (*Thunnus alalunga*, Bonn. 1788) population dynamics. Ph.D. diss., 200 p. [In Spanish.] Universidad Complutense de Madrid, Ciudad Universitaria, Madrid, Spain.
- Hurvich, C. M., and C. L. Tsai.
1995. Relative rates of convergence for efficient model selection criteria in linear regression. *Biometrika* 35:418–425.
- Kell, L. T., W. W. Crozier, and C. M. Legault.
2004a. Mixed and multi-stock fisheries: Introduction. *ICES J. Mar. Sci.* 61:1330.

- Kell, L. T., R. Scott, and E. Hunter.
2004b. Implications for current management advice for North Sea plaice: Part I. Migration between the North Sea and English Channel. *J. Sea Res.* 51:287–299.
- Koto, T.
1969. Studies on the albacore—XIV. Distribution and movement of the albacore in the Indian and the Atlantic Oceans based on the catch statistics of Japanese tuna longline fishery. *Bull. Far Seas Fish. Res. Lab.* 1:115–129.
- NRC (National Research Council).
1994. An assessment of Atlantic bluefin tuna, 166 p. National Academy Press, Washington D.C.
- Pawson, M. G., and S. Jennings.
1996. A critique of methods for stock identification in marine capture fisheries. *Fish. Res.* 25:203–217.
- Porch, C. E., S. C. Turner, and J. E. Powers.
2001. Virtual population analyses of Atlantic bluefin tuna with alternative models of transatlantic migration: 1970–1997. *Collect. Vol. Sci. Pap. ICCAT* 52:1022–1045.
- Ricker, W. E.
1981. Changes in the average size and average age of Pacific salmon. *Can. J. Fish. Aquat. Sci.* 38: 1636–1656.
- Rosenberg, A. A., and V. R. Restrepo.
1995. Uncertainty and risk evaluation in stock assessment advice for U.S. marine fisheries. *Can. J. Fish. Aquat. Sci.* 51: 2715–2720.
- Sarralde, R., F. X. Bard, and A. Hervé.
2002. Update of tropical east Atlantic albacore (*Thunnus alalunga*) purse seine bycatch information. [In Spanish.] *Collect. Vol. Sci. Pap. ICCAT* 55:245–250.
- Shiohama, T.
1971. Studies on measuring changes in the character of the fishing effort of the tuna longline fishery. Concentrations of the fishing effort to particular areas and species in the Japanese Atlantic fishery. *Bull. Far Seas Fish. Res. Lab.* 5:107–130.
- Stephenson, R. L.
1999. Stock complexity in fisheries management: a perspective of emerging issues related to population subunits. *Fish. Res.* 43:247–249.
- Suzuki, A.
1962. Serological studies of the races of tuna. VI. Bigeye-3 antigen occurred in the albacore. *Rep. Nankai Reg. Fish. Res. Lab.* 16:67–70.
- Takagi, M., T. Okamura, S. Chow, and N. Taniguchi.
2001. Preliminary study of albacore (*Thunnus alalunga*) stock identification inferred from microsatellite DNA analysis. *Fish. Bull.* 99:697–701.
- Turner, S. C.
1998. Stock structure and mixing. *Collect. Vol. Sci. Pap. ICCAT* 50:17–23.
- Ueyanagi, S.
1971. Larval distribution of tunas and billfishes in the Atlantic Ocean. *FAO Fisheries report* 71:297–305.
- Uozumi, Y.
1996. A historical review of Japanese longline fishery and albacore catch in the Atlantic ocean. *Collect. Vol. Sci. Pap. ICCAT* 43:261–268.
- Ward, R. D.
2000. Genetics in fisheries management. *Hydrobiologia* 420:191–201.

New information from fish diets on the importance of glassy flying squid (*Hyaloteuthis pelagica*) (Teuthoidea: Ommastrephidae) in the epipelagic cephalopod community of the tropical Atlantic Ocean

Yves Cherel (contact author)¹

Richard Sabatié²

Michel Potier³

Francis Marsac⁴

Frédéric Ménard⁴

¹ Centre d'Etudes Biologiques de Chizé
UPR 1934 du Centre National de la Recherche Scientifique BP 14
79360 Villiers-en-Bois, France
Email address for Y. Cherel: cherel@cebc.cnrs.fr

² Pôle Halieutique
Laboratoire d'Ecologie Halieutique, Agrocampus-Rennes
65 rue de Saint Briec
35042 Rennes Cedex, France

³ Institut de Recherche pour le Développement
Centre de La Réunion
UR 109 Thetis, BP 172
97492 Sainte Clotilde Cedex, Isle de La Réunion, France

⁴ Institut de Recherche pour le Développement
Centre de Recherche Halieutique Méditerranéenne et Tropicale
UR 109 Thetis, BP 171
34203 Sète Cedex, France

Squids of the family Ommastrephidae are a vital part of marine food webs and support major fisheries around the world. They are widely distributed in the open ocean, where they are among the most abundant in number and biomass of nektonic epipelagic organisms. In turn, seven of the 11 genera of this family (*Dosidicus*, *Illex*, *Martialia*, *Nototodarus*, *Ommastrephes*, *Sthenoteuthis*, and *Todarodes*) are heavily preyed upon by top marine predators, i.e., birds, mammals, and fish, and currently support fisheries in both neritic and oceanic waters (Roper and Sweeney, 1984; Rodhouse, 1997). Their commercial importance has made the large ommastrephids the target of many scientific investigations and their biology is consequently reasonably well-known (Nigmatullin et al., 2001; Zuyev et al., 2002; Bower and Ichii, 2005). In contrast, much less

information is available on the biology and ecological role of the smaller, unexploited species of ommastrephids (e.g., *Eucleoteuthis*, *Hyaloteuthis*, *Ornithoteuthis*, and *Todaropsis*).

Hyaloteuthis pelagica (Bosc, 1802), the glassy flying squid, is the smallest ommastrephid, reaching a maximum mantle length of 90 mm (Nesis, 1987). It appears to be an epipelagic species that is probably distributed in all tropical and subtropical oceans (Nesis and Nigmatullin, 1979; Wormuth, 1998). *Hyaloteuthis pelagica* is rarely captured, but was caught in large numbers during a cruise off Brazil, where it was the dominant ommastrephid captured in nets (Warneke-Cremer, 1986). Almost nothing is known about its trophic relationships, either as prey or predator (Nesis and Nigmatullin, 1979). Numerous remains of *H. pelagica*—from a few intact squids to

a fairly large number of accumulated beaks—were found in the stomachs of large predatory fishes during research cruises in the central Atlantic Ocean in autumn 2000. In this note, we describe the importance of *H. pelagica* in fish diets, thus adding new information about the abundance and trophic role of a poorly known ommastrephid species.

Materials and methods

Fieldwork was carried out in the central Atlantic Ocean during three cruises of the Japanese RV *Shoyo Maru* in October–December 2000 (Fig. 1). Cruise I took place in temperate waters of the north equatorial current (between 8–21°N and 42–29°W) and cruises II and III took place in tropical waters of the south equatorial divergence (between 2N–10°S and 13–26°W, and between 7–9°S and 9–24°W). Cruises were a part of the Bigeye Tuna Year Program (BETYP) that was undertaken under the auspices of the International Commission for the Conservation of Atlantic Tunas (ICCAT). The purpose of the cruises was to tag live tunas caught by longlines in order to investigate their migration pattern and behavior in relation to fish aggregating devices.

Fish were measured (eye-fork length for billfishes and fork length for other species) and dissected onboard. In the laboratory, each fish stomach was thawed, opened, and both accumulated (cephalopod beaks with no flesh attached) and fresh items were sorted. Fresh remains were divided into broad prey classes (fish, cephalopods, crustaceans, and others), and weighed to calculate their proportion by mass in the diet. Identification of cephalopod prey relied on the external morphological features of either intact specimens or beaks. Beaks

Manuscript submitted 2 March 2006
to the Scientific Editor's Office.

Manuscript approved for publication
24 May 2006 by the Scientific Editor.
Fish. Bull. 105:147–152 (2007).

(both lower and upper) were identified by reference to features given by Clarke (1986) and by comparison with material held in our own reference collection.

Well-preserved specimens of *H. pelagica* were identified from the special arrangement of luminous spots on the ventral side of the mantle (Nesis, 1987). Beaks from those specimens identified from the spots (reference beaks) allowed us to identify almost all ommastrephid beaks found in fish samples as belonging to *H. pelagica*. Importantly, wings of the lower beaks darkened at a small size, thus precluding misidentification with beaks of other ommastrephid species that darken at larger sizes, e.g., *Sthenoteuthis pteropus* (Clarke, 1986). Lower rostral length (LRL) of beaks was measured to 0.1 mm with a vernier caliper and the allometric equations given by Clarke (1986) were used to estimate dorsal mantle length (ML) and whole wet mass (M) from LRL. Specimens of *H. pelagica* were assumed to be adults at 46 mm ML and larger (Dunning and Brandt, 1985).

Dietary data are presented by using two calculation techniques, namely the frequency of occurrence and the percentage by number of each prey type. Data were statistically analyzed by using SYSTAT 9 (SPSS, Chicago, IL). Values given are means (\pm SD).

Results

Most (97%) of the fish caught on longlines belonged to 10 different species of large oceanic predatory fishes, including longnose lancetfish (*Alepisaurus ferox*), four scombrids (wahoo [*Acanthocybium solandri*], albacore [*Thunnus alalunga*], yellowfin tuna [*T. albacares*], and bigeye tuna [*T. obesus*]), swordfish (*Xiphias gladius*), and four istiophorids (sailfish [*Istiophorus albicans*], blue marlin [*Makaira nigricans*], and white marlin [*Tetrapturus albidus*], and longbill spearfish [*T. pfluegeri*]). Most of the fish (93%) contained fresh remains in their stomachs. Fish prey dominated the diet by mass (>50%) of eight predator species (Table 1). Fish and cephalopod items were almost equally important in the diet of white marlin, whereas fish, cephalopods, and crustaceans were the main food sources of albacore.

Cephalopods amounted to slightly more than 50% of the diet by mass in one fish species (white marlin) only. They were an important prey class (>10%) in five other species and were still a minor, but significant (≥ 5 –10%), portion of the food of the four remaining fishes (Table 1). Overall, cephalopods (both fresh and accumulated items) were found in most of the individuals (76%) and a total of 2701 cephalopod beaks were identified from the stomach of 105 fish. *Hyaloteuthis pelagica* was by far the most important cephalopod prey of the community of large predatory fishes, amounting

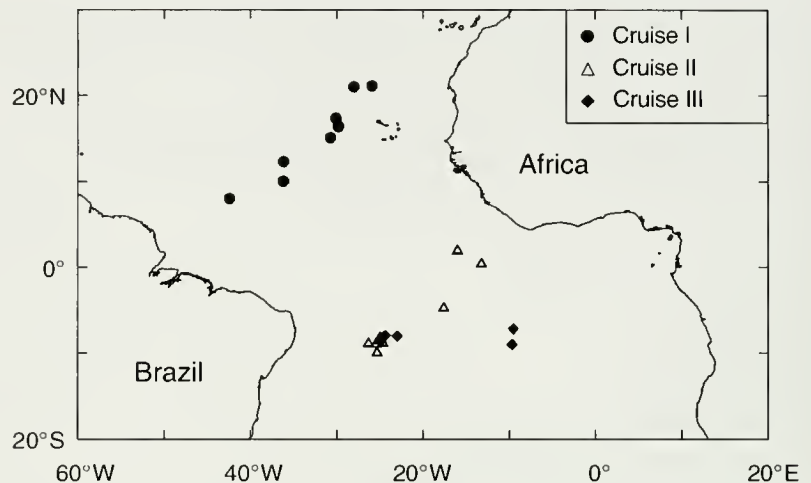


Figure 1

Locations of longline sets carried out in the central Atlantic Ocean during three cruises of the RV *Shoyo Maru* between October and December 2000.

to more than 50% of the total number of cephalopods (up to 93%) in six species (Table 2). Indeed, it was found to be the main cephalopod prey in all the fishes, except in bigeye tuna and lancetfish where it ranked second and third, respectively. *Hyaloteuthis pelagica* was much more abundant in the diet of fish caught in tropical waters (cruises II and III) than in the diet of individuals fished in temperate waters (cruise I) ($n=1937$ and 15 beaks, respectively).

Other important cephalopod prey (>10% by number) included the small onychoteuthid squid *Walvisteuthis* (= *Onykia*) *rancureli* in the diets of bigeye tuna and albacore, and the pelagic octopuses *Japetella diaphana* and common blanket octopus *Tremoctopus violaceus* in those of yellowfin and bigeye tunas, respectively. Three other ommastrephid squids were identified from fish stomach contents; they were two rare prey species, the Atlantic bird squid *Ornithoteuthis antillarum* and the orangeback flying squid *Sthenoteuthis pteropus*, as well as the bait, Argentine shortfin squid *Illex argentinus*.

All fishes fed upon the same size range of *H. pelagica*, including both juvenile and adult squids (Table 3, Fig. 2), but overall they segregated by preying on squids of different sizes (ANOVA on LRL, $F_{(6,907)}=16.36$, $P<0.0001$). *Post hoc* Tukey multiple comparison tests showed three groups of predators: yellowfin tuna and sailfish fed on smaller squids (51 mm and 3.9 g on average), bigeye tuna, white marlin, and longbill spearfish fed on larger individuals (60, 59, and 58 mm; 6.6, 6.2, and 5.7 g, respectively), and albacore and blue marlin fed on squids of intermediate sizes (54 mm and 4.7–4.8 g). Accordingly, bigeye tuna, white marlin, and longbill spearfish fed more on adult squids (89%, 92%, and 93% of the total number of *H. pelagica*, respectively) than did albacore and blue marlin (85% and 77%) and yellowfin tuna and sailfish (62% and 73%) (Table 3).

Table 1

Frequency of occurrence (FO) and proportion by mass (%) of four broad prey classes (fish, cephalopods, crustaceans, and others) recovered from the stomach contents of 10 species of predatory fishes sampled between October and December 2000 in the central Atlantic Ocean.

Species	No. of specimens	Length \pm SD (cm)	No. of stomachs with fresh remains	Fish		Cephalopods		Crustaceans		Others	
				FO	Mass	FO	Mass	FO	Mass	FO	Mass
Alepisauridae											
<i>Alepisaurus ferox</i>	29	120 \pm 15	26	18	67.8	9	9.8	19	13.6	9	8.8
Scombridae											
<i>Acanthocybium solandri</i>	7	136 \pm 18	7	6	63.5	2	7.5	0	0.0	6	29.0
<i>Thunnus alalunga</i>	16	109 \pm 6	15	11	31.5	9	31.7	15	29.7	5	7.1
<i>Thunnus albacares</i>	6	147 \pm 7	6	6	77.2	5	5.8	5	12.1	2	4.9
<i>Thunnus obesus</i>	24	107 \pm 22	24	24	77.0	17	20.2	13	2.7	2	0.1
Xiphiidae											
<i>Xiphias gladius</i>	8	126 \pm 32	6	6	89.3	3	10.3	2	0.4	0	0.0
Isiophoridae											
<i>Istiophorus albicans</i>	4	152 \pm 13	4	3	85.7	4	13.1	0	0.0	1	1.2
<i>Makaira nigricans</i>	8	180 \pm 25	5	3	95.2	2	4.7	0	0.0	3	0.2
<i>Tetrapturus albidus</i>	7	130 \pm 10	7	7	48.2	6	51.2	0	0.0	4	0.6
<i>Tetrapturus pfluegeri</i>	30	143 \pm 6	29	25	86.8	23	13.0	4	0.0	4	0.1

Table 2

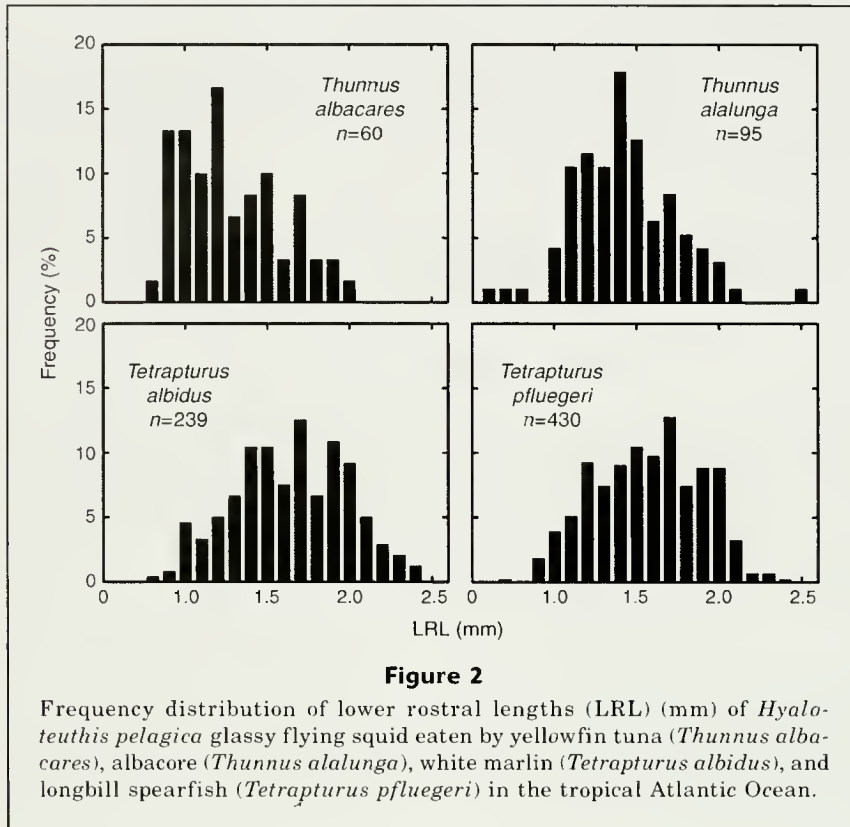
Number (and % composition by number) of the main cephalopod prey species found in the diet of Scombridae and Istiophoridae from the tropical Atlantic Ocean between October and December 2000. Only prey species contributing more than 5% by number are reported. *n* = number of stomachs examined.

Species	<i>Thunnus alalunga</i> <i>n</i> =15	<i>Thunnus albacares</i> <i>n</i> =5	<i>Thunnus obesus</i> <i>n</i> =19	<i>Istiophorus albicans</i> <i>n</i> =4	<i>Makaira nigricans</i> <i>n</i> =5	<i>Tetrapturus albidus</i> <i>n</i> =7	<i>Tetrapturus pfluegeri</i> <i>n</i> =29
Ommastrephidae							
<i>Hyaloteuthis pelagica</i>	194 (51.5)	133 (61.6)	45 (19.8)	78 (80.4)	101 (75.4)	481 (92.9)	897 (85.8)
Onychoteuthidae							
<i>Onychoteuthis banksi</i>	21 (5.6)	4 (1.9)	2 (0.9)	0 (0.0)	2 (1.5)	1 (0.2)	12 (1.1)
<i>Walvisteuthis rancureli</i>	63 (16.7)	5 (2.3)	62 (27.3)	1 (1.0)	9 (6.7)	0 (0.0)	7 (0.7)
Grimalditeuthidae							
<i>Grimalditeuthis bonplandi</i>	4 (1.1)	2 (0.9)	17 (7.5)	0 (0.0)	0 (0.0)	2 (0.4)	0 (0.0)
Tremoctopodidae							
<i>Tremoctopus violaceus</i>	3 (0.8)	35 (16.2)	3 (1.3)	8 (8.2)	7 (5.2)	11 (2.1)	19 (1.8)
Argonautidae							
<i>Argonauta argo</i>	6 (1.6)	15 (6.9)	2 (0.9)	8 (8.2)	4 (3.0)	21 (4.1)	82 (7.8)
Bolitaenidae							
<i>Japetella diaphana</i>	34 (9.0)	5 (2.3)	28 (12.3)	0 (0.0)	1 (0.7)	0 (0.0)	7 (0.7)
Other cephalopods	52 (13.8)	17 (7.9)	68 (30.0)	2 (2.1)	10 (7.5)	2 (0.4)	21 (2.0)
Total	377 (100.0)	216 (100.0)	227 (100.0)	97 (100.0)	134 (100.0)	518 (100.0)	1045 (100.0)

Discussion

This study is the first, to our knowledge, to point out the abundance of *H. pelagica* in the tropical pelagic ecosystem. In the central Atlantic Ocean, *H. pelagica*

was found as a prey of all the fish species that were investigated. When looking at both the proportion by mass of cephalopods in the fish diet (Table 1) and the proportion by number of *H. pelagica* in their cephalopod diet (Table 2), *H. pelagica* was a major prey of white

**Table 3**

Characteristics of *Hyaloteuthis pelagica* eaten by large predatory fish from the tropical Atlantic Ocean. Values given are means (\pm SD) with ranges in parentheses. LRL=lower rostral length, ML=mantle length, M=body mass.

Species	Number (n)	Measured LRL (mm)	Estimated ML (mm)	Estimated M (g)	Adults (ML >46 mm) (%)
<i>Alepisauridae</i>					
<i>Alepisaurus ferox</i>	2	1.6–1.8	60–64	6.1–7.3	100.0
<i>Scombridae</i>					
<i>Acanthocybium solandri</i>	3	2.1 \pm 0.2 (1.9–2.3)	71 \pm 5 (67–77)	9.7 \pm 2.0 (8.5–12.0)	100.0
<i>Thunnus alalunga</i>	95	1.4 \pm 0.3 (0.5–2.5)	54 \pm 8 (34–81)	4.7 \pm 2.1 (0.8–14.0)	85.2
<i>Thunnus albacares</i>	60	1.2 \pm 0.3 (0.8–1.9)	51 \pm 7 (39–67)	3.9 \pm 1.8 (1.5–8.5)	61.7
<i>Thunnus obesus</i>	18	1.6 \pm 0.5 (0.8–2.3)	60 \pm 11 (39–77)	6.6 \pm 3.2 (1.5–12.0)	88.9
<i>Xiphiidae</i>					
<i>Xiphias gladius</i>	5	1.9 \pm 0.2 (1.6–2.2)	67 \pm 6 (59–75)	8.4 \pm 2.0 (5.9–11.3)	100.0
<i>Istiophoridae</i>					
<i>Istiophorus albicans</i>	33	1.3 \pm 0.2 (0.9–1.8)	51 \pm 5 (42–64)	3.9 \pm 1.3 (2.0–7.3)	72.7
<i>Makaira nigricans</i>	39	1.4 \pm 0.4 (0.5–2.0)	54 \pm 9 (34–69)	4.8 \pm 2.2 (0.8–9.2)	76.9
<i>Tetrapturus albidus</i>	239	1.6 \pm 0.3 (0.7–2.3)	59 \pm 8 (38–78)	6.2 \pm 2.4 (1.4–12.4)	92.1
<i>Tetrapturus pfluegeri</i>	430	1.5 \pm 0.3 (0.7–2.4)	58 \pm 8 (37–79)	5.7 \pm 2.2 (1.2–12.8)	92.6

marlin, a common food item of albacore, longbill spearfish, and sailfish and a minor prey for the remaining fishes. However, more information is needed to assess the spatiotemporal importance of *H. pelagica* in the

fish community, because 1) all fish were caught during a relatively short period of time, and 2) a medium to low number of specimens per fish species were collected during the cruises.

The ommastrephid *Sthenoteuthis pteropus*, usually abundant in the tropical Atlantic Ocean, was surprisingly absent in fish diets in the present study. Two hypotheses may account for that apparent absence: either fish selected *H. pelagica* rather than *S. pteropus*, or *S. pteropus* was not an important and available nektonic prey organism at the time of sampling. The latter hypothesis is likely to be the best explanation because tunas and billfishes are known to be opportunistic predators. Moreover, the geographical distribution of *S. pteropus* shows that juvenile squids are not abundant in the central Atlantic Ocean where cruises of the present investigation took place (Warneke-Cremer, 1986; Zuev and Nikolsky, 1993). Instead, our study underlines the numerical importance of *H. pelagica*, together with *O. antillarum* (Vaske et al., 2004), in the area, and our numbers are in agreement with the large catches of the species with nets between 20°S and 31°S off Brazil during 1966 and 1968 (Warneke-Cremer, 1986).

The present study documents the largest number of *H. pelagica* ever reported, thus emphasizing the usefulness of marine predators to gain valuable information on the biology of their prey (Clarke, 1980; Cherel et al., 2004). Other ommastrephid species are important food items of various fishes, seabirds, and marine mammals (Clarke, 1996; Cherel and Klages, 1998), but *H. pelagica* was previously found only as a rare prey of squids (Shchetinnikov, 1992), fishes (Matthews et al., 1977; Okutani and Tsukada, 1988; Vaske et al., 2004), birds (Harrison et al., 1983), and cetaceans (Robertson and Chivers, 1997). In the same way, the squid *Grimalditeuthis bonplandi* and the pelagic octopods *T. violaceus* and *J. diaphana* were rarely found in significant numbers in the diet of cephalopod predators (Okutani and Tsukada, 1988; Le Corre et al., 2003), but we commonly found them as fish prey. Consequently, our study shows that these poorly known cephalopods, together with adults of *H. pelagica*, constitute a link in the transfer of energy from lower trophic levels (most likely mesozooplankton) to higher trophic levels (including tunas and billfishes) in the tropical Atlantic Ocean).

Acknowledgments

The authors thank P. Borsa, P. Dewals, and O. Maury for their help to collect scientific samples on board, and the captain and crew of the RV *Shoyo-Maru*.

Literature cited

- Bower, J. R., and T. Ichii.
2005. The red flying squid (*Ommastrephes bartramii*): a review of recent research and the fishery in Japan. *Fish. Res.* 76:39–55.
- Cherel, Y., G. Duhamel, and N. Gasco.
2004. Cephalopod fauna of subantarctic islands: new information from predators. *Mar. Ecol. Prog. Ser.* 266:143–156.
- Cherel, Y., and N. Klages.
1998. A review of the food of albatrosses. In *Albatross biology and conservation* (G. Robertson, and R. Gales, eds.), p 113–136. Surrey Beatty and Sons, Chipping Norton, Australia.
- Clarke, M. R.
1980. Cephalopoda in the diet of sperm whales of the Southern Hemisphere and their bearing on sperm whale biology. *Discovery Rep.* 37:1–324.
1986. A handbook for the identification of cephalopod beaks, 273 p. Clarendon Press, Oxford, England.
1996. The role of cephalopods in the world's oceans. *Phil. Trans. R. Soc. Lond. B* 351:977–1112.
- Dunning, M., and S. B. Brandt.
1985. Distribution and life history of deep-water squid of commercial interest from Australia. *Aust. J. Mar. Freshw. Res.* 36:343–359.
- Harrison, C. S., T. S. Hida, and M. P. Seki.
1983. Hawaiian seabird ecology. *Wildl. Monogr.* 85: 1–71.
- Le Corre, M., Y. Cherel, F. Lagarde, H. Lormée, and P. Jouventin.
2003. Seasonal and interannual variation in the feeding ecology of a tropical oceanic seabird, the red-tailed tropicbird *Phaethon rubricauda*. *Mar. Ecol. Prog. Ser.* 255:289–301.
- Matthews, F. D., D. M. Damkaer, L. W. Knapp, and B. B. Collette.
1977. Food of western North Atlantic tunas (*Thunnus*) and lancetfishes (*Alepisaurus*). NOAA Tech. Rep. NMSF SSRF-706, 19 p.
- Nesis, K. N.
1987. Cephalopods of the world. Squids, cuttlefishes, octopuses, and allies, 351 p. TFH Publs., Neptune City, NJ.
- Nesis, K. N., and C. M. Nigmatullin.
1979. The distribution and biology of the genus *Ornithoteuthis* Okada, 1927 and *Hyaloteuthis* Gray, 1849 (Cephalopoda: Oegopsida). *Bull. Moscow Soc. Nat.* 84:50–63. [In Russian.]
- Nigmatullin, C. M., K. N. Nesis, and A. I. Arkhipkin.
2001. A review of the biology of the jumbo squid *Dosidicus gigas* (Cephalopoda: Ommastrephidae). *Fish. Res.* 54:9–19.
- Okutani, T., and S. Tsukada.
1988. Squids eaten by lancetfish and tunas in the tropical Indo-Pacific Ocean. *J. Tokyo Univ. Fish.* 75:1–44.
- Robertson, K. M., and S. J. Chivers.
1997. Prey occurrence in pantropical spotted dolphins, *Stenella attenuata*, from the eastern tropical Pacific. *Fish. Bull.* 95:334–348.
- Rodhouse, P. G.
1997. Large and meso-scale distribution of the ommastrephid squid *Martialia hyadesi* in the Southern Ocean: a synthesis of information relevant to fishery forecasting and management. *Korean J. Polar Res.* 8:145–154.
- Roper, F. E., and M. J. Sweeney.
1984. Cephalopods of the world. An annotated and illustrated catalogue of species of interest to fisheries. FAO Species Catalogue 3:1–277.
- Shchetinnikov, A. S.
1992. Feeding spectrum of squid *Sthenoteuthis oualaniensis* (Oegopsida) in the eastern Pacific. *J. Mar. Biol. Assoc. U.K.* 72:849–860.
- Vaske Jr., T., C. M. Vooren, and R. P. Lessa.
2004. Feeding habits of four species of Istiophoridae (Pisces: Perciformes) from northeastern Brazil. *Environ. Biol. Fishes* 70:293–304.

Warneke-Cremer, C.

1986. Contributions to the systematics of ommastrephid squid (Mollusca, Cephalopoda, Teuthoidea) and their distribution in the Atlantic, based on the catches of FFS "Walter Herwig" made during 1966 and 1968. Mitteil. Inst. Seefisch. Hamburg 40:1-116. [In German.]

Wormuth, J. H.

1998. Workshop deliberations on the Ommastrephidae: a brief history of their systematics and a review of the systematics, distribution, and biology of the Genera *Mortialia* Rochebrune and Mabile, 1889, *Todaropsis* Girard, 1890, *Dosidicus* Steenstrup, 1857, *Hyaloteuthis* Gray, 1849, and *Eucleoteuthis* Berry, 1916. Smithsonian Contrib. Zool. 586:373-383.

Zuev, G. V., and V. N. Nikolsky.

1993. Ecological mechanisms related to intraspecific structure of the nektonic squid *Sthenoteuthis pteropus* (Steenstrup). In Recent advances in fisheries biology (T. Okutani, R. K. O'Dor, and T. Kubodera, eds.), p. 653-664. Tokai Univ. Press, Tokyo, Japan.

Zuyev, G., Ch. Nigmatullin, M. Chesalin, and K. Nesis.

2002. Main results of long-term worldwide studies on tropical nektonic oceanic squid genus *Sthenoteuthis*: an overview of the Soviet investigations. Bull. Mar. Sci. 71:1019-1060.

Measurements of total scattering spectra from bocaccio (*Sebastes paucispinis*)

Stéphane G. Conti (contact author)¹

Benjamin D. Maurer¹

Mark A. Drawbridge²

David A. Demer¹

Email address for S. G. Conti: sconti@ucsd.edu

¹ Southwest Fisheries Science Center
8604 La Jolla Shores Drive
La Jolla, California 92037

Present address for S. G. Conti: Marine Physical Laboratory
Scripps Institute of Oceanography
University of California San Diego
9500 Gilman Drive
La Jolla, California 92093-0238

² Hubbs-SeaWorld Research Institute
2595 Ingraham St.
San Diego, California 92109

Marine sportfishing in southern California is a huge industry with annual revenues totaling many billions of dollars. However, the stocks of lingcod and six rockfish species have been declared overfished by the Pacific Fisheries Management Council. As part of a multifaceted fisheries management plan, marine conservation areas, covering many million square nautical miles, have been mandated. To monitor the recovery of the rockfish stocks in these areas, scientists are faced with the following challenges: 1) multiple species of rockfish exist in these areas; 2) the species reside near or on the bottom at depths of 80 to 300 m; and 3) they are low in numerical density. To meet these challenges, multifrequency echosounders, multibeam sonar, and cameras mounted on remotely operated vehicles are frequently used (Reynolds et al., 2001). The accuracy and precision of these echosounder results are largely dependent upon the accuracy of the species classification and target strength estimation (MacLennan and Simmonds, 1992).

Broad bandwidth characterization of sound scatter from marine organisms has some potential for remotely classifying fish species (Conti and Demer, 2003), shapes and sizes

(Conti et al., 2005), behaviors (Conti et al., 2006b), and to validate models for target strength estimation (Demer and Conti, 2003). All of these studies have employed variants of a new method for measuring the broad bandwidth total scattering cross section (σ_T) of animals moving in a reverberant tank.

With the new method, the total scattering cross section (σ_T) of live animals in tanks is obtained from a comparison of the coherent and incoherent acoustical intensities reverberated in a tank (de Rosny and Roux, 2001, 2003). The accuracy of this measurement technique was shown by using standard metal spheres (Demer et al., 2003). This technique was successfully used on krill (Demer and Conti, 2003; Conti et al., 2006a), fish (Conti and Demer, 2003), and humans (Conti et al., 2004). In our study, we explored the potential and limitations of the method to characterize the broad bandwidth sound scattering from bocaccio (*Sebastes paucispinis*).

Materials and methods

The total scattering cross section, σ_T , of bocaccio was measured over acous-

tic frequencies ranging from 10 to 150 kHz with a group of fish ($n=20$) swimming freely in a large, insulated fiberglass tank at Hubbs-SeaWorld Research Institute, San Diego, CA, on 1 and 2 July 2004. The tank had 5.1 cm of foam insulation on the exterior, measured 2.44 m in diameter, and was filled with seawater to a depth of 1.37 m (V [volume]=6.4 m³). The pool was thermostated at approximately 12°C. The acoustic measurement technique and a variety of its applications have been well documented (de Rosny and Roux, 2001; Conti and Demer, 2003; Demer and Conti, 2003; Demer et al., 2003; Conti et al., 2004). However, the general procedure and details of these experiments are presented here for convenience and clarity.

Each of the 20 fish was handled one time, a week prior to the experiment, to measure their weight (W) and total length (L). These data were summarized and plotted in graphs (Table 1, Fig. 1).

An emitter transmitted M acoustical pulses into the tank every other second ($\delta T=2s$). The corresponding reverberation time-series $h_k(t)$ were simultaneously recorded on multiple receivers while the fish were swimming between consecutive shots. The boundaries, volume, as well as the positions of the emitter and the receivers in the tank remained identical during the measurements.

The time series $h_k(t)$ were composed of echoes from the boundaries of the tank and the fish. For two consecutive time series $h_k(t)$ and $h_{k+1}(t)$, the contributions from the boundaries of the tank were identical, whereas the contributions from the fish were not. The coherent

$$S_c(t) = \frac{1}{M} \sum_{k=1}^M h_k(t) h_{k+1}(t)$$

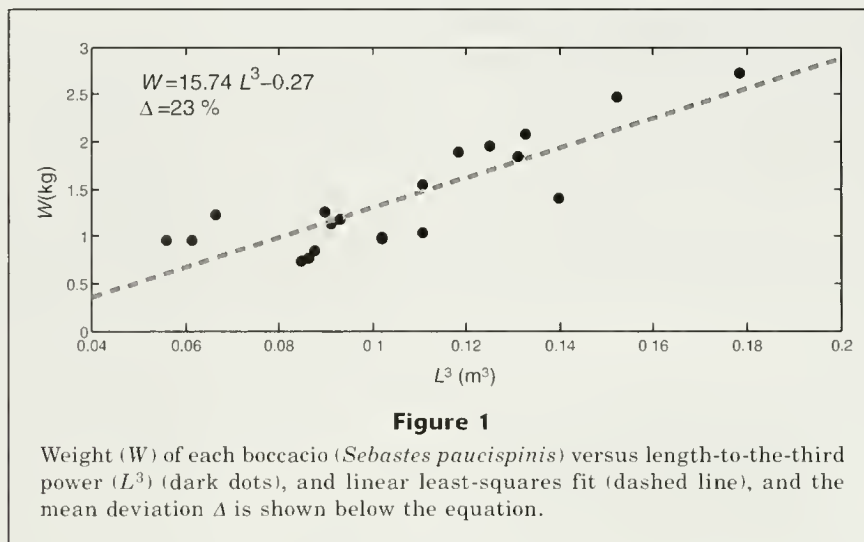
and incoherent

$$S_i(t) = \frac{1}{M} \sum_{k=1}^M h_k^2(t)$$

Manuscript submitted 19 July 2005
to the Scientific Editor.

Manuscript approved for publication
7 July 2006.

Fish. Bull. 105:153–157 (2007).



intensities in the tank were estimated from the M recorded time series. The coherent component represents the acoustical intensity reverberated by the fixed

boundaries of the tank. The incoherent component also accounted for the acoustical intensity scattered by the fish. When the positions of the fish were uncorrelated between consecutive pulses, the ratio $S(t)$ of the coherent to the incoherent intensities decreased exponentially with the scattering mean free path l_s of the fish (de Rosny and Roux, 2001):

$$S(t) = \left[\frac{S_c(t)}{S_i(t)} \right] \approx \exp\left(-t \frac{c}{l_s}\right) \approx \exp\left(-t \frac{cN\sigma_T}{V}\right),$$

where the bracketing $[\]$ designates the average for multiple receivers.

The scattering mean free path is related to the total scattering cross section of a single fish in the tank (σ_T), the sound speed (c), the number of fish (N), and the volume (V). Multiple receivers may be used simultaneously to reduce the heterogeneities of the acoustical field on the coherent and incoherent intensities in the tank. Knowing N , c , and V , σ_T (normalized to a single fish) was estimated from the exponential decay of $S(t)$. Thus, σ_T averaged over 10 to 150 kHz was estimated for a single bocaccio, and its total scattering spectrum was similarly estimated after filtering the recorded time series $h_k(t)$ into twenty narrow frequency bands. Each band corresponded to the bandwidth of the transmitted chirp, divided by twenty.

The signal acquisition system (Fig. 2) consisted of a function generator CompuGen 1100 (GageApplied, Montreal, Canada) internally clocked with two 16-bit CompuScope 1610 (GageApplied, Montreal, Canada) dual-channel acquisition boards in a portable computer. The internal clocking of the function generator and the acquisition boards allowed perfect timing between the emitted and the recorded signals. Ensembles of $M=100$ chirps were transmitted over 50 ms every other second for three frequency bandwidths from 10 to 40 kHz with an ITC1001B emitter ($f_c=25$ kHz); 30 to 70 kHz with an ITC1032 emitter ($f_c=50$ kHz); and 60 to 150 kHz with

Table 1

Total length (L) and weight (W), and the mean and standard deviation of each, for the 20 bocaccio (*Sebastes paucispinis*) used to measure the total scattering cross section over acoustic frequencies from 10 to 150 kHz in a laboratory tank at Hubbs SeaWorld Research Institute, San Diego, CA.

Fish number	Total length (L , mm)	Weight (W , kg)
1	467	0.99
2	444	0.85
3	480	1.03
4	467	0.97
5	453	1.18
6	442	0.77
7	519	1.4
8	439	0.73
9	450	1.13
10	500	1.95
11	448	1.25
12	510	2.08
13	480	1.54
14	508	1.84
15	534	2.47
16	563	2.73
17	491	1.88
18	394	0.95
19	382	0.95
20	405	1.23
Mean	468	1.37
Standard deviation	45.5	0.57

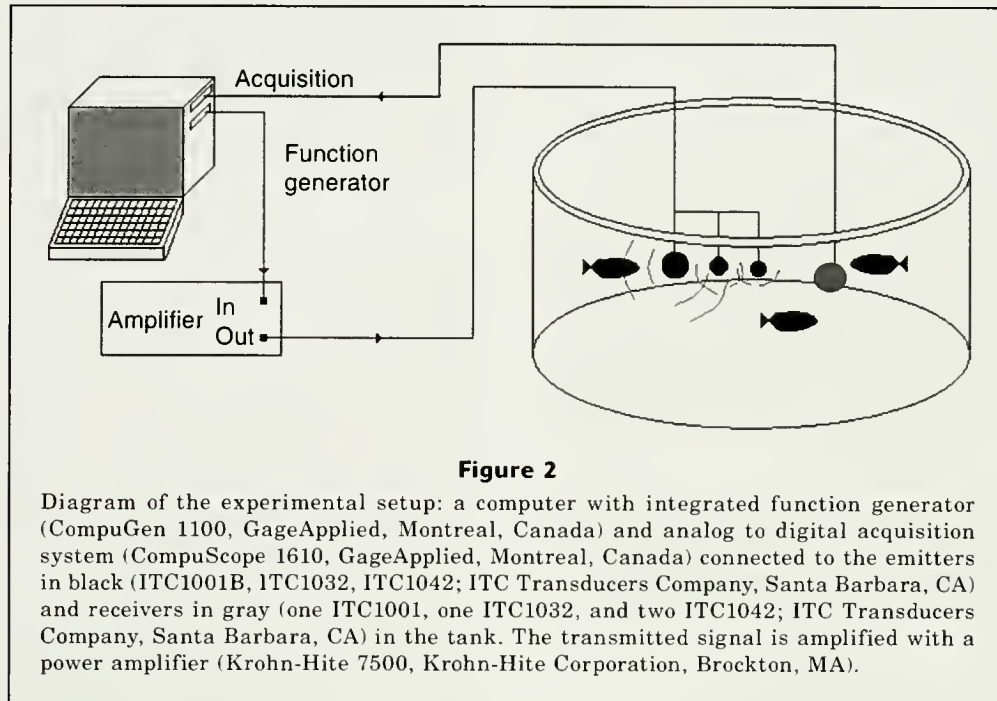


Figure 2

Diagram of the experimental setup: a computer with integrated function generator (CompuGen 1100, GageApplied, Montreal, Canada) and analog to digital acquisition system (CompuScope 1610, GageApplied, Montreal, Canada) connected to the emitters in black (ITC1001B, ITC1032, ITC1042; ITC Transducers Company, Santa Barbara, CA) and receivers in gray (one ITC1001, one ITC1032, and two ITC1042; ITC Transducers Company, Santa Barbara, CA) in the tank. The transmitted signal is amplified with a power amplifier (Krohn-Hite 7500, Krohn-Hite Corporation, Brockton, MA).

an ITC1042 emitter ($f_c=105$ kHz) (ITC Transducers Company, Santa Barbara, CA). The transducers were inserted from the top of the aquarium. The amplitude of the chirps from the function generator was 1 volt peak-to-peak, amplified 100 times (40 dB) with a Krohn-Hite 7500 amplifier (Krohn-Hite Corporation, Brockton, MA). The corresponding reverberation time series were recorded at a 500-kHz sampling rate, for at least 90 ms on a four transducer array consisting of one ITC1001, one ITC1032, and two ITC1042 transducers.

To increase the signal-to-noise ratio, the recorded reverberation time series were cross correlated with the transmitted signal to obtain the impulse responses $h_k(t)$. The measurements for the lowest ($f_c=25$ kHz) and highest ($f_c=105$ kHz) frequencies bands were repeated 11 times. The measurements for the center frequency ($f_c=50$ kHz) band were repeated 20 times. For $f_c=25$, 50, and 105 kHz, the total scattering cross sections were estimated from the signals on the ITC1001, ITC1032, and two ITC1042 receivers, respectively.

Results

The mean weight (W) and total length (L) of the 20 bocaccio were 1.37 kg (ranging from 0.73 to 2.73 kg; standard deviation (SD)=0.57 kg), and 468 mm (ranging from 382 to 563 mm; SD=45.5 cm), respectively (Table 1). Fish masses did not correlate well to fish lengths (Fig. 1). The mean deviation was about 25%, for fish weight to fish length-to-the-third-power. This fit may indicate heterogeneity in the shapes (i.e., long and thin versus short and wide) and could be observed from visual inspection of the fish.

Because the fish were not moving very actively during the experiments, the time between consecutive shots δT had to be increased to assure uncorrelated positions of the fish. This was effectively achieved by considering the shots k and $k+20$ instead of k and $k+1$ to estimate $S_c(t)$, resulting in $\delta T=40$ s between the shots. By increasing the time between shots, the measured total scattering cross section reached a stable plateau at $\sigma_T \approx 0.01$ m² for each of the considered frequency bands (Fig. 3). This plateau indicated that the positions of the fish were uncorrelated between shots, and the measured total scattering cross section was not biased by the correlation of fish positions (Conti et al., 2006a). The measurement variance was conspicuously higher in the lowest and highest frequency bands because of decreased signal-to-noise ratios. The differences in signal-to-noise ratio with frequency was due to the experimental setup at high frequency, and the lack of acoustic modes propagating in the tank at low frequencies. The total scattering cross section was equivalent to the one expected for a rigid sphere of diameter 90 mm in water (Fig. 4; Faran, 1951), which is of the order of the size of the swimbladder for the fish in the tank (Foote, 1979). The largest discrepancies between the measurements and expectations were at the lowest and highest frequencies, again because of lower signal-to-noise ratios.

The total scattering cross-sectional area was virtually the same for each of the three frequency bands because all three measurements were in the geometric scattering domain for these fish. In other words, in all three frequency bands the radius of the equivalent scattering sphere was greater than half the wavelength. In the geometric domain, the scattering cross-section increased with the square of the frequency, in contrast

to the frequency to the fourth power in the Rayleigh domain. For these fish, the transition from the Rayleigh to geometric regimes occurred at frequencies around 15 kHz (Fig. 4).

The spectra of σ_T are shown for over 60 narrow bandwidths (Fig. 4) after we averaged the results from all of the experiments. Each of the three frequency bands were resolved into 20 narrow bandwidths. Further narrowing of the filters on the reverberation time series served only to increase the standard deviation of the measurements without providing more information on the spectra. The mean σ_T was in agreement with the previous broad bandwidth average. The σ_T and its standard deviation increased at the lowest and highest frequencies, likely because of a decrease in signal-to-noise ratios.

The back scattering target strength $TS=10\log_{10}(\sigma_{bs})$ for these fish can be compared to the target strength from a rigid sphere in water of radius a for which the resonances are damped by the surrounding flesh. For this type of scatterer, the target strength at high

$$ka = \frac{2\pi f}{c} a$$

is equal to $10\log_{10}(\pi a^2)$. For a rigid sphere in water of diameter 90 mm, $10\log_{10}(\pi a^2) = -22\text{dB}$. The swimbladder

is gas filled and can be considered a hard scatterer and its resonances are damped by the surrounding flesh. As a first-order approximation, the theoretical predictions for the air bubble can be used to estimate the target strength of the fish by adjusting the radius of the rigid sphere to the size of the fish swimbladder.

Discussion

The mean σ_T from 10 to 150 kHz was measured from bocaccio with a mean length of 468 mm. It is roughly equivalent to that from a 90-mm-diameter rigid sphere in water. This result is in agreement with the approximate size of their swimbladder. Thus, the spectrum of the total scattering cross section for bocaccio can be measured with this technique.

Despite these positive results, the following should be considered for future experiments. These measurements were made against the frequency from a heterogeneous-size group of a single species of fish. As such, the results do not permit comparisons of σ_T with frequency, and animal species and morphological features (e.g., size, shape, length, sex, etc.). Measurements should be made of individual fish.

It should also be noted that the bocaccio in these experiments moved very slowly. Simply increasing the time to achieve incoherence between pulses may itself introduce systematic and random measurement error because of instabilities in the medium. That is, some additional incoherence can result from bubbles and fluctuations in the water temperature, sound speed, volume, and water surface. The magnitude of this incoherence could eclipse the differences in σ_T between individual fish. In these measurements, bubbles and motion of the air-water interface caused by breaking bubbles and fish motion were noticeable visually but had only minor effects on the data.

The most significant shortcoming of these experiments was a generally low signal-to-noise ratio because of the tank size and material properties. This low ratio caused appreciable measurement uncertainty at the lowest and highest frequencies. The water volume was large for the projected signal intensities, and the fiberglass boundaries were not very reflective in comparison to other materials such as stainless steel and glass used in previous experiments. Therefore, to obtain and compare measurements of σ_T from

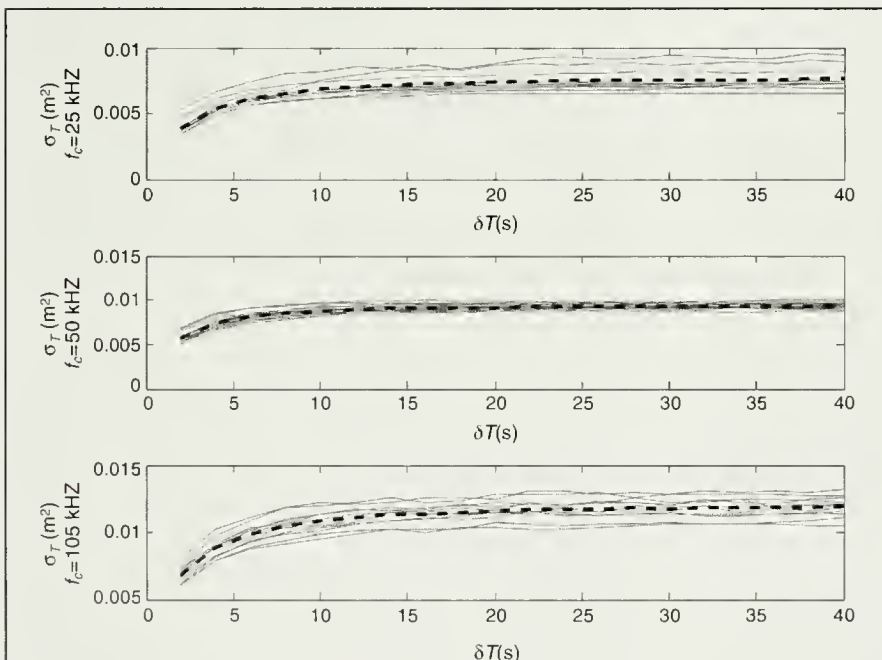


Figure 3

Total scattering cross section σ_T , normalized to one bocaccio (*Sebastes paucispinis*), versus time between shots, δT , for three frequency bands. The measurements (dotted lines) for the lowest and highest frequencies band were repeated 11 times, and 20 times for the center frequencies band, and averaged (dashed dark lines). For short time between shots, σ_T was biased because of slow fish motion. The measurements stabilized with increasing time between shots, δT .

rockfish of different species and sizes, future measurements should be made of individual fish in tank volumes appropriate to the size and the frequency range of the fish, insuring high signal-to-noise ratios and reverberation times. Because of fish handling constraints and access to only a single species of rockfish, it was not possible to do to include these measurements in the present study.

Acknowledgments

We are grateful to P. Sylvia and the rest of the staff at Hubbs-SeaWorld Research Institute for hosting the experiments, and to Chevron Corporation for sponsoring the research.

Literature cited

- Conti, S. G., and D. A. Demer.
2003. Wide-bandwidth acoustical characterization of anchovy and sardine from reverberation measurements in an echoic tank. *ICES J. Mar. Sci.* 60(3):617-624.
- Conti, S. G., D. A. Demer, and A. S. Brierley.
2005. Broadbandwidth sound scattering and absorption from krill (*Meganyctiphanes norvegica*), mysids (*Prounus flexuosus* and *Neomysis integer*) and shrimp (*Crangon crangon*). *ICES J. Mar. Sci.* 62(5):956-965.
- Conti, S. G., J. de Rosny, P. Roux, and D. A. Demer.
2006a. Scatterer motion characterization and estimation in a reverberant medium. *J. Acoust. Soc. Am.* 119(2):769-776.
- Conti, S. G., P. Roux, D. A. Demer, and J. de Rosny.
2004. Measurement of the scattering and absorption cross-section of the human body. *App. Phys. Lett.* 84(5):819-821.
- Conti, S. G., P. Roux, C. Fauvel, B. D. Maurer, and D. A. Demer.
2006b. Acoustic monitoring of fish density, behavior, and growth rate in a tank. *Aquaculture* 251(2-4):314-323.
- Demer, D. A., and S. G. Conti.
2003. Reconciling theoretical versus empirical target strengths of krill; effects of phase variability on the distorted wave Born approximation. *ICES J. Mar. Sci.* 60(2):429-434.
- Demer, D. A., S. Conti, J. De Rosny, P. Roux.
2003. Absolute measurements of total target strength from reverberation in a cavity. *J. Acoust. Soc. Am.* 113:1387-1394.
- de Rosny, J., and P. Roux.
2001. Multiple scattering in a reflecting cavity: application to fish counting in a tank. *J. Ac. Soc. Am.* 109:2587-2597.
- de Rosny, J., P. Roux, M. Fink, and J. H. Page.
2003. Field fluctuation spectroscopy in a reverberant cavity with moving scatterers. *Phys. Rev. Lett.* 90:9-4302.
- Faran, J. J.
1951. Sound scattering by solid cylinders and spheres. *J. Ac. Soc. Am.* 23(4):405-418.
- Foote, K. G.
1979. Fish target-strength-to-length regressions for application in fisheries research. Proceedings of the Ultrasonic International 19, Graz, Austria. 327-333 p. IPC Science and Technology Press Ltd., Guilford, England.
- MacLennan, D. N., and E. J. Simmonds.
1992. Fisheries acoustics, 325 p. Chapman and Hall, London.
- Reynolds, J. R., R. C. Highsmith, B. Konar, C. G. Wheat, and D. Doudna.
2001. Fisheries and fisheries habitat investigations using undersea technologies, OCEANS. MTS/IEEE Conference and Exhibition. In Proceedings of the Oceans 2001 conference; 5-8 November 2000, Honolulu, HI. Hawaiian Sea Grant Program, Univ. Hawaii at Manoa, Manoa, HI.

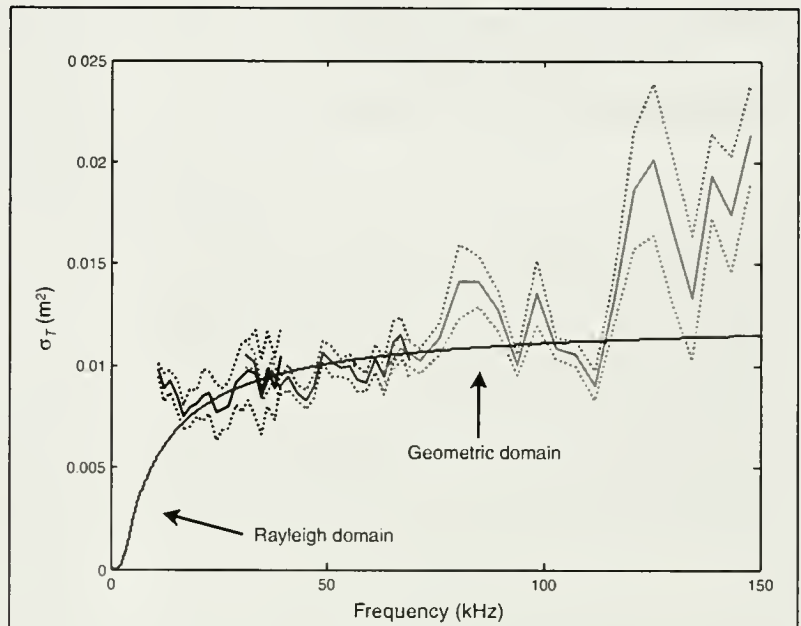


Figure 4

Total scattering spectra σ_T normalized to one boccacio (*Sebastes paucispinis*), over the full frequency band, low to high frequency bands (solid lines from dark to light), and one standard deviation error bounds for these measurements (dashed lines). The spectra were obtained after filtering the data in 20 narrow bands bins for each of the three frequency bands. Theoretical predictions for a 90-mm-diameter rigid sphere in water (Faran, 1951; solid line from 0 to 150 kHz), showing the transition between the Rayleigh and the geometric regimes.

Fishery Bulletin

Guidelines for authors

Content of manuscripts

Contributions published in *Fishery Bulletin* describe original research in marine fishery science, fishery engineering and economics, as well as the areas of marine environmental and ecological sciences (including modeling). Although all contributions are subject to peer review, responsibility for the contents of papers rests upon the authors and not upon the editor or publisher. *Submission of an article implies that the article is original and is not being considered for publication elsewhere.* Manuscripts must be written in English. Authors whose native language is not English are strongly advised to have their manuscripts checked by English-speaking colleagues prior to submission. **Articles** may range from relatively short contributions (10–15 typed, double-spaced pages, tables and figures not included) to extensive contributions (20–30 typed pages). **Notes** are reports of 5 to 10 pages without an abstract and describe methods or results not supported by a large body of data.

Manuscript preparation

Title page should include authors' full names and mailing addresses and the senior author's telephone, fax number, and e-mail address, and a list of key words to describe the contents of the manuscript. **Abstract** should be limited to 150 words (one-half typed page), state the main scope of the research, and emphasize the author's conclusions and relevant findings. Do not review the methods of the study or list the contents of the paper. Because abstracts are circulated by abstracting agencies, it is important that they represent the research clearly and concisely. **Text** must be typed in 12 point Times New Roman font throughout. A brief introduction should convey the broad significance of the paper; the remainder of the paper should be divided into the following sections: **Materials and methods**, **Results, Discussion (or Conclusions)**, and **Acknowledgments**. Headings within each section must be short, reflect a logical sequence, and follow the rules of multiple subdivision (i.e., there can be no subdivision without at least two items). The entire text should be intelligible to interdisciplinary readers; therefore, all acronyms, abbreviations, and technical terms should be written out in full the first time they are used. Include FAO common names for species in the list of keywords and in the introduction. Regional common names may be used throughout the rest of the text if they are different from FAO common names which can be found at <http://www.fishbase.org/search.html>. Follow the U.S. Government Printing Office Style Manual (1984 ed.) and the CBE Style Manual (6th ed.) for editorial style; for fish nomenclature follow the most current issue of the American Fisheries Society's Common

and Scientific Names of Fishes from the United States and Canada. Dates should be written as follows: 11 November 2000. Measurements should be expressed in metric units, e.g., 58 metric tons (t); if other units of measurement are used, please make this fact explicit to the reader. Write out the numbers zero through nine unless they form part of measurement units (e.g., nine fish but 9 mm).

Text footnotes should be inserted in 9-point font at the bottom of the page that displays the first citation of the footnote. Footnotes should be formatted in the same manner as citations. Footnote all personal communications, unpublished data, and unpublished manuscripts with full address of the communicator or author, or, as in the case of unpublished data, where the data are on file. Authors are advised to avoid references to nonstandard (gray) literature (such as internal, project, processed, or administrative reports, ICES Council Minutes, IWC Minutes or Working Papers, any "research" or "working" documents, laboratory or contract reports, Management Council reports, and manuscripts in review) wherever possible. If these references are used, present them as footnotes and list whether they are available at NTIS (National Technical Information Service) or at some other public depository. Cite all software and special equipment or chemical solutions used in the study, not in a footnote but within parentheses in the text (e.g., SAS, vers. 6.03, SAS Inst., Inc., Cary, NC).

Literature cited comprises published works and those accepted for publication in peer-reviewed literature (in press). Follow the name and year system for citation format in the "Literature cited" section. If there is a sequence of citations in the text, list chronologically: (Smith, 1932; Green, 1947; Smith and Jones, 1985). Abbreviations of serials should conform to abbreviations given in the Serial Sources for the BIOSIS Previews Database. Authors are responsible for the accuracy and completeness of all citations. Literature citation format: Author (last name, followed by first-name initials). Year. Title of report or manuscript. Abbreviated title of the series to which it belongs. Always include number of pages. If the authorship for a sequence of citations is identical, list works chronologically.

Tables and figures—general format

- Zeros should precede all decimal points for values less than one.
- Sample size, *n*, should be italicized.
- Capitalize the first letter of the first word in all labels within figures.
- Do not use overly large font sizes in maps and for units of measurements along axes in figures.
- Do not use bold fonts or bold lines in figures.
- Do not place outline rules around graphs.
- Do not use horizontal lines in graphs to indicate measurement units on axes.
- Use a comma in numbers of five digits or more (e.g. 13,000 but 3000).
- Maps should have a North arrow (or compass sign) and degrees latitude-longitude (e.g., 170°E)

Tables are often overused in scientific papers; it is seldom necessary or even desirable to present all the data associated with a study. Tables should not be excessive in size and must be cited in numerical order in the text. Headings should be short but ample enough to allow the table to be intelligible on its own. All unusual symbols must be explained in the table legend. Other incidental comments may be footnoted with italic footnote markers. Use asterisks to indicate probability in statistical data. Do not type table legends on a separate page; place them on the same page as the table data. *Do not submit tables in photo mode.*

Figures include line illustrations, photographs (or slides), and computer-generated graphs and must be cited in numerical order in the text. Graphics will aid in the comprehension of the text, but they should be limited to presenting patterns rather than raw data. Figures are costly to print and should be limited to six. Figures must be labeled with author's name and number of figure. Avoid placing labels vertically (except on *y*-axis). Figure legends should explain all symbols and abbreviations and should be double-spaced on a separate page at the end of the manuscript. Please note that we do not print graphs in color.

**FAILURE TO FOLLOW
THESE GUIDELINES
WILL DELAY
PUBLICATION
OF A MANUSCRIPT**

Copyright law does not apply to *Fishery Bulletin*, which falls within the public domain. However, if an

author reproduces any part of an article from *Fishery Bulletin* in his or her work, reference to source is considered correct form (e.g., Source: Fish. Bull 97:105).

Reprints are available free of charge to the senior author (50 copies) and to his or her laboratory (50 copies).

Submission

The Scientific Editorial Office encourages authors to submit their manuscripts as a *single* PDF (preferred), or Word (zipped) document by e-mail to Fishery.Bulletin@noaa.gov. Please use the subject heading "Fishery Bulletin manuscript submission." *Do not* send encrypted files. For further details on electronic submission, please contact the Scientific Editorial Office directly (see address below). Or you may send your manuscript on compact disc in one of the above formats along with four printed copies (one original plus three copies [stapled]) to the Scientific Editor, at the address shown below.

Dr. Adam Moles
Scientific Editor, *Fishery Bulletin*
11305 Glacier Hwy
Juneau, AK 99801-8626

Once the manuscript has been accepted for publication, you will be asked to submit a final software copy of your manuscript. When requested, the text and tables should be submitted in Word or Word Rich Text Format. Figures should be sent as PDF files, Windows metafiles, tiff files, or as EPS files. Send a copy of figures in original software if conversion to any of these formats yields a degraded version.





U.S. Department
of Commerce

Volume 105
Number 2
April 2007

Fishery Bulletin



**U.S. Department
of Commerce**

Carlos M. Gutierrez
Secretary

**National Oceanic
and Atmospheric
Administration**

Vice Admiral
Conrad C. Lautenbacher Jr.,
USN (ret.)

Under Secretary for
Oceans and Atmosphere

**National Marine
Fisheries Service**

William T. Hogarth
Assistant Administrator
for Fisheries



The *Fishery Bulletin* (ISSN 0090-0656) is published quarterly by the Scientific Publications Office, National Marine Fisheries Service, NOAA, 7600 Sand Point Way NE, BIN C15700, Seattle, WA 98115-0070. Periodicals postage is paid at Seattle, WA. POSTMASTER: Send address changes for subscriptions to *Fishery Bulletin*, Superintendent of Documents, Attn.: Chief, Mail List Branch, Mail Stop SSOM, Washington, DC 20402-9373.

Although the contents of this publication have not been copyrighted and may be reprinted entirely, reference to source is appreciated.

The Secretary of Commerce has determined that the publication of this periodical is necessary according to law for the transaction of public business of this Department. Use of funds for printing of this periodical has been approved by the Director of the Office of Management and Budget.

For sale by the Superintendent of Documents, U.S. Government Printing Office, Washington, DC 20402. Subscription price per year: \$36.00 domestic and \$50.40 foreign. Cost per single issue: \$28.00 domestic and \$35.00 foreign. See back for order form.

Fishery Bulletin

Scientific Editor

Adam Moles, Ph.D.

Associate Editor

Elizabeth Calvert

National Marine Fisheries Service, NOAA
11305 Glacier Highway
Juneau, Alaska 99801-8626

Managing Editor

Sharyn Matriotti

National Marine Fisheries Service
Scientific Publications Office
7600 Sand Point Way NE, BIN C15700
Seattle, Washington 98115-0070

Editorial Committee

Thomas Shirley	Texas A&M University
David Somerton	National Marine Fisheries Service
Mark Terceiro	National Marine Fisheries Service

***Fishery Bulletin* web site: www.fishbull.noaa.gov**

The *Fishery Bulletin* carries original research reports and technical notes on investigations in fishery science, engineering, and economics. It began as the Bulletin of the United States Fish Commission in 1881; it became the Bulletin of the Bureau of Fisheries in 1904 and the *Fishery Bulletin* of the Fish and Wildlife Service in 1941. Separates were issued as documents through volume 46; the last document was No. 1103. Beginning with volume 47 in 1931 and continuing through volume 62 in 1963, each separate appeared as a numbered bulletin. A new system began in 1963 with volume 63 in which papers are bound together in a single issue of the bulletin. Beginning with volume 70, number 1, January 1972, the *Fishery Bulletin* became a periodical, issued quarterly. In this form, it is available by subscription from the Superintendent of Documents, U.S. Government Printing Office, Washington, DC 20402. It is also available free in limited numbers to libraries, research institutions, State and Federal agencies, and in exchange for other scientific publications.

U.S. Department
of Commerce
Seattle, Washington

Volume 105
Number 2
April 2007

Fishery Bulletin

Contents

Articles

- 161–167 **Gentner, Brad**
Sensitivity of angler benefit estimates from a model of recreational demand to the definition of the substitute sites considered by the angler
- 168–179 **Anderson, Tara J., and Mary M. Yoklavich**
Multiscale habitat associations of deepwater demersal fishes off central California
- 180–188 **McClelland, Gary, and Jason Melendy**
Use of endoparasitic helminths as tags in delineating stocks of American plaice (*Hippoglossoides platessoides*) from the southern Gulf of St. Lawrence and Cape Breton Shelf
- 189–196 **Hamilton, Judy, and Brenda Konar**
Implications of substrate complexity and kelp diversity for south-central Alaskan nearshore fish communities
- 197–206 **Ward, Rocky, Kevin Bowers, Rebecca Hensley, Brandon Mobley, and Ed Belouski**
Genetic variability in spotted seatrout (*Cynoscion nebulosus*), determined with microsatellite DNA markers
- 207–233 **Smith-Vaniz, William F., and Kent E. Carpenter**
Review of the crevalle jacks, *Coranx hippos* complex (Teleostei: Carangidae), with a description of a new species from West Africa

MBLWHOI Library

JUN 19 2007

WOODS HOLE
Massachusetts 02543

The conclusions and opinions expressed in *Fishery Bulletin* are solely those of the authors and do not represent the official position of the National Marine Fisheries Service (NOAA) or any other agency or institution.

The National Marine Fisheries Service (NMFS) does not approve, recommend, or endorse any proprietary product or proprietary material mentioned in this publication. No reference shall be made to NMFS, or to this publication furnished by NMFS, in any advertising or sales promotion which would indicate or imply that NMFS approves, recommends, or endorses any proprietary product or proprietary material mentioned herein, or which has as its purpose an intent to cause directly or indirectly the advertised product to be used or purchased because of this NMFS publication.

- 234–248 **Trites, Andrew W., Donald G. Calkins, and Arliss J. Winship**
Diets of Steller sea lions (*Eumetopias jubatus*) in Southeast Alaska, 1993–1999
- 249–265 **Margulies, Daniel, Jenny M. Suter, Sharon L. Hunt, Robert J. Olson, Vernon P. Scholey, Jeanne B. Wexler, and Akio Nakazawa**
Spawning and early development of captive yellowfin tuna (*Thunnus albacares*)
- 266–277 **Zeller, Dirk, Shawn Booth, Gerald Davis, and Daniel Pauly**
Re-estimation of small-scale fishery catches for U.S. flag-associated island areas in the western Pacific: the last 50 years
- 278–291 **Somerton, David A., Peter T. Munro, and Kenneth L. Weinberg**
Whole-gear efficiency of a benthic survey trawl for flatfish
- Notes**
- 292–295 **Strange, Rex M., and Carol A. Stepien**
Yellow (*Perca flavescens*) and Eurasian (*P. fluviatilis*) perch distinguished in fried fish samples by DNA analysis
- 296–304 **Cooper, Daniel W., Katherine P. Maslenikov, and Donald R. Gunderson**
Natural mortality rate, annual fecundity, and maturity at length for Greenland halibut (*Reinhardtius hippoglossoides*) from the northeastern Pacific Ocean
- 305–309 **Roemer, Marja E., and Kenneth Oliveira**
Validation of back-calculation equations for juvenile bluefish (*Pomatomus saltatrix*) with the use of tetracycline-marked otoliths
- 310–311 **Guidelines for authors**
- 312 **Best Paper Awards**

Abstract—Fishery managers are mandated to understand the effects that environmental damage, fishery regulations, and habitat improvement projects have on the net benefits that recreational anglers derive from their sport. Since 1994, the National Marine Fisheries Service (NMFS) has worked to develop a consistent method for estimating net benefits through site choice models of recreational trip demand. In estimating net benefits with these models, there is a tradeoff between computational efficiency and angler behavior in reality. This article examines this tradeoff by considering the sensitivity of angler-welfare estimates for an increase in striped bass (*Morone saxatilis*) angling quality across choice sets with five travel distance cut-offs and compares those estimates to a model with an unrestricted choice set. This article shows that 95% confidence intervals for welfare estimates of an increase in the striped bass catch and keep rate overlap for all distance-based choice sets specified here.

Sensitivity of angler benefit estimates from a model of recreational demand to the definition of the substitute sites considered by the angler

Brad Gentner

NMFS Office of Science and Technology
Fisheries Statistics and Economics Division
1315 East West Highway
Silver Spring, Maryland 20910

Email address: brad.gentner@noaa.gov

Recreational angling is the second most popular outdoor sport nationwide when measured by number of participants. In 2004, 10.2 million anglers took 73.8 million recreational trips in the United States, exclusive of Alaska, Hawaii, and Texas (NMFS¹). In addition to participation, anglers spend \$20.4 billion dollars annually on trip-related and durable expenditures to pursue saltwater gamefish (Gentner et al., 2001), producing \$30.5 billion in economic impacts and supporting nearly 350,000 jobs (Steinback et al., 2004). Recreational fishing is an economically important activity and the National Marine Fisheries Service (NMFS) is mandated by law to examine changes in net benefits to anglers after the impact of environmental damage (oil spills, algal blooms, etc.), fishery regulations (bag limits, size limits, seasonal closures), and habitat improvement projects (damn removal, water quality improvements, etc.). Calculation of net benefits involves an examination of angler behavior when they make choices about taking recreational fishing trips.

Modeling angler trip demand involves observing anglers making recreation site choices and using a site choice model to estimate a recreational trip demand function. Site-choice models are typically estimated by using a random utility model (RUM). RUMs are used to estimate net benefits by looking at the cost of traveling to the site that anglers selected and comparing that cost to the cost of traveling to other sites in their choice set (set of sites considered by the an-

gler). Without any other information about the site, these models allow one to estimate the net benefits of access to that site which can be used to examine closures due to environmental damages or regulation. If site-quality information is available, such as catch rates or other measures of environmental quality, the net benefits of those ecosystem services can be estimated as well.

Since 1994, it has been the goal of the NMFS to develop a consistent method for estimating recreational site-choice models to increase the speed and efficiency of meeting legal mandates. To this end, NMFS has sponsored a good deal of research into RUMs of recreational site choice to value site closures and angling quality (the quality of the angling experience as measured by catch and keep rates) (Haab and Hicks, 1999, Jones and Lupi, 1999, Parsons et al., 1999). From this, and other work, the composition of an individual's choice set can impact net benefit estimates, giving rise to several difficulties when modeling angler net benefits. First, NMFS's RUM models concentrate on only single day trips, because it is difficult to disentangle the value of angling for anglers on trips that have

Manuscript submitted 24 August 2005
to the Scientific Editor.

Manuscript approved for publication
7 August 2006 by the Scientific Editor.

Fish. Bull. 105:161–167 (2007).

¹ NMFS (National Marine Fisheries Service). 2006. Fisheries Statistics and Economics Division. Marine Recreational Fisheries Statistical Survey Real Time Data Queries. Website: <http://www.st.nmfs.gov/st1/recreational/database/queries/index.html> (accessed on 13 August 2006).

multiple purposes. Because focus is strictly on single day trips, it would be incorrect to include sites in an angler's choice set if those sites are "too far" for the angler to consider when choosing a site for a single day trip. Second, a large number of sites in each individual's choice set can be computationally costly, particularly when a nested choice structure is appropriate, and increase the time it takes to bring policy analyses to the table. This problem may indicate that there is a tradeoff between computational efficiency and angler behavior in reality; a balance that will be examined here.

There is literature on the specification of choice sets based on many factors including distance. Parsons and Hauber (1998) estimated a freshwater recreational angler site choice model and found that there is little difference in the magnitude of welfare effects as one reduces the spatial scope of choice sets until a threshold of 1.6 hours one-way travel time is reached. This spatial scope translates into 32 mile and 80 mile distance thresholds, if one assumes a 20 mile per hour (mph) urban travel speed and a 50 mph highway travel speed, respectively. Below that threshold, welfare estimates inflate as the constraint tightens. Whitehead and Haab (1999) estimated a site choice model using a range of choice sets constructed with distance and site-quality metrics. They found that there is very little difference in the trip cost coefficients across distance-based choice sets that eliminate between 13% and 82% of the available sites. Hicks and Strand (2000) found that because the probability of choosing a site depends on the choice set, the likelihood function is also dependent on the choice set. If the choice set is incorrect, biased parameter estimates could be a consequence. The welfare estimates derived in the "Materials and methods" section below explicitly include the choice set and demonstrate this interaction.

This analysis will examine the sensitivity of welfare estimates in a RUM model of recreational demand across six distance-based definitions of site choice. This analysis will focus on a single species, striped bass (*Morone saxatilis*), from a single mode (the private rental boat mode) to avoid a nested choice structure. A simulation approach will be used to derive confidence intervals around these estimates in order to examine the significance of any differences found and to expand the literature that has previously been focused on only on the magnitude of the differences in welfare estimates.

Materials and methods

An angler chooses a fishing site from the set of all alternative sites if the utility of visiting that site is greater than the utility of visiting any other site in the global choice set. Denoting the set of all alternatives faced by any angler by $S = \{1, \dots, N\}$ as the choice set, the indirect utility of visiting site j is

$$U_j(q_j, y - p_j, \epsilon_j) = V_j(q_j, y - p_j) + \epsilon_j, \quad (1)$$

where U_j = an individual's utility;

V_j = the deterministic portion of utility;

y = income;

p = the cost of angling at site j ;

q = a vector of characteristics of site j ; and

ϵ_j = the unobservable portion of indirect utility.

In the RUM framework, an angler will choose site j from S if

$$V_j(q_j, y - p_j) + \epsilon_j \geq V_k(q_k, y - p_k) + \epsilon_k, j \in S, \forall k \in S, \quad (2)$$

where the indirect utility of visiting site j is greater than the indirect utility of visiting site k for all k in the global choice set, S .

The random portion of the random utility model stems from the unobservable portion of indirect utility, captured here in the error term ϵ_j . If this error term is assumed to be distributed in a type-I extreme value distribution, the above site choice framework can be modeled with the conditional logit model. Maddala (1983) has provided a complete derivation of the conditional logit model. Within this framework, the probability that i visits site j is given by

$$P_i(j) = P(j | j \in S) = \frac{e^{V_j(q_j, y - p_j)}}{\sum_{k \in S} e^{V_k(q_k, y - p_k)}}. \quad (3)$$

Up to this point it has been assumed that each angler faces the same choice set, S . This is not a necessary assumption and can be generalized to represent the possibility that i faces a choice set S_i that is a subset of the global choice set S . In this case the indirect utility comparison becomes

$$V_j(q_j, y - p_j) + \epsilon_j \geq V_k(q_k, y - p_k) + \epsilon_k, j \in S, \forall k \in S_i, S_i \subset S \quad (4)$$

and the probability that angler i chooses site j becomes

$$P_i(j) = \frac{e^{V_j(q_j, y - p_j)}}{\sum_{k \in S_i} e^{V_k(q_k, y - p_k)}}. \quad (5)$$

Because the goal of the present study is to examine the sensitivity of welfare estimates of a quality change to the specification of choice sets, it is necessary to show how the choice set enters the calculation of compensating variation (CV), or the level of income required to keep the angler at the same level of expected utility after the quality change. The following expression for CV is taken from the work of Bockstael et al. (1991), who examined the value of quality improvements in the demand for recreation, where β_y is the travel cost parameter.

$$CV = \frac{\ln\left(\sum_{k \in S_i} e^{v_k(q_k^1, p)}\right) - \ln\left(\sum_{k \in S_i} e^{v_k(q_k^0, p)}\right)}{\beta_y} \quad (6)$$

The summation of the indirect utilities is across the choice set facing each individual, S_i , and not the global choice set, S .

Since 1979, data have been collected on marine recreational angling during the Marine Recreational Fishery Statistics Survey (MRFSS). The MRFSS consists of two independent but complementary surveys: a field survey and a telephone survey, conducted annually in six two-month "waves." The field survey is an intercept survey of anglers conducted at fishing access sites and is designed to obtain a random sample of recreational trips for computing catch per unit of effort. Fish retained by interviewed anglers are sampled for length and weight. Fish not retained by the angler are not observed, but count data on this unobserved catch are collected. The data on harvest provide a picture of the size distribution of the kept fish from the stock. If a fishery is regulated by a minimum size limit, a catch-and-keep rate calculated from these data indicates the catchability of fish large enough to keep. As such, it is the observed rate at which anglers can catch and keep fish from a stock.

The intercept sample is stratified by state, wave, fishing mode, fishing area, catch type, and species. Specific data elements collected during the intercept survey include state, county, and zip code of angler's residence, hours fished, primary area fished, target species, gear used, and days fished in the last two and 12 months. During the intercept portion of the survey, data are collected on the length and weight of all fish species retained by the angler and the species and condition of all catch not retained by the angler. Upon completion of the base MRFSS, anglers in the Northeast (NE) (Maine, New Hampshire, Massachusetts, Rhode Island, Connecticut, New York, New Jersey, Delaware, Maryland, and Virginia) were asked to complete a short add-on questionnaire in 2000. This questionnaire provided information on whether or not the trip was a single-day or longer trip and, if it was a multiple-day trip, whether fishing was the primary purpose of the trip. Data were also collected on the angler's saltwater fishing experience (in number of years), boat ownership (whether owned or not), and whether or not the individual took time off without pay to take the fishing trip. If the individuals responded in the affirmative to the later, they were asked the number of hours in their work week and their personal income. The survey instrument is available at the NMFS web site (NMFS²).

In order to reduce the complexity of the modeling effort, the angler's choice to fish rather than participate in some other recreational activity, the angler's choice to fish in a private or rental boat mode, and the angler's decision regarding a species target are exogenous to the model. Because the area fished is not documented

in the MRFSS, a fishing site is defined as the point of fishing access. As mentioned previously, the treatment of all substitute sites can be quite costly from a data standpoint for a number of reasons. Because thousands of individual sites in the North East (NE) region are recognized in the MRFSS, estimation can be a lengthy process, particularly with nested models. In addition, not all species are sampled in all survey waves at all sites in all modes; therefore the calculation of historic catch rates at the individual site level results in many empty cells. To speed estimation and to fill some of these empty cells, all sites within a coastal county were aggregated into one site that represented that county. Across the NE, there are roughly 63 coastal counties, and therefore 63 sites. In order to examine whether this aggregation strategy induces any bias into the estimation of the conditional logit model, a variable (m) was created that represents the number of MRFSS sites aggregated into each new site. The rule that a county equals a site was not strictly followed in all cases. Some geographically diverse counties (i.e., those counties with both ocean frontage and bay frontage) were separated into two sites because of the different opportunities provided by these different types of water.

Both the historic five-year average catch rate (catch rate) and catch-and-keep rate (KRATE) were calculated for the boat mode for each wave and site combination. KRATE measures the catchability of a striped bass large enough to keep, incorporating the five-year average probability of catching a striped bass large enough to keep. The distinction between the catch rate and KRATE is particularly important for striped bass because this species is heavily regulated. Historic KRATE was used in the model because it represents the portion of the catch that an angler would be able to keep, not just the increase in overall catch. It is also the measure of angler quality used in the Whitehead and Haab (1999) study. Even after the site aggregation, some counties did not contain enough data points on striped bass catch from the boat mode over the 5-year period.

Whitehead and Haab (1999) replaced missing catch rates using the catch rate from the nearest neighboring site in some cases and with zero values, in other cases depending more or less on mode. Hicks et al. (1999) recognized this approach to be *ad hoc* and estimated his model using both nearest neighbor and zero value assignment, another *ad hoc* approach, and found that the treatment of missing values did not significantly affect the welfare estimates. He concluded that the zero assignment is perhaps less arbitrary because the empty cells actually convey information. That is, if there are no observations of average catch within a particular wave+mode+site+species combination, the site is not very productive over that combination. As a result, zero assignment requires less judgment by the researcher; therefore that is the approach used here.

Estimating any demand equation requires a price variable. Because recreational fishing experiences are not openly traded in markets, travel cost (both the actual cost of travel plus the opportunity cost of time) is

² NMFS (National Marine Fisheries Service). 2006. Fisheries Statistics and Economics Division. Survey Instruments. Website: http://www.st.nmfs.gov/st1/econ/surveys/survey_timeline.html (accessed on 13 August 2006).

used as the price. Round-trip travel cost (ttc) is calculated as the following;

$$ttc = (\$0.33 \times distance \times 2) + \left(\frac{(distance \times 2)}{40} + hrsf \right) \times lost_income \times w, \quad (7)$$

where $distance$ = the one-way distance from the anglers home zip code to the zip code, or latitude/longitude, of the intercept site.

This distance is multiplied by the Federal Travel Regulations reimbursement rate for private transportation (\$0.33) and includes both the fixed and variable costs of operating an automobile. The variable $lost_income$ is a dummy that takes the value of 1.0 if the individual did take time off work without pay to go fishing. If the individual lost income, their wage rate (w) is multiplied by the travel time plus the time on site ($hrsf$) and this amount is added to the travel cost (40 miles per hour is used as the average travel speed). Therefore, the opportunity cost of onsite time and travel time is only included if an individual took time off work to participate in fishing on a given day. If the individual is not losing income for the trip, his travel cost is simply round-trip distance multiplied by the fixed and variable costs of operating an automobile. As is typical for these MRFSS data sets, very few anglers (3.34%) report having foregone income to take the trip. To account for the opportunity cost of time for those anglers not losing income, travel time is used as a measure of time cost for those individuals. In order not to double count those that lost income taking a trip, the expression for travel time (tt) is

$$tt = \left(\frac{(distance \times 2)}{40} \right) (1 - lost_income). \quad (8)$$

Keeping only those anglers that have targeted or caught striped bass from the boat mode on a single day trip leaves 3630 usable observations.

With an aggregation strategy in place and the variables defined, the estimation of the conditional logit model follows. As a reminder, the choice of whether or not to take a fishing trip, which mode to fish in, and what species to pursue are made outside of this model. The angler then chooses the site that maximizes indirect utility from his or her set of substitutes. Every model carries a set of implicit assumptions. Angler behavior within this model is defined on a trip-by-trip basis and the angler is not allowed to modify the number of trips taken each season. Therefore, each choice is independent of the next, and unobservable utility, ε_j , is independent of any other trips. Additionally, the MRFSS intercept survey is assumed to approximate a random sample of trips. The author acknowledges these contentions with choice-based sampling in the MRFSS data, and this is an area of research that this author and NMFS scientists continue to explore.

Variables in the deterministic portion of indirect utility include travel cost (ttc), travel time (tt), log of the number of MRFSS intercept sites aggregated into the county site used in the model (m), and historic KRATE per trip for striped bass at site j (q_j). Indirect utility is

$$\beta_c ttc_{ij} + \beta_q q_j + \beta_t tt_{ij} + \beta_m \ln(m_j) + \varepsilon_j. \quad (9)$$

With this expression for indirect utility, the probability that angler i selects site j is

$$P_i(j) = \frac{e^{\beta_c ttc_{ij} + \beta_q q_j + \beta_t tt_{ij} + \beta_m \ln(m_j)}}{\sum_{k \in S_i} e^{\beta_c ttc_{ik} + \beta_q q_k + \beta_t tt_{ik} + \beta_m \ln(m_k)}} \quad (10)$$

and the expression for the change in compensating variation for a change in the historic catch and keep rate, after assuming a constant marginal utility of income, is the following:

$$\frac{1}{\beta_c} \left(\ln \left(\sum_{j \in S_i} \beta_c ttc_{ij} + \beta_q q_j^0 + \beta_t tt_{ij} + \beta_m \ln(m_j) \right) - \ln \left(\sum_{j \in S_i} \beta_c ttc_{ij} + \beta_q q_j^1 + \beta_t tt_{ij} + \beta_m \ln(m_j) + \varepsilon_j \right) \right), \quad (11)$$

where q^0 = the historic KRATE; and

q^1 = the KRATE after the environmental or policy change.

Table 1 provides descriptive statistics for all the variables to be used in the analysis and some angler-specific attributes in order to give the reader some background on these anglers. Throughout the range of this data collection, the bag limit for striped bass is two fish per day. On average, anglers catch far less than the limit. In fact, the base catch rate for anglers targeting or catching striped bass from the boat mode is less than one fish per trip. What is readily apparent is that there are some irrational anglers in this group, at least concerning travel time. The maximum travel time translates into a 798 mile one-way travel distance, which does not seem feasible for a one-day trip. Even after eliminating those anglers that admit to taking an "overnight" trip, there are obviously anglers that are away from home longer than 24 hours. One explanation is that these anglers live in the local area seasonally and have given the zip code of their permanent address, which is used to calculate travel distance. Another explanation arising from the author's experience in the field is that some of these anglers drive incredibly long distances and fish for 24 or more hours. They do not consider their trip to be an overnight trip because they are not staying in a hotel even though their round trip travel distance indicates that they were away from home for more than 24 hours. There were only 3 individuals in the data set with one-way travel distances greater than 500 miles and the results were not sensitive to leaving these outliers in the model. As a result they remain in the data set. Other statistics of note include the variable that

Table 1

Descriptive statistics for selected variables describing angler and trip characteristics from the only data set used in this study from the 2000 Marine Recreational Fisheries Statistical Survey economic add-on survey conducted in Maine, New Hampshire, Massachusetts, Rhode Island, Connecticut, New York, New Jersey, Delaware, Maryland, and Virginia.

Variable	Mean	Standard deviation	Minimum	Maximum
Used in model				
Travel cost (<i>ttc</i>) (US\$)	30.39	38.36	0.0	778.73
Travel time (<i>tt</i>) (hours)	1.99	2.15	0.0	39.93
Aggregation variable (<i>m</i>) (number of sites)	43.85	37.88	5.0	138.00
Catch-and-keep rate (<i>q</i>)	0.19	0.40	0.0	2.00
One-way travel distance (<i>distance</i>) (miles) (miles)	41.54	43.13	0.1	798
Not used in model				
Boat ownership (%)	0.73	0.44	0.0	1.00
Hours fished	4.20	1.88	0.5	22.00
Years fished	23.61	14.76	0.0	70.00
Catch rate (no. of fish)	0.89	1.64	0.0	10.67

looks at the aggregation of sites. On average there are almost 44 MRFSS intercept sites aggregated into the definition of a "site" used in the present study and a maximum of 138 sites and a minimum of five sites in a county. On average, anglers spend 4.2 hours on the water and 73% own the boat they are fishing from. Finally, this is a fairly experienced group, with an average of almost 24 years of saltwater fishing experience.

The final portion of this analysis yet to be discussed is the definition of distance-based choice sets. Haab and Hicks (1997) and Parsons and Hauber (1998) found that welfare estimates change little beyond a certain threshold. Up to a point, limiting an angler's choice set by using a distance-based metric only increases the realism of the choice that anglers consider in reality. Hicks et al. (1999) used such a designation in their analyses. Both included all sites within 150 miles, if the angler lived within 30 miles of the site selected, and all sites within 400 miles otherwise. The extreme rational limit for a one-day trip is probably 400 miles one-way. That distance translates into a 10 hour or 6 hour and 40 minute one-way travel time at 40 and 60 miles per hour, respectively. Whitehead and Haab (1999) used definitions of distance-based choice sets that ranged from 180 miles one-way to 360 miles one-way (3–6 hours one-way at 60 miles per hour), realizing that the 360 mile cut-off is likely not very realistic. These definitions probably drive the small difference in parameters across specifications, because eliminating sites outside of what anglers are really considering should have little effect (Whitehead and Haab, 1999).

To examine the definition of choice sets, this study examined much smaller cut-offs than those found in the previous literature that focused on saltwater angling. The cut-offs included the following: a full unrestricted choice set, and 300-, 250-, 200-, 150-, and 100-mile distance cut-offs. Initially, a 50-mile one-way distance cut-off was included, but, because of the site aggregation

strategy used, the only substitutes left in the choice set at the 50-mile cut-off were closer than the site that was chosen, for most anglers. If it is possible to estimate the model on an individual site basis, it would be possible to run smaller distance cutoffs without encountering this problem. In order not to also drop observations when applying these cut-offs, if an individual was observed to make a choice outside of the cut-off, that observation is retained. If all substitute sites for that individual are also outside of the cut-off, the next nearest site is included in that angler's choice set. Therefore, anglers have at least one substitute left in their choice set, no matter how restrictive the cut-off becomes. The average number of sites in each choice set is 63, 37.2, 30.5, 23.3, 16.9, and 10.6 for the six choice sets, from least restrictive to most restrictive, respectively. In percentage terms, these restrictions on the choice set eliminate between 40% and 93% of the available sites.

Estimation of the confidence intervals around these welfare estimates is calculated by taking 1000 random draws from a multivariate normal distribution parameterized by the vector of estimated parameters and their covariance matrix. Sorting these draws from highest to lowest and removing the upper and lower 2.5% and 5%, respectively, construct 95% and 90% confidence intervals (Krinsky and Robb, 1986).

Results

Table 2 contains the parameter estimates and standard errors of the six conditional logit models. All six models strongly reject the hypothesis that the coefficients are simultaneously equal to zero. Also, all coefficients in all models are statistically significant at the 99% level or better. In general, anglers prefer sites that are closer to home, both in terms of the cost of driving and the time cost (travel time multiplied by the individual's

Table 2
Parameter estimates for the six distance-based conditional logit models (standard errors in parentheses).

Variable	Choice set					
	Full	300-mile	250-mile	200-mile	150-mile	100-mile
Travel cost (<i>ttc</i>) (US\$)	0.06242 (0.00573)	-0.06240 (0.00573)	-0.06232 (0.00575)	-0.06176 (0.00582)	-0.05827 (0.00606)	-0.04150 (0.00682)
Travel time (<i>tt</i>) (hours)	-0.23226 (0.07753)	-0.23154 (0.07759)	-0.23216 (0.07782)	-0.23771 (0.07873)	-0.27057 (0.08186)	-0.36472 (0.09201)
Log of aggregation variable (<i>m</i>) (no. of sites)	0.68125 (0.02482)	0.68220 (0.02483)	0.68262 (0.02484)	0.68293 (0.02484)	0.68187 (0.02484)	0.67143 (0.02479)
Catch-and-keep rate (<i>q</i>) (no. of fish)	0.67653 (0.03792)	0.67535 (0.03794)	0.67584 (0.03795)	0.67506 (0.03795)	0.66885 (0.03794)	0.65325 (0.03820)
LR ¹	17,245.31	13,192.55	11,695.28	9,695.16	7,350.95	3,891.39
R ²	0.573	0.507	0.523	0.430	0.364	0.236

¹ Value of the likelihood ratio (LR) statistic testing the hypothesis that all betas = 0.

² McFadden's pseudo R².

wage rate). Additionally, anglers prefer sites that offer the possibility of catching and keeping more striped bass. Finally, with regard to the number of MRFSS sites aggregated into a site as defined in this study, anglers preferred to visit counties that contain more sites. Table 3 gives the mean CV for a one-fish increase in the catch-and-keep rate. A one-fish increase in the catch-and-keep rate is equivalent to the net benefits of an improvement in angling quality large enough to increase the keep rate by one fish or a regulation that allows increasing keep rates. A quality change significant enough to change KRATE by one fish would be unrealistic in the short term, considering the striped bass stock size distribution inferred from the catch rate and KRATE estimates (Table 1). Because KRATE incorporates the five-year average probability of catching a striped bass large enough to keep, this one-fish increase in KRATE models an angler's willingness to pay for a one-fish increase in the bag limit or an angler's willingness to pay for a special license allowing the retention of one striped bass more than the current two-fish limit.

This result supports Parson and Hauber's (1998) and Whitehead and Haab's (1999) results that there is indeed little difference in the definition of choice sets with the use of a distance metric. To examine the significance of the difference in welfare estimates, and not just the magnitude, 95% confidence intervals were calculated around each welfare measure (Krinsky and Robb, 1986). In fact, the mean of the smallest choice set is almost entirely contained within the 95% confidence interval of the next smallest choice set, and the entire lower bound for the smallest choice set is contained in the next smallest choice set. This is demonstrated graphically in Figure 1. From Figure 1, however, it

Table 3

Mean increase in angler benefits, measured by compensating variation (with 95% and 90% confidence intervals [CIs], for a one-fish increase in the catch-and-keep rate by distance-based choice set).

Choice set	Mean increase	95% CI		90% CI	
		Upper	Lower	Upper	Lower
Full	\$10.84	\$13.56	\$8.89	\$13.05	\$9.15
300-mile	\$10.82	\$13.57	\$8.86	\$13.04	\$9.13
250-mile	\$10.84	\$13.61	\$8.90	\$13.29	\$9.18
200-mile	\$10.93	\$13.79	\$8.95	\$13.30	\$9.23
150-mile	\$11.48	\$14.73	\$9.28	\$14.22	\$9.57
100-mile	\$15.74	\$23.57	\$11.65	\$22.05	\$12.23

appears that as the choice sets are truncated past the 150-mile threshold, welfare estimates rise—a similar result to that of Parson and Hauber (1998). Unfortunately, the aggregation strategy necessary when using the MRFSS data precludes an examination of a distance-based cut-off as small as that used in Parsons and Hauber's study (1998).

Conclusions

In general, as choice sets are restricted, the coefficient on cost goes up, its absolute value goes down, and its standard error goes up, but only slightly, until the point is reached where the aggregation strategy begins to impose an artificial restriction on the choice set with this data

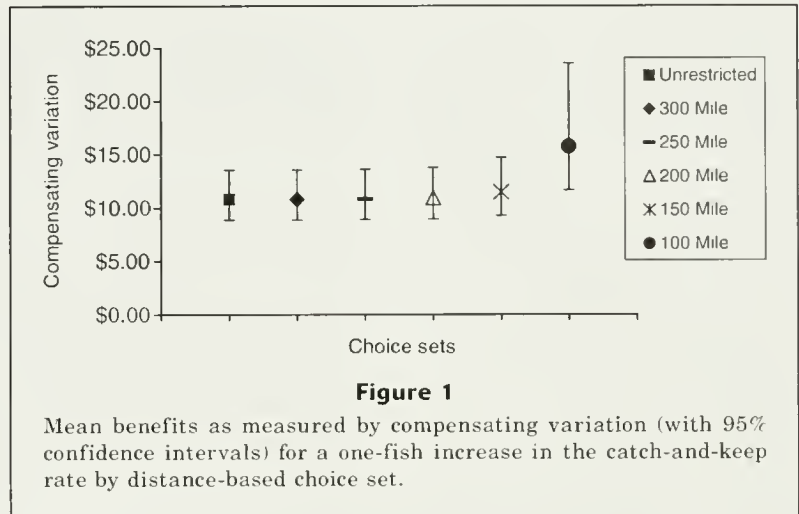
set. It would be interesting to examine the effect of the aggregation strategy by using the individual MRFSS intercept sites. It is possible that using average catch-and-keep rates calculated over a longer time series would result in far fewer empty cells, which are the main hurdle to using the individual MRFSS sites.

Mean one-way travel distance in the data set is 41.5 miles (Table 1). All of the choice sets at and above the 150 mile cut-off have an almost equal proportion of sites in the choice set and sites chosen at the cut-off point. That is, the percentage of substitutes within the cut-off and the percentage of sites chosen within the cut-off are equal (near 99% for both) for the full, 300-, 250-, and 200-mile choice sets. At the 150 mile cut-off this equality begins to fail and the percentage of chosen sites inside the cut-off fall to 98% and 94% for the 150- and 100-mile cut-offs, respectively. This fall is being driven partially by the aggregation strategy. Although this result has not been examined by the author, it is likely that the average distance for an angler to travel outside his county of residence is somewhere between 100 and 150 miles. Again, if the historic catch rate could be calculated to examine individual MRFSS sites, this aggregation restriction could be examined to determine the overall sensitivity of welfare estimates to the designation of distance-based choice sets.

In conclusion, when estimating the net benefits of quality changes for recreational anglers with the MRFSS data, it matters little how restrictive the choice sets become with a distance metric, as long as the researcher does not ask more of the aggregation strategy than it can provide. This result quantifies the significance of the difference in welfare estimates across aggregation strategies and indicates the strengths and the weaknesses of a nationwide data set on marine angling in estimating net benefits and thus makes policy analysis quicker and easier.

Literature cited

- Bockstael, N. E., K. E. McConnell, and I. E. Strand.
1991. Recreation. *In* Measuring the demand for environmental quality (J. Braden, and C. Kolstad, eds.), 227-268 p. North-Holland Pubs., Amsterdam, The Netherlands.
- Gentner, B. J., S. Steinback, and M. Price.
2001. Marine angler expenditures in the Pacific coast region, 2000. NOAA Tech. Memo. NMFS-F/SPO-49, 66 p.
- Haab, T., and R. Hicks.
1997. Accounting for choice set endogeneity in random utility models of site choice. *J. Environ. Econ. Manage.* 34:127-47.
- Haab, T., and R. Hicks.
1999. Choice set considerations in models of recreation demand. *Mar. Res. Econ.* 14:271-281.
- Hicks, R., A. B. Gautam, D. VanVoorhees, M. Osborn, and B. Gentner.
1999. *Thalassorama: an introduction to the NMFS marine recreational fisheries statistical survey with an emphasis on economic valuation.* *Mar. Res. Econ.* 14:375-385.
- Hicks, R., and I. E. Strand.
2000. The extent of information: Its relevance for random utility models. *Land Econ.* 76:374-385.
- Jones, C. A., and F. Lupi.
1999. The effects of modeling substitute activities on recreational benefit estimates. *Mar. Res. Econ.* 14:357-374.
- Krinsky, I., and A. L. Robb.
1986. On approximating the statistical properties of elasticities. *Rev. Econ. Stats.* 68:715-719
- Maddala, G. S.
1983. Limited dependent and qualitative variables in econometrics, 401 p. Economic Soc. Monographs. Cambridge Univ. Press, New York, NY.
- Parsons, G. R., D. M. Massey, and T. Tomasi.
1999. Familiar and favorite sites in a random utility model of beach recreation. *Mar. Res. Econ.* 14:299-315.
- Parsons, G. R., and A. B. Hauber.
1998. Spatial boundaries and choice set definition in a random utility model of recreation demand. *Land Econ.* 74:32-48.
- Steinback, S., B. Gentner, and J. Castle.
2004. Economic impacts of marine recreational angling in the United States. U.S. Dep. Commer., NOAA Prof. Pap. NMFS 2, 169 p.
- Whitehead, J. C., and T. C. Haab.
1999. Distance and catch based choice sets. *Mar. Res. Econ.* 14:283-299.



Abstract—Fish-habitat associations were examined at three spatial scales in Monterey Bay, California, to determine how benthic habitats and landscape configuration have structured deepwater demersal fish assemblages. Fish counts and habitat variables were quantified by using observer and video data collected from a submersible. Fish responded to benthic habitats at scales ranging from cm's to km's. At broad-scales (km's), habitat strata classified from acoustic maps were a strong predictor of fish assemblage composition. At intermediate-scales (m's–100 m's), fish species were associated with specific substratum patch types. At fine-scales (<1 m), micro-habitat associations revealed differing degrees of microhabitat specificity, and for some species revealed niche separation within patches. The use of habitat characteristics in ecosystem-based management, particularly as a surrogate for species distributions, will depend on resolving fish-habitat associations and habitat complexity over multiple scales.

Multiscale habitat associations of deepwater demersal fishes off central California

Tara J. Anderson (contact author)

Mary M. Yoklavich

Email address for T. J. Anderson: t.anderson@aims.gov.au

Fisheries Ecology Division
Southwest Fisheries Science Center
National Marine Fisheries Service
110 Shaffer Road,
Santa Cruz, California 95060

Present address (for T. J. Anderson): Australian Institute of Marine Science
PMB 3 Townsville MC
Queensland 4810, Australia

Measuring fish-habitat associations on a number of spatial scales is essential in determining the relative importance of habitat types and landscape configuration in structuring fish assemblages and populations. Many benthic habitat characteristics (e.g., substratum type, depth, relief) are important in explaining the local distribution and abundance patterns of demersal fishes (e.g., Jones and Syms 1998; Stephens et al., 2006). An organism's use of habitat may also change as a function of scale (Wiens, 1989). For example, fishes may make a considerable range of choices about their occupancy of specific habitats and may sample their environment at a range of spatial and temporal scales (Ault and Johnson, 1998; Syms and Jones, 1999). Habitat types (abiotic and biotic), however, are found within a large spatial domain (landscape) in which the configuration and connectivity between neighboring habitat areas may contribute to population structure (Forman, 1995). For example, landscape configuration and the degree of habitat patchiness may modify the distribution and movement of an organism, and the interactions among species (Addicott et al., 1987).

On the U. S. West Coast, demersal fishes, particularly rockfishes (*Sebastes*) are a dominant feature of the benthic ecosystem (Love and Yoklavich, 2006) and are important for both commercial and recreational fisheries

(Love, 2006). At broad spatial scales, traditional trawl surveys have documented a range of biogeographical and depth patterns for harvested demersal species (Gunderson and Sample, 1980; Weinberg, 1994; Williams and Ralston, 2002). Less research has been done on the role that benthic habitat variables, such as substratum type and relief, play in explaining the distribution and abundance of either commercial or noncommercial species. Strong relationships between demersal fish species and a range of habitat characteristics, particularly substratum type and abundance of giant kelp, have been identified in shallow (<30 m) coastal waters (Stephens et al., 2006). However, many demersal species in this system, particularly rockfish species, are found over extensive depth ranges beyond those that can safely be investigated with SCUBA (Love et al., 2002). The use of submersibles and remotely operated vehicles (ROVs), with sampling protocols similar to those of nearshore surveys (Stein et al., 1992; Adams et al., 1995; Yoklavich et al., 2000), provides the capabilities to make quantitative *in situ* observations of fish-habitat associations in deepwater (>30 m). Studies in which these tools are employed are also beginning to demonstrate characteristic habitat associations for deepwater demersal fish species (Love and Yoklavich, 2006). The importance of spatial scale in un-

Manuscript submitted: 16 June 2006
to the Scientific Editor.

Manuscript approved for publication
17 August 2006 by the Scientific Editor.
Fish. Bull. 105:168–179 (2007).

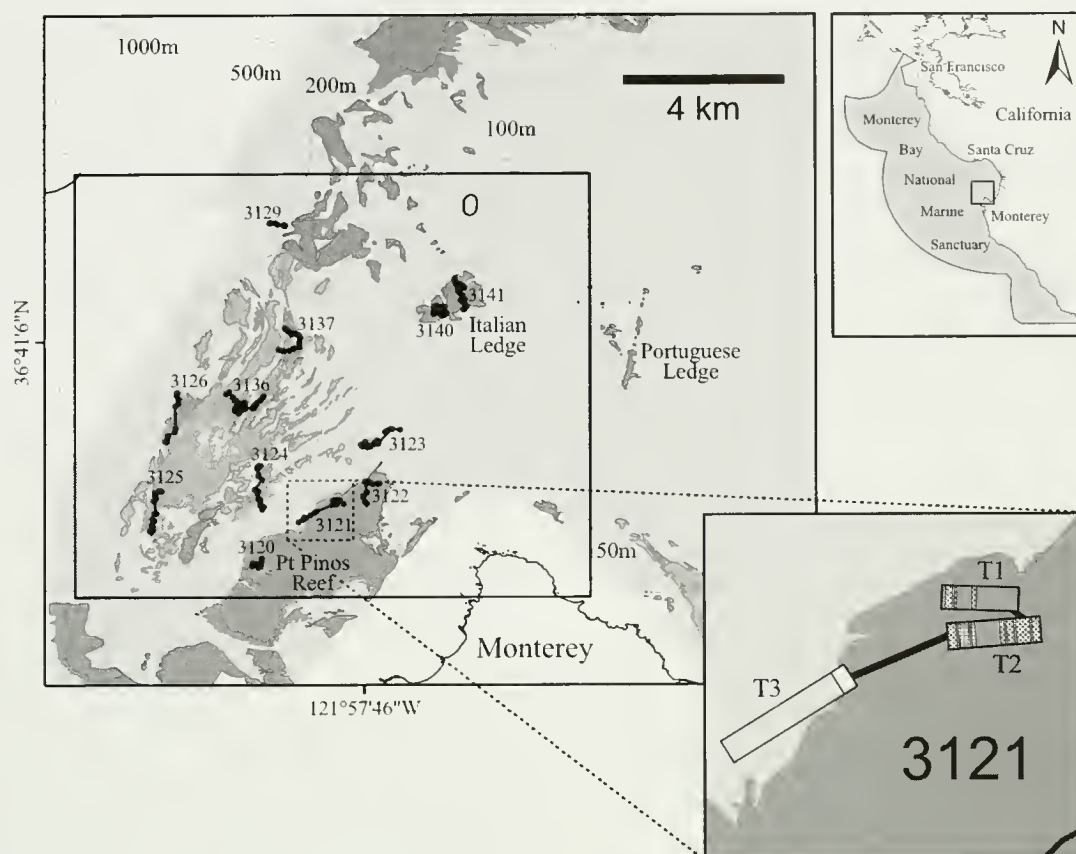


Figure 1

Seafloor map of the continental shelf in southern Monterey Bay, central California, depicting the three acoustically derived broad-scale strata and *Delta* submersible sampling locations (dive numbers 3120–3141). Hard substratum (i.e., complex outcrops) is depicted as dark gray areas. Mixed substratum (areas of hard mixed with soft) is depicted as medium gray areas. Soft substratum (i.e., areas of contiguous soft sediments) is depicted as light gray areas. White areas were not surveyed; box = 10×12 km study area. Bottom insert is an example of the observed intermediate-scale substratum types recorded within the three transects of dive 3121 (depicted by the three rectangles T1=transect 1, T2=transect 2, and T3=transect 3) in relation to the seafloor map of that area. Transects sampled in hard substratum (T1 and T2) were heterogeneous and were composed of mixed patches dominated by rock (dark gray), boulders (diagonal hatching) and cobbles (light gray checks). In contrast, transects run within soft substratum (T3) were more homogeneous, composed of either sand (white) or mud (light gray).

Understanding these associations, however, has received much less attention (Langton et al., 1995).

In this study, we examined the relationship between deepwater demersal fishes and benthic habitat variables at three spatial scales in an area encompassing a proposed marine protected area (MPA) in southern Monterey Bay, California. At the broad spatial scale of km's, habitat strata were identified from acoustic seafloor maps. Within these strata we conducted submersible transects and recorded both benthic habitat variables—such as substratum type, depth, relief, and habitat patchiness—and fish abundance and size. At the intermediate scale of 10–100's of meters, within-transect habitat measures, in combination with fish counts, provided measures of habitat patchiness and fish use of these patches. Finally, we assessed fine-scale or micro-

habitat (<1 m) fish-habitat associations by recording the habitat type located directly beneath each fish. These multiple spatial scales of habitat association were integrated to examine multiscale habitat and landscape requirements of these species.

Material and methods

Survey of fish habitat

To quantitatively sample demersal fishes and benthic habitats on the continental shelf in southern Monterey Bay (36°E, 121°S) (Fig. 1), *in situ* counts and habitat characterizations were made from the two-person *Delta* submersible. The submersible survey was conducted

from 9 through 12 October 1993 (boreal fall), between the hours of 07:30 (1 hour after sunrise) and 17:00 (1 hour before sunset). Thirty-three strip-transects (2 m wide by 10 minutes in duration) were surveyed within a 10×12 km study area (Fig. 1). During each transect, the scientific observer made observations from the central starboard porthole while the pilot drove the submersible about 1 m above the seafloor at a speed of 0.4–0.9 knots depending on currents and topography. Three broad-scale strata (hard, mixed, soft substratum), which had been identified from seafloor maps by using geophysical data (Eittreim et al., 2002; Anderson et al., 2005), were sampled at depths ranging from 72 to 252 m.

Within each 10-minute transect, all demersal fishes within 2 m of the submersible were identified to the lowest taxon, measured (total length was visually estimated to 5-cm size classes), and counted vocally by the scientific observer. An external starboard mounted Hi-8 video camera simultaneously recorded the seafloor along each transect and the scientific observers' vocal commentary on the audio track. A hand-held sonar gun was used to gauge transect width, and paired lasers, set 20 cm apart and projected into the observers' field of view, were used to gauge fish size. A *Pisces Video Plus II* data-logger (*Pisces Design*, San Diego, California) superimposed time, date, depth, and altitude of the submersible onto the video image. Final fish sizes and counts were derived from the videotape, by using the audio commentary as supporting information. All video analyses were conducted by the same person to reduce between-observer variability. Individual fish that could not be distinguished to species were assigned to a taxonomic group, for example: to subgenus (e.g., young-of-year *Sebastes* spp. [YOY], *Sebastes* spp. [rosy-like rockfish species]), genera (e.g., *Citharichthys* spp. [sanddabs], *Zaniolepis* spp. [combfishes]), family (e.g., Agonidae [poachers], Cottidae [sculpins]) or order (e.g., Pleuronectiformes [flatfishes]).

Benthic habitat characteristics within each transect (intermediate scale) were categorized and delineated from the videotape. Substratum composition (rocks, boulders >25.5 cm, cobbles [6.5–25.5 cm], sand, and mud) within a patch was categorized by using the dominant (primary=>50%) and subdominant (secondary=>20%) percentages of substratum cover used by Stein et al. (1992) and Yoklavich et al. (2000). For example, a patch comprising >50% rock and >20% boulders was classified as rock-boulder (RB); a patch comprising >70% rock was classified as rock-rock (RR). Patches were delineated from videotape where patch duration exceeded 3 seconds of elapsed video time (i.e., where patch size >1.7 m). Habitat relief within each patch was categorized as flat (0–5°), low (5–30°), or high (>30°). These methods adequately defined intermediate scale habitat composition and patchiness within transects (i.e., m's–100's m), yet logistically enabled long transects (max. 585 m) to be quantified. To describe fine-scale (<1 m) microhabitat use by demersal fish species, we recorded the type of substratum (rock, boulders, cobbles, sand, or mud) directly beneath each

fish. This multiscale approach enabled habitat associations at each scale to be recorded independently of associations at other scales.

Transect length, independent of submersible speed, was estimated by using the known distance between the lasers (i.e., 20 cm) as a ruler, by counting the number of lengths that occurred sequentially over a 15-s duration within each minute of videotape, and then multiplying by transect duration (i.e., 10 min). Patch lengths were calculated by using the same method but were multiplied by patch duration (elapsed time per patch).

Analysis

The categorical measures of substratum type were recoded as semiquantitative variables. Primary and secondary categories were recoded so that each substratum type within a patch was given a percent cover value of 0%, 20%, 50%, or 70%. For example, rock-rock (RR) was recoded as 70% rock (50%+20%) while all other substratum types scored a value of 0%; similarly boulder-cobble (BC) was recoded as 50% boulder, 20% cobble and all other types scored a value of 0%. Habitat relief was recategorized as an ordinal variable with values of 1, 2, and 3 that corresponded with flat, low, and high relief. The mean and standard error for substratum types and relief, and median depth were then calculated for each transect (broad-scale) and patch (intermediate-scale). Habitat patchiness at the broad-scale was represented by "patch number"—the number of patches within each transect, and "patch size"—calculated as the log(patch length) within each transect. Benthic habitat variables, with the exception of patch number and patch size, were $x^{0.5}$ transformed to improve data normality and linearity between variables. Principal components analysis (PCA) was run on the correlation matrix of the transformed transect-level data to evaluate the validity of the broad-scale strata classifications and to describe the relationship between benthic habitat variables over broad spatial scales.

To examine the relationship between fish and habitat, total abundance and species richness were calculated for all fish species and rockfish species at both transect (transect length×2 m width) and patch (patch length×2 m) scales: fish densities were then expressed as numbers per 1000 m² (transects), and 200 m² (patches). To examine the fish assemblage in relation to harvest potential, we classified species as either commercial (e.g., *Sebastes paucispinis* [bocaccio], *S. ruberrimus* [yelloweye rockfish], *S. flavidus* [yellowtail rockfish], *Ophiodon elongatus* [lingcod], and *Microstomus pacificus* [Dover sole]) or noncommercial (e.g., *S. wilsoni* [pygmy rockfish], *Rhinogobiops nicholsii* [blackeyed goby], and *Zaniolepis* spp.). We also categorized fishes as small (≤20 cm) or large (>20 cm). Individual species and taxon groups were included in analyses when they were present in more than 5% of all patches. Consequently, 21 taxa (15 species and six groups) from nine families were retained for analyses. The data on fish distributions were examined by using histograms and Taylor power

plots (i.e., $\log(\text{variance})$ versus $\log(\text{mean})$). Data were generally right-skewed and had a positive variance-mean relationship. The slope of the Taylor power plot was used to optimally decouple variance from mean by raising the data to the power of $((2-\text{slope})/2)$ (McArdle et al., 1990). Consequently, species abundance data were ($x^{0.25}$) transformed, total abundance was transformed by $\log_{10}(x+1)$, and a square root ($x^{0.5}$) transformation was applied to species richness. To examine broad-scale relationships between fish species and benthic habitat variables, we ran a canonical correlation analysis on the transect-level data matrix and then plotted the total structure coefficients of the fish in habitat space. The standardized redundancy output values of the model were used to measure the amount of variation for both fish species and benthic habitat variables.

To examine intermediate-scale relationships between fish species and benthic habitat variables, densities of fishes per patch types were examined. However, because all patch types were not equally available, we also standardized patch-use relative to habitat availability (patch selectivity) by subtracting proportional occurrence of each patch type from the proportional abundance for each species. Here, a positive association with a patch type revealed that more individuals were found in that patch type than would be expected given random habitat use (i.e., no selectivity). Conversely, a negative association revealed that fewer individuals were found in that patch type than would be expected by random habitat use. Finally, because microhabitat availability was not measured independently of fish presence, microhabitat use by fishes was restricted to graphical presentation.

Results

Seafloor composition

We sampled 11.15 linear km of seafloor within the 12×10 km survey region, using submersible strip-transect methods. At broad-scales, benthic habitat variables were grouped *a posteriori* in order to reliably distinguish hard, mixed, and soft strata (Fig. 2). Hard stratum comprised patchy "high-relief outcrops" of rock, boulders, and sand. In contrast, mixed stratum comprised "low-relief outcrops" of cobbles and mud. Soft stratum comprised "homogeneous mud." The three broad-scale habitat strata also varied in their depth distribution, and strata and depth were strongly collinear. High-relief outcrops were generally shallower (60–100 m) than low-relief outcrops (90–150 m), and although homogeneous mud occurred in most depth ranges, it was the only stratum surveyed in deep offshore locations (80–260 m). Benthic habitat variables within each of the three strata were also strongly collinear. For example, rock always co-occurred with boulders and sand, forming complex high-relief outcrops in shallower water (i.e., <100 m). Therefore, if a species was correlated at broad spatial scales with high-relief outcrops, differentiating the rela-

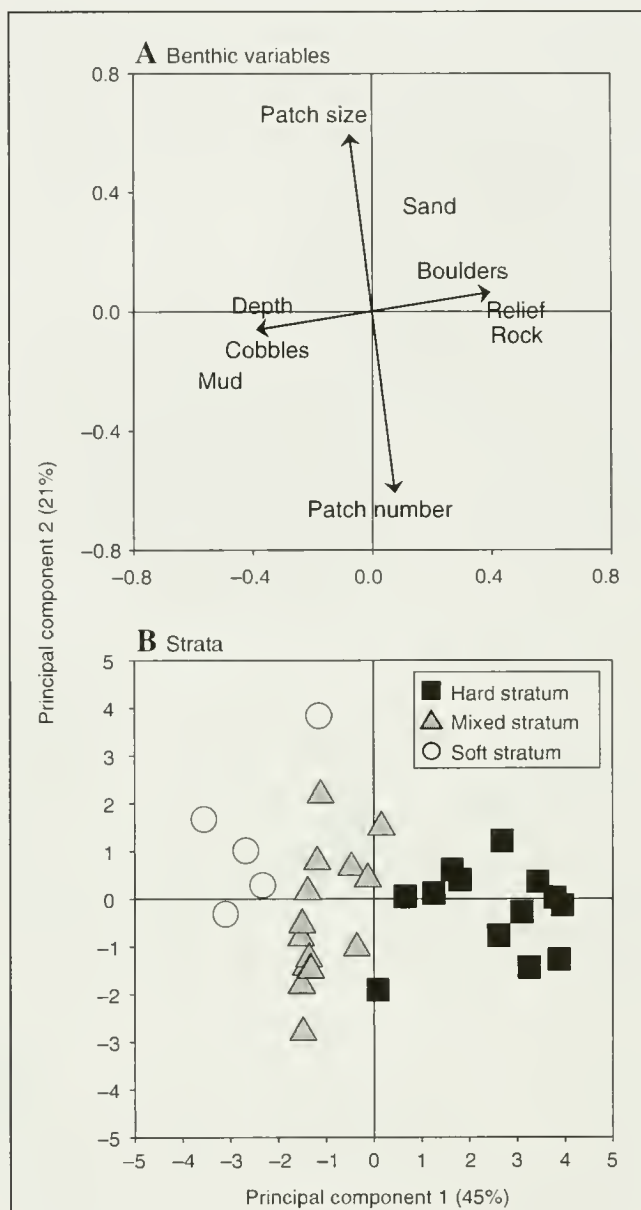


Figure 2

Principal components analysis of broad-scale benthic habitat characteristics: (A) correlation matrix of benthic variables; (B) projection of strata categories in ordination space.

tive importance of substratum composition, depth, or some corequisite would be problematic.

Variability in intermediate-scale habitat also was discernible (Fig. 3). Five substrata (rock, boulders, cobbles, sand, and mud) were recorded during this survey, which at intermediate scales were present in 21 of 25 possible paired "substratum patch types" (all but mud-sand, cobble-sand, sand-cobble, or sand-mud patch types were recorded). However, the proportional availability of these patch types differed between strata. For example, hard strata contained the highest number

of substratum types ($n=19$), where rock and boulders types were the most abundant (Fig. 3A). Mixed strata also contained a variety of patch types ($n=10$), but were devoid of rock and contained higher proportions of mud (Fig. 3B). Soft strata contained the fewest patch types ($n=3$), composed primarily of homogeneous mud, and small amounts of homogeneous sand and mud-cobble patch types (Fig. 3C).

Structure of fish assemblages and broad-scale fish-habitat associations

Sixty-two species of demersal fishes (from 21 families) totalling 21,184 fishes were recorded during this survey. Rockfishes were the most abundant portion of the demersal fish assemblage, representing 93% of all fish sampled (i.e., 24 rockfish species, totalling 19,668 rockfishes). Most fishes recorded (96%) were small (TL ≤ 20 cm) noncommercial species, dominated by small-bodied

(dwarf) rockfishes, such as *S. wilsoni* ($n=5857$, 28% of all fish sampled), *S. semicinctus* (halfbanded rockfish) ($n=5247$, 25%), and *S. hopkinsi* (squarespot rockfish) ($n=2747$, 13%). In comparison, both small (TL ≤ 20 cm) and large (TL > 20 cm) fishes of commercial species and large noncommercial species were uncommon (462 small-size commercial fish (2%); 295 large-size commercial fish (1%); and 79 large-size noncommercial fish (0.4%)).

Fish density and species richness varied between the three broad-scale strata. Hard stratum had the highest density of fish (1357 fishes per 1000 m²), followed by mixed stratum (862 fishes per 1000 m²), and both strata were dominated by rockfishes (90%, 98% respectively). Inversely, soft stratum had comparatively few fish (130 fishes per 1000 m²), dominated by nonrockfish species (63%). Small-size fishes accounted for the majority of demersal fishes within hard (98% of all fish sampled), mixed (99%), and soft (79%) strata. In comparison, large demersal fishes

(TL > 20 cm) were relatively uncommon in all three substrata; however, the hard stratum had higher densities (27 per 1000 m² [2% of all fishes in hard substratum]) than the soft (21 per 1000 m² [16%]), or mixed (4 per 1000 m² [0.5%]) strata. The mixed stratum had the highest number of species (44 species), where 64% of the species composition comprised non-rockfish species. The hard stratum had slightly fewer species (41 species) but comprised a more even mix of rockfish (54%) and nonrockfish (46%) species. Soft stratum had the fewest species of all three strata (19 species), of which most were nonrockfish species (74%). The number of commercially important species decreased as habitat complexity decreased: 18 commercial species (15 rockfish species) were recorded from hard substratum, compared with 16 (10 rockfish species) in mixed substratum, and 11 (5 rockfish species) in soft substratum.

Assemblage composition varied between the three broad-scale strata (Fig. 4). High-relief outcrops (hard stratum) were characterized by schools of small-bodied rockfishes (*S. hopkinsi*, *S. wilsoni*, and YOY), a suite of large-bodied rockfish (e.g., *S. paucispinis*, *S. flavidus*, *S. rubrivinctus* [flag rockfish], *S. rosaceus* [rosy rockfish], and *Sebastes* spp.), and a few non-rockfish species (e.g., *R. nicholsii* and *O. elongatus*). Low-relief outcrops (mixed stratum), in contrast, were characterized by schools of the small-bodied rockfish, *S. semicinctus*, two large-bodied rockfishes (*S. chlorostictus* [greenspotted rockfish] and *S. elongatus* [greenstriped rockfish]), and a variety of nonrockfish species (e.g., *Citharichthys* spp., *Zalembius rosaceus* [pink seaperch], *Zaniolepis* spp. [combfishes], *Argentina sialis* [Pacific argentine], and *O. elongatus*). Homogeneous mud areas (soft stratum) differed from high-relief and low-relief outcrops

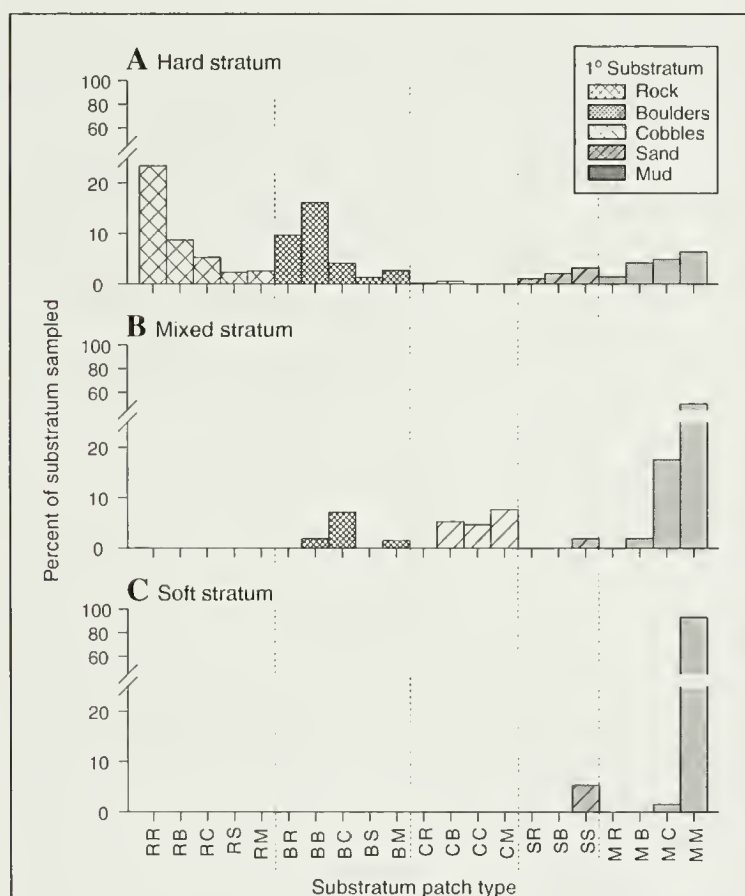


Figure 3

Intermediate-scale habitat characteristics: substratum patch composition within the three broad-scale habitat strata: (A) hard stratum, (B) mixed stratum, and (C) soft stratum. Substratum types recorded were R=rock, B=boulders, C=cobbles, S=sand, and M=mud. The first and second letters of each patch type (e.g., RR, RB, RC, to MM) represent primary (50%) and secondary (20%) substratum types, respectively.

by the characteristic presence of Pleuronectiformes and Agonidae.

Intermediate- and fine-scale fish-habitat associations

At the level of the individual fish species, a range of benthic habitat variables and spatial scales were important in explaining species-specific distributions. Intermediate-scale information on patch use, patch selectivity, along with fine-scale microhabitat use, revealed four types of species-specific groups (Fig. 5–8).

The first group, rock and boulder associates (e.g., *S. hopkinsi*, *S. flavidus*, and *S. paucispinis*) were species that at the intermediate-scale were strongly associated with patches of rock or boulders (or both) (Fig. 5). At the fine-scale, these three species were found on or above rocks (69%, 76%, and 30%, respectively) or boulders (28%, 24%, and 18%, respectively); *S. paucispinis* also used mud microhabitats (52%).

The second group, generalists (e.g., *S. wilsoni*, *S. rosaceus*, and *O. elongatus*) were species that at the intermediate-scale were associated with a variety of patch types (Fig. 6). However, when standardized by habitat availability, these species were strongly associated with patches of boulders, cobbles, and to a lesser extent, rock, and were negatively associated with patches of homogeneous mud. At the fine-scale, these species were also found on or above all possible microhabitat types and showed a flexibility in habitat use at all three spatial scales. Ontogenetic shifts in habitat use also were indicated. For example, small *O. elongatus*, (<25 cm; $n=54$) were more abundant in patches with mud or cobbles (e.g., 74% in mud-mud [MM], cobble-boulder [CB], and mud-cobble [MC]), whereas medium-size *O. elongatus* (25–50 cm; $n=57$) were found more frequently in patches with boulders (40%) and rock (32%). Larger individuals (>50 cm; $n=6$), on the other hand, were found in patches of rock (83%), indicating that *O. elongatus* move from mixed mud and cobble habitats to more complex rocky outcrops as they grow.

The third group, cobble-mud associates (e.g., *S. semicinctus*, *S. chlorostictus*, and *S. elongatus*) were species that at the intermediate-scale were found in patches containing various mixtures of cobbles, mud, and to a lesser extent, boulders (Fig. 7). At the fine-scale, these species were found over mud (66%, 54%, and 81%, respectively) or low-relief cobbles and boulders (pooled 33%, 47%, and 16%, respectively) indicating that mud habitats adjacent to or within mixed cobble-mud areas had inherent properties above either habitat in isolation.

Finally, the fourth group, soft-sediment associates (e.g., Pleuronectiformes, Agonidae, *Citharichthys* spp., and *R. nicholsii*) were species that at the intermediate-scale were strongly associated with patches containing

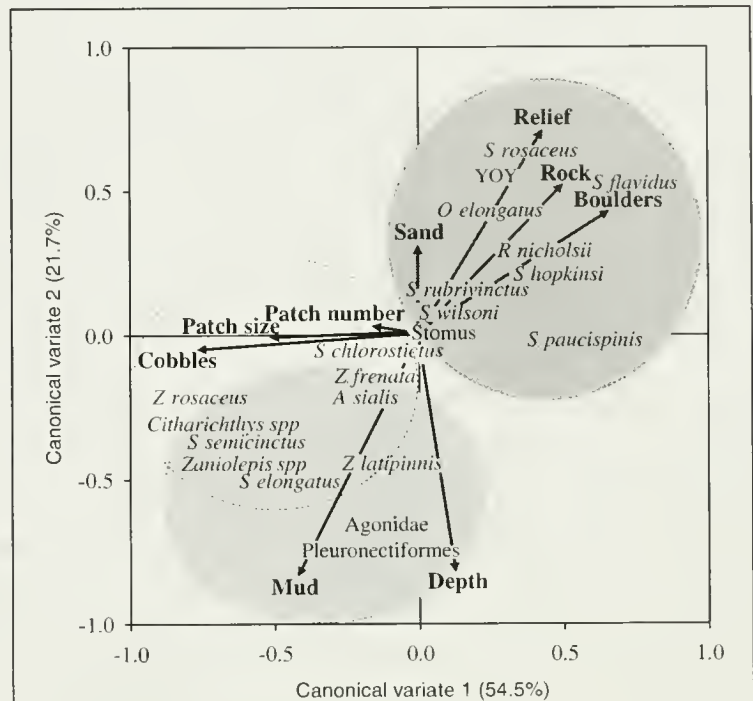


Figure 4

Broad-scale associations of the demersal fish assemblages with benthic habitat variables as discerned from canonical correlation analysis. Circles depict the three broad-scale strata (dark gray=hard, white=mixed, light gray=soft sediment), and are presented to assist in the visual association of species and benthic habitat variables. Vectors are the eigenvectors of the benthic habitat variables. YOY = young-of-year *Sebastes* spp., "Stomus" = *Sebastes* spp.; S = *Sebastes*; R = *Rhinogobius*; O = *Ophiodon*; Z = *Zaniolepis*; and A = *Argentina*.

mud or sand (Fig. 8). Pleuronectiformes, Agonidae, and *Citharichthys* spp. were all associated with homogeneous soft sediments at all spatial scales (Fig. 8, A–C). In contrast, *R. nicholsii* were found in a range of soft-sediment patch types (e.g., sand-boulder [SB], sand-sand [SS], mud-rock [MR], mud-boulder [MB], etc.) and microhabitats. However, homogeneous soft-sediment areas had few or no *R. nicholsii* (Fig. 8D), indicating that, for this species, sediment gaps within a rocky outcrop matrix had inherent properties above either rock or sediment habitats in isolation.

Discussion

The composition, complexity, and configuration of the seafloor at multiple scales allowed us to predict assemblage structure and species distributions across the continental shelf within southern Monterey Bay. Broad-scale habitat strata, which are routinely mapped by acoustic methods, showed clear distinctions in assemblage structure. Hard stratum, composed of high-relief outcrops, was occupied by a diverse range of demer-

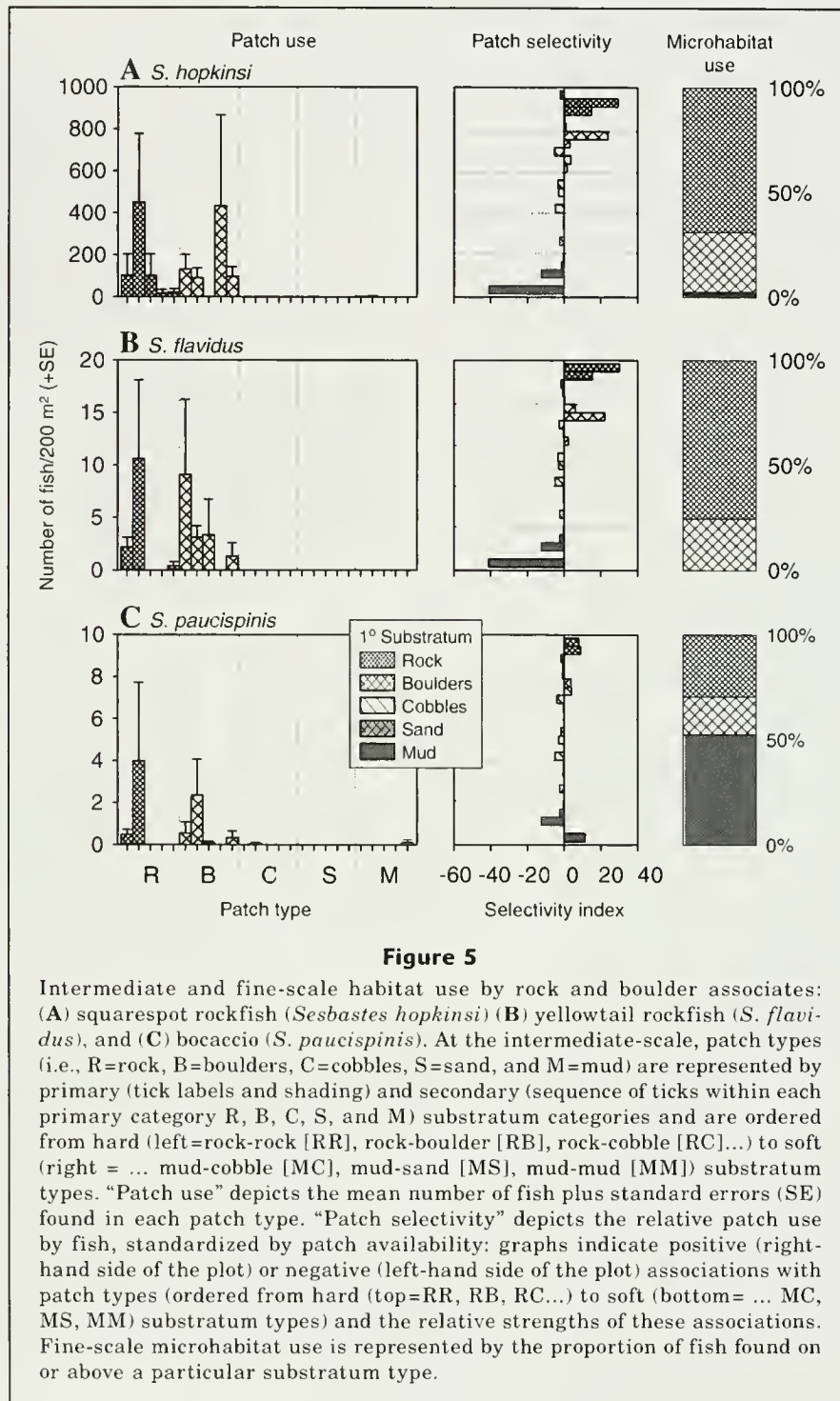


Figure 5

Intermediate and fine-scale habitat use by rock and boulder associates: (A) squarespot rockfish (*Sesbastes hopkinsi*) (B) yellowtail rockfish (*S. flavidus*), and (C) bocaccio (*S. paucispinis*). At the intermediate-scale, patch types (i.e., R=rock, B=boulders, C=cobbles, S=sand, and M=mud) are represented by primary (tick labels and shading) and secondary (sequence of ticks within each primary category R, B, C, S, and M) substratum categories and are ordered from hard (left=rock-rock [RR], rock-boulder [RB], rock-cobble [RC]...) to soft (right = ... mud-cobble [MC], mud-sand [MS], mud-mud [MM]) substratum types. "Patch use" depicts the mean number of fish plus standard errors (SE) found in each patch type. "Patch selectivity" depicts the relative patch use by fish, standardized by patch availability: graphs indicate positive (right-hand side of the plot) or negative (left-hand side of the plot) associations with patch types (ordered from hard (top=RR, RB, RC...) to soft (bottom= ... MC, MS, MM) substratum types) and the relative strengths of these associations. Fine-scale microhabitat use is represented by the proportion of fish found on or above a particular substratum type.

sal fish species dominated by small rockfish species. Although hard stratum was the least common of the three strata (Anderson et al., 2005), it supported the highest overall densities of fish, including more commercial species, than either mixed or soft strata. High fish densities, a dominance of small rockfish species, and the presence of large commercial species over high-relief outcrops have been recorded in other submersible

surveys in California (Yoklavich et al., 2000, 2002), Oregon (Stein et al., 1992), Washington (Jagiello et al., 2003), British Columbia (e.g., Murie et al., 1994), and Alaska (O'Connell and Carlile, 1993). For example, Yoklavich et al. (2000) found high numbers of large commercially important rockfish species (e.g., *S. paucispinis*, *S. ruberrimus*, *S. levis* [cowcod]) associated with discrete rocky outcrops in a submarine canyon

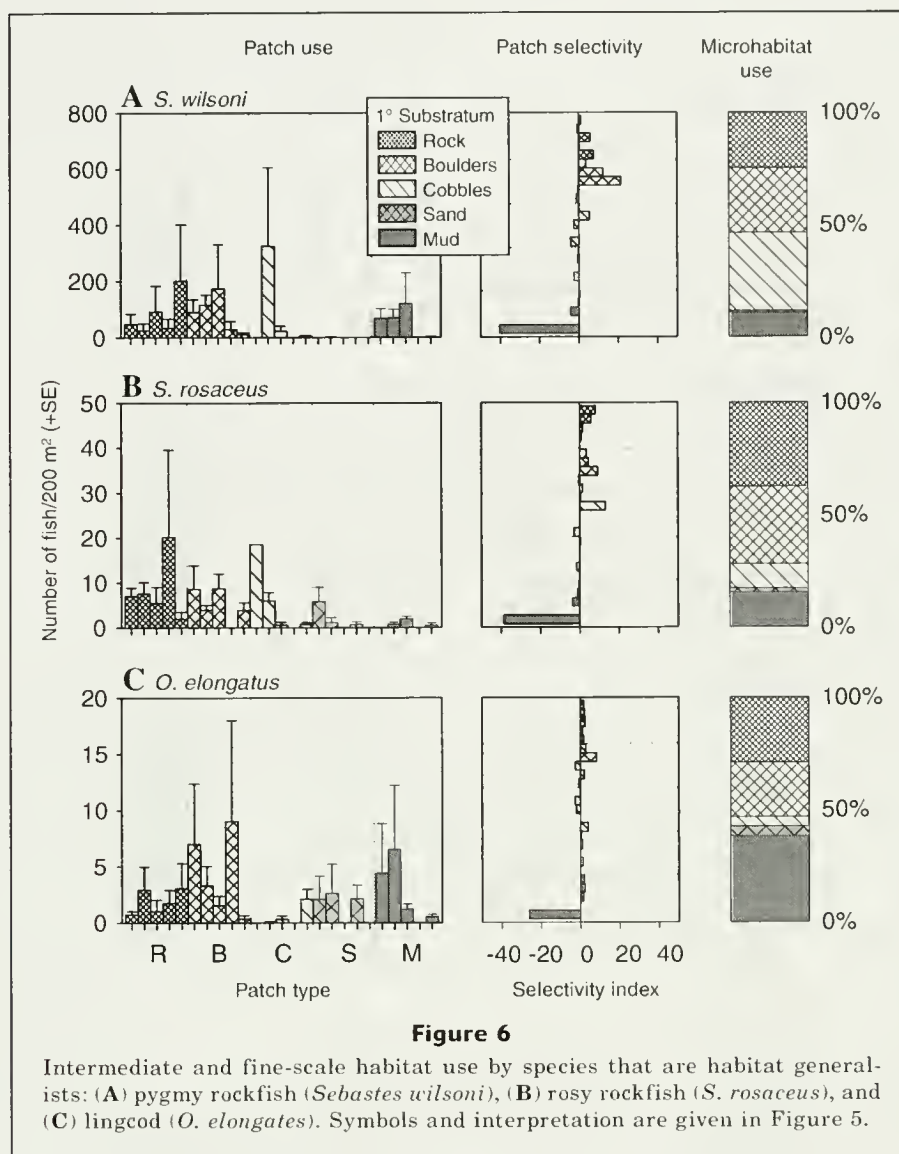
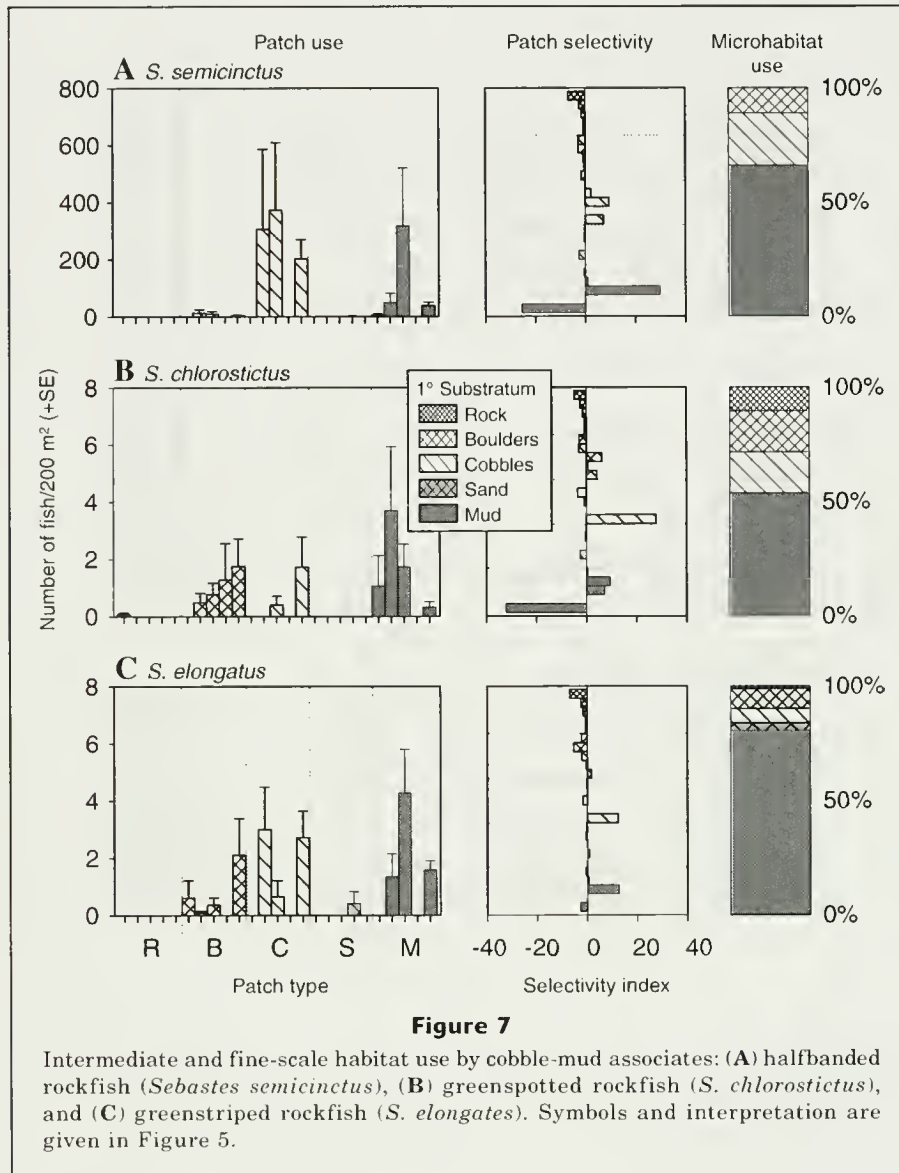


Figure 6
Intermediate and fine-scale habitat use by species that are habitat generalists: (A) pygmy rockfish (*Sebastes wilsoni*), (B) rosy rockfish (*S. rosaceus*), and (C) lingcod (*O. elongatus*). Symbols and interpretation are given in Figure 5.

off central California. Jagielo et al. (2003) compared trawlable and untrawlable habitats off Washington and found rockfishes (*Sebastes helvomaculatus* [rosethorn rockfish], *S. rubberimus*, *S. flavidus*, *Sebastes nigrocinctus* [tiger rockfish], and *Sebastes* spp.) were three times more abundant in untrawlable habitats. In more complex habitat systems, Stein et al. (1992) found high densities of juvenile *Sebastes* spp. and *S. flavidus* on the tops of high-relief rocky pinnacles on Heceta Bank, Oregon, whereas in the Gulf of Alaska, O'Connell and Carlile (1993) found the commercially important *S. rubberimus* in highest densities in complex habitats.

Mixed stratum, characterized by lower complexity and relief than areas of hard stratum, also comprised a distinctive demersal fish assemblage with high numbers of species. High diversity in these areas resulted from a combination of species unique to the mixed stratum (e.g., *S. semicinctus*), and species characteristic of both hard (e.g., *S. wilsoni*, *O. elongatus*, *S. rosaceus*) and

soft (e.g., Pleuronectiformes and Agonidae) strata. In addition to high diversity, some species (e.g., *S. chlorostictus*, *S. elongatus*, and *Z. frenata*) were also more abundant in the mixed stratum, indicating that some inherent property of heterogeneous habitats (e.g., multiple resource needs, higher levels of habitat fragmentation, and interface zones) may be important to these species. Similar findings have been reported in other submersible surveys. Stein et al. (1992), for example, found more species and higher densities of these species (e.g., *S. chlorostictus*, *S. wilsoni*) in patches with either "mud and boulder" or "mud and cobble" than in patches with mud, boulders, or cobbles in isolation. Species use of interface regions can also be inferred from previous studies even though habitat use at the microscale was not explicitly measured. For example, both Richards (1986) and Percy et al. (1989) reported higher numbers of *S. elongatus* in soft sediment areas adjacent to rocks. Similarly, Yoklavich et al. (2002) found that

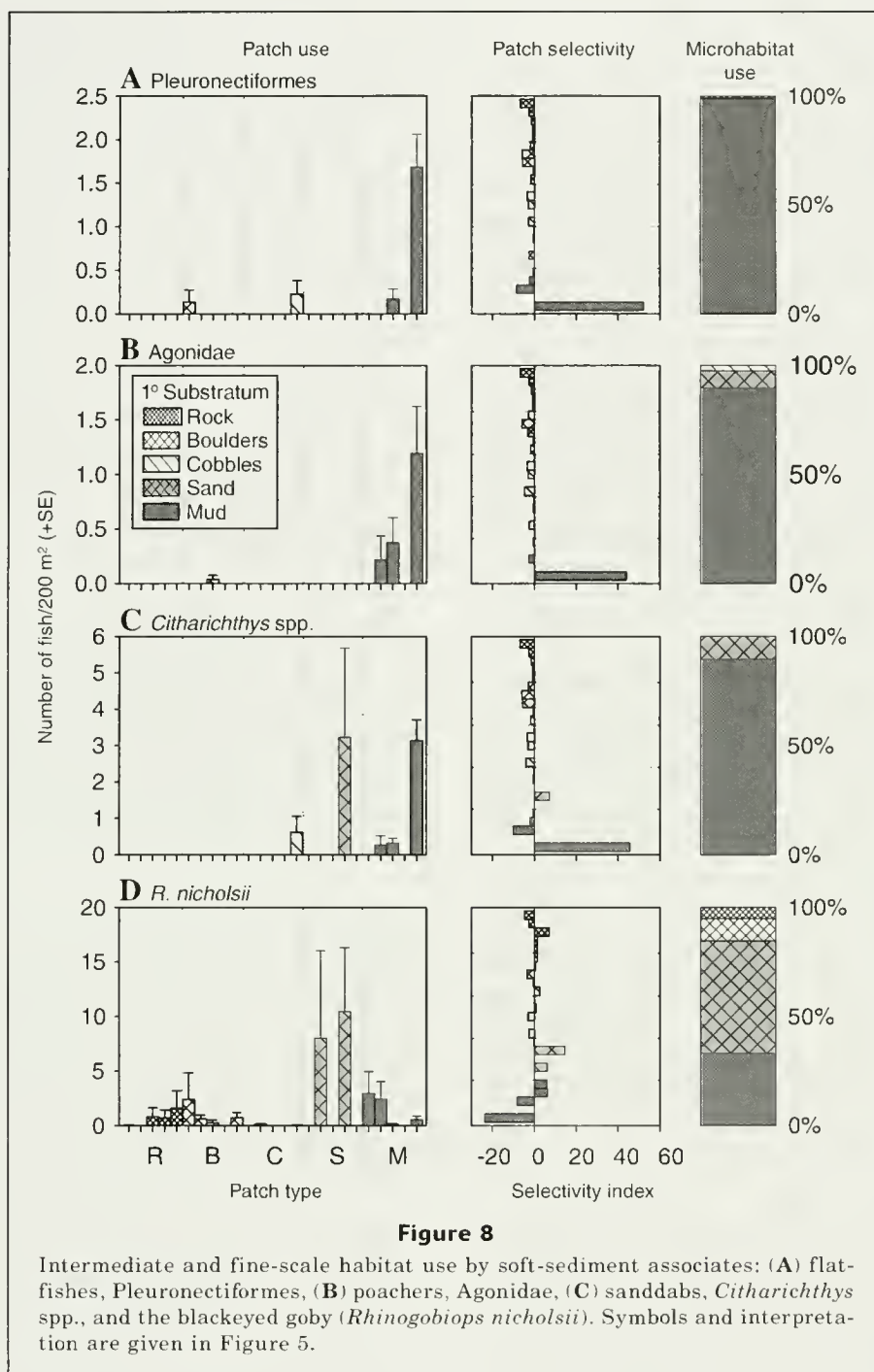


S. chlorostictus, along with other species, used habitats comprising a combination of rock and mud.

Soft substratum had the lowest habitat complexity and the lowest diversity and density of fishes of all three strata, although many of these species, particularly the Pleuronectiformes, are important commercial species. Stein et al. (1992), Yoklavich et al. (2000, 2002), and Jagielo et al. (2003) also recorded similar demersal fish assemblages in flat mud habitats (i.e., Pleuronectidae, namely *M. pacificus*, *Glyptocephalus zachirus* [rex sole], and *Lyopsetta exilis* [slender sole]), Agonidae, *Sebastes saxicola* [stripetail rockfish], Zorarcidae [eelpouts], and *Sebastolobus* spp. [thornyhead species]). Although demersal fish assemblages over trawlable habitats have been well documented by traditional fishery methods (e.g., Weinberg et al., 2002), biases in catchability between strata (because trawls may snag in complex habitats) mean that differences

in fish assemblage structure between soft, mixed, and hard strata have been difficult to identify. Although *in situ* submersible surveys facilitate these types of comparisons, some biases may still be present. For example, soft-sediment habitats reported in submersible studies (e.g., Stein et al., 1992; O'Connell and Carlile, 1993; Yoklavich et al., 2002) are often adjacent to, at the base of, or in the general vicinity of rock outcrops. As a result, it is unclear how the proximity of hard structure influences demersal fish composition and abundance, or whether these habitats are representative of soft-sediment areas where rock outcrops are not present. The analysis of submersible transects in relation to distance from rocks, or alternatively trawl surveys that include video or acoustic images of the benthos, may help to clarify these patterns.

All three spatial scales provided valuable information on how demersal fish species use benthic habitats.



For example, broad-scale strata supported characteristic fish assemblages. However, at intermediate scales (within a strata), species distribution varied by patch composition, patch size, and the neighborhood of surrounding patches. At fine scales, microhabitat use by fishes indicated which portions of habitat-patches were actually used (e.g., species A in cobbles and species B in mud, where both species were present within the same cobble-mud patch). A vital aspect of using a multiscaled approach, however, was that information from each spa-

tial scale could then be integrated to examine the relative importance of habitat types and their structural configuration, and this information also indicated that for some species the landscape context was important. For example, *R. nicholsii* was mainly found on sand or at the interface between sand and rock (microhabitat use), but these microhabitats were located within a range of rock and sediment patch types (intermediate-scale), which in turn were located within the complex hard stratum (broad-scale). This structure indicated

that for *R. nicholsii* sediment gaps within or adjacent to a rocky landscape were required.

On the other hand, *S. chlorostictus* and *S. elongatus* were both more abundant in the mixed stratum than in the hard stratum (broad scale) and were present together within mixed boulder, cobble, and mud substrata (intermediate scale). At fine scales, however, microhabitat use by these species differed; *S. elongatus* was common in the mud portion of these patches and *S. chlorostictus* was common over boulders and cobbles. These findings indicated that both species were interface associates, but within these interface regions different substratum types were used. The inclusion of microhabitat information within this multiscale approach provided a more comprehensive understanding of how demersal fish use benthic substrata. However, recording microhabitat use for each fish ($n=21,184$ fishes) was time consuming and therefore would likely negate its use in some studies. A recommended alternative method for recording microhabitat use might be to measure microhabitat use for a subset of fish per species, where subsamples are selected unbiasedly from the overall sample pool.

The ability to describe and predict fish-habitat relationships, as identified in this study, can be used to address area-based management concerns in several ways. For example, species captured by benthic trawl and long-line gear could be used to infer the presence of seafloor substratum types. Although this form of information is not novel, our study provides detailed quantitative species-habitat associations that validate this approach. For example, a benthic trawl that captures Pleuronectidae, Agonidae, *S. semicinctus*, *S. chlorostictus*, and *S. elongatus*, would indicate that the area trawled encompassed multiple strata (e.g., one or more areas of low-relief outcrop and homogenous mud). However, the proportions and spatial configuration of these strata would not be known unless a video camera, for example, was mounted on a benthic trawl (e.g., Abookire and Rose, 2005), or a seafloor substrata map was available for the area (e.g., Bellman et al., 2005).

Conversely, habitat could be used to predict community structure and species distributions. In this study, substratum type was a good indicator of distribution and abundance of many commercial and noncommercial fish species. However, the spatial arrangement and degree of habitat patchiness, in addition to substratum type, also were important predictive variables. Consequently, although areal estimates of substrata are likely to be effective for modeling the abundance and distribution of certain species (e.g., *S. rosaceus* and *S. flavidus*), accurately estimating other species will require additional knowledge of the spatial arrangement of these substrata. For example, species associated with sediment-rock interfaces, such as *S. chlorostictus*, *S. elongatus*, and *Z. frenata*, are likely to be modeled more effectively by estimating the perimeter of either an outcrop or specific habitat type. Likewise, the ability to model gap-associate species, such as *R. nicholsii*, will require information on the availability of

sediment-outcrop interfaces and sediment gaps within an outcrop matrix. For other species, such as young-of-year rockfish, a measure of habitat patchiness, in combination with areal estimates of substrata, may be required. The ability to map this level of habitat detail will depend to a large degree on a trade-off between data acquisition and resolution of the mapping tools used, and the amount of seafloor needed to be mapped (Anderson et al., 2005).

In conclusion, the overall success of area-based management strategies will reflect the ability of researchers to accurately measure the functional relationships between organisms and their habitat. Multiscale *in situ* surveys, such as this one, undertaken in multiple locations, in combination with larger-scale fishery surveys can improve our understanding of the role of benthic habitats in structuring demersal fishes across the broader U. S. West Coast. These insights, in turn, improve our ability to characterize and map essential fish habitat, estimate habitat availability, and predict multispecies distributions and habitat associations within specified areas such as marine protected areas. Importantly, this study also provides a quantitative baseline of demersal fish assemblage structure for both commercial and noncommercial species, which is critical for future comparisons of spatiotemporal abundance, diversity, and habitat use. This baseline is also vital for assessing the effects and value of increased protection of West Coast shelf ecosystems.

Acknowledgments

We thank G. Cailliet, R. Lea, M. Love, G. Moreno, R. Parrish, P. Reilly, L. Snook, R. Starr, D. Sullivan, the *Delta* Oceanographics (R. Slater, D. Slater, and C. Ijames) for logistical support and biological data collection. We thank M. Carr, C. Grimes, S. Ralston, C. Syms, B. Tissot, and W. Wakefield for their conversations and advice during the analysis and writing of this research, and Tim Simmonds and Guy Cochrane for graphical support. The manuscript was improved through the comments of M. Cappel, C. Grimes, T. Laidig, C. Syms, and three anonymous reviewers. This project was partially supported by NOAA's National Undersea Research Program, West Coast and Polar Undersea Research Center, University of Alaska, Fairbanks (Grants UAF-92-0063 and UAF-93-0036) and by a University of California, Santa Cruz postdoctoral fellowship to Tara Anderson, with joint funding from National Marine Fisheries Service, U. S. Geological Survey, and the National Marine Protected Areas Center Science Institute.

Literature cited

- Abookire, A. A., and C. S. Rose.
2005. Modifications to a plumb staff beam trawl for sampling uneven, complex habitats. *Fish. Res.* 71: 247-254.

- Adams, P. B., J. L. Butler, C. H. Baxter, T. E. Laidig, K. A. Dahlin, and W. W. Wakefield.
1995. Population estimates of Pacific coast groundfishes from video transects and swept-area trawls. *Fish. Bull.* 93:446–455.
- Addicott, J. F., J. M. Aho, M. F. Antoun, D. K. Padilla, J. S. Richardson, and D. A. Soluk.
1987. Ecological neighbourhoods: scaling environmental patterns. *Oikos* 49:340–346.
- Anderson, T. J., M. M. Yoklavich, and S. L. Eittrheim.
2005. Linking fine-scale groundfish distributions with large-scale seafloor maps: Issues and challenges of combining biological and geological data. *In* Benthic habitats and the effects of fishing (P. W. Barnes, and J. P. Thomas, eds.), p. 667–678. *Am. Fish. Soc. Symp.* 41, Bethesda, MD.
- Ault, T. R., and C. R. Johnson.
1998. Spatially and temporally predictable fish communities on coral reefs. *Ecol. Monogr.* 68:25–50.
- Bellman, M. A., S. A. Heppell, and C. Goldfinger.
2005. Evaluation of a US west coast groundfish habitat conservation regulation via analysis of spatial and temporal patterns of trawl fishing effort. *Can. J. Fish. Aquat. Sci.* 62:2886–2900.
- Eittrheim, S. L., R. J. Anima, and A. J. Stevenson.
2002. Seafloor geology of the Monterey Bay area continental shelf. *Mar. Geol.* 181:3–34.
- Forman, R. T. T.
1995. Land mosaics: the ecology of landscapes and regions, 632 p. Cambridge Univ. Press, Cambridge, U.K.
- Gunderson, D. R., and T. M. Sample.
1980. Distribution and abundance of rockfish off Washington, Oregon, and California during 1977. *Mar. Fish. Rev.* 42:2–16.
- Jagiello, T., A. Hoffmann, J. Tagart, and M. Zimmermann.
2003. Demersal groundfish densities in trawlable and untrawlable habitats off Washington: implications for the estimation of habitat bias in trawl surveys. *Fish. Bull.* 101:545–565.
- Jones, G. P., and C. Syms.
1998. Disturbance, habitat structure and the ecology of fishes on coral reefs. *Aust. J. Ecol.* 23:287–297.
- Langton, R. W., P. J. Auster, and D. C. Schneider.
1995. A spatial and temporal perspective on research and management of groundfish in the Northwest Atlantic. *Rev. Fish Sci.* 3:201–29.
- Love, M. S.
2006. Subsistence, commercial, and recreational fisheries. *In* The ecology of marine fishes: California and adjacent waters (L. G. Allen, D. J. Pondella, and M. H. Horn, eds.), p. 567–594. Univ. California Press, Berkeley, CA.
- Love, M. S., and M. Yoklavich.
2006. Deep rock habitats. *In* The ecology of marine fishes: California and adjacent waters (L. G. Allen, D. J. Pondella, and M. H. Horn, eds.), p. 411–427. Univ. California Press, Berkeley, CA.
- Love, M. S., M. Yoklavich, and L. Thorsteinson.
2002. The rockfishes of the northeast Pacific, 405 p. Univ. California Press, Berkeley and Los Angeles, CA.
- McArdle, B. H., K. J. Gaston, and J. H. Lawton
1990. Variation in the size of animal populations: patterns, problems and artifacts. *J. Anim. Ecol.* 59:439–454.
- Murie, D. J., D. C. Parkyn, B. G. Clapp, and G. G. Krause.
1994. Observations on the distribution and activities of rockfish, *Sebastes* spp., in Saanich Inlet, British Columbia, from the *Pisces IV* submersible. *Fish. Bull.* 92:313–323.
- O'Connell, V. M., and D. W. Carlile.
1993. Habitat-specific density of adult yelloweye rockfish *Sebastes ruberrimus* in the eastern Gulf of Alaska. *Fish. Bull.* 91:304–309.
- Pearcy, W. G., D. L. Stein, M. A. Hixon, E. K. Pikitch, W. H. Barss, and R. M. Starr.
1989. Submersible observations of deep-reef fishes of Heceta Bank, Oregon. *Fish. Bull.* 87:955–965.
- Richards, L. J.
1986. Depth and habitat distributions of three species of rockfish (*Sebastes*) in British Columbia: observations from the submersible PISCES IV. *Environ. Biol. Fishes* 17:13–21.
- Stein, D. L., B. N. Tissot, M. A. Hixon, and W. H. Barss.
1992. Fish-habitat associations on a deep reef at the edge of the Oregon continental shelf. *Fish. Bull.* 90:540–551.
- Stephens, J. S. Jr., R. J. Larson, and D. J. I. Podella.
2006. Rocky reefs and kelp beds. *In* The ecology of marine fishes: California and adjacent waters (L. G. Allen, D. J. Pondella, and M. H. Horn, eds.), p. 227–252. Univ. California Press, Berkeley, CA.
- Syms, C., and G. P. Jones.
1999. Scale of disturbance and the structure of a temperate fish guild. *Ecology* 80:921–940
- Weinberg, K. L.
1994. Rockfish assemblages of the middle shelf and upper slope off Oregon and Washington. *Fish. Bull.* 92:620–632.
- Weinberg, K. L., M. E. Wilkins, F. R. Shaw, and M. Zimmermann.
2002. The 2001 Pacific west coast bottom trawl survey of groundfish resources: estimates of distribution, abundance, and length and age composition. NOAA Tech. Memo. NMFS-AFSC-128, 140 p.
- Wiens, J. A.
1989. Spatial scaling in ecology. *Funct. Ecol.* 3:385–397.
- Williams, E. H., and S. Ralston.
2002. Distribution and co-occurrence of rockfishes (family: Sebastidae) over trawlable shelf and slope habitats of California and southern Oregon. *Fish. Bull.* 100:836–855.
- Yoklavich, M. M., G. M. Cailliet, R. N. Lea, H. G. Greene, R. M. Starr, J. de Marignac, and J. Field.
2002. Deepwater habitat and fish resources associated with the Big Creek Marine Ecological Reserve. *CalCOFI Rep.* 43:120–140.
- Yoklavich, M. M., H. G. Greene, G. M. Cailliet, D. E. Sullivan, R. N. Lea, and M. S. Love.
2000. Habitat association of deep-water rockfishes in a submarine canyon: an example of a natural refuge. *Fish. Bull.* 98:625–641.

Abstract—Endoparasitic helminths were inventoried in 483 American plaice (*Hippoglossoides platessoides*) collected from the southern Gulf of St. Lawrence, NAFO (North Atlantic Fisheries Organization) division 4T, and Cape Breton Shelf (NAFO subdivision 4Vn) in September 2004 and May 2003, respectively. Forward step-wise discriminant function analysis (DFA) of the 4T samples indicated that abundances of the acanthocephalans *Echinorhynchus gadi* and *Corynosoma strumosum* were significant in the classification of plaice to western or eastern 4T. Cross validation yielded a correct classification rate of 79% overall, thereby supporting the findings of earlier mark-recapture studies which have indicated that 4T plaice comprise two discrete stocks: a western and an eastern stock. Further analyses including 4Vn samples, however, indicated that endoparasitic helminths may have little value as tags in the classification of plaice overwintering in Laurentian Channel waters of the Cabot Strait and Cape Breton Shelf, where mixing of 4T and 4Vn fish may occur.

Use of endoparasitic helminths as tags in delineating stocks of American plaice (*Hippoglossoides platessoides*) from the southern Gulf of St. Lawrence and Cape Breton Shelf

Gary McClelland (contact author)

Jason Melendy

Fisheries and Oceans Canada
Gulf Fisheries Centre
343 University Avenue
Moncton, New Brunswick
E1C 9B6 Canada

Email address for G. McClelland: mccllellandg@dfo-mpo.gc.ca

American plaice (*Hippoglossoides platessoides*) are found in Northwest Atlantic waters along the continental shelf and upper continental slope from west Greenland to Rhode Island, favoring intermediate depths (90–250 m), cold waters (<0–1.5°C), and fine sand or mud bottom (Scott and Scott, 1988). American plaice has ranked second in importance to Atlantic cod (*Gadus morhua*) among groundfish landed in the southern Gulf of St. Lawrence (North Atlantic Fisheries Organization [NAFO] division 4T) over the past four decades, but commercial landings, which had ranged from 4907 to 11,780 t between 1965 and 1992 (Morin et al.¹), fell to 401 t by 2004 (Fisheries and Oceans Canada²). Commercial and research survey data show that declines in abundance of southern Gulf plaice since 1991 have occurred primarily in western 4T between the Gaspé Peninsula and the Magdalen Islands (see Fig. 1), and abundances east of the Magdalens have remained stable. The eastern and western 4T stocks monitored in recent assessments are consistent with the meristically indistinguishable “Miscou-Magdalen” and “Cape Breton” groups which Powles (1965) delineated through mark-recapture experiments. Powles (1965) suggested that the meristic uniformity of these two groups may be a consequence of larval drift because mature fish from the respective groups seldom

mix on their summer feeding grounds. More recently, Stott et al. (1992) found no evidence of population subdivision of Southern Gulf plaice in respect to allozyme variation and restriction fragment length polymorphisms in mitochondrial DNA.

As evident from commercial catch records and tag returns, 4T plaice, with the exception of some immature fish that remain in the shoals year round, migrate from summer feeding grounds on the Magdalen Shallows to deeper waters of the Laurentian Channel in winter (Powles, 1965). The winter distribution of plaice in the Laurentian Channel is continuous from the Gaspé to the Cabot Strait (Clay, 1991) and eastward along the Cape Breton Shelf (NAFO subdivision

¹ Morin, R., I. Forest, and G. Poirier. 2001. Status of NAFO Division 4T American plaice, February 2001. Canadian Science Advisory Secretariat Research Document. 2001/023, 70 p. Fisheries and Oceans Canada, Science Branch, Marine Fish Division, Gulf Region, P.O. Box 5030, Moncton, New Brunswick, Canada.

² Fisheries and Oceans Canada. 2005. American plaice in the southern Gulf of St. Lawrence (Division 4T). Fisheries and Oceans Canadian Science Advisory Secretariat Science. Advisory Report. 2005/008, 5 p. Maritime Provinces, Regional Advisory Process, Fisheries and Oceans Canada, P.O. Box 1006, Dartmouth, Nova Scotia, Canada.

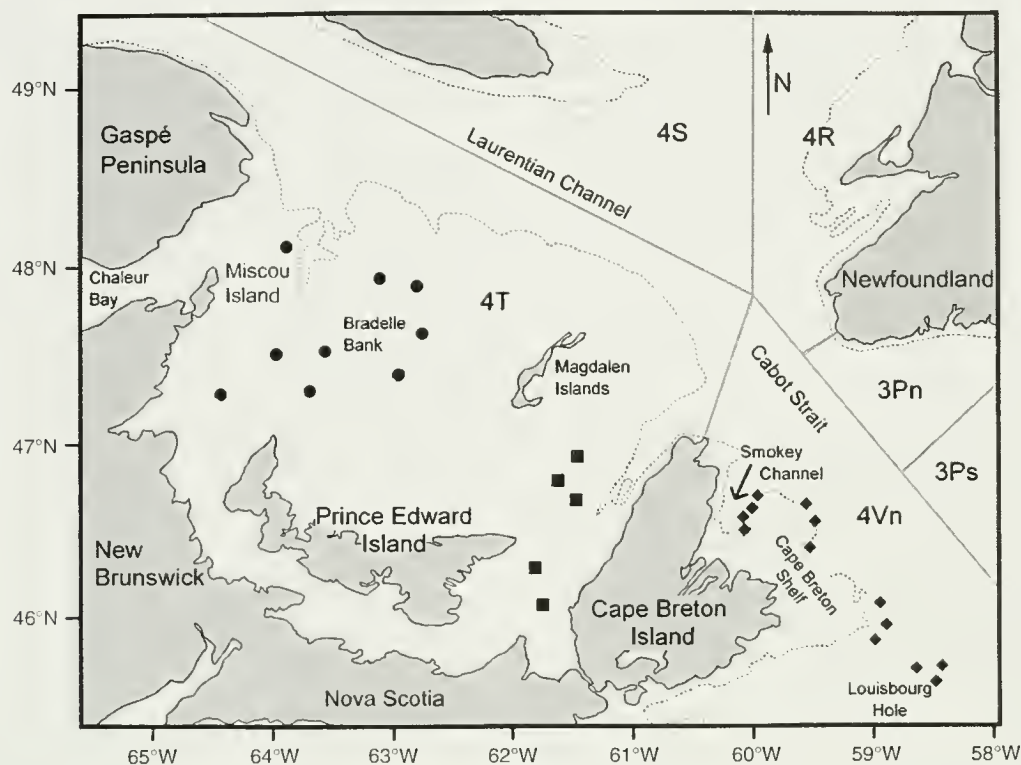


Figure 1

Map of eastern Canada indicating sites where American plaice (*Hippoglossoides platessoides*) were sampled in the southwestern (●) and southeastern (■) Gulf of St. Lawrence, and on or near the Cape Breton Shelf (◆). The depth contour (.....) is at 100 m. The pale gray lines demarcate North Atlantic Fisheries Organization divisions (4T, 4S, 4R) and subdivisions (3Pn, 3Ps, and 4Vn).

4Vn) (Swain et al., 1998). Clay (1991), noting the abundance of plaice in the Gulf portion of the Channel in January, surmised that southern Gulf plaice, unlike 4T cod, with which they are often closely associated, do not migrate through the Cabot Strait to over-winter in 4Vn. Length-at-age data from commercial landings indicate that plaice taken near the Cabot Strait late in the year are primarily from the slower growing eastern 4T (Cape Breton) stock (Tallman, 1991). A few older plaice tagged on Bradelle Bank, northwest of the Magdalen Islands, however, have been recovered in the Cabot Strait area in fall and winter (Powles, 1965). Clearly, tagging data and information on seasonal distributions from research surveys and commercial fisheries have provided little insight into the movements of 4T plaice stocks in the Laurentian Channel in winter and have not dispelled the possibility that 4T stocks may be exploited during the winter fishery within 4Vn.

Parasites as biological tags have often proven advantageous over more costly mark-recapture methods in studies of fish stock structure and migration (Williams et al., 1992) and are useful as markers in surveys for allocating quotas and combating illegal landings (Power et al., 2005). Parasite markers have shown potential in stock delineation of numerous demersal fish species (Marcogliese et al., 2003; MacKenzie and Abuanza,

2005; Melendy et al., 2005), including flatfish species such as Greenland halibut (*Reinhardtius hippoglossoides*) (Arthur and Albert, 1993; Boje et al., 1997), Pacific halibut (*Hippoglossus stenolepis*) (Blaylock et al., 2003), and winter flounder (*Pleuronectes americanus*) (McClelland et al., 2005). Although there have been no prior attempts to use parasite assemblages in describing the stock structure of American plaice, parasitological surveys of plaice in the Northwest Atlantic have identified a number of potential parasite tags. Scott (1975), for example, concluded that the enteric digeneans *Steringotrema ovacutum*, *Zoogonoides viviparous*, and *Felodistomum furcigerum* might prove useful as tags for plaice stocks from the southern Gulf of St. Lawrence, Scotian Shelf, and northeastern Gulf of Maine. Zubchenko (1985) remarked that species compositions and infection parameters of 20 protozoan and metazoan parasites of plaice from the Grand Bank, Flemish Cap, and northeastern Newfoundland and Labrador are peculiar to their geographic origin. Finally, studies of the temporal and geographic distributions of larval sealworm (*Pseudoterranova decipiens*) (Nematoda) in Atlantic Canadian groundfish have revealed significant disparities in prevalence and abundance of sealworm in neighboring plaice stocks (McClelland et al., 2000; McClelland and Martell, 2001b).

The primary objective of the present study was to investigate the possibility of using parasite markers to delineate the western and eastern 4T plaice stocks, evident in earlier mark-recapture experiments (Powles, 1965). In light of potential mixing of southern Gulf and Cape Breton Shelf plaice over-wintering in the Laurentian Channel, parasite tags were also employed in an effort to examine the discreteness of 4T and 4Vn stocks.

Materials and methods

Sampling of the host

American plaice, 31 to 40 cm in total length, were collected from two locations in the southern Gulf of St. Lawrence (NAFO division 4T) and from three locations on or near the Cape Breton Shelf (NAFO subdivision 4Vn) (Fig. 1). Samples from the southern Gulf were collected from the Canadian Coast Guard Ship (CCGS) *Alfred Needler* and the CCGS *Teleost* during a Fisheries and Oceans Canada (DFO) demersal fish survey in September of 2004, and plaice from the Cape Breton Shelf were sampled from the *Alfred Needler* in May 2003 during a dedicated survey of parasites and diseases in 4Vn groundfish. Fish were caught with a Western IIA otter trawl which was towed for 30 minutes at each station. A total of 483 plaice were collected, including 137 plaice taken at depths of 43 to 88 m in the western 4T division and 95 plaice sampled at depths of 49 to 70 m in eastern 4T division. In the 4Vn survey, 128 plaice were sampled from the eastern slope of the Smokey Channel, 46 along the eastern edge of the Cape Breton Shelf, and 77 in the Louisbourg Hole. "Channel," "Edge," and "Hole" samples were taken at depths ranging from 77 to 124 m, 72 to 158 m, and 77 to 135 m, respectively. Samples were frozen onboard in a walk-in freezer at -17°C and transferred on landing to a -20°C walk-in freezer at the Gulf Fisheries Centre (GFC), Moncton, New Brunswick, where they were stored for future examination.

Individual fish were thawed at room temperature and measured lengthwise to the nearest centimeter. External surfaces and gills were inspected by eye for signs of trauma and other disease conditions. Viscera were examined for endoparasitic helminths with a dissecting microscope, and fillets were removed and sliced into thin sections (McClelland and Martell, 2001a) for detection of larval digeneans and nematodes. All helminth parasites were counted with the exception of *Stephanostomum baccatum* metecercariae. Because the latter were often too numerous and too widely distributed in host tissues to be counted within a reasonable time frame, only their presence was noted.

Statistical analysis

Prevalence (P) and abundance (A) of individual parasite species were calculated according to the methods of Bush et al. (1997), with prevalence being the numbers of infected fish in a sample divided by the total number

of fish in a sample, expressed as a percentage, and abundance being the total number of parasites recovered from a sample divided by the total number of fish in a sample. Individual fish were coded 1 (infected), or 0 (uninfected) (Li, 1964; Neter et al., 1985) for analyses of prevalence, and a $\log(n+1)$ transformation was used to bring the distributions of parasite counts closer to normality (Sokal and Rohlf, 1969; Platt, 1975). Parasite infection parameters that best distinguished between sampling locations were selected by forward stepwise discriminant function analysis (DFA). The Kappa statistic (K) was used to determine the improvement over chance of DFA (Titus et al., 1984). Misclassification rates of DFAs were calculated by employing cross validation procedures described by Arthur and Albert (1993) and Boje et al. (1997). All statistical procedures were performed with Systat for windows, vers. 7.0 (SPSS Inc., Chicago, IL). Because the survey was confined to plaice in a narrow length range (31–40 cm TL) (McClelland et al., 2000), effects of host size on parasite infection parameters were not investigated. Plaice from the edge of the Cape Breton Shelf were not included in the DFA analysis because of the small sample size ($n=46$) and the fact that they were collected from two widely separated groups of trawl sets (Fig. 1); the northern ($n=21$) and southern ($n=25$) portions of the sample were more distant from each other than were the samples from Smokey Channel and Louisbourg Hole.

Results

Plaice sampled from the southern Gulf of St. Lawrence (NAFO Division 4T) and the Cape Breton Shelf and vicinity (NAFO subdivision 4Vn) ranged from 31 to 40 cm in total length (TL), but the great majority fell within the lower half of this range. Mean length of fish (\pm standard error) was 32.34 ± 0.180 cm ($n=137$) for plaice from the western 4T sample, and 32.31 ± 0.22 cm ($n=95$) for the eastern 4T sample. Mean lengths of 4Vn plaice were 33.17 ± 0.26 cm ($n=128$) and 32.88 ± 0.23 cm ($n=77$) for Smokey Channel and Louisbourg Hole fish, respectively.

Eleven species of endoparasitic helminths were identified during routine parasitological examinations of 483 plaice (Table 1), but the larval digeneans *Otodistomum* sp., plerocercoid larvae of an unknown cestode species, and the nematode *Hysterothylacium aduncum* were observed too infrequently ($<4\%$ prevalence in all samples) to be considered useful as biological tags (see MacKenzie and Abaunza, 1998). Forward stepwise DFA of infection parameters of the remaining species revealed that abundances of the acanthocephalans *Corynosoma strumosum* and *Echinorhynchus gadi* contributed significantly to the classification of plaice from the southwestern and southeastern Gulf of St. Lawrence ($K=0.57$) and that *E. gadi* abundance was the more significant variable (Table 2). Cross-validation yielded an overall rate of 79% correct classification (Table 3), and the lowest rate of misclassification (15%) was found in fish from the

western 4T division. Abundances of *C. strumosum* ($F=9.58$), the digenean *Fellodistomum* sp. ($F=11.61$), and the larval anisakine nematode *Pseudoterranova decipiens* ($F=8.89$), and prevalence of the larval digenean *Stephanostomum baccatum* ($F=8.64$) were significant factors in the classification of 4Vn plaice from Smokey Channel and Louisbourg Hole ($K=0.40$), and cross-validation resulted in an overall classification efficiency of 70% (Table 4).

Stepwise DFA of helminth infections in plaice from all four sampling locations indicated abundances of *E. gadi* ($F=35.80$), *C. strumosum* ($F=13.89$), *Fellodistomum* sp., ($F=5.81$), and *P. decipiens* ($F=4.75$) and the prevalence of *S. baccatum* ($F=5.71$) were significant markers ($K=0.30$) for the classification of plaice from the entire (4T–4Vn) survey area. The overall rate of correct classification, however, was only 48%, and 51% of the plaice from western 4T division were misclassified as 4Vn fish (Table 5). In a final analysis of samples from the east and west coasts of Cape Breton Island (eastern 4T and Smokey Channel, respectively), *E. gadi* abundance was again the most important marker selected ($F=59.10$), although abundances of the larval anisakine nematodes *Anisakis simplex* ($F=6.50$) and *Contracaecum osculatum* ($F=6.60$) also contributed significantly to classification ($K=0.49$). Cross-validation yielded a 77% rate of overall correct classification, but, although nearly all Smokey Channel plaice were classified correctly, more than half of the plaice from eastern 4T were misclassified as Smokey Channel fish (Table 6).

Table 1

Prevalence (P) (%) and abundance (A) of parasitic helminths in American plaice (*Hippoglossoides platessoides*) sampled from the southwestern (Western 4T) and southeastern (Eastern 4T) Gulf of St. Lawrence, Smokey Channel, edge of the Cape Breton Shelf, and Louisbourg Hole in 4Vn. Parasite, n/a=not available.

Species	Location (n)														
	Western 4T (n=137)			Eastern 4T (n=95)			Smokey Channel (n=128)			Edge of shelf (n=46)			Louisbourg Hole (n=77)		
	P	A		P	A		P	A		P	A		P	A	
Digenea															
Heminiriformes															
<i>Derogenes varicus</i>	4	0.04 ± 0.02		6	0.06 ± 0.03		3	0.17 ± 0.05		24	0.30 ± 0.09		16	0.17 ± 0.05	
<i>Otodistomum</i> sp. [†]	0	0		0	0		1	0.01 ± 0.01		2	0.02 ± 0.02		0	0	
Strigeiformes															
<i>Fellodistomum</i> sp.	29	0.89 ± 0.17		26	1.3 ± 0.38		45	2.6 ± 0.51		19	1.3 ± 0.93		17	0.46 ± 0.19	
Plagiorchiiformes															
<i>Stephanostomum baccatum</i> [†]	15	n/a		33	n/a		33	n/a		24	n/a		13	n/a	
Cestoda															
Cestoidea															
Unidentified cestode [†]	3	0.03 ± 0.01		1	0.02 ± 0.02		3	0.11 ± 0.09		0	0		4	0.04 ± 0.02	
Nematoda															
Ascaridida															
<i>Anisakis simplex</i> [†]	10	0.13 ± 0.03		8	0.08 ± 0.03		22	0.23 ± 0.04		15	0.19 ± 0.07		21	0.21 ± 0.05	
<i>Hysterothylacium Aduncum</i>	1	0.01 ± 0.0007		4	0.04 ± 0.02		2	0.02 ± 0.01		0	0		3	0.04 ± 0.03	
<i>Contracaecum osculatum</i> [†]	26	0.64 ± 0.18		15	0.31 ± 0.1		39	0.74 ± 0.17		9	0.11 ± 0.06		34	0.66 ± 0.17	
<i>Pseudoterranova decipiens</i> [†]	73	1.5 ± 0.12		67	1.34 ± 0.13		68	1.77 ± 0.18		60	1.4 ± 0.32		50	0.97 ± 0.15	
Acanthocephala															
Palaeacanthocephala															
<i>Echinorhynchus gadi</i>	7	0.1 ± 0.031		50	1.3 ± 0.3		4	0.09 ± 0.05		0	0		13	0.27 ± 0.1	
<i>Corynosoma strumosum</i> [†]	8	0.15 ± 0.06		30	0.5 ± 0.15		25	0.48 ± 0.1		33	1.6 ± 0.6		38	2.1 ± 0.9	

[†] Larval.

Discussion

Forward stepwise DFA of parasite tags has been successfully employed in describing the stock structure of various flatfish species. Arthur and Albert (1993) used

Table 2

Results of forward stepwise discriminant function analysis of samples of American plaice (*Hippoglossoides platessoides*) from the southern Gulf of St. Lawrence (North Atlantic Fisheries Organization Division 4T) showing the relative importance of abundances of two species of acanthocephalan in the classification of individual fish to western and eastern 4T stocks.

Variable	Standardized coefficient of first canonical variable	df	F score	Eigenvalue
<i>Echinorhynchus gadi</i>	0.862	230	71.48	0.46
<i>Corynosoma strumosum</i>	0.499	229	20.84	

Table 3

Cross-validation of American plaice (*Hippoglossoides platessoides*) from the western and eastern North Atlantic Fisheries Organization division 4T (southern Gulf of St. Lawrence) determined by discriminant function analysis of abundances of two species of acanthocephalans.

Location	Western 4T	Eastern 4T	% Correct
Western 4T	117	20	85
Eastern 4T	28	67	71
Totals	145	87	79

Table 4

Cross-validation of American plaice (*Hippoglossoides platessoides*) from the Smokey Channel and Louisbourg Hole, North Atlantic Fisheries Organization subdivision 4Vn, as revealed by discriminant function analyses of the prevalence or abundance of four helminth species (prevalence of *Stephanostomum baccatum*, and abundances of *Fellodistomum* sp., *Corynosoma strumosum*, and *Pseudoterranova decipiens*).

Location	Smokey Channel	Louisbourg Hole	% Correct
Smokey Channel	86	42	67
Louisbourg Hole	20	57	74
Totals	105	99	70

five species of larval helminth to classify widely separated stocks of Greenland halibut from the Saguenay fiord, St. Lawrence estuary, Labrador coast, and Baffin Island, and Boje et al. (1997) used six helminth species to gain insight into the stock structure of Greenland halibut from northeastern Newfoundland and Greenland. The overall correct classification rate was >99% in the former, and 77% in the latter study. Blaylock et al. (2003) used eight helminth species to describe the stock structure of Pacific halibut along the Pacific coast of North America from the Bering Sea to northern California and achieved an overall correct classification rate of 83%. In all three studies, accuracy of classification increased when the numbers of geographical categories were reduced by pooling sampling locations.

Although our survey was confined to a much smaller geographic area than those surveyed in the studies above, the accuracy of classification of plaice stocks from the southern Gulf of St. Lawrence (NAFO division 4T) is remarkably high (79%) (Table 3). DFA with only two markers, namely the abundances of the acanthocephalans *E. gadi* and *C. strumosum*, indicated that southern Gulf plaice consist of discrete western and eastern stocks on their summer feeding grounds; this result supports the results of earlier mark-recapture studies (Powles, 1965). Because the acanthocephalans are acquired passively in prey, and 4T plaice feed primarily in the Magdalen Shoals, spring through fall, while fasting in winter (Swain et al., 1998), these markers may also be employed in studies of seasonal migrations and mixing of the two stocks. Analysis of infection parameters of four helminth taxa (abundances of *C. strumosum*, the digenean *Fellodistomum* sp., the larval anisakine nematode *Pseudoterranova decipiens*, and prevalence of the larval digenean *Stephanostomum baccatum*) reveals a somewhat lower degree of discreteness (70% correct classification) between plaice from Smokey Channel and Louisbourg Hole, within NAFO subdivision 4Vn.

Abundances of *Fellodistomum* sp., *P. decipiens*, *E. gadi*, and *C. strumosum*, and prevalence of *S. baccatum* are significant factors in a DFA of plaice from all four locations, although the overall accuracy of classification falls to only 48% (Table 5). Although an improvement over random classification (25%), this latter result offers little encouragement for the use of parasites tags in future investigations of movements and possible mixing of 4T and 4Vn plaice overwintering in Laurentian Channel waters of the 4Vn subdivision. DFA of eastern 4T and Smokey Channel (4Vn) samples similarly seems to indicate that helminth tags would have little value in studies of the winter composition of plaice stocks in the Cabot Strait area. In this analysis, with the use of *E. gadi* and the larval nematodes *Anisakis simplex* and *Contracaecum osculatatum* as markers, 98% of the 4Vn plaice were classified correctly, but 52% of the plaice from southeastern 4T were misclassified as 4Vn fish. However, given the differences in infection parameters of *E. gadi* in eastern 4T (prevalence [P]=50%, abundance [A]=1.30) and Smokey Channel samples (P=4%,

Table 5

Cross-validation of American plaice (*Hippoglossoides platessoides*) from the western and eastern North Atlantic Fisheries Organization (NAFO) division 4T and from Smokey Channel and Louisbourg Hole in NAFO subdivision 4Vn, as revealed by discriminant function analyses of the prevalence or abundance of five species of parasitic helminth (prevalence of *Stephanostomum baccatum*, and abundances of *Fellodistomum* sp., *Corynosoma strumosum*, *Echinorhynchus gadi*, and *Pseudoterranova decipiens*).

Location	Western 4T	Eastern 4T	Smokey Channel	Louisbourg Hole	% Correct
Western 4T	57	10	37	33	42
Eastern 4T	14	48	15	18	51
Smokey Channel	28	5	64	31	50
Louisbourg Hole	18	8	11	40	52
Totals	117	71	127	122	48

A=0.09) (Table 1), this acanthocephalan may yet prove to be a useful marker for the detection of southeastern 4T migrants among plaice overwintering in Cabot Strait and 4Vn.

Parasites that contributed to the DFAs above meet MacKenzie's (1987) criteria for biological tags. None of the helminths are known to reproduce directly on or in plaice. Each of the markers is abundant in fish from at least one of the sampling areas, and there are significant geographical variations in the infection parameters of each species within the survey area. The third criterion, that the parasite must be long-lived in the host, is clearly met by five species of larval helminth that contribute significantly to classification. Metacercariae of *S. baccatum*, the larval anisakines *A. simplex*, *C. osculatum*, and *P. decipiens*, and cystacanths of *C. strumosum*, found variously in the body cavity and musculature, are believed to survive indefinitely in the fish host and have been used as markers in other studies of flatfish stock structure (Arthur and Albert, 1993; Boje et al., 1997; Blaylock et al., 2003).

Although the life spans of enteric helminths (*Fellodistomum* sp. and *E. gadi*, herein) in marine fish remain largely unknown, it is possible that species infecting cold-water hosts may persist for several months or even years (Margolis and Boyce, 1969)—sufficient time to meet MacKenzie's (1987) criterion for tag longevity. *Echinorhynchus gadi* infecting a relict population of Atlantic cod in Lake Mogil'noye, Russia, for example, recruit in the fall and die off in late summer and early fall of the following year (Kulachkova and Timofeyeva, 1993). Similarly, *E. lageniformis* survive for about a year in the intestines of starry flounder (*Platichthys stellatus*) in the coastal waters of Oregon (Olson and Pratt, 1971). In any event, parasites need not be long lived in order to be suitable as markers, and there are numerous precedents for use of enteric helminths as markers in studies of host stock structure (Williams et al., 1992). Khan and Tuck (1995) identified *E. gadi* as an important indicator of the discreteness of Newfoundland cod stocks, and Power et al. (2005) employed abundances of enteric digeneans in classifying bogue

Table 6

Cross-validation of American plaice (*Hippoglossoides platessoides*) to eastern North Atlantic Fisheries Organization (NAFO) division 4T and Smokey Channel (NAFO subdivision 4Vn) as revealed by discriminant function analyses of the abundances of three helminth species (abundances of *Echinorhynchus gadi*, *Anisakis simplex*, and *Contracaecum osculatum*).

Location	Eastern 4T	Smokey Channel	% Correct
Eastern 4T	46	49	48
Smokey Channel	3	125	98
Totals	49	174	77

(*Boops boops*) (Sparidae), a demersal species from Spanish fisheries.

Abundances of passively transmitted parasites are ultimately a function of host feeding behavior. Hence, geographical differences in intermediate-host abundance and frequency in plaice diets would manifest themselves as disparities in infection parameters of passively transmitted helminths in 4T and 4Vn plaice stocks. Digeneans, which mature in the digestive tract of marine fish, are usually acquired through the consumption of invertebrates (crustaceans, molluscs, polychaetes, and echinoderms, among other taxa) which harbor encysted metacercariae (Rohde, 2005). Brittle stars (Ophiuroidea), which are frequently exploited by both 4T and 4Vn plaice (Powles, 1965; Minet, 1975), are host to the metacercariae of *Fellodistomum* sp. (Koie, 1980), an important influence in our DFAs involving 4Vn plaice. Larval anisakine nematodes (*A. simplex*, *C. osculatum*, and *P. decipiens*), which proved significant in stock delineation herein, are acquired through predation on the parasite's invertebrate hosts, usually crustaceans (Rohde, 2005). Although the life cycle of *A. simplex* is largely pelagic, the larvae may be transmitted to de-

mersal fish, such as plaice, by diurnal vertical migrants (euphausiids, shrimp, etc.) which feed pelagically at night but are found near the seafloor by day (McClelland, 1990). Larval *P. decipiens* infections are acquired through consumption of various benthic invertebrates, including mysids, isopods, amphipods, decapods, and polychaetes (McClelland, 2002). The acanthocephalan *E. gadi*, which was the most significant species in the classification of 4T plaice stocks in this study, reach maturity in the intestines of dozens of species of marine fish in the North Atlantic and use gammaridean and caprellid amphipods and mysids as intermediate hosts (Marcogliese, 1994).

Among influences on digenean infection parameters in fish are the distributions and abundances of molluscan intermediate hosts, where the parasites perform one or more generations of asexual reproduction. Brittle stars, which transmit *Fellodistomum metacercariae* to plaice, become infected by feeding on cercariae which develop in bivalve mollusks (Koie, 1980). In contrast to the other helminths used as markers here, the digenean *S. baccatum*, an important component of DFAs involving 4Vn plaice, is transmitted actively, through penetration of the skin by cercariae (Wolfgang, 1955). Mollusks that host the asexual reproduction of *S. baccatum* to the cercarial stage are whelks, especially the common or waved whelk (*Buccinum undatum*), which is widely distributed and commercially exploited in eastern Canadian waters.

Infection parameters of larval helminths in 4T-4Vn plaice may also be influenced by temporal and spatial distributions of the final hosts. The digenean *S. baccatum* matures and reproduces in the intestines of large piscivorous fish such as sea raven (*Hemitripterus americanus*) and Atlantic halibut (*Hippoglossus hippoglossus*) (Wolfgang, 1955), and the anisakine nematode *A. simplex* matures and reproduces in the stomachs of cetaceans (Rohde, 2005). Adults of the anisakines *Contracaecum osculatum* and *P. decipiens*, and the acanthocephalan *C. strumosum* occur, respectively, in stomachs and intestines of seals. Surveys of various demersals in waters off Nova Scotia, Canada (Marcogliese and McClelland, 1992; McClelland et al., 2000; McClelland and Martell, 2001a&b) revealed that infection parameters of *P. decipiens* and *Corynosoma wegneri* increased with proximity to Sable Island, site of the largest grey seal (*Halichoerus grypus*) colony in the Northwest Atlantic.

Spatial disparities in prevalences and abundances of parasitic helminths in fish may also be traced to variation of physical parameters (temperature, salinity, depth, and bottom habitat) that influence distributions of the invertebrate precursor hosts (Williams and Jones, 1994). Our 4T plaice samples were collected at relatively uniform depths (43–88 m), and the substrates in both sampling areas ranged from sandy pelite to sandy gravel and had outcroppings of sandstone bedrock (see Loring and Nota³). The mean near-bottom temperature for sampling stations in eastern 4T was 1.62 (0.49–3.23)°C ($n=5$), but only 0.21 (–0.01–0.77)°C

($n=9$) for stations in western 4T. Near-bottom temperatures prevalent on the Magdalen Shoals are extremely low throughout the year (Swain et al., 1998), and small variations in temperature may have dramatic effects on the developmental and transmission rates of helminth parasites, as well as on the distributions and developmental rates of their poikilothermic intermediate hosts. Hence, the fact that acanthocephalan infections in southeastern Gulf plaice were much heavier than those found in plaice from the northwestern Magdalen Shoals may, to some extent, reflect the relative warmth of waters occupied in eastern 4T.

In summary, DFAs of abundances of the acanthocephalans *E. gadi* and *C. strumosum* support the findings of earlier mark-recapture studies (Powles, 1965), which indicate the presence of distinct northwestern (Miscou-Magdalen) and southeastern (Cape Breton) plaice stocks in the southern Gulf of St. Lawrence. Moreover, both parasite markers could be employed in future studies of migration and mixing of the two 4T stocks within 4T, and infection parameters of *E. gadi* alone may prove useful for detecting the presence of southeastern 4T migrants among stocks overwintering in Laurentian Channel waters of the Cabot Strait and 4Vn. The strength of our conclusions may be mitigated, however, by the fact that 4T and 4Vn plaice were sampled only during September and May, respectively, and samples from the two areas were taken more than a year apart. Hence, the possibility of seasonal or longer term variations in infection parameters of enteric helminths, e.g., *Fellodistomum* sp. and *E. gadi*, could not be investigated. Finally, given problems inherent in stepwise procedures (Power et al., 2005), statistical procedures employed in the present study, and in similar studies, could be improved upon. Power et al. (2005), for example, adopted an “all possible subsets” approach to selection of indicator parasites used in linear and quadratic discriminant analyses and in nonparametric classification of bogue landed at Spanish fishing ports. Efforts will be made to address these shortcomings in future surveys.

Acknowledgments

The authors are grateful to T. Hurlbut, Fisheries and Oceans Canada, Moncton, for supervising the collection of plaice samples during the 2004 groundfish cruise in the southern Gulf of St. Lawrence. We also thank R. Morin, Fisheries and Oceans Canada, Moncton, and four anonymous referees for their helpful comments and advice on earlier drafts of the manuscript.

³ Loring, D. H., and J. G. Nota. 1973. Morphology and sediments of the Gulf of St. Lawrence. Fisheries Research Board of Canada Bulletin, 182, 147 p. 116 Lisgart Street, Ottawa, Canada, K1A 0H3.

Literature cited

- Arthur, J. R., and E. Albert.
1993. Use of parasites for separating stocks of Greenland halibut (*Reinhardtius hippoglossoides*) in the Canadian northwest Atlantic. *Can. J. Fish. Aquat. Sci.* 50:2175–2181.
- Blaylock, R. B., L. Margolis, and J. C. Holmes.
2003. The use of parasites in discriminating stocks of Pacific halibut (*Hippoglossus stenolepis*) in the northeast Pacific. *Fish. Bull.* 101:1–9.
- Boje, J., F. Riget, and M. Køie.
1997. Helminth parasites as biological tags in population studies of Greenland halibut (*Reinhardtius hippoglossoides* (Walbaum)), in the northwest Atlantic. *ICES J. Mar. Sci.* 54:886–895.
- Bush, A. O., K. D. Lafferty, J. M. Lotz, and A. W. Shostak.
1997. Parasitology meets ecology on its own terms: Margolis et al. revisited. *J. Parasitol.* 83:575–583.
- Clay, D.
1991. Seasonal distribution of demersal fish (Osteichthyes) and skates (Chondrichthyes) in the southeastern Gulf of St. Lawrence. *In The Gulf of St. Lawrence: small ocean or big estuary?* (J. C. Therriault, ed.), p. 241–259. *Can. Spec. Pub. Fish. Aquat. Sci.* 113.
- Khan R. A., and C. Tuck.
1995. Parasites as indicators of stocks of Atlantic cod (*Gadus morhua*) off Newfoundland, Canada. *Can. J. Fish. Aquat. Sci.* 52:195–201.
- Koie, M.
1980. On the morphology and life-history of *Steringotrema pagelli* (Van Beneden, 1871) Ohdner, 1911 and *Fellodistomum fellis* (Olsson, 1868) Nicoll, 1909 [syn. *S. ovacutum* (Lebour, 1908) Yamaguti, 1953] (Trematoda, Fellodistomidae). *Ophelia* 19:215–236.
- Kulachkova, V. G., and T. A. Timofeyeva.
1993. The acanthocephalan *Echinorhynchus gadi* (Zoega) from relict cod of Lake Mogil'noye. *Can. Transl. Fish. Aquat. Sci.* no. 5602.
- Li, J. C. R.
1964. *Statistical inference*. Vol. 1, 658 p. Edwards Bros., Ann Arbor, MI.
- MacKenzie, K.
1987. Parasites as indicators of host populations. *Int. J. Parasit.* 17:345–352.
- MacKenzie, K., and P. Abaunza.
1998. Parasites as biological tags for stock discrimination of marine fish: a guide to procedures and methods. *Fish. Res.* 38:45–56.
2005. Parasites as biological tags. *In Stock identification methods. Applications in fisheries science.* (S. X. Cadrin, K. D. Friedland, and J. R. Waldman, eds.), p. 211–226. Elsevier Academic Press, San Diego, CA.
- Marcogliese, D. J.
1994. *Aeginina longocornis* (Amphipoda: Caprellidea), new intermediate host for *Echinorhynchus gadi* (Acanthocephala: Echinorhynchidae). *J. Parasitol.* 80:1043–1045.
- Marcogliese, D. J., E. Albert, P. Gagnon, and J. M. Sévigny.
2003. Use of parasites in stock identification of the deepwater redfish (*Sebastes mentella*) in the Northwest Atlantic. *Fish. Bull.* 101:183–188.
- Marcogliese, D. J., and G. McClelland.
1992. *Corynosoma wegneri* (Acanthocephala: Polymorphida) and *Pseudoterranova decipiens* (Nematoda: Ascaridoidea) larvae in Scotian Shelf groundfish. *Can. J. Fish. Aquat. Sci.* 49:2062–2069.
- Margolis, L., and N. P. Boyce.
1969. Life span, maturation and growth of two hemiurid trematodes, *Turbulovesicula lindbergi* and *Lecithaster gibbosus*, in Pacific salmon (Genus *Oncorhynchus*). *J. Fish. Res. Board Can.* 26:893–907.
- McClelland, G.
1990. Larval anisakine nematodes in various fish species from Sable Island Bank and vicinity. *In Population biology of sealworm (Pseudoterranova decipiens) in relation to its intermediate and seal hosts* (W. D. Bowen, ed.), p. 83–118. *Can. Bull. Fish. Aquat. Sci.* 222.
2002. The trouble with sealworms (*Pseudoterranova decipiens*, species complex, Nematoda): a review. *Parasitol.* 124(suppl.):183–203.
- McClelland, G., and D. J. Martell.
2001a. Surveys of larval seal-worm, *Pseudoterranova decipiens* infection in various fish species sampled from Nova Scotian waters between 1988 and 1996, with an assessment of examination procedures. *In Sealworms in the North Atlantic: ecology and population dynamics* (G. Desportes, and G. McClelland, eds.), p. 57–76. North Atlantic Marine Mammal Commission Scientific Publications, Tromsø, Norway.
2001b. Spatial and temporal distributions of larval seal-worm, *Pseudoterranova decipiens* (Nematoda: Anisakinae) in *Hippoglossoides platessoides* (Pleuronectidae) in the Canadian Maritime Region from 1993 to 1999. *In Sealworms in the North Atlantic: ecology and population dynamics* (G. Desportes, and G. McClelland, eds.), p. 77–94. North Atlantic Marine Mammal Commission Scientific Publications, Tromsø, Norway.
- McClelland, G., J. Melendy, J. Osborne, D. Reid, and S. Douglas.
2005. Use of parasite and genetic markers in delineating populations of winter flounder from the central and south-west Scotian Shelf and north-east Gulf of Maine. *J. Fish Biol.* 66:1082–1100.
- McClelland, G., R. K. Misra, and D. J. Martell.
2000. Spatial and temporal distributions of larval seal-worm (*Pseudoterranova decipiens*, Nematoda: Anisakinae), in *Hippoglossoides platessoides* (Pleuronectidae) in eastern Canada from 1980 to 1990. *ICES J. Mar. Sci.* 57:69–88.
- Melendy, J., G. McClelland, and T. Hurlbut.
2005. Use of parasite tags in delineating stocks of white hake (*Urophycis tenuis*) from the southern Gulf of St. Lawrence and Cape Breton Shelf. *Fish. Res.* 76: 392–400.
- Minet, J-P.
1975. Data on the biology of American plaice from the southern bank of Newfoundland and from the Cape Breton shelf. *Rev. Trav. Inst. Peches Marit. Nantes.* 38: 343–434.
- Neter, J., W. Wassermann, and M. H. Kutner.
1985. *Applied linear statistical models: regression, analysis of variance, and experimental design*, 1127 p. Richard Irwin Inc., Homewood, IL.
- Olson, R. E., and I. Pratt.
1971. The life cycle and larval development of *Echinorhynchus lageniformis* Ekbaum, 1938 (Acanthocephala: Echinorhynchidae). *J. Parasitol.* 57:143–149.
- Platt, N. E.
1975. Infestation of cod (*Gadus morhua* L.) with the larvae of codworm (*Terranova decipiens*) and herringworm, *Anisakis* sp. (Nematoda: Ascaridata) in North Atlantic and Arctic waters. *J. Appl. Ecol.* 12:437–450.

- Power, A. M., J. A. Balbuena, and J. A. Raga.
2005. Parasite infracommunities as predictors of harvest location of boogie (*Boops boops* L.): a pilot study using statistical classifiers. *Fish. Res.* 72:229-239.
- Powles, P.
1965. Life history and ecology of American plaice, (*Hippoglossoides platessoides* F.) in the Magdalen Shallows. *J. Fish. Res. Board Can.* 22:565-596.
- Rohde, K.
2005. *Marine Parasitology*, 565 p. Commonwealth Scientific and Industrial Research Organisation Publishing, Collingwood, Victoria, Australia.
- Scott, J. S.
1975. Geographic variation in incidence of trematode parasites of American plaice (*Hippoglossoides platessoides*) in the Northwest Atlantic. *J. Fish. Res. Board Can.* 32:547-550.
- Scott, W. B., and M. G. Scott.
1988. Atlantic fishes of Canada. *Can. Bull. Fish. Aquat. Sci.* 219:1-731.
- Sokal, R. R., and F. J. Rohlf.
1969. *Biometry*, 797 p. W.H. Freeman, San Francisco, CA.
- Stott, W., M. M. Ferguson, and R. F. Tallman.
1992. Genetic population structure of American plaice (*Hippoglossoides platessoides*) from the Gulf of St. Lawrence, Canada. *Can. J. Fish. Aquat. Sci.* 49:2538-2545.
- Swain, D. P., G. A. Chouinard, R. Morin, and K. F. Drinkwater.
1998. Seasonal variation in the habitat associations of Atlantic cod (*Gadus morhua*) and American plaice (*Hippoglossoides platessoides*) from the southern Gulf of St. Lawrence. *Can. J. Fish. Aquat. Sci.* 55:2548-2561.
- Tallman, R. F.
1991. Causes of within season decline in the size at age of American plaice, *Hippoglossoides platessoides*. In *The Gulf of St. Lawrence: small ocean or big Estuary?* (J. C. Therriault, ed.), p. 269-275. *Can. Spec. Pub. Fish. Aquat. Sci.* 113.
- Titus, K., J. A. Mosher, and B. K. Williams.
1984. Chance corrected classification for use in discriminant analysis: ecological applications. *Am. Midl. Nat.* 111:1-7.
- Williams, H., and A. Jones.
1994. *Parasitic worms of fish*, 593 p. Taylor and Francis Ltd., London, England.
- Williams, H. H., K. MacKenzie, and A. M. McCarthy.
1992. Parasites as biological indicators of the population biology, migrations, diet, and phylogenetics of fish. *Rev. Biol. Fish.* 2:144-176.
- Wolfgang, R. W.
1955. Studies of the trematodes *Stephonostomum bac-catum* (Nicoll, 1907) III. Its life cycle. *Can. J. Zool.* 33:113-128.
- Zubchenko, A. V.
1985. Parasitic fauna of American plaice (*Hippoglossoides platessoides*) from the Northwest Atlantic. *J. Northw. Atl. Fish. Sci.* 6: 165-171.

Abstract—Understanding the interactions between kelp beds and nearshore fish is essential because anthropogenic changes and natural variability in these beds may affect available habitat for fishes. In this study fish communities were investigated in south-central Alaska kelp beds characterized by a range of substrate complexity and varying densities of both perennial understory kelps and annual canopy kelps. Many of the observed fish species, as well as understory and canopy kelps, were positively associated with structurally complex substratum. Targeted canopy and understory kelp beds supported seasonal populations of adult and juvenile Pacific cod (*Gadus macrocephalus*), rockfishes (*Sebastes* spp.), and year-round populations of greenlings (*Hexagrammos* spp.). Monthly changes in kelp and fish communities reflected seasonal changes; the densities of some species were greatest during periods with higher temperatures. This work illustrates the importance of structurally complex kelp beds with persistent understory kelp populations as important fish habitat for several commercially and recreationally important fishes.

Implications of substrate complexity and kelp variability for south-central Alaskan nearshore fish communities

Judy Hamilton

Kachemak Bay National Estuarine Research Reserve
95 Sterling Highway, Suite 2
Homer, Alaska 99603

Email address: judy_hamilton@fishgame.state.ak.us

Brenda Konar

School of Fisheries and Ocean Sciences
University of Alaska Fairbanks
245 O'Neill Building
Fairbanks, Alaska 99775

Marine macroalgal communities in the shallow, rocky, nearshore zones are among the most productive aquatic biomes on earth and provide important habitat for invertebrates, fishes, and marine mammals (Steneck et al., 2002). Although the importance of kelp bed variability (including kelp density, distribution, and species composition) to fishes has been demonstrated in Alaskan waters (Dean et al., 2000; Hegwer, 2003; Hamilton, 2004; Calvert, 2005), the role of seasonality in these habitats is poorly understood, particularly in regions with seasonal extremes, such as the subarctic (but see Calvert, 2005). Furthermore, although the persistence and stability of kelp beds are at least partly determined by suitable space and substratum type (Dayton, 1985), the importance of overall habitat complexity (i.e., kelp cover and substrate topography) to kelp-associated fish species has not been investigated in Alaska.

Previous studies in Alaskan kelp beds have shown positive correlations between the presence of fishes and the density (or biomass) of understory algae (Dean et al., 2000; Hegwer, 2003; Hamilton, 2004). Researchers elsewhere have also agreed with these findings (Dayton, 1985) but have demonstrated relationships between fish density or biomass and the relative abundance of the canopy kelp *Macrocystis pyrifera* (Bodkin,

1986; Carr, 1994). *Macrocystis* forms dense stands that are generally stable and provide persistent habitat; beds composed of this perennial species exhibit relatively little seasonal and annual variation in structure (Dayton, 1985; Steneck et al., 2002). In contrast, northern Pacific canopy kelps are annuals (*Alaria fistulosa* and *Nereocystis luetkeana* [hereafter *Nereocystis*]) that afford much less midwater structure. As a result, vertical relief in northern Pacific kelp beds is often seasonally restricted to, and is more consistently provided by, physical structure of the seafloor and the perennial understory kelp species. The importance of physical structure (described by the measures of rugosity, substrate size, and verticality) to temperate and tropical reef fish assemblages has been documented (Aburto-Oropeza and Balart, 2001; Garcia-Charton and Perez-Ruzafa, 2001), but little is known about the importance of the physical structure of kelp and substrate to fishes in the northern Pacific rocky nearshore zones.

The objectives of this study were to assess relationships of fish to habitat structure and to seasonal variability in kelp communities. We determined the relationship of fishes to habitat structure (classified according to rugosity, size of substrate, and verticality) and kelp densities. Because north Pacific macroalgal communities vary

Manuscript submitted 10 September 2004 to the Scientific Editor.

Manuscript approved for publication 29 August 2006 by the Scientific Editor.

Fish. Bull. 105:189–196 2007.

seasonally with the growth and senescence of annual kelps, changes in the kelp communities were correlated with associated fish abundances.

Materials and methods

Study sites

This study was conducted in Kachemak Bay, the southernmost inlet on the western shore of the Kenai Peninsula, in south-central Alaska. Ten sites were chosen based on their structural characteristics and the presence of kelp communities (Fig. 1). All sites contained understory kelp, providing varying degrees of macroalgal cover, and five sites contained the canopy-forming kelp *Nereocystis*. A distance of at least 200 m (predominantly sandy bottom) separated all sites from each other. Sites were situated at a water depth of approximately 7 m.

Study design

At each site, transects ($n=3$) were surveyed monthly to quantify kelp densities and fish presence between May 2002 and September 2003. A haphazard starting point was selected for each transect from which a random direction was taken. Although visibility varied among sampling periods, transects were surveyed when visibility was at least a transect width (2 m on each side) or more and therefore such visibility was not included in the analyses. Because of turbidity and poor visibility at this site, MacDonald Spit was not sampled in July and November 2002 and Anisom Point was not sampled in October 2002. Each survey had two components (a kelp and a fish survey), which were conducted concurrently by two separate divers.

Physical habitat variables

Physical habitat variables (rugosity, substrate size, and verticality) were measured once for each site in September 2003. Rugosity and substrate size were measured for every quadrat at all sites during September 2003. Rugosity provides a measure of habitat complexity on a small spatial scale and is defined as the ratio of the true distance contour along the bottom to a one-meter horizontal distance (Leum and Choat, 1980). Rugosity was measured by using a 1-m bar with a series of 5-mm links attached at one end. The bar was held horizontally with the link end resting on the substrate. The links were then draped along the substrate beneath the bar. These links were counted

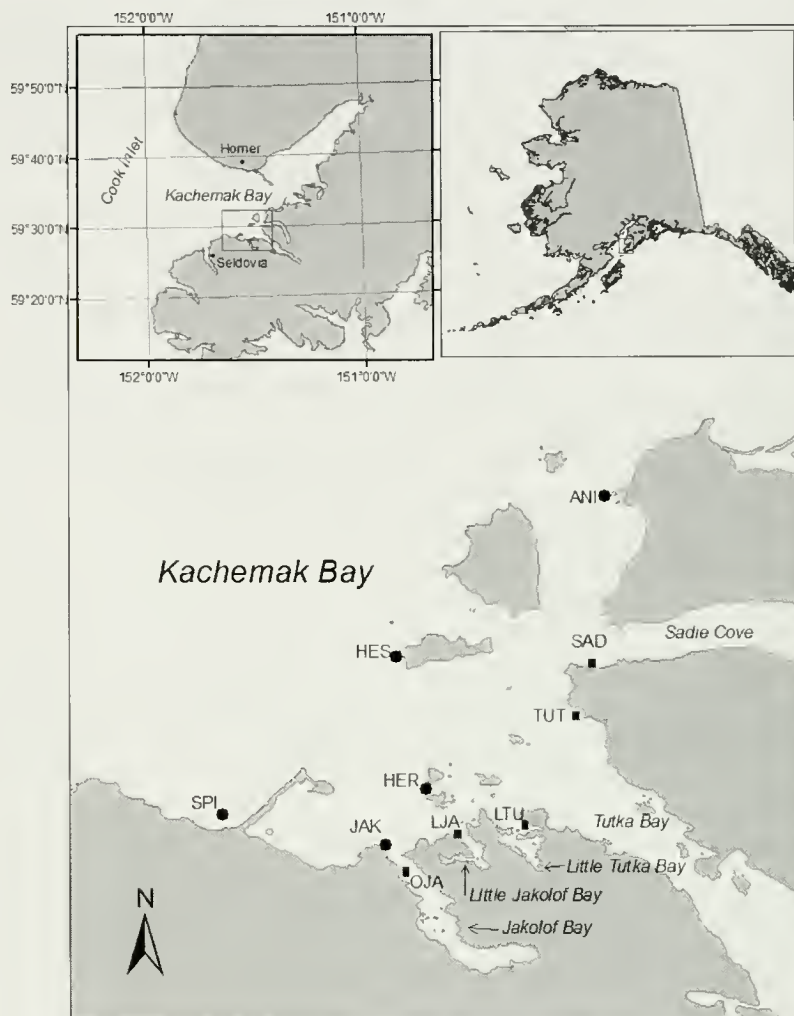


Figure 1

Location of Kachemak Bay and study sites. Sites characterized by high structural complexity of the substratum are denoted with a circle and low structural complexity sites are denoted with a square. Study sites are abbreviated as follows: ANI=Anisom Point; HER=Herring Islands; HES=Hesketh Island; JAK=Jakolof Bay; LJA=Little Jakolof Bay; LTU=Little Tutka Bay; OJA=Outside Jakolof Bay; SAD=Sadie Cove; SPI=MacDonald Spit; and TUT=Tutka Bay.

and a rugosity measure was calculated for each quadrat and averaged per transect. Substrate size was determined by measuring the diameter of samples of the bottom relief (e.g., sand, cobble, bedrock) that composed greater than 50% of the quadrat (Garcia-Charton and Perez-Ruzafa, 2001). When no substrate type dominated, the percentages and sizes of each substrate type were noted. These measurements were categorized from one (sand or silt) to five (bedrock) and an average value was calculated for each site. Verticality, a subjective measure ranging from one (for low structural relief) to five (high), was assigned to each site (Bodkin, 1986). Monthly water temperature was also measured at each site.

Surveys of kelp and fish

For surveys of kelp, randomly placed 0.25-m² quadrats ($n=10$) were examined per 120-m² transect. All understory kelps in each quadrat were counted and identified to species. Because all understory kelp species were structurally similar (in size and overall shape), they were grouped as “annual” (*Costaria costata*, *Cymathere triplicata*, and *Laminaria saccharina*,) or “perennial” (*Agarum clathratum*, *L. bongardiana*, and *L. yezoensis*) understory for statistical analyses. All data collected in May 2002 were omitted from the analyses involving kelp because understory data for that month were incomplete. Analyses were conducted on the average understory kelp densities per transect to enable comparison with the relatively sparse densities of the canopy kelp and fish communities. Because *Nereocystis* was relatively rare, all individuals were counted within each 120-m² band transect.

For fish surveys, all fishes observed within each transect and within one meter of the bottom (30 m × 4 m × 1 m = 120 m³) were enumerated and identified to species whenever possible. Because few fishes were observed, the three most abundant families (Hexagrammidae, Scorpaenidae, and Gadidae) were analyzed by family group. All other fishes were rarely observed and were grouped as “other fishes” for the analyses.

Statistical analyses

Statistical analyses were performed by using multivariate approaches and linear models with STATISTICA vers. 6 (Statsoft, Tulsa, OK). Cluster analyses were used to examine site variability in the kelp and fish communities and how this variability relates to structural complexity. Averages of all data were calculated by site across month and year for the ordination analyses. Kelp and fish densities were considered by species with the physical variables of rugosity, substrate size, and verticality. The Bray and Curtis dissimilarity coefficient (Bray and Curtis, 1957) was used and the Euclidean distance was calculated for physical variables, kelp, and fish. Water temperature did not vary among sites within months and was not used in our analysis. A one-way ANOVA was used for temporal variation of water temperature. Partial correlation analysis (with Pearson's correlation coefficient, r) was performed between kelp groups (based on average annual understory, perennial understory, and canopy kelp densities [no./120 m²]) and physical habitat data (rugosity, substrate size, and verticality; average values per 120 m²; water temperature: °C per month) while controlling for potentially intercorrelating variables. These results were considered significant at $\alpha < 0.05$. Because of the low number of fish observed, fish counts were converted to presence or absence data and logistic regression was applied. Independent variables were the four log-transformed physical variables (rugosity, substrate size, and verticality; \log_{10} [average values per 120 m²]; temperature: \log_{10} [value per month],) and the three log-transformed kelp groups (annual under-

story kelp, perennial understory kelp, and canopy kelp: \log_{10} [number of kelps per 120 m²]). Analyses were conducted separately for each fish family that composed at least 20% of total abundance (Hexagrammidae, Scorpaenidae, and Gadidae).

Results

Physical habitat variables

Substrate in the study sites varied from complex (rocky outcrops, large boulders, and bedrock) to homogeneous (small cobble and sand). The ten sites were partitioned by clustering techniques into two general structural complexity groups based on dissimilarities among the three measured structural characteristics (rugosity, substrate size, and verticality; Fig. 2A). Water temperature varied significantly among months ($F_{12,456}=1983.2$, $P < 0.001$). Temperature ranged from 1.8°C in winter to 11.0°C in summer and was the only physical variable that did not vary among sites. Water temperatures also differed significantly between years ($F_{1,456}=1028.6$, $P < 0.001$), and were higher in 2003 than 2002.

Surveys of kelp and fish

A comparison of cluster dendrograms revealed patterns of spatial variation among the kelp and fish groups that mirrored the substrate trends. When all biological data (understory and canopy kelp densities and fish presence) were averaged across months and years, five sites grouped with higher counts of kelp and fish exhibited the greatest structural complexity (Fig. 2, B [kelp] and C [fish]). Similarly, three of the structurally homogenous sites were grouped consistently with lower values for both kelp and fish. Two sites (LJA and OJA) showed inconsistencies in these groupings. Little Jakolof Bay (with a lower complexity designation) was in the higher macroalgal count group but in the lower fish abundance group. Outside Jakolof Bay (with a higher complexity designation) was in the lower density groups for both kelp and fish.

Kelp communities were variable in species composition and density over space and time and understory kelp communities were considerably denser than the canopy kelp. Understory kelps were present every month and perennial kelp dominated in all months except late October 2002 (Fig. 3). The annual understory kelp *C. costata* contributed at most 2% to the annual kelp relative abundance in any month, whereas *L. saccharina* composed at least 75%. Annual understory kelps were found in greatest densities during periods with warmer water temperatures; perennial kelps, however, were not significantly correlated with temperature (Table 1). Perennial understory kelps were found on all transects; an overall equal contribution was made by *A. clathratum* and the perennial *Laminaria* species (*L. bongardiana* and *L. yezoensis*, densities lumped together). Both annual and perennial understory kelps were found in

greatest densities in sites with higher values for rugosity and verticality, although, curiously, not for substrate size (Table 1). Five sites (ANI, HER, HES, OJA, and SPI) contained *Nereocystis* in 2002, compared to two

sites (HER and SPI) in 2003. Canopy kelp persisted throughout the winter at one site (HER). The greatest number of canopy kelp individuals was observed in October 2002, the lowest densities (fewer than 5 *Nereocystis*/120 m² transect) were observed from November through April, and no canopy kelp was observed in May 2003 (Fig. 4). Canopy kelp was more abundant during months with higher water temperatures and in sites with larger substrate and greater vertical relief, but, unlike the understory kelp, was negatively correlated with rugosity (Table 1).

The presence of some fishes was associated with season, year, physical habitat characteristics, and kelp. Four hundred twenty-two fishes representing 15 species from eight families were sighted on 34% ($n=171$) of transects surveyed. Three families (Hexagrammidae [greenlings], Scorpaenidae [rockfishes], and Gadidae [codfishes]) each composed at least 20% of the total abundance and together accounted for more than 80% of all fishes sighted. Infrequently sighted fishes included those in the families Pholidae (gunnels, 6%), Cottidae (sculpins, 3%), Pleuronectidae (flatfishes, 2%), and others (including ronquils, searchers, and unidentified fishes, 5%). Fish presence varied over time (Table 2); more fishes were sighted in 2003 (2.59 ± 6.92 fish/transect) than in 2002 (0.63 ± 0.96 fish/transect). More fish (considering all fish species pooled across months, years, and sites) were seen during periods with higher temperatures and in sites characterized by larger substrate and greater densities of annual understory and canopy kelp (Table 2). Greenlings (primarily kelp greenling [*Hexagrammos decagrammus*]) accounted for the majority of sightings (35% of total abundance) and their presence did not differ among months (Table 2). Greenlings were most commonly seen in sites with low rugosity values and larger substrate (i.e., boulder to bedrock), and during periods with warmer water temperatures and higher densities of annual understory kelps.

Schooling species, such as rockfishes (primarily the black rockfish [*S. melanops*]) and adult Pacific cod (*Gadus macrocephalus*), were observed infrequently. However, these groups accounted for the greatest number of fish seen on any one transect and exhibited the greatest variability in sightings per month in the fish groups, primarily during summer 2003 (Fig. 5). There was no difference in the presence of rockfishes among months, but there were significant temporal differences for codfishes (Table 2). Considering the major families observed in this study, only the presence of rockfishes showed significant annual variability (Table 2)—more in 2003 (1.23 ± 5.83 fish/transect) than in 2002 (0.08 ± 0.42 fish/transect). Both rockfishes and codfishes were most commonly seen during periods with higher water temperatures (Table 2). Although these results are based only on sightings of adult fishes, large schools (thousands of individuals) of juvenile codfishes (predominately *G. macrocephalus*) were observed at all sites during August and September 2002. The juvenile codfish schools observed in summer 2003

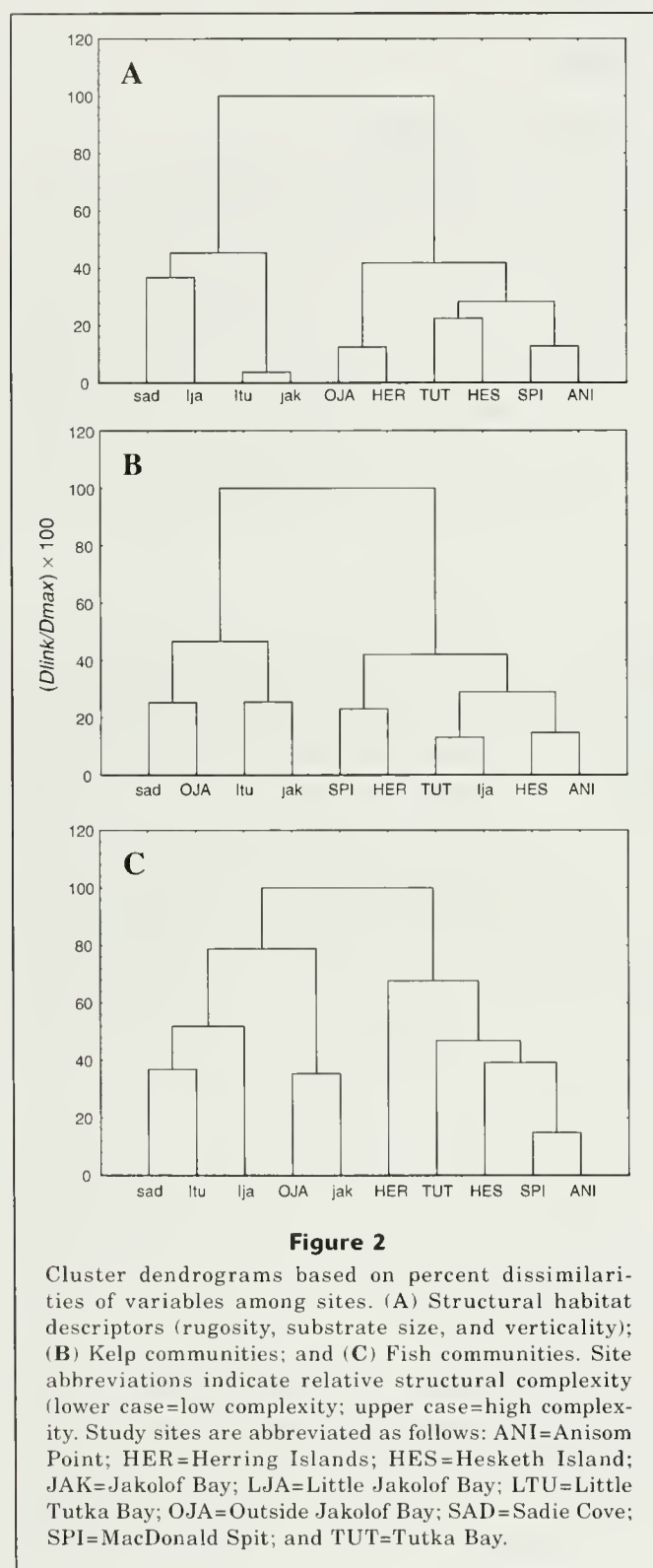


Table 1

Partial correlation analysis (Pearson's correlation coefficient, r) between physical variables and kelp groups ($n=473$ transects). Values are considered significant at $P < 0.05$. Rugosity provides a small-scale measure of habitat complexity and is the ratio of the true distance contour along the bottom to a one-meter horizontal distance. Substrate size is based on the average diameter of the substrate comprising the majority of a 0.25-m² quadrat. Verticality was assigned to each site on the basis of overall vertical relief.

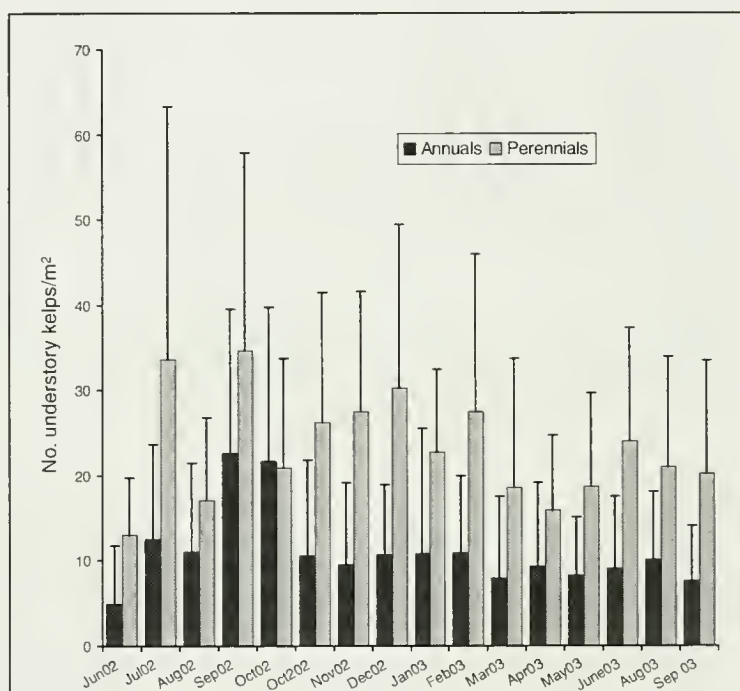
Kelp group	Temperature	Rugosity of substrate	Substrate size	Verticality of substrate
Canopy	0.18 $P < 0.001$	-0.32 $P < 0.001$	0.29 $P < 0.001$	0.09 $P < 0.001$
Annual understory kelp	0.17 $P = 0.001$	0.16 $P < 0.001$	0.01 $P = 0.790$	0.16 $P < 0.001$
Perennial understory kelp	0.02 $P = 0.685$	0.27 $P < 0.001$	-0.05 $P = 0.325$	0.26 $P < 0.001$

were composed of much fewer individuals (at most, tens of individuals/school). These juvenile codfishes were not included in any analyses in our study because of difficulties in accurately quantifying them.

Discussion

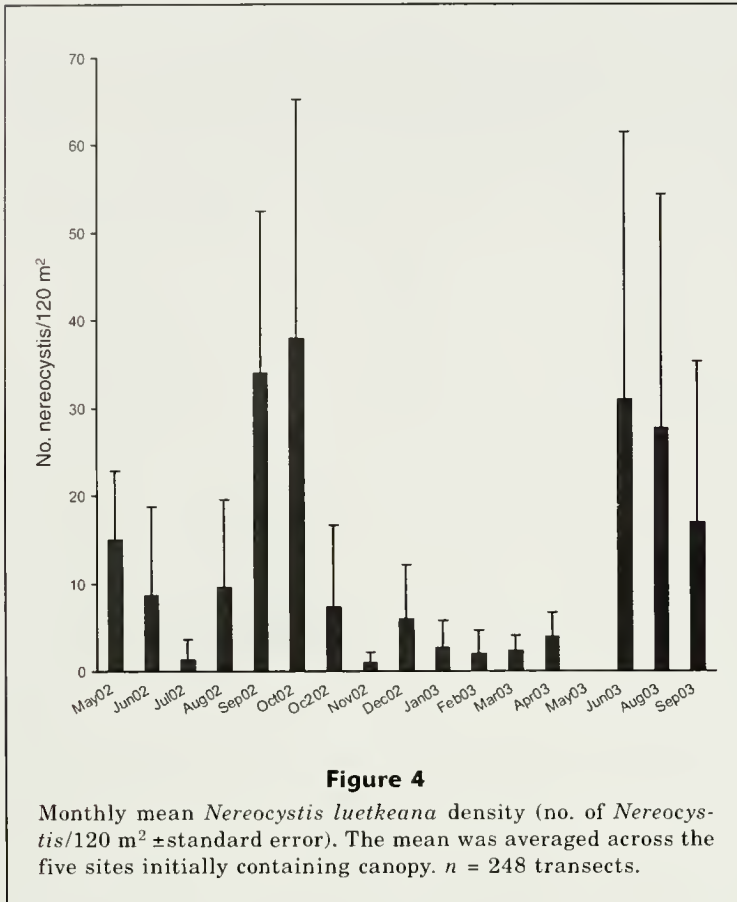
Structural habitat complexity is important to both fish and kelps in that greater physical habitat complexity is associated with greater overall densities of fish in these communities. In particular, greenlings associated most consistently with kelp beds that had a predominately rocky (i.e., large cobble/bedrock) and structurally complex bottom habitat. The association of the dominant fish species in our study with relatively larger substrate and higher rock relief may indicate that south-central Alaska kelp-bed fishes follow the same trend (of a strong association of fish with kelp and rocky substrate relief) documented elsewhere. For example, in California kelp beds, significant correlations exist between fish density and bottom relief (Ebeling et al., 1980; Bodkin, 1986). However, rockfishes in Puget Sound inhabited low-relief rocky kelp beds during summer (Matthews, 1990) and in Prince William Sound were positively associated with relief (Dean et al., 2000). Rockfishes and codfishes in the present study were never associated with any bottom structure, perhaps because of the sporadic sightings of these species. The lack of association of rockfishes and codfishes with any physical habitat variables or kelp may reflect the transient nature and seasonal association of these fishes with kelp. However, the rarity of any fishes observed higher than one meter above the substratum in the present study indicates that bottom structure may be important to the fishes observed in our study, if perhaps indirectly, by also being appropriate substratum for kelp habitat.

The variability of Alaska kelp communities and associated fish populations may be partially attributable

**Figure 3**

Monthly variation in the density (no. of plants/m² ± standard error) of understory kelp groups. $n = 503$ transects. Because surveys were conducted during alternate neap tide cycles throughout the 17 month study, two surveys occurred, at least partly, during October 2002.

to the extreme seasonal nature of the northern environment. Increased sightings of fish during periods characterized by warmer water indicate seasonal variability in fish communities associated with kelp communities. For example, although greenlings were observed in the shallow, rocky nearshore sites during every month in the present study, rockfishes and codfishes were rarely observed except in summer. Healthy understory kelp populations exist in this area on rocky substratum at depths of up to 16 m (first author, personal observ.) and fish populations may shift seasonally to similar



habitats in adjacent, deeper water. Puget Sound rockfishes tend to move to shallower water in summer and deeper water in winter (Moulton and Miller¹), possibly avoiding increased storm surge during winter months. Fish communities inhabiting seasonally and annually variable kelp beds in the north Pacific must be capable of enduring a wider variety of environmental variables over the course of a season, year, or lifetime than those occupying the relatively stable, perennial canopy-dominated kelp beds of more temperate zones. The importance and magnitude of seasonal cues vary among kelp and fish species throughout their ranges and the cues include temperature, photoperiod, turbidity, increased frequency of storms and surge in winter, and prey and nutrient availability (Ebeling et al., 1980, Dayton, 1985). However, the thresholds of many environmental factors are to some extent temperature-dependent (Dayton, 1985), providing an easily quantified surrogate variable for seasonality in the present study. Kelp beds (and associated fishes) at the

¹ Miller, B. S., and L. L. Moulton. 1988. Characterization of Puget Sound fishes for the EPA Bay Program, p. 77-84. In Proceedings, First Annual Meeting on Puget Sound Research, vol. 1, Seattle, WA, March 18-19, 1988. Puget Sound Action Team, Office of the Governor, P.O. Box 40900, Olympia WA 98504-0900.

Table 2

Logistic regression results on the presence of fishes by families and by total abundance. Only families composing greater than 20% of the total fish abundance are included. Independent variables are time (*n*=503 transects for tests of "month" or *n*=208 transects for test of "year," the comparison of June to September of years 2002 and 2003), kelp densities (canopy kelp and annual and perennial understory kelp groups; *n*=473 transects), and physical habitat variables (water temperature, rugosity, substrate size, and verticality). Only significant values (*P*<0.05) are reported.

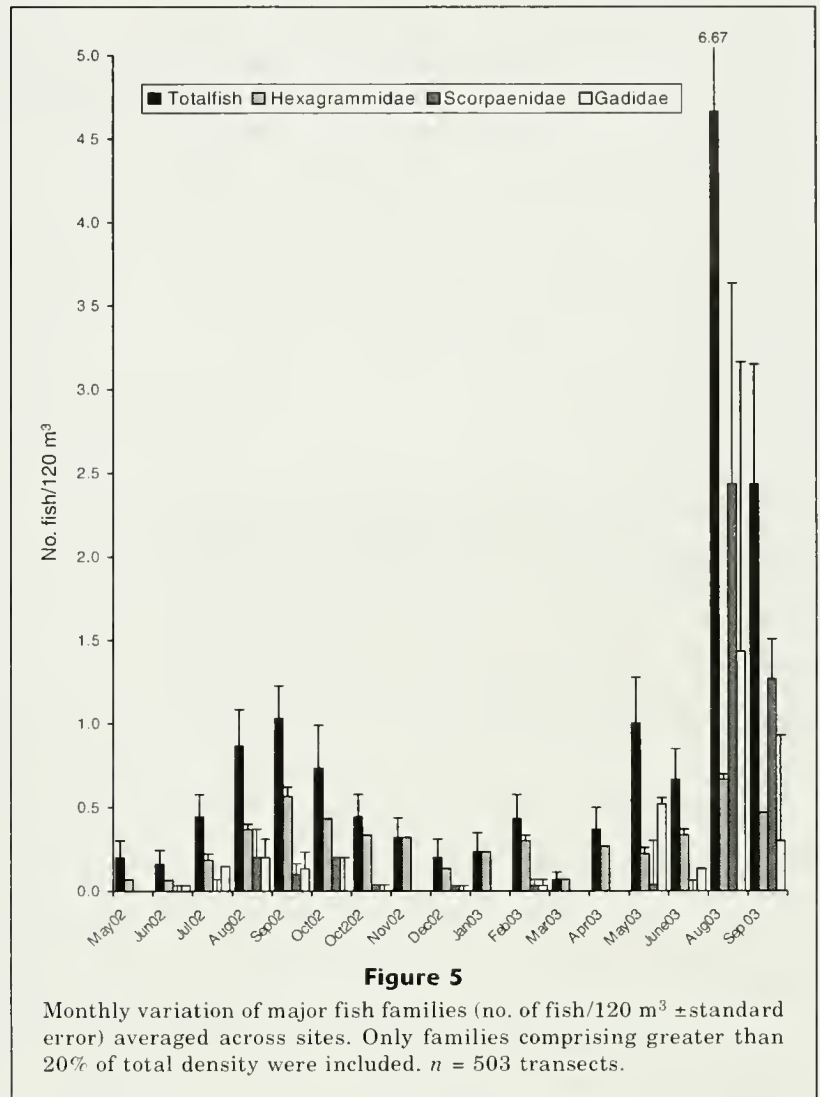
Analysis group	Independent variable	Parameter estimate	Standard error	Wald's χ^2	<i>P</i> -value
Hexagrammidae	Annual kelp understory	0.62	0.17	12.65	<0.001
	Water temperature	4.26	0.91	22.15	<0.001
	Rugosity	-2.48	1.15	4.66	0.031
	Substrate size	1.90	0.47	16.11	<0.001
Scorpaenidae	Year	0.64	0.29	4.67	0.031
	Water temperature	9.00	3.00	13.00	<0.001
Gadidae	Month	0.27	0.08	12.19	0.001
	Water temperature	4.28	1.62	6.96	0.008
Total fish	Month	0.08	0.03	10.19	0.001
	Year	0.28	0.13	4.61	0.032
	Canopy	0.66	0.32	4.37	0.037
	Annual understory	0.21	0.10	3.99	0.046
	Water temperature	5.12	0.78	43.13	<0.001
	Substrate size	0.80	0.38	4.49	0.034

northern edge of their range are subject to wide fluctuations in all of these factors, as well as wide inter-annual variation in intensity and duration of seasonal factors. It is these extremes that make studying these habitats difficult or impossible during all but summer months and result in the paucity of consistent seasonal data in northern Pacific systems.

Aerial surveys of kelp beds in Kachemak Bay during three consecutive summers (2000–2002) showed significant differences in size, location, and presence of *Nereocystis* canopy (Schoch and Chenlot, 2004), illustrating great interannual variability that may be apparent on relatively short temporal scales. Such variability was also observed in the present study, in that three of five sites originally containing canopy kelp did not recruit *Nereocystis* juveniles the second summer. Although this canopy kelp species is considered an annual, we observed *Nereocystis* individuals reproducing into a second summer.

Our findings of relatively more fishes inhabiting *Nereocystis* beds than understory-only kelp beds indicates that areas characterized by enhanced *Nereocystis* growth may have greater fish densities. In one northern California study, densities of kelp greenling in *Nereocystis* beds were four times greater than in the present study (Bodkin, 1986). *Nereocystis* beds in California were similarly more important to rockfishes (Bodkin, 1986; Love et al., 1991) than understory kelp alone. However, the existence of high understory kelp densities in the canopy-containing sites may be of greater importance to fishes than the canopy itself. In our study sites, both the greenlings and grouped fishes were positively associated with densities of annual understory. In addition, fishes in the present study were usually observed in close association with the understory and substratum as has been typical in other south-central Alaska studies (Rosenthal², Dean et al., 2000). The perennial-dominated understory of south-central Alaska kelp beds may provide a degree of habitat stability for some fishes for at least part of the year.

It is difficult to account for all factors influencing a natural system, particularly without knowing the recent history of the community. Because little is known



² Rosenthal, R. J. 1979. A preliminary assessment of composition and food webs for demersal fish assemblages in several shallow subtidal habitats in lower Cook Inlet, Alaska, 58 p. In Final report by Dames and Moore, Inc., 800 Cordova Street, Suite 101, Anchorage, AK 99501, for Alaska Department of Fish and Game. Commercial Fisheries Division, 211 Mission Rd., Kodiak, Alaska 99615.

about interactions between kelp and fish communities and their natural variability in south-central Alaska, investigation of more obvious, small-scale processes over an entire year is necessary. Physical factors, such as size of the kelp beds and related edge effects of the habitat, salinity fluctuations and freshwater runoff, degree and direction of exposure to light and tidal currents, and the frequency of storm events may play a significant role in structuring these dynamic communities. In addition, biological factors that may influence algal community structure include inter- and intra-species competition and herbivory. A growing body of evidence points to the importance of temporal and spatial scales in ecological processes (i.e., Dayton and Tegner, 1984; Wiens and Addicott, 1986; Foster, 1990). The structurally complex kelp beds surveyed in the present study appear to provide critical habitat throughout the year for greenling species. However, this habitat is also seasonally important to rockfishes and codfishes (both adult and juvenile).

This work provides a description and baseline information on the structural characteristics of south-central Alaska's nearshore kelp beds and associated fish communities, and provides insight on the importance of seasonality. These findings may enable managers to identify potentially important nearshore fish habitat from relatively easily quantified structural habitat variables. The identification of critical habitat areas for juvenile and adult fishes is essential for sustainable management, and the importance of habitat structure in and influence of seasonality on these habitats has been further illuminated by this work.

Acknowledgments

This publication is the result of research sponsored by Alaska Sea Grant with funds from the National Oceanic and Atmospheric Administration Office of Sea Grant, Department of Commerce, under grant no. NA 16RG2321 (project number R/31-09) and from the University of Alaska with funds appropriated by the state. We wish to thank S. Hills, G. Haas, and A. Blanchard, as well as numerous reviewers, divers, and logistical supporters for their priceless assistance.

Literature cited

- Aburto-Oropeza, O., and E. F. Balart.
2001. Community structure of reef fish in several habitats of a rocky reef in the Gulf of California. *Mar. Ecol.* 22:283-305.
- Bodkin, J. L.
1986. Fish assemblages in *Macrocystis* and *Nereocystis* kelp forests off central California. *Fish. Bull.* 84:799-807.
- Bray, J. R., and J. T. Curtis.
1957. An ordination of the upland forest communities of southern Wisconsin. *Ecol. Mono.* 27:325-329.
- Calvert, E. L.
2005. Kelp beds as fish and invertebrate habitat in southeastern Alaska. M.S. thesis, 113 p. Univ. Alaska Fairbanks, Juneau, AK.
- Carr, M. H.
1994. Effects of macroalgal dynamics on recruitment of a temperate reef fish. *Ecology* 75:1320-1333.
- Dayton, P. K., and M. J. Tegner.
1984. Catastrophic storms, El Nino, and patch stability in a southern California kelp community. *Science* 224:283-285.
- Dayton, P. K.
1985. Ecology of kelp communities. *Annu. Rev. Ecol. Sys.* 16:215-245.
- Dean, T. A., L. Haldorson, D. R. Laur, S. C. Jewett, and A. Blanchard.
2000. The distribution of nearshore fishes in kelp and eelgrass communities in Prince William Sound, Alaska: associations with vegetation and physical habitat characteristics. *Environ. Biol. Fishes* 57:271-287.
- Ebeling, A. W., R. J. Larson, W. S. Alevizon, and R. N. Bray.
1980. Annual variability of reef fish assemblages in kelp forests off Santa Barbara, California. *Fish. Bull.* 78:361-367.
- Foster, M. S.
1990. Organization of macroalgal assemblages in the northeast Pacific: the assumption of homogeneity and the illusion of generality. *Hydrobiologia* 192:21-33.
- Garcia-Charton, J. A., and A. Perez-Ruzafa.
2001. Spatial pattern and the habitat structure of a Mediterranean rocky reef fish local assemblage. *Mar. Biol.* 138:917-934.
- Hamilton, J. A.
2004. Kelp bed variability and fish population dynamics in Kachemak Bay, Alaska. M.S. thesis, 57 p. Univ. Alaska Fairbanks, Fairbanks, AK.
- Hegwer, C. L.
2003. Seasonal abundance and diversity of nearshore fishes around Steller sea lion haulouts of Kodiak Island. M.S. thesis, 76 p. Univ. Alaska Fairbanks, Fairbanks, AK.
- Leum, L. L., and J. H. Choat.
1980. Density and distribution patterns of the temperate marine fish *Cheliadactylus spectabilis* in a reef environment. *Mar. Biol.* 57:327-337.
- Love, M. S., M. H. Carr, and L. J. Haldorson.
1991. The ecology of substrate-associated juveniles of the genus *Sebastes*. *Environ. Biol. Fishes* 30:225-243.
- Matthews, K. R.
1990. A comparative study of habitat use by young-of-the-year, subadult, and adult rockfishes on four habitat types in central Puget Sound. *Fish. Bull.* 88:223-239.
- Schoch, G. C., and H. Chenelot.
2004. The role of estuarine hydrodynamics in the distribution of kelp forests in Kachemak Bay, Alaska. *J. Coast. Res.* 45:179-194.
- Steneck, R. S., M. H. Graham, B. J. Bourque, D. Corbett, J. M. Erlandson, J. A. Estes, and M. J. Tegner.
2002. Kelp forest ecosystems: biodiversity, stability, resilience, and future. *Environ. Cons.* 29:436-459.
- Wiens, J. A., and J. F. Addicott.
1986. Overview of the importance of spatial and temporal scale in ecological investigations. *In* Community ecology (J. Diamond, and T. J. Case, eds.), p. 145-153. Harper and Row, New York, NY.

Abstract—Variation in the allele frequencies of five microsatellite loci was surveyed in 1256 individual spotted seatrout (*Cynoscion nebulosus*) obtained from 12 bays and estuaries from Laguna Madre, Texas, to Charlotte Harbor, Florida, to St. John's River on the Florida Atlantic Coast. Texas and Louisiana collection sites were resampled each year for two to four years (1998–2001). Genetic differentiation was observed. Spotted seatrout from Florida waters were strongly differentiated from spotted seatrout collected in Louisiana and Texas. The greatest genetic discontinuity was observed between Tampa Bay and Charlotte Harbor, and Charlotte Harbor seatrout were most similar to Atlantic Coast spotted seatrout. Texas and Louisiana samples were not strongly structured within the northwestern Gulf of Mexico and there was little evidence of temporal differentiation within bays. These findings are contrary to those of earlier analyses with allozymes and mitochondrial DNA (mtDNA) where evidence of spatial differentiation was found for spotted seatrout resident on the Texas coast. The differences in genetic structure observed among these markers may reflect differences in response to selective pressure, or may be due to differences in underlying genetic processes.

Genetic variability in spotted seatrout (*Cynoscion nebulosus*), determined with microsatellite DNA markers

Rocky Ward (contact author)

Kevin Bowers

Rebecca Hensley

Brandon Mobley

Ed Belouski

Email address for R. Ward: rward@usgs.gov

Texas Parks and Wildlife Department

Coastal Fisheries Division

4200 Smith School Road

Austin, Texas 78744

Present address for R. Ward: Northern Appalachian Research Laboratory

USGS/Leetown Science Center

176 Straight Run Rd.

Wellsboro, Pennsylvania 16901

Spotted seatrout (*Cynoscion nebulosus*) support an important recreational fishery in the northern Gulf of Mexico and along the U.S. Atlantic Coast. Management of this fishery is multi-jurisdictional, employing a variety of strategies including reduction or elimination of commercial exploitation, adjustments of recreational fish-size limits and bag limits, closed seasons, and artificial spawning and stocking of fish (Vanderkooy and Muller, 2003). Effective management requires an understanding of the ecology, life history, and genetic structuring of a species. Understanding genetic population structure is important to every aspect of fishery management but is especially critical when stocking fish is the chosen management strategy. Stocking without regard for existing genetic variability within and among populations places the genetic integrity of the targeted species at risk (Allendorf et al., 1986). Genetic population structuring may be evidence of adaptation to past environmental differences, whereas genetic variability may enable a population to meet future environmental challenges.

Evidence of population structuring in spotted seatrout has been gained through morphological, physiological, and genetic examinations. Regional differences have been found in oto-

lith and scale structure, growth rate (Iverson and Tabb, 1962; however, see Murphy and Taylor, 1994 for a different interpretation), and in reproductive physiology (Brown-Peterson et al., 2002). Each of these studies found evidence of biologically significant regional differentiation—a finding consistent with observations of limited movement within and between bays (Music, 1981; Overstreet, 1983; Baker and Matlock, 1993) and between bays and adjacent nearshore waters (Baker et al., 1986).

Studies of genetic markers generally support the existence of population structuring among spotted seatrout in the northern Gulf of Mexico. Studies examining protein variation found evidence of weak (Ramsey and Wakeman, 1987; King and Pate, 1992) to strong (Weinstein and Yerger, 1976) population subdivision. The King and Pate (1992) study found indications of clinal variation in mean heterozygosity and in alleles of the aspartate aminotransferase-2 locus, indicating possible adaptation to environmental gradients on the Texas coast (King and Zimmerman, 1993). In each of the allozyme studies indications of isolation by distance were found, as was found in a survey in which mitochondrial DNA was used (mtDNA; Gold et al., 1999). In the

mtDNA study, significant heterogeneity was found in haplotype frequencies among collection sites, indicating that spotted seatrout were spatially differentiated. In contrast, Gold et al. (2003) found no significant differences in microsatellite DNA allele frequency among spotted seatrout inhabiting Texas bays. A similar study of microsatellite variation among spotted seatrout of the U.S. Atlantic and Florida Gulf coasts (employing different loci from those of Gold et al., 2003) found extensive spatial differences that coincided with known zoogeographic barriers (Wiley and Chapman, 2003). Surprisingly, the Indian River spotted seatrout sample on Florida's Atlantic coast was genetically more similar to the Choctawhatchee sample from the Florida Panhandle than to more northerly Atlantic Coast samples. The overall pattern that emerges from applications of molecular markers to the examination of spatial genetic variability in spotted seatrout is mixed. Most studies have found limited gene flow between adjacent bays and moderate population subdivision, and patterns of differentiation that may be described as "isolation by distance." The failure of the Gold et al. (2003) to find statistically significant genetic subdivision is surprising, given that studies employing allozymes and mtDNA have been successful in discerning genetic structuring and given that microsatellites are considered to be among the most capable genetic markers at resolving population level differentiation (Wright and Bentzen, 1994). Gold et al. (2003) focused on the northwestern Gulf of Mexico, and their geographically limited examination may have restricted the ability of the marker to discern patterns in the spatial variability of spotted seatrout. It is also possible that underlying genetic properties of the markers accounted for the differences in observed variation, or that some markers (i.e., allozymes) were able to detect genetic adaptation to environmental gradients which microsatellites, assumed to be selectively neutral, were not.

The present study is an attempt to re-examine genetic variability in spotted seatrout in the northern Gulf of Mexico. As did Gold et al. (2003) (who also examined a portion of the present data), we used microsatellite markers. Samples from Louisiana and the Gulf and Atlantic coasts of Florida were added in an attempt to give a greater spatial perspective that may be useful in evaluating the observed genetic variability among populations. In addition, samples from multiple years were included for Texas and Louisiana bays, allowing for evaluation of the stability and robustness of detected genetic structure.

Materials and methods

A total of 1256 individuals were examined. Sample collection sites are shown in Figure 1. All Texas sites were sampled in three consecutive years, 1998–2000, except Corpus Christi Bay which was sampled across four years, 1998–2001. The Louisiana site was sampled in 1999 and in 2000, and the Florida sites were sampled

only in 2000. Texas and Florida samples were obtained through routine resource sampling efforts of Texas Parks and Wildlife Department and Florida Department of Natural Resources personnel, respectively, and Louisiana samples were donated by licensed recreational anglers. Soft dorsal-fin tissue was removed from the fish, placed in 95% ethanol, and stored at room temperature until processed. Genomic DNA was extracted by using the PureGene DNA isolation kit and protocols (Gentra Systems, Inc., Minneapolis, MN).

Primers designed to amplify three microsatellites (*Soc12*, *Soc50*, and *Soc243*) originally developed for red drum (*Sciaenops ocellatus*) by Turner et al. (1998) were employed. Two additional primer pairs (*Cne133* and *Cne133'*) were designed by sequencing products of the *Soc133* (Turner et al., 1998) forward and reverse primers and then identifying internal primer sequences that amplified separate repeat regions within the original *Soc133* amplicon. Primer sequences for *Cne133* and *Cne133'* and protocols for amplification and interpretation are discussed in Gold et al. (2003).

Summary statistics were generated by using the Microsoft Excel add-on Microsatellite Toolkit (Park, 2001) and ARLEQUIN, version 2.001 (Schneider et al., 2000), which was also employed to test frequencies for deviations from Hardy-Weinberg equilibrium by using exact tests performed with Markov-chain randomization (Guo and Thompson, 1992). Permutations with 1000 resamplings (Manly, 1991) were used to generate probability values (*P*) for each test of Hardy-Weinberg equilibrium for each microsatellite locus in each sample. ARLEQUIN was also used to test for linkage between microsatellite loci, and significance of *P*-values was estimated by 1000 resamplings. Critical values for interpreting significance levels for simultaneous inferential comparisons were adjusted by using the sequential Bonferroni approach (Rice, 1989).

Allelic distribution homogeneity of each microsatellite was assessed with exact tests implemented with the statistical package GENETOP, version 3.4 (Raymond and Rousset, 1995), and significance was estimated by permutation with 1000 resamplings for each comparison. Population subdivision was estimated with Weir and Cockerham's (1984) theta (θ) as generated in FSTAT, version 2.9.3 (Goudet, 1995), and a bootstrap procedure in FSTAT was employed to calculate a 95% confidence interval (CI). Although the use of theta is contingent on the assumption of an infinite-alleles mutation model (Kimura and Crow, 1964), it has been shown to compare favorably with other measures of genetic subdivision when employed with microsatellite data (Ruzzante, 1998). The significance of population differentiation across all loci was estimated as the combined probability of *P*-values for Fisher's exact tests for individual loci. Separate analyses were made for data sets that comprised 13 samples defined by site and collection date and 13 samples defined by site alone, with date combined across all year classes.

A hierarchical analysis of gene diversity was performed by using the analysis of molecular variance

model (AMOVA; Michalakis and Excoffier, 1996) in ARLEQUIN (Excoffier et al., 1992). The components of genetic diversity attributable to variance between regions (Atlantic versus Gulf of Mexico), variance among sampling sites within regions, temporal variance among years within sampling sites, and variance among individuals within samples were estimated. The significance of each variance component was tested with nonparametric permutation procedures (~1000 permutations; Excoffier et al., 1992). In addition, genetic differentiation among all collection sites for each sampling year and between pairs of populations within sampling years was estimated by using the theta statistic of Weir and Cockerham (1984) accessed on FSTAT (Goudet, 1995).

Cavalli-Sforza and Edwards' chord distance (D_C ; Cavalli-Sforza and Edwards, 1967) was used to reconstruct phylogenetic relationships among collection sites. Estimations of D_C were obtained with the statistical package NJBPOP (Cornuet et al., 1999). Takezaki and Nei (1996) found D_C to be a better estimate of genetic divergence with microsatellite DNA data than with measures based on the step-wise mutation model. This estimate is not based on the assumption of a constant population size or a constant mutation rate among loci (Takezaki and Nei, 1996) and appears to accurately resolve closely related populations (Paetkau et al., 1997; Angers and Bernatchez, 1998). A phenogram was generated from the chord-distance matrix with the neighbor-joining (N-J) algorithm. Robustness of each node was evaluated by bootstrapping over loci for 2000 replications (Hedges, 1992) with the SEQBOOT program on PHYLIP, version 3.5c (Felsenstein, 1995). The PHYLIP program CONSENSE then was used to generate a consensus tree which was drawn with the program TREEVIEW (Page, 1996).

Results

The number of alleles per sample (Table 1) exceeded those reported for the same loci in red drum (*Sciaenops ocellatus*), the species of origin for the markers (Turner et al., 1998). Mean observed heterozygosity (H_o) ranged from 0.21 to 0.39, and there were no statistically significant deviations from Hardy-Weinberg expectations at any locus and sample combination after Bonferroni adjustment. Without the Bonferroni correction, allele frequencies at 16 of 165 comparisons would have failed to

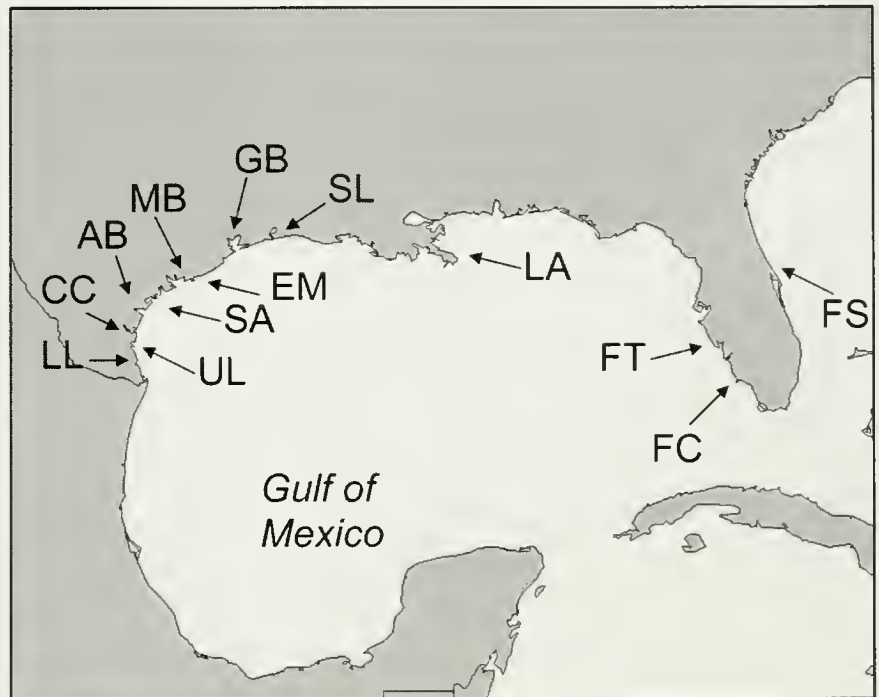


Figure 1

Sampling localities for spotted seatrout (*Cynoscion nebulosus*) examined from the northern Gulf of Mexico and the Atlantic Coast of Florida. LL = lower Laguna Madre; UL = upper Laguna Madre; CC = Corpus Christi Bay; AB = Aransas Bay; SA = San Antonio Bay; MB = Matagorda Bay; EM = east Matagorda Bay; GB = Galveston Bay; SL = Sabine Lake; LA = Grand Isle, Louisiana; FT = Tampa Bay, Florida; FC = Charlotte Harbor, Florida; FS = St. John's River, Florida.

meet expectations. This included all loci except Soc243, which was observed to be in Hardy-Weinberg equilibrium in all samples. Soc012 most often failed to meet Hardy-Weinberg expectations; six of 33 samples were out of equilibrium before Bonferroni adjustment. Observed heterozygosity was lower than expected in 14 of the 16 locus-and-sample combinations that failed to meet Hardy-Weinberg expectation before adjustment. Statistically significant linkage disequilibrium was noted for one pair of loci in one sample (*Cne133'* with *Soc12* in sample GB99) after Bonferroni adjustments. If the unadjusted critical value ($\alpha=0.05$) was applied, 15 of 330 comparisons were statistically significant. Interestingly, the associated loci *Cne133* and *Cne133'* did not exhibit linkage disequilibrium for any sample.

After Bonferroni adjustment, exact tests for allele distribution homogeneity across all 33 samples demonstrated statistically significant differentiation for all microsatellite loci except *Soc50*, which approached statistical significance ($P=0.05$). All theta estimates were significantly greater than zero after Bonferroni adjustments, as was the overall theta of 0.116 (95% CI, 0.007–0.073; $P<0.001$), indicating significant genetic differentiation across both the spatial and temporal dimensions sampled in this study. When spatial samples were collapsed to form 13 spatial samples, all loci except *Soc50* exhibited statistically significant deviations from

Table 1

Summary statistics for spotted seatrout (*Cynoscion nebulosus*) samples included in a survey of microsatellite variation. n = number of individuals in sample; n_a = number of alleles; P_{HW} = probability of meeting Hardy-Weinberg expectations (with Bonferri-corrected critical value of $\alpha = 0.0003$).

Sample location	Sample acronym	n	n_a P_{HW}	Soc 12	Soc 50	Soc 243	Cne 133	Cne 133'
St. Johns River, Florida 2000	FS00	26	n_a 0.32	3	2	3	3	3
Charlotte Harbor, Florida 2000	FC00	22	n_a 0.18	3	2	2	3	2
Tampa Bay, Florida 2000	FT00	40	n_a 0.18	3	2	2	4	2
Grand Isle, Louisiana 1999	LA99	60	n_a 0.46	3	2	3	4	3
Grand Isle, Louisiana 2000	LA00	39	n_a 0.69	3	3	2	3	2
Sabine Lake, Texas 1998	SL98	23	n_a 0.157	3	2	2	3	2
Sabine Lake, Texas 1999	SL99	36	n_a 0.61	3	3	3	3	2
Sabine Lake, Texas 2000	SL00	30	n_a 1.00	3	3	3	3	2
Galveston Bay, Texas 1998	GB98	28	n_a 0.03	4	2	2	3	2
Galveston Bay, Texas 1999	GB99	37	n_a 0.61	3	3	3	3	2
Galveston Bay, Texas 2000	GB00	40	n_a 0.03	3	5	3	3	3
E. Matagorda Bay, Texas 1998	EM98	33	n_a 0.91	4	2	2	3	2
E. Matagorda Bay, Texas 1999	EM99	40	n_a 0.47	4	2	2	3	2
E. Matagorda Bay, Texas 2000	EM00	40	n_a 0.33	3	2	2	3	2
Matagorda Bay, Texas 1998	MB98	40	40 0.22	3	3	3	3	2
Matagorda Bay, Texas 1999	MB99	40	40 0.36	3	2	2	3	2
Matagorda Bay, Texas 2000	MB00	40	40 0.36	3	2	3	4	2
San Antonio Bay, Texas 1998	SA98	40	n_a 0.03	3	3	3	3	2
San Antonio Bay, Texas 1999	SA99	40	n_a 0.84	3	3	3	3	3
San Antonio Bay, Texas 2000	SA00	40	n_a 0.01	4	4	2	3	2
Aransas Bay, Texas 1998	AB98	40	n_a 1.00	3	2	3	3	3
Aransas Bay, Texas 1999	AB99	39	n_a 0.43	4	3	3	4	2
Aransas Bay, Texas 2000	AB00	40	n_a 0.04	3	2	3	4	2
Corpus Christi Bay, Texas 1998	CC98	40	n_a 0.61	3	2	3	3	2
Corpus Christi Bay, Texas 1999	CC99	50	n_a 0.04	3	4	3	3	2

continued

Table 1 (continued)

Sample location	Sample acronym	<i>n</i>	n_a P_{HW}	Soc 12	Soc 50	Soc 243	<i>Cne</i> 133	<i>Cne</i> 133'
Corpus Christi Bay, Texas 2000	CC00	40	n_a P_{HW}	3 0.10	2 0.33	4 0.25	3 1.00	3 0.19
Corpus Christi Bay, Texas 2001	CC01	35	n_a P_{HW}	3 0.59	4 0.02	4 0.71	4 0.74	3 1.00
Upper Laguna Madre, Texas 1998	UL98	40	n_a P_{HW}	3 0.05	2 1.00	3 0.33	3 1.00	2 1.00
Upper Laguna Madre, Texas 1999	UL99	40	n_a P_{HW}	3 0.07	3 0.05	4 0.16	3 0.04	3 1.00
Upper Laguna Madre, Texas 2000	UL00	40	n_a P_{HW}	3 0.31	4 1.00	4 0.36	4 1.00	2 1.00
Lower Laguna Madre, Texas 1998	LL98	38	n_a P_{HW}	4 0.06	3 0.13	2 1.00	3 0.79	2 0.01
Lower Laguna Madre, Texas 1999	LL99	40	n_a P_{HW}	3 0.55	3 1.00	5 1.00	4 0.04	2 1.00
Lower Laguna Madre, Texas 2000	LL00	40	n_a P_{HW}	3 0.84	2 1.00	3 0.31	3 1.00	2 0.39

homogeneous allele distributions and the overall test was significant ($P_{exact} < 0.001$). Estimated theta values were statistically significant after Bonferroni adjustment, except *Cne*133'. The overall estimate of theta ($\theta = 0.057$, 95% CI, 0.005–0.062) was lower than the estimate including both spatial and temporal dimensions ($\theta = 0.116$), indicating that temporal differences likely contributed to overall population differentiation in spotted seatrout.

Analysis of molecular variance indicated a statistically significant 4.11% of the among-sample genetic variance was attributable to differences between Gulf and Atlantic samples ($P = 0.04$). Statistically significant variance was also detected among sampling sites within the Gulf of Mexico (0.49% of the total variance, $P < 0.001$). No significant genetic variance attributable to temporal differences was found within bays ($P = 0.42$). An overall F_{ST} of 0.046 was estimated, which was statistically significant ($P < 0.001$).

We found no significant differences among Texas bays in the 1998 collections (Table 2). In 1999, spotted seatrout from Texas and Louisiana were not differentiated except for the Galveston Bay samples that differed significantly from all other samples. Analyses of year 2000 collections, which included samples from Texas, Louisiana, and Florida, revealed differences between Florida samples and all samples from Louisiana and Texas. The Louisiana sample differed from most Texas samples, and within Texas most samples were genetically undifferentiated, except for samples Galveston Bay which were significantly different from those of all bays, except Sabine Lake and Corpus Christi. Finally, the upper and lower Laguna Madre samples were statistically different from each other. Temporally, the only statistically significant differences among years

were seen among Louisiana and Galveston Bay samples. The overall theta within sampling years ranged from less than 0.006 in 1998 to 0.080 in 2000, perhaps reflecting the increased genetic variability introduced by the Florida samples in the 2000 data set. The statistically insignificant differentiation among sampling years within bays, with the exception of the Louisiana and Galveston Bay, supports the notion that temporal differentiation, at least on the limited scale reported in our study, may be ignored and temporal samples can be collapsed within bays. The genetic structure of spotted seatrout in Galveston Bay is highly differentiated, both temporally and spatially, showing significant differences in 1999 and 2000 with almost all other bays.

The topology of the neighbor-joining tree based on D_C for 34 site and year groups (Fig. 2) was poorly supported by bootstrap replications and demonstrated little correspondence to geographic and temporal patterns. An exception was the separation of samples FC00 and FS00 (Charlotte Bay and St. John's River, FL, respectively; acronyms are defined in Table 1) from samples collected in the northern and western Gulf. When groupings were collapsed across years (Fig. 3), the distinctiveness of the Florida samples from the southern Gulf Coast and the Atlantic Coast continued to be supported. Spotted seatrout from Florida's Tampa Bay (FT00) were found to be more closely related to spotted seatrout from Louisiana and Texas than to spotted seatrout in the other Florida samples. Texas and Louisiana samples formed a well-differentiated grouping; however, within that grouping, there was little correspondence between genetic differentiation and geographic location. One exception was the south coast of Texas (Corpus Christi Bay and the upper and

lower Laguna Madre), which formed a weakly supported clade.

A statistically significant ($P < 0.001$) correlation between D_C and geographic distance was observed ($r = 0.90$) and thus supported the isolation-by-distance hypothesis. The greatest geographic distance between adjacent collection sites was observed between Charlotte Harbor and St. John's River; however, when the St. John's River sample was excluded from the analysis, a significant positive relationship was still evident ($r = 0.80$, $P < 0.001$). The correlation between D_C and geographic distance within the western Gulf of Mexico (Texas and Louisiana) remained positive ($r = 0.42$) and statistically significant ($P = 0.05$).

Discussion

Spotted seatrout inhabiting a series of sites from the lower Laguna Madre of Texas to St. John's River on the

Atlantic Coast of Florida were genetically differentiated by analyses of allele frequencies of five microsatellite markers. Samples from Florida waters were strongly differentiated from spotted seatrout from Louisiana and Texas, and the statistically significant correlation between geographic distance and genetic distance was due primarily to these differences. Within Florida, the Charlotte Harbor spotted seatrout is genetically more similar to the Atlantic Coast spotted seatrout from St. John's River than to the neighboring Tampa Bay spotted seatrout, which is genetically more similar to Texas and Louisiana than to other Florida fish of the same species. Differences in allele frequency between Charlotte Harbor and Tampa Bay samples represented the greatest discontinuity observed in this study. This putative population structure is congruent with Wiley and Chapman's (2003) findings of distinct population subdivision among Atlantic Coast spotted seatrout, although details of that structure may be difficult to reconcile. Wiley and Chapman (2003) found spotted

Table 2

Results of tests for homogeneity in allele distributions among samples of spotted seatrout (*Cynoscion nebulosus*). Pairwise- θ estimates for 1998 samples (above diagonal), 1999 samples (below diagonal), and 2000 samples (lower matrix). θ^F is θ calculated across all sampling periods within a bay. * indicates statistical significance ($\alpha = 0.05$) after adjustment for multiple comparisons (Rice, 1989). Acronyms for within-bay samples collapsed across years are the two letters (e.g., LA99+LA00=LA). Definitions for abbreviations for sample locations (LA, SL, etc.) are given in Table 1.

Sample location	LA	SL	GB	EM	MB	SA	AB	CC	UL	LL		
SL	-0.007	0.000	0.026	-0.011	-0.010	-0.003	0.011	0.015	0.012	0.002		
GB	0.092*	0.070*	0.000	0.019	0.010	0.009	0.006	0.009	0.004	0.029		
EM	0.009	0.002	0.053*	0.000	-0.007	0.006	-0.003	0.019	0.018	0.020		
MB	0.007	0.007	0.083*	0.000	0.000	-0.008	-0.001	0.002	-0.001	0.005		
SA	-0.004	-0.006	0.078*	-0.001	-0.006	0.000	0.008	-0.002	-0.005	0.000		
AB	0.008	0.001	0.089*	-0.004	-0.000	-0.001	0.000	0.009	0.008	0.024		
CC	-0.006	-0.008	0.079*	0.001	-0.004	-0.011	-0.001	0.000	0.000	0.010		
UL	0.003	-0.002	0.081*	-0.001	0.011	-0.002	0.000	0.001	0.000	0.003		
LL	0.005	0.002	0.072*	-0.009	-0.006	-0.003	-0.006	-0.003	0.000	0.000		
	FC	FT	LA	SL	GB	EM	MB	SA	AB	CC	UL	LL
FS	0.007	0.326*	0.108*	0.061*	0.110*	0.039*	0.077*	0.053*	0.053*	0.0532*	0.031*	0.081*
FC		0.341*	0.136*	0.077*	0.145*	0.031*	0.085*	0.054*	0.059*	0.068*	0.043*	0.081*
FT			0.245*	0.185*	0.257*	0.263*	0.195*	0.229*	0.219*	0.236*	0.288*	0.136*
LA				0.057	0.011	0.084*	0.067*	0.058*	0.039	0.029	0.093*	0.063*
SL					0.065	0.006	0.012	-0.006	0.003	-0.001	0.016	0.003
GB						0.105*	0.104*	0.083*	0.072*	0.050	0.115*	0.083*
EM							0.011	-0.003	0.004	0.004	-0.007	0.019
MB								0.009	-0.004	0.013	0.016	0.001
SA									-0.006	-0.005	0.004	0.013
AB										-0.004	0.008	0.008
CC											0.013	0.016
UL												0.034*
θ^F			0.065*	0.004	0.049*	<0.001	-0.004	-0.002	<0.001	0.013	0.001	0.013

seatrout from Indian River, Florida (which is near St. John's River), to be genetically more similar to spotted seatrout from Choctawhatchee Bay in the Florida Panhandle than to other Atlantic Coast fish of the same species. The analyses of the two studies, taken together, indicate at least two distribution breaks in the eastern Gulf and the Atlantic, the first between Georgia and the upper Atlantic Coast of Florida and a second between Charlotte Harbor and Tampa Bay. The clustering of populations observed by Wiley and Chapman (2003) between Indian River and Choctawhatchee Bay may, in light of our finding of a genetic discontinuity between the intervening Charlotte Harbor and Tampa Bay, reflect relative differences in genetic affinity discerned by the two data sets. Resolution of this possible incongruence will require examination of numerous sampling sites collected from both the Atlantic and Gulf coasts of Florida.

Spotted seatrout inhabiting the northwestern Gulf of Mexico from the Laguna Madre to Grand Isle, Louisiana, were not found to be subdivided into discernible stocks or populations and there was little indication of temporal differentiation within bays. Exceptions to this lack of temporal differentiation were seen in Galveston Bay and in Louisiana. Temporal differences in these two sites may be due to sampling error (although the n for each year's sample in the two sites appear to be adequate), or these two large regions may harbor populations that are temporally or spatially genetically structured. Some indications of geographically coherent spatial patterns were observed among spotted seatrout in the northwestern Gulf of Mexico. For example, there was an indication that this species on the lower coast is genetically differentiated, albeit weakly, from conspecifics inhabiting bays on the middle and upper Texas coast. This finding is similar to that found in allozyme (King and Pate, 1992) and mtDNA data (Gold et al., 1999) where differences between Laguna Madre samples and more northerly bays were observed. Galveston Bay spotted seatrout were also found to be genetically divergent, being genetically distinct from spotted seatrout in all other bays in 1999 and most bays in 2000. Galveston Bay was, in addition, one of two sites where the genetic structure of spotted seatrout was found to be temporally heterogeneous. Gold et al. (2003) found the upper Texas Coast to be a region of genetic transition; a notable shift in allele frequencies of the *Soc201* locus was evident between Matagorda Bay and Sabine Pass—a span that includes Galveston Bay.

The lack of genetic population subdivision in the northwestern Gulf is consistent with the observed decrease in heterozygosity in relation to Hardy-Weinberg expectations. Similar heterozygote deficiencies in white seabream (*Diplodus sargus*) (Lenfant and Planes, 2002) were hypothesized to represent mixing of genetically disparate individuals during some stage of recruitment (the Wahlund effect). This phenomenon may be characteristic of many marine fishes, especially those with local populations recruited from a larval stage with highly dispersive capabilities. Spotted seatrout,

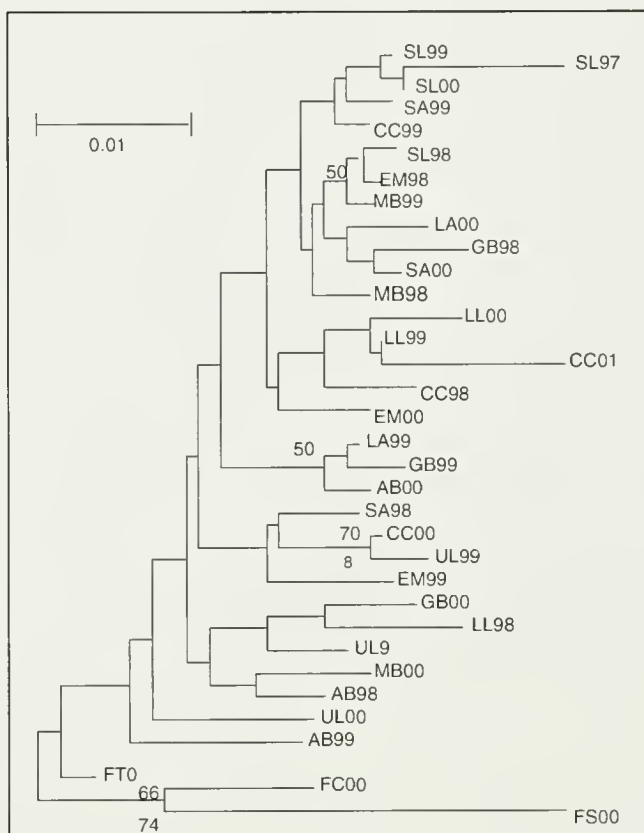
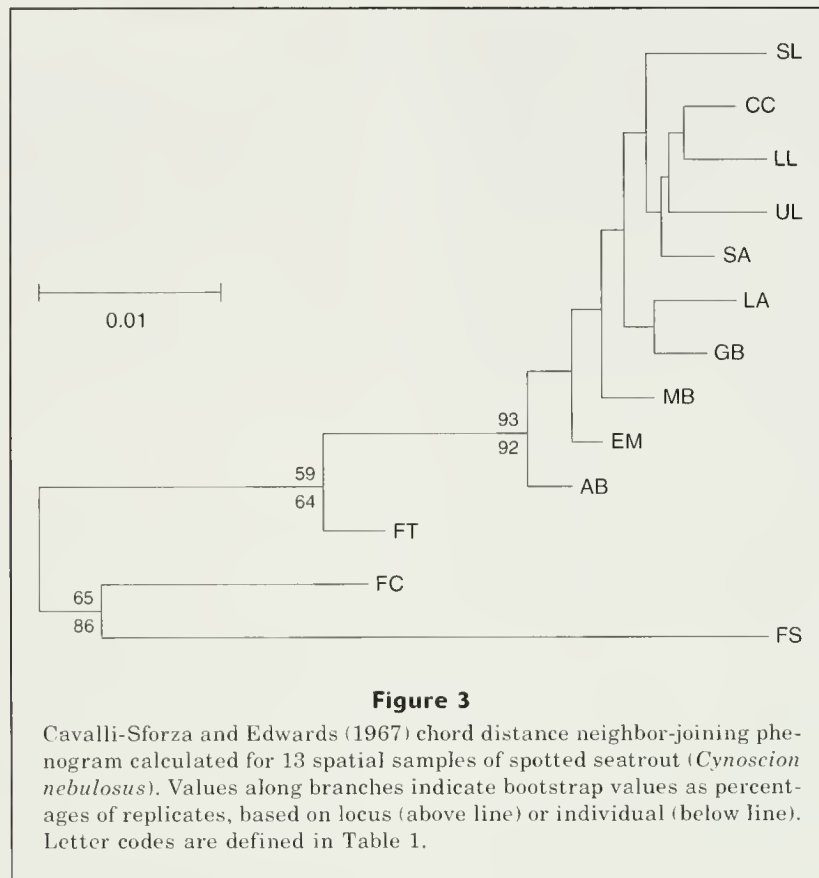


Figure 2

Cavalli-Sforza and Edwards (1967) chord distance neighbor-joining phenogram calculated for 33 spatial and temporal samples of spotted seatrout (*Cynoscion nebulosus*). Values along branches indicate bootstrap values as percentages of replicates, based on locus (above line) or individual (below line). Letter codes are defined in Table 1.

due to its unique life history characteristics, is not an obvious example of a marine species expected to exhibit high gene flow. Spotted seatrout are confined to nearshore waters, spend most of their life within an estuarine habitat, and spawn and select their nursery area within the estuary (McMichael and Peters, 1989). Results of tagging studies support the hypothesis of a natal bay affinity based on spotted seatrout life history (e.g., Baker and Matlock, 1993). Stock structure among spotted seatrout was detected by the studies of morphology, physiology, (Iverson and Tabb, 1962), and genetics (Gold et al., 1999, and references therein). This population structure was not detected in the Gold et al. (2003) or the present analyses of variation in microsatellite DNA loci—markers expected to yield a high-resolution analysis of population-level genetic variability. The differences observed between microsatellite variability and that seen in allozymes (Weinstein and Yerger, 1976; Ramsey and Wakeman, 1987; King and Pate, 1992) and mtDNA (Gold et al., 1999) may reflect different evolutionary processes (Gold et al., 2003).



Microsatellites are assumed to be selectively neutral, whereas the allozyme and mtDNA markers used in earlier studies are potentially subject to selection and thus may present different patterns for the same region (Hellberg et al., 2002). King and Zimmerman (1993) suggested the cline in *AAT-2* observed by King and Pate (1992) may reflect adaptation to temperature or salinity gradients along the Texas Coast. Microsatellite markers would not, in the absence of linkage to loci affected by selection, be subject to such processes. It is also possible, as Gold et al. (2003) suggested, that the earlier allozyme and mtDNA studies provided evidence, not of genetic differentiation of populations inhabiting neighboring bays, but rather of a general confirmation of the isolation-by-distance model, where greatest genetic differences are found between the most peripheral sampling sites.

Currently, about 5 million fingerling spotted seatrout are stocked per year into Texas bays and estuaries. Neither Florida nor the other states of the eastern Gulf of Mexico have implemented large-scale spotted seatrout stocking programs; however such efforts are being considered. The genetic population structure observed in studies of allozymes (Weinstein and Yerger, 1976; Ramsey and Wakeman, 1987; King and Pate, 1992) and mtDNA (Gold et al., 1999) argue for a cautious policy concerning the stocking of spotted seatrout. Gold et al. (2003) suggested the gene flow observed

in microsatellite markers argued against the current Texas policy of stocking only into the bay from which broodfish were procured. Allowing stocking into both the bay of broodfish origin and into adjacent bays would meet this suggestion of simulated gene flow and still protect the putative population subdivision detected by the earlier studies. Should stocking programs in Florida or elsewhere in the northeastern Gulf be implemented, it is critical, considering the level of population subdivision observed in the present study and that of Wiley and Chapman (2003), that fine-scale genetic surveys in the eastern Gulf be accomplished. It is also obvious that inter-regional transfers of spotted seatrout should be strictly avoided.

Acknowledgments

This research was partially funded by the Federal Aid to Sportfish Restoration Program, project F-36-R. Samples were provided by staff of the Coastal Fisheries Division of Texas Parks and Wildlife Department, the Florida Fish and Wildlife Conservation Commission, and A. Landry and W. Dailey of Texas A&M University, Galveston. I. Blandon, W. Karel, and J. Burr provided laboratory assistance. A debt of gratitude is owed L. McEachron and R. Colura of Texas Parks and Wildlife Department, who supported and guided this work.

Literature cited

- Allendorf, F., N. Ryman, and F. Utter.
1986. Genetics and fishery management: past, present, and future. In Population genetics and fishery management (N. Ryman, and F. Utter, eds.), p 1-19. Washington Sea Grant Program, Seattle, WA.
- Angers, B., and L. Bernatchez.
1998. Combined use of SMM and non-SMM methods to infer fine structure and evolutionary history of closely related brook charr (*Salvelinus fontinalis*, Salmonidae) populations from microsatellites. *Mol. Biol. Evol.* 15:143-159.
- Baker, W. B., Jr., and G. C. Matlock.
1993. Movement of spotted seatrout in Trinity Bay, Texas. *Northeast Gulf Sci.* 13:29-34.
- Baker, W. B., Jr., G. C. Matlock, L. W. McEachron, A. W. Green, and H. E. Hegen.
1986. Movement, growth, and survival of spotted seatrout tagged in Bastrop Bayou, Texas. *Contr. Mar. Sci.* 29:91-101.
- Brown-Peterson, N. J., M. S. Peterson, D. L. Nieland, M. D. Murphy, R. G. Taylor, and J. R. Warren.
2002. Reproductive biology of female spotted seatrout, *Cynoscion nebulosus*, in the Gulf of Mexico: differences among estuaries? *Environ. Biol. Fishes* 63:405-415.
- Cavalli-Sforza, L. L., and A. W. F. Edwards.
1967. Phylogenetic analysis models and estimation procedures. *Am. J. Human Gen.* 19:233-257.
- Cornuet, J.-M., S. Piry, G. Luikart, and M. Solignac.
1999. New methods employing multilocus genotypes to select or exclude populations as origins of individuals. *Genetics* 153:1989-2000.
- Excoffier, L., P. E. Smouse, and J. M. Quattro.
1992. Analysis of molecular variance inferred from metric distances among DNA haplotypes: application to human mitochondrial DNA restriction data. *Genetics* 131:479-491.
- Felsenstein, J.
1995. PHYLIP (Phylogeny Inference Package), version 3.57c. Univ. Washington, Seattle, WA.
- Gold, J. R., L. R. Richardson, and C. Furman.
1999. Mitochondrial DNA diversity and population structure of spotted seatrout (*Cynoscion nebulosus*) in coastal waters of the southeastern United States. *Gulf Mex. Sci.* 1999:40-50.
- Gold, J. R., L. B. Stewart, and R. Ward.
2003. Population structure of spotted seatrout (*Cynoscion nebulosus*) along the Texas Gulf Coast, as revealed by genetic analysis. In *Biology of the spotted seatrout* (S. A. Bartone, ed.), p. 17-29. CRC Press, Boca Raton, FL.
- Goudet, J.
1995. F-STAT (version 1.2): A computer program to calculate F-statistics. *J. Hered.* 86:485-486.
- Guo, S., and E. Thompson.
1992. Performing the exact test of Hardy-Weinberg proportion from multiple alleles. *Biometrics* 48:361-372.
- Hedges, S. B.
1992. The number of replications needed for the accurate estimation of the bootstrap *P* value in phylogenetic studies. *Mol. Biol. Evol.* 9:366-369.
- Hellberg, M. E., R. S. Burton, J. E. Neigel, and S. R. Palumbi.
2002. Genetic assessment of connectivity among marine populations. *Bull. Mar. Sci.* 70:273-290.
- Iverson, E. S. and D. C. Tabb.
1962. Subpopulations based on growth and tagging studies of spotted seatrout, *Cynoscion nebulosus*, in Florida. *Copeia* 1962:544-548.
- Kimura, M., and J. F. Crow.
1964. The number of alleles that can be maintained in a finite population. *Genetics* 49:725-738.
- King, T. L., and H. O. Pate.
1992. Population structure of spotted seatrout inhabiting the Texas Gulf Coast: an allozymic perspective. *Trans. Am. Fish. Soc.* 121:746-756.
- King, T. L., and E. G. Zimmerman.
1993. Clinal variation at aspartate aminotransferase-2 in spotted seatrout, *Cynoscion nebulosus* (Cuvier), inhabiting the northwestern Gulf of Mexico. *Animal Gen.* 24:59-61.
- Lenfant, P., and S. Planes.
2002. Temporal genetic changes between cohorts in a natural population of a marine fish, *Diplodus sargus*. *Biol. J. Linn. Soc.* 76:9-20.
- Manly, B. J. F.
1991. Randomization and Monte Carlo methods in biology, 281 p. Chapman and Hall, New York, NY.
- McMichael, R. H., Jr., and K. M. Peters.
1989. Early life history of spotted seatrout, *Cynoscion nebulosus* (Pisces: Sciaenidae), in Tampa Bay, Florida. *Estuaries* 12:98-110.
- Michalakis, Y., and L. Excoffier.
1996. A generic estimation of population subdivision using distances between alleles with special reference to microsatellite loci. *Genetics* 142:1061-1064.
- Murphy, M. D., and R. G. Taylor.
1994. Age, growth, and mortality of spotted seatrout in Florida waters. *Trans. Am. Fish. Soc.* 123:482-497.
- Music, J. L., Jr.
1981. Seasonal movement and migration of spotted seatrout (*Cynoscion nebulosus*). *Estuaries* 4:280.
- Overstreet, R. M.
1983. Aspects of the biology of the spotted seatrout, *Cynoscion nebulosus*, in Mississippi. *Gulf Res. Rep.* (suppl. 1):1-43.
- Paetkau, D., L. P. Waits, P. L. Clarkson, L. Craighead, and C. Strobeck.
1997. An empirical evaluation of genetic distance statistics using microsatellite data from bear (*Ursidae*) populations. *Genetics* 147:1943-1957.
- Page, R. D. M.
1996. TREEVIEW: an application to display phylogenetic trees on personal computers. *Comp. Appl. Biosci.* 12:357-358.
- Park, S. D. E.,
2001. Trypanotolerance in west African cattle and the population genetic effects of selection. Ph.D. diss., 241 p. Univ. Dublin, Dublin, Republic of Ireland.
- Ramsey, P. R., and J. M. Wakeman.
1987. Population structure of *Sciaenops ocellatus* and *Cynoscion nebulosus* (Pisces: Sciaenidae): biochemical variation, genetic subdivision and dispersal. *Copeia* 1987:682-695.
- Raymond, M., and F. Rousset.
1995. GENEPOP (vers. 1.2): population genetics software for exact tests and ecumenicism. *J. Genet.* 86:248-249.
- Rice, W. R.
1989. Analyzing tables of statistical tests. *Evolution* 43:223-225.

- Ruzzante, D. E.
1998. A comparison of several measures of genetic distance and population structure with microsatellite data: bias and sampling variance. *Can. J. Fish. Aquat. Sci.* 55:1-14.
- Schneider, S., D. Roessli, and L. Excoffier.
2000. ARLEQUIN, vers. 2.000: a software for population genetics data analysis. Genetics and Biometrics Laboratory, Department of Anthropology and Ecology, Univ. Geneva, CP 511 1211 Geneva 24, Switzerland.
- Takezaki, N., and M. Nei.
1996. Genetic distances and reconstruction of phylogenetic trees from microsatellite DNA. *Genetics* 144:389-399.
- Turner, T. F., L. R. Richardson, and J. R. Gold.
1998. Polymorphic microsatellite DNA markers in red drum (*Sciaenops ocellatus*). *Mol. Ecol.* 7:1771-1773.
- Vanderkooy, S. J., and R. G. Muller.
2003. Management of spotted seatrout and fishery participants in the U.S. *In* Biology of the spotted seatrout (S. A. Bartone, ed.), p. 227-245. CRC Press, Boca Raton, FL.
- Weinstein, M. P., and R. W. Yerger.
1976. Electrophoretic investigation of subpopulations of the spotted seatrout, *Cynoscion nebulosus* (Cuvier), in the Gulf of Mexico and Atlantic Coast of Florida. *Comp. Biochem. Physiol.* 54B:97-102.
- Weir, B. S., and C. C. Cockerham.
1984. Estimating *F*-statistics for the analysis of population structure. *Evolution* 38:1358-1370.
- Wiley, B. A., and R. W. Chapman.
2003. Population structure of spotted seatrout, *Cynoscion nebulosus*, along the Atlantic Coast of the U.S. *In* Biology of the spotted seatrout (S. A. Bartone, ed.), p. 31-40. CRC Press, Boca Raton, FL.
- Wright, J. M., and P. Bentzen.
1994. Microsatellites: genetic markers for the future. *Rev. Fish Biol. Fish.* 4:384-388.

Abstract—The *Caranx hippos* species complex comprises three extant species: crevalle jack (*Caranx hippos*) (Linnaeus, 1766) from both the western and eastern Atlantic oceans; Pacific crevalle jack (*Caranx caninus*) Günther, 1868 from the eastern Pacific Ocean; and longfin crevalle jack (*Caranx fischeri*) new species, from the eastern Atlantic, including the Mediterranean Sea and Ascension Island. Adults of all three species are superficially similar with a black blotch on the lower half of the pectoral fin, a black spot on the upper margin of opercle, one or two pairs of enlarged symphyseal canines on the lower jaw, and a similar pattern of breast squamation. Each species has a different pattern of hyperostotic bone development and anal-fin color. The two sympatric eastern Atlantic species also differ from each other in number of dorsal- and anal-fin rays, and in large adults of *C. fischeri* the lobes of these fins are longer and the body is deeper. *Caranx hippos* from opposite sides of the Atlantic are virtually indistinguishable externally but differ consistently in the expression of hyperostosis of the first dorsal-fin pterygiophore. The fossil species *Caranx carangopsis* Steindachner 1859 appears to have been based on composite material of *Trachurus* sp. and a fourth species of the *Caranx hippos* complex. Patterns of hyperostotic bone development are compared in the nine (of 15 total) species of *Caranx sensu stricto* that exhibit hyperostosis.

Review of the crevalle jacks, *Caranx hippos* complex (Teleostei: Carangidae), with a description of a new species from West Africa

William F. Smith-Vaniz (contact author)¹

Kent E. Carpenter²

Email address for W. F. Smith-Vaniz: bill_smith-vaniz@usgs.gov

¹ U.S. Geological Survey

7920 NW 71st Street
Gainesville, Florida 32653

Present address: Division of Ichthyology
Florida Museum of Natural History
Dickinson Hall, Museum Road
University of Florida
Gainesville, Florida 32611-7800

² Department of Biological Sciences

Old Dominion University
Norfolk, Virginia 23529

Species of the *Caranx hippos* complex or crevalle jacks (Fig. 1) are fished commercially or recreationally in coastal waters throughout their range. Recognized as “superb light tackle species” by the International Game Fish Association (IGFA, 2006), they are important apex predators in inshore tropical waters—all species attaining maximum sizes approaching or exceeding 22.7 kg (50 lb). They are also commonly exhibited in public aquaria and books on marine fishes usually include accounts of them for the areas where these species are found. Despite this importance, there has been considerable confusion regarding the taxonomy and geographic distributions of these species. Gill and Kemp (2002) discussed the potentially serious implications for fishery and conservation managers of an inadequate taxonomic understanding of putatively widespread shore-fish species. Blaber (2002) noted that one of the major obstacles to ecological research in developing countries is the difficulty associated with correct identification of tropical marine and estuarine fishes, which is exacerbated by an overall decline in funding throughout the world for taxonomic research.

In a general review of the phenomenon of hyperostosis in fishes, including those of the allopatrically distributed and externally nearly identical species *Caranx hippos* (Linnaeus) (Atlantic Ocean) and *C. caninus* Günther (eastern Pacific Ocean), Smith-Vaniz et al. (1995) determined that patterns of hyperostotic bone development were often species-specific. These findings stimulated us to re-evaluate the taxonomic status of specimens from the eastern Atlantic identified as *Caranx hippos*, which we herein recognize as actually representing two species. The primary objectives of this research were to describe a new species of West African *Caranx* that has been routinely misidentified as *C. hippos*, to provide diagnoses and comparisons for all members of the *Caranx hippos* complex, and to determine their geographic distributions.

This study has been hampered by the scarcity of preserved adults of *Caranx hippos* from the eastern Atlantic. This scarcity is not surprising because natural history museums and institutional fish collections do not exist in any coastal West African country, and preservation and shipment of large fish specimens from the region

are logistically difficult. Color photographs of *Caranx hippos* provided by the International Game Fish Association and numerous colleagues indicate that adults of this species are relatively common locally, especially during October to February. We urge fishery biologists and others who have the opportunity to obtain adults of fishes that mature at relatively large sizes to help ensure that at least a few such specimens are available in major research collections.

Taxonomic history

The genus *Caranx* was established by Lacépède (1801, p. 57) and the type-species *Caranx carangua* Lacépède was apparently first designated by Desmarest (1856, p. 242) as *Caranx carougus* [sic] Bloch, which is a junior synonym of *Scomber hippos* Linnaeus. Two other generic or subgeneric names have been applied to these species (*Tricropterus* Rafinesque, 1810 and *Carangus* Girard, 1858), but both are junior synonyms of *Caranx* because the type species of these nominal taxa is also *Scomber carangus* Bloch.

Caranx hippos was first described (Linnaeus, 1766) from Carolina as *Scomber hippos*. The putative holotype, a right half-skin (Wheeler, 1985), was included in one of the last shipments of dried fish specimens sent to Linnaeus by the colonial physician Alexander Garden (Sanders, 1997). Synonyms of *Caranx hippos* (see species account) are either unnecessary replacement names or Linnaeus's original description was not considered. Nichols (1920), because his superficial description of his new Brazilian subspecies, *Caranx hippos tropicus*, was based on too few specimens, failed to appreciate the range of variation in the species, and other workers have correctly disregarded this trinomial. In his description of the eastern Pacific *Caranx caninus*, Günther (1867, 1868) did not compare this species with any other species. Jordan and Gilbert (1883), Jordan (1895), and Gilbert and Starks (1904) all concluded that this nominal species was indistinguishable from the western Atlantic *C. hippos*. In their major work on the fishes of Panama, Meek and Hildebrand (1925) also did not recognize *C. caninus* as a valid species, stating "a careful comparison of our large series from the two coasts discloses no differences of importance." Hildebrand (1946) continued to recognize fish from both oceans as conspecific. Berry (1974) stated that eastern Pacific and western Atlantic specimens of *Caranx hippos* are essentially identical. Eschmeyer and Herald (1983) stated that *C. caninus* might not be a valid species. Eschmeyer (1998)

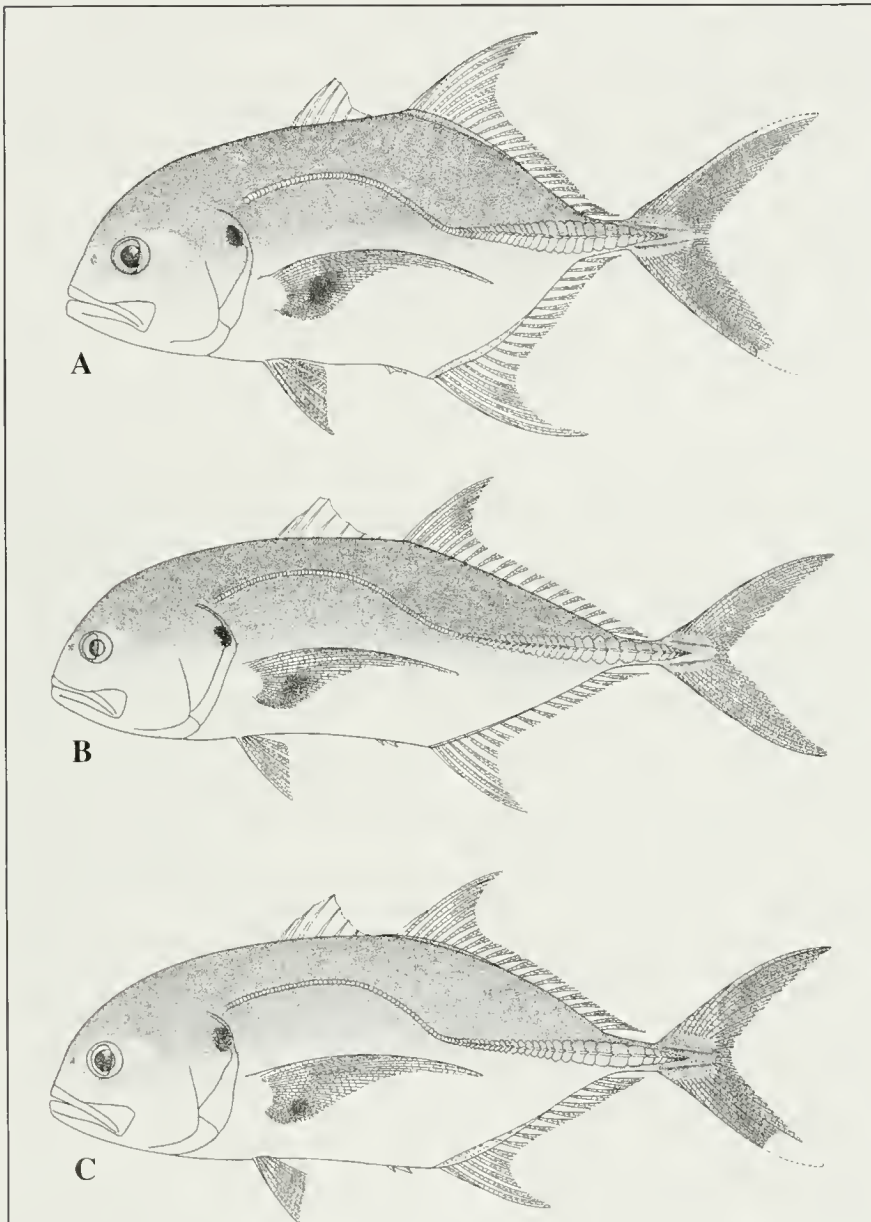


Figure 1

The *Caranx hippos* species complex: (A) longfin crevalle jack (*C. fischeri*), 358 mm FL, BMNH 1927.12.7.49, Ascension Island; (B) crevalle jack (*C. hippos*), 390 mm FL, USNM 33247, Florida, Dixie Co., Swanee River; (C) Pacific crevalle jack (*C. caninus*), 359 mm FL, USNM 127918, Peru, Lobos de Tierra Island. Illustrations by Tracy D. Pedersen.

and Castro-Aguirre et al. (1999) both treated it as a synonym of *C. hippos*; however, the former subsequently recognized *C. caninus* as a valid species (Eschmeyer¹).

Most recent authors have recognized a single eastern Atlantic member of this species group, which has been uncritically referred to as *Caranx hippos* (Fowler, 1936; Bini, 1968; Hureau and Tortonese, 1973; Bauchot and Pras, 1980; Smith-Vaniz and Berry, 1981; Smith-Vaniz, 1986; Smith-Vaniz et al., 1990; Bauchot, 1992). In the few cases where two species were recognized (Cadenat, 1960; Blache et al., 1970; Okera, 1978), the scientific names used for both species were misapplied. The name *C. carangus* Valenciennes [*sic*] (the account given in Cuvier and Valenciennes, 1833 is not an original description) was used for the true *C. hippos* and the superficially similar new species (*C. fischeri*) was routinely misidentified as *C. hippos*.

Materials and methods

Abbreviations used for institutional depositories and cooperative organizations are as follows: American Museum of Natural History, New York (AMNH); Academy of Natural Sciences of Philadelphia (ANSP); The Natural History Museum, London (BMNH); California Academy of Natural Sciences, San Francisco (CAS, CAS-SU); Food and Agricultural Organization of the United Nations, Rome (FAO); International Game Fish Association, Dania Beach, Florida (IGFA); Institut Royal des Sciences Naturelles de Belgique, Brussels (IRSNB); Musée Royal des de l'Afrique Centrale, Tervuren (MRAC); Museum National d'Histoire Naturelle, Paris (MNHN); Naturhistorisches Museum, Wien (Vienna), Austria (NMW); South African Institute of Aquatic Biodiversity (formerly J. L. B. Smith Institute of Ichthyology), Grahamstown (SAIAB); Scripps Institution of Oceanography, La Jolla (SIO); Florida Museum of Natural History, Gainesville (UF); National Museum of Natural History, Washington, D. C. (USNM); Universität Hamburg (ISH, ZMH); Zoological Museum, University of Copenhagen (ZMUC).

Parenthetical expressions in material examined include number of specimens, if more than one, followed by the size range in millimeters fork length (FL); cleared and stained specimens are indicated as "C&S." Localities are abbreviated and listed only by major geographic areas for *Caranx caninus* and western Atlantic *C. hippos*. Except for those given in the scatter plots, measurements are of limited value in distinguishing members of the *hippos* complex (and then only for specimens >200 mm FL). Total lengths (TL) are given when that was the only length measurement reported in cited references. All measurements are in mm unless specified as cm. Measurements expressed

in percent fork length or head length, are given only in the description of the new species *Caranx fischeri*. Fork length is measured from the front of the upper lip to the tip of shortest median caudal-fin ray. Body depths are measured from the anterior base of the spinous dorsal fin (D10) to the origin of the pelvic fin (P20) and from the anterior base of the spine at the origin of the dorsal-fin lobe (D20) to the anterior base of the anal-fin spine at the origin of the anal-fin lobe (A20). Lengths of the dorsal- (D2) and anal-fin (A2) bases are straight-line measurements from either the D20 or A20 to the posterior base of the terminal fin ray of the respective fin. Head length is measured from the front of the upper lip to the posterior end of the opercular flap. Snout length is measured from the anterior end of the upper lip to the anterior edge of the eye. Eye diameter is the greatest bony diameter. Upper jaw length is taken from the anterior end of the upper lip to the posterior end of the maxilla. The curved part of the lateral line is measured as a chord (straight-line distance) of the arch extending from the upper edge of the opercle to its junction with the straight part; the straight part of the lateral line is measured from its junction with the curved part to its termination on the caudal-fin base (end of last scute). Scutes are defined as scales that have a raised horizontal ridge or a small to moderate projecting spine on the posterior margin ending in a point not exceeding a 120° angle; for detailed description and illustrations of scute formation and development in *Caranx crysos* (Mitchill) see Berry (1960). All scutes were counted, including those extending onto the caudal-fin base. Pectoral-fin ray counts do not include the dorsal-most spine-like element. Gill raker counts are from the first gill arch (usually on the right side), and the raker at the angle is included in the lower-limb count; rudimentary gill rakers, with the diameter of their bases greater than their height, are defined as tubercles or short rakers. The anterior dorsal-fin pterygiophore formula indicates the interdigitation pattern of supraneurals and pterygiophores within interneural spaces; neural spines are indicated by slashes, supraneural (predorsal) bones by an "S," pterygiophores by "2" (pterygiophores with two supernumerary rays and a serially associated ray) or "1" (no supernumerary ray and one serially associated ray).

Results

Taxonomy and distributions

Some recent authors (Amezcu-Linares, 1996; Randall, 1996; McBride and McKown, 2000) still follow Briggs (1960) in erroneously reporting a worldwide distribution in tropical and subtropical latitudes for *Caranx hippos*, although Nichols (1920) had correctly concluded that records of the species from the Indian and western Pacific oceans were based on misidentifications. Other authors (Talwar and Kacker, 1984; Krishnan and Mishra, 1994; Mishra et al., 1999; Khan, 2003;

¹ Eschmeyer, W. N. Catalog of fishes, on-line edition. Website: <http://www.calacademy.org/research/ichthyology/catalog/> (accessed June 2006).

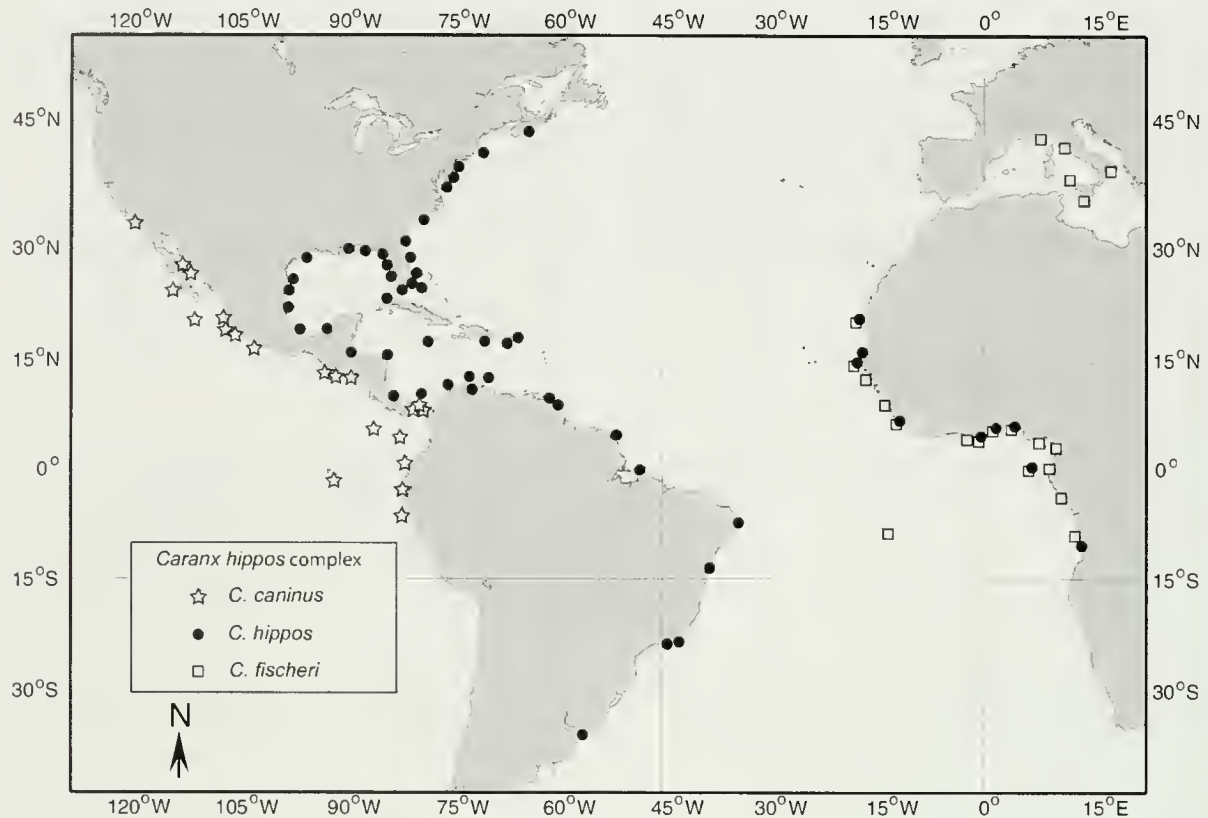


Figure 2

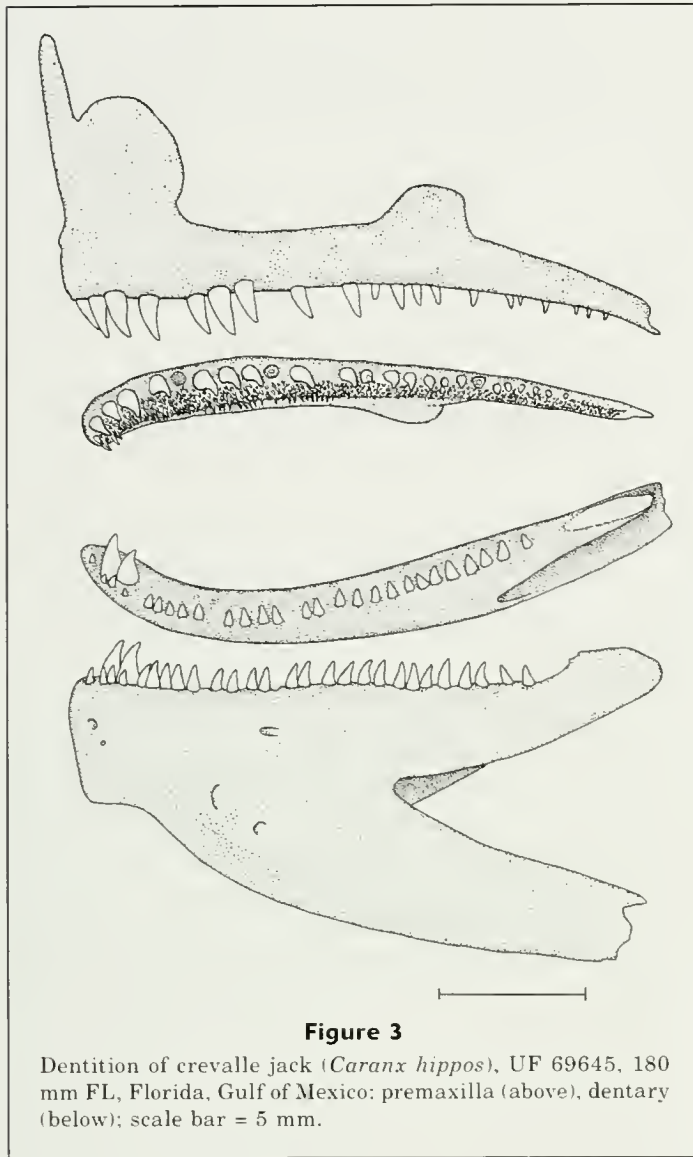
Distribution of members of the crevalle jack (*Caranx hippos*) complex: (Mediterranean locality records for longfin crevalle jack (*C. fischeri*) are based solely on literature reports; discussion of geographic distribution appears in individual species accounts).

Mishra and Krishnan, 2003) reported *C. hippos* as *C. carangus* (Bloch) from the Indian Ocean based on misidentifications of *Caranx heberi* (Bennett). What was once considered to be a single widespread species is herein recognized as consisting of three species (Fig. 2). For almost a century, most ichthyologists and fishery biologists who have worked on West African crevalle jacks have failed to distinguish the new species *Caranx fischeri* described herein from *C. hippos*, although both species are commonly taken together.

Adults of *Caranx hippos* from opposite sides of the Atlantic Ocean are indistinguishable externally but exhibit consistent differences in the degree of development of the hyperostosis in the first dorsal-fin pterygiophore and neural spines of some of the anterior vertebrae (see "Geographic variation" in *C. hippos* species account). Although we consider these predictable ontogenetic and consistent site-specific patterns obvious evidence of genetic divergence associated with bone metabolism, an important consideration is the unknown functional significance of hyperostosis. In light of this, we believe it would be premature to recognize the eastern Atlantic population of *C. hippos* as taxonomically distinct. No formal change in classification should be made in the absence of collaborative molecular data.

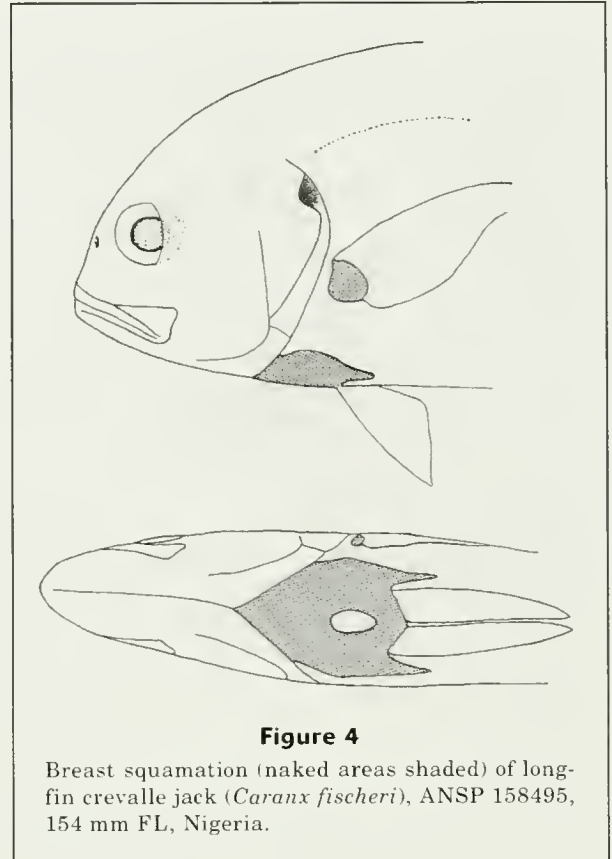
The *Caranx hippos* complex

The *C. hippos* species complex can be diagnosed by the following combination of characters: a pair of strong symphyseal dentary canines (Fig. 3); breast naked ventrally except for a small oblong patch of prepelvic scales (Fig. 4) which forms at about 30 mm FL; rounded black blotch on the lower rays of the pectoral fin in adults; large black opercular spot; and vertebrae 10 precaudal + 14 caudal. Only the black blotch on the pectoral fin is unique to these species. Adults of the horse-eye jack, *Caranx latus* Agassiz, occasionally have a somewhat similarly placed dusky blotch on the pectoral fin (although the dark area is different in character and never as well defined as in *C. hippos*), and this similarity in appearance has occasionally resulted in field misidentifications, especially by scuba divers unfamiliar with both species. The typical breast squamation pattern of the *C. hippos* species complex is not duplicated in any other Atlantic or eastern Pacific species of *Caranx*, although it occurs in three Indo-west Pacific species: commonly in *C. ignobilis* (Försskål) and *C. papuensis* Alleyne and Macleay, and less frequently in *C. heberi*. Dentition has been used as an important diagnostic character of carangid genera, but comparison of the dentition of a large number of



carangid species reveals an almost complete continuum of dentition types that in some cases does not agree with traditional generic assignments. In all members of the *C. hippos* complex the upper jaw has an outer row of strong canines (widely spaced in adults) and an inner band of small villiform teeth that is widest anteriorly. The lower jaw has a single row of strong conical teeth that are smaller anteriorly, and one or two pairs of noticeably enlarged inner symphyseal canines. Enlarged symphyseal dentary canines are absent in the following species of *Caranx*: *C. crysos*, *C. caballus* Günther, *C. melampygus* Cuvier, *C. papuensis*, and *C. senegallus* Cuvier. Gill (1862) proposed the genus *Paratractus* for *Caranx pisquetus* Cuvier, a junior synonym of *C. crysos*, primarily because of the absence of symphyseal canines.

Some recent authors follow Randall (1996) in assigning several common Atlantic carangids to the genus *Carangoides* Bleeker, but we maintain traditional usage for reasons given by Smith-Vaniz et al. (1999, p. 237).



Hyperostosis in *Caranx* species

Hyperostosis appears to have been an integral part of the evolutionary history of the *Caranx hippos* complex, but the pattern of expression is surprisingly different in each species (Table 1). Hyperostosis involves the expansion or swelling of certain bones into globose, gall-like structures characterized by cellular bone foci and bone-resorbing osteoclasts.

In most carangids the condition is usually apparent only in relatively large individuals (but can be detected histologically in smaller individuals) and the onset in different bone foci is typically sequential rather than simultaneous. A large number and size range of individuals of each species usually must be examined before the ontogenetic pattern can be precisely determined. Although Smith-Vaniz et al. (1995) were unable to determine the functional significance of hyperostosis, they found no histological evidence of hyperostosis as a pathologic condition and concluded that the intraspecific predictability and site-specificity of hyperostosis in a taxonomically diverse group of marine fishes was indicative of genetic control.

A detailed description of hyperostosis in *Caranx* is beyond the scope of this article, but to appreciate the context of its site-specificity and distribution in the *C. hippos* complex we briefly discuss its known occurrence in the genus. We found no evidence of hyperostosis in adults of six species: *C. heberi*, *C. ignobilis*, *C. lugubris*

Table 1

Comparison of hyperostosis in the *Caranx hippos* species complex. Sizes are minimum fork length at which hyperostosis is usually developed in all individuals.

Hyperostotic bones	<i>C. fischeri</i> (E. Atlantic)	<i>C. hippos</i> (E. Atlantic)	<i>C. hippos</i> (W. Atlantic)	<i>C. caninus</i> (E. Pacific)
Posttemporal	yes >20 cm, Fig. 5	none	none	none
Cleithrum	none	well-developed, >35 cm Fig. 10	well-developed, >35 cm Figs. 9, B-C	none
Neural spines	none	slight, 56 cm	well-developed, >40 cm Figs. 9, B-C, 13	none
Pleural ribs	well-developed >34 cm (usually ribs 5-7), Figs. 5, B-C	slight, 56 cm (ribs 6-8)	well-developed, >38 cm (usually ribs 6-8), Figs. 9, B-C	none or 5th rib only, Fig. 14A (in 6 of 16 spec. >34cm)
Pelvic girdle	none	well-developed, 56 cm	well-developed, >50 cm	well-developed, >45 cm
1st pterygiophore of dorsal fin	none Figs. 5, 11	slight, Figs. 10, 11, 12A	well-developed, Figs. 9, 11, 12B	well-developed, Figs. 11, 14
1st pterygiophore of anal fin	none not convex anteriorly convex anteriorly,	none not convex anteriorly	none not convex anteriorly, Fig. 15	well-developed, >40 cm Figs. 14, 15

Poey, *C. melampygus*, *C. papuensis*, and *C. tille* Cuvier. In addition to *C. fischeri*, hyperostotic posttemporal bones are present in large individuals of the blue runner (*C. crysos*) and green jack (*C. caballus*) allopatric species that are possibly conspecific. *Caranx hippos* is exceptional in that the neural spines of at least vertebrae 6-12 are hyperostotic in large adults. The ventral end of the cleithrum is hyperossified in large *C. hippos*, *C. latus*, and *C. sexfasciatus*, but the shape of the hyperossification is noticeably different (wider and shorter) in the latter two species, which also differ from *C. hippos* in having two separate regions of hyperostosis on the cleithrum. The pelvic bones are hyperossified only in *C. hippos* and *C. caninus*. In large adults of *C. caninus* and western Atlantic *C. hippos* the first pterygiophore of the spinous dorsal fin becomes so enlarged that it resembles an oblong swollen fruit; but see discussion of geographic variation associated with hyperostosis of this pterygiophore in *C. hippos* species account. Even in small individuals of both species (where no pterygiophore swelling is evident), this bone is noticeably wider in lateral profile than in similar size individuals of *C. fischeri*, a species that never develops hyperostosis in this pterygiophore. The only site of hyperostosis in *C. senegallus* (largest specimen examined was 30 cm FL) is the posterior part of the supraoccipital crest. Hyperostosis is extensive in *C. bucculentus* Alleyne and Macleay and includes the entire supraoccipital crest, first supraneural, first pterygiophore of the dorsal and anal fins, and a pair of patches on the caudal fin near its base. The ribs on precaudal vertebrae 5-7 (*C. fischeri*) or 6-8 (*C. hippos*) exhibit extensive hyperostosis in relatively large individuals, but *C. fischeri* differs in that only the distal half of each rib is hyperossified. The only apparent contradiction to the consistent site

specificity of hyperostosis in the *C. hippos* group is the pattern of occurrence seen on ribs of *C. caninus*. Ribs of the fifth precaudal vertebra appear "normal" in nine specimens (359-643 mm FL), are strongly and uniquely hyperostotic in six others (335-431 mm FL), and in SIO 65-176A (670 mm FL) there is a slight but noticeable swelling only in the middle part of the rib. Even more unexpectedly, in two of six individuals only one rib of these bilaterally paired structures was strongly hyperostotic and its counterpart rib exhibited no hyperostosis.

Caranx carangopsis Steindachner, described from mid-Miocene deposits near Vienna, Austria, also deserves mention. Heckel (1852) recognized the distinctiveness of this fossil species and gave it a scientific name, but the subsequent description was prepared entirely by Steindachner (1859) who must be credited as author of the species. The original description is based on an incomplete series of disarticulated bones, some of which are clearly hyperostotic, from several individuals estimated to have been about 0.9 meters in length. The scientific name refers to the presumed close relationship of this fossil species to *C. carangus* (= *C. hippos*)—a relationship based, in part, on the occurrence of hyperostotic bones (including the ribs, some of the vertebrae, and the first dorsal-fin pterygiophore) in both species. The text descriptions and illustrations of the massively swollen first pterygiophore and pleural ribs of *C. carangopsis* agree reasonably well with those of western Atlantic *C. hippos*, but do not resemble that characteristic of eastern Atlantic *C. hippos*. Steindachner's (1859) accurate description (footnote on p. 690) of the swollen neural spines of the vertebrae in a 1220 mm TL *C. carangus* (= *C. hippos*) also contrasts sharply with his illustrations (pl. 7, Figs. 1-3) of the very differ-

ent thickened vertebrae of *C. carangopsis*. These fossil vertebrae are similar to those of hyperostotic *Trachurus trachurus* Linnaeus (see Desse et al., 1981), suggesting that the original description of *C. carangopsis* is likely based on material (deposited at NMW) from two carangid genera.

Biology, fisheries, fish size, and edibility

Remarkably little information has been published on the biology of members of the *Caranx hippos* complex. Both Kwei (1978) and McBride and McKown (2000) discussed the importance of estuaries as nurseries for juvenile *C. hippos*, and such importance undoubtedly also applies to the other species. The former work is a comprehensive reference on the biology and fisheries of the "crevalle jack" in West Africa; unfortunately no photographs or meristic data were included that can be used to confirm the identification of species. *Caranx hippos* may well have been the most abundant species in the study, but *C. fischeri* is also very common in the region and almost certainly was included in some of the samples.

Noting the occurrence of smallest juveniles in his study, Berry (1959) stated that off the southeastern Atlantic coast of North America spawning probably occurred offshore from March to September. Kwei (1978) reported juveniles present in Ghanaian lagoons (Keta region) during every month of the year and re-entering the sea at sizes ≥ 12 cm FL. Large shoals of *Caranx* entered Ghanaian inshore waters from September to December, spawning appeared to be protracted, and peak spawning activity (determined from limited data) occurred from October to late January. Low frequency of ripe fish from inshore waters indicated that spawning occurred offshore. Thompson and Munro (1983) reported collecting seven "ripe" *C. hippos*, four males and three females, in the vicinity of Jamaica. The smallest ripe males and females were 55 and 66 cm FL, respectively. Adults were found occasionally in reef habitats and reproductively active fish were taken in May, July, and November. Hildebrand (1939) recorded seven females (67–98 cm TL) with large or developing roe and 11 males (69–88 cm TL), most with developed testes, during 20–24 February 1935 from Gatun Locks, Panama Canal. McBride and KcKown (2000) reported young-of-the-year *C. hippos*, < 4.0 cm FL, present in subtropical estuaries (North Carolina to Florida) from June to November and discussed literature indicating that 9°C was likely the lower lethal temperature for the species. Franke and Acero (1993) suggested that *C. caninus* spawns throughout the year, peaking in January–February and August. Examining 96 specimens, they reported a 1:1 sex ratio, and the smallest mature males and females were 67 and 65 cm TL, respectively.

All species of the crevalle jack complex are major predators of small schooling fishes in coastal areas. In the western Atlantic (Florida, Louisiana, and Texas), Saloman and Naughton (1984) reported that small jacks fed primarily on clupeids and larger fish fed usually on clupeids, carangids, and sparids, but penaeoid

shrimps, crabs, and other invertebrates were also consumed. Clupeids (*Sardinella* and *Engraulis*) were also the dominant prey of *C. hippos* in the Gulf of Guinea, and juvenile shrimps contributed 50–80% of the diet of juvenile fish during the dry season (Kwei, 1978).

Most commercial landings of crevalle jack in the western Atlantic are from Florida, and annual catches of 221 to 320 t (metric tons) were recorded during 2000–2004 (NMFS²). In the eastern Atlantic, where data for *C. hippos* and *C. fischeri* are combined under "crevalle jack," commercial landings are reported only from Angola, Ghana, São Tome, and Principe, and for years 1995–2004 ranged from 2233 to 10,054 t (FAO, 2006). In the Gulf of Guinea, beach seine and set net fisheries for crevalle jack historically supported a large dried or salted fish industry. Okera (1978) reported *C. hippos* (as *C. carangus*) to be one of the dominate pelagic species in the beach seine fishery at Lumley, Sierra Leone, and that 80–100 cm TL fish were most common during September–October. Catches from Ghana in the mid 1950s to early 1960s and from Angola in the 1970s exceeded 15,000 t during some years, but such large catches no longer occur (FAO statistical data in Froese and Pauly³).

With regard to fighting ability of the crevalle jack, Shipp (1986) stated "there is no tougher game to be had in shallow coastal waters with light tackle than this species." *Caranx hippos* is more important in recreational fisheries in the United States (statistics based only on Atlantic Coast, Gulf of Mexico, excluding Texas and Puerto Rico) and for years 2000–2004 annual catches ranged from 409 to 1030 t (NMFS²). Recreational fishing also occurs in West Africa for both *C. hippos* and *C. fischeri* (Schratwieser⁴).

The IGFA All-Tackle world-record *C. hippos*, from Barra do Kwanza, Angola, was caught in December 2000, weighed 26.5 kg (58 lb 6 oz) and was 114 cm FL and 129 cm TL; several other fish almost as large have also been recorded from West Africa. One *C. fischeri* caught at Ozouri Zimbani, Gabon, in January 1989, weighed 20.9 kg, and was approximately 100 cm FL and 127 cm TL. An even larger one (see Fig. 8C), released without being measured or weighed (est. weight 26 kg) was caught in Loango National Park (Iguela Lagoon mouth), Gabon, in December 2005. The IGFA All-Tackle world-record *C. caninus* was caught at Playa Zancudo, Costa Rica, in March 1997, weighed 19.7 kg, and was 101.6 cm TL.

Crevalle jacks are strong fast-swimming predators with large quantities of red muscle and consequently

² NMFS (National Marine Fisheries Service). 2006. Fisheries Statistics Division. Website: <http://www.st.nmfs.gov/st1/> (accessed August 2006).

³ Froese, R., and D. Pauly, eds. FishBase world wide web electronic publication. Website: <http://www.fishbase.org> version (07/2006) (accessed August 2006).

⁴ Schratwieser, J. 2006. Personal commun. International Game Fish Association, 300 Gulf Stream Way, Dania Beach, Florida, 33004.

their flesh is generally considered coarse and relatively unpalatable. Small individuals are more flavorful and bleeding immediately after capture is recommended. According to Shipp (1986), some of the better seafood cooks make delectable marinated specialties using *C. hippos*.

Caranx fischeri, new species

Longfin crevalle jack

(Figs. 1A, 4–7, 8, A–C, 11; Tables 1–4)

Caranx hippos (not of Linnaeus): Clark, 1915:385 (listed; Ascension Island); Fowler, 1919:254 (brief description; not distinct from American examples); Norman and Irvine, 1947:140, Fig. 65 (biology; artisanal fishery; Ghana); Tortonese, 1952:302, Figs. 11–12 (description; Mediterranean specimens and records); Franca, 1954:24, pl. 3 Figs. 2–3 (description; Luanda, Angola); Poll, 1954:131, Fig. 37, pl. 4, Figs. 1 and 3 (description); Cadenat, 1960:1392 (compared with "*C. carangus*"=*C. hippos*); Cadenat, 1961:240 (listed); Bauchot and Blanc, 1963:43, Fig. 2c (in part, composite description, also includes *C. hippos*; distribution); Daget and Stauch, 1968:40 (listed; Congo); Williams, 1968:252 (maximum reported size 75 cm); Blache et al., 1970:313, Fig. 818 (identification key; distinguished from "*C. carangus*"=*C. hippos*); Daget and Ittis, 1965:238, Fig. 152 (description; Ivory Coast); Tortonese, 1975:156, Fig. 64 (description; Mediterranean records, after Tortonese, 1952); Okera, 1978:85 (beach seine fishery, occasionally taken with "*C. carangus*"=*C. hippos*; Sierra Leone); Smith-Vaniz and Berry, 1981: unpaginated; Fig. (in part, composite description; distribution); Bianchi, 1986:49, Fig., color pl. II, Fig. 10 (habitat; biology; fisheries utilization; Angola); Smith-Vaniz, 1986:824, Fig. (in part, composite diagnosis; habitat; distribution); Bellemans et al., 1988:46, Fig., color pl. 2, Fig. 10 (local names; habitat); Papaconstantinou, 1988:95 (compiled; Greek seas); Edwards and Glass, 1987:1377 (unconfirmed records, St. Helena); Edwards, 1990:97, Fig. 48 (compiled description; unconfirmed occurrence at St. Helena); Smith-Vaniz et al., 1990:732 (in part, composite synonymy; distribution); Afonso et al., 1999:73 (listed; Gulf of Guinea); Bilecenoglu et al., 2002:84 (Aegean and Turkish seas; compiled); Edwards et al., 2003:2238 (J. R. Irvine's Ghanaian specimens).

Caranx carangus (non Bloch): Ehrenbaum, 1915:65 (misidentification, in part, Fig. of *C. hippos* after Goode, 1984; description; Cameroon); Chabanaud and Monod, 1927:18, Fig. 24 (listed, rare; Port Etienne, Mauritania); Collignon et al., 1957:192, Fig. 47 (brief description).

Holotype ANSP 140256 (328 mm FL), Cameroon, Douala, 22 Aug 1978, obtained by P. J. P. Whitehead.

Paratypes One-hundred twenty-eight specimens (33–530 mm FL) from 56 collections. SENEGAL:

IRSNB 829 (530), Dakar, Madeleine Island, 9 Nov 1949, G. Marlier; MNHN 1978-260 (313), coast of Senegal. GUINEA: ISH 163/62 (227), 9°45'N, 13°55'W, 17 m. SIERRA LEON: ANSP 158497 (237), Freetown, 8°29'24"N, 13°11'30"W, 6 m, hook and line, 9 Feb 1968, RV *Undaunted* Cr. 6801, G. Beardsley; ANSP 158498 (239), 7°07'N, 11°57'30"W, 18–21 m, Guinea Trawling Survey I, RV *La Rafale*, Trans. 12, sta. 1, 13 Nov 1963; BMNH 1928.8.3.14 (164.5), "Sierra Leone," J. Hornell; USNM 279566 (2, 163–203), St. Anne Banana Islands, 15–25 m, Feb 1986, G. Naylor. LIBERIA: USNM 193784 (121), Mesurado River beach, 6°19'N, 10°48'W, 24 May 1952, G. C. Miller; USNM 193790 (148) and USNM 193792 (102), Mesurado River beach, 20 Jun 1952, G. C. Miller; USNM 193779 (2, 148–163), Monrovia, Freeport, 5 May 1953, G. C. Miller. IVORY COAST: MNHN 1978-200 (253). GHANA: BMNH 1930.8.26.49-50 (2, 91–139), Accra, Mar 1930, F. R. Irvine (Irvine 53); BMNH 1938.12.15.48 (114), Volta River, Amedica, May 1938, F. R. Irvine (Irvine 237); BMNH 1939.7.12.12 (271), Prampram, Sep 1938, F. R. Irvine (Irvine 316); CAS-SU 64645 (118), Volta River; CAS-SU 64648 (124), Lower Volta River, Jun–Jul 1963, W. Titiati; CAS-SU 64700 (69), Battor River, 2 Mar 1964, T. R. Roberts; CAS-SU 66674 (41), Volta River at Amedia, 8 Mar 1963, T. R. Roberts; CAS-SU 69861 (2, 35–40), mouth of Volta River at Little Ada, 12 Jan 1963, T. R. Roberts; USNM 373240 (17, 33–52), Volta River at Big Ada, 9 Mar 1960, G. W. Bane; USNM 300660 (113), Tema Nunga, 18 May 1962, G. W. Bane; USNM 373242 (22, 37–52), beach at Tema fishing harbor, 15 Dec 1959, G. W. Bane; USNM 365702 (16, 71–90), Dix Cove Amaful, 25 Jan 1961, G. W. Bane; USNM 373244 (56), Ahiaho River W. of Amanful. Takoradi, 4 Feb 1961, Amegah; USNM 368973 (3, 49–88), Ashantee, Beyah River, 27 Nov 1889, W. H. Brown, U.S. Eclipse African Exped. TOGO: ZMH 14575 (155), lagoon near Anecto, "Dr. Liebl," summer 1909. BENIN: MNHN 1967-826 (198), 6°15'N, 2°38'E, 23 m, 27 Jul 1964, A. Crosnier and J. Marteau. NIGERIA: BMNH 1968.11.15.31-32 (2, 85–169), Lagos Lagoon, 1967, S. O. Fagade; ANSP 158495 (3, 154–163), 4°15'N, 6°49'E, 15 m, Guinea Trawling Survey II, RV *Thierry*, trans. 43, sta. 1, 5 Apr 1964; CAS 38373 (135), 6°21'N, 2°54'E, 15 m, Guinea Trawling Survey II, RV *Thierry*, trans. 36, sta. 1, 19 Mar 1964; CAS 38375 (2, 145–160), 4°28'N, 5°07'E, 19 m, Guinea Trawling Survey II, RV *Thierry*, trans. 41, sta. 7, 2 Apr 1964; CAS 38395 (2, 146–150), 5°15'N, 5°09'E, Guinea Trawling Survey II, RV *Thierry*, trans. 40, sta. 1, 30 Mar 1964; ISH 1147/64 (145), 5°09'N, 4°39'W, 20 m; ZMUC P.46362 (450), Bonny River, 22 Feb 1946, "Atlantidae" sta. 111; MNHN 1896-327 (153), Campagne Touree; BMNH 1956.9.6.68 (183), Lagos Tarkwe, F. Williams. CAMEROON: ANSP 140288 (156), Victoria, 23 Aug 1978, FAO; BMNH 1936.12. 29.7 (172), Victoria, Cross River; D. Tovey; CAS-SU 15883 (2, 41–44), Bwanjo, Bwanjo River, 15 Sep 1936, A. I. Good; CAS-SU 15884 (150), Kribi, 25 Oct 1938, A. I. Good; CAS-SU 15885 (171), Kribi, 23 Feb 1940, A. I. Good; CAS-SU 18221 (77), Mbode, 23 Dec 1940, A. I. Good; CAS-SU 18222 (82), Kribi, Kribi River, 24 Sep

1940, A. I. Good; CAS-SU 64900 (70), Kirbi, Kirbi River, 23 Nov 1940, A. I. Good; MNHN 1978-336 (147), Depierre; MNHN 1982-1093 (117), Yabassi, Depierre, 1980. UF 142347 (2, 144–155), 2°28'N, 9°44'E, 15–16 m, Guinea Trawling Survey II, RV *Thierry* Trans. 49, sta. 1, 25 Apr 1968; USNM 304197 (81), S. Korup at coast, Rio del Rey, 10 Mar 1988, G. M. Reid; ZMH 14576 (135), Douala, J. V. Eitzen, 1912–1913. EQUATORIAL GUINEA: ANSP 158493 (4, 173–197), Bioko (Fernando Po) 3°35'N, 9°19'E, 30 m, Guinea Trawling Survey II, RV *Thierry*, trans. 47, sta. 2, 18 Apr 1964; UF 142348 (2, 52–64), Bioko (Fernando Po), fresh water pool on SE end of island, 25 Sep 1959, G. W. Bane. GABON: CAS 38376 (197), 0°21'N9°15'E, 20 m, Guinea Trawling Survey II, RV *Thierry*, trans. 52, sta. 1, 7 May 1964; BMNH 1896.5.5.14 (102), Corisco Island, M.H. Kingsley. CONGO: BMNH 1899.2.20.3 (173), Manyanga; BMNH 1899.11.27.87 (348), Banana; M. Delhez; MRAC 36 (403), Banana, 1896, Lt. E. Wilverth; MRAC 87428 (367), Banana, 1952, Major Marée. ASCENSION ISLAND: BMNH 1927.12.7.49 (358), J. Simpson.

Other material Centro Oceanográfico de Canarias, Tenerife, uncataloged (310), Benin, trawled in 38 m, 28 Jul 2002, FAO; SAIAB 26541 (130), Gulf of Guinea between Cameroon and Bioko; SAIAB 26541 (7, 138–233), Gulf of Guinea; MNHN 1978-235 (317), coast of tropical French Africa.

Diagnosis A member of the *Caranx hippos* complex with the following combination of characters: segmented dorsal-fin rays 21–23 (exceptionally 24); segmented anal-fin rays 17–19, usually 18; posttemporal bones hyperossified in specimens larger than 20 cm FL (Fig. 5); cleithrum, first pterygiophore of dorsal and anal fins, and neural spines of vertebrae relatively slender and never hyperossified; in specimens >20 cm FL, heights of longest dorsal- and anal-fin rays both 0.7–1.3 in head length; in adults, anal-fin lobe white anteriorly and remainder of fin gray to brown.

Description Total range of values given first, followed by values for holotype in parentheses: dorsal-fin rays VIII-I, 21–24 (22); anal-fin rays II-I, 17–19 (18); pectoral-fin rays 18–21 (21); vertebrae 10 pre-caudal + 14 caudal; curved lateral-line scales 50–73 (69); straight lateral-line scales 0–16 (4); straight lateral-line scutes 24–41 (35); total scales + scutes in straight lateral line 32–47 (39); developed gill rakers 2–7 (3) upper, 14–17 (14) lower, 16–24 (17) total; rudimentary gill rakers 0–4 (4) upper, 0–3 (3) lower, 4–8 (7) total; rudimentary + developed gill rakers 20–25 (24) total.

Posttemporal bones distinctly hyperossified in specimens larger than 20 cm FL (Fig. 5); cleithrum, pelvic bone, first pterygiophore of dorsal and anal fins, and vertebral neural spines not hyperossified, the latter

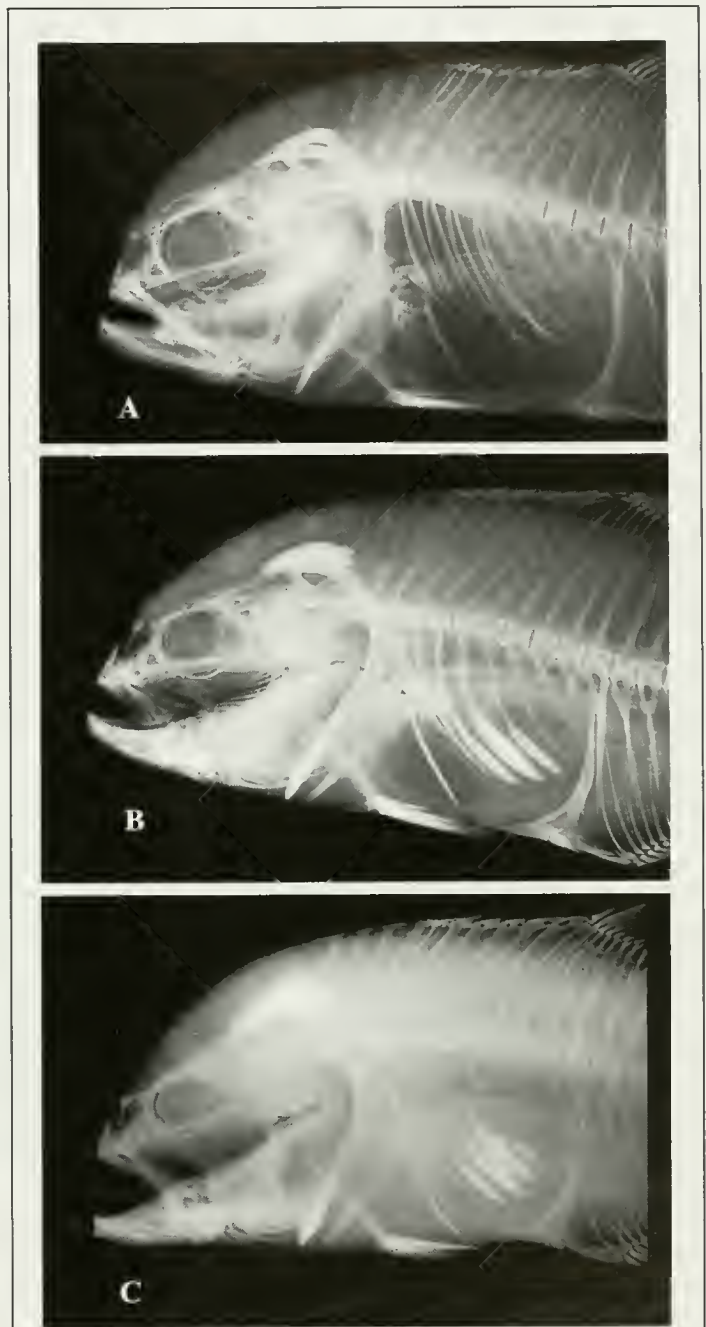
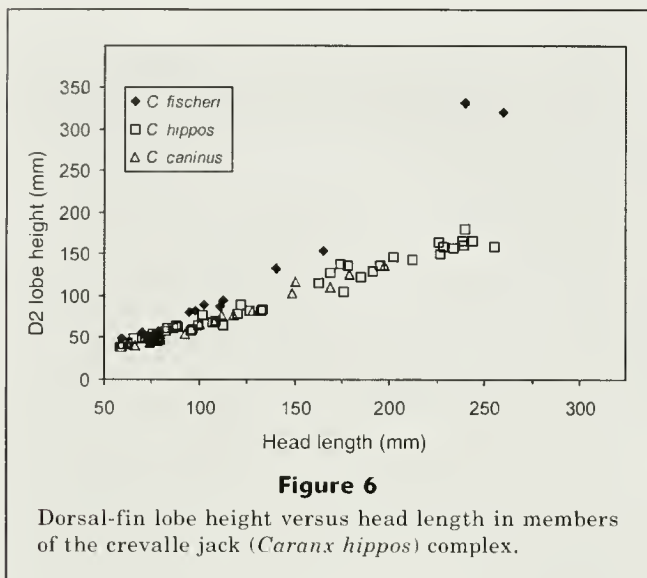


Figure 5

Radiographs of longfin crevalle jack (*Caranx fischeri*) exhibiting hyperostotic bones (pale areas of hyperostotic bones are slightly computer enhanced): (A) BMNH 1939.7.12.12, 271 mm FL, Gold Coast; (B) BMNH 1899.11.27.87, 348 mm FL, Congo; (C) ZMUZ P.46362, 450 mm FL, Nigeria.

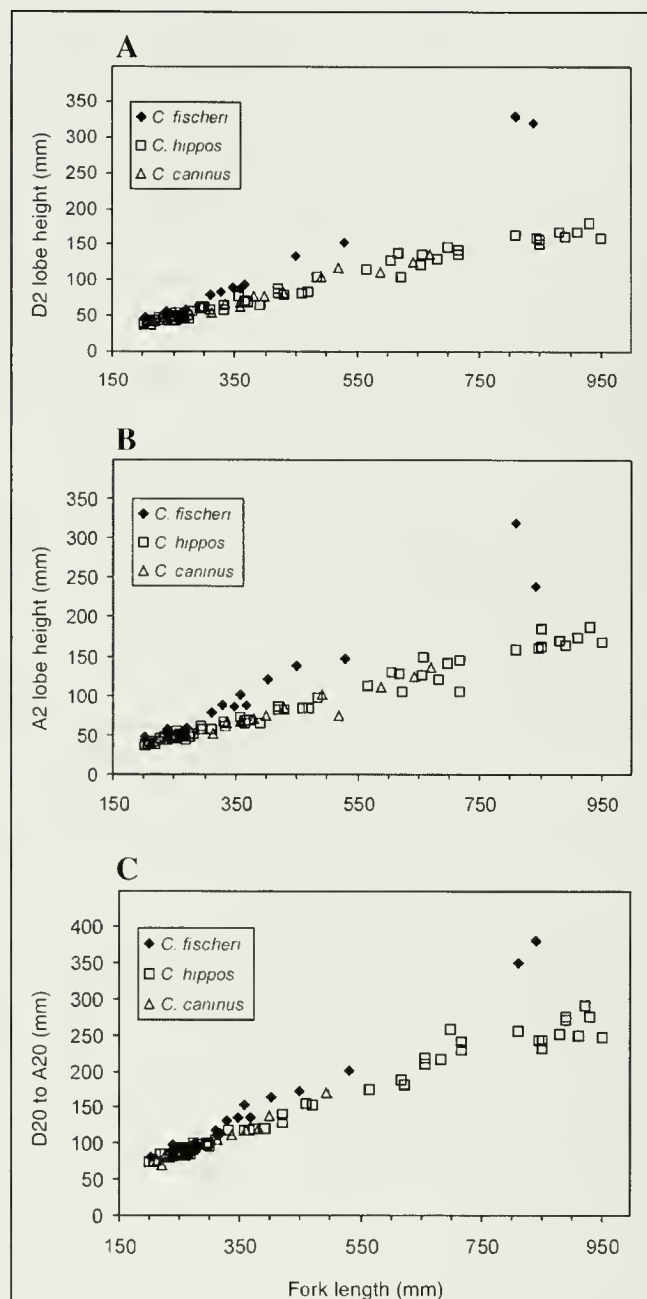
relatively slender; in specimens ≥ 34 cm FL distal half of pleural ribs of vertebrae 5–7 hyperostotic; anterior dorsal-fin pterygiophore formula S/S-S/2+1/1; supraneurals relatively robust proximally; first anal-fin pterygiophore elongated anteroventrally.



Body robust and compressed; head blunt—upper profile strongly convex, lower profile only slightly curved anteriorly; caudal peduncle slender. Breast naked ventrally to origin of pelvic fins, except for a small oval or oblong patch of scales in front of pelvic fins (Fig. 4); laterally, naked area sometimes extending slightly behind pelvic fins as a narrow wedge and always separated from naked base of pectoral fin by a narrow-to-broad band of scales; maxilla, lacrimal and dorsum of head naked; cheeks, preopercle, and opercle covered with scales; bases of dorsal and anal fins have a narrow scaly sheath anteriorly. Junction of curved and straight parts of lateral line below segmented dorsal-fin rays 5–10 (9); length of curved lateral line 0.93–1.47 (0.97) in straight lateral line. Dorsal fins well separated; first spine of spinous dorsal fin very slender and closely applied to second spine, posterior 1–4 spines partially or completely embedded in large adults; third spine longest and much shorter than height of second dorsal-fin lobe. Height of second dorsal-fin lobe 0.7–1.3 (1.2) in head length; height of anal-fin lobe 0.7–1.3 (1.1) in head length; heights of both fin lobes longer than head in large adults (Figs. 6–7). Pectoral fin of adults long and falcate, 0.8–0.9 (0.8) in head length.

Upper jaw 2.2–2.3 (2.2) in head length, extending to or slightly behind posterior margin of eye; eye diameter 4.0–6.1 (4.3) in head length, and adipose eyelid well-developed, especially posteriorly, in adults. Upper jaw with an outer row of strong canines (widely spaced in adults) and an inner band of small villiform teeth that are widest anteriorly; lower jaw with a single row of strong conical teeth that are smaller anteriorly and one (occasionally two) pair of noticeably enlarged inner symphyseal canines. Vomerine tooth patch triangular-shaped, without a median posterior extension, and sparsely covered with small teeth.

Measurements of 14 paratypes, 203–530 mm, and the holotype as percentages of FL: snout to D1O 40.7–43.9



(41.6); snout to D2O 55.7–59.8 (57.0); snout to P2O 29.8–34.3 (30.2); snout to A2O 55.5–60.2 (58.8); D1O to P2O 33.4–39.0 (35.5); D2O to A2O 35.3–42.6 (40.2); D2 base 31.2–34.1 (32.2); A2 base 28.4–32.5 (28.7); curved lateral-line length 27.6–36.0 (34.3); straight lateral-line length 32.1–43.8 (33.3); height of dorsal-fin lobe 21.6–29.6 (25.3); height of anal-fin lobe 22.7–30.6 (26.8); pelvic-fin length 13.6–15.7 (13.9); pectoral-fin length 33.7–38.7

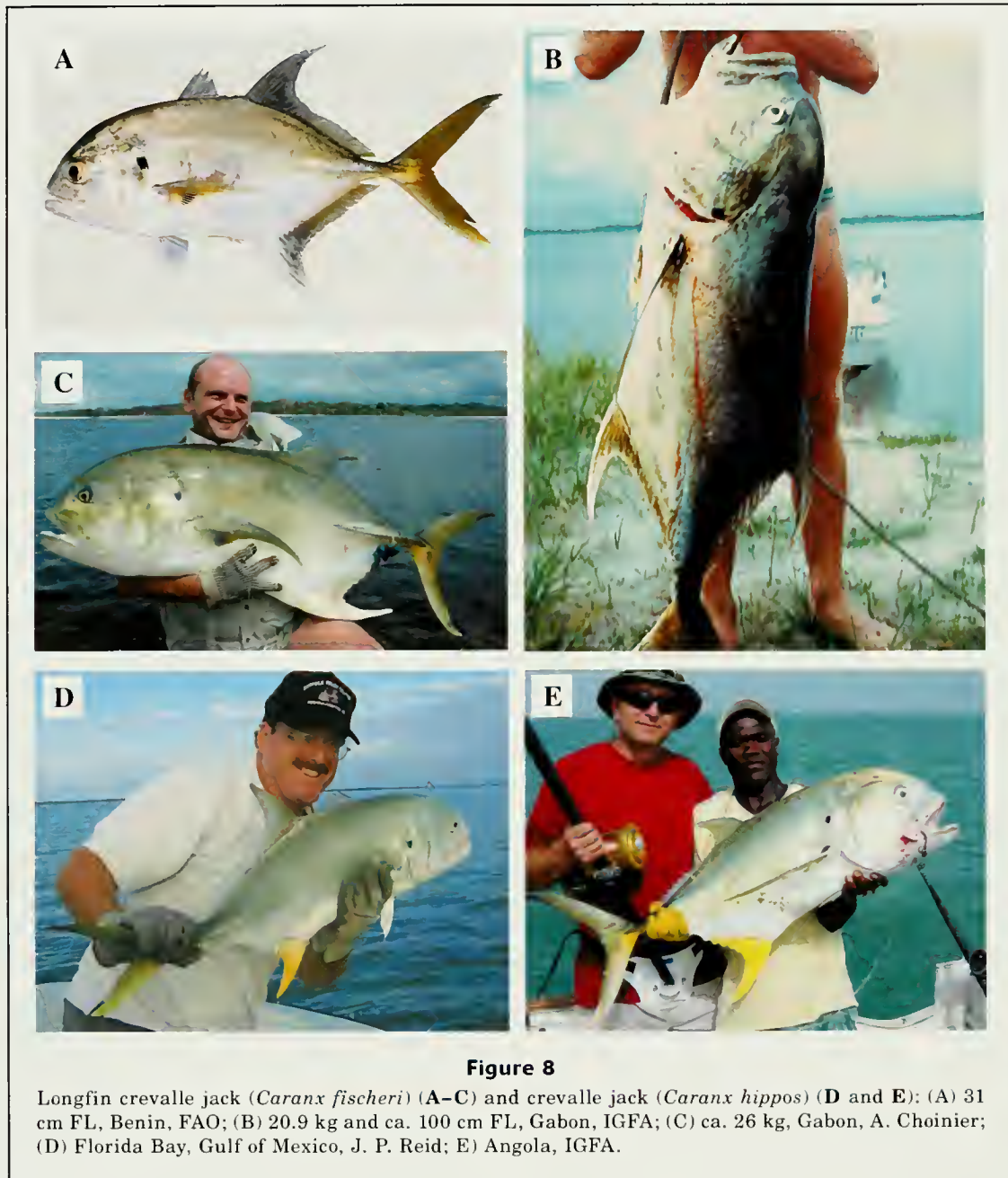


Figure 8

Longfin crevalle jack (*Caranx fischeri*) (A–C) and crevalle jack (*Caranx hippos*) (D and E): (A) 31 cm FL, Benin, FAO; (B) 20.9 kg and ca. 100 cm FL, Gabon, IGFA; (C) ca. 26 kg, Gabon, A. Choinier; (D) Florida Bay, Gulf of Mexico, J. P. Reid; (E) Angola, IGFA.

(36.4); head length 29.0–31.6 (29.9). As percentages of head length: postorbital head length 49.5–57.4 (50.5); snout length 24.4–28.4 (26.1); eye diameter 16.4–25.2 (23.1); upper jaw length 43.1–46.3 (45.2).

Fresh coloration of adults (Fig. 8, A–C) olive to greenish-blue dorsally, changing to silvery white on lower sides and ventrally; prominent black spot, approximately diameter of pupil, posteriorly on opercle at level of eye; an oval black spot on lower pectoral-fin rays and in upper axil of pectoral fins; dorsal fin dark brown; anal-fin lobe mostly white, especially anteriorly, and remainder of fin brownish-yellow; pelvic fins white and caudal fin brownish-yellow.

In preserved adults, the dark spot on the opercle and dark blotch on lower pectoral-fin rays are readily apparent, the latter on rays 6 or 7 to 14–16 (counting ventrally). The relatively pale anterior of the anal-fin lobe in comparison to the remainder of the fin is also evident. Small juveniles have five dusky bands on body; lack the dark blotch on the pectoral fin, have a heavily pigmented spinous dorsal fin and the dorsal-fin lobe is dark distally. Two juveniles, 35–40 mm FL (CAS-SU 69861) collected near the mouth of the Volta River, Ghana, had the identical pigmentation of 28 specimens of *C. hippos* (CAS-SU 64646) taken in the same collection, including some in the same size range. Berry

Table 2
Frequency distributions of segmented dorsal- and anal-fin rays in the *Caranx hippos* species complex.

Species	Dorsal-fin rays								Anal-fin rays					
	19	20	21	22	23	24	<i>n</i>	\bar{x}	16	17	18	19	<i>n</i>	\bar{x}
<i>C. fischeri</i>			31	93	10	1	135	21.9		17	104	14	135	18.0
<i>C. hippos</i> (E. Atlantic)	28	35					63	19.6	54	9			63	16.1
<i>C. hippos</i> (W. Atlantic)	18	130	13				161	20.0	103	58			161	16.4
<i>C. caninus</i>	28	66	6				100	19.8	69	31			100	16.3

Species	Dorsal + anal rays										Pectoral-fin rays				
	35	36	37	38	39	40	41	42	43	<i>n</i>	\bar{x}	18	19	20	21
<i>C. fischeri</i>				15	18	83	13	5	1	135	39.8	1	12	57	12
<i>C. hippos</i> (E. Atlantic)	26	30	7							63	35.7	1	18	21	1
<i>C. hippos</i> (W. Atlantic)	22	79	51	9						161	36.3	3	68	50	2
<i>C. caninus</i>	25	47	22	6						100	36.1		15	38	8

(1959) included excellent illustrations of young *C. hippos* and *C. latus*. As both he and Laroche et al. (2006) discussed, small juveniles of these two species can not be distinguished solely by pigmentation. Thus, as might be expected, juveniles of *C. fischeri* and *hippos* also apparently cannot be distinguished by color pattern.

Comparisons and relationships The unique pigmentation of the pectoral fin in adults, pattern of breast squamation (a relatively small number of *C. hippos* and *C. caninus* are atypical in having the naked area of the breast continue without interruption to the pectoral-fin base), and the relatively large symphyseal dentary canines, which are shared by all members of the *hippos* complex, indicate their common ancestry. Of the three extant species, *C. fischeri* is readily distinguished by typically having more dorsal- and anal-fin rays (Table 2), and in specimens >20 cm FL the anterior dorsal- and anal-fin rays are relatively longer, and the body is deeper. The pattern of bones that exhibit hyperostosis is markedly different from that of the other species (Table 1), in neither of which is the posttemporal bone hyperossified. The anal-fin lobe is white anteriorly in adults of *C. fischeri*, in contrast to the uniformly lemon yellow lobe of *C. hippos*. Adults of *C. hippos* also differ in having the underside of the caudal peduncle bright yellow.

The presence of hyperostosis in a particular bone is presumed to be a derived condition (and conversely, the absence of hyperostosis is uninformative). On the basis of shared character states 5–6 (Table 1), *C. hippos* and *C. caninus* are considered to be sister species, and the geologically recent (~3.1 mya) rise of the Panamanian Isthmus was the likely vicariant event leading to the isolation and subsequent speciation of *C. caninus*. The common ancestor of *C. fischeri* and *C. hippos-caninus* presumably originated in the proto-Atlantic Ocean; and the sympatric occurrence of both *C. fischeri* and *C.*

hippos in the eastern Atlantic is likely indicative of an earlier phylogenetic origin.

Distribution African coast from Mauritania south at least to Moçamedes, southern Angola (Franca, 1954), and at least historically it was present in the Mediterranean Sea (Fig. 2). The collection of an adult *C. fischeri* from Ascension Island indicates at least the occasional vagrant occurrence at insular localities. Unconfirmed historical reports of *C. hippos* from both Ascension (Clark, 1915) and St. Helena (Edwards, 1990) are likely based on misidentifications, possibly of *C. fischeri*.

Tortonese (1952) discussed historical Mediterranean specimens dating from the 1890s in the Giglioli Collection and Genova Museum and he identified these specimens as *Caranx hippos*. Our efforts to locate these or recent Mediterranean specimens of *C. hippos* have been unsuccessful (see Tortonese, 1973, for status of historical fish collections in Italy). Data that Tortonese (1952) provided for two of his five specimens, as well as an accompanying photograph of one of them, confirm their identification as *C. fischeri*. We assume that all five specimens were conspecific, and all Tortonese's Mediterranean distributional records are plotted in Figure 2. Papaconstantinou (1988) and Bilecenoglu et al. (2002) cited a few additional unconfirmed literature records of *C. hippos* from the Mediterranean, which we presume were also based on misidentifications of *C. fischeri*; these records are not shown on the distribution map (Fig. 2). See discussion of probable erroneous recent photographic record of *C. hippos* from the Mediterranean in the following species account.

This species is often found in brackish water, sometimes ascending rivers. The paratype series includes collections, mostly of juveniles, from three different river drainages. In their account of *C. hippos*, Norman and Irvine (1947) quoted a secondary source as report-

ing that local fishermen say that *Afāfā* fish (probably *C. fischeri*) swim far up rivers to spawn.

Etymology We take great pleasure in naming this new species *Caranx fischeri* in honor of our friend and colleague Dr. Walter Fischer (retired) for his vision and dedication in initiating the Species Identification and Data Programme of the Food and Agriculture Organization of the United Nations (Fischer, 1989). In numerous ways this program has been an invaluable resource for marine fisheries biologists and ichthyologists generally.

***Caranx hippos* (Linnaeus, 1766)**

Crevalle jack

(Figs. 1B, 3, 6–7, 8, D–E, 9–13, 15; Tables 1–4)

Scomber hippos Linnaeus, 1766:494 (original description; Carolina; putative holotype Linn. Soc. Lond. 130 [Garden no. 16]); Wheeler, 1985:55 (type status).

Scomber carangus Bloch, 1793:69, pl. 340 (original description; Antilles; syntype ZMB 1542).

Caranx erythrurus Lacépède, 1801:58, 68 (no locality stated; based on *Caranx hippos* Linnaeus and other sources).

Caranx carangua Lacépède, 1801:59, 74 (original description; Martinique, West Indies; no type, based on a drawing by Plumier).

Caranx antillarum Bennett, 1840:282 (unnecessary replacement name for *Scomber carangus* Bloch 1793).

Caranx defensor DeKay, 1842:120, pl. 24, Fig. 72 (original description; New York; type whereabouts unknown).

Carangus esculentus Girard, 1858:168 (name only); Girard, 1859:23, pl. 11, Figs. 1–3 (description; Brazos Santiago, Texas; apparently an unnecessary replacement name for *Scomber carangus* Bloch to avoid “Strickland tautonymy” when Girard provided the new genus name *Carangus*).

Caranx hippos: Goode, 1884:323, pl. 99 (biology, edibility, distribution); Devincenzi, 1924:215, pl. 232, Fig. 1 (description; Rio de la Plata, Uruguay); Hildebrand, 1939:26 (sexual maturity; Panama Canal); Ginsburg, 1952:93, pl. 5, Fig. C (synonymy; description; distribution; Gulf of Mexico); Berry, 1959:503, Figs. 81–85 (juvenile description); Postel, 1959:157 (listed; Mauritania); Bauchot and Blanc, 1963:43 (composite description, also includes *C. fischeri*; distribution); Vergara, 1972 (osteology and relationships of Cuban *Caranx* spp.); Menezes and Figueiredo, 1980:4, Fig. 4 (brief description; Brazil); Smith-Vaniz and Berry, 1981:unpaginated (in part; composite description; distribution); Uyeno et al., 1983:332, color photo (description, Suriname); Shipp, 1986:118, Fig. 133 (habits; edibility; Gulf of Mexico); Scott and Scott, 1988:376 (Canadian occurrence); Smith-Vaniz et al., 1990:732 (composite synonymy; distribution); Cervigón, 1993:63, Figs. 24–25 (description; distribution; Venezuela); Randall, 1996:142, Fig. 173 (brief description; Caribbean); Murdy et al., 1997:165, Fig.

151 (description distribution; ecology; Chesapeake Bay); Debelius, 1997:159, unnumbered color Fig. (Balearic Islands, Spain; locality probably erroneous); Smith-Vaniz et al., 1999:238 (erroneous occurrence records; Bermuda); McBride and McKown, 2000:528 (seasonal dispersal patterns of juveniles between subtropical and temperate habitats; east coast of North America); Brito et al., 2002:220 (misidentification of *C. latus*; Canary Islands); Klein-MacPhee, 2002:415, Fig. 222 (description; early life history; Gulf of Maine); Laroche et al., 2006:1462, Figs. (early stages; early postflexion larvae indistinguishable from *C. latus*).

Carangus hippos: Jordan and Evermann, 1902:306, unnumbered photograph (color description; “everywhere a food-fish of considerable importance”).

Caranx hippos tropicus Nichols, 1920:45 (original description; Para, Brazil; holotype AMNH 3889).

Caranx africanus (not of Steindachner): Poll, 1954: pl. 4, Fig. 4 (misidentification; Banana, Congo).

Caranx carangus: Cuvier and Valenciennes, 1833:91, pl. 57, Fig. 2 (description); Duméril, 1861:262 (listed; Gorée); Steindachner, 1870:704 (Senegal); Peters, 1877:836 (listed; Congo); Pellegrin, 1907:90, Fig. 7 (Dakar); Monod, 1927:699, Figs. 16–22B (Cameroon); Cadenat, 1950:171, Fig. 103 (Senegal); Cadenat, 1960:1392 (compared with “*C. hippos*”=*C. fischeri*; Ghana and Nigeria); Williams, 1968:252 (maximum reported size 120 cm); Blache et al., 1970:313, Fig. 819 (identification key; distinguished from “*C. hippos*”=*C. fischeri*); Okera, 1978:84 (abundance in beach seine fishery; Sierra Leone).

Diagnosis This species is a member of the *Caranx hippos* complex and has the following combination of characters: segmented dorsal-fin rays 19–21; segmented anal-fin rays 16 or 17; posttemporal bones never hyperossified; cleithra hyperossified distally in adults ≥ 35 cm FL (Figs. 9, 10); first pterygiophore of dorsal fin (Figs. 11, 12) and neural spines of some vertebrae (Fig. 13) noticeably (western Atlantic) or slightly to moderately (eastern Atlantic) hyperossified in adults ≥ 50 cm FL; first pterygiophore of anal fin not hyperossified in large adults; pleural ribs 6–8 hyperossified in large adults; in specimens >20 cm FL, heights of longest dorsal- and anal-fin rays 1.3–2.1 and 1.2–2.0, respectively, in head length; anal-fin lobe and underside of caudal peduncle bright yellow in adults.

Remarks Nichols and Roemhild (1946) gave frequency counts of dorsal- and anal-fin rays for 42 specimens of *C. hippos* from the western Atlantic Ocean. Their counts of 15 anal soft rays (3 specimens) and 18 dorsal soft rays (2 specimens) were not duplicated (see Table 2) in our material that was based on a total of 161 western Atlantic and 63 eastern Atlantic specimens. Because Berry (1959, Table 21) recorded the same range of soft rays (based on 132 western Atlantic *C. hippos*) that we also recorded, we conclude that the outlier counts given in the earlier study are erroneous.

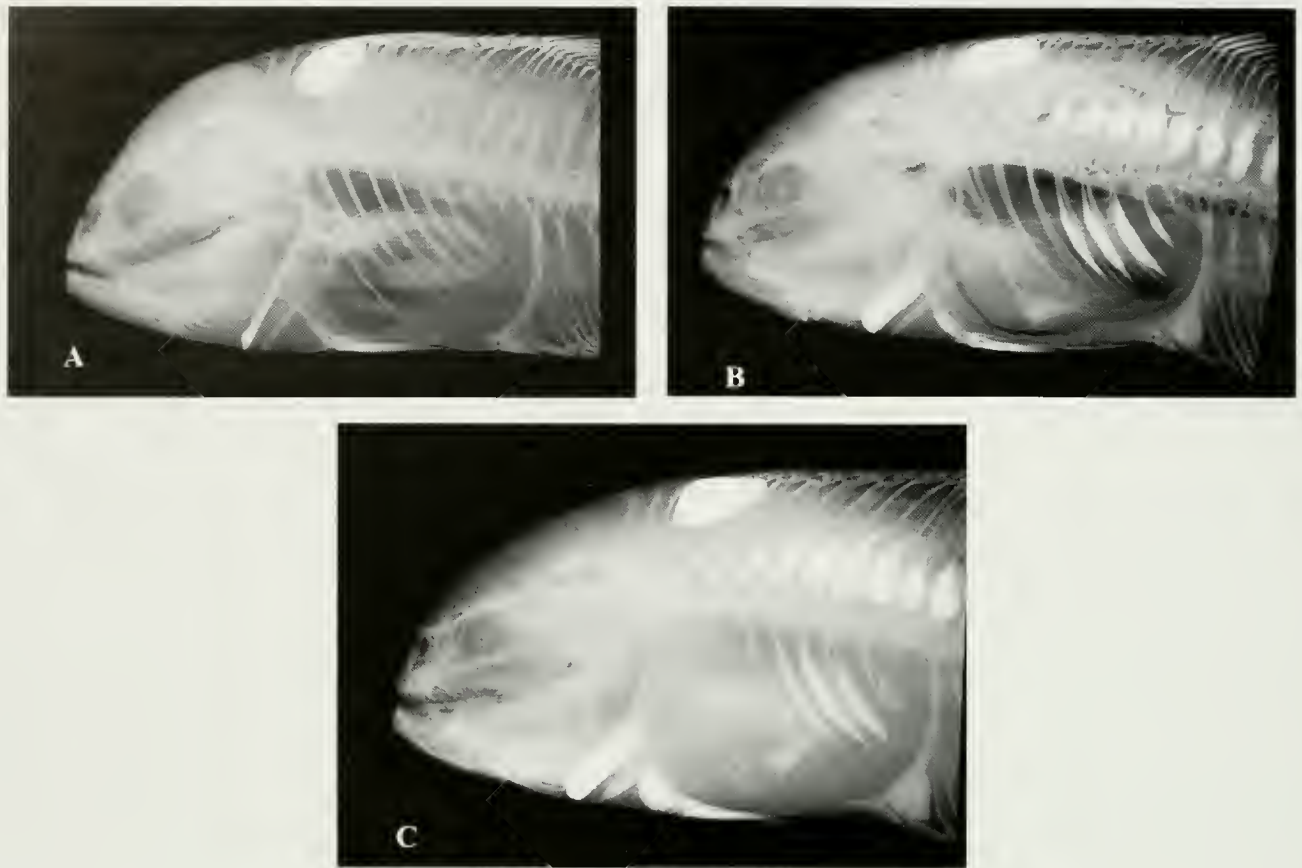


Figure 9

Radiographs of crevalle jack (*Caranx hippos*) exhibiting hyperostotic bones (pale areas of hyperostotic bones are slightly computer enhanced): (A) AMNH 58046, 274 mm FL, Brazil; (B) USNM 132964, 400 mm FL, Cuba; (C) USNM 114618, 557 mm FL, Guatemala.

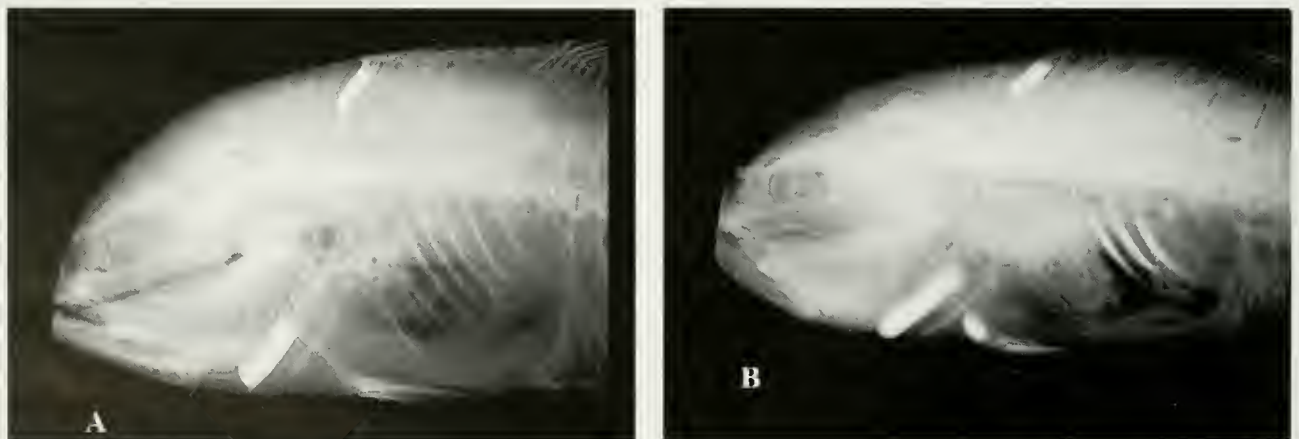


Figure 10

Radiographs of crevalle jack (*Caranx hippos*) exhibiting hyperostotic bones (pale areas of hyperostotic bones are slightly computer enhanced): (A) MNHN 1978-216, 331 mm FL, Mauritania; (B) ZMUC 25, 565 mm FL, Senegal.

Comparisons Although long confused with *Caranx fischeri*, as discussed under "Comparisons and relationships" in the account of that species, *C. hippos* is easily distinguished. However, *C. hippos* and *C. caninus* are so similar externally that many authors considered them to be taxonomically identical or only subspecifically distinct. They have broadly overlapping mensural (Figs. 6–7) and meristic values (Tables 2–4), but the pattern of hyperostosis (Table 1) is surprisingly different in the two species. They differ in four character states (Table 1, characters 2–4, 6) and share three others (Table 1, characters 5–6), although even in one of these (Table 1, character 5), the relative degree of hyperostosis is different (Fig. 11), namely the expansion of the first dorsal-fin pterygiophore being more pronounced in *C. caninus*. The color of the anal fin of a living fish is lemon yellow in *C. hippos* and is either uniformly white or brownish-orange in *C. caninus*. The underside of the caudal peduncle in adults of *C. hippos* is mostly yellow, a trait that *C. caninus* lacks.

Distribution This species is found on both sides of the Atlantic Ocean but is largely restricted to continental shelf areas (Fig. 2). In the western Atlantic it is found from Nova Scotia only as rare waifs (Scott and Scott, 1998) to Rio de la Plata, Uruguay (Devincenzi, 1924), but is absent from Bermuda (Smith-Vaniz et al., 1999) and most of the Lesser Antilles. Confirmed insular locality records based on museum specimens include those for Jamaica and the Bahamas (Andros Island), and we have photographic documentation for the Virgin Islands (St. Thomas) near the southern end of the shallow Puerto Rico shelf, where the species is relatively common. *Caranx hippos* is a regular summer visitor as far north as Woods Hole, Massachusetts (Klein-MacPhee, 2002), and young-of-the-year inhabit temperate estuaries of New York and New Jersey from July to November. McBride and McKown (2000) presented data indicating that these juveniles are spawned in subtropical latitudes and, aided by the Gulf Stream, disperse northward to coastal nurseries. Although the species is incapable of surviving the winter north of Cape Hatteras, growth rates and seasonal changes in distribution of this species indicate that some individuals successfully migrate southward to suitable over-wintering habitat and retain their potential contribution to the spawning population.

In the eastern Atlantic *C. hippos* is known from Mauritania to Angola, but historical records for the Mediterranean Sea (Tortonese, 1952, 1975) are based on misidentifications of *C. fischeri*, as presumably are additional unconfirmed records cited by Papaconstantinou (1988) and Bilecenoglu et al. (2002). The photograph (Debelius, 1997, p. 159) of a large school of adult *Caranx*, identified in the caption as *C. hippos* and stated to have been taken at the Balearic Islands, Spain, may have been a substitution and this locality record for the species could not be confirmed (Debelius⁵). Reports of *C. hippos* from the Canary Islands are based on misidentifications of *C. latus*; and

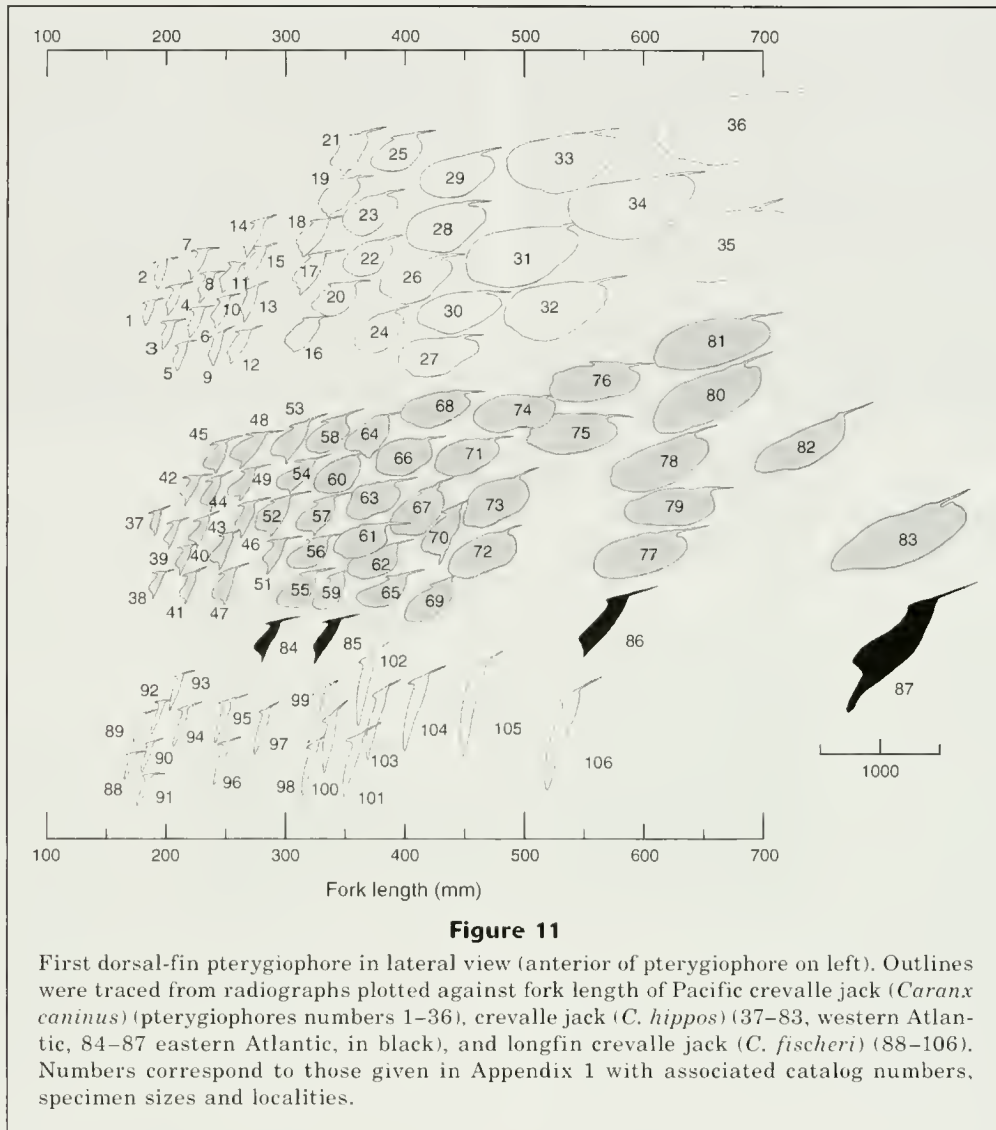
records of the species from the Azores (Arruda, 1997), Cape Verde Islands (Osório, 1911), and St. Helena (Melliss, 1875; Edwards and Glass, 1987; Edwards, 1990) are unreliable and can not be confirmed.

Adults are found inshore and frequently in upstream brackish waters (Klein-MacPhee, 2002) but are most common in salinities higher than 30 ppt (Gunter, 1945). Juveniles appear to use estuaries as nurseries in both temperate and tropical areas. Most reports of the species from freshwater are unreliable because of previous confusion with *C. fischeri* or are misleading (Herald and Strickland, 1949) because Homosassa Springs, Florida, has high alkalinity from the ionic composition of bicarbonate spring effluents. Gunter (1945) recorded juveniles and adults from Texas in salinities from 4.8 to 36.4 ppt. Smith (1985) reported that crevalle jacks are common summer residents in the Lower Hudson River, New York, and "in 1982 they were especially abundant as far upstream as River Mile 68 in early October and were still present at River Mile 66 in early November." McBride and McKown (2000) observed individuals in the Hudson River during July–October 1986–1993 at the freshwater interface (about 1 ppt), about 90–100 km inland.

Geographic variation Juveniles and adults of *C. hippos* from opposite sides of the Atlantic Ocean are virtually identical externally, including life coloration (Fig. 8, D–E), but differ notably in relative development of hyperostosis of the first pterygiophore of the dorsal fin. This bone is much less robust in adults of eastern Atlantic *C. hippos* (Figs. 11, 12). There is some variation in relative development of this pterygiophore in large western Atlantic specimens, but in all those we have examined (including a number of partially articulated skeletons at the AMNH not listed below) it is dorsolaterally expanded in marked contrast to the slender profile of the bone in eastern Atlantic specimens (Fig. 12). The basal halves of the neural spines of some of the anterior vertebrae (usually vertebrae 5–12) are also consistently and strongly expanded (Fig. 9, B–C) in large adults from the western Atlantic. The neural spines are only slightly hyperossified in a 56-cm-FL specimen (Figs. 10B, 13) from Senegal. They were more expanded (although much less so than in similar-size western Atlantic specimens) in a 90-cm specimen from Angola that had been partially dissected and photographed at our request so that we could ascertain the condition of the neural spines.

Caranx hippos has an essentially continental distribution (there are no confirmed records from any oceanic island) and populations on opposite sides of the Atlantic presumably are isolated and have little genetic connectivity, thus some geographic differentiation might be expected. *Caranx senegallus* and *C. fischeri* are both eastern Atlantic endemics, but other Atlantic species of *Caranx* with ampho-Atlantic distributions (*C.*

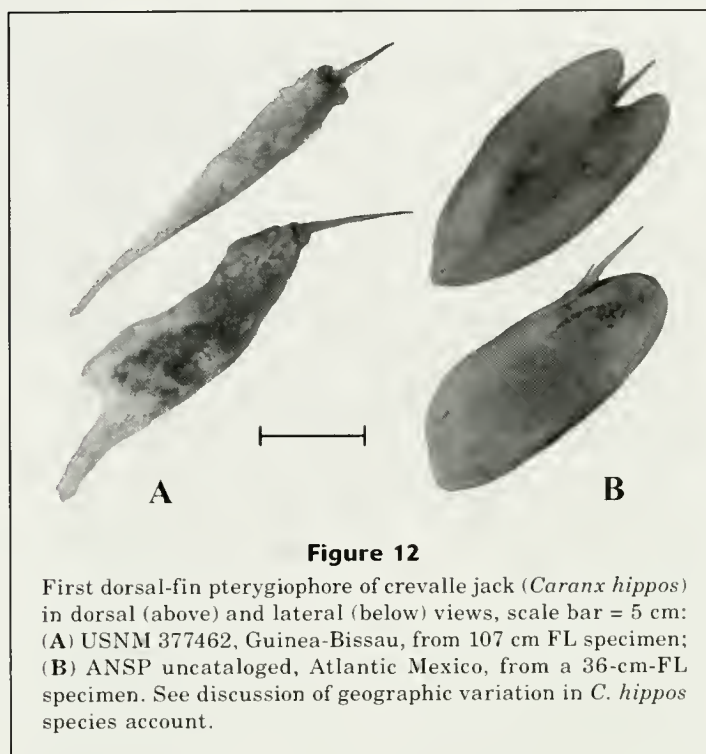
⁵ Debelius, H. 2004. Personal commun. IKAN-Unterwasserarchiv, Waldschulstrasse 166, 65933, Frankfurt, Germany.



crisos, *C. latus*, and *C. lugubris*) commonly are found at insular localities, including Ascension Island on the mid-Atlantic ridge.

Material examined Two hundred fifty-one specimens (29.5–1070 mm FL) from 103 collections (western Atlantic localities abbreviated). MASSACHUSETTS: ANSP 165909 (4, 152–189); USNM 10431 (4, 262–276); USNM 13656 (265); USNM 126812 (2, 54–69). RHODE ISLAND: ANSP 98280 (2, 175–179); USNM 21654 (274). NEW JERSEY: ANSP 97864 (3, 176–189); ANSP 121305 (2, 167–175); ANSP 105515 (173); ANSP 165911 (118); USNM 37022 (187); USNM 45120 (133); USNM 64053 (186). DELAWARE: USNM 187280 (5, 102–120), Indian River. VIRGINIA: ANSP 52647 (167). NORTH CAROLINA: UF 124148 (153) and UF 124400 (154), Onslow Bay. SOUTH CAROLINA: UF 124149 (122). GEORGIA: UF 126976 (2, 132–133). FLORIDA: CAS 216873 (1015); ANSP 33039 (188); ANSP 93821 (366);

ANSP 151093 (6, 186–208); CAS 216873 (1015); USNM 12681 (3, 254–269); USNM 22855 (622); USNM 29986 (372); USNM 53335 (263); USNM 57225 (260); USNM 57294 (2, 176–187); USNM 57295 (2, 172–175); USNM 154847 (167), St. Johns River; USNM 184871 (366); USNM 332457 (2, 390–421), Swanee River, salinity 14 ppt; USNM 362541 (3, 430–490), Caloosahatchee River; USNM 62289 (219); USNM 163601 (227). ALABAMA: ANSP 162288 (9, 810–950); USNM 157710 (4, 138–154). TEXAS: ANSP 99176 (5, 96–105); USNM 708 (10, 30–93); USNM 118497 (122); USNM 144017 (153). BAHAMAS: ANSP 102112 (2, 293–297); ANSP 102762 (657). CUBA: USNM 9867 (177); USNM 19821 (2, 357–386); USNM 132964 (2, 303–400). JAMAICA: USNM 32080 (725). DOMINICAN REPUBLIC: ANSP 81949 (114). PUERTO RICO: ANSP 151589 (254); ANSP 151590 (182). MEXICO: ANSP 159674 (5, 655–717); ANSP 156991 (9, 159–174); USNM 39278 (311); USNM 50473 (281). GUATEMALA: USNM 114580 (333); USNM



114594 (420), 2 mi above mouth of Rio Sarstoon; USNM 114618 (7, 326–557); USNM 134378 (92); USNM 157572 (196). HONDURAS: ANSP 158504 (5, 227–251). COSTA RICA: USNM 89073 (122); USNM 94155 (114). PANAMA: ANSP 45238 (2, 119–136); USNM 79965 (287); USNM 79981 (440); USNM 128657 (2, 350–364); USNM 128658 (334). COLOMBIA: USNM 94769 (2, 142–158); USNM 290077 (247). CURACAO: USNM 34914 (263). VENEZUELA: ANSP 161642 (2, 202–209); USNM 121801 (9, 136–213). GUYANA: USNM 186190 (357). FRENCH GUIANA: ANSP 148238 (294). BRAZIL: AMNH 3889 (300), Para Mkt., holotype of *Caranx hippos tropicus*; AMNH 58046 (274); ANSP 121329 (102); CAS 11861 (178); CAS-SU 22133 (4, 223–235); CAS-SU 51828 (2, 216–235); CAS-SU 51830 (231); CAS-SU 53013 (300); CAS-SU 53015 (311); CAS-SU 53016 (3, 316–319); CAS-SU 53025 (233); CAS-SU 53026 (232); CAS-SU 53080 (2, 605–617); CAS-SU 53082 (2, 534–555). MAURITANIA: MNHN 1978-216 (331), Port Etienne. SENEGAL: BMNH 1900.6.28.302–303 (2, 95–109), St. Louise, M. P. Delhez; ZMUC 25 (565), Senegal, Dakar, Dec 1927, H. Madsen. GUINEA-BISSAU: USNM 377462 (estimated 107 cm) anterior dorsal-fin pterygiophore, May 2004, P. Sebile. LIBERIA: ANSP 158494 (16, 29.5–35.0), 6°31′–7°07′N, 11°29′–11°57′30″W, surface dip net, 12 Nov 1963, B. B. Collette, sta. BBC 888. GHANA: CAS-SU 64646 (28, 34.8–68.4), mouth of Volta River at Little Ada, 12 Jan 1963, T. R. Roberts; USNM 373239 (3, 33–52), Volta River at Big Ada, 9 Mar 1960, G. W. Bane; USNM 42228 (71), Ashantee, Beyah River, 27 Nov 1889, W. H. Brown; USNM 373241 (3, 48–57), beach at Tema fishing harbor, 15 Dec 1959, G. W. Bane;

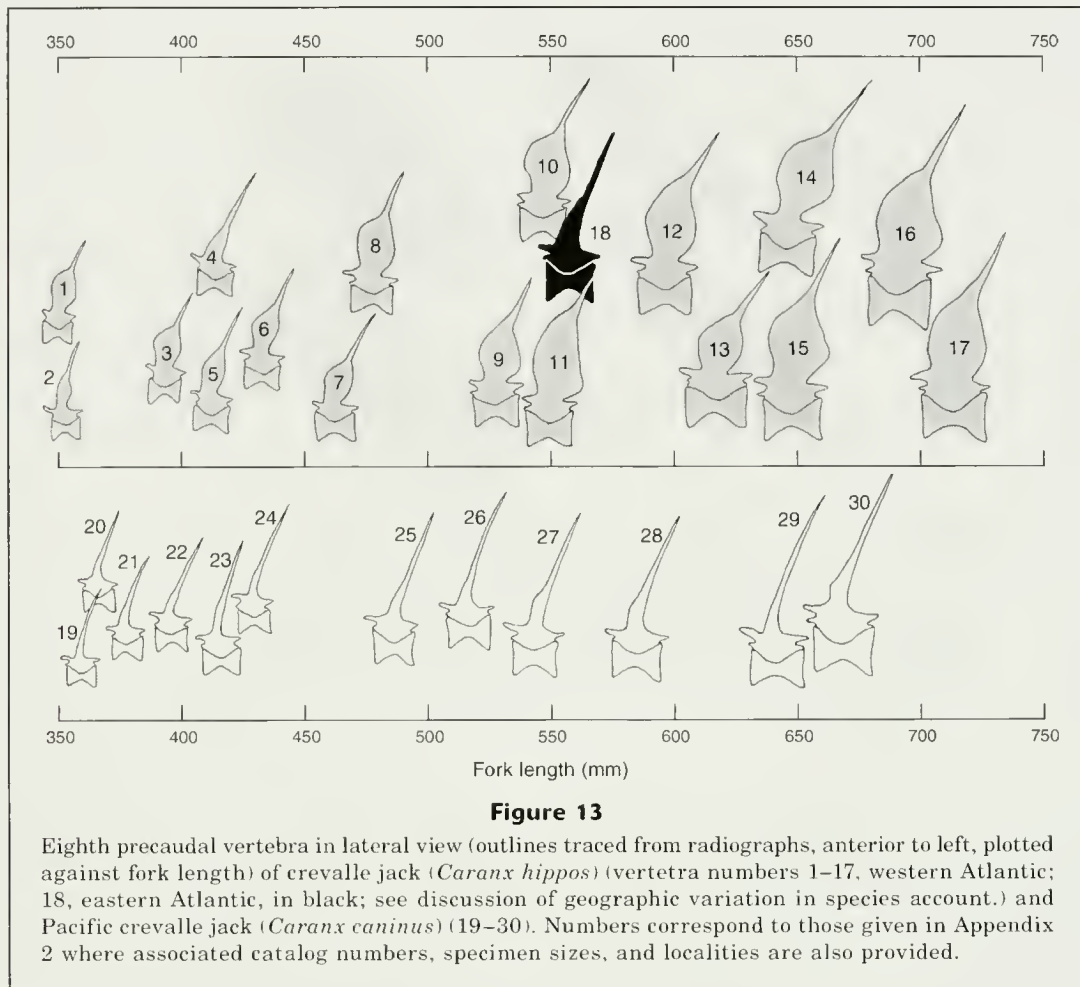
USNM 373247 (66), 0.4 km above mouth of Rio Hwini, Takoradi, 26 Nov 1959, G. W. Bane; USNM 300496 (78), Takoradi swimming pool, 10 Aug 1961, G. W. Bane; USNM 368825 (65), Takoradi Fisheries Station bay, 14 Aug 1961, G. W. Bane. NIGERIA: MNHN 1896-328 (150), Campagne Toutee; BMNH 1968.11.15.29-30 (2, 93–94), Lagos Lagoon, 1967, S. O. Fagade. EQUATORIAL GUINEA: MNHN 1893-14 (155), Pobeguini. CONGO: MNHN 1967-0286 (88), Tchitemo, May 1964, A. Stauch. WEST AFRICA: MNHN 1978-230 (274) “coast of tropical French Africa.”

Caranx caninus Günther, 1867

Pacific crevalle jack

(Figs. 1C, 6–7, 11, 13–15; Tables 1–4)

Caranx caninus Günther, 1867:601 (original description; Panama; holotype BMNH 1863.12.16.19); Günther, 1868:432 (expanded description); Walford, 1937:72, color pl. 51, Fig. A (diagnosis; comparison with *C. hippos*; habits); Walford, 1974:15 (“disagreement among ichthyologists as to whether species is distinct from *C. hippos*”; distribution); Eschmeyer and Herald, 1983, Fig. 40 (diagnosis; possible synonym of *C. hippos*; distribution); Allen and Robertson, 1994:126, pl. VIII-4 (color photograph; brief description); Franke and Acero, 1993:57 (size at sexual maturity; Colombia); Grove and Lavenberg, 1997:362, Figs. 37 (color), 192, 193 (brief description; Galapagos); Garrison, 2000:166, color photograph (uncommon; Costa Rico, Cocos Island); Lea and Rosenblatt, 2000:122 (occurrence in San Diego Bay).



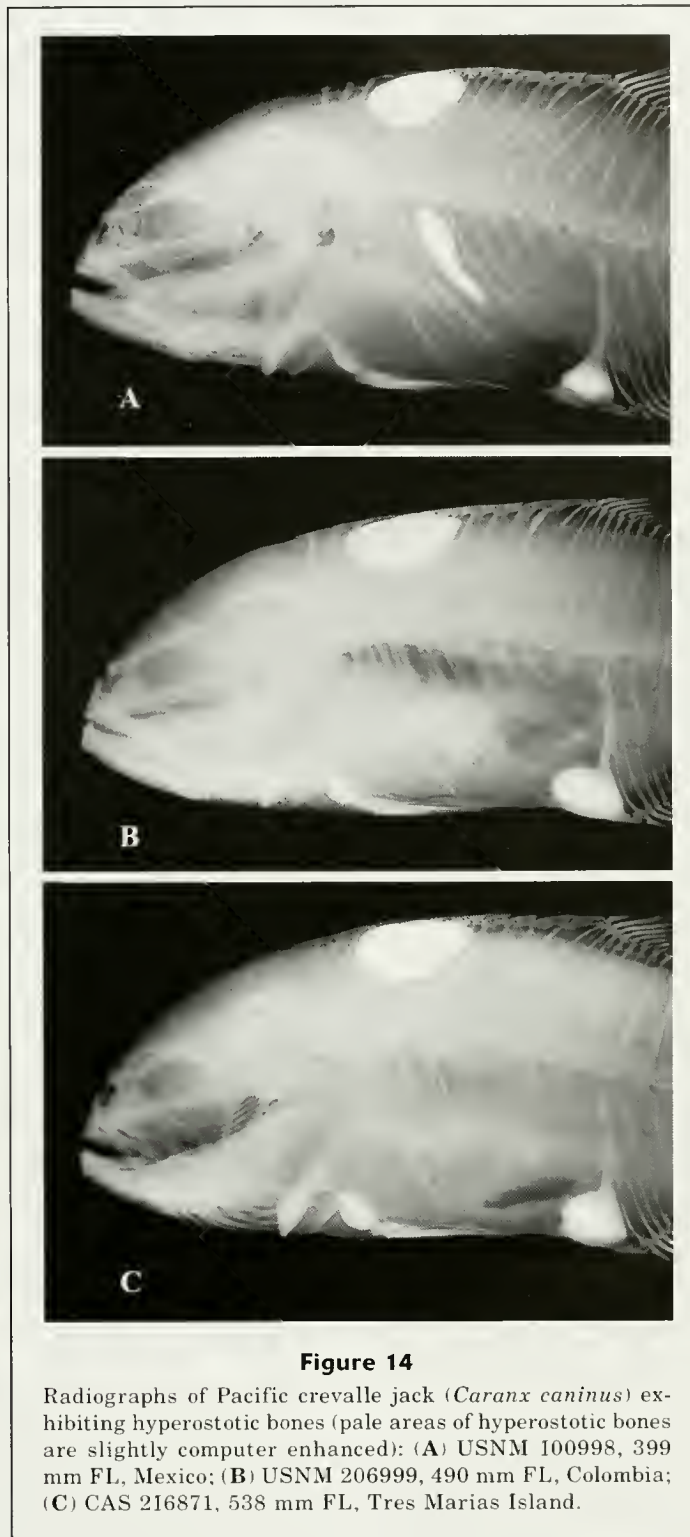
Caranx hippos (not of Linnaeus): Jordan and Gilbert, 1883:201 (synonymy; in part; *C. caninus* listed as synonym); Jordan, 1895:432 (misidentification in part; important food fish, occasionally entering estuaries; specimens from west coast and Havana indistinguishable; Mazatlan); Gilbert and Starks, 1904:77 (misidentification in part; Pacific and Atlantic specimens compared and considered conspecific; Panama Bay); Nichols, 1920:44 (Gulf of California fish indistinguishable from those from Atlantic coast); Meek and Hildebrand, 1925:350 (misidentification in part; distribution "Panama, common on both coasts of tropical America"); Hildebrand, 1946:208 (description; Peru); Fierstine, 1968:1, Figs.1–5 (description of dorsal-fin pterygiophore hyperostosis in Miocene deposits and living *Caranx*); Berry, 1974:240 (eastern Pacific and western Atlantic specimens essentially identical); Amezcua-Linares, 1996:88, unnumbered Fig. (description; biology; Mexico); Castro-Aquirre and Balart, 2002:166 (listed; Revillagigedo Islands).

Caranx (Tricropterus) hippos: Hiyama, 1937:33, color pl. 12 ("often identified to *C. caninus* Günther; reaches 2 feet, abundant, good food fish").

Caranx hippos caninus: Nichols, 1937:58 (specimens from Ecuador compared with Atlantic *C. hippos*); Hobson, 1968:63, fig. 25 (predatory behavior; Gulf of California).

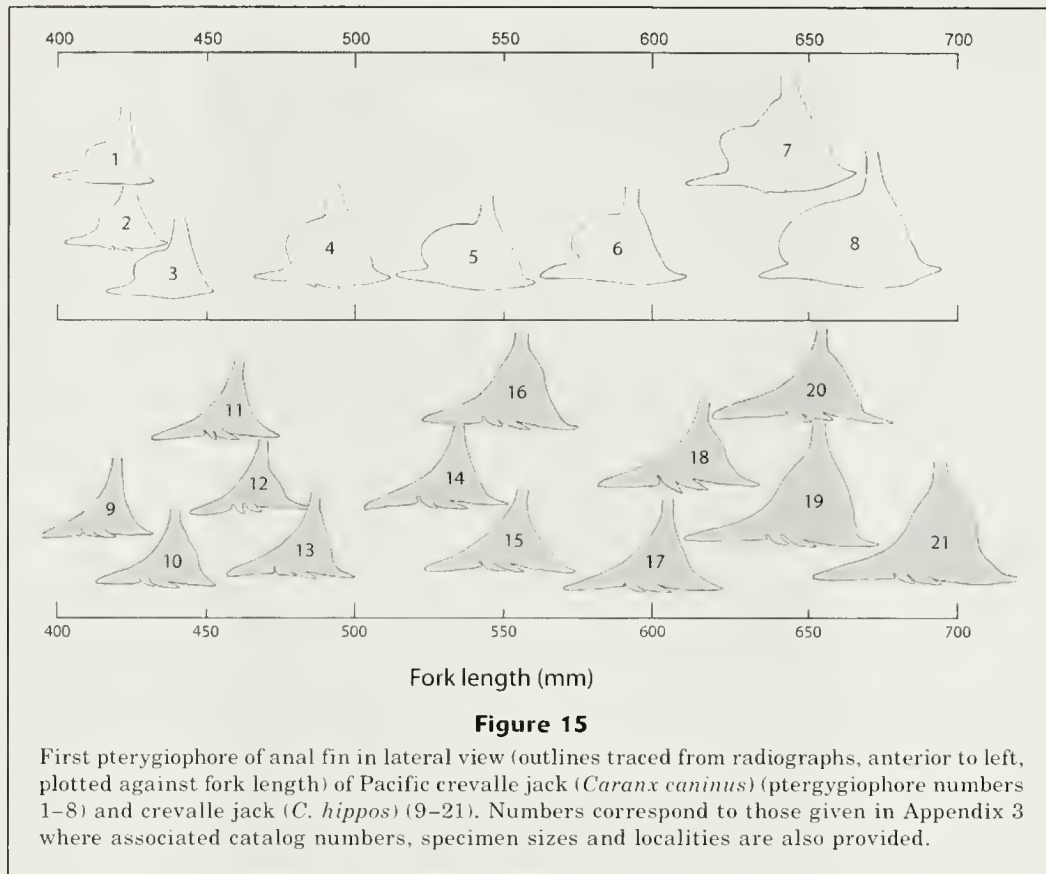
Diagnosis A member of the *Caranx hippos* complex with the following combination of characters: segmented dorsal-fin rays 19–21 (Table 2); segmented anal-fin rays 16 or 17; posttemporal bones, cleithra, and neural spines of vertebrae never hyperossified (Fig. 14); first pterygiophore of dorsal fin distinctly hyperossified in adults ≥ 38 cm FL (Figs. 11, 14); first pterygiophore of anal fin distinctly hyperossified, and having a convex anterior profile, in adults > 40 cm FL (Figs. 14, B–C, 15); either none or 5th pleural rib only hyperossified (Fig. 14A) in adults ≥ 38 cm FL; in specimens > 20 cm FL, heights of longest dorsal- and anal-fin rays 1.3–1.7 and 1.3–2.0 mm, respectively, in head length; and anal-fin lobe varying from entirely white to brownish-orange in adults.

Comparisons *Caranx caninus* and *C. hippos* have identical or broadly overlapping mensural and meristic values (Tables 2–4), although *C. caninus* usu-



ally has more lateral-line scutes. Differences in development of hyperostosis (Table 1) are the most useful distinguishing characters (see comparisons in account of *C. hippos*). The color of the anal fin also differs in these two species. In *C. hippos* the anal

fin is consistently lemon yellow, fading in postmortem individuals to orange-yellow. The anal fin of *C. caninus* varies from uniformly white to brownish-orange, and often some of the interradial membranes are dark brown. According to photographs of angler-



caught fish, the underside of the caudal peduncle of *C. caninus* is never bright yellow as in *C. hippos*, and in fish with uniformly white anal fins the caudal peduncle is also white.

Remarks We have not had the opportunity to study *C. caninus* in the field although we have examined many color photographs of recently caught adults. The pronounced differences in color of the anal fin in this species (see above) indicate the possibility of sexual dichromatism but determining the sex of large *Caranx* is best done with freshly caught specimens. The striking and inconsistent occurrence of hyperostosis of the third rib in this species (see Table 1) is also puzzling and the possibility that its presence or absence in adults may be sex linked and should be investigated.

Distribution This species is restricted to the eastern tropical Pacific (Fig. 2), ranging north to San Diego Bay, California, where its occurrence is associated with El Niño events (Lea and Rosenblatt, 2000), and from Mexico south to Lobos de Tierra Island, Peru (6°27'S); also known from the Galapagos, Malpelo, Cocos, and Revillagigedo islands, but it is unrecorded from Cliperton Atoll (Robertson and Allen, 1996). Meek and Hildebrand (1925) reported the species, as *C. hippos*, from tidal streams at Corozal and Balboa, Panama.

Material examined One hundred ten specimens (59-670 mm FL) from 51 collections. CALIFORNIA: SIO 75-383 (643), San Diego Bay. TRES MARIAS IS.: CAS 216871 (538); MEXICO: ANSP 144417 (25, 98-176); ANSP 158506 (4, 248-313); CAS 66825 (155); CAS 11112 (329); CAS-SU 55737 (2, 180-182); CAS 216872 (421); SIO 62-61 (3, 372-420); SIO 62-2725 (377); SIO 65-176A (670); SIO 65-182 (431); USNM 28293 (304); USNM 29556 (152); USNM 29617 (156); USNM 47143 (185); USNM 47144 (213); USNM 47145 (191); USNM 100991 (381); USNM 100998 (399); USNM 101006 (261); USNM 205166 (307). GUATEMALA: USNM 114469 (8, 77-233); EL SALVADOR: ANSP 136539 (172); ANSP 144401 (220); ANSP 144406 (169); USNM 220728 (2, 240-248); USNM 367522 (185); USNM 367542 (156); USNM 367671 (81); USNM 367946 (8, 61-77); USNM 367968 (63); USNM 367990 (166). PANAMA: ANSP 144409 (163); CAS 42539 (333); CAS 66826 (177); CAS 89955 (201); USNM 82080 (7, 75-187); USNM 79984 (2, 335-348); USNM 128659 (520); USNM 226417 (4, 59-112); USNM 321987 (2, 67-84). COLOMBIA: ANSP 144413 (164); USNM 206999 (493). ECUADOR: ANSP 158998 (137); CAS 66938 (212). GALAPAGOS IS.: USNM 89751 (2, 109-121), Indefatigable Id. PERU: SIO 58-83 (588); USNM 127917 (158); USNM 127918 (359); USNM 127919 (360).

Table 3
Frequency distributions of lateral-line scales and scutes in the *Caranx hippos* species complex.

Species	Curved lateral-line scales													n	\bar{x}	SD
	50 51	52 53	54 55	56 57	58 59	60 61	62 63	64 65	66 67	68 69	70 71	72 73	74 75			
<i>C. fischeri</i>	1	—	3	6	6	6	11	8	9	3		1		54	62.1	4.5
<i>C. hippos</i> (E. Atlantic)						1	1	3	1	5	—	1		12	66.2	3.3
<i>C. hippos</i> (W. Atlantic)			1	1	3	7	7	12	14	13	10	4	1	73	66.0	4.1
<i>C. caninus</i>		1	1	—	5	3	9	10	8	4	2	1		44	61.8	4.1
Species	Straight lateral-line scales										n	\bar{x}	SD			
	0 0	1 2	3 4	5 6	7 8	9 10	11 12	13 14	15 16							
<i>C. fischeri</i>	5	6	21	12	19	6	—	—	1					70	5.5	2.8
<i>C. hippos</i> (E. Atlantic)	1	1	4	5	3	2	—	—	1					17	5.9	3.4
<i>C. hippos</i> (W. Atlantic)	4	10	21	19	13	8	5	1	1					82	5.4	3.2
<i>C. caninus</i>	8	9	17	11	7	1	1							54	3.8	2.7
Species	Straight lateral-line scutes												n	\bar{x}	SD	
	24 25	26 27	28 29	30 31	32 33	34 35	36 37	38 39	40 41	42 43	44 45	46 47				
<i>C. fischeri</i>	3	3	15	8	19	17	2	2	1					70	31.8	3.3
<i>C. hippos</i> (E. Atlantic)	4	1	—	6	3	1	2							17	29.9	4.2
<i>C. hippos</i> (W. Atlantic)	1	4	12	26	27	8	3	1						82	31.2	2.4
<i>C. caninus</i>			1	—	—	8	15	16	7	5	1	1		54	38.1	2.9
Species	Straight lateral-line scales + scutes												n	\bar{x}	SD	
	28 29	30 31	32 33	34 35	36 37	38 39	40 41	42 43	44 45	46 47	48 49					
<i>C. fischeri</i>			11	7	24	17	6	3	—	2				70	37.0	3.1
<i>C. hippos</i> (E. Atlantic)	1	1	1	4	4	4	1	1						17	35.8	3.5
<i>C. hippos</i> (W. Atlantic)	1	2	10	18	17	18	12	3	1					82	36.7	3.1
<i>C. caninus</i>	1	—	—	1	4	4	14	13	8	8	1			54	41.9	3.6

Acknowledgments

The study would not have been possible without the generous cooperation of the following individuals who variously facilitated loans and access to specimens, helped with literature, provided accommodations and technical assistance during visits, and general encouragement: M. L. Bauchot, the late F. H. Berry, B. Brown, G. H. Burgess, D. Catania, B. B. Collette, W. E. Eschmeyer, P. C. Heemstra, G. Kelly, T. Iwamoto, R. N. Lea, G. Lenglet, J. G. Lundberg, J. Maclaine, J. G. Nielsen, S. G. Poss, P. Pruvost, R. H. Robins, R. H. Rosenblatt, M. H. Sabaj, J. Schratwieser, O. Schultz, D. G. Smith, V. G. Springer, the late P. J. P. Whitehead, H. Wilkens, and J. T. Williams. Color photographs of *Caranx* spp. were

provided by P. Afonso, A. Edwards, G. Kelly (IGFA), J. P. Reid, R. N. Lea, M. Lambouf (FAO), I. Nicholson, E. Truter, and P. Wirtz.

We especially thank H. L. Jelks whose expertise with Photoshop and Adobe Illustrator programs greatly improved the quality of Figures 2, 8, 11–13, and 15, and S. Reardon for digital photography of Figure 12A. We especially thank P. Sebile for his courtesy, with cooperation of the International Game Fish Association, in obtaining and sending us the anterior dorsal-fin spines and pterygiophores of a huge (131 cm TL) *Caranx hippos* from Guinea-Bissau. This material was critical in confirming our preliminary impression that certain aspects of hyperostosis were consistently different in eastern and western Atlantic populations of this species.

Table 4
Frequency distributions for gill raker counts in the *Caranx hippos* species complex.

Species	Upper limb gill rakers																		\bar{x}				
	Rudiments					Developed								Total									
	0	1	2	3	4	5	2	3	4	5	6	7	8	4	5	6	7	8		9			
<i>C. fischeri</i>																							
<10 cm FL	18	5	—	1	1			1	1	—	17	6			13	11	1						
>10 cm FL	9	13	7	10	6			3	14	7	4	16	1	1	5	22	17						
<i>C. hippos</i> (E. Atl.)																							
<10 cm FL	8	12	—	3	4				5	2	1	12	7			4	21	2					
>10 cm FL		2	1	2	1			1	2	—	2	1			1	—	2	2	1				
<i>C. hippos</i> (W. Atl.)																							
<10 cm FL	2	1	—	1	1				2	—	—	1	2			1	4						
>10 cm FL	31	28	14	18	9	7	4	11	14	14	26	34	4			10	63	34					
<i>C. caninus</i>																							
<10 cm FL	9	2	1								1	5	6				3	9					
>10 cm FL	9	14	12	10	8	3			4	14	6	9	18	5			1	16	36	3			
Species	Lower limb gill rakers																		\bar{x}				
	Rudiments				Developed						Total												
	0	1	2	3	13	14	15	16	17	18	16	17	18	19	20								
<i>C. fischeri</i>																							
<10 cm FL	4	11	10			3	11	7	4			7	18							16.7			
>10 cm FL		2	35	8		14	26	5					10	28	7					17.0			
<i>C. hippos</i> (E. Atl.)																							
<10 cm FL		13	11	3	1	11	14	1				24	3							16.1			
>10 cm FL			5	1	1	4	1				5	1							16.2				
<i>C. hippos</i> (W. Atl.)																							
<10 cm FL		1	2	2			2	2	1			1	3	1						17.0			
>10 cm FL	1	9	80	17	1	35	57	13	1			29	65	13						16.9			
<i>C. caninus</i>																							
<10 cm FL	4	8							2	6	4		3	9					17.8				
>10 cm FL	2	13	38	3			1	10	35	9	1	4	14	31	6	1			17.8				
Species	Total gill rakers																		\bar{x}				
	Total developed										Total developed + rudiments												
	16	17	18	19	20	21	22	23	24	25	26	20	21	22	23	24	25	26		27	28		
<i>C. fischeri</i>																							
<10 cm FL			1	1	—	—	11	6	4	2				5	10	10					23.2		
>10 cm FL	2	6	13	4	5	11	3	1					2	2	9	14	15	3			23.0		
<i>C. hippos</i> (E. Atl.)																							
<10 cm FL			3	3	2	6	8		4	1				4	21	2					23.0		
>10 cm FL	1	2	1	—	2							1	—	2	2	—	1					22.5	
<i>C. hippos</i> (W. Atl.)																							
<10 cm FL	1	1	—	1	—		1	1							2	3					23.6		
>10 cm FL	4	6	11	14	12	25	25	9	1						7	15	55	24	6			24.1	
<i>C. caninus</i>																							
<10 cm FL							1	1	4	2	4					2	2	8			25.5		
>10 cm FL				1	7	12	5	8	12	10	1				2	7	19	21	6	1			25.4

Literature cited

- Afonso, P., F. M. Porteiro, R. S. Santos, J. P. Barreiros, J. Worms, and P. Wirtz.
1999. Coastal marine fishes of São Tomé Island (Gulf of Guinea). *Bull. Univ. Azores* 17A:65–92.
- Allen, G. R., and D. R. Robertson.
1994. *Fishes of the tropical eastern Pacific*, 332 p. Crawford House Press, Bathurst, New South Wales, Australia.
- Amezcu-Linares, F.
1996. Peces demersales de la plataforma continental del Pacífico central de México, 184 p. Instituto de ciencias del Mar y Limnología, UNAM/Comisión Nacional para el Conocimiento y Uso de la Biodiversidad, México, D.F.
- Arruda, L. M.
1997. Checklist of the marine fishes of the Azores. *Arq. Mus. Bocage* (n. s.) 3 (2):13–164.
- Bauchot, M. L.
1992. Carangidae. In *Faune des poissons d'eaux douces et saumâtres d'Afrique de l'Ouest*, vol. 2 (C. Lévêque, D. Paugy, and G. G. Teugels, eds.), p. 671–875. ORSTOM, Paris.
- Bauchot, M. L., and M. Blanc.
1963. Poissons marins de l'Est Atlantique tropical II. Percoides (Téléostéens Perciformes). 2e partie. *Atlantide Rep.* 7:37–61.
- Bauchot, M. L., and A. Pras.
1980. *Guide des poissons marins d'Europe*, 427 p. Delachaux et Niestlé, Lausanne-Paris, France.
- Bellemans, M., A. Sagna, W. Fischer, and N. Scialabba.
1988. Fiches FAO d'identification des espèces pour les besoins de la pêche. *Guide des ressources halieutiques du Sénégal et de la Gambie (espèces marines et d'eaux saumâtres)*, 223 p. FAO, Rome.
- Bennett, F. D.
1840. *Narrative of a whaling voyage round the globe, from the year 1833 to 1836*, vol. 2., 395 p. London.
- Berry, F. H.
1959. Young jack crevalles (*Caranx* species) off the south-eastern Atlantic coast of the United States. *Fish. Bull.* 59:417–535.
1960. Scale and scute development of carangid fish *Caranx crysos* (Mitchill). *Quart. J. Fla. Acad. Sci.* 23:59–66.
1974. Crevalle *Caranx hippos*. In *McClane's new standard fishing encyclopedia and international angling guide* (A. J. McClane, ed.), p. 240–241. Holt, Rinehart, and Winston, New York, NY.
- Bianchi, G.
1986. Fichas FAO de identificação de espécies para propósitos comerciais. *Guia de campo para as espécies comerciais marinhas e de águas salobras de Angola*, 184 p. FAO, Rome.
- Bilecenoglu, M., E. Taskavak, S. Mater, and M. Kaya.
2002. Checklist of the marine fishes of Turkey. *Zootaxa* 113:1–194.
- Bini, G.
1968. *Atlante dei pesci delle coste Italiane*, vol. 5. Ostetti. Mondo Sommerso, 175 p. Edizioni Calderini, Bologna, Italy.
- Blaber, S. J. M.
2002. 'Fish in hot water': the challenges facing fish and fisheries research in tropical estuaries. *J. Fish Biol.* 61 (suppl. A):1–20.
- Blache, J., J. Cadenat, and A. Stauch.
1970. Clés de détermination des poissons de mer signalés dans l'Atlantique orientale entre le 20e parallèle nord et le 15e parallèle sud. *Faune Trop.* 18:1–479.
- Bloch, M. E.
1793. *Naturgeschichte der ausländischen Fische*, vol. 7, 144 p. Berlin.
- Briggs, J. C.
1960. Fishes of worldwide (circumtropical) distribution. *Copeia* 1960:171–180.
- Brito, A., P. J. Pascual, J. M. Falcón, A. Sancho, and G. González.
2002. Peces de las Islas Canarias catálogo comentado e ilustrado, 419 p. Francisco Lemus, La Laguna, Tenerife, Canary Is.
- Cadenat, J.
1950. Poissons de mer du Sénégal. *Init. afr.* 3:1–345.
1960. Notes d'ichtyologie ouest-africaine. XXX. Poissons de mer ouest-africains observés du Sénégal au Cameroun et plus spécialement au large des Côtes de Sierra Leone et du Ghana. *Bull. Inst. fr. Afr. noire*, (A) 22 (4):1358–1420.
1961. Notes d'ichtyologie ouest-africaine. XXXIV. Liste complémentaire des espèces de poissons de mer (provenant des côtes de l'Afrique occidentale) en collection à la section de biologie marine de l'IFAN à Gorée. *Bull. Inst. fr. Afr. noire*, (A) 23(1):231–245.
- Castro-Aguirre, J. L., and E. F. Balart.
2002. La ictiofauna de las Islas Revillagigedo y sus relaciones zoogeográficas, con comentarios acerca de su origen y evolución. In *Libro Jubilar en Honor al Dr Salvador Contreras Balderas (Lozano-Vilano M de Lourdes, ed.)* p. 153–170. Universidad Autónoma de Nuevo Leon, Monterey, Mexico.
- Castro-Aguirre, J. L., H. S. Espinosa Pérez, and J. J. Schmitter-Soto.
1999. Ictiofauna estuarino-Lagunar y vicaria de México. *Colección Textos Politécnicos. Serie Biotecnologías*:1–711.
- Cervigón, F.
1993. Los peces marinos de Venezuela, vol. 2., 499 p. Fundación Científica Los Roques, Caracas, Venezuela.
- Chabanaud, P., and T. Monod.
1927. Les poissons de Port-Étienne, contribution à la faune ichthyologique de la région du Cap Blanc (Mauritanie Française). *Bull. Com. Étud. Hist. Scient. Afr. Occid. Fr.* [1926] 9:225–287.
- Clark, R. S.
1915. Scottish National Antarctic Expedition: "Scotia" collection of Atlantic fishes. *Rep. scient. Results Scott. natn. Antarct. Exped.* 4 (16):379–401.
- Collignon, J., M. Rossignol, and C. Roux.
1957. Mollusques, crustacés, poissons marins des côtes d'A.E.F. en collection au Centre d'Océanographie de l'Institut d'Études Centrafricaines de Pointe-Noire, 396 p. Paris.
- Cuvier, G., and A. Valenciennes.
1833. *Histoire naturelle des poissons*, vol. 9, 519 p. F. G. Levrault, Paris.
- Daget, J., and A. Iltis.
1965. Poissons de Côte D'Ivoire (eaux douces et saumâtres). *Mém. Inst. Fr. Afr. Noire*, (74):385 p.
- Daget, J., and A. Stauch.
1968. Poissons d'eaux douces et saumâtres de la région côtière du Congo. *Cah. ORSTOM, Hydrobiol.* 2 (2):21–50.
- Debelius, H.
1997. *Mediterranean and Atlantic fish guide*, 305 p. IKAN, Frankfurt, Germany.

- DeKay, J. E.
1842. Zoology of New-York, or the New-York fauna; comprising detailed descriptions of all the animals hitherto observed within the state of New-York, with brief notices of those occasionally found near its borders, and accompanied by appropriate illustrations. Part IV. Fishes, 415 p. W. & A. White & J. Visscher, Albany, NY.
- Desmarest, E.
1856. Reptiles et poissons. In Encyclopédie d'histoire naturelle; ou, traité complet de cette science d'après les travaux des naturalistes les plus éminents de toutes les époques, etc. . . . par le Dr. Chenu. Encyclopédie d'histoire naturelle, vol. 19. (J. G. Chenu, ed.), 360 p. Paris.
- Desse, G., F.-J. Meunier, M. Peron, and J. Laroche.
1981. Hyperostose vertébrale chez l'animal. *Rhumatologie*, 33 (2):105-119.
- Devincenzi, G. J.
1924. Peces del Uruguay. II. Nuestra fauna ictológica según nuestras colecciones. *Anales del Museo N. de Montevideo*, ser. 2, 1 (5):139-290.
- Duméril, A. H. A.
1861. Reptiles et poissons de la Côte occidentale d'Afrique. *Archs. Mus. Hist. Nat. (Paris)* 10 [1858]: 241-268.
- Edwards, A. J.
1990. Fish and fisheries of Saint Helena Island, 152 p. Centre for Tropical Coastal Management Studies, Univ. Newcastle upon Tyne, Newcastle, England.
- Edwards, A. J., A. C. Gill, and P. O. Abohweyere.
2003. A revision of F. R. Irvine's Ghanaian marine fishes in the collections of the Natural History Museum, London. *J. Fish Biol.* 37:2213-2267.
- Edwards, A. J., and C. W. Glass.
1987. The fishes of Saint Helena Island, South Atlantic Ocean. II. The pelagic fishes. *J. Nat. Hist.* 21:1367-394.
- Ehrenbaum, E.
1915. Über küsten Fische von Westafrika, besonders von Kamerun, 85 p. Hamburg, Germany.
- Eschmeyer, W. N.
1998. Catalog of fishes, 2905 p. Calif. Acad. Sci., Spec. Publ. 1, San Francisco, California.
- Eschmeyer, W. N., and E. S. Herald.
1983. A field guide to Pacific coast fishes of North America, 336 p. Peterson Field Guide Series, No. 28. Houghton Mifflin Co., Boston, MA.
- FAO (Food and Agriculture Organization of the United Nations).
2006. Yearbook of fishery statistics—capture production 2004. 98(1):1-560. FAO, Rome.
- Fierstine, H. L.
1968. Swollen dorsal fin elements in living and fossil *Caranx* (Teleostei: Carangidae). *Cont. Sci. Los Angeles Co. Mus.* 137:1-10.
- Fischer, W.
1989. The significance of FAO's biosystematics program in the enhancement of world fisheries. *Aquatic Sci.* 1(4):683-692.
- Fowler, H. W.
1919. The fishes of the United States "Eclipse" Expedition to West Africa. *Proc. U. S. Natl. Mus.* 56 (2294): 195-292.
1936. The marine fishes of West Africa. *Bull. Am. Mus. Nat. Hist.* 70:1493 p.
- Franca, P. da.
1954. Contribuição para o conhecimento dos Carangídeos (Carangidae, Pomatomidae e Coryphaenidae) de Angola. *An. Junta Invest. Ultramar* 9 (2):3-52.
- Franke, R., and A. Acero P.
1993. Peces Carangídeos del Parque Gorgona. *Pacífico Colombiano (Osteichthyes: Carangidae, Nematis-tiidae y Coryphaenidae)*. *Rev. Biol. Mar., Valparaíso* 28:51-73.
- Garrison, G.
2000. Peces de la Isla del Cocos [Isla del Cocos fishes], 393 p. INBio, Santo Domingo de Heredia, Costa Rica.
- Gilbert, C. H., and E. C. Starks.
1904. The fishes of Panama Bay. *Mem. Calif. Acad. Sci.* part 4:1-304.
- Gill, A. C., and J. M. Kemp.
2002. Widespread Indo-Pacific shore-fish species: a challenger for taxonomists, biogeographers, ecologists, and fishery and conservation managers. *Environ. Biol. Fish.* 65:165-174.
- Gill, T. N.
1862. Note on some genera of fishes of western North America. *Proc. Acad. Nat. Sci. Phila.* 14:329-332.
- Ginsburg, I.
1952. Fishes of the family Carangidae of the northern Gulf of Mexico and three related species. *Publ. Inst. Mar. Sci.* 2:41-117.
- Girard, C. F.
1858. Notes upon various new genera and new species of fishes, in the museum of the Smithsonian Institution, and collected in connection with the United States and Mexican boundary survey: Major William Emory, Commissioner. *Proc. Acad. Nat. Sci. Phila.* 10:167-171.
1859. Ichthyology. In United States and Mexican boundary survey, under the order of Lieut. Col. W. H. Emory, Major First Cavalry and United States commissioner. U.S. and Mexican Boundary Serv. 2 (2):1-85, Fishes pls. 1-41.
- Goode, G. B.
1884. The food fishes of the United States. In *The Fisheries and Fishery Industries of the United States*. U.S. Comm. Fish Fish. Rept., Sect. 1 (3):163-682.
- Grove, J. S., and R. J. Lavenberg.
1997. The fishes of the Galápagos Islands, 863 p. Stanford Univ. Press, Palo Alto, California.
- Gunter, G.
1945. Studies on marine fishes of Texas. *Publ. Inst. Mar. Sci. Univ. Texas.* 1:1-100.
- Günther, A.
1867. On the fishes of the states of Central America, founded upon specimens collected in fresh and marine waters of various parts of that country by Messrs. Salvin and Godman and Capt. J. M. Dow. *Proc. Zool. Soc. Lond.* 1866 (3):600-604.
1868. An account of the fishes of the states of Central America, based on collections made by Capt. J. M. Dow, F. Godman, Esq., and O. Salvin, Esq. *Trans. Zool. Soc. Lond.* 6(7):377-494.
- Heckel, J. J.
1852. *Caranx carangopsis* und fossile Delphin-wirbel. *Jahrbuch Geol. Reichsanstalt, Vienna* 3 (2):160-161.
- Herald, E. S., and R. R. Strickland.
1949. Annotated list of the fishes of Homosassa Springs, Florida. *Quart. J. Fla. Acad. Sci.* (1948) 11: 99-101.
- Hildebrand, S. F.
1939. The Panama Canal as a passageway for fishes,

- with lists and remarks on the fishes and invertebrates observed. *Zoologica* 24 (1):15-45.
1946. A descriptive catalog of the shore fishes of Peru. *Bull. U. S. Natl. Mus.* 189, 530 p.
- Hiyama, Y.
1937. Marine fishes of the Pacific coast of Mexico. (T. Kumada, ed.), 75 p. Nissan Fisheries Institute, Odawara, Japan.
- Hobson, E. S.
1968. Predatory behavior of some shore fishes in the Gulf of California. *Fish Wildlife Serv. Res. Rep.* 73: 1-92.
- Hureau, J. C., and E. Tortonese.
1973. Carangidae. In Check-list of the fishes of the north-eastern Atlantic and the Mediterranean (CLOF-NAM), vol. 1 (Hureau, J. C., and T. Monod, eds.), p. 373-384. UNESCO (United Nations Educational, Scientific, and Cultural Organization), Paris.
- IGFA (International Game Fish Association).
2006. World record game fishes, 2006 ed., 384 p. IGFA, Dania Beach, FL.
- Jordan, D. S.
1895. The fishes of Sinaloa. *Proc. Calif. Acad. Sci.* (ser. 2)5:377-514.
- Jordan, D. S., and B. W. Evermann.
1902. American food and game fishes, 573 p. Doubleday, Page & Company, New York, NY.
- Jordan, D. S., and C. H. Gilbert.
1883. A review of the American Caranginae. *Proc. U. S. Natl. Mus.* 6:188-207.
- Khan, R. A.
2003. Fish faunal resources of Sunderban estuarine system with special reference to the biology of some commercially important species. *Rec. Zool. Surv. India, Misc. Publ., Occas. Pap.* 209:1-150.
- Klein-MacPhee, G.
2002. Jacks. Family Carangidae. In Bigelow and Schroeder's fishes of the Gulf of Maine, 3rd ed. (B. B. Collette, and G. Klein-MacPhee, eds.), p. 411-427. Smithsonian Press, Washington, D.C.
- Krishnan, S., and S. S. Mishra.
1994. On a collection of fish from middle and south Andaman group of islands. *Rec. Zool. Surv. India* 94 (2-4):265-306.
- Kwei, E. A.
1978. Food and spawning activity of *Caranx hippos* (L.) off the coast of Ghana. *J. Nat. Hist.* 12:195-215.
- Lacépède, B. G. E.
1801. Histoire naturelle des poissons, vol. 3, 558 p. Plassan, Paris.
- Laroche, W.A., J. G. Ditty, J. T. Lamkin, and S. R. Whiteraft.
2006. Carangidae: jacks. In Early stages of Atlantic fishes: an identification guide for the western central North Atlantic, vol. 2 (W. J. Richards, ed.), p.1439-1509. CRC Press, Boca Raton, FL.
- Lea, R. N., and R. H. Rosenblatt.
2000. Observations on fishes associated with the 1997-98 El Niño off California. *Calif. Coop. Oceanic Fish. Invest. Rep.* 41:117-129.
- Linnaeus, C.
1766. Systema naturae sive regna tria naturae, secundum classes, ordines, genera, species, cum characteribus, differentiis, synonymis, locis. Laurentii Salvii, Holmiae. 12th ed., 1(1):1-532.
- McBride, R. S., and K. A. Mckown.
2000. Consequences of dispersal of subtropically spawned crevalles jacks, *Caranx hippos*, to temperate estuaries. *Fish. Bull.* 98:528-538.
- Meek, S. E., and S. F. Hildebrand.
1925. The marine fishes of Panama. Part II. *Field Mus. Nat. Hist. Publ. Zool. Ser.* 15 (226):331-707.
- Melliss, J. C.
1875. Class V. Pisces. In St. Helena: a physical, historical and topographical description of the island, including its geology, fauna, flora, and meteorology, p. 100-113. Reeve & Co., London.
- Menezes, N. A., and J. L. Figueiredo.
1980. Manual de peixes marinhos do sudeste do Brasil. IV. Teleostei (3):1-96.
- Mishra, S. S., R. Gouda, L. Nayak, and R. P. Panigrahy.
1999. A check list of the marine and estuarine fishes of south Orissa, east coast of India. *Rec. Zool. Surv. India* 97 (3):81-90.
- Mishra, S. S., and S. Krishnan.
2003. Marine fishes of Pondicherry and Karaikal. *Rec. Zool. Surv. India, Occ. Pap.* 216:1-52.
- Monod, T.
1927. Pisces I, pisces marini. In Contributions à l'étude de la faune du Cameroun, part 2 (T. Monod, ed.), p. 643-742. Soc. Edit. Geogr. Marit. Colon., Paris.
- Murdy, E. O., R. S. Birdsong, and J. A. Musick.
1997. Fishes of Chesapeake Bay, 324 p. Smithsonian Inst. Press, Washington, D.C.
- Nichols, J. T.
1920. On the range and geographic variation of *Caranx hippos*. *Copeia* (83):44-45.
1937. On *Caranx hippos* (Linnaeus) from Ecuador. *Copeia* 1937:58-59.
- Nichols, J. T., and J. Roemhild.
1946. Fin-count variation in *Caranx hippos* (Linnaeus). *Marine Life, Occas. Papers* 1(5):15-17.
- Norman, J. R., and F. R. Irvine.
1947. Marine fishes. In F. R. Irvine, The fishes and fisheries of the Gold Coast, p. 81-220. Crown Agents, London.
- Okera, W.
1978. Fishes taken by the beach seines fishing at Lumley, Freetown (Sierra Leone). *J. Fish Biol.* 12:81-88.
- Osório, B.
1911. Peixes colhido nas visinhanças do archipelago de Cabo Verde. *Mems Mus. Bocage* 3:37-49.
- Papaconstantinou, C.
1988. Check-list of marine fishes of Greece, 257 p. Fauna Graeciae IV, Hellenic Zoological Society, Athens.
- Peters, W. (C. H.).
1877. Übersicht der während der von 1874 bis 1876 unter dem Commando des Hrn. Capitän z. S. Freiherrn von Schleinitz ausgeführten Reise S. M. S. Gazelle gesammelten und von der Kaiserlichen Admiralität der Königlichen Akademie der Wissenschaften übersandten Fische. *Monatsb. Akad. Wiss. Berlin* 1876:831-854.
- Pellegrin, J.
1907. Mission des pêcheries de la côte occidentale d'Afrique, 2e memoire. *Act. Soc. Linn. Bordeaux* 62:71-102.
- Poll, M.
1954. Poissons. IV. Téléostéens acanthoptérygiens (Ière partie). *Résult. Scient. Exped. Océanogr. Belg. Eaux côt. Afr. Atlant. Sud* (1948-49) 4(3B):1-390.

- Postel, E.
1959. Liste commentée des poissons signalés dans l'Atlantique tropico-oriental nord, du Cap Spartel au Cap Roxo, suivie d'un bref aperçu sur leur repartition bathymétrique et géographique. *Bull. Soc. Scient. Bretagne* 34 (1/2):129-170.
- Randall, J. E.
1996. Caribbean reef fishes, 3rd ed., 368 p. TFH Publications, Inc., Neptune, NJ.
- Robertson, D. R., and G. R. Allen.
1996. Zoogeography of the shorefish fauna of Clipperton Atoll. *Coral Reefs* (1996) 15:121-131.
- Saloman, C. H., and S. P. Naughton.
1984. Food of crevalle jack (*Caranx hippos*) from Florida, Louisiana, and Texas. NOAA Tech. Memo. NMFS-SEFC-134, 34 p.
- Sanders, A. L.
1997. Alexander Garden (1730-1791), pioneer naturalist in colonial America. In *Collection building in ichthyology and herpetology* (T. W. Pietsch, and W. D. Anderson Jr., eds.), p. 409-437. *Am. Soc. Ich. Herp., Spec. Publ.* 3.
- Scott, W. B., and M. G. Scott.
1988. Atlantic fishes of Canada. *Can. Bull. Fish. Aquat. Sci.* 219, 731 p.
- Shipp, R. L.
1986. Dr. Bob Shipp's guide to fishes of the Gulf of Mexico, 256 p. 20th Century Printing Co., Mobile, AL.
- Smith, C. L.
1985. The inland fishes of New York State, 522 p. New York State Dept. Environ. Conserv., Albany, NY.
- Smith-Vaniz, W. F.
1986. Carangidae. In *Fishes of the north-eastern Atlantic and Mediterranean (FNAM)*, vol. 2 (Whitehead, P. J. P., M.-L. Bauchot, J.-C. Hureau, J. Nielsen, and E. Tortonese, eds.), p. 815-844. UNESCO (United Nations Educational, Scientific, and Cultural Organization) Paris.
2003. Carangidae. In *FAO species identification sheets for fishery purposes* (K. E. Carpenter, ed.), p. 1426-1468. Western Central Atlantic. FAO, Rome.
- Smith-Vaniz, W. F., and F. H. Berry.
1981. Carangidae. In *FAO species identification sheets for fishery purposes*, vol. 1 (W. Fischer and G. Bianchi, eds.), unnumbered p. 1-7+74. Eastern Central Atlantic. FAO, Rome.
- Smith-Vaniz, W. F., B. B. Collette, and B. E. Luckhurst.
1999. Fishes of Bermuda: history, zoogeography, annotated checklist, and identification keys. *Am. Soc. Ich. Herp., Spec. Publ.* 4, 424 p.
- Smith-Vaniz, W. F., J. C. Quéro, and M. Desoutter.
1990. Carangidae. In *Check-list of the fishes of the eastern tropical Atlantic (CLOFETA)*, vol. 2 (Quéro, J. C., J. C. Hureau, C. Karrer, A. Post, and L. Saldanha, eds.), p. 729-755. UNESCO, Paris.
- Smith-Vaniz, W. F., L. S. Kaufman, and J. Glowacki.
1995. Species-specific patterns of hyperostosis in marine teleost fishes. *Mar. Biol.* 121:573-580.
- Steindachner, F.
1859. Beiträge zur Kenntniss der fossilen Fisch-Fauna Österreichs. *Sitzungsber. Akad. Wiss Wien* 37:673-703.
1870. Zur Fischfauna des Senegal. Erste Abtheilung. *Sitzungsber. Akad. Wiss Wien* 60 (1) [1869]:669-714.
- Talwar, P. K., and R. K. Kacker.
1984. Commercial sea fishes of India, 997 p. *Zool. Surv. India, Calcutta.*
- Thompson, R., and J. L. Munro.
1983. The biology, ecology, and bionomics of the jacks, Carangidae. In *Caribbean Coral Reef Fishery Resources* (J. L. Munro, ed.), p. 82-93. International Center for Living Aquatic Resources Management, Manila, Philippines.
- Tortonese, E.
1952. Monografia dei Carangini viventi nel Mediterraneo (Pisces Perciformes). *Ann. Mus. Civ. Stor. Nat. Giacomo Doria* 65:259-324.
1973. The ichthyological collections now existing in Italy. *Ann. Mus. Civ. Stor. Nat. Giacomo Doria* 79: 108-116.
1975. Osteichthyes (Pesci ossei). Parte seconda. Edizioni Calderini, Bologna. *Fauna Ital.* 11:1-636.
- Uyeno, T., K. Matsuura, and E. Fujii, eds.
1983. Fishes trawled off Suriname and French Guiana, 519 p. JAMARC (Japan Marine Fishery Resources Research Center), Tokyo.
- Vergara, R.
1972. Analisis taxonomico y consideraciones filogeneticas sobre las especies Cubanas del genero *Caranx* (teleostel, Perciformes, Carangidae). *Cent. Inst. Pesq. Cuba* (34):1-137.
- Walford, L. A.
1937. Marine game fishes of the Pacific Coast from Alaska to the Equator, 205 p. Univ. Calif. Press, Berkeley, CA.
1974. Marine game fishes of the Pacific Coast from Alaska to the Equator, p. 1-19. [i-xxix+1-205], pls. 1-69. Reprint of 1937 edition for the Smithsonian Institution by T.F.H. Publications, Inc., Neptune, NJ.
- Wheeler, A.
1985. The Linnaean fish collection in the Linnaean Society of London. *Zool. J. Linn. Soc.* 84:1-76.
- Williams, F.
1968. Report on the Guinean Trawling Survey. Vol. 1: General report. Lagos:1-828.

Appendix 1

Catalog numbers, localities, and sizes (mm FL) of specimens used for outline drawings of the first dorsal-fin pterygiophore in Figure 11. Numbers in bold correspond to the numbers for the pterygiophores illustrated in Figure 11.

Caranx caninus: 1, ANSP 144406 (169) El Salvador; 2, USNM 114469 (178) Guatemala; 3, USNM 820080 (187) Panama; 4, USNM 47145 Gulf of California (192); 5, USNM 114469 Guatemala (197); 6, CAS 66938 Ecuador (212); 7, USNM 47144 Gulf of California (213); 8, ANSP 144401 El Salvador (220); 9, USNM 114469 Guatemala (227); 10, USNM 114469 Guatemala (233); 11, USNM 200728 El Salvador (240); 12, ANSP 158506 Mexico, Sinalosa (248); 13, ANSP 158506 Mexico, Sinalosa (258); 14, USNM 101006 Mexico (261); 15, ANSP 158506 Mexico, Sinalosa (262); 16, USNM 28293 Mexico (304); 17, USNM 205166 Baja California (307); 18, ANSP 158506 Mexico, Sinalosa (313); 19, CAS 42539 3°53'N, 105°10'W (333); 20, CAS 11112 Mexico (329); 21, US-

NM 79884 Panama (348); **22**, USNM 127918 Peru (359); **23**, USNM 127919 Peru (360); **24**, SIO 62-61 Mexico, Isabel Island (371); **25**, USNM 100991 Mexico (381); **26**, USNM 100998 Mexico (399); **27**, SIO 62-61 Mexico, Isabel Island (419); **28**, CAS 216872 Baja California (421); **29**, SIO 65-182 (431); **30**, SIO-62-61 Mexico, Isabel Island (438); **31**, USNM 206999 Colombia (490); **32**, USNM 128659 Panama (520); **33**, CAS 216871 Tres Marias Island (538); **34**, SIO 58-83 Peru (588); **35**, SIO 75-383 California, San Diego (643); **36**, SIO 65-176A Baja California (670).

Caranx hippos: **37**, USNM 57294 (176) Florida; **38**, ANSP 97864 (176) New Jersey; **39**, ANSP 97864 (189) New Jersey; **40**, ANSP 151093 (198) Florida; **41**, USNM 121801 (205); Venezuela **42**, ANSP 151093 Florida (207); **43**, USNM 121801 (213) Venezuela; **44**, CAS 122133 (223) Brazil; **45**, CAS 122133 (228) Brazil; **46**, ANSP 158504 (233) Honduras; **47**, CAS 122133 (235) Brazil; **48**, ANSP 151589 (254) Puerto Rico; **49**, ANSP 158504 (251) Honduras; **50**, USNM 12681 (254) Key West; **51**, USNM 12681 (269) Key West; **52**, AMNH 3889 (274) Brazil; **53**, ANSP 148238 (294) French Guiana; **54**, ANSP 102112 (298) Brazil; **55**, AMNH 3889 (300) Brazil; **56**, CAS 153016 (316) Brazil; **57**, CAS 153016 (319) Brazil; **58**, USNM 114618 (326) Guatemala; **59**, USNM 114618 (332) Guatemala; **60**, USNM 128658 (334) Panama; **61**, USNM 128658 (350) Panama; **62**, USNM 114618 (360) Guatemala; **63**, USNM 128657 (364) Panama; **64**, ANSP 93821 (366) Florida; **65**, USNM 29986 (372) Rhode Island; **66**, USNM 19821 (386) Cuba; **67**, USNM 132964 (400) Cuba; **68**, USNM 114594 (420) Guatemala; **69**, USNM 332457 (421) Florida; **70**, USNM 362541 (430) Florida; **71**, USNM 79981 Panama (440); **72**, USNM 362541 (460) Florida; **73**, USNM 362541 (470) Florida; **74**, USNM 114816 (485) Guatemala; **75**, CAS 153082 (534) Brazil; **76**, CAS 153082 (555) Brazil; **77**, CAS 153080 (605) Brazil; **78**, CAS 153080 (617) Brazil; **79**, USNM 22855 Gulf of Mexico (622); **80**, ANSP 159674 (655) Mexico; **81**, ANSP 102762 (657) Bahamas; **82**, USNM 32080 (725) Jamaica; **83**, CAS 216873 (1015) Florida; **84**, MNHN 1978-230 (274) "tropical West Africa"; **85**, MNHN 1978-216 (331) Western Sahara; **86**, ZMUC 25 (565) Senegal, Dakar; **87**, USNM 377462 (1070 estimated, 130 cm TL measured), Guinea-Bissau.

Caranx fischeri: **88**, CAS 38375 (159) Nigeria; **89**, USNM 27566 (163) Sierra Leone; **90**, CAS-SU 15885 (171) Cameroon; **91**, ANSP 158493 (173) Gulf of Guinea, Bioko; **92**, ANSP 158493 (182) Bioko; **93**, ANSP 158493 (197) Bioko; **94**, USNM 279566 (203) Sierra Leone; **95**, ANSP 158497 (237) Sierra Leone; **96**, ANSP 158498 (239) Sierra Leone; **97**, BMNH 1939.7.12.12 (271) Gold Coast; **98**, MNHN 1978-260 (313) Senegal; **99**, MNHN 1978-235 (317) "tropical West Africa"; **100**, ANSP 140256 (328) Cameroon; **101**, BMNH 1899.11.27.87 (348) Congo; **102**, BMNH 1927.12.7.49 (358) Ascension Island; **103**, MRAC 87428 (367) Congo; **104**, MRAC 36 (403) Congo; **105**, ZMUC P.46362 (450) Nigeria; **106**, IRSNB 829 (530) Senegal.

Appendix 2

Catalog numbers, localities, and sizes (mm FL) of specimens used for the outline drawings of the eighth precaudal vertebra in Figure 13. Number in bold correspond to the numbers for the vertebrae illustrated in Figure 13.

Caranx hippos: **1**, USNM 19821 (357), Cuba; **2**, USNM 114618 (360), Guatemala; **3**, USNM (400) Cuba; **4**, USNM 11490 (420) Guatemala; **5**, USNM 3324557 (421) Florida, Swanee River; **6**, USNM 79981 (440), Panama, Colon; **7**, USNM 362541 (470), Florida, Caloosahatchee River; **8**, USNM 115618 (485), Guatemala; **9**, CAS-SU (534) Brazil; **10**, CAS-SU 53082 (555) Brazil; **11**, USNM 114618 (557) Guatemala; **12**, CAS-SU 53080 (605) Brazil; **13**, USNM 22855 (622) Florida, Pensacola; **14**, ANSP 159674 (655) Mexico, Carmen; **15**, ANSP 102762 (657) Bahamas, Andros Island; **16**, ANSP 159674 (698) Mexico, Carmen; **17**, ANSP 159674 (717) Mexico, Carmen; **18**, ZMUC (565) Senegal, Dakar

Caranx caninus: **19**, USNM 127918 (359) Peru, Lobos de Tierra; **20**, SIO-62-61 (371) Mexico, Isabel Island; **21**, USNM 10099 (381), Mexico, Petarabo Bay; **22**, USNM 100998 (399) Mexico; **23**, SIO 62-61 (419) Mexico, Isabel Id.; **24**, SIO 65-182 (431) Mexico, Baja; **25**, USNM 206999 (490) Colombia, Baja Utria; **26**, USNM 128659 (520) Panama, Miraflores Lock; **27**, CAS 216871 (538) Tres Marias Is.; **28**, SIO 58-83 (588) Peru; **29**, SIO 75-383 (643), San Diego Bay; **30**, SIO 65-176A (670), Baja California.

Appendix 3

Catalog numbers, localities, and sizes (mm FL) of specimens used for the outline drawings of the first anal-fin pterygiophore in Figure 15. Numbers in bold font correspond to the numbers for the pterygiophores seen in Figure 15.

Caranx caninus: **1**, SIO-62-61 (419) Mexico, Isabel Island; **2**, CAS 216872 (421) Baja California; **3**, SIO-62-61 (438) Mexico, Isabel Island; **4**, USNM 206999 (490) Colombia; **5**, CAS 21871(538) Tres Marias Island; **6**, SIO 58-83 (588) Peru; **7**, SIO 75-383 (643) California, San Diego; **8**, SIO 65-176A (670) Baja California.

Caranx hippos: **9**, USNM 114594 (420) Guatemala; **10**, USNM 79981 (440) Panama, Colon; **11**, USNM 362541 (460) Florida, Coloosahatchee River; **12**, USNM 362541 (470), Florida, Coloosahatchee River; **13**, USNM 114618 (485) Guatemala; **14**, CAS-SU 53082 (534) Brazil; **15**, CAS-SU 53082 (534) Brazil; **16**, USNM 114618 (557), Guatemala; **17**, CAS-SU 53082 (555) Brazil; **18**, CAS-SU 53080 (617) Brazil; **19**, ANSP 159674 (655) Mexico; **20**, ANSP 102762 (657) Bahamas; **21**, ANSP 159674 (698) Mexico.

Abstract—The diet of Steller sea lions (*Eumetopias jubatus*) was determined from 1494 scats (feces) collected at breeding (rookeries) and nonbreeding (haulout) sites in Southeast Alaska from 1993 to 1999. The most common prey of 61 species identified were walleye pollock (*Theragra chalcogramma*), Pacific herring (*Clupea pallasii*), Pacific sand lance (*Ammodytes hexapterus*), Pacific salmon (Salmonidae), arrowtooth flounder (*Atheresthes stamias*), rockfish (*Sebastes* spp.), skates (Rajidae), and cephalopods (squid and octopus). Steller sea lion diets at the three Southeast Alaska rookeries differed significantly from one another. The sea lions consumed the most diverse range of prey categories during summer, and the least diverse during fall. Diet was more diverse in Southeast Alaska during the 1990s than in any other region of Alaska (Gulf of Alaska and Aleutian Islands). Dietary differences between increasing and declining populations of Steller sea lions in Alaska correlate with rates of population change, and add credence to the view that diet may have played a role in the decline of sea lions in the Gulf of Alaska and Aleutian Islands.

Diets of Steller sea lions (*Eumetopias jubatus*) in Southeast Alaska, 1993–1999

Andrew W. Trites¹

Donald G. Calkins²

Arliss J. Winship¹

Email address for A. W. Trites: trites@zoology.ubc.ca

¹ Marine Mammal Research Unit, Fisheries Centre
Room 247, AERL – Aquatic Ecosystems Research Laboratory
2202 Main Mall, University of British Columbia
Vancouver, BC, Canada V6T 1Z4

² Alaska Department of Fish and Game
333 Raspberry Road
Anchorage, Alaska 99518-1599

Steller sea lion (*Eumetopias jubatus*) populations in the Aleutian Islands and Gulf of Alaska began declining in the mid-1970s and were listed as endangered under the U.S. Endangered Species Act in 1997 (NMFS¹; Trites and Larkin, 1996; Loughlin, 1998). The cause of the population decline is uncertain but may be linked to a decrease in the quantity, quality, or availability of prey, in turn caused either by commercial fisheries or by a natural change in the ecosystem (Alaska Sea Grant, 1993; DeMaster and Atkinson, 2002; Trites et al., 2007). Stomach contents and scat analysis indicate that the diets of the declining population may have changed from primarily small, fatty, schooling fishes (such as capelin (*Malotus villosus*) and sand lance (*Ammodytes hexapterus*)) in the 1950s to one increasingly dominated by walleye pollock (*Theragra chalcogramma*), Atka mackerel (*Pleurogrammus monopterygius*), and flatfish (Pleuronectidae) in the 1970s, 1980s, and 1990s (Mathisen et al., 1962; Thorsteinson and Lensink, 1962; Pitcher, 1981; Calkins and Goodwin¹; Merrick et al., 1997; Sinclair and Zeppelin, 2002).²

Merrick et al. (1997) found a positive relationship between the rate of population change and the diversity of summer Steller sea lion diets in the declining population during the early 1990s. Regions that had the highest

rates of decline had the lowest diversities of diet. The greater the diet diversity, the slower the rate of population decline. Additional diet data (through to 2001) supported the conclusion that diet diversity had some influence on population success (Sinclair and Zeppelin, 2002; Sinclair et al., 2005). Merrick et al. (1997) hypothesized that animals with less diverse diets may have experienced difficulty obtaining enough prey. Others have hypothesized that consumption of larger proportions of lower energy-dense prey may have exacerbated the effect of diet diversity by increasing the food requirements of sea lions (Alverson, 1992; Rosen and Trites, 2000; Trites and Donnelly, 2003). Sea lions with less diverse, low energy-dense diets may also have been more sensitive to changes in overall prey abundance, and could have theoretically incurred higher rates of predation from killer

¹ NMFS (National Marine Fisheries Service). 1992. Recovery plan for the Steller sea lion (*Eumetopias jubatus*), 92 p. Prepared by the Steller Sea Lion Recovery Team for the National Marine Fisheries Service, 1315 East-West Highway, Silver Spring, MD 20910-3282.

² Calkins, D. G., and E. Goodwin. 1988. Investigation of the declining sea lion population in the Gulf of Alaska, 76 p. Unpublished report. Alaska Department of Fish and Game, 333 Raspberry Road, Anchorage, AK 99518-1599.

whales if they had to forage for longer periods of time.

Population trends in Southeast Alaska have been opposite to those observed in the Gulf of Alaska (Trites and Larkin, 1996; Calkins et al., 1999; Pitcher et al., 2007). The robustness of the Southeast population compared to the other regions of Alaska may reflect a difference in diet. One explanation for this finding is that Steller sea lions in Southeast Alaska eat a wider range of prey and therefore have a more diverse diet. Another is that low energy-density prey (such as pollock) do not comprise a significant portion of the sea lion diet in Southeast Alaska.

Our goal was to determine the diets of Steller sea lions in Southeast Alaska. We sought to test two hypotheses: 1) diet in Southeast Alaska is the most diverse of all regions inhabited by Steller sea lions; and 2) pollock is not an important prey species in Southeast Alaska. We also wanted to document prey associations and seasonal changes in diet.

Materials and methods

There are three major breeding areas (rookeries) and over 45 major non-breeding areas (haulouts) in Southeast Alaska. We collected 1494 scats from 12 haulouts and all three rookeries from 1993 through 1999 (Fig. 1). Some areas, such as the Forrester rookery, were sampled every year, and others were sampled less frequently (Table 1). We grouped our analyses into rookeries and haulouts, and then into subgroups by sample size, location, and frequency of sampling. Haulouts consisted of 12 nonbreeding sites in the inside protected waters of Southeast Alaska (Fig. 1). Rookeries consisted of the three breeding areas in Southeast Alaska (Forrester Island, Hazy Island, and White Sisters Islands).

Scats were generally collected opportunistically, when rookeries and haulouts were disturbed in order to count pups or for other research purposes. Each scat was placed in a zip-lock plastic bag and frozen in a 5-gallon plastic bucket before it was shipped to the Food and Energy Consumption Laboratory at the Vancouver Aquarium Marine Science Centre for cleaning. Only scats that were big enough or solid enough to likely contain prey remains were collected, and only one scat was collected from any group of scats if there was any doubt about whether the scat came from more than one Steller sea lion. Each thawed scat was transferred to a plastic jar and soaked in water for 1–6 days. Periodic

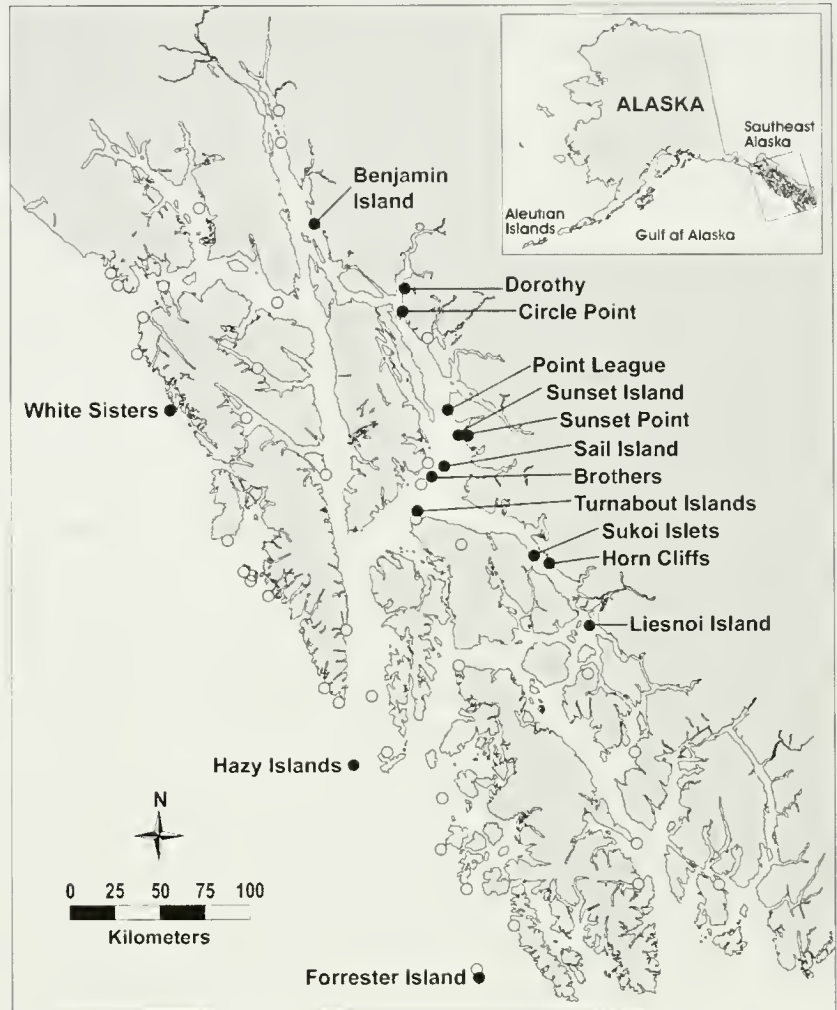


Figure 1

Major rookeries (White Sisters, Hazy Island, and Forrester Island) and haulouts (all other sites) of Steller sea lions (*Eumetopias jubatus*) in Southeast Alaska during 1993–99. Labeled sites indicate where scats were collected.

shaking of the jars ensured that the scats broke down and formed a uniform slurry at the bottom of the jar. Volume was recorded from graduated markings on each jar. An elutriator removed most of the water-soluble elements (Bigg and Olesiuk, 1990) before the remaining sample was washed through a fine mesh screen.

Prey species were identified at Pacific IDENTifications Inc. (Victoria, BC) from cleaned and dried hard parts; the types of hard parts that were present and the species from which they came were also noted. Prey hard parts recovered from scats were compared with hard parts from a reference collection of identified skeletal and nonskeletal hard parts. Otoliths and all other hard parts were identified to the lowest possible taxon. Hard parts that were digested beyond recognition or were not diagnostic for prey taxa were not included in our analysis (e.g., ribs). Some recovered structures, such as otoliths or squid beaks, could be used to estimate

the type and number of prey consumed, but other hard parts, such as scales, teeth, branchials, and gill rakers, could only be used to quantify the type of prey consumed.

Scats that were empty or contained prey that could not be identified with certainty were not analyzed. These represented few of the scats collected (56 of 1494, 4%). Unrecognizable hard parts could have been from

Table 1

Total number of Steller sea lion (*Eumetopias jubatus*) scats collected in Southeast Alaska during 1993–99 by year, location, and month. Note that North Rocks, Cape Horn Rocks, and Sea Lion Rocks are part of the Forrester Island rookery complex.

Year	Location	Jan	Feb	Mar	Apr	May	Jun	Jul	Aug	Sep	Oct	Nov	Dec	Total
1993	Benjamin Is.	0	0	0	0	0	0	0	0	0	0	28	0	28
1993	Brothers	0	0	0	0	0	0	0	0	0	7	27	0	34
1993	Cape Horn Rocks	0	0	0	0	0	5	0	0	0	0	0	0	5
1993	Hazy	0	0	0	0	0	27	0	0	0	0	0	0	27
1993	North Rocks	0	0	0	0	0	8	0	0	0	0	0	0	8
1993	Pt. League	0	0	0	0	0	0	0	0	0	0	38	0	38
1993	Sail Is.	0	0	0	0	0	0	0	0	0	0	80	0	80
1993	Sea Lion Rocks	0	0	0	0	0	9	8	0	0	0	0	0	17
	Total	0	0	0	0	0	49	8	0	0	7	173	0	237
1994	Cape Horn Rocks	0	0	0	0	0	29	0	0	0	0	0	0	29
1994	Hazy	0	0	0	0	0	0	54	0	0	0	0	0	54
1994	North Rocks	0	0	0	0	0	32	0	0	0	0	0	0	32
1994	Sea Lion Rocks	0	0	0	0	0	73	0	0	0	0	0	0	73
1994	White Sisters	0	0	0	0	0	0	49	0	0	0	0	0	49
	Total	0	0	0	0	0	134	103	0	0	0	0	0	237
1995	Benjamin Is.	0	0	0	0	0	0	0	0	0	16	0	0	16
1995	Brothers	0	0	0	0	0	0	0	0	0	25	0	14	39
1995	Cape Horn Rocks	0	0	0	0	0	30	0	0	0	0	0	0	30
1995	Circle Pt.	0	0	0	0	0	0	0	0	0	12	0	22	34
1995	Horn Cliff	0	0	0	0	0	0	0	0	0	10	0	0	10
1995	North Rocks	0	0	0	0	0	68	0	0	0	0	0	0	68
1995	Pt. League	0	0	0	0	0	0	0	0	0	13	0	14	27
1995	Sail Is.	0	0	0	0	0	0	0	0	0	26	0	6	32
1995	Sea Lion Rocks	0	0	0	0	0	30	0	0	0	0	0	0	30
1995	Sukoi Is.	0	0	0	0	0	0	0	0	0	7	0	0	7
1995	Sunset Is.	0	0	0	0	0	0	0	0	0	0	0	4	4
1995	Sunset Pt.	0	0	0	0	0	0	0	0	0	0	0	22	22
1995	Turnabout Is.	0	0	0	0	0	0	0	0	0	10	0	2	12
	Total	0	0	0	0	0	128	0	0	0	119	0	84	331
1996	Benjamin Is.	4	0	10	0	0	0	0	0	0	0	0	0	14
1996	Brothers	0	0	15	20	18	0	0	0	0	0	0	0	53
1996	Cape Horn Rocks	0	0	0	0	0	11	13	0	0	0	0	0	24
1996	Dorothy	0	0	0	11	0	0	0	0	0	0	0	0	11
1996	Horn Cliff	0	0	0	0	12	0	0	0	0	0	0	0	12
1996	Liesnoi Is.	0	0	0	0	22	0	0	0	0	0	0	0	22
1996	North Rocks	0	0	0	0	0	0	21	0	0	0	0	0	21
1996	Pt. League	0	0	11	0	14	0	0	0	0	0	0	0	25
1996	Sail Is.	0	0	0	0	11	0	0	0	0	0	0	0	11
1996	Sea Lion Rocks	0	0	0	0	0	8	0	0	0	0	0	0	8
1996	Sunset Pt.	0	0	20	13	0	0	0	0	0	0	45	0	78
1996	Turnabout Is.	0	0	34	0	0	0	0	0	0	0	0	0	34
	Total	4	0	90	44	77	19	34	0	0	0	45	0	313

continued

species not in the reference skeleton collection at the time of identification or could have been too far digested to be identifiable.

We grouped the identified species of prey into eight categories for statistical analysis. These included gadids, forage fish, salmon (*Salmonidae*), flatfish, rockfish (*Sebastes* spp.), cephalopods, hexagrammids, and other prey (Fig. 2). Scats that contained more than one species from a particular group were scored as containing only a single occurrence of that group. For example, a scat containing both Pacific herring (*Clupea pallasii*) and sand lance was scored as having a single occurrence of forage fish. Hexagrammids do not inhabit the waters of Southeast Alaska in significant numbers but were included as a prey category so that diets could be compared across regions of the North Pacific where hexagrammids are consumed in greater numbers (Merrick et al., 1997; Sinclair and Zeppelin, 2002).

The diversity of the diet was calculated for the eight prey groups by using the Shannon-Wiener species diversity index (Ricklefs and Miller, 2000), which yields a value between 1 and 8, where a value of 1 indicates that only one of the eight groups was consumed, and a value of 8 indicates that all eight were equally consumed. Merrick et al. (1997) used this index to determine the dietary diversity of Steller sea lions that consumed seven prey groups in the Gulf of Alaska and Aleutian Islands. We therefore pooled rockfish with other prey to create the same seven categories used by Merrick et al. (1997) to compare the diversity of diet across all regions of Alaska. We compared our estimate of dietary diversity to those presented by Merrick et al. (1997) for diet data collected between 1990 and 1995. However, we recalculated the diet diversities presented in their paper (from their split-sample frequency of oc-

currence data) because of a calculation error in their published values.

Seasonal diets were calculated for rookeries in summer (Forrester Island, Jun–Aug, 1993–99) and haulouts in fall (Sep–Nov, 1993 and 1995–96), winter (Dec–Feb, 1996–1997), and spring (Mar–May 1996). Average summer diet (Jun–Aug) was calculated from the three rookeries—weighted by the average number of pups counted at each site during 1993–1997 (pup counts serving as an index of population size; Trites and Larkin, 1996; Pitcher et al., 2007). The summer data were weighted to indicate what the average Steller sea lion ate in Southeast Alaska, rather than to describe what the average rookery diet was. Fall, winter, and spring diets were given equal weight and averaged to describe the nonsummer diet (haulouts, Sep–May) because animals are more evenly distributed during the nonbreeding season and haulout counts were not available for each of the seasons.

The relative importance of prey in the diet was quantified as “simple” and “split-sample” frequency of occurrences. The simple frequency of occurrence indicates what proportion of scats contains any particular prey type. They do not sum to 100%. For example, 80% of the scats examined may contain gadids, and 50% may contain forage fish—meaning that some scats contained both prey types, and others contained only gadids or only forage fish. The second method we used, the split-sample frequency of occurrence (Olesiuk et al., 1990; Olesiuk, 1993), yields the proportion of the overall diet made up of any single prey type. These proportions do sum to 100%. With the split-sample method, it is assumed that the scat contained remains from all prey consumed in the previous meal and that the prey were consumed in equal volumes.

Table 1 (continued)

Year	Location	Jan	Feb	Mar	Apr	May	Jun	Jul	Aug	Sep	Oct	Nov	Dec	Total
1997	Cape Horn Rocks	0	0	0	0	0	25	0	0	0	0	0	0	25
1997	North Rocks	0	0	0	0	0	25	0	0	0	0	0	0	25
1997	Sea Lion Rocks	0	0	0	0	0	25	0	0	0	0	0	0	25
1997	Sunset Pt.	0	32	0	0	0	0	0	0	0	0	0	0	32
1997	Turnabout Is.	0	27	0	0	0	0	0	0	0	0	0	0	27
	Total	0	59	0	0	0	75	0	0	0	0	0	0	134
1998	Cape Horn Rocks	0	0	0	0	0	0	27	0	0	0	0	0	27
1998	Hazy	0	0	0	0	0	0	70	0	0	0	0	0	70
1998	North Rocks	0	0	0	0	0	0	21	0	0	0	0	0	21
1998	Sea Lion Rocks	0	0	0	0	0	0	21	0	0	0	0	0	21
	Total	0	0	0	0	0	0	139	0	0	0	0	0	139
1999	Hazy	0	0	0	0	0	0	60	0	0	0	0	0	60
1999	North Rocks	0	0	0	0	0	6	33	0	0	0	0	0	39
1999	Sea Lion Rocks	0	0	0	0	0	4	0	0	0	0	0	0	4
	Total	0	0	0	0	0	10	93	0	0	0	0	0	103
	Grand Total	4	59	90	44	77	415	377	0	0	126	218	84	1494

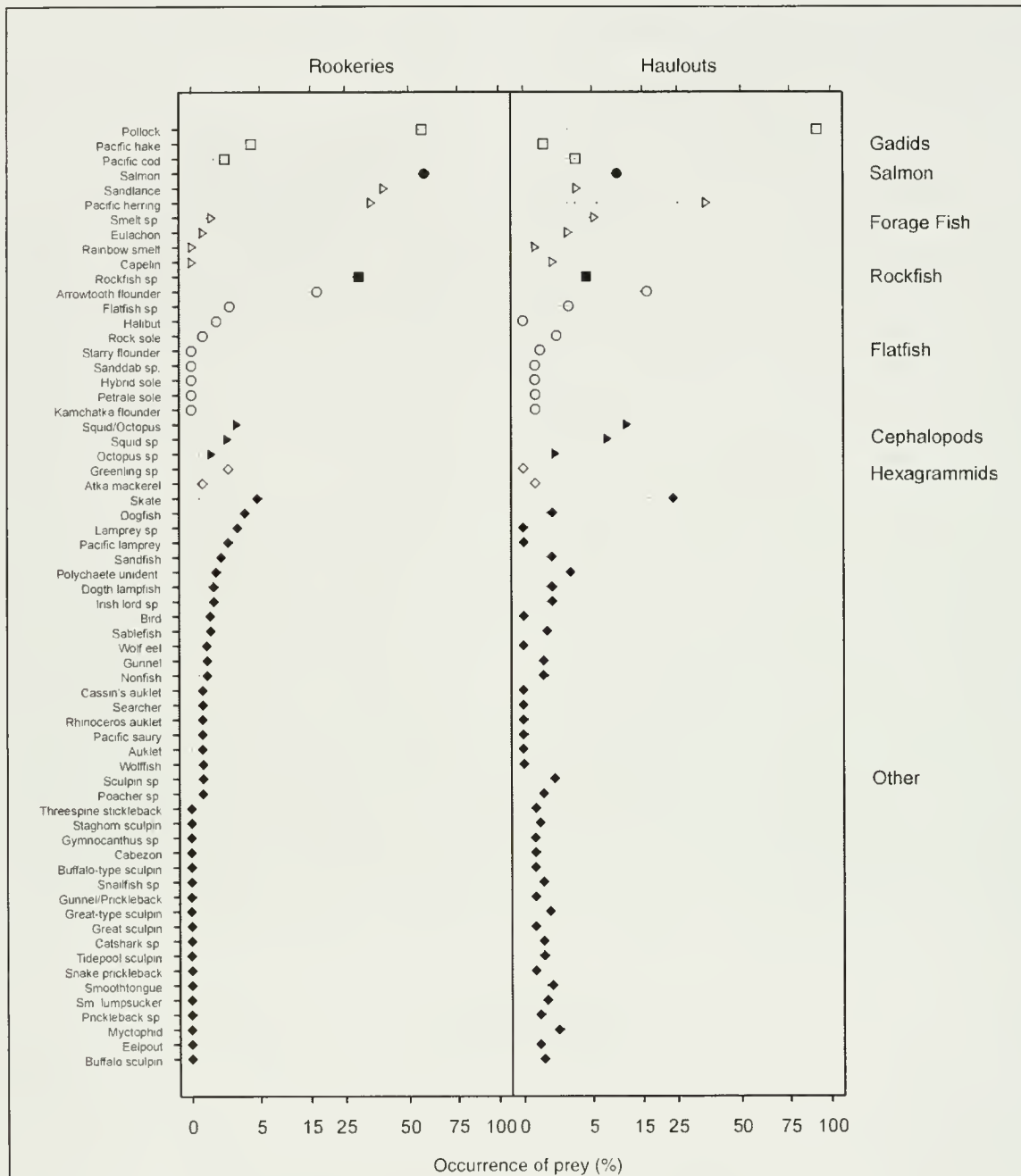


Figure 2

Frequency of occurrence of individual prey species in Steller sea lion (*Eumetopias jubatus*) scats from three Southeast Alaskan rookeries (Forrester, Hazy, and White Sisters; $n=752$) in summer (Jun–Aug) and haulouts ($n=686$) during the rest of the year (Sep–May, 1993–99). Data were pooled across months, years, and sites. Plotted data were transformed (square-root transformed) to improve the visual resolution at lower frequencies of occurrence. The eight symbols identify the eight groups of species used to calculate diet diversity.

Statistical analyses were performed on the simple frequency of occurrences to determine whether diets varied by sites and time (across years). We used a contingency table analysis for the total number of scats containing particular prey categories

(Pearson χ^2 , $\alpha \leq 0.05$). The cephalopod and hexagrammid prey categories were not considered in these analyses because of their low frequencies of occurrence. Differences in the number of categories of prey consumed on each foraging trip (i.e., the number of prey

groups per scat) were compared by using analysis of variance.

Associations between prey groups recovered from individual scats were identified by calculating partial correlation coefficients for each pair of prey groups by using presence and absence data with each scat as a replicate (Zar, 1996). This analysis was performed for all scats collected at the three rookeries during the summer and for all scats collected at the haulouts during autumn–spring. Partial correlations were considered significant at $P=0.05$. Prey associations were illustrated by using the *hclust* function of S-Plus 2000 (Mathsoft Inc., Seattle, WA) and using the “average” clustering method and the distance between two prey groups as equal to 1 minus the partial correlation coefficient of those two prey.

Results

A total of 61 species of prey were identified from all of the scats examined. The most common prey (i.e., those that occurred in more than 5% of all the scats examined) in order of frequency were walleye pollock, Pacific herring, sand lance, salmon, arrowtooth flounder (*Atheresthes stomias*), rockfish (*Sebastes* spp.), skates (Rajidae), squid, and octopus (Fig. 2, Table 2). Species of salmon, rockfish, squids, and octopus could be identified only to family, and other species, such as Pacific herring or walleye pollock, could be identified to species. Unfortunately not all recovered hard parts could be identified to the species level.

Steller sea lion diets at the Forrester Island rookeries were significantly different from one another in 1994 and 1998 ($P<0.001$), but the differences between the diets at Forrester Island and those at Hazy Island in 1993 and 1999 were not significant ($P=0.06$, 0.36 , respectively; Fig. 3). At White Sisters, mature females consumed primarily forage fish followed by gadids; whereas at Hazy Island, gadids were the dominant prey. Further south at Forrester Island, the diet was more evenly distributed between forage fish, salmon, and gadids. Scats were collected in multiple years at Forrester Island and Hazy Island and showed little difference in diet over time within each site ($P=0.30$, 0.11 , respectively).

Outside of the breeding season, the diet of Steller sea lions in Southeast Alaska was dominated by gadids (primarily pollock; Figs. 4 and 5, Table 3). The abundance of salmon in the diet dropped from summer to fall (Fig. 4, Table 3) when the runs of salmon presumably passed into the river systems. Forage fish were found in 37% of the scats collected in the fall (Sep–Nov), in 43% of scats in the winter, 47% in spring, and in 62% of scats in the summer (Fig. 4). Squid and octopus were more important in fall and winter (22% on average) than during summer. Rockfish were consumed relatively frequently during the summer but were largely absent in the diet from fall to spring, presumably because they were not present or accessible in significant numbers. “Other” fishes (primarily

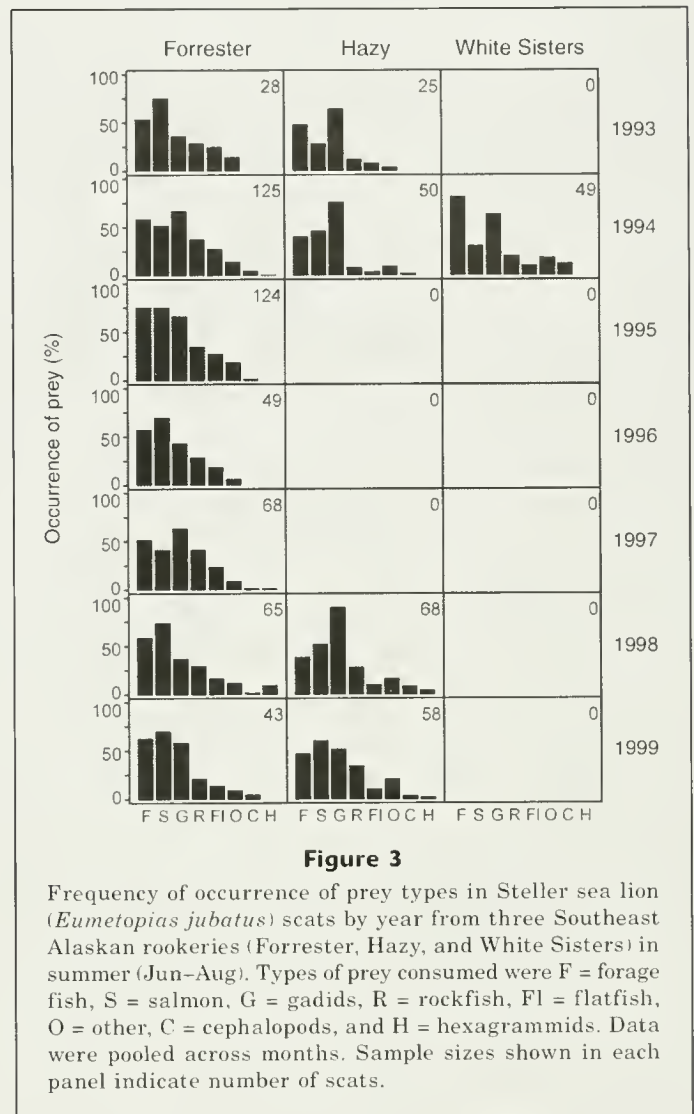


Figure 3

Frequency of occurrence of prey types in Steller sea lion (*Eumetopias jubatus*) scats by year from three Southeast Alaskan rookeries (Forrester, Hazy, and White Sisters) in summer (Jun–Aug). Types of prey consumed were F = forage fish, S = salmon, G = gadids, R = rockfish, Fl = flatfish, O = other, C = cephalopods, and H = hexagrammids. Data were pooled across months. Sample sizes shown in each panel indicate number of scats.

skates, see Fig. 2) rose in importance from summer to fall (13% to 24% respectively), peaking at 50% in winter (Fig. 4). Gadids, forage fishes, and other fishes were the dominant prey during winter. In terms of diet diversity (dd), Steller sea lions consumed the most diverse range of prey categories during summer at rookeries (dd=5.34 on a scale of 1–8), and the least diverse during fall while at haulouts (dd=3.53).

Most scats contained at least two prey groups, and one scat contained remains from all eight groups (Fig. 6). The mean number of prey groups per scat ranged from 2.1 to 2.6 depending on season (Fig. 6). In general, the distributions were skewed towards fewer prey groups occurring together in a single scat in fall and spring, and were more normally distributed in summer and winter. The number of prey types per scat was not significantly different between fall and spring or between summer and winter ($P>0.05$; Tukey-Kramer test) but did differ significantly between these seasonal pairings. Those scats with only a single identifiable prey type

Table 2

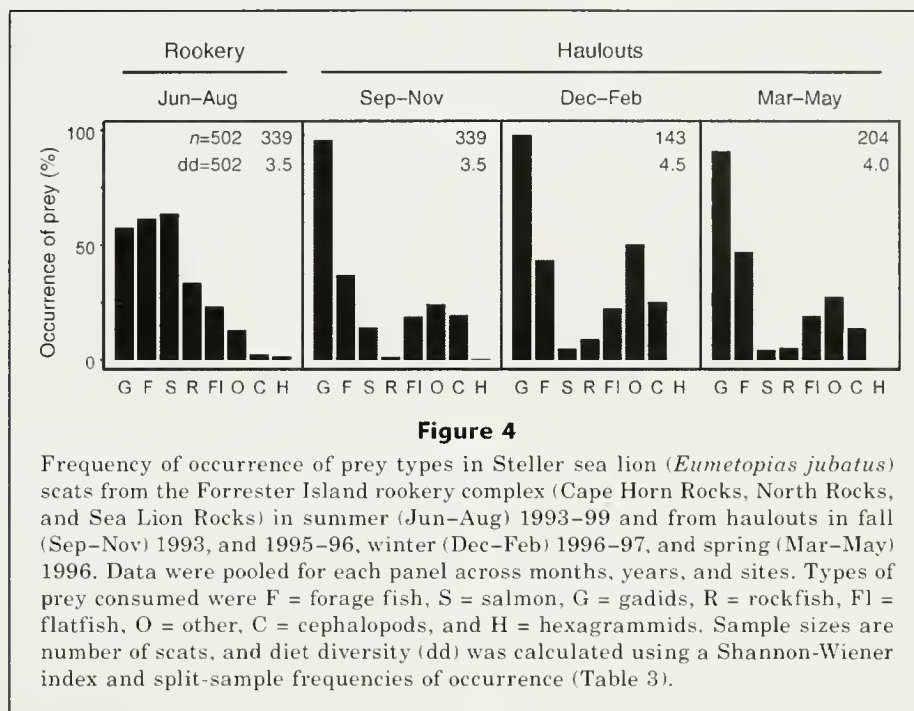
Frequency of occurrence of prey types in Steller sea lion (*Eumetopias jubatus*) scats from Southeast Alaska. Samples were from rookeries (Forrester, Hazy, and White Sisters) in summer (Jun–Aug) 1993–99 and from haulouts in fall (Sep–Nov) 1993 and 1995–96, winter (Dec–Feb) 1996–97, and spring (Mar–May) 1996. The rookery data (summer) were pooled across months (and sites within the Forrester complex) but averaged across years and rookeries (weighted by pup counts). Haulout data were pooled across months and sites but averaged across years.

Species	Frequency of occurrence in diet (%)				Species	Frequency of occurrence in diet (%)			
	Summer n=752	Fall n=339	Winter n=143	Spring n=204		Summer n=752	Fall n=339	Winter n=143	Spring n=204
Gadids					Other species				
Walleye pollock	56.4	90.6	96.5	88.7	Skate	4.7	17.7	45.5	18.1
Pacific hake	3.9	0.9	0.0	0.0	Dogfish	3.1	1.5	0.0	0.5
Pacific cod	1.2	2.4	2.1	4.4	Lamprey spp.	2.3	0.0	0.0	0.0
Salmonids					Pacific lamprey	1.5	0.0	0.0	0.0
Salmon	57.7	14.2	4.9	4.4	Sandfish	0.9	0.6	0.0	2.0
Forage fish					Polychaete unident.	0.7	0.6	6.3	2.5
Pacific sand lance	38.8	3.8	2.8	1.5	Dogth lampfish	0.5	0.0	0.7	2.5
Pacific herring	34.0	31.3	39.9	38.2	Irish lord spp.	0.5	0.6	1.4	1.0
Smelt spp.	0.4	5.0	2.8	7.4	Sablefish	0.4	1.2	0.0	0.0
Eulachon	0.1	0.0	2.1	5.4	Wolfeel	0.3	0.0	0.0	0.0
Rainbow smelt	0.0	0.3	0.0	0.0	Gunnel	0.3	0.3	0.7	0.5
Capelin	0.0	0.6	0.0	2.0	Searcher	0.1	0.0	0.0	0.0
Rockfish					Pacific saury	0.1	0.0	0.0	0.0
Rockfish spp.	29.8	1.5	9.1	5.4	Wolffish	0.1	0.0	0.0	0.0
Flatfish					Sculpin spp.	0.1	1.5	1.4	0.0
Arrowtooth flounder	16.8	16.2	20.3	13.2	Poacher spp.	0.1	0.9	0.0	0.0
Flatfish spp.	1.6	1.8	2.1	2.9	Threespine stickleback	0.0	0.0	0.0	0.5
Halibut	0.7	0.0	0.0	0.0	Staghorn sculpin	0.0	0.0	0.0	1.0
Rock sole	0.1	0.9	0.7	2.0	Gymocanthus spp.	0.0	0.0	0.0	0.5
Starry flounder	0.0	0.0	0.0	1.0	Cabezon	0.0	0.0	0.0	0.5
Sanddab spp.	0.0	0.0	0.0	0.5	Buffalo-type sculpin	0.0	0.0	0.0	0.5
Hybrid sole	0.0	0.0	0.0	0.5	Snailfish spp.	0.0	0.0	0.7	1.0
Petrale sole	0.0	0.3	0.0	0.0	Gunnel/Prickleback	0.0	0.0	0.7	0.0
Kamchatka flounder	0.0	0.3	0.0	0.0	Great-type sculpin	0.0	0.0	1.4	1.5
Cephalopods					Great sculpin	0.0	0.0	0.7	0.0
Squid/Octopus	2.1	11.2	20.3	4.4	Catshark spp.	0.0	0.0	1.4	0.5
Squid spp.	1.3	8.0	4.9	7.8	Tidepool sculpin	0.0	0.3	0.7	0.5
Octopus spp.	0.4	1.2	0.0	1.5	Snake prickleback	0.0	0.3	0.0	0.0
Hexagrammids					Smoothtongue	0.0	0.3	2.8	0.5
Greenling spp.	1.5	0.0	0.0	0.0	Small lumpsucker	0.0	0.6	0.7	0.5
Atka mackerel	0.1	0.3	0.0	0.0	Prickleback spp.	0.0	0.3	0.0	0.5
					Myctophid	0.0	1.2	3.5	0.0
					Eelpout	0.0	0.3	0.0	0.5
					Buffalo sculpin	0.0	0.9	0.0	0.0

more likely contained gadids (mostly pollock) than any other species.

There was a positive relationship between scat size (volume) and the numbers of prey types each scat contained for samples <250 mL (which represented about 50% of the scats collected). Beyond this volume, numbers of prey types per scat appeared to be independent of scat size (Fig. 7).

In terms of which prey groups occurred most frequently together, the highest partial correlation among prey groups was between salmon and forage fish (rookeries: $r=0.23$, $r_{0.05(2),744}=0.07$, $P<0.05$; haulouts: $r=0.189$, $r_{0.05(2),678}=0.08$, $P<0.05$; Fig. 8). Gadids and cephalopods were also significantly correlated in scats from both rookeries ($r=0.11$) and haulouts ($r=0.08$), whereas gadids were negatively correlated with occurrences of salmon

**Table 3**

Split-sample frequency of occurrence of prey types in Steller sea lion (*Eumetopias jubatus*) scats from Southeast Alaska. Samples were from rookeries (Forrester, Hazy, and White Sisters) in summer (Jun–Aug) 1993–99 and from haulouts in fall (Sep–Nov) 1993 and 1995–96, winter (Dec–Feb) 1996–1997, and spring (Mar–May) 1996. The rookery data (summer) were pooled across months (and sites within the Forrester complex) but averaged across years and rookeries (weighted by pup counts). Haulout data were pooled across months and sites, but were averaged across years.

Season	Prey category (%)							
	Cephalopods	Flatfish	Forage fish	Gadids	Hexagrammids	Other	Rockfish	Salmon
Winter (Dec–Feb)	8.1	7.6	13.5	49.1	0.0	15.9	4.5	1.2
Spring (Mar–May)	5.0	7.6	21.0	52.5	0.0	10.5	2.0	1.4
Summer (Jun–Aug)	0.8	6.4	21.9	27.3	0.4	4.3	11.7	27.3
Fall (Sep–Nov)	7.0	6.2	12.5	62.2	0.1	8.4	0.4	3.3

from rookeries ($r = -0.16$) and with forage fish from scats collected at haulouts ($r = -0.10$).

Plotting our estimate of dietary diversity for Southeast Alaska during summer with values recalculated for other regions of Alaska revealed a significant relationship between diet diversity and the rate of population change during 1990–94 (Fig. 9). High rates of population decline correlated with low levels of diet diversity.

Discussion

The Southeast Alaska population of Steller sea lions grew considerably since the first census of 100 animals was made at Forrester Island in the 1920s (Rowley,

1929). Subsequent counts were 350 sea lions (nonpups) in 1945 (Imler and Sarber, 1947), and 2500 in 1957 (Mathisen and Lopp, 1963). The total population in 1992 (including pups) was estimated at 10,003 (Trites and Larkin, 1996), and an annual growth rate of 6% was estimated (1979–97; Calkins et al., 1999). Steller sea lions were first noted breeding on White Sisters (3 pups) and Hazy Island (30 pups born) in 1979. In 1997, 205 pups were counted at White Sisters, 1157 were counted at Hazy, and 2798 were counted at Forrester Island. Small numbers of pups have since been noted at Graves Rocks and Biali Rocks (Pitcher et al., 2007).

It is not clear why Steller sea lion populations grew through the 20th century in Southeast Alaska. One possible explanation is that predation by killer whales

or hunting by native peoples was reduced. Another is that these sea lions may have begun consuming more abundant prey or they had a higher quality diet that enhanced birth and survival rates. Unfortunately there is little or no information to shed light on this important question.

There are few data available on fish stocks preyed upon by sea lions or on the diet of Steller sea lions in Southeast Alaska prior to the 1990s. Pollock does not appear to have been abundant in fishery surveys and was not thought to be present in commercially available quantities. However, Imler and Sarber (1947) reported that pollock were found in five of the seven stomachs taken in the vicinity of the Brothers Islands and White Sisters Islands in 1946—and accounted for 68% of the stomach contents by volume. The only other dietary information comes from the stomachs of five Steller sea lions shot at Forrester Island in May 1986 (Calkins and Goodwin¹); for these sea lions Pacific cod (*Gadus macrocephalus*) accounted for the largest single

prey occurrence at 58% of the total volume, and pollock accounted for 32% of the contents by volume and were present in three stomachs.

The scats we collected during the 1990s revealed that gadids were an important part of the diet and that pollock was the predominant gadid. Relatively few Pacific cod were noted (Fig. 2). Pollock were the most frequently occurring food item in all scats examined from haulouts during the nonbreeding season and were second only to salmon by frequency of occurrence in all scats taken from rookeries during the breeding season. Pollock may have been important in the diet of Steller sea lions in the 1940s and 1980s, but the sample sizes taken at that time are inadequate to draw a firm conclusion or to determine whether diet changed over time (Trites and Joy, 2005).

Attempts to reconstruct the size of the pollock consumed during the 1990s in Southeast Alaska from the lengths of bones recovered in the scats revealed that adult fish (>45 cm fork length) were present more frequently in the diets of Steller sea lions on the outer coast sites than they were present in the diets of Steller sea lions from the inside waters (Tollit et al., 2004a). The largest proportions of fish consumed were of adult and subadult sizes. Juvenile pollock (≤ 20 cm) contributed insignificantly to the overall sea lion diet (Tollit et al., 2004a).

Potential biases

The use of scats, like all measures to quantify diet, entails caveats. Fortunately, the assumptions that underlie our analyses in Southeast Alaska also underlie the interpretation of scats we sought to compare them with from the Gulf of Alaska and Aleutian Islands. Some of the limitations that can restrict the interpretation of the dietary data from scats collected during the 1990s from all parts of Alaska are also greatly reduced by the large sample sizes (>1000 scats) collected in both regions (Trites and Joy, 2005). However, greater caution must be exerted when comparing stomach contents of Steller sea lions shot from the 1950s–1980s with scats collected during the 1990s, particularly for species such as squid and octopus whose beaks can be caught on the stomach lining and are often regurgitated rather than passed through the intestinal tract.

Our seasonal diet estimates largely compared what lactating females were eating during summer with what lactating females and all other age and sex classes were eating during fall, winter, and spring. Whether or not the different age groups forage in different areas or have different prey preferences is not known. It should also be noted that the seasonal descriptions of diet came from samples that were primarily collected in two time periods—February to July (1996–99) and June to December (1993–95). Our conclusions about seasonal changes in diet could therefore be biased if significant changes occurred in the prey field over our decade of sampling. We assumed that feeding conditions remained relatively stable during the 1990s; our conclusions were based on

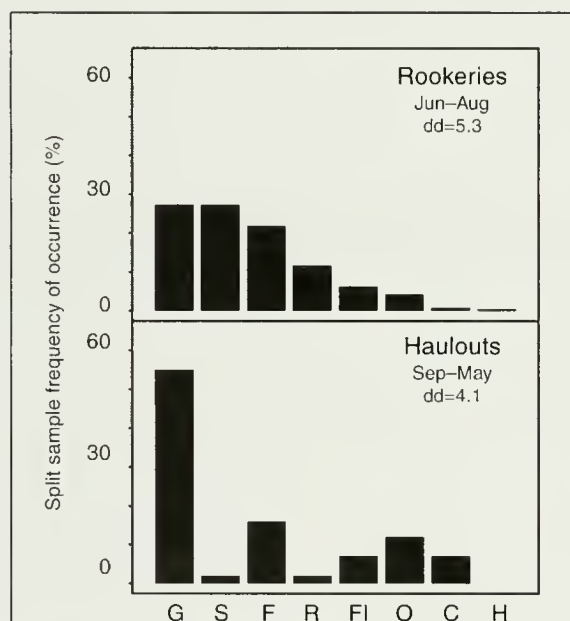
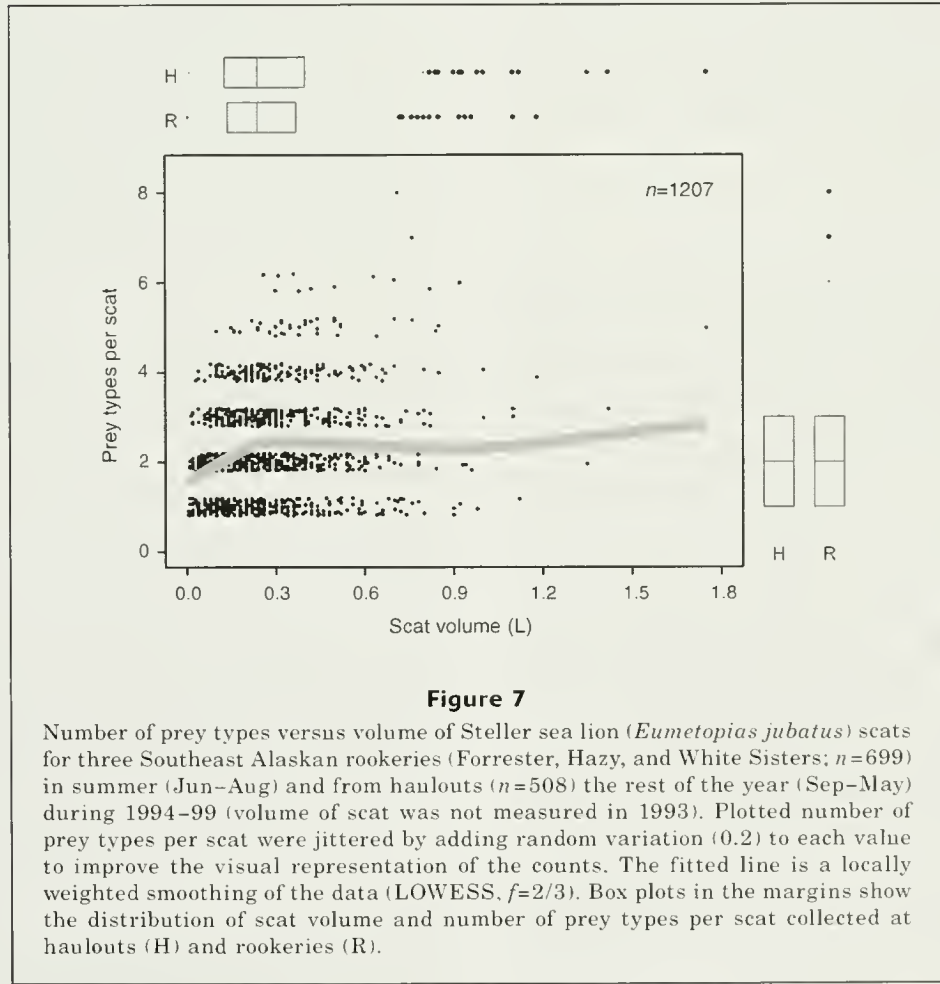
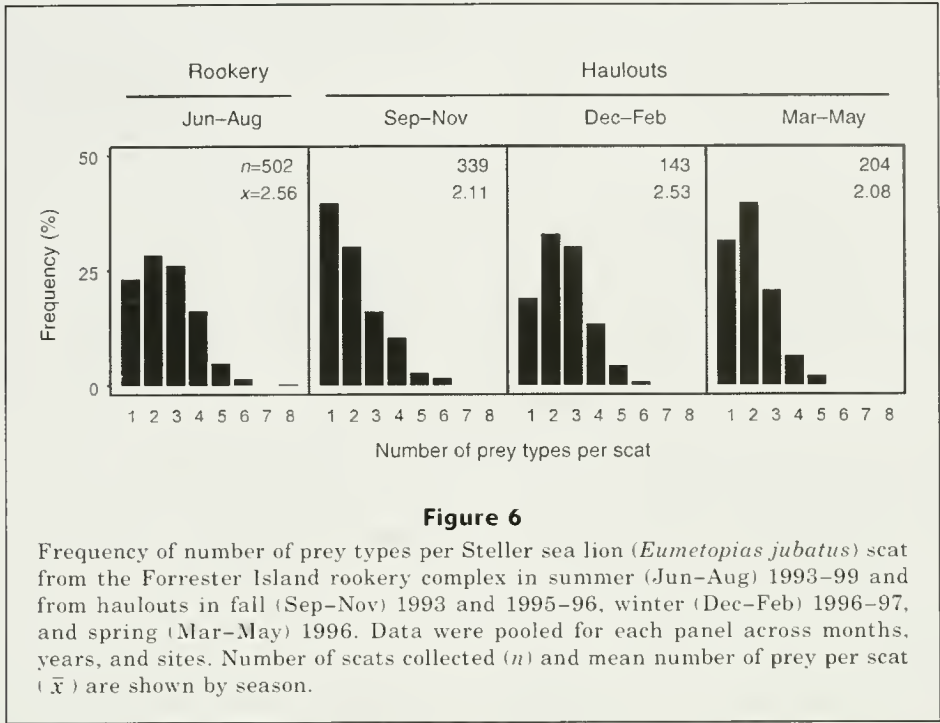


Figure 5

Split-sample frequency of occurrence of prey types in Steller sea lion (*Eumetopias jubatus*) scats from Southeast Alaskan rookeries (Forrester, Hazy, and White Sisters) in summer (Jun–Aug) and from haulouts the rest of the year (Table 1). Diet at rookeries is the weighted average (by the average 1993–97 pup counts) of the three mean rookery diets (averaged across years). The haulout diet is the average of the three mean seasonal diets (averaged across years). Diet diversity (dd) was calculated by using a Shannon-Wiener index. Types of prey consumed were F = forage fish, S = salmon, G = gadids, R = rockfish, Fl = flatfish, O = other, C = cephalopods, and H = hexagrammids.



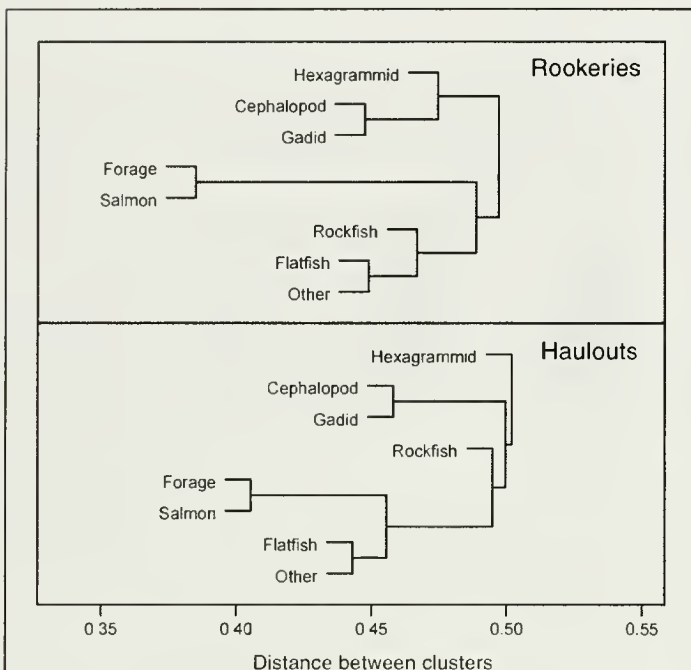


Figure 8

Hierarchical clustering trees of prey groups found in Steller sea lion (*Eumetopias jubatus*) scats from three Southeast Alaskan rookeries (Forrester, Hazy, and White Sisters) in summer (Jun–Aug) and from haulouts the rest of the year (Sep–May). Distances between pairs of prey groups were defined as $(1 - \text{partial correlation coefficient})/2$ and clustering was done using “hclust” software (S-Plus 4.0) (MathSoft Inc., Cambridge, MA).

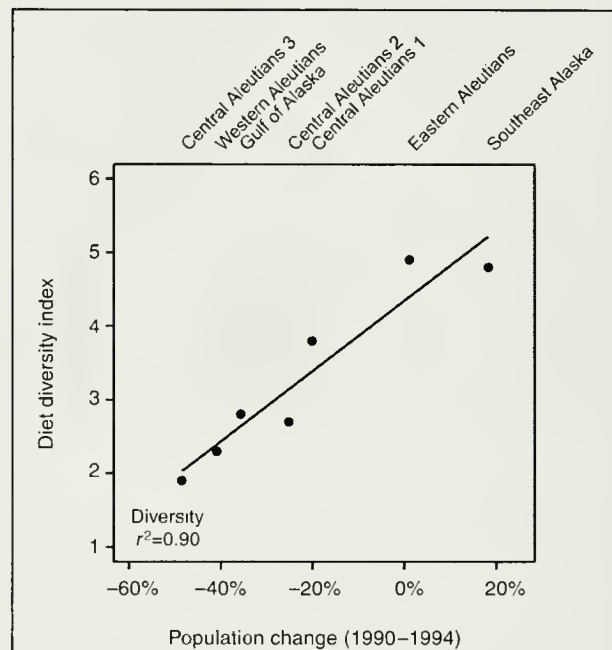


Figure 9

Diet diversity versus rate of population change of Steller sea lions (*Eumetopias jubatus*) between 1990 and 1994 (total number of adults and juveniles counted on rookeries during the summer; Strick et al., 1997) by region of Alaska. The fitted line is a least squares linear regression. Diet diversity was calculated using split-sample frequency of occurrence and a Shannon-Wiener index. The locations and all the data used to calculate diet diversity (except for Southeast Alaska) were taken from Merrick et al. (1997). Data from Southeast Alaska reflect the mean summer rookery diet of Steller sea lions and rockfish were grouped with the “other” prey type.

the consistency of the annual summer diet at Forrester Island (which was sampled in all years, Fig. 2) and on the relative stability of ocean conditions during the 1990s (which is believed to determine the relative abundances of suites of prey available to sea lions and other species; Benson and Trites, 2002; King, 2005; Trites et al., 2007). Thus we feel that the seasonal description of diet accurately reflects what Steller sea lions were eating in Southeast Alaska during the 1990s.

A bias could have been introduced in our analysis if the sizes of collected scats differed significantly between haulouts and rookeries, and if the number of prey species recovered was correlated with the size of scats. In checking this potential source of error, we found numbers of prey types per scat were positively related to size for scats <250 mL but were independent of scat size beyond this volume (Fig. 7). In general, there was little difference in the sizes of scats and numbers of species recovered from rookeries and haulouts, and thus there was no apparent effect of size of scat on our results.

By inferring the dietary importance of prey species from their frequencies of occurrence in scats one implicitly assumes that the probability of finding prey in scats is proportional to the number or mass of that prey consumed, and that this proportionality does not vary

among prey species. However, controlled feeding studies with captive Steller sea lions, and other pinnipeds, have shown that the types and proportions of prey hard parts that pass through the digestive tract vary, depending on the species of prey and the size of prey (Cottrell and Trites, 2002; Tollit et al., 2003; Tollit et al., 2004b). Pollock bones, for example, tend to be more robust than the bones of other species and have a higher likelihood of being recovered than the more fragile bones of other species, such as sand lance. However, smaller schooling species, such as sand lance, are likely to be consumed in higher numbers than pollock, and the greater consumption of these smaller species would increase the likelihood of some of the smaller bones passing through the digestive tract. Thus, the probability of detecting different prey species in scats can vary. Recording the presence of all identifiable hard parts as we did (i.e., not relying only on otoliths) significantly reduces the likelihood of any species passing undetected (Cottrell and Trites, 2002).

Captive feeding experiments indicate that the average scat probably contains the remains of prey con-

sumed over a number of days (Tollit et al., 2003). In other words, a scat likely does not represent a single meal, but is probably a composite of one or more feeding trips. Frequency of occurrence (Figs. 2–4) represents the probability that a particular prey type was consumed and does not represent the number or mass of prey consumed. However, with large sample sizes, the ranked importance of any particular prey type appears to equate with frequency of occurrence or numbers of prey (Sinclair et al., 1994; Antonelis et al., 1997; Sinclair and Zeppelin, 2002). The split-sample frequency of occurrence technique is another approach that deals with these biases by assuming that all prey species identified in a scat were consumed in equal mass and that each scat contributes an equal amount of information to the overall diet (Fig. 5, Table 3). Split-sample estimates tend to correlate with simple frequencies of occurrence to give a reasonable proportional description of diet, even when the assumption that all prey in a meal were consumed in equal quantities is not always true.

Prey associations

The remains found in sea lion scats likely delineate associations and distributions of prey species by region. In Southeast Alaska, the hard parts recovered from scats indicate that Steller sea lion prey were not randomly distributed, given that some prey species were found together more frequently than expected (if estimated occurrence was based on chance alone). For example, occurrences of gadids tended to be associated with occurrences of cephalopods (Fig. 8), whereas salmon were found most often with forage fishes (herring and sand lance). An association was also noted between flatfish and “other” species (primarily skates—Figs. 2 and 8). These associations may reflect groups of prey that are commonly associated with each other because of habitat similarities (e.g., depth or substrate similarities).

Associations of prey in scats may also reflect prey-specific foraging strategies of individual Steller sea lions. In some cases, prey associations may reflect secondary prey, whereby a species was consumed by the prey species actually targeted by the sea lion. Hard remains of a fish may occur in a sea lion scat not because it was depredated directly but because it had been consumed by a fish that was then eaten by a sea lion. In our case, 10 of over 60 species were found in more than 5% of the scats and were presumably preferred prey that were directly targeted by the sea lions (Fig. 2). The low frequencies of the remaining 50+ species (Fig. 2) may reflect preferred species that were in low abundance in Southeast Alaska, or they might indicate incidental prey and those that had been consumed by their preferred prey.

Eastern versus western diets

Our systematic survey of Steller sea lion diets in Southeast Alaska during the 1990s was prompted by a desire to gain insight into a possible dietary basis for the

population decline that occurred in the Gulf of Alaska and Aleutian Islands. Dietary differences of Steller sea lions between the two regions may help to explain why one population declined while the other increased.

The most common prey of 61 species identified in Southeast Alaska in frequency of occurrence were wall-eye pollock, Pacific herring, sand lance, salmon, arrowtooth flounder, rockfish, skates, squid, and octopus. Looking further afield (west) we found that Steller sea lions targeted a similar suite of species in the Gulf of Alaska in the 1990s as those we noted in Southeast Alaska, although the relative abundances of each differed considerably (Sinclair and Zeppelin, 2002; Trites et al., 2007). The most common prey reported in the Gulf of Alaska in order of importance were pollock, salmon, Pacific cod, arrowtooth flounder, sand lance, herring, and Irish lords (*Hemilepidotus* sp.). Further west in the Aleutian Islands, however, Atka mackerel, salmon, cephalopods, Pacific cod, Irish lords, and pollock dominated the sea lion diet.

It is unclear what role pollock and Atka mackerel stocks alone have played in the different trajectories of Steller sea lion populations. Pollock were consumed in the Kodiak area—both prior to what was thought to be the beginning of the decline (Pitcher, 1981) and after the decline was under way (Calkins and Goodwin¹). Calkins and Goodwin¹ noted that although sea lions ate more pollock in the Kodiak area after their decline in terms of frequency of occurrence, the pollock they ate were significantly smaller after the decline began. No similar data are available for Southeast Alaska.

Since the mid 1970s, pollock has been one of the most dominant species in the Bering Sea and Gulf of Alaska ecosystems (Livingston, 1993; Trites et al., 1999; Conners et al., 2002). Unfortunately, little is known about the relative importance of pollock in the Southeast Alaska ecosystem. Pollock have been little exploited, and relatively little is known about their distribution in Southeast Alaska. Surveys conducted during 1950–62 (Alverson et al., 1964) and again during 1976–77 (Parks and Zenger, 1978) caught 64–129 lbs of pollock per hour in select areas of Southeast Alaska using a 400-mesh eastern otter trawl. The 1950–1962 surveys covered only outside waters from Hazy Islands to Dixon Entrance, whereas the later surveys were distributed throughout both inside and outside waters. Parks and Zenger (1978) estimated pollock biomass in Frederick Sound at 0.94 t/nmi². A more recent unpublished estimate indicates that the biomass may have been as much as seven times this level in Frederick Sound in 2001 (Sigler³). Thus, pollock would appear to be an important species in the ecosystem within some areas of Southeast Alaska.

The most striking difference between the diets of Steller sea lions in the different regions of Alaska is the diversity of prey consumed. Steller sea lions feed-

³ M. Sigler. 2004. Personal commun. National Oceanic and Atmospheric Administration, National Marine Fisheries Service, Auke Bay Lab, 11305 Glacier Highway, Juneau, AK, 99801.

ing in the Gulf of Alaska and Aleutian Islands during summer had diversity indices of 2–3, compared to 5.3 in Southeast Alaska (Fig. 5, Merrick et al., 1997; Sinclair and Zeppelin, 2002). Summer diets were dominated in the Aleutian Islands by a single species (Atka mackerel) and there were small amounts of other prey in the diet. In the Gulf of Alaska, the dominant prey was pollock, followed by salmon (Sinclair and Zeppelin, 2002). Dietary diversity remained low in the Gulf and Aleutian Islands from summer to winter (Sinclair and Zeppelin, 2002), but dropped in Southeast Alaska from 5.3 to 4.1 (Fig. 5). Winter diets in Southeast Alaska were dominated by pollock. However, the average scat from Southeast Alaska contained at least two prey species. In other words, pollock was rarely consumed alone and, when consumed, was usually accompanied by at least one other species type, such as herring, salmon, sand lance, flatfish, or skates (Figs. 2 and 6).

The inclusion of our data from Southeast Alaska with those from Merrick et al. (1997) provided the same conclusion, namely that the numbers of sea lions declined more slowly and even increased as diversity of diet increased (Fig. 9). Steller sea lions that consumed the least diverse diet experienced the greatest population declines. However, it is not clear whether diet diversity is a proxy for energy content of the sea lion diet as suggested by Winship and Trites (2003), or whether it captures some other biologically meaningful measure of nutrition. Nor is it clear whether the diet diversity index reflects depths of nearest ocean passes to rookeries (with diet diversity increasing with shallower depths; Sinclair et al., 2005), or whether it could be a relative measure of prey distribution and density.

The relative importance of pollock in the diet of Steller sea lions in Southeast Alaska was not expected. However, pollock is not as dominant in the sea lion diet in Southeast Alaska as it is in other regions, and appears to usually be accompanied by other types of energy-rich prey (Fig. 4). It may be easier for sea lions with a more diverse or energy-rich diet to obtain sufficient prey to meet their energy requirements (Trites, 2003; Rosen and Trites, 2004; Trites et al., 2006). They may also be less sensitive to changes in overall prey abundance and may spend less time foraging under risk of predation.

The increase in Steller sea lion numbers in Southeast Alaska since the 1970s contrasts sharply with the declines observed in the Gulf of Alaska. The difference between the diets of Steller sea lions in the two regions is one possible explanation underlying the population trends. Stomach samples collected in the Bering Sea and Gulf of Alaska before the population decline (1950s–mid-1970s) indicate that their diet might have once resembled that of sea lions in Southeast Alaska during the 1990s (Alverson, 1992; Merrick et al., 1997; Sinclair and Zeppelin, 2002). However, the small number of stomachs sampled and the nonstandard methods used to collect them make it difficult to compare pre- and post-decline periods over broad areas. A change in diet during the population decline

may be related to large-scale changes in oceanographic conditions (regime shifts) that may have affected the relative abundances of different suites of species (Wilderbuer et al., 2002; King, 2005; Trites et al., 2007). In terms of oceanic regimes, the marine ecosystems of the eastern North Pacific appear to group into two broad domains (California to Southeast Alaska, and the Gulf of Alaska to western Aleutian Islands) that are out of phase with each other as they alternate between anomalous warm and cool states (regimes). Finer-scale analyses should be undertaken to determine how the declines and increases of different prey and predator species line up in time and space with changes in oceanographic events.

Conclusions

A comparison of our dietary data with dietary data collected from other regions of Alaska indicated that Steller sea lions consumed a relatively similar suite of schooling species, most notably pollock, salmon, herring, sand lance, rockfish, and squid. However, in terms of frequency of occurrence, there were marked differences between Southeast Alaska during the 1990s and regions where sea lions have declined. Diets in Southeast Alaska were more diverse and may have had a higher energy content overall. Pollock is part of a normal sea lion diet but is less dominant in Southeast Alaska than in the Gulf of Alaska and Bering Sea where population declines occurred. The difference in diets between the regions is potentially a useful clue for determining why population trends of Steller sea lions have diverged in Alaska. This difference in diets also underlines the overall importance of continuing to assess and monitor sea lion diets.

Acknowledgments

We are grateful to the many people who helped collect and clean the scat, and would particularly like to acknowledge and thank W. Cunningham, D. McAllister, B. Porter, D. Porter, and S. Stanford. We thank P. Rosenbaum for managing our scat collection, and S. Crockford (Pacific IDentifications) for identifying the prey and patiently answering our questions. We are also grateful to M. Rehberg and S. Heaslip for assisting with the map, and M. Sigler for his insights into pollock distribution in Southeast Alaska. Useful comments and suggestions on earlier drafts of our manuscript were made by D. Tollit, D. Rosen, and three anonymous reviewers. Laboratory space was provided by the Vancouver Aquarium Marine Science Centre, and funding was provided by the National Oceanic and Atmospheric Administration to the North Pacific Marine Science Foundation and to the Alaska Department of Fish and Game. Additional support was also provided by the North Pacific Marine Science Foundation through the North Pacific Universities Marine Mammal Research Consortium. Research was conducted under U.S. Marine Mammal Act and Endan-

gered Species Act permits 965 and 358-1564 issued to the Alaska Department of Fish and Game.

Literature cited

- Alaska Sea Grant.
1993. Is it food? Addressing marine mammal and sea bird declines, 65 p. Alaska Sea Grant Rep. 93-01. Univ. Alaska Fairbanks, Fairbanks, AK.
- Alverson, D. L.
1992. A review of commercial fisheries and the Steller sea lion (*Eumetopias jubatus*): the conflict arena. *Rev. Aquat. Sci.* 6:203-256.
- Alverson, D. L., A. T. Pruter, and L. L. Ronholt.
1964. A study of demersal fishes and fisheries of the northeast Pacific Ocean, 190 p. H. R. MacMillan Lectures in Fisheries, Univ. British Columbia, Vancouver, BC.
- Antonelis, G. A., E. H. Sinclair, R. R. Ream, and B. W. Robson.
1997. Inter-island variability in the diet of female northern fur seals (*Callorhinus ursinus*) in the Bering Sea. *J. Zool., Lond.* 242:435-451.
- Benson, A. J., and A. W. Trites.
2002. Ecological effects of regime shifts in the Bering Sea and eastern North Pacific Ocean. *Fish. Fish.* 3:95-113.
- Bigg, M. A., and P. F. Olesiuk.
1990. An enclosed elutriator for processing marine mammal scats. *Mar. Mamm. Sci.* 6:350-355.
- Calkins, D. G., D. C. McAllister, K. W. Pitcher, and G. W. Pendleton.
1999. Steller sea lion status and trend in Southeast Alaska: 1979-1997. *Mar. Mamm. Sci.* 15:462-477.
- Connors, M. E., A. B. Hollowed, and E. Brown.
2002. Retrospective analysis of Bering Sea bottom trawl surveys: regime shift and ecosystem reorganization. *Prog. Oceanogr.* 55:209-222.
- Cottrell, P. E., and A. W. Trites.
2002. Classifying prey hard part structures recovered from fecal remains of captive Steller sea lions (*Eumetopias jubatus*). *Mar. Mamm. Sci.* 18:525-539.
- DeMaster, D., and S. Atkinson, eds.
2002. Steller sea lion decline: is it food II?, 80 p. Univ. Alaska Sea Grant, AK-SG-02-02, Fairbanks, AK.
- Imler, R. H., and H. R. Sarber.
1947. Harbor seals and sea lions in Alaska, 23 p. U.S. Fish and Wildlife Service, Special Report no. 28.
- King, J. R., ed.
2005. Report of the study group on "Fisheries and ecosystem response to recent regime shifts," 168 p. PICES Scientific Report no. 28, Victoria, BC.
- Livingston, P. A.
1993. Importance of predation by groundfish, marine mammals and birds on walleye pollock *Theragra chalcogramma* and Pacific herring *Clupea pallasii* in the eastern Bering Sea. *Mar. Ecol. Prog. Ser.* 102:205-215.
- Loughlin, T. R.
1998. The Steller sea lion: a declining species. *Bios. Cons.* 1:91-98.
- Mathisen, O. A., R. T. Baade, and R. J. Lopp.
1962. Breeding habits, growth and stomach contents of the Steller sea lion in Alaska. *J. Mammal.* 43:469-477.
- Mathisen, O. A., and R. J. Lopp.
1963. Photographic census of the Steller sea lion herds in Alaska, 1956-58, 20 p. U.S. Fish and Wildlife Service, Special Scientific Report F-424.
- Merrick, R. L., M. K. Chumbley, and G. V. Byrd.
1997. Diet diversity of Steller sea lions (*Eumetopias jubatus*) and their population decline in Alaska: a potential relationship. *Can. J. Fish. Aquat. Sci.* 54:1342-1348.
- Olesiuk, P. F.
1993. Annual prey consumption by harbor seals (*Phoca vitulina*) in the Strait of Georgia, British Columbia. *Fish. Bull.* 91:491-515.
- Olesiuk, P. F., M. A. Bigg, G. M. Ellis, S. J. Crockford, and R. J. Wigen.
1990. An assessment of the feeding habits of harbour seals (*Phoca vitulina*) in the Strait of Georgia, British Columbia, based on scat analysis, 135 p. *Can. Tech. Rep. Fish. Aquat. Sci.* no. 1730.
- Parks, N. B., and H. H. Zenger.
1978. Trawl surveys of groundfish resources in the eastern Gulf of Alaska and southeastern Alaskan waters 1976-77, 53 p. Northwest and Alaska Fisheries Science Center Processed Report.
- Pitcher, K. W.
1981. Prey of the Steller sea lion, *Eumetopias jubatus*, in the Gulf of Alaska. *Fish. Bull.* 79:467-472.
- Pitcher, K. W., P. F. Olesiuk, R. F. Brown, M. S. Lowry, S. J. Jeffries, J. L. Sease, W. L. Perryman, C. E. Stinchcomb, and L. F. Lowry.
2007. Abundance and distribution of the eastern North Pacific Steller sea lion (*Eumetopias jubatus*) population. *Fish. Bull.* 105:102-115.
- Ricklefs, R. E., and G. L. Miller.
2000. *Ecology*, 4th ed., 822 p. W. H. Freeman and Company, New York, NY.
- Rosen, D. A. S., and A. W. Trites.
2000. Pollock and the decline of Steller sea lions: testing the junk-food hypothesis. *Can. J. Zool.* 78:1243-1258.
- Rosen, D. A. S., and A. W. Trites.
2004. Satiation and compensation for short-term changes in food quality and availability in young Steller sea lions (*Eumetopias jubatus*). *Can. J. Zool.* 82:1061-1069.
- Rowley, J.
1929. Life history of sea lions on the California coast. *J. Mammal.* 10:1-36.
- Sinclair, E. H., T. R. Loughlin, and W. Pearcy.
1994. Prey selection by northern fur seals (*Callorhinus ursinus*) in the eastern Bering Sea. *Fish. Bull.* 92:132-156.
- Sinclair, E. H., S. E. Moore, N. A. Friday, T. K. Zeppelin, and J. M. Waite.
2005. Do patterns of Steller sea lion (*Eumetopias jubatus*) diet, population trend and cetacean occurrence reflect oceanographic domains from the Alaska Peninsula to the central Aleutian Islands? *Fish. Oceanogr.* 14:223-242.
- Sinclair, E. H., and T. K. Zeppelin.
2002. Seasonal and spatial differences in diet in the western stock of Steller sea lions (*Eumetopias jubatus*). *J. Mammal.* 83:973-990.
- Strick, J. M., L. W. Fritz, and J. P. Lewis.
1997. Aerial and ship-based surveys of Steller sea lions (*Eumetopias jubatus*) in Southeast Alaska, the Gulf of Alaska and Aleutian Islands during June and July 1994. NOAA Tech. Memo. NMFS-AFSC-71, 55 p.

- Thorsteinson, F. V., and C. J. Lensink.
1962. Biological observations of Steller sea lions taken during an experimental harvest. *J. Wildl. Manage.* 26:353-359.
- Tollit, D. J., S. G. Heaslip, and A. W. Trites.
2004a. Sizes of walleye pollock (*Theragra chalcogramma*) consumed by the eastern stock of Steller sea lions (*Eumetopias jubatus*) in Southeast Alaska from 1994-1999. *Fish. Bull.* 102:522-532.
- Tollit, D. J., S. Heaslip, T. Zepplelin, R. Joy, K. Call, and A. W. Trites.
2004b. A method to improve size estimates of walleye pollock (*Theragra chalcogramma*) and Atka mackerel (*Pleurogrammus monopterygius*) consumed by pinnipeds: digestion correction factors applied to bones and otoliths recovered in scats. *Fish. Bull.* 102:498-508.
- Tollit, D. J., M. Wong, A. J. Winship, D. A. S. Rosen, and A. W. Trites.
2003. Quantifying errors associated with using prey skeletal structures from fecal samples to determine the diet of Steller's sea lion (*Eumetopias jubatus*). *Mar. Mamm. Sci.* 19:724-744.
- Trites, A. W.
2003. Food webs in the ocean: who eats whom and how much? In *Responsible Fisheries in the Marine Ecosystem* (M. Sinclair, and G. Valdimarsson, eds.), p. 125-143. FAO, Rome, and CABI Publishing, Wallingford, UK.
- Trites, A. W., and C. P. Donnelly.
2003. The decline of Steller sea lions *Eumetopias jubatus* in Alaska: a review of the nutritional stress hypothesis. *Mamm. Rev.* 33:3-28.
- Trites, A. W., and R. Joy.
2005. Dietary analysis from fecal samples: how many scats are enough? *J. Mammal.* 86:704-712.
- Trites, A. W., and P. A. Larkin.
1996. Changes in the abundance of Steller sea lions (*Eumetopias jubatus*) in Alaska from 1956 to 1992: How many were there? *Aquat. Mamm.* 22:153-166.
- Trites, A. W., P. A. Livingston, S. Mackinson, M. C. Vasconcellos, A. M. Springer, and D. Pauly.
1999. Ecosystem change and the decline of marine mammals in the eastern Bering Sea: testing the ecosystem shift and commercial whaling hypotheses, 106 p. Fisheries Centre Research Reports no. 7(1).
- Trites, A. W., A. J. Miller, H. D. G. Maschner, M. A. Alexander, S. J. Bograd, J. A. Calder, A. Capotondi, K. O. Coyle, E. D. Lorenzo, B. P. Finney, E. J. Gregr, C. E. Grosch, S. R. Hare, G. L. Hunt, J. Jahncke, N. B. Kachel, H.-J. Kim, C. Ladd, N. J. Mantua, C. Marzban, W. Maslowski, R. Mendelssohn, D. J. Neilson, S. R. Okkonen, J. E. Overland, K. L. Reedy-Maschner, T. C. Royer, F. B. Schwing, J. X. L. Wang, and A. J. Winship.
2007. Bottom-up forcing and the decline of Steller sea lions (*Eumetopias jubatus*) in Alaska: assessing the ocean climate hypothesis. *Fish. Oceanogr.* 16:46-67.
- Trites, A. W., B. P. Porter, V. B. Deecke, A. P. Coombs, M. L. Marcotte, and D. A. S. Rosen.
2006. Insights into the timing of weaning and the attendance patterns of lactating Steller sea lions (*Eumetopias jubatus*) in Alaska during winter, spring, and summer. *Aquat. Mamm.* 32:85-97.
- Wilderbuer, T. K., A. B. Hollowed, W. J. Ingraham, P. D. Spencer, M. E. Conners, N. A. Bond, and G. E. Walters.
2002. Flatfish recruitment response to decadal climatic variability and ocean conditions in the eastern Bering Sea. *Prog. Oceanogr.* 55:235-247.
- Winship, A. J., and A. W. Trites.
2003. Prey consumption of Steller sea lions (*Eumetopias jubatus*) off Alaska: How much prey do they require? *Fish. Bull.* 101:147-167.
- Zar, J. H.
1996. *Biostatistical analysis*, 3rd ed., 662 p. Prentice-Hall, Inc., Englewood Cliffs, NJ.

Abstract—In this study we describe the courtship and spawning behaviors of captive yellowfin tuna (*Thunnus albacares*), their spawning periodicity, the influence of physical and biological factors on spawning and hatching, and egg and early-larval development of this species at the Achotines Laboratory, Republic of Panama, during October 1996 through March 2000. Spawning occurred almost daily over extended periods and at water temperatures from 23.3° to 29.7°C. Water temperature appeared to be the main exogenous factor controlling the occurrence and timing of spawning. Courtship and spawning behaviors were ritualized and consistent among three groups of broodstock over 3.5 years. For any date, the time of day of spawning (range: 1330 to 2130 h) was predictable from mean daily water temperature, and 95% of hatching occurred the next day between 1500 and 1900 h. We estimated that females at first spawning averaged 1.6–2.0 years of age. Over short time periods (<1 month), spawning females increased their egg production from 30% to 234% in response to short-term increases in daily food ration of 9% to 33%. Egg diameter, notochord length (NL) at hatching, NL at first feeding, and dry weights of these stages were estimated. Water temperature was significantly, inversely related to egg size, egg-stage duration, larval size at hatching, and yolksac larval duration.

Spawning and early development of captive yellowfin tuna (*Thunnus albacares*)

Daniel Margulies (contact author)¹

Jenny M. Suter¹

Sharon L. Hunt¹

Robert J. Olson¹

Vernon P. Scholey²

Jeanne B. Wexler¹

Akio Nakazawa³

Email address for D. Margulies: dmargulies@iattc.org

¹ Inter-American Tropical Tuna Commission
8604 La Jolla Shores Drive
La Jolla, California 92037-1508

² Inter-American Tropical Tuna Commission
Achotines Laboratory, Las Tablas
Los Santos Province, Republic of Panama

³ Overseas Fishery Cooperation Foundation
Sankaido Building, 9-13 Akasaka 1, Minato-ku
Tokyo 107-0052, Japan

The yellowfin tuna (*Thunnus albacares*) is found worldwide in tropical and subtropical oceans. Yellowfin tuna reproduction is characterized by serial batch spawning and asynchronous oocyte development that is typical of tunas (Schaefer, 2001a). Yellowfin tuna are broadcast spawners and exhibit extremely high batch and annual fecundities over protracted spawning seasons (McPherson, 1991; Schaefer 1996, 1998).

Tuna reproduction has been studied predominantly through histological analyses of the gonads of fish sampled at sea. Estimates have been made of either spawning seasons, spawning intervals, fecundities, or energetic costs of spawning for yellowfin tuna (Joseph, 1963; McPherson, 1991; Schaefer, 1996), skipjack tuna, *Katsuwonus pelamis* (Goldberg and Au, 1986; Hunter et al., 1986; Schaefer, 2001b), bigeye tuna, *Thunnus obesus* (Nikaido et al., 1991), albacore, *Thunnus alalunga* (Ramon and Bailey, 1996), and southern bluefin tuna, *Thunnus maccoyii* (Farley and Davis, 1998). Egg and early larval development of tunas has been described in a number of identification guides

or descriptive reviews (Nishikawa and Rimmer, 1987; Ambrose, 1996; Richards, 2006). Most descriptions of early life stages of tunas are based on examinations of specimens collected at sea.

Our knowledge of the spawning dynamics and early development of tunas remains incomplete, and most of our understanding comes from studies of cultured tunas. Before 1980, there were several small-scale efforts in Japan to artificially spawn tunas and to rear the larvae and juveniles (Harada¹). In the past decade several programs have been developed worldwide to induce spawning and to rear tunas in captivity. Maturation and spawning of tuna broodstock in sea pens in Japan has been described

¹ Harada, T. 1980. Progress and future prospects in tuna culturing studies. In Proceedings of the 1979 Japan Tuna Research Conference, Shimizu, Japan, p. 50–58. [Engl. Transl. no. 50 by T. Otsu, 1980, 8 p., avail. Pacific Islands Fisheries Science Center, National Marine Fisheries Service, 2570 Dole Street, Honolulu, HI 96822.]

for yellowfin (Masuma et al.²) and bluefin tuna, *Thunnus thynnus* (Miyashita et al., 2000a). Spawning of captive yellowfin tuna in landbased tanks in Bali occurred in late 2004 (Nakazawa³). Descriptions of larval and juvenile development stemming from these culturing programs have been presented for yellowfin tuna (Kaji et al., 1999; Margulies et al., 2001; Wexler et al., 2001) and bluefin (Kaji et al., 1996; Miyashita et al., 2001).

Little is known about the spawning behavior of tunas or the influence of physical factors on spawning or egg and larval development. Almost nothing is known about the manner in which tunas aggregate for spawning, their courtship and spawning behaviors, the duration of spawning events, or the effects of physical variables on spawning dynamics or early life stage development. Since 1996, the Inter-American Tropical Tuna Commission (IATTC) has maintained a spawning population of yellowfin tuna in large landbased tanks at the Achotines Laboratory in Panama (Scholey et al., 2001; Wexler et al., 2003). Our broodstock yellowfin tuna have spawned over protracted time periods (nearly year-round on a daily basis) since October of 1996. This spawning pattern has provided a unique opportunity to study the daily spawning dynamics of this species over multiple years. In this article we describe the courtship and spawning behaviors of captive yellowfin tuna, their spawning periodicity, the influence of physical and biological factors on spawning and hatching, and the egg and early-larval development of this species.

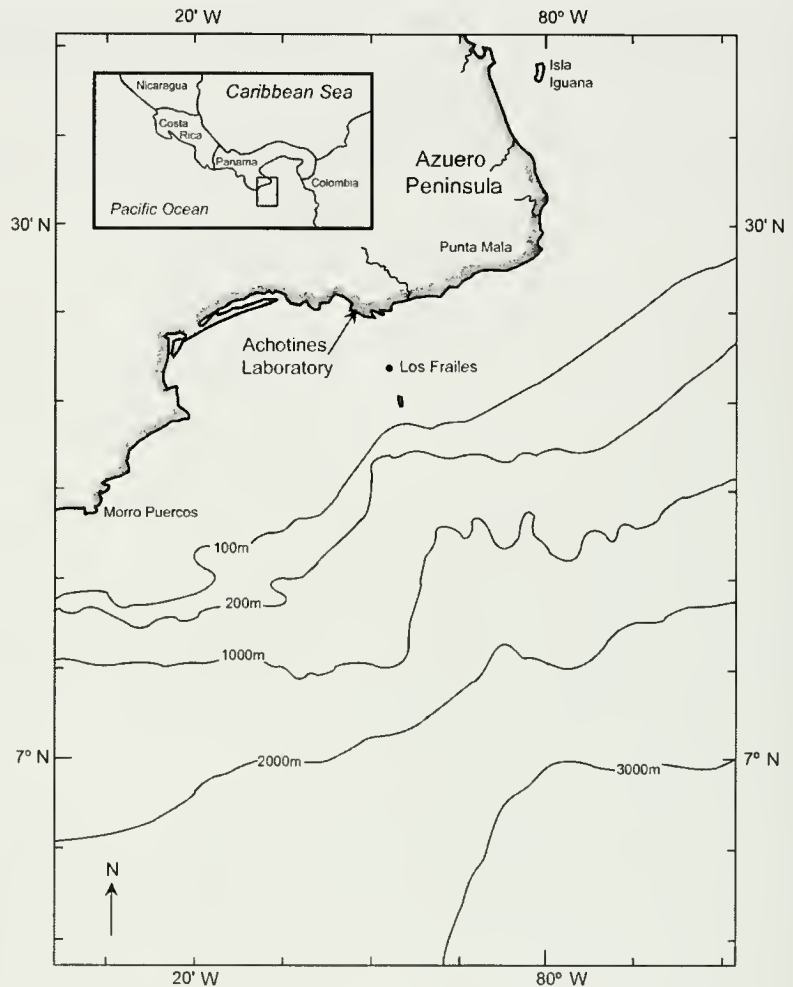


Figure 1

Location of the Inter-American Tropical Tuna Commission's Achotines Laboratory, Republic of Panama.

Materials and methods

Development of the broodstock

The yellowfin tuna broodstock was developed at the IATTC's Achotines Laboratory, located at the southern tip of the Azuero Peninsula of Panama in the northwestern portion of the Panama Bight in the Pacific Ocean (Fig. 1). The broodstock was developed in collaboration with the Overseas Fishery Cooperation Foundation (OFCF) of Japan. The design of the seawater system, plus specific details of the capture, handling, and feeding procedures

for the broodstock yellowfin tuna are described by Wexler et al. (2003). We began collecting this species in coastal waters in the vicinity of the Laboratory in early 1996, and initially placed 55 individuals in the main broodstock tank (concrete, in-ground, 17 m diameter, 6 m deep) in June and September of 1996. We captured an additional 24 fish in September and October 1996 and maintained them in a smaller (8.5 m diameter, 6 m deep) in-ground tank as a reserve group. The tanks received filtered seawater by intake lines that extended outside Achotines Bay, and both tanks received biological filtration and partial recirculation. The water delivery for the main broodstock tank flowed through an aeration tower (400 m³/h) designed to aerate and degas the makeup and recirculated water entering the tank. We installed several translucent panels in the roof above the main tank to allow exposure to the natural photoperiod. Water temperature, salinity, dissolved oxygen (DO), and oxygen saturation in the tanks were recorded on a daily basis. We measured ammonia, nitrite, nitrate, and carbon dioxide on a weekly or semi-weekly basis.

² Masuma, S., N. Tezuka, K. Teruya, M. Oka, M. Kanematsu, and H. Nikaido. 1993. Unpubl. data. Yaeyama Experimental Station, Japan Sea Farming Association, 148 Ohta Ishigaki, Okinawa 907 Japan.

³ Nakazawa, A. 2004. Personal commun. OFCF (Overseas Fishery Cooperation Foundation), Sankaido Bldg. 9-13, Akasaka 1, Minato-ku, Tokyo 107-0052, Japan.

We fed the broodstock a controlled diet of market squid (*Loligo opalescens*), Argentine shortfin squid (*Illex argentinus*), Pacific thread herring (*Opisthonema* spp.), Pacific anchoveta (*Cetengraulis mysticetus*), and bigscale anchovy (*Anchovia macrolepidota*). The daily ration was usually divided into 50% squid and 50% fish.

Nonlinear least-squares procedures were used to obtain growth parameters for the yellowfin broodstock (Tomlinson⁴) in order to estimate growth rates and sizes at age and length (Wexler et al., 2003).

Spawning

During October 1996, the fish in the main broodstock tank began to exhibit courtship behavior in the late afternoons (see subsection "Spawning behavior"). We began monitoring the broodstock tank for egg production during this time. On 8 October 1996, we collected fertilized eggs in the tank for the first time. The fish spawned sporadically throughout October and November 1996, and by December 1996 were spawning daily. Using the estimated ages of wild yellowfin tuna in the eastern Pacific Ocean (Wild, 1986) and applying them to the lengths and weights of our broodstock fish (Wexler et al., 2003), we estimated the average age of the broodstock fish at the time of first spawning. During 1999–2000, we estimated the spawning periodicity and age at first-spawning of individual females. We compared the mitochondrial DNA genotypes of the female broodstock with those of their offspring (eggs and yolk sac larvae) on a weekly basis from August 1999 through August 2000. Mitochondrial DNA analysis was conducted by using polymerase chain reaction/restriction fragment length polymorphism (PCR/RFLP) methods. The genetic analysis is described in greater detail in Niwa et al. (2003).

To determine the time of spawning each day, we checked approximately every 15 minutes for fertilized eggs at the surface of the tank with a hand-held dipnet, usually beginning in mid-afternoon because the fish most often spawned during the late afternoon or evening. Yellowfin tuna eggs, when fertilized, are positively buoyant and rise to the surface in a tank. The time at which eggs were first caught in the dipnet was noted as the "time of spawning." This is a conservative estimate because the fish spawned at different depths and locations in the tank, and we always sampled for eggs at the same location in the tank. We recorded the temperature of the broodstock tank at the time of spawning.

Although we did not anticipate spawning to occur in the reserve tank, the yellowfin tuna began spawning after 7 to 8 months in captivity in mid-April 1997. After the initial spawning in the reserve tank, we monitored the tank daily for fertilized eggs. In October 1997, we collected eggs spawned by the one remaining pair of

fish to study Mendelian inheritance of nuclear DNA variants (Chow et al., 2001). We sacrificed the breeding pair after six spawning events and took samples of their muscle tissue for genetic analysis.

Spawning behavior

When the fish spawned before sunset, we made visual observations to describe the courtship and spawning behavior. In addition, we used an underwater video camera connected to a surface video recorder to tape the spawning behavior. On several occasions, we positioned the camera at a depth of 1 to 4 m in different locations and at different angles in the main broodstock tank. The camera recorded continuously for approximately 1 h. We viewed the video tapes and chose footage that showed both courtship and spawning behaviors for behavioral analysis.

Egg collection

In early 1997, we constructed an egg-collection system with three PVC pipes, placed at different depths between the water surface and 70 cm below the surface, so that eggs were siphoned into a square egg-collection basket (1 m × 1 m) made of porous fabric (mesh size 200 μ m). We also collected eggs with dipnets and with an egg seine that sampled the entire surface of the tank. In early 1998, we attached a stationary drift net (trapezoidal opening 70 cm height × 20 cm [top width] and 40 cm [bottom width] × 1.6 m long) to one of the siphons to further standardize the egg collections. We considered the siphon system (1997) and the drift net+siphon system (1998–2000) as equivalent sampling systems because the same area in the water column (70 cm × 20 cm) was sampled, siphoned into the same egg collection basket (1 m × 1 m), and sampled daily for the same period.

We collected and counted eggs from each spawning event approximately two hours after the estimated time of spawning. We washed the eggs from the collection basket into a 20-L container. We then set the egg collection basket back into place until the next morning, when we made a second, supplementary collection. We included the second collections in the daily estimates of egg numbers, but these eggs were not used in developmental or experimental analyses.

To determine the number of eggs collected, we brought the egg collection container to 10 L of water volume and lightly agitated the mixture until the eggs were well distributed. We took three 5-mL samples with a wide-mouthed pipette and placed them in three separate glass counting dishes. We counted the individual eggs in each of the three dishes under a dissecting microscope, calculated the mean, and estimated by extrapolation the total number of eggs in the container. Standardized egg production in the main tank was calculated daily as the number of eggs collected divided by the total biomass of females assumed to be spawning (all those ≥ 20 kg) in the tank.

⁴ Tomlinson, P. 2001. Personal commun. Inter-American Tropical Tuna Commission, 8604 La Jolla Shores Drive, La Jolla, CA 92037.

Determination of egg stage and average egg size

We determined the stage of development of the eggs (egg stage) and measured the egg diameter and oil globule diameter of 30 fresh, randomly selected eggs from each standard collection made at 2 h after fertilization. We measured the eggs to the nearest 0.1 mm with a dissecting microscope fitted with an ocular micrometer. Eggs were classified developmentally according to the terms used by Fritzsche (1978). Egg-stage duration was estimated as the time period from fertilization to 50% hatching (defined below).

Incubation of eggs

We incubated the eggs in conical fiberglass tanks containing 300 L of 1- μ m-filtered, UV-sterilized seawater. Through mid-1997, the incubation tanks were exposed to ambient air temperatures and indirect ambient light. Beginning in mid-1997, the incubation tanks were housed in a room with indirect fluorescent lighting and at a constant temperature. The incubation tanks were in total darkness during the night, and were never exposed to direct sunlight or overhead fluorescent light at any time. We used tanks with both flow-through and closed systems for incubation, but we detected no notable differences in hatching success between the two systems. We rinsed the eggs in a 500- μ m sieve before placing them in the incubation tanks to eliminate any potentially harmful organisms such as *Benedenia* trematodes or parasitic copepods that might have transferred with the egg sample from the broodstock tank. Beginning in January 1997, we recorded the daily temperatures of the incubation tanks approximately four times between initial stocking and the time of hatching.

Determination of time at hatching

To determine the time at 50% hatching, we collected a sample of eggs from the incubation tank at 15-min intervals, beginning about 12 to 15 h (depending on water temperature) after the estimated time of spawning. When 50% of the eggs in the sample were hatched, we recorded the time. Approximately 2 hours after 50% hatching, we made a final estimate of the mean hatching rate. We took three 300-mL samples from the incubation tank and counted the total number of dead and live eggs and yolksac larvae. Live unhatched eggs, which made up a small portion (<5%) of the samples, were considered to be almost ready to hatch because our experience has shown that the majority of these eggs eventually hatch. The estimated final percent hatching was calculated as

$$\text{Final \% hatching} = (\text{no. larvae} + \text{no. live eggs}) / (\text{no. larvae} + \text{no. live eggs} + \text{no. dead eggs} + \text{no. dead larvae}) \times 100.$$

Collection of yolksac larvae

After all the larvae were hatched (final hatching), we made morphometric measurements on 20 randomly selected yolksac-stage larvae from each daily cohort. For each larva we measured total length (TL), notochord length (NL), yolk length, yolk height, and oil globule diameter to the nearest 0.1 mm.

Developmental series

Periodically we followed the development of a daily cohort of eggs and larvae from fertilization to first-feeding (normally a duration of 3.5 days). We initiated a developmental series whenever the daily mean temperature of the broodstock tank changed by at least 1°C. Each developmental series entailed sampling eggs at 15-min intervals for the first 4 hours after fertilization, at 1-h intervals for the next 6 h, and then at 2-h intervals until the time at 50% hatching. After final hatching, we sampled yolksac larvae at 6-h intervals until the larvae were ready to feed. We considered a larva to be at first-feeding stage when its retina was pigmented, the alimentary tract was formed, and the mouth was fully developed. We took morphometric measurements on 20–30 fresh eggs and yolksac larvae, as described previously. At first feeding, we measured 20 live larvae for TL, NL, the height and length of any remaining yolk, and the diameter of the oil globule. We measured mouth width on freshly fixed (5% formalin) first-feeding larvae because of the difficulty in obtaining accurate mouth measurements on live specimens.

Dry weights of eggs, yolksac larvae, and first-feeding larvae

For each developmental series examined, we obtained fresh dry weights of 20–30 eggs, yolksac larvae, and first-feeding larvae. We used 8-mm diameter aluminum pans that were dried in an oven at 60°C for 24 h, desiccated for 24 h, and then individually weighed to the nearest 0.1 μ g on a microbalance. After measuring, we rinsed the larvae and eggs multiple times with distilled water to remove salts and particulate matter. We placed an individual egg or larva in a preweighed aluminum pan, dried it at 60°C for 48 h, desiccated it for 48 h, and then weighed the specimen to the nearest 0.1 μ g.

Data analysis

We analyzed spawning parameters and the characteristics of eggs and early-stage larvae in relation to biological and physical data, including water temperature, time of day, and lunar cycle, from October 1996 through March 2000. We analyzed the relationships of daily ration and female size with egg size and egg production. We considered 20 kg as the minimum size for actively spawning females, based on the size at first-spawning from the genetic analysis (Niwa et al., 2003) and our observations of courtship and spawning behaviors. We

analyzed egg parameters possibly affected by size of females (standardized egg production, egg size) only during the period from June 1997 through July 1999. During this period only the original broodstock group was spawning, and we estimated that the majority of females in the tank were actively spawning (i.e., ≥ 20 kg each). This eliminated any confounding effects due to newly introduced immature females. Statistical analyses of the data included linear regression, correlation, and multiple regression, and followed the methods of Zar (1984). Statistical programs were run in Microsoft Excel and S-Plus 6.0 (Mathsoft, Inc., Seattle, WA).

Results

The spawning patterns and subsequent egg and larval development are described only for the fish in the main broodstock tank in the first 11 subsections. A short synopsis of the spawning patterns of the fish in the reserve tank is presented in the last subsection.

Broodstock fish

A total of 55 yellowfin tuna were initially stocked in the main broodstock tank in June and September of 1996. At stocking, the fish ranged in length from 51 to 78 cm fork length (FL) (mean of 62 cm FL) and weighed between 3 and 8 kg (mean of 5 kg). The sex composition of the original 55 fish (determined later at death) was 54% female and 46% male. Spawning first occurred in the main broodstock tank on 8 October 1996. At that time, there were 24 females (ranging from 6 to 16 kg and 65 to 93 cm FL) and 20 males (ranging from 6 to 14 kg and 66 to 86 cm FL) in the tank. From observations of courtship behavior during the first 2 to 4 months of spawning, it appeared that only a small group of larger individuals (generally >80 cm FL) was spawning. This pattern changed over time, as more of the broodstock fish attained reproductive size, and by mid-1997 it appeared from the courtship behavior that most of the broodstock fish were participating in the spawning. By mid-1997, there were 19 females (ranging from 13 to 30 kg and 87 to 108 cm FL, averaging 20 kg and 98 cm FL) and 16 males (ranging from 15 to 30 kg and 89 to 112 cm FL, averaging 22 kg and 99 cm FL) in the main tank. Using the estimated ages of wild yellowfin tuna in the eastern Pacific Ocean (Wild, 1986) and applying them to the lengths and weights of our broodstock fish (Wexler et al., 2003), we estimated that the average age of the broodstock fish in mid-1997 was approximately 2 years.

The broodstock population ranged in number from 55 (in September 1996) to five (in July 1999). In mid-August of 1999, we added 14 fish (ranging from 8 to 15 kg and 74 to 89 cm FL) to the main tank to supplement the spawning group. In February of 2000, we added another group of six fish (ranging from 4 to 14 kg and 58 to 71 cm FL) to the tank. The longest time that any individual fish from these broodstock groups survived

in captivity was 4.7 years, although average survival in captivity was 1.9 years. Estimated ages of broodstock fish at death averaged 3.1 years and ranged from 1.4 to 6.1 years. Mortalities occurred gradually over time—most often caused by strikes against the tank wall—during the early morning hours before feeding. The average size of the broodstock fish increased over time, and reached a maximum in mid-August 1999. At that time, there were four females (ranging from 46 to 77 kg and 141 to 150 cm FL, averaging 67 kg and 147 cm FL) and one male (50 kg and 133 cm FL) in the main tank. Several of these fish attained sizes >85 kg and 155 cm FL at the time of their deaths in March and October 2000. Estimated growth rates in length for the broodstock fish ranged from 0.9 to 4.0 cm/month and decreased with increasing lengths of the fish. Estimated growth rates in weight ranged from 0.8 to 1.6 kg/month for fish <19 kg and 1.7 to 1.9 kg/month for sizes >19 kg (Wexler et al., 2003).

Water temperature, spawning, and egg incubation

The mean daily water temperature in the main broodstock tank fluctuated with the ocean temperatures and ranged from 20.1° to 29.7°C, averaging 27.3°C (SD=1.5) (Fig. 2A). Periods of reduced temperatures occurred each year during the coastal upwelling season from January through March. Spawning occurred when the daily mean tank temperature was 23.3° to 29.7°C, and averaged 27.7°C (SD=1.1) at the time of spawning (Fig. 2A). The minimum spawning temperature during most years and seasons was about 24.0°C. The daily mean water temperature decreased to 24.0°C or below during three of the four years of the study; however, only two spawnings occurred at mean temperatures below 24.0°C. During most years, spawning occurred daily and continuously for several months, but spawning ceased when tank temperatures decreased below 24°C (March 1997, March 1999, and February 2000) or decreased by at least 0.5°C for at least one week (December 1997, October 1998, and August 1999). The cessation of spawning in October 1998 extended for 5.5 months. During this period, water temperatures were sufficient for spawning, although they were steadily decreasing (from 28°C to <24 °C) during most of the period.

The mean water temperatures in the egg incubation tanks ranged from 21.9° to 29.8°C, averaging 27.6°C (SD=1.0) (Fig. 2B). The pattern of incubation temperatures closely paralleled the pattern of mean daily water temperatures for the main broodstock tank, although the incubation temperatures did not decrease as much as those of the main broodstock tank during the upwelling period in early 1997 (because of the influence of higher air temperatures on the incubation tanks). From January 1997 through March 2000, incubation temperatures and the broodstock tank temperatures were highly correlated ($r=0.74$, $df=886$, $P<0.001$), and we considered the two data sets as equally representative of water temperatures observed in the laboratory.

Seawater characteristics and spawning

Spawning in the main broodstock tank occurred at salinities of 26 to 36 ppt, but during most months salinities ranged from 30 to 34 ppt. Dissolved oxygen ranged from 65% to 107% of saturation but usually exceeded 80% of saturation. The seawater pH ranged from 7.6 to 8.3, and ammonia was always below detection levels. During periods of cessation of spawning, salinities were generally stable between 30 and 34 ppt, and dissolved oxygen, pH, and ammonia were also within normal ranges.

Courtship and spawning behavior

The daily courtship and spawning behavior of the broodstock fish followed a consistent pattern. Courtship behavior usually began in the afternoon, and spawning occurred most often in the late afternoon or evening. The courtship behavior was usually initiated with a loose aggregation by most of the fish in the central, bottom area of the tank, although at times some pairing behavior was observed before formation of the aggregation. Smaller groups of fish (two to five individuals per group) would break off from the main aggregation and exhibit

courtship behavior that included paired swimming, chasing, and bursts of speed throughout the tank. The paired swimming and chasing was often in the pattern of loops throughout the water column. A courtship group consisted of a single fish, presumed to be a female, followed closely by one to three fish, assumed to be males. During the courtship process males would often flash vertical bars (also termed feeding bars by tuna biologists) along the sides of their bodies. Fish presumed to be females would often release concentrated discharge trails from their vents during the late stages of courtship. Courtship behaviors would continue unabated for 1 to 4 h prior to actual spawning.

Two to eight spawning groups would eventually break off from the courtship aggregation and spawning would take place nearly simultaneously in the tank. When the fish spawned, they would typically swim in an ever-tightening circle—one female in front and one to five males following closely behind in single file. During actual spawning we always observed the trailing individuals releasing milt. As the females in each group began to release their eggs, they would tighten their swimming circle and the males would do the same while they released milt. This action resulted in the entire spawning group swimming in a very tight circle, which appeared to facilitate the mixing of eggs and milt. During spawning, the swimming speeds of the fish usually decreased, compared to the speeds during courtship, but at times swimming would remain quite rapid while eggs and milt were released. The fish within spawning groups moved horizontally as they spawned, but the fish often added some vortex-like movement upward through the water column as spawning occurred. Within each group, spawning was usually completed within 30 to 45 sec. The entire spawning event was often finished within 60 to 90 sec, although at times spawning events would continue for up to 5 to 10 min.

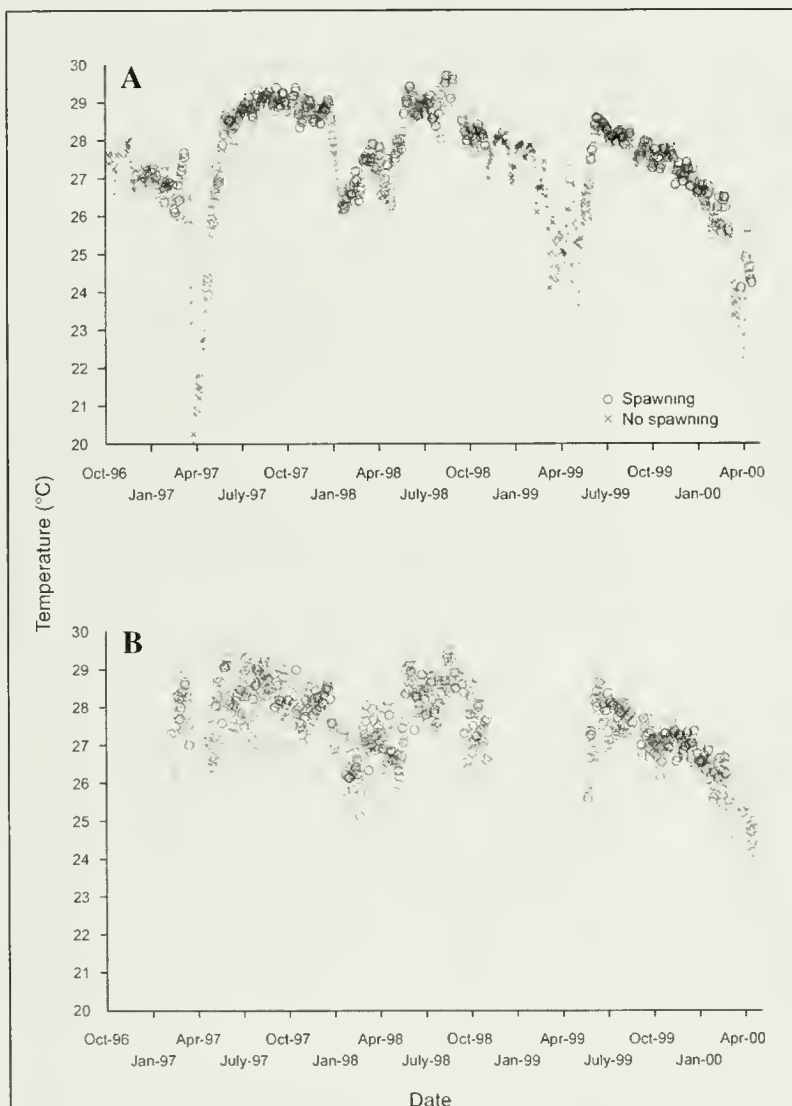


Figure 2

Mean daily water temperature in (A) the main broodstock tank, and (B) the incubation tanks from October 1996 through March 2000. In (A), plotted symbols are individual dates on which there was either spawning (indicated by o) or no spawning (indicated by x). In (B), plotted symbols are individual dates on which egg incubation occurred.

Spawning periodicity and size and age at first-spawning

The yellowfin tuna broodstock spawned 963 times, at almost daily frequencies, over the study period, although not all the fish were sexually mature during the entire period. Genetic analysis of female broodstock and their eggs and larvae (Niwa et al., 2003) corroborated our observations and videotape analysis of courtship and spawning behaviors and spawning frequencies. The mitochondrial DNA analysis confirmed that multiple females were contributing to individual spawns over protracted time periods (weeks to months). From August 1999 through August 2000, there were ten identified females in the tank. We identified up to six female genotypes in egg or larval samples on individual spawning dates, and we observed the same genotypes for at least five females on successive sampling dates over 1 to 3 months. The spawning frequencies estimated by this analysis were undoubtedly conservative because the sampling was not conducted every day, even though spawning was occurring daily.

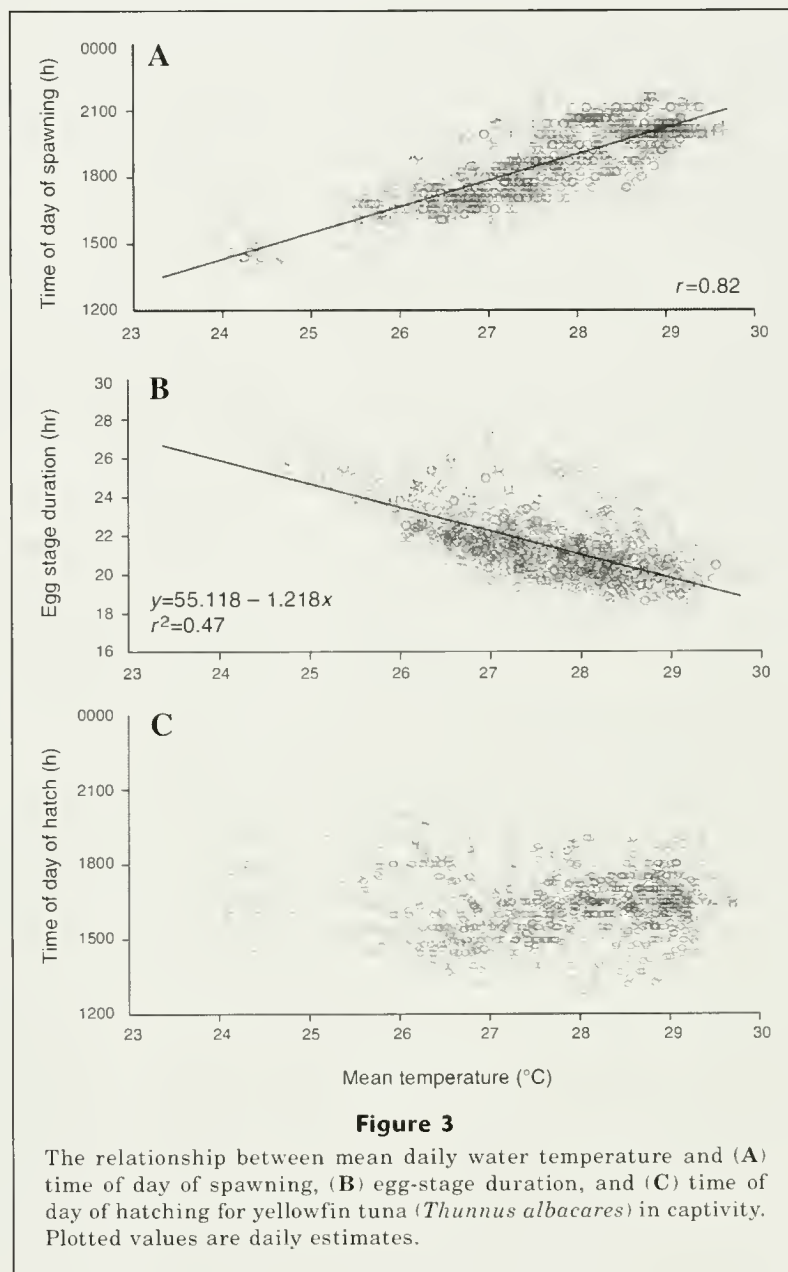
When spawning first occurred (8 October 1996), we estimated that the average age of the broodstock females was 1.6 years (range 1.3–2.0 years, $n=24$). For the 1999–2000 period, we estimated that the weight of a female at first spawning was 12 to 28 kg and its size was 75 to 112 cm FL. These measurements correspond to an average age of 2.0 years (range 1.6–2.8 years, $n=7$), where the majority of females would be slightly younger than 2.0 years.

Timing of spawning and hatching

The time of day that spawning occurred ranged from 1330 to 2130 h, and was most frequent between 1600 and 2100 h (Fig. 3A). The time of day of spawning was strongly and positively correlated ($r=0.82$, $df=937$, $P<0.001$) with mean daily water temperature. For example, at mean daily water temperatures of 25°C or below, spawning occurred in the afternoon between 1330 h and 1745 h. At temperatures near 27°C, spawning took place near 1800 h, and at water temperatures of 27.5°C or above, spawning occurred at night between 1845 h and 2130 h.

Egg-stage duration was inversely related to mean incubation temperature (Fig. 3B). Mean egg-stage duration ranged from a maximum of 28 h at 24°C to a minimum of 18 h at 29°C or above. The relationship was best described by a highly significant linear regression ($r^2=0.47$, $df=827$, $P<0.001$).

Water temperature imposed opposite effects on the time of day of spawning (direct relationship) and egg-



stage duration (inverse relationship), and the net effect of these relationships was a narrow range for the time of day at hatching (Fig. 3C). Over the 3.5-yr study period, the eggs hatched between 1300 h and 2145 h. However, over 95% of the hatch times occurred in a narrow time frame between 1500 h and 1900 h, regardless of water temperature.

Egg production and daily ration

For the original broodstock group, there was no definitive relationship between standardized egg production and mean size of spawning females, nor was there a significant overall correlation between standardized egg production and daily ration over the entire study

period ($r=0.15$, $df=564$, $P>0.10$). However, over short time periods (<1 month), the spawning females increased their egg production in response to short-term increases in daily ration. Over the period of June 1997 through July 1999, we varied the daily ration of food for the broodstock fish from approximately 1.0% to 4.5% body wt/day. During eight periods, we purposely increased daily food ration from 9% to 33% over time durations of 3 to 14 days. The rations were usually increased in response to greater food requirements, signaled by increasing feeding activity, or in attempts to effect increased egg production. During all eight of these periods, the standardized egg production in the tank increased from 30% to 234% (Fig. 4). There was a time lag until peak egg production occurred (indicated by numbers in parentheses in Fig. 4) after the initial increase in ration. Egg production increased, and peaked from 4 to 21 (average of 12) days after the introduction of increased rations. The percentage increase in egg production tended to be greater with greater increases in daily ration, but the relationship was not significant ($r=0.36$, $df=7$, $P>0.10$). The increases in egg production occurred over a range of water temperatures from 27.3° to 29.4°C; however, there was no clear association between water temperature and standardized egg production.

Spawning and photoperiod

Given the tropical latitude of the Achotines Laboratory (7°25'N), photoperiod was relatively constant during the study. From October 1996 through March 2000, day length varied by only 53 min, and changed by only 3 to 12 min/month (U.S. Naval Observatory Astronomical Applications Database⁵). No strong relationships between either frequency of spawning or standardized egg production and photoperiod were apparent. Cessations in spawning associated with short-term decreases in tank water temperature (in December 1997, October 1998, and August 1999) occurred during periods of decreasing photoperiod, while cessations in spawning due to water temperature decreases below the apparent-minimum for spawning (<24°C) (in March 1997, March 1999, and February 2000) occurred during periods of increasing photoperiod.

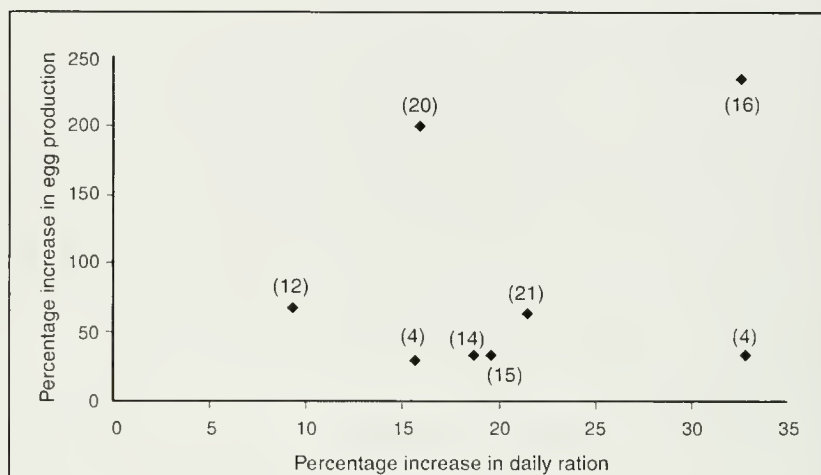


Figure 4

Increases in egg production by female yellowfin tuna (*Thunnus albacares*) broodstock during eight periods of planned increases in daily ration. Each period is represented by a plotted symbol. For each period, the value in parenthesis is the elapsed number of days from the initial increase in ration until the peak egg production was observed.

Spawning and lunar phase

Spawning occurred almost daily and showed no definitive relationship with lunar phase on a daily or monthly basis. Also, there was no significant correlation between standardized egg production and lunar phase ($r=0.10$, $df=564$, $P>0.20$). In each of the 26 months for which standardized egg production was calculated (June 1997 through July 1999), the monthly maxima egg production occurred equally during the first two quarters (new moon to half-moon) and last two quarters (half-moon to full moon) of each lunar cycle. However, over the 2-year period, the maximum egg production from individual spawns occurred most often at greater illumination phases of the moon. Of the 20 spawns with the greatest standardized egg production, 90% occurred during the third or fourth quarters (i.e., half-moon to full-moon), although only one of these 20 spawns occurred directly on a full moon.

Egg-stage duration and egg size

Egg-stage duration increased with larger egg size, although the predictive power of the linear regression was low ($r^2=0.09$, $df=837$, $P<0.001$). Water temperature, as presented previously (Fig. 3B), exhibited a strong inverse relationship with egg stage duration. We used stepwise regression to build a model to predict egg-stage duration as a function of egg size and temperature:

$$Y = 27.96 (\pm 1.69 \text{ SE}) + 29.05 (\pm 1.55) D - 1.28 (\pm 0.04) DT$$

$(r^2=0.58, df=826, P<0.001),$

⁵ U.S. Naval Observatory Astronomical Applications Database. 2002. Table of sunrise/sunset, Astronomical Applications Dept., Data Services. Website: <http://aa.usno.navy.mil/data> (accessed August 2002).

Table 1

Morphometric measurements and dry weights of eggs, yolk-sac larvae, and first-feeding larvae of yellowfin tuna (*Thunnus albacares*).

Eggs	Egg diameter (mm)	Oil globule (mm)	Weight (μg)	
Mean	0.97	0.22	42.8	
Standard error	<0.01	<0.01	0.4	
Minimum	0.85	0.15	33.6	
Maximum	1.13	0.28	59.7	
<i>n</i>	27,343	27,359	197	
Yolksac larvae	Total length (mm)	Notochord length (mm)	Weight (μg)	
Mean	2.61	2.51	30.1	
Standard error	<0.01	<0.01	0.4	
Minimum	2.10	2.00	25.0	
Maximum	3.6	2.90	40.8	
<i>n</i>	15,832	15,849	132	
First-feeding larvae	Total length (mm)	Notochord length (mm)	Mouth width (mm)	Weight (μg)
Mean	3.49	3.32	0.262	21.7
Standard error	<0.01	<0.01	<0.01	0.4
Minimum	2.90	2.70	0.225	13.8
Maximum	4.10	3.90	0.350	29.6
<i>n</i>	272	272	126	105

where Y = egg stage duration (h),
 D = mean egg diameter, and
 T = mean incubation temperature ($^{\circ}\text{C}$).

The diameter of individual fertilized eggs ranged from 0.85 to 1.13 mm and averaged 0.97 mm (Table 1). Each egg contained a single oil globule that averaged 0.22 mm in diameter. The dry weight of individual eggs ranged from 34 to 60 μg and averaged 43 μg (Table 1). Mean daily egg diameter was inversely related to water temperature during the period when the original broodstock (stocked in 1996) were spawning (Fig. 5A; $df=892$, $P<0.001$), although there was considerable scatter about the regression ($r^2=0.23$). Mean egg diameter was significantly correlated ($r=0.45$, $df=553$, $P<0.001$) with the mean weight of spawning females (all females ≥ 20 kg) in the original broodstock group (Fig. 5B).

Larval size at hatching and hatching success

At hatching, the larvae averaged 2.5 mm NL (range 2.0–2.9 mm NL; $SD=0.16$) (Table 1). Larvae at hatching had unpigmented eyes, no alimentary tract nor mouth, and exhibited a large, elliptical yolk mass containing a single posterior oil globule. The dry weight of individual larvae at hatching ranged from 25 to 41 μg , averaging 30 μg ($SD=4$) (Table 1). Mean larval length at hatching was positively correlated ($r=0.46$, $df=498$, $P<0.001$) with

mean egg diameter (Fig. 6A), and negatively correlated ($r=-0.27$, $df=774$, $P<0.05$) with mean incubation temperature (Fig. 6B).

The percentage hatching of eggs spawned in captivity ranged from 9.5% to 99.0% and averaged 83% ($SD=14.7\%$). In general, the hatching success was high, with over 84% of the hatchings occurring at rates $>70\%$. The percentage hatching showed no relationship with either water temperature or larval length.

Egg and early larval development

Yellowfin tuna egg development was rapid. The developmental duration from fertilization to hatching followed a curvilinear pattern (Fig. 7), and the egg-stage duration was temperature dependent (Fig. 3B). At a modal incubation temperature of 27.0°C , egg-stage duration was 21.65 h (Fig. 7). At 27.0°C , cell cleavage occurred <1 h after fertilization, early embryo gastrulation occurred about 6 h after fertilization, the embryo first formed after 8 h of development, and the embryo was in the tail-free stage approximately 17 h after fertilization. The specific gravity of fertilized eggs changed with development. Upon fertilization, eggs were positively buoyant and would rise to the surface neuston layer of the broodstock tank. Eggs remained positively buoyant into the tail-free stage, but 2 to 4 h (dependent on temperature) before hatching the specific gravity changed and the eggs became negatively buoyant until they hatched. The nega-

tive buoyancy in the late egg stage was observed at all salinities at which incubation occurred (26 to 36 ppt).

The duration of the yolk sac larval stage was inversely (but weakly) related to temperature and ranged from 56 h at 29.0°C to 65 h at 23.5°C. Eye pigmentation and mouth formation in larvae occurred almost simultaneously, and at the stage of mouth formation there was usually only a trace of yolk remaining. First-feeding larvae averaged 3.3 (SD = 0.18) mm NL (range 2.7–3.9 mm) and weighed between 14 and 30 μg (average 22 μg) (Table 1). The mouth width of first-feeding larvae ranged from 225 to 350 μm , averaging 262 μm (Table 1).

Spawning in the reserve tank

The fish in the smaller reserve tank began spawning in mid-April 1997. At that time there were four females and four males in the tank. When spawning first commenced, the females ranged from approximately 7.0 to 10.5 kg (average 9 kg) and 70 to 74 cm FL (average 72 cm), while the males ranged from 5.5 to 9.0 kg (average 7.5 kg) and 62 to 74 cm FL (average 66 cm). We did not determine how many fish were involved in the initial spawning, but it appeared from courtship behavior that only a few of the larger individuals were participating in spawning during the first 1 to 2 months. Spawning continued into October 1997, when we sacrificed the one remaining pair of fish. At the time of death, the female was 16 kg and 94 cm FL and the male was 12 kg and 79 cm FL. We did not monitor the numbers or characteristics of eggs or larvae in the reserve tank. Spawning in the reserve tank occurred over a water temperature range of 24.4° to 29.2°C.

Discussion

The spawning by the yellowfin tuna broodstock at the Achotines Laboratory, beginning in 1996, represents the first occurrence worldwide of sustained spawning by yellowfin tuna in landbased facilities. Over 3.5 years, the broodstock fish spawned in our large broodstock tank (1362 m³) at near-daily frequencies over extended time periods. In general, the fish spawned as long as they received adequate daily rations of food and the water temperature was 24°C or higher. The reserve group also spawned for a 6-month period in a tank of reduced volume (270 m³).

Courtship and spawning behaviors

No courtship behavior or spawning aggregation has ever been observed in tunas in nature. The sustained spawning by the yellowfin tuna broodstock in this study allowed us to observe and analyze reproductive behavior that has not been described previously. The courtship and spawning behavior of the captive yellowfin tuna was ritualized and consistent among three groups of broodstock fish over almost four years. The courtship behavior (chasing by males, paired swimming) always occurred after the initial formation of a central aggregation of participating fish. During the actual spawning events, males were not monogamous to single spawning groups and would often move from

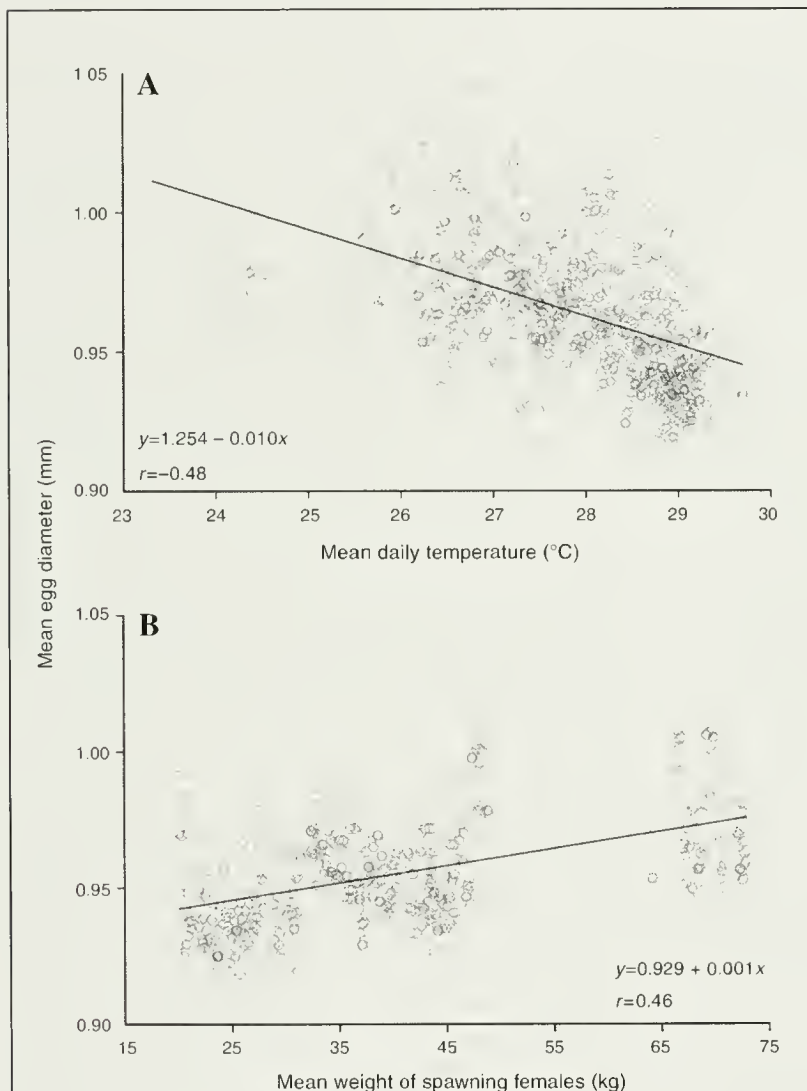


Figure 5

(A) The relationship between mean egg diameter and mean daily water temperature, and (B) the relationship between mean egg diameter and mean weight of spawning females of yellowfin tuna (*Thunnus albacares*) in captivity.

one spawning female to another. Spawning behavior (swimming in tightening circles with females in the lead position) ensured that eggs and milt would be well mixed. Most spawning groups moved over a range of depths in the broodstock tank, so it is likely in nature that yellowfin tuna in spawning groups move vertically to some degree during release of gametes.

The aggregations and courtship behavior usually occurred unabated for several hours before spawning and represented a significant energetic investment by the broodstock fish. The daily energetic cost of maturing a batch of eggs for a single spawning by yellowfin tuna sampled at sea was estimated at 1.06% of body weight by Schaefer (1996), but that estimate did not include the energetic costs of courtship or spawning behavior. If the behavior of our captive spawning group is representative of yellowfin tuna behavior in nature, then we believe that yellowfin tuna in the wild probably form large spawning aggregations and individual fish may invest considerable time (1 to 4 h) and energy (costs unknown) on daily courtship and spawning activities.

The behavior of the yellowfin tuna broodstock is predictable on a daily basis, which would indicate that a synchronization mechanism is inherent to the behavior. Most of the courtship and spawning behavior of the fish appeared to be driven by female behavior (i.e., females led, males followed). In teleost fishes, the release of eggs and milt during spawning is synchronized by the release of pheromones, predominantly by females (Liley et al., 1991). Sex hormones and hormone metabolites are water soluble and indicate the sender's reproductive status. Pheromones studied to date appear to be of two types, steroids and prostaglandins, and they are released by females in concentrated urine trails (Stacey, 1984, 1991). Female yellowfin tuna in our spawning group often released discharge trails during the courtship process just before spawning, and at times we misinterpreted these trails as egg emissions. Given the ritualized nature of the courtship and spawning behavior of both sexes in our broodstock, most of the discharge trails during late-courtship may have been pheromone releases by the females, although future confirmation with biochemical or immunoassay analyses would be required.

Diel patterns of spawning and egg hatching

The diel timing of spawning by the broodstock yellowfin tuna was finely tuned to water temperature and, com-

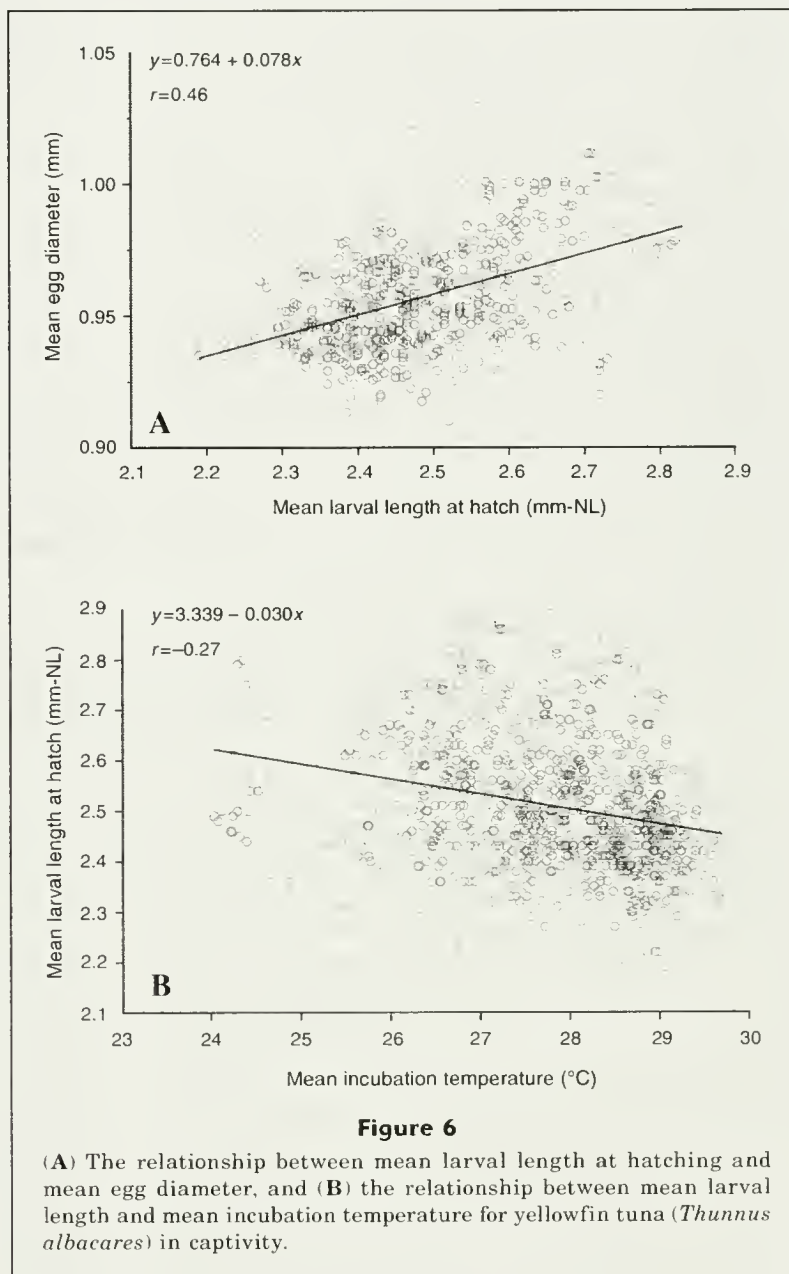


Figure 6

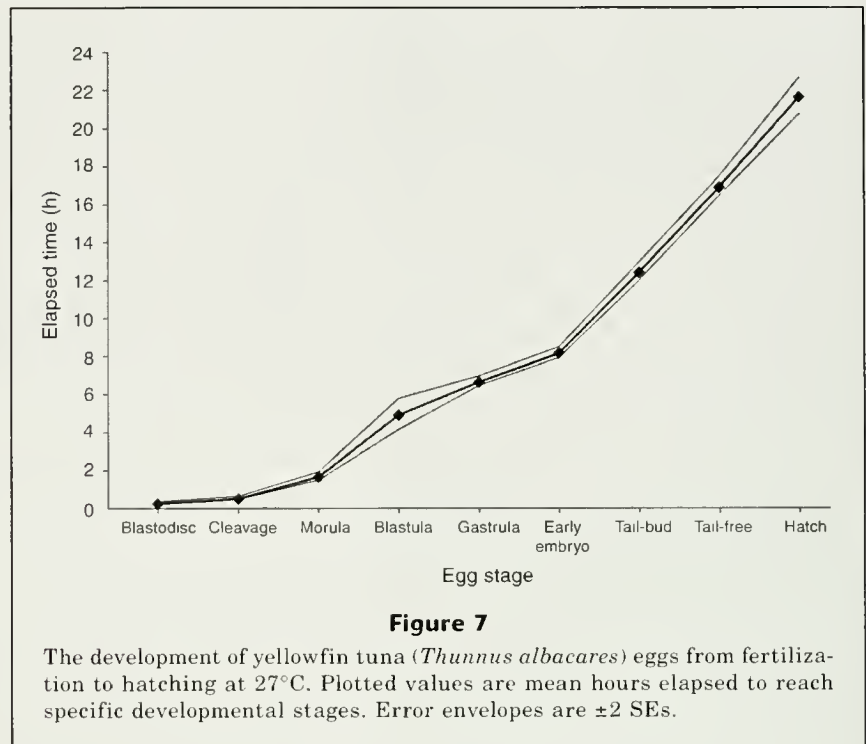
(A) The relationship between mean larval length at hatching and mean egg diameter, and (B) the relationship between mean larval length and mean incubation temperature for yellowfin tuna (*Thunnus albacares*) in captivity.

bined with the strong inverse relationship between water temperature and egg duration, resulted in a predictable and narrow range in the time of hatching. The majority of spawning occurred after sunset and at higher (generally $>27^{\circ}\text{C}$) water temperatures. However, when water temperatures decreased, the broodstock fish spawned earlier in the day. This temporal shift resulted in nearly all hatching occurring in the late afternoon or early evening. We believe that this pattern for the diel timing of spawning and hatching is important and has adaptive significance for the early life history of yellowfin tuna. In nature, the maintenance of a conservative time for egg hatching would ensure that newly hatched yellowfin larvae spend the first 12 to 15 h after hatching in dimming light or darkness. Because yolksac larvae of marine

fishes are vulnerable to predation by planktivorous fishes and invertebrates (Bailey and Houde, 1989), minimizing the amount of time spent in daylight appears to be a mechanism for maximizing survival for yolk sac larvae.

This temporal pattern of hatching would also minimize the exposure of yellowfin tuna yolk sac larvae to the ultraviolet effects of sunlight. Although the vertical distribution of yellowfin tuna yolk sac larvae in the ocean has not been described, feeding-stage larvae of yellowfin tuna are found predominantly in the upper mixed layer (Leis et al., 1991; Boehlert and Mundy, 1994). The deleterious effects (mostly genetic damage) of ultraviolet radiation are strongest in the upper mixed layer and may affect yolk sac larvae more than other early life stages of marine fishes (Vetter et al., 1999). Thus, any adaptation that reduces the amount of time yellowfin tuna yolk sac larvae spend in daylight increases their chances of survival.

Most tunas are reported to be nocturnal spawners, according to histological analyses of the ovaries of adult fishes caught at sea (McPherson, 1991; Nikaido et al., 1991; Schaefer, 1998, 2001a). Our experimental results indicate that the view that yellowfin tuna spawn exclusively at night should be reconsidered. The assumption of nocturnal spawning by tunas in past studies has been based on histological analyses of oocyte development and new postovulatory follicles in the ovaries of adult fishes in the wild (collected predominantly at sea surface temperatures $>27^{\circ}\text{C}$), but the actual water temperatures encountered by the fish before and during spawning were not known. Our results indicate that yellowfin tuna respond to variations in water temperature by altering their time of spawning and that the diel changes in spawning time are precise and predictable. The ability to control the timing of spawning by adults may be mediated by the timing of the release of sex hormones and maturation processes in response to water temperature. It is possible that our results are simply an artifact of captivity because our broodstock fish were confined to a tank and not able to thermoregulate by changing water depth or location as wild fish can. However, we believe that our experimental evidence for the control of the timing of spawning by yellowfin is compelling. The adaptive significance of this spawning pattern is most likely related to the ultimate effects of temperature on development rates of eggs and yolk sac larvae (i.e., maintenance of a consistent time of hatching to maximize early larval survival). In the only other similar study on tunas, Miyashita et al. (2000a) reported that cultured bluefin tuna also spawned predominantly before sunset. Daily mean water temperatures in their



4-yr study ranged from 21.6° to 29.2°C, and the mean temperatures during the spawning season ranged from 23.6° to 27.0°C.

Spawning cues

Spawning substrate, food availability, water temperature, photoperiod, and lunar cycle can strongly influence many functions of the teleost reproductive system (Bye, 1984; Stacey, 1984). We consider each of these potential cues for reproduction in yellowfin tuna

Because yellowfin tuna are pelagic spawners, they have no specific substrate requirements. The yellowfin tuna in our study received controlled daily rations to fuel daily spawning costs (Wexler et al., 2003). Under the nonlimiting food conditions that we provided, no relationship was apparent between spawning occurrence and food abundance. However, this pattern of spawning in captivity does not rule out the possibility that the timing of yellowfin tuna reproduction in tropical or subtropical waters could be influenced by seasonal fluctuations in food abundance, such as those associated with seasonal upwelling. Some species of tropical and subtropical marine fishes exhibit reproductive cycles that coincide with periods of upwelling or increased productivity and food availability (Bye, 1984). Tunas in tropical regions usually spawn year-round, but those occurring in the subtropics exhibit seasonal spawning patterns (Fritzsche, 1978; Schaefer, 1998), whereas bluefin tuna and albacore migrate to warm waters to spawn in distinct areas during restricted periods (Collette and Nauen, 1983). Our yellowfin tuna broodstock

did not exhibit any patterns of spawning occurrence that were related to food abundance in captivity (but see the following subsection on "Egg production and daily rations").

Our focus on the processes controlling maturation and spawning of captive yellowfin tuna has centered on the influences of water temperature, photoperiod, and lunar cycle. Water temperature appeared to provide the main exogenous control over the occurrence and timing of spawning of captive yellowfin tuna. The fish spawned over a range of daily mean temperatures from 23.3° to 29.7°C. Spawning occurred at daily mean temperatures <24°C on only two out of 963 dates (single spawning events at 23.3° and 23.9°C), and spawning became intermittent or ceased within 24 hours after those two dates. This thermal range for spawning of yellowfin tuna is similar to that reported from collections at sea of reproductively active adults (Schaefer, 1998) and early-stage larvae (Nishikawa et al., 1985; Boehlert and Mundy, 1994; Lauth and Olson, 1996). In general, tunas spawn at water temperatures $\geq 24^\circ\text{C}$ (Collette and Nauen, 1983), although larvae of bullet or frigate tunas (or larvae of both) (*Auxis* spp.) and skipjack tuna have been collected at sea at temperatures near 22°C (Richards and Simmons, 1971; Boehlert and Mundy, 1994). In their study of spawning of captive bluefin tuna in Japan, Miyashita et al. (2000a) reported spawning temperatures from 21.6° to 29.2°C.

This study is the first to investigate the relationship on a daily basis between water temperature and spawning by yellowfin tuna over a protracted period. Our results indicate that the sensory ability of yellowfin tuna to detect ambient water temperature and the associated feedback mechanisms involved in neuroendocrine control of ovulation and spawning behavior are rapid and characterized by subdaily response times. Spawning usually ceased within one day after water temperatures decreased by only 0.1 to 0.2°C, and usually recommenced in less than one day after similar minute changes in water temperature. The broodstock altered the time of day of spawning predictably in relation to water temperature, but this behavioral change in the time of day of spawning occurred only after several days of exposure to changes in water temperature. Maturation and spawning in female fishes, in particular the initiation of vitellogenesis, oogenesis, and ovulation, is under hormonal control (Goetz, 1983). Sensory inputs to neuroendocrine control of reproduction include information on external water temperature transmitted via temperature-sensitive afferent nerve fibers (Van der Kraak et al., 1998). The spawning periodicity of the broodstock and their ability to adjust the time of day of spawning in response to water temperature indicate that yellowfin tuna have the ability to rapidly integrate sensory information on water temperature and, often within hours, adjust the hormonal control of final maturation processes and spawning.

Our analysis of spawning by the yellowfin tuna broodstock did not indicate a strong influence of lunar cycles on the timing of spawning or egg production within

monthly periods. We originally anticipated some lunar periodicity to spawning because many tropical marine species exhibit lunar spawning rhythms that usually peak around the new moon or full moon (spring tides) (Johannes, 1978; Bye, 1984). Peak spawning on new or full moons in the tropics may be an adaptation to maximize offshore transport of eggs and larvae by spring tides away from increased predation pressure in coastal habitats (Johannes, 1978). Our captive yellowfin tuna, however, were exposed only to lunar cycles in captivity, but not to tidal influences. The mean daily egg production from individual spawnings in our study was highest during phases of greater lunar illumination. This trend in egg production could be viewed as evidence that yellowfin tuna increase their spawning efforts just prior to full moons, but the trend from our data is not definitive. Although adult yellowfin tuna in nature sometimes aggregate around islands and seamounts (Boehlert and Mundy, 1994), spawning by yellowfin tuna is widespread throughout the tropical and subtropical oceans (Nishikawa et al., 1985). Because yellowfin tuna often spawn in pelagic open-ocean habitats, they may not require the same level of synchronization with lunar cycles to aid in egg and larval dispersal as that required by coastal tropical species.

Photoperiod is an important environmental cue for spawning in temperate fish species (Lam, 1983). However, in the tropics, photoperiod hardly varies throughout the year and is usually not a major factor in the control of maturation and spawning of tropical fishes (Lam, 1983). Photoperiod changed very little during our study, and the yellowfin tuna broodstock showed no detectable responses to slight changes in day length.

Egg production and daily rations

Yellowfin tuna in this study exhibited the ability to boost egg production in response to periodic increases in daily food rations. Egg production peaked over periods of 1 to 3 weeks (average 12 days) after food rations were increased. These increases in daily egg production sometimes exceeded 200%, providing strong evidence that yellowfin can convert peaks in exogenous energy consumption into higher egg production in a matter of days or weeks. The adaptive significance of this reproductive pattern is obvious. The ability to increase egg production in response to greater food abundance in oceanic habitats would provide yellowfin tuna with the opportunity to exploit patchy food resources and periodic increased production that can occur in the vicinity of islands, seamounts, and in coastal or equatorial upwelling zones. Results from several field studies, where the abundance of tuna larvae was examined, support our laboratory results. Boehlert and Mundy (1994) suggested that increased abundance of *Thunnus* spp. larvae on the leeward side of Oahu, Hawaii, may be related to greater forage for adult tunas in that region. Lauth and Olson (1996) reported peak abundance of *Euthynnus lineatus* and *Auxis* spp. larvae during periods of peak seasonal upwelling and secondary production in the Panama

Bight, and they suggested that spawning adult tunas may increase batch fecundities in response to greater forage.

Yellowfin tuna are multiple-spawning fish, and their fecundity is not fixed at the beginning of any spawning period (Schaefer, 2001a). Batch fecundity of yellowfin tuna can vary annually or geographically (Schaefer, 1998), although information on daily patterns in batch fecundity of tunas is lacking. Wootton (1979) reported one of the few studies to demonstrate a positive relationship between batch fecundity and daily food ration in nonscombrid species. Our results with captive yellowfin tuna agree with Wootton's data and indicate that over short time periods yellowfin tuna can boost egg production in response to increased food abundance.

Size and age at first spawning and sex ratios

Our estimates of the range of sizes at first spawning for our female yellowfin tuna in 1999–2000 (12 to 28 kg, 75 to 112 cm FL) (Niwa et al., 2003) are not directly comparable to estimates from some studies of wild yellowfin tuna because of slight differences in the reproductive conditions measured. We estimated size at first spawning, whereas estimates from studies of wild fish have included estimates of size at maturity and size of reproductively active fish. Size at maturity, although related to size at first-spawning, is a more conservative estimate than size at first-spawning and does not indicate true reproductive activity. Schaefer (1998) reported that the minimum length of reproductively-active wild fish observed in the eastern Pacific Ocean was 60 cm FL. Fifty percent of the fish in that study were mature at 92 cm FL, and the portion spawning per day at that size was 0.61. McPherson (1991) estimated that the mean length at maturity of yellowfin tuna in the western Pacific Ocean was 108 cm FL. In general, the sizes of reproductively active fish reported for wild yellowfin tuna are comparable to our estimates of size at first spawning. Also, Schaefer's (1998) estimate of 92 cm FL as the length at 50% maturity for wild fish is similar to the average length of our broodstock fish in mid-1997, when we estimated that most of our fish appeared to be spawning.

It appears that the majority of our broodstock began spawning at slightly earlier ages than did the wild yellowfin tuna. Schaefer (1998) estimated the age at first maturity of yellowfin tuna in the eastern Pacific Ocean to be approximately 2 years. Our estimates of age at first spawning for the original broodstock fish ranged from 1.3 to 2.0 years, and averaged 1.6 years, and the estimated age at first spawning for the 1999–2000 females ranged from 1.6 to 2.8 years and averaged 2.0 years. However, the majority of these females were estimated to be slightly younger than 2 years. The more precocious spawning by most of the captive fish was most likely due to greater food rations and higher growth rates compared to those of wild fish during the first 1–2 years in captivity. Our results indicate that

fish size, rather than age, is the best predictor of reproductive status of yellowfin tuna.

The sex ratio of the original group of yellowfin tuna in this study was initially 1.2:1.0 (female:male), and females remained slightly more abundant in the spawning group over 3.5 years. A dominance by males in larger length classes has been reported for wild yellowfin tuna, and has been attributed to potential differences in natural mortality rates between the sexes (Suzuki, 1994; Wild, 1994). We saw no evidence of greater mortality in larger females in our broodstock group. However, mortality rates in captivity are expected to be less than in nature because food is not limiting and predators are absent.

Egg and larval development

Yellowfin tuna eggs and newly hatched larvae are morphologically typical of marine pelagic fishes. Fertilized yellowfin tuna eggs average about 1 mm in diameter, and the larvae hatch at a relatively small size (ca. 2.5 mm SL). The weight data that we present in this study are either the first (yolksac larvae, first-feeding larvae) or second (eggs) published estimates for tuna. Yellowfin eggs weigh about 43 μg dry, and weight loss occurs during the embryonic phase, and larvae lose about 33% of the original total weight at hatching and almost 50% of the original weight at first-feeding. The weight loss is due to utilization of yolk and oil during the egg and yolksac stages.

Scombrid early life history is characterized by high mortality rates, high metabolic rates, and exponential growth (Davis et al., 1991; Margulies, 1993; Wexler et al., 2001). Yellowfin tuna larvae at first feeding are intermediate in size (3.3 mm SL, 22 μg in this study) compared to other scombrid larvae (Tanaka et al., 1996), and they exhibit a large scope for growth as juveniles (Kaji et al., 1999; Wexler et al., 2007). Given the low initial weights of yellowfin eggs and yolksac larvae and the high growth rates of larvae and early-juveniles, the potential for weight gain from the egg stage to the stage at first-recruitment for yellowfin (30 cm FL, 6 months of age, IATTC⁶) is very high and approaches a gain in weight from $\times 10^6$ to $\times 10^7$.

Water temperature influences almost every aspect of the egg and yolksac larval stages of yellowfin tuna. Water temperature is inversely related (significantly) to egg size, egg-stage duration, larval size at hatching, and yolksac larval duration. Inverse developmental relationships between water temperature and the sizes and durations of egg and yolksac stages are common in marine fishes (Blaxter, 1969) and have also been reported for cultured bluefin tuna (Miyashita et al., 2000a, 2000b). These inverse relationships are most likely the result of slower responses of ontogenetic pro-

⁶ IATTC (Inter-American Tropical Tuna Commission). 2000. Annual report of the Inter-American Tropical Tuna Commission, 1998, 357 p. 8604 La Jolla Shores Drive, La Jolla, CA 92037.

cesses to lower water temperature during oogenesis and embryonic stages (Chambers, 1997). At lower water temperatures, the durations of developmental stages are longer, and eggs and hatched larvae are larger.

An interesting aspect of egg development in yellowfin tuna is the change in buoyancy as the eggs develop. Fertilized eggs are positively buoyant throughout development until a few hours before hatching, when they become negatively buoyant. We assume that the onset of negative buoyancy occurs as the chorion of the egg begins to break down and more water diffuses into the egg. Just before hatching, the chorion of fish eggs is slowly liquefied by proteolytic enzymes (Blaxter, 1969), and it is likely that this process occurs also in late-stage yellowfin tuna eggs. The change in buoyancy of eggs has not been studied extensively in tunas. Mayo (1973) reported a similar change in buoyancy in the eggs of seven taxa of scombrids from Florida waters, and we have observed a similar pattern in fertilized eggs of black skipjack (*Euthynnus lineatus*, first author, personal commun.). In nature, the adaptive significance of negative buoyancy in late-stage eggs is not clear, but presumably the process of sinking just before hatching would remove the late-stage eggs and newly hatched yolk sac larvae from the neuston layer and reduce mortality caused by wave action, wind, and damage from ultraviolet radiation.

Egg size increased with female yellowfin tuna size. This is a common trait in many fish species, although a direct relationship is apparent in some stocks but not in others (Hempel and Blaxter, 1967; Marteinsdottir and Able, 1988; Chambers and Leggett, 1996). The relationship between egg size and female size is relatively unstudied in tunas and is probably less important, in terms of reproductive potential, than the relationship between fecundity and female age and size (Chambers, 1997).

For aquaculture purposes, the relationship of egg size to female size in our study could be used to determine the optimum size of broodstock females required to produce maximum egg sizes. For our original broodstock group, the largest females produced the largest eggs and larvae. However, larger egg size or hatching size had no relationship with hatching success in our study. Whether larger sizes at hatching confer some greater fitness for yellowfin tuna during prerecruit stages in nature is unclear, and may depend on processes of growth, feeding, and development that occur later during development. The ecological implications of the effects of size during early life stages of yellowfin tuna or other tuna species remain unknown and would require detailed investigations of spawning and early life history traits in wild tuna populations.

Acknowledgments

We thank the talented and dedicated staff of the Achotines Laboratory for their hard work to ensure the success of this project. The Overseas Fishery Coopera-

tion Foundation of Japan provided the majority of the funding for the expansion of the seawater and tank systems, and they were also our collaborative partners in the development of the yellowfin tuna spawning project. S. Masuma (Fisheries Research Agency of Japan), C. Farwell and D. Thomasberg (Monterey Bay Aquarium), and H. Yoneshima (Kinki University) provided technical advice on the culture of tunas in captivity. In Panama, R. Martans, A. Franco, E. Diaz, and A. Cano (Direccion General de Recursos Marinos y Costeros) provided administrative support. R. Jope and K. Bentler (formerly of the IATTC) assisted with project logistics and purchasing. C. Montez (IATTC) skillfully prepared the figures. P. Tomlinson (IATTC) provided invaluable advice on growth curve fitting and bootstrap procedures. W. Bayliff provided helpful review comments. We wish to thank A. Suda for his assistance in the early development of the project. We would also like to thank the former and present Directors of the IATTC, J. Joseph and R. Allen, and the Chief Scientist of the Tuna-Billfish program, R. Deriso, for their support of this study.

Literature cited

- Ambrose, D. A.
1996. Scombridae: mackerels and tunas. *In* Guide to the early stages of fishes in the California Current region (H. G. Moser, ed.), p. 1270-1285. Calif. Coop. Ocean. Fish. Inves., CALCOFI Atlas No. 33.
- Bailey, K. M., and E. D. Houde.
1989. Predation on eggs and larvae of marine fishes and the recruitment problem. *Adv. Mar. Biol.* 25:1-83.
- Blaxter, J. H. S.
1969. Development: eggs and larvae. *In* Fish physiology (S. Hoar, and D. J. Randall, eds.), p. 177-252. Academic Press Inc., New York, NY.
- Boehlert, G. W., and B. C. Mundy.
1994. Vertical and onshore-offshore distributional patterns of tuna larvae in relation to physical habitat features. *Mar. Ecol. Prog. Ser.* 107:1-13.
- Bye, V. J.
1984. The role of environmental factors in the timing of reproductive cycles. *In* Fish reproduction: strategies and tactics (G. W. Potts, and R. J. Wootton, eds.), p. 187-205. Academic Press Inc., London, UK.
- Chambers, R. C.
1997. Environmental influences on egg and propagule sizes in marine fishes. *In* Early life history and recruitment in fish populations (R. C. Chambers, and E. A. Trippel, eds.), p. 63-102. Chapman and Hall, London, UK.
- Chambers, R. C., and W. C. Leggett.
1996. Maternal influences on variation in egg sizes in temperate marine fishes. *Am. Zool.* 36:180-196.
- Chow, S., V. P. Scholey, A. Nakazawa, D. Margulies, J. B. Wexler, R. J. Olson, and K. Hazama.
2001. Direct evidence for Mendelian inheritance of the variations in the ribosomal protein gene introns in yellowfin tuna (*Thunnus albacares*). *Mar. Biotechnol.* 3: 22-26.
- Collette, B. B., and C. E. Nauen.
1983. FAO species catalogue, vol. 2. Scombrids of the

- world: An annotated and illustrated catalogue of tunas, mackerels, bonitos and related species known to date. FAO Fish. Synop. 125, vol. 2, 137 p.
- Davis, T. L. O., V. Lyne, and G. P. Jenkins.
1991. Advection, dispersion and mortality of a patch of southern bluefin tuna larvae *Thunnus maccoyii* in the East Indian Ocean. Mar. Ecol. Prog. Ser. 73:33-45
- Farley, J. H., and T. L. O. Davis.
1998. Reproductive dynamics of southern bluefin tuna, *Thunnus maccoyii*. Fish. Bull. 96:223-236.
- Fritzsche, R. A.
1978. Development of fishes of the Mid-Atlantic Bight: An atlas of egg, larval, and juvenile stages, V, Chaetodontidae through Ophidiidae. U.S. Dep. Interior, Fish Wildl. Serv., Biol. Serv. Prog. FWS/OBS-78/12, 340 p.
- Goetz, F. W.
1983. Hormonal control of oocyte final maturation and ovulation in fishes. In Fish physiology, vol. 9B, Reproduction: behavior and fertility control (W. S. Hoar, D. J. Randall, and E. M. Donaldson, eds.), p. 117-170. Academic Press, Inc., New York, NY.
- Goldberg, S. R., and D. W. K. Au.
1986. The spawning of skipjack tuna from southeastern Brazil as determined from histological examination of ovaries. In Proceedings of the ICCAT conference on the International Skipjack Year Program (P. E. K. Symons, P. M. Miyake, and G. T. Sakagawa, eds.), p. 277-284. International Commission for the Conservation of Atlantic Tunas, Madrid, Spain.
- Hempel, G., and J. H. S. Blaxter.
1967. Egg weight in Atlantic herring (*Clupea harengus* L.). J. Cons., Cons. Int. Explor. Mer 31:170-195.
- Hunter, J. R., B. J. Macewicz, and J. R. Sibert.
1986. The spawning frequency of skipjack tuna, *Katsuwonus pelamis*, from the South Pacific. Fish. Bull. 84:895-903.
- Johannes, R. E.
1978. Reproductive strategies of coastal marine fishes in the tropics. Environ. Biol. Fish. 3:65-84.
- Joseph, J.
1963. The fecundity of yellowfin tuna (*Thunnus albacares*) and skipjack (*Katsuwonus pelamis*) from the eastern Pacific Ocean. Inter-Am. Trop. Tuna Comm., Bull. 7:255-292.
- Kaji, T., M. Tanaka, M. Oka, H. Takeuchi, S. Ohsumi, K. Teruya, and J. Hirokawa.
1999. Growth and morphological development of laboratory-reared yellowfin tuna *Thunnus albacares* larvae and early juveniles, with special emphasis on the digestive system. Fish. Sci. 65:700-707.
- Kaji, T., M. Tanaka, Y. Takahashi, M. Oka, and N. Ishibashi.
1996. Preliminary observations on development of Pacific bluefin tuna *Thunnus thynnus* (Scombridae) larvae reared in the laboratory, with special reference to the digestive system. Mar. Freshw. Res. 47:261-269.
- Lam, T. J.
1983. Environmental influences on gonadal activity in fish. In Fish physiology, vol. 9B, Reproduction: behavior and fertility control (W. S. Hoar, D. J. Randall, and E. M. Donaldson, eds.), p. 65-116. Academic Press, Inc., New York, NY.
- Lauth, R. R., and R. J. Olson.
1996. Distribution and abundance of larval Scombridae in relation to the physical environment in the north-western Panama Bight. Inter-Am. Trop. Tuna Comm., Bull. 21:127-167.
- Leis, J. M., T. Trnski, M. Harmelin-Vivien, J.-P. Renon, V. Dufour, M. K. El Moudni, and R. Galzin.
1991. High concentrations of tuna larvae (Pisces: Scombridae) in near-reef waters of French Polynesia (Society and Tuamotu Islands). Bull. Mar. Sci. 48:150-158.
- Liley, N. R., K. H. Olsen, and C. J. Foote.
1991. Reproductive pheromones in rainbow trout, *Oncorhynchus mykiss*, and kokanee salmon, *O. nerka*. In Proceedings of the fourth international symposium on the reproductive physiology of fish (A. P. Scott, J. P. Sumpter, D. E. Kime, and M. S. Rolfe, eds.), p. 188-193. FishSymp 91, Dept. Animal Plant Sci., The University of Sheffield, Sheffield, UK.
- Margulies, D.
1993. Assessment of the nutritional condition of larval and early juvenile tuna and Spanish mackerel (Pisces: Scombridae) in the Panama Bight. Mar. Biol. 115: 317-330.
- Margulies, D., J. B. Wexler, K. T. Bentler, J. M. Suter, S. Masuma, N. Tezuka, K. Teruya, M. Oka, M. Kanematsu, and H. Nikaido.
2001. Food selection of yellowfin tuna, *Thunnus albacares*, larvae reared in the laboratory. Inter-Am. Trop. Tuna Comm., Bull. 22: 9-51.
- Marteinsdottir, G., and K. W. Able.
1988. Influence of egg size on embryos and larvae of *Fundulus heteroclitus* (L.). J. Fish. Biol. 41:883-896.
- Mayo, C. A.
1973. Rearing, growth, and development of the eggs and larvae of seven scombrid fishes from the Straits of Florida. Ph.D. diss., 127 p. Univ. Miami, Miami, FL.
- McPherson, G. R.
1991. Reproductive biology of yellowfin tuna in the eastern Australian fishing zone, with special reference to the north-western Coral Sea. Aust. J. Mar. Freshw. Res. 42: 465-477.
- Miyashita, S., O. Murata, Y. Sawada, T. Okada, Y. Kubo, Y. Ishitani, M. Seoka, and H. Kumai.
2000a. Maturation and spawning of cultured bluefin tuna, *Thunnus thynnus*. Suisanzoshoku 48:475-488.
- Miyashita, S., Y. Sawada, T. Okada, O. Murata, and H. Kumai.
2001. Morphological development and growth of laboratory-reared larval and juvenile *Thunnus thynnus* (Pisces: Scombridae). Fish. Bull. 99:601-616.
- Miyashita, S., Y. Tanaka, Y. Sawada, O. Murata, N. Hattori, K. Takii, Y. Mukai, and H. Kumai.
2000b. Embryonic development and effects of water temperature on hatching of the bluefin tuna, *Thunnus thynnus*. Suisanzoshoku 48:199-207.
- Nikaido, H., N. Miyabe, and S. Ueyanagi.
1991. Spawning time and frequency of bigeye tuna, *Thunnus obesus*. Nat. Res. Inst. Far Seas Fish., Bull. 28:47-73.
- Nishikawa, Y., M. Honma, S. Ueyanagi, and S. Kikawa.
1985. Average distribution of larvae of oceanic species of scombroid fishes, 1956-1981. Far Seas Fish. Res. Lab., S. Ser. 12, 99 p.
- Nishikawa, Y., and D. W. Rimmer.
1987. Identification of larval tunas, billfishes and other scombroid fishes (suborder Scombroidei): an illustrated guide, 20 p. CSIRO Mar. Lab. Rep. 186.
- Niwa, Y., A. Nakazawa, D. Margulies, V. P. Scholey, J. B. Wexler, and S. Chow.
2003. Genetic monitoring for spawning ecology of captive yellowfin tuna (*Thunnus albacares*) using mitochondrial DNA variation. Aquaculture 218:387-395.

- Ramon, D., and K. Bailey.
1996. Spawning seasonality of albacore, *Thunnus alalunga*, in the south Pacific Ocean. *Fish. Bull.* 94: 725-733.
- Richards, W. J.
2006. Scombridae: mackerels and tunas. In *Early stages of Atlantic fishes*, vol. 2, An identification guide for the western central north Atlantic (W. J. Richards, ed.), p. 2187-2227. CRC Press, Taylor and Francis Group, Boca Raton, FL.
- Richards, W. J., and D. C. Simmons.
1971. Distribution of tuna larvae (Pisces, Scombridae) in the northwestern Gulf of Guinea and off Sierra Leone. *Fish. Bull.* 69:555-568.
- Schaefer, K. M.
1996. Spawning time, frequency, and batch fecundity of yellowfin tuna, *Thunnus albacares*, near Clipperton Atoll in the eastern Pacific Ocean. *Fish. Bull.* 94:98-112.
1998. Reproductive biology of yellowfin tuna (*Thunnus albacares*) in the eastern Pacific Ocean. *Inter-Am. Trop. Tuna Comm., Bull.* 21:201-272.
2001a. Reproductive biology of tunas. In *Fish physiology*, vol. 19, Tuna: physiology, ecology, and evolution (B. A. Block, and E.D. Stevens, eds.), p. 225-270. Academic Press, San Diego, CA.
2001b. Assessment of skipjack tuna (*Katsuwonus pelamis*) spawning activity in the eastern Pacific Ocean. *Fish. Bull.* 99:343-350.
- Scholey, V. P., D. Margulies, R. Olson, J. Wexler, J. Suter, and S. Hunt.
2001. Lab culture and reproduction of yellowfin tuna in Panama. *Global Aqua. Advoc.* 4(2):17-18.
- Stacey, N. E.
1984. Control of the timing of ovulation by exogenous and endogenous factors. In *Fish reproduction: strategies and tactics* (G. W. Potts, and R. J. Wootton, eds.), p. 207-222. Academic Press Inc., London, UK.
1991. Hormonal pheromones in fish: status and prospects. In *Proceedings of the fourth international symposium on the reproductive physiology of fish* (A. P. Scott, J. P. Sumpter, D. E. Kime, and M. S. Rolfe, eds.), p. 177-181. *FishSymp 91*, Dept. Animal Plant Sci., The University of Sheffield, Sheffield, UK.
- Suzuki, Z.
1994. A review of the biology and fisheries for yellowfin tuna, *Thunnus albacares*, in the western and central Pacific Ocean. *FAO Fish. Tech. Pap.* 336 (2):108-137.
- Tanaka, M., T. Kaji, Y. Nakamura, and Y. Takahashi.
1996. Developmental strategy of scombrid larvae: high growth potential related to food habits and precocious digestive system development. In *Survival strategies in early life stages of marine resources* (Y. Watanabe, Y. Yamashita, and Y. Oozeki, eds.), p. 125-139. A. A. Balkema, Rotterdam, The Netherlands.
- Van der Kraak, G., J. P. Chang, and D. M. Janz.
1998. Reproduction. In *The Physiology of fishes* (D. H. Evans, ed.), p. 465-488. CRC Press LLC, Boca Raton, FL.
- Vetter, R. D., A. Kurtzman, and T. Mori.
1999. Diel cycles of DNA damage and repair in eggs and larvae of northern anchovy, *Engraulis mordax*, exposed to solar ultraviolet radiation. *Photochem. Photobiol.* 69:27-33.
- Wexler, J. B., S. Chow, T. Wakabayashi, K. Nohara, and D. Margulies.
2007. Temporal variation of *in situ* growth of yellowfin tuna (*Thunnus albacares*) larvae in the Panama Bight, 1990-97. *Fish. Bull.* 105:1-18.
- Wexler, J. B., D. Margulies, S. Masuma, N. Tezuka, K. Teruya, M. Oka, M. Kanematsu, and H. Nikaido.
2001. Age validation and growth of yellowfin tuna, *Thunnus albacares*, larvae reared in the laboratory. *Inter-Am. Trop. Tuna Comm., Bull.* 22:52-91.
- Wexler, J. B., V. P. Scholey, R. J. Olson, D. Margulies, A. Nakazawa, and J. M. Suter.
2003. Tank culture of yellowfin tuna, *Thunnus albacares*: developing a spawning population for research purposes. *Aquaculture* 220:327-353.
- Wild, A.
1986. Growth of yellowfin tuna, *Thunnus albacares*, in the eastern Pacific Ocean based on otolith increments. *Inter-Am. Trop. Tuna Comm., Bull.* 18: 423-482.
1994. A review of the biology and fisheries for yellowfin tuna, *Thunnus albacares*, in the eastern Pacific Ocean. *FAO Fish. Tech. Pap.* 336 (2):52-107.
- Wootton, R. J.
1979. Energy costs of egg production and environmental determinants of fecundity in teleost fishes. *Symp. Zool. Soc. Lond.* 44:133-159.
- Zar, H. H.
1984. *Biostatistical analysis*, 2nd ed., 718 p. Prentice-Hall, Inc., Englewood Cliffs, NJ.

Abstract—Nearshore fisheries in the tropical Pacific play an important role, both culturally and as a reliable source of food security, but often remain under-reported in statistics, leading to undervaluation of their importance to communities. We re-estimated nonpelagic catches for Guam and the Commonwealth of the Northern Mariana Islands (CNMI), and summarize previous work for American Samoa for 1950–2002. For all islands combined, catches declined by 77%, contrasting with increasing trends indicated by reported data. For individual island entities, re-estimation suggested declines of 86%, 54%, and 79% for Guam, CNMI, and American Samoa, respectively. Except for Guam, reported data primarily represented commercial catches, and hence under-represented contributions by subsistence and recreational fisheries. Guam's consistent use of creel surveys for data collection resulted in the most reliable reported catches for any of the islands considered. Our re-estimation makes the scale of under-reporting of total catches evident, and provides valuable baselines of likely historic patterns in fisheries catches.

Re-estimation of small-scale fishery catches for U.S. flag-associated island areas in the western Pacific: the last 50 years

Dirk Zeller (contact author)¹

Shawn Booth¹

Gerald Davis²

Daniel Pauly¹

Email address (for D. Zeller): d.zeller@fisheries.ubc.ca

¹ Fisheries Centre
2202 Main Mall
University of British Columbia
Vancouver, V6T 1Z4, Canada

² National Oceanic and Atmospheric Administration
National Marine Fisheries Service
1601 Kapiolani Blvd.
Honolulu, Hawaii 96814-4700

Small-scale nearshore fisheries in the tropical Pacific are of fundamental importance for subsistence, social and cultural purposes, in addition to providing food, trade, and recreational resources (e.g., Dalzell et al., 1996). These fisheries commonly play a vital role in providing a secure supply of protein on many Pacific Islands. Yet, catches for the small-scale fisheries in these islands are typically not estimated by the fisheries agencies. This lack of data on estimated catch applies especially to the non-commercial sectors (e.g., subsistence and recreational) and is generally justified by real or perceived difficulties and costs associated with quantification of these very spatially dispersed fisheries. Hence, extractions of these marine resources are usually underestimated in official statistics, as are their economic and social importance (Zeller et al., 2006b).

An approach to retroactively estimate catches in cases where reliable time series data are lacking applies a “re-estimation” approach to approximate historic catch time series (Zeller et al., 2006a). Such an approach typically requires subjective inferences and interpolations. This approach is justified, despite data uncertainties,

given the less acceptable alternative outcome, namely that subsequent users of the available data will interpret nonreported or missing data as zero catches.

Without accounting for total catches from all sectors, it is not possible to obtain any comprehensive measure of the formal and informal economic value of these resources, or of the risks excessive fishing may represent to an island entity. The lack of these two measures is of concern, given that human population growth rates in many Pacific island countries are high and natural resources in these islands are limited. Furthermore, the growing shift from predominantly subsistence to market-based cash-oriented economies, as well as increasing development since World War II, has contributed to declines in coastal marine resources. Although localized overfishing may be responsible for some of these observed declines, anthropogenic factors such as coastal development, pollution, and poor watershed management have likely also contributed to the degradation and reduction of coastal habitat and in the productivity of the resource (Friedlander and DeMartini, 2002).

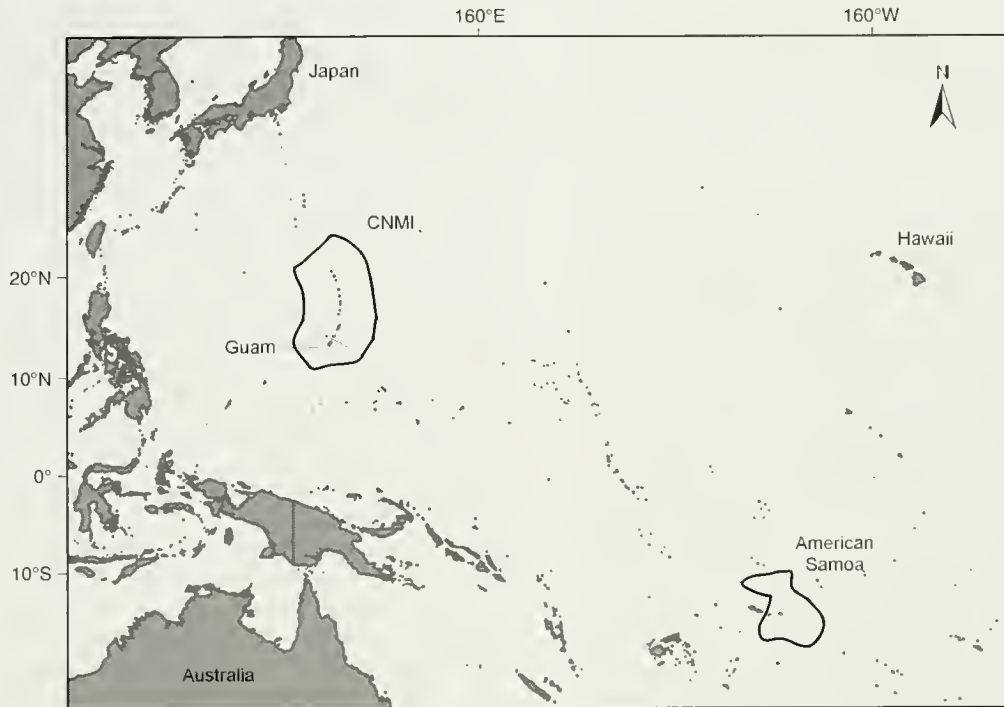


Figure 1

Location and Exclusive Economic Zones (areas outlined) of the major U.S. flag-associated island areas in the western Pacific covered in this study: Guam, Commonwealth of the Northern Mariana Islands (CNMI), and American Samoa. The Pacific Remote Island Areas (minor islands) also under U.S. flag jurisdiction are excluded from present consideration (Zeller et al.³). Map courtesy of A. Kitchingman and C. H. Close, *Sea Around Us* Project, Fisheries Centre, University of British Columbia.

This is particularly true close to human population centers on main islands, whereas the status of stocks in more remote areas is generally better. Obviously, places that have not experienced widespread development may still suffer stock declines because over-fishing alone can deplete fishery resources on coral reefs.

The U.S. National Oceanic and Atmospheric Administration National Marine Fisheries Service (NOAA-NMFS), through its Western Pacific Fishery Information Network (WPacFIN¹), provides data collection, assimilation, and technical reporting support to U.S. flag-associated island areas in the Pacific (Fig. 1). The coverage of this electronic information source only dates back to the early 1980s and differs between islands. There is near-complete coverage for some areas, such as Guam, and very limited coverage for others, such as Commonwealth of the Northern Mariana Islands (CNMI). For the U.S. western Pacific region, this centralized data depository is largely the result of the development of WPacFIN programs in each of

the island areas in the early 1980s. All the islands considered here have few legislative requirements for reporting of catches; however, some, such as American Samoa, have instituted legal mandates that require the number of fish sold be reported. Generally, the focus of reported data has been primarily on commercial harvests (e.g., the small-boat based fisheries of American Samoa) and have not covered other sectors, such as the shore-based fisheries (Zeller et al., 2006a).

However, many small-scale studies have been undertaken to assess these missing sectors, reporting local catches or catch rates for specific periods, locations, or gear types (e.g., Craig et al., 1997). Such data sources can form the foundation for deriving catches, catch rates per unit of area, or per capita catch rates during a given time interval for these sectors of the fishery. These time-point estimates provide anchor points of concrete data upon which total catch estimates can be based. Once all such data have been extracted from their disparate sources, interpolations can be employed to fill in the periods for which quantitative data are missing. Thus, the key aspect of the approach used here is psychological, and managers have to overcome the notion that no information is available, which is not only an incorrect assumption when dealing with fisheries but a profoundly misleading one

¹ Western Pacific Fishery Information Network (WPacFIN). NOAA-National Marine Fisheries Service, Pacific Islands Fisheries Science Center, 2570 Dole Street, Honolulu, 96822-2396. Website: <http://www.pifsc.noaa.gov/wpacfin> (accessed 1 November 2005).

(Pauly²). Here, we report on work undertaken for the U.S. Western Pacific Regional Fishery Management Council to account for unreported catches (Zeller et al.³).

Island areas

Guam Guam (13°28'N, 144°45'E) is the southernmost island in the Mariana Archipelago (Fig. 1), and has a potential coral reef ecosystem habitat area to 100 fathom (183 m) depth, within an Exclusive Economic Zone (EEZ), of approximately 276 km² (including offshore banks). Of this area, 202.8 km² are associated with the island of Guam directly (Rohmann et al., 2005). Guam's coral reef fisheries are both economically and culturally important and have been historically significant in the diet of the human population (Hensley and Sherwood, 1993). Limitations were placed on the indigenous population with regards to any large-scale fisheries development during the Japanese occupation period (Smith⁴). These limitations, together with the destruction of the Japanese fishing infrastructure at the end of WWII, resulted in a heavy reliance on subsistence fisheries in Guam into the late 1940s. The near-shore coral reefs around Guam are considered heavily fished and degraded, and concerns about overfishing were raised as early as 1970 (Hensley and Sherwood, 1993). Most of the less accessible offshore banks, however, appear to be in better condition.

Guam's domestic fisheries can be divided into two sectors (ignoring tuna transshipment and distant water fleet catches of large pelagics): small boat-based fisheries (Myers, 1993) and shore-based fisheries (Hensley and Sherwood, 1993). Because there are few full-time commercial fishermen, there is little distinction between commercial, subsistence, and recreational fishing, and many fishing trips contribute to all three segments. In the past, tidal fish-weirs were used in Guam, although their numbers declined over the decades, and the use of weirs ceased in 1989.

Catch data for both fisheries sectors have been estimated by the Guam Division of Aquatic and Wildlife Resources (DAWR) since the mid-1960s through the use of two separate creel surveys: a marina-based boat-centered creel survey (offshore survey), and a shore-based creel survey (inshore survey). The reporting of fish weir catches was mandated as part of weir-operating permits but the data were likely incomplete. Various expansion

methods have been applied in the past to raise the creel survey data to island-wide catch estimates, but these have been standardized since the mid-1980s in collaboration with WPacFIN. However, specifics of the method and thoroughness of a survey, of data handling, and of analyses have varied during the earlier periods. Since the early 1980s, these survey data have been reported through WPacFIN, and are the most comprehensive series of catch estimates used in the present study.

Commonwealth of the Northern Mariana Islands (CNMI)

The Commonwealth of the Northern Mariana Islands (CNMI, Fig. 1) consists of a 680 km chain of 14 volcanic islands, extending northward from Rota (14°9'N, 145°12'E) to Farallon De Pajaros (20°32'N, 144°54'E). Over 99% of the human population (69,000 in 2000) is concentrated on the three southern main islands of Saipan, Tinian, and Rota. The population has increased rapidly since the 1980s, driven by fewer restrictions on immigration and by the prosperity from the main industries—tourism and garment manufacturing.

CNMI are a group of islands with fringing reefs (surrounding most islands) and offshore coral reef banks and ridges. The conditions of local reefs vary; heavy fishing pressure is considered a problem for the sustainability of the reefs on the main islands, particularly the island of Saipan, because of its large population and more extensive coastal development.

Following WWII and the expulsion of the active Japanese fisheries, subsistence fisheries again dominated the catch. Because of the loss of most Japanese fishing vessels, and decades of Japanese restrictions on indigenous fishing outside local reefs, early subsistence catches were focused on near-shore and lagoon-based resources. Subsistence fishing for near-shore resources was an important daily activity for the local population well into the 1970s, whereas commercial and recreational fleet developments did not start until the 1960s, and westernized economic development did not accelerate until the 1970s and 1980s. The local economic boom starting in the late 1980s, driven by tourism and garment manufacturing, did not result in significant growth of the commercial fisheries sector. Thus, the local fishing industry supplied only a small part of the total seafood demand in the 1990s, and imports accounted for a growing part of the supply. Growth in recreational fisheries came instead with increased westernization of the economy which, combined with increased availability of boats, blurred the boundaries between subsistence and recreational fishing. Thus, each fishing trip today may have commercial and subsistence, as well as recreational aspects.

The Division of Fish and Wildlife (DFW) for CNMI conducted a data collection system for commercial catches since the mid-1970s but reported data have only been available since the early 1980s through WPacFIN. The estimated commercial landings in Saipan are based on a voluntary dealer purchase receipt collection system and are adjusted by WPacFIN for the remainder of CNMI. The noncommercial sector (subsistence and

² Pauly, D. 1998. Rationale for reconstructing catch time series. EC Fisheries Cooperation Bulletin 11:4–10.

³ Zeller, D., S. Booth, and D. Pauly. 2005. Reconstruction of coral reef- and bottom-fisheries catches for U.S. flag island areas in the Western Pacific, 1950 to 2002. Western Pacific Regional Fishery Management Council, 1164 Bishop St., Suite 1400, Honolulu, HI 96813. Website: <http://www.wpacouncil.org/bottomfish.htm> (accessed 17 October 2006).

⁴ Smith, R. O. 1947. Survey of the fisheries of the former Japanese mandated islands. Fishery Leaflet 273, U.S. Fish and Wildlife Service, Department of the Interior, 1849 C Street, NW, Washington, DC 20240, 105 p.

recreational fishing) has been subject to limited monitoring since 1984 and day-time creel surveys have been undertaken for the Saipan lagoon only. However, these data have not been analyzed or expanded for estimation of CNMI-wide noncommercial catches and were not available to us.

American Samoa American Samoa is the only U.S. territory south of the equator (14°20'S, 170°W, Fig. 1), and its small-scale fisheries consist of shore-based and boat-based sectors (Zeller et al., 2006a). A clear separation between commercial and noncommercial aspects in each fishery is difficult because fish from either sector can be sold or retained for personal consumption (Craig et al., 1993). The existing catch data on the predominantly commercial boat-based sector by the American Samoa Department of Marine and Wildlife Resources (DMWR) has been reported through WPacFIN since the early 1980s. The noncommercial sector, especially as relating to shore-based fisheries, is not monitored and catches are not reported on a regular basis. However, a short-lived DMWR survey of shore-based fisheries, as well as other local studies, was conducted sporadically on this sector between 1980 and 2002. Recently, total nonpelagic fisheries catches for both sectors were re-estimated back to 1950 by Zeller et al. (2006a), and these findings will be relied upon in the present study.

Aims

The purpose of our study was to assemble available information and data on catches of the small-scale, near-shore fisheries for nonpelagic species of the major U.S. flag-associated island areas in the western Pacific for 1950–2002, namely Guam, the Commonwealth of the Northern Mariana Islands (CNMI), and, in summary form, for the previously estimated catches for American Samoa (Zeller et al., 2006a). Although American Samoa's catches were published separately (Zeller et al., 2006a), they are summarized in the present study for completeness. The U.S. State of Hawaii was excluded from present considerations because the economic, social and noncommercial fishery conditions and data differed substantially from those of the other islands, and required a different method for reconstructing the data. Also excluded was the information available for the limited (predominantly recreational) catches taken on the Pacific Remote Island Areas (PRIAs or minor islands) reported on elsewhere (Zeller et al.³). The aim was to derive estimates of likely total removal of marine resources for the 1950–2002 period. The present re-estimation excludes pelagic species (i.e., tunas and billfishes) that are the target of large-scale fisheries, even if these species are also caught by small-scale, local sectors. Small-scale fisheries in our study targeted both deeper water species (such as lutjanids, lethrinids, and serranids), as well as coastal, reef-associated small pelagic species (such as carangids, including the culturally important big-eye scad [*Selar crumenophthalmus*]).

Materials and methods

The catch re-estimation approach utilized here consists of six general steps based on work done for the Western Pacific Regional Fishery Management Council (Zeller et al.³) and Zeller et al. (2006a):

- 1 Identification of existing reported catch times series, e.g., local reports, and data presented by the Western Pacific Fishery Information Network (WPacFIN¹) on behalf of local agencies;
- 2 Identification of sectors, time periods, species, gears, etc. not covered by (1), i.e., missing catch data, via literature searches and consultations;
- 3 Search for available alternative information sources to supply the missing catch data in (2), through extensive literature searches and consultations with local experts;
- 4 Development of data anchor points in time for missing data items, and their expansion to island- or country-wide catch estimates;
- 5 Interpolation for time periods between data anchor points for total catch, generally with per capita catch rates; and
- 6 Estimation of final total catch times series estimates for total catch, combining reported catches (1) and interpolated, island-expanded missing data series (5).

Island areas differed in terms of fisheries sectors, their coverage of reported data, and available alternative information. Details of available alternative information sources for each island area, all reference material for data sources used (non-refereed publications), and the specifics of data anchor point estimation can be found in a report to the U.S. Western Pacific Regional Fishery Management Council (Zeller et al.³).

Guam

Catches for both boat- and shore-based fisheries sectors have been estimated by DAWR since the mid-1960s through the use of two creel surveys (offshore survey and inshore survey). In the more recent years, DAWR applied expansion methods to extrapolate island-wide catch estimates from creel survey data. The fish weir catch estimates were likely incomplete.

Because domestic fisheries in Guam are generally part commercial, part subsistence, and part recreational, the re-estimation approach taken was not by differentiation of the commercial and noncommercial sectors, but rather by following the creel-survey distinction between boat-based (offshore survey) and shore-based (inshore survey) estimations of catches (Table 1). Given our focus on nonpelagic fisheries, we excluded the trolling section for large pelagic species from the offshore catch reports and retained bottom-fishing and boat-based spear-fishing catches. Comparisons of supply and demand, with the use of reported catch (including pelagic taxa), as well as estimates of imported

seafood and domestic seafood consumption rates, were undertaken to estimate potentially unreported catches, as well as to estimate total likely catch for the 1950–64 period for which no other reported information was available (see “Supply versus demand” heading below, Table 2).

Offshore boat-based catches

1965–82: The offshore catch estimates for this time period, which pre-dates WPacFIN reporting, were drawn from the creel survey data as reported in DAWR annual

reports. Procedures for expanding survey data to island-wide catches, as listed or applied by the various data sources, were generally accepted. For example, reports from earlier years indicated under-reporting due to sampling design limitations of the creel surveys by a minimum factor of two, and we adjusted the reported catch estimates correspondingly for these years (Zeller et al.³).

1983–2002: We relied on the island-wide expanded catch estimates as provided by WPacFIN, based on offshore creel surveys undertaken by DAWR. These data

Table 1

Data sources, available time series data, and data anchor points for catch re-estimation for Guam. DAWR: Division of Aquatic and Wildlife Resources; WPacFIN: Western Pacific Fishery Information Network. X=yes.

Sector	Year(s)	Source	Official data (reported)	Missing data (unreported)	Catch (t)
Offshore, boat-based	1965–82	Guam DAWR offshore creel survey reports	X		1–36
Offshore, boat-based	1983–2002	WPacFIN, DAWR	X		43–65
Inshore, shore-based	1965–81	Guam DAWR inshore creel survey reports	X		145–102
Inshore, shore-based	1982–84	Hensley and Sherwood (1993)		X	92–141
Inshore, shore-based	1985–2002	WPacFIN, DAWR	X		179–63
Offshore and inshore	1950	Reported consumption rate ¹		X	957

¹ Adjusted for imports and consumption of pelagic species.

Table 2

Data sources and data anchor points for import and consumption estimation, forming part of the supply (reported catch and estimated imports) and demand (consumption estimates) approach used for catch re-estimation for Guam.

Supply or demand	Item	Year(s)	Source	Comments	Annual per capita rate (kg)	Guam total (kg)
Supply	Import	1950	Assumption	Half of adjusted 1980 rate ¹	10.6	636,850
Supply	Import	1980	Import rate	17.7 kg/person/year, adjusted for cooler-shipped fish by 20%	21.2	2,250,204
Supply	Import	1999	Dept. of Commerce		19.5	2,962,380
Supply	Import	2000	Dept. of Commerce		20.5	3,180,014
Supply	Import	2002	Dept. of Commerce		20.9	3,359,137
Demand	Consumption	1950	Assumption	Same as 1980, adjusted for pelagics	26.6	1,593,940
Demand	Consumption	1980	Consumption rate	Adjusted for pelagics	26.1	2,766,977
Demand	Consumption	1985–2002	Assumption	Consumption = imports + reported catches	22.6–21.7	2,595,204–3,488,267

¹ This accounts for the lower air-and boat-based travel between islands in 1950 compared to 1980.

were reported by taxon, and thus allowed us to exclude large pelagic species.

Inshore, shore-based catches

1965–81: The inshore catch data for this period were based on the inshore creel survey data as reported in the DAWR annual reports, including the often separately reported estimates for octopus and shellfish (based on reef-gleaning), fish weirs, and the highly irregular, seasonal catches of juvenile rabbitfishes (*Siganidae*) and big-eye scad. Procedures for expanding the catches were accepted as reported at the time. We applied or accepted adjustment factors for nonsurveyed periods as provided or used by the fishery data sources (Zeller et al.³). The years 1980 and 1981 were deemed poorly reported because of limited survey coverage. Therefore, we replaced the reported catches for 1980 and 1981 with the average catches for 1978–79 and 1982–83, respectively.

1982–84: Data from Hensley and Sherwood (1993) were used for the 1982–84 period because WPacFIN has reported inshore catches only since 1985. It should be noted that these data did not include those from night fisheries and therefore under-represented actual catches.

1985–2002: We used the island-wide expanded catch estimates from the inshore creel survey, as undertaken by DAWR, and provided by WPacFIN.

Supply (imports and catches) versus demand (consumption) To assess whether the reported catches as outlined above accounted for the likely total catches and to derive estimates of likely catches for the undocumented 1950–64 period, we compared estimates of total supply (reported catches plus estimated imported catches) with demand as approximated by consumption estimates. For the purpose of supply and demand estimation, we included catches of pelagic species as provided by WPacFIN and DAWR, with a fixed amount of 39 t/year carried back from 1959 to 1950, based on DAWR's estimated annual pelagic catch for 1960–62.

Imports Information on reported imports was available for 1999 and 2002 (Guam Department of Commerce⁵), which were converted to per capita rates (1999: 19.5 kg/person; 2002: 20.9 kg/person) using human population statistics (U.S. Census Bureau⁶), and for 1980 as an estimated annual per capita import rate of 17.7 kg (Table 2). There is a long-standing tradition of bringing fish into Guam as part of personal travel. A large, but unknown portion of these imports are so-called cooler-shipped fish and are primarily from the Federated States of Micronesia, Palau, and the Republic of the Marshall Islands. These imports have been poorly recorded, especially

in the earlier periods. To account for under-reporting of cooler-shipped imports in earlier years, we adjusted the 1980 annual per capita import rate by 20%, to 21.2 kg. For 1950, we assumed a level of import of half of the adjusted 1980 import rate (i.e., 10.6 kg; Table 2), to account for the much lower air- and boat-based travel between the various islands in 1950 compared to 1980. We linearly interpolated import rates between the 1950, 1980, 1999, and 2002 import data anchor point estimates and expanded these to total import estimates using human population statistics.

Another factor that may have influenced rates of import and harvest is aquaculture. There is potentially a considerable (but unknown) volume of locally farmed tilapia, catfish, and milkfish that is sold without regulation through small-scale markets and road-side vendors, and these products are not reported or recorded. Currently, it is not possible to estimate the impact of aquaculture on the present estimation of catches.

Demand Estimates of demand were based on the reported annual per capita consumption rate of 27 kg of seafood for 1980 (Zeller et al.³)—a rate that was carried back unaltered to 1950. We thus assumed the same relative consumption patterns for 1950 as for 1980, which may underestimate the seafood consumption patterns for 1950, and thus is adding a conservative component to our estimation. We accounted for the consumption of pelagic species by removing the reported catches of pelagic species for each year from total consumption for that year, and subsequently derived estimated nonpelagic per capita consumption rates with population statistics (Table 2).

For 1985–2002, we assumed that total consumption was accounted for by the sum of reported catches plus estimated imported catches. Total consumption was adjusted by removing the reported pelagic catches, and the 1985–2002 per capita nonpelagic consumption rates were derived with human population statistics (Table 2).

For the 1981–84 period, we interpolated per capita nonpelagic consumption rates between the 1980 and 1985 data anchor points. The growing concern about market dumping of incidental bycatch from the pelagic transshipment fleet onto the local seafood market was not considered in the present study because it is thought to be a relatively recent phenomenon. It would be reflected in declining commercial reported catch data because it replaces local fish in the commercial market supply.

Supply versus demand To derive estimates of catches for the 1950–64 period, we assumed that domestic seafood supply was either locally caught, relying heavily on subsistence fishing, or was part of the cooler-shipped imports. Given the assumed imports, the likely total local catches were derived as the difference between import estimates and consumption estimates (Table 2). Thus, in 1950, an assumed per capita import of 10.6 kg of seafood and an estimated per capita consump-

⁵ Guam Department of Commerce. 2005. Website: <http://www.admin.gov.gu/commerce> (accessed 15 January 2005).

⁶ U.S. Census Bureau. 2005. Website: <http://www.census.gov/cgi-bin/ipc/idbsprd> (accessed 15 January 2005).

Table 3

Data sources, available time series data, and data anchor points for catch re-estimation for the Commonwealth of the Northern Mariana Islands. WPacFIN=Western Pacific Fishery Information Network; DFW=Division of Fish and Wildlife.

Sector	Year(s)	Source	Official data (reported)	Missing data (unreported)	Catch (t)
Commercial	1960	No commercial fishing		X	0
Commercial	1983–2002	WPacFIN, DFW	X		76–106
Noncommercial	1950	Per capita consumption		X	456 ¹
Noncommercial	1984	Proportion of total catch		X	166 ²
Noncommercial	1993–2002	Proportion of total catch		X	87–106 ³

¹ Reported per capita seafood consumption of 0.45 kg/day was reduced by 50% to remain a conservative estimate.

² In 1984 noncommercial catches represented about 63% of total catches, corresponding to a noncommercial to commercial ratio of 1.7:1.

³ By the early 1990s, the noncommercial catch accounted for about 50% of total catches. This ratio was carried to 2002.

tion rate of 26.6 kg, implied a per capita catch rate of 16.0 kg for 1950.

For the 1965–84 period, the difference between reported catches and supply/demand estimates was interpreted as unreported catches (e.g., unrecorded night fisheries catches in the early 1980s), and were added to the reported catches (since 1965), resulting in the final re-estimated total catches.

Catch rates We converted re-estimated catches into per capita catch rates using human population statistics and catch per unit area of the depth-defined potential coral reef ecosystem habitat area (*sensu* Rohmann et al., 2005). Given that most nonpelagic catches come from areas relatively close to Guam, we used the potential reef area estimate (to 100 fathom=183 m depth) for reefs associated directly with the island of Guam (202.8 km²), not the reef area estimate for the EEZ (276 km²; Rohmann et al., 2005). The reef area may slightly underestimate the area for bottom-fisheries, particularly for the post-1980 period, when an increasing proportion of commercial bottomfish catches (up to 30%) likely originated from offshore banks.

CNMI

Commercial catches Estimates based on data collected by DFW of commercial landings for recent years (1981–2002) were available through WPacFIN. Given uncertainty surrounding the low catches reported for the first few years of this data series, only the period from 1983 through 2002 was used (Table 3). Because the collected data relate to Saipan only, WPacFIN uses an adjustment factor of 20% to expand to CNMI total catches, which is thought to account for much of the known under-recording of commercial landings. Because there was little local commercial fisheries development in the CNMI until the 1960s, we assumed commercial catches were zero in 1960 (Table 3) and linearly interpolated catches between 1960 and the 1983 value as reported by WPacFIN.

Noncommercial catches Noncommercial catches are not reported in CNMI. Although limited monitoring has existed since 1984 for the Saipan lagoon only, these data have not been analyzed and were not available to us.

1950–83: Subsistence fishing was an important daily activity in the Northern Marianas after WWII, and it was estimated that in the late 1940s the local population traditionally consumed nearly 0.45 kg/person/day, implying an annual per capita seafood consumption of over 165 kg (Smith⁴). Although this rate of consumption may appear a high estimate, other Pacific islands have reported similarly high annual per capita consumption rates as recently as the late 1990s, e.g., Kiribati (183 kg), Palau (124 kg), Federated States of Micronesia (119 kg), or Tuvalu (113 kg) (Gillett⁷). To account for lower fish consumption by the small nonindigenous population, the likely inclusion of pelagic species in the reported consumption rate, and U.S. military food support after WWII, as well as to remain conservative in our estimation, we reduced this rate by over 50% to 72.6 kg/person/year (0.2 kg/person/day) as the assumed per capita consumption rate for 1950 (Table 3). Furthermore, given that virtually no vessels were available for exploitation of offshore resources shortly after WWII, we assumed that noncommercial catches in 1950 were based almost exclusively on near-shore resources. We linearly interpolated the per capita catch rates between this 1950 level and the catch rate estimated for 1984 (see below) and expanded these to a total noncommercial catch estimate with the use of human population census data.

1984–2002: In 1984, noncommercial catches were thought to have accounted for approximately 63% of total catches, which corresponded to a noncommercial-

⁷ Gillett, R. 2002. Pacific Island fisheries: regional and country information. RAP Publication 2002/13, 168 p. Asia-Pacific Fishery Commission, FAO Regional Office for Asia and the Pacific, Maliwan Mansion, Phra Atit Road, Bangkok 10200, Thailand.

Table 4
American Samoa reconstructed catch summary, by decade. Summarized from Zeller et al. (2006a).

Year	Official reported catch (t)	Unreported catch (t)	Total estimated catch (t)
1950	—	752	752
1960	—	635	635
1970	—	596	596
1980	41	368	409
1990	10	312	322
2000	42	152	195
2002	34	121	155

to-commercial catch ratio of 1.7:1 (Table 3). By the early 1990s, approximately 50% of total catches were thought to be not reported because they constituted noncommercial catches. Thus, the noncommercial catch value for the time period 1993–2002 was set equal to the total commercial catches (Table 3). Thus, we assumed higher reliance on noncommercial fishing in the early 1980s compared to the 1990s. We interpolated the proportion of noncommercial catches between 1984 and 1993 and expanded them by using reported commercial catches.

Catch rates Re-estimated catches were converted to per capita catch rates by using human population census data, and to catch per unit area of the depth-defined potential coral reef ecosystem habitat area (*sensu* Rohmann et al., 2005). Total potential coral reef area to a depth of 100 fathoms (183 m) for CNMI is 476 km² (Rohmann et al., 2005). Given that most fishing in CNMI occurs near the three main islands, the coral reef area estimate for these islands (331.2 km²) was used here also (Rohmann et al., 2005).

American Samoa

Total catches for nipelagic species for American Samoa have been re-estimated independently by Zeller et al. (2006a), and are summarized by decade in Table 4. American Samoan catches were included in the present study for completeness in the re-estimation of total time series catches for the U.S. flag-associated Pacific island areas.

Results

The catch re-estimation for nipelagic species for the major U.S. flag-associated island areas in the western Pacific combined (excluding Hawaii) indicated two main points (Fig. 2A):

- 1 a substantial discrepancy between officially reported catch data and potential total catches as re-

estimated here and by Zeller et al. (2006a). For the time period for which reported data existed (1965–2002), such data may have yielded an underestimate of likely total catches by as much as a factor of 4.55. This discrepancy was largest in early years; and

- 2 a potential decline of 77% occurred in total catches, from an estimated 2165 t in 1950 to 496 t in 2002. This decline contrasted with the trend observed from the data reported by individual island entities—namely an increasing trend from 147 t in 1965 to 269 t in 2002.

Individual islands

For Guam, the re-estimation indicated a decline of 86% in catches of nipelagic species over the 50-year time period considered here. There was also a 2.5-fold difference between the re-estimated catches and the reported statistics for the 1965–2002 period, driven by under-reporting of catches in earlier periods. Guam's ongoing commitment to and consistent application of creel surveys to estimate total catches has resulted in what may be the most reliable estimates of total catches for any of the islands considered here, at least since the mid-1980s (Fig. 2B). Based on the re-estimated data, the annual per capita catch rates for Guam's coral reef and bottom-fisheries may have declined from 16.0 kg to 0.8 kg between 1950 and 2002 (Table 5). Catch rates per area of potential coral reef habitat (to 100 fathom=183 m depth) appear to have declined from 4.7 t/km²/year to 0.6 t/km²/year between 1950 and 2002 (Table 5).

For CNMI, the re-estimated catches indicated a decline of about 54% in catches of nipelagic species between 1950 and 2002. Comparing the catches reported by CNMI from WPacFIN with the re-estimated total catches, we found a 2.2-fold under-reporting of potential total catches by the reported data, compared to the re-estimated totals for the 1983–2002 time period of coverage by WPacFIN (Fig. 2C). Taking into account CNMI's rapid human population growth over the last two decades, we surmise that the annual per capita catch rate may have declined from a high of 72.6 kg in

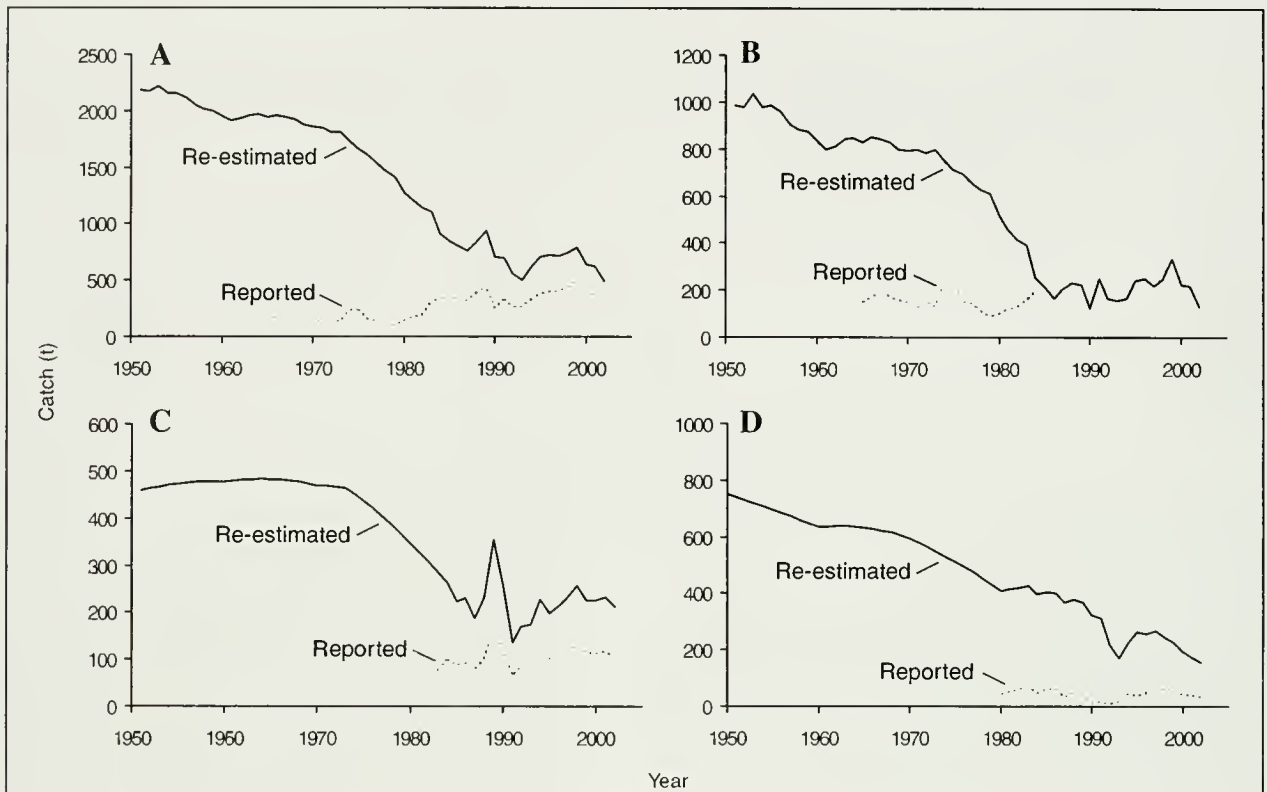


Figure 2

Re-estimated catches of small-scale, coral-reef fisheries for the major U.S. flag-associated island areas in the western Pacific (Guam, Commonwealth of the Northern Mariana Islands [CNMI], and American Samoa), versus the statistics officially reported by these island entities through the Western Pacific Fishery Information Network. Both the under-representation of likely total catches, as well as the likely decline in catches is evident in each case. Total re-estimated catches (A) summed over all the major U.S. flag-associated island areas of the western Pacific considered here; (B) for Guam versus the catches reported by Division of Aquatic and Wildlife Resources; (C) for CNMI versus the statistics officially reported by Division of Fish and Wildlife; and (D) for American Samoa versus the statistics officially reported by Department of Marine and Wildlife Resources (Figure 2D modified from Zeller et al., 2006a).

Table 5

Catch rates for the re-estimated small-scale fishery catches for Guam and the Commonwealth of the Northern Mariana Islands (CNMI), excluding pelagic species. Catch estimates are presented as per capita catch rates, and as catch per surface area of potential coral reef habitat to a depth of 100 fathom (183 m, Rohmann et al., 2005).

Year	Per capita catch (kg/year)		Catch/area (t/km ² /year)		
	Guam	Commonwealth of the Northern Mariana Islands	Guam (202.8 km ²)	Commonwealth of the Northern Mariana Islands	
				All islands (476 km ²)	Main islands (331.2 km ²)
1950	16.0	72.6	4.7	1.0	1.4
1960	12.5	53.9	4.1	1.0	1.4
1970	9.4	37.9	3.9	1.0	1.4
1980	4.9	20.5	2.5	0.7	1.0
1990	1.0	5.8	0.6	0.5	0.8
2000	1.4	3.2	1.1	0.5	0.7
2002	0.8	2.9	0.6	0.4	0.6

1950 to 2.9 kg by 2002 (Table 5). Given that over 99% of the human population of CNMI lives around the three main islands, the catch per reef habitat area was assessed for both the entire CNMI reef area (476 km²) and also for the reef areas of the three main islands (331.2 km²). Thus, between 1950 and 2002, estimated annual catch per km² reef area appears to have declined from 1.0 t to 0.4 t, and from 1.4 t to 0.6 t for the entire CNMI reef area (476 km²) and main islands reef areas (331.2 km²), respectively (Table 5).

The historic fisheries catches for American Samoa, as re-estimated by Zeller et al. (2006a), indicated a potential decline of about 79% in small-scale fisheries catches of nonpelagic species between 1950 and 2002 (Fig. 2D; modified from Zeller et al., 2006a). There was also a 7-fold difference between the re-estimated catches and the reported data for the 1980–2002 time period.

Discussion

Local and regional fisheries experts often acknowledge that they are aware of the limited nature of much of the official data, but rarely are willing or able to quantify the missing catches. Our re-estimation makes the potential scale of under-reporting of total extractions of marine resources evident. Specifically, our study illustrates not only the potential discrepancy by a factor of 4.55 between what was reported and what may have been caught (for the period of data reporting), but also indicates the potential scale of declines (77% overall for all areas combined) in total catches over the last 50 years. Although the historic catch estimates proposed here obviously do not represent a formal stock assessment, they are useful as baselines of potential historic patterns and trends in fisheries catches.

Regarding our comparison of catch data to those from official, reported fisheries, we acknowledge that most fisheries statistics were originally designed as an economic development and monitoring tool, where there was a common focus on commercial catches (with the exception of Guam). Nevertheless, reported data are being increasingly used to present national and global fisheries conditions and status and trends of resources. Thus, the under-representation of likely total catches as indicated here may lead directly to an erroneous interpretation of the status of fisheries within the U.S. flag-associated islands. Significantly, the situation of under-reporting contributes to the continued marginalization of small-scale fisheries (Pauly, 1997), and the ongoing under-valuation of the direct and indirect economic and social contribution of noncommercial (e.g., subsistence, and increasingly recreational) fisheries to the economic well-being of these islands (Zeller et al., 2006b). Such underestimations of catch histories may also have repercussions for the move towards ecosystem-based fisheries management.

The general approach used here, which relies on anchor points of data obtained from a variety of peer-reviewed and non-refereed data sources, moderated by

conservative assumptions, and interpolated for missing-data years, results in catch estimates that accounted for all fisheries sectors. We acknowledge that our estimates clearly are not statistically rigorous in the sense of approximating “true” time-series values, which are obviously not known. However, given our conservative approach to estimation, the present estimates are less wrong than the current default of reporting zero catch for fisheries sectors not considered in official figures. Ignoring the catches of noncommercial sectors of fisheries in the U.S. flag-associated island areas of the western Pacific has likely resulted in a skewed picture of the historic catch trends, as well as the magnitude of catches for nonpelagic, near-shore resources in these islands.

Catch estimation procedures such as ours are associated with high data uncertainty; this is the nature of alternative, non-standardized data sources. The paucity of data for the earlier periods was an acknowledged shortcoming to our approach; nevertheless, our approach is based on the best data and information available. We endeavored to remain conservative in our estimation throughout the period of examination; thereby incorporating a precautionary aspect into the data. Our conservative approach can be placed into context by the following consideration.

The re-estimation of catches for Guam, as undertaken here, indicates a decline in catches of 86%, and a 2.5-fold discrepancy between the re-estimated catches and the reported statistics over the time period for which DAWR reported data exist (1965–2002). The validity of the differences between reported and re-estimated catches is supported by the observation that, at least for the earlier periods, the catch data as reported by our sources (and forming the reported data) were “probably several times” less than the actual yields (Zeller et al.³).

Concerns about our approach to the unreported catches can be placed into perspective through an alternative, albeit less rigorous estimation (Zeller et al.³). In 1977, 38.6% of households in Guam were considered to have at least one family member who fished, and mean monthly catch per surveyed household was 32.7 kg, or 392 kg/year. With an average of 5 people per household and a population of 110,000 in 1977 for Guam, these figures imply 22,000 households (110,000 people/5 people per household), of which 38.6% (i.e., 8492 households) had active fishermen. These actively fishing households alone could thus have caught 3,328,864 kg in 1977 (8492 households with catch rate of 392 kg). Accounting for pelagic fish in their catch (45.8% of reported catches in 1977 were caught with pelagic gear), this calculation would imply a nonpelagic catch of 1,804,244 kg for 1977 ($3,328,864 \text{ kg} \times [1 - 0.458]$). This admittedly very indirect estimate is 2.76 times our total reconstructed nonpelagic catch estimate of 654,345 kg for 1977, and 12.6 times the DAWR reported catch of 143,220 kg. Thus, this indirect approximation supports our contention that our re-estimation approach was conservative, and total catches in the earlier periods were considerably higher than those of the reported data.

We appreciate that using linear interpolation of per capita catch rates between anchor points (particularly if widely spaced in time) may introduce additional data uncertainties associated with potential behavioral (changes in lifestyle and dietary preferences) and socioeconomic (move towards cash-economy) changes in the human population over that time period. This uncertainty in turn may lead to over- or underestimation of catches for a given year, for the period between anchor points. However, given the bounds provided by the anchor point data, such uncertainties would primarily influence the shape of the resultant catch curve for the period between each set of anchor points. Given the paucity of other supportive data, the only reliable alternative approach would have been a simple linear interpolation of catches between anchor points. On closer examination of our reconstructed data (see Fig. 2, the source of present data [Zeller et al.³], and Zeller et al., 2006a), such linear interpolation would only result in relatively small differences compared to our present approach. For example, a simple linear interpolation of anchor point catches would have smoothed the slight rise in reconstructed catches for CNMI between 1950 and 1980 (Fig. 2C). Overall, however, the broad conclusions and general trends observed here would not have been substantially affected.

The area catch rates as estimated here indicate catch rates ranging from 0.4 to 4.7 t/km²/year. These estimates are all at or near the lower end of the only other comprehensive range of estimates (0.3–64 t/km²/year) established for the Pacific region (Dalzell and Adams, 1997). However, all area catch rates are heavily influenced by the definition of coral reef area, which here was taken as depth defined (100 fathoms=183 m) potential coral reef ecosystem habitat as defined by Rohmann et al. (2005), which may represent overestimates of true coral reef habitats around each island. Nevertheless, the present estimates indicate that our reconstructed catch estimates, even for the early years, may likely be feasible in a broader ecological context.

Although the overall finding of our study was that of declining total catches, such declining catches may not necessarily be the result of excessive fishing alone because other factors may also contribute to the decline. These include changes in lifestyles, cash incomes, and dietary preferences of the local populations (as indicated above), as well as habitat degradation and pollution resulting from environmentally insensitive developments (Friedlander and DeMartini, 2002). All these factors can potentially lead to declines in the size of fish stocks and catches. Nevertheless, our results do indicate likely substantial changes over the last 50+ years in fisheries catches and should form important baselines for a move towards ecosystem-based resource and habitat management in the U.S. western Pacific region, particularly as other lines of evidence (e.g., declines in mean size of fish) also indicate that overfishing or stock declines may indeed be occurring in many areas (e.g., Craig et al., 1993).

Finally, and in our opinion significantly, we suggest strongly that all responsible agencies should be required to implement and maintain regular estimation procedures to account for and report all catches taken by all fisheries sectors. According to the data from the present study, Guam may offer a good example and starting point for such considerations. Guam has established an active commitment to creel surveys during the last 20+ years as a mechanism to estimate total catches. It is to be hoped that this commitment will continue. Given the high costs of creel surveys (which are the most suitable method for estimating highly dispersed and de-centralized noncommercial fisheries), resource-limited developing countries should give considerations to regular, albeit nonannual surveys for estimation of noncommercial catches. Well executed and comprehensive noncommercial catch estimates undertaken every 2–5 years are better than the current scenario of virtually no data collection.

Management agencies and policy makers should consider the distinctly different baselines of past catches as presented in this study, as they shed new light on issues and concerns for fisheries sustainability and ecosystem conservation. Furthermore, re-estimations, as presented here, illustrate the importance of small-scale and noncommercial fisheries sectors and indicate a need to account for all fisheries catches in official statistics.

Acknowledgments

We thank the Western Pacific Regional Fishery Management Council for funding the present study. The data provided by D. Hamm from the Western Pacific Fishery Information Network (WPacFIN) at the Pacific Islands Fishery Science Centre, NMFS, NOAA, are greatly appreciated. Critical comments by R. Clarke, E. DeMartini, D. Fenner, T. Graham, D. Hamm, K. Lowe, and W. Walsh contributed significantly to this study and are greatly appreciated. The statements, findings, conclusions, and recommendations are those of the authors and do not necessarily reflect the views of NOAA, Guam DAWR, American Samoa DMWR, or CNMI DFW. D. Zeller, S. Booth and D. Pauly acknowledge the support of the Pew Charitable Trusts for funding the *Sea Around Us* project at the University of British Columbia Fisheries Centre.

Literature cited

- Craig, P., B. Ponwith, F. Aitaoto, and D. Hamm.
1993. The commercial, subsistence, and recreational fisheries of American Samoa. *Mar. Fish. Rev.* 55: 109–116.
- Craig, P., J. H. Choat, L. M. Axe, and S. Saucerman.
1997. Population biology and harvest of the coral reef surgeonfish *Acanthurus lineatus* in American Samoa. *Fish. Bull.* 95:680–693.
- Dalzell, P., T. J. H. Adams, and N. V. C. Polunin.
1996. Coastal fisheries in the Pacific islands. *Oceanogr. Mar. Biol. Ann. Rev.* 34:395–531.

- Dalzell, P., and T. J. H. Adams.
1997. Sustainability and management of reef fisheries in the Pacific Islands. *Proc. 8th Int. Coral Reef Sym.* 2:2027-2032.
- Friedlander, A., and E. E. DeMartini.
2002. Contrasts in density, size, and biomass of reef fishes between the northwestern and the main Hawaiian Islands: the effects of fishing down apex predators. *Mar. Ecol. Prog. Ser.* 230:253-264.
- Hensley, R. A., and T. S. Sherwood.
1993. An overview of Guam's inshore fisheries. *Mar. Fish. Rev.* 55:129-138.
- Myers, R. F.
1993. Guam's small-boat-based fisheries. *Mar. Fish. Rev.* 55:117-128.
- Pauly, D.
1997. Small-scale fisheries in the tropics: marginality, marginalization, and some implications for fisheries management. *In* Global trends: fisheries management (E. K. Pikitch, D. D. Huppert, and M. P. Sissenwine, eds.), p. 40-49. *Am. Fish. Soc. Symp.* 20, Bethesda, MD.
- Rohmann, S. O., J. J. Hayes, R. C. Newhall, M. E. Monaco, and R. W. Grigg.
2005. The area of potential shallow-water tropical and subtropical coral ecosystems in the United States. *Coral Reefs* 24:370-383.
- Zeller, D., S. Booth, P. Craig, and D. Pauly.
2006a. Reconstruction of coral reef fisheries catches in American Samoa, 1950-2002. *Coral Reefs* 25:144-152.
2000b. Fisheries contributions to GDP: underestimating small-scale fisheries in the Pacific. *Mar. Res. Econ.* 21:355-374.

Abstract—Whole-gear efficiency (the proportion of fish passing between the otter doors of a bottom trawl that are subsequently captured) was estimated from data collected during experiments to measure the herding efficiency of bridles and doors, the capture efficiency of the net, and the length of the bridles sufficiently close to the seafloor to elicit a herding response. The experiments were focused on four species of flatfish: arrowtooth flounder (*Atheresthes stomias*), flathead sole (*Hippoglossoides elassodon*), rex sole (*Glyptocephalus zachirus*), and Dover sole (*Microstomus pacificus*). Whole-gear efficiency varied with fish length and reached maximum values between 40% and 50% for arrowtooth flounder, flathead sole, and rex sole. For Dover sole, however, whole-gear efficiency declined from a maximum of 33% over the length range sampled. Such efficiency estimates can be used to determine catchability, which, in turn, can be used to improve the accuracy of stock assessment models when the time series of a survey is short.

Whole-gear efficiency of a benthic survey trawl for flatfish

David A. Somerton (contact author)

Peter T. Munro

Kenneth L. Weinberg

National Marine Fisheries Service, NOAA
Alaska Fisheries Science Center
7600 Sand Point Way NE
Seattle, Washington 98115

Email address for D. A. Somerton: david.somerton@noaa.gov

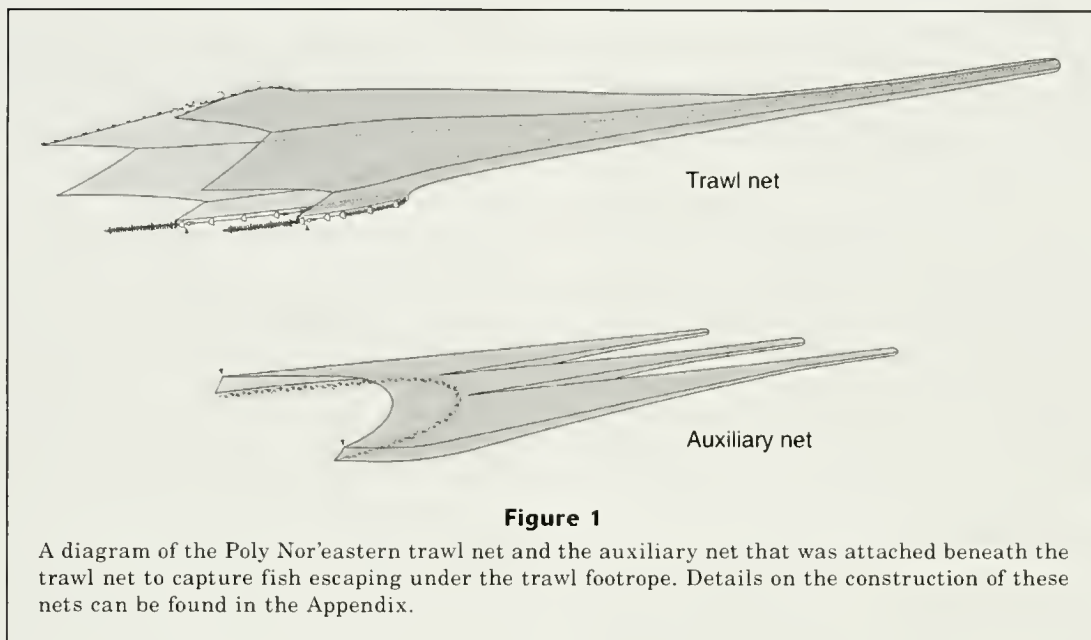
Fish density can be estimated from bottom trawl catch-per-swept-area data if there is knowledge of the whole-gear efficiency (the proportion of fish that are captured within the area spanned by the trawl doors). One approach to the estimation of whole-gear efficiency is to consider it as a function of three separate and underlying trawling processes: vertical and horizontal herding of fish, retention of fish by the net, and escapement of fish beneath the trawl footrope, which are often more tractable to field experimentation and estimation. Perhaps the earliest example of this approach was the development of a mathematical model by Dickson (1993a) for the efficiency of trawl gear in capturing fish and the application of this model for capturing Atlantic cod (*Gadus morhua*) and haddock (*Melanogrammus aeglefinus*; Dickson, 1993b) with the use of experimental data on herding (Engås and Godø, 1989a) and on escapement under the footrope (Engås and Godø, 1989b). Somerton and Munro (2001) proposed a modification to Dickson's (1993a) model for application to flatfish to account for the observation that flatfish herding is restricted to the length of the lower bridle that is sufficiently close to the bottom to elicit a behavioral response (Main and Sangster, 1981b). A variant of this model was then applied to seven species of North Pacific flatfish to estimate the efficiency of the capture process that was due to herding (Somerton and Munro, 2001). Although this application was followed

by experiments to estimate escapement under the footrope for some of the same flatfish species (Munro and Somerton, 2002), the flatfish efficiency model was never used to combine the herding and escapement estimates and thereby produce an estimate of whole-gear efficiency. In this article, we again use the flatfish trawl efficiency model, extended by developing an estimator for the variance of efficiency, and apply the model to new experimental data for four flatfish species (flathead sole [*Hippoglossoides elassodon*], rex sole [*Glyptocephalus zachirus*], Dover sole [*Microstomus pacificus*], and arrowtooth flounder [*Atheresthes stomias*]) to estimate whole-gear efficiency for the Poly Nor'eastern trawl, which is used by the Alaska Fisheries Science Center (AFSC) on its bottom trawl surveys of the Gulf of Alaska and the Aleutian Islands region.

Materials and methods

The Poly Nor'eastern trawl

The Poly Nor'eastern trawl, pictured in Figure 1 and detailed in the Appendix, has the following basic features: the net has a four-seam design and has a 27.2-m headrope and a 36.5-m footrope equipped with 36-cm diameter bobbins to allow operation on moderately rocky terrain. The trawl doors are "V" style measuring 1.8 m by 2.7 m and weighing 816 kg each. Tailchains constructed of two 3-m



lengths of 13-mm long-link chain are joined to a single 19-mm diameter steel cable, known as the tailchain extension, that is varied in length to suit the needs of each vessel. Tailchain length is the combined length of the chain and extensions. Tailchain extensions are connected to the leading edge of each wing with three bridles measuring 54.9 m in length and constructed of 16-mm steel cable. The net mesh in the lower section of each wing ends 6.1 m behind the end of the footrope (Fig. 1; Appendix); the footrope in this section will be referred to as the wing extension.

Trawl efficiency model for flatfish

For flatfish, which are unlikely to escape through the small-mesh, codend liner, or over the headrope, the catch of a trawl (N) can be expressed as the sum of the catches of fish originating from the net and bridle paths (Dickson, 1993a; Somerton and Munro, 2001)¹:

$$N = k_n DLW_n + k_n h DLW_{on}, \quad (1)$$

where

- D = fish density;
- L = tow length;
- W_n = the width of the net path;
- W_{on} = the width of the bridle path contacted by the bridle;
- k_n (net efficiency) = the proportion of fish within net path that are captured; and

h (herding coefficient) = the proportion of fish within the bridle contact path that are herded into the net path.

Because h is relative to W_{on} , which will vary with trawl design, for comparative purposes a more convenient measure of herding is the bridle efficiency (k_b) or the proportion of fish that are herded from the entire bridle path (Dickson, 1993a). Bridle efficiency can be calculated from the herding coefficient by using

$$k_b = \frac{hW_{on}}{W_d - W_n}, \quad (2)$$

where W_d = the width of the door path.

k_b = the average bridle efficiency in the area swept by the entire bridle (i.e., wing tip to door); and

h = the bridle efficiency only in the area actually contacted by the lower bridle.

Trawl efficiency (E) can then be derived from Equation 1 by dividing by the total number of fish within the door path (i.e., DLW_d).

$$E = \frac{k_n(W_n + hW_{on})}{W_d}. \quad (3)$$

Of the five quantities needed to evaluate this expression, two (W_n , and W_d) are routinely measured on bottom trawl surveys, but three (k_n , h , and W_{on}) require separate field experiments for their estimation. In this study, k_n was estimated with the data obtained from a net efficiency experiment which consisted of attaching

¹ In Somerton and Munro (2001) the parameter W_{on} in Equation 1 was instead represented by the equivalent, but more complex, expression: $W_d - W_n - W_{off}$ where W_{off} is the width of the bridle path not contacted by the bridle.

an auxiliary net under the trawl net to capture those fish escaping beneath the footrope—a method similar to that used in the studies of Engås and Godø (1989a), Walsh (1992), and Munro and Somerton (2002). Bridle efficiency (k_n) and the herding coefficient (k_h) were estimated from the data obtained from a herding experiment which consisted of repeatedly conducting trawl hauls where W_d was varied by varying the length of the bridles as has been done in the studies of Engås and Godø (1989b), Ramm and Xiao (1995), and Somerton and Munro (2001). The width of the area contacted by the bridle was estimated from the data obtained from an experiment by using bottom contact sensors to measure the off-bottom distance along the lower bridle—a distance that was reported for the Poly Nor'eastern trawl in Somerton (2003).

Net efficiency experiment

The net efficiency experiment was conducted during 2–10 July 1996 in the Gulf of Alaska, off the southeast side of Kodiak Island (58°30'N, 149°30'W) at 135–151 m depth with a 45-m chartered stern trawler, the FV *Golden Dawn*. An auxiliary net, described in the Appendix and patterned after those described in Engås and Godø (1989b) and Walsh (1992), was attached under the trawl net (Fig. 1). Trawling procedures followed normal survey protocols that included towing only during daylight hours for 15 minutes at a vessel speed of 1.5 m/sec. Catches from the trawl and the auxiliary net were kept separate, sorted by species, weighed, and all individuals were measured for total length (TL) in centimeters.

The auxiliary net, which was constructed of smaller 10.2-cm stretch mesh polyethylene netting, had a 24.8-m long headrope that was lashed directly to the fishing line of the trawl net (i.e., the forward edge of the netting) excluding the wing extension sections of the trawl footrope. The auxiliary net also had a 28.0-m long, 1.3-cm diameter chain footrope, strung with 12.7-cm rubber disks (Fig. 1), that was attached to the trawl footrope at the junctions of the roller gear and wing extensions, thus allowing the auxiliary footrope to move independently of the trawl footrope and to follow it with a separation distance of approximately 1–2 m at its center. The auxiliary net was designed so that the common intermediate section was attached to three separate codends, each having a 3.2-cm stretch mesh liner.

Experimental tows to verify that trawl performance was not altered by the attachment of the auxiliary net preceded the tows used for the measurement of net efficiency. During all of the experimental tows, a video camera, supplied with a 50 W light, was positioned in front of the footrope along the centerline of the trawl so that it had an oblique view and allowed an approximate measurement of the distance between the center of the footrope center and the sea floor. Initially, 10 tows were made with the trawl without the auxiliary net attached. When the same procedure was used for the trawl with the auxiliary net attached, the video recording indicated that the off-bottom distance of the footrope at its

center was greater. By trial and error, additional weight (chain) was attached to the center of the footrope until the off-bottom distance appeared equal to that of the trawl footrope without the auxiliary net. A total of 53.4 kg of chain was attached across the centermost 6.1 m of the footrope.

Estimating k_n from the experimental data

Net efficiency, k_n , was estimated as a function of fish length, l , by fitting an analytical model to the capture probability, P (i.e., proportion of fish passing between the trawl wing tips that are caught), and fish length data pooled over tows. Four competing models, each representing a different capture process, were considered (Munro and Somerton, 2001). The first three are parametric models, which, in order of increasing complexity, are expressed as

$$\text{2-parameter logistic, } P = \frac{1}{1 + e^{-(\alpha + \beta l)}}, \quad (4)$$

$$\text{3-parameter logistic, } P = \gamma \left(\frac{1}{1 + e^{-(\alpha + \beta l)}} \right), \quad (5)$$

4-parameter logistic,

$$P = \gamma \left(\frac{1}{1 - \delta} \right) \left(\frac{1 - \delta}{\delta} \right)^\delta \left(\frac{e^{-\delta(\alpha + \beta l)}}{1 + e^{-(\alpha + \beta l)}} \right), \quad (6)$$

where α , β , γ , and δ are free parameters to be estimated.

The maximum likelihood procedure for fitting these models, detailed in Munro and Somerton (2001), was based on the assumption that the entry of individual fish into either the trawl net or the auxiliary net could be described as a binomial statistical process. The fourth model is a nonparametric model, the cubic spline, which was fitted by using an S+ (S-PLUS, Insightful Corporation, Seattle, WA) function that determined the effective number of parameters of the spline function with cross validation (Venerables and Ripley, 1994). Of the four competing models, the best fitting model was selected as the one producing the lowest value of the Akaike Information Criterion (AIC; Burnham and Anderson, 1998). Ninety-five percent confidence intervals about the capture probabilities as a function of fish length were estimated by using the bootstrapping method (Efron and Tibshirani, 1993) where entire hauls were used as the units of data resampled.

Herding experiment

The herding experiment was conducted 10–19 May 1998 aboard a 30.6-m stern trawler, the FV *Hickory Wind*, near Kodiak Island in the Gulf of Alaska at depths ranging from 126 to 183 m. A blocked sampling design was

used to minimize the effects of the spatial variation in fish density on catch. In each geographical block, three nearby, but nonoverlapping, trawl hauls were made with each of three bridle lengths (chosen in random order). Bridles lengths measured 36.6 m, 54.9 m (the standard used on AFSC bottom trawl surveys), and 73.1 m. Tailchain length was 6.1 m. Trawling was conducted during daylight hours for 30 min at 1.5 m/sec. On all hauls, door spread, wing spread, and headrope height were measured simultaneously and continuously with an acoustic trawl mensuration system. Tow length was measured as the straight-line distance between the GPS positions of the first and last footrope contact with the bottom; this distance was determined by using a bottom contact sensor (Somerton and Weinberg, 2001) attached to the center of the footrope. The catch from each haul was first sorted to species, weighed in the aggregate, and then all flatfish were measured for TL in centimeters.

Estimates of W_{on} for the three bridle lengths were calculated from the estimates of the length of bridle contact with the bottom, L_{on} , provided by the bridle contact experiment described in Somerton (2003). Although the lengths of the bridles in this experiment were the same as those in the herding experiment, the length of the tailchains was 10.4 m longer because the length of the tailchain extensions vary with the size of a vessel. Consequently, the distance between the wing tip and the door differed between experiments. Because the cable used for the tail chain extension is quite similar in diameter to that used for the bridles (i.e., 19 mm [tail chain] vs. 16 mm [bridle]), the resulting difference in length is essentially the same as a constant addition to the three bridle lengths. We assumed that the effect of such a change in total bridle length was reflected only in L_{on} and that the portion of the bridle that was off bottom, L_{off} , did not differ between the bridle measurement and herding experiments. Thus L_{on} for the herding experiment was estimated as the total bridle length (bridle length + tail chain length) for the herding experiment minus L_{off} from the bridle contact experiment. A value of W_{on} was then estimated for each bridle length as

$$W_{on} = 2 \sin(\alpha) L_{on}, \quad (7)$$

where α = the average bridle angle at each bridle length during the herding experiment.

$\sin(\alpha)$ was computed for each haul as

$$(W_d - W_n) / 2L_t,$$

where L_t = the total length of the bridle plus the tail-chain (i.e., wingtip to door distance); and W_d and W_n = the haul mean values of door and wing spread.

Variance of W_{on} was estimated by using the delta method (Seber, 1973) and assuming no covariance between $\sin(\alpha)$ and L_{on} . This variance is expressed as

$$\text{Var}(W_{on}) = 4 \left(\sin(\alpha)^2 \text{Var}(L_{on}) + L_{on}^2 \text{Var}(\sin(\alpha)) \right). \quad (8)$$

$\text{Var}(\sin(\alpha))$ for each bridle length was calculated as the between-haul variability in $\sin(\alpha)$, and $\text{Var}(L_{on})$ was obtained from Somerton (2003).

Estimating h from the experimental data

The herding coefficient was estimated by fitting a modified version of Equation 1 to the experimental data on W_n , W_{on} , and catch (in numbers). The first modification, which is considered more fully in Somerton and Munro (2001), consists of introducing a new parameter, k , defined as the product of D and k_n , that is allowed to vary among blocks. The second modification is to allow length dependency in k and h . The modified equation is

$$N_{ijk} = k_{ik} (LW_n)_{ij} + k_{ik} h_k (LW_{on})_{ij} + \epsilon_{ijk}, \quad (9)$$

where subscript i refers to block number, j to bridle length within block, k to fish length class, and ϵ_{ijk} is a normally distributed error term.

For each fish-length class, fitting Equation 9 to the herding data required estimation of $n+1$ parameters, where n is the number of blocks sampled (i.e., a unique value of k for each block and a common value of h for all blocks). Because the model is nonlinear in the parameters (h and k are multiplied together), it was fitted to data by using nonlinear regression (Venables and Ripley, 1994). Fish length classes used in the calculations were chosen such that the number of observations of length was approximately equal among classes, and differed among species due to differences in the number and size range of sampled fish. After h was estimated, k_b was calculated for the standard bridle length with Equation 2. Variance of k_b was estimated by using a bootstrapping process designed to include among-block variability in catch and trawl measurements as well as the uncertainty in the estimated value of W_{on} . First, a bootstrap replicate of catch and trawl measurement data was obtained by randomly choosing, with replacement, blocks of data, each containing a single haul at each bridle length, from the n blocks sampled (blocks rather than hauls were randomized to preserve the within-block correlation in catch). Second, for each bridle length, a value of W_{on} was computed by using a normal random number generator with values of the mean and variance of W_{on} reported in Somerton (2003). Third, h was then estimated by fitting Equation 9 by using nonlinear regression, and k_b was estimated from h by using Equation 2. Fourth, the process was repeated 100 times and the variance of k_b was estimated as the variance among the replicates. Although the model that we used allows for length-dependent herding, herding may not be a length-dependent process in all species. To determine if k_b varied with fish length, the estimated length-specific values of k_b were regressed on the midpoints of the length intervals.

Table 1

Selectivity model selection and estimated parameters of the best fitting model. The value of the Akaike Information Criterion (AIC) is shown for each of four possible models described in Munro and Somerton (2001): 2-parameter logistic, 3-parameter logistic, 4-parameter logistic, and cubic spline models. The estimated parameters of the best fitting model, that is, the one with the lowest value of the AIC, are shown. Parameter notation (α, β, γ) is the same as in Equations 4–6 in the text. Although, for arrowtooth flounder (*Atheresthes stomias*) the best fitting model is the cubic spline, the parameters of the best fitting parametric model are also included for use at lengths >20 cm.

Species	AIC				Estimated parameters		
	2-parameter logistic	3-parameter logistic	4-parameter logistic	Cubic spline	α	β	γ
Arrowtooth flounder (<i>Atheresthes stomias</i>)	6568.8	6502.0	6504.0	6382.7	-2.65	0.156	0.966
Flathead sole (<i>Hippoglossoides elassodon</i>)	1804.3	1794.7	1796.7	1863.4	-3.66	0.208	0.861
Rex sole (<i>Glyptocephalus zachirus</i>)	1642.8	1594.0	1596.0	1634.9	-7.45	0.376	0.873
Dover sole (<i>Microstomus pacificus</i>)	1245.9	1247.9	1249.9	1256.6	2.27	-0.055	

Estimating whole-gear efficiency

Estimates of trawl efficiency, by 1 cm length categories, were obtained by substituting into Equation 3 the estimates of mean W_n and W_d for the standard bridle length from the herding experiment, k_n from the net efficiency experiment, h from the herding experiment, and W_{on} from the bridle measurement experiment. Variance of E , which was derived from Equation 2 by using the delta method (Seber, 1973) and by assuming no covariance between any of the parameters, was calculated as

$$\begin{aligned}
 V(E) = & \left(\frac{W_n + hW_{on}}{W_d} \right)^2 V(k_n) + \left(\frac{k_n}{W_d} \right)^2 V(W_n) + \\
 & \left(\frac{k_n W_{on}}{W_d} \right)^2 V(h) + \left(\frac{k_n h}{W_d} \right)^2 V(W_{on}) + \\
 & \left(\frac{k_n (W_n + hW_{on})}{W_d^2} \right)^2 V(W_d).
 \end{aligned} \quad (10)$$

The variance variables $V(W_n)$, and $V(W_d)$ were estimated as the variance of these dimensions during the herding experiment. Variance variables $V(k_n)$, $V(h)$, and $V(W_{on})$ were calculated as described earlier.

Results

Net efficiency experiment

All four species of flatfish were present in each of the 34 tows successfully completed. Total number and size range of measured fish were the following: 9512; 5–84 cm TL (arrowtooth flounder); 1701; 6–45 cm TL (flathead sole); 2142; 10–61 cm TL (rex sole); and 949; 30–57 cm TL (Dover sole).

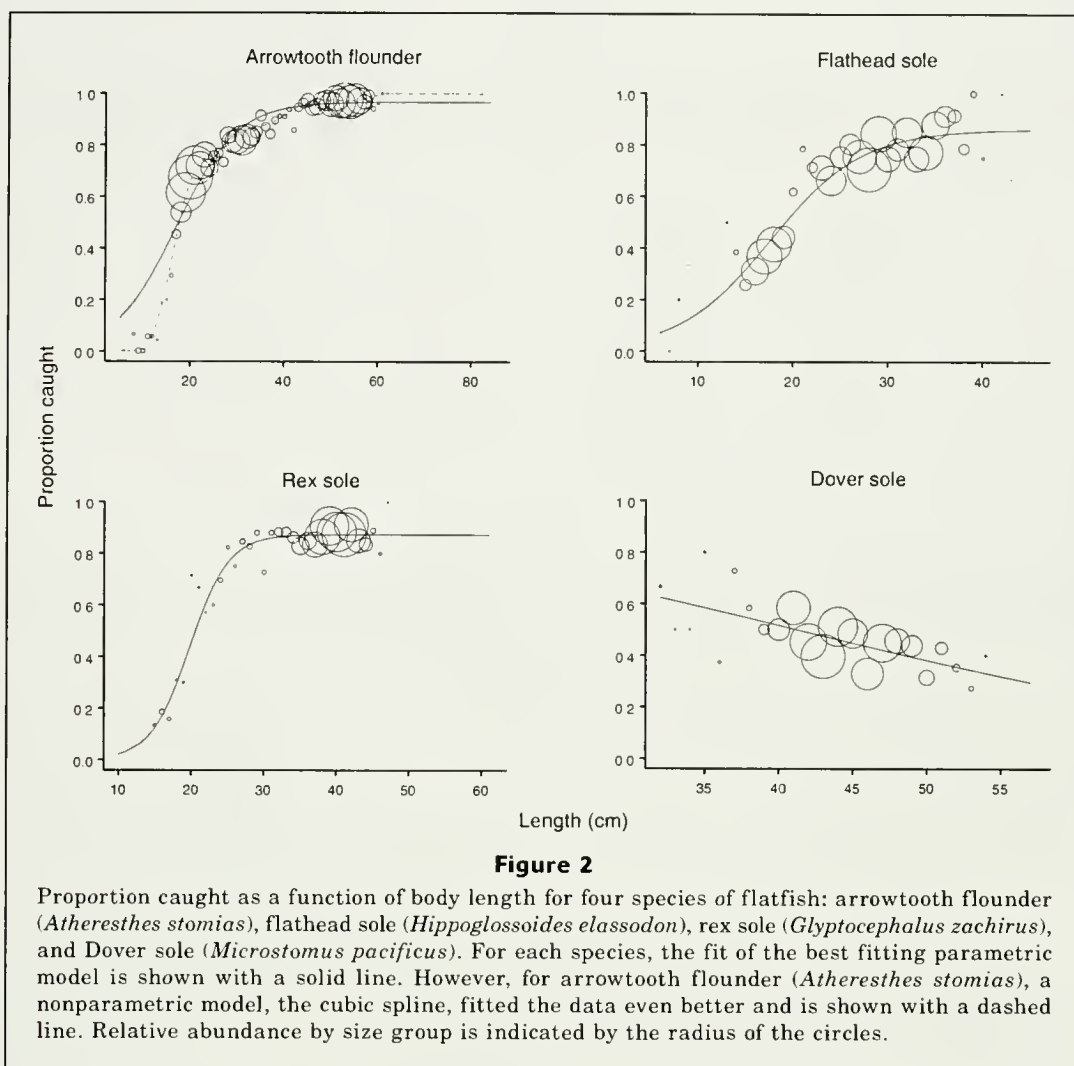
Estimates of k_n

The best fitting model of k_n as a function of length differed among the four flatfish species. For arrowtooth flounder, the best fitting model was the cubic spline (Table 1, Fig. 2), primarily because of its flexibility to fit the selectivity of small (<20 cm TL) fish. At larger sizes (>20 cm TL), however, the best fitting parametric model was the 3-parameter logistic model. The cubic spline model fitted almost equally well (Fig. 2); therefore, we have also included the parameter estimates of this model in Table 1. For flathead sole and rex sole, the best fitting selectivity model was the 3-parameter logistic with a maximum capture probability substantially below that for arrowtooth flounder (Table 1; Fig. 2), indicating that the escapement beneath the footrope for these species is substantial even at the largest sizes. For Dover sole, the best fitting model was the 2-parameter logistic model, with the parameters chosen such that the predicted capture probability decreased monotonically, and nearly linearly, over the observed length range of fish.

Herding experiment

Seventeen geographic blocks, each containing three hauls, were successfully completed. For arrowtooth flounder, 11,510 fish were measured and all 17 blocks had nonzero catches at all bridle lengths. For the remaining species, the statistics are as follows: flathead sole (6632 measurements, 17 blocks), rex sole (620 measurements, 13 blocks), and Dover sole (392 measurements, 12 blocks).

The width of the area contacted by the bridles (W_{on}) increased dramatically with increasing bridle length (Table 2), primarily because of the increase between the short and standard bridle length. At the shortest bridle length, the estimated value of W_{on} indicated that the lower bridle was typically lifted off the bottom along its entire length. Other aspects of trawl geometry changed with increasing bridle length. Wingspread



decreased slightly (0.4 m; Table 2) as bridle length increased, but the decrease was not significant; bridle angle (i.e., the angle between the bridles and the direction of travel (α)) decreased significantly with increasing bridle length.

Estimates of k_b

Tests for length dependency in the herding process, based on the linear regression of k_b on fish length, indicated that the slopes were positive in all four cases (Table 3; Fig. 3), but significant only for arrowtooth flounder. Because the significance of the relationship for arrowtooth flounder is primarily due to the conspicuously lower value of k_b at the smallest length class (Fig. 3), we consider the evidence for an increase in k_b with size as credible, but still equivocal.

Length dependency in the herding process should lead to differences in the size distribution as bridle length is changed; however, size distributions for each species appeared quite similar for each of the three bridle lengths (Fig. 4) and none of the species had a significant

($P < 0.05$) difference in mean size among bridle lengths. Consequently, k_b was considered as length invariant in the calculation of efficiency for all four species.

Length-invariant estimates of k_b were similar for the three sole species, ranging from 0.22 for rex sole to 0.24 for Dover sole (Table 4). These values are slightly larger than the estimated value of 0.17 for arrowtooth flounder. The values of the herding coefficient (h), or the herding efficiency in relation to the area swept by the lower bridle, were considerably higher than the values of k_b . For the three sole species, h ranged from 0.53 for rex sole to 0.58 for Dover sole. Again, these values were higher than the h estimate of 0.39 for arrowtooth flounder. Thus, roughly 40–50% of the flatfish encountering the lower bridle were ultimately herded into the path of the net.

Whole-gear trawl efficiency

Trawl efficiency estimates for arrowtooth flounder, flathead sole, and rex sole increased with increasing fish length and reached maxima of 0.45, 0.42, and 0.43,

Table 2

Trawl configuration parameters for the herding experiment. Included are the bridle lengths that were used, the means (and standard deviations) of the door width (W_d), wing width (W_n), bridle angle (α), bridle width ($W_d - W_n$), and bridle width in contact with the bottom (sea floor) (W_{on}).

Bridle length (m)	Door width (m) W_d	Wing width (degrees) W_n	Bridle angle (m) α	Bridle width (m) $W_d - W_n$	Bridle width on bottom (m) W_{on}
73.1	54.1 (3.4)	15.9 (0.6)	13.9 (1.0)	38.2 (2.8)	16.7 (2.1)
54.9	47.8 (2.7)	16.1 (0.6)	15.0 (1.0)	31.6 (2.1)	13.5 (2.5)
36.6	39.8 (1.8)	16.3 (0.5)	16.0 (1.0)	23.5 (1.4)	0.0 (0.0)

Table 3

Fit of a linear model to estimates of the bridle herding coefficient (k_b) as a function of fish length. The number of fish length bins, the slope of the regression line fit to k_b and length data, and the probability that the slope equaled zero is shown for each species. Significance of the slope ($P < 0.05$) indicates that herding changes with fish size.

Species	Number of length bins	Slope of regression line	$P(\text{slope}=0)$
Arrowtooth flounder (<i>Atheresthes stomias</i>)	8	0.0035	0.039
Flathead sole (<i>Hippoglossoides elassodon</i>)	6	0.0033	0.616
Rex sole (<i>Glyptocephalus zachirus</i>)	5	0.0057	0.554
Dover sole (<i>Microstomus pacificus</i>)	4	0.0184	0.150

Table 4

Estimates of r^2 for the fit of the model (Eq. 9) without length dependency, and the values of h , k_b (Eq. 2), and the standard deviation (SD) of K_b for each of the four species of flatfish.

Species	r^2	h	k_b	SD(k_b)
Arrowtooth flounder (<i>Atheresthes stomias</i>)	0.71	0.391	0.167	0.038
Flathead sole (<i>Hippoglossoides elassodon</i>)	0.98	0.555	0.237	0.047
Rex sole (<i>Glyptocephalus zachirus</i>)	0.84	0.531	0.222	0.066
Dover sole (<i>Microstomus pacificus</i>)	0.62	0.576	0.239	0.162

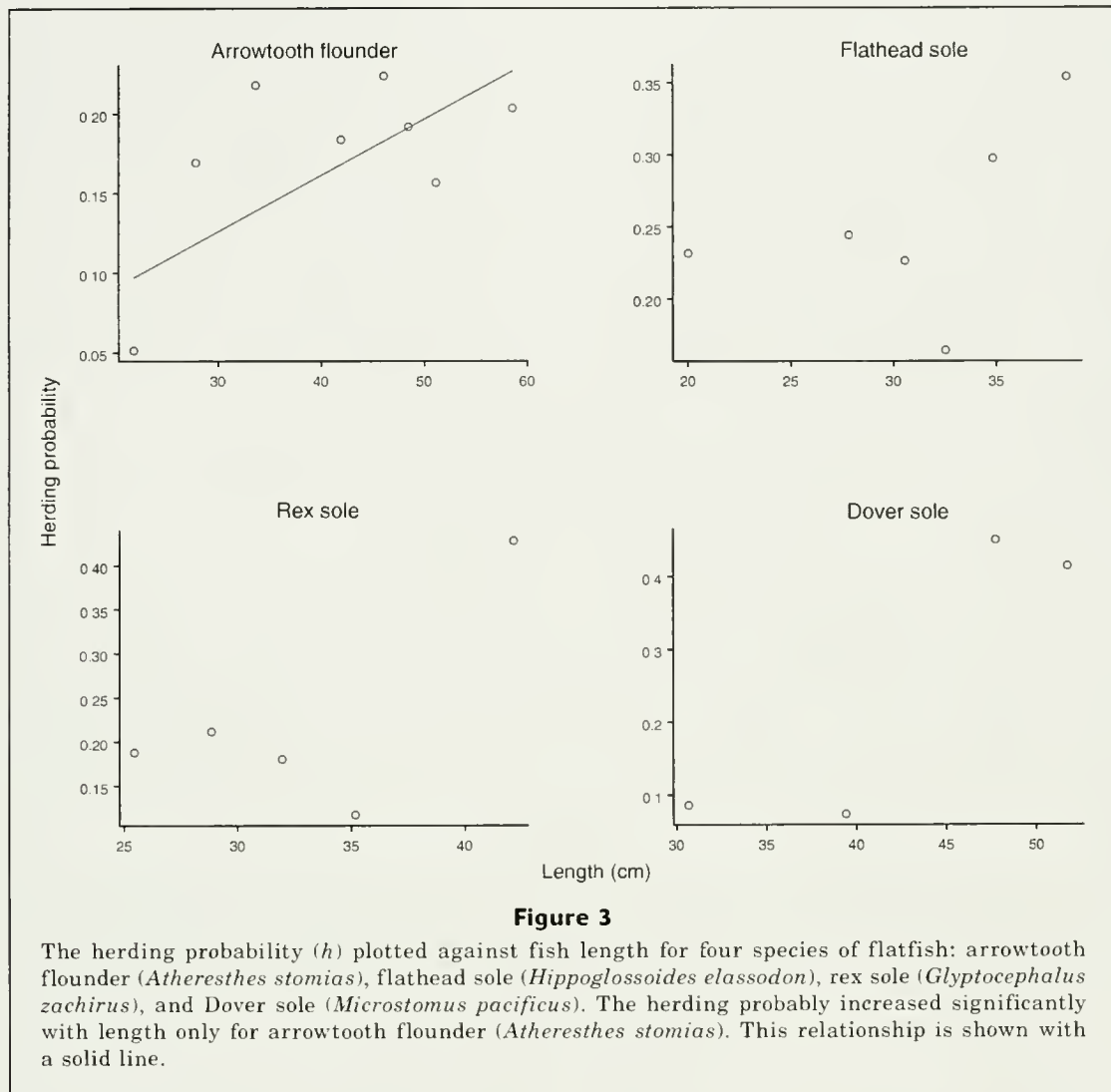
respectively (Fig. 5), indicating that slightly more than 40% of the largest individuals that passed between the doors of the trawl were ultimately caught. In contrast, the efficiency estimates for Dover sole were considerably lower over the sampled size range and monotonically decreased with increasing fish length.

Discussion

Net efficiency

For three of the four flatfish species (i.e., arrowtooth flounder, flathead sole, rex sole), net efficiency (k_n)

increased monotonically with fish size. For Dover sole, however, net efficiency declined over the sampled size range and was considerably lower than that for the other species in the larger commercial sizes. This unusual pattern is likely the result of two factors. First, small individuals, which are likely better at escaping under the footrope, were not sampled; consequently, the left-hand, ascending, portion of the selection curve is not defined. Second, the decline in capture probability with increasing size indicates that this species is behaviorally more adept at escaping under the footrope, probably by swimming ahead of the footrope, then dropping to the bottom, and allowing the footrope to pass over. Although distinct species-specific escape responses to a footrope



have been reported (Bublitz, 1996), our video recordings were insufficiently clear for us to distinguish species and therefore we could not determine the mechanism leading to the decline in capture probability. Regardless of the mechanism, a decline in net efficiency with increasing size has been previously reported for another flatfish (i.e., yellowtail flounder, *Limanda ferruginea*; Walsh, 1992).

Assumptions with the net efficiency experiment

The auxiliary net did not extend across the full width of the trawl net, but only across the center 78% of the width where the mesh of the trawl net attaches to the footrope. Our use of the estimated net efficiency in this section as a proxy for that of the total net spread, which is measured at the junction of the upper bridle and wing tip, is based on the assumption that the average escapement in the unsampled section is the same as that in the sampled section. From video observations (K. Weinberg,

unpubl. data), it is evident that flatfish encountering these outer portions of the footrope tend to be herded toward the center of the footrope rather than pass under or over the footrope. Although we have no quantitative data on the change in escapement rate across the width of the trawl, we believe that our extrapolation of the measured escapement rate into the unsampled portion of the net spread potentially results in a slight underestimate of net efficiency.

Herding

One would expect herding to be a length-dependent process because the swimming endurance of fish, and therefore their ability to maintain position in front of the bridle, increases with body size (Winger et al., 1999). Our evidence for length-dependent herding, however, is equivocal. All four of the species had a positive slope in the regression of k_b on body length (Table 2), but in only one case, arrowtooth flounder, was

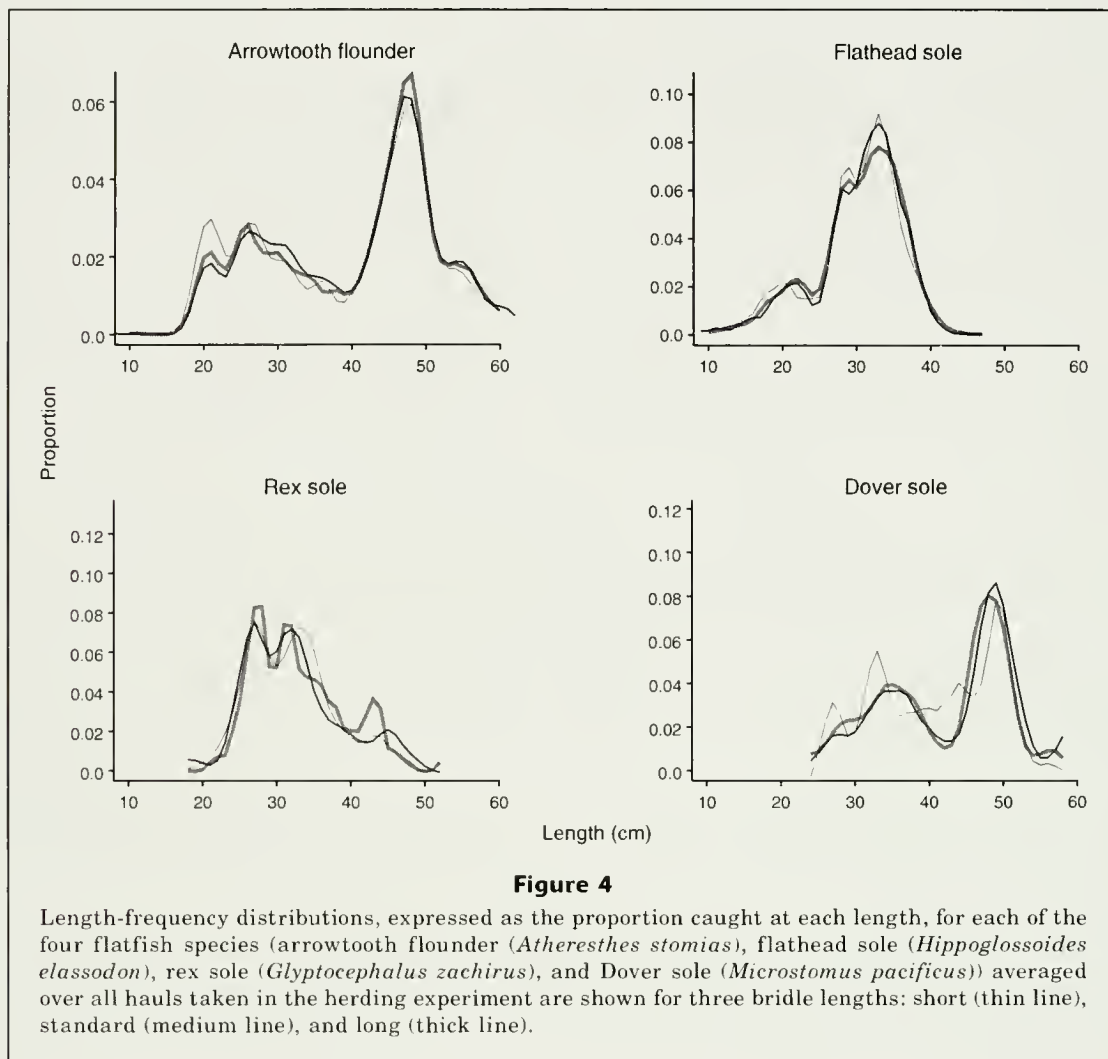


Figure 4

Length-frequency distributions, expressed as the proportion caught at each length, for each of the four flatfish species (arrowtooth flounder (*Atheresthes stomias*), flathead sole (*Hippoglossoides classodon*), rex sole (*Glyptocephalus zachirus*), and Dover sole (*Microstomus pacificus*)) averaged over all hauls taken in the herding experiment are shown for three bridle lengths: short (thin line), standard (medium line), and long (thick line).

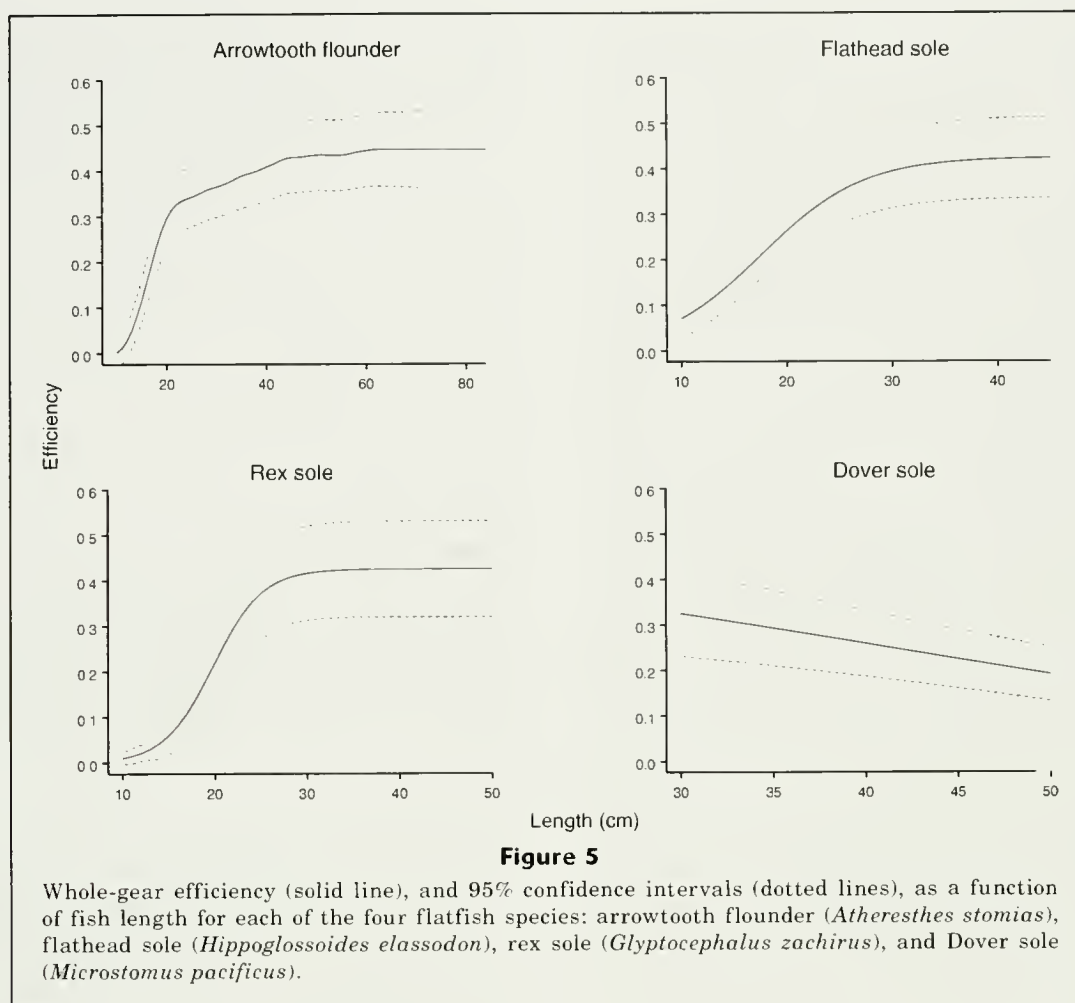
the slope statistically significant and this significance was dependent on the relatively low value of k_b in the smallest size interval. In previous studies, evidence for length-dependent herding has been inconsistent. Although Engås and Godø (1989a) observed increases in bridle efficiency with fish length for Atlantic cod and haddock, Somerton and Munro (2001) found either no change or decreases in bridle efficiency for seven species of flatfish, and Ramm and Xiao (1995) found no evidence of length dependent herding for any of a variety of species.

An alternative way of detecting length-dependent herding is through the changes in mean length of the catch as bridle length is changed, because the processes leading to the differences in herding ability with fish size would be intensified with increases in bridle length. Although Engås and Godø (1989a) and Andrew et al. (1991) found an increase in fish length with increasing bridle length, Somerton and Munro (2001) found a decrease in fish length. Because, in the present study, we observed no significant changes in mean size with bridle length (Fig. 4), even for arrowtooth flounder,

which had a significant increase in k_b with length, length-dependency in the herding process is, at best, weak for flatfish sampled with the Poly Nor'eastern trawl and is therefore unlikely to contribute substantially to size selectivity.

Although estimates of k_b for the four species were pairwise not significantly different from each other, the estimates for flathead sole, rex sole, and Dover sole were very similar (Table 3), but considerably greater than the estimate for arrowtooth flounder. From an ecological perspective, similarity in the herding coefficients for the three sole species makes sense because all eat sessile or slow moving prey taken from the bottom and are likely relatively slow swimmers that stay close to the bottom when herded, whereas arrowtooth flounder eats relatively large pelagic fish (Yang and Nelson, 2000) and is likely a stronger, more agile swimmer that readily leaves the bottom.

The k_b estimates for the three sole species are also quite similar to the estimates that we obtained previously for the 83-112 Eastern trawl (flathead sole, 0.24; rex sole, 0.22; Dover sole, 0.27; Somerton and Munro,



2001). Although the two trawls have bridles that are identical in length and thickness, we found the similarity in the k_b estimates surprising because the bridles on the Poly Nor'eastern trawl are obscured over their entire length by mud clouds during trawling (Somerton, 2003), whereas those on the 83-112 Eastern trawl are mostly unobscured and likely visible to fish. This indicates that either the lower bridle, even in a mudcloud, is more visible to a flatfish than it seems to be when viewed with a video camera or that visibility of the lower bridle is not particularly important for flatfish herding—at least for the type of bridles used on AFSC bottom survey trawls.

For flathead, rex, and Dover sole, 55% (average value of h) of the individuals within the bridle contact path and 23% of the individuals within the entire bridle path were herded into the net path. Assuming that herded fish have the same probability of being captured as fish originally in the net path, then the herded fish comprise about 32% of the catch. For arrowtooth flounder, herded fish comprise 25% of the catch. This finding indicates that herding contributes substantially to the catch of these species and cannot be ignored when computing swept area estimates of abundance.

Assumptions with the herding experiment

The objective of the herding experiment was to change the size of the area experiencing a herding stimulus without altering other aspects of trawl geometry or performance. However, as in our previous experiment (Somerton and Munro, 2001), and those of Ramm and Xiao (1996) and Engås and Godø (1989a), both the net width and the bridle angle changed in response to the change in bridle length (Table 2). Because of these unintended changes in trawl geometry, the width of the bridle area did not change in proportion to the change in bridle length. Thus, the increase in the width of the bridle path (i.e., $W_d - W_n$) was 8.1 m between the short length and standard length bridles, but only 6.6 m between the standard length and the long length bridles. A better design for a herding study would be one in which the incremental changes in bridle path width, or, better yet W_{on} , were approximately equal among bridle lengths. By studying bridle geometry as a function of bridle length, it should be possible to choose the correct experimental bridle lengths to achieve this equality.

One assumption with the herding model is that flatfish are stimulated to herd by the bridles only from the

footrope attachment of the lower bridle out to a distance L_{on} , but not beyond. This is an over simplification of the herding process, but in our previous study (Somerton and Munro, 2001) video recordings substantiated this assumption. Because the bridles are obscured by the mudclouds on the Poly Nor'eastern trawl, not only were we unable to verify the fish reaction to the bridles but the mud clouds themselves may have provided a herding stimulus as they reportedly do for some roundfish (Main and Sangster, 1981a, 1981b). If so, the effective length of the bridle over which herding occurs could be longer than L_{on} . We attempted to answer this question by positioning a video camera to allow us to observe flatfish behavior at the inner edge of the mud cloud, but were unsuccessful.

Another assumption is that the estimates of L_{on} can be extrapolated from the bridle measurement experiment to the herding experiment. On all vessels that we use for experiments, the tailchain extensions are adjusted in length depending on the size of the vessel and storage location of the doors when out of water. On the herding and bridle measurement experiments, the difference in the sizes of the vessels was so large that the tailchain length was approximately 10 m longer in the bridle measurement experiment. Because the cable used for the tail chain extensions is quite similar in diameter to that used for the bridles (i.e., 19 vs. 16 mm), the difference in tailchain length can be viewed as an equivalent difference in bridle length. Although unsubstantiated, our belief is that the combined forces on the lower bridle are such that a lengthening of the bridle by 10 m would result in a minimal change in the length of the bridle held off the bottom and therefore simply add a 10-m increment to L_{on} .

Whole-gear efficiency

We are aware of two previous studies in which whole-gear efficiency and the efficiency of the subsidiary trawling processes were experimentally estimated. One of these studies, that of Dickson (1993b), focused on Atlantic cod and haddock and therefore produced results that were not directly comparable to ours. The other, that of Harden Jones et al. (1977), is comparable because it was focused on a flatfish (plaice, *Pleuronectes platessa*) and used a bottom trawl similar in design to the Poly Nor'eastern trawl. In the latter study, gear efficiency was estimated by determining the fate (i.e., capture or escape) of individual fish tagged with acoustic transponders which allowed them to be located with a sector scanning sonar. For all fish passing between the doors, 44% were subsequently caught. This result is quite similar to the maximum efficiency of the Poly Nor'eastern trawl for three of the species in our study (mean=43%). In the Harden Jones et al. (1977) study, fish entering the trawl within the bridle path (between the wings and doors) had a 22% chance of being caught and fish entering the trawl within the net path had a 61% chance of being caught. Again, based on the maximum efficiency of the Poly Nor'eastern trawl, there

was a 19% mean chance of being caught (calculated as $k_b k_n$) for fish entering the trawl within the bridle path and a 90% chance of being caught for fish entering the net path. Thus, compared with the Harden Jones et al. (1977) study, the bridle efficiency of the Poly Nor'eastern trawl for flatfish was less, net efficiency was greater, but the whole-gear efficiency was nearly the same.

For some bottom trawl surveys, including those conducted by the AFSC, swept area calculations are based on wing spread rather than door spread and the selectivity or catchability parameters in stock assessment models are formulated according to this convention. To convert efficiency estimates presented here to the estimates appropriate for the net spread convention, the values must be multiplied by the quotient of the door spread and net spread, which for the Poly Nor'eastern trawl is approximately equal to 3 (47.8 m/16.1 m).

Such efficiency estimates can be used to estimate survey catchability, which, in turn, can be used to constrain the survey catchability parameter in stock assessment models. In situations when the survey time series is relatively short, constraining the catchability parameter can lead to improved predictions of stock biomass and harvest rate (Somerton et al., 1999).

Literature cited

- Andrew, N. L., K. J. Graham, S. J. Kennelly, and M. K. Broadhurst
1991. The effects of trawl configuration on the size and composition of catches using benthic prawn trawls off the coast of New South Wales, Australia. *ICES J. Mar. Sci.* 48:201-209.
- Bublitz, G. G.
1996. Quantitative evaluation of flatfish behavior during capture by trawl gear. *Fish. Res.* 25:293-304.
- Burnham, K. P., and D. R. Anderson
1998. Model selection and inference: practical information-theoretic approach, 353 p. Springer-Verlag, New York, NY.
- Dickson, W.
1993a. Estimation of the capture efficiency of trawl gear. I: development of a theoretical model. *Fish. Res.* 16: 239-253.
1993b. Estimation of the capture efficiency of trawl gear. II: testing a theoretical model. *Fish. Res.* 16: 255-272.
- Efron, B., and R. Tibshirani
1993. An introduction to the bootstrap, 436 p. Chapman and Hall, New York, NY.
- Engås, A., and O. R. Godø
1989a. The effect of different sweep lengths on the length composition of bottom-sampling trawl catches. *J. Cons. Int. Explor. Mer* 45:263-268.
1989b. Escape of fish under the fishing line of a Norwegian sampling trawl and its influence on survey results. *J. Cons. Int. Explor. Mer* 45:269-276.
- Harden Jones, F. R., A. R. Margetts, M. G. Walker, and G. P. Arnold
1977. The efficiency of the granton otter trawl determined by sector-scanning sonar and acoustic transponding tags. *Rapp. P-v. Reun. Cons. Explor. Mer* 170:45-51.

- Main, J., and G. I. Sangster
1981a. A study of the sand clouds produced by trawl boards and their possible effect on fish capture. *Scott. Fish. Res. Rep.* 20:1-20.
- 1981b. A study of the fish capture process in a bottom trawl by direct observations from a towed underwater vehicle. *Scott. Fish. Res. Rep.* 23:1-23.
- Munro, P. T., and D. A. Somerton
2001. Maximum likelihood and non-parametric methods for estimating trawl footrope selectivity. *ICES J. Mar. Sci.* 58:220-229.
2002. Estimating net efficiency of a survey trawl for flatfishes. *Fish. Res.* 55:267-279.
- Ramm, D. C., and Y. Xiao
1995. Herding in groundfish and effective pathwidth of trawls. *Fish. Res.* 24:243-259.
- Seber, G. A. F.
1973. The estimation of animal abundance, 343 p. Hafner Press, New York, NY.
- Somerton, D.
2003. Bridle efficiency of a survey trawl for flatfish: measuring the length of the bridles in contact with the bottom. *Fish. Res.* 60:273-279.
- Somerton, D. A., and P. Munro
2001. Bridle efficiency of a survey trawl for flatfish. *Fish. Bull.* 99:641-652.
- Somerton, D. A., and K. L. Weinberg
2001. The affect of speed through the water on footrope contact of a survey trawl. *Fish. Res.* 53:17-24.
- Somerton, D., J. Ianelli, S. Walsh, S. Smith, O. R. Godø, and D. Ramm.
1999. Incorporating experimentally derived estimates of survey trawl efficiency into the stock assessment process: a discussion. *ICES J. Mar. Sci.* 56:299-302.
- Venerables, W. N., and B. D. Ripley
1994. *Modern applied statistics with S-plus*, 462 p. Springer-Verlag, New York, NY.
- Walsh, S. J.
1992. Size-dependent selection at the footgear of a groundfish survey trawl. *N. Am. J. Fish. Manage.* 12: 625-633.
- Winger, P. D., P. He, and S. J. Walsh
1999. Swimming endurance of American plaice (*Hippoglossoides platessoides*) and its role in fish capture. *ICES J. Mar. Sci.* 56:252-265.
- Yang, M. S., and M. W. Nelson
2000. Food habits of the commercially important groundfishes in the Gulf of Alaska in 1990, 1993, and 1996. NOAA Tech. Memo. NMFS-AFSC-112, 174 p.
- ate sections) and has a double 8.9-cm (4-mm thickness) codend with a 3.2-cm nylon mesh liner. The 27.2-m headrope supports twenty 30.5-cm diameter and four 20.3-cm diameter trawl floats that provide 220 kg of total lift. The webbing is hung from a 24.9-m bolsh line consisting of 0.95-cm diameter bare stranded wire wrapped with 0.95-cm diameter polypropylene rope, that attaches to a 24.7-m chain (1.6-cm long-link) fishing line. The 24.2-m, 1.9-cm diameter stranded-wire footrope is rigged with three sections of roller gear that attach to the fishing line with 25-cm pieces of 0.95-cm chain. The 12.2-m center section of the roller gear consists of eight 36-cm rubber bobbins separated by 10-cm rubber disks. To either side of the center segment is a 6.0-m section that consists of four 36-cm rubber bobbins separated by pieces of rubber hose to protect the wire footrope. In addition, 5.9-m footrope wing extensions consisting of 1.9-cm diameter stranded-wire rope with 10-cm and 20-cm rubber disks span the lower "flying" wing section on each side of the net. Riblines, constructed of 1.9-cm diameter Duralon 2 in 1 braided rope (Samson Inc., Ferndale, WA), are hung along 98% of the stretched length of the netting.
- The net is connected to a pair of 1.8×2.7 m steel "V" doors, weighing approximately 816 kg each, by two 3-m door legs, consisting of 1.6-cm long-link chain; a 12.2-m door leg extension, consisting of 1.9-cm diameter bare stranded wire; and triple 54.9-m bridles, consisting of 1.6-cm diameter bare stranded wire, on each side of the net. Additional 46-cm and 23-cm-long extensions, consisting of 1.3-cm long-link chain, connect the upper and middle bridles to the respective wing tips of the trawl.

Auxiliary net for Poly Nor'eastern trawl gear The auxiliary net is a 2-seam trawl fitted with small side panels designed to help maintain steady footrope contact with the bottom during periods of intermittent contact by the Poly Nor'eastern footrope; it also fitted with three codends for catch retention should the net sustain damages (Appdx. Fig. 2). The 24.8-m headrope, constructed of 1.9-cm diameter double braid polyester rope, is lashed to the survey trawl bolsh line. The 28.0-m footrope, constructed of 1.3-cm long-link chain passing through 12.7-cm diameter rubber disks, is lashed to the 1.9-cm diameter double braid polyester fishing line from which the netting is hung. A delta plate located just aft of each survey trawl wing extension is used to connect both the front ends of the headrope and the fishing line to the trawl footrope.

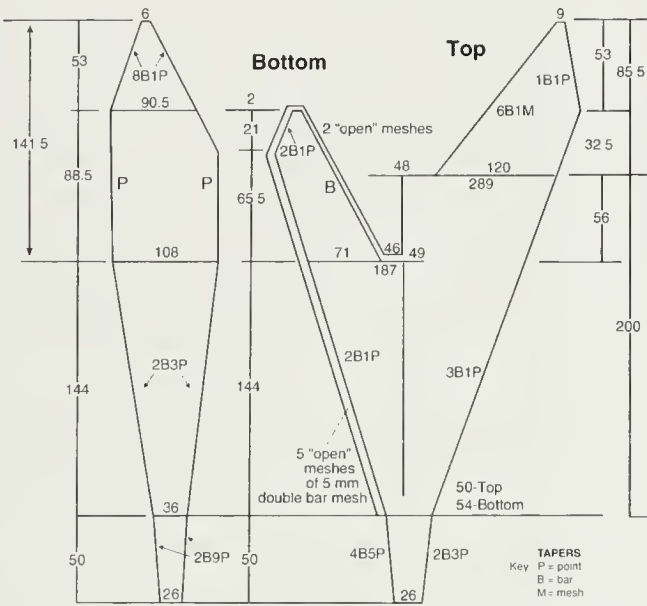
With the exception of the 8.9-cm stretched-mesh codends, the net is constructed of 10.2-cm stretched-mesh polyethylene web (4 mm in body and codend and 5 mm in the wings and mouth area of the lower panel). For added protection, netting was doubled on the leading wing edges of the upper panel, the wings and mouth areas of the lower panel, the forward meshes of the side panels, the aft 10 meshes of the intermediate section, and throughout the codends. Riblines, constructed of 1.6-cm diameter poly dacron twisted rope, were hung along 92.5% of the stretched length of the netting.

Appendix

Description and construction diagram for the trawl and the auxiliary net

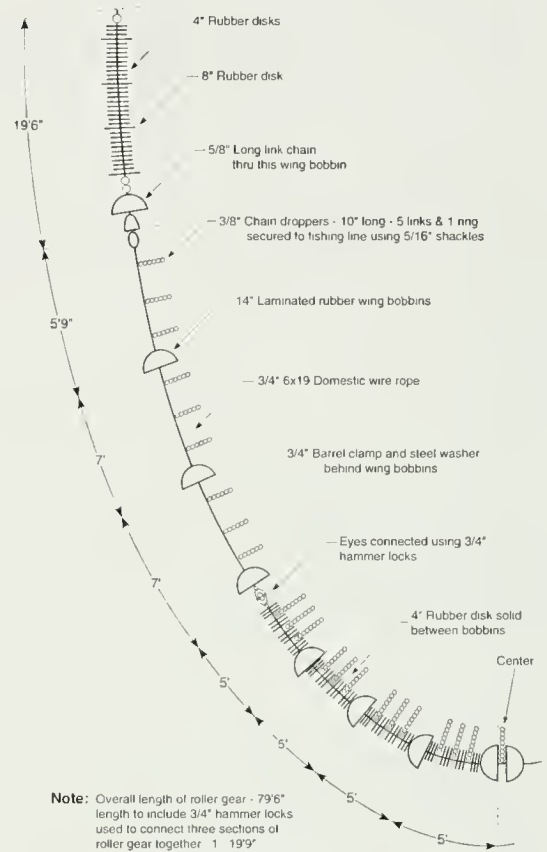
Poly Nor'eastern survey bottom trawl The Poly Nor'eastern is a high-rise, 4-seam, trawl rigged with rubber bobbin roller gear designed for use on moderately rocky terrain (Appdx. Fig.1). The net is constructed of 12.7-cm stretched-mesh polyethylene web (4-mm thickness top and sides, 5-mm thickness in the bottom and intermedi-

Side panel

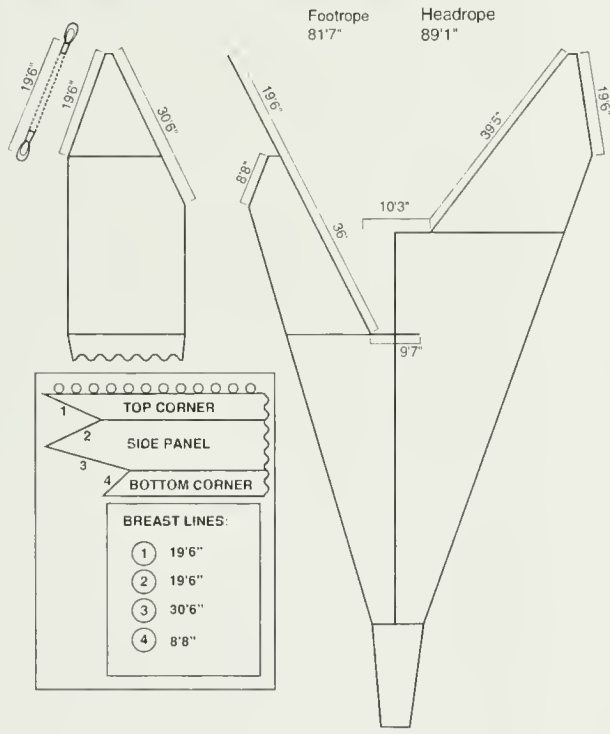


Web: Chaffing strip along inside of bottom wings and busom cut 8 meshes wide. 5 mm double bar mesh, goring 3 meshes on each side (leaving 2 open meshes). Secure 3 mesh of gore on inside (bar cut) of bottom wings, and securing other gore to footrope (bolsh).

Bobbin roller gear

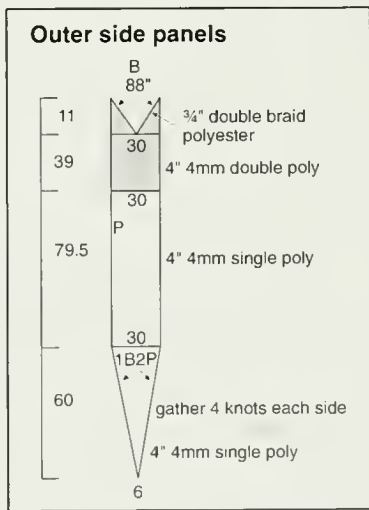
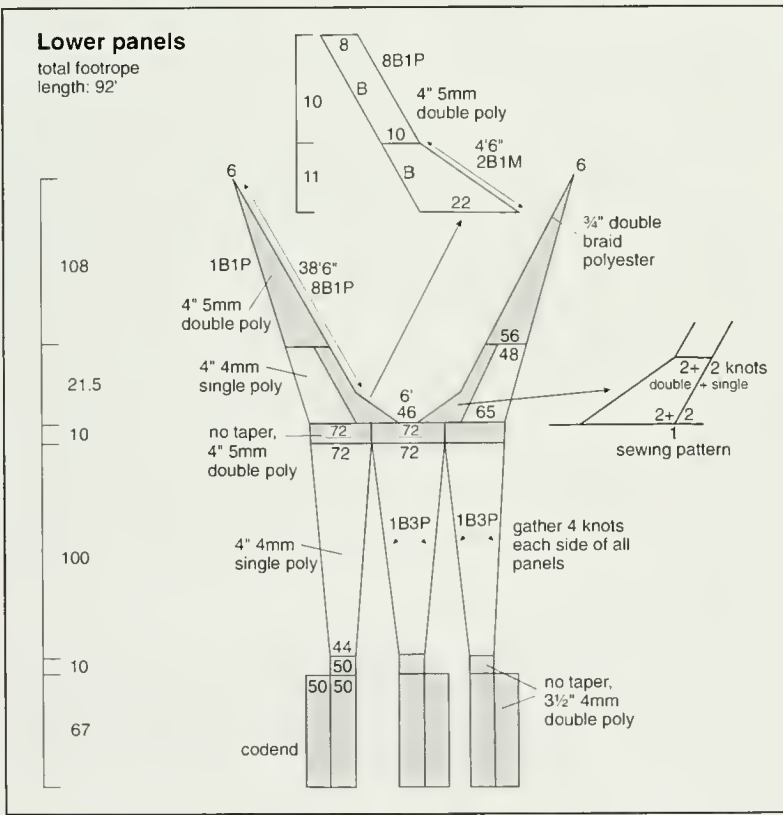
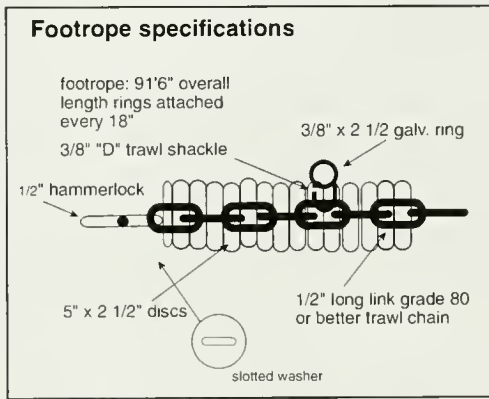
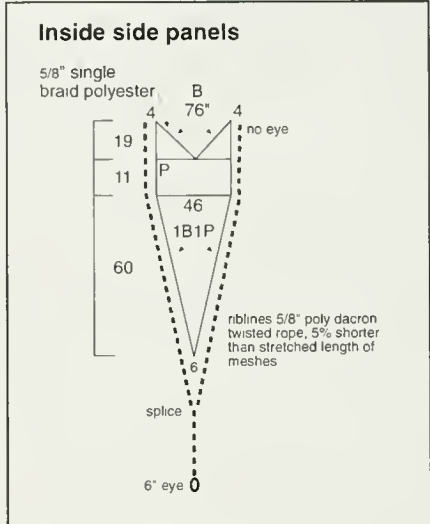
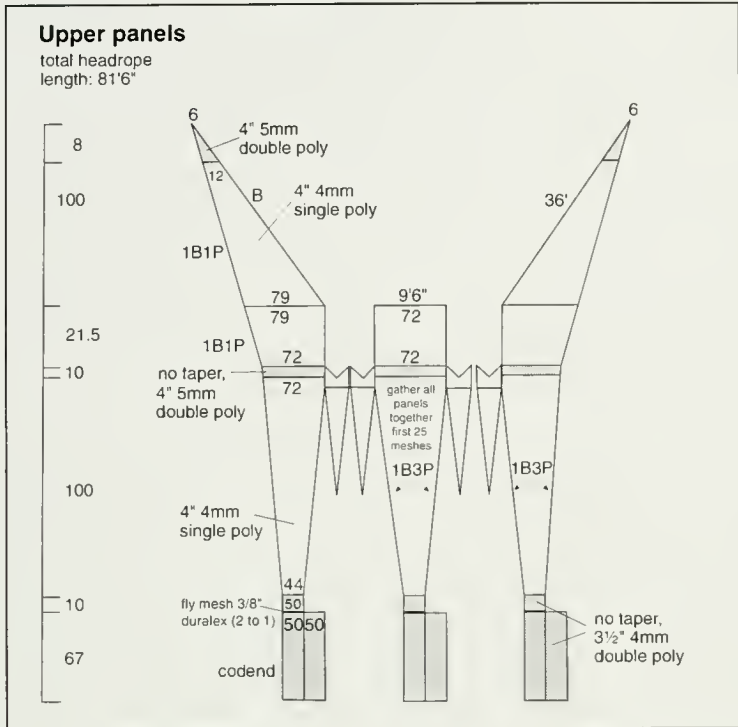


Framing lines for Poly Nor'easter trawl



Appendix Figure 1

Diagram of the Poly Nor'easter bottom trawl.



Tapers
 Key: P = point
 B = bar
 M = mesh
 [shaded box] double mesh

Appendix Figure 2

Diagram of the auxiliary net that was attached under the Poly Nor'easter bottom trawl to capture fish escaping under the footrope.

Yellow (*Perca flavescens*) and Eurasian (*P. fluviatilis*) perch distinguished in fried fish samples by DNA analysis

Rex M. Strange

Carol A. Stepien (contact author)

Email address for C. A. Stepien: Carol.Stepien@utoledo.edu

Great Lakes Genetics Laboratory
Lake Erie Center and Department of Environmental Sciences
The University of Toledo
6200 Bayshore Road
Toledo, Ohio 43618

DNA techniques are increasingly used as diagnostic tools in many fields and venues. In particular, a relatively new application is its use as a check for proper advertisement in markets and on restaurant menus. The identification of fish from markets and restaurants is a growing problem because economic practices often render it cost-effective to substitute one species for another. DNA sequences that are diagnostic for many commercially important fishes are now documented on public databases, such as the National Center for Biotechnology Information's (NCBI) GenBank.¹ It is now possible for most genetics laboratories to identify the species from which a tissue sample was taken without sequencing all the possible taxa it might represent.

We were contacted by reporters from a news agency, who were interested in determining whether yellow perch "fish fries" in their local restaurants were, in fact, local yellow perch (*Perca flavescens* Mitchell) taken from the Great Lakes. In recent years it has become economically desirable to substitute Eurasian perch (*P. fluviatilis* Linnaeus) or some other species for yellow perch because of the decline of stocks of yellow perch in the Great Lakes and because of rising prices, both of which raise truth-in-advertising questions. Such cases of substitution usually involve replacement with less expensive fish species, which are difficult to detect in fillets (see Ward, 2000).

We agreed to attempt to identify the fish using DNA techniques because the Great Lakes Genetics Laboratory has several on-going projects involving evolutionary genetics of yellow perch and other percids (e.g., Faber and Stepien, 1997; Ford and Stepien, 2004). However, instead of the fresh frozen fillets that we expected, the reporters sent us breaded and deep fried fish fillets taken from served dinners. We decided to attempt to identify the species of the fish, despite our initial misgivings as to whether useful amounts of DNA could be extracted from deep-fried material. In the present study, we outline a procedure with molecular tools and an analysis that allows the identification of any species for which sequences are documented on GenBank.¹

Materials and methods

We removed approximately 10 mg of muscle tissue from below the breading of each fried fillet, submerged the tissue in an ethanol (95%) wash, and allowed the wash to sit overnight at room temperature. No other attempt was used to remove any residual cooking oil. Samples were then air-

dried before digestion with proteinase K. After complete digestion, DNA was isolated by using standard phenol-chloroform extractions, alcohol precipitation, and two washes with 70% ethanol. From experience, we found that the final pellet of DNA was smaller than the DNA yield we would expect from uncooked material; therefore we suspended the pellet with 30 μ L (microliters) of dd (deionized distilled) H₂O rather than the 100 μ L we typically use.

The polymerase chain reaction (PCR) was used to amplify a fragment (approximately 400 base pairs) of the mitochondrial cytochrome *b* gene with the following universal primers described by Palumbi (1996): L14724 (5'-GTG ACT TGA AAA ACC ACC GTT G-3') and Kocher et al. (1989): H15149 (5'-TGC AGC CCC TCA GAA TGA TAT TTG TCC TCA-3'). We chose this particular fragment for two reasons: 1) cytochrome *b* is commonly used in systematic studies of fishes and a wide variety of fish taxa are documented in the GenBank¹ data base, including percids (e.g., Song et al., 1998; Near, 2002; Sloss et al., 2004); and 2) our previous experience has shown that PCR amplification of smaller fragments is often more successful than amplification of larger fragments, especially when dealing with degraded samples such as extracts from deep-fried fillets.

The PCR mixture consisted of a total volume of 50 μ L, with concentrations of 1.5 mM (milli Molar) MgCl₂, 1.0 μ M (micro Molar) of each primer, and 1.0 U (units) of *Taq* polymerase. Amplification parameters consisted of an initial denaturation at 94°C for 2.5 min, followed by 35 cycles of denaturation (94°C, 1 min), primer annealing (52°C, 1 min), and polymerase extension (72°C, 1 min). A final extension at 72°C for 7 min was included to reduce the number of partial strands. Amplification products were then purified by running the entire product

¹ GenBank. 2006. National Center for Biotechnology Information (NCBI), National Institutes of Health, 8600 Rockville Pike, Bethesda, MD 20894. Website: <http://www.ncbi.nlm.nih.gov> (accessed 14 February 2006).

Manuscript submitted 16 June 2006 to the Scientific Editor's Office.

Manuscript approved for publication 6 September 2006 by the Scientific Editor. *Fish. Bull.* 105:292–295 (2007).

on a 2% agarose gel in TAE (Tris-acetate-EDTA, p.H. 8.0) buffer. The band was made visible with ethidium bromide staining and was then excised and purified in a spin column. The resulting gel-purified PCR product was then used as a template for another round of PCR with identical parameters. Samples consisting of 250 ng (nanograms) of purified PCR product and 16 pmol (pico moles) of primer (L14724) were sequenced on an automated ABI 3700 sequencer (Applied Biosystems Inc., Fullerton, CA).

Because we did not know the identity of the species in the fish fillets, each sequence was submitted to a BLAST (basic local alignment search tool) search on the NCBI GenBank¹ database, which provides the identification of species by sequences. After we were confident that the identities of the species in the fillets were limited to the genus *Perca*, the sequences were aligned sequentially with cytochrome *b* sequence data from all three species of *Perca* (e.g., *P. flavescens*, *P. fluviatilis*, and *P. schrenkii*), and two outgroup percid taxa (walleye [*Sander vitreus*] and ruffe [*Gymnocephalus cernuus*]) by using the computer program CLUSTALX² (Thompson et al., 1997). A tree of the relationships among the sequences was constructed by using maximum likelihood estimates of sequence divergences with a neighbor-joining network (Saitou and Nei, 1987) as implemented in the computer program PHYLIP (PHYLogeny Inference Package; Felsenstein³).

Results and discussion

Our extraction procedure yielded DNA usable for PCR and subsequent sequencing, although the extractions were degraded and of relatively low molecular weight. Thirteen complete cytochrome *b* sequences representing all three species of *Perca* were found documented on GenBank¹ (Table 1). Yellow perch is one of three described species of this genus, for which a substantial fishery exists in the Great Lakes, although fish stocks have declined at some localities.⁴ The natural distribution of yellow perch extends from Nova Scotia south along the Atlantic coast of North America to South Carolina, and west to Montana (Scott and Crossman, 1973; Craig, 2000). The Eurasian perch is very similar morphologically to *P. flavescens*, is found throughout most of

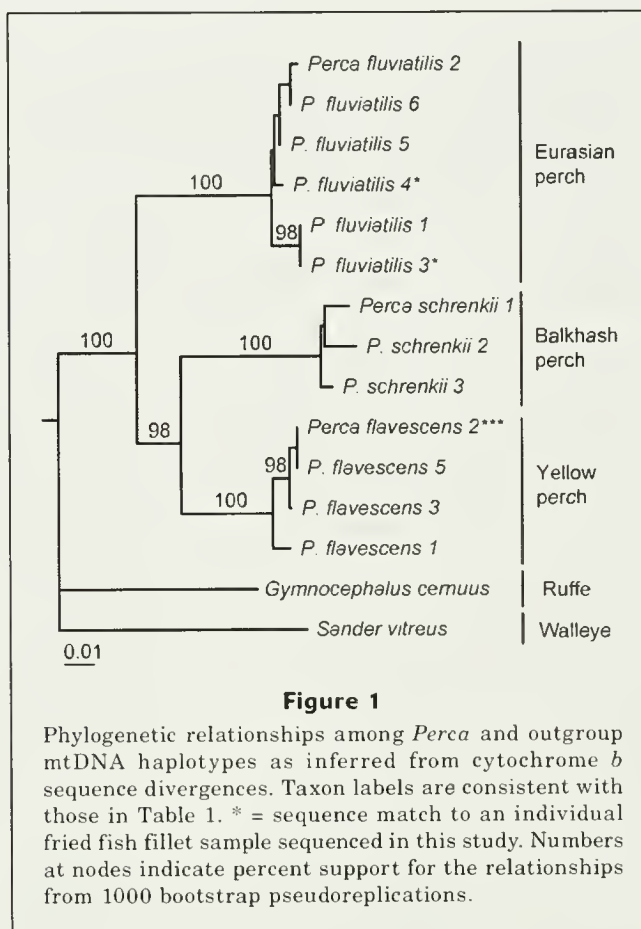


Figure 1

Phylogenetic relationships among *Perca* and outgroup mtDNA haplotypes as inferred from cytochrome *b* sequence divergences. Taxon labels are consistent with those in Table 1. * = sequence match to an individual fried fish fillet sample sequenced in this study. Numbers at nodes indicate percent support for the relationships from 1000 bootstrap pseudoreplications.

northern Europe and Asia (Craig, 2000; Maitland, 2000), and also represents a commercially important species. A third species, *P. schrenkii* Kessler, is restricted to the eastern portion of Kazakhstan and does not contribute to the world market.

Each species of *Perca* is represented by unique nucleotide cytochrome *b* sequences and has marked divergences (Fig. 1). Three of our five samples matched one of the cytochrome *b* sequences of the yellow perch *P. flavescens* (designated as *flavescens* 2), and two matched sequences of the Eurasian perch *P. fluviatilis* (denoted as *fluviatilis* 3 and *fluviatilis* 4). It is noteworthy that large genetic divergences separate the mtDNA cytochrome *b* sequences of *P. flavescens* and *P. fluviatilis*. These two species differ at 130 sites (11.4%; Song et al., 1998; Sloss et al., 2004), and intraspecific variation for each is an order of magnitude less (Fig. 1; also see Billington, 1993). Thus, it is unlikely that our identifications were in error.

Although one would expect that most of the perch fillets at local markets are caught locally, the supply of and demand for North American and Eurasian perch determines which species is the most economical to serve. Importers and exporters trade fish from both sides of the ocean and the price fluctuates seasonally for both species. Winter is the low supply period for both,

² Gibson, T., D. Higgins, J. Thompson, and F. Jeanmougin. 2006. ClustalX. Plate-forme de bio-informatique (Bio-informatique platform), I.G.B.M.C., 1 rue Laurent Fries, 67404 Illkirch, Cedex, France. Website: <http://bips.u-strasbg.fr/fr/Documentation/ClustalX> (accessed 14 February 2006).

³ Felsenstein, J. 1995. Department of Genome Sciences, University of Washington, Box 357730, Seattle, Washington, USA 98195-7730. Website: <http://evolution.genetics.washington.edu/phylip/general.html> (accessed 20 February 2006).

⁴ Johnson, T. B. 2006. Personal commun. Ontario Ministry of Natural Resources, Glenora Fisheries Station, R.R. #4, 21 Hatchery Lane, Picton, Ontario, Canada K0K 2T0.

Table 1

Taxonomic assignment and GenBank (Footnote 1 in the main text) accession numbers for each of the diagnostic mitochondrial cytochrome *b* sequences used in our comparisons with unknown fried fish fillets. Sequences from ruffe (*Gymnocephalus cernuus*) and walleye (*Sander vitreus*) were used for outgroup comparison. Taxonomic labels are consistent with the labeling on the tree in Figure 1. Each asterisk denotes that a single fried fish fillet sample was matched to this known sequence. * = one sample matched; *** = three samples matched.

Taxon	Haplotype designation	GenBank accession number
Yellow perch	<i>Perca flavescens</i> 1	AY374280
	<i>P. flavescens</i> 2***	AF546115
	<i>P. flavescens</i> 3	AF386600
	<i>P. flavescens</i> 4	AF045357
Eurasian perch	<i>Perca fluviatilis</i> 1	AY374281
	<i>P. fluviatilis</i> 2	AF546117
	<i>P. fluviatilis</i> 3*	AF546116
	<i>P. fluviatilis</i> 4*	AY929376
	<i>P. fluviatilis</i> 5	AF386599
	<i>P. fluviatilis</i> 6	AF045358
Balkash perch	<i>Perca schrenkii</i> 1	AF546120
	<i>P. schrenkii</i> 2	AF546119
	<i>P. schrenkii</i> 3	AF546118
Ruffe	<i>Gymnocephalus cernuus</i>	AF386598
Walleye	<i>Sander vitreus</i>	AF386602

but prices quickly fall as the ice clears from the Great Lakes.⁴ In North America, the fishery in Lake Michigan (near Milwaukee, Wisconsin) crashed by 2000 and most perch taken in the past from the Great Lakes are presently taken from Lake Erie.^{4,5,6}

Lake Erie itself is divided into four quota zones across both U.S. and Canadian waters, of which Zone 2 (comprising the west-central basins) has the largest U.S. allowable quota.^{4,5,6} Most of those perch are landed and processed in Wheatley, Ontario, where the largest processing plants are located.^{4,6} Current landed prices for North American yellow perch are about Can \$2.00/lb, whereas the market price for processed fish runs about Can \$8–9/lb.⁴ Eurasian perch have been sold in North American markets for over 20 years, and presently are cheaper than North American yellow perch, selling for Can \$2–3/lb.⁴ Thus, restaurants in the Great Lakes area that advertise yellow perch “fish fries” may be unlikely to offer economical all-you-can-eat dinners and stay in business without imported Eurasian perch. Our results illustrate that use of mtDNA sequencing is an economic and effective method to identify the species in

fillets for perch (and other species), even in the case of genetic material that has been deep fried.

Acknowledgments

We thank T. Johnson (Ontario Ministry of Natural Resources) and T. Bader (Ohio Division of Wildlife) for information regarding the Lake Erie perch fishery and the importation of Eurasian yellow perch. We also thank R. Knight (Ohio Division of Wildlife) for providing valuable comments on the manuscript, along with Great Lakes Genetic Laboratory graduate students A. Haponski and M. Neilson and research technician R. Lohner for help. This study was supported by grants to C. Stepien from the Lake Erie Protection Fund no. 00-15, NOAA Sea Grant no. R/LR-7 through Ohio Sea Grant, and USEPA CR-83281401-0. RMS was supported as a postdoctoral researcher in the Great Lakes Genetics Laboratory. This is contribution number 2007-04 from the Lake Erie Center.

Literature cited

- Billington, N.
1993. Genetic variation in Lake Erie yellow perch (*Perca flavescens*) demonstrated by mitochondrial DNA analysis. *J. Fish Biol.* 43:941–943.
- Baldwin, N. S., R. W. Saalfeld, M. R. Dochoda, H. J. Buettner, and R. L. Eshenroder. 2002. Commercial Fish Production in the Great Lakes 1867–2000. Website: <http://www.glf.org/databases/commercial/commerc.php> (accessed on 26 July 2006).
- Bader, T. J. 2005. Personal commun. Ohio Division of Wildlife, Fairport Fish Research Unit, 1190 High St., Fairport Harbor, OH, USA 44077.
- Craig, J. F.
2000. Percid fishes: systematics, ecology, and exploitation, 352 p. Blackwell Science, Oxford, UK.

- Faber, J. E., and C. A. Stepien.
1997. The utility of mitochondrial DNA control region sequences for analyzing phylogenetic relationships among populations, species, and genera of the Percidae. *In* Molecular systematics of fishes (T. D. Kocher, and C. A. Stepien, eds.), p. 129-134. Academic Press, San Diego, CA.
- Ford, A. M., and C. A. Stepien.
2004. Genetic variation and spawning population structure in Lake Erie yellow perch, *Perca flavescens*: a comparison with a Maine population. *In* Proceedings of Percis III, the 3rd international symposium on percid fishes (T. P. Barry, and J. A. Malison, eds.), p. 131-132. Univ. Wisconsin Sea Grant Institute, Madison, WI.
- Kocher, T. D., W. K. Thomas, A. Meyer, S. V. Edwards, S. Paabo, F. X. Villablanca, and A. C. Wilson.
1989. Dynamics of mitochondrial DNA evolution in animals: amplification and sequencing with conserved primers. *Proc. Natl. Acad. Sci. USA* 86:6196-6200.
- Maitland, P. S.
2000. Guide to freshwater fish of Britain and Europe, 256 p. Octopus Publ. Group, Ltd., London, UK.
- Near, T. J.
2002. Phylogenetic relationships of *Percina* (Percidae: Etheostomatinae). *Copeia* 2002:1-14.
- Palumbi, S. R.
1996. Nucleic acids II: The polymerase chain reaction. *In* Molecular systematics, 2nd ed. (D. M. Hillis, C. Moritz, and B. K. Mable, eds.), p. 205-247. Sinauer Assoc., Sunderland, MA.
- Saitou, N., and M. Nei.
1987. The neighbor-joining method: a new method for reconstructing phylogenetic trees. *Mol. Biol. Evol.* 4:406-425.
- Scott, W. B., and E. J. Crossman.
1973. Freshwater fishes of Canada, 966 p. Fish. Res. Board Can., Ottawa, Canada.
- Sloss, B. L., N. Billington, and B. M. Burr.
2004. A molecular phylogeny of the Percidae (Teleostei, Perciformes) based on mitochondrial DNA sequence. *Mol. Phylogenet. Evol.* 32:545-562.
- Song, C. B., T. J. Near, and L. M. Page.
1998. Phylogenetic relations among percid fishes as inferred from mitochondrial cytochrome *b* DNA sequence data. *Mol. Phylogenet. Evol.* 10:343-353.
- Thompson, J. D., T. J. Gibson, F. Plewnial, F. Jeanmougin, and D.G. Higgins.
1997. The CLUSTALX windows interface: flexible strategies for multiple sequence alignment aided by quality analysis tools. *Nucleic Acids Res.* 22:4673-4680.
- Ward, R. D.
2000. Genetics in fisheries management. *Hydrobiologia* 420:191-201.

Natural mortality rate, annual fecundity, and maturity at length for Greenland halibut (*Reinhardtius hippoglossoides*) from the northeastern Pacific Ocean

Daniel W. Cooper (contact author)¹

Katherine P. Maslenikov²

Donald R. Gunderson²

Email address (for D. W. Cooper): dan.cooper@noaa.gov

¹ Alaska Fisheries Science Center F/AKC 2
7600 Sand Point Way NE
Seattle, Washington 98115-0700.

² University of Washington
School of Aquatic and Fishery Sciences
1122 NE Boat Street
Seattle, Washington 98195.

Mortality, fecundity, and size at maturity are important life history traits, and their interactions determine the evolution of life history strategies (Roff, 1992; Stearns, 1992; Charnov, 2002). These same traits are also important for population dynamics models (Hunter et al., 1992; Clark, 1999). It is increasingly important to accurately determine Greenland halibut (*Reinhardtius hippoglossoides*) life history traits and to correctly assess the status of its stocks because low recruitment or low biomass estimates have led to catch restrictions in the Bering Sea and Aleutian Islands (Ianelli et al.¹), the Northeastern Arctic (Ådlandsvik et al., 2004), and the Northwest Atlantic (Bowering and Nedreaas, 2000).

Mortality has been estimated for stocks of Greenland halibut from the Northwest Atlantic (Bowering, 1983) and from the Bering Sea (Ianelli et al.¹) from population age structures where a maximum age near 20 years has been assumed. However, recent age validation (Treble et al.²) and a

new aging technique (Gregg et al., 2006) indicate that Greenland halibut may have a lower mortality rate and live longer. Fecundity estimates (Gundersen et al., 2000) and length at maturity estimates (Morgan et al., 2003) vary by geographic area and year for Greenland halibut in the Atlantic. Fecundity of Greenland halibut from the Bering Sea has been estimated once (D'yakov, 1982), and no estimates for Greenland halibut maturity at length have been reported from Alaskan waters.

A significant and positive relationship between natural mortality rate (M) and annual reproductive effort, as measured by gonadosomatic index ($GSI = \text{ovary weight} / \text{somatic body weight}$), was found for 28 fish stocks of a variety of species ($M = 1.79 \times GSI$, $r^2 = 0.75$) (Gunderson, 1997). This GSI- M relationship can provide an estimate of M independent of age data, and is desirable for Greenland halibut because age data are still

controversial for this species. The objectives of this study are to estimate annual fecundity, length at 50% maturity, and the rate of instantaneous natural mortality (M) by using GSI for Greenland halibut from the Bering Sea and Aleutian Islands.

Materials and methods

Ovaries were collected by fishery observers and scientists from the National Marine Fisheries Service (NMFS) in the Bering Sea and Aleutian Islands (Table 1, Fig. 1). Fork length (cm) and somatic weight (kg) (ovaries and stomach contents removed) were recorded at sea. Total weight was approximated by adding somatic weight and the estimated fresh ovary weight.

Ovaries were removed and placed in a 10% formalin solution buffered with sodium bicarbonate. Twenty-eight ovaries were weighed (± 2 g) before being placed in formalin. The fresh weight was later compared to formalin weight to determine a conversion factor when fresh weight was not available. Ovaries were removed from the 10% buffered formalin, blotted dry, and weighed (± 0.001 g). When possible, a whole cross section was removed from one lobe of an ovary for histological analysis. If the ovary cross section was too large to fit on a slide, a wedge-shaped sample was removed which included tissue from the center of the ovary to the ovarian wall. Ovary tissue samples were embedded in paraffin, sectioned at 4 μm , and stained with hematoxylin and eosin. All 56 specimens smaller than 40 cm were obviously immature because of their very small ovaries; therefore histological examination was completed on only six of these specimens to verify that they were immature.

¹ Ianelli, J. N., T. K. Wilderbuer, and D. Nichol. 2005. Stock assessment and fishery evaluation: Bering Sea and Aleutian Islands Greenland turbot. Website: <http://www.afsc.noaa.gov/refm/docs/2005/BSAIGturbot.pdf> (accessed on 28 June 2006).

² Treble, M. A., S. E. Campana, R. J. Wastle, C. M. Jones, and J. Boje. 2005. An assessment of age determination methods, with age validation of Greenland halibut from the Northwest Atlantic. NAFO SCR Doc. 05/43, 22 p. Northwest Atlantic Fisheries Organization, P.O. Box 638, Dartmouth, Nova Scotia, Canada B2Y 3Y9.

Manuscript submitted 18 March 2005 to the Scientific Editor's Office.

Manuscript approved for publication 8 September 2006 by the Scientific Editor. Fish. Bull. 105:296–304 (2007).

Each slide was analyzed for the oocyte stages present and for postovulatory follicles (POFs) according to the descriptions and images from Gunderson (2003) (Fig. 2). Maturity stages were assigned according to Gunderson et al. (2003).

Length-GSI relationship and instantaneous rate of natural mortality

For the GSI-M relationship, Gunderson (1997) defined GSI as the point in ovarian development when the ovaries had attained maximum weight due to vitellogenesis, but had not gained nonenergetic weight (due to hydration). For this study, fish with ovaries in maturity stage vitellogenesis 4 (Fig. 2) were used in the GSI-M estimate. Fish with ovaries containing hydrated oocytes or POFs were excluded. Fedorov (1968) found that dry weights of oocytes corresponding to the vitellogenesis-4 stage (yolk-filled oocyte in the trophoplasmic growth stage) were equal to dry weights of hydrated ova; this result indicates that yolk deposition is completed at the vitellogenesis-4 stage.

The length of the average mature female in an unexploited population is required for Gunderson's (1997) GSI-M relationship. The foreign trawl fishery prior to 1988 showed the best selectivity for fish in the widest size range (Ianelli and Wilderbuer³). Foreign trawl fishery data from the NMFS Observer program (Berger⁴) were analyzed, and the oldest complete data set (1977–87) was chosen to best approximate the true nature of the Greenland halibut population in the absence of fishing pressure. The mean length of mature females was determined from the weighted length by using data on the abundance at each length as weights.

Potential annual fecundity

To test for homogeneity of vitellogenic oocyte density throughout the ovaries, subsamples were selected from nine fish at three locations (anterior, middle, and posterior) on each ovary lobe (eyed side and blind side) for a total of six subsamples per fish. Cross sections were taken through the ovary and included the ovarian wall. For the anterior and middle sections, one half of the cross section was used as the subsample. The posterior cross sections of the ovary were much smaller and therefore the entire cross section was used. The subsamples had a mean weight of 2.07 grams (standard error [SE]=0.14) and a mean number of 553 vitellogenic

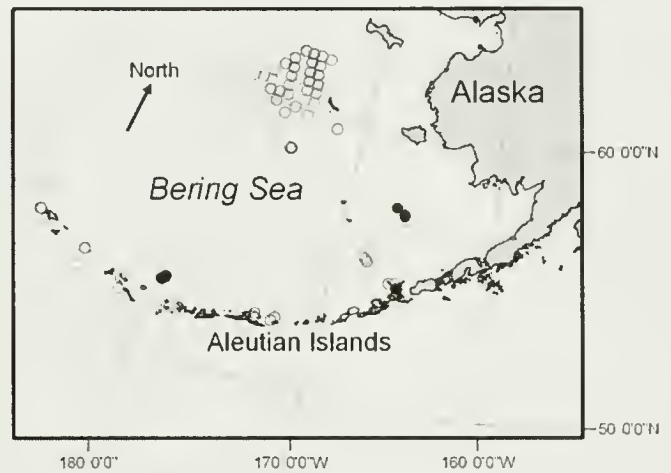


Figure 1

Map of locations where Greenland halibut (*Reinhardtius hippoglossoides*) were collected for ovary samples. Open circles mark locations where fish were collected for the ovary samples. Filled circles mark locations where fish were collected for the natural mortality (*M*) estimate.

Table 1

Number of Greenland halibut (*Reinhardtius hippoglossoides*) females collected by month and year.

Month	Year					Total
	1999	2000	2002	2003	2004	
January						
February						
March					19	19
April						
May						
June		13	3	1		17
July		44	8	101		153
August						
September	78	42				120
October		2				2
November						
December						
Total	78	101	11	102	19	311

oocytes (SE=43.11). Oocyte density (number of oocytes/gram of ovarian tissue) and diameters of 50 of the most advanced oocytes per fish were recorded.

Two-way ANOVAs were used to test for differences in oocyte density and diameter between ovarian lobes and among ovarian locations. Paired *t*-tests were used to identify differences among ovarian locations when the ANOVA detected significant differences.

Greenland halibut are reported to have determinate fecundity (Gunderson et al., 2001; Junquera et al.,

³ Ianelli, J. N., and K. T. Wilderbuer. 1995. Greenland turbot (*Reinhardtius hippoglossoides*) stock assessment and management in the Eastern Bering Sea. In Proceedings of the International Symposium on North Pacific flatfish, p. 407–441. Alaska Sea Grant report 95-04. Univ. Alaska Sea Grant College Program, P. O. Box 755040, Fairbanks, AK 99775.

⁴ Berger, J. 2002. Personal commun. Alaska Fisheries Science Center, National Marine Fisheries Service, 7600 Sand Point Way NE, Seattle, WA 98115.

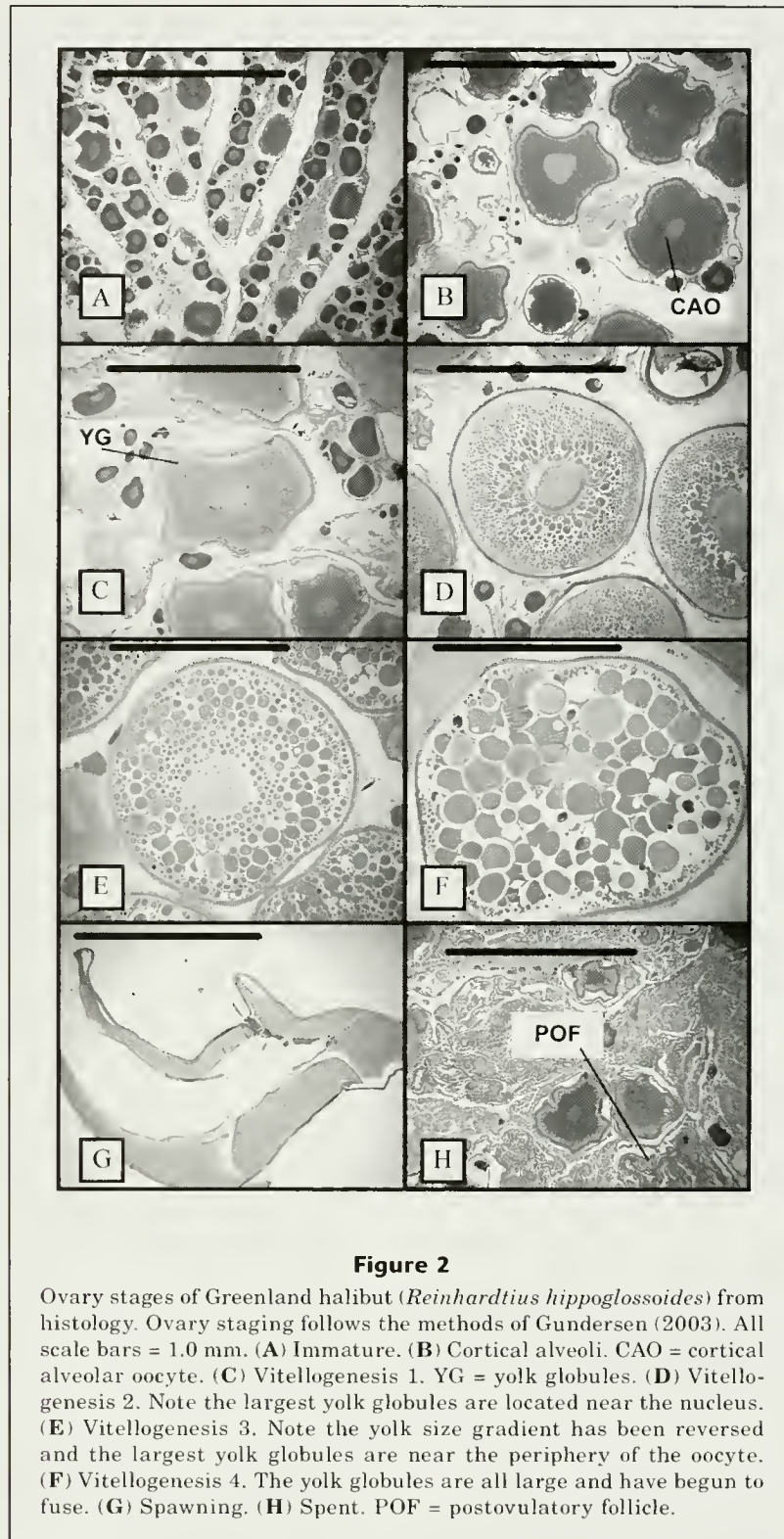


Figure 2

Ovary stages of Greenland halibut (*Reinhardtius hippoglossoides*) from histology. Ovary staging follows the methods of Gundersen (2003). All scale bars = 1.0 mm. (A) Immature. (B) Cortical alveoli. CAO = cortical alveolar oocyte. (C) Vitellogenesis 1. YG = yolk globules. (D) Vitellogenesis 2. Note the largest yolk globules are located near the nucleus. (E) Vitellogenesis 3. Note the yolk size gradient has been reversed and the largest yolk globules are near the periphery of the oocyte. (F) Vitellogenesis 4. The yolk globules are all large and have begun to fuse. (G) Spawning. (H) Spent. POF = postovulatory follicle.

2003). To confirm this for Greenland halibut in the Bering Sea, oocyte diameters were measured to determine if there is a hiatus in size between developing and reserve oocytes. Mean diameters of nonvitellogenic

and vitellogenic oocytes were measured from whole oocyte tissue samples. All vitellogenic oocytes in a tissue sample of known weight were counted. The oocytes were placed in a dish on top of a sampling grid. All

oocytes touching the lines of the sampling grid were measured until 50 nonvitellogenic and 50 vitellogenic oocytes had been measured. Nonvitellogenic oocytes were reported as percent frequency, whereas vitellogenic oocytes were reported as number of vitellogenic oocytes per gram of ovary tissue. Because oocyte diameter may vary by ovary location (see "Results" section), all oocyte measurements were taken from the middle location of the ovaries.

To select ovaries suitable for fecundity estimates, the diameters of six vitellogenic oocytes sectioned through the nucleus were measured from the histological sections by using a microscopic image analysis system. Because oocytes were not perfectly round, oocyte diameter was calculated from oocyte area with the following equation:

$$\text{Diameter} = 2\sqrt{\frac{\text{Oocyte Area}}{\pi}}$$

Females with the mean diameter of vitellogenic oocytes smaller than 1000 μm were excluded from the fecundity estimate because not all oocytes to be spawned in the current year could be identified (see "Results" section). To exclude fish that had already begun spawning, samples containing POFs or ova were excluded.

Fecundity was estimated gravimetrically by counting vitellogenic oocytes from weighed subsamples of ovarian tissue. The weight of the thick ovarian wall could not be discounted; therefore subsamples were cut with a proportionately weighted piece of ovarian wall attached. This procedure was accomplished by using either an entire cross section of the ovary, or a wedge-shaped sample cut from an entire cross section. Because small oocyte density differences were found between the posterior location and the anterior+middle locations, and between the eyed and blind lobes (see "Results" section), four subsamples were taken for each fish. The posterior region of each lobe and the area between the middle and anterior locations of each lobe were sampled. Weighting factors for the posterior and for the middle and anterior locations of the ovary were determined by calculating the proportional mass of these locations of the ovaries for 26 fish. The average proportional mass for the posterior and for the middle and anterior locations was 0.11 and 0.89 (SE: 0.0048), respectively. When divided by two (to account for the two ovary lobes), the average weighting factors for the posterior blind and eyed lobes = 0.06, and the average weighting factor of the anterior and middle locations for the blind and eyed lobes = 0.44. Fecundity of each female was estimated from the four subsamples by using the fecundity equation with weighting factors from Nichol and Acuna (2001) to account for the smaller proportional mass of the posterior sections.

The fraction of vitellogenic oocytes undergoing atresia was estimated for 174 fish from histological cross sections. The total number of vitellogenic oocytes and the number of atretic vitellogenic oocytes (Hunter and Macewicz, 1985) for each histological section were

counted. The fraction of vitellogenic oocytes undergoing atresia was estimated as the number of atretic vitellogenic oocytes divided by the total number of vitellogenic oocytes.

Length at maturity

Maturity was determined histologically, by using all fish 40 cm and larger, and a subsample ($n=6$) of females less than 40 cm. Maturity stages were determined according to the method of Gunderson (2003).

Results

Length-GSI relationship and instantaneous rate of natural mortality

The conversion factor between ovary fresh weight and weight after fixation and storage in formalin was:

$$\text{Fresh} = (1.437 \times \text{Formalin}) + 6.8276, \quad (n=28, r^2=0.9903),$$

where *Fresh* = fresh ovary weight (g); and

Formalin = ovary weight after storage in formalin (g).

Maturity stages increased from spring (March) to summer (June and July) and again to autumn (September and October) (Fig. 3). In March, mature females were spawning, spent, or beginning vitellogenesis for the next spawning season. Most fish were in the vitellogenesis-1 stage. By June–July, the ovaries had advanced until most were in the vitellogenesis-2 stage, although some were also in stages vitellogenesis 1 and 3. By September–October, the majority of mature ovaries were in vitellogenesis-3 stage, although some had progressed to vitellogenesis 4 and a small percentage (4%) of the mature females collected in September were ready to spawn (presence of hydrated oocytes) or showed signs of recent spawning (presence of ova or POFs). The largest mean oocyte diameter ($n=6$ for histological examination) for any female with oocytes before hydration was 1720 μm .

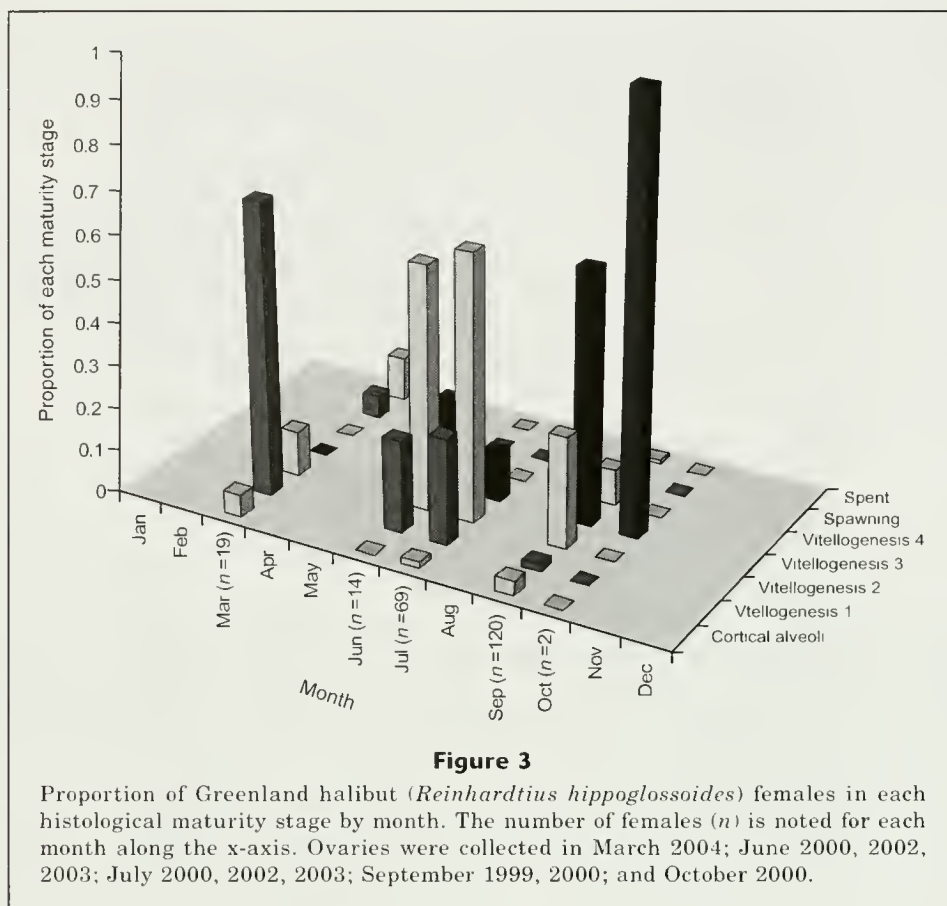
The mean length of mature females was 79.2 cm during 1977–87, and the GSI data were derived from females smaller and greater than 79.2 cm. The GSI was very poorly correlated with length ($r^2=0.04$), and we used the mean GSI (0.063, $\sigma^2=0.000018$) in our sample to obtain a natural mortality estimate of $M = 0.112$. The variance of M ($\text{Var } \hat{M}$, 0.0002) was estimated according to the method of Gunderson et al. (2003) with the following equation:

$$\text{Var } \hat{M} = (\overline{\text{GSI}})^2 \text{Var}(\hat{k}) + \hat{k}^2 \text{Var}(\overline{\text{GSI}}),$$

where $\text{Var } \hat{M}$ = the variance of mortality;

$\overline{\text{GSI}}$ = mean value of GSI; and

\hat{k} = constant from the GSI-M regression (Gunderson, 1997).



The final estimate of instantaneous natural mortality (*M*) in our study had a standard error of 0.0138, yielding a 95% confidence interval of 0.08–0.14).

Potential annual fecundity

When nine females were tested for the difference in mean oocyte density by ovary location, the difference was significant (two-way ANOVA, $P < 0.01$, $df = 2$, $F = 19.7$). Mean oocyte densities were 280, 276, and 240 in the anterior, middle, and posterior locations in ovaries, respectively. Paired *t*-tests indicated that the posterior location had a significantly lower oocyte density than middle ($P < 0.001$) or anterior locations ($P < 0.001$), whereas the middle and anterior locations were not significantly different from each other ($P = 0.19$). Oocyte density was also slightly lower in the eyed (259 eggs/gram) than in the blind lobe (272 eggs/gram; two-way ANOVA, $P = 0.034$, $df = 1$, $F = 4.8$).

Mean oocyte diameters also varied significantly by ovary location (two-way ANOVA, $P = 0.047$, $df = 2$, $F = 3.4$). Mean oocyte diameters for the anterior, middle, and posterior locations were 1611, 1627, and 1609 μm , respectively. We observed two distinct and separate oocyte size-frequency modes corresponding to nonvitellogenic and vitellogenic oocytes when the average vitellogenic oocyte diameter exceeded 1000 μm (Fig. 4). On the basis of these results, we decided to include only those

samples where the mean vitellogenic oocyte diameter was greater than 1000 μm ($n = 6$ oocytes per specimen for histological examination).

Potential annual fecundity data conformed more closely to a linear regression on total weight:

$$Fec = 13.438 (Wt_{total}(g)) - 436.4438 \quad r^2 = 0.6206, n = 47$$

where Fec = fecundity; and
 Wt_{total} = total weight,

than to a nonlinear regression on length (Fig. 5):

$$Fec = 0.0266 (ForkLength(\text{cm}))^{3.3654}, \quad r^2 = 0.4969, n = 47$$

where Fec = fecundity; and
 $ForkLength$ = fork length.

The highest fractions of atretic vitellogenic oocytes occurred in females with oocytes in early stages of vitellogenesis. Once the largest cohort of vitellogenic oocytes reached a diameter of 750 μm , the fraction of atresia was greater than 0.20 for only one of 153 specimens. Over 77% of females with developing oocytes had fractions of atresia of 0.05 or less, and over 90% of females had fractions of atresia of 0.10 or less. For fish that met oocyte diameter criteria for fecundity estimates

Table 2

Greenland halibut (*Reinhardtius hippoglossoides*) female length (cm) at 50% maturity determined in the present study and in other studies. Examination method column indicates whether visual macroscopic gonad inspection or histological examination was used to assign maturity stages.

Study	Examination method	Area	Length
This study	Histological	Bering Sea, Aleutian Islands	65–70
Walsh and Bowering (1981)	Histological and visual	Northern Labrador	75–80
Nielsen and Boje ¹	Histological	West Greenland Fjords	65
Junquera et al. (1999)	Visual, checked with histological	Flemish Cap (N. Atlantic)	64.5–69.5
Gundersen (2003)	Visual, checked with histological	Barents Sea	57.8
Morgan et al. (2003)	Visual	Gulf of St. Lawrence 1978–1981	58.2
Morgan et al. (2003)	Visual	Gulf of St. Lawrence 1996–2000	48.2
Morgan et al. (2003)	Visual	Labrador-eastern Newfoundland	78.5
Morgan et al. (2003)	Visual	Eastern Greenland	62.7
Morgan et al. (2003)	Visual	Iceland	64
Morgan et al. (2003)	Visual	Barents Sea (Norwegian data)	57.3
Morgan et al. (2003)	Visual	Barents Sea (Russian data)	60.6

¹ Nielsen, J. G., and J. Boje. 1995. Sexual maturity of Greenland halibut at West Greenland based on visual and histological observations. NAFO SCR Doc. 95/18, 7 p. Northwest Atlantic Fisheries Organization, P.O. Box 638, Dartmouth, Nova Scotia, Canada B2Y 3Y9.

(mean diameter of vitellogenic oocytes >1000 μm), the mean fraction of atretic vitellogenic oocytes was 0.04 (standard deviation [SD]=0.05, $n=108$).

Length at maturity

All females smaller than 65 cm were categorized as immature, although few females were collected between 51 and 60 cm (2 females between 61 and 65 cm, and 4 females between 56 and 60 cm). All females larger than 70 cm were categorized as mature.

Discussion

Maturity at length

No precise estimate of female length at 50% maturity was possible because of a scarcity of collected samples near the presumed length at 50% maturity. The data indicate length at 50% maturity is somewhere between 65 and 70 cm and is higher than the 60 cm value currently used in stock assessment (Ianelli et al.¹). Estimates for female length at 50% maturity for this species in other geographic regions range from 48–80 cm (Table 2).

Fecundity

Atresia followed the same general pattern as reported by Gundersen (2003) and did not have a large effect on annual fecundity. Fecundity at length from our study was somewhat higher than that reported by D'yakov (1982) from samples collected in 1978 in the Bering Sea.

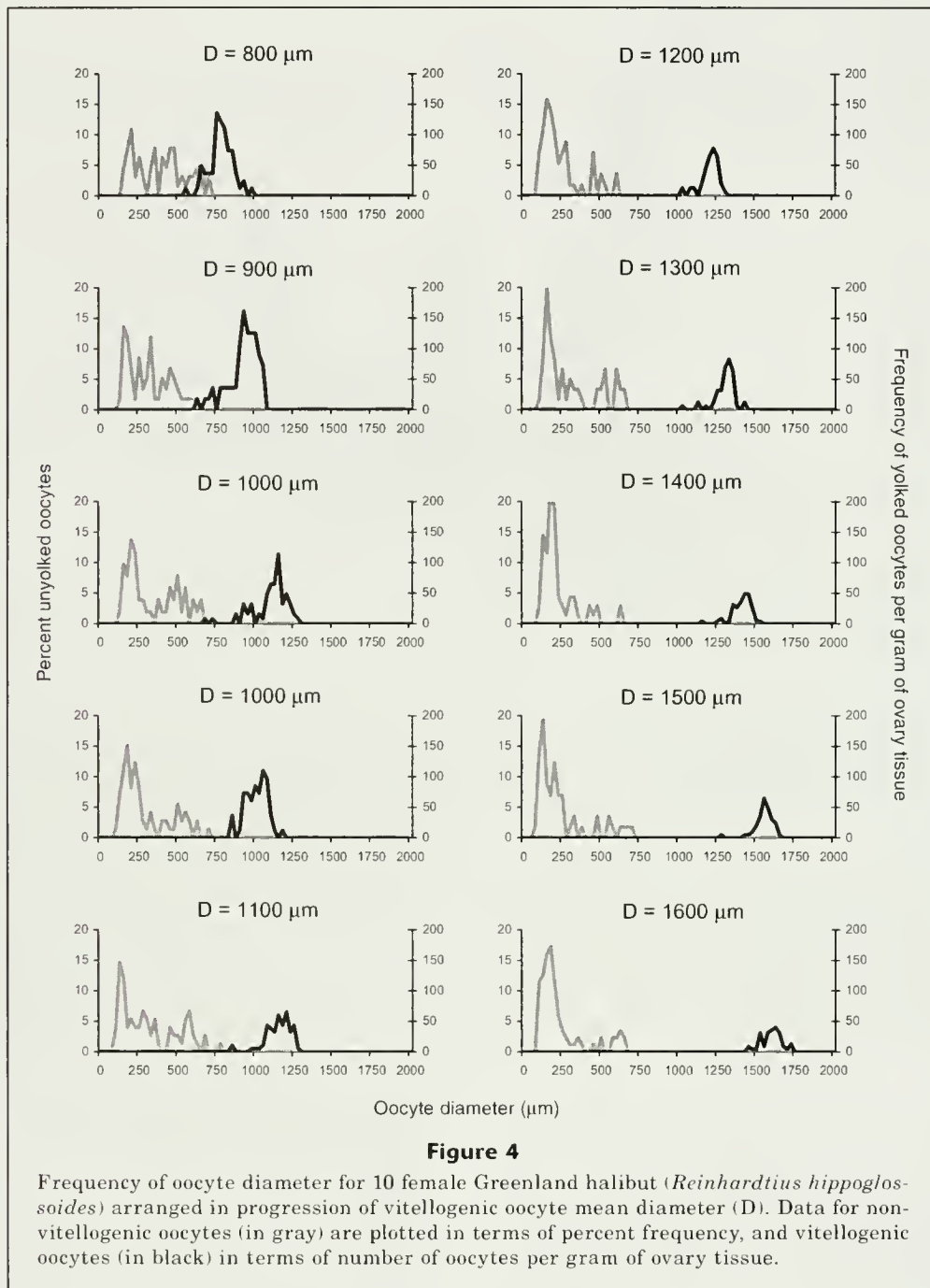
The results from both our study and D'yakov's study (1982) fall within reported ranges of fecundity from other regions; however there is strong variation between the regions in fecundity at length (Fig. 5). Gundersen (2003) hypothesized a geographic variation in fecundity for Greenland halibut. This variation may be caused by a trade-off between egg size and fecundity (Roff, 1992). The largest vitellogenic oocytes before hydration in our study were about 1700 μm , compared to 2800 μm reported by Gundersen (2003) for samples collected in the Barents Sea. Fecundity estimates by Gundersen (2000) from samples collected in the Barents Sea in 1996, 1997, and 1998 were all lower than the fecundity estimates from our study (Fig. 5).

Length-GSI relationship and instantaneous rate of natural mortality

The estimated rate of instantaneous natural mortality of 0.112 from our study is lower than the value of M currently used in the Bering Sea and Aleutian Islands stock assessment. The stock assessment uses a maximum age of 21 to estimate M to be 0.18 (Ianelli et al.¹).

Our estimate for M corresponds more closely with results from Gregg et al. (2006) who aged Greenland halibut from the Bering Sea up to 36 years, corresponding to an M of 0.115. A recent age validation study has revealed that Greenland halibut in the Atlantic live up to 33 years, which is also older than previous estimates (Treble et al.²). Overestimating M may result in unsustainably high target harvest rates (Clark, 1999).

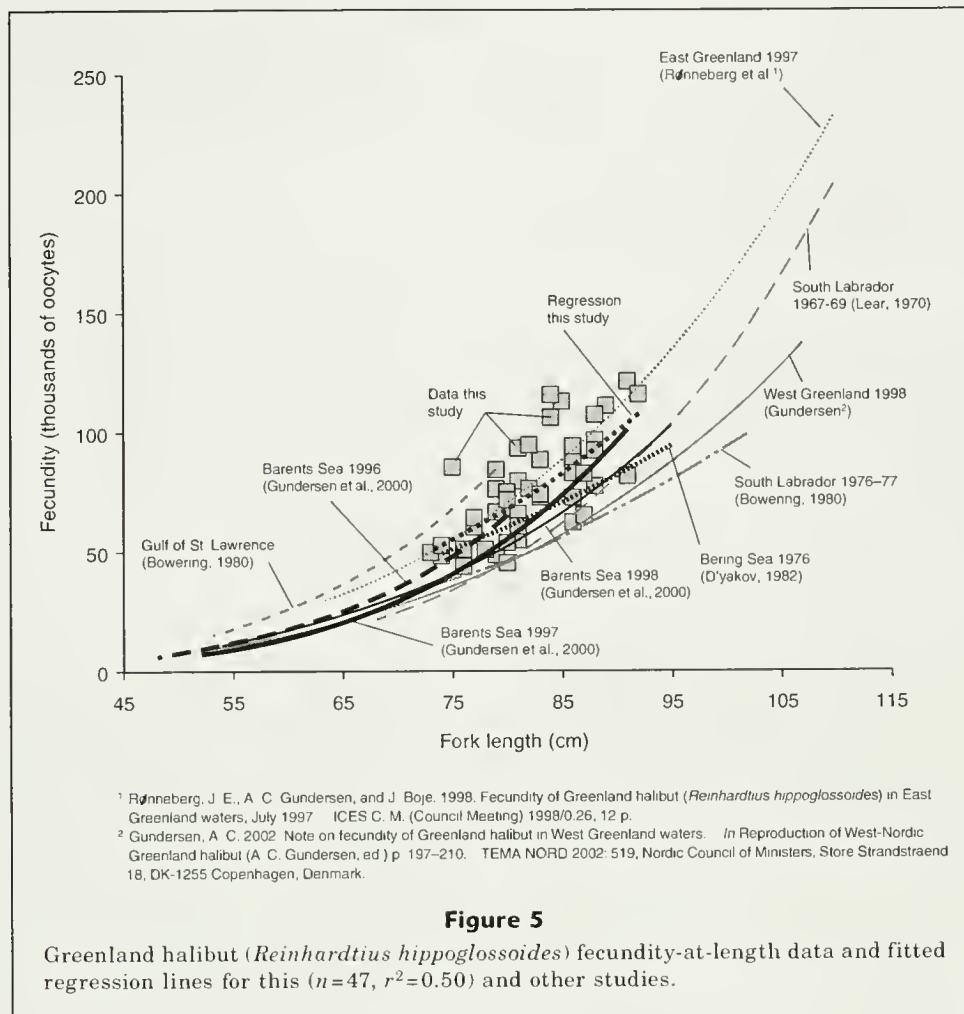
This study provides a length range for estimated length at 50% maturity, annual fecundity, and an



estimate of instantaneous natural mortality independent of age data for a species with an uncertain age structure. Fecundity was higher and eggs were smaller in Greenland halibut from Alaskan waters than the reported values for the Barents Sea. This may be due to a trade-off between number of eggs and egg size (Roff, 1992). Based on the energy invested in annual reproduction (GSI), Greenland halibut mortality (M) appears lower than the values used currently in population models.

Acknowledgments

We thank the scientists of Resource Assessment and Conservation Engineering division of the Alaska Fishery Science Center, and the following fishery observers for ovary collections: J. Bennett, K. Fleming, R. Hutson, C. Hilderbrandt, N. Goddard, A. Randi, and S. Rothamel. D. Kimura, S. McDermott, and D. Nichol provided valuable comments on manuscript drafts. This publication was funded by the Joint Institute for the Study



of the Atmosphere and Ocean (JISAO) under NOAA Cooperative Agreement no. NA17RJ1232, contribution no. 1088.

Literature cited

- Ådlandsvik, B., A. C. Gundersen, K. H. Nedreaas, A. Stene, and O. L. Albert.
2004. Modeling the advection and diffusion of eggs and larvae of Greenland halibut (*Reinhardtius hippoglossoides*) in the north-east Arctic. *Fish. Oceanogr.* 13:403-415.
- Bowring, W. R.
1980. Fecundity of Greenland halibut, *Reinhardtius hippoglossoides* (Walbaum), from Southern Labrador and Southeastern Gulf of St. Lawrence. *J. Northwest Atl. Fish. Sci.* 1:39-43.
1983. Age, growth, and sexual maturity of Greenland halibut, *Reinhardtius hippoglossoides* (Walbaum), in the Canadian Northwest Atlantic. *Fish. Bull.* 81:599-611.
- Bowring, W. R., and K. H. Nedreaas.
2000. A comparison of Greenland halibut (*Reinhardtius hippoglossoides* (Walbaum) fisheries and distribution in the Northwest and Northeast Atlantic. *Sarsia* 85:61-76.
- Charnov, E. L.
2002. Reproductive effort, offspring size, and benefit/cost ratios in the classification of life histories. *Evol. Ecol. Res.* 4:749-758.
- Clark, W. G.
1999. Effects of an erroneous natural mortality rate on a simple age-structured stock assessment. *Can. J. Fish. Aquat. Sci.* 56:1721-1731.
- D'yakov, Y. P.
1982. The fecundity of the Greenland halibut, *Reinhardtius hippoglossoides* (Pleuronectidae), from the Bering Sea. *J. Ichthyol.* 22(5):59-64.
- Fedorov, K. Y.
1968. Oogenesis and the sexual cycle of the Greenland halibut. [In Russian]. *Tr. Palyarn. Nauchno-Issled. Proekt. Inst. Morsk. Rybn. Khoz. Okeanogr.* 23:425-450.
- Gregg, J. L., D. M. Anderl, and D. K. Kimura.
2006. Improving the precision of otolith-based age estimates for Greenland halibut (*Reinhardtius hippoglossoides*) with preparation methods adapted for fragile sagittae. *Fish. Bull.* 104:643-648.
- Gundersen, A. C.
2003. Sexual maturity, fecundity and nursery grounds of Northeast Arctic Greenland halibut (*Reinhardtius*

- hippoglossoides* (Walbaum). Ph. D. diss., 166 p. Univ. Bergen, Bergen, Norway.
- Gundersen, A. C., K. H. Nedreaas, O. S. Kjesbu, and O. T. Albert.
2000. Fecundity and recruitment variability of Northeast Arctic Greenland halibut during 1980–1998, with emphasis on 1996–1998. *J. Sea Res.* 44:45–54.
- Gundersen, A. C., J. E. Ronnegerg, and J. Boje.
2001. Fecundity of Greenland halibut (*Reinhardtius hippoglossoides* Walbaum) in East Greenland waters. *Fish. Res.* 51:229–236.
- Gunderson, D. R.
1997. Trade-off between reproductive effort and adult survival in oviparous and viviparous fishes. *Can. J. Fish. Aquat. Sci.* 54:990–998.
- Gunderson, D. R., M. Zimmermann, D. G. Nichol, and K. Pearson.
2003. Indirect estimates of natural mortality rate for arrowtooth flounder and darkblotched rockfish. *Fish. Bull.* 101:175–182.
- Hunter, J. R., and B. J. Macewicz.
1985. Rates of atresia in the ovary of captive and wild northern anchovy, *Engraulis mordax*. *Fish. Bull.* 83:119–136.
- Hunter, J. R., B. J. Macewicz, N. C. Lo, and C. A. Kimbrell.
1992. Fecundity, spawning, and maturity of female Dover sole, *Microstomus pacificus*, with an evaluation of assumptions and precision. *Fish. Bull.* 90:101–128.
- Junquera, S., E. Roman, J. Morgan, M. Sainza, and G. Ramilo.
2003. Time scale of ovarian maturation in Greenland halibut (*Reinhardtius hippoglossoides*, Walbaum). *ICES J. Mar. Sci.* 60:767–773.
- Junquera, S., E. Roman, X. Paz, and G. Ramilo.
1999. Changes in Greenland halibut growth, condition, and fecundity in the Northeast Atlantic (Flemish Pass, Flemish Cap and Southern Grand Bank). *J. Northwest Atl. Fish. Sci.* 25:17–28.
- Lear, W.A.
1970. Fecundity of Greenland halibut (*Reinhardtius hippoglossoides*) in the Newfoundland-Labrador area. *Fish. Res. Board Can.* 27:1880–1882.
- Morgan, M. J., W. R. Bowering, A. C. Gundersen, A. Hoines, B. Morin, O. Smirnov, and E. Hjørleifsson.
2003. A comparison of the maturation of Greenland Halibut (*Reinhardtius hippoglossoides*) from populations throughout the North Atlantic. *J. Northwest Atl. Fish. Sci.* 31:99–112.
- Nichol, D. G., and E. I. Acuna.
2001. Annual and batch fecundities of yellowfin sole, *Limanda aspera*, in the eastern Bering Sea. *Fish. Bull.* 99:108–122.
- Roff, D. A.
1992. The evolution of life histories: theory and analysis, 535 p. Chapman and Hall, New York, NY.
- Stearns, S. C.
1992. The evolution of life histories, 249 p. Oxford Univ. Press, New York, NY.
- Walsh, S. J., and W. R. Bowering.
1981. Histological and visual observations on oogenesis and sexual maturity in Greenland halibut off Northern Labrador. *NAFO (North Atlantic Fisheries Organization) Sci. Counc. Stud.* 1:71–75.

Validation of back-calculation equations for juvenile bluefish (*Pomatomus saltatrix*) with the use of tetracycline-marked otoliths

Marja E. Roemer

Department of Biology
University of Massachusetts Dartmouth
North Dartmouth, Massachusetts 02747

Kenneth Oliveira (contact author)

Department of Biology
University of Massachusetts Dartmouth
285 Old Westport Road
North Dartmouth, Massachusetts 02747

E-mail address for K. Oliveira: Koliveira@umassd.edu

In recent years, a decrease in the abundance of bluefish (*Pomatomus saltatrix*) has been observed (Fahay et al., 1999; Munch and Conover, 2000) that has led to increased interest in a better understanding the life history of the species. Estimates of several young-of-the-year (YOY) life history characteristics, including the importance and use of estuaries as nursery habitat (Kendall and Walford, 1979) and size-dependant mortality (Hare and Cowen, 1997), are reliant upon the accuracy of growth determination. By using otoliths, it is possible to use back-calculation formulae (BCFs) to estimate the length at certain ages and stages of development for many species of fishes. Use of otoliths to estimate growth in this way can provide the same information as long-term laboratory experiments and tagging studies without the time and expense of rearing or recapturing fish. The difficulty in using otoliths in this way lies in validating that 1) there is constancy in the periodicity of the increment formation, and 2) there is no uncoupling of the relationship between somatic and otolith growth.

To date there are no validation studies demonstrating the relationship between otolith growth and somatic growth for bluefish. Daily increment formation in otoliths has been documented for larval (Hare and Cowen, 1994) and juvenile bluefish (Nyman and Conover, 1988).

Hare and Cowen (1995) found age-independent variability in the ratio of otolith size to body length in early age bluefish, although these differences varied between ontogenetic stages. Furthermore, there have been no studies where an evaluation of back-calculation methods has been combined with a validation of otolith-derived lengths for juvenile bluefish.

This study uses tetracycline-marked YOY bluefish otoliths to achieve two objectives: 1) to validate the relationship between somatic and otolith growth for juvenile bluefish, and 2) to compare the effectiveness of the Dahl-Lea equation, Fraser-Lee equation, scale proportional hypothesis (SPH), and body proportional hypothesis (BPH) length back-calculation formulae.

Materials and methods

Young-of-the-year bluefish were collected by beach seine (15 m × 1.2 m × 6 mm mesh) from Clarks Cove in Buzzards Bay, Massachusetts, in July and August 2005. The fish were anesthetized with eugenol (clove oil), measured for fork length (FL), weighed, injected with tetracycline hydrochloride (75 mg/kg body weight), and individually marked with visible implant elastomer (VIE) tags (Northwest Marine Technology, Shaw Island, WA). The fish were maintained in a

970 liter flow-through seawater tank for 1 month at ambient water temperature and fed with chopped squid and fish once daily to satiation. After 32 days, the fish were remeasured, reweighed, and their sagittal otoliths were removed for analysis. In addition, 417 YOY juvenile bluefish between 62 and 182 mm FL were collected from southeastern Massachusetts during the years 2004 and 2005 and were used to develop models of the relationship between otolith radius and fork length. ANCOVA was used to compare the slopes of the otolith-size–body-size relationship between wild fish and experimental fish to determine if the experimental conditions caused uncoupling of the relationship.

Otoliths were prepared for analysis as in Oliveira (1996) with two modifications; a 0.48-mm section was cut through the nucleus and visibility of the microstructure was enhanced by soaking the section in trypsin solution. Cross-sectioned bluefish otoliths have an occluded area in the center which obscures observation of the microstructure of the otolith. To clear this region, a procedure was developed in which the sections were placed in 2% trypsin solution for approximately 48 to 72 hours to remove excess protein. This procedure cleared the masked area and enhanced visibility of the rings.

Otoliths were observed on a computer monitor at 100× magnification so that the entire otolith from primordia to ventral edge could be viewed. Measurements were taken by using the Image-Pro Plus 5.0 image analysis software (Media Cybernetics, Silver Spring, MD). Two radial measurements were made on each otolith. The first measurement, R_c , was defined as the distance from the primordium to the ventral edge of the otolith (Fig. 1) and represents the radius of the otolith at the end of the experiment. Because bluefish otoliths develop a curvature that increases

Manuscript submitted 8 May 2006
to the Scientific Editor's Office.

Manuscript approved for publication
13 October 2006 by the Scientific Editor.

Fish. Bull. 105:305–309 (2007).

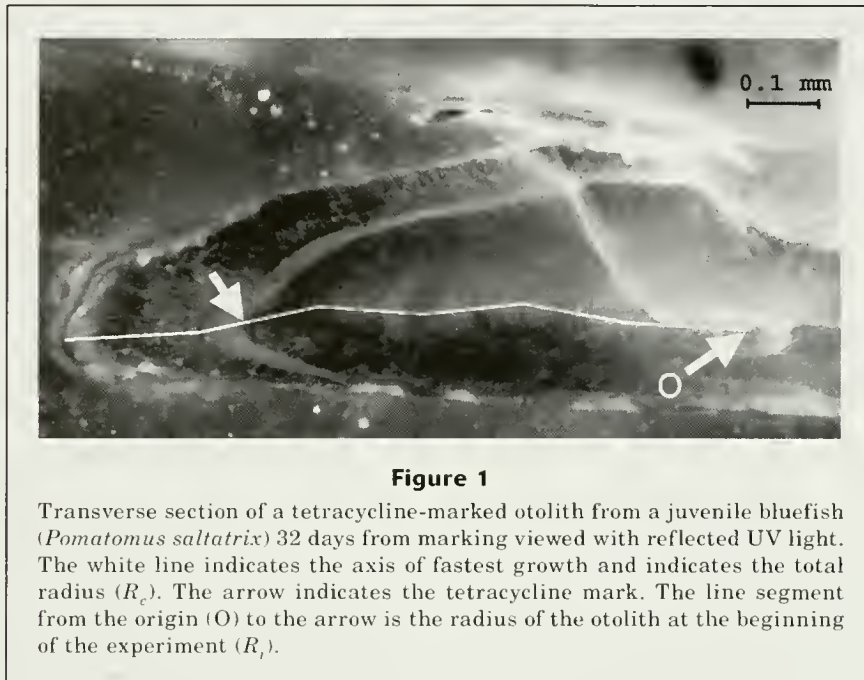


Figure 1

Transverse section of a tetracycline-marked otolith from a juvenile bluefish (*Pomatomus saltatrix*) 32 days from marking viewed with reflected UV light. The white line indicates the axis of fastest growth and indicates the total radius (R_c). The arrow indicates the tetracycline mark. The line segment from the origin (O) to the arrow is the radius of the otolith at the beginning of the experiment (R_t).

with age, a straight line measurement from nucleus to edge would not reflect the true radius and therefore would bias the estimation of growth increments associated with the curvatures. In order to account for this curvature, radial measurements were made along the axis of fastest growth, which was the sum of several straight line measurements from the nucleus to the edge. The second measurement, R_t , was defined as the distance from the primordium to the inner edge of the tetracycline mark deposited on the otolith, along the axis of fastest growth, and represents the radius of the otolith at the time of injection.

The frequency of ring deposition was also determined. The sectioned otoliths were observed at 400 \times magnification under reflected UV light. When necessary, computer images were enhanced by alternating changes in contrast, and further digital magnification was used to observe rings. The tetracycline mark was located and then the UV light was turned off and the number of rings between the tetracycline-marked ring to the edge of the otolith were counted in normal transmitted light. Two replicates were made for otolith daily ring counts.

Back-calculation formulae

Growth rates from bluefish were estimated by using four back-calculation growth models as described in Francis (1990). In these equations, L_t is the initial fork length of the fish and L_c is the fork length of the fish at the end of the experiment.

The Dahl-Lea equation (based on the study of Lea [1910]) is a simple linear ratio of scale growth to body growth, with the assumption that the two are in exact proportion.

$$L_t = L_c \left(\frac{R_t}{R_c} \right). \quad (1)$$

The Fraser-Lee equation (based on the approach described by Fraser [1916]) is similar to the Dahl-Lea equation but with the Fraser-Lee equation there is the assumption that each back-calculation line passes through the point c , resulting in Equation 2. The value c was calculated as the intercept of the regression of otolith radius and body length (Fig. 2).

$$L_t = c + (L_c - c) \left(\frac{R_t}{R_c} \right). \quad (2)$$

With the SPH (Whitney and Carlander, 1956) there is the assumption of a constant proportional deviation from the mean in scale size such that if the scale is ten percent larger than average for a fish of that length, then it will be ten percent larger throughout the life of the fish. The a and b values for the SPH were calculated as the intercept and the slope of the regression of otolith radius (y) against fork length (x) (Fig. 2). In its linear form, the SPH is expressed as follows:

$$L_t = \left(\frac{-a}{b} \right) + \left(L_c + \frac{a}{b} \right) \left(\frac{R_t}{R_c} \right). \quad (3)$$

The BPH (Whitney and Carlander, 1956) is similar in principal to the SPH but carries that assumption that if a fish is ten percent smaller than an average fish with that size scale, it will be ten percent smaller throughout its life. For the BPH, c is as in Equation 2 and d was

calculated as the slope of fork length (y) plotted against otolith radius (x). In linear form the BPH is expressed as follows:

$$L_t = L_c \left(\frac{c + dR_t}{c + dR_c} \right) \quad (4)$$

The otolith radii and fork lengths were fitted to linear, quadratic, and cubic regression models. The data fitted all the models similarly: r^2 for the linear and quadratic functions were 0.86 and the cubic function had an r^2 of 0.85. A visual comparison of residuals between linear and nonlinear models showed the data to be homoscedastic and therefore the linear model was chosen because of its parsimony. Using these formulae, we estimated the lengths of individual bluefish at the start of the experiment and then compared our estimates to the actual measured lengths. The best model for estimating growth was determined by using paired t -tests. All statistical analyses were made with SPSS, vers. 13.0 (SPSS, Inc., Chicago, IL). For all comparisons $P < 0.05$ was considered significant.

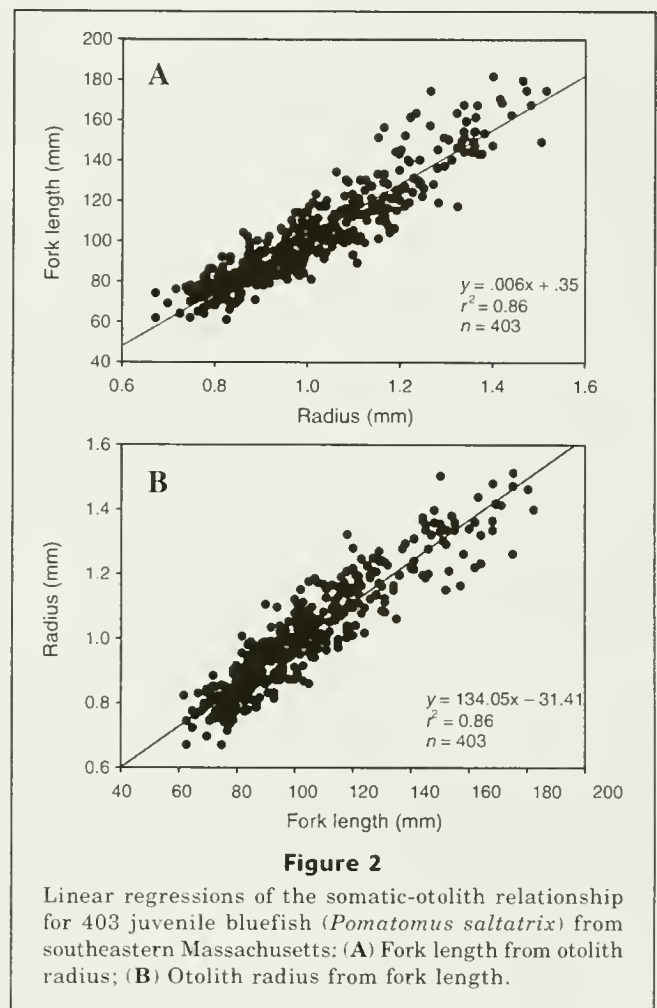
Results

Seventy-seven fish were injected with tetracycline and 13 produced readable otoliths that could be used for age and growth analyses. Mortality was high in the first day of the experiment when 26 fish died. Five fish that appeared to be diseased were also removed from the experiment. An additional 21 fish that survived did not show the tetracycline mark and 12 fish had unreadable otoliths. Growth increments were distinguishable and the number of observed rings after the tetracycline injection was within 5% of the number of days in captivity for all tetracycline-injected fish. All replicate counts were within two days of the number of days in captivity.

Some fish died before the 32-day intended experimental time period, and two distinct groups of fish that died were evident. Group 1 included the seven fish that survived at least three weeks (23–32 days) and group 2 included the six fish which lived one week or less (3–7 days). Group 2 did not survive the entire study period but did have the same growth patterns as group-1 fish. For this reason, the data were analyzed as 1) pooled data (all 13 fish), and 2) data from group 1 (7 fish).

Measured growth estimates from all fish varied between 0.4 and 3.0 mm FL/day (Table 1). There was no significant difference ($P = 0.13$) in otolith growth rates and body growth rates for the wild fish used to develop the BCFs and the experimental fish, indicating that uncoupling of the relationship did not occur under experimental conditions.

The closest estimate of the measured L_t came from the Dahl-Lea equation, showing no significant difference ($P = 0.48$) between the estimates and the initial lengths of the bluefish. The estimates from the Fraser-Lee equation, BPH, and SPH were all significantly different from the measured initial length ($P < 0.01$). The



Dahl-Lea equation estimated the L_t by a mean absolute difference of 2.0% \pm 0.6 standard error (SE) and had a tendency to over-estimate the initial lengths. The Fraser-Lee equation and the BPH were similar in their estimations, tending to under-estimate length by 2.9% \pm 0.9 SE and 3.0% \pm 0.9, respectively. The SPH underestimated lengths by a mean of 5.3% \pm 1.4 SE.

Our analysis of the same data without group-2 fish produced results similar to the results with the pooled data. The Dahl-Lea equation estimations were not significantly different from the L_t ($P = 0.41$), whereas the other three equations were significantly different from the measured length (≤ 0.02). Percent differences for all the equations were slightly higher for group-1 fish alone than for the pooled fish. Dahl-Lea estimates differed from the measured lengths by 3.1% \pm 0.9 SE, the Fraser-Lee and BPH estimates both differed by 4.7% \pm 1.3 SE, and the SPH differed by 8.6% \pm 1.7 SE.

Discussion

The agreement between the number of daily rings and the days after injection indicates that the observed ring

Table 1

Summary of variables and back-calculation equation results for tetracycline-injected juvenile bluefish (*Pomatomus saltatrix*). BPH = body proportional hypothesis, SPH = scale proportional hypothesis, L_i = initial fork length of fish, L_f = final fork length of fish, R_i = initial radius of otolith, and R_f = final radius of otolith. * Indicates a significant difference from the measured initial fork length (L_i) ($P < 0.05$).

Fish number	Days after injection	L_i	L_f	Growth (mm)	Growth rate (mm/day)	R_f	R_i	Dahl-Lea	Fraser-Lee*	BPH*	SPH*
1	32	84.0	116.0	32.0	1.0	1.0	0.8	86.1	78.0	77.3	72.2
2	32	89.0	120.0	31.0	1.0	1.2	0.9	94.6	87.9	88.1	83.1
3	32	89.0	112.0	23.0	0.7	0.9	0.7	94.6	89.6	88.2	86.1
4	25	91.0	105.0	14.0	0.6	1.1	0.9	88.7	83.7	84.3	80.3
5	23	93.0	102.0	9.0	0.4	1.0	0.9	92.9	90.1	90.1	88.1
6	23	93.0	108.0	15.0	0.7	1.0	0.8	89.7	84.4	84.0	80.6
7	23	101.0	115.0	14.0	0.6	1.1	0.9	101.6	97.9	97.8	95.3
8	7	118.0	121.0	3.0	0.4	1.2	1.2	118.2	117.5	117.6	117.0
9	4	122.0	125.0	3.0	0.8	1.2	1.1	122.2	121.5	121.5	121.0
10	4	128.0	130.0	2.0	0.5	1.1	1.1	127.7	127.1	127.1	126.7
11	3	127.0	129.0	2.0	0.7	1.2	1.2	126.4	125.7	125.7	125.2
12	3	118.0	127.0	9.0	3.0	1.2	1.1	119.7	117.8	117.8	116.6
13	3	133.0	136.0	3.0	1.0	1.1	1.0	130.8	129.6	129.3	128.7
Mean		106.6	118.9	12.3	0.9			107.2	103.9	103.8	101.6

formation occurred daily. This is in agreement with Nyman and Conover (1988) who used tetracycline to validate that rings were formed daily in juvenile bluefish. This finding indicates that the tetracycline mark was formed directly after the injection and that the number of rings, after tetracycline marking, corresponded with the number of days in the study period.

The Dahl-Lea equation provided the most accurate estimate of the initial size of the bluefish at the start of the experiment. This is the simplest equation and is based solely on the linearity of the otolith-size-body-size relationship. The accuracy of the estimation may be due to bluefish being a fast growing species. Wright et al. (1990) found that faster growing salmon smolts fit a linear growth model more favorably than slower growing conspecifics. It is possible that daily otolith growth is conservative, to a certain extent, as found by Panfili and Tomás (2001), but that the width of the daily growth increments may be a function of metabolism as postulated by Wright et al. (1990) or a function of temperature (Mosegaard et al., 1988). Therefore, species with high metabolisms, such as bluefish, may be expected to show a more direct relationship between otolith growth and somatic growth than a fish with a slower metabolism.

The Fraser-Lee equation underestimated the true initial lengths of the fish by a mean of 2.8%. This underestimate may be due the length-intercept constant c in the to the Fraser-Lee equation. When this constant is given a biological interpretation of zero, the equation is the same as the Dahl-Lea equation; therefore the interpretation of c is important in determining the accuracy of the Fraser-Lee and BPH equations. The c calculated by the linear regression was a negative

value, -31.41 ; the underestimation was likely caused by changes in the otolith-size-body-size relationship during different life stages.

Hare and Cowen (1997) found significant differences between different ontogenetic stages during the bluefish larval period. These differences would explain why the regression of the otolith radius on fork length data did not predict a biologically reasonable y -intercept, although the data were strongly linear: the ratios during the juvenile and larval stages were different. When applying BCFs a biological intercept may be more useful and could make the Fraser-Lee BCF the more accurate equation. However, because otolith formation occurs during the early egg stage (0–24 hours) (Hare and Cowen, 1994), it would be problematic to get an accurate mean length at time of formation. Given that this measurement is likely to be less than the 2.0–2.4 mm hatching size (Klein-MacPhee, 2002) and that the otolith growth to somatic growth relationship is linear, forcing an intercept of zero should provide reasonably accurate length estimations.

In summary, this study was designed to validate and compare back-calculation methods for a fast growing juvenile bluefish, rather than to characterize bluefish growth. All four back-calculation formulae did result in close estimates ($\leq 8.6\%$) of the true initial length regardless of growth rate (0.4 to 3.0 mm FL/day). Although the sample sizes were not adequate to properly explore the observed variability in growth rate the fact that the precision of the BCFs was not affected by growth rate illustrates a link between the rate of otolith growth and body growth, at least in the short term. In the case of bluefish, the results of this study indicate that the relationship between otolith growth

and body growth is linear for juveniles. The Dahl-Lea equation is the most parsimonious BCF equation and best approximated the true growth rate of juvenile bluefish, therefore making it the best suited method for estimating growth rate during the juvenile phase of this species. However it should be noted that the linear model used to develop the BCFs may not hold true for larval development or for annual growth of adults; more complex models may be needed to accurately estimate the amount of growth beyond year one. Caution must also be used in applying the equation because the lack of significant difference between the Dahl-Lea-predicted lengths and true initial lengths of the fish may have been due to the small sample size. If the linear relationship between somatic and otolith growth is, in fact, influenced by growth rate, then the Dahl-Lea equation may prove to be useful in back-calculating length for other fast-growing species of fishes.

Acknowledgments

This research was funded by the National Marine Fisheries Service/CMER grant no. NOAA Ref. NA04NMF4550380. We thank T. Rajaniemi for her advice and assistance with statistical analysis and S. Cadrin for reading an earlier draft of this manuscript.

Literature cited

- Fahay, M. P., P. L. Berrien, D. L. Johnson, and W. W. Morse.
1999. Essential fish habitat source document: Bluefish, *Pomatomus saltatrix*, life history and habitat characteristics. NOAA Tech. Memo. NMFS-NE-144, 68 p.
- Francis, R. I. C. C.
1990. Back-calculation of fish length: a critical review. *J. Fish Biol.* 36:883-902.
- Fraser, C. Mcl.
1916. Growth of the spring salmon. *Trans. Pacif. Fish. Soc.* 1915:29-39.
- Hare, J. A., and R. K. Cowen.
1994. Ontogeny and otolith microstructure of bluefish *Pomatomus saltatrix* (Pisces: Pomatomidae). *Mar. Biol.* 118:541-550.
1995. Effect of age, growth rate, and ontogeny on the otolith size-fish size relationship in bluefish, *Pomatomus saltatrix*, and the implications for back-calculation of size in fish early life history stages. *Can. J. Fish. Aquat. Sci.* 52:1909-1922.
1997. Size, growth, development, and survival of the planktonic larvae of *Pomatomus saltatrix* (Pisces: Pomatomidae). *Ecology* 78:2415-2431.
- Kendall, A. W. Jr., and L. A. Walford.
1979. Sources and distribution of bluefish, *Pomatomus saltatrix*, larvae and juveniles off the east coast of the United States. *Fish. Bull.* 77:213-227.
- Klein-MacPhee, G.
2002. Bluefish. Family Pomatomidae. In Bigelow and Schroeder's Fishes of the Gulf of Maine, 3rd ed. (B. B. Collette, and G. MacPhee, eds.), p. 400-406. Smithsonian Institution Press, Washington, DC.
- Lea, E.
1910. On the methods used in the herring-investigations. *Con. Perm. Int. L'explor. Mer* 53:7-174.
- Mosegaard, H., H. Svedang, and K. Taberman.
1988. Uncoupling of somatic and otolith growth rates in Atlantic char (*Salvelinus alpinus*) as an effect of differences in temperature response. *Can. J. Fish. Aquat. Sci.* 45:1514-1524.
- Munch, S. B., and D. O. Conover.
2000. Recruitment dynamics of bluefish (*Pomatomus saltatrix*) from Cape Hatteras to Cape Cod, 1973-1995. *ICES J. Mar. Sci.* 57:393-402.
- Nyman, R. M., and D. O. Conover.
1988. The relation between spawning season and the recruitment of young-of-the-year bluefish, *Pomatomus saltatrix*, to New York. *Fish. Bull.* 86:237-250.
- Oliveira, K.
1996. Field validation of annular growth rings in the American eel, *Anguilla rostrata*, using tetracycline-marked otoliths. *Fish. Bull.* 94:186-189.
- Panfili, J., and J. Tomás.
2001. Validation of age estimation and back-calculation of fish length based on otolith microstructures in tilapias (Pisces, Cichlidae). *Fish. Bull.* 99:139-150.
- Whitney, R. R., and K. D. Carlander.
1956. Interpretation of body-scale regression for computing body length of fish. *J. Wild. Mgmt.* 20:21-27.
- Wright, P. J., N. B. Metcalfe, and J. E. Thorpe.
1990. Otolith and somatic growth rates in Atlantic salmon parr, *Salmo salar* L: evidence against coupling. *J. Fish Biol.* 36:241-249.

Fishery Bulletin

Guidelines for authors

Content of manuscripts

Contributions published in Fishery Bulletin describe original research in marine fishery science, fishery engineering and economics, as well as the areas of marine environmental and ecological sciences (including modeling). Although all contributions are subject to peer review, responsibility for the contents of papers rests upon the authors and not upon the editor or publisher. *Submission of an article implies that the article is original and is not being considered for publication elsewhere.* Manuscripts must be written in English. Authors whose native language is not English are strongly advised to have their manuscripts checked by English-speaking colleagues prior to submission. **Articles** may range from relatively short contributions (10–15 typed, double-spaced pages, tables and figures not included) to extensive contributions (20–30 typed pages). **Notes** are reports of 5 to 10 pages without an abstract and describe methods or results not supported by a large body of data.

Manuscript preparation

Title page should include authors' full names and mailing addresses and the senior author's telephone, fax number, and e-mail address, and a list of key words to describe the contents of the manuscript. **Abstract** should be limited to 150 words (one-half typed page), state the main scope of the research, and emphasize the author's conclusions and relevant findings. Do not review the methods of the study or list the contents of the paper. Because abstracts are circulated by abstracting agencies, it is important that they represent the research clearly and concisely. **Text** must be typed in 12 point Times New Roman font throughout. A brief introduction should convey the broad significance of the paper; the remainder of the paper should be divided into the following sections: **Materials and methods**, **Results, Discussion (or Conclusions)**, and **Acknowledgments**. Headings within each section must be short, reflect a logical sequence, and follow the rules of multiple subdivision (i.e., there can be no subdivision without at least two items). The entire text should be intelligible to interdisciplinary readers; therefore, all acronyms, abbreviations, and technical terms should be written out in full the first time they are used. Include FAO common names for species in the list of keywords and in the introduction. Regional common names may be used throughout the rest of the text if they are different from FAO common names which can be found at <http://www.fishbase.org/search.html>. Follow the U.S. Government Printing Office Style Manual (1984 ed.) and the CBE Style Manual (6th ed.) for editorial style; for fish nomenclature follow the most current issue of the American Fisheries Society's Common

and Scientific Names of Fishes from the United States and Canada. Dates should be written as follows: 11 November 2000. Measurements should be expressed in metric units, e.g., 58 metric tons (t); if other units of measurement are used, please make this fact explicit to the reader. Write out the numbers zero through nine unless they form part of measurement units (e.g., nine fish but 9 mm).

Text footnotes should be inserted in 9-point font at the bottom of the page that displays the first citation of the footnote. Footnotes should be formatted in the same manner as citations. Footnote all personal communications, unpublished data, and unpublished manuscripts with full address of the communicator or author, or, as in the case of unpublished data, where the data are on file. Authors are advised to avoid references to nonstandard (gray) literature (such as internal, project, processed, or administrative reports, ICES Council Minutes, IWC Minutes or Working Papers, any "research" or "working" documents, laboratory or contract reports, Management Council reports, and manuscripts in review) wherever possible. If these references are used, present them as footnotes and list whether they are available at NTIS (National Technical Information Service) or at some other public depository. Cite all software and special equipment or chemical solutions used in the study, not in a footnote but within parentheses in the text (e.g., SAS, vers. 6.03, SAS Inst., Inc., Cary, NC).

Literature cited comprises published works and those accepted for publication in peer-reviewed literature (in press). Follow the name and year system for citation format in the "Literature cited" section. If there is a sequence of citations in the text, list chronologically: (Smith, 1932; Green, 1947; Smith and Jones, 1985). Abbreviations of serials should conform to abbreviations given in the Serial Sources for the BIOSIS Previews Database. Authors are responsible for the accuracy and completeness of all citations. Literature citation format: Author (last name, followed by first-name initials). Year. Title of report or manuscript. Abbreviated title of the series to which it belongs. Always include number of pages. If the authorship for a sequence of citations is identical, list works chronologically.

Tables and figures—general format

- Zeros should precede all decimal points for values less than one.
- Sample size, *n*, should be italicized.
- Capitalize the first letter of the first word in all labels within figures.
- Do not use overly large font sizes in maps and for units of measurements along axes in figures.
- Do not use bold fonts or bold lines in figures.
- Do not place outline rules around graphs.
- Do not use horizontal lines in graphs to indicate measurement units on axes.
- Use a comma in numbers of five digits or more (e.g. 13,000 but 3000).
- Maps should have a North arrow (or compass sign) and degrees latitude-longitude (e.g., 170°E)

Tables are often overused in scientific papers; it is seldom necessary or even desirable to present all the data associated with a study. Tables should not be excessive in size and must be cited in numerical order in the text. Headings should be short but ample enough to allow the table to be intelligible on its own. All unusual symbols must be explained in the table legend. Other incidental comments may be footnoted with italic footnote markers. Use asterisks to indicate probability in statistical data. Do not type table legends on a separate page; place them on the same page as the table data. *Do not submit tables in photo mode.*

Figures include line illustrations, photographs (or slides), and computer-generated graphs and must be cited in numerical order in the text. Graphics will aid in the comprehension of the text, but they should be limited to presenting patterns rather than raw data. Figures are costly to print and should be limited to six. Figures must be labeled with author's name and number of figure. Avoid placing labels vertically (except on *y*-axis). Figure legends should explain all symbols and abbreviations and should be double-spaced on a separate page at the end of the manuscript. Please note that we do not print graphs in color.

**FAILURE TO FOLLOW
THESE GUIDELINES
WILL DELAY
PUBLICATION
OF A MANUSCRIPT**

Copyright law does not apply to *Fishery Bulletin*, which falls within the public domain. However, if an

author reproduces any part of an article from *Fishery Bulletin* in his or her work, reference to source is considered correct form (e.g., Source: Fish. Bull 97:105).

Reprints are available free of charge to the senior author (50 copies) and to his or her laboratory (50 copies).

Submission

The Scientific Editorial Office encourages authors to submit their manuscripts as a *single* PDF (preferred), or Word (zipped) document by e-mail to Fishery.Bulletin@noaa.gov. Please use the subject heading "Fishery Bulletin manuscript submission." *Do not* send encrypted files. For further details on electronic submission, please contact the Scientific Editorial Office directly (see address below). Or you may send your manuscript on compact disc in one of the above formats along with four printed copies (one original plus three copies [stapled]) to the Scientific Editor, at the address shown below.

Dr. Adam Moles
Scientific Editor, *Fishery Bulletin*
11305 Glacier Hwy
Juneau, AK 99801-8626

Once the manuscript has been accepted for publication, you will be asked to submit a final software copy of your manuscript. When requested, the text and tables should be submitted in Word or Word Rich Text Format. Figures should be sent as PDF files, Windows metafiles, tiff files, or as EPS files. Send a copy of figures in original software if conversion to any of these formats yields a degraded version.

Announcement of the NMFS (National Marine Fisheries Service) best paper awards

The National Marine Fisheries Service best scientific paper awards for 2006 were awarded to the following authors:

**Butler, John, Melissa Neuman,
Deanna Pinkard, Rikk Kvitek,
and Guy Cochrane**

The use of multibeam sonar mapping techniques to refine population estimates of the endangered white abalone (*Haliotis sorenseni*)

Fishery Bulletin 104:521–532

Maloney, Nancy E.

Sablefish, *Anaplopoma fimbria*, populations on Gulf of Alaska seamounts

Marine Fisheries Review 66(3):1–12





U.S. Department
of Commerce

Volume 105
Number 3
July 2007

Fishery Bulletin



**U.S. Department
of Commerce**

Carlos M. Gutierrez
Secretary

**National Oceanic
and Atmospheric
Administration**

Vice Admiral
Conrad C. Lautenbacher Jr.,
USN (ret.)

Under Secretary for
Oceans and Atmosphere

**National Marine
Fisheries Service**

William T. Hogarth
Assistant Administrator
for Fisheries



The *Fishery Bulletin* (ISSN 0090-0656) is published quarterly by the Scientific Publications Office, National Marine Fisheries Service, NOAA, 7600 Sand Point Way NE, BIN C15700, Seattle, WA 98115-0070. Periodicals postage is paid at Seattle, WA. POSTMASTER: Send address changes for subscriptions to *Fishery Bulletin*, Superintendent of Documents, Attn.: Chief, Mail List Branch, Mail Stop SSOM, Washington, DC 20402-9373.

Although the contents of this publication have not been copyrighted and may be reprinted entirely, reference to source is appreciated.

The Secretary of Commerce has determined that the publication of this periodical is necessary according to law for the transaction of public business of this Department. Use of funds for printing of this periodical has been approved by the Director of the Office of Management and Budget.

For sale by the Superintendent of Documents, U.S. Government Printing Office, Washington, DC 20402. Subscription price per year: \$36.00 domestic and \$50.40 foreign. Cost per single issue: \$28.00 domestic and \$35.00 foreign. See back for order form.

Fishery Bulletin

Scientific Editor

Adam Moles, Ph.D.

Associate Editor

Elizabeth Siddon

Ted Stevens Marine Research Institute
Auke Bay Laboratories
Alaska Fisheries Science Center
17109 Pt. Lena Loop Road
Juneau, Alaska 99801

Managing Editor

Sharyn Matriotti

National Marine Fisheries Service
Scientific Publications Office
7600 Sand Point Way NE, BIN C15700
Seattle, Washington 98115-0070

Editorial Committee

Jeffrey M. Leis	Australian Museum, Sydney, Australia
Thomas Shirley	Texas A&M University
David Somerton	National Marine Fisheries Service
Mark Terceiro	National Marine Fisheries Service

***Fishery Bulletin* web site: www.fishbull.noaa.gov**

The *Fishery Bulletin* carries original research reports and technical notes on investigations in fishery science, engineering, and economics. It began as the Bulletin of the United States Fish Commission in 1881; it became the Bulletin of the Bureau of Fisheries in 1904 and the *Fishery Bulletin* of the Fish and Wildlife Service in 1941. Separates were issued as documents through volume 46; the last document was No. 1103. Beginning with volume 47 in 1931 and continuing through volume 62 in 1963, each separate appeared as a numbered bulletin. A new system began in 1963 with volume 63 in which papers are bound together in a single issue of the bulletin. Beginning with volume 70, number 1, January 1972, the *Fishery Bulletin* became a periodical, issued quarterly. In this form, it is available by subscription from the Superintendent of Documents, U.S. Government Printing Office, Washington, DC 20402. It is also available free in limited numbers to libraries, research institutions, State and Federal agencies, and in exchange for other scientific publications.

U.S. Department
of Commerce
Seattle, Washington

Volume 105
Number 3
July 2007

Fishery Bulletin

Contents

Articles

- 313–326 Auth, Toby D., Richard D. Brodeur, and Kathleen M. Fisher
Diel variation in vertical distribution of an offshore ichthyoplankton community off the Oregon coast
- 327–336 Curtis, Janelle M. R.
Validation of a method for estimating realized annual fecundity in a multiple spawner, the long-snouted seahorse (*Hippocampus guttulatus*), using underwater visual census
- 337–347 Benson, Scott R., Karin A. Forney, James T. Harvey, James V. Carretta, and Peter H. Dutton
Abundance, distribution, and habitat of leatherback turtles (*Dermochelys coriacea*) off California, 1990–2003
- 348–355 Bengtson, John L., Alana V. Phillips, Elizabeth A. Mathews, and Michael A. Simpkins
Comparison of survey methods for estimating abundance of harbor seals (*Phoca vitulina*) in glacial fjords
- 356–367 DeMartini, Edward E., James H. Uchiyama, Robert L. Humphreys Jr., Jeffrey D. Sampaga, and Happy A. Williams
Age and growth of swordfish (*Xiphias gladius*) caught by the Hawaii-based pelagic longline fishery
- 368–378 Anderson, Joel D.
Systematics of the North American menhadens: molecular evolutionary reconstructions in the genus *Brevoortia* (Clupeiformes: Clupeidae)

The conclusions and opinions expressed in *Fishery Bulletin* are solely those of the authors and do not represent the official position of the National Marine Fisheries Service (NOAA) or any other agency or institution.

The National Marine Fisheries Service (NMFS) does not approve, recommend, or endorse any proprietary product or proprietary material mentioned in this publication. No reference shall be made to NMFS, or to this publication furnished by NMFS, in any advertising or sales promotion which would indicate or imply that NMFS approves, recommends, or endorses any proprietary product or proprietary material mentioned herein, or which has as its purpose an intent to cause directly or indirectly the advertised product to be used or purchased because of this NMFS publication.

MBLWHOI Library

SEP 7 2007

WOODS HOLE
Massachusetts 02543

- 379–389 Schaefer, Kurt M., and Daniel W. Fuller
Vertical movement patterns of skipjack tuna (*Katsuwonus pelamis*) in the eastern equatorial Pacific Ocean, as revealed with archival tags
- 390–395 Golet, Walter J., Andrew B. Cooper, Robert Campbell, and Molly Lutcavage
Decline in condition of northern bluefin tuna (*Thunnus thynnus*) in the Gulf of Maine
- 396–407 Stark, James W.
Geographic and seasonal variations in maturation and growth of female Pacific cod (*Gadus macrocephalus*) in the Gulf of Alaska and Bering Sea
- 408–417 Garrison, Lance P.
Interactions between marine mammals and pelagic longline fishing gear in the U.S. Atlantic Ocean between 1992 and 2004
- 418–425 Melville-Smith, Roy, and Simon de Lestang
Changes in egg production of the western rock lobster (*Panulirus cygnus*) associated with appendage damage
- 426–435 Able, Kenneth W., and Thomas M. Grothues
Diversity of estuarine movements of striped bass (*Morone saxatilis*): a synoptic examination of an estuarine system in southern New Jersey

Notes

- 436–439 Renshaw, Mark A., Eric Saillant, Siya Lem, Philip Berry, and John R. Gold
Microsatellite multiplex panels for genetic studies of gray snapper (*Lutjanus griseus*) and lane snapper (*Lutjanus synagris*)
- 440–444 Kane, Joseph, and Jacquelyn L. Anderson
Effect of towing speed on retention of zooplankton in bongo nets
- 445–445 Guidelines for submission

Abstract—We examined the diel vertical distribution, concentration, and community structure of ichthyoplankton from a single station 69 km off the central Oregon coast in the northeast Pacific Ocean. The 74 depth-stratified samples yielded 1571 fish larvae from 20 taxa, representing 11 families, and 128 fish eggs from 11 taxa within nine families. Dominant larval taxa were *Sebastes* spp. (rockfishes), *Stenobrachius leucopsarus* (northern lampfish), *Tarletonbeania crenularis* (blue lanternfish), and *Lyopsetta exilis* (slender sole), and the dominant egg taxa were *Sardinops sagax* (Pacific sardine), *Icichthys lockingtoni* (medusafish), and *Chauliodus macouni* (Pacific viperfish). Larval concentrations generally increased from the surface to 50 m, then decreased with depth. Larval concentrations were higher at night than during the day, and there was evidence of larval diel vertical migration. Depth stratum was the most important factor explaining variability in larval and egg concentrations.

Diel variation in vertical distribution of an offshore ichthyoplankton community off the Oregon coast

Toby D. Auth (contact author)¹

Richard D. Brodeur²

Kathleen M. Fisher³

Email address for T. D. Auth: toby.auth@noaa.gov

¹ Cooperative Institute for Marine Resources Studies
Oregon State University, Hatfield Marine Science Center
2030 Marine Science Drive
Newport, Oregon 97365

² Northwest Fisheries Science Center
NOAA Fisheries, Hatfield Marine Science Center
2030 Marine Science Drive
Newport, Oregon 97365

³ National Ocean Service
NOAA, The Center for Operational Oceanographic Products and Services
1305 East-West Highway
Silver Spring, Maryland 20910

Early life stages of fishes have long been studied to gain insight into adult spawning locations and biomass (Hunter et al., 1993), trophic interactions between fish larvae and their surrounding zooplankton and piscivore communities (Hunter and Kimbrell, 1980), and the relationship between early life processes and subsequent recruitment success (Bradford, 1992; Houde, 1997). Knowledge of the diel vertical distribution of fish eggs and larvae is critical to understanding the structure and ecological interactions of ichthyoplankton communities, and for the development of appropriate sampling strategies (Gray, 1998). Furthermore, variation in the diel vertical distributions of different larval fish taxa and their associated predator and prey fields may influence the occurrence, degree, and timing of competitive, trophic, and environmental interactions (Neilson and Perry, 1990). In addition, an understanding of the differences in ichthyoplankton depth distribution and concentration is essential for accurate quantitative estimates of whole water-column abundance when the depth to be sampled is limited (Ahlstrom, 1959; Comyns and Lyczkowski-Shultz, 2004). Also, because in many surveys sampling is

conducted during both night and day, it is often necessary to separate diel (e.g., visual net avoidance by larvae during daylight conditions) and depth effects when analyzing variable ichthyoplankton distributions (Ahlstrom, 1959; Boehlert et al., 1985).

Larvae of many fish species are known to perform diel vertical migrations (Ahlstrom, 1959; Neilson and Perry, 1990). These migrations can follow several different patterns; the most common is movement into the upper water column during night and into deeper water during the day (Shoji et al., 1999; Tsukamoto et al., 2001). However, the reverse pattern has also been observed (Lyczkowski-Shultz and Steen, 1991; Brodeur and Rugen, 1994). In addition, some fish larvae have been found to disperse during the night and aggregate during the day (Brewer and Kleppel, 1986; Munk et al., 1989).

In the present study the diel variation in vertical distributions and concentrations of fish eggs and larvae was examined by repeatedly sampling fish eggs and larvae from a single offshore station off the central Oregon coast in the northeast Pacific Ocean. We used univariate and multivariate statistical techniques such as ANO-

Table 1

Date, time (Pacific daylight-savings time [PDT]), and number of depth-stratified samples collected during each sampling period. All hauls were conducted at the same station (HH-05), located at 44°00'N, 125°00'W at a station depth of 950 m.

Haul	Date	Time	Day or night	Number of depth-stratified samples
HH-05A	3 Aug 2000	1600	Day	8
HH-05B	5 Aug 2000	2356	Night	8
HH-05C	6 Aug 2000	0330	Night	8
HH-05D	6 Aug 2000	0630	Day	8
HH-05E	6 Aug 2000	1623	Day	9
HH-05F	7 Aug 2000	0343	Night	9
HH-05G	7 Aug 2000	0633	Day	7
HH-05B	11 Aug 2002	0350	Night	9
HH-05C	11 Aug 2002	0722	Day	8

VA, diversity and evenness indices, multidimensional scaling, and cluster analyses to assess the influence of water depth, diel migration, temperature, and salinity on the occurrence and concentration of dominant ichthyoplankton taxa and assemblages. This is the first examination of diel variation in the vertical distributions of ichthyoplankton in the northern California Current since Boehlert et al. (1985), and the only work of its kind for an offshore assemblage. In addition, no similar study has been conducted examining fish egg diel vertical distributions and assemblages in this region. Results from this study are intended to supplement previous spatial and temporal analyses of Oregon coast ichthyoplankton (Richardson and Percy, 1977; Auth and Brodeur, 2006)—analyses that were based on samples collected along the Newport Hydrographic (NH) line (44°39'N) over many years.

Materials and methods

Sampling procedures

Ichthyoplankton samples were collected from a single station (HH-05) approximately 69 km off of Heceta Head (44°00'N, 125°00'W) along the central Oregon coast in 950 m of water. Sampling cruises in August 2000 and 2002 resulted in the collection of 74 depth-stratified samples from nine diel hauls: five during the day and four at night (Table 1). Samples collected after the beginning of civil twilight (~0445 Pacific daylight-savings time [PDT]) were considered day samples, whereas those collected after the end of civil twilight (~2006 PDT) were considered night samples. A multiple opening and closing net and environmental sensing system (MOCNESS; Wiebe et al., 1976) with a 1.2-m² mouth opening and 333- μ m mesh nets was used to collect ichthyoplankton at 7–9 discrete depths. The MOCNESS was fished as a continuous oblique tow from a depth of 350 m to the surface at a retrieval rate of 20–30 m/min and a ship speed of 1.0–1.5 m/s. Ship and retrieval speeds were

continually adjusted during each tow so as to maintain the mouth opening at a 45° angle for an effective mouth opening of 1 m² at all times. Mean water volume filtered by each net was 210 m³ (standard error [SE]=18.0), but was always greater in nets from deeper strata and less in nets fished in the upper 50 m. Because strata had unequal depth ranges, towing times were different for each stratum. Throughout the water column during each tow, we recorded volume of water filtered, temperature, salinity, depth of the net, length of wire out, and angle of the net mouth relative to the geoid.

Ichthyoplankton samples were preserved at sea in a 10% buffered-formalin seawater solution. Fish eggs and larvae from each sample were completely sorted, counted, and identified to the lowest taxonomic level possible in the laboratory with a dissecting microscope. The lesser of either all larvae or a random subsample of 50 individuals from each species in each sample was measured to the nearest 0.1 mm standard length (SL) (or notochord length for preflexion larvae) using an ocular micrometer mounted on the sorting microscope.

It should also be noted that *Sebastes* spp. were not identifiable below the generic level based on meristics and pigmentation patterns (see Richardson and Percy [1977] and Matarese et al. [1989] for a more complete discussion of this problem); therefore no species-specific inferences are intended for this taxon in this study. Recent work has allowed the identification of rockfishes to species level based on mitochondrial markers (Gray et al., 2006), and this identification should enable future researchers to discern specific patterns in larval rockfish distribution and abundance.

Data analyses

Fish egg and larval concentrations for each depth-stratified sample (D_i) were expressed as the number of individuals per 1000 m³. Weighted mean water-column densities for each haul (D_{Haul}) were calculated according to the following equation:

$$D_{Haul} = \sum D_i r_i / \sum r_i, \quad (1)$$

where r_i = the depth range (m) of each depth-stratified sample.

Weighted mean depths (WMDs) of dominant larval taxa were calculated according to the following equation (Pearre, 1973):

$$WMD = \sum n_i d_i / \sum n_i, \quad (2)$$

where n_i = the number of individuals in each depth-stratified sample; and

d_i = the mean depth (m) of each sample.

To facilitate vertical distribution analyses, the water column was divided into seven depth strata: 0–10, 10–20, 20–50, 50–100, 100–150, 150–200, and 200–350 m. The weighted mean density of eggs and larvae in all samples collected in each depth stratum per haul were calculated as the strata densities for each haul. A type-II ANOVA model was used to test the null hypothesis that egg and larval densities did not differ between day and night periods or between depth strata, and that there was no interaction among these factors (Dunn and Clark, 1974; Lough and Potter, 1993). ANOVA and a Tukey's multiple range test were applied to the $\log_e(n+0.1)$ -transformed haul and depth-strata densities to test for significant differences between day and night periods and depth strata. Weighted mean (based on density) larval lengths of important species were also calculated for each haul and depth stratum, and were similarly tested for significant differences between day and night periods and depth strata.

Taxa diversity and evenness for day and night and total diversity and evenness for each depth stratum were analyzed for all identifiable egg ($n=11$) and larval ($n=20$) taxa. The Shannon-Wiener diversity index (H') was used to measure egg and larval diversity, where higher H' values denote greater diversity. Taxa evenness was assessed by using Pielou's evenness index (J'), which ranges from zero to one, with the maximum J' value indicating that all taxa are represented in the same relative concentrations. Both H' and J' were calculated according to the formulas of Shannon and Weaver (1949) and Krebs (1989).

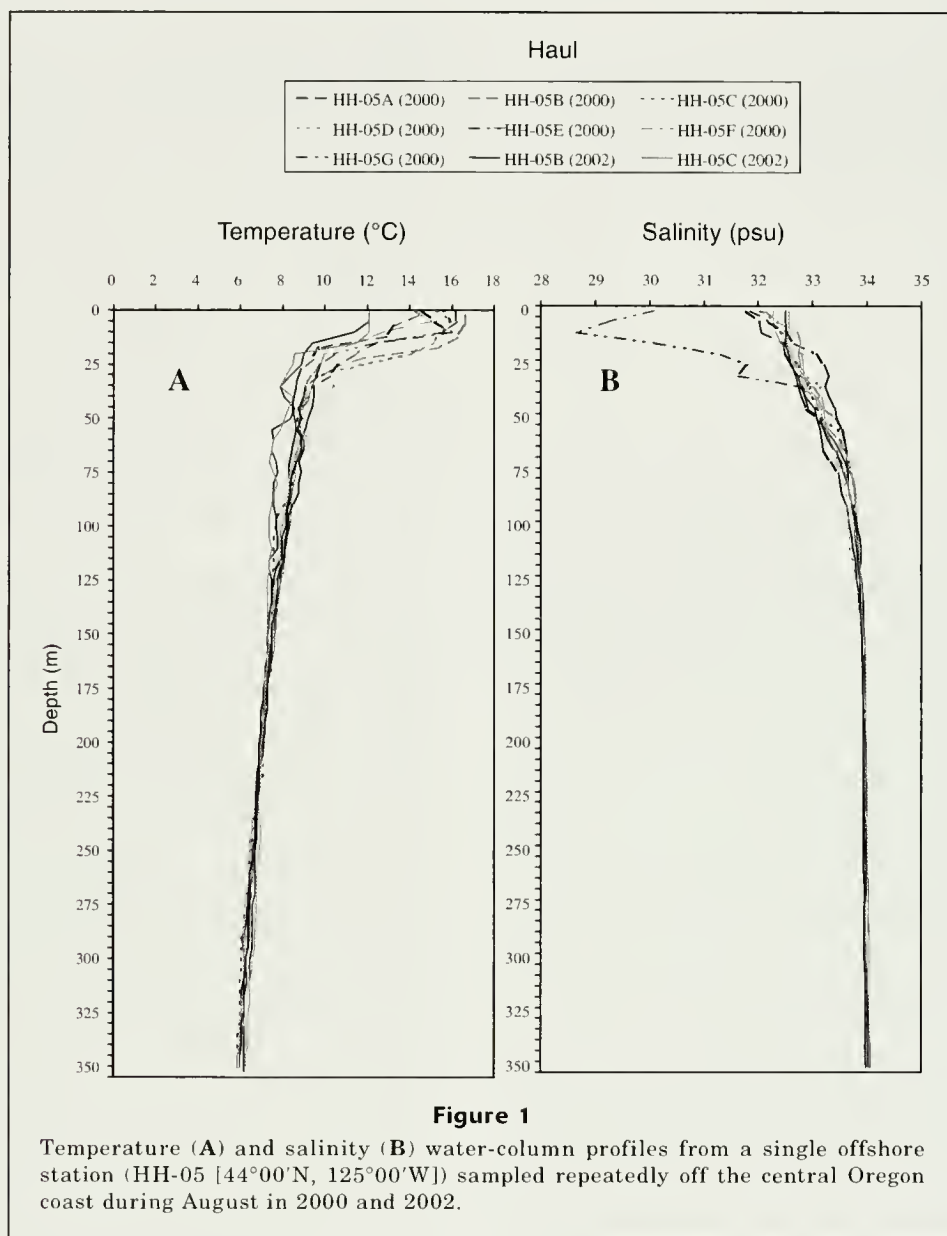
On Field et al.'s (1982) recommendation, we performed a hierarchical cluster analyses in conjunction with non-metric multidimensional scaling (MDS) ordinations to identify assemblages by potential taxa, depth-strata, and diel egg and larval concentrations. For analyses of taxa assemblages, only those egg ($n=4$) and larval ($n=12$) taxa found during more than 5% of the sampling events were included, whereas all identifiable egg ($n=10$) and larval ($n=19$) taxa were included in the other assemblage analyses. Concentrations for each egg and larval taxon were averaged for each diel tow (eggs: $n=8$; larvae: $n=9$) and each depth stratum from all tows (eggs: $n=22$; larvae: $n=53$), which constituted the sampling units in the respective multivariate matrices.

Sampling units for which no taxa were found were excluded from the analyses.

Dendrograms of egg and larval taxa, depth strata, and diel presence were created using hierarchical, group-averaged clustering from Bray-Curtis ranked similarities on standardized, fourth root-transformed egg and larval concentrations (Clarke and Warwick, 2001). Dendrograms were cut to produce ecologically interpretable clusters when they were apparent. In order to verify our interpretations of the dendrograms, we performed nonmetric MDS ordinations using similarity matrices from the cluster analyses, with 20 random restarts each to minimize stress levels. A two-dimensional ordination approach was adopted because stress levels were sufficiently low (≤ 0.08) in all cases and were not appreciably reduced by the addition of a third dimension, and the results were sufficiently interpretable ecologically in two-dimensional space (Clarke and Warwick, 2001).

A nonparametric, multivariate procedure (BIO-ENV) was used to analyze the relationship between select environmental variables and egg and larval community structures. The details of the BIO-ENV algorithm and its suitability for use in analyzing the interactions of biological and environmental data are described by Clarke and Gorley (2001) and Clarke and Warwick (2001). Two separate analyses were performed: one with a similarity matrix of depth-stratified samples by egg taxa (24 samples \times 9 taxa), and the other with a similarity matrix of depth-stratified samples by larval taxa (61 samples \times 19 taxa). These matrices were analyzed in association with three environmental variables: mean depth (m), mean temperature ($^{\circ}\text{C}$), and mean salinity of each depth-stratified sample. Both BIO-ENV analyses were performed by using the Spearman rank correlation method on the normalized Euclidean distance similarity matrices of the $\log_e(n+0.1)$ -transformed, nonstandardized environmental variables by depth-stratified samples (Clarke and Gorley, 2001). All diversity, evenness, cluster, MDS, and BIO-ENV analyses were performed by using PRIMER statistical software (PRIMER, vers. 5.2.9, PRIMER-E Ltd, Plymouth, UK).

Pairwise correlation analyses were also conducted to assess the relationship between concentrations of several prominent egg (*Sardinops sagax* [Pacific sardine], *Icichthys lockingtoni* [medusafish], and *Chauliodus macouni* [Pacific viperfish]) and larval (*Sebastes* spp. [rockfishes], *Stenobranchius leucopsarus* [northern lampfish], *Tarletonbeania crenularis* [blue lanternfish], and *Lyopsetta exilis* [slender sole]) taxa as well as total eggs and larvae and the environmental variables salinity and temperature. Mean egg and larval densities, salinity, and temperature per depth-stratified sample were used as variable measures. Before inclusion in the analyses, egg and larval concentrations were $\log_e(n+0.1)$ -transformed to normalize the data and homogenize residual variances. Statistical significance was determined at $\alpha = 0.05$. All ANOVA and correlation analyses were performed using the statistical software JMP (JMP, vers. 5.1., SAS Inst., Inc., Cary, NC).



Results

Hydrography

The water column at the sampling station was similarly stratified for each of the nine diel hauls, and a thermocline was centered approximately at 20 m (Fig. 1, A and B). Mean water temperature was 14.7°C (standard deviation [SD]=1.6) at the surface, and decreased to 6.2°C (SD=0.2) at 350 m. Salinity increased from a mean of 31.9 psu (SD=0.7) at the surface to 34.0 psu (SD=0.03) at 350 m. The unusually low salinities recorded in the upper 35 m of the water column during the last haul in 2000 (HH-05G) may have resulted from an infusion of low-salinity Columbia River plume water from the north.

Egg concentrations and distributions

A surprisingly small sum of 128 fish eggs representing 11 taxa from nine families was collected throughout the study. Three taxa were dominant according to total mean concentration and frequency of occurrence from all depth-stratified samples: *S. sagax* (3.42/1000 m³; 0.07), *I. lockingtoni* (2.00/1000 m³; 0.14), and *C. macouni* (1.07/1000 m³; 0.12). Together these three taxa accounted for over 71% of the total mean egg concentration. *Trachurus symmetricus* (jack mackerel) eggs were found at a high concentration (241.29/1000 m³) in a single daytime surface (0–10 m) sample in 2000 but were found in only two other samples and at much lower densities (6.80 and 17.54/1000 m³). These two samples were collected from two depths

Table 2

Day, night, and total mean densities (number/1000 m³) of fish eggs collected at all different depth strata from a single offshore station off the central Oregon coast in 2000 and 2002 (1 standard error in parentheses). For between-stratum comparisons of each taxon within each diel category, different superscripts indicate significant differences (ANOVA, $P < 0.05$).

Taxa	Depth (m)							Total
	0–10	10–20	20–50	50–100	100–150	150–200	200–350	
Day								
Total eggs	159.90 (79.0) ^a	31.01 (14.1) ^{ab}	18.60 (4.1) ^a	0.70 (0.7) ^b	0 (0) ^b	0 (0) ^b	1.30 (1.3) ^b	13.43 (5.8)
<i>Sardinops sagax</i>	84.11 (78.9)	6.26 (6.3)	1.36 (1.4)	0 (0)	0 (0)	0 (0)	0 (0)	5.99 (5.6)
<i>Lipolagus ochotensis</i>	2.10 (2.1)	0 (0)	0 (0)	0 (0)	0 (0)	0 (0)	0 (0)	0.14 (0.1)
<i>Chauliodus macouni</i>	2.14 (2.1) ^{ab}	9.39 (6.3) ^{ab}	8.70 (2.5) ^a	0 (0) ^b	0 (0) ^b	0 (0) ^b	0 (0) ^b	1.74 (0.8)
<i>Merluccius productus</i>	0 (0)	0 (0)	0 (0)	0 (0)	0 (0)	0 (0)	0 (0)	0 (0)
<i>Trachipterus altivelus</i>	0 (0)	2.09 (2.1)	4.45 (4.4)	0 (0)	0 (0)	0 (0)	0.43 (0.4)	0.75 (0.4)
<i>Trachurus symmetricus</i>	50.36 (47.8)	3.51 (3.5)	1.36 (1.4)	0 (0)	0 (0)	0 (0)	0 (0)	2.10 (1.9)
<i>Ichthyos lockingtoni</i>	14.76 (7.9)	6.26 (6.3)	1.37 (1.4)	0.70 (0.7)	0 (0)	0 (0)	0 (0)	1.83 (0.7)
<i>Tetragonurus cuvieri</i>	0 (0)	0 (0)	1.37 (1.4)	0 (0)	0 (0)	0 (0)	0 (0)	0.14 (0.1)
<i>Lyopsetta exilis</i>	0 (0)	0 (0)	0 (0)	0 (0)	0 (0)	0 (0)	0 (0)	0 (0)
<i>Microstomus pacificus</i>	0 (0)	0 (0)	0 (0)	0 (0)	0 (0)	0 (0)	0.87 (0.9)	0.28 (0.3)
Undetermined spp.	6.42 (6.4)	3.51 (3.5)	0 (0)	0 (0)	0 (0)	0 (0)	0 (0)	0.44 (0.3)
Night								
Total eggs	42.42 (40.2)	26.66 (11.2)	1.02 (1.0)	0.95 (1.0)	0 (0)	0.67 (0.7)	0.58 (0.6)	3.65 (2.2)
<i>Sardinops sagax</i>	0 (0)	7.28 (7.3)	0 (0)	0 (0)	0 (0)	0 (0)	0 (0)	0.21 (0.2)
<i>Lipolagus ochotensis</i>	0 (0)	0 (0)	0 (0)	0 (0)	0 (0)	0 (0)	0 (0)	0 (0)
<i>Chauliodus macouni</i>	0 (0)	3.64 (3.6)	1.02 (1.0)	0 (0)	0 (0)	0 (0)	0 (0)	0.24 (0.1)
<i>Merluccius productus</i>	0 (0)	3.88 (3.9)	0 (0)	0 (0)	0 (0)	0 (0)	0 (0)	0.14 (0.1)
<i>Trachipterus altivelus</i>	0 (0)	0 (0)	0 (0)	0 (0)	0 (0)	0 (0)	0 (0)	0 (0)
<i>Trachurus symmetricus</i>	0 (0)	0 (0)	0 (0)	0 (0)	0 (0)	0 (0)	0 (0)	0 (0)
<i>Ichthyos lockingtoni</i>	34.28 (32.0)	11.87 (7.5)	0 (0)	0 (0)	0 (0)	0 (0)	0 (0)	2.21 (1.9)
<i>Tetragonurus cuvieri</i>	2.71 (2.7)	0 (0)	0 (0)	0 (0)	0 (0)	0 (0)	0 (0)	0.14 (0.1)
<i>Lyopsetta exilis</i>	0 (0)	0 (0)	0 (0)	0.95 (1.0)	0 (0)	0 (0)	0 (0)	0.13 (0.1)
<i>Microstomus pacificus</i>	0 (0)	0 (0)	0 (0)	0 (0)	0 (0)	0.67 (0.7)	0.58 (0.6)	0.31 (0.3)
Undetermined spp.	5.43 (5.4)	0 (0)	0 (0)	0 (0)	0 (0)	0 (0)	0 (0)	0.28 (0.3)
Total								
Total eggs	107.69 (49.3) ^a	29.08 (8.7) ^{ab}	10.78 (3.8) ^{abc}	0.81 (0.5) ^{bc}	0 (0) ^c	0.33 (0.3) ^c	0.98 (0.7) ^{bc}	9.08 (3.6)
<i>Sardinops sagax</i>	46.73 (44.1)	6.71 (4.4)	0.76 (0.8)	0 (0)	0 (0)	0 (0)	0 (0)	3.42 (3.1)
<i>Lipolagus ochotensis</i>	1.17 (1.2)	0 (0)	0 (0)	0 (0)	0 (0)	0 (0)	0 (0)	0.08 (0.08)
<i>Chauliodus macouni</i>	1.19 (1.2) ^{ab}	6.83 (3.8) ^{ab}	5.28 (1.9) ^a	0 (0) ^b	0 (0) ^b	0 (0) ^b	0 (0) ^b	1.07 (0.5)
<i>Merluccius productus</i>	0 (0)	1.72 (1.7)	0 (0)	0 (0)	0 (0)	0 (0)	0 (0)	0.06 (0.06)
<i>Trachipterus altivelus</i>	0 (0)	1.16 (1.2)	2.47 (2.5)	0 (0)	0 (0)	0 (0)	0.24 (0.2)	0.42 (0.2)
<i>Trachurus symmetricus</i>	27.98 (26.7)	1.95 (1.9)	0.76 (0.8)	0 (0)	0 (0)	0 (0)	0 (0)	1.17 (1.1)
<i>Ichthyos lockingtoni</i>	23.43 (14.1) ^a	8.75 (4.6) ^{ab}	0.76 (0.8) ^b	0.39 (0.4) ^b	0 (0) ^b	0 (0) ^b	0 (0) ^b	2.00 (0.8)
<i>Tetragonurus cuvieri</i>	1.21 (1.2)	0 (0)	0.76 (0.8)	0 (0)	0 (0)	0 (0)	0 (0)	0.14 (0.1)
<i>Lyopsetta exilis</i>	0 (0)	0 (0)	0 (0)	0.42 (0.4)	0 (0)	0 (0)	0 (0)	0.06 (0.06)
<i>Microstomus pacificus</i>	0 (0)	0 (0)	0 (0)	0 (0)	0 (0)	0.33 (0.3)	0.74 (0.5)	0.30 (0.2)
Undetermined spp.	5.98 (4.1)	1.95 (1.9)	0 (0)	0 (0)	0 (0)	0 (0)	0 (0)	0.37 (0.2)

(10–20 and 20–50 m, respectively) in the same haul (HH-05A).

Fish egg concentrations varied across depth-stratified and diel scales (Table 2). However, depth stratum was the only significant factor explaining variation in *C. macouni*, *I. lockingtoni*, and total egg densities in the type-II ANOVA model ($P < 0.05$). Almost 91% of the

total egg abundance was found in the upper 100 m of the water column. Egg densities were generally highest near the surface and decreased with depth. There were no *S. sagax*, *C. macouni*, or *I. lockingtoni* eggs found at depths >100 m.

Mean total water-column concentrations were greater during the day than at night for *S. sagax* (5.99/1000 m³

[day]; 0.21/1000 m³ [night]), *C. macouni* (1.74/1000 m³ [day]; 1.07/1000 m³ [night]), and total eggs (13.43/1000 m³ [day]; 3.65/1000 m³ [night]), although differences were not significant (ANOVA, $P > 0.05$). However, *I. lockingtoni* eggs occurred in slightly higher concentrations in the water column at night (2.21/1000 m³) than during the day (1.83/1000 m³). Egg concentrations were generally higher during the day than at night at each depth stratum for most taxa (Table 2).

Larval concentrations and distributions

A total of 1571 fish larvae representing 20 taxa from 11 families were collected throughout the study. Three families accounted for 97.4% of the total standardized larval concentration: Scorpaenidae (55.6%), Myctophidae (35.6%), and Pleuronectidae (6.2%). Within these families, four taxa were dominant based on total mean concentration and frequency of occurrence from all depth-stratified samples: *Sebastes* spp. (57.75/1000 m³; 0.42), *S. leucopsarus* (25.23/1000 m³; 0.45), *T. crenularis* (8.81/1000 m³; 0.35), and *L. exilis* (3.78/1000 m³; 0.15). Several other taxa were documented at relatively high frequencies but at lower mean concentrations: *Glyptocephalus zachirus* (rex sole) (2.10/1000 m³; 0.18), *Protomyctophum thompsoni* (northern flashlightfish) (1.17/1000 m³; 0.16), *I. lockingtoni* (1.01/1000 m³; 0.11), *Diaphus theta* (California headlightfish) (0.91/1000 m³; 0.11), and *Liparis fucensis* (slipskin snailfish) (0.66/1000 m³; 0.11).

Larval concentrations varied across depth-stratified and diel scales (Table 3). For *S. leucopsarus* larvae, both factors and their interaction term (depth, diel presence, and depth×diel presence) in the type-II ANOVA model were significant ($P < 0.05$). However, depth stratum was the only significant factor explaining variation in *L. exilis*, *Sebastes* spp., *T. crenularis*, and total larval densities in the model. More than 96% of the total larval abundance was distributed in the upper 100 m of the water column. Mean concentrations of *Sebastes* spp., *S. leucopsarus*, *T. crenularis*, and total larvae generally increased from the surface to the 20–50 m depth, then declined steadily as depth increased. No *Sebastes* spp. larvae were collected below 100 m. In addition, *L. exilis* larvae were found only in the 20–100 m depth range, where concentrations were greater than 3× higher in the 20–50 than in the 50–100 m depth stratum.

Mean larval densities were generally greater at night than during the day at all but one depth stratum for *Sebastes* spp., *S. leucopsarus*, *T. crenularis*, and total larvae (Table 3). These differences were significant for *S. leucopsarus* and total larvae at the 0–10 and 10–20 m depth strata (ANOVA, $P < 0.05$). However, higher larval densities were found during the day than at night for *Sebastes* spp., *S. leucopsarus*, and total larvae at the 50–100 m depth stratum. In addition, *L. exilis* larvae were found at higher densities during the day than at night at all depths at which they were collected.

Analysis of the dominant larval taxa depth distributions over a 16-h period revealed evidence of diel verti-

cal migration (Fig. 2). Weighted mean depth (WMD) of *L. exilis* and *Sebastes* spp. larvae increased from 2324 to 1550 PDT, whereas larval *S. leucopsarus* WMD decreased slightly between 2324 and 0303 PDT before increasing as the day progressed. In contrast, *T. crenularis* larvae appeared to move up in the water column from 2324 to 0604 PDT but were not found in any sample from the haul conducted at 1550 PDT.

Weighted mean standard lengths (SL) of *L. exilis*, *Sebastes* spp., *S. leucopsarus*, and *T. crenularis* larvae generally increased with depth (Table 4). Mean SL for *S. leucopsarus* larvae collected during night and during both day and night combined was significantly greater at the 20–100 m than at the 10–20 m depth stratum (ANOVA, $P < 0.05$). *Lyopsetta exilis*, *Sebastes* spp., and *T. crenularis* larvae collected at night were generally the same size or larger than those collected during the day at each depth stratum, although these differences were not significant (ANOVA, $P > 0.05$).

Diversity and evenness

Larval and egg diversity and evenness varied across depth strata. Larval diversity generally increased with depth. Egg diversity increased from the surface to 20 m then declined with increasing depth. Egg and larval evenness generally increased with depth before declining slightly at the 200–350 m depth stratum. Egg diversity and evenness could not be assessed at the 100–150 and 150–200 m depth strata because no eggs were found between 100 and 150 m, and only one egg (*Microstomus pacificus* [Dover sole]) was found at the 150–200 m depth stratum. There was no appreciable difference in egg and larval diversity and evenness between day and night samples.

Assemblages

Several taxa and depth assemblages were identified on the basis of cluster analyses and MDS, although no diel assemblages were apparent (Fig. 3, A–C). Larval taxa separated out into four assemblages (Fig. 3A). In more than 5% of the samples too few egg taxa ($n = 4$) were present to permit identification of any assemblages. Cluster analyses and MDS also indicated the presence of two egg and larval depth assemblages: <100 m and >100 m (Fig. 3, B and C).

Environmental relationships

BIO-ENV and correlation analyses revealed significant relationships between several environmental factors and egg and larval mean concentrations. A depth-stratified BIO-ENV analysis, which included mean depth (m), mean temperature (°C), and mean salinity of each depth-stratified sample, showed that depth alone explained 46% of the variability in mean egg concentrations and 44% in larval concentrations. No multiple-factor combination explained more variability in egg or larval concentration data. Pairwise correlation analyses revealed significant

Table 3

Day, night, and total mean densities (number/1000 m³) of fish larvae collected at different depth strata from a single offshore station off the central Oregon coast in 2000 and 2002 (1 SE in parentheses). For between stratum comparisons of each taxon within each diel category, different alphabetic superscripts indicate significant differences (ANOVA, $P < 0.05$). For diel comparisons of each taxon within each depth stratum, different numeric superscripts indicate significant differences (ANOVA, $P < 0.05$).

Taxa	Depth (m)								Total
	0–10	10–20	20–50	50–100	100–150	150–200	200–350		
Day									
Total larvae	247.47 (22.6) ^{abc}	2130.11 (71.3) ^{ab}	324.49 (104.4) ^a	150.55 (59.3) ^a	6.27 (2.6) ^{bcd}	1.93 (1.3) ^d	2.97 (0.8) ^{cd}	75.05 (20.1)	
<i>Sardinops sagax</i>	0 (0)	0 (0)	0 (0)	0 (0)	0 (0)	0 (0)	0 (0)	0 (0)	
<i>Pseudobathylagus milleri</i>	0 (0)	0 (0)	0 (0)	0 (0)	0 (0)	0 (0)	0.43 (0.4)	0.19 (0.2)	
<i>Chauliodus macouni</i>	0 (0)	0 (0)	0 (0)	0 (0)	1.59 (1.6)	0 (0)	0 (0)	0.11 (0.1)	
<i>Tactostoma macropus</i>	2.09 (2.1)	0 (0)	0 (0)	0 (0)	0 (0)	0 (0)	0 (0)	0.14 (0.1)	
<i>Lestidiops ringens</i>	0 (0)	0 (0)	0 (0)	0 (0)	0 (0)	0 (0)	0 (0)	0 (0)	
<i>Myctophidae</i> spp.	0 (0)	0 (0)	0 (0)	0 (0)	0 (0)	0 (0)	0 (0)	0 (0)	
<i>Protomyctophum thompsoni</i>	0 (0)	0 (0)	0 (0)	1.70 (1.1)	3.92 (1.5)	0 (0)	0.62 (0.4)	0.88 (0.3)	
<i>Tarletonbeania crenularis</i>	0 (0) ^c	12.98 (9.6) ^{abc}	26.69 (13.8) ^a	18.63 (13.9) ^{ab}	0.76 (0.8) ^{abc}	0 (0) ^{bc}	0.26 (0.3) ^{bc}	8.40 (5.1)	
<i>Nannobranchium regale</i>	0 (0)	2.46 (2.5)	0 (0)	0 (0)	0 (0)	0 (0)	0 (0)	0.14 (0.1)	
<i>Stenobranchius leucopsarus</i>	20 (0) ^b	23.13 (3.1) ^b	55.79 (34.4) ^a	46.50 (16.4) ^a	0 (0) ^b	0 (0) ^b	0.79 (0.5) ^b	15.42 (5.3)	
<i>Diaphus theta</i>	0 (0)	2.46 (2.5)	0 (0)	0 (0)	0 (0)	0 (0)	0 (0)	0.14 (0.1)	
<i>Brosmophycis marginata</i>	0 (0)	3.13 (3.1)	0 (0)	0 (0)	0 (0)	0 (0)	0 (0)	0.14 (0.1)	
<i>Sebastes</i> spp.	33.45 (26.0) ^{ab}	85.61 (51.0) ^{ab}	190.12 (54.4) ^a	64.04 (38.6) ^a	0 (0) ^b	0 (0) ^b	0 (0) ^b	38.73 (8.9)	
<i>Liparis fucensis</i>	0 (0)	0 (0)	2.69 (1.6)	2.60 (1.7)	0 (0)	0.53 (0.5)	0 (0)	0.81 (0.4)	
<i>Ichthythys lockingtoni</i>	8.47 (5.2)	10.94 (5.1)	0 (0)	0 (0)	0 (0)	0 (0)	0 (0)	1.28 (0.6)	
<i>Citharichthys sordidus</i>	0 (0)	0 (0)	0 (0)	0 (0)	0 (0)	0 (0)	0 (0)	0 (0)	
<i>Glyptocephalus zachirus</i>	0 (0)	9.39 (9.4)	8.43 (5.2)	4.65 (4.7)	0 (0)	0 (0)	0 (0)	2.21 (0.7)	
<i>Lyopsetta exilis</i>	0 (0) ^b	0 (0) ^b	40.77 (25.7) ^a	11.72 (5.1) ^a	0 (0) ^b	0 (0) ^b	0 (0) ^b	5.60 (2.7)	
<i>Microstomus pacificus</i>	0 (0)	0 (0)	0 (0)	0.70 (0.7)	0 (0)	1.40 (1.4)	0.87 (0.5)	0.66 (0.3)	
Undetermined spp.	3.45 (3.5)	0 (0)	0 (0)	0 (0)	0 (0)	0 (0)	0 (0)	0.19 (0.2)	
Night									
Total larvae	1293.20 (131.3) ^a	1667.70 (153.9) ^a	630.54 (281.2) ^a	84.33 (41.4) ^{ab}	13.21 (7.8) ^b	3.66 (1.2) ^b	2.68 (1.0) ^b	139.73 (42.4)	
<i>Sardinops sagax</i>	4.42 (2.7)	0 (0)	0 (0)	0 (0)	0 (0)	0 (0)	0 (0)	0.27 (0.2)	
<i>Pseudobathylagus milleri</i>	0 (0)	0 (0)	0 (0)	0 (0)	0 (0)	0 (0)	0 (0)	0 (0)	
<i>Chauliodus macouni</i>	0 (0)	0 (0)	0 (0)	3.26 (1.1)	0.94 (0.9)	0 (0)	0 (0)	0.58 (0.3)	
<i>Tactostoma macropus</i>	0 (0)	0 (0)	0 (0)	0 (0)	0 (0)	0 (0)	0 (0)	0 (0)	
<i>Lestidiops ringens</i>	0 (0)	0 (0)	0 (0)	1.45 (1.4)	0 (0)	0 (0)	0 (0)	0.14 (0.1)	
<i>Myctophidae</i> spp.	0 (0)	0 (0)	3.05 (3.1)	1.90 (1.9)	0 (0)	0 (0)	0 (0)	0.68 (0.4)	
<i>Protomyctophum thompsoni</i>	0 (0)	0 (0)	0 (0)	3.61 (2.5)	8.30 (4.8)	1.29 (1.3)	0 (0)	1.52 (0.7)	
<i>Tarletonbeania crenularis</i>	1.34 (1.3) ^{ab}	27.65 (19.4) ^{ab}	38.98 (27.9) ^a	19.26 (10.7) ^a	3.02 (3.0) ^{ab}	0.67 (0.7) ^{ab}	0 (0) ^b	9.34 (5.5)	
<i>Nannobranchium regale</i>	5.43 (5.4)	12.36 (12.4)	2.03 (1.2)	0 (0)	0 (0)	0 (0)	0 (0)	0.94 (0.4)	
<i>Stenobranchius leucopsarus</i>	15.09 (2.2) ^{abc}	1248.31 (170.3) ^a	175.64 (61.7) ^a	34.70 (19.4) ^{ab}	0 (0) ^c	1.71 (1.0) ^{bc}	1.59 (0.6) ^{bc}	37.50 (13.3)	

continued

Table 3 (continued)

Taxa	Depth (m)								Total
	0-10	10-20	20-50	50-100	100-150	150-200	200-350		
Night (continued)									
<i>Diaphus theta</i>	3.05 (1.8)	11.52 (3.9)	9.20 (6.7)	0 (0)	0 (0)	0 (0)	0 (0)	0 (0)	1.88 (1.0)
<i>Bromophycis marginata</i>	0 (0)	0 (0)	0 (0)	0 (0)	0 (0)	0 (0)	0 (0)	0 (0)	0 (0)
<i>Sebastes</i> spp.	263.65 (124.1) ^a	356.70 (176.9) ^a	379.92 (209.6) ^a	14.96 (12.0) ^{ab}	0 (0) ^b	0 (0) ^b	0 (0) ^b	0 (0) ^b	81.52 (25.7)
<i>Liparis fucensis</i>	0 (0)	0 (0)	0 (0)	3.23 (1.9)	0 (0)	0 (0)	0 (0)	0 (0)	0.47 (0.3)
<i>Ichthythys lockingtoni</i>	6.45 (4.8)	0 (0)	1.02 (1.0)	0 (0)	0 (0)	0 (0)	0 (0)	0 (0)	0.67 (0.5)
<i>Citharichthys sordidus</i>	1.70 (1.7)	0 (0)	0 (0)	0 (0)	0 (0)	0 (0)	0 (0)	0 (0)	0.13 (0.1)
<i>Glyptocephalus zachirus</i>	2.07 (2.1)	11.17 (6.9)	7.15 (4.5)	0 (0)	0.94 (0.9)	0 (0)	0.81 (0.8)	0 (0)	1.96 (1.0)
<i>Lypsetta exilis</i>	0 (0) ^b	0 (0) ^b	9.23 (3.5) ^a	1.95 (2.0) ^{ab}	0 (0) ^b	0 (0) ^b	0 (0) ^b	0 (0) ^b	1.50 (0.5)
<i>Microstomus pacificus</i>	0 (0)	0 (0)	2.28 (1.3)	0 (0)	0 (0)	0 (0)	0.29 (0.3)	0 (0)	0.34 (0.2)
Undetermined spp.	0 (0)	0 (0)	2.04 (2.0)	0 (0)	0 (0)	0 (0)	0 (0)	0 (0)	0.28 (0.3)
Total mean									
Total larvae	156.68 (69.8) ^a	369.04 (119.5) ^a	460.51 (138.2) ^a	121.11 (37.4) ^a	9.74 (4.0) ^b	2.80 (0.9) ^b	2.84 (0.6) ^b	103.80 (23.3)	
<i>Sardinops sagax</i>	1.96 (1.3)	0 (0)	0 (0)	0 (0)	0 (0)	0 (0)	0 (0)	0.12 (0.1)	
<i>Pseudobathylagus milleri</i>	0 (0)	0 (0)	0 (0)	0 (0)	0 (0)	0 (0)	0.24 (0.2)	0.11 (0.1)	
<i>Chauliodus macouni</i>	0 (0)	0 (0)	0 (0)	1.45 (0.7)	1.26 (0.9)	0 (0)	0 (0)	0.32 (0.1)	
<i>Toctostoma macropus</i>	1.16 (1.2)	0 (0)	0 (0)	0 (0)	0 (0)	0 (0)	0 (0)	0.08 (0.08)	
<i>Lestidiops ringens</i>	0 (0)	0 (0)	0 (0)	0.64 (0.6)	0 (0)	0 (0)	0 (0)	0.06 (0.06)	
<i>Myctophidae</i> spp.	0 (0)	0 (0)	1.36 (1.4)	0.85 (0.8)	0 (0)	0 (0)	0 (0)	0.30 (0.2)	
<i>Protomyctophum thompsoni</i>	0 (0)	0 (0)	0 (0)	2.55 (1.2)	6.11 (2.5)	0.64 (0.6)	0.34 (0.2)	1.17 (0.3)	
<i>Tarletonbeania crenularis</i>	0.60 (0.6) ^c	19.50 (9.7) ^{abc}	32.15 (13.7) ^a	18.91 (8.6) ^{ab}	1.89 (1.5) ^{bc}	0.33 (0.3) ^c	0.15 (0.1) ^c	8.81 (3.5)	
<i>Nannobranchium regale</i>	2.41 (2.4)	6.86 (5.5)	0.90 (0.6)	0 (0)	0 (0)	0 (0)	0 (0)	0.50 (0.2)	
<i>Stenobranchius leucopsarus</i>	2.26 (1.3) ^{bc}	112.1 (81.8) ^{ab}	109.06 (37.5) ^a	41.25 (11.9) ^a	0 (0) ^c	0.85 (0.6) ^{bc}	1.14 (0.4) ^{bc}	25.23 (7.2)	
<i>Diaphus theta</i>	1.35 (0.9)	6.49 (2.6)	4.09 (3.2)	0 (0)	0 (0)	0 (0)	0 (0)	0.91 (0.5)	
<i>Bromophycis marginata</i>	0 (0)	1.74 (1.7)	0 (0)	0 (0)	0 (0)	0 (0)	0 (0)	0.08 (0.08)	
<i>Sebastes</i> spp.	135.76 (66.3) ^{ab}	206.09 (90.6) ^{ab}	274.47 (96.2) ^a	42.22 (22.6) ^b	0 (0) ^c	0 (0) ^c	0 (0) ^c	57.75 (13.7)	
<i>Liparis fucensis</i>	0 (0)	0 (0)	1.50 (1.0)	2.88 (1.2)	0 (0)	0.27 (0.3)	0 (0)	0.66 (0.2)	
<i>Ichthythys lockingtoni</i>	7.57 (3.4)	6.08 (3.3)	0.45 (0.5)	0 (0)	0 (0)	0 (0)	0 (0)	1.01 (0.4)	
<i>Citharichthys sordidus</i>	0.76 (0.8)	0 (0)	0 (0)	0 (0)	0 (0)	0 (0)	0 (0)	0.06 (0.06)	
<i>Glyptocephalus zachirus</i>	0.92 (0.9)	10.18 (5.7)	7.86 (3.3)	2.58 (2.6)	0.47 (0.5)	0 (0)	0.36 (0.4)	2.10 (0.5)	
<i>Lypsetta exilis</i>	0 (0) ^b	0 (0) ^b	26.75 (14.7) ^a	7.38 (3.3) ^a	0 (0) ^b	0 (0) ^b	0 (0) ^b	3.78 (1.6)	
<i>Microstomus pacificus</i>	0 (0)	0 (0)	1.02 (0.7)	0.39 (0.4)	0 (0)	0.70 (0.7)	0.61 (0.3)	0.52 (0.2)	
Undetermined spp.	1.92 (1.9)	0 (0)	0.91 (0.9)	0 (0)	0 (0)	0 (0)	0 (0)	0.23 (0.2)	

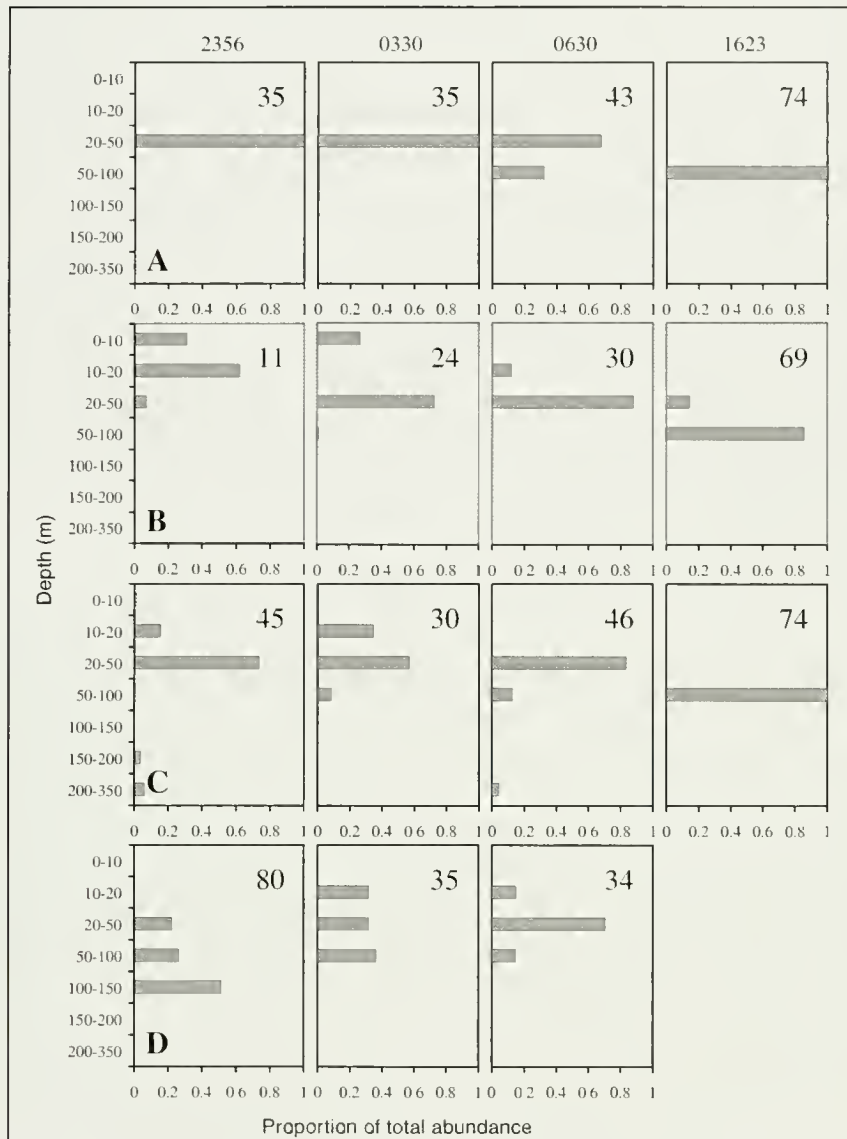


Figure 2

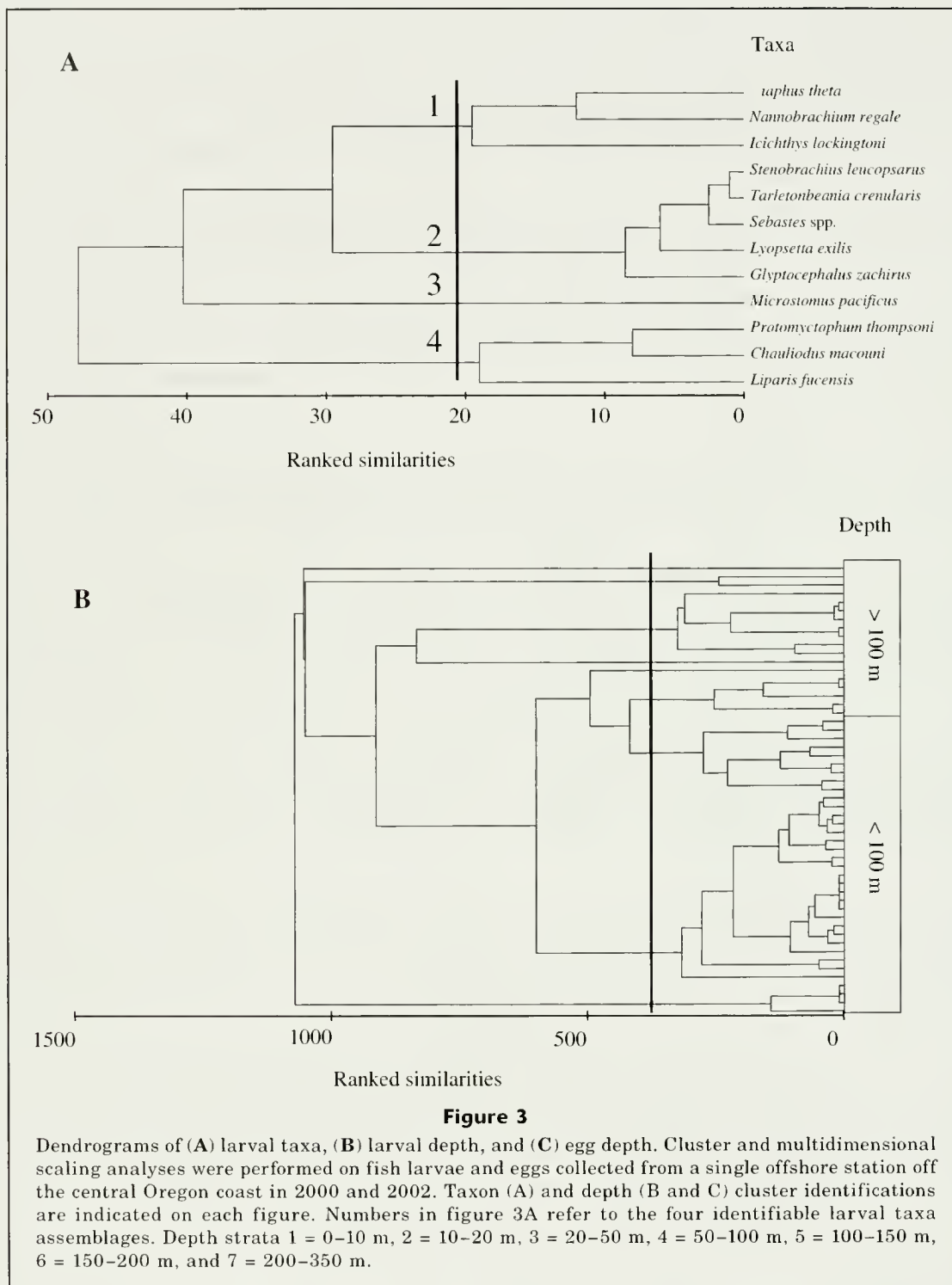
Diel differences in the proportion of total abundances for (A) *Lyopsetta exilis*, (B) *Sebastes* spp., (C) *Stenobranchius leucopsarus*, and (D) *Torlettonbeania crenularis* larvae, collected at different depth strata during a 16-h period at a single offshore station off the central Oregon coast on 5–6 August 2000. No *T. crenularis* larvae were collected in the 1623 PDT haul. The times at which the first MOCNESS net of each haul was opened are given above the panels. Numbers in the upper right corner of each panel represent the weighted mean depth (m) of larvae collected in each haul. During the sampling period, sunset occurred at 2033 and sunrise at 0610 PDT.

correlations between temperature and mean concentrations of *Sebastes* spp. and total larvae, *C. macouni*, *I. lockingtoni*, and total eggs. Significant negative correlations were seen between these same taxa and salinity, and temperature and salinity were negatively correlated with each other ($P < 0.05$) (Table 5). Mean concentrations of *L. exilis*, *S. leucopsarus*, and *T. crenularis* larvae, and *S. sagax* eggs were also positively correlated with temper-

ature and negatively correlated with salinity, although the correlations were not significant ($P > 0.05$).

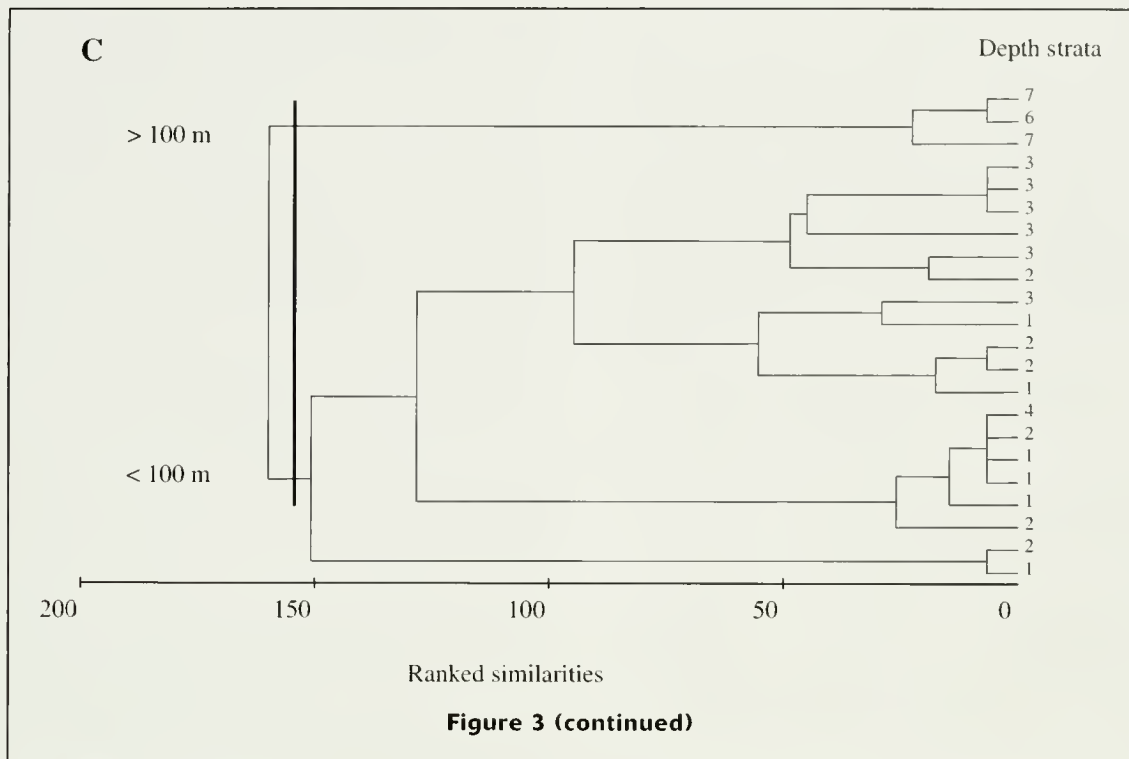
Discussion

The species composition, assemblages, and dominant taxa identified in this study were similar to those found



in other studies conducted during the summer in offshore waters off the central Oregon coast (Richardson, 1973; Richardson and Percy, 1977; Brodeur et al., 1985; Auth and Brodeur, 2006). This similarity may indicate that the composition of dominant larval fishes in this area is resilient to dramatic environmental fluctuations such as those observed during the last 35 years in the

northern California Current (Schwing and Moore, 2000; Grantham et al., 2004). It also provides evidence in support of the hypothesis of Auth and Brodeur (2006) that past sampling of ichthyoplankton along the NH line during the summer is indeed representative of summer ichthyoplankton assemblages elsewhere along the Oregon coast.

**Table 4**

Day, night, and total mean standard lengths (mm) of fish larvae collected at different depth strata from a single offshore station off the central Oregon coast in 2000 and 2002 (1 SE in parentheses). For between stratum comparisons of each taxon within each diel category, different superscripts indicate significant differences (ANOVA, $P < 0.05$).

Taxa	Depth (m)						Total	
	0–10	10–20	20–50	50–100	100–150	150–200		200–350
Day								
<i>Lyopsetta exilis</i>	—	—	8.7 (0.6)	10.3 (0.5)	—	—	—	9.1 (0.4)
<i>Sebastes</i> spp.	4.1 (1.4)	5.1 (0.2)	6.6 (0.7)	7.4 (1.4)	—	—	—	6.2 (0.5)
<i>Stenobranchius leucopsarus</i>	—	13.6	9.3 (0.9)	9.5 (0.6)	—	—	14.7 (0.3)	9.5 (0.5)
<i>Tarletonbeania crenularis</i>	—	9.2 (2.2)	8.9 (1.1)	10.7 (1.4)	14.3	—	16.3	9.6 (0.7)
Night								
<i>Lyopsetta exilis</i>	—	—	9.6 (0.4)	8.6	—	—	—	9.4 (0.4)
<i>Sebastes</i> spp.	6.4 (0.2)	6.2 (0.5)	7.9 (0.5)	10.0 (2.3)	—	—	—	6.9 (0.3)
<i>Stenobranchius leucopsarus</i>	5.6 (0.7) ^{ab}	7.6 (0.2) ^b	9.7 (0.8) ^a	11.4 (0.3) ^a	—	14.8 (0.0) ^{ab}	15.4 (0.9) ^{ab}	8.8 (0.4)
<i>Tarletonbeania crenularis</i>	8.7	7.7 (0.3)	9.4 (0.5)	12.1 (0.9)	13.4	16.0	—	9.6 (0.6)
Total mean								
<i>Lyopsetta exilis</i>	—	—	8.8 (0.4)	10.1 (0.5)	—	—	—	9.1 (0.3)
<i>Sebastes</i> spp.	6.1 (0.5)	6.0 (0.4)	7.4 (0.4)	7.5 (1.1)	—	—	—	6.7 (0.3)
<i>Stenobranchius leucopsarus</i>	5.6 (0.7) ^{ab}	7.7 (0.4) ^b	9.6 (0.5) ^a	10.2 (0.5) ^a	—	14.8 (0.0) ^{ab}	15.1 (0.6) ^{ab}	8.9 (0.3)
<i>Tarletonbeania crenularis</i>	8.7	8.3 (0.9)	9.2 (0.6)	11.3 (0.8)	13.5 (0.4)	16.0	16.3	9.6 (0.4)

However, in our study we collected no *Engraulis mordax* (northern anchovy) eggs or larvae, which usually comprise a significant portion of the offshore ichthyoplankton in August (Richardson and Pearcy, 1977). *Engraulis mordax* larvae have been associated with

warmer, less saline, offshore surface waters from the Columbia River (Richardson, 1973; Auth and Brodeur, 2006). This warmer surface water did not appear to have occurred as far south as our sampling station, except perhaps during the last haul in 2000 (HH-05G) (Fig. 2).

Table 5

Correlation coefficients for the depth-stratified sample means ($n=74$) of eleven variables sampled during the day and night from a single station (HH-05) off the Oregon coast in August 2000 and 2002: water temperature ($^{\circ}\text{C}$), salinity (kg/m^3), and \log_e -transformed densities (number/1000 m^3) of *Lyopsetta exilis*, *Sebastes* spp., *Stenobranchius leucopsarus*, *Tarletonbeania crenularis*, and total fish larvae, and *Chauliodus macouni*, *Ichthyos lockingtoni*, *Sardinops sagax*, and total fish eggs. *= $P<0.05$, **= $P<0.001$, ***= $P<0.0001$.

	Temperature	Salinity
Salinity	-0.82***	
<i>Lyopsetta exilis</i>	0.03	-0.09
<i>Sebastes</i> spp.	0.48***	-0.51***
<i>Stenobranchius leucopsarus</i>	0.16	-0.18
<i>Tarletonbeania crenularis</i>	0.15	-0.14
Total larvae	0.57***	-0.53***
<i>Chauliodus macouni</i>	0.24*	-0.40**
<i>Ichthyos lockingtoni</i>	0.63***	-0.47***
<i>Sardinops sagax</i>	0.20	-0.23
Total eggs	0.55***	-0.51***

In addition, we found evidence that *S. sagax* spawn in this region, as documented since the 1990s (Emmett et al., 2005; Auth and Brodeur, 2006). Similarly, we collected *T. symmetricus* eggs, which are normally found off southern California but which have been reported off southern Oregon by Kendall and Clark¹, off Washington by Ahlstrom (1956), and most recently in the Columbia River plume by Parnel et al.²

Our finding that the vast majority (96%) of fish larvae were present in the upper 100 m of the water column has been supported by several other studies (Brodeur and Rugen, 1994; Suntsov, 2002; Sabatés, 2004; Auth and Brodeur, 2006). This finding has significant implications for strategies to sample ichthyoplankton off Oregon and potentially throughout the California Current. *Sebastes* spp. primarily occurred in the 10–50 m depth range, as previously reported (Ahlstrom, 1961; Boehlert et al., 1985; Sakuma et al., 1999; Auth and Brodeur, 2006), whereas *L. exilis* larvae were found between 20 and 100 m as observed by Auth and Brodeur (2006) and during daytime collections made by Boehlert et al. (1985). Also, myctophid larvae within the subfamily Myctophinae (*T. crenularis*) were found at greater

depths than those within the subfamily Lampanyctinae (*S. leucopsarus*) as reported by Sassa et al. (2002), although the vast majority was still found above 100 m.

One implication from these findings is that sampling in the upper 100 m of the water column should be sufficient to characterize pelagic summer ichthyoplankton abundances and distributions of the majority of fish taxa along the northeastern Pacific coast (Brodeur and Rugen, 1994; Auth and Brodeur, 2006). A further implication is that sampling strategies without discrete vertical strata, which expend additional effort collecting ichthyoplankton below 100 m, may underestimate larval fish abundances by using samples from largely uninhabited portions of the water column.

Differences in the abundance and size of fish larvae collected in diel samples have often led researchers to suspect bias due to net avoidance, resulting in underestimation of larvae (especially larger larvae) collected during the day (Richardson and Percy, 1977; Boehlert et al., 1985). These differences can vary depending on such factors as gear type, size, and tow speed. The present study supports this contention, particularly for the upper 20 m of the water column, where light penetration is of greatest concern. Sakuma et al. (1999) found that total adjusted catches of *Sebastes* spp. larvae off the central California coast were significantly greater at night than during the day. Richardson and Percy (1977) observed that large *Sebastes* spp. larvae (9–11 mm) were collected exclusively during the night, while smaller larvae (3–4 mm) were collected during both day and night at the 0–50 m depth off the central Oregon coast. However, they did not find evidence of daytime net avoidance for *S. leucopsarus* (5–11 mm) or *Isopsetta isolepis* (butter sole) (14–23 mm) larvae collected during the same study. In addition, Laroche and Richardson (1979) found no evidence of increased net avoidance by larger *Parophrys vetulus* (English sole) larvae collected during the day versus night off the Oregon coast. However, considering results from the present and similar studies on differences in diel ichthyoplankton abundance (Ahlstrom, 1959), we believe that ichthyoplankton sampling should be conducted primarily at night if at all possible to eliminate any potential bias due to net avoidance. Net avoidance should at least be factored into any model estimating abundances and depth distributions of larvae collected during both day and night.

As noted earlier, diel vertical migration (DVM) has been well documented for larvae of many marine fish species. A variety of theories have been put forth to explain DVM in larval fish, including predator avoidance (Hunter and Sanchez, 1976; Yamashita et al., 1985), the pursuit of zooplankton prey (Fortier and Leggett, 1983; Munk et al., 1989), facilitated larval transport in varying tidal currents (Norcross and Shaw, 1984; Hare and Govoni, 2005), optimization of the energetic advantage gained by larvae at certain depths in thermally stratified water (Wurtsbaugh and Neverman, 1988; Neilson and Perry, 1990), and the pursuit of optimum light conditions for larval survival (Heath et al., 1988). Although this study was not designed to

¹ Kendall, A. W., Jr., and J. Clark. 1982. Ichthyoplankton off Washington, Oregon, and northern California April–May 1980. AFSC Proc. Rep. 82-11, 44 p. National Oceanic and Atmospheric Administration, Alaska Fisheries Science Center, 7600 Sand Point Way NE, Seattle, WA 98115.

² Parnel, M. M., R. L. Emmett, and R. D. Brodeur. 2006. Interannual and seasonal variation in ichthyoplankton collected off the Columbia River. Unpubl. manuscript, 20 p. Oregon State Univ., Hatfield Marine Science Center, 2030 SE Marine Sci. Dr., Newport, OR 97365.

determine the underlying causes of the DVM of larval fish, it does provide some evidence for type-I DVM (up at night, down during the day) for *S. leucopsarus* and *Sebastes* spp. larvae (and to a lesser extent for *L. exilis* larvae), and type-II DVM (down at night, up during the day) for *T. crenularis* larvae (Fig. 3). Evidence for either type of DVM for larval *Sebastes* spp. has not been found in previous studies (Sakuma et al., 1999; Bjorkstedt et al., 2002). This new type-I DVM could help explain the retention of *Sebastes* spp. larvae close to settlement areas along and inshore from the shelf as observed by Auth and Brodeur (2006)—a retention that is due to the ability of larvae to regulate their position in the water column and to take advantage of selective Ekman transport (Sakuma and Larson, 1995).

Acknowledgments

We thank the captains and crews of all research vessels participating in this study for their cooperation and assistance in the sampling. Collection of all MOCNESS tows discussed in this paper was made possible through two grants to W. Peterson from the U. S. GLOBEC program (NA 67RJ10151 and NA 86OP0589). We are indebted to the Peterson Zooplankton Group for their efforts in collecting data at sea and for archiving the samples. In this regard, special thanks to J. Keister, M. Vance, L. Feinberg, T. Shaw, J. Lamb, A. Røestad, and D. Swenson. We also thank M. Busby, D. Blood, and A. Matarese of the Alaska Fisheries Science Center Recruitment Studies Program for their help in identifying eggs and larvae. We thank G. Boehlert, B. Mundy, A. Moles, and three anonymous reviewers for critical reviews of the manuscript. Funding was provided by NOAA's Stock Assessment Improvement Program, Fisheries and the Environment Initiative, and the Northeast Pacific GLOBEC Program. This is contribution number 512 of the U.S. GLOBEC Program.

Literature cited

- Ahlstrom, E. H.
1956. Eggs and larvae of anchovy, jack mackerel, and Pacific mackerel. *Fish. Bull.* 5:33–42.
1959. Vertical distribution of pelagic fish eggs and larvae off California and Baja California. *Fish. Bull.* 60:107–46.
1961. Distribution and relative abundance of rockfish (*Sebastes* spp.) larvae off California and Baja California. *ICNAF Spec. Pub.* 3:169–176.
- Auth, T. D., and R. D. Brodeur.
2006. Distribution and community structure of ichthyoplankton off the coast of Oregon, USA, in 2000 and 2002. *Mar. Ecol. Prog. Ser.* 319:199–213.
- Bjorkstedt, E. P., L. K. Rosenfeld, B. A. Grantham, Y. Shkedy, and J. Roughgarden.
2002. Distributions of larval rockfishes *Sebastes* spp. across nearshore fronts in a coastal upwelling region. *Mar. Ecol. Prog. Ser.* 242:215–228.
- Boehlert, G. W., D. M. Gadomski, and B. C. Mundy.
1985. Vertical distribution of ichthyoplankton off the Oregon coast in spring and summer months. *Fish. Bull.* 83:611–621.
- Bradford, M. J.
1992. Precision of recruitment predictions from early life stages of marine fishes. *Fish. Bull.* 90:439–453.
- Brewer, G. D., and G. S. Kleppel.
1986. Diel vertical distribution of fish larvae and their prey in nearshore waters of southern California. *Mar. Ecol. Prog. Ser.* 27:217–226.
- Brodeur, R. D., D. M. Gadomski, W. G. Pearcy, H. P. Batchelder, and C. B. Miller.
1985. Abundance and distribution of ichthyoplankton in the upwelling zone off Oregon during anomalous El Niño conditions. *Estuarine Coastal Shelf Sci.* 21:365–378.
- Brodeur, R. D., and W. C. Rugen.
1994. Diel vertical distribution of ichthyoplankton in the northern Gulf of Alaska. *Fish. Bull.* 92:223–235.
- Clarke, K. R., and R. N. Gorley.
2001. Primer v5: user manual/tutorial, 91 p. PRIMER-E Ltd., Plymouth, UK.
- Clarke, K. R., and R. M. Warwick.
2001. Change in marine communities: an approach to statistical analysis and interpretation, 2nd ed., 172 p. PRIMER-E Ltd., Plymouth, UK.
- Comyns, B. H., and J. Lyczkowski-Shultz.
2004. Diel vertical distribution of Atlantic croaker, *Micropogonias undulatus*, larvae in the northcentral Gulf of Mexico with comparisons to red drum, *Sciaenops ocellatus*. *Bull. Mar. Sci.* 74:69–80.
- Dunn, O. J., and V. A. Clark.
1974. Applied statistics: Analysis of variance and regression, 387 p. John Wiley, New York, NY.
- Emmett, R. L., R. D. Brodeur, T. W. Miller, S. S. Pool, P. J. Bentley, G. K. Krutzikowsky, and J. McCrae.
2005. Pacific sardine (*Sardinops sagax*) abundance, distribution and ecological relationships in the Pacific Northwest. *Calif. Coop. Oceanic Fish. Invest. Rep.* 46:122–143.
- Field, J. G., K. R. Clarke, and R. M. Warwick.
1982. A practical strategy for analyzing multispecies distribution patterns. *Mar. Ecol. Prog. Ser.* 8:37–52.
- Fortier, L., and W. C. Leggett.
1983. Vertical migrations and transport of larval fish in a partially mixed estuary. *Can. J. Fish. Aquat. Sci.* 40:1543–1555.
- Grantham, B. A., F. Chan, K. J. Nielsen, D. S. Fox, J. A. Barth, J. Huyer, J. Lubchenco, and B. A. Menge.
2004. Upwelling-driven nearshore hypoxia signals ecosystem and oceanographic changes in the northeast Pacific. *Nature* 429:749–754.
- Gray, C. A.
1998. Diel changes in vertical distributions of larval fishes in unstratified coastal waters off southeastern Australia. *J. Plankton Res.* 20:1539–1552.
- Gray, A. K., A. W. Kendall Jr., B. L. Wing, M. G. Carls, J. Heifetz, Z. Li, and A. J. Gharrett.
2006. Identification and first documentation of larval rockfishes in southeast Alaskan waters was possible using mitochondrial markers but not pigmentation patterns. *Trans. Am. Fish. Soc.* 135:1–11.
- Hare, J. A., and J. J. Govoni.
2005. Comparison of average larval fish vertical distributions among species exhibiting different transport

- pathways on the southeast United States continental shelf. *Fish. Bull.* 103:728-736.
- Heath, M. R., E. W. Henderson, and D. L. Baird.
1988. Vertical distribution of herring larvae in relation to physical mixing and illumination. *Mar. Ecol. Prog. Ser.* 47:211-228.
- Houde, E. D.
1997. Patterns and consequences of selective processes in teleost early life histories. In *Early life history and recruitment in fish populations* (R. C. Chambers, and E. A. Trippel, eds.), p. 172-196. Chapman and Hall, London.
- Hunter, J. R., and C. Kimbrell.
1980. Egg cannibalism in the northern anchovy, *Engraulis mordax*. *Fish. Bull.* 78:811-816.
- Hunter, J. R., and C. Sanchez.
1976. Diel changes in swim bladder inflation of the larvae of the northern anchovy *Engraulis mordax*. *Fish. Bull.* 74:847-855.
- Hunter, J. R., N. C.-H. Lo, and L. A. Fuiman.
1993. Advances in the early life history of fishes: Part 2, Ichthyoplankton methods for estimating fish biomass. *Bull. Mar. Sci.* 53:723-935.
- Krebs, C. J.
1989. *Ecological methodology*, 654 p. Harper Collins Publishers, New York, NY.
- Laroche, J. L., and S. L. Richardson.
1979. Winter-spring abundance of larval English sole, *Parophrys vetulus*, between the Columbia River and Cape Blanco, Oregon during 1972-1975 with notes on occurrences of three other pleuronectids. *Estuarine Coastal Mar. Sci.* 8:455-476.
- Lough, R. G., and D. C. Potter.
1993. Vertical distribution patterns and diel migrations of larval and juvenile haddock *Melanogrammus aeglefinus* and Atlantic cod *Gadus morhua* on Georges Bank. *Fish. Bull.* 91:281-303.
- Lyczkowski-Shultz, J., and J. P. Steen Jr.
1991. Diel vertical patterns in abundance and distribution of red drum (*Sciaenops ocellatus*) larvae in the northcentral Gulf of Mexico. *Fish. Bull.* 89:631-641.
- Matarese, A. C., A. W. Kendall Jr., D. M. Blood, and B. M. Vinter.
1989. Laboratory guide to early life history stages of northeast Pacific fishes. NOAA Tech. Rep. NMFS 80, 652 p.
- Munk, P., T. Kiørboe, and V. Christensen.
1989. Vertical migrations of herring, *Clupea harengus*, larvae in relation to light and prey distribution. *Environ. Biol. Fishes.* 26:87-96.
- Neilson, J. D., and R. I. Perry.
1990. Diel vertical migrations of marine fishes: an obligate or facultative process? *Adv. Mar. Bio.* 26:115-168.
- Norcross, B. L., and R. F. Shaw.
1984. Oceanic and estuarine transport of fish eggs and larvae: a review. *Trans. Am. Fish. Soc.* 113:153-165.
- Pearre, S., Jr.
1973. Vertical migration and feeding in *Sagitta elegans*. *Ecology* 54:300-314.
- Richardson, S. L.
1973. Abundance and distribution of larval fishes in waters off Oregon, May-October 1969, with special emphasis on the northern anchovy, *Engraulis mordax*. *Fish. Bull.* 71:697-711.
- Richardson, S. L., and W. G. Pearcy.
1977. Coastal and oceanic larvae in an area of upwelling off Yaquina Bay, Oregon. *Fish. Bull.* 75:125-145.
- Sabatés, A.
2004. Diel vertical distribution of fish larvae during the winter-mixing period in the Northwestern Mediterranean. *ICES J. Mar. Sci.* 61:1243-1252.
- Sakuma, K. M., and R. J. Larson.
1995. Distribution of pelagic metamorphic-stage sanddabs *Citharichthys sordidus* and *C. stigmaeus* within areas of upwelling off central California. *Fish. Bull.* 93:516-529.
- Sakuma, K. M., S. Ralston, and D. A. Roberts.
1999. Diel vertical distribution of postflexion larval *Citharichthys* spp. and *Sebastes* spp. off central California. *Fish. Oceanogr.* 8:68-76.
- Sassa, C., H. G. Moser, and K. Kawaguchi.
2002. Horizontal and vertical distribution patterns of larval myctophid fishes in the Kuroshio Current region. *Fish. Oceanogr.* 11(1):1-10.
- Schwing, F. B., and C. Moore.
2000. 1999—A year without summer for California or a harbinger of a climate shift? *Eos Trans. AGU* 81:301, 304-305.
- Shannon, C. E., and W. Weaver.
1949. *The mathematical theory of communication*, 543 p. Univ. Illinois Press, Urbana, IL.
- Shoji, J., T. Maehara, and M. Tanaka.
1999. Diel vertical movement and feeding rhythm of Japanese Spanish mackerel larvae in the Central Seto Inland Sea. *Fish. Sci.* 65:726-730.
- Suntsov, A. V.
2002. Vertical and horizontal distribution of ichthyoplankton off Peru in February 1982. *J. Ichthyol.* 42(5): 391-399.
- Tsukamoto, Y., H. Zenitani, R. Kimura, Y. Watanabe, and Y. Oozeki.
2001. Vertical distribution of fish larvae in the Kuroshio and Kuroshio-Oyashio transition region in early summer. *Bull. Natl. Res. Inst. Fish. Sci.* 16:39-56.
- Wiebe, P. H., K. H. Burt, S. H. Boyd, and A. W. Morton.
1976. A multiple opening/closing net and environmental sampling system for sampling zooplankton. *J. Mar. Res.* 34:313-326.
- Wurtsbaugh, W. A., and D. Neverman.
1988. Post-feeding thermotaxis and daily vertical migration in a larval fish. *Nature* 333:846-848.
- Yamashita, Y., D. Kitagawa, and T. Aoyama.
1985. Diel vertical migration and feeding rhythm of the larvae of the Japanese sand-eel *Ammodytes personatus*. *Bull. Jap. Soc. Sci. Fish.* 51:1-5.

Abstract—The long-snouted seahorse (*Hippocampus guttulatus*) (Cuvier, 1829), was used to validate the predictive accuracy of three progressively realistic models for estimating the realized annual fecundity of asynchronous, indeterminate, multiple spawners. Underwater surveys and catch data were used to estimate the duration of the reproductive season, female spawning frequency, male brooding frequency, and batch fecundity. The most realistic model, a generalization of the spawning fraction method, produced unbiased estimates of male brooding frequency (mean \pm standard deviation [SD]=4.2 \pm 1.6 broods/year). Mean batch fecundity and realized annual fecundity were 213.9 (\pm 110.9) and 903.6 (\pm 522.4), respectively. However, females prepared significantly more clutches than the number of broods produced by males. Thus, methods that infer spawning frequency from patterns in female egg production may lead to significant overestimates of realized annual fecundity. The spawning fraction method is broadly applicable to many taxa that exhibit parental care and can be applied nondestructively to species for which conservation is a concern.

Validation of a method for estimating realized annual fecundity in a multiple spawner, the long-snouted seahorse (*Hippocampus guttulatus*), using underwater visual census

Janelle M. R. Curtis

Email address: j.curtis@fisheries.ubc.ca

Department of Biology

McGill University

1205 Dr. Penfield Avenue, Montréal

Québec, Canada H3A 1B1

Present address: Project Seahorse

Fisheries Centre

University of British Columbia

2202 Main Mall, Vancouver

British Columbia, Canada V6T 1Z4

Reliable estimates of fecundity for multiple spawning fishes are difficult to obtain because of the logistic challenges associated with monitoring the reproductive activity of mature individuals over extended periods of time (Parrish et al., 1986). Fecundity estimates require knowing the number of young produced per spawning event (batch fecundity), as well as the number of batches of young produced per year (annual spawning frequency) (Hunter et al., 1986; Lowerre-Barbieri et al., 1996). Consequently, estimates of annual fecundity for multiple spawners often are derived from the sampling of ovaries to evaluate temporal patterns in the development and maturation of oocytes (Hunter and Leong, 1981; Murua and Saborido-Rey, 2003). However, the reliability of histological assessments is limited for estimating the annual fecundity of fishes with asynchronous oocyte development and indeterminate recruitment (e.g., anchovies, *Engraulis* spp.) (Brown-Peterson et al., 1988, Murua and Saborido-Rey, 2003). In these fishes, no one cohort of oocytes is dominant, and yolked oocytes forming new clutches are recruited from previtellogenic stages on a continual basis throughout the reproductive season (Wallace and Selman, 1981).

To obtain estimates of annual fecundity in asynchronous, indeterminate spawners, batch fecundity and spawning frequency are estimated by using different approaches. Batch fecundity can be obtained directly from the number of eggs released per spawning event or from the number of hydrated eggs present in the ovary immediately before spawning. Spawning frequency can be obtained indirectly by using a plot of the fraction of females spawning (indicated by the presence of hydrated eggs or new postovulatory follicles in the ovaries) over time (spawning fraction method, Hunter and Leong, 1981; Murua and Saborido-Rey, 2003).

Estimates of annual fecundity based on the number of eggs produced per year are reliable provided populations are sampled adequately and appropriately (DeMartini and Fountain, 1981; Hunter and Leong, 1981), and egg production is an unbiased proxy for the actual number of offspring produced. Histological methods for estimating annual fecundity may overestimate the actual number of young produced, or realized annual fecundity, if estimates do not correct for losses due to atresia, inability of females to secure mates, low fertilization efficiency,

Manuscript submitted: 27 April 2006
to the Scientific Editor's Office.

Manuscript approved for publication
25 October 2006 by the Scientific Editor.
Fish. Bull. 105:327–336 (2007).

or clutch predation (Weddle and Burr, 1991; Cole and Sadovy, 1995). Such estimates of "potential" annual fecundity are usually difficult to validate because of the challenges of monitoring early life history stages (e.g., eggs, embryos, larvae) over time and space. In many species that provide parental care, however, both mating and brooding may be directly observed (e.g., Vincent and Giles, 2003). Such species provide an opportunity to validate indirect inferences based on egg production and to obtain more accurate estimates of the actual number of young produced (e.g., Cole and Sadovy, 1995). Seahorses are asynchronous, indeterminate multiple spawners that provide obligate paternal care in a sealed brood pouch (Boisseau, 1967; Wallace and Selman, 1981). Although numerous studies have investigated aspects of seahorse reproductive behavior (e.g., Vincent and Sadler, 1995; Perante et al., 2002), annual fecundity has been estimated for only one wild seahorse population (White's seahorse, *Hippocampus whitei*, Vincent and Giles, 2003) by dividing the duration of the reproductive season by the brooding period (time required for a male to brood a clutch of eggs), and multiplying this estimate of spawning frequency by the average brood size (i.e., batch fecundity). Implicit in this method are three assumptions: 1) the time between release of young and remating is negligible, an assumption that was supported by observations of rapid remating in *H. whitei* (Vincent and Sadler, 1995), 2) individuals reproduce continuously from the beginning until the end of the reproductive season, and 3) there is no variation in brood size (a potentially unrealistic assumption, Vincent and Giles [2003]). If validated, this method could be used to estimate the realized annual fecundity of several *Hippocampus* spp. (IUCN¹) with data that already exist (Foster and Vincent, 2004).

In this article, I used European long-snouted seahorses (*Hippocampus guttulatus*) (Cuvier, 1829), to validate three progressively realistic models for estimating spawning frequency and realized annual fecundity. The objectives of this study were 1) to estimate the batch fecundity and spawning frequency of *H. guttulatus*, 2) to identify correlates of fecundity, and 3) to evaluate the predictive accuracy of the three models. The simplest model is the calculation employed by Vincent and Giles (2003). The second model includes an estimate of interbrood interval. The most realistic model is a generalization of the "spawning fraction" method (Hunter and Leong, 1981) that could be applied nondestructively to estimate realized annual fecundity in species of conservation concern. The study objectives were addressed by using fishery-independent sampling and underwater visual census in a locally abundant and unexploited population of *H. guttulatus*.

Materials And Methods

Species description

The life history and ecology of seahorses has been reviewed by Foster and Vincent (2004). *Hippocampus guttulatus* inhabits seagrass- and macroalgae-dominated communities in the Mediterranean Sea and the north-eastern Atlantic Ocean (Lourie et al., 1999). Individuals begin reproducing at approximately 1 year of age and live 4 to 5.5 years (Boisseau, 1967; Curtis and Vincent, 2006). Adults range in size from 110 to 210 mm standard length (sum of head, trunk, and tail lengths, Lourie et al., 1999) and from 2.4 to 22.5 g wet mass (Curtis and Vincent, 2006). Male and female seahorses mate monogamously within reproductive cycles: the female deposits an entire clutch of eggs into the male's brood pouch (Jones et al., 1998). Brooding male *H. guttulatus* (i.e., with full pouches) have been captured from March to October (Boisseau, 1967; Reina-Hervás, 1989) and in January (Lo Bianco, 1888). The ovarian structure of *H. guttulatus* indicates that females produce multiple clutches per year (Boisseau, 1967).

Sampling

This study was carried out in the Ria Formosa lagoon in southern Portugal (36°59'N, 7°51'W). The Ria Formosa is a shallow, productive coastal lagoon characterized by high water turnover rates, seagrass beds, sand flats, salt marshes, and a network of channels and tidal creeks (Machás and Santos, 1999; Curtis and Vincent, 2005). Data employed in this study were derived from fisheries-independent samples of fish community structure (Erzini et al.²) and from underwater visual censuses of tagged *H. guttulatus* on a small focal study site (Curtis and Vincent, 2006). Seahorses captured during fisheries-independent sampling were collected monthly from September 2000 to July 2002 (except January 2002) at 53 stations throughout the western part of the Ria Formosa lagoon by using small beach seines, push nets, or beam trawls (Erzini et al.²), and then frozen. Data from all the captured seahorses were opportunistically recorded and included the standard length, life history stage, sex, reproductive state, wet mass, and brood size of males with full pouches (details provided in Curtis, 2004; Curtis and Vincent, 2006). Brood sizes were obtained by dissecting the full pouches of captured males and counting all of the developing embryos. Broods with embryos captured during the earliest stages of development (<stage 10, *sensu* Boisseau, 1967) were

¹ IUCN (World Conservation Union). 2006. 2006 IUCN Red List of Threatened Species. IUCN Species Survival Commission, 219c Huntingdon Road, Cambridge CB3 0DL, United Kingdom. Website: <http://www.redlist.org> (accessed 31 May 2006).

² Erzini, K., L. Bentes, R. Coelho, C. Correia, P. G. Lino, P. Monteiro, J. Ribeiro, and J. M. S. Gonçalves. 2002. Recruitment of sea breams (Sparidae) and other commercially important species in the Algarve (southern Portugal). Final Report, 178 p. Commission of the European Communities DG XIV/C/1. Directorate-General for Fisheries and Maritime Affairs, Unit for Information and Communication, European Commission, B-1049, Brussels, Belgium.

excluded from the analyses because eggs and small embryos were in poor condition due to freezing and were therefore difficult to count. For the same reason, it was not possible to estimate clutch sizes by examining the ovaries of captured adult females. Data were recorded from a total of 1264 adult males and 1211 adult females captured with the fishing gears (Erzini et al.²).

Underwater visual censuses of tagged *H. guttulatus* were also carried out on a 10 m × 10 m focal study grid established in June 2001. The grid was located 5 m from the intertidal zone next to a permanent pier located within the Ria Formosa Natural Park at a depth of 1.3 to 6.1 m (additional details provided in Curtis, 2006; Curtis and Vincent, 2006). Tagged seahorses exhibited high site fidelity to small home ranges averaging 20 m² during multiple years (Curtis and Vincent, 2006). The juveniles released by eight tagged males on the grid were also counted and used to estimate brood size as in Vincent and Giles (2003). The eight brooding males were placed in cages (0.3 m high × 0.45 m wide, 0.5 mm mesh) *in situ* for a maximum of 48 h each between 18 July and 16 August 2002 (Curtis and Vincent, 2006). The mesh allowed water and small zooplankton to flow through the cages, while retaining newborn juveniles. After juveniles were born, the cages were slowly brought to the surface and emptied into large tanks filled with seawater where the total number of juveniles was counted. Males and their juveniles were released at their original capture site within 12 hours of birth.

Three models for estimating annual fecundity

The assumptions of rapid remating and continuous reproduction during the reproductive season were examined by using three progressively realistic models to estimate realized annual fecundity: the continuous reproduction (CR) model, the intermittent reproduction (IR) model, and the intermittent and seasonal reproduction (ISR) model.

Continuous reproduction (CR) model

In the simplest model, individuals were assumed to reproduce continuously from the beginning to the end of the reproductive season, from March to October (Boisseau, 1967; Reina-Hervás, 1989). Annual fecundity, $f_{b,yr}$, was estimated by using mean estimates of the brooding period, t_b , and brood size, f_b :

$$f_{b,yr} = f_b \times t_s / t_b, \quad (1)$$

where $f_{b,yr}$ = the total number of young produced per male per year; and

t_s = the duration of the reproductive season.

In the CR model, f_b and t_b were assumed to be constant throughout t_s , and the interbrood interval, t_{ib} , was 0. The brooding period, t_b , was estimated by monitoring changes in the reproductive state of tagged adult males

on the grid using underwater visual census. In 2001 and 2002, 553 *H. guttulatus* (264 males, 254 females, 35 juveniles) were individually tagged with visible implanted fluorescent elastomer (VIE tags, Northwest Marine Technologies, Inc., Shaw Island, WA) (Curtis, 2006; Curtis and Vincent, 2006). A total of 163 underwater visual censuses (2–5 person-hours/dive) were carried out with SCUBA on the grid during two census periods: from 17 July to 26 October 2001 and from 23 May to 12 September 2002. On average, one underwater visual census was carried out every 1 to 2 days during each of these census periods. During underwater visual censuses, observers swam ~1 m above the substrate and searched for tagged seahorses. The date, tag, life history stage, sex, size (trunk length, converted to standard length by using equations developed for *H. guttulatus*, Curtis and Vincent 2005, 2006), and reproductive state of all tagged seahorses were noted. The reproductive state of adult males (full or empty brood pouch) was determined by visual (and in ambiguous cases, manual) inspection.

Changes in reproductive state were plotted as a function of census date for each tagged male. Because of high seahorse density on the grid (1.5/m²; Curtis and Vincent, 2006), it was not feasible to verify the status of all individuals during each dive; therefore, t_b was estimated by recording the minimum and maximum possible durations of each brooding period, as graphically depicted in Figure 1. Unmated male *H. guttulatus* occasionally mimic males that are close to releasing juveniles by temporarily and completely filling their pouches with water during reproductive displays to females (J. Curtis, personal observ.). Reproductive interactions between male and female *H. guttulatus* generally occurred within two hours of sunrise and lasted on average 4.8 min ± 3.3 SD (standard deviation) (J. Curtis, unpubl. data). Therefore putative brooding periods were included in the analysis only when a male was observed ≥ 3 times with a full pouch during a period bracketed by observations of an empty pouch. The minimum and maximum possible brooding periods were averaged within and among all males.

Intermittent reproduction (IR) model

This model expanded the continuous reproduction model by incorporating a mean estimate of the interbrood interval, t_{ib} , which was assumed to be constant throughout the reproductive season:

$$f_{b,yr} = f_b \cdot t_s / (t_b + t_{ib}), \quad (2)$$

where t_{ib} = the time elapsed between release of young and deposition of a new clutch of eggs into the male's brood pouch.

The interbrood interval was estimated by using a similar approach to that employed to estimate the brooding period (Fig. 1): the maximum and minimum possible durations of each interbrood interval were recorded and

averaged within and among tagged males observed on the grid in 2001 and 2002.

For comparison, the annual frequency of clutches prepared by tagged females was also estimated by monitoring the time required to prepare eggs, t_c , and the interval between inferred clutches, t_{ic} (Fig. 1). Female trunk girth was used as an indicator of reproductive status (Vincent and Sadler, 1995; Perante et al., 2002). Females whose trunks were bulging between trunk rings (occasionally with visible eggs) were assumed to be preparing a clutch of eggs for mating. Within monogamous pairs of *H. comes* (Perante et al., 2002) and *H. whitei* (Vincent and Sadler, 1995), changes in female trunk girth were significantly correlated with changes in the reproductive state of their male partner. Therefore trunk girth was assumed to be a reliable proxy for clutch preparation in *H. guttulatus*. Because female sea pony (*Hippocampus fuscus*), prepared and released their eggs within approximately three days (Vincent, 1990), t_{ic} was estimated only during periods when female *H. guttulatus* were observed on average at least once every two to three days.

Intermittent and seasonal reproduction (ISR) model

This model is more realistic than the two previous models because information about seasonal trends in reproductive activity is incorporated, rather than the assumption that there is constant reproduction throughout the reproductive season. This model was adapted from the spawning fraction method used to estimate the average number of spawnings per year among female northern anchovy (Hunter and Leong, 1981). A Gaussian curve was fitted to the fraction of mature males with full pouches in the catch data plotted against sampling month by using nonlinear regression, as in Curtis and Vincent (2006). The area beneath this curve corresponds to an estimate of the total number of days the average adult male brooded embryos per year, t_{b-yr} . The mean number of broods produced per male each year (i.e., annual spawning frequency), s_{b-yr} , was estimated as t_{b-yr}/t_b . Annual fecundity was then calculated as $f_b s_{b-yr}$. Similarly, the ISR model was applied to the proportion of adult females preparing eggs, where the number of clutches produced by females each year, s_{c-yr} , was estimated as the total time spent preparing clutches of eggs, t_{c-yr} , divided by the time required to prepare a single clutch, t_c . In order to characterize among-population differences in *H. guttulatus* spawning frequency, this method was also applied to male catch data reported from the Arcachon Basin, France (Boisseau, 1967).

Model validation

An independent estimate of the brooding period (21 days; Boisseau, 1967) was used to evaluate the predictive accuracy of the CR and ISR models. The CR model was used to predict the expected number of broods produced by males, s_{b-cen} , during the census periods from 18 July to 26 October (2001, 112 days) and 23 May to 12 September (2002, 108 days). Similarly, the curve fitted to the male catch data using the ISR model was used to calculate the predicted number of broods produced by males during these two census periods. Because the only estimate of the time females take to prepare eggs, t_c (used to estimate the number of clutches produced by females in the ISR model) was based on the underwater visual census data, the ISR model could not be used to predict the total expected number of clutches produced by females during the census periods. Therefore, the ISR model was used to predict the total number of days females spent preparing eggs during the census periods, t_{c-cen} . Expected values of s_{b-cen} and t_{c-cen} based on the CR and ISR models were compared to the mean values of s_{b-cen} and t_{c-cen} directly observed on the grid during the corresponding census periods. The IR model could not be validated because there was no independent estimate of interbrood interval, t_{ib} , for *H. guttulatus*.

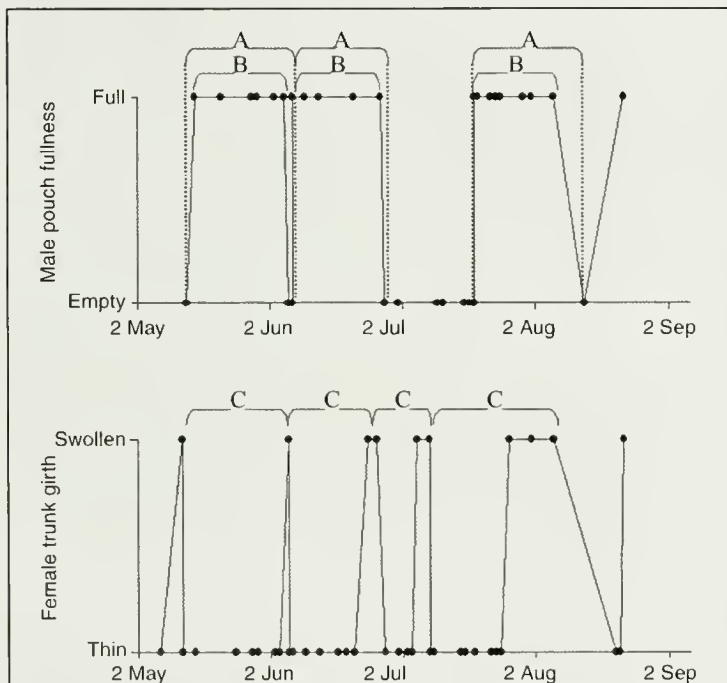


Figure 1

Examples of the changes in reproductive state from May to September 2002 in one marked male (**top**) and one marked female (**bottom**) *Hippocampus guttulatus* (long-snouted seahorse) during the census period in 2002. Males have full pouches when brooding eggs and embryos. Females whose trunks were bulging between trunk rings (i.e., swollen) were assumed to be preparing a clutch of eggs. Brackets marked with an A indicate the maximum duration of three brooding periods, and brackets marked with a B indicate minimum durations. One brief and one lengthy interbrood interval are evident. The interclutch intervals, inferred from changes in female trunk girth are also denoted with brackets marked with a C.

Correlates of fecundity

The influences of body size, water temperature, season, and lunar phase on batch fecundity and reproductive activity (i.e., the proportion of spawning males and females) were investigated. Daily and mean monthly water temperatures in the Ria Formosa were recorded with an Onset HOBO Temperature logger (Onset Computer, Bourne, MA) placed 0.3 m above the substrate on the grid from June 2001 to September 2002. All means are reported with one standard deviation or 95% confidence intervals (95% CI). Statistical procedures were carried out with SPSS 10.0.7 (SPSS Inc., Chicago, IL).

Results

Continuous reproduction (CR) model

Nonlinear regression indicated that the size of male *H. guttulatus* was a significant predictor of brood size, f_b , which varied from 10 to 567 embryos or juveniles, with a mean of 213.9 ± 110.9 ($n=117$, caged and dissected males pooled). Both standard length ($r^2=0.29$, $P<0.0001$, $n=117$) and wet mass ($r^2=0.20$, $P<0.003$, $n=39$) significantly predicted f_b (Fig. 2). Brood size was not correlated with mean monthly temperature ($r^2=0.00$, $P=0.90$, $n=117$) but was weakly correlated with Julian day in 2001 ($r^2=0.06$, $P=0.015$, $n=106$).

A total of 4550 records were collected from the 553 individually tagged *H. guttulatus* in 2001 and 2002 for an average of 8.2 records per individual (maximum 87). On the grid, 94% of resighted, mature males mated at least once within a census period. The mean brooding period, t_b , was $21.4 (\pm 5.5)$ days ($n=80$ intervals from 73 males, median=20.0 days). Temperature was not a significant predictor of t_b ($r^2=0.004$, $F_{[1,55]}=0.22$, $P>0.05$), despite reports of an inverse relationship between temperature and brooding period in other seahorse species (Vincent and Sadler, 1995; Foster and Vincent, 2004).

The CR model produced the highest estimates of annual spawning frequency, s_{b-yr} , and realized annual fecundity, f_{b-yr} . Assuming continuous reproduction from March to October (245 days), male *H. guttulatus* was predicted to produce 11.5 broods annually. Mean annual fecundity was estimated as approximately 2450 young per year (Table 1).

Intermittent reproduction (IR) model

The interbrood interval, t_{ib} , ranged from 0 to 61 days and had a mean of $12.9 (\pm 8.2)$ days ($n=98$ intervals from 58 males; median=10.5 days) (Table 1). Size did not influence the number of broods produced by males during the census periods (Kruskal-Wallis test,

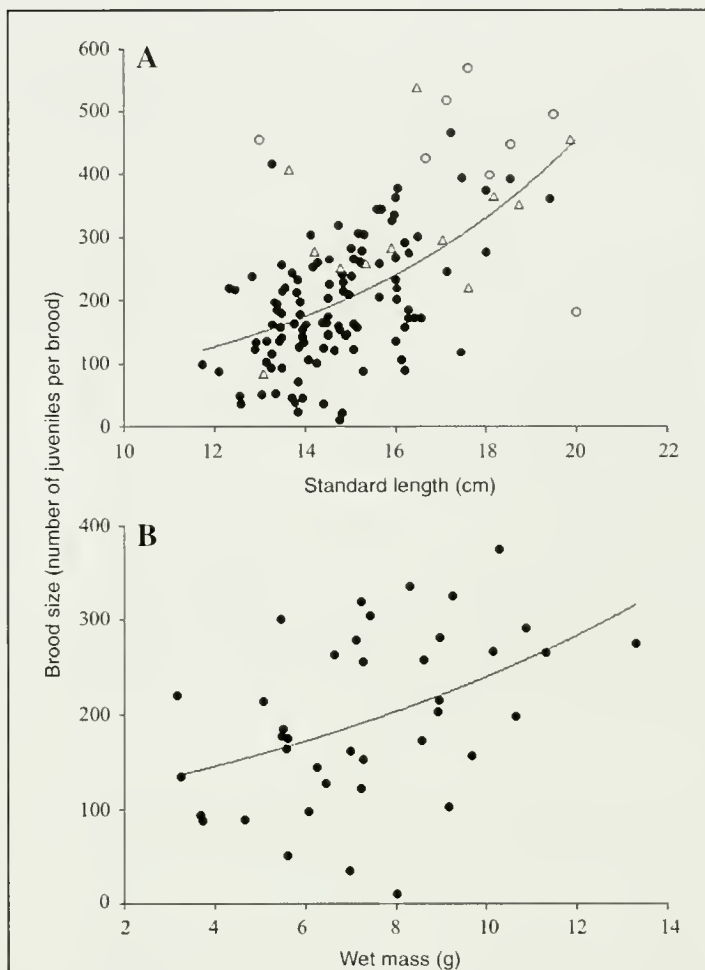


Figure 2

Relationship between *Hippocampus guttulatus* (long-snouted seahorse) male size and brood size (solid circles represent embryos dissected from brood pouches, open circles represent live juveniles born in cages): (A) standard length ($n=117$), and (B) wet mass ($n=40$). Equations of the fitted line in (A) and (B) are $y=18.7e^{0.16x}$ and $y=104.3e^{0.08x}$, respectively. Open triangles in (A) represent mean clutch sizes of female *Hippocampus guttulatus* in 12 length classes (Americano, D. 2004. Aspects of the reproductive biology of *Hippocampus guttulatus* (Cuvier, 1829) [In Portuguese], Undergraduate thesis, 51 p. Universidade do Algarve, Faro, Portugal.)

$\chi^2=3.0$, $n=73$, $df=5$, $P=0.7$) and temperature was not a significant predictor of t_{ib} ($r^2=0.001$, $F_{[1,97]}=0.07$, $P=0.79$). Incorporating t_{ib} into the IR model led to substantially lower estimates of spawning frequency and annual fecundity than predicted by the CR model: $7.14 (\pm 4.89)$ broods per year and $1527 (\pm 1309)$ young per year, respectively (Table 1).

All resighted, mature females prepared at least one clutch of eggs within a census period on the grid. The mean number of days females had hydrated eggs, t_c , was $2.58 (\pm 2.66)$ days ($n=72$ inferred clutches), indicating that females required at least 2.5 days to prepare

Table 1

Parameter values (\pm standard deviation) and model predictions from three progressively realistic models for the Ria Formosa population of *Hippocampus guttulatus* (long-snouted seahorse). Estimates are also given for the Arcachon Basin population by using the intermittent and seasonal reproduction model.

Model	Continuous reproduction (CR)	Intermittent reproduction (IR)	Intermittent and seasonal reproduction (ISR)	Intermittent and seasonal reproduction (ISR)
Population	Ria Formosa	Ria Formosa	Ria Formosa	Arcachon Basin
Parameters				
Reproductive season t_s (days)	245 ¹	245 ¹	250 ²	102 ²
Brooding period t_b (days)	21.4 (± 5.6)	21.4 (± 5.6)	21.4 (± 5.6)	21 ³
Interbrood interval t_{ib} (days)	0	12.9 (± 8.2)		
Time spent brooding t_{b-yr} (days)			90.4	20.7
Brood size (batch fecundity) f_b	213.9 (± 110.9)	213.9 (± 110.9)	213.9 (± 110.9)	232 (± 82.8) ³
Predictions				
Spawning frequency s_{b-yr}	11.5 (± 2.9)	7.14 (± 4.89)	4.22 (± 1.09)	0.98
Annual fecundity f_{b-yr}	2449.2 (± 1415.9)	1527.2 (± 1309.8)	903.6 (± 522.4)	227.4 (± 81.6)

¹ Assuming 8 months from March through October (Reina-Hervás, 1989).

² Period when $\geq 1\%$ of mature males were predicted to have full pouches.

³ Values reported in Boisseau (1967).

eggs for mating. Although there was no significant difference between the brooding period, t_b , of males and female interclutch interval, t_{ic} (21.06 \pm 6.6 days, $n=102$ intervals from 26 females; median=20 days) (t -test, $df=180$, $t=-0.36$, $P=0.72$), females produced significantly more clutches than males brooded during both underwater visual census periods (2001: $df=37$, $t=3.32$, $P=0.002$; 2002: $df=62$, $t=7.16$, $P<0.0001$, Table 2). Assuming that the duration of the reproductive season is the same for both sexes and that the IR model is correct, the estimate of the interclutch interval indicates that the average female prepared 11.63 (± 3.65) clutches per year. Temperature was not a significant predictor of t_{ic} ($r^2=0.02$, $F_{[1,101]}=1.66$, $P=0.2$).

Intermittent and seasonal reproduction (ISR) model

The reproductive activity of males varied significantly within years ($r^2=0.78$, $F_{[2,19]}=39.28$, $P<0.0001$, Fig. 3A). *Hippocampus guttulatus* males reproduced during most of the year and peaked in reproductive activity from June through August. No reproductively active males were captured from December 2000 to March 2001, or in February 2002. Male reproductive activity was also significantly and positively correlated with water temperature ($r^2=0.55$, $F_{[1,12]}=13.32$, $P=0.004$), which varied seasonally from 10–28°C (mean annual temperature=18.2°C). There was no effect of lunar phase on male reproductive activity ($r^2=0.01$, $F_{[2,50]}=0.26$, $P=0.78$), as inferred by Boisseau (1967). The fraction of mature females that were preparing eggs also varied seasonally ($r^2=0.21$, $F_{[2,17]}=3.59$, $P=0.05$, Fig. 3B). Temperature was weakly correlated with female reproductive

activity ($r^2=0.30$, $F_{[1,12]}=4.80$, $P=0.05$), but lunar phase was not ($r^2=0.04$, $F_{[2,50]}=1.15$, $P=0.33$).

Incorporation of seasonal variation in reproductive activity into the ISR model resulted in estimates of s_{b-yr} and f_{b-yr} that were 63.1% smaller than those predicted by the CR model. The ISR model predicted that the total time an average male *H. guttulatus* spent brooding embryos per year in the Ria Formosa was 90.4 days, giving an estimate of male annual spawning frequency, s_{b-yr} , of 4.22 broods per year (Table 1). Similarly, the total time females spent preparing eggs per year was 13.51 days, giving an estimate of female annual spawning frequency, s_{c-yr} , equal to 5.23 clutches per year. These estimates of annual spawning frequency were at least four times greater than estimates from the Arcachon Basin population. During the reproductive season, which lasted 3.5 months (Fig. 4), the average male had a full pouch for 20.7 days, indicating that, on average, males in the Arcachon Basin population bred only once a year (Table 1).

Model validation

The number of broods predicted by the CR model for the 2001 and 2002 census periods, s_{b-cen} , was significantly greater than observed directly with underwater visual census (Table 2), indicating that this model produces upwardly biased estimates of spawning frequency for *H. guttulatus*. By contrast, the more realistic ISR model produced expected values of s_{b-cen} and the total number of days female spent with hydrated eggs, t_{c-cen} , which were within 95% confidence intervals for the observed mean values on the grid in both 2001 and 2002. This

latter inference is supported by close correspondence between observed male and female reproductive activity observed over time on the grid and the values predicted by the ISR model (Fig. 3).

Discussion

This article presents the first estimates of realized annual fecundity in a population of wild European long-snouted seahorses (*H. guttulatus*) and validates a potentially nondestructive application of the spawning fraction method (Hunter and Leong, 1981) for estimating spawning frequency. Results indicate that estimates of spawning frequency and annual fecundity based on egg production alone may lead to significant overestimates of realized annual fecundity and thus underscore the importance of testing assumptions when using proxies for estimating fecundity in multiple spawning fishes.

Batch fecundity

A significant relationship between male size and brood size of *H. guttulatus* means that size-specific realized annual fecundities can be calculated and converted to age-specific fecundities (e.g., Curtis, 2004) by using a length-at-age model developed for *H. guttulatus* (Curtis and Vincent, 2006). Among fishes, fecundity is strongly size-dependent (Davis and West, 1993; Lowerre-Barbieri et al., 1996). Female size is typically used to predict clutch size in fishes (Bagenal, 1978), including syngnathids (Teixeira and Musick, 2001; Vincent and Giles, 2003), but male dimensions can be also be used to predict brood size in fishes that provide paternal care, such as syngnathids (Strawn, 1958; Teixeira and Musick, 2001) and mouthbrooding cardinalfishes (Okuda et al., 1998; Kolm, 2002). Because both the volume of the female's abdominal cavity and volume of the male's sealed brood pouch potentially limit the number or size (or both) of embryos that can be successfully produced by seahorses (Boisseau, 1967), correlations between the dimensions of both parents and brood size likely reflect mutual mate selection for size (Vincent and Sadler, 1995; Teixeira and Musick, 2001; Vincent and Giles, 2003). A positive correlation between the standard lengths of *H. guttulatus* males and females engaged in courtship behavior on the grid (J. Curtis, unpubl. data), indicates that mating is size-assortative in this population.

Annual spawning frequency

The underwater visual census data indicate that on average, female *H. guttulatus* prepared significantly more clutches of eggs (1.2–1.7 times as many) than males brooded in the Ria Formosa in 2001 and 2002 (Table 2). This means that estimates of spawning frequency and annual fecundity based on female egg production (e.g.,

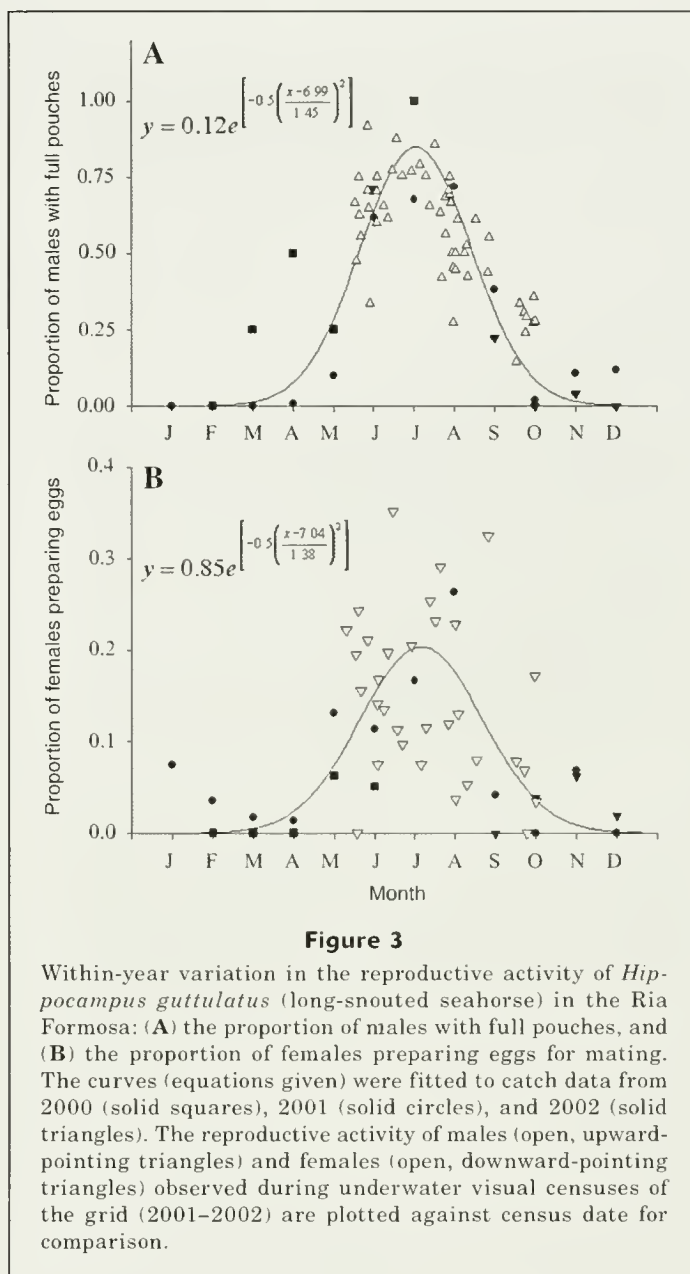


Figure 3

Within-year variation in the reproductive activity of *Hippocampus guttulatus* (long-snouted seahorse) in the Ria Formosa: (A) the proportion of males with full pouches, and (B) the proportion of females preparing eggs for mating. The curves (equations given) were fitted to catch data from 2000 (solid squares), 2001 (solid circles), and 2002 (solid triangles). The reproductive activity of males (open, upward-pointing triangles) and females (open, downward-pointing triangles) observed during underwater visual censuses of the grid (2001–2002) are plotted against census date for comparison.

histological assessments) may significantly overestimate the actual number of young produced. Brood production by males was probably not limited by the availability of mature females because sex ratios were slightly biased in favor of females (Curtis and Vincent, 2006), and the interclutch intervals of females were equal to the brooding periods of males. Significantly longer interbrood intervals for the population of male *H. guttulatus* in the present study may have derived in part from depredation by other fishes during egg transfer to male brood pouches. This depredation occurred during one of three matings witnessed on the grid. Approximately 1% of male *H. guttulatus* in the Ria Formosa had holes in their pouch. Such injuries indicate that other predators

Table 2

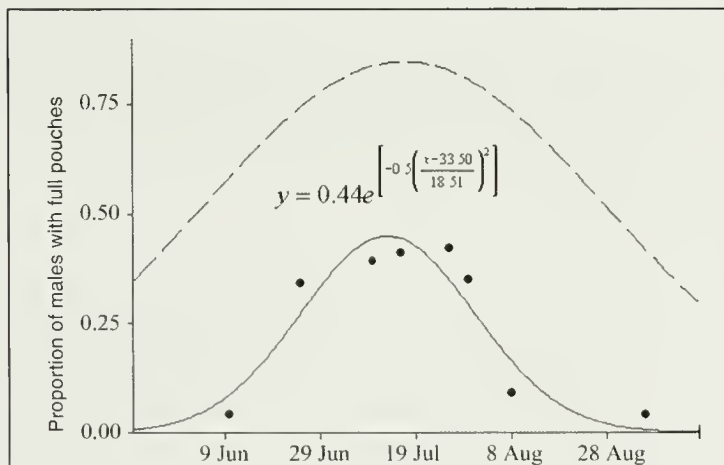
Predicted and observed number of broods (males) and clutches (females) produced during underwater visual census periods in 2001 and 2002. Expected values were calculated by estimating the area beneath fitted curves in Figure 3 that corresponded to census periods in 2001 and 2002. Observed values (mean \pm standard deviation) were taken from n males and females that were tagged and monitored throughout the entire census period. * = greater than upper 95% confidence limit of mean observed value.

	2001		2002	
	17 Jul–26 Oct	n	23 May–12 Sept	n
Males				
Observed number of broods (95% confidence interval)	2.07 \pm 1.10 (0–4.22)	28	2.72 \pm 0.86 (1.03–4.40)	45
Continuous reproduction (CR) model				
Predicted number of broods	5.33*		5.14*	
Intermittent and seasonal reproduction (ISR) model				
Predicted days with full pouch	56.65		71.59	
Predicted number of broods	2.69		3.40	
Females				
Observed number of clutches (95% confidence interval)	3.40 \pm 1.07 (1.30–5.49)	10	4.66 \pm 1.23 (2.24–7.07)	18
Observed days with prepared eggs (95% confidence interval)	8.51 \pm 3.37 (1.88–15.11)		11.58 \pm 5.13 (1.52–21.65)	
Intermittent and seasonal reproduction (ISR) model				
Predicted days with prepared eggs	8.14		10.46	

may also deplete eggs or developing embryos directly from the pouch (Curtis, 2004). A wounded wild *H. whitei* male had a hole in his pouch that precluded mating for nearly three reproductive cycles (~60 days, Vincent and Sadler, 1995). The degree to which predation affects reproductive success in *H. guttulatus* is unknown, but

reproductive success in other fishes that provide male parental care is strongly affected by interspecific predation (e.g., Cole and Sadovy, 1995).

A fourfold difference in estimated spawning frequency between the Arcachon Basin (one brood per year) and the Ria Formosa (4.2 broods per year) indicates that realized annual fecundity varies among *H. guttulatus* populations. Spawning frequencies are positively correlated with temperature in many marine fishes (Bone et al., 1995), including darters (Gale and Deutsch, 1985). Variation in spawning frequency among northern anchovy populations was also linked to energetic constraints (4–20 spawnings per year, Hunter and Leong, 1981). With an estimated mean spawning frequency of once per year and a shorter reproductive season, *H. guttulatus* in the Arcachon Basin may be more vulnerable to environmental stochasticity than the Ria Formosa population. Spawning that occurs multiple times within a reproductive season confers fitness benefits, particularly for small-bodied fishes inhabiting variable environments. By spawning fewer times in variable environments, the risk of catastrophic losses of eggs and larvae due to temporarily poor environmental conditions are increased (Nikolsky, 1963; McEvoy and McEvoy, 1992).

**Figure 4**

Within-year variation in the reproductive activity of *Hippocampus guttulatus* (long-snouted seahorse) in the Arcachon Basin from June to September 1952. The equation for the solid line fitted to the data from Boisseau (1967) is given. The dashed line is fitted to catch data from the Ria Formosa lagoon (see Fig. 3A).

Trends in reproductive activity

Peaks in the reproductive activity of male and female *H. guttulatus* in the Ria Formosa lagoon

corresponded to months with warmer water temperatures and higher primary and secondary production (Sprung, 1994a, 1994b), as observed in other fishes (Bye, 1984; Milton and Blaber, 1990). The duration of the reproductive season in the Ria Formosa lagoon (March–November) was similar to that reported for populations in southern Spain at a similar latitude (March–October, 36.7°N; Reina-Hervás, 1989) but was almost twice as long as in the higher latitude Arcachon Basin population (May–September, 44.7°N; Boisseau, 1967). Among-population differences in the duration of the reproductive season may be attributable to differences in temperature regimes (Robert et al., 1993) and photoperiod. Although Boisseau (1967) suggested that peaks in *H. guttulatus* reproductive activity occurred during full moons in the Arcachon Basin, there was no evidence of a correlation between lunar phase and reproduction in the Ria Formosa.

Models for estimating realized annual fecundity

Neither assumption of the CR model (rapid remating and continuous reproduction) was met empirically for *H. guttulatus* (Table 1, Fig. 3). This means that accurate estimates of realized annual fecundity in other seahorse species of conservation concern (Foster and Vincent 2004; IUCN¹) may require further biological research. Annual spawning frequency and realized annual fecundity may be overestimated by as much as 270% when the assumptions of rapid remating or continuous reproduction have not been met (Table 1). Assumptions inherent in the CR model may be more likely to hold for monogamous species with short interbrood intervals (e.g., *H. whitei*; Vincent and Sadler, 1995) that breed year round in tropical environments (e.g., *H. comes*; Perante et al., 2002). Incorporating an estimate of interbrood interval into the IR model produced intermediate estimates of annual spawning frequency. However, estimates of interbrood intervals required considerable effort because of the need to monitor changes in the reproductive activity of individually tagged seahorses. Use of the ISR model circumvented the need to directly estimate interbrood intervals (see “Material and methods” section) and led to unbiased estimates of spawning frequency for both males and females.

The success of the ISR model in predicting observed estimates of male spawning frequency and the number of days females spent preparing eggs indicates that this model, based on the spawning fraction method developed by Hunter and Leong (1981), may be broadly applicable to all organisms for which batch fecundity and the time to prepare or brood a clutch of eggs are known. This model is suitable for species with broods that can be readily and periodically surveyed by using either fisheries-independent catches or underwater visual census techniques. Although fisheries-independent collections were opportunistically used in this study to estimate brood sizes and the fraction of spawning males and females, reliable estimates of these values were also obtained nondestructively by caging brood-

ing males to count batch fecundity directly, and by monitoring changes in the fraction of spawning males and females over time with underwater visual censuses (Fig. 3). For species at risk that can be surveyed periodically during the reproductive season with non-destructive fisheries-independent sampling (e.g., underwater visual census), the generalized spawning fraction method becomes a potentially effective and appropriate means of estimating spawning frequency and realized annual fecundity.

Acknowledgments

This is a contribution from Project Seahorse. I thank K. Erzini and J. Ribeiro for providing their seahorse catches, the Parque Natural da Ria Formosa for logistic support, and R. Adams, H. Balasubramanian, K. Bigney, J. d'Entremont, B. Gunn, S. Lemieux, C.-M. Lesage, E. Murray, J. Nadeau, S. Overington, M. Veillette, K. Wieckowski, and S. V. Santos for excellent assistance. C. Hall, D. O'Brien, and A. Vincent provided valuable comments on this manuscript. Funding was provided by Guylian, Natural Science and Engineering Research Council, Fonds Québécois de la Recherche sur la Nature et les Technologies, and McGill University.

Literature Cited

- Bagenal, T. B.
1978. Aspects of fish fecundity. *In Ecology of freshwater fish production* (S. D. Gerking, ed.), p. 75–101. Blackwell Scientific Publications, Oxford, UK.
- Boisseau, J.
1967. Hormonal regulation of incubation in a male vertebrate: research on seahorse reproduction. [In French]. Ph. D. diss., 379 p. Univ. Bordeaux, Bordeaux, France.
- Bone, Q., N. B. Marshall, and J. S. H. Blaxter (eds.).
1995. *Biology of fishes*, 2nd ed., 288 p. Blackie Academic and Professional, London.
- Brown-Peterson, N., P. Thomas, and C. R. Arnold.
1988. Reproductive biology of the spotted seatrout, *Cynoscion nebulosus*, in south Texas. *Fish. Bull.* 86: 373–388.
- Bye, V. J.
1984. The role of environmental factors in the timing of reproductive cycles. *In Fish reproduction: strategies and tactics* (G. W. Potts, and R. J. Wootton, eds), p. 188–205. Academic Press, London.
- Cole, K. S., and Y. Sadovy.
1995. Evaluating the use of spawning success to estimate reproductive success in a Caribbean reef fish. *J. Fish Biol.* 47:181–191.
- Curtis, J. M. R.
2004. Life history, ecology and conservation of European seahorses. Ph. D. thesis, 213 p. McGill Univ., Montreal, Canada.
2006. Visible implant elastomer color determination, tag visibility, and tag loss: Potential sources of error for mark-recapture studies. *N. Am. J. Fish. Manage.* 26:327–337.

- Curtis, J. M. R., and A. C. J. Vincent.
2005. Distribution of sympatric seahorse species along a gradient of habitat complexity in a seagrass-dominated community. *Mar. Ecol. Prog. Ser.* 291:81–91.
2006. Life history of an unusual marine fish: survival, growth and movement patterns of the European long-nouted seahorse, *Hippocampus guttulatus* (Cuvier 1829). *J. Fish Biol.* 68:707–733.
- Davis, T. L. O., and G. J. West.
1993. Maturation, reproductive seasonality, fecundity, and spawning frequency in *Lutjanus vittus* (Quoy and Gaimard) from the North West shelf of Australia. *Fish. Bull.* 91:224–236.
- DeMartini, E. E., and R. K. Fountain.
1981. Ovarian cycling frequency and batch fecundity in the queenfish, *Seriphus politus*—attributes representative of serial spawning fishes. *Fish. Bull.* 79: 547–560.
- Foster S., and A. C. J. Vincent.
2004. The life history and ecology of seahorses, *Hippocampus* spp.: implications for conservation and management. *J. Fish Biol.* 65:1–61.
- Gale, W., and W. Deutsch.
1985. Fecundity and spawning frequency of captive tessellated darters—fractional spawners. *Trans. Am. Fish. Soc.* 111:35–40.
- Hunter, J. R., and R. Leong.
1981. The spawning energetics of female northern anchovy, *Engraulis mordax*. *Fish. Bull.* 79: 215–230.
- Hunter, J. R., B. J. Macewicz, and J. R. Sibert.
1986. The spawning frequency of skipjack tuna, *Katsuwonus pelamis*, from the south Pacific. *Fish. Bull.* 84:895–903.
- Jones, A. G., C. Kvarnemo, G. I. Moore, L. W. Simmons, and J. C. Avise.
1998. Microsatellite evidence for monogamy and sex-biased recombination in the Western Australian seahorse *Hippocampus angustus*. *Mol. Ecol.* 7:1497–1505.
- Kolm, N.
2002. Male size determines reproductive output in a paternal mouthbrooding fish. *Anim. Behav.* 63:727–733.
- Lo Bianco, S.
1888. Biological note on the period of sexual maturity of animals in the Gulf of Napoli [In Italian]. *Mitte. Zool. Stat. Neapel.* 8:385–440.
- Lourie, S. A., A. C. J. Vincent, and H. J. Hall.
1999. Seahorses: An identification guide to the world's species and their conservation, 214 p. Project Seahorse, London.
- Lowerre-Barbieri, S. K., M. E. Chittenden Jr., and L. R. Barbieri.
1996. Variable spawning activity and annual fecundity of weakfish in Chesapeake Bay. *Trans. Am. Fish. Soc.* 125:532–545.
- Machás, R., and R. Santos.
1999. Sources of organic matter in Ria Formosa revealed by stable isotope analysis. *Acta. Oecol. Int. J. Ecol.* 20:463–469.
- McEvoy, L. A., and J. McEvoy.
1992. Multiple spawning in several commercial fish species and its consequences for fisheries management, cultivation and experimentation. *J. Fish Biol.* 41(Suppl. B):125–136.
- Milton, D. A., and M. Blaber.
1990. Maturation, spawning seasonality, and proximate spawning stimuli of six species of tuna baitfish in the Solomon Islands. *Fish. Bull.* 89:221–237.
- Murua, H., and F. Saborido-Rey.
2003. Female reproductive strategies of marine fish species of the north Atlantic. *J. Northw. Atl. Fish. Sci.* 33: 23–31.
- Nikolsky, G. V.
1963. The ecology of fishes, 353 p. Academic Press, New York, NY.
- Okuda, N., I. Tayasu, and Y. Yanagisawa.
1998. Determinate growth in a paternal mouthbrooding fish whose reproductive success is limited by buccal capacity. *Evol. Ecol.* 12:681–699.
- Parrish, R. H., D. L. Mallicoate, and R. A. Klingbeil.
1986. Age dependent fecundity, number of spawnings per year, sex ratio, and maturation stages in northern anchovy, *Engraulis mordax*. *Fish. Bull.* 84:503–517.
- Perante, N. C., M. G. Pajaro, J. J. Meeuwig, and A. C. J. Vincent.
2002. Biology of a seahorse species *Hippocampus comes* in the central Philippines. *J. Fish Biol.* 60:821–837.
- Reina-Hervás, J. A.
1989. Contribution to the study of the family Syngnathidae (Pisces) along the southeast coast of Spain [In Spanish]. *Arq. Mus. Bocage* 1:325–334.
- Robert, R., G. Trut, and J. L. Laborde.
1993. Growth, reproduction and gross biochemical composition of the Manila clam *Ruditapes philippinarum* in the Bay of Arcachon, France. *Mar. Biol.* 116:291–299.
- Sprung, M.
1994a. High larval abundances in the Ria Formosa (Southern Portugal)—methodological or local effect? *J. Plankton Res.* 16:151–160.
- 1994b. Macrobenthic secondary production in the intertidal zone of the Ria Formosa—a lagoon in Southern Portugal. *Est. Marine Coastal Shelf. Sci.* 38:539–558.
- Strawn, K.
1958. Life history of the pigmy seahorse, *Hippocampus zosterae* Jordan and Gilbert, at Cedar Key, Florida. *Copeia* 1:16–22.
- Teixeira, R. L., and J. A. Musick.
2001. Reproduction and food habits of the lined seahorse, *Hippocampus erectus* (Teleostei: Syngnathidae) of Chesapeake Bay, Virginia. *Brazil. J. Biol.* 61:79–90.
- Vincent, A. C. J.
1990. Reproductive ecology of seahorses. Ph. D. diss., 101 p. Cambridge Univ., Cambridge, UK.
- Vincent, A. C. J., and B. Giles.
2003. Correlates of reproductive success in a wild population of *Hippocampus whitei*. *J. Fish. Biol.* 63:344–355.
- Vincent, A. C. J., and L. M. Sadler.
1995. Faithful pair bonds in wild seahorses, *Hippocampus whitei*. *Anim. Behav.* 50: 1557–1569.
- Wallace, R. A., and K. Selman.
1981. Cellular and dynamic aspects of oocyte growth in teleosts. *Am. Zool.* 21:325–343.
- Weddle, G. K., and B. M. Burr.
1991. Fecundity and the dynamics of multiple spawning in darters: an in-stream study of *Etheostoma rafinesquei*. *Copeia* 1991:419–433.

Abstract—Leatherback turtles (*Dermochelys coriacea*) are regularly seen off the U.S. West Coast, where they forage on jellyfish (Scyphomedusae) during summer and fall. Aerial line-transect surveys were conducted in neritic waters (<92 m depth) off central and northern California during 1990–2003, providing the first foraging population estimates for Pacific leatherback turtles. Males and females of about 1.1 to 2.1 m length were observed. Estimated abundance was linked to the Northern Oscillation Index and ranged from 12 (coefficient of variation [CV]=0.75) in 1995 to 379 (CV=0.23) in 1990, averaging 178 (CV=0.15). Greatest densities were found off central California, where oceanographic retention areas or upwelling shadows created favorable habitat for leatherback turtle prey. Results from independent telemetry studies have linked leatherback turtles off the U.S. West Coast to one of the two largest remaining Pacific breeding populations, at Jamursba Medi, Indonesia. Nearshore waters off California thus represent an important foraging region for the critically endangered Pacific leatherback turtle.

Abundance, distribution, and habitat of leatherback turtles (*Dermochelys coriacea*) off California, 1990–2003

Scott R. Benson (contact author)¹

Karin A. Forney²

James T. Harvey³

James V. Carretta⁴

Peter H. Dutton⁴

Email address for S. R. Benson: Scott.Benson@noaa.gov

¹ Protected Resources Division
Southwest Fisheries Science Center, NMFS, NOAA
c/o MLML Norte
7544 Sandholdt Rd.
Moss Landing, California 95039

² Protected Resources Division
Southwest Fisheries Science Center, NMFS, NOAA
110 Shaffer Road
Santa Cruz, California 95060

³ Moss Landing Marine Laboratories
8272 Moss Landing Road
Moss Landing, California 95039

⁴ Protected Resources Division
Southwest Fisheries Science Center, NMFS, NOAA
8604 La Jolla Shores Drive
La Jolla, California 92037

The leatherback turtle (*Dermochelys coriacea*) is listed as a critically endangered species on the World Conservation Union Red List 2006 (IUCN¹). The Pacific population is at risk of extirpation because of over-harvest of eggs, commercial and residential development on nesting beaches, and incidental bycatch in fisheries (Spotila et al., 2000). Declines have been documented at nesting beaches in the eastern Pacific and throughout the Indo-Pacific region, where there has been a complete loss of the Malaysian nesting population (Chan and Liew, 1996), severe declines at nesting beaches in Costa Rica (Spotila et al., 2000) and Mexico (Sarti et al., 1996), and lesser declines at western Pacific nesting beaches (Hitipeuw et al., 2007).

Research on leatherback turtles in the Pacific has typically been limited to nesting beaches and few studies have been conducted in foraging areas. In the eastern North Pacific,

the leatherback turtle is the most common sea turtle sighted north of Mexico (Stinson, 1984), although no nesting occurs at these latitudes. Sightings and incidental capture data indicate that this species is found as far north as Alaska but has been most frequently encountered off the coast of central California (Stinson, 1984; Starbird et al., 1993). Genetic analyses of tissues from leatherback turtles stranded on California beaches or caught incidentally in the California-Oregon drift gillnet fishery indicate that these turtles originate from nesting beaches in the western Pacific (Dutton et al., 2000, 2007). Thus, leatherback turtles travel thousands of kilometers from western Pacific beaches to forage on season-

Manuscript submitted 21 August 2006 to the Scientific Editor's Office.

Manuscript approved for publication 29 November 2006 by the Scientific Editor. Fish. Bull. 105:337–347 (2007).

¹ IUCN (World Conservation Union). 2006. Species Survival Commission. Red List database 2006. Website: <http://www.iucnredlist.org/> (accessed 19 November 2006).

ally abundant jellyfish (Scyphomedusae) along the West Coast of North America (Eisenberg and Frazier, 1983; Shenker, 1984), where coastal upwelling creates a dynamic and highly productive ecosystem.

The California Current ecosystem is dominated by seasonal upwelling that is most intense between Pt. Conception and Cape Mendocino and gradually abates between July and October (Bakun et al., 1974). Previous studies of sighting patterns have linked leatherback turtle distribution and occurrence off the West Coast of North America to sea surface temperatures of 15–16°C during late summer and early fall (Stinson, 1984; Starbird et al., 1993). In particular, Monterey Bay, California, was identified as an area where leatherback turtles can be found during August, according to incidental sighting information collected by recreational boaters, researchers, and whale-watching operators. The spatially biased nature of these observations, however, precluded the estimation of overall leatherback turtle density and abundance.

In this study, we report the results of systematic aerial surveys conducted over coastal California waters between 1990 and 2003 and provide the first estimates of abundance for foraging leatherback turtles along the California coast. We also describe the density, distribution, and interannual variability of leatherback turtles off California during the peak period of occurrence in late summer and fall, examine oceanographic factors related to their occurrence in this region, and evaluate the potential significance of this foraging area to the western Pacific stock. Knowledge of leatherback foraging habitats is essential for the recovery of this critically endangered species, and the results of this study provide a basis for identifying and examining other potential foraging regions in the northeastern Pacific.

Materials and methods

Field methods

Aerial line-transect surveys for marine mammals and sea turtles were conducted between 15 August and 15 November in 10 of 14 years between 1990 and 2003. The primary objective of these surveys was to estimate abundance and trends of harbor porpoise (*Phocoena phocoena*), a small, cryptic nearshore cetacean; however, turtle sightings were also recorded systematically. Surveys were restricted to good weather days, defined as days with clear to partly cloudy skies and winds of less than about 12 kt (Beaufort sea states of 0–3). The transects followed a zigzag pattern designed to survey systematically between the coast and the 92-m (50-fathom) isobath, located less than 30 km offshore, and covering the primary habitat for harbor porpoise (Fig. 1). During each survey year, 26 transects between Pt. Conception and the Russian River (38°27'N) were replicated 4–8 times, depending on weather conditions. An additional 17 transects were surveyed 1–3 times a year

off northern California between the Russian River and the California-Oregon border. Total transect length was 916 km, and under good weather conditions all transects were surveyed in two days. The full set of 43 transects was surveyed during the years 1990, 1991, 1993, 1995, 1997, 1999, and 2002. A subset of the transect lines (between Pt. Sur and Pt. Arena) was surveyed during 2000, 2001, and 2003 to provide further information on leatherback turtle occurrence off central California during these years.

Details of the survey methods have been reported elsewhere (Forney et al., 1991), and only a summary of key methods is provided here. The survey platform was a high-wing, twin-engine Partenavia P-68 aircraft, with two bubble windows for lateral viewing and a belly port for downward viewing. The survey team consisted of three observers (one on the left, right, and belly) and one data recorder. Distances to sighted animals were calculated from the declination angle to the sighting when abeam of the aircraft (obtained with a hand-held clinometer) and the aircraft's altitude. Surveys were flown at 167–185 km/h (90–100 kt) airspeed and 213 m (700 ft) altitude. Sighting information and environmental conditions, including Beaufort sea state, percentage cloud cover, and horizontal sun position (to measure glare direction) were recorded and updated throughout the survey by using a laptop computer connected to the aircraft's LORAN or GPS navigation system.

Visibility of submerged leatherback turtles is dependent upon water clarity and color contrast of the animals. When viewed from the air, this species generally exhibits considerable contrast to the surrounding waters within the California study area. To approximate the visibility of turtles at varying depths below the surface, a calibration experiment was conducted by using a set of multiple light-colored Secchi disks submerged at 1 m, 2 m, 3 m, and 4 m depth. During overflights, observers recorded the maximum visible Secchi disk depth. The proportion of time leatherback turtles spent within the visible depth range was estimated from dive data obtained during 2005 on free-swimming turtles, using a suction cup apparatus containing a VHF transmitter and a Lotek LTD 1110 time-depth-recorder (TDR) (Lotek, St. John's, Newfoundland, Canada). The suction cup apparatus (280 g weight in air) was attached to the dorsal surface of three leatherback turtles by using a pole from a small vessel, without capturing or handling the animal. The TDRs recorded depth every 5 sec at a resolution of 0.5 m and with an accuracy of $\pm 1\%$. Tagged turtles were tracked for several hours until the tag disengaged from the animal or was actively removed with the pole, creating little or no disturbance to the animal. Potential posttagging effects were examined by visually inspecting the full dive profile, and by analysis of variance to test for differences in the time spent within the estimated visual depth range between the first 30 minutes and subsequent 30-minute periods. All deployments occurred during daylight hours between 12:00 and 16:30 local time.

Analytical methods

For analysis of regional patterns of leatherback turtle density and distribution, the study area was divided into five geographic strata, near prominent features of the coastline, to capture variation in bathymetric and oceanographic characteristics (Fig. 1): north coast (3765 km²), Pt. Arena (772 km²), Gulf of the Farallones (4189 km²), Monterey Bay (908 km²), and south central California (1849 km²).

Leatherback turtle sighting rates were evaluated for potential effects of sea state, glare, and cloud cover, by using a two-way extension of the Kruskal-Wallis nonparametric analysis of variance (Scheirer et al., 1976), because these factors can influence one's ability to detect marine animals. Glare conditions were categorized as either optimal, when the sun position was behind the aircraft or directly ahead and did not affect the primary field of view, or marginal, when the sun position was just ahead of or perpendicular to the aircraft's travel direction. Cloud cover was divided into four categories: clear (<25% cloud cover), partly cloudy (26–50%), mostly cloudy (51–75%), and overcast (76–100%). Data collected in sea states greater than Beaufort 3 were excluded from the analysis; cloud cover and glare did not appear to exhibit any effect (see "Results" section) and were not considered further.

The detection function of leatherback turtles was estimated from the pooled perpendicular distances by using DISTANCE software (Thomas et al.²). Truncation of the 5–10% most distant sightings was investigated but it did not improve precision or model fit, and the final models included all data without truncation. Hazard, half-normal, and uniform models with and without cosine adjustment terms were fit to the ungrouped perpendicular distance data. The best model was selected according to Akaike's information criterion, AIC (Akaike, 1973), and visual inspection of goodness-of-fit.

The density (D) and abundance (N) of leatherback turtles within each geographic stratum, j , were estimated by using standard line-transect formulae (Buckland et al., 2001):

$$D_j = \frac{n_j f(0)}{2L_j g(0)}, \quad (1)$$

$$N_j = D_j A_j, \quad (2)$$

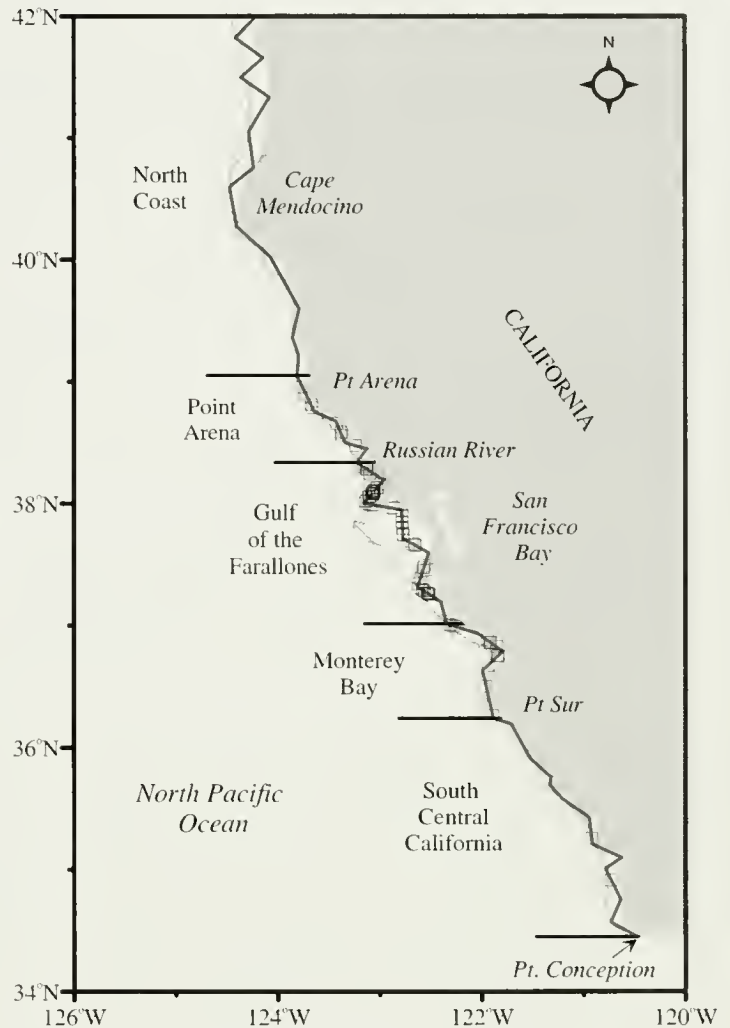


Figure 1

California study area with survey transects and geographic strata. Open squares represent locations of leatherback turtle (*Dermochelys coriacea*) sightings during systematic surveys. Thin gray line denotes the 90-m isobath.

where n_j = the total number of turtles seen during systematic surveys;

$f(0)$ = the probability density function evaluated at zero perpendicular distance;

L_j = the linear distance surveyed in km;

$g(0)$ = the probability of detection at zero perpendicular distance, estimated from leatherback turtle dive data (see below); and

A_j = the area size in km².

Although we attempted to complete each transect the same number of times, weather conditions often resulted in uneven coverage. To avoid this potential within-stratum source of bias, encounter rates (n_j/L_j) for each geographic stratum were calculated from the individual transect encounter rates, weighted according to the proportional contribution of each transect:

² Thomas, L., J. L. Laake, S. Strindberg, F. F. C. Marques, S. T. Buckland, D. L. Borchers, D. R. Anderson, K. P. Burnham, S. L. Hedley, J. H. Pollard, and J. R. B. Bishop. 2004. Distance 4.1. Release 2. Research Unit for Wildlife Population Assessment, University of St. Andrews, UK. Website: <http://www.ruwpa.st-and.ac.uk/distance/> (accessed 19 November 2006).

Table 1

Number of leatherback turtle (*Dermochelys coriacea*) sightings and kilometers of trackline surveyed by geographic stratum, 1990–2003 (SC=South Central California, MB=Monterey Bay, GF=Gulf of the Farallones, PA=Pt. Arena, NC=North Coast).

	1990	1991	1993	1995	1997	1999	2000	2001	2002	2003
No. of leatherback turtles										
SC	0	0	0	1	0	0	0	0	1	0
MB	4	0	0	1	0	1	2	0	8	0
GF	21	1	5	0	11	12	1	3	11	4
PA	3	0	0	0	2	5	0	0	0	0
NC	0	2	1	0	0	0	0	0	0	0
Total	28	3	6	2	13	18	3	3	20	4
Km surveyed										
SC	1605	922	1643	1197	1492	1317	0	0	1652	0
MB	655	509	860	730	860	585	74	368	812	334
GF	1316	293	1273	1030	1343	1026	197	482	1664	668
PA	343	107	287	192	328	327	12	179	475	27
NC	806	517	762	477	814	777	0	0	549	0
Total	4724	2347	4826	3626	4837	4032	283	1030	5151	1030

$$\frac{n_j}{L_j} = \sum_{i=1}^k \frac{t_{ij}}{T_j} \frac{n_{ij}}{L_{ij}}, \quad (3)$$

where k = the total number of transects within geographic stratum j ;

t_{ij} = the length (in km) of the i th transect in stratum j ;

T_j = the total length of all transects in stratum j ;

n_{ij} = the number of turtles seen on transect i in stratum j ; and

L_{ij} = the actual distance flown on transect i within stratum j .

The probability of detecting a leatherback turtle at zero perpendicular distance, $g(0)$, is primarily influenced by the proportion of time a turtle is unavailable to be seen by the aerial survey team because it is diving (availability bias; Marsh and Sinclair, 1989). In other cases, animals may be present at or near the surface, but missed by observers for other reasons, such as fatigue or poor viewing conditions (perception bias). In this study, no correction was available for perception bias. Availability bias was estimated from leatherback turtle dive data and the estimated visible depth range from the visibility calibration experiment. Variances for D and N were calculated on basis of the variances of n , $f(0)$, and $g(0)$, according to the method of Buckland et al. (2001). The variance in number of sightings, n , was expected to differ by year and stratum because of differences in mean turtle density; however, it was not possible to calculate stratum-specific and year-specific variances empirically because not all transects were replicated in all years. The variance of leatherback turtle detections, therefore, was assumed to follow a Poisson distribution, with $\text{var}(n) = n$. The variance of $f(0)$ was estimated analytically with DISTANCE soft-

ware, and the variance of $g(0)$ was estimated from the individual $g(0)$ estimates for the three tagged turtles.

Overall abundance estimates for the entire study area were calculated as the sum of the stratum-specific abundance estimates for the seven full survey years: 1990, 1991, 1993, 1995, 1997, 1999, and 2002. During the three years when surveys were flown only off central California (2000, 2001, and 2003), coastwide abundance of leatherback turtles was estimated as the sum of the abundances for the Monterey Bay and Gulf of the Farallones strata, divided by the mean proportion of the total abundance found in these two strata during full survey years. The variance in this proportion was estimated across years ($n=7$) and incorporated into the variance of N and D by using standard formulae. Abundance estimates were examined for trends and potential large-scale environmental influences by linear least squares regression that included year and the 12-month average Northern Oscillation Index (NOI; Schwing et al., 2002) as predictor variables. Regressions were performed for all years, and for the subset of seven full survey years, because there was greater uncertainty in the abundance estimates for 2000, 2001, and 2003.

Results

Survey summary

A total of 31,885 km were surveyed in Beaufort sea states of 0–3 during 1990–2003 (Table 1), and annual totals ranged from 2347 to 5151 km during the full survey years when all strata were surveyed, and from 283 to 1030 km during the partial survey years, when only waters between Pt. Sur and Pt. Arena were surveyed. Weather conditions varied by year and were the primary deter-

minant of the level of survey coverage achieved. Leatherback turtle encounter rates were identical for Beaufort sea states 0–1, 2, and 3 (0.003 turtles/km). Cloud cover and glare categories did not have a significant effect on encounter rates ($P=0.08$ and $P=0.23$, respectively).

The number of leatherback turtles seen per year ranged from 2 to 28, and totaled 100 individuals for all years (Table 1). The majority of turtles were subjectively estimated to be 5–7 ft (1.5–2.1 m) in total length, but only three smaller individuals (3.5–4.5 ft; 1.1–1.4 m) and one very large individual, estimated to be about 7.5 ft (2.3 m), were also recorded. Whenever possible, the presence of a long tail (indicating an adult male) was noted; however, this feature was often difficult to determine from the aircraft. In particular, males with tails of intermediate length may have had a greater likelihood of being recorded as “tail length undetermined.” The proportion of identified males, 6 of 44 (14%), therefore, is a minimum proportion of males in the study area. Greatest concentrations of leatherback turtles were observed in the Gulf of the Farallones stratum, but turtles were observed in all geographic strata (Fig. 1).

Estimation of line-transect parameters

All three detection function models yielded similar estimates of $f(0)$, and AIC values were within one point. The Hazard rate model (Buckland et al., 2001) was selected because it provided the best fit, especially near the transect line (Fig. 2), yielding an estimated $f(0)=4.465$ (coefficient of variation, $CV=0.136$).

During the visibility calibration experiment, only the Secchi disk at 1 m depth was visible to the aerial observers; therefore, the depth at which leatherback turtles were detected was estimated to be about 1 m. Time-depth recorders (TDRs) were attached to three turtles (1 male, 2 females) on 29 September (for 153 minutes), 30 September (167 minutes), and 13 October, 2005 (229 minutes). There was no visible reaction by the turtles to the application of the tag, and the proportion of time spent within 1 m of the surface did not differ between the first 30 minutes and subsequent 30-minute periods of tag deployment ($P=0.08$). The parameter $g(0)$ was, therefore, estimated from the complete TDR dive record as the average proportion of time leatherbacks spent at or above 1 m depth. The three individuals exhibited a remarkably similar proportion of time spent within the upper meter of the sea surface (Table 2), and $g(0)$ was estimated as 0.471 ($CV=0.029$). Corrected estimates of abundance thus are about twice the uncorrected values (Fig. 3).

Abundance and density

Estimated leatherback turtle abundance was variable among years (Fig. 3; Table 3), ranging from 12

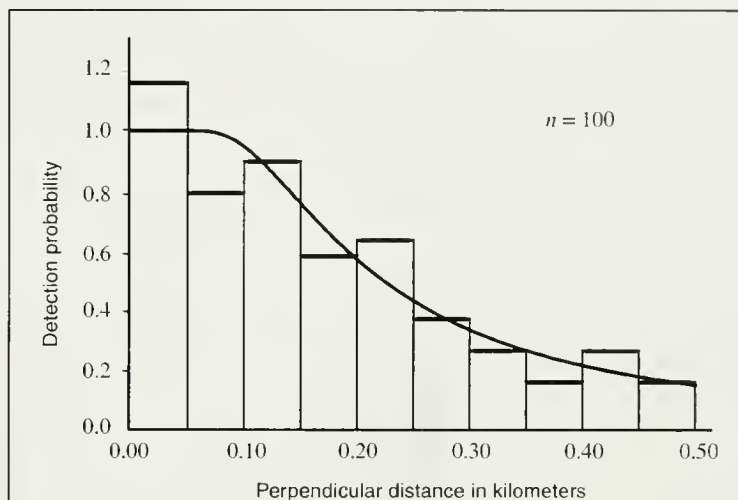


Figure 2

Detection probability function (Hazard rate model) and distribution of perpendicular distances for 100 leatherback turtle (*Dermodochelys coriacea*) sightings.

($CV=0.74$) during 1995 to 379 ($CV=0.23$) during 1990. The greatest proportion of turtles was encountered within the two central California strata (Monterey Bay and Gulf of the Farallones), accounting for an average of 72% (range 31–97%, $CV=0.37$) of the total abundance. In partial survey years, when only these two strata were surveyed, total abundance within the study area was estimated as the central California abundance divided by the mean percentage (72%). For all years combined, estimated leatherback turtle abundance averaged 140 ($CV=0.17$) within the central California strata and 178 ($CV=0.15$) for the entire study area (Table 3). Although the Gulf of the Farallones stratum contributed the most to overall abundance because of its larger size, turtle densities were only slightly less for the Monterey Bay and Pt. Arena strata (Table 3). The South Central California and North Coast strata had the lowest densities. Monthly encounter rates of leatherback turtles by stratum (Fig. 4) were consistent with past reports of frequent sightings in Monterey Bay during August (Starbird et al., 1993); however, in our study, encounter rates were also high during September in the Monterey Bay and Gulf of the Farallones strata, and during October within the Gulf of the Farallones. Encounter rates decreased markedly throughout the study area during November. Interannual variability was least during September, and regionally within the Gulf of the Farallones stratum.

The estimates of abundance of leatherback turtles off California (Fig. 3) did not exhibit a trend between 1990 and 2003 ($P=0.19$ when data for all ten survey years were used, $P=0.41$ including only the seven coastwide survey years) but appeared to be related to the average annual NOI (Schwing et al., 2002), i.e., there were positive index values associated with greater leatherback turtle abundance and vice versa (Fig. 5; $P=0.03$ when

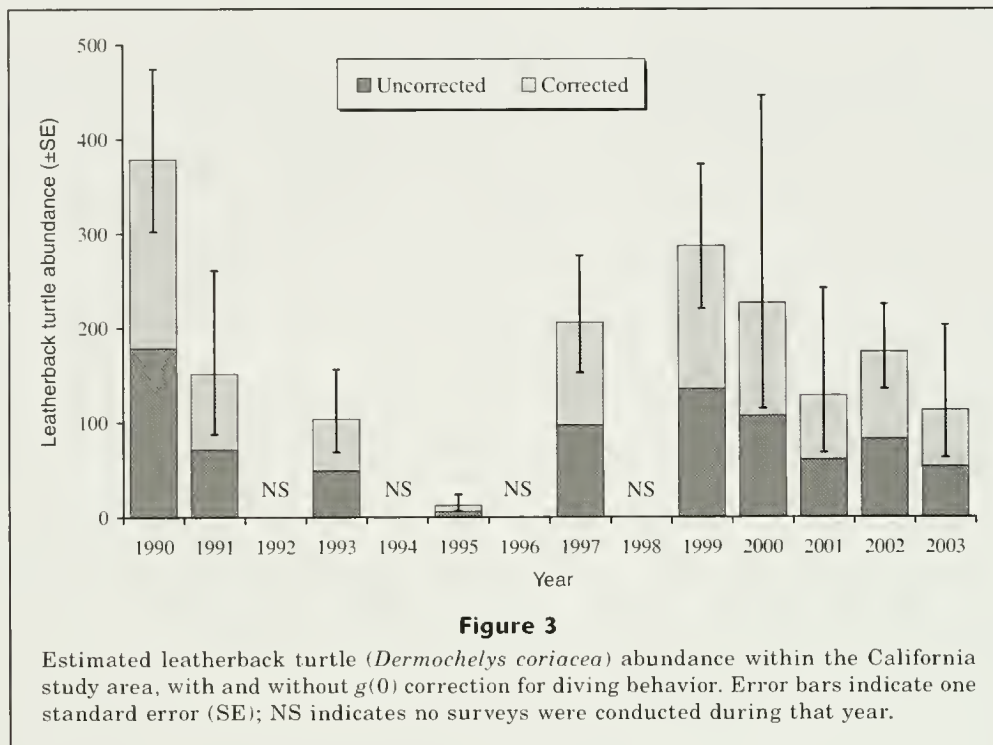


Figure 3

Estimated leatherback turtle (*Dermochelys coriacea*) abundance within the California study area, with and without $g(0)$ correction for diving behavior. Error bars indicate one standard error (SE); NS indicates no surveys were conducted during that year.

Table 2

Proportion of time spent in upper 5 meters of the water column by three foraging leatherback turtles (*Dermochelys coriacea*) tagged with time-depth recorders off central California during 2005. Dates and deployment times are provided for each turtle. "No. of intervals" represents the number of samples recorded by the depth logger (every 5 sec) within each depth category. The proportion of intervals within the upper 1 m was used for $g(0)$ estimation. CV = coefficient of variation.

Depth (m)	29 Sep 2005 (12:20–14:53)		30 Sep 2005 (13:28–16:16)		13 Oct 2005 (12:06–15:54)		Average	
	No. of intervals	Proportion of intervals	No. of intervals	Proportion of intervals	No. of intervals	Proportion of intervals	Proportion of intervals	CV
At surface	804	0.437	876	0.436	1099	0.400	0.425	0.029
≤1	35	0.456	124	0.498	164	0.460	0.471	0.029
≤2	104	0.513	260	0.628	219	0.540	0.560	0.062
≤3	63	0.547	123	0.689	150	0.595	0.610	0.069
≤4	220	0.666	229	0.803	287	0.699	0.723	0.057
≤5	76	0.708	92	0.849	91	0.732	0.763	0.057
>5	538	1.000	303	1.000	735	1.000	1.000	—

including all ten survey years; $P=0.04$ for only the seven coastwide survey years).

Discussion

The results of this study demonstrate the importance of neritic waters off California to foraging leatherback turtles and provide the first estimates of abundance for a Pacific foraging population of this critically endangered

species. The aerial line-transect surveys, although not originally designed to census this species, provided quantitative data during the summer and fall peak season of occurrence (Starbird et al., 1993). Absolute abundances of foraging Pacific leatherback turtles were estimated for the first time by applying a new telemetry-based correction factor to account for submerged animals. Corrected densities in this study were 2.1 times greater than uncorrected densities. This contrasts markedly with the correction factor of 7.6 derived from dive data for a single leatherback turtle off St. Croix, U.S. Virgin Islands

Table 3

Estimated density and abundance of leatherback turtles (*Dermochelys coriacea*) by year and geographic stratum (SC=South Central California, MB = Monterey Bay, GF=Gulf of the Farallones, PA=Pt. Arena, NC=North Coast. Central CA includes MB and GF). CV = Coefficient of variation.

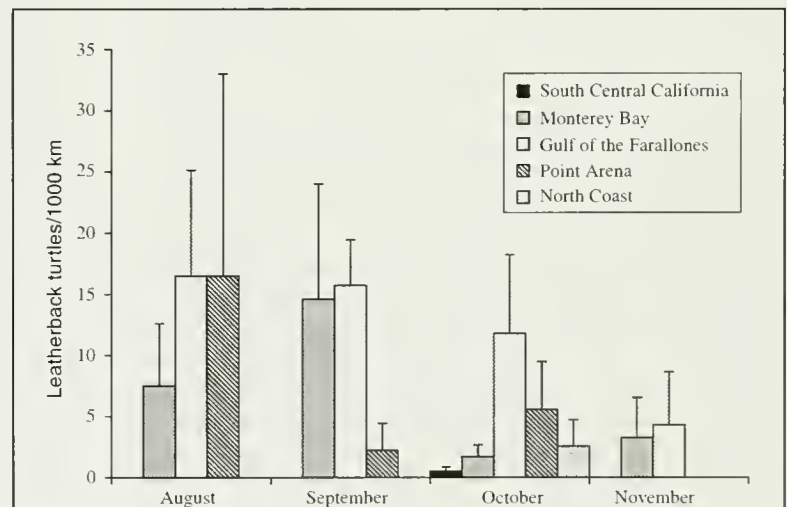
	1990	1991	1993	1995	1997	1999	2000 ¹	2001 ¹	2002	2003 ¹	Mean	CV
Density (no./100 km²)												
SC	0.0	0.0	0.0	0.4	0.0	0.0	—	—	0.3	—	0.1	0.72
MB	2.8	0.0	0.0	0.5	0.0	1.0	7.2	0.0	4.9	0.0	1.3	0.29
GF	7.7	1.1	1.9	0.0	4.3	5.4	2.3	2.2	3.0	1.9	3.6	0.18
PA	4.1	0.0	0.0	0.0	3.5	6.6	0.0	0.0	0.0	0.0	2.3	0.35
NC	0.0	2.8	0.6	0.0	0.0	0.0	—	—	0.0	—	0.3	0.59
Total area	3.3	1.3	0.9	0.1	1.8	2.5	2.0	1.1	1.5	1.0	1.6	0.15
Abundance												
SC	0	0	0	8	0	0	—	—	6	—	2	0.72
MB	25	0	0	4	0	9	66	0	45	0	15	0.29
GF	321	47	80	0	179	227	97	92	124	81	125	0.18
PA	32	0	0	0	27	51	0	0	0	0	14	0.35
NC	0	105	23	0	0	0	—	—	0	—	18	0.59
Total area	379	151	104	12	205	287	226	129	175	113	178	0.15
CV	0.23	0.59	0.43	0.74	0.30	0.27	0.77	0.70	0.26	0.64		
Central CA	347	47	80	4	179	236	162	92	169	81	140	0.17
CV	0.24	1.01	0.47	1.01	0.33	0.31	0.67	0.59	0.26	0.52		
% of total	92%	31%	78%	36%	87%	82%	—	—	97%	—	72%	0.37

¹ In these years, only central California was surveyed. Abundance estimates for the total area were extrapolated from central CA estimates based on the mean proportion of leatherbacks in central California during full survey years.

(Keinath and Musick, 1993) and applied to aerial survey density estimates for Atlantic leatherback turtles (Keinath et al., 1996). The correction used in the Keinath and Musick study, however, was based on the proportion of time the transmitter was above the water surface (and wave action), not the estimated proportion of time a turtle would have been visible to an aerial survey team (to about 1 m depth), as in this study. Furthermore, St. Croix represents a nesting area, and leatherback diving behavior may differ between nesting and foraging areas.

Average uncorrected densities of leatherback turtles off California during our study (0.75 turtles/100 km²) are within the range of 0.21 to 2.2 leatherback turtles/100 km² reported during 1978–82 along the U.S. Atlantic coast (Shoop and Kenney, 1992), although the Atlantic study reported monthly estimates, not a seasonal average, and encompassed a larger study area. Average uncorrected densities in a smaller foraging area off North Carolina during August–November 1986–91 (0.80 leatherback turtles/100 km²; Keinath et al., 1996), were similar to those observed in this study.

Leatherback turtles along the U.S. West Coast are part of the western Pacific genetic stock (Dutton et al.,

**Figure 4**

Average monthly leatherback turtle (*Dermochelys coriacea*) encounter rates (turtles / 1000 km surveyed) by geographic stratum, 1990–2003. Error bars indicate one standard error.

2000, 2007), which is known to nest in Papua (Indonesia), Papua New Guinea, Solomon Islands, and on other western Pacific islands (Dutton et al., 2007). The western Pacific metapopulation was estimated to contain

roughly 1800 nesting females in 1995 (Spotila et al., 1996); however, a more comprehensive evaluation indicates that the total western Pacific metapopulation may contain 2700–4500 breeding females (Dutton et al., 2007). Satellite telemetry studies have linked leatherback turtles foraging along the U.S. West Coast with one of the two largest remaining nesting beaches, Jamursba Medi (Papua, Indonesia) (Benson et al., 2007a), which experiences peak nesting activity during the austral winter. No links to the U.S. West Coast have been identified for animals nesting during the austral summer at nearby Wermon, Papua, Indonesia (S. Benson and P. Dutton, unpubl. data) or in Papua New Guinea (Benson et al., 2007b).

In a recent analysis of nest counts at Jamursba Medi, an average of about 750 females were estimated to nest annually between 1993 and 2004 (Hitipeuw et al., 2007). Efforts are underway to determine the relationship between the number of females nesting annually and the total number of females in the Jamursba-Medi nesting population; however, it is thought that this population currently has at least 1000–2000 nesting females (Spotila et al., 1996; Dutton et al., 2007). Capture studies off central California during 2000–2005 documented that about 67.5% (27 of 40) of foraging leatherback turtles were female (S. Benson and P. Dutton, unpubl. data). Our average annual estimate of 178 leatherback turtles along the California coast, therefore, should correspond to approximately 120 females. It is difficult, however, to evaluate this number in relation to the total Jamursba-Medi nesting population, because insufficient data are available on migration intervals between nesting beaches and foraging grounds. If each nesting year corresponds to one year at the California foraging grounds, then an average of about 16% of Jamursba-Medi females (120 divided by 750) potentially use the California foraging area; however there is evidence that leatherback turtles do not alternate nesting and foraging at such regular intervals. Remigration intervals to nesting beaches can range up to seven years (Price et al., 2004; Dutton et al., 2005), and some turtles have returned to forage off the U.S. West Coast during consecutive years without nesting (S. Benson and P. Dutton, unpubl. data). Further studies of remigration patterns and foraging site fidelity of western Pacific leatherback turtles will be required to resolve the proportion of these turtles that forage off California.

Estimates of foraging abundance in this study vary markedly among years (Fig. 3) and have a number of known sources of downward bias. First, the California study area includes only the nearshore environment to a water depth of about 92 m (50 fm), but leather-

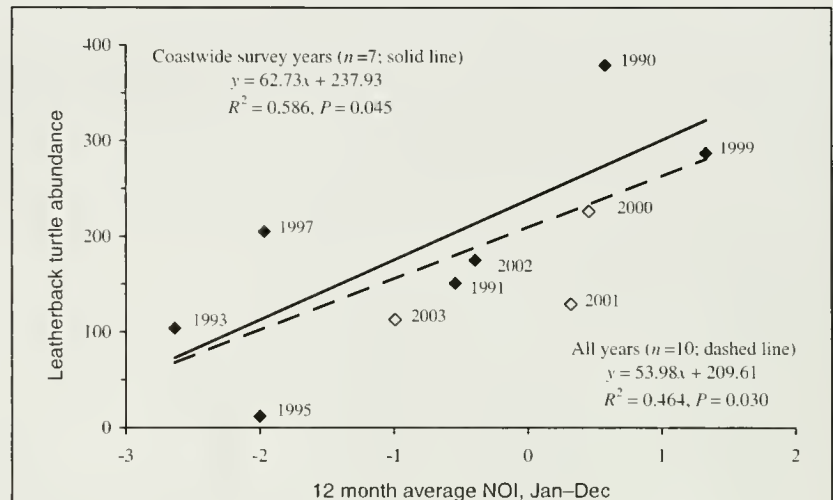


Figure 5

Regression of estimated leatherback turtle (*Dermochelys coriacea*) abundance versus 12 month average Northern Oscillation Index (NOI; Schwing et al., 2002) for the period January–December of each survey year (indicated next to the points). Filled symbols represent years in which surveys were conducted coastwide; open symbols represent years in which estimates of coastwide abundance were based on central California abundance (see “Materials and methods” section).

back turtles also have been captured incidentally in drift gill nets set in deeper waters (Julian and Beeson, 1998; Carretta et al., 2005). Second, the estimate calculated in this article represents an average snapshot abundance, and will be an underestimate of the true number of individuals using the area to the extent that residence times in the study area are less than our three-month study season. For example, if leatherback turtles forage within the study area for two months, then turtles observed in August would likely be different individuals from those observed during October or November, but average line-transect densities would only reflect the presence of a single turtle. Similarly, if leatherback turtle density is not constant throughout the three-month study period, the pooled estimate presented in this study will be lower than the peak seasonal abundance. Lastly, no estimate of perception bias was available for leatherback turtles in this study; however, small groups of small dolphins and porpoises are missed about 33% of the time (Forney et al., 1995). Therefore, it is likely that the detection of available turtles along the transect line is less than 100%.

The estimate of $g(0)$ developed in this study is the first to be based on dive records of leatherback turtles within a foraging region. Although the three turtles exhibited remarkably similar proportions of time within near-surface waters (Table 2), there is some uncertainty in the estimate because it is based on limited afternoon deployments ($n=3$) within a single year (2005). Furthermore, the depth to which turtles are visible to aerial observers may vary in space and time, as turbidity changes. The estimated $g(0) = 0.471$ should, therefore,

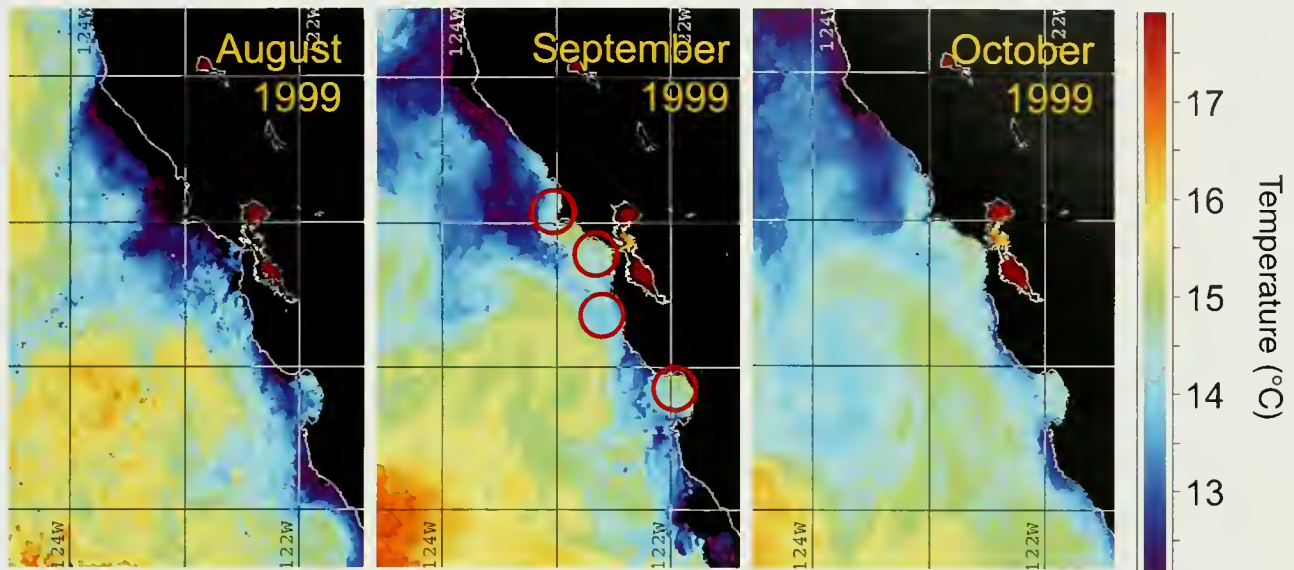


Figure 6

Pattern of upwelling and retention along the central California coast, illustrated with monthly satellite-derived sea surface temperature images for August, September, and October 1999. Leatherback turtles (*Dermochelys coriacea*) and Scyphomedusae were primarily found in areas of retention (circled in middle panel). High resolution monthly composite satellite images courtesy of NOAA CoastWatch, West Coast Node.

be considered provisional, pending further TDR deployments and calibration experiments.

Leatherback turtle populations at many Pacific nesting beaches have decreased dramatically during the last decade (Spotila et al., 2000), but decreases at Jamursba-Medi have been less pronounced (Hitipeuw et al., 2007), and the abundance of turtles foraging off California does not exhibit a trend between 1990 and 2003 (Fig. 3). The California study area is a dynamic upwelling environment that exhibits great interannual variability in oceanographic conditions (Chelton et al., 1982; McGowan et al., 1998) and distribution of marine vertebrates (e.g., Ainley et al., 1993; Benson et al., 2002). Links have been proposed elsewhere between large-scale environmental indices, such as the Southern Oscillation Index and the North Atlantic Oscillation, and sea turtles (Limpus and Nicholls, 1988; Rivalan, 2004) or their prey (Lynam et al., 2004). In this study, leatherback turtle abundance off California exhibited a positive relationship with the average annual NOI (Fig. 5). Positive NOI values correspond with conditions favorable to upwelling along the California coast, leading to increased zooplankton production (Schwing et al., 2002) and the development of large aggregations of gelatinous zooplankton (Graham, 1994), which are known to be the primary prey of leatherback turtles (Eisenberg and Frazier, 1983).

Although we did not measure underlying physical and biological processes, central California has been the focus of numerous oceanographic studies that shed light on potential trophic links between physical processes

and leatherback turtles. Strong northwest winds during late spring and early summer lead to wind-driven upwelling (Bakun et al., 1974), particularly near points and headlands. These prominences can interact with local hydrographic features to create localized retention areas (upwelling shadows; Graham, 1994), where nutrient-rich, upwelling-modified water is entrained nearshore, particularly during wind relaxation. This process creates favorable conditions for phytoplankton growth and increases retention of zooplankton, larval fish, crabs, and gelatinous organisms (Wing et al., 1995; Graham et al., 2001). Dense aggregations of jellyfish (Scyphomedusae), primarily *Chrysaora fuscescens*, *C. colorata*, and *Aurelia* spp., have been observed regularly in these nearshore regions (Graham, 1994; this study). Similar processes have been reported off Oregon, where Scyphomedusae become denser and larger in size during summer, when the movement of surface and near-surface waters concentrates plankton in nearshore retention areas (Shenker, 1984). During our surveys, Scyphomedusae were common in retention areas between Pt. Reyes and Monterey Bay (Fig. 6), where leatherback turtles were most frequently encountered and observed feeding on *C. fuscescens*, *C. colorata*, and *Aurelia* spp. (Starbird et al., 1993; this study). We hypothesize that variability in the expression of these physical and trophic processes leads to interannual and seasonal variability in observed leatherback turtle abundance off central California, with densities greatest during periods of significant upwelling and subsequent relaxation events.

Previous researchers have linked leatherback turtle occurrence at high latitudes to the 15–16°C isotherm (Stinson, 1984; McMahon and Hays, 2006). Off central California, this reported pattern may reflect the presence of >15°C waters during summer and fall relaxation events and in upwelling shadows where jellyfish aggregations are found (Graham, 1994; Graham and Largier, 1997), rather than a physiological limitation of leatherback turtles. The broad shallow area of retention in the Gulf of the Farallones consistently exhibited greater abundances of leatherback turtles during our study. In contrast, few turtles were observed south of Pt. Sur, where the shelf is extremely narrow and cooler waters dominate along a nearly straight coastline where there are limited retention zones.

Many questions remain unanswered regarding the role of physical and biological factors and their influence on leatherback turtle abundance and distribution along the U.S. West Coast. Upwelling shadows and relaxation events probably affect leatherback turtle occurrence, but directed studies are needed to establish trophic links. Furthermore, the potential influence and role of the San Francisco Bay outflow on this nearshore foraging area is unknown. Results of this study provide a means for designing finer-scale surveys in key index areas of reliable leatherback turtle occurrence, such as the Gulf of the Farallones and Monterey Bay. Aerial surveys of these index areas should be coupled with telemetry studies and investigations of environmental variables that affect leatherback turtle foraging behavior to provide insights into the relevant trophic processes.

Ultimately, successful conservation efforts for leatherback turtles must include both protection of nesting beaches and mitigation of at-sea threats in foraging areas and along migratory routes. This study has demonstrated that waters off central California are a critical foraging area for one of the largest remaining Pacific nesting populations. Fortunately, threats such as coastal gillnet and longline fisheries that may incidentally catch leatherback turtles have largely been eliminated within our nearshore study area although pelagic driftnet and longline fisheries remain along the migratory pathways to and from the coast (e.g., Spotila et al., 1996; Carretta et al., 2005). Continued efforts to identify and characterize Pacific foraging areas are critical for mitigating at-sea threats, monitoring population trends, and, ultimately, for the successful recovery of Pacific leatherback turtle populations.

Acknowledgments

This study could not have been completed without the dedicated support of many aerial observers, whom we thank sincerely. S. Eckert originally noted the significance of leatherback turtle sighting data collected during these nearshore surveys and encouraged us to initiate the analyses presented here. Aspen Helicopters, Inc. provided aircraft and pilots, and Moss Landing Marine Laboratories Marine Operations provided small boat

support. Captain J. Douglas' exceptional boat handling skills were key to the success of the telemetry studies. Suction-cup telemetry was conducted under ESA permit no. 1227. Surveys were conducted under National Marine Fisheries Service permit nos. 748 and 773-1437, and National Marine Sanctuary permit nos. GFNMS / MBNMS-03-93, MBNMS-11-93, GFNMS / MBNMS / CINMS-09-94, GFNMS / MBNMS / CINMS-04-98-A1, and MULTI-2002-003. Financial support and personnel were provided by the National Marine Fisheries Service (Southwest Fisheries Science Center, Southwest Region, and Office of Protected Resources), Monterey Bay National Marine Sanctuary, and the California Department of Fish and Game. We thank J. Barlow, E. Calvert, A. Moles, J. Musick, F. Schwing, J. Seminoff, and three anonymous reviewers for their helpful reviews of this manuscript.

Literature cited

- Ainley, D. G., W. J. Sydeman, R. H. Parrish, and W. H. Lenarz.
1993. Oceanic factors influencing distribution of young rockfish (*Sebastes*) in central California: a predator's perspective. *CalCOFI Rep.* 34:133–139.
- Akaike, H.
1973. Information theory and an extension of the maximum likelihood principle. *In* Second international symposium on information theory (B. N. Petran and F. Csàaki, eds.), p. 267–281. Akadèmiai Kiado, Budapest, Hungary.
- Bakun, A., D. R. McLain, and F. V. Mayo.
1974. The mean annual cycle of coastal upwelling off western North America as observed from surface measurements. *Fish. Bull.* 72:843–844.
- Benson, S. R., D. A. Croll, B. Marinovic, F. P. Chavez, and J. T. Harvey.
2002. Changes in the cetacean assemblage of a coastal upwelling ecosystem during El Niño 1997–98 and La Niña 1999. *Prog. Oceanogr.* 54:279–291.
- Benson, S. R., P. H. Dutton, C. Hitipeuw, B. Samber, J. Bakarbessy, and D. Parker.
2007a. Post-nesting migrations of leatherback turtles (*Dermochelys coriacea*) from Jamursba-Medi, Bird's Head Peninsula, Indonesia. *Chelonian Conserv. Biol.* 6(1):150–154.
- Benson, S. R., K. M. Kisokau, L. Ambio, V. Rei, P. H. Dutton, and D. Parker.
2007b. Beach use, internesting movement, and migration of leatherback turtles, *Dermochelys coriacea*, nesting on the north coast of Papua New Guinea. *Chelonian Conserv. Biol.* 6(1):7–14.
- Buckland, S. T., D. R. Anderson, K. P. Burnham, J. L. Laake, D. L. Borchers, and L. Thomas.
2001. Introduction to distance sampling: estimating abundance of biological populations, 432 p. Oxford Univ. Press, Inc., New York, NY.
- Carretta, J. V., T. Price, D. Petersen, and R. Read.
2005. Estimates of marine mammal, sea turtle, and seabird mortality in the California drift gillnet fishery for swordfish and thresher shark, 1996–2002. *Mar. Fish. Rev.* 66(2):21–30.
- Chan, E. H., and H. C. Liew.
1996. Decline of the leatherback population in Tereng-

- ganu, Malaysia, 1956–1995. *Chelonian Conserv. Biol.* 2(2):196–203.
- Chelton, D. B., P. A. Bernal, and J. A. McGowan. 1982. Large-scale interannual physical and biological interaction in the California Current. *J. Mar. Res.* 40:1095–1125.
- Dutton, D. L., P. H. Dutton, M. Chaloupka, and R. H. Boulon. 2005. Increase of a Caribbean leatherback turtle *Dermochelys coriacea* nesting population linked to long-term nest protection. *Biol. Conserv.* 126(2):186–194.
- Dutton, P. H., A. Frey, R. LeRoux, and G. Balazs. 2000. Molecular ecology of leatherbacks in the Pacific. In *Sea turtles of the Indo-Pacific. Research, management and conservation* (N. Pilcher, and G. Ismael, eds.), p. 248–253. Asean Academic Press Ltd, London, UK.
- Dutton, P. H., C. Hitipeuw, M. Zein, S. R. Benson, G. Petro, J. Pita, V. Rei, L. Ambio, and J. Bakarbesy. 2007. Status and genetic structure of nesting populations of leatherback turtles (*Dermochelys coriacea*) in the western Pacific. *Chelonian Conserv. Biol.* 6(1):47–53.
- Eisenberg, J. F., and J. Frazier. 1983. A leatherback turtle (*Dermochelys coriacea*) feeding in the wild. *J. Herpetol.* 17:81–82.
- Forney, K. A., J. Barlow, and J. V. Carretta. 1995. The abundance of cetaceans in California coastal waters. Part II: Aerial surveys in winter and spring of 1991 and 1992. *Fish. Bull.* 93:15–26.
- Forney, K. A., D. A. Hanan, and J. Barlow. 1991. Detecting trends in harbor porpoise abundance from aerial surveys using analysis of covariance. *Fish. Bull.* 89:367–377.
- Graham, W. M. 1994. The physical oceanography and ecology of upwelling shadows. Ph.D. diss., 205 p. Univ. California, Santa Cruz, CA.
- Graham, W. M., and J. L. Largier. 1997. Upwelling shadows as nearshore retention sites: the example of northern Monterey Bay. *Cont. Shelf Res.* 17(5):509–532.
- Graham, W. M., F. Pagès, and W. M. Hamner. 2001. A physical context for gelatinous zooplankton aggregations: a review. *Hydrobiologia* 451:199–212.
- Hitipeuw, C., P. H. Dutton, S. R. Benson, J. Thebu, and J. Bakarbesy. 2007. Population status and internesting movement of leatherback turtles (*Dermochelys coriacea*) nesting on the northwest coast of Papua, Indonesia. *Chelonian Conserv. Biol.* 6(1):28–36.
- Julian, F., and M. Beeson. 1998. Estimates of marine mammal, turtle and bird mortality for two California gillnet fisheries: 1990–1995. *Fish. Bull.* 96:271–284.
- Keinath, J. A., and J. A. Musick. 1993. Movements and diving behavior of a leatherback turtle, *Dermochelys coriacea*. *Copeia* 1993: 1010–1017.
- Keinath, J. A., J. A. Musick, and D. E. Barnard. 1996. Abundance and distribution of sea turtles off North Carolina. OCS Study/MMS 95-0024, 156 p. U. S. Department of the Interior, Minerals Management Service, Gulf of Mexico OCS Region, 1201 Elmwood Park Boulevard, New Orleans, LA 70123-2394.
- Limpus, C. J., and N. Nicholls. 1988. The Southern Oscillation regulates the annual numbers of green turtles (*Chelonia mydas*) breeding around northern Australia. *Austral. J. Wildl. Res.* 15(2):157–161.
- Lynam, C. P., S. J. Hay, and A. S. Brierley. 2004. Interannual variability in abundance of North Sea jellyfish and links to the North Atlantic Oscillation. *Limnol. Oceanogr.* 49:637–643.
- Marsh, H., and D. F. Sinclair. 1989. Correcting for visibility bias in strip transect aerial surveys of aquatic fauna. *J. Wildl. Manage.* 53:1017–1024.
- McGowan, J. A., D. R. Cayan, and L. M. Dorman. 1998. Climate-ocean variability and ecosystem response in the Northeast Pacific. *Science* 281:210–217.
- McMahon, C. R., and G. C. Hays. 2006. Thermal niche, large-scale movements and implications of climate change for a critically endangered marine vertebrate. *Global Change Biol.* 12:1–9.
- Price, E. R., B. P. Wallace, R. D. Reina, J. R. Spotila, F. V. Paladino, R. Piedra, and E. Vélez. 2004. Size, growth, and reproductive output of adult female leatherback turtles *Dermochelys coriacea*. *Endang. Species Res.* 5:1–8.
- Rivalan, P. 2004. Population dynamics of leatherback turtles in French Guiana: Research on relevant factors and application to the establishment of conservation strategies. [In French.] Ph.D. diss., 249 p. Univ. Paris XI Orsay, Paris.
- Sarti, L., S. A. Eckert, N. García, and A. R. Barragan. 1996. Decline of the world's largest nesting assemblage of leatherback turtles. *Mar. Turtle Newsl.* 74:2–5.
- Scheirer, C. J., W. S. Ray, and N. Hare. 1976. The analysis of ranked data derived from completely randomized factorial designs. *Biometrics* 32:429–434.
- Schwing, F. B., T. Murphree, and P. M. Green. 2002. The Northern Oscillation Index (NOI): a new climate index for the northeast Pacific. *Prog. Oceanogr.* 53(2):115–139.
- Shenker, J. M. 1984. Scyphomedusae in surface waters near the Oregon coast, May–August, 1981. *Estuar. Coastal Shelf Sci.* 19:619–632.
- Shoop, C. R., and R. D. Kenney. 1992. Seasonal distributions and abundances of loggerhead and leatherback sea turtles in waters of the northeastern United States. *Herpetol. Monogr.* 6:43–67.
- Spotila, J. R., A. E. Dunham, A. J. Leslie, A. C. Steyermark, P. T. Plotkin, and F. V. Paladino. 1996. Worldwide population decline of *Dermochelys coriacea*: Are leatherback turtles going extinct? *Chelonian Conserv. Biol.* 2(2):209–222.
- Spotila, J. R., R. D. Reina, A. C. Steyermark, P. T. Plotkin, and F. V. Paladino. 2000. Pacific leatherback turtles face extinction. *Nature* 405:529–530.
- Starbird, C. H., A. Baldrige, and J. T. Harvey. 1993. Seasonal occurrence of leatherback sea turtles (*Dermochelys coriacea*) in the Monterey Bay region, with notes on other sea turtles, 1986–1991. *Calif. Fish Game* 79(2):54–62.
- Stinson, M. L. 1984. Biology of sea turtles in San Diego Bay, California, and the north eastern Pacific Ocean. M.S. thesis, 578 p. San Diego State Univ., San Diego, CA.
- Wing, S. R., J. L. Largier, L. W. Botsford, and J. F. Quinn. 1995. Settlement and transport of benthic invertebrates in an intermittent upwelling system. *Limnol. Oceanogr.* 40:316–329.

Abstract—The importance of glacial ice habitats to harbor seals (*Phoca vitulina*) in Alaska has become increasingly apparent. However, enumerating harbor seals hauled out on ice in glacial fjords has been difficult. At Johns Hopkins Inlet in Glacier Bay, Alaska, we compared a shore-based counting method to a large-format aerial photography method to estimate seal abundance. During each aerial survey, shore-based observers simultaneously counted seals from an observation post. Both survey methods incurred errors in double-counting and missing seals, especially when ice movements caused seals to drift between survey zones. Advantages of shore-based counts included the ability to obtain multiple counts for relatively little cost, distinguish pups from adults, and to distinguish mobile seals from shadows or glacial debris of similar size. Aerial photography provided a permanent record of each survey, allowing both a reconciliation of counts in overlapping zones and the documentation of the spatial distribution of seals and ice within the fjord.

Comparison of survey methods for estimating abundance of harbor seals (*Phoca vitulina*) in glacial fjords

John L. Bengtson (contact author)¹

Alana V. Phillips¹

Elizabeth A. Mathews²

Michael A. Simpkins^{1,3}

E-mail: John.Bengtson@noaa.gov

¹ National Marine Mammal Laboratory
Alaska Fisheries Science Center
National Marine Fisheries Service, NOAA
7600 Sand Point Way NE
Seattle, Washington 98115

² University of Alaska Southeast
Department of Natural Sciences
11120 Glacier Highway
Juneau, Alaska 99801

³ Marine Mammal Commission
4340 East-West Highway, Rm. 905
Bethesda, Maryland 20814

Harbor seals (*Phoca vitulina*) in Alaska occupy a geographically extensive range and topographically diverse haul-out habitats. They are present in U.S. waters from approximately 172°E to 130°W (over 3500 km east to west) and from 51°N to 61°N (over 1000 km north to south), hauling out on a variety of substrates including sand, rock, and, in Alaska, glacial ice. Alaska harbor seal populations have declined at several locations since the late 1970s. For example, counts of harbor seals at Tugidak Island (southwest of Kodiak Island, Alaska) declined 85% between 1976 and 1988 (Pitcher, 1990), and counts in Prince William Sound indicate population declines of approximately 63% between 1984 and 1997 (Frost et al., 1999). Additional evidence indicates that harbor seal numbers near Kodiak Island, including those at Tugidak Island, increased 6.6%/yr during 1993–2001 (Small et al., 2003), but that seals in Prince William Sound have continued to decline 3.3%/yr during 1988–99 (Ver Hoef and Frost, 2003). In Glacier Bay, Alaska, harbor seal numbers declined by 75% (–14.5%/yr) during 1992–2002 at terrestrial resting sites and by 64% (–9.6%/yr) from 1992 to 2001 in Johns Hopkins Inlet, the primary breeding site, which

is a glacial fjord where seals haul out on floating ice (Mathews and Pendleton, 2006). Because it is estimated that 10% or more of harbor seals in Alaska use glacial ice habitats during the molting season (August–September) (J. L. Bengtson, unpubl. data), there is a pressing need to develop reliable survey methods to assess harbor seal abundance in such areas. Here we evaluate two such survey methods: counts from shore-based observations and counts from large-format aerial photography.

Shore-based surveys of harbor seals in two glacial fjords in Glacier Bay National Park, Alaska, have been made from elevated shore sites over the past three decades (Calambokidis et al., 1987; Mathews, 1995; Mathews and Pendleton, 2006) and in Aialik Bay, a glacial fjord in the Gulf of Alaska (Hoover, 1983). In 1997, Mathews et al.¹ conducted a pilot

¹ Mathews, E. A., W. L. Perryman, and L. B. Dzinich. 1997. Use of high-resolution, medium-format aerial photography for monitoring harbor seal abundance at glacial ice haulouts, 15 p. Unpubl. report to Glacier Bay National Park and Preserve, P. O. Box 140, Gustavus, AK 99826. Website: <http://www.uas.alaska.edu/biology/faculty/mathews/publications.html> (accessed 1 December 2006).

study in Johns Hopkins Inlet, Glacier Bay, and determined that it was feasible to count harbor seals on glacial ice from medium-format aerial photographs, and comparisons of these counts were made to simultaneous shore counts. In our study, we employed higher resolution (large-format) film, conducted three simultaneous aerial and shore surveys (vs. one in the pilot study), and used data from different altitudes to assess sources of counting error within aerial photographs.

Aerial surveys of harbor seals are most often conducted when peak numbers are hauled out, which usually occurs during the annual molt in late summer. During such surveys, low altitude (100–300 m) photographs of harbor seal groups are obtained, from which seal counts are made (Olesiuk et al., 1990; Boveng et al., 2003). Surveying seals in glacial fjords is more difficult than on terrestrial sites because the moving, large expanses of scattered ice on which seals haul out offer little spatial reference to aid in counting seals. Furthermore, there is often insufficient maneuvering room for low-altitude aerial surveys in the fjords. The main objective of our study was to compare the relative effectiveness of shore-based and aerial survey methods to estimate harbor seal abundance.

Materials and methods

Study area

Johns Hopkins Inlet is located in the northwest arm of Glacier Bay (58°N, 138°30'W) in southeastern Alaska (Fig. 1). At the head of the inlet is an active tidewater glacier that is currently advancing. The fjord walls are steep, rising to 640 m and 884 m within one km of the western and eastern shores, respectively. Harbor seals rest, nurse, and molt on ice calved from the glacier. Pieces of ice occupied by seals are typically around 8–24 m², although they vary widely in size and can be much larger (up to ~890 m², $n=105$) (E. A. Mathews, unpubl. data). Ice that has above-water features taller than about 2 m is rarely occupied. The percent of ice cover in the inlet was estimated by shore observers before seal counts during August for the years 1995–2001; for most surveys, 6–25% or 26–50% of the inlet was covered by ice ($n=83$ shore surveys). Approximately 60–70% of harbor seals in Glacier Bay use glacial ice in Johns Hopkins Inlet during the pupping, breeding, and molting periods from spring to early fall (Mathews, 1995).

Shore-based surveys

Observers counted seals from an elevated (~35 m) site located along the western shore of the inlet about 2.5 km from the terminus of Johns Hopkins Glacier (Fig. 2A).



Figure 1

Map of Glacier Bay, Alaska, showing Johns Hopkins Inlet (shaded).

From this site, the observers' field of view comprised approximately 9 km (from the glacier to Jaw Point). The northwestern edge of the inlet and a small area near the northwest edge of the glacier face were not visible to the shore observers because of obstruction by headlands and other geographic features (i.e., "blind spots," Fig. 2A). Ice in the inlet more commonly drifted closer to the east than the west shore because of current and wind patterns; therefore, the location of the observation site along the western shore was selected as the observation site. Two of the four observers involved in this study simultaneously counted seals 2 or 3 times each day between 12 and 23 August 2001 and 9 and 26 August 2002. Seals on ice and in the water were tallied, but only seals on ice were included in this analysis. Observers conducted shore-based counts of harbor seals in Johns Hopkins Inlet during, or within an hour of, the aerial surveys conducted on 15 and 16 August 2001, and 15 August 2002. Surveys targeted the period around solar noon when the largest number of seals hauls out on glacial ice (Hoover, 1983; Calambokidis et al., 1987).

Observers counted seals using 20×60 binoculars mounted on tripods. After each tripod was leveled, observers locked the vertical orientation of the tripod head and counted all seals in the field of view as the

binoculars were pivoted horizontally in one direction. To facilitate systematic counting in the study area, observers visually divided the field of view into three or four subareas using markers such as landmarks or natural breaks in the ice as viewed from the observation site. When a marker came into the field of view, the binoculars were lowered exactly one field of view, locked again, and a pass in the opposite direction was made (Mathews, 1995). Each of the subareas typically required only two nonoverlapping, parallel passes across ice habitat to completely cover the width of a subarea. Counts from all subareas were summed for each observer to estimate total counts, and the two observers' total counts were then averaged to estimate the total count for each survey. The variance for each survey's total count was estimated as the variance among the two observers' total counts.

Aerial surveys

Aerial surveys were conducted from a twin engine aircraft on 15 and 16 August 2001 and 15 August 2002 by

a commercial photographic surveying company (Aeromap U.S., Anchorage, AK). In 2001, each aerial survey over Johns Hopkins Inlet was completed in three transects: two transects at 1465 m altitude covering the entire inlet, and an additional transect at 915 m covering the central portion of the inlet a second time from Johns Hopkins Glacier to the point north of Jaw Point (Fig. 2B). In 2002, the survey aircraft flew two transects at 1465 m covering Johns Hopkins Inlet from the glacier to Jaw Point; a lower-altitude, central transect was not flown (Fig. 2C). Shore observers observed no reaction by the seals (e.g., entering the water) to the aerial surveys.

During each survey, large-format (23×23 cm) photographic images were taken automatically at a predetermined rate on Agfa Aviphot Color X100 PE1 negative film (Agfa Corp., Ridgefield Park, NJ), with a belly-mounted Zeiss RMK TOP 15 camera (Carl Zeiss, Inc., Thornwood, NY) with forward-motion compensation (15 August 2001) or with a Zeiss RMK A 15/23 camera (Carl Zeiss, Inc., Thornwood, NY) (16 August 2001 and 15 August 2002). We did not notice any substantial im-

provement with the use of forward-motion compensation. The resulting photographic frame widths (i.e., the on-the-ground width of the area photographed in each photo frame) were 2200 m for high-altitude (1465 m) images and 1400 m for low-altitude (915 m) images. The images had approximately 10% endlap (i.e., overlapping duplication of the same area in separate, successive images) within transects, 20% sidelap between high-altitude transects, and 75% sidelap between the central transect and the neighboring high-altitude transects in 2001. Large-format negatives were scanned at 1600 dpi (the maximum resolution available to us) with a digital scanner and converted to positive-color digital images. The pixel resolutions of the resulting digital images were 0.10 m and 0.15 m for low- and high-altitude transects, respectively. At that resolution, we found that seals could be identified from the scanned imagery, and we were satisfied with this resolution for the purposes of counting seals.

Seals were counted from the digital images by using the "geospatial light table" feature of ERDAS Imagine 8.6 software (Leica GeoSystems Inc., Atlanta, GA). No distinction was made between adults, pups, or juvenile seals. A virtual mosaic was created by delineating overlapping zones on adjacent images based on the relative positions of identifiable pieces of ice. This mosaic allowed the analyst to account for ice movement when counting seals. In some cases, delineation of overlapping zones was difficult, particularly

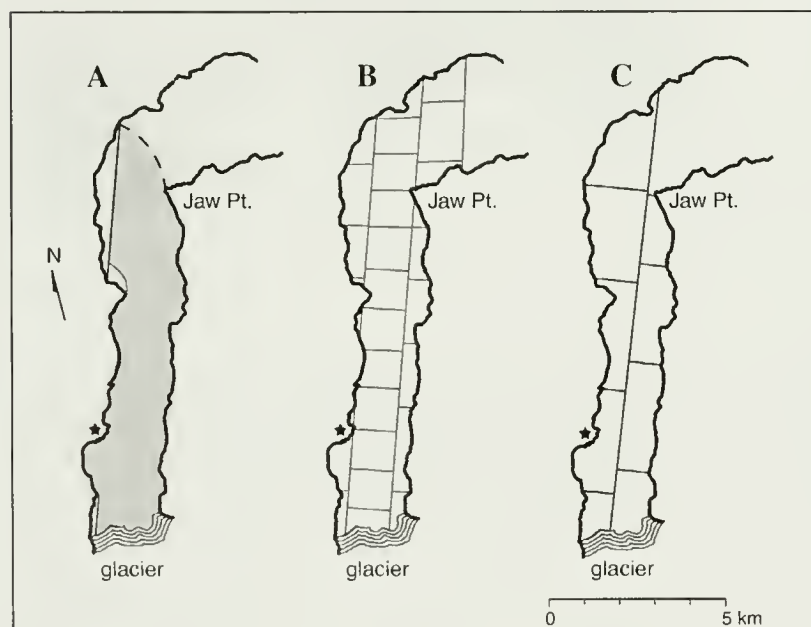


Figure 2

Survey coverage of Johns Hopkins Inlet, Glacier Bay, achieved by each survey type in this study. (A) Field of view (shaded area) observed from shore-based observation site (indicated with a star). Note that the northwestern edge of the inlet and a small area near the glacier are obscured from view ("blind spots") by geographical features. The outer range of visibility varied with conditions and is denoted by a dashed, curved line. (B) Photographic coverage of aerial transects flown on 15 and 16 August 2001. The straight lines in the inlet reflect the approximate boundaries between photographs. For simplicity, only the nonoverlapping areas (i.e., no endlap or sidelap) of each image are shown. The central transect was flown at a lower altitude (915 m) than the two adjacent transects (1465 m). (C) Photographic coverage of aerial transects (1465 m altitude) flown on 15 August 2002; the overlap between neighboring photographs was ignored.

Table 1

Shore-based and aerial photographic counts of harbor seals (*Phoca vitulina*) at Johns Hopkins Inlet, Glacier Bay, Alaska, in 2001 and 2002. Means, standard errors (SE), and coefficients of variation (CV) are derived from two simultaneous counts during each shore-based census and from three independent counts of aerial survey imagery (times are given in local solar time).

Date	Survey type	Survey time (h)	Mean count	SE	CV
15 Aug 2001	Shore-based	1406–1449	1970	57.0	0.029
	Aerial	1457–1512	1581	20.0	0.013
16 Aug 2001	Shore-based	1401–1439	1906	192.5	0.101
	Aerial	1421–1442	1294	25.6	0.020
15 Aug 2002	Shore-based	1249–1349	1562	4.0	0.003
	Aerial	1231–1245	1511	46.6	0.031

when ice moved substantially during the time that elapsed between neighboring photographs. Seals in overlapping zones were counted only once (i.e., only counted in one of the overlapping images). In 2001, the resolution in the low-altitude transects was superior to that in the high-altitude transects; therefore we counted all seals within the low-altitude imagery first and then added counts of seals in the nonoverlapping portions of the high-altitude imagery. Three replicate total counts were calculated for each survey by counting the seals in each image three separate times and tallying the resulting counts for each replicate. All replicates were counted by a primary analyst, and at least one week elapsed between each replicate count to minimize bias caused by the analyst remembering the location of seals from previous replicate counts. The number of images analyzed varied between surveys, depending on the survey tracks flown and the distribution of ice. Sixty-two total images were analyzed: 15 August 2001=21 images, 16 August 2001=30 images, and 15 August 2002=11 images. A subsample of five images from Johns Hopkins Inlet was also counted by a secondary analyst to provide independent verification of counts. The mean count (of the three counts by the primary analyst) for each image was calculated, and the mean counts for all images from each survey were summed to estimate the total survey count. The variance of the total count estimate was estimated as the sum of the variances for each mean count included in the total estimate.

Comparison of detection rates at different altitudes

To compare the detection rates in low- and high-altitude imagery from 2001, we counted all seals in the overlapping zones of low- and high-altitude images. Next, we visually compared the location of each seal in the overlapping portions of low- and high-altitude images and classified seals as either 1) counted in both images or 2) counted in only one of the images. Seals counted in only one of the images were further categorized as follows: 1) light-colored seal not detected in the other image, 2) seal in a group not resolved as an individual in the other image, 3) seal definitely not present in the

other image (e.g., seal went into the water or hauled out between transects), or 4) shadow or dirty ice classified as a seal in other image. These comparisons were conducted to help us understand the relative accuracy of counting seals from images taken at different altitudes. The less accurate high-altitude counts were not used when estimating mean counts for each survey; mean counts were estimated by triplicate counts with priority given to low-altitude counts as described above.

Results

Comparison of total counts

In 2001, counts made from shore were consistently higher than counts made with the use of aerial photography (Table 1). In contrast, both counting methods produced similar results in 2002. The standard errors and coefficients of variation (CV) presented in Table 1 reflect variance between counts by shore-based observers or between independent counts of aerial photographs. Although the CVs for counts of individual images were generally larger than the CVs for total estimates, 91% of the CVs for individual images were less than 0.1. Of the five images counted by a secondary analyst, all counts were within 8% of the mean of the three replicate counts conducted by the primary analyst. Imprecision or inaccuracies in counts caused by the distance of seals from the observation site or the altitude of the aerial survey were not easily quantified, although altitude-related errors were evaluated separately by comparing counts of seals in overlapping low- and high-altitude images.

Spatial distribution of seals in Johns Hopkins Inlet

The distribution of seals in Johns Hopkins Inlet was different during each of the surveys and appeared to be associated with the pattern of ice in the inlet. Generally, seals were found in aggregations, although solitary seals were frequently observed outside of the main seal concentrations (Fig. 3). On 15 August 2001, seals were distributed in groups of 200–500 animals, ranging

from 1 to 6 km from the glacier terminus (Fig. 3A). On 16 August 2001, a large group of 800–900 seals was aggregated in a band stretching from 0.5 km from the glacier terminus to the shore-based observation site, and another group of 300–400 seals was found 3–5 km from the glacier (Fig. 3B). On 15 August 2002, all of the seals were within 3 km of the glacier face between the glacier and the shore-based observation site (Fig. 3C). Of these, a group of 350–450 seals was observed on the southwest side of the inlet, and the remaining 1100–1200 seals formed a dense concentration on the east side of the inlet. No seals were located in the blind areas (from the view point of the shore-based observers) on any of the three survey days (Figs. 2A and 3).

Comparison of detection rates at different altitudes

An examination of seals in overlapping zones of low- and high-altitude images revealed a difference in the rates of seal detection between the two altitudes. Seals were more easily detected and confirmed to be seals in the low-altitude imagery; therefore, seals identified in low-altitude imagery were considered to be “true” observations for comparison to seals counted in high-altitude imagery. For the 15 August 2001 survey, 32.7% of the seals counted in the low-altitude images (i.e., “true” seals) were misclassified in high-altitude images: 8.6% were counted as seals when no seals were present (i.e., shadows or dirty ice misidentified as seals) and 24.1% were not counted as seals when seals were present (i.e., 23.3% were dark seals dismissed as shadows or

dirty ice, 0.5% were light-colored seals that were not detected, and 0.3% were so close to other seals that they could not be identified from their neighbors). In the 16 August 2001 survey, 34.3% of the seals counted in the low-altitude images were misclassified in the high-altitude images, including 12.5% that were shadows or dirty ice misidentified as seals and 21.8% that were not detected in the high-altitude imagery (21.5% dark seals and 0.3% light-colored seals). The net effect of the misclassifications was that counts from higher-altitude images were underestimates of the number of seals compared to counts from lower altitudes (i.e., the proportion of seals missed exceeded the proportion of false identifications).

Discussion

Comparison of total counts

Both shore-based and aerial counts indicated that more than 1500 seals haul out on glacial ice in Johns Hopkins Inlet in mid-August, making the inlet one of the most important haul-out sites in Glacier Bay (as suggested by Mathews [1995]). The total number of seals that use the inlet might be substantially larger because some unknown proportion of seals was in the water (i.e., not hauled out on ice) during the surveys. In 2001, counts made from shore were consistently higher than counts made with aerial photography (Table 1). In contrast, both counting methods produced similar results in 2002. Several sources of error for each method likely contributed to these inconsistencies in results between the two methods.

Sources of error for each survey method

Both counting methods were susceptible to common errors of either double-counting or missing seals. These errors were most likely to occur within overlapping zones between neighboring photographic images, between parallel passes with binoculars, or between shore-based counts of subareas. If overlapping zones were not accurately delineated, individual seals within the overlapping zone could be counted twice, or missed entirely. The permanent record provided by photography provided the best opportunity to minimize such errors by allowing for careful delineation of overlapping zones based on the relative positions of identifiable pieces of ice on adjacent images. The shore-based method did not allow re-identification of individual pieces of ice; therefore shore-based observers attempted to eliminate overlapping by adjusting binoculars carefully. Seals could be missed, however, if the binoculars were

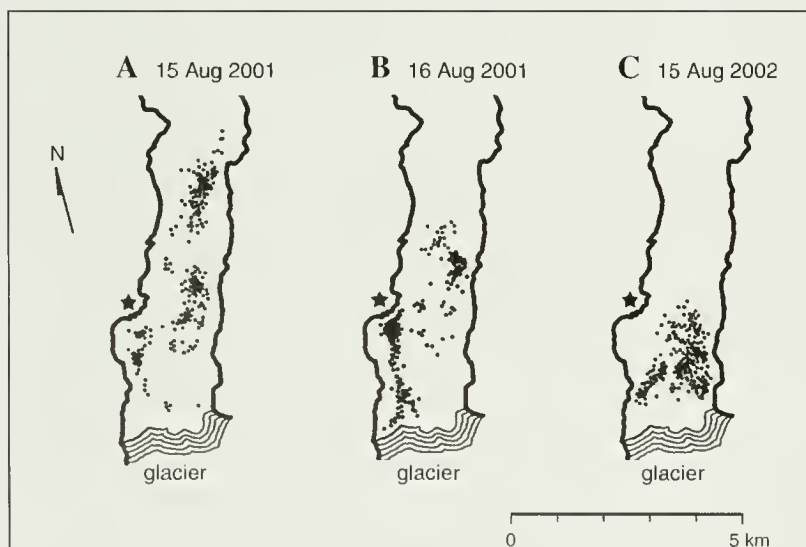


Figure 3

Relative distribution of patches of harbor seals (*Phoca vitulina*) in Johns Hopkins Inlet, Glacier Bay, determined by aerial photography, on (A) 15 August 2001, (B) 16 August 2001, and (C) 15 August 2002. Dots indicate groups of seals and are meant to illustrate generalized locations of seals, rather than a precise indication of seal abundance. The shore-based observation site is indicated with a star.

Table 2

Comparison of the percent difference ($[(\text{shore-based count} - \text{aerial photography count})/\text{shore-based count}]$) in the number of harbor seals (*Phoca vitulina*) counted by two survey methods. Potential sources of error for harbor seal counts in Johns Hopkins Inlet included maximum distance between harbor seals and shore observers, degree of clumping of harbor seals on ice, and the degree of movement of ice.

Date	Percent difference in counting method	Maximum distance between seals and shore site (km)	Degree of seal clumping	Degree of ice movement
15 Aug 2001	25%	4.25	moderate	high
16 Aug 2001	47%	2.40	high	high
15 Aug 2002	3%	2.75	low	high

lowered more than one field of view. Similarly, seals could be counted twice, if the binoculars were lowered less than one field of view before the second survey pass.

Counting errors could be caused by movement of ice on which seals were hauled out. Shore-based observers could not track the movement of ice between parallel passes; therefore some counting errors caused by ice movements were unavoidable. Depending on ice drift patterns, seals that were already counted could drift into an uncounted zone and be double counted, or uncounted seals could drift into a counted zone and be missed. On both days surveyed in 2001, we observed considerable movement of ice between aerial transects, particularly along the eastern side of the inlet, farthest away from the shore-based observation site. Thus, it is likely that seals would have drifted between the shore-based observers' counting areas, resulting in either missed or double counts. In contrast, the ice was less mobile during the 2002 survey day. Ice did not drift much between adjacent photographic images along a transect because only 5–10 seconds elapsed between each image. However, ice sometimes drifted substantially between images along neighboring transects, which were typically separated by 10–15 minutes. Although such ice movements sometimes made identification of individual seals between neighboring images more difficult, spatial clues from recognizable pieces of ice aided identification and made us confident that seals on moving ice were properly counted.

The distribution of seals could also influence counting errors for both survey methods. In 2001, ice was distributed up to 4.5–6 km from the glacier terminus and seal distribution was clumped (Fig. 3, A and B). In contrast, during the 2002 survey day the ice was more densely packed near the glacier terminus and seals were more evenly distributed (Fig. 3C). The distance between the shore observers and seals was also expected to affect shore counts, and to produce greater error as distance increased. Our results, however, did not exhibit a clear pattern in the percent difference between counting methods and distance between shore observers and seals. In 2001, seals were

within 4.25 km of observers on 15 August and within 2.4 km on 16 August; during the 2002 survey seals were located within 2.75 km (Table 2). Overall, the counts recorded by both methods were most similar when ice movement and seal clumping were minimal (Table 2).

Counting errors could also be caused by misidentifying seals as shadows or dirty ice. Occasionally, ice ridges cast shadows that looked remarkably like seals. Some glacial ice contained veins of dirt that also had the similar shape and color of seals. When comparing seals identified in overlapping imagery from the two aerial survey altitudes, we found that 22–24% of seals counted in the low-altitude (high-resolution) imagery either were not detected or were dismissed as shadows or dirty ice in counts of the high-altitude imagery. However, 9–13% of seals counted in the high-altitude imagery were actually shadows or dirty ice, according to the low-altitude imagery. These two types of errors tended to offset each other, although high-altitude counts still exhibited a general bias toward 10–15% lower seal counts. As a result, the aerial counts (especially from high-altitude imagery) likely produce underestimates of the actual number of seals hauled out on ice. The aerial counts from 2001 were based primarily on low-altitude counts, and, thus probably represent less biased estimates than the counts for the 2002 survey, which was based solely on high-altitude imagery. No correction was applied to the high-altitude counts because the likelihood of misidentifying or missing seals varied according to conditions specific to each image (e.g., dirty ice and shadows); therefore applying a correction based on images from one part of the fjord probably was not applicable to images from other parts of the fjord, let alone images from an entirely different day. Further, no correction was available for the proportion of seals misidentified or missed in the low-altitude imagery and for an unknown number of seals that were in the water during the surveys.

Shore-based observers had the advantage of a three-dimensional “live” view of seals and were able to distinguish between actively moving seals and shadows

or dirty ice, although this advantage probably diminished with distance. Stationary seals could still be difficult to distinguish at any distance, although their characteristic profiles and the reflectivity of their fur helped to distinguish seals from rocks or dirt of similar size. As was the case for the aerial estimates, no correction was available for seals missed or misidentified by shore-based observers, and some unknown number of seals were in the water during the observation periods.

Advantages of each method

Shore-based counts The main benefit associated with counting harbor seals from land is the ability to obtain multiple counts throughout the day, and on successive days, relatively inexpensively.¹ Counts can also be made from land under suboptimal weather conditions, when aerial surveys are impossible or when the resulting photographs would be of poor quality. Repeated surveys allow an assessment of changes in seal counts related to covariates such as time of day, ice conditions, and weather (Mathews and Pendleton, 2006). The number of harbor seals counted on ice in Johns Hopkins Inlet varies from day to day and thus increases the probability that a small number of aerial surveys could yield misleading results. For example, on 10 consecutive days in August 1999 the number of seals counted from shore near midday ranged from 1465 to 2534. If surveys are conducted when pups are nursing (generally during June in Alaskan waters), shore observers can identify seal pups based on size, shape, and relative position of seals within a group hauled out on ice. By August, however, almost all pups are weaned and the number of seals in groups on ice is much larger than in June, making it much more difficult to distinguish weaned pups or juveniles from adults except at very close range. With the aerial surveys there were also difficulties in distinguishing pups and juveniles (i.e., the resolution of the aerial photographs in the August study was not high enough to distinguish weaned pups, and no large-format aerial surveys were conducted during June when dependent pups are more likely to be distinguishable from adults).

Aerial photography Large-format aerial photography allows investigators to count seals from a set of images taken at a consistent distance (altitude) from the seals without potential "blind spots" caused by land or ice features. Photographs can be taken with overlapping images so that a mosaic of the complete study area can be obtained for each sampling event, and so that ice movement can be taken into account. The ability to view seals from a vertical perspective, rather than obliquely from a shore-based observation site, removes many of the potential biases associated with sighting seals at variable distances from the shoreline. The photographs also represent a permanent record of the distribution of the seals within a fjord—a record that allows recounts or re-analyses of images. For example,

the primary analyst was able to count seals in each image independently three times to estimate variance in the number of seals recorded; a secondary analyst was also able to count seals in a subsample of the same images to provide an independent verification of the final estimates. Aerial photography also offers one the ability to evaluate the spatial distribution of seals within a study area in relation to other seals (e.g., social interactions) and to environmental features (e.g., ice types or shifting ice patterns). A final advantage of using aerial photography is that researchers are not required to establish and maintain a remote field camp throughout the study period.

Future surveys of harbor seals in glacial fjords

The development of reliable methods for surveying harbor seal abundance in glacial ice habitats is a fundamental requirement for estimating the population size of these seals in Alaska. Conventional aerial surveys of harbor seals at terrestrial haul-out sites indicate that approximately 180,000 seals may be found at terrestrial sites. Preliminary counts of harbor seals from large-format photographs taken in glacial ice habitats throughout Alaska indicate that as many as 20,000 to 25,000 additional harbor seals may be using glacial ice habitats (J. L. Bengtson, unpubl. data). If 10% or more of Alaska's harbor seal population are using glacial ice habitats at various times of the year, monitoring trends in seal abundance in these areas will be very important to resource managers and to subsistence hunters in the Alaska Native community. In some regions, a much larger proportion of harbor seals may use glacial ice habitats. Within Glacier Bay, an average of 72% of harbor seals surveyed between 1992 and 2001 (2400–4700 seals per year) were found within glacial fjords during the breeding season (Mathews and Pendleton, 2006). At present, there are about 20 sites in Alaska where harbor seals are known to haul out in glacial ice habitats. Several of these fjords are of special interest to resource managers because 1) some local seal populations may be declining, 2) the fjords are important hunting areas to Alaska Natives, and 3) logistical difficulties have hampered past efforts to monitor changes in seal abundance with standard survey methods.

In the future, which survey methods seem most appropriate for monitoring the abundance of harbor seals in glacial ice habitats? Both shore-based counts and aerial photography are valuable methods for monitoring seals in glacial fjords, and each method has different limitations and potential applications. Unlike Johns Hopkins Inlet, many glacial fjords in Alaska do not have an overlook with such a full view of seal habitat, and thus large-format aerial photography may be the only option for surveying seals in these important breeding areas. The present study demonstrates that large-format aerial photography is a promising method for surveying the abundance of harbor seals using glacial ice habitats in Alaska.

Acknowledgments

L. Dzinich, O. Harding, K. Blejwas, and N. Tex provided field assistance with shore-based counts at Johns Hopkins Inlet. Funding for this project was provided by the National Park Service to E. A. Mathews and J. L. Bengtson and by the National Oceanic and Atmospheric Administration and the National Park Service to J. L. Bengtson. We thank M. Kralovec and M. B. Moss at the Glacier Bay National Park for their support in helping to secure funding. S. Slade at Leica GeoSystems provided technical assistance for Erdas Imagine for the aerial photography counts. S. Tackley produced Figures 2 and 3. This manuscript was improved by comments from J. K. Jansen, J. M. Waite, and three anonymous reviewers. This research was conducted under Marine Mammal Protection Act permits 527-1461, 782-1355, and 782-1676.

Literature cited

- Boveng, P. L., J. L. Bengtson, D. E. Withrow, J. C. Cesarone, M. A. Simpkins, K. J. Frost, and J. J. Burns.
2003. The abundance of harbor seals in the Gulf of Alaska. *Mar. Mamm. Sci.* 19(1):111-127.
- Calambokidis, J., B. L. Taylor, S. D. Carter, G. H. Steiger, P. K. Dawson, and L. D. Antrim.
1987. Distribution and haul-out behavior of harbor seals in Glacier Bay, Alaska. *Can. J. Zool.* 65:1391-1396.
- Frost, K. J., L. F. Lowry, and J. M. Ver Hoef.
1999. Monitoring the trend of harbor seals in Prince William Sound, Alaska, after the *Exxon Valdez* oil spill. *Mar. Mamm. Sci.* 15(2):494-506.
- Hoover, A. A.
1983. Behavior and ecology of harbor seals (*Phoca vitulina richardsi*) inhabiting glacial ice in Aialik Bay, Alaska. M.S. thesis, 132 p. Univ. Alaska, Fairbanks, AK.
- Mathews, E. A.
1995. Longterm trends in abundance of harbor seals (*Phoca vitulina richardsi*) and development of monitoring methods in Glacier Bay National Park, Southeast Alaska. In Proceedings of the third Glacier Bay science symposium, Glacier Bay National Park & Preserve, P.O. Box 140, Gustavus, Alaska, U.S.A., Sept. 15-18, 1993 (D. R. Engstrom, ed.) p. 254-263. U.S. National Park Service, Anchorage, AK.
- Mathews, E. A., and G. W. Pendleton.
2006. Declining trends in harbor seal (*Phoca vitulina*) numbers at glacial ice and terrestrial haulouts in Glacier Bay National Park, 1992-2002. *Mar. Mamm. Sci.* 22(1):167-189.
- Olesiuk, P. F., M. A. Bigg, and G. M. Ellis.
1990. Recent trends in the abundance of harbor seals, *Phoca vitulina*, in British Columbia. *Can. J. Fish. Aquat. Sci.* 47:992-1003.
- Pitcher, K. W.
1990. Major decline in the number of harbor seals (*Phoca vitulina*) on Tugidak Island, Gulf of Alaska. *Mar. Mamm. Sci.* 6(2):121-134.
- Small, R. J., G. W. Pendleton, and K. W. Pitcher.
2003. Trends in abundance of Alaska harbor seals, 1983-2002. *Mar. Mamm. Sci.* 19(2):344-362.
- Ver Hoef, J., and K. J. Frost.
2003. A Bayesian hierarchical model for monitoring harbor seal changes in Prince William Sound, Alaska. *Environ. Ecol. Sta.* 10:210-219.

Abstract—We verified the age and growth of swordfish (*Xiphias gladius*) by comparing ages determined from annuli in fin ray sections with daily growth increments in otoliths. Growth of swordfish of exploitable sizes is described on the basis of annuli present in cross sections of the second ray of the first anal fins of 1292 specimens (60–260 cm eye-to-fork length, EFL) caught in the region of the Hawaii-based pelagic longline fishery. The position of the initial fin ray annulus of swordfish was verified for the first time with the use of scanning electron micrographs of presumed daily growth increments present in the otoliths of juveniles. Fish growth through age 7 was validated by marginal increment analysis. Faster growth of females was confirmed, and the standard von Bertalanffy growth model was identified as the most parsimonious for describing growth in length for fish greater than 60 cm EFL. The observed growth of three fish, a year-old in size when first caught and then recaptured from 364 to 1490 days later, is consistent with modeled growth for fish of this size range. Our novel approach to verifying age and growth should increase confidence in conducting an age-structured stock assessment for swordfish in the North Pacific Ocean.

Age and growth of swordfish (*Xiphias gladius*) caught by the Hawaii-based pelagic longline fishery

Edward E. DeMartini (contact author)

James H. Uchiyama

Robert L. Humphreys Jr.

Jeffrey D. Sampaga

Happy A. Williams

Email address for E. E. DeMartini: Edward.Demartini@noaa.gov

Pacific Islands Fisheries Science Center
National Marine Fisheries Service, NOAA
2570 Dole Street
Honolulu, Hawaii 96822-2396

Swordfish (*Xiphias gladius*) constitute an economically important fishery resource and have historically supported many large-scale commercial fisheries throughout the world's oceans. During the 1990s, however, declining catches and average sizes of swordfish in Atlantic and Mediterranean fisheries indicated possible or likely overexploitation of these populations, and the status and management of these stocks became a highly publicized issue.

Swordfish began to be a major species targeted by the Hawaii-based pelagic longline fishery in 1990 and continued as such through the late 1990s, with landings peaking at 4000–6000 t in 1991–93 (Ito et al., 1998). This longline fishery targeted swordfish within, and adjacent to, fronts of the Subtropical Convergence Zone north of Hawaii during winter and late spring (Bigelow et al., 1999). Beginning in 1999, gear restrictions were imposed and in mid-2001 a moratorium on shallow-set (swordfish style) longlining within the swordfish fishery grounds north of the equator was instated to reduce interactions of fishing gear with, and incidental take of, protected species—primarily loggerhead turtles (*Caretta caretta*). The moratorium was lifted in March 2004 and a regulated (by annual effort cap, gear restrictions, take limit) longline fishery was reinstated.

A preliminary stock assessment for swordfish caught in the North Pacific Ocean, based on surplus production models, was conducted in early 1999 and was updated in early 2002 to include body length composition. No age-structured assessment as yet exists for swordfish in the central North Pacific. With the subsequent re-opening of the Hawaii-based fishery, there has been renewed interest in swordfish management in the North Pacific and a recognized need for a more robust, age-structured basis for stock assessment and documentation of age distributions and growth rates. For example, Sun et al. (2005) recently assessed the population status of swordfish taken by the tuna longline fishery in the waters around Taiwan in the western North Pacific.

Our objectives in this study were the following: 1) to evaluate the accuracy and precision of our age estimates; 2) to provide several complementary data supporting a predictable periodicity (on a yearly basis) of annulus formation in cross sections of anal-fin rays of swordfish caught in the region of the Hawaii-based longline fishery and examine evidence verifying our age estimates for these specimens; and 3) to estimate sex-specific patterns of size-at-age and growth to provide input for pending age-structured assessments of swordfish stock(s) in the central North Pacific.

Manuscript submitted 21 September 2006 to the Scientific Editor's Office.

Manuscript approved for publication 20 December 2006 by the Scientific Editor. Fish. Bull. 105:356–367 (2007).

Materials and methods

Collections and measurements of fish

All swordfish used for age determination in this study were collected from within the general region of the Hawaii-based pelagic longline fishery (Ito et al., 1998; DeMartini et al., 2000, Fig. 2 therein). About 95% of the specimens used were caught by commercial longlines during March 1994–June 1997; specimen collections were conducted and fish measurements were recorded by National Oceanic and Atmospheric Administration (NOAA) Fisheries, Southwest Region observers. The remaining 5% of the fish were caught on research cruises conducted during April–May 1992 and 1993, September 1996, and March–April 1997. Fish were measured (eye-to-fork length, EFL, in cm) before dressing (removal of head, entrails, tail, and fins) at sea. As they were dressed, sex was scored according to macroscopic criteria and later validated by microscopic evaluation of histological preparations of gonads for subsamples of the fish (DeMartini et al., 2000). When the fins of swordfish were removed at sea, either a portion or the entire first anal fin was collected and frozen. The braincase section, including the region of the semicircular canals was collected from juvenile and young adult swordfish, either when fish were beheaded at sea or when whole frozen bycatch specimens were thawed and dissected ashore. Additional larval and early young-of-year specimens (4 mm to 20 cm EFL) were collected by a neuston trawl (5-mm and 0.505-mm mesh in wings and codend, respectively) leeward of Hawaii Island during 1995–97; intact specimens were stored frozen before otolith extraction.

Laboratory processing and specimen examination

Frozen first anal fins were thawed, and the second spiny ray was selected (Berkeley and Houde, 1983), removed, and cleaned of all tissue. It was then dried in a dehydrator for 24–48 h at about 60°C, and three adjacent, transverse sections were cut with a low-speed saw. The first cut was made according to standard protocol (Ehrhardt et al., 1996) but at a newly defined position (distal end of the medial suture, hereafter “suture terminus”) located about 15% of the distance beyond the basal condyle. Subsequent cuts were made distal to the first, spaced to provide wafers ≈1 mm thick (Uchiyama et al., 1998). The location chosen for the cuts was different from the conventional standard (i.e., at a distance above the basal condyle equal to one-half the condyle width= $d/2$) currently used in swordfish aging studies (Sun et al., 2002). The unconventional cut was necessary because the condyle of the second ray is often severed or lost during the removal of fins by fishermen at sea. A small series of matched (same fish) fin ray samples were cut at the suture terminus and at the $d/2$ positions; some of these were also cut immediately distal to the condyle (basal cut) and the numbers of annuli were counted and compared. Cross sections of rays were preserved in mounting media on glass microscope slides and stored

(without cover slips) in sealed boxes. Otoliths (sagittae) were dissected from frozen larvae and young adults at the NOAA Fisheries, Pacific Islands Fisheries Science Center (Honolulu Laboratory), and stored dry after having been cleaned, rinsed with water, and dried with 95% ethanol (EtOH).

Fin ray annuli, each defined as a single pair of opaque and translucent bands completely encircling the cross-section hemisphere without partial and split checks (Ehrhardt et al., 1996; Sun et al., 2002), were enumerated. At first examination, about 1% of all cross sections were deemed unreadable and discarded. The distances separating the distal edges of the translucent band of each annulus were measured, the opaque versus translucent nature of cross-section edges was noted, and marginal increment ratios (MIRs) were measured in marginal increment analysis (Campana, 2001). A series of MIRs was calculated for each specimen of age 1 or older by using the formula (Prince et al., 1988; Sun et al., 2002):

$$MIR = (R_{tot} - R_n) / (R_n - R_{n-1}),$$

where R_{tot} = total radius of fin ray specimen; and R_n and R_{n-1} = the distance from ray focus to the n th and $(n-1)$ th annuli, respectively.

The focus was identified at the proximal confluence of growth striations (Ehrhardt et al., 1996). Because only one image analyzer was available and multiple readers had to work concurrently, several methods were used to examine specimens: 1) slide-mounted ray cross sections were viewed with a dissecting microscope (10–60×) by reflected light against a black background; 2) grey-scale TIFF file images of slide-mounted cross sections were prepared by using a digital camera system (Sony DKC-5000 and VCL-713BXS macro-zoom lens; Sony USA, New York, NY), processed to enhance contrast and sharpness using Adobe PhotoShop vers. 3, and viewed by means of two shareware available in the public domain (NIH Image vers. 1.58; National Institutes of Health, Bethesda, MD; and Scion Image vers. Beta 4.0.2; Scion Corporation, Frederick, MD), for MAC and PC, respectively. Annuli were counted independently by two primary readers (1 and 2) without reference to length, sex, or month of capture. Each reader made two or more readings, spaced by at least several months to cloak the identity of individual specimens. Presumed daily growth increments (DGIs) were enumerated by using digitized composite images (scanning electron micrographs of sagittae) (Humphreys, 2000).

If known-age specimens are unavailable for use in calibrating age assignments, a reference collection should be evaluated and a consensus or majority agreement used to provide a reference standard (Campana, 2001). We therefore enlisted the services of four other North and South Pacific laboratories that either recently had or were presently conducting aging studies of swordfish (Institute of Oceanography, National Taiwan University [NTU]; the National Research Institute of Far Seas

Fisheries [NRIFSF], Japan; the Centro de Investigacion Cientifica y de Educacion Superior de Ensenada [CICESE], Mexico; and the Instituto de Fomento Pesquero [IFOP], Chile). They provided 20 representative and usable fin ray specimens for swordfish caught by their respective regional fisheries. Specimens spanned all available months of capture and body sizes of both sexes.

Specimens were processed in identical fashion within each laboratory (e.g., the $d/2$ cut was used by the Honolulu Laboratory for select Hawaii-based fishery specimens). Digitized images of all 100 specimens were prepared at the Honolulu Laboratory and file images were distributed among laboratories. Most laboratories conducted multiple readings by two or more readers, thus enabling evaluation of precision and bias within and among laboratories.

Statistical analyses

Conventional descriptive statistics (Zar, 1984) were used to evaluate several interrelated data necessary for verification or corroboration of annular periodicity and size-at-age. We evaluated interrelations among fin ray radius (in mm) and estimated age (in days) based on enumeration of DGIs and EFL (in cm). Regression models were fitted by using nonlinear least squares (Marquardt algorithm) and the best model was chosen on the basis of relative r^2 values (proc nlin, SAS, vers. 8, SAS Inst., Inc., Cary, NC). Likely sexual dimorphisms in relationships (Sun et al., 2002) were evaluated with ANCOVA (proc glm; SAS, vers. 8, SAS Inst., Inc., Cary, NC).

Standard graphical methods and statistics (Campana, 2001) were used to evaluate between- and within-reader bias (age-bias plots) and precision gauged by the coefficient of variation (CV: deviation [=SD] (100/mean) (Campana et al., 1995; Campana, 2001). Observer bias (accuracy) also was evaluated partly in terms of the majority agreement standard generated by the aforementioned inter-laboratory calibration exercise. Precision was evaluated by comparing the repeatability of estimates made by readers 1 and 2 for both the specimen series provided by the inter-laboratory exercise and the much larger group of specimens that were used for the main study described in this article. CVs were compared both within- and between-readers.

Growth was described by fitting fin ray-based age estimates to back-calculated body length-at-age by using von Bertalanffy growth formulas (VBGFs). Both standard and generalized VBGFs (Richards, 1959) were evaluated:

$$\begin{aligned} \text{Standard VBGF: } L_t &= L_\infty (1 - e^{-k(t-t_0)}); \\ \text{Generalized VBGF: } L_t &= L_\infty (1 - e^{-K(1-m)(t-t_0)^{1/(1-m)}}); \end{aligned}$$

where L_t = mean eye-to-fork length (EFL, in cm) at age t ;

L_∞ = asymptotic length;

t = a specific age;

t_0 = hypothetical age at length zero;

k and K = growth coefficients; and
 m = fitted fourth parameter.

Individual length-at-age was back-calculated by using method II of Sun et al. (2002) which is based on the formula of Ehrhardt et al. (1996):

$$EFL_t = (R_n/R_{tot})^b EFL,$$

where EFL_t = back-calculated eye-to-fork length at age t ;

R_n and R_{tot} are as previously defined; and
 b = parameter derived from the relation of EFL to R_{tot} .

EFL was related to R_{tot} using the power equation,

$$EFL = a R_{tot}^b,$$

where a , b = fitted parameters.

This model was chosen because of the obvious curvilinearity of the relationship. Sex effects were evaluated by using ANCOVA.

Likelihood ratio (LR) tests (Cerrato, 1990; Quinn and Deriso, 1999) were used to evaluate the effects of sex and type of VBGF model for describing the length-at-age relationship. For LR test statistics, the additivity of untransformed data was assumed and the statistics were calculated as two times the log-likelihood:

$$LR = [-n/2] [\ln(2\pi[SSE/n]) + 1],$$

where SSE = error sum of squares; and
 n = number of age classes.

In both cases, LR test statistics were compared against χ^2 with $df = 1$ by using the Akaike information criterion.

Results

Accuracy and precision

A pilot evaluation of the two methods used for viewing fin ray preparations (microscope, digital image analyzer) indicated nearly congruent results (mean difference only 0.12 ± 0.087 yr or 3% of a mean age of 3.8 years; matched-pairs t -test; $t=1.38$; $P=0.17$). Directly viewed and image analyzed preparations were therefore considered equivalent (no bias from methods) and were pooled in all subsequent analyses.

Age-bias plots for readers 1 and 2 indicated variable deviations, small in relation to the age estimates, which lacked major pattern over the range of all putative ages. Reader 1's mean age estimates regressed on reader 2's age estimates deviated insignificantly from a slope of 1 and an intercept of 0, even if additional positive deviations for ages > 8 were included (Table 1A). Readers

Table 1

Summary statistics from a comparison of the (A) bias (accuracy), and (B) precision (repeatability) of swordfish (*Xiphias gladius*) ages estimated by readers 1 and 2; precision was evaluated both between- and within-readers. Bias and precision were evaluated by age-bias plots and coefficient of variation (CV), respectively (Campana et al., 1995; Campana, 2001). Sexes were pooled in (A) because the effect of sex insignificantly influenced aging differences between readers, both for ages <8 and for all ages (ANCOVA: $P=0.21$ and 0.06 , respectively). H_0 = null hypothesis. SE = standard error.

A Hypothesis	Main study data subset	Parameter estimate \pm SE (test statistic)	df	Prob > F
Bias				
H_0 : slope = 1	ages < 8	0.985 ± 0.034	1,6	0.67
H_0 : intercept = 0		($F=0.20$)	1,6	0.85
		0.015 ± 0.078		
		($F=0.04$)		
H_0 : slope = 1	all ages	1.010 ± 0.019	1,10	0.93
H_0 : intercept = 0		($F=0.01$)	1,10	0.62
		-0.006 ± 0.070		
		($F=0.27$)		
B				
Type	Specimen series	Median CV ¹	Number of fish	
Precision				
Within-reader, reader 2	inter-laboratory ²	9.7	100	
Within-reader, reader 1	main study	13.3	377	
Within-reader, reader 2	main study	12.9	790	
Between-reader	inter-laboratory	15.7	100	
Between-reader	main study	10.8	1055	

¹ Weighted equally over all age groups.

² Unavailable for reader 1, who made only one set of readings.

1 and 2 aged specimens used in the inter-laboratory calibration exercise with negligible (<2%) deviation from the majority agreement standard. The age assignments of both readers 1 and 2 were henceforth used for growth analyses. If the readers did not agree, reader 2 re-examined the specimen to resolve the discrepancy. Specimens with unresolvable ages were omitted from subsequent analysis.

Age estimates were adequately precise, as well as accurate. CVs of within- and between-reader age estimates were generally 10–15 % (Table 1B). CVs of the inter-laboratory and main study readings were similar, as were the within- and between-reader CVs within each series (Kruskal-Wallis 1-way ANOVAs; all $P>0.3$).

Verification and validation of annuli

The results of marginal increment analysis (Fig. 1) provided consistent quantitative support for the contention that fin rays form a single pair of opaque and translucent bands per year (Campana, 2001). Formation of the annulus is complete by September in central North Pacific swordfish; MIRs were wider in June and narrower in September (for fish of both sexes) than during the rest of the year (2-way ANOVA on

sex and month; interaction effect: $F=0.80$, $df=11,732$, $P=0.64$; month effect: $F=2.05$, $df=11,743$, $P=0.02$). The pattern generally applied to fish of all ages through at least age-group 7 of adequate sample sizes (Fig. 1), although considerable variability existed throughout the year.

Verification and corroboration of annuli (Kalish et al., 1995; Campana, 2001) were further explored using several complementary methods. These consisted of comparisons of ages that were based on otolith sagittae and fin rays from matched (same) fish and on quantitative relations among fin ray cross-section dimensions, fish body length, and ages based on sagittal DGIs and fin ray annuli. Measurements of total and incremental radii in fin ray cross-sections were obtained for a total 1336 swordfish (733 females, range 46–260 cm EFL; 603 males, range 36–229 cm EFL). Numbers of DGIs on sagittae were enumerated for a total 63 larval, older juvenile, and small adult swordfish of the two sexes (range 4–135 cm EFL). The EFL-at-age relation was described for 49 fish (range 4–133 cm EFL) for which there were adequately precise DGI counts. Fin ray preparations were available for 50 specimens with matched DGI counts.

Total cross-section radius of the second ray of the first anal fin was significantly related to fish age in days for

older juveniles and small adults (Fig. 2). The best fitted power equation relationship:

$$R_{\text{tot}} = 0.0197 \text{ DGI}^{0.7877}, r^2 = 0.877,$$

predicted an R_{tot} of 2.055 ± 0.069 (mean \pm SE) mm at an age of 365 days. For a larger sample of fish aged to be 1 yr old by using fin rays, the radius R_1 (the just-completed first annulus) was 2.23 ± 0.091 mm from the focus on cross sections cut as described and was unrelated to sex of fish (Student's $t=0.88$; $n=71$ fish; $P=0.38$).

Cross sections taken at the suture terminus were located about 14% of the conforming total length (distal surface) of the ray above the condyle. In a comparison between cross sections from matched (same) fish, where the cross sections were taken at our suture terminus and the $d/2$ position for 115 specimens (sexes pooled) ranging from 82–241 cm EFL, the conventional cross-section radius was located at a shorter average distance (about 10%) above the condyle. Total radii of cross sections produced by the two different types of cuts nec-

essarily differed slightly (by 3%; ANCOVA; $P<0.001$) but were independent of fish size and sex (ANCOVA; $P=0.6$ and 0.3 , respectively). Despite these numeric differences, there was no discernible average difference in annuli counts with sections cut at the suture terminus and $d/2$ positions. Core regions of basal cut sections were obscure in 77% of the specimens whose ages ranged from 1 to 11 years (ages estimated by using suture terminus sections). Either the first annulus was missing or the section could not be aged for 21% of the basal cut specimens. Ages averaged 0.8 yr younger with basal sections (matched-pairs signed-ranks test; $P<0.01$) for 25 of the specimens whose age estimates differed between basal and distal sections, and averaged 0.2 yr younger overall. For basal cuts only, mean back-calculated body lengths at age 1 yr, based on the presumed "first annulus," differed in predicted fashion among age groups (i.e., they were greater for older fish in which the real first annulus was more apt to be missing with age (2-way ANOVA on age-group and type of section; age-group effect: $P<0.0001$; Penha et al., 2004).

Daily growth of young swordfish based on counts of DGIs on otoliths strongly corroborated our estimates of size-at-age for age-group 0 (age 0+) and yearling fish based on fin ray cross sections (Fig. 3). Body length was nonlinearly related to presumed age in days and the most parsimonious, best fit was the hyperbolic, two-parameter relation:

$$EFL = (136.6 \text{ DGI}) / (140.8 + \text{DGI}), r^2=0.937, n=49.$$

This best fit relation indicated a body length of 98.6 ± 3.0 (95 % CI) cm EFL at an age of 365 days (Fig. 3).

Development of growth model

The relations between EFL and cross-section fin ray radius were strongly curvilinear, and doubly log-transformed data differed in elevation for females and males (ANCOVA; $F_{1,1333}=6.41$; $P=0.01$) but shared a common slope (ANCOVA; $F_{1,1332}=0.84$; $P=0.36$). For R_{tot} measured in mm and EFL (in cm), the best fit relations were

$$\begin{aligned} \text{Females } EFL &= 64.3725 R_{\text{tot}}^{0.5539}, r^2=0.939; \\ \text{Males } EFL &= 66.3090 R_{\text{tot}}^{0.5175}, r^2=0.936. \end{aligned}$$

R_{tot} regressed on EFL indicated that R_1 should be about 2.16 mm, using the independent length-at-age 1-yr estimate of 98.6 cm EFL. An R_1 of 2.055 mm would be equivalent to a length of about 96 cm EFL (Figs. 2 and 3).

Table 2 lists our sex-specific, back-calculated EFL-at-age estimates. Summary statistics for the corresponding estimates of ray radii are provided in Table 3 for males and females, respectively, by age group and averaged over all age groups. We estimated an age of 0.58 yr (213 days) at an observed mean EFL of 82.2 cm from the otolith-based length-at-age relation (Fig. 3) and used this estimate to represent the mean length of age-group-0 fish ≥ 60 cm EFL in the aged population.

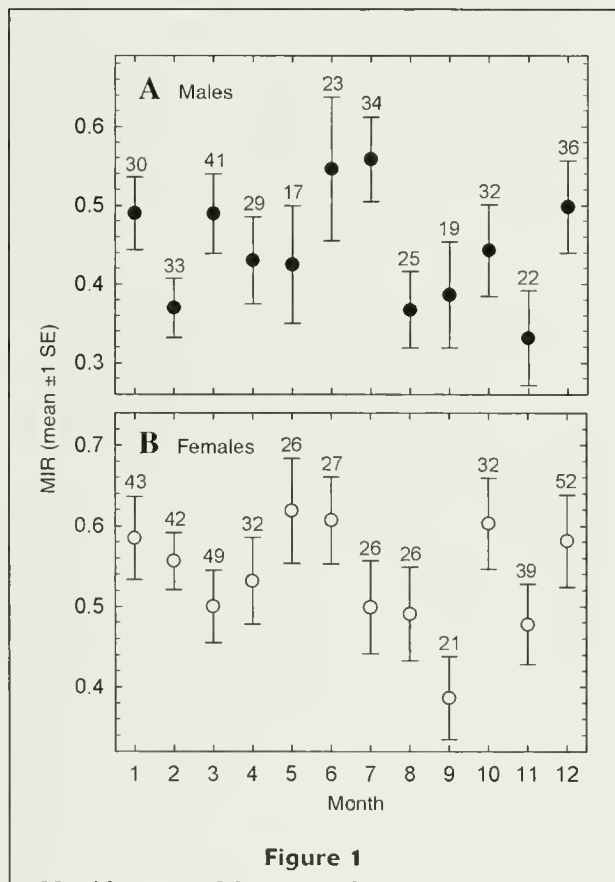


Figure 1

Monthly means of the marginal increment ratio (MIR) for (A) male and (B) female swordfish (*Xiphias gladius*) caught in the region of the Hawaii-based pelagic longline fishery during 1993–97. Vertical lines indicate ± 1 standard error (SE). Number of fish specimens is noted above each monthly estimate. Code to months: 1 = January, 2 = February, ... 12 = December.

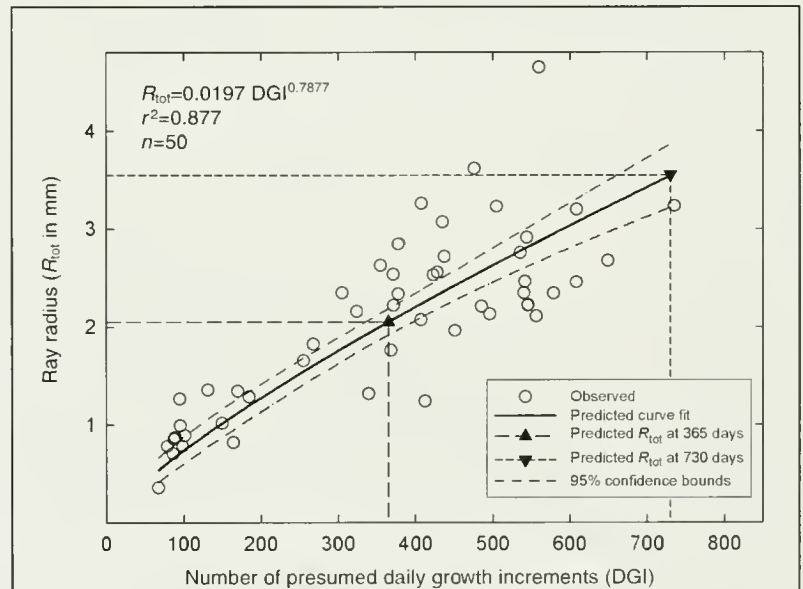
Table 2

Summary of eye-to-fork length (EFL, cm) statistics and estimated mean back-calculated lengths-at-age for swordfish (*Xiphias gladius*) of each sex and age-group, caught in the region of the Hawaii-based pelagic longline fishery during 1993–97. SD=standard deviation.

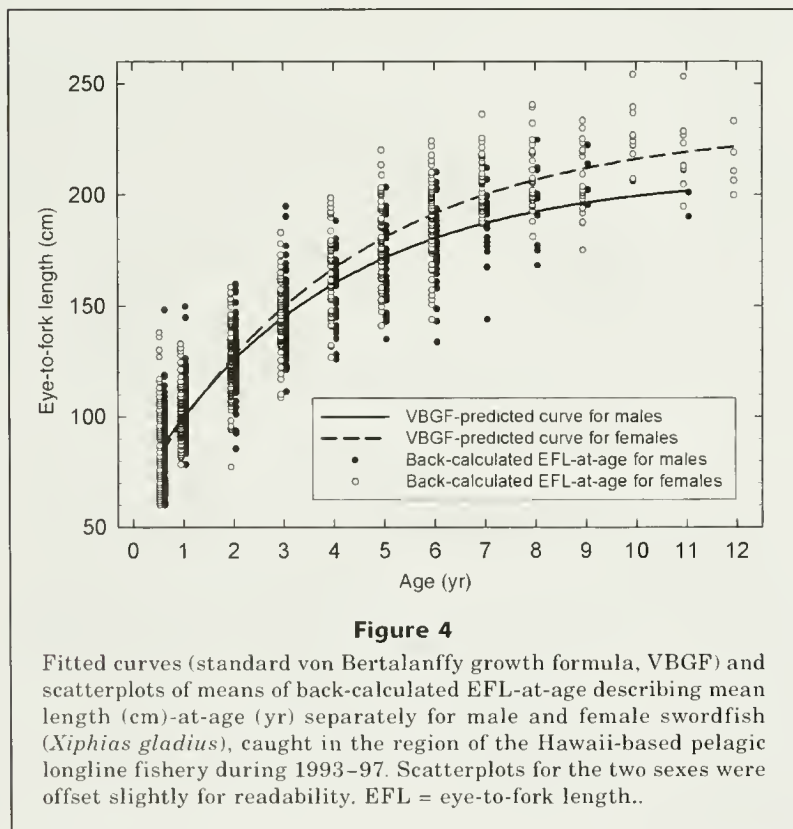
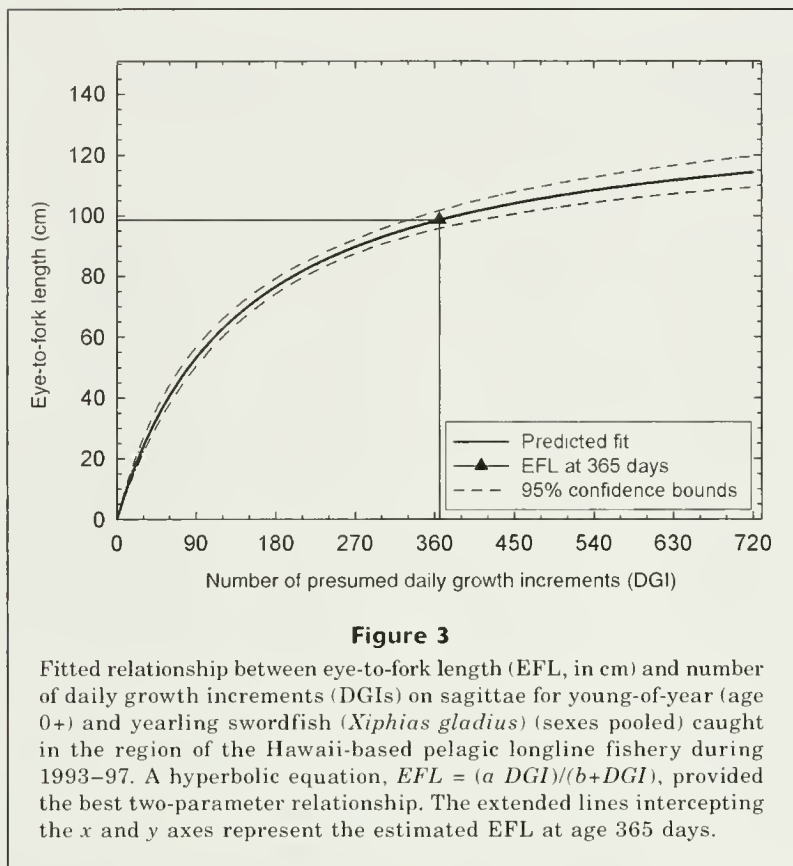
Age group	Males			Females		
	Sample size	Back-calculated EFL	Mean \pm SD EFL	Sample size	Back-calculated EFL	Mean \pm SD EFL
0	136		82.1 \pm 18.4	137		82.3 \pm 18.8
1	145	102.0	114.3 \pm 13.2	114	100.5	115.1 \pm 14.2
2	97	127.4	137.0 \pm 13.5	109	126.3	138.3 \pm 15.1
3	69	147.9	155.3 \pm 16.0	64	147.7	155.4 \pm 15.5
4	41	159.9	164.1 \pm 14.2	58	167.1	171.4 \pm 18.2
5	29	166.3	172.8 \pm 18.0	59	179.6	185.3 \pm 18.0
6	34	174.7	181.0 \pm 17.6	63	189.7	195.0 \pm 17.8
7	15	188.4	189.7 \pm 17.2	36	204.7	209.9 \pm 12.4
8	10	196.7	197.3 \pm 19.7	29	208.5	212.3 \pm 15.4
9	4	202.2	212.5 \pm 12.9	20	208.0	210.3 \pm 16.6
10				12	223.4	228.0 \pm 15.6
11	2	197.5	198.5 \pm 6.4	9	219.6	222.8 \pm 17.6
12				5	216.0	218.2 \pm 14.5

Back-calculated lengths-at-age were used to evaluate length versus age by using several versions of the von Bertalanffy growth model, for a total 1292 fish (712 females, 580 males) ≥ 60 cm EFL. Less than 4% of all fin ray preparations were deemed unreadable and not used. Age-group-0 fish (0.58 yr; 82.3 cm [females], 82.1 cm [males]) were included in the model fits. Male and female swordfish clearly grow in length at different rates after age 1 (Table 4; likelihood-ratio test; $P < 0.001$; Table 5A). Furthermore, for central North Pacific swordfish spanning the length range of most fish in the commercial catch (60-cm EFL as an average minimum), the standard three-parameter VBGF fit the length-at-age data more efficiently than Richards' generalized VBGF (likelihood-ratio test; males: $P > 0.2$, females: $P = 0.5$; Table 5B). Hence, the standard VBGF is the more parsimonious growth model and should be applied to the sexes separately for central North Pacific swordfish of exploitable sizes (Table 4; Fig 4).

Three fish, whose ship-side, visually estimated weights were equivalent to lengths of 88, 98, and 93 cm EFL when initially tagged and released, were recaptured after 364, 610, and 1490 days at liberty and had grown 38, 58, and 90 cm, respectively, based on round weights at market (Uchiyama et al., 1998). The sex of none of these fish was determined when they were tagged

**Figure 2**

Scatterplot and fitted relationship between the total cross-section radius (R_{tot} , in mm) of the second ray of the first anal fin and the number of daily growth increments (DGI; estimated age in presumed days based on microincrement counts) on sagittae for the same young-of-year and yearling swordfish (*Xiphias gladius*) (sexes pooled) caught in the region of the Hawaii-based pelagic longline fishery during 1993–97. The power equation, $R_{tot} = a DGI^b$, was used to model the fitted relationship. The extended lines intercepting the x and y axes represent the estimated radii at ages 365 and 730 days. Confidence in the R_{tot} at age 730 days (3.5–3.6 mm) is low because of the poor readability of DGIs at and beyond this age, for fish of either or both sexes.



or recaptured. If estimated length increments are related to a fit of the standard VBGF (sexes pooled) for central North Pacific swordfish, the growth trajectories of these fish agreed reasonably well with those expected for fish of their sizes at liberty for the observed durations (Fig. 5).

Discussion

Verification and validation of age

Our comparisons of ages based on annuli in fin ray sections and DGIs in otoliths, coupled with those of ray radii and otolith ages, represent a novel approach to verifying the age and growth of swordfish and other species for which validation is difficult. The good agreement we observed between our estimates of size at age 365 days based on otoliths and of size at age 1 yr based on fin rays provides a strong partial verification of our aging protocols for young swordfish. Our detailed cross-validation of fin ray annuli against otolith DGIs has conclusively identified the location of the first annulus on swordfish fin rays for the first time. Marginal increment analysis further corroborates that a single annulus forms once each year in anal-fin rays and is complete for swordfish through age 7 caught in the central North Pacific by the end of the spawning period in late summer (DeMartini et al., 2000), when somatic condition is lowest (Uchiyama et al., 1999). Others have similarly observed that the time of annulus formation occurs at the end of the growing season for swordfish in the western North Pacific (Sun et al., 2002) and eastern South Pacific (Cerna¹), although other drains on physiological condition, such as migration, may be involved (Sun et al., 2002). We also present final proof that basal cross sections of fin rays underestimate ages as a result of partial or complete resorption of the first annulus, as first proposed by Berkeley and Houde (1983) and subsequently observed by Tserpes and Tsimenides (1995) and others. Our comparison of age readings derived from basal, $d/2$, and suture terminus cuts of anal-fin rays demonstrates the equivalence of the latter two types of ray cross sections.

¹ Cerna, F. J. 2006. Unpubl. data. Sección Edad y Crecimiento, División de Investigación Pesquera, Instituto de Fomento Pesquero, Blanco 839, Valparaiso 5a Region, Chile.

Table 3

Mean R_n (radius from focus to distal edge of each annulus) for each age-group of male and female swordfish (*Xiphias gladius*) caught in the region of the Hawaii-based pelagic longline fishery during 1993–97. Roman numerals indicate the number of presumed annuli. SD = standard deviation. "Increment" refers to the increase in mean R_n from the preceding annulus.

Males Age-group (yr)	Sample size	Mean R_n (mm) from focus to distal edge of each annulus											
		I	II	III	IV	V	VI	VII	VIII	IX	X	XI	
0	136												
1	145	2.22											
2	97	2.23	3.34										
3	68	2.20	3.38	4.30									
4	41	2.17	3.36	4.32	5.04								
5	29	2.19	3.33	4.35	5.11	5.76							
6	33	2.09	3.27	4.25	5.09	5.87	6.43						
7	15	2.39	3.41	4.27	4.98	5.62	6.15	6.61					
8	10	2.08	3.23	4.19	4.87	5.53	6.09	6.57	6.96				
9	4	2.28	3.24	4.23	5.24	5.85	6.50	7.15	7.76	8.22			
10	—												
11	2	2.02	3.15	3.86	4.96	5.54	6.17	6.59	6.91	7.28			8.03
Mean		2.19	3.30	4.22	5.04	5.69	6.26	6.73	7.21	7.75			8.03
SD		0.11	0.09	0.15	0.12	0.15	0.18	0.28	0.48	0.66			—
Increment			1.11	0.92	0.82	0.65	0.57	0.47	0.48	0.54			0.28

Females Age-group (yr)	Sample size	Mean R_n (mm) from focus to distal edge of each annulus											
		I	II	III	IV	V	VI	VII	VIII	IX	X	XI	XII
0	137												
1	114	2.22											
2	108	2.26	3.37										
3	63	2.15	3.36	4.28									
4	58	2.15	3.25	4.22	4.99								
5	58	2.27	3.42	4.40	5.28	5.95							
6	63	2.17	3.28	4.29	5.25	6.04	6.65						
7	36	2.24	3.42	4.47	5.42	6.16	6.79	7.25					
8	29	2.23	3.31	4.24	5.14	5.88	6.56	7.19	7.62				
9	20	2.15	3.27	4.20	5.06	5.75	6.39	6.98	7.48	7.89			
10	12	2.13	3.23	4.19	5.08	5.94	6.60	7.21	7.75	8.24	8.67		
11	9	2.18	3.11	4.02	4.99	5.77	6.52	7.19	7.71	8.14	8.56	8.90	
12	5	2.28	3.31	4.33	5.14	5.71	6.40	6.97	7.45	7.90	8.34	8.70	9.08
Mean		2.20	3.30	4.27	5.15	5.90	6.56	7.13	7.60	8.04	8.52	8.80	9.08
SD		0.05	0.09	0.12	0.14	0.16	0.14	0.12	0.13	0.17	0.17	0.14	
Increment			1.10	0.97	0.88	0.75	0.66	0.57	0.47	0.44	0.48	0.28	0.28

Selection of growth model

Unlike swordfish caught in waters near Taiwan (Sun et al., 2002), swordfish of exploitable size in the central North Pacific near Hawaii grow in length at rates described by the standard, rather than generalized, VBGF. We suggest that this model primarily reflects the different size structure of catches from the two regions. By truncating the application of our growth model at the approximate minimum size of fish caught by the Hawaii-based longline fishery (60-cm EFL), we eliminate the markedly allometric growth effects that half-year-old and younger fish have on the ascending limb of the VBGF curve. The disproportionately low body mass of

young juveniles reflects the fact that swordfish, perhaps like most pelagic fishes that are reliant on swimming speed as their primary antipredator adaptation (and unlike typical nonpelagic fish with less pronounced allometric growth), must experience intense selection for growth in length (swimming speed) at the expense of growth in mass during the juvenile stage. A related issue is the fact that swordfish >180–200 cm EFL are more abundant in the Hawaiian than in Taiwanese fisheries, and these larger fish provide an extended scope for resolving the asymptote of VBGF models, especially the standard VBGF which lacks a fourth parameter (shape function) to help resolve curvature of the ascending limb. Not surprisingly, growth of swordfish caught

Table 4

Parameter estimates (\pm standard error, SE) for the standard von Bertalanffy and the generalized von Bertalanffy growth formulas (VBGFs) fitting mean back-calculated eye-to-fork length (EFL)-at-age against age for male and female swordfish (*Xiphias gladius*) ≥ 60 cm EFL caught in the region of the Hawaii-based longline fishery during 1993–97. L_{∞} = asymptotic length; k and K = growth coefficients; t_0 = hypothetical age at length zero; m = fitted fourth parameter; n = number of age-classes. r^2 = coefficient of determination; n = sample size.

Parameter	Standard VBGF		Generalized VBGF	
	Male	Female	Male	Female
L_{∞}	208.9 \pm 5.60	230.5 \pm 3.94	221.0 \pm 20.1	227.2 \pm 6.18
k	0.271 \pm 0.034	0.246 \pm 0.019		
K			0.070 \pm 0.080	0.524 \pm 0.871
t_0	-1.37 \pm 0.259	-1.24 \pm 0.167	-0.15 \pm 0.576	-2.41 \pm 2.968
m			-1.27 \pm 1.122	0.448 \pm 0.771
r^2	0.989	0.995	0.991	0.995
n	11	12	11	12
P	<0.001	<0.001	<0.001	<0.001

Table 5

Summary statistics for likelihood ratio (LR) tests evaluating (A) potential differences between the estimated von Bertalanffy growth (VBGF) parameters for male and female swordfish (*Xiphias gladius*), and (B) the standard versus generalized VBGF models of length-on-age for males and females caught in the region of the Hawaii-based pelagic longline fishery during 1993–97. H_0 = null hypothesis.

	Sexes pooled		By sex (male+female)	
	Standard	Generalized	Standard	Generalized
A Male versus female				
Log-likelihood	-64.7		-79.1	
χ^2 (prob $> \chi^2$)	28.8 (<0.001)			
Conclusion	Reject H_0 male = female			
	Male		Female	
	Standard	Generalized	Standard	Generalized
B Standard versus generalized VBGF				
Log-likelihood	-30.7	-29.9	-34.0	-33.8
χ^2 (prob $> \chi^2$)	1.62 ($P > 0.2$)	0.46 ($P = 0.5$)		
Conclusion	Accept H_0 standard = generalized		Accept H_0 standard = generalized	

by the Chilean longline fishery (Cerna¹), like those caught near Hawaii, is better described by the standard VBGF, and large swordfish are also abundant in the relatively undeveloped Chilean fishery. Chapman's five-parameter version of the generalized VBGF would be the most appropriate for describing size-at-age of swordfish only if there was a compelling reason to fit the growth curve through zero length at zero age (see Arocha et al., 2003).

Our growth-at-liberty data for tagged-recaptured swordfish in the central North Pacific, albeit limited to only three fish, are consistent with modeled growth of small- to medium-size adult fish. Restrepo (1990) and Brown (1995) provide the only other data of this type for swordfish, limited to fish caught in the Atlantic

Ocean and Gulf of Mexico. The usefulness of such data is limited because of inaccuracies in estimates of body size at time of first capture (Restrepo, 1990)—as it was for our tagged swordfish—and uncertain units of size measurement (Brown, 1995), but some general growth patterns are nonetheless evident. For nearly 100 swordfish with a median length of about 100 cm at initial capture and of 135 cm when recaptured after a median period at liberty of 1.5 years, the growth rate was about 24 cm per yr (Brown, 1995). Given that body size when a fish is tagged is usually overestimated (Restrepo, 1990), and this body size yields an underestimate of incremental growth at liberty and given also the likely faster growth of swordfish in the Pacific—especially the central North Pacific—see below, the average growth in-

crement (35 cm per yr) that we observed for the three tagged-recaptured fish, yearlings in size when first caught and at liberty for 1, 2, and 4 years, is reasonable, as well as consistent, with our modeled growth trajectories for fish of this size range. We nonetheless caution, however, that these few consistencies by themselves do not verify our growth curves.

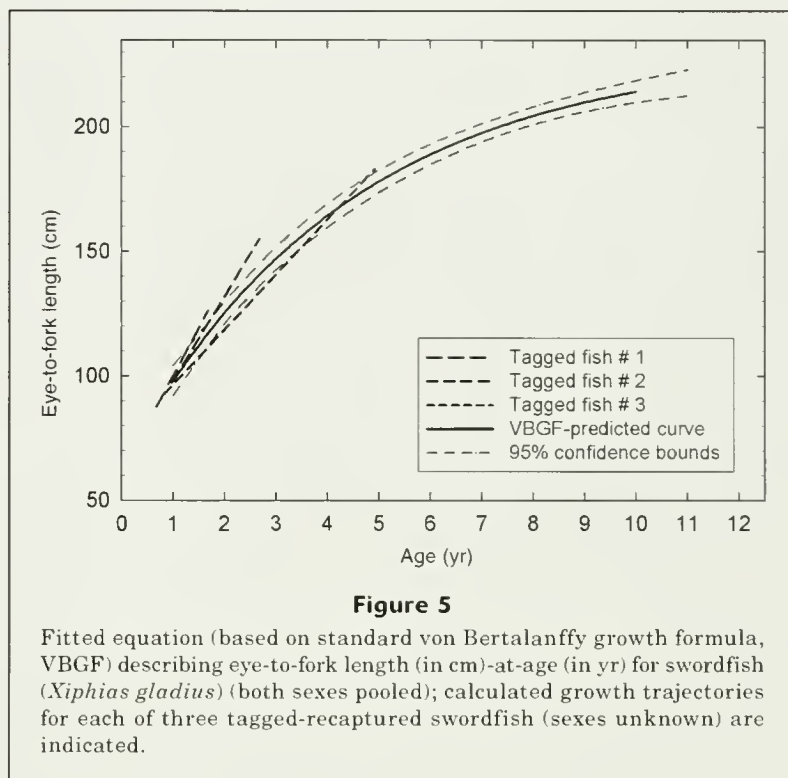
Sexually dimorphic growth

By now there can be no doubt that female swordfish grow faster and attain larger maximum body sizes than do males in the Pacific (Castro-Longoria, 1995; Sun et al., 2002; Cerna¹; this study), as many others (e.g., Berkeley and Houde, 1983) have observed for swordfish in the Atlantic. That females on average live longer than males is less certain, and this uncertainty will likely persist because of the rarity of the largest, oldest fish captured by fisheries—especially in developed fisheries—and associated difficulties in validating estimates of their ages. Even though sexually dimorphic growth does not become prominent in either body length or fin rays until after age 1, it is obvious that the sexes should be evaluated separately in stock assessments (Wang et al., 2005) for retained swordfish (generally greater than 1 yr old in most fisheries) whenever landings data allow. The sexual differences in body size and growth that we observed reinforce the argument that sex-specific, age-based stock assessments are needed for swordfish.

The greater probability of error in estimating the ages of larger swordfish affects females disproportionately as the larger-bodied fish. Sex-specific stock assessments need to explicitly evaluate the greater uncertainty of age estimates for the largest, mostly female, fish as well as the more generally recognized influences of gear bias on the capture efficiency (hence sex ratio) for male and female swordfish of different sizes.

Unresolved issues and future research needs

In prior studies of swordfish age and growth there has been the conspicuous need to validate the periodicity of annulus formation for all age groups present in a fishery, including the oldest age groups, which are typically relegated to a catch-all plus group that complicates stock assessment computations (Restrepo and Powers, 1991). Validation of the age and growth of these largest, oldest fish likewise has been a problem in our study, and our estimates of growth-at-liberty for tag-recaptured fish only provide insights into growth (not absolute age) of juveniles and young adults. There is still great need to verify the accuracy of age estimates for swordfish in older age-groups. Radiometric aging (Watters et al.,



2006), one alternative method for aging the hard parts of large, old fish, is inappropriate for swordfish because the oldest living tissue is reabsorbed within fin rays and because their tiny otoliths provide insufficient material for analysis of individual fish. Resolution of the problem would almost certainly require a dedicated, large-scale, and expensive conventional tagging effort targeting large and old fish, preferably one in which a rigorous protocol is implemented for accurately estimating size at initial capture and labeling body size at time of release with a fluorescent biomarker. Such a study is unlikely to be implemented unless greater reductions in stock sizes, increases in value, or (more likely) both in concert, justify the great cost of such an enterprise. Of course, such a study could provide data on fish movements whose importance might dwarf that of age and growth validation.

Geographic variation in growth rates is evident for swordfish in regional Pacific fisheries. Size-at-age is appreciably greater for swordfish caught in the region of the Hawaii-based fishery (versus the Taiwanese fishery) and the regional difference includes juvenile and small adult, as well as larger adult fish. For example, the mean length at age 1 of swordfish in the Taiwanese fishery is about 96 cm lower-jaw-to-fork length, which is equivalent to only 83 cm EFL (Sun et al., 2002), whereas the mean length at age 1 in the Hawaii-based fishery is 99 cm EFL. The results of our study indicate that swordfish caught in the central North Pacific grow in length at a rate faster than swordfish caught by several other Pacific regional fisheries (Fig. 6), and this

finding was confirmed by readers from other laboratories during the inter-laboratory exercise. Faster growth in the central North Pacific (versus the western North Pacific) may reflect the high planktonic productivity of swordfish feeding grounds in the Subtropical Convergence Zone (Seki et al., 2002), perhaps similar to that in the productive upwelling region off Chile in the eastern South Pacific. Consistent with this observation, data on body condition (weight-at-length) indicate that central North Pacific swordfish are heavier at a given length than swordfish from the western North Pacific (Uchiyama et al., 1999; Sun et al., 2002). Regional differences in growth rates are also apparent for swordfish

throughout the Atlantic and Mediterranean (Tserpes and Tsimenides, 1995; Ehrhardt et al., 1996; Alici and Oray, 2001).

Stock structure is still incompletely understood for Pacific swordfish and regional variations in growth rates complicate rather than resolve the issue. Present understanding of the population genetics of swordfish indicates that separate stocks exist in the North and South Pacific and that there likely is some stock structuring between east and west in the North Pacific (Reeb et al., 2000). Detailed comparisons among the nuclear (microsatellite) DNAs and mtDNAs of planktonic spawning products (eggs and larvae) and fish of exploitable sizes, coupled with analyses of phenotypic traits like growth and environmental markers, such as trace element signatures in otoliths (Humphreys et al., 2005), are needed for swordfish collected from all regional fisheries in order to fully resolve the stock issue for swordfish in the Pacific.

Acknowledgments

We gratefully acknowledge C.-L. Sun (National Taiwan University), K. Yokawa (National Research Institute of Far Seas Fisheries), O. Sosa-Nishizaki (Centro de Investigacion Cientifica y de Educacion Superior de Ensenada), and F. Cerna (Instituto de Fomento Pesquero) for their cooperation in implementing the inter-laboratory calibration exercise mandated at the Second Meeting of the Interim Scientific Committee for Tuna and Tuna-like Fishes in the North Pacific (ISC2) held January 15–23, 1999, in Honolulu, Hawaii. We also thank M. McCracken for statistical advice, D. Yamaguchi for assistance with preparing all of the final figures, and P. Kleiber, D. Kobayashi, R. Nishimoto, C. Boggs, and three anonymous reviewers for constructive criticisms of a draft of the manuscript.

Literature cited

- Alici, T. Z., and I. K. Oray.
2001. Age and growth of swordfish (*Xiphias gladius* L., 1758) in the eastern Mediterranean Sea. *Int. Comm. Conserv. Atl. Tunas, Coll. Vol. Sci. Pap.* 52:698–707.
- Arocha, F., C. Moreno, L. Beerkircher, D. W. Lee, and L. Marciano.
2003. Update on growth estimates for swordfish, *Xiphias gladius*, in the northwestern Atlantic. *Int. Comm. Conserv. Atl. Tunas, Coll. Vol. Sci. Pap.* 55(4):1416–1429.
- Berkeley, S. A., and E. D. Houde.
1983. Age determination of broadbill swordfish, *Xiphias gladius*, from the Straits of Florida, using anal fin spine sections. *NOAA Tech. Rep. NMFS* 8:137–143, 211 p.

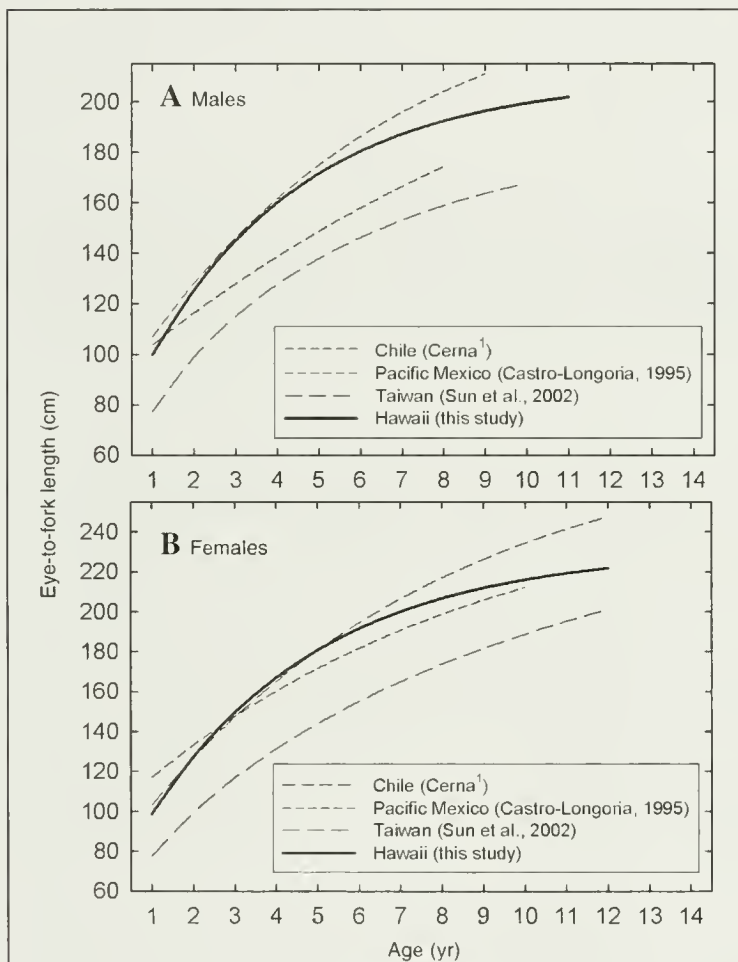


Figure 6

Fitted curves describing body length-at-age relationships for (A) male and (B) female swordfish (*Xiphias gladius*) captured by three other regional Pacific fisheries; length-at-age curves for swordfish caught in the region of the Hawaii-based fishery are provided for comparison. To facilitate the comparison, lower jaw-to-fork lengths were converted to eye-to-fork lengths (EFL). EFL-at-age relationships were fitted by using parameters of the standard von Bertalanffy growth formula (VBGF) in all cases except that of Taiwan, for which the generalized VBGF was used, as recommended by Sun et al. (2002).

- Bigelow, K. A., C. H. Boggs, and X. He.
1999. Environmental effects on swordfish and blue shark catch rates in the US North Pacific longline fishery. *Fish. Oceanogr.* 8:178–198.
- Brown, C. A.
1995. Preliminary examination of size and location data for U.S. tagged and recaptured swordfish. *Int. Comm. Conserv. Atl. Tunas, Coll. Vol. Sci. Pap.* 44(3): 217–224.
- Campana, S. E.
2001. Accuracy, precision and quality control in age determination, including a review of the use and abuse of age validation methods. *J. Fish Biol.* 59:197–242.
- Campana, S. E., M. C. Annand, and J. I. McMillan.
1995. Graphical and statistical methods for determining the consistency of age determinations. *Trans. Am. Fish. Soc.* 124:131–138.
- Castro-Longoria, R.
1995. Analysis of age, growth, and gonadal maturity of swordfish, *Xiphias gladius*, in the Mexican Pacific longline fishery. Ph. D. diss., 114 p. Departamento de Ecología, Division de Oceanología, Centro de Investigación Científica y de Educación Superior de Ensenada, Ensenada, Mexico [In Spanish].
- Cerrato, R. M.
1990. Interpretable statistical tests for growth comparisons using parameters in the von Bertalanffy equation. *Can. J. Fish. Aquat. Sci.* 47:1416–1426.
- DeMartini, E. E., J. H. Uchiyama, and H. A. Williams.
2000. Sexual maturity, sex ratio, and size composition of swordfish, *Xiphias gladius*, caught by the Hawaii-based pelagic longline fishery. *Fish. Bull.* 98:489–506.
- Ehrhardt, N. M., R. J. Robbins, and F. Arocha.
1996. Age validation and growth of swordfish, *Xiphias gladius*, in the northwest Atlantic. *Int. Comm. Conserv. Atl. Tunas, Coll. Vol. Sci. Pap.* 45(2):358–367.
- Humphreys, R. L., Jr.
2000. Otolith-based assessment of recruitment variation in a North Pacific seamount population of armorhead *Pseudopentaceros wheeleri*. *Mar. Ecol. Prog. Ser.* 204:213–223.
- Humphreys, R. L., Jr., S. E. Campana, and E. E. DeMartini.
2005. Otolith elemental fingerprints of juvenile Pacific swordfish (*Xiphias gladius* L.). *J. Fish Biol.* 66:1660–1670.
- Ito, R., R. A. Dollar, and K. E. Kawamoto.
1998. The Hawaii-based longline fishery for swordfish, *Xiphias gladius*. In *Biology and fisheries of swordfish, Xiphias gladius* (I. Barrett, O. Sosa-Nishizaki, and N. Bartoo, eds.), p. 77–88. NOAA Tech. Rep. NMFS 142, 276 p.
- Kalish, J. M., R. J. Beamish, E. B. Brothers, J. M. Casselman, R. I. C. C. Francis, H. Modgaard, J. Panfili, E. D. Prince, R. E. Thresher, C. A. Wilson, and P. J. Wright.
1995. Glossary for otolith studies. In *Recent developments in fish otolith research*. (D. H. Secor, J. M. Dean, and S. E. Campana, eds.), p. 723–729. Belle W. Baruch Library in Marine Science Number 19. Univ. So. Carolina Press, Columbia, SC.
- Penha, J. M. F., L. A. F. Mateus, and M. P. Petrere, Jr.
2004. A procedure to improve confidence in identification of the first annulus in fin-spines of fishes. *Fish. Manage. Ecol.* 11:135–137.
- Prince, E. D., D. W. Lee, and S. A. Berkeley.
1988. Use of marginal increment analysis to validate the anal spine method for ageing Atlantic swordfish and other alternatives for age determination. *Int. Comm. Conserv. Atl. Tunas, Coll. Vol. Sci. Pap.* 27:194–201.
- Quinn, T. J., II, and R. B. Deriso.
1999. *Quantitative fish dynamics*, 542 p. Oxford Univ. Press, New York, NY.
- Reeb, C. A., L. Arcangeli, and B. A. Block.
2000. Structure and migration corridors in Pacific populations of the swordfish *Xiphias gladius*, as inferred through analyses of mitochondrial DNA. *Mar. Biol.* 136:1123–1131.
- Restrepo, V.
1990. An update of swordfish tagging data for use in growth analyses. *Int. Comm. Conserv. Atl. Tunas, Coll. Vol. Sci. Pap.* 32:360–370.
- Restrepo, V. R., and J. E. Powers.
1991. A comparison of three methods for handling the “plus” group in Virtual Population Analysis in the presence of ageing errors. *Int. Comm. Conserv. Atl. Tunas, Coll. Vol. Sci. Pap.* 35(2):346–354.
- Richards, F. J.
1959. A flexible growth function for empirical use. *J. Exp. Bot.* 10:290–300.
- Seki, M. P., J. J. Polovina, D. R. Kobayashi, R. R. Bidigare, and G. T. Mitchum.
2002. An oceanographic characterization of swordfish (*Xiphias gladius*) longline fishing grounds in the springtime subtropical North Pacific. *Fish. Oceanogr.* 11:251–266.
- Sun, C.-L., S.-P. Wang, C. E. Poreh, and S.-Z. Yeh.
2005. Sex-specific yield per recruit and spawning stock biomass per recruit for the swordfish, *Xiphias gladius*, in the waters around Taiwan. *Fish. Res.* 71:61–69.
- Sun, C.-L., S.-P. Wang, and S.-Z. Yeh.
2002. Age and growth of the swordfish (*Xiphias gladius* L.), in the waters around Taiwan determined from anal-fin rays. *Fish. Bull.* 100:822–835.
- Tserpes, G., and N. Tsimenides.
1995. Determination of age and growth of swordfish, *Xiphias gladius* L., 1758, in the eastern Mediterranean using anal-fin spines. *Fish. Bull.* 93:594–602.
- Uchiyama, J. H., E. E. DeMartini, and H. A. Williams.
1999. Length-weight interrelationships for swordfish *Xiphias gladius* L. caught in the central North Pacific. NOAA Tech. Memo. NMFS-SWFSC-284, 82 p.
- Uchiyama, J. H., R. A. Skillman, J. D. Sampaga, and E. E. DeMartini.
1998. A preliminary assessment of the use of hard parts to age central Pacific swordfish, *Xiphias gladius*. In *Biology and fisheries of swordfish, Xiphias gladius* (I. Barrett, O. Sosa-Nishizaki, and N. Bartoo, eds.), p. 261–273. NOAA Tech. Rep. NMFS 142, 276 p.
- Wang, S.-P., C.-L. Sun, A. E. Punt, and S.-Z. Yeh.
2005. Evaluation of a sex-specific age-structured assessment method for the swordfish, *Xiphias gladius*, in the North Pacific Ocean. *Fish. Res.* 73:79–97.
- Watters, D. L., D. E. Kline, K. H. Coale, and G. M. Cailliet.
2006. Radiometric age confirmation and growth of a deep-water marine fish species: the bank rockfish, *Sebastes rufus*. *Fish. Res.* 81:251–257.
- Zar, J. H.
1984. *Biostatistical analysis*, 2nd ed., 718 p. Prentice-Hall, Englewood Cliffs, NJ.

Abstract—Evolutionary associations among the four North American species of menhadens (*Brevoortia* spp.) have not been thoroughly investigated. In the present study, classifications separating the four species into small-scaled and large-scaled groups were evaluated by using DNA data, and genetic associations within these groups were explored. Specifically, data from the nuclear genome (microsatellites) and the mitochondrial genome (mtDNA sequences) were used to elicit patterns of recent and historical evolutionary associations. Nuclear DNA data indicated limited contemporary gene flow among the species, and also indicated higher relatedness within the small-scaled and large-scaled menhadens than between these groups. Mitochondrial DNA sequences of the large-scaled menhadens indicated the presence of two ancestral lineages, one of which contained members of both species. This result may indicate genetic divergence (reproductive isolation) followed by secondary contact (hybridization) between these species. In contrast, a single ancestral lineage indicated incomplete genetic divergence between the small-scaled menhaden. These results are discussed in the context of the biology and demographics of each species.

Systematics of the North American menhadens: molecular evolutionary reconstructions in the genus *Brevoortia* (Clupeiformes: Clupeidae)

Joel D. Anderson

Email address: Joel.Anderson@tpwd.state.tx.us
Perry R. Bass Marine Fisheries Research Station
Texas Parks and Wildlife Department
HC02 Box 385
Palacios, Texas 77465.

The North American species of menhaden (*Brevoortia* spp. Gill, 1861) support large commercial fisheries on the eastern Atlantic and Gulf of Mexico (hereafter, Gulf) coasts. Historically, this industry represented as much as 40% of all commercial landings in the United States (Vaughan and Merriner, 1991), and the Gulf menhaden (*B. patronus* Goode, 1878) supported, by weight, one of the largest single fisheries in the United States. In addition, menhaden are one of the most important participants in estuarine and nearshore food webs along the Atlantic coast (Gottlieb, 1998) and support various recreational fisheries in the Gulf and Atlantic (Kroger and Guthrie, 1972; Scharf and Schlicht, 2000; Bethea et al., 2004).

There are four species of menhaden present in North American waters, three of which are found in the Gulf of Mexico (Fig. 1). These species are further classified into two general groups, the small-scaled and large-scaled menhadens. These groups are named according to the relative size of scales adjacent to the lateral line but also reflect contrasts in other morphological characteristics (Dahlberg, 1970), population demographics (Christmas and Gunter, 1960), and migratory behavior (Gunter, 1945; Simmons, 1957; Tolan and Newstead, 2004). The Gulf menhaden (*B. patronus*) and Atlantic menhaden (*B. tyrannus* Latrobe, 1802) are members of the large-scaled group. *Brevoortia patronus* occurs wholly in the Gulf of Mexico, and dominates the men-

haden fishery in the Gulf, with other menhaden species representing less than 1% of the annual catch (Ahrenholz, 1981). *Brevoortia tyrannus* is a semimigratory species found in large schooling populations and is targeted by a second reduction fishery. This species is found only on the Atlantic coast, and does not inhabit the Gulf (Ahrenholz, 1991). The small-scaled menhadens, yellowfin menhaden (*B. smithi* Hildebrand, 1941) and finescale menhaden, (*B. gunteri* Hildebrand, 1948), are present in smaller population sizes and have slightly overlapping distributions in the Gulf. *Brevoortia gunteri* has a distribution range restricted entirely to the northern and western Gulf coastal region. In contrast, *B. smithi* exists mainly in the eastern Gulf, although it ranges north on the Atlantic coast to Cape Lookout, North Carolina (Reintjes, 1959; Ahrenholz, 1991). *Brevoortia smithi* overlaps the eastern range of *B. patronus*, and also overlaps the southern range *B. tyrannus*. Considerable hybridization is thought to occur between *B. patronus* and *B. smithi* along the west coast of Florida, and between *B. tyrannus* and *B. smithi* along the east coast of Florida (Turner, 1969; Hettler, 1984).

Although the evolutionary relationships among the four North American menhaden species have not been explicitly examined, early investigations in species morphology indicated that *B. tyrannus* and *B. patronus* were Atlantic and Gulf complements of one another, and that *B. gunteri* and *B.*

smithi were western and eastern Gulf cognates (Christmas and Gunter, 1960). Dahlberg (1970) conducted an extensive morphological investigation of the Atlantic and Gulf menhadens, including compilation of older data as well as 14 novel physical character assessments that provided morphological support for the notion of small-scaled and large-scaled groups. Subsequent morphological assessments of menhaden at various life stages support this generally accepted taxonomic arrangement (Hettler, 1984; Ahrenholz, 1991; Tolan and Newstead, 2004). Avise et al. (1989) and Bowen and Avise (1990) examined mitochondrial DNA (mtDNA) fingerprints of the large-scaled menhaden complex (*B. patronus*+*tyrannus*), and two divergent lineages of large-scaled menhadens were identified, one of which was shared between the two species, and the other occurring only in *B. tyrannus*. Avise (1992) suggested that this type of pattern is what would be expected from historical divergence, followed by secondary contact between the species. Anderson and McDonald (2007) used microsatellites to characterize populations of western Gulf menhadens (*B. patronus* and *B. gunteri*) and found significant genetic differences between these species. However, the latter work was limited in its phylogenetic scope because 1) it included only two of the four species of *Brevoortia* found in North America, and 2) it did not include genomic or mtDNA sequence data, which are typically more reliable than microsatellites in discerning relationships among species.

In the present study, the taxonomic relationships among the four North American menhaden species are examined by using both nuclear satellite DNA (microsatellites) and mitochondrial DNA sequences (mtDNA). Microsatellites are short runs of repetitive sequence (usually a two to four base motif repeated multiple times) that tend to be highly variable in vertebrates, are codominant (both parental copies of the marker can be scored for progeny), and are selectively neutral. Because of these properties, they are used extensively for examinations of population structure, paternity, and kinship in vertebrates (Wright and Bentzen, 1994; Jarne and Lagoda, 1996). Five DNA microsatellites were scored in populations of menhaden comprising the range of the four North American species. In addition, mtDNA sequencing was conducted on a short segment of the mtDNA control region for a subset of menhaden representing the four species. Mitochondrial DNA assays are beneficial because the mitochondrial genome of fishes is presumably not affected by recombination, and direct maternal lineages can be examined in contrast to the potentially admixed genotypes of nuclear DNA. In addition, genome-wide genetic studies (i.e., those that include both nuclear and mitochondrial data) are favored over single-locus or single-genome treatments because different genetic loci may yield conflicting results (Hare and Avise, 1998). These data revealed distinctive patterns which, when examined in the context of the biogeographic setting of each species, broaden the existing information with which the evolutionary history of North American menhadens may be elucidated.

Materials and methods

Sample collection and DNA isolation

Fin clips from individual menhaden were collected from bay systems covering the extent of the North American range of *Brevoortia* (Fig. 1) from 2002 through 2004 (see Brown et al., 1996 for a discussion of the implications and assumptions of pooling multiple year genetic data in clupeids). Adult fish samples from Texas were collected with a 184 m gill net partitioned into four sections ranging in mesh sizes from 76 mm to 152 mm, and all juveniles and young adult menhaden were collected in bag-seine hauls. Menhaden from locations outside of Texas were obtained through appropriate state and federal agencies (see "Acknowledgments" section). Fin tissue was excised from larger fish and placed in 70% ethanol; for smaller fish, whole individuals were preserved in ethanol. DNA was extracted from 200 mg of each fin clip or whole fish by using a Puregene[®] miniprep kit (Gentra Systems, Minneapolis, MN) and following the manufacturer's instructions.

Microsatellite data set

Genomic DNA from 20 sampling locales (Fig. 1) was used as a template to amplify microsatellite loci by touchdown polymerase chain reaction (PCR) with fluorescent end-labeled forward primers. Primer pairs were designed around microsatellite regions initially isolated from another clupeid, American shad (*Alosa sapidissima* Wilson, 1811); these primers have subsequently been evaluated for examinations of the genus *Brevoortia* (Anderson and McDonald, 2007). PCR products were electrophoresed with a Beckman-Coulter CEQ[™] 8000 automated capillary system, with a 400 base pair (bp) standard (Beckman Coulter, Inc., Fullerton, CA), according to the manufacturer's suggested protocol. Microsatellite allele sizes were estimated with Beckman-Coulter fragment analysis software (Beckman Coulter, Inc., Fullerton, CA), by using allelic bins that were based on the analysis of 1276 DNA samples from the four North American menhaden species collected over four years (data not shown).

The freeware program FSTAT vers. 2.9.3.2 (Goudet, 1995) was used to calculate observed (H_o) and expected (H_e) heterozygosity and allelic diversity (k_o), and to identify microsatellite loci which deviated significantly from Hardy-Weinberg equilibrium expectations (HWE). Deviation from HWE was tested by calculating the inbreeding coefficient (F_{is}) in the overall data set, and within each individual sampling locale. Statistical significance was assessed in a randomization procedure with 100 iterations. For this analysis, 13 populations of *B. patronus* ($n=20$) ranging from southern Texas to southern Florida were used. Individuals were then pooled into species and sampling locales ($n=20$ in each sampling locale, in locales where two species were captured, 20 of each species were used). The genetic divergence (F_{st} , Weir and Cockerham, 1984) among the four



Figure 1

Geographic range of the four menhaden species: Gulf menhaden (*Brevoortia patronus*)—smooth gray line, Gulf; Atlantic menhaden (*B. tyrannus*)—dotted gray line, Atlantic; fine-scale menhaden (*B. gunteri*)—dotted black line, western Gulf; and yellowfin menhaden (*B. smithi*)—dashed black line, eastern Gulf). Sample sites are indicated by black boxes.

species, and among all populations, was determined by using FSTAT software. A neighbor-joining (N-J) dendrogram was constructed with genetic divergence as a distance metric, and populations were revealed as terminal nodes by using the freeware program MEGA, vers. 2.1 (Kumar et al., 2001).

With a small subset of the data (to accommodate differences in sample size among species), we used a Bayesian procedure, as implemented in the freeware program Structure 2.1 (Pritchard et al., 2000), to examine historical admixture among species. Admixture may be defined as any measure of combination and introgression of genotypes (through hybridization) between two distinctive genetic sources, such as definitive populations, subspecies, or species. Structure 2.1 uses a Markovian chain Monte Carlo method (MCMC) to assign individuals to population clusters such that satisfaction of Hardy-Weinberg and linkage equilibrium expectations are maximized within populations. Because of the mechanics of the MCMC method, each iteration in a simulation is necessarily connected to the previous iteration, and therefore initial iterations are subject to the stochastic nature of random sampling. In order to account for this, data from simulations should not be collected until summary statistics begin to converge (to “burn-in”). A burn-in length of 10,000 repetitions was

chosen by examination of summary statistics for convergence in preliminary runs. A run length of 100,000 repetitions was chosen after several preliminary trials, after which parameter values were evaluated for consistency. For all analyses, the admixture model was used, and allele frequencies were assumed to be independent among species. Although this procedure allows estimation of the number of populations present (K), while simultaneously assigning individuals, we constrained the population number to $K = 4$, to reflect the prior assumption that only four species were present. Individuals were then assigned profiles that included the proportion of their genotype contributed by each species cluster. These profiles were then aligned by species in order to visually examine the influence of genetic admixture upon species groups.

Multilocus expected heterozygosity, estimated from microsatellite allele frequencies, was used to generate relative estimates of the value $N_e\mu$ for each of the four species, where N_e is the effective population size and μ represents the overall mutation rate, assuming a stepwise mutation model (Valdes et al., 1993). The estimator θ_F (Xu and Fu, 2004) was used to approximate $N_e\mu$ and was calculated as follows:

$$\theta_F = 0.5 (F^{-2} - 1),$$

where F = multilocus mean homozygosity ($1 - H_e$).

Although estimates of N_e from small genetic samples are notoriously inaccurate and may do a poor job of reflecting overall census size, relative estimates of N_e have been used to test evolutionary hypotheses (Nielsen, 1997), and theoretically may be used to examine relative differences in multiple populations at the same loci. The assumptions of the present study are that the mutation rate (μ) is not significantly different among the four examined species, and that genetic variability is related to population size. For this analysis, four loci were used because of the highly significant deviation from equilibrium frequencies that was observed at locus AF39660 (see "Results" section).

Sequencing data set

Sequencing templates were generated with PCR by using primers specific to an 840-bp fragment of the mtDNA control region. The heavy strand primer (HN20) was a previously described universal primer (Bernatchez and Danzmann, 1993) (5'-CGGGGTTTGACATGAATAT), whereas the light strand primer (940r) was a novel sequence primer designed specifically for menhaden (3'-TGTAATACTAGTGCAGATGGTAC). Each sample was amplified twice, and the amplicons were combined before purification to assure a high quality, concentrated product. PCR products were purified by using QIAquick® PCR purification kits (Qiagen Inc., Valencia, CA). The resulting purified fragments were used in two sequencing reactions in a nested design. The novel heavy strand primer (520f) was internal (5'-GGAACCAAATGCCAGGAATAGT), whereas the light strand primer was the same used in PCR. This nested design resulted in fragments which overlapped one another for 360 bp and which resided within the original 840-bp PCR fragment. Sequences were electrophoresed and analyzed on a Beckman-Coulter CEQ™ 8000 capillary sequencer by using default module (LFR-1) parameters (Beckman Coulter, Inc., Fullerton, CA). Raw sequences were trimmed and edited, and forward and reverse sequences were conjoined by using the software package Sequencher™ vers. 4.2 (Gene Codes Corp., Ann Arbor, MI). Whole sequences were then aligned by using Clustal X freeware (Jeanmougin et al., 1998). Sequences were submitted to GenBank by means of Sequin freeware (National Center for Biotechnology Information, Bethesda, MD) as batch submissions (accession numbers EF119342-EF119454).

Sequence data were obtained from 113 individuals from the four species (*B. tyrannus*, $n=37$; *B. smithi*, $n=32$; *B. patronus*, $n=30$; *B. gunteri*, $n=14$), and samples were selected to represent the full geographic range of each species (sampling locations in Maine, New Jersey, Virginia, North Carolina, Atlantic and Gulf Florida, and Texas). Sequence statistics, including nucleotide diversity (π) and haplotype diversity (h), were estimated for each species, and the genetic similarity among populations (measured using D_a , Nei, 1987) was calculated by using the freeware program DnaSP 4.0 (Rozas et al.,

2003). The variances of sequence diversity estimates were used to construct 95% confidence intervals around each mean. The averaged frequency of each base and the estimated ratio of transitions to transversions (ts/tv) were calculated with the freeware program DAMBE (Data Analysis in Molecular Biology and Evolution, Xia and Xie, 2001). Because of the extreme level of variation found in menhaden mtDNA, both in this study and in a previous study (Bowen and Avise, 1990), we employed a mutation saturation test as instituted in DAMBE. With this analysis, we compared the genetic distance between sequences to the number of transitions and transversions occurring between them. When all pairwise comparisons of sequences were plotted in this manner, mutation saturation was indicated by a plateau at which transversions approach or outnumber transitions at higher genetic distances. The genetic distance employed for this analysis ($K2P$) is described in Kimura (1980).

Both transitions and transversions were included in phylogenetic analyses. Before evolutionary reconstruction of haplotypes, the freeware program Modeltest 3.7 (Posada and Crandall, 1998) was used to determine the model of sequence evolution which had the highest likelihood. Briefly, 56 nested models of evolution were tested against raw sequence data with the program PAUP 4.0b1 (Phylogenetic Analysis Using Parsimony, available from Sinauer Associates, Inc., Sunderland, MA). Modeltest was then used to perform hierarchical likelihood ratio testing (hLRT) in order to identify the model with the highest likelihood. Concurrently, the Akaike information criterion (AIC) weights of the four most likely models were also examined during model selection. The appropriate model was subsequently used in a maximum-likelihood (ML) procedure in PAUP 4.0b1, with 10 replicates, to reconstruct an unrooted haplotype phylogeny. Because of the enormous computational load associated with maximum likelihood of highly variable loci, a concurrent N-J tree was constructed by using the 2-parameter distance of Kimura (1980); this tree was bootstrapped (1000 replicates over nucleotides, Felsenstein, 1985) to evaluate the significance of major interior nodes that correlated with nodes on the maximum-likelihood tree.

Results

Microsatellite data set

Microsatellite samples were distributed from southern Texas to the Gulf of Maine, the northern extent of *B. tyrannus*. *Brevoortia tyrannus* was sampled in three locations (all Atlantic coast), *B. smithi* in two locations (one Atlantic, one eastern Gulf), *B. patronus* in 14 locations (all Gulf coast), and *B. gunteri* in three locations (all western Gulf coast). Of the five microsatellite markers used in this study, all had observed levels of heterozygosity that were lower than anticipated under Hardy-Weinberg expectations when tested by using samples

Table 1

Short tandem repeat locus statistics (listed by National Center for Biotechnology Information accession number) averaged over 13 populations of Gulf menhaden (*Brevoortia patronus*, $n=260$). Statistics include the DNA base motif (each allele is distinguished by "x" number of repetitions of the motif), observed (H_o) and expected (H_e) heterozygosity, number of alleles (k_a), and deviation from Hardy-Weinberg expected genotype frequencies (measured by deviation of F_{is} from 0).

Locus	Primer sequence	Motif	H_o	H_e	k_a (overall)	F_{is} (overall)
AF049462	F: GGAGGCACAGGTGTGGTATT R: TTTGGAGGGAGAGAAACGTC	[GTT] _x	0.84	0.93	31	0.09
AF039658	F: TAATAAACCCCGTTGGGACA R: GCTGATGTTCTCCATCTCC	[CAA] _x	0.78	0.87	23	0.10
AF039657	F: GCCATTACTCCAAGTTGCTTTT R: CGTGGCACAACATAGTCATCA	[CTT] _x	0.70	0.73	20	0.05
AF039661	F: TGCTTTAATCCGGAATGGAC R: GGGGAGTGAGAGAACGAGTG	[CTTT] _x	0.15	0.20	10	0.24
AF039660	F: GGAGCTCAGCACATCTCTCC R: CTGACATGGCCAGTAGGTT	[GTTT] _x	0.26	0.58	13	0.55*

* indicates that F_{is} is significantly different from zero in a majority of *B. patronus* populations sampled after correction for multiple tests, determined by a randomization procedure with 1000 iterations.

of *B. patronus* individuals from the Gulf of Mexico ($n=260$, Table 1). One locus (AF39661) had a high overall value of F_{is} , but was not significantly different than zero based on randomization tests. However, a second locus (AF39660) had lower than expected heterozygosity at a significant level in a majority of the populations assayed. Whether the explanation for decreased levels of heterozygosity is biological or simply sampling error is unclear; however analyses excluding this marker had little effect on tree topology or other results. Multilocus estimates of genetic divergence (F_{st}) were lowest within the pre-defined menhaden groups; that is, the level of divergence seen in the comparisons between *B. patronus*+*tyrannus* and *B. smithi*+*gunteri* was lower than any other pairwise comparisons among species (Table 2). Similarly, the N-J tree constructed from microsatellite data was deeply bifurcated (Fig. 2) and the two major groupings on this tree corresponded to populations of small-scaled and large-scaled menhaden, exclusively. Four major clusters on this tree corresponded to the populations of each of the four assayed species. The greatest level of within-species divergence was observed between the Atlantic and Gulf populations of *B. smithi*. The divergence among these populations was an order of magnitude higher than the mean divergence from comparisons among populations of the same species, and was 5.5 standard deviations removed from the mean of all F_{st} comparisons combined ($F_{st}^{smithi}=0.0523$, $F_{st}^{overall}=0.0054$, $\sigma^2=0.0094$).

Bayesian analysis of population structure resulted in four well-defined clusters corresponding to the four assayed species (Fig. 3). However, no single species

Table 2

Genetic divergence among Atlantic menhaden (*Brevoortia tyrannus*), Gulf menhaden (*B. patronus*), yellowfin menhaden (*B. smithi*), and finescale menhaden (*B. gunteri*), as measured by using multilocus microsatellite data (F_{st} , above the diagonal) and mtDNA sequence similarity among populations (D_a , below the diagonal).

	<i>B. tyrannus</i>	<i>B. patronus</i>	<i>B. smithi</i>	<i>B. gunteri</i>
<i>B. tyrannus</i>	0	0.110	0.448	0.412
<i>B. patronus</i>	0.005	0	0.411	0.378
<i>B. smithi</i>	0.077	0.093	0	0.355
<i>B. gunteri</i>	0.071	0.088	0.004	0

contained exclusively one cluster; each species had individuals with composite genotypes including influence from other clusters. In particular, admixture among the two large-scaled species was indicated by individuals of each species in which a majority of the genotype was contributed by the complimentary species. A smaller level of admixture was indicated in the small-scaled species. However, one interesting result was a single individual *B. gunteri* which had 0.723 of its genotype contributed by the *B. patronus* cluster. This is significant in that, although the possibility of hybridization in the western Gulf has not been ruled out (Anderson and McDonald, 2007), a verified F1 *B. patronus*+*gunteri* hybrid has not been documented in the Gulf.

Estimates of genetic variability including H_e , k_a , and θ_F were higher in large-scaled species of menhaden than in small-scaled species (Table 3). Multilocus expected heterozygosity ranged from 0.672 in *B. patronus* and

Table 3

Genetic diversity estimates over four nuclear loci (AF49462, AF39658, AF39657, and AF39661) and the mtDNA control region locus, for Atlantic menhaden (*Brevoortia tyrannus*), Gulf menhaden (*B. patronus*), finescale menhaden (*B. gunteri*), and yellowfin menhaden (*B. smithi*). The diversity estimates include allelic diversity (k , alleles/locus) at each microsatellite locus and overall (k_a), multilocus expected heterozygosity (H_e), relative effective population size estimated from multi-locus heterozygosity (θ_F), the 95% confidence range of mtDNA nucleotide diversity (π), and the 95% confidence range of mtDNA haplotype diversity (h). Sample sizes were equal ($n=39$) in all comparisons unless otherwise noted.

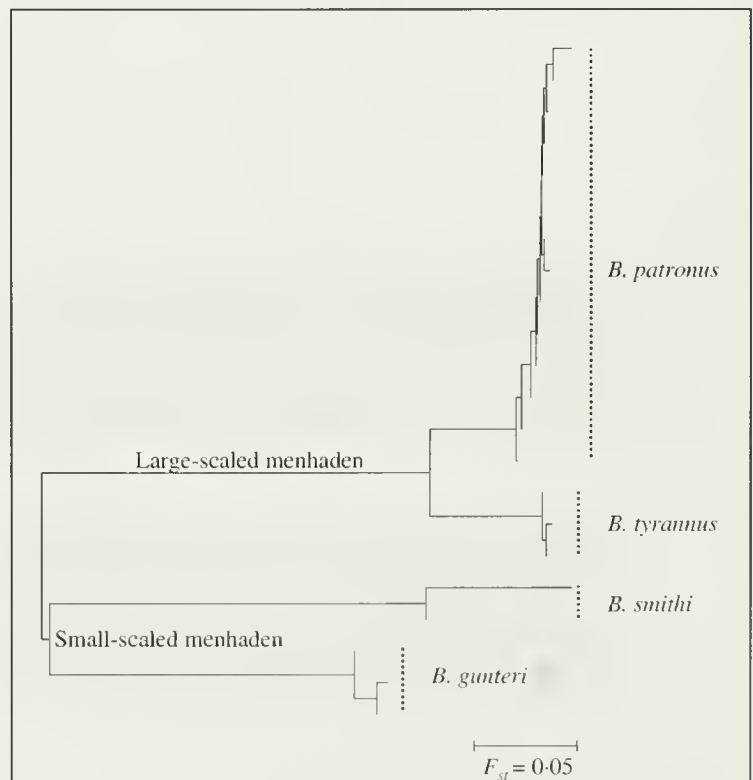
Species	AF49462 (k)	AF39658 (k)	AF39657 (k)	AF39661 (k)	k_a	H_e	θ_F	π	h
<i>Brevoortia tyrannus</i>	20	14	15	3	13.0	0.67	4.15	0.064–0.086 ($n=37$)	0.99–1.00 ($n=37$)
<i>Brevoortia patronus</i>	19**	16**	9**	4**	12.0	0.67	4.15	0.046–0.054 ($n=30$)	0.99–1.00 ($n=30$)
<i>Brevoortia gunteri</i>	11	11	3	1	6.5	0.41	0.90	0.038–0.055 ($n=14$)	0.95–1.00 ($n=14$)
<i>Brevoortia smithi</i>	8	4	2	2	4.0	0.37	0.76	0.030–0.037 ($n=32$)	0.92–1.00 ($n=32$)

** Allelic counts for *B. patronus* are different from those presented in Table 1 because fewer individuals were used to account for smaller sample sizes in the three remaining species.

B. tyrannus, to 0.413 in *B. gunteri* and 0.370 in *B. smithi*. This disparity is due to near fixation of alleles in both small-scaled species at a single locus which is highly polymorphic in both large-scaled species (AF39657), but also reflects decreased variability at all marker loci. As a result, the estimates of θ_F in large-scaled species were four to five times larger than those for small-scaled species.

Sequencing data set

The mtDNA sequencing data set indicates an enormous amount of genetic variation in the control region of menhaden (Table 3), although this variation was not evenly distributed across the entire alignment. In particular, regions of sequence conservation in the data set were directly adjacent to highly degenerate regions more typical of the mitochondrial control region of clupeids (Grant et al., 1998). Over a total dataset of 360 bp, 149 sites were polymorphic, and pairwise sequence comparisons resulted in an average of 28.7 nucleotide differences among haplotypes. Of 113 individuals assayed, 106 haplotypes were identified in the four species. Despite this high level of sequence divergence, only three single-base deletions were detected in the multiple alignment of 113 individuals (deletions were treated as missing data). The control region of menhaden is A-T rich (contains greater than 50% adenine and thymine bases), with averaged base frequencies of A = 0.269, T = 0.487, C (cytosine) = 0.156, and G (guanine) = 0.167, and with no evidence for heterogeneity of base frequencies among taxa ($\chi^2=59.40$, $P=1.00$).

**Figure 2**

Neighbor-joining dendrogram of populations ($n=20$, in each population) of Gulf menhaden (*Brevoortia patronus*), Atlantic menhaden (*B. tyrannus*), finescale menhaden (*B. gunteri*), and yellowfin menhaden (*B. smithi*). The distance metric used for neighbor-joining was F_{st} (Weir and Cockerham, 1984), which is the estimated proportion of genetic variance that is due to between-population effects.

The estimated ts/tv ratio was 2.1:1. As was the case in comparisons using microsatellites, the mtDNA distance among species (D_a) was lowest in comparisons between species within small-scaled and large-scaled groups (Table 2).

Hierarchical likelihood ratio tests indicated that the K81uf+I+ Γ model (Kimura, 1981) was the most appropriate model of sequence evolution at the control region locus. This model also had the second highest AIC weight, at 0.23. The K81uf+I+ Γ model approxi-

mates the rate of heterogeneity across sites (a property which can simply be described as unequal probabilities of mutations among sites) by using a gamma distribution, after variant sites have been removed. Haplotype phylogenies generated with both the M-L method and the N-J cluster method indicated three divergent lineages of menhadens (Fig. 4), and these lineages were identical in haplotype membership between the two tree-building methods. The first lineage had 99% bootstrap support and included haplotypes contributed from both *B. patronus* and *B. tyrannus*. This main group of large-scaled haplotypes ($n=59$) was characterized primarily by transitions and had minimal (<7) transversions among haplotypes. A second, small group of divergent Atlantic menhaden occurred in the haplotype phylogeny, with 100% bootstrap support. This second group comprised the remaining eight large-scaled haplotypes and differed from the first group by 14+ transversions per haplotype, likely the result of mutation saturation. Plots of transitions and transversions indicated that this data set was saturated; the rate of transversions begins to rival that of transitions at approximately a Kimura distance of 0.10 (Fig. 5A). Although saturation is indicated in cases where divergent haplotype clades are compared, saturation is not indicated in comparisons involving within-clade comparisons (Fig. 5, B–D). Thus, the main effect of saturation on this data set was on longer (more divergent) branches. A third lineage on the maximum likelihood tree had 100% bootstrap support and consisted of haplotypes contributed by *B. gunteri* and *B. smithi* in paraphyly. Haplotypes in this clade indicated incomplete sorting of mtDNA haplotypes within the small-scaled menhadens. However, there was clear evidence for genetic divergence between this group and both large-scaled clades, and 100% bootstrap support for monophyly of the small-scaled haplotypes.

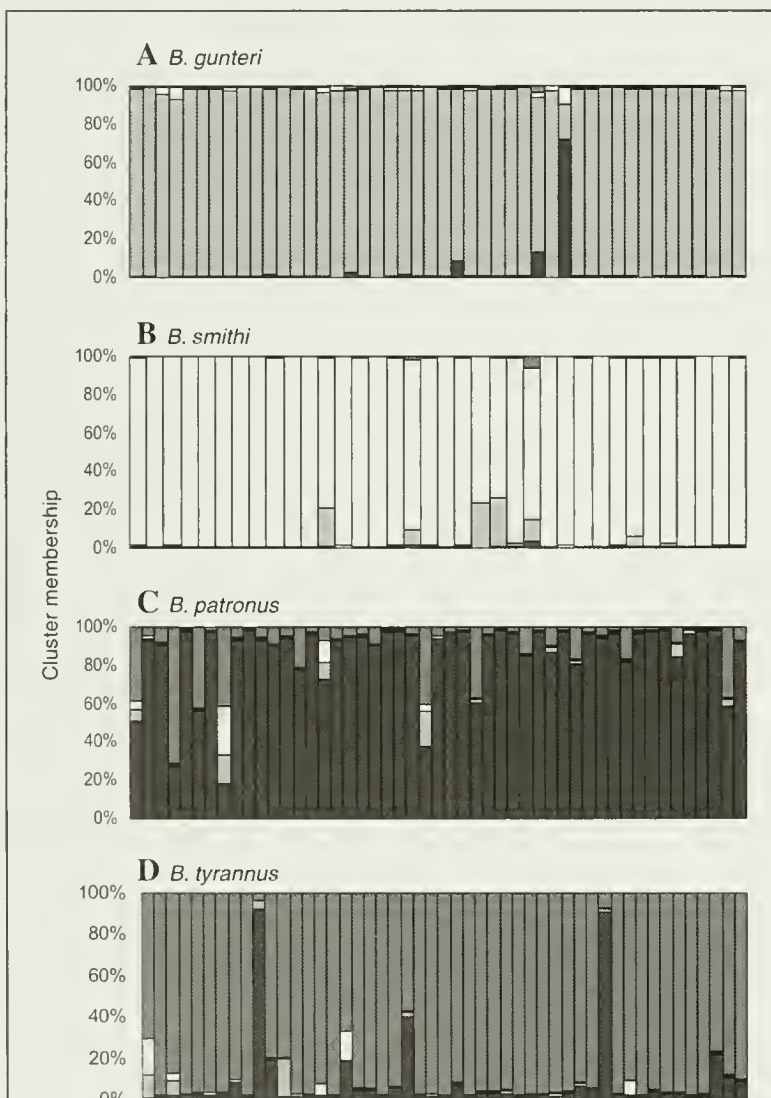


Figure 3

Bayesian assignment tests resulted in recovery of four putative source populations of genotypic data. Individuals were separated into their respective species groups (A–D), and genetic identity was assigned based upon the percentage of an individual's genotype contributed by each of the four source populations, as indicated on the y-axis. Genetic source populations are represented by light grey (finescale menhaden [*Brevoortia gunteri*]), white (yellowfin menhaden, [*B. smithi*]), black (Gulf menhaden [*B. patronus*]), and dark grey (Atlantic menhaden [*B. tyrannus*]).

Discussion

The morphological differences among the four North American menhaden species have been examined previously at egg, larval, juvenile, and adult stages (Dahlberg, 1970 [and references therein]; Hettler, 1984; Ahrenholz, 1991; Tolan and Newstead, 2004), and previous classifications have the species divided between small-scaled and large-scaled groups (Dahlberg, 1970). The results presented here reinforce the conventional hypothesis that *B. smithi* and *B. gunteri* share recent common ancestry as do *B. patronus* and *B. tyrannus*. Both classes of genetic markers showed

significant genetic divergence between the two menhaden types, and this distinction is reinforced by demographic characteristics shared within these groups. Specifically, overall census sizes (Christmas and Gunter, 1960), species ranges (Christmas and Gunter, 1960), and migratory behavior (Gunter, 1945; Simmons, 1957; Tolan and Newstead, 2004) are markedly different between the small-scaled and large-scaled species pairs, yet similar between species within these pairs. The differences in the demographics of small-scaled and large-scaled menhaden are reflected in nuclear-based estimates of $N_{e,u}$, which are four to five times larger in large-scaled species. Smaller population sizes, and relatively shorter overall coastal ranges, are reflected in the lower genetic variability of small-scaled menhaden compared to large-scaled menhaden. In addition, nutritional and trophic differences among these species in the western Gulf have previously been documented (Castillo-Rivera et al., 1996; Castillo-Rivera and Kobelkowsky, 2000) and may represent mechanisms for the divergence of population demographic parameters among these groups.

In both the present study and the study of Bowen and Avise (1990), high levels of genetic variation were detected in the mtDNA genome of menhaden. Indeed, because of the high mutation rate of the mtDNA region surveyed in this study, saturation was a likely source of bias in comparisons among divergent lineages. A second similarity between this study and that of Bowen and Avise (1990) is the presence of two divergent large-scaled haplotype groups, one that is confined to *B. tyrannus*, and a second which includes haplotypes from both species. Avise (1992) suggested that a likely explanation for this pattern is recent gene flow between these species, rather than incomplete lineage sorting. A Bayesian population assignment of nuclear genotypes seems to support the possibility of admixture between these species, with individuals from both species containing genetic signatures of the complementary group. Epperly (1989, [and references therein]), suggested the existence of two subpopulations of *B. tyrannus* in the Atlantic: one on the southern Atlantic coast (below 40°N) and a subpopulation north of Long Island, New York. Juveniles from these subpopulations differed in meristic and morphological characteristics, and also had different biochemical profiles (Epperly, 1989). Epperly (1989) suggested that the spawning times for these two subpopulations

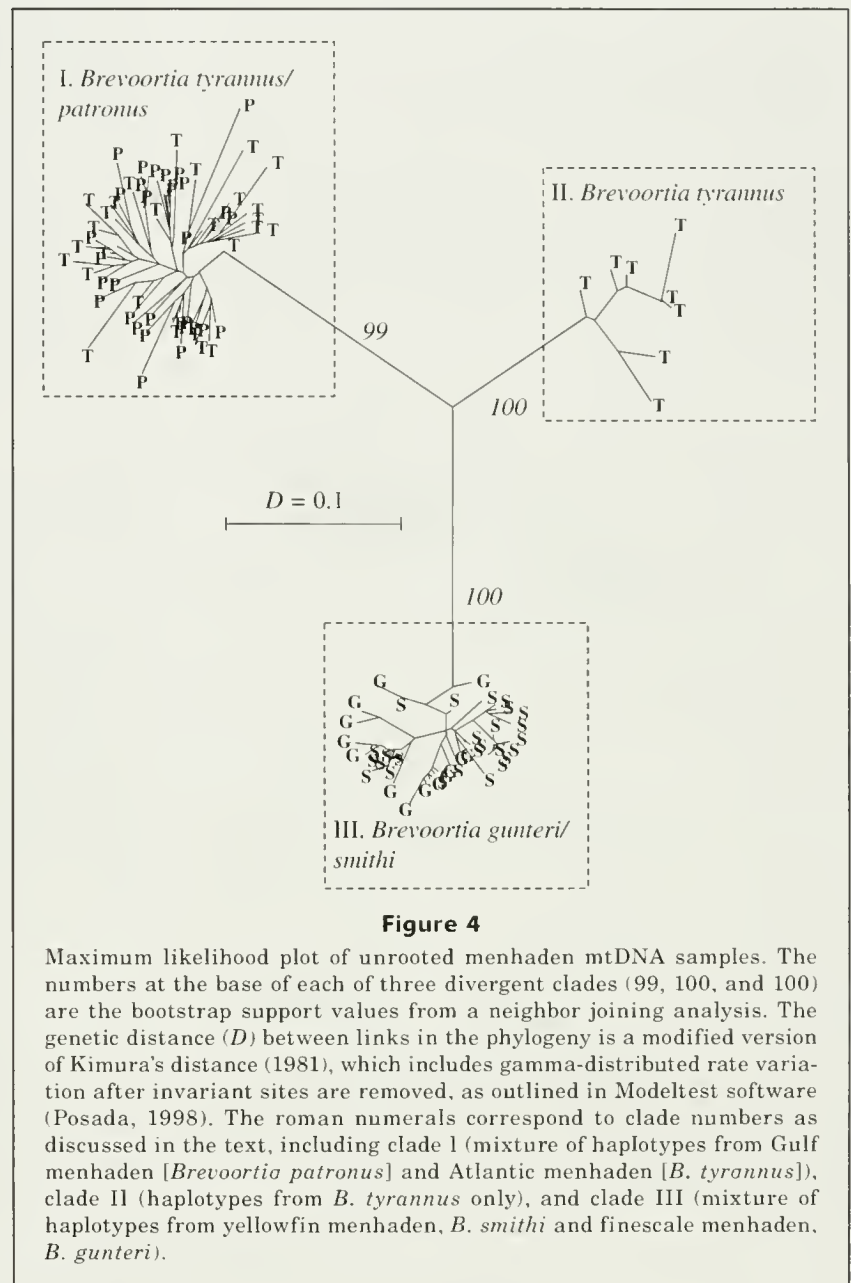


Figure 4

Maximum likelihood plot of unrooted menhaden mtDNA samples. The numbers at the base of each of three divergent clades (99, 100, and 100) are the bootstrap support values from a neighbor joining analysis. The genetic distance (D) between links in the phylogeny is a modified version of Kimura's distance (1981), which includes gamma-distributed rate variation after invariant sites are removed, as outlined in Modeltest software (Posada, 1998). The roman numerals correspond to clade numbers as discussed in the text, including clade I (mixture of haplotypes from Gulf menhaden [*Brevoortia patronus*] and Atlantic menhaden [*B. tyrannus*]), clade II (haplotypes from *B. tyrannus* only), and clade III (mixture of haplotypes from yellowfin menhaden, *B. smithi* and finescale menhaden, *B. gunteri*).

may be different, allowing for recruitment to occur in these areas at different times of the year. Variance in spawning times may be a mechanism for maintenance of divergence between haplotype clades for large-scale menhaden recovered in this study. However, it is likely that the variation in morphology and biochemistry seen in northern and southern forms of Atlantic menhaden is affected by the influence of recurrent gene flow between this species and its Gulf cognate. Avise (1992) demonstrated a broad-scale demographic break between Atlantic and Gulf forms of both terrestrial and marine vertebrates (including menhaden); however, in many species, haplotypes representative of Gulf forms were present in individuals collected in the southern Atlan-

tic. Locales farther north in the Atlantic lack the Gulf haplotypes; in this scenario it would be expected that Atlantic menhaden collected farther north would lack the Gulf menhaden influence. Indeed, in the divergent group of Atlantic menhaden examined in the present study, four of the eight haplotypes came from juveniles collected from the northernmost sampling locale (Maine). The remaining haplotypes came from a single adult from a northern locale (New Jersey), two adults from southern locales (North Carolina), and a southern locale juvenile (North Carolina).

Previous treatments have recognized two subpopulations of *B. smithi* in the Gulf and Atlantic, and Hildebrand (1963) characterized the eastern Gulf *B. smithi* as intermediate in form between *B. gunteri* and the Atlantic form of *B. smithi*. An interesting note in our data set is the large divergence estimate between two sampled populations of *B. smithi* obtained in the microsatellite analysis. This estimate of divergence between these populations ($F_{st}^{smithi}=0.0523$) is the largest of any comparison and is an order of magnitude greater than the mean comparison among populations of the same species ($F_{st}^{mean}=0.0054$). *Brevoortia smithi* is the only species of menhaden that has significantly large populations in both the Gulf and Atlantic, and populations of this species are rare towards the southern tip of Florida (Reintjes, 1959; Dahlberg, 1970). Thus, vicariance may play a role in divergence between these populations. It is clear that biological differences between Atlantic and Gulf forms of *B. smithi* extend into the genetic data presented here, resulting in long branches in the microsatellite-based topology. In addition, the smaller relative census sizes of small-scaled menhaden species has likely resulted in a faster and more distinctive pattern of divergence among populations of these species than what has occurred in large-scaled species. Further investigation is needed in order to determine if the genetic divergence between Gulf and Atlantic forms of *B. smithi* is genome-wide.

A final peculiarity of the data was a single individual *B. gunteri* which had a genotype that indicated influence from *B. patronus* (Fig. 3). Specifically, this individual had an estimated 72.3% of its genotype contributed by a cluster roughly representative of *B. patronus*, whereas all other individuals of this species had less than a 10% contribution from this cluster (averaged around 2.7%). Although high rates of hybridization between *B. smithi* and both large-scaled menhaden species have been documented in peninsular Florida (Turner, 1969; Hettler, 1984), hybrids between *B. gunteri* and *B. patronus* have not been documented (Anderson and McDonald, 2007). Visual inspection of the individual in question yielded no morphological evidence of hybridization. In addition, Bayesian assignment can be expected to perform better if more loci are sampled. Although five microsatellite loci were adequate to recover evidence for population structure in the present data set, individual assignments based on limited genetic loci will comprise a high level of uncertainty

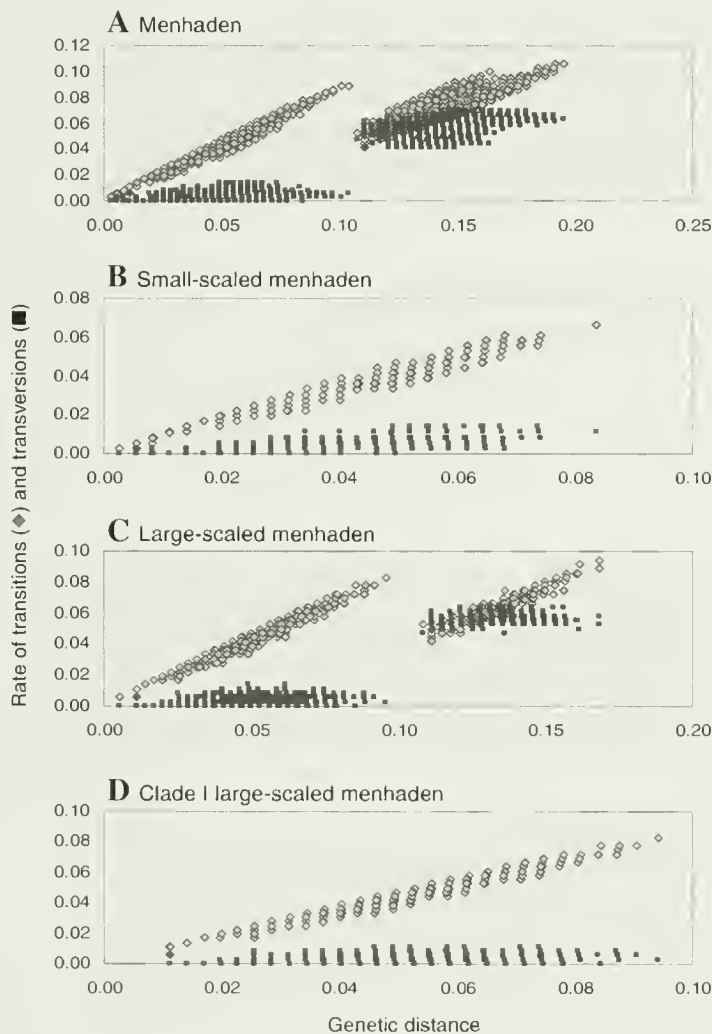


Figure 5

Saturation plots of menhaden mtDNA data. The x-axis represents Kimura (1980) distances between sequences, whereas the y-axis represents the rate of transitions (◆) and transversions (■). A saturation plot was constructed for (A) mtDNA samples from all four species, (B) samples from small-scaled menhaden only (yellowfin menhaden [*Brevoortia smithi*] and finescale menhaden [*B. gunteri*]), (C) samples from large-scaled menhaden only (Gulf menhaden [*B. patronus*] and Atlantic menhaden [*B. tyrannus*]), and (D) large-scaled menhaden from mtDNA clade I only.

(Corander et al., 2006). However, given the result here and a similar individual possible occurrence documented in Anderson and McDonald (2007), rare hybridization events between *B. gunteri* and *B. patronus* cannot be ruled out.

Acknowledgments

The following are to be acknowledged for their assistance in completing this work. B. Mobley, K. Anderson, and H. Hendrickson provided technical laboratory assistance. B. Bumguardner, B. Karel, M. Fisher, J. Mambretti, T. Stelly, D. McDonald, S. Grant, and four anonymous reviewers provided thoughtful comments on the manuscript. Texas samples were collected by numerous individuals during routine monitoring of Texas estuarine ecosystems by staff of Texas Parks and Wildlife Department, Coastal Fisheries Division. The following provided samples from outside of Texas: R. McMichael and the staff of the fisheries-independent monitoring program at the Florida Fish and Wildlife Conservation Commission, especially T. Tuckey, D. Adams, and C. Idelberger; J. W. Smith at the National Marine Fisheries Service, National Oceanic and Atmospheric Administration, Beaufort Laboratory in Beaufort, NC; and B. Tarbox at the Southern Maine Community College. This research was funded in part by a Federal Aid in Sport Fish Restoration Grant (F-144-R).

Literature cited

- Ahrenholz, D. W.
1981. Recruitment and exploitation of Gulf menhaden, *Brevoortia patronus*. *Fish. Bull.* 79:325–335.
1991. Population biology and life history of the North American menhadens, *Brevoortia* spp. *Mar. Fish. Rev.* 53:3–19.
- Anderson, J. A., and D. L. McDonald.
2007. Morphological and genetic investigations of two western Gulf of Mexico menhadens (*Brevoortia* spp.). *J. Fish Biol.* 70(S):139–147.
- Avise, J. C.
1992. Molecular population structure and the biogeographic history of a regional fauna: a case history with lessons for conservation biology. *Oikos* 63:62–76.
- Avise, J. C., B. W. Bowen, and T. Lamb.
1989. DNA fingerprints from hypervariable mitochondrial genotypes. *Mol. Biol. Evol.* 6:258–269.
- Bernatchez, L., and R. G. Danzmann.
1993. Congruence in control-region sequence and restriction-site variation in mitochondrial DNA of brook charr (*Salvelinus fontinalis* Mitchell). *Mol. Biol. Evol.* 10:1002–1014.
- Bethea, D. M., J. A. Buckel, and J. K. Carlson.
2004. Foraging ecology of the early life stages of four sympatric shark species. *Mar. Ecol. Prog. Ser.* 268:245–264.
- Bowen, B. W., and J. C. Avise.
1990. Genetic structure of Atlantic and Gulf of Mexico populations of sea bass, menhaden and sturgeon: influence of zoogeographic factors and life-history patterns. *Mar. Biol.* 107:371–381.
- Brown, B. L., J. M. Epifanio, P. E. Smouse, and C. J. Kubiak.
1996. Temporal stability of mtDNA haplotypes frequencies in American shad stocks: to pool or not to pool across years? *Can. J. Fish. Aquat. Sci.* 53:2274–2283.
- Castillo-Revera, M., and A. Kobelkowsky.
2000. Distribution and segregation of two sympatric *Brevoortia* species (Teleostei:Clupeidae). *Estuar. Coast. Shelf Sci.* 50:593–598.
- Castillo-Revera, M., A. Kobelkowsky, and V. Zamayoá.
1996. Food resource partitioning and trophic morphology of *Brevoortia gunteri* and *B. patronus*. *J. Fish Biol.* 49:1102–1111.
- Christmas, J. Y., and G. Gunter.
1960. Distribution of menhaden, genus *Brevoortia*, in the Gulf of Mexico. *Trans. Am. Fish. Soc.* 89:338–343.
- Corander, J., P. Marttinen, and S. Mäntyniemi.
2006. A Bayesian method for identification of stock mixtures from molecular marker data. *Fish. Bull.* 104:550–558.
- Dahlberg, D. W.
1970. Atlantic and Gulf of Mexico menhadens, genus *Brevoortia* (Pisces: Clupeidae). *Bull. Fla. Mus. Nat. Hist. Biol. Sci.* 15:91–162.
- Epperly, S. P.
1989. A meristic, morphometric and biochemical investigation of Atlantic menhaden, *Brevoortia tyrannus* (Latrobe). *J. Fish Biol.* 35:139–152.
- Felsenstein, J.
1985. Confidence limits on phylogenies: An approach using the bootstrap. *Evolution* 39:783–791.
- Gottlieb, S. J.
1998. Ecological role of Atlantic menhaden (*Brevoortia tyrannus*) in Chesapeake Bay and implications for management of the fishery. M.S. thesis, 126 p. Univ. of Maryland, College Park, MD.
- Goudet, J.
1995. FSTAT (vers. 1.2): a computer program to calculate F-statistics. *J. Hered.* 86:485–486.
- Grant, W. S., A. M. Clark, and B. W. Bowen.
1998. Why restriction fragment length polymorphism analysis of mitochondrial DNA failed to resolve sardine (*Sardinops*) biogeography: insights from mitochondrial DNA cytochrome *b* sequences. *Can. J. Fish. Aquat. Sci.* 55:2539–2547.
- Gunter, G.
1945. Studies on marine fishes of Texas. *Publ. Inst. Mar. Sci.* 1:1–190.
- Hare, M. P., and J. C. Avise.
1998. Population structure in the American oyster as inferred by nuclear gene genealogies. *Mol. Biol. Evol.* 15:119–128.
- Hettler, W. F.
1984. Description of eggs, larvae, and early juveniles of gulf menhaden, *Brevoortia patronus*, and comparisons with Atlantic menhaden, *B. tyrannus*, and yellowfin menhaden, *B. smithi*. *Fish. Bull.* 82:85–95.
- Hildebrand, S. F.
1963. Family Clupeidae. In *Fishes of the western North Atlantic Memoir 1, Part 3* (Y. H. Olsen, ed.), p.257–454. Sears Foundation Mar. Res., Yale Univ., New Haven, CT.
- Jarne, P., and J. L. Lagoda.
1996. Microsatellites, from molecules to populations and back. *Trends Ecol. Evol.* 11:424–429.

- Jeanmougin, F., J. D. Thompson, M. Gouy, D. G. Higgins, and T. J. Gibson.
1998. Multiple sequence alignment with Clustal X. *Trends Biochem. Sci.* 23:403-405.
- Kimura, M. A.
1980. Simple method for estimating evolutionary rates of base substitutions through comparative studies of nucleotide sequences. *J. Mol. Evol.* 16:111-120.
1981. Estimation of evolutionary distances between homologous nucleotide sequences. *Proc. Nat. Acad. Sci.* 78:454-458.
- Kroger, R. L., and J. F. Guthrie.
1972. Effect of predators on juvenile menhaden in clear and turbid estuaries. *Mar. Fish Rev.* 34:78-80.
- Kumar, S., K. Tamura, I. B. Jakobsen, and M. Nei.
2001. Mega2: Molecular Evolutionary Genetics Analysis Software. *Bioinformatics* 12:1244-1245.
- Nei, M.
1987. *Molecular evolutionary genetics*, 1st ed., 512 p. Columbia Univ. Press, New York, NY.
- Nielsen, R.
1997. A likelihood approach to populations samples of microsatellite alleles. *Genetics* 146:711-716.
- Posada, D., and K. A. Crandall.
1998. Modeltest: testing the model of DNA substitution. *Bioinformatics* 14:817-818.
- Pritchard, J. K., M. Stephens, and P. Donnelly.
2000. Inference of population structure using multilocus genotype data. *Genetics* 155:945-959.
- Reintjes, J. W.
1959. Continuous distribution of menhaden along the south Atlantic and Gulf coasts of the United States. *Proc. Gulf Carib. Fish. Inst.* 12:31-35.
- Rozas, J., J. C. Sanchez-DelBarrio, X. Messeguer, and R. Rozas.
2003. DnaSP, DNA polymorphism analyses by the coalescent and other methods. *Bioinformatics* 19:2496-2497.
- Scharf, F. S., and K. K. Schlicht.
2000. Feeding habits of red drum (*Sciaenops ocellatus*) in Galveston Bay, Texas: Seasonal diet variation and predator-prey size relationships. *Estuaries* 23:128-139.
- Simmons, E. G.
1957. An ecological survey of the upper Laguna Madre of Texas. *Publ. Inst. Mar. Sci. Univ. Tex.* 4:156-200.
- Tolan, J. M., and D. A. Newstead.
2004. Descriptions of larval, prejuvenile, and juvenile fin-escape menhaden (*Brevoortia gunteri*) (family Clupeidae), and comparisons to Gulf menhaden (*B. patronus*). *Fish. Bull.* 102:723-732.
- Turner, W. R.
1969. Life history of menhadens in the eastern Gulf of Mexico. *Trans. Am. Fish Soc.* 98:216-224.
- Valdes, A. M., M. Slatkin, and N. B. Freimer.
1993. Allele frequencies at microsatellite loci: the stepwise mutation model revisited. *Genetics* 133:737-749.
- Vaughan, D. S., and J. V. Merriner.
1991. Assessment and management of Atlantic and Gulf menhaden stocks. *Mar. Fish Rev.* 53:47-55.
- Weir, B. S., and C. C. Cockerham
1984. Estimating F-statistics for the analysis of population structure. *Evolution* 38:1358-1370.
- Wright, J. M., and P. Bentzen.
1994. Microsatellites: genetic markers for the future. *Rev. Fish Biol.* 4:384-388.
- Xia, X., and Z. Xie.
2001. DAMBE: Data analysis in molecular biology and evolution. *J. Heredity* 92:371-373.
- Xu, H., and Y. X. Fu.
2004. Estimating effective population size or mutation rate with microsatellites. *Genetics* 166:555-563.

Abstract—Thirty-three skipjack tuna (*Katsuwonus pelamis*) (53–73 cm fork length) were caught and released with implanted archival tags in the eastern equatorial Pacific Ocean during April 2004. Six skipjack tuna were recaptured, and 9.3 to 10.1 days of depth and temperature data were downloaded from five recovered tags. The vertical habitat-use distributions indicated that skipjack tuna not associated with floating objects spent 98.6% of their time above the thermocline (depth=44 m) during the night, but spent 37.7% of their time below the thermocline during the day. When not associated with floating objects, skipjack tuna displayed repetitive bounce-diving behavior to depths between 50 and 300 m during the day. The deepest dive recorded was 596 m, where the ambient temperature was 7.7°C. One dive was particularly remarkable because the fish continuously swam for 2 hours below the thermocline to a maximum depth of 330 m. During that dive, the ambient temperature reached a low of 10.5°C, and the peritoneal cavity temperature reached a low of 15.9°C. The vertical movements and habitat use of skipjack tuna, revealed in this study, provide a much greater understanding of their ecological niche and catchability by purse-seine fisheries.

Vertical movement patterns of skipjack tuna (*Katsuwonus pelamis*) in the eastern equatorial Pacific Ocean, as revealed with archival tags

Kurt M. Schaefer (contact author)

Daniel W. Fuller

Email address for K. M. Schaefer: kschaef@iattc.org

Inter-American Tropical Tuna Commission
8604 La Jolla Shores Drive
La Jolla, California 92037-1508

Limited information on the vertical movements of skipjack tuna (*Katsuwonus pelamis*) is available from analyses of catch data for tuna long-line gear (Yabe et al., 1963), ultrasonic telemetry (Dizon et al., 1978; Schaefer and Fuller, 2005; Matsumoto et al.¹), and archival tags (Ogura²). These studies have indicated that skipjack tuna inhabit predominantly the mixed layer but make occasional brief dives below the thermocline.

Skipjack tuna are distributed throughout the world's tropical and subtropical oceans (Collette and Nauen, 1983; Matsumoto et al., 1984). In the eastern Pacific Ocean (EPO), catches of this species have occurred from about 34°N off southern California to about 27°S off northern Chile. The species is limited to surface temperatures of about 17° to 30°C (Wild and Hampton, 1994). Skipjack tuna are one of three principal targets of a large-scale purse-seine fishery in the EPO and are caught mostly in association with floating objects between about 10°N and 15°S. The purse-seine catch of skipjack tuna in the EPO during 1995–2004 averaged 197 thousand metric tons (t) (range: 129 to 295 thousand t), which is 160% greater than the average of 76 thousand t (range: 51 to 95 thousand t) during the previous 10-year period (Anonymous, 2005).

The anatomical and physiological adaptations of skipjack tuna characterize them as highly efficient opportunists for exploiting their oceanic vertical habitat. Their body shape, fin configurations, and musculature

are close to optimum for relatively fast, sustained, and burst swimming (Magnuson, 1978; Altringham and Shadwick, 2001). They lack a swim bladder (Godsil and Byers, 1944), are capable of physiological thermoregulation (Dizon and Brill, 1979), and have relatively rapid gastric evacuation rates (Magnuson, 1969).

Skipjack tuna possess a well-developed large central rete, in addition to epaxial and hypaxial vessels and retia (Stevens et al., 1974; Graham and Dickson, 2001). The counter-current retia provide a thermoconserving mechanism enabling metabolic heat to be retained within the muscles and thus elevate body temperatures above that of ambient water temperatures (Graham, 1975; Stevens and Neill, 1978). The anatomical specializations enhance the thermal inertia of this species and

¹ Matsumoto, T., H. Okamoto, and M. Toyonaga. 2006. Behavioral study of small bigeye, yellowfin and skipjack tunas associated with drifting FADs using ultrasonic coded transmitter in the central Pacific Ocean. Information Paper 7, 25 p. Second regular session of the scientific committee. Western and Central Pacific Fisheries Commission, P.O. Box 2356, Kolonia, Pohnpei FM 96941.

² Ogura, M. 2003. Swimming behavior of skipjack, *Katsuwonus pelamis*, observed by the data storage tag at the northwestern Pacific, off northern Japan, in summer of 2001 and 2002. Working Paper SKJ-7, 10 p. Sixteenth meeting of the standing committee on tuna and billfish, Sec. Pac. Comm., Noumea, New Caledonia, B.P. D5 Noumea Cedex, New Caledonia.

enable this species to slow the cooling rate of the body. Thermal inertia allows skipjack tuna to undertake brief dives into cooler waters below the thermocline to exploit deep prey resources or to escape predators (Neill et al., 1976; Stevens and Neill, 1978).

The objectives of this investigation were to elucidate vertical movement patterns of and habitat use by skipjack tuna in the equatorial EPO. By examining the behavioral and physiological constraints and environmental variables that define skipjack tuna vertical habitat, we can improve our ecological understanding and provide useful data for inclusion in stock assessments.

Materials and methods

Tag releases

Thirty-three skipjack tuna were captured, tagged, and released during 9–10 April 2004 in close proximity to a Tropical Atmosphere–Ocean (TAO) mooring at 1°59'N 95°19'W in the equatorial EPO. The estimated depth of the seafloor at the TAO mooring was 3091 m. Tagging was conducted on the chartered FV *Her Grace*, a 17.7-m pole-and-line fishing vessel. The tagged fish (tagged from an aggregation estimated at 10 t of skipjack tuna), remained associated with the tagging vessel as it drifted away from the TAO mooring at 0520 h on 11 April 2004 until 0940 h and about 15 km west of the mooring, when the aggregation dispersed as the vessel departed at about a cruising speed of 8 kt.

The archival tags (ATs) used in this study were model LTD_1100 (Lotek Wireless Inc., St. John's, Newfoundland, Canada). The tag is a rectangular solid, measuring 8 mm × 16 mm × 27 mm, and weighing 5 g in air. Information on how to report the recovery of the tag and how to claim the associated reward (US\$50) was printed in Spanish on a label encased in the epoxy of the tag.

Depth and temperature data were stored in the memory of the ATs at 28-s intervals. At this sampling rate, the memory of each AT (64 KB) was capable of storing 10.7 days of data. The maximum depth sensing was 1000 m (with a resolution of 0.4%, and an accuracy of ±1%). The temperature sensing range was from -5° to 35°C, with a resolution of 0.2°C and an accuracy of better than 0.3°C.

Skipjack tuna were captured with fishing rods and reels ($n=18$) and handline gear ($n=9$) equipped with chrome jigs and barbless hooks during the night, and with pole-and-line gear ($n=6$) and by chumming live bait during the day. Each fish was lifted directly into a padded aluminum cradle that was covered with wet smooth vinyl. The fish were placed ventral side up, their eyes were immediately covered with a wet synthetic chamois, the hook was removed, and the condition of the fish was determined. If the fish was in excellent condition (i.e., no damage to the eyes or gills and no significant bleeding), the surgery required for implanting an

AT was initiated. An incision about 2 cm long was made with a sterile surgical scalpel blade in the abdominal wall about 1/3 of the distance between the anus and the base of the pelvic fins and about 2 cm to the left of the centerline of the fish. Special care was taken to cut through the dermis and only partially through the muscle, but not into the peritoneal cavity. A gloved finger was inserted into the incision and forced through the muscle into the peritoneal cavity. The tag, sterilized in Betadine solution, was inserted through the incision into the peritoneal cavity, and a 13-cm length of 64-kg spectra line was tied to the tag that protruded outside. The incision was closed with three staples, by using a surgical staple gun.

After implantation of the AT, each fish was also tagged with one numbered 12.5-cm green plastic dart tag (Hallprint, Victor Harbor, Australia), by using tubular stainless steel applicators. Tags were inserted into the dorsal musculature with the barbed heads passing between the pterygiophores below the base of the second dorsal fin, from either side of the fish.

The 33 skipjack tuna released with ATs were measured to the nearest centimeter (mean=66.9 cm fork length (FL), range: 53–73 cm). The fish were then picked up by hand from the cradle and released back into the ocean. The total time that fish were out of the water was less than 1 min. All fish released with ATs were observed to swim away from the vessel after release, and all appeared to be in good condition.

Tag recoveries

Six of 33 skipjack tuna released in 2004 were recaptured (18.2%), but just five of the archival tags were recovered. Data on the fish lengths, release and recapture dates and locations, numbers of days at liberty, and linear displacements of the six fish are given in Table 1. Recapture locations ranged from 341 km to 2548 km and 123° (southeast) to 260° (west) of the release location. Of the six fish recaptured, four were initially caught by using fishing rods and reels, one by using handline gear, and one by using pole-and-line gear.

Data processing

Data were downloaded from the tags, and initial exploratory data analyses were conducted with software provided by the tag manufacturer. For the five skipjack tuna, the behavior for each day at liberty was classified as associated or unassociated with floating objects, on the basis of behavioral characteristics from ultrasonic telemetry observations of skipjack tuna associated with floating objects (reported by Schaefer and Fuller [2005]). For each day at liberty, surface-oriented and deep diving behavior were also classified. Behavior associated with floating objects was characterized by tunas remaining primarily at depths of less than 50 m during the day. Behavior unassociated with floating objects was defined as the behavior of fish that made 10 or more dives to depths greater than 150 m during the daytime within

Table 1

Release and recapture information for six skipjack tuna (*Katsuwonus pelamis*) from which five archival tags were recovered. Archival tag 6553 was not recovered. The lengths given for each skipjack tuna were those recorded at the time of tagging. The release and recapture locations are given in decimal degrees. The linear displacements, in kilometers and directions (degrees), from the release to the recapture locations are given.

Tag no.	Length (cm)	Release		Recapture		Linear displacement		
		Date	Location	Date	Location	Days at liberty	Kilometers	Direction
4881	67	10 Apr 2004	1.98°N 95.32°W	18 Oct 2004	0.17°S 103.18°W	190	906	255°
4885	68	9 Apr 2004	1.98°N 95.32°W	30 Aug 2004	3.33°S 106.07°W	142	1332	244°
4908	67	9 Apr 2004	1.98°N 95.32°W	14 Nov 2004	2.42°S 117.82°W	218	2548	260°
4930	66	10 Apr 2004	1.98°N 95.32°W	6 May 2004	1.25°S 92.35°W	25	487	137°
6553	68	9 Apr 2004	1.98°N 95.32°W	25 May 2004	4.25°S 92.25°W	45	772	153°
6740	69	9 Apr 2004	1.98°N 95.32°W	21 June 2004	0.33°N 92.73°W	72	341	123°

a 24-h period. Surface-oriented behavior was defined as the behavior of fish that remained less than 10 m below the surface for periods greater than 10 minutes. Deep-diving behavior was defined as the behavior of fish that whose dives exceeded 500 m in depth. The quantitative characteristics describing the different types of behavioral events were derived from the AT records for the five fish.

The AT data sets were separated into periods of nighttime and daytime by the times of nautical twilight. Nighttime was classified as the period between the time of the first evening record after nautical twilight until the time of the last morning record before nautical twilight. The individual data sets for night and day were used in evaluations of diel differences in behavior and in habitat use.

The depth data obtained from the archival tags were analyzed in conjunction with ambient ocean temperatures, as measured by a calibrated Sea-Bird SBE 39 time-temperature-depth probe (Sea-Bird Electronics, Seattle, WA) deployed on 9 April 2004 to about 500 m depth near the TAO mooring at which the fish were tagged and released. For ambient temperatures at depths greater than 500 m we utilized the temperatures measured by a CTD (conductivity-depth-temperature) probe deployed off the National Oceanic and Atmospheric Association (NOAA) ship *Ka'imimoana* by the TAO Project Office (NOAA/Pacific Marine Environmental Laboratory) on 15 April 2004 to 1000 m depth near the same TAO mooring. These two temperature-depth profiles to depths of about 500 m, obtained from hydrocasts conducted six days apart, were virtually identical.

Results

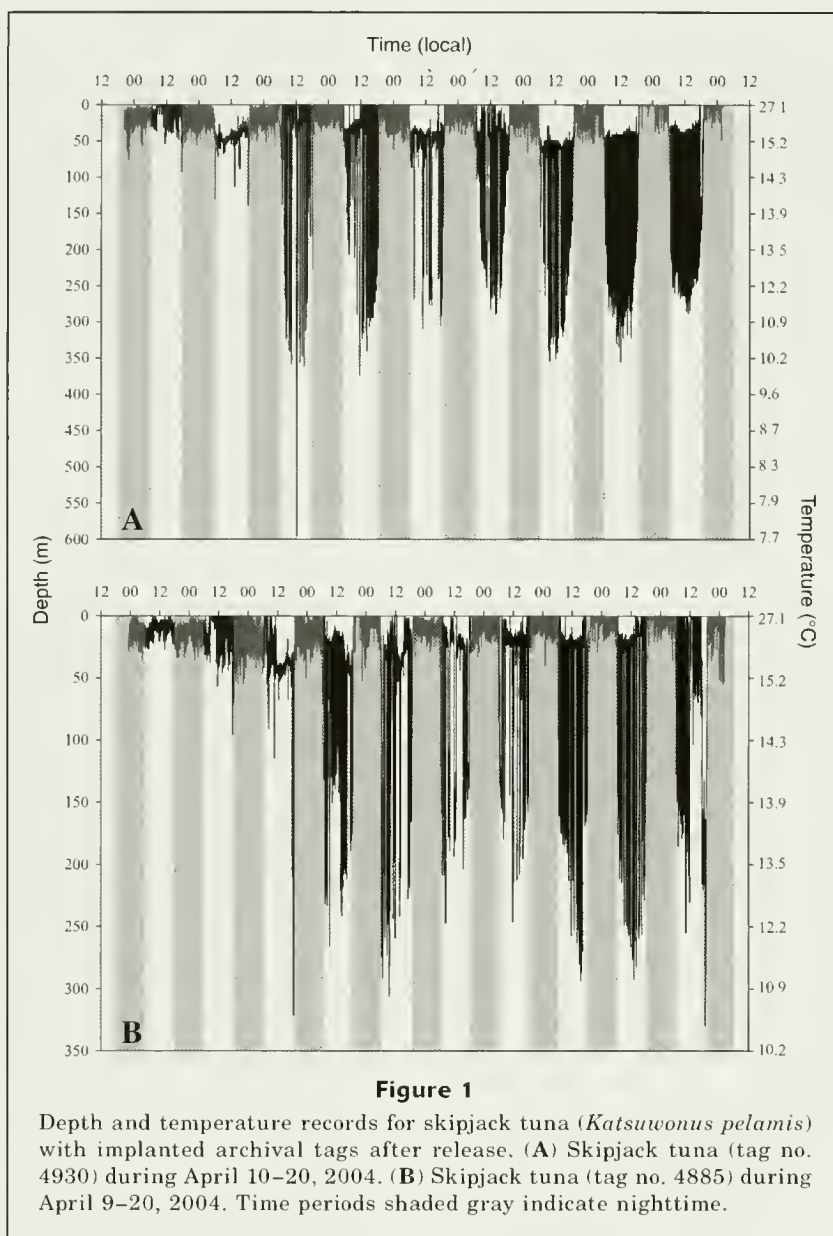
Behavior patterns

Evaluations of the complete AT depth records, which ranged from 9.3 to 10.1 days, for the five skipjack tuna

(Table 1; tag numbers: 4881, 4885, 4908, 4930, 6740) indicated that all five fish remained associated with the drifting vessel, following separation from the TAO mooring, until the vessel departed the area at 0940 h on 11 April 2004. Within 48 h of the time of separation, all five fish demonstrated distinct behavior unassociated with a floating object, including repetitive bounce diving during the day, and for each of the six subsequent days of the AT depth records. The variability in the daytime unassociated behavior patterns for each of the five fish during the approximate 8 days of AT depth records, following separation from the vessel, indicated that all five fish did not remain together.

The depth records for two representative fish (Fig. 1) showed similarities for both day and night for the first 48-h period, including a change in behavior when the vessel departed. The following day, both fish showed deeper average swimming depths, and the day after that both fish began to show repetitive bounce-diving behavior which continued for the remaining 7 days. The first day in which bounce diving occurred for a skipjack tuna (tag no. 4930), included the deepest dive, to a depth of 596 m, recorded for any of the five fish. During the last 3 days of depth records, in addition to the distinct diel differences seen for both fish, the average depth after a dive for the fish with tag 4930 (mean=47.1 m, 95% confidence interval (CI)=1.1) was significantly deeper (ANOVA: $F=3.9$, $P<0.05$) than for the fish with tag 4885 (mean=20.3 m, 95% CI=3.7). These depth differences and behavior patterns indicate that these two similar-size skipjack tuna did not remain together for long after their separation from the vessel.

Evaluations of the depth records for the five skipjack tuna carrying ATs in the equatorial EPO resulted in the discrimination of four distinct behaviors: 1) behavior associated with floating objects (abbreviated to "associated behavior" in this article; 2) behavior unassociated with floating objects (abbreviated to "unassociated behavior", 3) deep diving behavior, and 4) surface-oriented behavior. For the five archival tag data



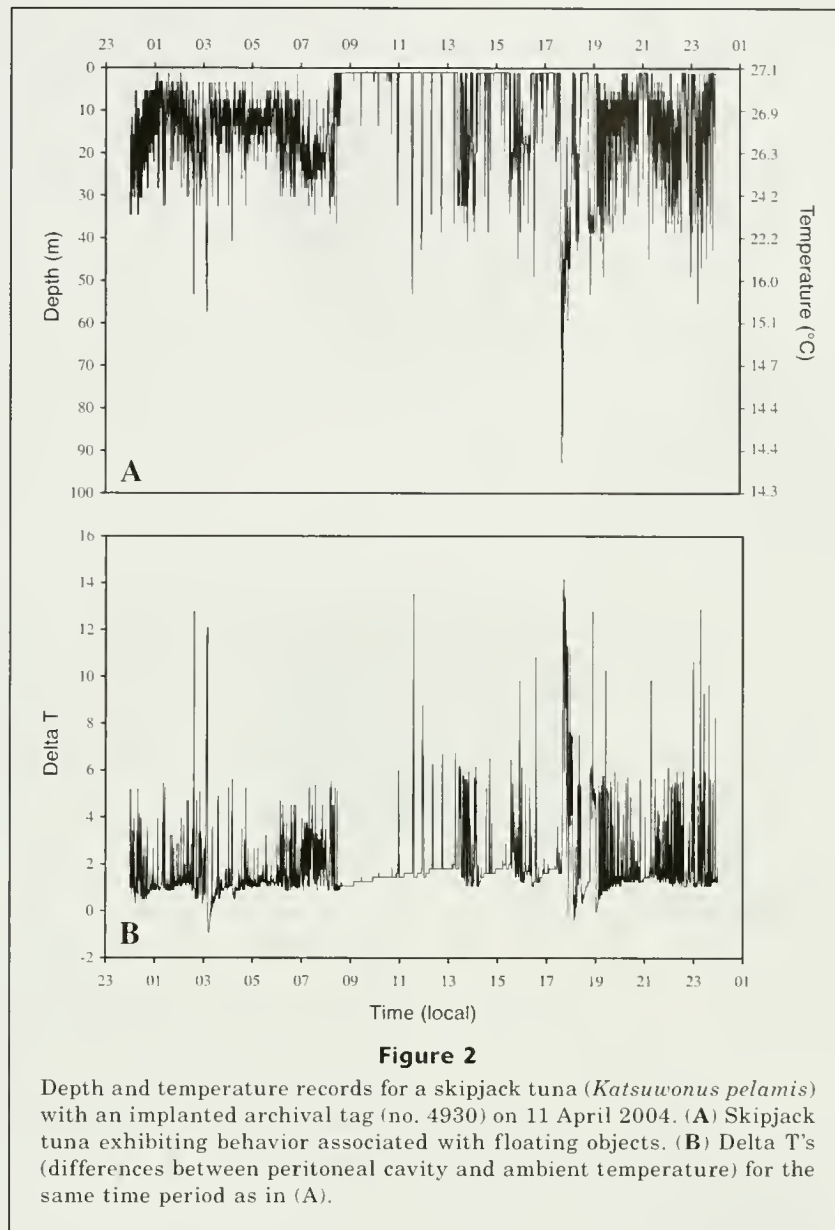
sets, behavior types 1, 2, 3, and 4 were evaluated for each day at liberty, and the descriptive characteristics presented.

Behavior associated with floating objects

The behaviors of the skipjack tuna released at the TAO mooring were distinct and discernible from the behaviors 48 h after the tuna separated from the mooring and the vessel. When the fish were associated with the mooring and the vessel, they remained primarily between the surface and 50 m during the night and day (Fig. 2A). The mean swimming depths were 13.6 m (range: 1–57.4 m) at night and 10.8 m (range: 1–92.3 m) during the day. Shortly before dusk, several dives to about 90 m were recorded, which were followed by an apparent change in

the vertical movements during the night. The greater frequency of vertical movements observed during the night (1900 h to 0700 h) within the mixed layer probably represented foraging activity on prey organisms of the deep-scattering layer (DSL).

The delta T values, differences between the peritoneal cavity temperatures and the ambient temperatures (Fig. 2B), corresponding to the simultaneous depth records (Fig. 2A), showed an average of 2.2°C (95% CI=0.1°C, range: -0.4 to 14.1°C) during the day, and an average of 1.8°C (95% CI=0.1°C, range: -0.9 to 12.9°C) during the night. The depths of the mixed layer and the thermocline (depth of the 20°C isotherm) (Fiedler, 1992) were approximately 15 and 44 m, respectively. Whenever skipjack tunas made dives in excess of the thermocline depth, the delta T values were observed



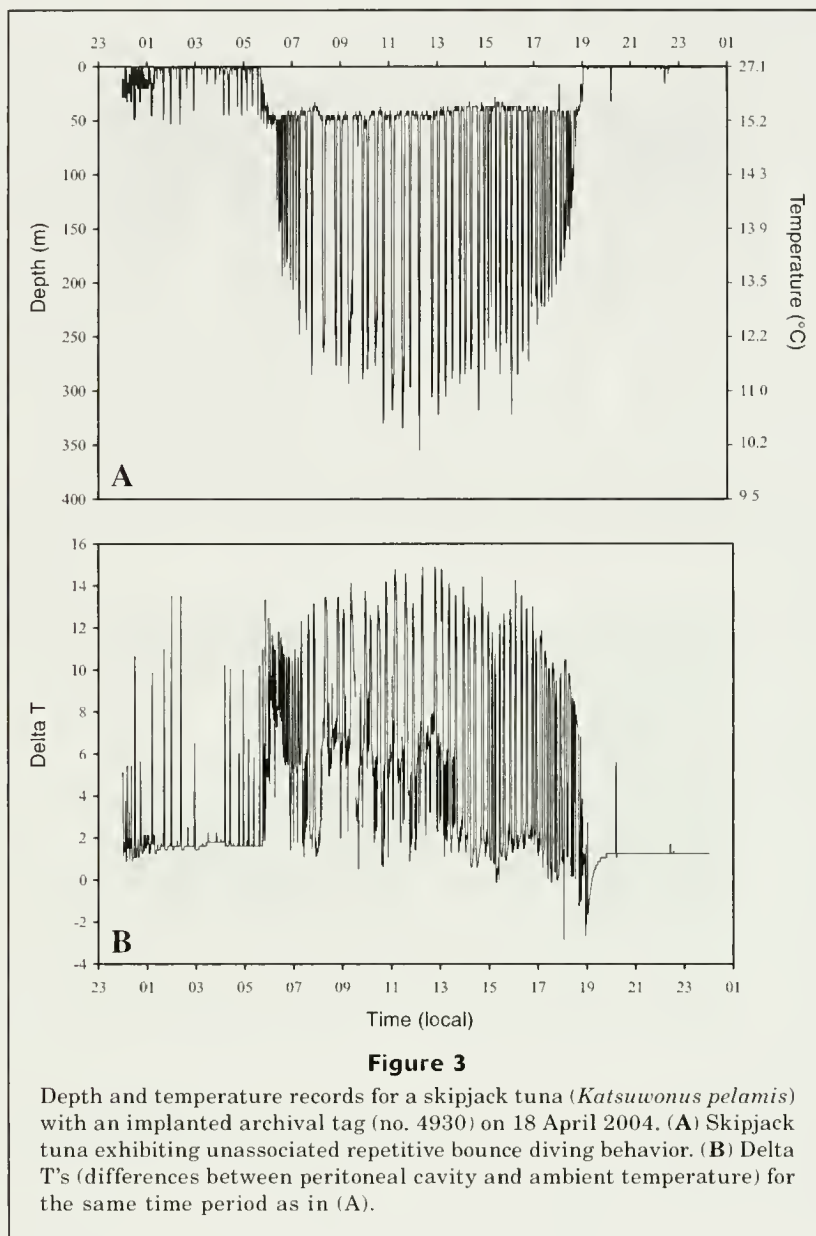
to spike upward, indicative of the thermal excess of the peritoneal cavity in relation to the ambient temperature.

Behavior unassociated with floating objects

Within 48 hours after the skipjack tuna were unassociated with the vessel, they showed a distinct change in their vertical movements and behavior, exhibiting repetitive bounce diving between about 50 and 300 m during the day (Figs. 1 and 3A). They remained close to the surface at night, primarily within 50 m, showing distinct diel differences in behavior. Figure 3A shows 50 dives in excess of 150 m, and an average duration of 6.8 min (range: 3 to 17 min). The mean depth of these dives was 257 m (range: 153–355 m). During ascents

following dives the fish returned to an average depth of 44 m, the approximate depth of the thermocline, before undertaking another dive. The delta T values (Fig. 3B), corresponding to the simultaneous depth records (Fig. 3A), showed an average of 1.9°C (95% CI=0.09°C, range: 0.8–13.5°C) during the night when the fish were primarily in the mixed layer. The delta T values during the day corresponding to the maximum depths of bounce dives were an average of 12.2°C (95% CI=0.3°C, range: 10.2–13.9°C). At the maximum depths of these bounce dives, the mode of the minimum ambient temperature experienced was 11.7°C and the peritoneal cavity temperature was 25.1°C.

For the five skipjack tuna, during days of unassociated repetitive bounce diving behavior, the mode for the time the first dive of the day occurred was 07:10 h (95%



CI=00:25 h) (Fig. 4A), the mean number of dives made per day was 21.2 (95% CI=4.9) (Fig. 4B), the mean duration of dives was 10.0 min (95% CI=0.9 min), and the mean depth of all dives was 230 m (95% CI=5.7) (Fig. 4C).

One skipjack tuna (tag no. 4885) made an extraordinary dive below the thermocline that lasted 119 min at 1700 h on 19 April 2004. From a depth of 36 m (22.3°C) with a peritoneal cavity temperature of 24.1°C, the fish dived to about 180 m (13.7°C) where it presumably foraged for 1 h 12 min. The fish then dived fairly rapidly to a maximum depth of 330 m (10.5°C) from which it gradually ascended toward the surface, remaining below the thermocline for another 47 min. From echosounder data collected aboard the vessel, it appeared that this fish was tracking the slowly ascending DSL

and foraging on prey during this period. The minimum peritoneal cavity temperature observed in this study of 15.9°C was recorded continuously over a period of 7 minutes as this skipjack tuna ascended from 197 to 105 m depth.

Deep diving behavior

Only one of the five skipjack tuna (tag no. 4930) dived in excess of 500 m on 13 April 2004, beginning at 12:16 (Fig. 5). The maximum depth was 596 m, with a duration of 14 min in excess of 300 m (11.0°C), and 1 min 52 seconds in excess of 500 m (8.3°C). The dive profile shows that the fish dived initially to about 300 m where it remained for 4 minutes before continuing to 596 m and returning after about 2 minutes to between

300 m and 250 m, where it remained for about 12 minutes before returning to depths within the mixed layer. The peritoneal cavity temperature and delta T were 28.7°C and 3.8°C, respectively, at the beginning of the dive, 26.1°C and 18.4°C at the bottom of the dive, and 21.8°C and 9.8°C before the quick ascent at 12:38 h from 271 m to above the thermocline.

Surface-oriented behavior

For unassociated behavior, the mean number of surface-oriented events per day ranged from 5 to 23 (grand mean=9.4, 95% CI=2.4). The greatest number and longest duration of surface-oriented events occurred between 01:00 and 12:00 h (Fig. 6, A and B). The duration of events ranged from 10 to 214 min (mean=48.8 min, 95% CI=6.2 min) (Fig. 6 C).

Vertical habitat use

The vertical habitat use by the five skipjack tuna, for unassociated behavior, is presented as composite distributions by night and day along with the thermal profile in Figure 7. The vertical habitat-use distributions indicated that the fish remained above the depth of the thermocline (44 m) during the night 98.6% of the time but spent 37.7% of their time below the thermocline during the day.

Discussion

The results obtained in our study are useful for evaluating vertical movement patterns and habitat use for skipjack tuna on temporal scales previously undocumented. Knowledge about skipjack tuna movements, behavior, and habitat use, when tuna are associated and unassociated with floating objects, specifically in oceanic regions where large-scale industrial purse-seine fisheries operate, are important for understanding the ecology of this species, assessing catchability of the species for inclusion in stock assessments, and for evaluating potential modifications in fishing techniques for reduction of the bycatches of nontarget species.

In the present study, the vertical movement patterns of skipjack tuna when associated with floating objects were similar to those reported by Schaefer and Fuller (2005) for both skipjack and bigeye (*Thunnus obesus*) tunas associated with floating objects in the equatorial EPO. In both studies, the behavior of skipjack tuna was characterized by swimming depths predominantly shallower than the depth of the thermocline, throughout the day and night, and average nighttime depths were slightly deeper than those during the day. A plausible explanation for the greater average depths at night than during the day in these studies is the observed nighttime vertical distribution of the DSL and the foraging behavior of these tunas while associated with the moored buoys and the drifting vessel in this study area (Schaefer and Fuller, 2005). Ultrasonic telemetry

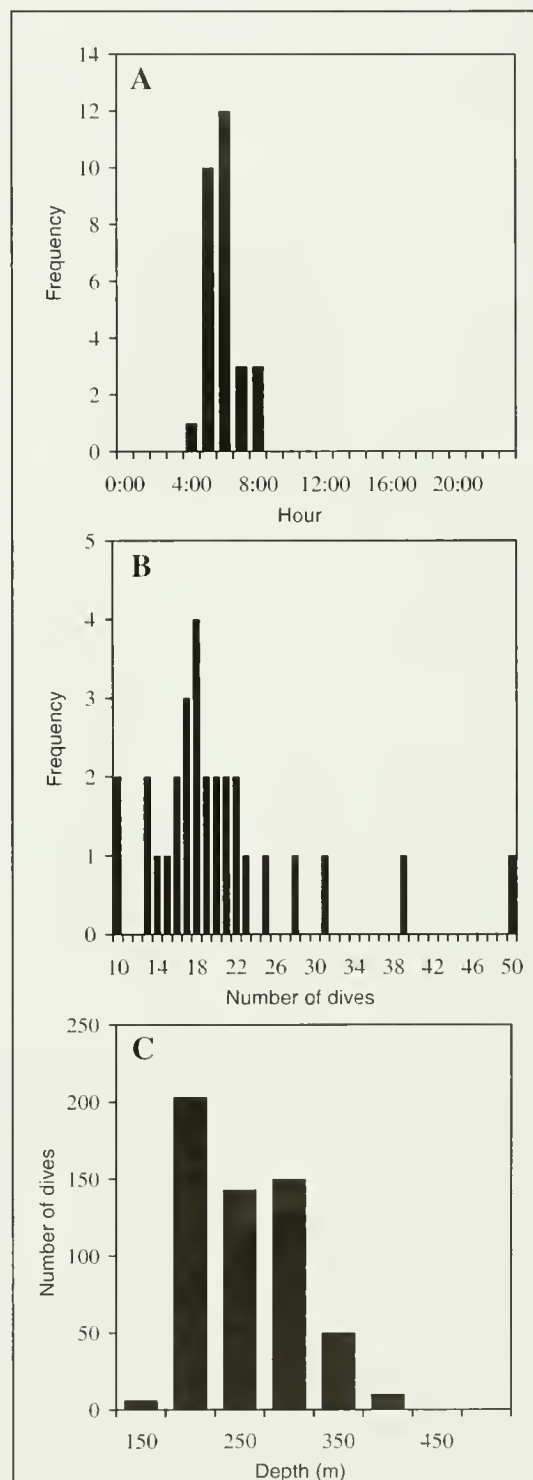
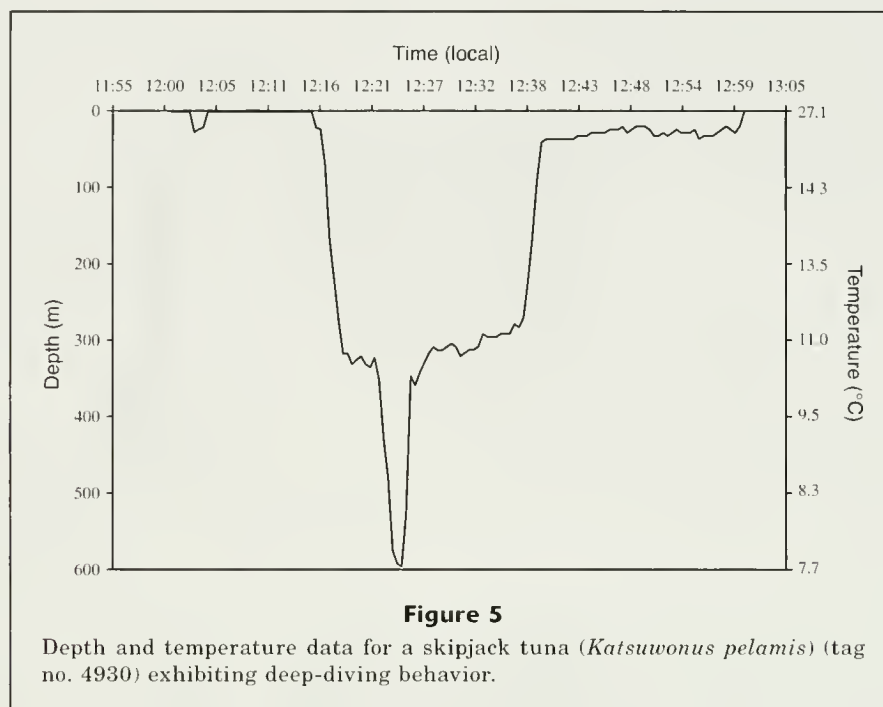


Figure 4

Summary of frequency data for repetitive bounce diving behavior not associated with floating objects for five skipjack tuna (*Katsuwonus pelamis*) over all dives. (A) Time the first dive of the day occurred. (B) Total number of dives for each day. (C) Depth of all dives.



studies on the simultaneous behavior of skipjack, big-eye, and yellowfin (*Thunnus albacares*) tunas associated with drifting fish aggregation devices in the central Pacific Ocean also revealed that skipjack tuna swimming depths are predominantly shallower than the thermocline depth, about 115 m, throughout the day and night, but average nighttime depths are shallower than those during the daytime (Matsumoto et al.¹).

The vertical movement patterns observed in this study for unassociated behavior of skipjack tuna, seen mostly as relatively high frequency repetitive bounce diving between dawn and dusk, was unexpected on account of the data from previously published studies (Matsumoto et al., 1984). There are, however, most likely other vertical movement patterns for skipjack tuna when unassociated with floating objects, from that observed in the present study. This pattern is probably dependent on the spatial and temporal habitat as well as forage availability. In the first published paper on acoustic tracking of tunas (Yuen, 1970), ultrasonic transmitters were used to study the behavior and movements of skipjack tuna off Hawaii. One individual, tracked for 8 days, undertook daily cyclical movements away from and back to a bank at consistent times, and from these movements Yuen (1970) first suggested that skipjack tuna can navigate and have a sense of time. The method Yuen (1970) used was suitable only to conclude that the fish remained close to the surface at night but could be found at various depths during the day. In a subsequent tracking study in Hawaiian waters, three skipjack tuna tagged with ultrasonic transmitters spent time between the surface (23.5°C) and 263 m (13.5°C) during the day, but remained above 75 m (22°C) depth at night (Dizon et al., 1978). Vertical positions of the

skipjack tuna were determined only every 3 minutes, but indicated many rapid vertical movements, including some to depths below the thermocline. Although the three tracked skipjack tuna spent 85% of the time in water above 20°C (about 160 m), there were brief dives to temperatures between 12° and 14°C. The data retrieved from seven archival tags recovered from skipjack tuna released off northern Japan indicated that their nighttime movements were normally between the surface and depths of about 30 m, but during the daytime they exhibited frequent dives to depths below the thermocline and below ambient temperatures of 12°C; the greatest depth was reported to be 267 m (Ogura²). The lowest peritoneal cavity temperatures recorded in that study were around 17°C, whereas in the present study it was about 16°C. Skipjack tuna held in land-based tanks in Hawaii subjected to gradually lowered temperatures resulted in one mortality at 17°C, and none survived at 15°C for more than a few hours (Dizon et al., 1977).

A relatively dense DSL was observed at night on the echosounder during the time the skipjack tuna were associated with the vessel in this study. Skipjack tuna associated with a TAO mooring in this study area have been documented to be feeding at night near the surface on prey organisms of the DSL (Schaefer and Fuller, 2005). The repetitive bounce diving observed in the present study for unassociated skipjack tuna during the day apparently reflects foraging activity on prey organisms of the diurnally migrating DSL (Kuznetsov et al., 1982). The profile in Figure 3A of repetitive bounce diving shows a higher frequency of dives during the first hour at around dawn when the DSL is descending and during the 1.5 h period preceding dusk during

the ascent of the DSL. Sonic tracking studies have also shown that the diel vertical migrations of bigeye tuna are closely associated with vertical movements of organisms of the DSL (Josse et al., 1998; Dagorn et al., 2000). When in areas with a high density DSL it appeared that skipjack tuna were also commonly foraging on DSL prey organisms near the surface at night and at depths well below the thermocline during the day. Depths of the DSL in the eastern tropical Pacific have been reported to be 300–400 m during the day and 0–100 m at night (Fiedler et al., 1998). Variation in daytime DSL depths is probably a function of light penetration (which is regulated by biological production) and absorption of light by chlorophyll and phaeopigments (Tont, 1976).

The depths and temperatures to which skipjack tuna were repetitively bounce diving during the day in this study were mostly between 200 to 300 m and 10.9° to 13.5°C, respectively. In the same general area of the equatorial EPO, bigeye tuna unassociated with floating objects have been reported to undertake prolonged dives to similar depths and temperatures during the day to forage on DSL prey organisms (Schaefer and Fuller, 2002). A recent study of yellowfin tuna behavior off northern Mexico in the EPO, based on archival tag data, has revealed that yellowfin tuna are also capable of exploiting the vertical habitat below the thermocline by repetitively bounce diving during the day between about 150 and 250 m and between 11°C and 13.5°C, respectively (Schaefer et al., in press).

An ecological benefit of endothermy in tunas is an expanded thermal niche, including exploitation of vertical habitat by skipjack tuna (Block, 1991; Graham and Dickson, 2001). There are several anatomical and physiological differences between skipjack and bigeye tunas (Brill and Bushnell, 2001; Graham and Dickson, 2001) that would explain why skipjack, unlike large bigeye (Holland and Sibert, 1994), are unable to remain for extensive periods at optimal foraging depths below the thermocline. Instead they exhibit repetitive bounce diving behavior to employ both behaviorally and physiologically induced thermoregulation for partial independence from cold water effects on temperature-dependent functions (Graham and Dickson, 2004). Thermal inertia also helps stabilize body temperatures during dives, and larger bigeye tuna have been shown to have slower cooling rates than smaller individuals (Schaefer and Fuller, 2002). The heart rates of tunas are reduced by lower temperatures and hypoxia; therefore excursions below the thermocline may be limited by the diminished capacity of the heart to supply the oxygen requirements of the endothermic tissues (Brill and Bushnell, 2001; Blank et al., 2004).

Skipjack tuna surface-oriented behavior was observed in this study to occur primarily between 0100 h and 1200 h. Skipjack tuna within large multispecies aggregations associated with floating objects have previously been reported to show monospecific horizontal separation and “breezing” (rippling of the water surface) behavior near dawn (Schaefer and Fuller, 2005). Informa-

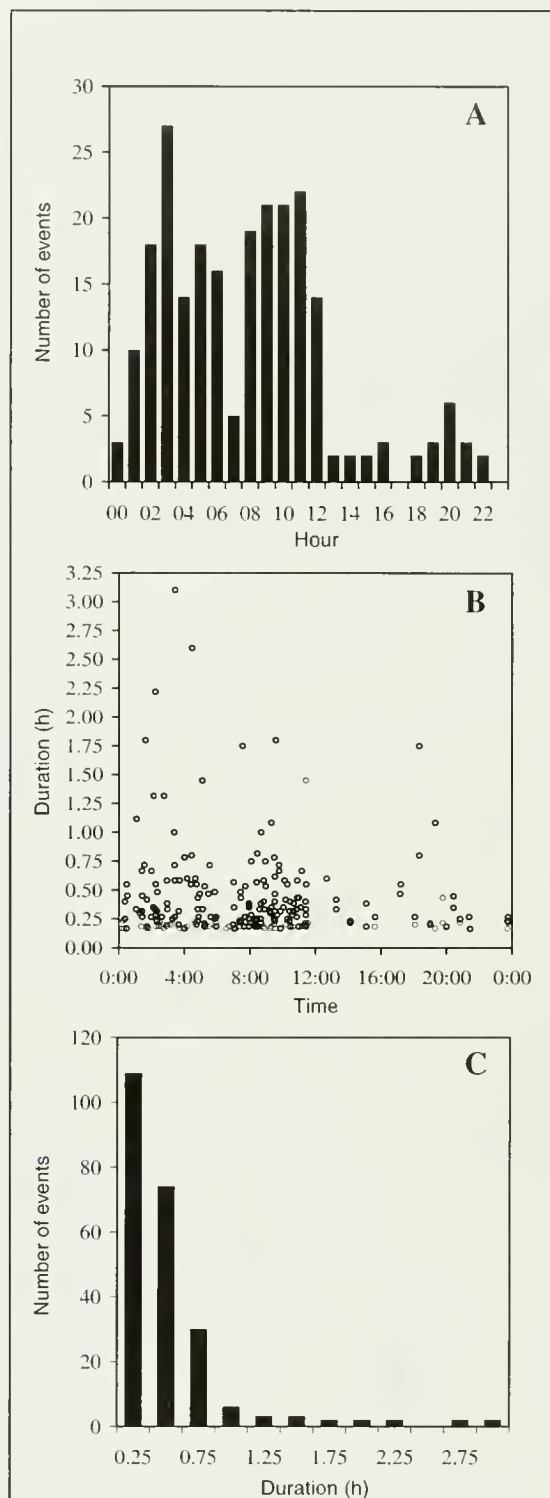


Figure 6

Summary of surface-oriented events for skipjack tuna (*Katsuwonus pelamis*). (A) Hour of the day at which the events occurred. (B) Beginning time and duration of each event. (C) Duration of events.

tion on surface-oriented behavior of skipjack is relevant to understanding catchability (vertical vulnerability plus spatial vulnerability) by purse-seine vessels and may be useful to incorporate into the standardization of catch and effort data. In addition, this information on occurrence and duration of surface-oriented behavior is useful for evaluating optimal detection periods for the use of remote-sensing techniques for conducting fisheries-independent abundance estimation of this species with the use of airborne optical equipment, including LIDAR (light detection and ranging) (Gauldie et al., 1997).

Large-scale studies with archival tags are needed to improve our understanding of skipjack tuna movements, behavior, and habitat use, all of which, in turn, will provide useful information for stock assessments of this valuable resource. Elucidating skipjack tuna behavior may also permit the design of optimal fishing strategies for this species, including the reduction

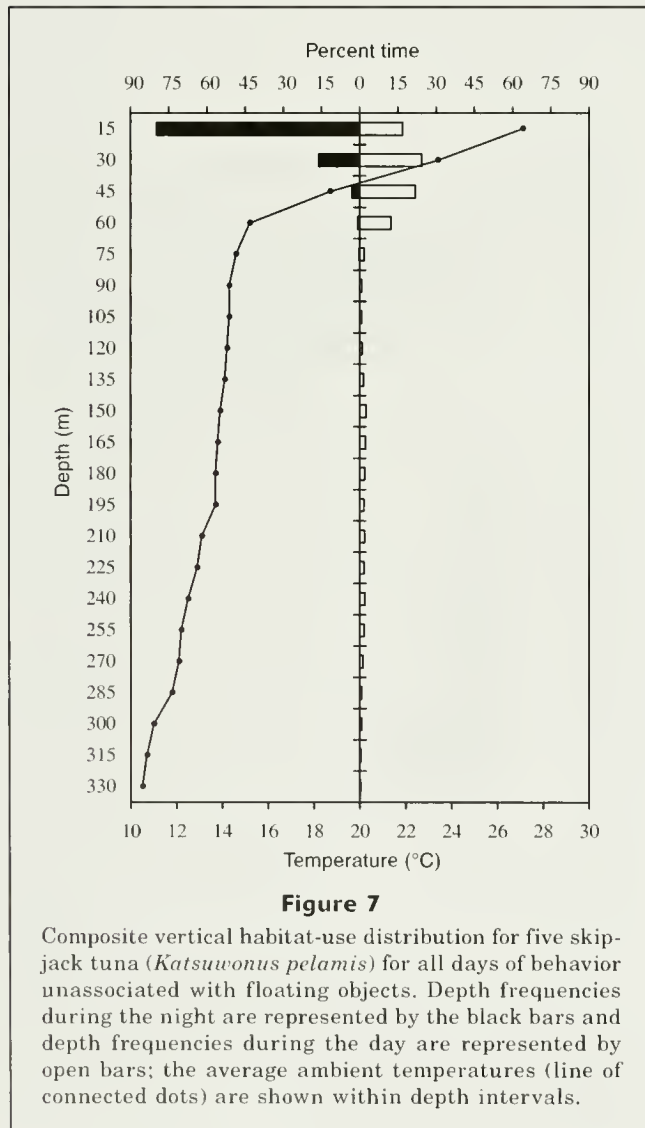
of current bycatch levels associated with purse-seine fishing around floating objects. Archival tags are now capable of storing data for multiple years; this capacity provides a remarkable opportunity to evaluate ontogenetic changes and the influence of seasonal and annual environmental variability on the behavioral characteristics of tuna.

Acknowledgments

This research was made possible through financial contributions by the Japan Fisheries Agency, Taiwan Fisheries Agency, and the United States Tuna Foundation. We are grateful to vessel owners, captains, fishermen, unloaders, industry representatives, and Inter-American Tropical Tuna Commission field office staff in Ecuador for assistance in recovering the archival tags. We appreciate the constructive comments on drafts of the manuscript provided by W. Bayliff, E. Calvert, A. Moles, M. Scott, and three anonymous reviewers.

Literature cited

- Altringham, J. D., and R. E. Shadwick.
2001. Swimming and muscle function. *In* Tuna physiology, ecology, and evolution. Fish physiology series, vol. 19 (B. A. Block, and E. D. Stevens, eds.), p. 313–344. Academic Press, San Diego, CA.
- Anonymous.
2005. Tunas and billfishes in the eastern Pacific Ocean in 2004. Fishery Status Report No. 3. Inter-Am. Trop. Tuna Comm., 119 p.
- Blank, J. M., J. M. Morrisette, A. M. Landeira-Fernandez, S. B. Blackwell, T. D. Williams, and B. A. Block.
2004. In situ cardiac performance of Pacific bluefin tuna hearts in response to acute temperature change. *J. Exp. Biol.* 207:881–890.
- Block, B. A.
1991. Endothermy in fish: thermogenesis, ecology, and evolution. *In* Biochemistry and molecular biology of fishes, vol. 1 (P. W. Hochachka, and T. P. Mommsen, eds.), p. 269–311. Elsevier Publishing, New York, NY.
- Brill, R. W., and P. G. Bushnell.
2001. The cardiovascular system of tunas. *In* Tuna physiology, ecology and evolution, Fish physiology series, vol. 19 (B. A. Block, and E. D. Stevens, eds.), p. 79–120. Academic Press, San Diego, CA.
- Collette, B. B., and C. E. Nauen.
1983. FAO species catalogue. Vol. 2: Scombrids of the world: an annotated and illustrated catalogue of tunas, mackerels, bonitos, and related species known to date. FAO Fish. Synop. 125, 137 p. FAO, Rome.
- Dagorn, L., P. Bach, and E. Josse.
2000. Movement patterns of large bigeye tuna (*Thunnus obesus*) in the open ocean, determined using ultrasonic telemetry. *Mar. Biol.* 136:361–371.
- Dizon, A. E., and R. W. Brill.
1979. Thermoregulation in tunas. *Am. Zool.* 19:249–265.
- Dizon, A. E., R. W. Brill, and H. S. H. Yuen.
1978. Correlations between environment, physiology, and activity and the effects on thermoregulation in



- skipjack tuna. *In* The physiological ecology of tunas (G. D. Sharp, and A. E. Dizon, eds.), p. 233–259. Academic Press, New York, NY.
- Dizon, A. E., W. H. Neill, and J. J. Magnuson.
1977. Rapid temperature compensation of volitional swimming speeds and lethal temperatures in tropical tunas (Scombridae). *Environ. Biol. Fish.* 2:83–92.
- Fiedler, P. C.
1992. Seasonal climatologies and variability of eastern tropical Pacific surface waters. NOAA Tech. Rep. NMFS 109, 65 p.
- Fiedler, P. C., J. Barlow, and J. Gerrodette.
1998. Dolphin prey abundance determined from acoustic backscatter data in eastern Pacific surveys. *Fish. Bull.* 96:237–247.
- Gauldie, R. W., S. K. Sharma, and C. E. Helsey.
1997. LIDAR applications to fisheries monitoring problems. *Can. J. Fish. Aquat. Sci.* 53:1459–1468.
- Godsil, H. C., and R. D. Byers.
1944. A systematic study of the Pacific tunas. *Calif. Div. Fish Game, Fish Bull.* 60, 131 p.
- Graham, J. G.
1975. Heat exchange in the yellowfin tuna, *Thunnus albacares*, and skipjack tuna, *Katsuwonus pelamis*, and the adaptive significance of elevated body temperatures. *Fish. Bull.* 72:219–229.
- Graham, J. B., and K. A. Dickson.
2001. Anatomical and physiological specializations for endothermy. *In* Tuna physiology, ecology, and evolution, Fish physiology series, vol. 19 (B. A. Block, and E. D. Stevens, eds.), p. 121–165. Academic Press, San Diego, CA.
2004. Tuna comparative physiology. *J. Exp. Biol.* 207:4015–4024.
- Holland, K. N., and J. R. Sibert.
1994. Physiological thermoregulation in bigeye tuna, *Thunnus obesus*. *Environ. Biol. Fish.* 40:319–327.
- Josse, E., P. Bach, and L. Dagorn.
1998. Simultaneous observations of tuna movements and their prey by sonic tracking and acoustic surveys. *Hydrobiologia* 371/372:61–69.
- Kuznetsov, I. L., S. R. Stefanov, and V. I. Savagov.
1982. A migrating sound scattering layer in the equatorial Pacific Ocean. *Oceanology* 22:702–703.
- Magnuson, J. J.
1969. Digestion and food consumption by skipjack tuna (*Katsuwonus pelamis*). *Trans. Am. Fish. Soc.* 98:379–392.
1978. Locomotion by scombrid fishes: hydromechanics, morphology, and behavior. *In* Fish physiology series, vol. 7 (W. S. Hoar, and D. J. Randall, eds.), p. 239–313. Academic Press, New York, NY.
- Matsumoto, W. M., R. A. Skillman, and A. E. Dizon.
1984. Synopsis of biological data on skipjack tuna, *Katsuwonus pelamis*. NOAA Tech. Rep. NMFS Circ. (451), 92 p.
- Neill, W. H., R. K. C. Chang, and A. E. Dizon.
1976. Magnitude and ecological implications of thermal inertia in skipjack tuna, *Katsuwonus pelamis* (Linnaeus). *Environ. Biol. Fish.* 1:61–80.
- Schaefer, K. M., and D. W. Fuller.
2002. Movements, behavior, and habitat selection of bigeye tuna (*Thunnus obesus*) in the eastern equatorial Pacific, ascertained through archival tags. *Fish. Bull.* 100:765–788.
2005. Behavior of bigeye (*Thunnus obesus*) and skipjack (*Katsuwonus pelamis*) tunas within aggregations associated with floating objects in the equatorial eastern Pacific. *Mar. Biol.* 146:781–792.
- Schaefer, K. M., D. W. Fuller, and B. A. Block.
In press. Movements, behavior, and habitat utilization of yellowfin tuna (*Thunnus albacares*) in the north-eastern Pacific Ocean, ascertained through archival tag data. *Mar. Biol.*
- Stevens, E. D., H. M. Lam, and J. Kendall.
1974. Vascular anatomy of the counter-current heat exchanger of skipjack tuna. *J. Exp. Biol.* 61:145–153.
- Stevens, E. D., and W. H. Neill.
1978. Body temperature relations of tunas, especially skipjack. *In* Fish physiology series, vol. 7 (W. H. Hoar, and D. J. Randall, eds.), p. 316–359. Academic Press, New York, NY.
- Tont, S. A.
1976. Deep scattering layers: patterns in the Pacific. *Calif. Coop. Ocean Fish. Investig. Rep.* 18:112–117.
- Wild, A., and J. Hampton.
1994. A review of the biology and fisheries for skipjack tuna, *Katsuwonus pelamis*, in the Pacific Ocean. *FAO Fish. Tech. Pap.* 336(2):1–51.
- Yabe, H., Y. Yabuta, and S. Ueyanagi.
1963. Comparative distribution of eggs, larvae and adults in relation to biotic and abiotic environmental factors. *FAO Fish. Rep.* 6(3):979–1009.
- Yuen, H. S. H.
1970. Behavior of skipjack tuna, *Katsuwonus pelamis*, as determined by tracking with ultrasonic devices. *J. Fish. Res. Board Can.* 27:2071–2079.

Abstract—The northern bluefin tuna (*Thunnus thynnus*) is a highly mobile apex predator in the Gulf of Maine. Despite current stock assessments that indicate historically high abundance of its main prey, Atlantic herring (*Clupea harengus*), commercial fishermen have observed declines in the somatic condition of northern bluefin tuna during the last decade. We examined this claim by reviewing detailed logbooks of northern bluefin tuna condition from a local fishermen's co-operative and applying multinomial regression, a robust tool for exploring how a categorical variable may be related to other variables of interest. The data set contained >3082 observations of condition (fat and oil content and fish shape) from fish landed between 1991 and 2004. Energy from stored lipids is used for migration and reproduction; therefore a reduction in energy acquisition on bluefin tuna feeding grounds could diminish allocations to growth and gamete production and have detrimental consequences for rebuilding the western Atlantic population. A decline in northern bluefin tuna somatic condition could indicate substantial changes in the bottom-up transfer of energy in the Gulf of Maine, shifts in their reproductive or migratory patterns, impacts of fishing pressure, or synergistic effects from multiple causes.

Decline in condition of northern bluefin tuna (*Thunnus thynnus*) in the Gulf of Maine

Walter J. Golet (contact author)¹

Andrew B. Cooper¹

Robert Campbell²

Molly Lutcavage¹

Email address for W. J. Golet: wgolet@cisunix.unh.edu

¹ Large Pelagics Research Center, Room 177
Spaulding Hall, College Rd.
University of New Hampshire
Durham, New Hampshire 03824

² Yankee Fisherman's Co-op
Seabrook, New Hampshire 03874

The Gulf of Maine is a highly productive region of the northwest Atlantic where substantial aggregations of forage fish attract northern bluefin tuna (*Thunnus thynnus*) and other top predators, including sharks, marine mammals, and seabirds. Atlantic herring (*Clupea harengus*), Atlantic mackerel (*Scomber scomber*), and sand lance (*Ammodytes dubius*) form a major part of this prey base (Bigelow and Schroeder, 1953). As seasonal migrants, northern bluefin tuna arrive in the Gulf of Maine in limited numbers in late May and early June (Bigelow and Schroeder, 1953; Mather et al., 1995). Fish landed in the Gulf of Maine during June and early July are typically lean and have little to no perigonadal or body fat reserves (Estrada et al., 2005; Goldstein et al., in press). Presumably, energy stores of mature northern bluefin tuna entering the Gulf of Maine have been exhausted after spawning, a time when shifts in fat and energy stores are pronounced (Mourente et al., 2001) and mesenteric lipid stores are used for gametogenesis and for subsequent migration to feeding grounds.

Given its size, speed, and wide thermal tolerance, the northern bluefin tuna is a formidable predator, capable of exploiting diverse prey species. Having visceral retes that warm the stomach (Carey et al., 1971) and digestive enzymes with

fast turnover rates, northern bluefin tuna can rapidly process prey (Stevens and McLeese, 1984). During the 1950s and 1970s, individual northern bluefin tuna gained 7% (Rivas, 1955) and 10% (Butler¹), respectively, of their body mass per month on the northwest Atlantic feeding grounds. The majority of this mass gain was reflected in the accumulation of intramusculature and perigonadal fat stores, which presumably provide the necessary reserves for migration to the spawning grounds and subsequent gamete production following their departure from the Gulf of Maine in late September to mid November (Lutcavage and Kraus, 1995; Wilson et al., 2005).

Recent observations by fishermen, brokers, and co-operative managers have identified two declining trends in the Gulf of Maine commercial northern bluefin tuna fishery. First, there appears to be fewer mature fish now than in the last decade. Hundreds of surface schools were detected

Manuscript submitted 23 June 2006 to the Scientific Editor's Office.

Manuscript approved for publication 16 January 2007 by the Scientific Editor.
Fish. Bull. 105:390–395 (2007)

¹ Butler, M. J. A. 1974. Prince Edward Island bluefin tuna research program 1974. Prince Edward Island marine fisheries and training center and department of tourism, parks, and conservation, Prince Edward Island, 65 p. Agriculture, Fisheries and Aquaculture P. O. Box 2000, Charlottetown, Prince Edward Island, Canada C1A7N8.

annually between 1994 and 1996 in aerial surveys (Lutcavage and Kraus, 1995), but catches in 2004 and 2005 decreased dramatically, and only 30% of the commercial quota was landed in the New England region. Second, coincident with the reduction in catch, over the past decade fishermen and dealers have reported a decline in fish quality irrespective of season. Fish landed in September and October had the same somatic condition as those landed in June, indicating that northern bluefin tuna are not establishing the fat reserves they once did. Given that energy allocation is a key factor in growth, maturation, reproduction, and migration in long-lived fishes (Marshall et al., 1999; Rideout et al., 2005; Jørgenson et al., 2006), a decline in the somatic condition of northern bluefin tuna would be expected to affect the population.

Catch rates of highly migratory species, especially northern bluefin tuna, have fluctuated over the years in many different regions of the world (Anderson and Piatt, 1999; Ravier and Fromentin, 2001). These top pelagic predators may have altered their distribution because of environmental shifts (Anderson and Piatt, 1999), or may have suffered localized depletion because of fishing pressures (Tiews, 1978; Fromentin and Powers, 2005). Although these causes may explain why northern bluefin tuna distribution or abundance in the Gulf of Maine has changed, they do not account for the apparent decline in quality of those fish remaining in the area. In this study, we examined records of the fat and oil content and shape of northern bluefin tuna captured in the Gulf of Maine from 1991 to 2004 in order to investigate whether the observations of a decline in quality (as advanced by commercial fishermen and dealers) represents a significant change in somatic condition of these fish.

Materials and methods

Fish condition is most often assessed through the use of Fulton's *K* or linear regression, both of which give a quantitative value to the physical condition of fish. Such analyses were not possible in this study because individual lengths and weights were not recorded for many of the fish. As a substitute, we used grade data from brokers in the commercial northern bluefin tuna fishery who grade every fish before purchase. This procedure is quite involved and often requires schooling or an apprenticeship to learn the trade. Grading involves a qualitative assessment of the condition of fish, defined by the characteristics of freshness, color, fat and oil content, and fish shape (Bestor, 2004). Fat grade is assessed by evaluating the amount of marbling in a tail cut sectioned between the third and fourth finlet, the thickness of the midsection, and the amount of fat present in a small core of muscle (near the mid-line) extracted for biopsy. Shape grade is determined by the overall appearance of the fish, the more rotund the better. A good quality fish will receive high marks in all categories. Even though different graders may use different terms, ranking of

fish quality is consistent between experienced graders (Foote²).

We used two of these characteristics, fat and oil content and fish shape, as proxies for fish condition. Fish with large fat reserves and rotund appearance are presumably feeding in excess of their daily metabolic requirements and hence, are in good condition. Fat and oil content and fish shape are reasonable proxies to assess condition because, unlike freshness and color, they cannot be altered by either the time fishermen are at sea or type of gear used.

Detailed logbooks were obtained from a local fishermen's co-operative that consisted of 3834 observations of fat and oil content and 3082 observations of shape from fish landed between 1991 and 2004. Fish ranged in size from the commercial minimum of 185 cm curved fork length (CFL) to 300 cm CFL and weighed from 54 kg to 351 kg dressed (i.e., after head, gill plate, and internal organs were removed). All of the grading was carried out by the same individual using the same grade scale for the entire 14-year period.

To examine temporal trends in fish quality, as defined separately by fat and oil content and fish shape, we used multinomial logit regression with fat and oil grade or shape grade as the dependent variable, and month and year as independent variables. The multinomial logit model estimates the probability of a fish being in grade *j* in month *m* and year *y* as

$$\pi_j(m,y) = \frac{\exp(\eta_j(m,y))}{\sum_{v_i} \exp(\eta_i(m,y))}$$

where $\eta_j(m,y)$ is a linear equation consisting of the variables for month (*m*) and year (*y*) and any month-year interactions.

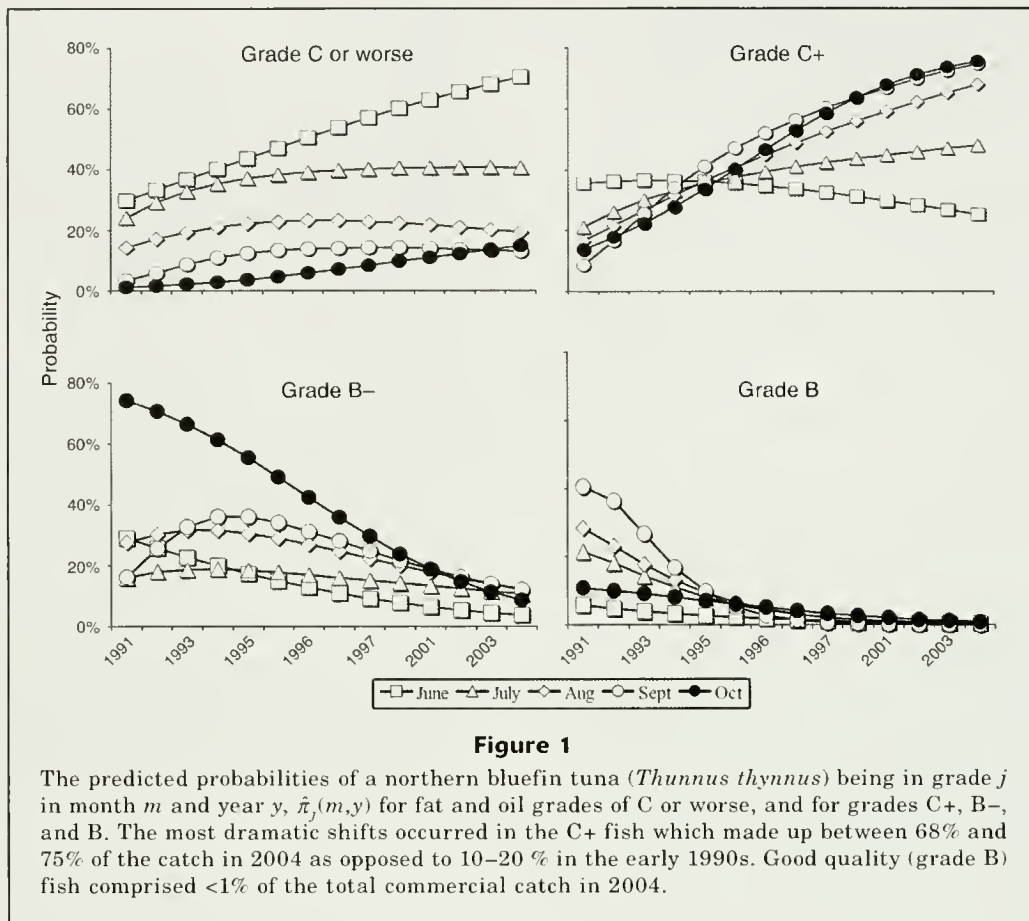
The coefficients for these variables can take on different values for each grade (McCullagh and Nelder, 1989). For example, if we treat month as a categorical variable, $\eta_j(m,y)$ can be written as

$$\eta_j(m,y) = \beta_{0,j} + (\beta_{1,k,j} \times m_k) + (\beta_{2,j} \times y) + (\beta_{3,k,j} \times m_k \times y)$$

where $B_{0,j}$ = the intercept for grade *j*;
 $B_{1,k,j}$ = the coefficient for the effect of month *k* on grade *j*;
 m_k = an indicator variable denoting the month as a categorical variable;
 $B_{2,j}$ = the effect of year on grade *j*; and
 $B_{3,k,j}$ = the interaction between month *k* and year *y*.

The model was fitted by using the multinomial command in the NNET library of S-PLUS vers. 6.2 (Insightful Corporation, Seattle, WA). The significance of each variable was tested by using likelihood ratios for nested

² Foote, J. 2005. Personal commun. Jensen Tuna Inc., 8 Seafood Way, Boston, MA 02210.



models, and Akaike's information criterion (AIC) for non-nested models.

Results

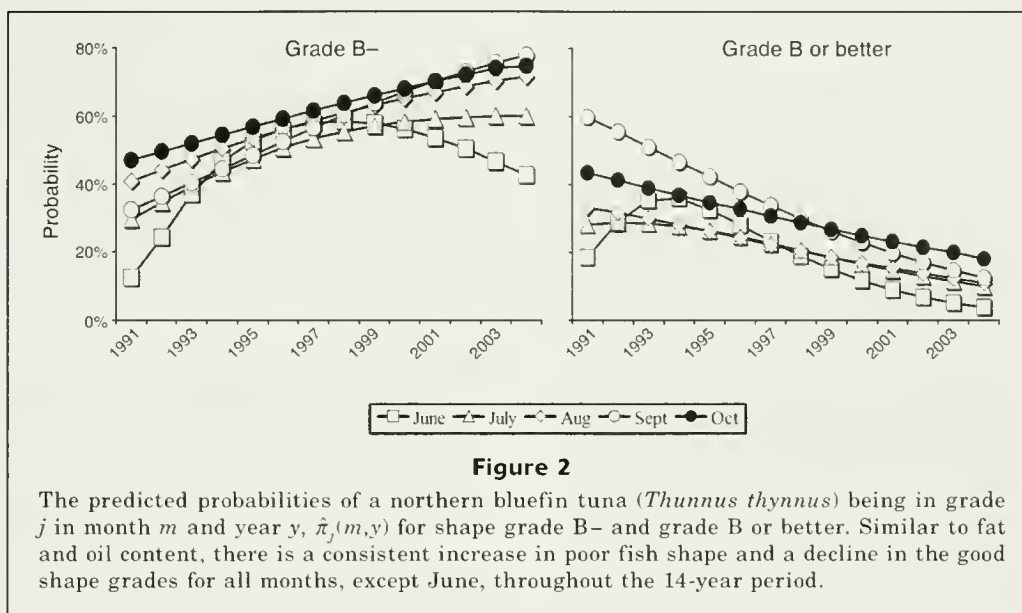
Our analysis identified significant declines in the somatic condition (fat and oil content and fish shape) of northern bluefin tuna in the Gulf of Maine. For fat and oil content, the effect of month, year, and the month-year interaction were each significant (all $P < 0.0001$; $\chi^2_4 = 429$, $\chi^2_4 = 1088$, and $\chi^2_4 = 29.95$, respectively). Fish landed in the month of June arrived in poorer condition than they did in the early 1990s (Fig. 1). For example, the probability of landing a poor quality fish (grade C or worse) in June 1991 was 30% compared with 70% in 2004. Similar, but more striking results were observed in the C+ category during August and September (Fig. 1). In 1991, the probability of landing a fish in the C+ category was 16% and 9% for August and September, respectively. In 2004, the probability increased to 68% and 76% in the C+ category for August and September, respectively. Good quality fish, such as B or better now comprise <1% of the commercial catch at this particular co-operative (Fig. 1).

For fish shape, the effect of month, year, and the month-year interaction were each significant (all

$P < 0.0001$; $\chi^2_3 = 207$, $\chi^2_3 = 388$, and $\chi^2_3 = 47.18$, respectively). Results for shape were similar to fat and oil content, likely because shape and fat and oil content are closely related (fat fish should have a more rotund shape). The probability of landing a fish that received a B- (lesser quality) grade for shape increased by 30%, 32%, 43%, and 28% from 1991 to 2004 for the months of July, August, September, and October, respectively (Fig. 2). For the same time period, fish with a good shape (B or better) decreased by 18%, 22%, 47%, and 25% for the months of July, August, September, and October, respectively (Fig. 2).

Discussion

Our multinomial regression analysis demonstrated highly significant declines in the fat and oil content and shape of northern bluefin tuna landed in the Gulf of Maine over the last 14 years, corroborating the observations of fishermen. Northern bluefin tuna arrive in leaner condition and are not increasing their fat stores on the feeding grounds as they did in the early 1990s. This was particularly true in late summer and early fall, when fish usually fatten and become more rotund (Butler¹).



Seasonal migrations of adult northern bluefin tuna are believed to be bound by reproduction and feeding constraints: spawning in warm ($>24^{\circ}\text{C}$) regions in spring and early summer followed by dispersal to continental shelves at higher latitudes for intensive foraging through late fall (Rivas, 1955; Clay, 1991). Their body condition also varies through this cycle: feeding periods presumably put individuals into positive lipid balance, creating energy stores for gonadal development and metabolism (Medina et al., 2002; Carruthers et al., 2005). Since the mid 1990s, mixed size classes of northern bluefin tuna appeared in North Carolina coastal waters from December to February (Block et al., 2001), extending the range of their inshore foraging on Atlantic menhaden (*Brevoortia tyrannus*) and possibly other species. If the temporal or spatial aspects of migration, reproduction, and feeding patterns have changed over the past decade, alterations in the somatic and bioenergetic condition of fish feeding in the Gulf of Maine could be expected. Other possible explanations for changes in somatic and bioenergetic condition of fish include increased growth rates due to selective fishing pressure (Polacheck et al., 2004), or skipped spawning to increase growth (Jørgensen et al., 2006), but the general declines in condition in fish of such large body size are difficult to explain based on intrinsic changes in growth. This is particularly true in this study where every fish was larger than 110 cm, the size at which the seasonal length-weight relationship begins to decrease (Mather et al., 1995) and northern bluefin tuna gain more in mass than length.

In pelagic fishes, migrations require a substantial energetic cost (Harden Jones, 1984), and migration distance has been linked to body size and available fat stores (Nøttestad et al., 1999). The longstanding migration paradigm is that western Atlantic northern

bluefin tuna spawn in the Gulf of Mexico and Straits of Florida from April to June and then migrate northward along the continental shelf to New England and Canadian waters (Rivas, 1955; Mather et al., 1995; Block et al., 2005). A substantial increase in migrants from the Eastern Atlantic may explain why the condition of fish in this region has declined. Northern bluefin tuna migrating to the Gulf of Maine from the eastern Atlantic would have to swim a greater distance, travel against major currents and through unproductive waters using more stored energy than individuals coming from western Atlantic spawning grounds. To date, there is insufficient data to confirm that such a shift has occurred (Fromentin and Powers, 2005). Another possibility is that the timing and location of spawning has shifted. The long held assumption that the New England assemblage spawns exclusively in the Gulf of Mexico and adjacent regions (Rivas, 1955; Block et al., 2005) may be incorrect (Lutcavage et al., 1999; Fromentin and Powers, 2005; Goldstein et al., in press). If fish are spawning outside of these traditional spawning grounds during May and June (Mather et al., 1995; Lutcavage et al., 1999; Wilson et al., 2005), or at different times, their somatic condition and lipid allocations would be expected to shift from historical patterns (Rajasilta, 1992).

Given that northern bluefin tuna spend up to five months on the feeding grounds, a decline in somatic condition intuitively points to changes in the forage base and energy transfer within the Gulf of Maine. Northern bluefin tuna exploit several trophic levels, including krill, before arrival in the Gulf of Maine (Estrada et al., 2005), but while there, they forage extensively on herring (Chase, 2002), which has the highest energy density of prey in the region (Lawson et al., 1998). The observed decline in condition could result

from a decrease in the amount, quality, or availability of herring (Marshall et al., 1999; Diamond and Devlin, 2003), or an increase in the energy required for northern bluefin tuna to acquire and process sufficient amounts of prey (Marshall et al., 1999; Nøttestad et al., 1999; Carruthers et al., 2005).

Atlantic herring spawning stocks in the Gulf of Maine and Georges Bank-Nantucket Shoals are at historically high levels (Overholtz et al.³); this fact argues against a reduction in herring abundance as a causal factor for the declining condition in northern bluefin tuna. A reduction in the energy density of herring itself, as seen in seabird-herring-copepod ecosystem studies (Diamond and Devlin, 2003; Durant et al., 2003) are other possible reasons for the decline. A coincident decline in northern bluefin tuna and Atlantic herring condition in the Gulf of St. Lawrence indicate that similar changes are occurring in other Northwest Atlantic shelf systems. In view of changes also detected in other predators, such as seabirds, and in the distribution and abundance of baleen whales, there appears to be a major shift in energy transfer and dynamics across the Gulf of Maine ecosystem over a period when oceanographic changes linked to the North Atlantic Oscillation were also evident (Greene and Pershing, 2003).

If the abundance of forage fish has been reduced, dispersed into smaller schools, or shifted, northern bluefin tuna would have to expend more energy in search of prey, shift their diet to less energetic prey (i.e., the junk food hypothesis [Piatt and Anderson, 1996; Golet et al., 2002]), or move to regions with a greater biomass of forage fish (Anderson and Piatt, 1999). Northern bluefin tuna are arriving in poorer condition than they were 10–14 years ago, and despite long residency in the area they are no longer attaining the good condition of previous decades. Of additional concern is that after disappearances in the North Sea and in some historic locations on the Canadian Atlantic shelf, northern bluefin tuna have not returned to these areas (Tiews, 1978; Clay and Hurlbut, 1989).

Condition data alone do not allow us to identify the cause of observed declines in this top predator, but decreased energy stores on feeding grounds could reduce energetic allocations to growth and reproduction, as observed in gadids in the northwest Atlantic and elsewhere (Marshall et al., 1999; Lambert and Dutil, 2000), and may have unexpected and detrimental consequences for rebuilding the northern bluefin tuna population. Given that northern bluefin tuna are currently overexploited throughout most of their range, it is essential to identify root causes for these declines on one of their most important foraging grounds in the western Atlantic.

Acknowledgments

This work was supported by a National Oceanic and Atmospheric Administration Grant NA04NMF4550391 to M. Lutcevage. We thank M. Perkins for all his work processing the bluefin tuna, and several anonymous reviewers for their constructive comments that improved our manuscript.

Literature cited

- Anderson, P. J., and J. F. Piatt.
1999. Trophic reorganization in the Gulf of Alaska following ocean climate regime shift. *Mar. Ecol. Prog. Ser.* 189:117–123.
- Bestor, T. C.
2004. Tsukiji. The fish market at the center of the world, p. 257–258. Univ. California Press, Berkeley and Los Angeles, CA.
- Bigelow, H. B., and W. C. Schroeder.
1953. Fishes of the Gulf of Maine. *Fish. Bull. Wild. Ser.* 53:1–577.
- Block, B. A., H. Dewar, S. B. Blackwell, T. D. Williams, E. D. Prince, C. J. Farwell, A. Boustany, S. L. H. Teo, A. Seitz, A. Walli, and D. Fudge.
2001. Migratory movements, depth preferences, and thermal biology of Atlantic bluefin tuna. *Science* 293:1310–1314.
- Block, B. A., S. L. H. Teo, A. Walli, A. Boustany, M. J. W. Stokesbury, C. Farwell, K. Weng, H. Dewar, and T. D. Williams.
2005. Electronic tagging and population structure of Atlantic bluefin tuna. *Nature* 434:1121–1126.
- Carey, F. G., J. M. Teal, J. W. Kanwisher, K. D. Lawson, and J. S. Beckett.
1971. Warm-bodied fish. *Am. Zool.* 11:137–145.
- Carruthers, E. H., J. D. Neilson, C. Waters, and P. Perley.
2005. Long-term changes in the feeding of *Pollachius virens* on the Scotian Shelf: responses to a dynamic ecosystem. *J. Fish Biol.* 66:327–347.
- Chase, B. C.
2002. Differences in the diet of Atlantic bluefin tuna (*Thunnus thynnus*) at five seasonal feeding grounds on the New England continental shelf. *Fish. Bull.* 100:168–180.
- Clay, D.
1991. Atlantic bluefin tuna (*Thunnus thynnus thynnus* (L.)): a review. *In* World meeting on stock assessment of bluefin tunas: strengths and weaknesses (R. B. Deriso, and W. H. Bayliff, eds), p. 89–180 p. Inter-Am. Trop. Tuna Comm., La Jolla, CA.
- Clay, D., and T. Hurlbut.
1989. Catch and effort for Canadian Atlantic bluefin tuna (*Thunnus thynnus* L.). *ICCAT Coll. Vol. Sci. Pap.* 30:335–342.
- Diamond, A. W., and C. M. Devlin.
2003. Seabirds as indicators of changes in marine ecosystems: Ecological monitoring on Machias Seal Island. *Environ. Monit. Assess.* 88:153–175.
- Durant, J. M., T. Anker-Nilssen, and N. C. Stenseth.
2003. Trophic interactions under climate fluctuations: the Atlantic puffin as an example. *Proc. R. Soc. Lond., Ser. B: Biol. Sci.* 270:1461–1466.
- Estrada, J. A., M. Lutcevage, and S. R. Thorrold.
2005. Diet and trophic position of Atlantic bluefin tuna

³ Overholtz, W. J., L. D. Jacobson, G. D. Melvin, M. Cieri, M. Power, D. Libby, and K. Clark. 2004. Stock assessment of the Gulf of Maine-Georges Bank Atlantic herring complex, 2003. *Northeast Fish. Sci. Cent. Ref. Doc.* 04-06, 300 p.

- (*Thunnus thynnus*) inferred from stable carbon and nitrogen isotope analysis. *Mar. Biol.* 147:37–45.
- Fromentin, J. M., and J. E. Powers.
2005. Atlantic bluefin tuna: population dynamics, ecology, fisheries and management. *Fish Fish. Ser.* 6:281–306.
- Goldstein, J., S. Heppell, A. Cooper, S. Brault, and M. Lutcavage.
In press. Variability in the reproductive status and body condition of Atlantic bluefin tuna in the Gulf of Maine, 2000–2002. *Mar. Biol.*
- Golet, G. H., P. E. Seiser, A. D. McGuire, D. D. Roby, J. B. Fischer, K. J. Kuletz, D. B. Irons, T. A. Dean, S. C. Jewett, and S. H. Newman.
2002. Long-term direct and indirect effects of the Exxon Valdez oil spill on pigeon guillemots in Prince William Sound, Alaska. *Mar. Ecol. Prog. Ser.* 241:287–304.
- Greene, C. H., and A. J. Pershing.
2003. The flip-side of the North Atlantic Oscillation and modal shifts in slope-water circulation patterns. *Limnol. Oceanogr.* 48:319–322.
- Harden Jones, F. R.
1984. A view from the ocean. In *Mechanisms of migration in fishes* (J. D. McCleave, G. P. Arnold, J. J. Dodson, and W. H. Neill, eds.), 26 p. Plenum Press, New York, NY.
- Jørgensen, C., B. Ernande, Ø. Fiksen, and U. Dieckmann.
2006. The logic of skipped spawning in fish. *Can. J. Fish. Aquat. Sci.* 63:200–211.
- Lambert, Y., and J. Dutil.
2000. Energetic consequences of reproduction in Atlantic cod (*Gadus morhua*) in relation to spawning level of somatic energy reserves. *Can. J. Fish. Aquat. Sci.* 57:815–825.
- Lawson, J. W., A. M. Magalhães, and E. H. Miller.
1998. Important prey species of marine vertebrate predators in the northwest Atlantic: proximate composition and energy density. *Mar. Ecol. Prog. Ser.* 164:13–20.
- Lutcavage, M., R. W. Brill, G. B. Skomal, B. C. Chase, and P. W. Howey.
1999. Results of pop-up satellite tagging of spawning size class fish in the Gulf of Maine: Do North Atlantic bluefin tuna spawn in the mid-Atlantic? *Can. J. Fish. Aquat. Sci.* 56:173–177.
- Lutcavage, M., and S. Kraus.
1995. The feasibility of direct photographic assessment of giant bluefin tuna, *Thunnus thynnus*, in New England waters. *Fish. Bull.* 93:495–503.
- Marshall, C. T., N. A. Yaragina, Y. Lambert, and O. S. Kjesbu.
1999. Total lipid energy as a proxy for total egg production by fish stocks. *Nature* 402:288–290.
- Mather, F. J., J. M. Mason Jr., and A. Jones.
1995. Historical document: life history and fisheries of Atlantic bluefin tuna. NOAA Tech. Memo. NMFS-SEFSC-370, 412 p.
- McCullagh, P., and J. A. Nelder.
1989. Generalized linear models, 511 p. Chapman and Hall, London.
- Medina, A., F. J. Abascal, C. Megina, and A. Garcia.
2002. Stereological assessment of reproductive status of female Atlantic northern bluefin tuna during migration to the Mediterranean spawning grounds through the Strait of Gibraltar. *J. Fish Biol.* 60:203–217.
- Mourente, G., C. Megina, and E. Díaz-Salvago.
2001. Lipids in female northern bluefin tuna (*Thunnus thynnus* L.) during sexual maturation. *Fish. Physiol. Biochem.* 24:351–363.
- Nottestad, L., J. Giske, J. C. Holst, and G. Huse.
1999. A length-based hypothesis for feeding migration in pelagic fish. *Can. J. Fish. Aquat. Sci.* 56:26–34.
- Piatt, J. F., and P. Anderson.
1996. Response of common murre to the Exxon Valdez oil spill and long-term changes in the Gulf of Alaska marine ecosystem. *Am. Fish. Soc. Symp.* 18:720–737.
- Polacheck, T., J. P. Eveson, and G. M. Laslett.
2004. Increase in growth rates of southern bluefin tuna (*Thunnus maccoyii*) over four decades:1960–2000. *Can. J. Fish. Aquat. Sci.* 61:307–322.
- Rajastilta, M.
1992. Relationship between food, fat, sexual maturation, and spawning time of Baltic herring (*Clupea harengus*) in the Archipelago Sea. *Can. J. Fish. Aquat. Sci.* 49:644–654.
- Ravier, C., and J.-M. Fromentin.
2001. Long-term fluctuations in the Eastern Atlantic and Mediterranean bluefin tuna population. *ICES J. Mar. Sci.* 58:1299–1317.
- Rideout, R. M., G. A. Rose, and M. P. M. Burton.
2005. Skipped spawning in iteroparous fishes. *Fish. Ser.* 6:50–72.
- Rivas, L. R.
1955. A comparison between giant bluefin tuna (*Thunnus thynnus*) from the straits of Florida and the Gulf of Maine with reference to migration and population identity. *Proc. Gulf and Caribbean Fish. Inst. Seventh Ann. Sess.* 133–149.
- Stevens, E. D., and J. M. McLeese.
1984. Why bluefin tuna have warm tummies: temperature effect on trypsin and chymotrypsin. *Am. J. Physiol-Reg I.* 246:R487–R494.
- Tiews, K.
1978. On the disappearance of bluefin tuna in the North Sea and its ecological implications for herring and mackerel. *Rapp. P-V. Réun. Cons. Int. Explor. Mer* 172:301–309.
- Wilson, S. G., M. E. Lutcavage, R. W. Brill, M. P. Genovese, A. B. Cooper, and A. W. Everly.
2005. Movements of bluefin tuna (*Thunnus thynnus*) in the northwestern Atlantic recorded by pop-up satellite archival tags. *Mar. Biol.* 146:409–423.

Abstract—This study investigates the temporal stability of length- and age-at-maturity estimates for female Pacific cod (*Gadus macrocephalus*) in the Gulf of Alaska and eastern Bering Sea. Females reached 50% maturity (A_{50}) at 4.4 years in the Gulf of Alaska and at 4.9 years in the eastern Bering Sea. Total body length at 50% maturity (LT_{50}) was significantly smaller (503 mm) in the Gulf of Alaska than in the eastern Bering Sea (580 mm). The estimated length- and age-at-maturity did not differ significantly between winter and spring in either the Gulf of Alaska (1999) or Bering Sea (2003) areas. The results of this study raised the spawning biomass estimate of female Alaskan Pacific cod from 298×10^3 t for 2005 to 499×10^3 t for 2006. The increased spawning biomass estimate resulted in an increased over-fishing limit for Pacific cod.

Geographic and seasonal variations in maturation and growth of female Pacific cod (*Gadus macrocephalus*) in the Gulf of Alaska and Bering Sea

James W. Stark

Email address: jim.stark@noaa.gov

Resource Assessment and Conservation Engineering Division
Alaska Fisheries Science Center
NOAA/National Marine Fisheries Service
7600 Sand Point Way NE
Seattle, Washington 98115

Pacific cod (*Gadus macrocephalus*) was the fourth most important commercial species landed in the United States during 2003 by volume, and catches totaled 27×10^4 metric tons (t) and had a value of \$160 million. The Pacific cod stocks in Alaska were not considered to be overfished in 2005 (Thompson and Dorn, 2005; Thompson et al., 2005). Pacific cod range from California, around the North Pacific Rim, to the Sea of Japan (Hart, 1973). In Alaska, this species is found along the continental shelf and upper slope, primarily at depths <300 m (Matarese et al., 2003). The objectives of this study were to determine the length- and age-at-maturity, as well as growth of female Pacific cod, in order to provide for significantly improved stock management in the Gulf of Alaska, eastern Bering Sea, and Aleutian Islands. Previous estimates of Pacific cod length-at-maturity were based on visual (macroscopic) observations of ovaries taken during the spawning season (Welch and Foucher, 1988; Thompson et al., 2005), or on a gonadosomatic index (*IG*) (Teshima, 1985; Hattori et al., 1992).

The macroscopic observation and *IG* methods can introduce sampling bias through misclassifications of the stage of oocyte maturity (Hunter et al., 1992). The macroscopic method of maturity classification is contingent upon differentiating between ova that contain yolk (mature ova) which can appear transparent to the naked eye, and opaque ova that do not con-

tain yolk. The change in opacity is the result of yolk sequestering within the ova, resulting in distension and transparency of the chorion (external covering of the ova). Opacity is more difficult to discern in the small ova that are produced by smaller fish. Therefore, the macroscopic method of classification can result in a bias against smaller fish.

With macroscopic classification, there is also a bias against specimens in early vitellogenesis, because during this period only a small quantity of yolk has been sequestered within the ova, resulting in an opaque chorion that is not distended. With macroscopic observation methods, an ovary containing only postovulatory follicles and opaque ova would be classified as immature; postovulatory follicles can be detected only through the use of histological methods.

Macroscopic observations also have the disadvantage of generally being conducted under less than ideal lighting and weather conditions. Maturity classifications based on histological examination are not subject to these biases because the maturity classifications are based on a comprehensive microscopic assessment of ova and associated structures, such as postovulatory follicles, under controlled laboratory conditions. Histological methods provide a high probability that yolk sequestered within ova will be detected because ova are sectioned and stained with eosin that renders yolk pink.

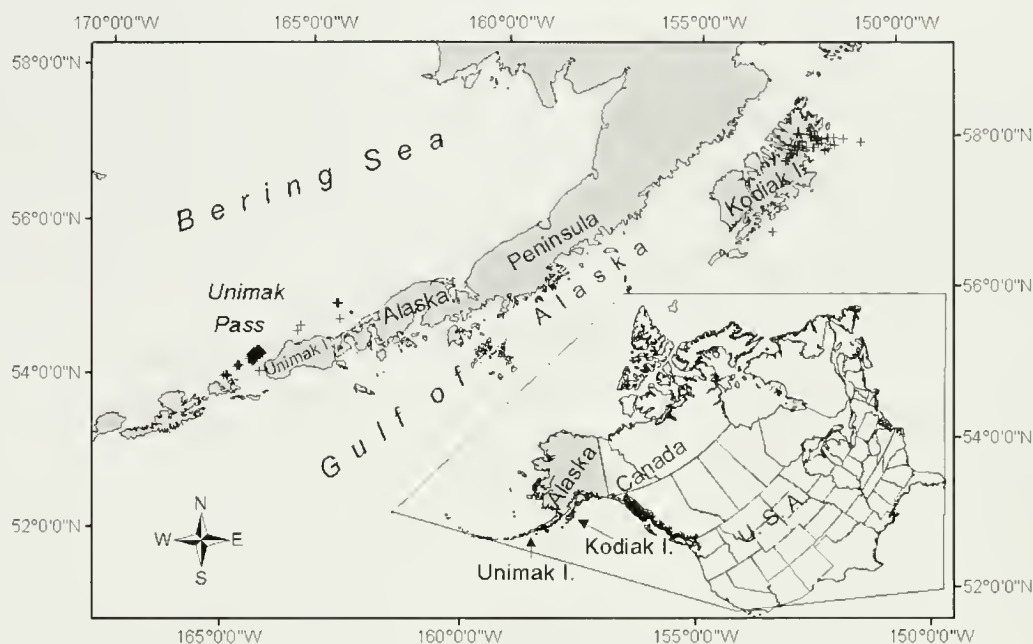


Figure 1

Locations (+) sampled by survey crews of the National Oceanic and Atmospheric Administration Alaska Fisheries Science Center from October 1998 through January 2004 for Pacific cod (*Gadus macrocephalus*).

Materials and methods

Ovaries and otoliths were collected from Pacific cod in two geographic areas, the Gulf of Alaska and eastern Bering Sea (Fig. 1). Seasonal sampling was used to estimate the time of spawning, rate of ovary development, and length- and age-at-maturity for female Pacific cod. The first area, located in the central Gulf of Alaska, was sampled during October 1998, January 1999, and April 1999 (Table 1) during a cooperative seasonal maturity study conducted by the Alaska Department of Fish and Game (ADFG) and the National Oceanic and Atmospheric Administration Alaska Fisheries Science Center (NOAA/AFSC). The area was sampled with bottom trawl gear again in June 1999 during the annual ADFG crab survey and during the commercial fishery in January 2004. Seawater temperature, and depth data were collected with a calibrated trawl-mounted microbaththermograph. The second area, within Unimak Pass and the adjacent southeastern Bering Sea, was sampled during the January, February, and March 2003 AFSC Pacific cod pot study. Growth was determined by using the cod length- and geographic area-stratified otolith collections from the 2003 AFSC area wide surveys in the Gulf of Alaska and eastern Bering Sea (Table 1). Otoliths were aged by using the methods developed during 2002 for Pacific cod (Roberson et al., 2005; Thompson and Dorn, 2005) by personnel of the AFSC Age and Growth Program.

In both the Gulf of Alaska and Bering Sea collections, ovaries were removed and placed in individu-

ally labeled cloth bags and stored in a solution of 4% buffered formaldehyde. The ovary samples for the Gulf of Alaska consisted of whole ovaries and samples from the Bering Sea area were excised ovarian cross-sections (minimum of two 16.4-mm-diameter samples per individual). For each whole ovary sample, a section was taken from the posterior region of the ovary. From 50 of these specimens, two additional sections were taken from the anterior and median regions.

Oocytes within each ovary were classified into five histological stages based on criteria used by Hunter et al. (1992) and Stark and Somerton (2002). The five stages were perinucleus, cortical alveoli, vitellogenesis, hydrated oocytes, and postovulatory follicles. Individual ovaries were classified according to the most advanced stage of oocytes present in the histological sections. Individuals classified as spawners were those with ovaries containing either hydrated oocytes or post-ovulatory follicles. Mature individuals were defined by using two different classification criteria in order to compare results from each method. One method classified mature specimens as those with ovary stages ranging from vitellogenesis through postovulatory follicles. The other method included the additional stage of cortical alveoli ovaries in the mature category.

Ovarian development was compared across months, by tabulating the proportion of fish classified within each of the five histological stages only for females that had reached the minimum total body length (LT) at maturity, as determined by a length-at-maturity analysis. A selection of samples from the entire length range of

Table 1

Summary of data on samples collected by the National Oceanic and Atmospheric Administration Alaska Fisheries Science Center used to estimate maturity and growth of Pacific cod (*Gadus macracephalus*). Categories include date of sample collections, location of sample collections, sources of sample collections, types and numbers (*n*) of specimen samples. The ovaries and otoliths used to estimate length- and age-at-maturity and timing of the reproductive cycle were taken from specimens collected in the Gulf of Alaska (GOA) and Bering Sea (BS). The GOA sampling was conducted during surveys extending from October 1998 to June 1999, and additional specimens were collected from a seafood processing plant (referred to as "Plant" in table) during 2004. The BS ovary and otolith specimens were collected during the 2003 Pacific cod surveys. The length data and the otoliths (of both sexes) used to estimate growth were collected during the 2003 bottom trawl surveys conducted in the GOA and BS.

Period of sample collections	Location of sample collections	Source of sample collections	No. of specimens sampled for histological examination of ovaries	No. of specimens aged
For maturity estimates				
October 1998	GOA	Survey	59	58
January 1999	GOA	Survey	107	104
April 1999	GOA	Survey	60	57
June 1999	GOA	Survey	66	48
January 2004	GOA	Plant	50	50
	GOA	Total	342	317
January 2003	BS	Survey	30	29
February 2003	BS	Survey	133	129
March 2003	BS	Survey	96	92
	BS	Total	259	250
	GOA and BS	Total	601	567
For growth estimates				
May–July 2003	GOA	Survey females		375
May–July 2003	GOA	Survey males		336
June–July 2003	BS	Survey females		676
June–July 2003	BS	Survey males		684
	GOA and BS	Total		2071

mature females allowed the investigation of the full seasonal progression of ovary development. The proportion of females in spawning condition was estimated for each month by dividing the sum of the fish classified as spawning by the sum of the fish classified as mature. The length- and age-at-maturity estimates that were chosen as representing the standard for each area were based on specimens collected during the prespawning or initial yearly spawning period, January 1999 and 2004 and February 2003. By January and February, all specimens that would mature that year had matured according to the results of seasonal sampling from this study. The data from January of 1999 and 2004 were combined to obtain length- and age-at-maturity estimates with the lowest variance. The monthly length and age composition of females in mature condition were estimated by using standard length- and age-at-maturity analysis.

Maturity as a function of length was estimated by fitting a logistic function to the maturity data with generalized linear modeling (Venables, 1997); for this procedure, S-Plus software (vers. 2000 Professional release 3, Math-

Soft Inc., Cambridge, MA) was used. The significance of between-area, between-month, and between-classification methods differences were tested by fitting the model of maturity as a function of L_T with a term distinguishing area, month, and method and by recalculating without each term. Significance of the area, month, and method terms were determined by using analysis of deviance (Venables, 1997). Length at 50% maturity was also estimated by evaluating the fitted model at 50% maturity and algebraically solving for length. The variance of $L_{T_{50}}$ was estimated for each area, month, and method by using bootstrapping (Efron and Tibshirani, 1993) based on 200 resamplings, with replacement, of the maturity and length data. Between-area, between-month, and between-method differences in $L_{T_{50}}$ were then tested with a *z*-test (Sokal, 1969). With these same procedures, maturity was described as a function of age, and spawning was estimated as a function of L_T , age, month, and ambient water temperature.

With the use of S-Plus software, length-at-age was described by the von Bertalanffy growth function, which incorporated nonlinear least-squares fitted to

L_T and age data (Venables, 1997). Between-sex and between-area differences in growth were tested by first fitting the von Bertalanffy model with a term distinguishing sex and area and again tested for the combined sexes and areas. The likelihood ratio of the two models was then determined for each category (Kimura, 1980). Significance of the likelihood ratio was tested to determine if growth differed by sex or area.

The gonadosomatic index (I_G) was calculated from the specimens sampled for maturity as the ratio of gonad weight (W_G) to body weight (W) with the gonads removed ($IG=100 W_G/W$). The body weight portion of the data included food contents for the Gulf of Alaska specimens, whereas stomachs were emptied for all 250 Bering Sea specimens that were weighed. However, weight of the stomach contents represented less than 1% of the total body weight for the Bering Sea specimens. A z -test (Sokal, 1969) was performed with S-Plus software to determine if there were between-area and between-month differences in I_G .

Results

The results provided information on the relationship between ovary growth and maturation for Pacific cod in the Gulf of Alaska and Bering Sea. The I_G data were available for 95% of the Gulf of Alaska specimens and 99% of the Bering Sea specimens sampled for maturity. For both areas, the I_G cycled according to the season (Fig. 2). The observed I_G was highest during the winter months (Jan=4.24 I_G and February=8.48 I_G), declined through the spring (March=6.37 I_G and April=3.50 I_G), and reached the lowest levels in early summer (June=1.02 I_G). Maturation of the population of oocytes to be spawned the following year occurred at a slow rate through October (1.74 I_G).

Similarly linked to the Pacific cod spawning cycle, was the development of oocytes within the ovaries (Fig. 3), which was consistent in all quadrants of each ovary. By January, over 70% of the sampled ovaries were in the vitellogenesis stage of development in preparation for spawning, in both the Gulf of Alaska and Bering Sea Pacific cod. Females that had vitellogenesis-stage oocytes during the spring were expected to develop and spawn those oocytes that year. By June, all stocks of vitellogenesis-stage oocytes had been exhausted. In the Gulf of Alaska, over half of the female Pacific cod spawned during April and June. Pacific cod spawning began during February in the Bering Sea area, and

Table 2

Length-at-maturity results based on samples of ovaries (n) collected between the late prespawning and initial spawning period for female Pacific cod (*Gadus macrocephalus*) in the Gulf of Alaska (GOA) and Bering Sea (BS) areas, by date of collection. The parameters of the logistic equation that were used to fit the data are given: B (slope of the line) and A (Y intercept), variance (the square of the standard deviation of B and A), covariance (the product of the standard deviations of B and A and the coefficient of correlation between them), length (mm) at which 50% of females were expected to reach sexual maturity (L_{T50}), and variance of L_{T50} .

Sampling statistics	Gulf of Alaska	Bering Sea
	January 1999 and 2004	February 2003
n	157	133
B	0.0222	0.0132
A	-11.1425	-7.6248
Variance (B)	2.0649	1.3807
Variance (A)	6.5528	3.2433
Covariance (B,A)	-0.0002	0.0001
L_{T50} (mm)	502.5543	579.9599
Variance (L_{T50})	212.5733	309.3380

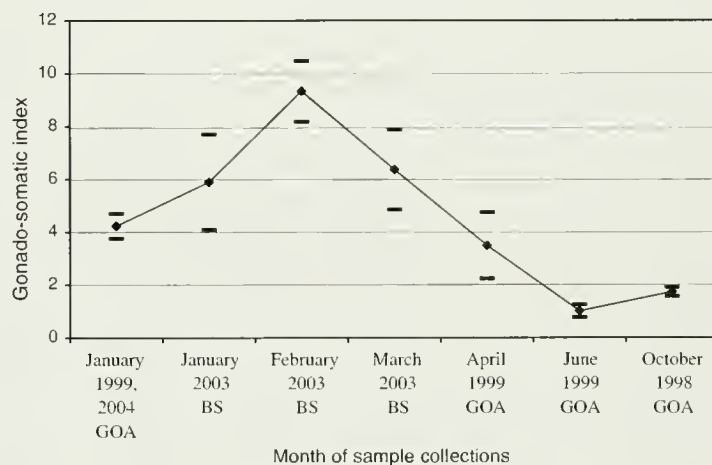


Figure 2

Mean gonadosomatic index of female Pacific cod (*Gadus macrocephalus*). Sample sites were located in the Gulf of Alaska (GOA) during January 1999 and 2004, April and June 1999, and October 1998 (total $n=327$), and the Bering Sea (BS) during January, February, and March 2003 (total $n=261$). The 95% confidence intervals are represented by bars located adjacent to each data point.

approximately 10% of the fish population participated. During October, 5% of female Pacific cod had vitellogenesis-stage ovaries, whereas 95% of Gulf of Alaska cod were in earlier stages of maturation. The likelihood of female Pacific cod spawning was significantly

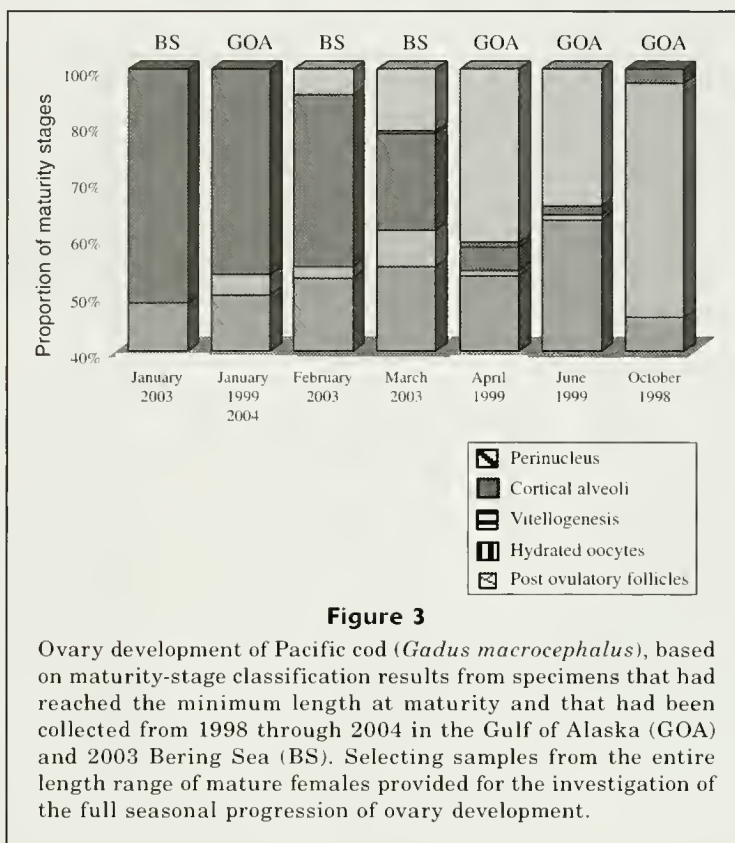


Figure 3

Ovary development of Pacific cod (*Gadus macrocephalus*), based on maturity-stage classification results from specimens that had reached the minimum length at maturity and that had been collected from 1998 through 2004 in the Gulf of Alaska (GOA) and 2003 Bering Sea (BS). Selecting samples from the entire length range of mature females provided for the investigation of the full seasonal progression of ovary development.

($P < 0.001$) associated with the time of month and not significantly associated with L_T ($P = 0.06$), age ($P = 0.06$), or ambient water temperature ($P = 0.21$). However, by April and June in the Gulf of Alaska, L_T was slightly ($P = 0.01$) associated with the likelihood of spawning. Spawners ranged in L_T from 420 mm to 1060 mm. The age-at-spawning ranged from 4 year olds up to the oldest females taken, at 10 years of age. Spawning female Pacific cod were found in all areas, including bays and offshore gullies, sampled during April and June 1999 in the Gulf of Alaska. Ambient seawater temperatures were similar in 1999 during January and April (2.21°C to 6.10°C), and increased only slightly in June (3.7°C to 7.01°C).

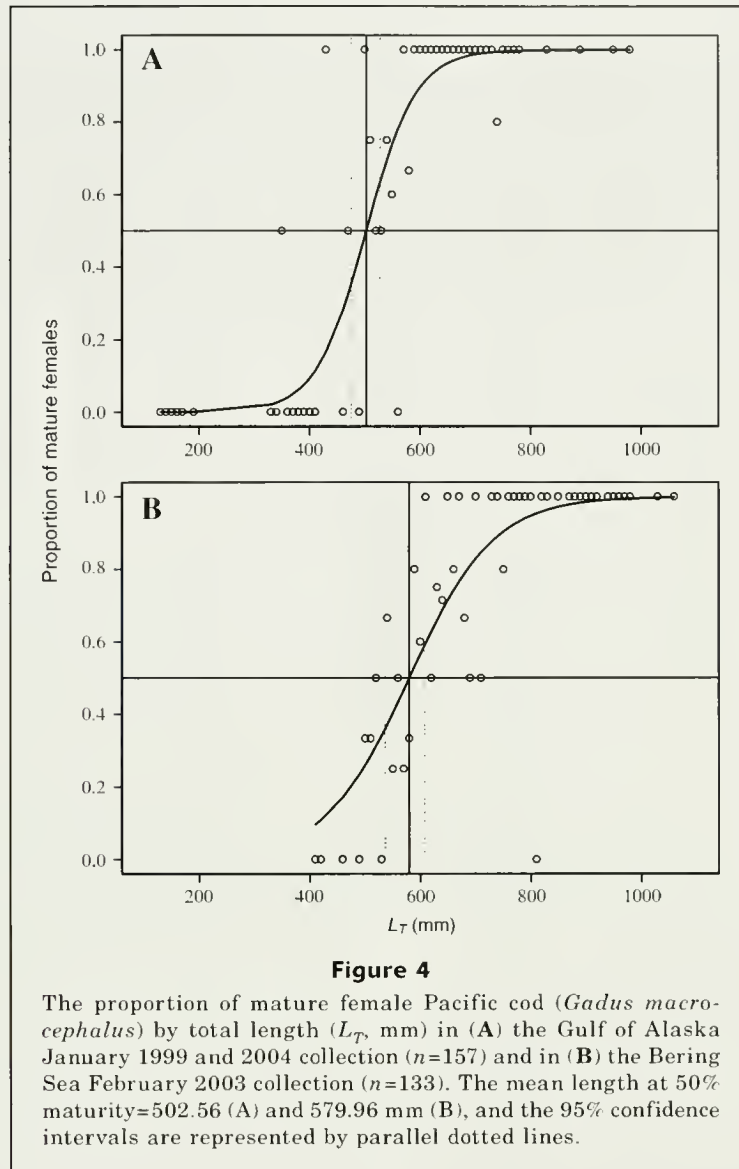
The estimates of L_{T50} did not differ significantly between the two histology-based methods used to define mature females, except for a slight difference ($P = 0.02$) with January Gulf of Alaska estimates, which used the combined data from 1999 and 2004. The January L_{T50} estimates were 503 mm based on a mature classification that did not include cortical alveoli (CA) stage ovaries, and 437 mm when CA-stage ovaries were included as part of the mature category.

However, there was a significant area difference ($P < 0.001$, Fig. 4, Table 2) between the January 1999, 2004 Gulf of Alaska L_{T50} (503 mm) and the February 2003 Bering Sea L_{T50} (580 mm). In both areas, the estimates of length-at-maturity did not differ significantly between months, with the exception of a slight differ-

ence ($P = 0.03$) between January (496 mm) and June (601 mm) 1999. In the present study the expected L_T range of mature female P. cod was adequately assessed from a sample L_T distribution that extended to 130 mm L_T in the Gulf of Alaska and 350 mm L_T in the Bering Sea (Table 3) and on the documentation of only a single specimen smaller than 420 mm L_T .

The estimated age at which 50% of the females reached maturity (A_{50}) did not differ significantly between the two histological methods for assigning maturity. With either method, the A_{50} differed slightly ($P = 0.02$) between the Gulf of Alaska (4.4 years) and Bering Sea (4.9 years, Table 4, Fig. 5). However, within each area, the estimated ages at maturity did not differ significantly between months ($P > 0.16$). Similarly, the January 1999 and 2004 Gulf of Alaska female cod ages at maturity did not differ significantly ($P = 0.19$).

The otoliths taken during the 2003 AFSC bottom trawl surveys of the Gulf of Alaska ($n = 711$) and eastern Bering Sea ($n = 1360$) provide the largest and most comprehensive collection of age data available for female and male Pacific cod. The otolith specimens were selected by region, sex, and L_T . Pacific cod had wide variations in age at length (Fig. 6, Table 5). Based on these collections, the von Bertalanffy growth function differed significantly ($P < 0.001$) between the Gulf of Alaska and Bering Sea for both males and females (Table 5). Female Pacific cod length at age was smaller in the Gulf of Alaska than in the Bering Sea. The Gulf



of Alaska female Pacific cod growth differed significantly ($P<0.001$) from the growth of males. The rate of growth declined more with age for males than for females in the Gulf of Alaska (Fig. 6). However, in the Bering Sea, male growth was nearly as rapid ($P=0.015$) as that of females. Males were estimated to reach a slightly smaller maximum theoretical L_∞ of 1044 mm in the Gulf of Alaska than in the Bering Sea (1101 mm).

Discussion

This study provides the most extensive and representative estimates of female Pacific cod length- and age-at-maturity and growth available. This is the first Pacific cod study to rely on histological methods to assess ovary maturity, and the first to make temporal comparisons of maturity. It is the first northeast Pacific Ocean study

to assess Pacific cod age-at-maturity. Before this study, managers of the Alaska Pacific cod fishery (Thompson and Dorn, 2005; Thompson et al., 2005) used a female L_{T50} estimate of 670 mm from macroscopic maturity classifications made by commercial fishery observers on specimens collected after March in 1993 and 1994. However, the macroscopic maturity classification method can introduce sampling bias and misclassifications. In contrast, in this study, it was determined that the most representative method for estimating L_{T50} relied on making histological maturity assessments of large numbers of ovary samples from a wide L_T range of specimens collected before the late spawning period.

The results from this study are similar to the results from studies conducted in other areas. The estimated female Pacific cod A_{50} differed only slightly between the Gulf of Alaska and Bering Sea study areas and were similar to the ages estimated for Sea

Table 3

Total length (mm) and age (years) composition of female Pacific cod (*Gadus macrocephalus*) specimens collected in the Gulf of Alaska (GOA) during January 1999 and 2004 and in the Bering Sea (BS) during February 2003 to estimate the length and age at which 50% reached sexual maturity. The objective was to collect a minimum of five specimens per length class, subject to availability. n = number of fish in the sample.

Length (mm)	GOA n	BS n	Length (mm)	GOA n	BS n	Age (years)	GOA n	BS n
130	1		660	4	5	1	6	
140	1		670	4	2	2	3	
150	1		680	8	6	3	20	3
160	1		690	5	2	4	16	16
170	1		700	4	2	5	32	32
190	1		710	6	6	6	42	22
330	1		720	8		7	26	30
340	1		730	8	1	8	6	18
350	2		740	5	5	9	2	6
360	3		750	2	5	10	1	2
370	5		760	5	3			
380	7		770	2	1			
390	3		780	1	2			
400	3		790		3			
410	4	1	800		4			
420		2	810		1			
430	1		820		3			
460	1	3	830	1	2			
470	2		850		1			
490	1	1	870		1			
500	1	3	880		3			
510	4	3	890	1	2			
520	4	2	900		1			
530	4	1	910		1			
540	4	3	920		1			
550	5	4	940		1			
560	1	2	950	1	1			
570	2	4	960		1			
580	3	3	970		1			
590	3	5	980	1	1			
600	4	5	1030		1			
610	4	2	1060		1			
620	2	4						
630	5	2						
640	4	3						
650	1	4						

of Okhotsk (5 years of age, Rovnina et al., 1997) and Sea of Japan (4 years of age, Hattori et al., 1992) female Pacific cod. Results from previous studies support the between-area differences in female Pacific cod length-at-maturity found during the present study. Like Gulf of Alaska Pacific cod, female Pacific cod from Canadian waters were estimated to mature at a smaller L_{T50} (median 450 mm during the 1970s and 550 mm during the 1960s; Welch and Foucher, 1988) than Bering Sea Pacific cod. The Bering Sea estimate of L_{T50} was within the range estimated for

the Sea of Okhotsk female Pacific cod (550 mm L_T to 600 mm L_T ; Rovnina et al., 1997). In the present study, no significant differences were found in female Pacific cod L_{T50} or A_{50} for any of the months sampled, within either the Gulf of Alaska or Bering Sea areas. The temporal agreement for female Pacific cod A_{50} and L_{T50} estimates indicates they are reliable. Results were also similar between the two histology-based methods of classifying mature female Pacific cod, indicating that either method could be used to define A_{50} or L_{T50} .

Table 4

Age-at-maturity results based on ovary samples (n) collected between the late prespawning and initial spawning periods for female Pacific cod (*Gadus macrocephalus*) in the Gulf of Alaska (GOA) and Bering Sea (BS) areas, by date of collection. The parameters of the logistic equation that were used to fit the data are given: B (slope of the line) and A (Y intercept), variance (the square of the standard deviation of B and A), covariance (the product of the standard deviations of B and A and the coefficient of correlation between them), age (years) at which 50% of females were expected to reach sexual maturity (A_{50}), and variance of A_{50} .

Sampling statistics	Gulf of Alaska	Bering Sea
	January 2003 and 2004	February 2003
n	154	129
B	1.9632	0.9654
A	-8.5395	-4.7143
Variance (B)	0.0145	0.0065
Variance (A)	2.1246	1.3680
Covariance (B,A)	0.0059	0.0013
A_{50}	4.3499	4.8832
Variance (A_{50})	0.0224	0.0663

Spawning participants sampled during this study, included female Pacific cod as small as 420 mm L_T in the Gulf of Alaska and 460 mm in the Bering Sea area. In comparison, cod (*Gadus morhua*) from the northwest Atlantic Ocean initiated spawning in 1995 at 400 mm—a decline from 500 mm in 1992 (Saborido-Rey and Junquera, 1998).

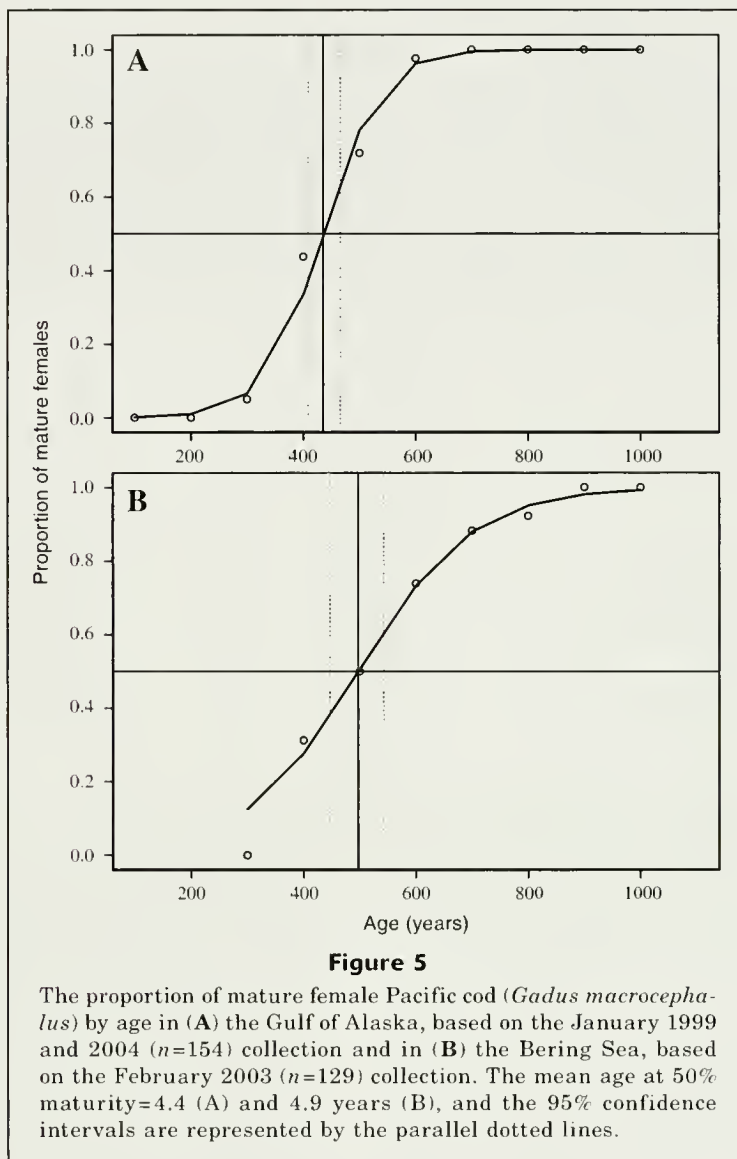
Spawning is an annual occurrence for female Pacific cod according to the results of seasonal ovary development, the I_G cycle, and the wide range in age and body length composition of the spawning population each month. This conclusion was consistent with that from Teshima's (1985) study, which found that the Bering Sea Pacific cod gonadosomatic index increased in November and December because of maturation and that spawning was not expected to occur until the following year. Similarly, Atlantic cod individuals have an annual reproductive cycle (Norberg et al., 2004) and spawn despite being raised in captivity under conditions of starvation (Kjesbu et al., 1991).

Based on results from this study, the spawning activity for female Pacific cod is believed to begin during late winter and peak during the spring. This estimated period of peak spawning, based on results summarizing ovarian maturities by month of collection, is validated by larval abundance estimates from the Gulf of Alaska and Bering Sea ichthyoplankton surveys conducted since 1980 by the AFSC (Matarese et al., 2003). Similarly, the Sea of Okhotsk population is estimated to have a peak spawning period that includes the months of March and May, based on a 1995 study (Rovnina et al., 1997). Spawning probably ends in early summer in the Gulf of Alaska, as indicated by

the lack of any specimens in June with vitellogenesis-stage ovaries.

The likelihood of female Pacific cod spawning was strongly associated ($P < 0.001$) with the time of month, and later in the spawning season, spawning was associated ($P = 0.01$) with L_T . There were no associations with spawning and age, or ambient water temperature; consequently these factors probably do not regulate the timing of spawning for Pacific cod. Similarly, seawater temperature was not the most important environmental cue regulating the maturation and spawning of Atlantic cod and other commercially cultured Atlantic Ocean fish species, including rainbow trout (*Oncorhynchus mykiss*), Atlantic halibut (*Hippoglossus hippoglossus*) and sole (*Solea solea*) (Norberg et al., 2004). For these cultured Atlantic species, photoperiod is the most important regulator of the reproductive cycle. Pacific cod maturation and spawning was significantly associated with time of month, as determined by this study, which would indicate that photoperiod may regulate the reproductive cycle in this species. Photoperiod should be similar for both the Gulf of Alaska and Bering Sea study areas sampled by this survey, given their similar latitudes (Fig. 1), and could account for the similarity in the timing of spawning within the Gulf of Alaska and Bering Sea waters found during this study and during the ichthyoplankton surveys.

Regardless of where spawning occurs, the reproductive effort by the fish represents a substantial investment, based on ovary weight that represents up to 30% of the total female Pacific cod body weight and Atlantic cod body weight (Lambert and Dutil, 2000). Pacific cod have among the highest fecundities of any tele-

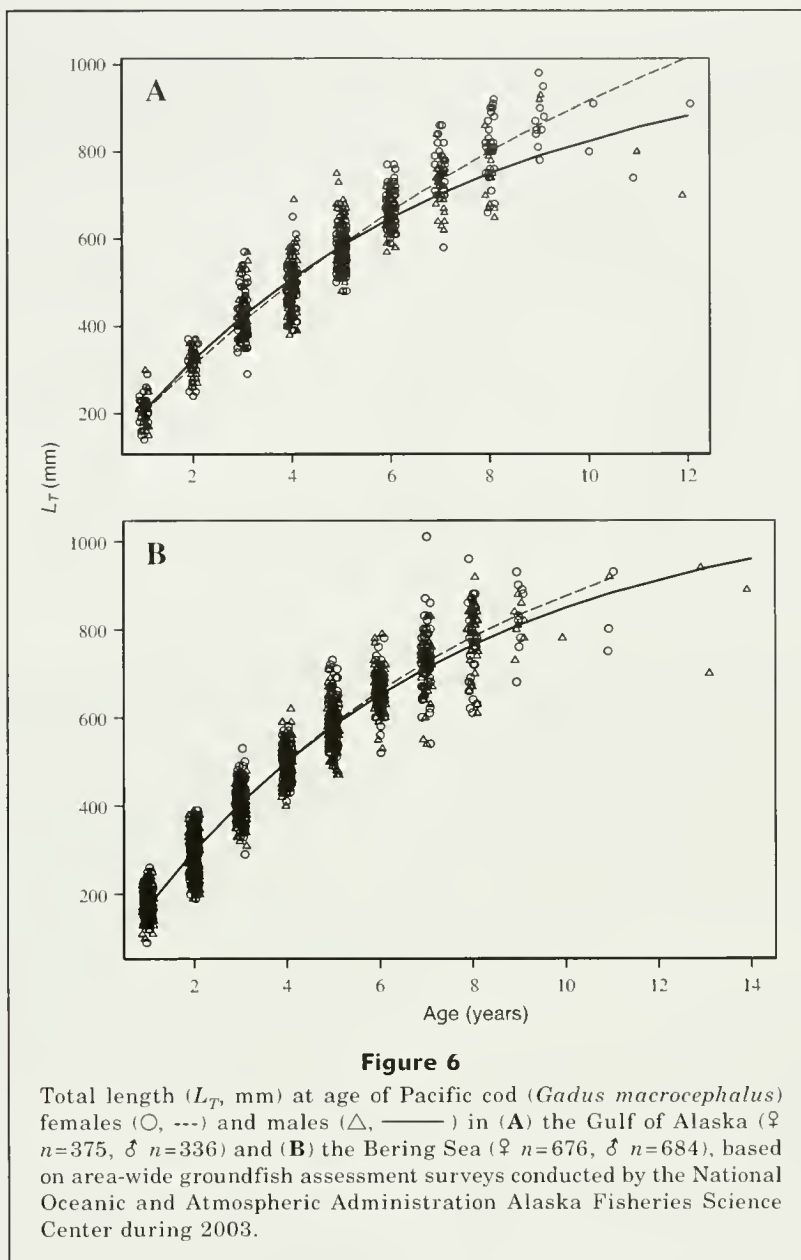


ost (Waiwood, 1982; Foucher and Tyler, 1990) and can produce up to 5.7 million ova each year. However, it appears that the metabolic costs of spawning do not diminish female Pacific cod growth.

Female Pacific cod growth does not significantly decline upon reaching A_{50} in either the Gulf of Alaska or Bering Sea. Males in the Gulf of Alaska area reach a smaller maximum length than females. Similarly, in the eastern Sea of Okhotsk, male Pacific cod reach a smaller total length than females (Rovnina et al., 1997). In contrast male Pacific cod in the Bering Sea area reach a maximum length similar to that of females, and female Pacific cod grow significantly faster in the Bering Sea than in the Gulf of Alaska. The growth results support the maturity-at-length results in the present study that indicate a much larger L_{T50} for the Bering Sea females. Longevity, however, is similar for Gulf of Alaska and Bering Sea Pacific cod and does not differ between sexes. Pacific cod growth probably

occurs primarily during the summer and fall, as does growth in Atlantic cod (Norberg et al., 2004), and not during the winter through early summer months, the period used by the present study to assess length- and age-at-maturity.

With the estimates of A_{50} and L_{T50} from this study, the spawning stock biomass of female Pacific cod for the Gulf of Alaska and eastern Bering Sea increased from the 2005 estimate of 300×10^3 t that was based on a previous study, to an 2006 estimate of 500×10^3 t (Thompson and Dorn, 2005; Thompson et al., 2005). The spawning biomass estimates are of critical importance for stock management models from which are determined the allowable commercial catch quotas of Pacific cod in the northeast Pacific Ocean and Bering Sea (Thompson and Dorn, 2005; Thompson et al., 2005). The increased spawning stock biomass estimates of female Pacific cod resulting from this study support the establishment of higher over-fishing limits for Pacific



cod than would have otherwise occurred. As a result, the revised 2006 management plan increased the estimated spawning stock biomass by 80% in the Gulf of Alaska and by 10% in the eastern Bering Sea and Aleutian Islands, over the 2005 plan estimates. These increases offset declines in the estimated biomass of Pacific cod over 2 years of age for the Gulf of Alaska (4%) and for the eastern Bering Sea and Aleutian Islands (19%) during the same period. Consequently, the recommended over-fishing limit increased 51% in the Gulf of Alaska and declined only 18% in the Bering Sea and Aleutian Islands.

Although temporal stability was found for Pacific cod A_{50} and L_{T50} estimates in the present study, maturity

assessments should be conducted on a periodic basis in the future to ensure that managers continue to receive representative estimates of Pacific cod A_{50} and L_{50} and timing of spawning, which are essential for rational stock management. Maturity assessments would be particularly important during periods of significant change in climate or habitat.

Acknowledgments

Thanks to the following Alaska Fisheries Science Center personnel for their contributions: D. Somerton, G. Stauffer, R. Nelson, A. Hollowed, D. Nichol,

Table 5

Length-at-age described by the von Bertalanffy growth equation for male and female Pacific cod (*Gadus macrocephalus*) in the Gulf of Alaska (GOA) and Bering Sea (BS). Also provided are sample size (n) and parameters L_{∞} (length at maximum age in mm), k (estimated growth increment), t_0 (theoretical age when fish length is 0). Numbers in parentheses represent the number of fish in the sample.

	Gulf of Alaska		Bering Sea	
	Males	Females	Males	Females
n	347	389	684	676
L_{∞} (mm)	1043.7900	1567.2000	1100.630	1203.9400
var (L_{∞})	3564.9736	24716.8707	1281.3393	2641.7441
k	0.1498	0.0825	0.1449	0.1277
var (k)	0.0003	0.0002	0.0001	0.0001
t_0	-0.4670	-0.6712	-0.1814	-0.2233
var (t_0)	0.0182	0.0246	0.0032	0.0042
cov (L_{∞}, k)	-0.9892	-2.0091	-0.3052	-0.4808
cov (L_{∞}, t_0)	-6.1381	-20.3573	-1.4960	-2.5903
cov (k, t_0)	0.0020	0.0018	0.0004	0.0005

E. Acuna, R. MacIntosh, C. Armistead, J. Haaga, M. Wilkins, S. Neidetcher, L. Logerwell, P. Munro, C. Johnston, M. Nelson, G. Duker, and J. Lee. Thanks to the following Alaska Department of Fish and Game staff for sample collections: J. Blackburn, D. Urban, D. Pengilly, K. Phillips, T. Dinnocenzo, I. MacIntosh, M. Ruccio, D. Jackson, the Captain R. Kutchick, and crew of the RV *Resolution*. K. MacIntosh from the Alaska Groundfish Databank collected the plant samples.

Literature cited

- Efron, B., and R. J. Tibshirani.
1993. An introduction to the bootstrap, 436 p. Chapman and Hall, New York, NY.
- Foucher, R. P., and A. V. Tyler
1990. Estimation of the fecundity of Pacific cod *Gadus macrocephalus*. Can. Man. Rep. Fish. Aquat. Sci. 2088, 49 p.
- Hart, L.
1973. Pacific fishes of Canada. Fish. Res. Board Can. Bull. 180,740 p.
- Hattori, T., Y. Kasurai, and K. Shimazaki.
1992. Maturation and reproductive-cycle of female Pacific cod in waters adjacent to the southern coast of Hokkaido, Japan. Nihon. Suisan. Gakkai-Shi 58:2245-2252.
- Hunter, J. R., B. J. Macewicz, N. C. H. Lo, and C. A. Kimbrell.
1992. Fecundity, spawning, and maturity of female Dover sole, *Microstomus pacificus*, with an evaluation of assumptions and precision. Fish. Bull. 90:101-128.
- Kimura, D. K.
1980. Likelihood methods for the von Bertalanffy growth curve. Fish. Bull. 77:765-776.
- Kjesbu, O. S., J. Klungsoyr, H. Kryvi, P. R. Witthames, and M. Greer-Walker.
1991. Fecundity, atresia, and egg size of captive Atlantic cod (*Gadus morhua*) in relation to proximate body composition. Can. J. Fish. Aquat. Sci. 48:2333-2343.
- Lambert, Y., and J. D. Dutil.
2000. Energetic consequences of reproduction in Atlantic cod *Gadus morhua* in relation to spawning level of somatic energy reserves. Can. J. Fish. Aquat. Sci. 57:815-825.
- Matarese, A. C., D. M. Blood, S. J. Picquelle, and J. L. Benson.
2003. Atlas of abundance and distribution patterns of ichthyoplankton from the Northeast Pacific Ocean and Bering Sea ecosystems based on research conducted by the Alaska Fisheries Science Center 1972-1996. U.S. Dep. Commer. NOAA Prof. Pap. NMFS 1, 281 p.
- Norberg, B., C. L. Brown, O. Halldorsson, K. Stensland, and B. T. Bjornsson.
2004. Photoperiod regulates the timing of sexual maturation, spawning, sex steroid and thyroid hormone profiles in the Atlantic cod *Gadus morhua*. Aquaculture 229:451-467.
- Roberson, N. E., D. K. Kimura, D. R. Gunderson, and A. M. Shimada.
2005. Indirect validation of the age-reading method for Pacific cod (*Gadus macrocephalus*) using otoliths from marked and recaptured fish. Fish. Bull. 103:153-160.
- Rovnina, O. A., N. V. Klovach, A. I. Glubokov, and A. P. Selyutin.
1997. On the biology of Pacific cod *Gadus macrocephalus* in the eastern part of the Sea of Okhotsk. J. Ichthyol. 37:21-26. Translated from Russian [1997 Voprosy Ikhtologii 37:27-32] by Interperiodica Publishing, Russia.
- Saborido-Rey, F., and S. Junquera.
1998. Histological assessment of variations in sexual maturity of cod (*Gadus morhua* L.) at the Flemish Cap (north-west Atlantic). ICES J. Mar. Sci. 55:515-521.
- Sokal, R. R.
1969. Biometry, 776 p. W.H. Freeman and Company, San Francisco, CA.
- Stark, J. W., and D. A. Somerton.
2002. Maturation, spawning and growth of rock soles off Kodiak Island in the Gulf of Alaska. J. Fish Biol. 61:417-431.
- Teshima, K.
1985. Maturation of Pacific cod in the eastern Bering Sea. Bull. Jap. Soc. Sci. Fish. 51:21-31.

- Thompson, G. G., and M. W. Dorn.
2005. Stock assessment and fishery evaluation: Bering Sea and Aleutian Island cod, 90 p. North Pacific Fishery Management Council. Anchorage, AK.
- Thompson, G. G., H. H. Zenger, and M. W. Dorn.
2005. Stock assessment and fishery evaluation: Gulf of Alaska Cod, 112 p. North Pacific Fishery Management Council. Anchorage, AK.
- Venables, W. N.
1997. Modern applied statistics with S-Plus, 548 p. Springer-Verlag, New York, NY.
- Waiwood, K. G.
1982. Growth history and reproduction in Atlantic cod (*Gadus morhua*). In Proceedings of the international symposium on reproductive physiology of fish (C. J. J. Richter, and H. J. Th. Goos, eds.), 256 p. Pudoc Press, Wageningen, The Netherlands.
- Welch, D. W., and R. P. Foucher.
1988. A maximum-likelihood methodology for estimating length-at-maturity with application to Pacific cod (*Gadus macrocephalus*) population dynamics. Can. J. Fish. Aquat. Sci. 45(2):333-343.

Abstract—The U.S. East Coast pelagic longline fishery has a history of interactions with marine mammals, where animals are hooked and entangled in longline gear. Pilot whales (*Globicephala* spp.) and Risso's dolphin (*Grampus griseus*) are the primary species that interact with longline gear. Logistic regression was used to assess the environmental and gear characteristics that influence interaction rates. Pilot whale interactions were correlated with warm water temperatures, proximity to the shelf break, mainline lengths greater than 20 nautical miles, and damage to swordfish catch. Similarly, Risso's dolphin interactions were correlated with geographic location, proximity the shelf break, the length of the mainline, and bait type. The incidental bycatch of marine mammals is likely associated with depredation of the commercial catch and is increased by the overlap between marine mammal and target species habitats. Altering gear characteristics and fishery practices may mitigate incidental bycatch and reduce economic losses due to depredation.

Interactions between marine mammals and pelagic longline fishing gear in the U.S. Atlantic Ocean between 1992 and 2004

Lance P. Garrison

Email address: Lance.Garrison@noaa.gov

National Marine Fisheries Service
Southeast Fisheries Science Center
75 Virginia Beach Dr.
Miami, Florida 33149

Marine mammal mortalities and injuries occur in gillnet fisheries (Perrin et al., 1994), trawl fisheries (Fertl and Leatherwood, 1997), and longline fisheries (e.g., Garrison, 2005; Kock et al., 2006). The U.S. East Coast pelagic longline fishery targeting swordfish, tunas, and sharks has long been the focus of bycatch reduction efforts for nontarget fish species (e.g., billfish; Goodyear, 1999) and for marine turtles (Watson et al., 2005). In addition, marine mammal bycatch in the pelagic longline fishery is common, particularly of pilot whales (*Globicephala* spp.) and Risso's dolphins (*Grampus griseus*). An estimated average of 132 (CV [coefficient of variation]=0.49) pilot whales and 45 (CV=0.38) Risso's dolphins either died or were seriously injured because of interactions with pelagic longline gear each year between 1999 and 2003 (Waring et al., 2006). These numbers account for 63% of the total commercial fishery-related mortality for pilot whales and 88% for Risso's dolphins along the U.S. East Coast. The total fishery mortality for pilot whales approaches the potential biological removal (PBR) benchmark (PBR=249 for pilot whales and 129 for Risso's dolphins), and it exceeds the requirement that mortality caused by commercial fishing approach insignificant levels as mandated by the U.S. Marine Mammal Protection Act (MMPA) (Waring et al., 2006).

In addition to marine mammal conservation concerns, the occurrence of depredation, or marine mammals feeding on the catch or bait from commercial fishing gear, is an emerging global issue. Depredation has been observed

on both bottom and pelagic longlines by killer whales (*Orcinus orca*; Secchi and Vaske, 1998; Kock et al., 2006), false killer whales (*Pseudorca crassidens*), pilot whales, and sperm whales (*Physeter macrocephalus*; Kock et al., 2006). Fishermen in the Atlantic longline fleet indicate that damage to commercial catch by pilot whales is common (Angliss and DeMaster, 1998). Depredation has a direct economic impact on commercial fishermen by removing commercially valuable catch.

Identification of the fishing practices and environmental processes that drive interactions between marine mammals and longline fishing gear is important to understanding and reducing both incidental mortality and depredation. In this study, pelagic longline fishery observer data collected between 1992 and 2004 were analyzed to describe the number of interactions, seasonal and spatial patterns, and the types of interactions associated with serious injuries and mortalities of marine mammals. Logistic regression was used to examine factors affecting the probability of interactions with pilot whales and Risso's dolphins. The results of these analyses will help managers make informed decisions to reduce both marine mammal bycatch and economic losses due to depredation.

Materials and methods

Pelagic observer program

The U.S. East Coast pelagic longline fishery has been observed since 1992.

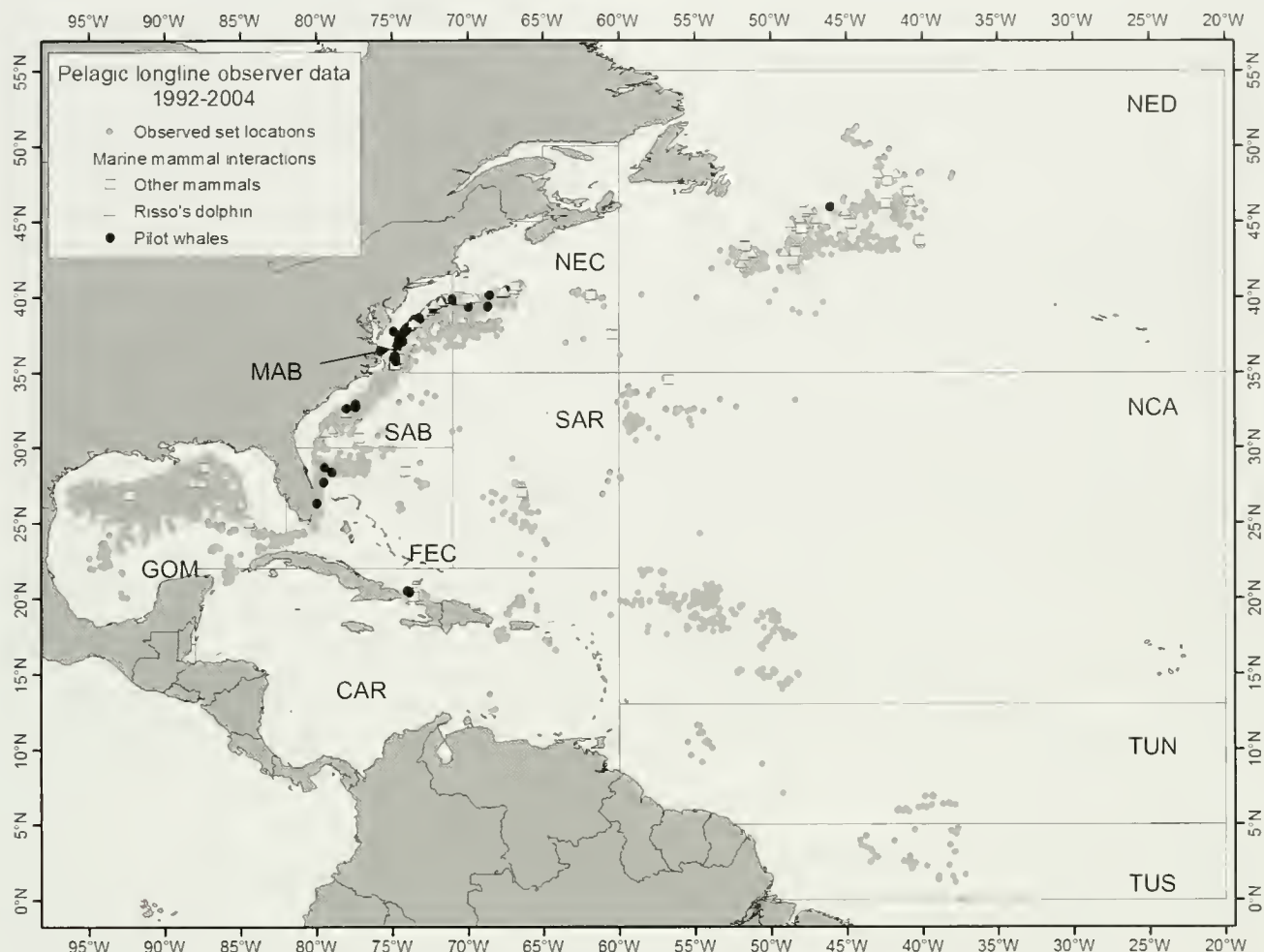


Figure 1

Locations of observed pelagic longline sets and marine mammal interactions from 1992 through 2004. Abbreviations indicate pelagic longline statistical fishing areas: CAR=Caribbean, FEC= Florida East Coast, GOM=Gulf of Mexico, NEC=Northeast Coastal, NED=Northeast Distant, NCA=North Central Atlantic, MAB=Mid-Atlantic Bight, SAB=South Atlantic Bight, SAR=Sargasso Sea, TUN=Tuna North, and TUS=Tuna South.

Observer coverage was allocated randomly among fishing vessels by calendar quarter and fishing area. Achieved annual observer coverage typically ranged between 3–4% of longline sets between 1992–2001 and was near 7% during 2002–04. The observers collected detailed information on gear characteristics, set and haul locations, environmental data, and composition of the fish catch. Observers also documented incidental takes of marine mammals including estimated lengths and written descriptions of each animal and its interaction with the fishing gear (Beerkircher et al., 2004).

During 2001–04, the Northeast Distant (NED) fishing area (Fig. 1) was closed to the longline fishery because of concerns over marine turtle bycatch. An experimental program was initiated, in cooperation with the fishing industry, to explore potential gear and bait combinations to reduce interactions with marine turtles. During the study, fishermen used larger circle hooks rather than traditional, smaller, straight-shanked “J” hooks

(Watson et al., 2005). There was 100% observer coverage of this experimental fishing. Because the fishing operations were prescribed by experimental design, and differed from standard commercial fishing operations, data from these experimental sets, including data on marine mammal interactions, were excluded from the current analysis.

Observed marine mammal interactions

When a marine mammal interacted with the longline gear (i.e., was hooked or entangled), the observers noted the condition of the captured animal and the type of fishing gear, documented efforts to remove the animal from the gear, and recorded the behavior of the animal after release. Observer comments were summarized to assess the most frequent types of interactions with longline gear. Two species of pilot whales inhabit the waters along the U.S. East Coast: the short-finned pilot

whale (*G. macrorhynchus*) and long-finned pilot whale (*G. melas*). However, the two could not be reliably distinguished at sea by the observers and therefore were combined in this analysis.

Determination of serious injury to marine mammals

The MMPA requires that incidental mortality of and serious injury to marine mammals during commercial fishing operations be reduced below the PBR benchmark. Serious injury has been defined as an injury likely to result in mortality (Angliss and DeMaster, 1998). A workshop of National Marine Fisheries Service (NMFS) and nongovernmental experts was convened in 1997 to evaluate the types of injuries occurring in commercial fisheries and to develop guidelines to determine if a given marine mammal observed interacting with commercial fishing gear was seriously injured. For small cetaceans, including pilot whales and other delphinids, it was concluded that animals that ingested hooks, that were released with significant amounts of trailing fishing gear, that were swimming abnormally, or that suffered severe external trauma would be considered seriously injured (Angliss and Demaster, 1998). Serious injury determinations were made by NMFS staff on a case-by-case basis after reviewing the observations and comments of fishery observers.

Logistic regression analysis

Logistic regression was used to evaluate the effects of environmental conditions and fishing practices on the probability of interactions with pilot whales and Risso's dolphins. The vast majority (>85%) of interactions with marine mammals involved only one individual with a set. Therefore, the data were transformed to a binary response variable indicating whether or not a marine mammal interaction was observed.

Only longline sets made along the U.S. Atlantic and Caribbean coasts, including the Florida East Coast (FEC), South Atlantic Bight (SAB), Mid-Atlantic Bight (MAB), Northeast Coastal (NEC), and Caribbean (CAR) fishing areas (Fig. 1), were included in this analysis because interaction rates in most other areas were extremely low or zero. Although Risso's dolphin interactions were observed during experimental fishing in the NED, the fishing characteristics of these sets were different from those of the normal commercial fishing operations. Therefore, sets observed in the NED (experimental and nonexperimental) were excluded from the analysis. This included two observed interactions with Risso's dolphins and none with pilot whales in nonexperimental fishing. The analysis focused on the Atlantic fishing areas with the highest overall interaction rates with pilot whales and Risso's dolphin and comprised 3187 observed longline sets.

Explanatory variables were drawn from a broad suite of data collected during each set by the fishery observer (Table 1), or they were derived from the date and location of the set (Table 1). Variables were categorized

broadly as environmental conditions, space or time variables, gear characteristics, fishing effort level, and catch characteristics. However, each was considered independently in developing the best fitting, most parsimonious logistic regression model following strategies for model selection outlined in Hosmer and Lemeshow (1989). Briefly, each variable was examined individually to assess its explanatory power, and the subset of significant single terms was included in the initial model. Following this initial exploratory step, the single terms and all two-way interactions were examined by using stepwise selection. The explanatory power and significance of each potential model term was examined through chi-square tests and Akaike's information criterion (AIC; Hosmer and Lemeshow, 1989; McCullagh and Nelder, 1989). Terms were retained in the model if they were significant (at a P -value <0.10) based upon chi-square tests and if their addition resulted in a reduction in AIC. The resulting models were examined for overdispersion by using the ratio between the residual model chi-square and degrees of freedom (Burnham et al., 1987; McCullagh and Nelder, 1989). For both the pilot whale model and the Risso's dolphin model, this ratio was approximately equal to one, which indicated no significant problems with overdispersion and hence accurate estimates of variance for model parameters.

Results

Observed marine mammal interactions

Between 1992 and 2004, a total of 200 interactions between marine mammals and pelagic longline gear were observed. Of these, there were 10 observed mortalities and 94 observed serious injuries (Table 2). One hundred of the observed interactions were with pilot whales, 64 were with Risso's dolphin, and all other species had six or fewer observed interactions. Other marine mammal interactions of note occurred with a killer whale, unidentified beaked whales (family Ziphiidae), a pygmy or dwarf sperm whale (*Kogia* spp.), a northern bottlenose whale (*Hyperoodon ampullatus*), and two baleen whales (Table 2).

The majority of marine mammal interactions were observed near the shelf break along the U.S. Atlantic coast between North Carolina and Georges Bank (Fig. 1). Pilot whale interactions were concentrated in the MAB fishing area between North Carolina and New Jersey, whereas Risso's dolphin interactions primarily occurred in the NEC region (Fig. 1). Thirteen Risso's dolphins, one pilot whale, and eight additional animals of various species interacted with fishing gear during experimental fishing operations in the NED during 2001–03 (Fig. 1).

The observed interaction rates (number of sets with a marine mammal interaction/number of observed sets) fluctuated across the time series. The highest rates were observed during 1992–95 and in the most recent years from 2000 through 2004 (Fig. 2A). There were generally low interaction rates and very few pilot whale

Table 1

Environment, space or time, gear type, fishing effort, and catch variables examined in logistic regression analyses of the probability of marine mammal interactions in the U.S. pelagic longline fishery. The fishing areas included in the study were the following: Florida East Coast (FEC), Mid-Atlantic Bight (MAB), South Atlantic Bight (SAB), Northeast Coastal (NEC), and Caribbean (CAR) (see Fig. 1).

Type of variable	Variable name	Description
Environment	Average temperature	Average of sea surface temperature reported by observer at beginning and end of haul and set
Environment	Water depth	Water depth based on average location of set determined from a global bathymetry grid
Environment	Wave height	Recorded by observers at time of set
Environment	Wind speed	Recorded by observers at time of set
Environment	Weather conditions	Calm, cloudy, mild storm, stormy—recorded by observers at time of set
Space or time	Distance from 200-m isobath	Distance of the set (km) from the 200-m isobath
Space or time	Average location	Average of latitude and longitude for beginning set, end set, beginning haul, end haul
Space or time	Month	Calendar month of beginning set
Space or time	Quarter	Calendar quarter of beginning set
Space or time	Year	Calendar year of beginning set
Space or time	Fishing area	Fishing area of set: includes FEC, MAB, SAB, NEC, CAR
Space or time	Geographic area	Combined area categories MAB versus other areas
Space or time	Lunar phase	Lunar age since full moon
Gear type	Hook shape	Type(s) of hooks reported on the set. Categories include J-hook only, C-hook only, or both types
Gear type	Hook size	Size categories of hooks on the set were 7/0, 8/0, 9/0, 10/0, 12/0, 16/0, and 18/0
Gear type	Light sticks	Binary variable, whether or not light sticks were used on the set
Gear type	Bait type	Type(s) of bait recorded. Includes fish only, squid only, or both
Gear type	Live bait	Binary variable, whether or not live bait was used on the set
Gear type	Hook depth	Average of reported minimum and maximum hook depths (fathoms)
Gear type	Day set	Binary variable, whether or not set occurred during daylight
Gear type	Day soak	Binary variable, whether or not gear soaked during daylight
Gear type	Day haul	Binary variable, whether or not haulback occurred during daylight
Effort	Mainline length	Mainline length reported in miles
Effort	Number of hooks	Number of hooks set
Effort	Set duration	Number of hours to set the gear
Effort	Soak duration	Number of hours the gear soaked between the end of the set and the beginning of the haul
Effort	Haul duration	Number of hours spent hauling the gear
Effort	Total duration	Estimated number of hours the average hook was in the water (1/2 set duration + soak duration + 1/2 haul duration)
Effort	Hook density	Number of hooks/mainline length
Effort	Hook hours	Number of hooks×total duration
Catch	Bigeye tuna (<i>Thunnus obesus</i>)	Bigeye tuna catch (numbers)
Catch	Sharks	Shark catch (numbers)
Catch	Swordfish (<i>Xiphias gladius</i>)	Swordfish catch (numbers)
Catch	Other tunas	Other tuna catch (numbers)
Catch	Yellowfin tuna (<i>Thunnus albacores</i>)	Yellowfin tuna catch (numbers)
Catch	All tunas	Sum of yellowfin tuna, bigeye tuna, and other tunas
Catch	Damage	Binary variable, whether or not damage to the catch was observed
Catch	Swordfish damage	Binary variable, whether or not damage to swordfish catch was observed
Catch	Tuna damage	Binary variable, whether or not damage to tuna catch was observed

Table 2

Marine mammal interactions with pelagic longline fishing gear between 1992 and 2004. The totals include interactions observed during experimental fishing in the Northeast Distant Water (NED) fishing area. Determination of serious injury was based on observer descriptions and National Marine Fisheries Service criteria (Angliss and Demaster, 1998).

Species	Total captured	Total observed dead	Total seriously injured
Pilot whale (<i>Globicephala</i> spp.)	100	4	52
Risso's dolphin (<i>Grampus griseus</i>)	64	6	30
Common dolphin (<i>Delphinus delphi</i>)	6	0	0
Bottlenose dolphin (<i>Tursiops truncatus</i>)	6	0	2
Unidentified dolphin	4	0	2
Unidentified marine mammal	4	0	2
Unidentified beaked whales (<i>Mesoplodon</i> spp.)	3	0	1
Pantropical spotted dolphin (<i>Stenella attenuata</i>)	3	0	0
Atlantic spotted dolphin (<i>Stenella frontalis</i>)	2	0	2
Striped dolphin (<i>Stenella coeruleoalba</i>)	2	0	0
Unidentified whale	1	0	1
Northern bottlenose whale (<i>Hyperoodon ampullatus</i>)	1	0	1
Unidentified baleen whale	1	0	0
Killer whale (<i>Orcinus orca</i>)	1	0	0
Minke whale (<i>Balaenoptera acutorostratus</i>)	1	0	0
Pygmy or dwarf sperm whale (<i>Kogia</i> spp.)	1	0	1

Table 3

Types of serious injuries observed in marine mammals interacting with pelagic longline fishing gear between 1992 and 2004.

Species	Mouth hooked	Animal released with entangling gear	Mouth hooked and animal released with entangling gear	Total
Pilot whales (<i>Globicephala</i> spp.)	3	19	30	52
Risso's dolphin (<i>Grampus griseus</i>)	7	12	11	30
Other species	1	3	8	12
Totals	11	34	49	94

interactions were observed during 1996–98. Interaction rates for both pilot whales and Risso's dolphins peaked during the late summer and fall (Fig. 2B).

Types of serious injury

Of the 94 observed serious injuries, there were 60 cases where marine mammals were released with hooks remaining in the mouth. In 49 of these cases, monofilament line (typically 15–60 feet in length) remained with the animal (Table 3). In the remaining 11 cases, the animal was released with less than five feet of monofilament line and with the hook remaining in the mouth. In four of the 11 documented mortalities, the animal was hooked in the mouth.

There were 34 serious injuries in which the animal was released entangled with fishing gear that did not involve ingestion of a hook (Table 3). The majority of these cases were injuries to animals that became

entangled in the mainline which typically consists of 700-lb test monofilament. In most of these cases, the animal was released with multiple wraps of mainline around its tail or body, and the gear remained with the animal after the line was cut. In five of the 10 documented mortalities, the animal was entangled in the mainline. Fishermen were typically able to cut the mainline away from entangled animals. Thus, the majority of animals entangled in the mainline were released without entangling gear, and these animals were not considered to be seriously injured.

Logistic regression results: Pilot whales

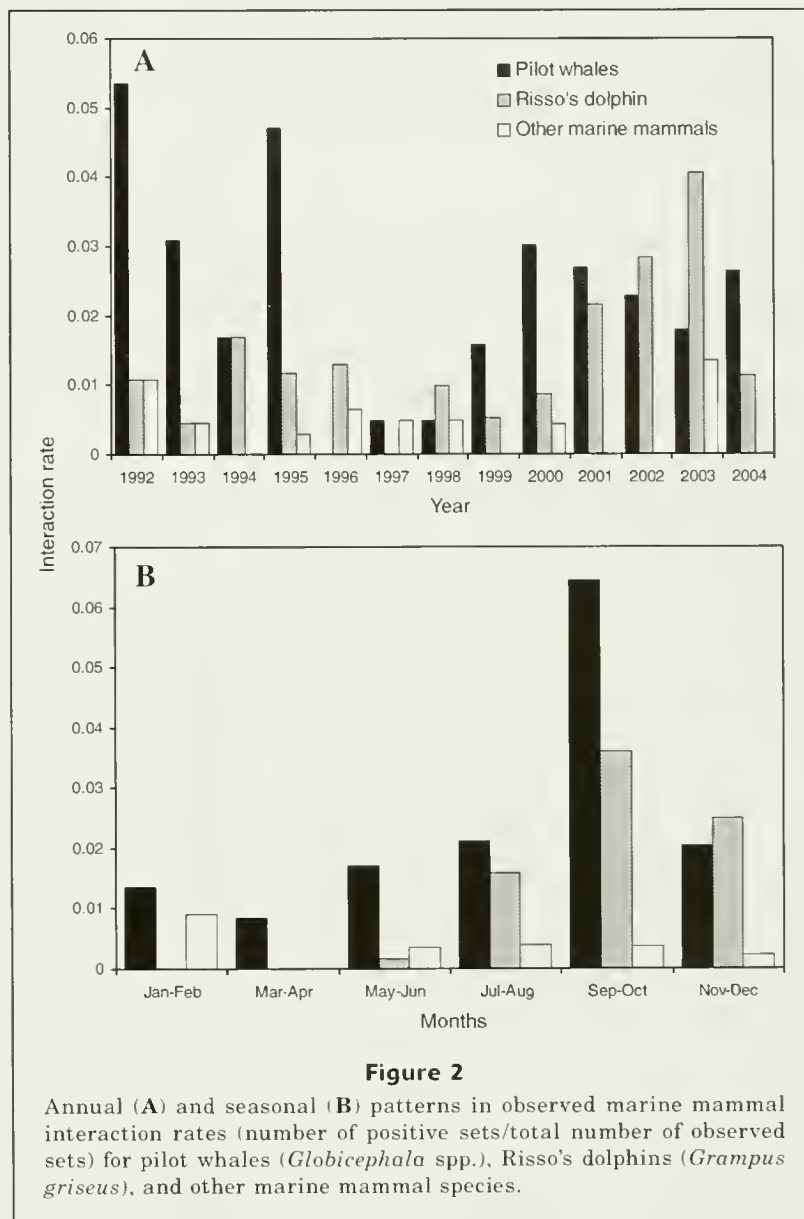
Geographic area (MAB vs. other areas; chi-square=31.24, df=1, $P<0.0001$), distance from the 200-m isobath (chi-square=11.31, df=1, $P=0.0008$), and observed damage to the swordfish catch (chi-square=7.26, df=1, $P=0.0071$) were significant factors correlated with the occurrence

of pilot whale interactions with longline gear. A linear term for water temperature was also highly significant and, on inspection of initial regression results, there was a unimodal relationship between water temperature and interaction rate. Water temperature ($\chi^2=8.53$, $df=1$, $P=0.0035$) and its second-order term ($\chi^2=7.87$, $df=1$, $P=0.0050$) were included in the model and were statistically significant. There was also an apparent nonlinear relationship with mainline length, with a step increase in interaction rate for mainlines greater than 20 nautical miles in length. The continuous mainline length variable was replaced with a binary response (mainline ≥ 20 miles). This variable was highly significant ($\chi^2=13.24$, $df=1$, $P=0.0003$) and provided greater explanatory power and a better model fit than the continuous variable. The final model was highly significant (total $\chi^2=146.67$, $df=6$, $P<0.0001$), and both examination of residuals and goodness-of-fit tests indicated strong model fit.

Interactions with pilot whales were much more likely to occur in the MAB fishing area than in other regions. Both mainline length and damage to swordfish catch on the set also significantly increased the probability of observing a pilot whale interaction (Fig. 3). There was a strong decrease in the probability of a pilot whale interaction with increasing distance from the 200-m isobath (Fig. 4), and this trend was apparent in the MAB and other regions. No pilot whale interactions were observed in sets greater than 30 km away from the 200-m isobath. The correlation with water temperature was generally weaker than that for other factors; however, there was a peak in interaction rates in warm waters between 70 and 80°F in the MAB and between 75 and 85°F in the other geographic areas. This warm water peak was associated with late summer and fall in these regions.

Logistic regression results: Risso's dolphins

Risso's dolphin interaction rates were significantly higher in the MAB ($\chi^2=4.56$, $df=1$, $P=0.0328$) and the NEC fishing areas ($\chi^2=13.03$, $df=1$, $P=0.0003$) than in areas farther south. The highest interaction rates overall were observed in the NEC. As with pilot whales, distance from the 200-m isobath ($\chi^2=4.58$, $df=1$, $P=0.0306$) and damage to swordfish catch ($\chi^2=4.68$, $df=1$, $P=0.0297$) were important explanatory factors. However, overall, the strength of these effects was weaker than that for pilot whales.



The mainline length effect, although improving the explanatory power of the model, was not a statistically significant factor ($\chi^2=3.284$, $df=1$, $P=0.07$). The use of fish bait, either alone or in addition to squid bait, significantly decreased the probability of observing a Risso's dolphin interaction ($\chi^2=4.33$, $df=1$, $P=0.0375$). The overall model was highly significant ($\chi^2=71.68$, $df=6$, $P<0.0001$) and provided a good fit to the data.

The bait effect was apparent only in the observed data from the MAB region and the southern Atlantic areas and was not observed in the NEC region, but the positive correlation with damage to swordfish catch was observed across all regions (Fig. 5). The negative correlation with distance from the 200-m isobath for Risso's dolphins was somewhat weaker than that for

pilot whales; however, no interactions were observed in waters greater than 30 km from the 200-m isobath, with the exception of one interaction observed in the south Atlantic areas (Fig. 6).

Discussion

Interactions of marine mammals with pelagic longlines are concentrated primarily in the MAB and NEC fishing areas along the shelf break. Interaction rates were

consistent across the time series, with the exception of the period between 1996–99. There was relatively low observer coverage in the MAB fishing area during these years, and the low observed interaction rates may be a sampling artifact. Pilot whales and Risso's dolphins are the primary species interacting with the longline fishery, and mortality and serious injury of these species are a significant conservation concern. Assessing the impact of fishery-induced mortality on the two pilot whale species (longfin and shortfin pilot whales) is difficult because the species cannot be distinguished in either assessment surveys or when caught on fishing gear. Thus, although the total fishery mortality is below the PBR limit for the combined species, it is possible that the longline fishery disproportionately impacts one species. The shortfin pilot whale (*G. macrorhynchus*) generally has a more southern distribution than the longfin pilot whale (*G. melas*), and therefore the impact of the longline fishery may be more severe than current stock assessments indicate. Research is currently underway to determine the spatial distributions of the two species in order to assess their status more accurately.

Approximately equal proportions of interactions involve hookings versus entanglement in the mainline for both species. Hooking almost exclusively involves the animal being hooked in the mouth. In most cases, the animal is released after the gangion line is either cut or broken; however the animal either trails or is entangled in a significant amount of monofilament line upon release. These animals are considered seriously injured and likely to die, and hence they are of greatest concern for conservation and management agencies. Marine turtle interactions with longlines also generally involve the animal swallowing the hook or being hooked externally. Therefore, developing and implementing guidelines for the removal of hooks and careful release of turtles is a major focus of management efforts (Watson et al., 2005). The challenges for release of marine mammals are more severe because larger animals can break gangion lines before these animals can be brought close to the boat, and there can be considerable risk of injury to the vessel crew. However, the development of equipment and protocols to more effectively remove ingested hooks from marine mammals would be an important step to reduce the severity of injuries.

The shape of the hook had no effect on marine mammal interaction rates in these analyses. This factor was examined closely because of recent changes in longline fishery gear—changes mandated to reduce the catch and mortality of endangered sea turtles. As of August 2004, all U.S. East Coast pelagic longline fishermen were required to use larger circle hooks rather than “J” hooks. In the data examined in the present

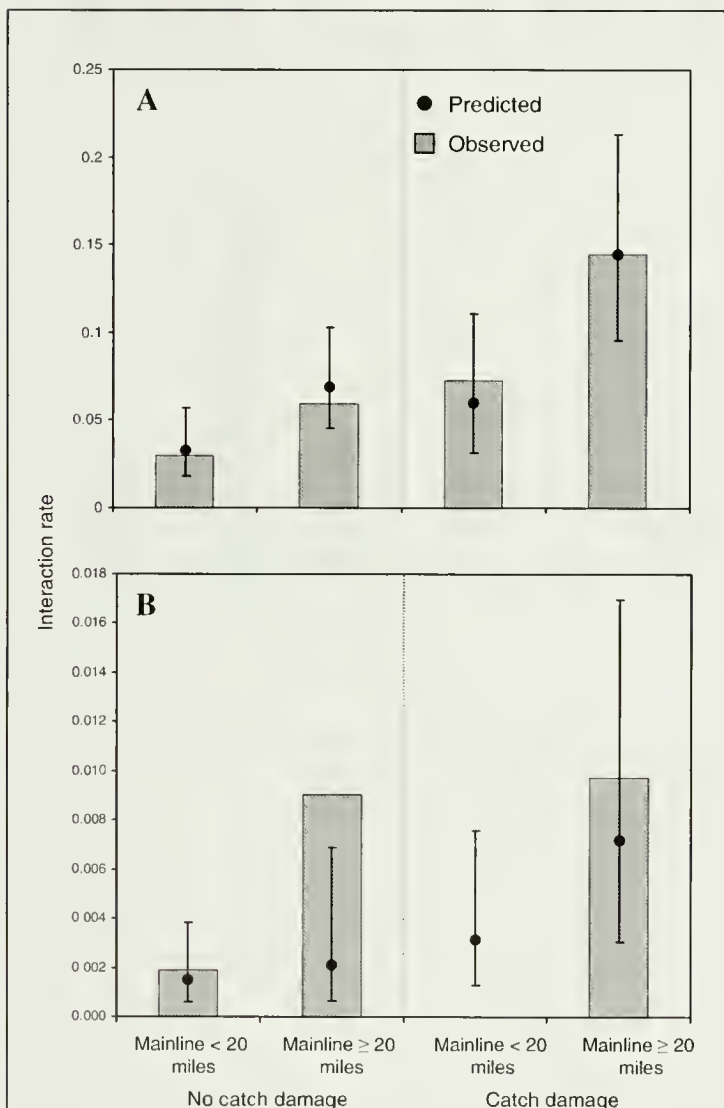


Figure 3

Predicted (black dots) and observed (bars) interaction rates with pilot whales (*Globicephala* spp.) by mainline-length category and observed catch damage for the Mid-Atlantic Bight fishing area (A) and other fishing areas (B). Error bars indicate 95% confidence intervals of predicted values. Note the difference in y-axis scale.

study, there were relatively few circle hooks observed in the fishery and thus there was limited power to test this potential gear effect. Marine mammal interactions with the fishery will continue to be closely monitored to verify that actions to reduce turtle interactions do not inadvertently increase marine mammal interactions.

The logistic regression results demonstrate that longline fishery interactions with both pilot whales and Risso's dolphins are largely driven by environmental factors and spatial overlap of marine mammals and fishery operations. Pilot whales are concentrated along the shelf break between the 200- and 1000-m isobaths, and the highest densities are found between Cape Hatteras, NC, and New Jersey and along the southern flank of Georges Bank (Payne and Heineemann, 1993; Mullin and Fulling, 2003; Waring et al., 2006). Risso's dolphins are similarly concentrated along the shelf break, but they have a more northern distribution from New Jersey to southern New England (Waring et al., 2006). Both species are found along the southeast Atlantic U.S. coast from North Carolina to Florida; however, they have much lower densities and are not as strongly associated with the shelf break (Mullin and Fulling, 2003; Waring et al., 2006) as in the former region. The fishery effort is similarly concentrated along the shelf break in both the MAB and NEC (Fig. 1; Abercrombie et al., 2005). Fishery effort is generally concentrated just north of Cape Hatteras, NC, during the winter months from January through April. The fishery then expands northward and overall effort increases through the MAB and NEC fishing areas, reaching peak effort levels during September and October and remaining high through December.

The strong overlap between fishery effort and high marine mammal presence is related to prey distribution. The pelagic longline fishery targets tunas and swordfishes that feed on small fish and squids. Both pilot whales and Risso's dolphins are also pelagic predators, and squids are a major component of their diets (Overholtz and Waring, 1991; Gannon et al., 1997; Kruse et al., 1999). Both longfin (*Loligo pealei*) and shortfin (*Illex illecebrosus*) squids are primary prey items, and both concentrate near the convergence zone of shelf-slope waters during summer and autumn (Brodziak and Hendrickson, 1999). The high interaction rate in the MAB area during summer and fall, and in warmer water temperatures, is therefore likely a function of environmental features driving availability of squid and small pelagic fishes that are prey for both the target fish species and marine mammals.

For both pilot whales and Risso's dolphins, there was a correlation between observed damage to swordfish catch and the likelihood of an interaction with a marine mammal. It should be noted that damage to catch may

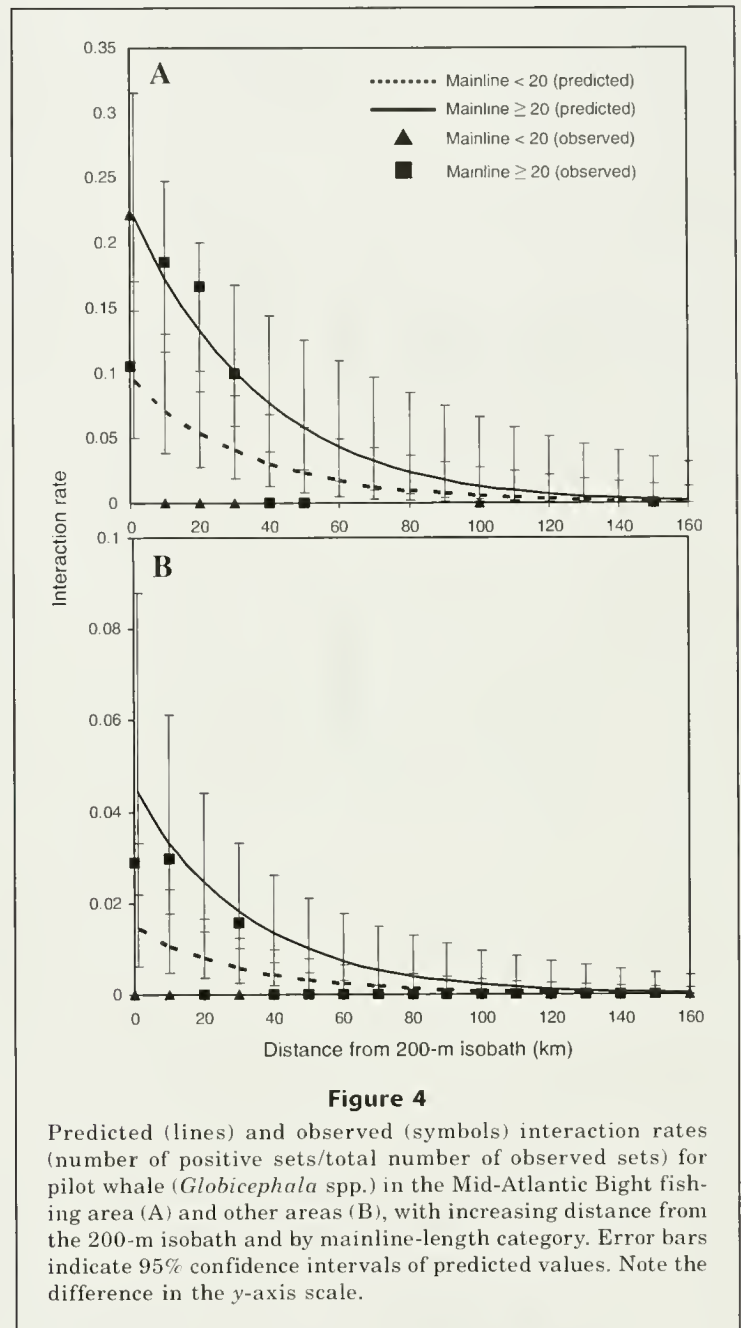
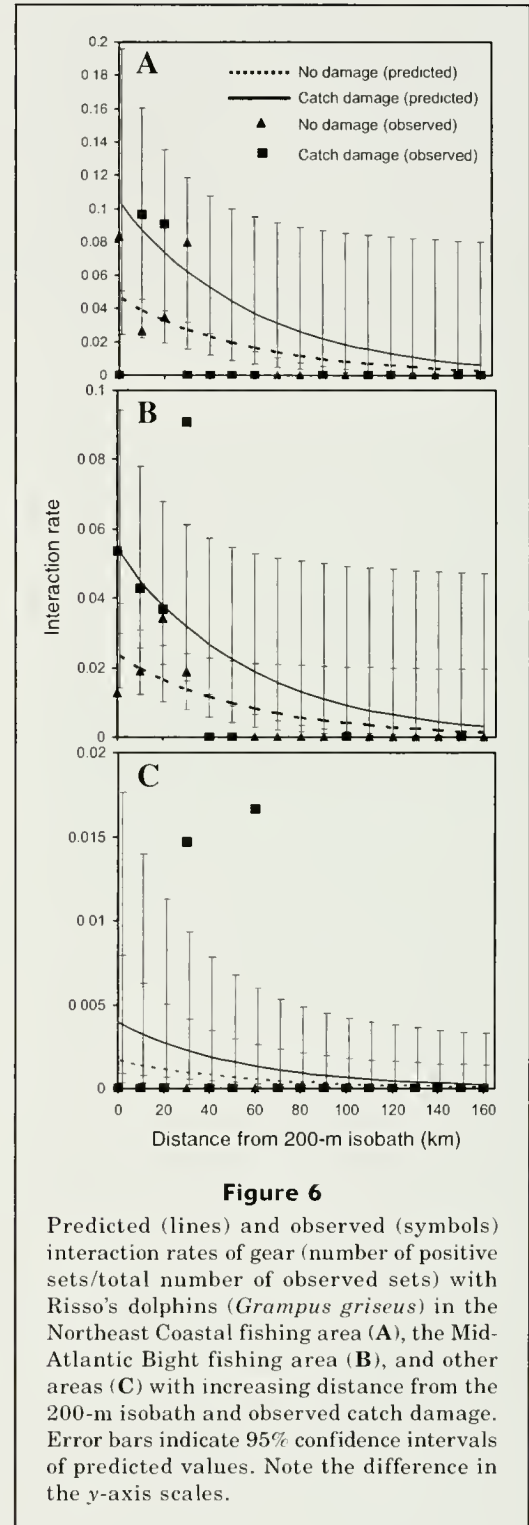
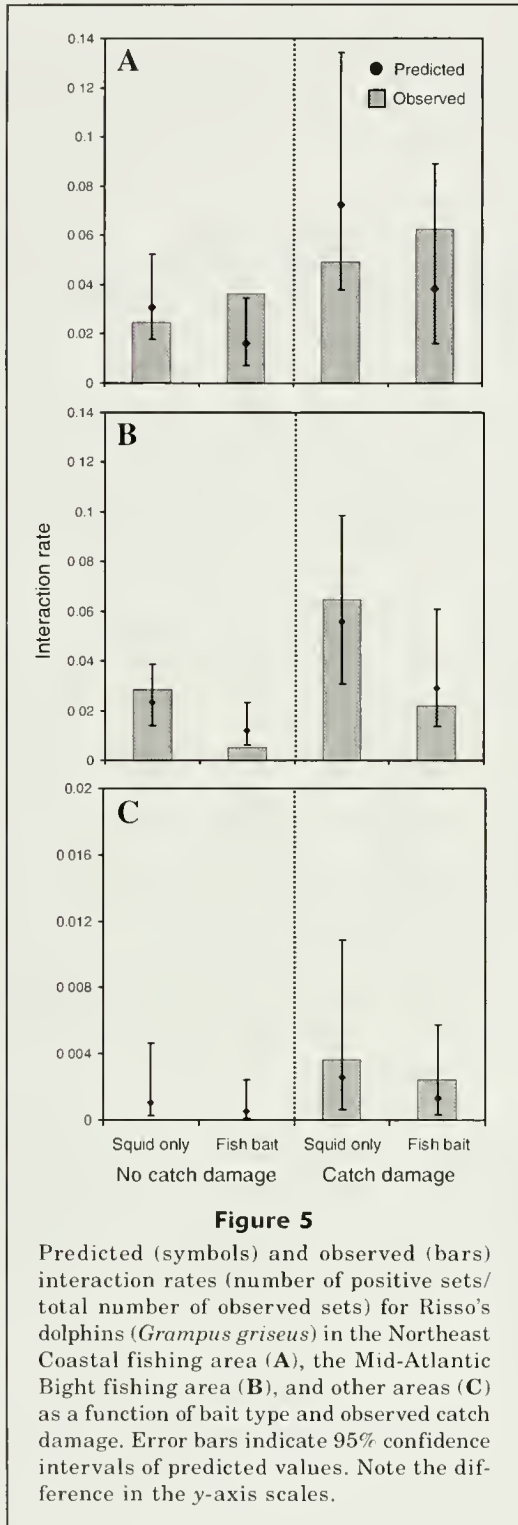


Figure 4

Predicted (lines) and observed (symbols) interaction rates (number of positive sets/total number of observed sets) for pilot whale (*Globicephala* spp.) in the Mid-Atlantic Bight fishing area (A) and other areas (B), with increasing distance from the 200-m isobath and by mainline-length category. Error bars indicate 95% confidence intervals of predicted values. Note the difference in the y-axis scale.

also be related to feeding by sharks, as well as by marine mammals. The strong correlation with damage to catch indicates that marine mammals are likely feeding upon the catch or bait. Similarly, the negative correlation between fish bait and Risso's dolphin interactions indicates that the animals were attracted to gear with squid bait as a ready food source.

The consistent effect of mainline length may also be related to depredation of catch on the longline gear. Longer mainlines represent a larger, more attractive food source or may be more easily detectable. Marine mammals therefore likely spend a longer time around the gear, creating greater opportunities for hooking



or entanglement. In other regions, sperm whales and killer whales are thought to respond to the sound of the vessel engines and winches when bottom longlines are hauled back on board (Kock et al., 2006). Longer haulback times associated with longer mainlines may thus further increase the opportunity for marine mam-

mals to detect fishing gear. Improving the understanding of how and why marine mammals are attracted to longline gear will help both to reduce the economic losses due to depredation of catches and the impacts of commercial fishing activities on marine mammal populations.

Marine mammal bycatch in longline gear is driven to a large extent by the overlap of marine mammal and pelagic fish habitat with the area of longline fishery operations. In addition, this analysis demonstrates that longer mainlines had a significantly higher bycatch rate than shorter mainlines. Reducing mainline lengths below 20 nautical miles, particularly within the seasons and areas where interactions occur, has the potential to reduce the rate of interactions and the impact of the longline fishery on pilot whale and Risso's dolphin populations. This management option, along with a suite of other measures, is currently being considered by NMFS within the framework of the Pelagic Longline Take Reduction plan.

Acknowledgments

I am indebted to the diligent efforts of the observers who have participated in the Pelagic Longline Observer Program throughout its history. C. Brown, D. Abercrombie, L. Beerkircher, and D. Lee of the National Marine Fisheries Service, Southeast Fisheries Science Center provided invaluable assistance. The analytical approach was developed in cooperation with members of the Pelagic Longline Take Reduction Team who made many useful suggestions and provided insights into the operation of the fishery. I would like to recognize the late N. Beideman, commercial fisherman and head of the Blue Water Fisherman's Association, for his contributions to the conservation of protected species during pelagic longline fishing operations. This work is a contribution of the Protected Species and Biodiversity Division, Southeast Fisheries Science Center, National Marine Fisheries Service.

Literature cited

- Abercrombie, D. L., H. A. Balchowsky, and A. L. Paine.
2005. 2002 and 2003 annual summary: large pelagic species. NOAA Tech. Memo. NMFS-SEFSC-529, 33 p.
- Angliss, R. P., and D. P. DeMaster.
1998. Differentiating serious and non-serious injury of marine mammals taken incidental to commercial fishing operations: Report of the serious injury workshop 1-2 April, 1997, Silver Spring, Maryland. NOAA Tech. Memo. NMFS-OPR-13, 48 p.
- Beerkircher, L. R., C. J. Brown, D. L. Abercrombie, and D. W. Lee.
2004. SEFSC Pelagic Observer Program Data Summary for 1992-2002. NOAA Tech. Memo. NMFS-SEFSC-522, 25 p.
- Burnham, K. P., D. R. Anderson, G. C. White, C. Brownia, and K. Pollack.
1987. Design and analysis methods for fish survival experiments based on release-recapture. American Fisheries Society, Monograph 5, 433 p. Am. Fish. Soc., Bethesda, MD.
- Brodziak, J., and L. Hendrickson.
1999. An analysis of environmental effects on survey catches of squids *Loligo pealei* and *Illex illecebrosus* in the northwest Atlantic. Fish. Bull. 97:9-24.
- Fertl, D., and S. Leatherwood.
1997. A review of cetacean interactions with trawls. J. NW Atl. Fish. Sci. 22:209-218.
- Gannon, D. P., A. J. Read, J. E. Craddock, K. M. Frstrup, and J. R. Nicolas.
1997. Feeding ecology of long-finned pilot whales *Globicephala melas* in the western North Atlantic. Mar. Ecol. Prog. Ser. 148:1-10.
- Garrison, L. P.
2005. Estimated bycatch of marine mammals and turtles in the U.S. Atlantic pelagic longline fleet during 2004. NOAA Tech. Memo. NMFS-SEFSC-531, 57 p.
- Goodyear, C. P.
1999. An analysis of the possible utility of time-area closures to minimize billfish bycatch by U.S. pelagic longlines. Fish. Bull. 97:243-255.
- Hosmer, D. W., and S. Lemeshow.
1989. Applied logistic regression, 307 p. John Wiley and Sons, Inc., New York, NY.
- Kock, K.-H., M. G. Purves, and G. Duhamel.
2006. Interactions between cetaceans and fisheries in the Southern Ocean. Polar Biol. 29:379-388.
- Kruse, S., D. K. Caldwell, and M. C. Caldwell.
1999. Risso's dolphin—*Grampus griseus* (G. Cuvier 1812). In Handbook of marine mammals (S. H. Ridgeway, and R. Harrison, eds.), p. 183-212. Academic Press, San Diego, CA.
- McCullagh, P., and J. A. Nelder.
1989. Generalized linear models, 511 p. Chapman and Hall, London.
- Mullin, K. D., and G. L. Fulling.
2003. Abundance of cetaceans in the southern U.S. north Atlantic ocean during summer 1998. Fish. Bull. 101:603-613.
- Overholtz, W. M., and G. T. Waring.
1991. Diet composition of pilot whales *Globicephala* sp. and common dolphins *Delphinus delphis* in the mid-Atlantic bight during spring 1989. Fish. Bull. 89:723-728.
- Payne, P. M., and D. W. Heinemann.
1993. The distribution of pilot whales (*Globicephala* sp.) in the shelf/shelf edge and slope waters of the northeastern United States, 1978-1998. Reports of the International Whaling Commission (special issue 14):51-68.
- Perrin, W. F., G. P. Donovan, and J. Barlow.
1994. Gillnets and cetaceans. International Whaling Commission. Special issue 15, p. 1-53.
- Secchi, E. R., and T. Vaske.
1998. Killer whale (*Orcinus orca*) sightings and depredation on tuna and swordfish longline catches. Aquat. Mamm. 24:117-122.
- Waring, G. T., E. Josephson, C. P. Fairfield, and K. M. Foley.
2006. U.S. Atlantic and Gulf of Mexico marine mammal stock assessments—2005. NOAA Tech. Memo. NMFS-NE-194, 352 p.
- Watson, J. W., S. P. Epperly, A. K. Shah, and D. G. Foster.
2005. Fishing methods to reduce sea turtle mortality associated with pelagic longlines. Can. J. Fish. Aquat. Sci. 62:965-981.

Abstract—Data collected during fishery-independent sampling programs were used to examine the impact of appendage damage (indicated by lost or regenerated legs and antennae) on the reproductive output of female western rock lobster (*Panulirus cygnus*). Most of the damaged females sampled had one (53%), two (27%), or three (13%) appendages that had been lost or that were regenerating. Appendage damage was associated with the reduced probability of a female developing ovigerous setae; and if setae were produced, with the reduced probability that females would produce more than one batch of eggs within a season. These effects were more pronounced as the number of damaged appendages increased. From data collected in 2002, it was estimated that the total number of eggs produced by mature females caught in the fishery was significantly reduced ($P < 0.001$) by 3–9% when the impact of appendage damage was included.

Changes in egg production of the western rock lobster (*Panulirus cygnus*) associated with appendage damage

Roy Melville-Smith (contact author)

Simon de Lestang

Email address for R. Melville-Smith: rmsmith@fish.wa.gov.au

Department of Fisheries (Western Australia)
Western Australian Marine Research Laboratories
39 Northside Drive
Hillarys, Western Australia 6025, Australia

Western rock lobster (*Panulirus cygnus*) are found only off Western Australia, where they form the basis of an intensive commercial fishery (Phillips and Melville-Smith, 2005). One result of the high exploitation rates experienced by western rock lobster (Brown and Caputi, 1985, 1986), and other decapod species (Krouse, 1976; Smith and Howell, 1987), is the damage sustained by the catch that is returned to the water. Damage, whether caused by aggression between conspecifics trapped in pots, desiccation on board boats before processing, or rough handling during sorting, is generally a combination of dehydration, broken body parts, and the loss of entire appendages. Apart from the mortality of animals due to processing, both the growth rate and fecundity of the surviving animals can be significantly reduced (Davis, 1981; Brouwer et al., 2006). Damaged animals appear to reallocate energy stores towards regenerating damaged appendages and away from growth and reproduction (Norman and Jones, 1992; Juanes and Smith, 1995; Mariappan and Balasundaram, 2001).

In the western rock lobster fishery, sustainability of the resource has been achieved by management regulations that include limited entry to the commercial fishery, a closed fishing season from July to mid-November, and return to the water of all lobsters that are outside the maximum and minimum legal size limits or that are in a breeding condition (i.e., bearing ovigerous setae) (Caputi et al., 2000; de Lestang and Melville-Smith,

2006). Anecdotally, these regulations are believed to result in 55% of the *P. cygnus* catch being returned to the sea. This species is especially susceptible to autotomizing (dropping) limbs (Brown and Caputi, 1983, 1985): 40–80 tonnes of legs are estimated to be lost from the landed catch of *P. cygnus* each year (Davidson and Hosking, 2002).

We used data from a variety of existing and new sources to examine the effect of appendage loss and regeneration (both antennae and legs) on the reproductive biology of female *P. cygnus*. We believe this study to be the first comprehensive assessment of the impact that appendage damage has on the reproductive output of a decapod species. This study assesses the impact of appendage damage on the proportion of females developing ovigerous setae, the proportion of females that will produce one or more batches of eggs within a breeding season, and the number of eggs in a batch.

Materials and methods

Sampling regime

Data were collected during a fishery-independent breeding stock survey (hereafter referred to as “the survey”), which has been conducted annually at three localities (Lancelin, Dongara, and Abrolhos Islands) and intermittently at three others (Fremantle, Jurien, and Kalbarri) since 1992. The commercial fishery in Western Aus-

tralia is divided into three management zones: the Abrolhos Islands (zone A), north coastal (zone B), and south coastal (zone C) (Fig. 1). In some cases data were pooled into these zones for analysis.

The surveys were undertaken over the course of ten days before the start of the commercial lobster fishing season on 15 November. This period is very close to the annual peak of the egg-bearing season, which is considered to occur in November of each year (Chubb, 1991). Because this survey was designed to be repeatable, the same fishing gear (batten pots with closed escape gaps), bait (a combination of north sea herring [*Clupea harengus*] and Australian salmon [*Arripis truttaceus*]), and locations (same GPS coordinates) were used. The results are therefore directly comparable between years. For more details on the survey sampling regime see Chubb (2000).

Measurements and records

During the surveys, the carapace length (CL) of each lobster was measured to the nearest 1 mm from midpoint between the preorbital spines down the mid-dorsal line to the posterior edge of its carapace. The presence of gonopores on the base of the fifth pair of pereopods was used to identify males. For females, the presence of ovigerous setae attached to the endopodites, the visual appearance of the ovaries through the dorsothoracic musculature, the presence and developmental stage of external ova attached to the setae, and the presence of a spermatophoric mass attached to the fifth abdominal segment were recorded. These data have been used to predict whether a female would produce one or two batches of eggs in a spawning season (such females are known as “single breeders” and “double breeders, respectively”)—see Melville-Smith and de Lestang (2005) for a full description of this method).

Loss and regeneration of antennae and limbs were also recorded during the survey as either an old loss, new loss, or as a regenerated appendage and all three categories were grouped collectively and referred to as “appendage damage.” Old loss was identified by dark melanization at the site of the lost appendage and new loss by exposed flesh without melanization. Although new leg losses were recorded, nearly all were considered to have resulted from capture and handling during the survey and therefore were excluded from our analysis of the impact of appendage damage on reproductive output. Regenerated limbs of *P. cygnus* were only easily identifiable in the first intermoult period after the limb was lost and were distinguished by being greenish in color and noticeably smaller or thinner than existing limbs. Because old and new losses have been recorded since 1992 and

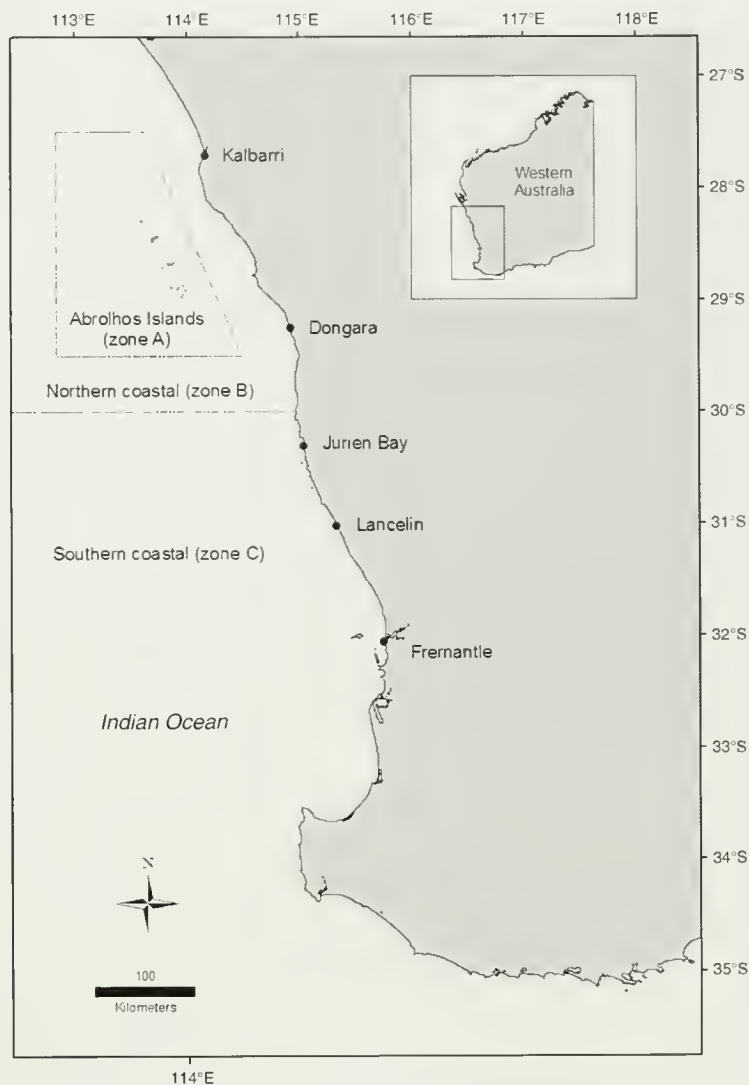


Figure 1

Management zones (zone A, Abrolhos Islands; zone B, northern coastal; zone C, southern coastal) in the western rock lobster (*Panulirus cygnus*) fishery, and six sites (five on the coast of Western Australia and one comprising the Abrolhos Islands) used for fishery-independent breeding stock surveys and commercial monitoring of the catch.

regenerated limbs have been recorded since 2001, we used only the data collected since the 2001 survey. The incidence of old losses, new losses, and regenerated appendages between zones, sex, and carapace size was compared by using ANOVA.

Effect of appendage damage on fecundity estimates

Because most of the lobsters sampled in zone A (the Abrolhos Islands) during the 2001–03 surveys were larger than the size at maturity (Melville-Smith and de Lestang, 2006), data derived from sampling in this location were used to examine whether the incidence of old appendage-losses and regenerated appendages affects the reproductive state of female *P. cygnus*.

The batch fecundity (number of eggs in one batch) of 50 female *P. cygnus* with early-stage eggs that ranged in carapace length (CL) from 67.1 to 96.2 mm was determined. Twenty-three females had either one or two damaged appendages and 27 had no damaged appendages; females with early-stage eggs and more than two damaged appendages were seldom caught and therefore were not assessed. The endopodites with eggs were removed from the lobsters and dried in an oven for 24 hours. The eggs were then separated from the setae and weighed to the nearest 0.0001 g. Three subsamples of each brood (each of ~0.05 g) were taken and weighed. The number of eggs in each subsample was counted to determine the mean number of eggs per gram of dry egg weight, and the mean of these values was used to estimate the total number of eggs in the brood. The mean fecundity per spawning season was compared for females with and without appendage damage after standardizing for carapace length with ANCOVA.

The total number of eggs produced by all mature female *P. cygnus* caught during the 2002 survey in each of the three commercial fishing zones was estimated by using an equation that incorporates the number of broods of eggs produced each spawning season and the effects of appendage damage on the likelihood of spawning once or twice.

$$(TF = NB \times F \times PO_{DA}),$$

where TF = the total fecundity (number of eggs produced) by mature females;

NB = the probability of a female producing one or two broods each spawning season, on the basis of their CL;

F = s the relationship of fecundity to carapace length; and

PO = the probability that females with damaged appendages DA will produce eggs.

$$P_1 = (1 / 1 + \exp(-\ln(19) \times (CL - SB_{50}) / (SB_{95} - SB_{50}))),$$

$$P_2 = (1 / 1 + \exp(-\ln(19) \times (CL - DB_{50}) / (DB_{95} - DB_{50}))),$$

where SB_{50} and SB_{95} = the CLs at which 50 and 95%, respectively, of the population at each location produced one brood of eggs (P_1); and

DB_{50} and DB_{95} = the CLs at which 50 and 95%, respectively, of the population at each location produced two broods of eggs (P_2) per spawning season (de Lestang and Melville-Smith, 2006).

Results

Frequency of appendage damage in 2001–05 surveys

The percentage of western rock lobster with damaged appendages in the 2001–05 survey catches decreased as

Table 1

Percentage of all female and male western rock lobster (*Panulirus cygnus*) with old damage, or regenerated appendages, in the three management zones of the fishery. Data are from the 2001–05 fishery-independent breeding stock survey.

Sex	Fishing zone		
	Zone A	Zone B	Zone C
Female	17.8%	12.4%	20.9%
Male	18.9%	8.7%	17.2%

the number of damaged appendages increased (Fig. 2, A–C). For example, in zone A, about 82% of all female and male *P. cygnus* in the catches had no appendage damage, whereas about 9%, 4%, and 2% of both sexes had one, two, and three damaged appendages, respectively. Only 1% of the catch of each sex had four damaged appendages and less than 0.5% of all lobsters had more than five damaged appendages.

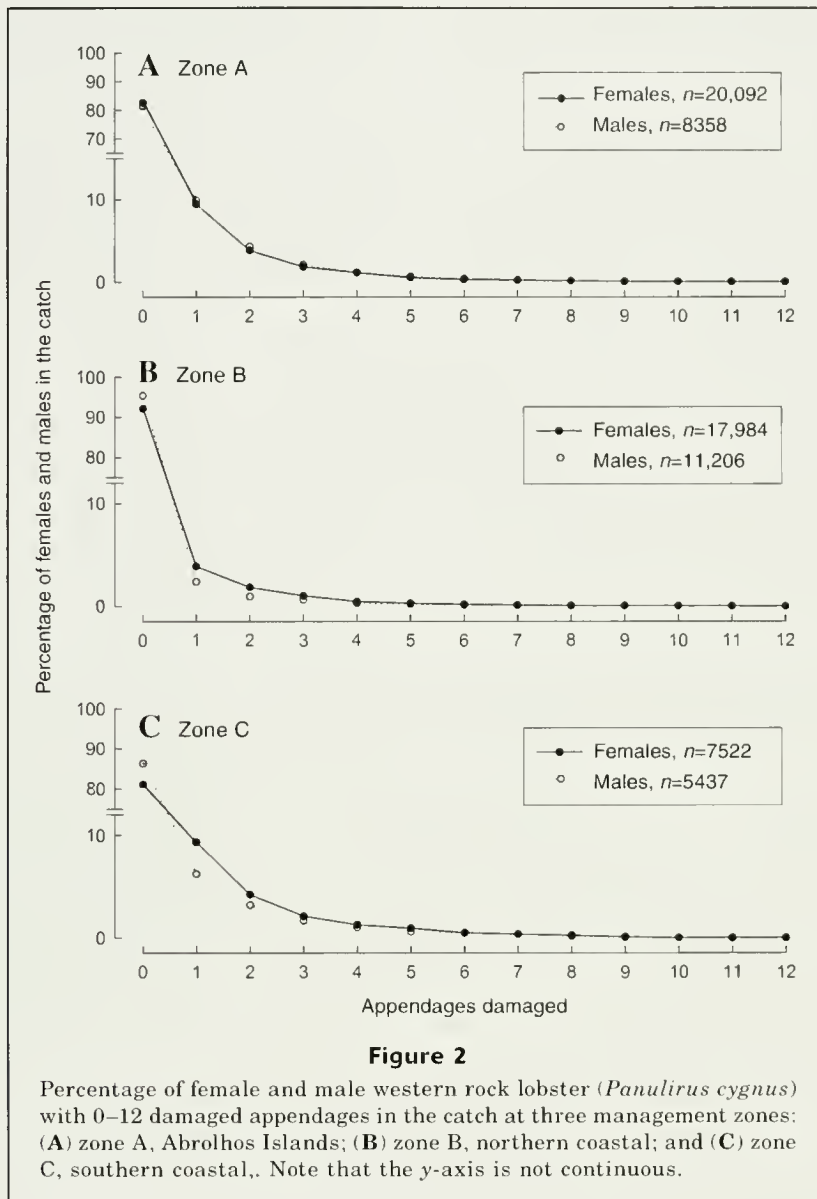
The incidence of appendage damage was significantly different between zones ($P < 0.001$) and both zones A and C had higher incidences than zone B (Table 1). In addition, within zones B and C, significantly ($P < 0.001$) more females than males were caught with appendage damage. There was no significant difference ($P = 0.14$) in the incidence of appendage damage for females and males caught at the Abrolhos Islands.

Relationship between appendage damage and carapace length

The incidence of new appendage loss differed significantly ($P < 0.001$) between the two sexes in the various size classes (Fig. 3A). New appendage loss in females remained at about 17% in all the size classes, whereas in males this loss decreased from 15% to 8% in the first four size classes, then increased substantially to 28% and 20% in the larger size classes (110–119 and 120–129 mm CL, respectively).

The incidence of old appendage loss also differed significantly ($P < 0.001$) between sexes in different size classes (Fig. 3B). Old appendage damage was slightly more common as females increased in size, i.e., from 7% to 11% between the 60–69 and 100–109 mm CL size classes. This increase also occurred for males but to a much greater extent, i.e., from 4% to 23% between the 60–69 and 100–109 mm CL size classes. The incidence of old appendage damage in males then declined slightly over the two largest size classes (110–119 and 120–129 mm CL) 22 and 16%, respectively (Fig. 3B).

Regenerated appendages in the catches of lobster differed significantly ($P < 0.001$) between sex and size classes (Fig. 3C). Regenerated appendages were more commonly recorded for females than for males, but regenerated appendages for each sex remained relatively



constant at about 4% and 3%, respectively, in all size classes below 120 mm CL. Above this size class, the incidence of regenerated appendages increased markedly in females (10%) and declined to zero for males (Fig. 3C).

The influence of appendage damage on egg production

The proportions of female *P. cygnus* (CL>65 mm) from the Abrolhos Islands that were classified as having ovigerous setae, as being single breeders, and as being double breeders, all declined with increasing appendage damage (Fig. 4, A–C). A consistent trend existed between the various reproductive states and the magnitude of their appendage damage. For females at the Abrolhos Islands above the size at maturity, the likelihood of developing ovigerous setae declined with the number of appendages

damaged: 98% likelihood (one appendage damaged), 95% (two), 80% (five), and 58% (six). This likelihood continued to decline until it reached zero for all females with either 11 or 12 damaged appendages (Fig. 4A).

For ovigerous females with damaged appendages, the likelihood of producing either one or two batches of eggs each spawning season declined more rapidly than the likelihood of developing ovigerous setae. Females with one damaged appendage were 20% and 19% less likely to produce one or two batches of eggs, respectively, whereas those with five damaged appendages were around 85% and 65% less likely to produce one or two batches of eggs, respectively. Females with more than seven damaged appendages did not produce eggs (Fig. 4, B and C). Equations describing the relationships between appendage damage and the likelihood of spawning once for single breeders and twice for double

breeders were not significantly ($P=0.42$) different from each other and were thus combined to produce a single equation to describe the likelihood of producing one or two broods of eggs:

$$PO_{DA} = \exp[-0.31 \times \ln(DA + 1) + 0.742] - 1.$$

The above relationship between appendage damage and the likelihood of lobsters developing ovigerous setae, or the likelihood of lobsters producing one or two broods

of eggs at the Abrolhos Islands, was very similar in the other two coastal management zones.

The influence of appendage damage on fecundity

The mean fecundity per spawning season of female *P. cygnus* with a standardized CL of 77.0 mm did not differ significantly ($P>0.05$) between females with and without damaged appendages (i.e., $249,885 \pm 7873$ eggs and $234,164 \pm 7094$ eggs, respectively). Furthermore, regressions between fecundity (F) and carapace length (CL) of female *P. cygnus* with and without damaged appendages (Fig. 5) did not differ from each other ($P>0.05$) and were both very similar to the relation of carapace length to fecundity recorded for this species by Chubb (1991).

The effect of damaged appendages on the number of eggs produced per spawning season by female *P. cygnus* at the Abrolhos Islands was greater for large than for small females (Fig. 6). For example, two damaged appendages reduced the fecundity of a 70-mm-CL lobster by about 114,000 eggs, whereas the fecundity of a 120-mm-CL lobster was reduced by about 1,000,000 eggs (Fig. 6).

The total number of eggs produced in the 2002 survey was estimated for each of the three management zones separately for females with and without appendage damage. The inclusion of appendage damage significantly (all $P<0.001$, paired t -test) reduced egg production estimates by 8.5%, 3%, and 9% in zones A, B, and C, respectively.

Discussion

The incidence of appendage damage

The proportions of lobsters with damaged appendages varied markedly between sexes, sizes, and locations sampled. However, the timing and frequency within a year that molting takes place for the sexes, and for different-size animals, plays only a relatively minor role in influencing these differences. Female western rock lobsters generally molt twice a year: February–March and again in May. A significant proportion of large breeding females occasionally skip the February–March molt, but all take part in the May molt (de Lestang and Melville-Smith, 2006).

New appendage damage occurred around the time of capture and could mostly be attributed to the survey sam-

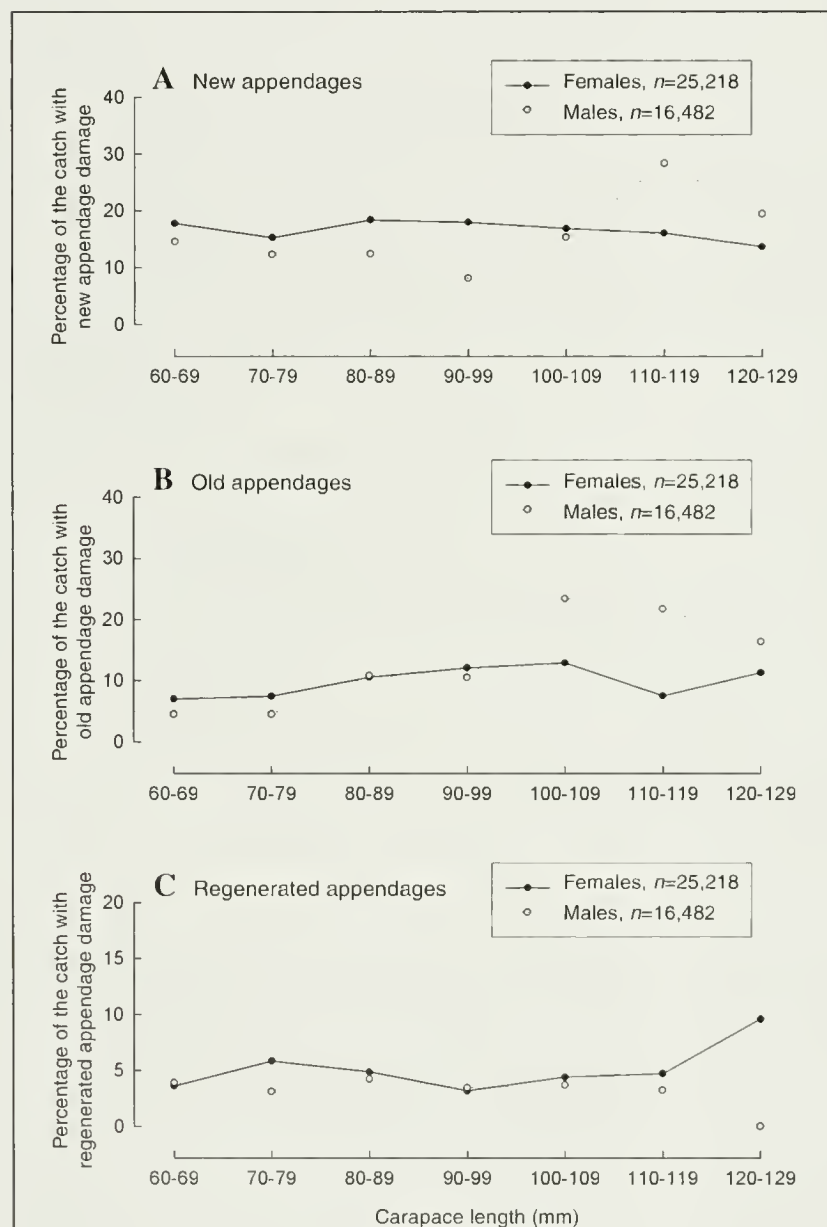


Figure 3

Percentage of female and male western rock lobster (*Panulirus cygnus*) in different size classes with (A) new or (B) old appendage loss, or (C) with regenerated appendages. The analysis uses 2001–05 fishery-independent breeding stock survey data from all five coastal sites.

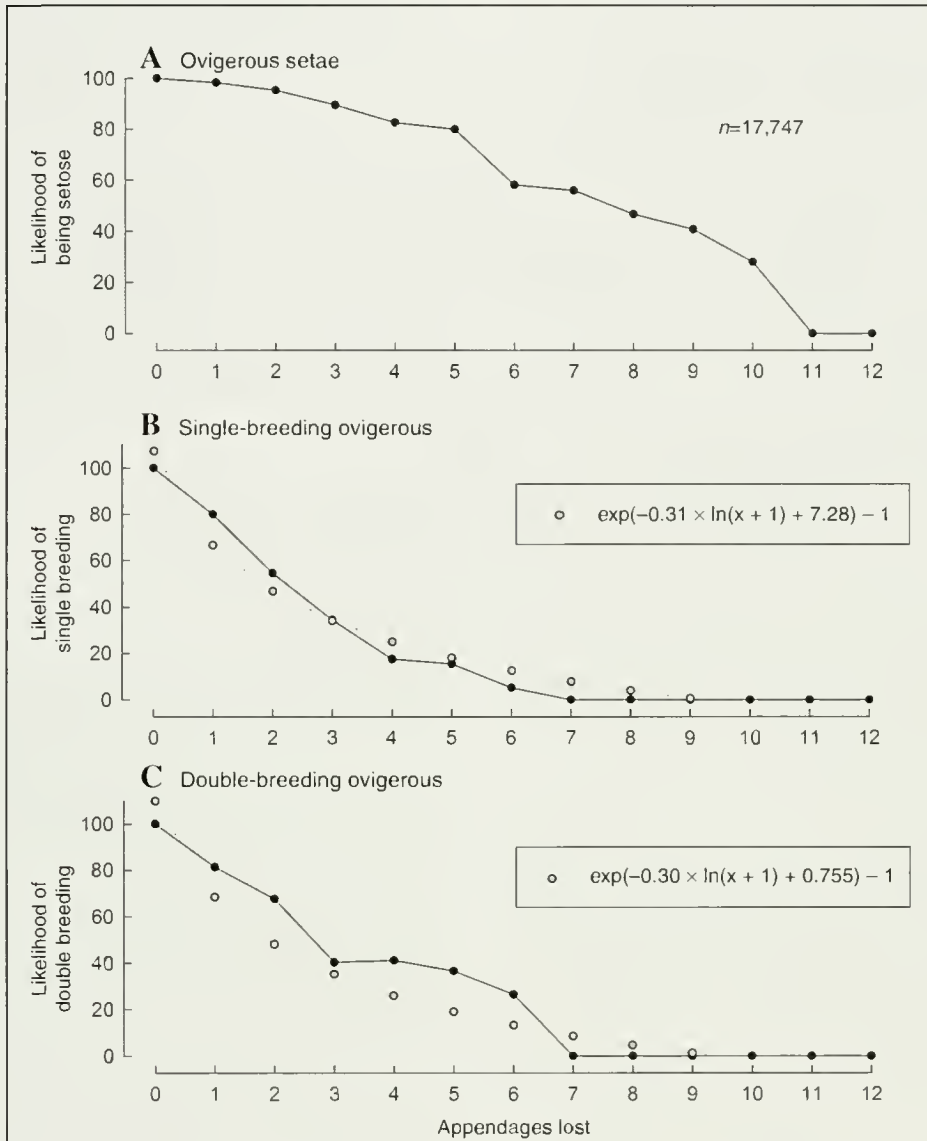
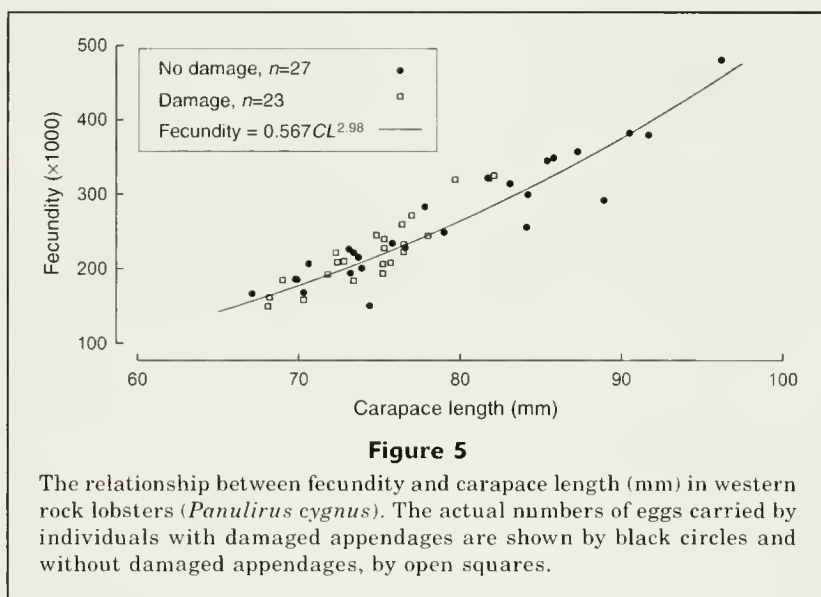


Figure 4

Likelihood of female western rock lobster (*Panulirus cygnus*) with (A) ovigerous setae, (B) or being single-breeding ovigerous individuals, and (C) double-breeding individuals, with 0–12 appendages damaged. Data are from the 2001–05 fishery-independent breeding stock surveys at the Abrolhos Islands (zone A) for all females >65 mm CL combined. Equations in (B) and (C) refer to fitted relationships describing the likelihood of breeding with appendage loss.

pling methods, either to capture in the pots or handling on deck. The slightly higher proportions of females than males recorded with new damage are possibly the result of the longer handling time needed to make additional observations, such as recording the presence or absence of eggs and spermatophores and visually assessing the condition of the ovary. In contrast to new appendage damage, the events that resulted in old damage and regenerated appendages occurred before the survey and, in the latter case (regenerated appendages), before the lobster's last molt, i.e., about May (de Lestang and

Melville-Smith, 2006). It is therefore likely that much of this damage is inflicted during the commercial fishing season, possibly as a result of capture and handling. It is thus not surprising that the lobsters showing the greatest incidence of regenerated appendages are females above the maximum legal size (115 mm CL in zone C and 105 mm CL in zones A and B); many of these animals were likely handled and returned to the water many times during a season. Predators may be an additional cause of appendage damage. The fact that the incidence of old appendage damage increased in



both sexes with size may indicate that larger individuals are more likely to survive the attack of a predator, although perhaps with the loss of appendages.

The effect of appendage damage on reproductive output

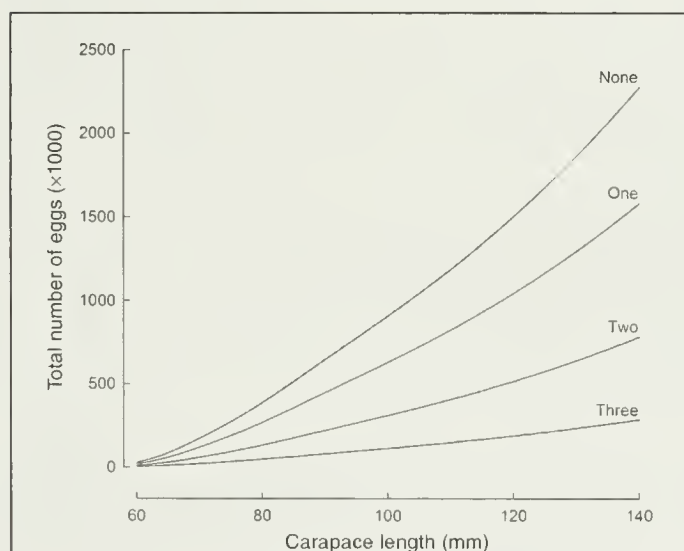
Appendage damage can lead to an associated reduction in the reproductive output of female *P. cygnus* directly, namely as reduced proportions of females that develop ovigerous setae, and as a reduction in the proportions of

ovigerous females that will produce one or two batches of eggs within a season. Reproductive output is also affected indirectly when females with appendage damage do not molt into breeding condition (with ovigerous setae); a female above the legal minimum size without ovigerous setae can be legally retained by commercial and recreational fishermen and thus her contribution to the broodstock is removed.

The significant reduction in reproductive output of female *P. cygnus* with appendage damage is not surprising, because regeneration places large demands on energy reserves, often in the form of a reallocation of resources that were originally destined for reproduction and growth (Démeusy, 1965; Norman and Jones, 1992; Juanes and Smith, 1995). Moreover, if appendage damage is extensive, the process of regenerating multiple appendages may result in a long-term reallocation and an overall increase in energy demand (McVean, 1982).

Most *P. cygnus* caught during the survey were intact when examined; less than 15% of the entire catch had damaged appendages. This 15% was probably due, in part, to management measures based on previous work on the effects of appendage damage (Brown and Caputi, 1985, 1986) to initiate changes aimed at reducing limb loss. Methods for limiting appendage damage even further are being developed, i.e., cold stunning (Davidson and Hoskin, 2002). However, even with the best intentions, some appendage damage through handling is unavoidable.

This study has highlighted that management measures aimed at protecting the western rock lobster broodstock inevitably result in the animals being handled more than once (or multiple times) in the course of the fishing season, and the damage to appendages caused by handling produces a significant, and previously unrecognized, effect on the overall egg production of this resource. These effects need



to be taken into account when considering the benefits of these management measures in this and other crustacean fisheries.

Acknowledgments

Thanks are expressed to research staff and crew of the RV *Naturaliste* for assistance with sampling. R. Campbell, N. Caputi, C. Lawrence, V. Mawson, and J. Penn provided constructive criticisms to earlier drafts of the paper. This work was undertaken as part of Fisheries Research and Development Corporation Project 2003/005. All experiments were conducted in compliance with the current laws of Australia.

Literature cited

- Brouwer, S. L., J. C. Groeneveld, and B. Blows.
2006. The effects of appendage loss on growth of South African west coast rock lobster *Josus lalandii*. *Fish. Res.* 78:236–242.
- Brown, R. S., and N. Caputi.
1983. Factors affecting the recapture of undersize western rock lobster *Panulirus cygnus* George returned by fishermen to the sea. *Fish. Res.* 2:103–128.
- Brown, R. S., and N. Caputi.
1985. Factors affecting the growth of undersize western rock lobster *Panulirus cygnus* George returned by fishermen to the sea. *Fish. Bull.* 83:67–574.
- Brown, R. S., and N. Caputi.
1986. Conservation and recruitment of the western rock lobster (*Panulirus cygnus*) by improving survival and growth of undersize rock lobsters captured and returned by fishermen to the sea. *Can. J. Fish. Aquat. Sci.* 43:2236–2242.
- Caputi, N., C. F. Chubb, N. G. Hall, and R. S. Brown.
2000. Measurement of catch and fishing effort in the western rock lobster fishery. In *Spiny lobsters fisheries and culture* (B. F. Phillips, and J. Kittaka, eds.), p. 334–356. Fishing News Books, Oxford.
- Chubb, C. F.
1991. Measurement of spawning stock levels for the western rock lobster, *Panulirus cygnus*. *Rev. Invest. Mar.* 12:223–233.
2000. Reproductive biology: issues for management. In *Spiny lobsters fisheries and culture* (B. F. Phillips and J. Kittaka, eds.), p. 245–275. Fishing News Books, Oxford.
- Davidson, G., and W. Hosking.
2002. Development of a method for alleviating leg loss during post-harvest handling of rock lobsters. In *Proceedings of the fourth annual rock lobster enhancement and aquaculture subprogram/rock lobster post-harvest subprogram* (R. van Barneveld, and B. Phillips, eds.), p. 85–89. Rock Lobster Enhancement and Aquaculture Subprogram Publication No. 7. Barneveld Nutrition Pty Ltd. Springwood, Queensland, Australia.
- Davis, G. E.
1981. Effects of injuries on spiny lobsters, *Panulirus argus*, and implications for fishery management. *Fish. Bull.* 78:979–984.
- de Lestang, S., and R. Melville-Smith.
2006. Interannual variation in the moult cycle and size at double breeding of mature female western rock lobster *Panulirus cygnus*. *ICES J. Mar. Sci.* 63:1631–1639.
- Démeusy, N.
1965. Somatic growth and reproductive function in the female brachyuran decapod *Carcinus maenas* Linn. [In French.] *Arch. Zool. Exp. Gen.* 106:625–663.
- Juanes, F., and L. D. Smith.
1995. The ecological consequences of limb damage and loss in decapod crustaceans: a review and prospectus. *J. Exp. Mar. Biol. Ecol.* 193:197–223.
- Krouse, J. S.
1976. Incidence of cull lobsters, *Homarus americanus*, in commercial and research catches off the Maine coast. *Fish. Bull.* 74:717–724.
- Mariappan, P., and C. Balasundaram.
2001. Limb autotomy along with exuvium in freshwater prawn, *Macrobrachium malcolmsonii*. *Indian J. Animal Sci.* 71:1001–1002.
- McVean, A.
1982. Autotomy. In *The biology of crustaceans, neural integration and behaviour* (D. C. Sandeman, and H. L. Atwood, eds.), p. 107–246. Academic Press Inc., New York, NY.
- Melville-Smith, R., and S. de Lestang.
2005. Visual assessment of the reproductive condition of female western rock lobsters (*Panulirus cygnus*). *N. Z. J. Mar. Freshw. Res.* 39:557–567.
2006. Spatial and temporal variation in the size at maturity of the western rock lobster *Panulirus cygnus*. *Mar. Biol.* 150:183–195.
- Norman, C. P., and M. B. Jones.
1992. Reproductive ecology of the velvet swimming crab, *Necora puber* (Brachyura: Portunidae), at Plymouth. *J. Mar. Biol. Assoc. U.K.* 73:379–389.
- Phillips, B. F., and R. Melville-Smith.
2005. Sustainability of the western rock lobster fishery: a review of past progress and future challenges. *Bull. Mar. Sci.* 76:485–500.
- Smith, E. M., and P. T. Howell.
1987. The effects of bottom trawling on American lobsters *Homarus americanus* in Long Island Sound. *Fish. Bull.* 85:737–744.

Abstract—We determined the distribution of multiple ($n=68$; 508–978 mm total length [TL]) striped bass (*Morone saxatilis*) along the estuarine salinity gradient in the Mullica River–Great Bay in southern New Jersey over two years to determine the diversity of habitat use and the movements of striped bass. Ultrasonically tagged fish were detected in this estuarine area by means of wireless hydrophones deployed at four gates inside the entrance of the study area and farther up to tidal freshwater (38 km). Numerous individuals frequently departed and returned to the estuary, primarily in the spring and late fall over periods of 15–731 days at liberty. The period of residency and degree of movement of individuals to and from the estuary varied extensively among seasons and years. The diversity of movements in and out of, as well as within, the estuary differed from the less-complex patterns reported in earlier studies, perhaps because of the comprehensive and synoptic nature of this study.

Diversity of estuarine movements of striped bass (*Morone saxatilis*): a synoptic examination of an estuarine system in southern New Jersey

Kenneth W. Able (contact author)

Thomas M. Grothues

Email address for K. W. Able: able@marine.rutgers.edu

Marine Field Station, Institute of Marine and Coastal Sciences
Rutgers University
800 c/o 132 Great Bay Boulevard
Tuckerton, New Jersey 08087-2004

Striped bass (*Morone saxatilis*) are an economically and ecologically important species along most coasts of the United States, and especially along the east coast and into Canada (Klein-MacPhee, 2002). The degree to which this species uses estuaries along the east coast appears to vary among and within estuaries. From North Carolina southward most striped bass remain in rivers and estuaries (Haeseker et al., 1996; Bjorgo et al., 2000), as does the northernmost population in the Gulf of St. Lawrence (Coutant, 1985). North of North Carolina to the Bay of Fundy, striped bass can be highly migratory (Waldman et al., 1990; Rulifson and Dadswell, 1995). Much of the research effort in this region has focused on the coastal migrations and there has been less effort on within-estuary movements. Both coastal and within-estuary movements have become more important to understand because 1) the recovery of the species (Wooley et al., 1990; Richards and Rago, 1999), especially at the current higher densities, may influence its movement patterns, and 2) there is the possibility that there are distinct contingents, including estuarine residents, that are critical to understanding stock structure for fishes in general (Begg and Waldman, 1999), but especially for striped bass (Secor et al., 2001).

In the past, most attempts to examine estuarine movements have been based on fish caught in local fisheries (Rulifson and Dadswell, 1995) and tagged-recaptured fish (Boreman and Lewis, 1987; Waldman et

al., 1990). However, in recent years the development of otolith microchemistry has helped scientists to recognize the importance of distinct substocks or contingents and their migrations (Secor, 1999) that have the potential to be indicative of homing (Thorrold et al., 2001; Gillanders, 2005). These concepts have been applied to striped bass as well, and resident, mesohaline, and coastal migratory contingents have been recognized within the same estuarine and river system (Secor, 1999; Zlokovitz et al., 2003), as well as the annual variation in the migratory patterns of these contingents (Morris et al., 2003). Additionally, the development of biotelemetry in general (Cooke et al., 2004; Heupel et al., 2006) and smaller ultrasonic tags and passive receivers has increased the possibility for more accurate and frequent detection of fish and has enhanced our ability to study fish movements (Arnold and Dewar, 2001; Sibert and Nielsen, 2001). These efforts conducted on striped bass previously focused on introduced populations in freshwater reservoirs (e.g., Jackson and Hightower, 2001; Young and Isley, 2002), with exceptions in North Carolina (Haeseker et al., 1996; Carmichael et al. 1998), Maryland (Hocutt et al., 1990), and New Jersey (Tupper and Able, 2000). More detailed studies are necessary to determine how estuarine and ocean use varies among individuals over seasons and years. This is especially necessary because much of the past focus has been on large estuarine and river systems such as the

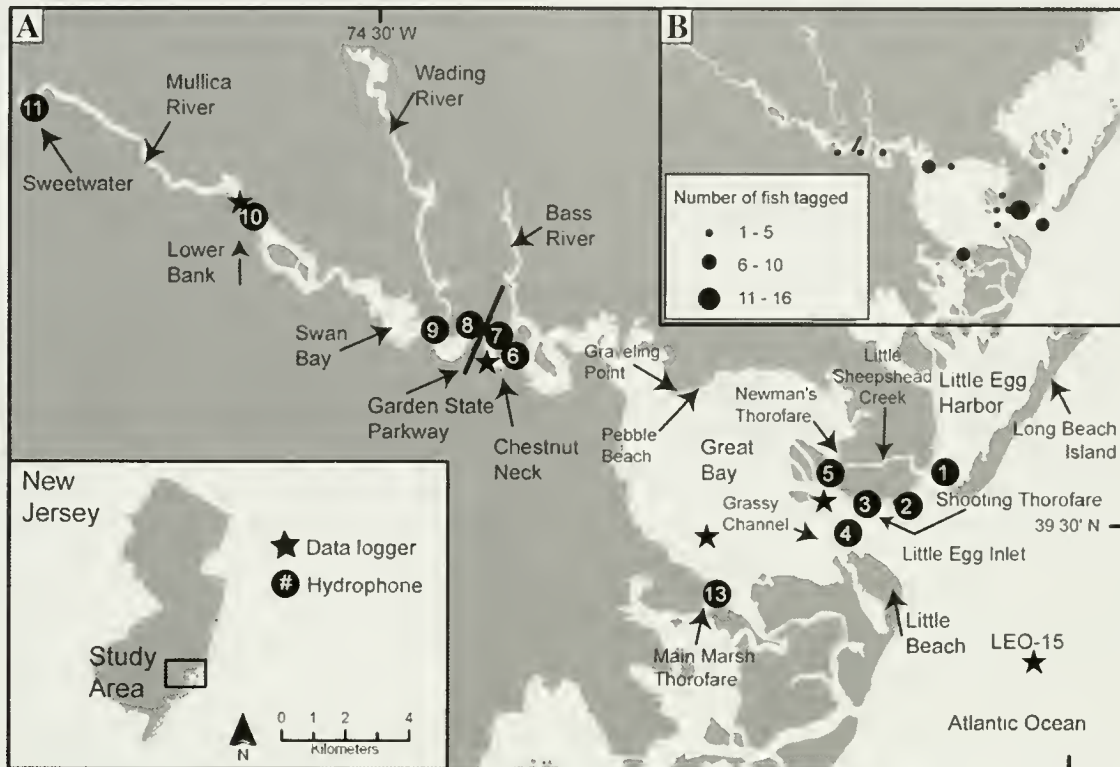


Figure 1

Mullica River–Great Bay study site and important localities (A) and location of fish tagging and release sites (B) during 2003 and 2004. Hydrophone 12 was not deployed during this period and is not shown.

Hudson River (Secor et al., 2001; Zlokovitz et al., 2003) or Chesapeake Bay (Secor, 2000a, 2000b). Relatively little attention has been directed to small coastal bay and estuarine systems that, owing to scale, may have very different dynamics.

The purpose of this study was to determine the annual, seasonal, and episodic patterns of residency and movements for large juvenile and adult striped bass along an estuarine gradient in a small drowned-river-valley estuary. Although most previous telemetry and tracking studies focused on one fish at a time, the estuarine system used in the present study allowed for synoptic observations of numerous individuals. Throughout this study there was an emphasis on individual behavior, an approach that has provided important insight into the stock structure of other fishes (Sutherland, 1996; Slotte and Fiksen, 2000).

Materials and methods

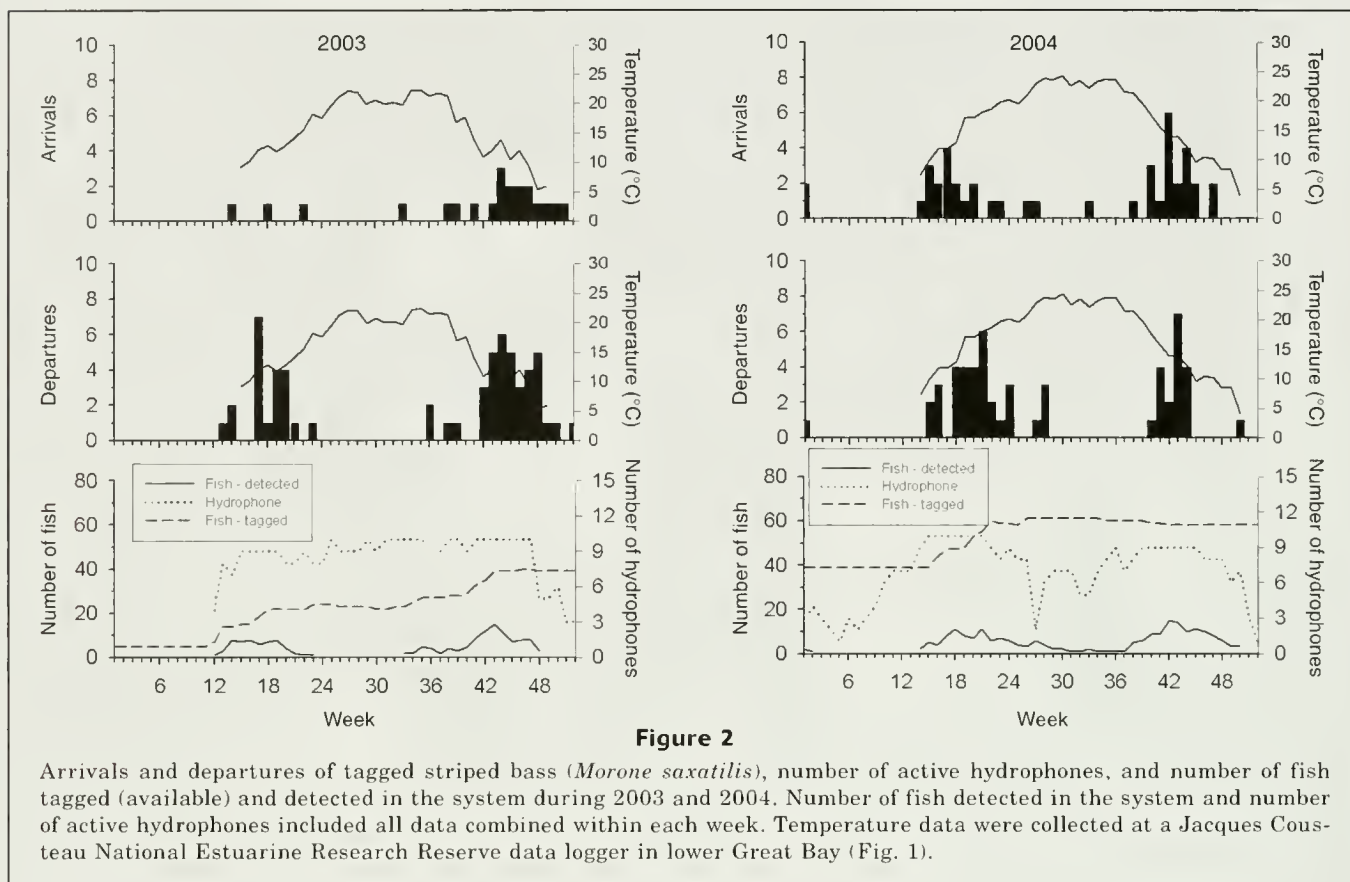
Study site

The Mullica River–Great Bay estuary (Fig. 1) is one of the few remaining relatively undisturbed estuaries in the northeastern United States because there is little agricultural or industrial development in the watershed and human population density is relatively low (Kennish,

2004). This relatively small watershed (1474 km²; Kennish, 2004) that comprises several tributaries (Batsto, Wading, and Bass Rivers) is part of the Jacques Cousteau National Estuarine Research Reserve (JCNERR) and drains the Pinelands National Reserve at a mean monthly stream flow of approximately 1.7 to 4.2×10^8 L/d (Rhodehamel, 1998) (Fig. 1). Much of the 280 km of shoreline in this watershed consists of cordgrass (*Spartina alterniflora*) dominated salt marsh, and has a tidal range between 0.7 m (in Little Egg Harbor) and 1.1 m (near the mouth of Great Bay). Mean salinity of 29 at the entrance to the bay drops sharply to about 8 within 30 linear km upriver; the inflection point corresponds to a steep decrease in pH from 8.0 to 6.0 owing to tannins leached from the pine-forested watershed (Kennish, 2004). The majority of water exits into the ocean through the narrow but deep (20 m) Little Egg Inlet and to a lesser extent through the Main Marsh Thorofare, an intra-estuarine connection that is part of the Intra-Coastal Waterway (ICW) (Chant et al., 1996).

Estuarine observatory

Wireless hydrophones were deployed at a series of gates in order to enhance detection of tagged striped bass while in residence or moving along the estuarine gradient (Fig. 1). At the entrance to the estuary (Little Egg Inlet) hydrophones 2, 3, and 4 (recorded as positioned



at 0 km) were arranged to take advantage of local topography, such as at sand bars, channels, etc. to detect fish moving along several passages. The entrance to Little Egg Harbor was monitored by hydrophone 1 (considered to be 0 km from the inlet for the purposes of this study). This same hydrophone, along with no. 5, also served to identify fish moving through a deep (to 7 m) channel (Little Sheepshead Creek) between Little Egg Harbor and Great Bay. The channel exiting Great Bay to the south (Main Marsh Thorofare) was monitored by hydrophone 13 (4.5 km from the inlet), although this hydrophone was deployed later than the others. Hydrophone 5 (4.5 km from the inlet) also served to monitor fish passing through the deepest channel in Great Bay (Newmans Thorofare). The next gate upstream was located in the Mullica River (hydrophones 6, 7, 8, 9; approximately 18 km from the inlet). Hydrophones 6 and 8 were removed after a test period because they were largely redundant. Farther upstream the next gate consisted of a single hydrophone (no. 10; 28.3 km from the inlet) just above the saltwater-freshwater interface. On occasion, another hydrophone (no. 11; 38.1 km from the inlet) was deployed farther upstream in tidal freshwater. The total number of hydrophones deployed over the period of the study is indicated in Figure 2. Additional details of this estuarine system (referred to as an "observatory") are provided in Grothues et al. (2005). Our ability to detect tagged fish in certain portions of

the estuary was affected by the times of hydrophone deployment and, occasionally, by aperiodic retrieval of the hydrophones because of poor weather conditions (ice formation in the winter of 2003–04) or equipment malfunction (Fig. 2).

Striped bass bearing surgically implanted acoustic transmitters (76.8 KHz) with an individual identification code were detected when they came within range (approximately 500 m; Grothues et al., 2005) of moored wireless hydrophones (WHS-1100, Lotek Wireless, Inc., St. Johns, Newfoundland, Canada), which were suspended at a depth of 3.2 m where surrounding total water depth reached a depth of 10 m. Wireless hydrophones transmitted received sound in the 76.8 KHz band by a VHF radio frequency unique to the unit (between 148 and 152 MHz) to shore-based receivers for the interpretation and logging of the data in real time (see Grothues et al., 2005, for additional details). The JCNERR study area also provided useful infrastructure for routine environmental monitoring. Permanent instrumentation included data loggers used to record salinity, temperature, pH, and water depth (Kennish and O'Donnell, 2002) along the estuarine gradient (Fig. 1).

Tagging technique

Fish were collected by hook and line from 2 November 2002 to 2 November 2004 in the study area. Immedi-

ately after capture, each individual was anesthetized in a cooler containing 0.4–0.6 g/liter of MS-222 (Sigma-Aldrich Corporation, St. Louis, MO). A transmitter (CAFT 16-3, Lotek Wireless Inc., St. Johns, Newfoundland, Canada) was then surgically implanted in the body cavity. The incision was closed with absorbable ethalon monofilament sutures and treated with antibiotic ointment. An external tag (Floy Tag, Inc., Seattle, WA), with printed contact information, was anchored into the flesh to allow fishermen to report capture later to the study crew. While still anesthetized, the fish was measured (mm total length, TL), injected with Liquamycin®Pfizer at 0.1 mg/kg fish weight as a prophylactic against latent infection. Each fish was then placed in clean, ambient water until it showed normal swimming ability at which time it was released at the capture site. On occasion, fish were held for short periods of time (two hours) before release. However, one fish was held for four days at Rutgers University Marine Field Station (RUMFS) before surgery and then taken to the site of capture and released.

Data analyses

The sampling unit (n) used in the analyses of telemetry data was an individual tagged fish because this approach places equal importance on the movements of each fish (Rogers and White, in press). For the purpose of this study, immigration of a tagged fish occurred when the first detection of a fish tagged in 2002 was recorded after January 2003 at or near an entrance to the estuary. Emigration was determined by detection at one of the entrances to the estuary followed by no detections of that individual for two consecutive weeks, presumably because it left the estuary for the ocean or an adjacent bay. In order to measure swimming speed, we used the last detection at a hydrophone at one gate and the first detection at the next gate to determine time of travel and distance between hydrophones.

Results

Environmental parameters

Pronounced seasonal changes in temperature and dissolved oxygen occurred consistently throughout the estuary, and salinity and pH decreased in the river (Fig. 3). Temperatures approached, and probably reached, 0°C during both winters but reached maximum temperatures of approximately 25°C farther up the estuary during summer. Temperatures near Little Egg Inlet were consistently cooler than elsewhere in the estuary during both years. Dissolved oxygen values followed the same seasonal trend, except that values were highest in the winter, near 14 mg/L, and lowest in the summer, at 4–6 mg/L, but in both years values at Little Egg Inlet were higher than farther up the estuary. The salinity varied distinctly with distance up the estuary. The values at Little Egg Inlet averaged 28.6 (16.8–32.7)

during both years, whereas those upstream at Chestnut Neck (mean=13.8, range 0.9–24.4) and Lower Bank (mean=2.1, range 0–13.4) were much lower. Although there were no data collected at Sweetwater during the 2005 study period, the salinity values averaged 0.1 (range: 0.02–5.1). The estuary differs from many others in the Middle Atlantic Bight in that pH values in the upper portions of the study area are naturally low (Lower Bank, mean 5.9, range=4–7.4). These values tended to be lowest in the spring and winter, presumably because of higher runoff associated with more precipitation and because of lower salinities at that time of the year.

General characteristics of ultrasonically tagged fish

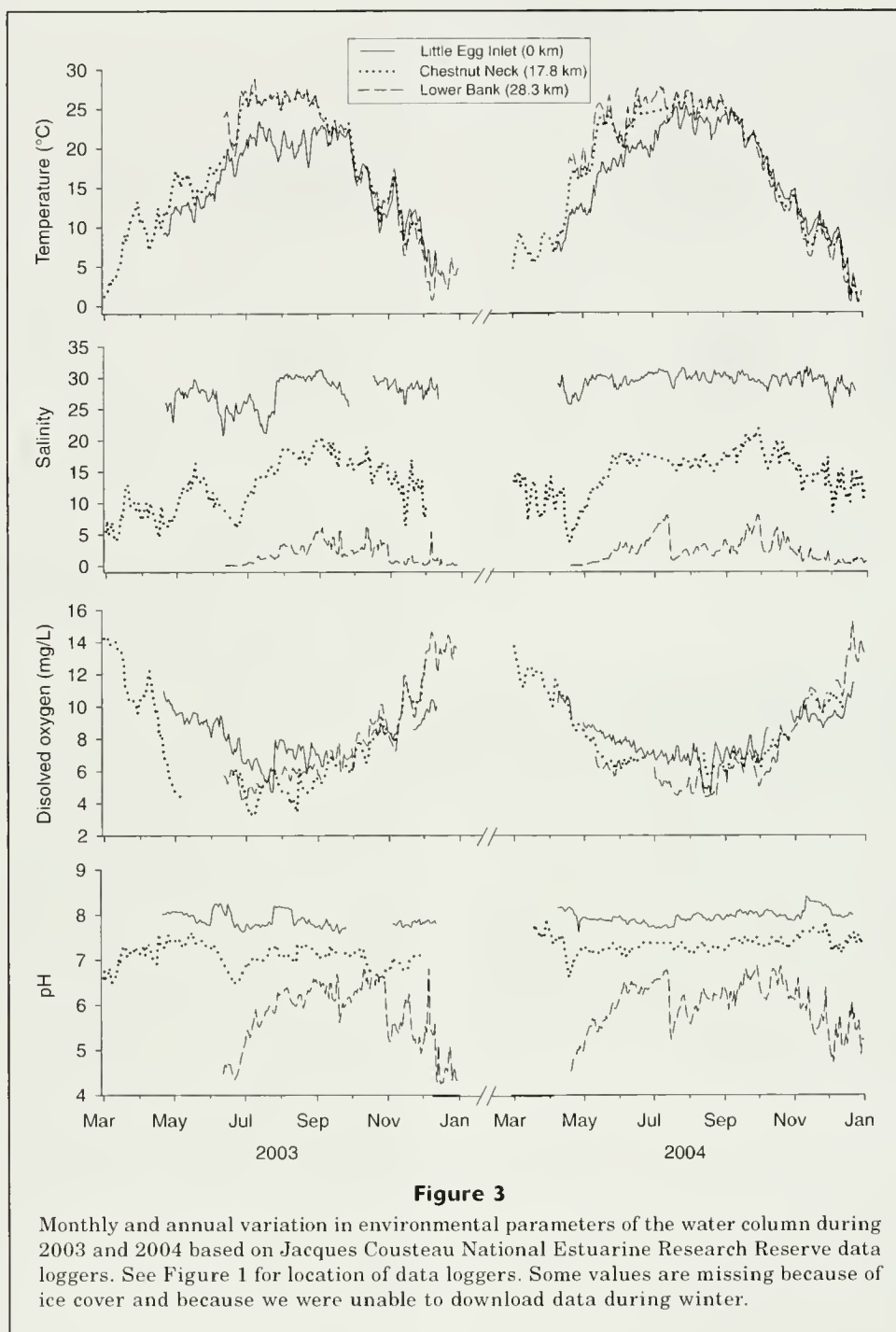
During the study period, 68 striped bass (range 483–978 mm TL) were tagged and tracked through the Mullica River–Great Bay study area. Most of these fish were tagged in Great Bay ($n=61$), especially in the lower bay near Little Egg Inlet and Shooting Thorofare, although a number were also tagged at Graveling Point and Pebble Beach (Fig. 1B). Most fish were tagged in the fall and spring of 2003 and spring of 2004. The duration of detection of these tagged fish varied greatly among individuals. Some individuals ($n=3$) were detected only immediately after tagging and not again. Some were detected only during one season or one year ($n=3$), others ($n=5$) were detected in both years, and two individuals were detected for almost the entire duration of this study. The mean duration in the study area for fish tagged in 2003 was 43.5 days and in 2004 was 20.0 days. Several fish were captured by anglers within the estuary ($n=4$), outside the estuary elsewhere in New Jersey ($n=5$), on the south shore of Long Island ($n=1$), coastal New Hampshire ($n=1$) and one was detected by similar hydrophones in the Saco River, Maine (Carter¹).

The overlap in time between hydrophone deployment and the time of initial tagging of each fish and their exit and re-entry into the estuary determined the frequency and duration of tag detections (Fig. 2). Overall the rate of detection was high; over 97% of all tagged fish were detected after tagging. The number of detections for each individual varied markedly and ranged from 22 to 75,603 contacts; the total number of contacts for all fish was 501,760 over the course of the study. Of the fish tagged and subsequently detected, duration at liberty varied from 15 to 731 days. Most fish were detected by more than one hydrophone and numerous individuals were detected by 2–10 hydrophones.

Annual and seasonal visits to the estuary

The patterns of estuarine use by tagged striped bass were diverse and varied by individual, season, and year. We characterized individual tagged fish by their use of the estuary, either as resident fish (never detected

¹ Carter, J. 2005. Personal observ. Department of Life Sciences, Univ. New England, 11 Hills Beach Road, Biddeford, ME 04005.



leaving the estuary), seasonal inlet visitors (detected only at the inlet gate by hydrophones 1-4), seasonal estuarine visitors, (within the estuary gate at hydrophones 13, 5-9), or as seasonal river visitors (within the river gate at hydrophones 10, 11) (Fig. 1). The consistency of these four patterns varied with individual fish. Of the total number of tagged fish that could be classified ($n=64$), 67.1% displayed a single pattern, 31.2% displayed two patterns, and 1.5% exhibited three of the

above patterns. Of these patterns there were 105 total classifications. The residents made up 2.8% of all estuarine use patterns. The seasonal inlet visitors made up 36.1%, seasonal estuarine visitors made up 49.5%, and seasonal river visitors made up 11.4% of all estuarine-use patterns. Of these, 58% of all tagged fish ($n=67$) that left the system returned in later seasons (42%) and years (16%) (proportions were standardized to two-year tags at large for one year).

Seasonal occurrence in the estuary was the result of departure and re-entry of individual fish (Fig. 2). The number of departures for individuals ranged from 0 to 7, whereas arrivals ranged from 0 to 6. In both years most departures and arrivals occurred in the spring and during the fall and early winter and not during mid-winter or summer. In 2003, most departures ($n=27$) from the estuary occurred between weeks 12 and 21 (late March–May) and again between weeks 39 and 48 (late September–mid November), whereas in 2004 departures ($n=14$) occurred later, during weeks 17–23 (mid May–mid June) and later ($n=4$) in weeks 27 and 45 (mid July and early November (Fig. 2). In 2003, most arrivals ($n=4$) were detected during weeks 40–46 (beginning October and early November) and earlier ($n=2$) during weeks 16–20 (mid May–beginning June), whereas in 2004 most arrivals ($n=7$) occurred during weeks 12–20 (mid March–beginning June) and later ($n=17$) during weeks 37–46 (mid September–mid November).

The departure and arrival times (Fig. 2) corresponded with the seasonal increase and decrease, respectively, of estuarine inlet temperatures (Fig. 3). In both years the number of departures (21% of total fish) and arrivals (21%) was low at temperatures $<10^{\circ}\text{C}$ and $>20^{\circ}\text{C}$, respectively. During the period between these temperatures (when 79% of both departures and arrivals occurred), departures occurred at a mean of 13.9°C and arrivals occurred at a mean of 14.0°C . These temperatures typically occurred during the spring and fall (Fig. 3).

Patterns of arrival and departure were especially interesting for several individuals that revisited the study area during 2003 and 2004. The best evidence for frequent, seasonal re-entry and departure from the study estuary comes from the redetection of six striped bass tagged on 2 April 2003 at Graveling Point (Fig. 4). Of these, four returned and departed on several occasions. For three of these individuals (tags 95, 97, 99) the pattern of the timing of return and departure was nearly the same over several seasons (winter 2003, spring and winter 2004). Another individual (with tag 96) was redetected only once, but it reappeared (spring 2004) at the same time as the other individuals. Even those fish that were not redetected during a later season or year typically departed the estuary at the same ap-

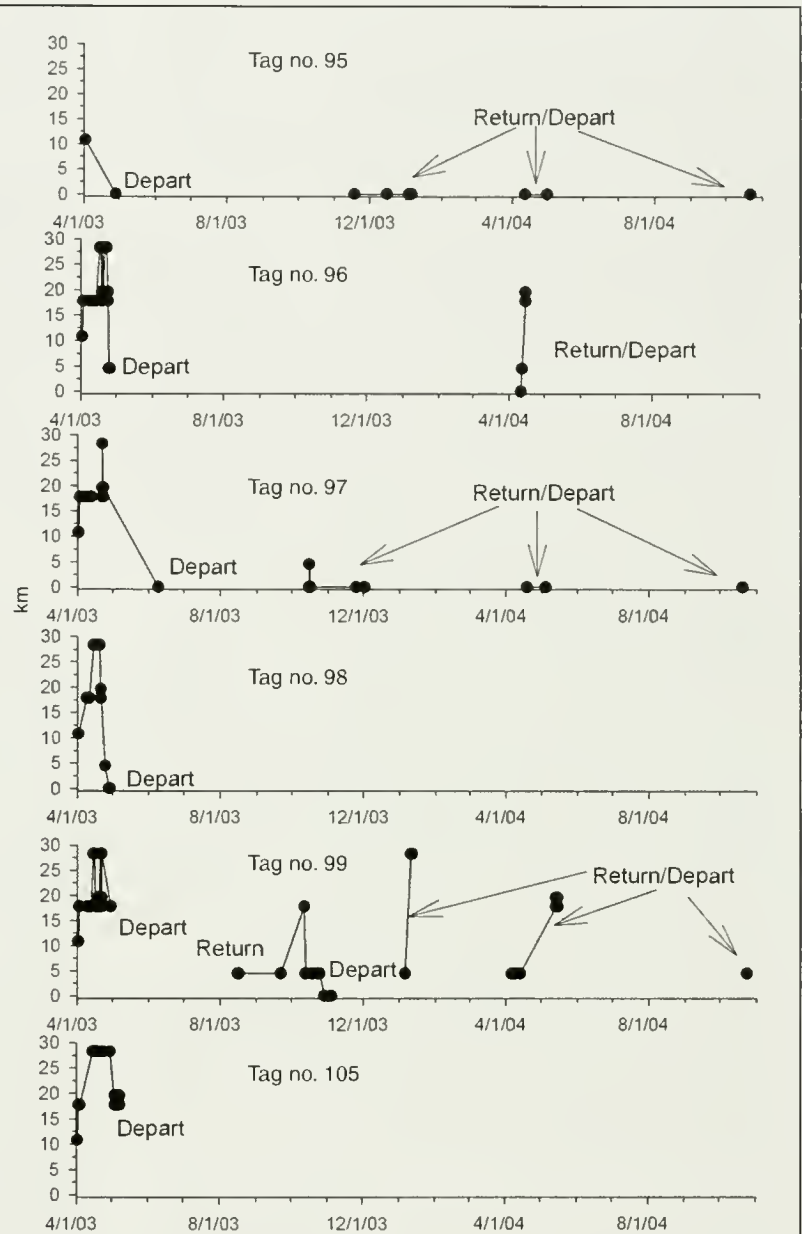


Figure 4

Occurrence and distribution of selected individual striped bass (*Morone saxatilis*) tagged on 2 April 2003 at Graveling Point. Filled circles indicate when there were detections by hydrophones. Distance upstream is from Little Egg Inlet gate (hydrophones 1–4, 13, reported as 0 km from the inlet) to Chestnut Neck gate (hydrophones 6–8, 18 km from the inlet), Lower Bank gate (hydrophone 10, 28 km from the inlet), and Sweetwater gate (hydrophone 12, 38 km from the inlet).

proximate time (spring 2003 and spring 2004) as the other fish (Fig. 2). The close agreement in seasonal arrival to and departure from the estuary is probably the result of seasonal migrations during which fish enter this estuary, and probably other estuaries, on their migration south in the winter and north in the spring.

For fish that left the estuary, the last detection was most frequent in the vicinity of Little Egg Inlet where most detections occurred at hydrophones 2 (33%), 1 (23%), and 4 (20%). Other final detections also occurred within the estuary at hydrophones 6 (9%), 7 (6%), 13 (3%), 5 (3%), and 8 (<1%). The last detection at relatively long distances from the inlet (hydrophones 6, 7, 8) may have resulted from departures during periods before hydrophone 13 was deployed.

Spatial and temporal patterns of striped bass within the estuary

Fish moved, as evidenced by hydrophone detections at selected gates, in a variable manner with respect to areas in the study site, seasons, and years (Figs. 4 and 5). Fish were frequently detected in the polyhaline portions near the inlet and in the estuary and less consistently in the river. The distribution of fish in the estuary varied by season; fish were detected at the inlet gate (hydrophones 1–4) during all seasons, whereas fish detected in spring were more frequently found farther up at the estuary gate (hydrophones 5–9, 13) or farther upstream at the river gate (hydrophones 10–11). However, few fish were detected during the winter at any gate. These general patterns of estuarine use varied between years. A strong peak in estuarine users occurred in the spring (weeks 14–21) of 2003, but there were fewer users in 2004. Modest peaks in inlet and estuarine users occurred in the fall (weeks 34–48) in both years. The sole peak in river use occurred in spring (weeks 14–20) of 2003.

The degree of residency and movements within the estuary varied among individuals over time for a given individual. Some individuals were resident in one portion of the estuary for long periods of time. This finding was substantiated by the long duration of detections for some individuals in the vicinity of the inlet. For example, two fish ($n=1273$ contacts and 280 cumulative hours of detection) spent 91% and 58% of their time, respectively, at the inlet, even though they were detected at two other gates. Together these types of patterns account for the preponderance of detections in the vicinity of the inlet and for the somewhat lower detections upstream. Another fish, with one of the longer time records ($n=1190$ hours of detection) was detected at all gates in the study area. Alternatively, some fish were consistently detected farther up the estuary. For example, one fish ($n=154.5$ hours detected) was detected frequently in the vicinity of Chestnut Neck (75% of the time).

Other individuals, although not detected as frequently, appeared to be resident for relatively long periods.

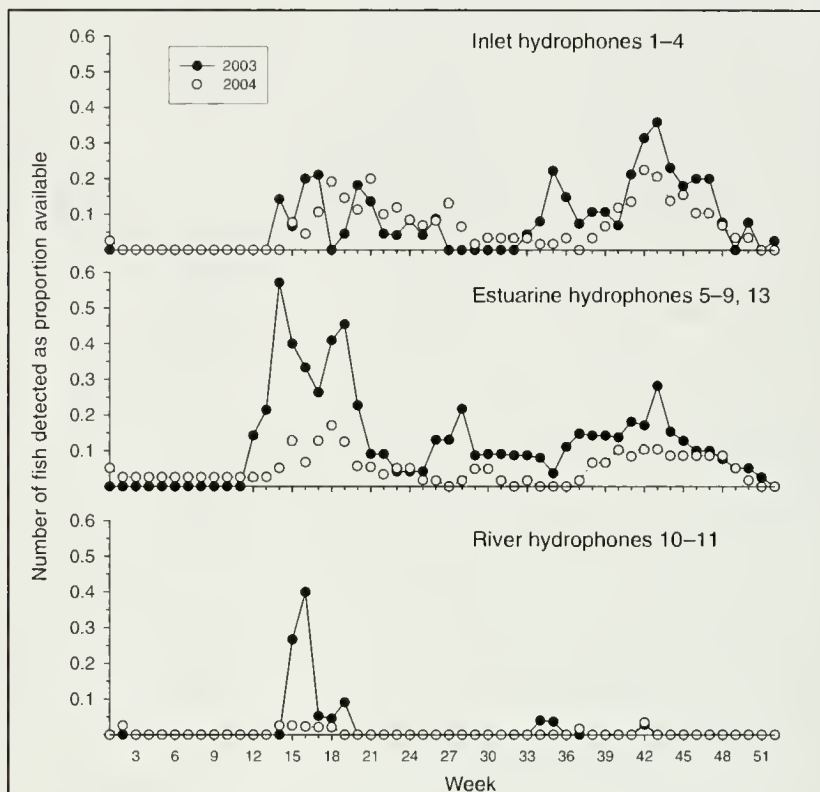


Figure 5

Annual variation in number of fish detected, by week in the inlet, by estuary, and at river gates. See Figure 1 for locations of gates.

For example, two fish were consistently found farther up the estuary over several months and we interpreted this period as residency. The lack of frequent detections implies that this residency occurred in areas between hydrophone gates. Active telemetry of individual fish confirms this interpretation (Ng, 2006; Ng et al., in press). Movements in the study area were often dynamic; individual fish moved large distances over short periods. Several individuals moved quickly upstream after being tagged lower in the estuary during the spring. Of six individuals tagged on 2 April 2003, five moved upstream 7–10 km into the area of the freshwater-saltwater interface (near Lower Bank, approximately 28.3 km from Little Egg Inlet) or farther into completely freshwater in the vicinity of Sweetwater (approximately 38.1 km from Little Egg Inlet) (Fig. 4). These same upstream movements occurred for 3 of 4 fish tagged at Graveling Point on 2 May 2003. More extensive movements were detected for all 3 fish tagged on 22 April 2004 at Little Egg Inlet. All of these fish moved 17–19 km upstream and were detected at the same locations as those of the previous fish.

Upstream movements were relatively quick. The speed of fish passing upstream from Little Egg Inlet to Chestnut Neck ranged from 0.3 to 2.4 km/h ($n=10$ fish) and from Chestnut Neck to Lower Bank ranged from 0.09 to 0.5 km/h ($n=11$ fish). The subsequent movement down-

stream followed quickly (within a few days) for most fish, but the range of speeds during these movements overlapped with the speed of upstream movements from Lower Bank to Chestnut Neck (0.1–0.3 km/h, $n=11$ fish) and from Chestnut Neck to Little Egg Inlet (0.1–2.2 km/h, $n=12$). Perhaps the slower movements between Chestnut Neck and Lower Bank reflect the steeper gradients in salinity, temperature, and especially pH in this region (Fig. 3). Although most of these movements occurred during the spring, others of similar magnitude occurred at other times of the year, as was the case for one fish during the winter of 2004 (Tag no. 99, Fig. 4).

Discussion

Annual and seasonal visits to the estuary

The seasonal visits of many tagged striped bass to this estuary reflect their seasonal migrations up and down the east coast of the United States. This seasonal migration to the south in the fall and winter and to the north in the spring and summer has been observed from prior tag-recapture studies (e.g., Boreman and Lewis, 1987; Waldman et al., 1990). The coastal ocean migrations of larger juvenile and adult striped bass must influence the timing and duration of their occurrence in estuaries. These patterns differ along the east coast of the United States and thus have to be taken into consideration when evaluating occurrences in the study area. In general, populations from North Carolina and southward are considered riverine and do not make coastal migrations, whereas those from Chesapeake Bay to the Bay of Fundy are generally considered to be anadromous and highly migratory (see Rulifson and Dadswell, 1995; Haeseker et al., 1996; Bjorgo et al., 2000 for reviews of the relevant literature), with the exception of the population of the St. Lawrence estuary which is believed to be resident (Coutant, 1985). Thus, it is not surprising that large juvenile and adult striped bass from the Mullica River–Great Bay estuary frequently left the estuary for extended periods. This interpretation is supported by the recapture by hook and line of fish we tagged in the study area at a variety of locations along the coast (northern New Jersey, south shore of Long Island, New Hampshire) and implies the same seasonal migration pattern. Further support is based on the detection of one striped bass tagged in the Mullica River–Great Bay and later detected in the Saco River, Maine, in a similar observation site (Carter²) and fish tagged at Saco River, Maine, that have been detected in the southern New Jersey study estuary ($n=3$) (Able and Grothues, pers. observ.). Earlier tag-recapture studies found striped bass in the Mullica River–Great Bay estuarine system that

had been tagged on the south shore of Long Island and northern New Jersey (Clark, 1968).

This study is one of the few that presents data on the high (58%) and seasonal rate of return to an estuary. Most of these returns occurred in the spring and fall when water temperatures were 10–20°C. Annual returns to the same estuary have also been reported in Chesapeake Bay tributaries for a few individuals ($n=9$) where the returns were assumed to be related to spawning (Hocutt et al., 1990). Many of the instances of fidelity of tagged striped bass to the Mullica River–Great Bay system were the result of detections at the inlet and not farther up the estuary. One possible interpretation is that these fish enter numerous inlets during the north and south coastal ocean migrations, thus providing the relatively high frequency of detections at the study site. This idea could be tested at observation sites in other estuaries.

Spatial and temporal patterns within the estuary

Movements within the estuary were frequently dynamic and were most likely to occur in the spring and fall. The spring movements of several fish tagged near Little Egg Inlet and near Chestnut Neck were commonly upstream to the vicinity of the freshwater-saltwater interface (Fig. 4). These were typically quick movements followed by similarly rapid movements downstream and into the ocean. The short duration in the riverine portion of the study area may reflect the avoidance of the low pH that typically occurs in this system (Fig. 3). These brief visits in the study area were very different from those found in a pilot study ($n=4$ males, 5 females) in upper Chesapeake Bay tributaries, which indicated a long residence time in the spawning areas (30 days) at least for males (Hocutt et al., 1990). Similarly, in the Roanoke River in North Carolina males remained on the spawning grounds for 21–22 days and females for 8–11 days in different years (Carmichael et al., 1998). The timing and types of movement in the study area, although consistent with an upstream movement for spawning, do not appear to be consistently successful. Some spawning does occur in the upstream portion of the estuary (see Hoff³ for accounts of egg and larvae collections). However, numerous collections in this estuary with a variety of gears, such as otter trawls (Martino and Able, 2003), seines (Able et al., 1996), traps (Able et al., 2006), and weirs (Able et al., 1996), have yielded less than 20 young-of-the-year (YOY) (<100 mm FL) striped bass. Over the same period, we have frequently collected numerous YOY striped bass in

² Carter, J. 2005. Unpubl. data. Department of Life Sciences, Univ. New England, 11 Hills Beach Road, Biddeford, ME 04005.

³ Hoff, H. K. 1976. The life history of striped bass, *Morone saxatilis* (Walbaum), in the Great Bay–Mullica River estuary and in the vicinity of Little Egg Inlet. In *Ecological studies in the bays and other waterways near Little Egg Inlet and in the ocean in the vicinity of the proposed site for the Atlantic Generating Station, New Jersey* (C. D. Milstein, and D. L. Thomas, eds.), p. 43–53. Progress Report for the period January–December 1975. Public Service Electric and Gas Company, 80 Park Plaza T-17-A, Newark, NJ 07101.

similar sampling programs in Delaware Bay (Nemerson and Able, 2003) and in the New York–New Jersey Harbor Estuary (Able and Duffy-Anderson, 2006). The short period of residency in upstream portions of the Mullica River may indicate the testing and then rejection of the area as a spawning site.

This study confirms that there are multiple ways in which striped bass use small estuaries, such as that of the study area, as there are multiple ways in which striped bass use larger systems such as the Hudson River (e.g., Secor et al. 2001). Further, the movement patterns observed in this study may be more diverse and variable than previously reported because the same fish can exhibit different patterns in different seasons and years. This diversity implies that the behavior at the individual level may be as, or more important (Sutherland, 1996; Slotte and Fikson, 2000) than, that at the level of the stock, contingent, or population level and thus is necessary to understand how striped bass use estuarine ecosystems and how biologists can manage natural populations.

Acknowledgments

Numerous technicians from the Rutgers University Marine Field Station assisted in the deployment and maintenance of hydrophone moorings, tagging of fish, and data compilation, especially R. Nichols and M. Greaney. Several recreational fishermen shared their local knowledge and helped extensively with tagging including D. Messerschmid and G. Delaporte. Personnel of the Jacques Cousteau National Estuarine Research Reserve, especially G. Sakowicz, provided access to environmental data. Several anonymous reviews provided helpful comments on an earlier draft. Financial support for the development and deployment of the hydrophones came from the Rutgers University/National Marine Fisheries Service Bluefish/Striped Bass program. This research was conducted under Rutgers University Animal Use Protocol no. 88-042. This paper is Rutgers University Institute of Marine and Coastal Sciences Contribution no. 2006-16.

Literature cited

- Able, K. W., and J. T. Duffy-Anderson.
2006. Impacts of piers on juvenile fishes in the lower Hudson River. *In* The Hudson River Estuary (J. S. Levinton, and J. R. Waldman, eds.), p. 428–440. Cambridge Univ. Press, New York, NY.
- Able, K. W., M. P. Fahay, D. A. Witting, R. S. McBride, and S. M. Hagan.
2006. Fish settlement in the ocean vs. estuary: comparison of pelagic larval and settled juvenile composition and abundance from southern New Jersey, USA. *Estuar. Coast. Shelf Sci.* 66:280–290.
- Able, K. W., D. A. Witting, R. S. McBride, R. A. Rountree, and K. J. Smith.
1996. Fishes of polyhaline estuarine shores in Great Bay-Little Egg Harbor, New Jersey: a case study of seasonal and habitat influences. *In* Estuarine shores: evolution, environments and human alternations (K. F. Nordstrom, and C. T. Roman, eds.), p. 335–353. John Wiley and Sons, Ltd., Chichester, England.
- Arnold, G. P., and H. Dewar.
2001. Electronic tags in marine fisheries research: a 30 year perspective. *In* Electronic tagging and tracking in marine fisheries (J. R. Siebert, and J. L. Nielsen, eds), p. 7–64. Kluwer Academic Publ., Dordrecht, The Netherlands.
- Begg, G. A., and J. R. Waldman.
1999. An holistic approach to fish stock identification. *Fish. Res.* 43: 35–44.
- Bjorgo, K. A., J. J. Isley, and C. S. Thomason.
2000. Seasonal movement and habitat use by striped bass in the Combahee River, South Carolina. *Trans. Am. Fish. Soc.* 129:1281–1287.
- Boreman, J., and R. R. Lewis.
1987. Atlantic coastal migration of striped bass. *Am. Fish. Soc. Symp.* 1:331–339.
- Carmichael, J. T., S. L. Haeseker, and J. E. Hightower.
1998. Spawning migration of telemetered striped bass in the Roanoke River, North Carolina. *Trans. Am. Fish. Soc.* 127:286–297.
- Chant, R., M. C. Curran, K. W. Able, and S. M. Glenn.
1996. Delivery of winter flounder (*Pseudopleuronectes americanus*) larvae to settling habitats in coves near tidal inlets. *Estuar. Coast. Shelf Sci.* 51:529–541.
- Clark, J.
1968. Seasonal movements of striped bass contingents of Long Island Sound and the New York Bight. *Trans. Am. Fish. Soc.* 97(4):320–343.
- Cooke, S. J., S. G. Hinch, M. Wikelski, R. D. Andrews, L. J. Kuchel, T. G. Wolcott, and P. J. Butler.
2004. Biotelemetry: a mechanistic approach to ecology. *Trends Ecol. Evol.* 19(6):334–343.
- Coutant, C. C.
1985. Striped bass, temperature, and dissolved oxygen: a speculative hypothesis for environmental risk. *Trans. Am. Fish. Soc.* 114:31–61.
- Gillanders, B. M.
2005. Using elemental chemistry of fish otoliths to determine connectivity between estuarine and coastal habitats. *Est. Coast. Shelf Sci.* 64:47–57.
- Grothues, T. M., K. W. Able, J. McDonnell, and M. M. Sisak.
2005. An estuarine observatory for real-time telemetry of migrant macrofauna: design, performance, and constraints. *Limnol. Oceanogr. Methods* 3:275–289.
- Haeseker, S. L., J. T. Carmichael, and J. E. Hightower.
1996. Summer distribution and condition of striped bass within Albemarle Sound, North Carolina. *Trans. Am. Fish. Soc.* 125:690–704.
- Heupel, M. R., J. M. Semmes, and A. J. Hobday.
2006. Automated acoustic tracking of aquatic animals: scales, design and deployment of listening station arrays. *Mar. Freshw. Res.* 57:1–13.
- Hocutt, C. H., S. E. Seibold, R. M. Harrell, R. V. Jesien, and W. H. Bason.
1990. Behavioral observations of striped bass (*Morone saxatilis*) on the spawning grounds of the Choptank and Nanticoke Rivers, Maryland, USA. *J. Appl. Ichthyol.* 6:211–222.
- Jackson, J. R., and J. E. Hightower.
2001. Reservoir striped bass movements and site fidelity

- in relation to seasonal patterns in habitat quality. *N. Am. J. Fish. Manag.* 21:34–45.
- Kennish, M. J.
2004. Jacques Cousteau National Estuarine Research Reserve. *In* Estuarine research monitoring, and resource protection (M. J. Kennish, ed.), p. 59–115. CRC Press, Baton Raton, FL.
- Kennish, M. J., and S. O'Donnell.
2002. Water quality monitoring in the Jacques Cousteau National Estuarine Research Reserve System. *Bull. New Jersey Acad. Sci.* 47(2):1–14.
- Klein-MacPhee, G.
2002. Striped bass (*Morone saxatilis*, Walbaum 1792). *In* Bigelow and Schroeder's Fishes of the Gulf of Maine (B. B. Collette, and G. Klein-MacPhee, eds.), p. 377–389. Smithsonian Institution Press, Washington, DC.
- Martino, E., and K. W. Able.
2003. Fish assemblages across the marine to low salinity transition zone of a temperate estuary. *Est. Coast. Shelf Sci.* 56(5–6):967–985.
- Morris, J. A., R. A. Rulifson, and L. H. Toburen.
2003. Life history strategies of striped bass, *Morone saxatilis*, populations inferred from otolith microchemistry. *Fish. Res.* 62: 53–63.
- Nemerson, D. M., and K. W. Able.
2003. Spatial and temporal patterns in the distribution and feeding habits of *Morone saxatilis*, in marsh creeks of Delaware Bay, USA. *Fish. Manag. Ecol.* 20: 337–348.
- Ng, C.
2006. Habitat utilization and movement patterns of adult striped bass, *Morone saxatilis*, in a southern New Jersey estuary using acoustic telemetry. M.S. thesis. 91 p. Rutgers, the State University of New Jersey, New Brunswick, NJ.
- Ng, C., K. W. Able, and T. M. Grothues.
In press. Habitat use, site fidelity and movement of adult striped bass in a southern New Jersey estuary based on acoustic telemetry. *Trans. Am. Fish. Soc.*
- Rhodehamel, E. C.
1998. Hydrology of the New Jersey Pine Barrens. *In* Pine Barrens: ecosystem and landscape (R. T. T. Forman, ed.), p. 147–167. Rutgers Univ. Press, New Brunswick, NJ.
- Richards, R. A., and P. J. Rago.
1999. A case history of effective fishery management: Chesapeake Bay striped bass. *N. Am. J. Fish. Manag.* 19:356–375.
- Rogers, K. B., and G. C. White.
In press. Analysis of movement and habitat use from telemetry data. *In* Analysis and interpretation of freshwater fisheries data (M. L. Brown, and C. S. Guy, eds.). American Fisheries Society, Bethesda, MD.
- Rulifson, R. A., and M. J. Dadswell.
1995. Life history and population characteristics of striped bass in Atlantic Canada. *Trans. Am. Fish. Soc.* 124:477–507.
- Secor, D. H.
1999. Specifying divergent migrations in the concept of stock: the contingent hypothesis. *Fish. Res.* 43: 13–34.
2000a. Longevity and resilience of Chesapeake Bay striped bass. *J. Mar. Sci.* 57:808–815.
2000b. Spawning in the nick of time? Effect of adult demographics on spawning behavior and recruitment of Chesapeake Bay striped bass. *ICES J. Mar. Sci.* 57:403–411.
- Secor, D. H., J. R. Rooker, E. Zlokovitz, and V. S. Zdanowicz.
2001. Identification of the riverine, estuarine, and coastal contingents of Hudson River striped bass based upon elemental fingerprints. *Mar. Ecol. Prog. Ser.* 211:245–253.
- Slotte, A., and O. Fiksen.
2000. State-dependent spawning migration in Norwegian spring-spawning herring. *J. Fish Biol.* 56: 138–162.
- Sibert, J. R., and J. L. Nielsen (eds).
2001. Electronic tagging and tracking in marine fisheries, 484 p. Kluwer Academic Publishers, Dordrecht, The Netherlands.
- Sutherland, W. J.
1996. From individual behavior to population biology. 224 p. Oxford Univ. Press, New York, NY.
- Thorrold, S. R., C. Latkoczy, P. K. Swart, and C. M. Jones.
2001. Natal homing in a marine fish metapopulation. *Science* 291:297–299.
- Tupper, M., and K. W. Able.
2000. Movements and food habits of striped bass (*Morone saxatilis*) in Delaware Bay (USA) salt marshes: comparison of a restored and a reference marsh. *Mar. Biol.* 137:1049–1058.
- Waldman, J. R., D. J. Dunning, Q. E. Ross, and M. T. Mattson.
1990. Range dynamics of Hudson River striped bass along the Atlantic coast. *Trans. Am. Fish. Soc.* 119: 910–919.
- Wooley, C. M., N. C. Parker, B. M. Florence, and R. W. Miller.
1990. Striped bass restoration along the Atlantic coast: a multistate and federal cooperative hatchery and tagging program. *Am. Fish. Soc. Symp.* 7:775–781.
- Young, S. P., and J. J. Isley.
2002. Striped bass annual site fidelity and habitat utilization in J. Strom Thurmond Reservoir, South Carolina-Georgia. *Trans. Am. Fish. Soc.* 131:828–837.
- Zlokovitz, E. R., D. H. Secor, and P. M. Piccoli.
2003. Patterns of migration in Hudson River striped bass as determined by otolith microchemistry. *Fish. Res.* 63: 245–259.

Microsatellite multiplex panels for genetic studies of gray snapper (*Lutjanus griseus*) and lane snapper (*Lutjanus synagris*)

Mark A. Renshaw

Eric Saillant

Siya Lem

Philip Berry

John R. Gold

Email address for M. A. Renshaw: mrenshaw@ag.tamu.edu

Center for Biosystematics and Biodiversity

Texas A&M University, TAMU-2258

College Station, Texas 77843-2258

Microsatellites are codominantly inherited nuclear-DNA markers (Wright and Bentzen, 1994) that are now commonly used to assess both stock structure and the effective population size of exploited fishes (Turner et al., 2002; Chistiakov et al., 2006; Saillant and Gold, 2006). Multiplexing is the combination of polymerase chain reaction (PCR) amplification products from multiple loci into a single lane of an electrophoretic gel (Olsen et al., 1996; Neff et al., 2000) and is accomplished either by co-amplification of multiple loci in a single reaction (Chamberlain et al., 1988) or by combination of products from multiple single-locus PCR amplifications (Olsen et al., 1996). The advantage of multiplexing microsatellites lies in the significant reduction in both personnel time (labor) and consumable supplies generally required for large genotyping projects (Neff et al., 2000; Renshaw et al., 2006).

In this note, we report the development of multiplex panels of microsatellites that will facilitate population-level genetic studies of both gray (*Lutjanus griseus*) and lane (*L. synagris*) snappers. The overexploitation of Gulf red snapper (*L. campechanus*) in U.S. waters and the increasing restrictions on both commercial and recreational red snapper catches (Gillig et al., 2001) have led to increased fishing pressure on other snapper species (Fischer et al.,

2005), including both gray (Burton, 2001; Fischer et al., 2005) and lane snappers (GMFMC¹). Although neither species has yet been classified as "overfished" or subject to "overfishing," the increased exploitation of the two species could jeopardize these snapper resources in the future. In this study, we optimized multiplex panels for gray and lane snappers from among microsatellite markers designed originally for red snapper by Gold et al. (2001) and vermilion snapper (*Rhomboplites aurorubens*) by Bagley and Geller (1998).

Materials and methods

Samples of gray and lane snappers were obtained off the west coast of Florida during April of 2004. Fin clips and pieces of liver were preserved in 95% ethanol, brought to the laboratory, and stored at room temperature. Genomic DNA was extracted by using an alkaline-lysis method (Saillant et al., 2002) and stored at -20°C .

Microsatellites were first evaluated in single-locus (simplex) reactions in order to determine the size range and ease of scoring of PCR products in each species. PCR amplifications were performed in 11.5- μL volumes comprising 1.5 μL of DNA (approximately 50 ng), 1 μL of 10 \times reaction buffer [50 mM KCl, 10 mM Tris, 1% Triton-X 100], 0.75 U *Taq* DNA polymerase (Invitrogen, Carlsbad, CA), 200 μM of each dNTP, 1 mM MgCl_2 , and various quantities of PCR primers. One PCR primer of each pair was labeled with one of three fluorescent dyes from set D (Applied Biosystems, Foster City, CA): FAM, HEX, or NED. Fragment analysis was carried out on an ABI PRISM 377 automated DNA sequencer (Applied Biosystems, Foster City, CA). Allele size was estimated by using the GENESCAN-400HD [ROX] size standard (Applied Biosystems, Foster City, CA); allele size estimation was performed with GENESCAN 3.1.2 (Applied Biosystems, Foster City, CA) and allele calling was performed in GENOTYPER, version 2.5 (Applied Biosystems, Foster City, CA). Multiplex tests were performed only on those microsatellites that amplified successfully and yielded PCR products that were easy to score; loci not meeting these criteria were eliminated from subsequent analyses.

Initial multiplex PCR amplifications were performed by using the three multiplex panels designed to amplify 20 microsatellite loci in red snapper (Renshaw et al., 2006). At first, PCR primer concentrations followed those outlined in Renshaw et al. (2006), and changes were made according to the relative success of amplifications at each microsatellite within a particular multiplex. Microsatellites that failed to amplify in multiplex reactions were optimized in simplex reactions. Additional PCR

¹ GMFMC (Gulf of Mexico Fishery Management Council). 2005. Final amendment to the FMPs for: reef fish (Amendment 25) and coastal migratory pelagics (Amendment 17) for extending the charter vessel/headboat permit moratorium (including SEIS/RIR/IRFA), 111 p. Gulf of Mexico Fishery Management Council, 3018 North U.S. Highway 301, Suite 1000, Tampa, FL 33619-2272.

Table 1

Technical details on amplification of microsatellite loci in gray snapper (*Lutjanus griseus*) and lane snapper (*L. synagris*). Included in the table are the multiplex polymerase chain reaction (PCR) panel, primer quantities, and fluorescent dye labels (Set D; Applied Biosystems, Foster City, CA). PCR protocols, including appropriate annealing temperatures, correspond to those outlined in Renshaw et al. (2006). Primer sequences for *Lca* and *Prs* microsatellites are given in Gold et al. (2001); those for *Ra* microsatellites are given in Bagley and Geller (1998).

Species	Panel	Microsatellite	Quantity (pmol)	ABI dye	PCR protocol
<i>Lutjanus griseus</i>	1	<i>Lca</i> 20	5	FAM	Touchdown II
		<i>Lca</i> 43	4	FAM	56°
		<i>Prs</i> 260	1.5	FAM	53°
	2	<i>Ra</i> 1	3.5	HEX	50°
		<i>Prs</i> 137	7	FAM	Touchdown II
		<i>Prs</i> 275	6	FAM	54°
		<i>Prs</i> 328	0.8	FAM	52°
	3	<i>Ra</i> 6	2	NED	50°
		<i>Lca</i> 22	2.5	FAM	Touchdown I
		<i>Lca</i> 91	8	FAM	56°–50.5°
	simplex	<i>Lca</i> 107	6.5	HEX	50°
	simplex	<i>Prs</i> 221	5	HEX	Same as panel 2
	simplex	<i>Prs</i> 240	5	HEX	Same as panel 3
simplex	<i>Ra</i> 7	5	NED	Same as panel 3	
<i>Lutjanus synagris</i>	1	<i>Lca</i> 20	5	FAM	Touchdown II
		<i>Prs</i> 248	5	NED	52°
		<i>Prs</i> 260	1.5	FAM	50°
		<i>Prs</i> 303	1.5	NED	48°
		<i>Ra</i> 1	7.5	NED	
	2	<i>Ra</i> 4	5	HEX	
		<i>Prs</i> 275	4	FAM	Touchdown II
		<i>Prs</i> 328	1	FAM	52°
		<i>Ra</i> 2	3.5	FAM	50°
	3	<i>Ra</i> 6	3	NED	48°
		<i>Lca</i> 22	1	FAM	Touchdown II
		<i>Lca</i> 91	8	FAM	52°
		<i>Prs</i> 240	9	HEX	50°
<i>Prs</i> 333		3	HEX	48°	
	<i>Ra</i> 7	5	NED		

primers (*Ra* 1, *Ra* 2, and *Ra* 4) designed by Bagley and Geller (1998) for vermilion snapper microsatellites were tested in simplex reactions as described above and labeled with one fluorescent dye to allow integration into one of the three multiplex panels.

Multiplex PCR amplifications initially followed the Touchdown I and II protocols outlined in Renshaw et al. (2006). Touchdown PCR protocols enable the amplification of multiple loci with different optimal annealing temperatures. The former (Touchdown I) protocol involved a one-half degree drop in annealing temperature with each subsequent cycle, for a total of 12 cycles, followed by 30 cycles at a bottom annealing temperature that was 6°C below the initial annealing temperature; the latter (Touchdown II) protocol featured a three-step drop in annealing temperature with seven cycles at an initial annealing temperature, followed by seven cycles at a lower annealing temperature, followed by 28 cycles

at a bottom annealing temperature that was 4–6°C below the initial annealing temperature. Changes were made to optimize multiplex panels individually for each species. These changes included 1) removal of various primers and addition of others, and 2) modification of annealing temperatures and species-specific differences in primer concentrations.

Once multiplex or simplex protocols were developed for the two species, DNA from 28 individuals of each species was assayed across all optimized loci. Genetic variability of microsatellites in each species was measured by the number of alleles, expected heterozygosity (gene diversity), and observed heterozygosity. Fisher's exact test was used to evaluate loci for significant departures from Hardy-Weinberg equilibrium expectations. Three common causes for genotyping errors—null alleles, large allele dropout, and stuttering—were assessed with MICRO-CHECKER (Van Oosterhout et al., 2004).

Table 2

Summary data for microsatellites amplified from 28 gray snapper (*Lutjanus griseus*) and 28 lane snapper (*L. synagris*). Data for each microsatellite include number of alleles (N_A), size range (in base pairs) of detected alleles, expected (H_E) and observed (H_O) heterozygosity, and probability (P_{HW}) of conformity to Hardy-Weinberg equilibrium expectations. *Lca* and *Prs* microsatellites were developed initially for red snapper (*L. campechanus*) (Gold et al., 2001), and *Ra* microsatellites were developed initially for vermilion snapper (*Rhomboplites aurorubens*) (Bagley and Geller, 1998).

Species	Microsatellite	N_A	Size range	H_E/H_O	P_{HW}
<i>Lutjanus griseus</i>	<i>Lca</i> 20	4	216–222	0.707/0.643	0.721
	<i>Lca</i> 22	5	242–252	0.593/0.500	0.050
	<i>Lca</i> 43	2	176–188	0.195/0.214	1.000
	<i>Lca</i> 91	2	134–136	0.036/0.036	1.000
	<i>Lca</i> 107	6	112–144	0.771/0.750	0.266
	<i>Prs</i> 137	7	127–141	0.794/0.679	0.075
	<i>Prs</i> 221	4	235–245	0.566/0.714	0.448
	<i>Prs</i> 240	4	210–220	0.642/0.679	0.963
	<i>Prs</i> 260	9	105–129	0.847/1.000	0.060
	<i>Prs</i> 275	5	156–168	0.548/0.571	0.343
	<i>Prs</i> 328	3	202–206	0.527/0.464	0.842
	<i>Ra</i> 1	7	149–171	0.594/0.571	0.081
	<i>Ra</i> 6	15	113–155	0.926/0.679	0.000
	<i>Ra</i> 7	3	154–158	0.200/0.143	0.127
<i>Lutjanus synagris</i>	<i>Lca</i> 20	12	234–262	0.810/0.571	0.009
	<i>Lca</i> 22	8	234–256	0.712/0.679	0.257
	<i>Lca</i> 91	7	139–153	0.601/0.679	0.263
	<i>Prs</i> 240	5	192–202	0.592/0.538	0.484
	<i>Prs</i> 248	17	224–260	0.938/0.893	0.402
	<i>Prs</i> 260	4	92–120	0.292/0.321	1.000
	<i>Prs</i> 275	2	154–156	0.036/0.036	1.000
	<i>Prs</i> 303	4	135–141	0.690/0.643	0.724
	<i>Prs</i> 328	5	198–214	0.631/0.571	0.499
	<i>Prs</i> 333	12	152–180	0.870/0.821	0.327
	<i>Ra</i> 1	9	141–163	0.806/0.893	0.587
	<i>Ra</i> 2	6	82–100	0.704/0.821	0.972
	<i>Ra</i> 4	9	59–99	0.787/0.821	0.660
	<i>Ra</i> 6	4	118–124	0.384/0.464	0.770
<i>Ra</i> 7	4	177–187	0.612/0.536	0.578	

Results and discussion

A total of 14 microsatellites (11 in three multiplex panels and 3 in simplex reactions) were optimized for gray snappers, and 15 microsatellites (in three multiplex panels) were optimized for lane snappers. The multiplex and simplex formats are presented in Table 1 and include for each microsatellite the fluorescent label (Applied Biosystems, Foster City, CA), primer quantity, PCR protocol, and optimized annealing temperatures. Genotype summary data from 28 individuals (in both species) are given in Table 2; data for each microsatellite include number of alleles, size range of alleles detected, expected and observed heterozygosity, and probability of conformity to Hardy-Weinberg equilibrium expectations.

For gray snappers, the number of alleles per microsatellite ranged from two (*Lca* 43 and *Lca* 91) to 15 (*Ra* 6), and expected and observed heterozygosity per microsat-

ellite ranged from 0.036 (*Lca* 91) to 0.926 (*Ra* 6) and from 0.036 (*Lca* 91) to 1.000 (*Prs* 260), respectively. Only one microsatellite (*Ra* 6) deviated significantly ($P < 0.05$) from Hardy-Weinberg equilibrium expectations after sequential Bonferroni correction (Rice, 1989). Analysis with MICRO-CHECKER (Van Oosterhout et al., 2004) indicated the possible occurrence of null alleles at *Ra* 6.

For lane snappers, the number of alleles per microsatellite ranged from two (*Prs* 275) to 17 (*Prs* 248), and expected and observed heterozygosity per microsatellite ranged from 0.036 (*Prs* 275) to 0.938 (*Prs* 248) and from 0.036 (*Prs* 275) to 0.893 (*Prs* 248 and *Ra* 1), respectively. None of the 15 microsatellites deviated significantly from Hardy-Weinberg equilibrium expectations after sequential Bonferroni correction (Rice, 1989). Analysis with MICRO-CHECKER indicated the possibility of null alleles at one microsatellite (*Lca* 20) where the probability

of deviation from Hardy-Weinberg equilibrium expectations was significant ($P=0.009$) before Bonferroni correction. One locus, *Lca* 91, exhibited a one base-pair shift (rather than the two base-pair shifts expected from dinucleotide repeats) in samples of lane snapper; this difference in shift could generate scoring problems in future genotyping efforts.

The costs of large genotyping projects can be substantially reduced through the combination of multiple loci in single PCR amplifications (Renshaw et al., 2006). The reduction in costs could enable researchers to increase sample sizes, possibly allowing for the inclusion of additional year classes for temporal studies or could extend a proposed sampling range to include more of the geographic distribution of a species. The multiplex panels and simplex reactions developed in the present study will provide critical tools for future population-level genetic studies designed to identify fishery management units and to monitor changes in genetic effective population size for both gray and lane snappers.

Acknowledgments

We thank the crew of the RV *Tommy Munro* (Florida Fish and Wildlife Research Institute) and M. Murphy, B. Mahmoudi, and R. Lehnert for assistance in sampling, and C. Bradfield and D. Ebel for assistance in the laboratory. Work was supported by the Marfin Program of the U.S. Department of Commerce (Grant NA04-NMF-4330074), and by the Texas Agricultural Experiment Station (Project H-6703). This article is number 54 in the series "Genetic Studies in Marine Fishes" and is contribution number 147 of the Center for Biosystematics and Biodiversity at Texas A&M University.

Literature cited

- Bagley, M. J., and J. B. Geller.
1998. Characterization of microsatellite loci in the vermillion snapper *Rhomboplites aurorubens* (Percoidae: Lutjanidae). *Mol. Ecol.* 7:1089–1090.
- Burton, M. L.
2001. Age, growth, and mortality of gray snapper, *Lutjanus griseus*, from the east coast of Florida. *Fish. Bull.* 99:254–265.
- Chamberlain, J. S., R. A. Gibbs, J. E. Ranier, P. N. Nguyen, and C. T. Caskey.
1988. Deletion screening of the Duchenne muscular dystrophy locus via multiplex DNA amplification. *Nucleic Acids Res.* 16:11141–11156.
- Chistiakov, D. A., B. Hellems, and F. A. M. Volckaert.
2006. Microsatellites and their genomic distribution, evolution, function and applications: a review with special reference to fish genetics. *Aquaculture* 255:1–29.
- Fischer, A. J., M. S. Baker Jr., C. A. Wilson, and D. L. Nieland.
2005. Age, growth, mortality, and radiometric age validation of gray snapper (*Lutjanus griseus*) from Louisiana. *Fish. Bull.* 103:307–319.
- Gillig, D., W. L. Griffin, and T. Ozuna Jr.
2001. A bioeconomic assessment of Gulf of Mexico red snapper management policies. *Trans. Am. Fish. Soc.* 130:117–129.
- Gold, J. R., E. Pak, and L. R. Richardson.
2001. Microsatellite variation among red snapper (*Lutjanus campechanus*) from the Gulf of Mexico. *Mar. Biotechnol.* 3:293–304.
- Neff, B. D., P. Fu, and M. R. Gross.
2000. Microsatellite multiplexing in fish. *Trans. Am. Fish. Soc.* 129:584–593.
- Olsen, J. B., J. K. Wenburg, and P. Bentzen.
1996. Semiautomated multilocus genotyping of Pacific salmon (*Oncorhynchus* spp.) using microsatellites. *Mol. Mar. Biol. Biotechnol.* 5:259–72.
- Renshaw, M. A., E. Saillant, S. C. Bradfield, and J. R. Gold.
2006. Microsatellite multiplex panels for genetic studies of three species of marine fishes: red drum (*Sciaenops ocellatus*), red snapper (*Lutjanus campechanus*), and cobia (*Rachycentron canadum*). *Aquaculture* 253:731–735.
- Rice, W. R.
1989. Analyzing tables of statistical tests. *Evolution* 43:223–225.
- Saillant, E., A. Fostier, P. Haffrey, B. Menu, J. Thimonier, and B. Chatain.
2002. Temperature effects and genotype-temperature interactions on sex determination in the European sea bass (*Dicentrarchus labrax* L.). *J. Exp. Zool.* 292:494–505.
- Saillant, E., and J. R. Gold.
2006. Population structure and variance effective size of red snapper (*Lutjanus campechanus*) in the northern Gulf of Mexico. *Fish. Bull.* 104:136–148.
- Turner, T. F., J. P. Wares, and J. R. Gold.
2002. Genetic effective size is three orders of magnitude smaller than adult census size in an abundant, estuarine-dependent marine fish (*Sciaenops ocellatus*). *Genetics* 162:1329–1339.
- Van Oosterhout, C., W. F. Hutchinson, D. P. M. Willis, and P. Shipley.
2004. MICRO-CHECKER: software for identifying and correcting genotyping errors in microsatellite data. *Mol. Ecol. Notes* 4:535–538.
- Wright, A. J., and P. Bentzen.
1994. Microsatellites: genetic markers for the future. *Rev. Fish Biol. Fish.* 4:384–388.

Effect of towing speed on retention of zooplankton in bongo nets

Joseph Kane (contact author)

Jacquelyn L. Anderson

Email address for J. Kane: jkane@whsun1.wh.who.edu

National Oceanic and Atmospheric Administration
National Marine Fisheries Service
Northeast Fisheries Science Center
28 Tarzwell Drive
Narragansett, Rhode Island 02882-1152

Long-term time series of zooplankton data provide invaluable information about the fluctuations of species abundance and the stability of marine community structure. These data have demonstrated that environmental variability have a profound effect on zooplankton communities across the Atlantic basin (Beaugrand et al., 2002; Frank et al., 2005; Pershing et al., 2005). The value of these time series increases as they lengthen, but so does the likelihood of changes in sampling or processing methods. Sampling zooplankton with nylon nets is highly selective and biased because of mesh selectivity, net avoidance, and damage to fragile organisms. One sampling parameter that must be standardized and closely monitored is the speed of the net through the water column. Tow speed should be as fast as possible to minimize net avoidance by the organisms, but not so fast as to damage soft bodied zooplankters or extrude them through the mesh (Tranter et al., 1968; Anderson and Warren, 1991).

The bongo plankton sampler (Posgay and Marak, 1980) has been used by many investigators to monitor plankton populations throughout the world's oceans (e.g., Lough et al., 1985; Kane, 1993; Licandro et al., 2001). Tow speed on bongo surveys has ranged from approximately 1 to 4 knots, depending on the target population of the survey program. With the growing interest in long-term time series, the purpose of our study was to evaluate differences in catches with bongo nets towed at two

of the common speeds: 1.5 and 3.5 knots. If the differences can be quantified, zooplankton data collected at the two towing speeds could be used to compare or extend time series at the regional level. We made replicate collections at the two different tow speeds and compared species composition, community structure, and overall biomass.

Materials and methods

Plankton samples were collected aboard the RV *Delaware II* from March 29 to April 9 1999 in north-eastern U.S. continental shelf waters (Fig. 1). Initially a cross-shelf transect of 10 stations was surveyed, extending from the island of Martha's Vineyard out to just beyond the 200-m isobath. For the remainder of the cruise, samples were collected at 29 stations in a saw tooth pattern throughout the Georges Bank region, most within the 200-m isobath.

At each sampling location two consecutive hauls were conducted with a 61-cm bongo frame fitted with a white colored 0.333-mm mesh net towed obliquely to a maximum depth of 200 m or to within 5 m from the bottom and back to the surface. Wire was payed out at 50 m/min and retrieved at 20 m/min during both tows and a conductivity-temperature-depth (CTD) probe was attached above the bongo to measure sampling depth. A flowmeter was suspended in the center of the bongo frame to measure the volume of water filtered during each

tow. The first tow was performed at a ship speed of 1.5 knots, which varied slightly at times to maintain an approximately 45° wire angle. The sampler was depressed with a simple 45-kg lead ball. After the first tow had been completed, the vessel returned to the exact location where the tow was initiated. The gear was redeployed with a wedge-shaped 1.2-m 108-kg vfin depressor and towed at 3.5 knots without regard to the wire angle. Specimens from all samples were preserved in 5% formalin.

In the laboratory, biomass was measured by displacement volume. The plankton sample, with preserving liquid, was measured in a graduated cylinder, poured through a mesh cone into a second cylinder, and drained until the interval between drops was 15 seconds. The liquid in the second cylinder was measured and the displacement volume of the sample was the difference between readings. Samples were then reduced to approximately 500 organisms by subsampling with a modified box splitter. Zooplankton were sorted, counted, and identified to the lowest possible taxa. Abundance and biomass were expressed as number/100 m³ and cubic centimeters/100 m³, respectively.

Abundance of dominant taxa, defined as those contributing on average >1% to the total abundance, were compared between tow speeds. Survey mean abundance values were tested for significant differences by using the conventional paired *t*-test, and its nonparametric counterpart, the Wilcoxon test, was used to compare median abundance levels. The stage distribution of the five most abundant copepods was also examined for significant differences by using the same statistical methods.

Zooplankton community structures from the two tow speeds were compared by using multivariate statisti-

Manuscript submitted 12 Decembbber 2006 to the Scientific Editor's Office.

Manuscript approved for publication 14 March 2007 by the Scientific Editor.
Fish. Bull. 105:440–444 (2007).

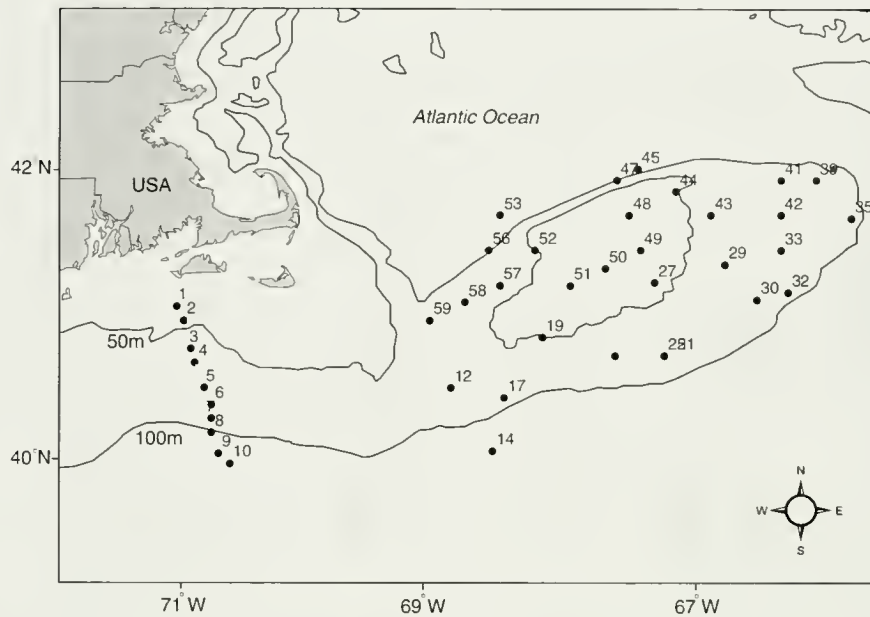


Figure 1

Locations surveyed with the RV *Delaware II* for effect of towing speed on retention of zooplankton in bongo nets. Sampling was conducted from March 29 to April 1999 at two tow speeds: 1.5 and 3.5 knots. Locations are labeled with the station number.

cal and ordination techniques from the PRIMER 6.1.5 software package (PRIMER-E Ltd, Plymouth, UK). Initially, data were log transformed and the biotic relationship between any two samples was represented by the Bray-Curtis index (Bray and Curtis, 1957), which measures the similarity (or dissimilarity) in species composition. The triangular matrix of similarity between each sample was then classified into groups by using two techniques: 1) hierarchical agglomerative cluster analysis, and 2) nonmetric multidimensional scaling (MDS). Clusters of samples that were found to be statistically significant ($P < 0.05$) by the similarity profile test (SIMPROF) and also to be isolated by low stress (< 0.20) MDS ordinations, were judged to be samples with similar zooplankton community structure. The significance of the resultant groupings was tested by using the nonparametric permutation procedure ANOSIM (analysis of similarity).

Results

Nine taxa dominated the zooplankton community captured during the survey (Table 1). All dominant taxa were common to both tow speeds and their mean abundance ranked in nearly the same order. The only difference was found for the copepods *Temora longicornis* and *Oithona* spp., which were the seventh and eighth most abundant taxa in the 1.5-knot tows, and eighth and seventh most abundant in the 3.5-knot tows (Table 1).

The mean and median abundance levels of the dominant species were not significantly different ($P > 0.05$) between tow speeds.

The copepodite stage distributions of the dominant copepods were equally represented at the two tow speeds. Mean abundance levels of all *Calanus finmarchicus* life stages and *Pseudocalanus* spp. stage-V copepodites were nearly identical from both hauls (Fig. 2) and not significantly different ($P > 0.05$). Slightly higher mean numbers of late-stage copepodites of *Metridia lucens*, *Centropages typicus*, and *Centropages hamatus*, and adults of *Pseudocalanus* spp. were captured at the higher tow speed (Fig. 2), but the values also were not significantly different ($P > 0.05$). These similar mean numbers for the various life-stages indicate that there was no substantial difference in the size of particles retained or extruded by the nets at the two tow speeds.

Ordinations of zooplankton community structures from the two speeds were very similar. Cluster analysis of data from both tow speeds produced five significant ($P < 0.05$) groupings that were also evident in the low-stress MDS plots (Fig. 3). These station clusters for the two tow speeds were nearly identical, both reflecting the different depth strata and areas sampled during the survey. The two large clusters were essentially inshore and offshore station groupings, and the remaining three were different deepwater (> 200 m) sites (Figs. 1 and 3). The community composition of the samples collected at the two speeds was not significantly different (ANOSIM procedure, $P = 0.40$).

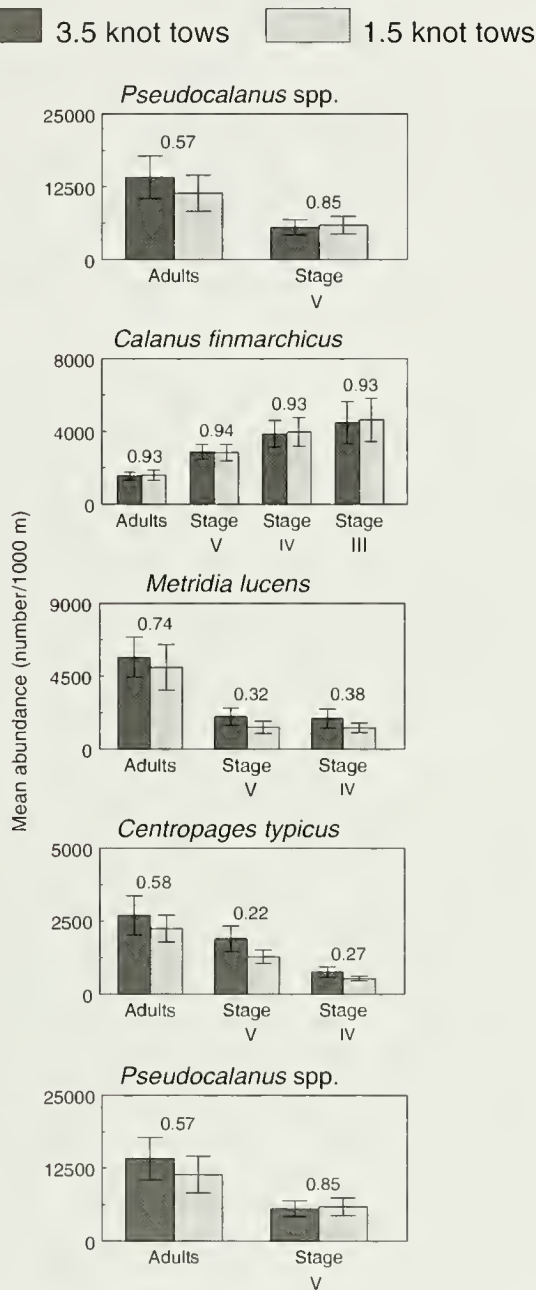


Figure 2

Comparison of mean abundance at 3.5 and 1.5 knot tow speeds for different life stages of the five dominant copepods sampled during the cruise. Only the mean abundance of adults and copepodite stages (denoted as stage III, IV, or V) that were captured quantitatively with the 0.333-mm mesh nets are shown. Mean values for the two tow speeds were not significantly different (P values from t -test results are given above each tested pair). Error bars represent one standard error. Please note that y-axis scales are different.

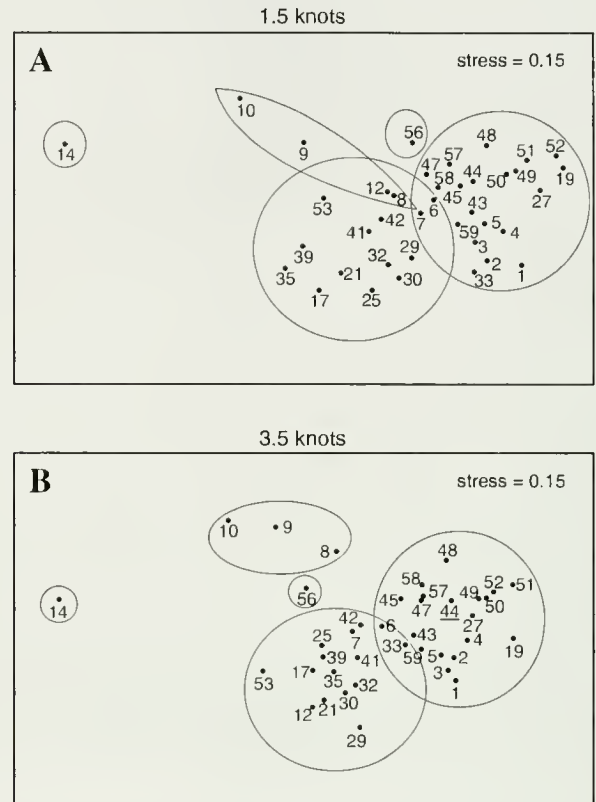


Figure 3

Nonmetric multidimensional scaling (MDS) plots produced after calculation of Bray-Curtis similarity index on log-transformed zooplankton station abundance data obtained with the bongo sampler towed at (A) 1.5 knots and (B) 3.5 knots. Encircled groups are stations strongly grouped by cluster analysis. The stress value is a measure of the strength of the MDS plot and is considered meaningful if <2.0 .

In contrast to species abundance, mean and median displacement volume values from the 1.5-knot tows were significantly different ($P < 0.05$) from the faster tows, averaging 40% higher (Table 1). Because mean and median total zooplankton counts at the two speeds were not significantly different ($P > 0.05$), the increased biomass could be caused by items not counted in slower tows. These could include phytoplankton, Cnidaria fragments, and general detritus that would have been extruded through the nets at higher speed tows.

Discussion

The degree of similarity between the overall catches at the two speeds was remarkable given the variation normally associated with replicate plankton tows (Wiebe and Holland, 1968). None of the survey mean and median abundance values of dominant taxa were significantly

Table 1

Average abundances (no./100 m³) and proportions of the dominant taxa (arranged in order of mean abundance in the tow) collected from tows traveled at 1.5 and 3.5 knots. Placed below them are the mean and median abundance values for total zooplankton and displacement volume values (cc/100 m³) for each tow speed.

Abundance rank	Taxa	Frequency of occurrence	Mean abundance	Median abundance	Mean proportion	Cumulative %
1.5 knots						
1	<i>Pseudocalanus</i> spp.	100.0	18,696	10,956	28.6	28.6
2	<i>Calanus finmarchicus</i>	100.0	17,478	9929	26.7	55.3
3	<i>Metridia lucens</i>	97.4	8812	6417	13.4	68.8
4	<i>Centropages typicus</i>	97.4	4067	2149	6.2	75.0
5	<i>Centropages hamatus</i>	76.9	3775	3327	5.7	80.8
6	Balanidae	66.7	3424	873	5.2	86.1
7	<i>Oithona</i> spp.	89.7	2971	1496	4.6	90.6
8	<i>Temora longicornis</i>	92.3	2352	1888	3.6	94.2
9	<i>Sagitta elegans</i>	79.5	719	567	1.1	95.3
	Total zooplankton		65,367	49,230		
	Displacement volume		53	49		
3.5 knots						
1	<i>Pseudocalanus</i> spp.	100	20,653	14,210	28.9	28.9
2	<i>Calanus finmarchicus</i>	100	17,023	8601	23.8	52.8
3	<i>Metridia lucens</i>	94.9	10,867	7401	15.2	68.0
4	<i>Centropages typicus</i>	97.4	5354	2001	7.5	75.5
5	<i>Centropages hamatus</i>	82.1	5199	2357	7.3	82.8
6	Balanidae	64.1	3823	846	5.4	88.1
7	<i>Temora longicornis</i>	94.9	2704	1606	3.8	91.9
8	<i>Oithona</i> spp.	89.7	2053	1830	2.9	94.8
9	<i>Sagitta elegans</i>	64.1	895	1034	1.3	96.1
	Total zooplankton		71,388	65,815		
	Displacement volume		38	35		

different and the rank abundances were nearly identical. Furthermore, nearly identical life-stage distributions were derived for the dominant copepod species at the two tow speeds. There was no significant effect of tow speed on zooplankton community structure.

Catches in most tows at a single location showed good agreement between the catches of taxa at the two speeds, although occasionally there were large differences between species abundance. One reason for this discrepancy may be sampling error attributed to water movement. Although the vessel returned to the exact location where the 1.5-knot tows began, the same specific water parcel was not precisely sampled by the faster tow. Furthermore, the patchiness of zooplankton also makes it difficult to sample exactly the same community with duplicate tows. Nonetheless, these differences were averaged out when several stations were pooled and mean or median abundances were calculated.

Direct comparison between displacement volume measurements made at the two speeds is not recommended. It appears that at the slower tow speed unaccounted material is collected that is extruded through

the net meshes at higher speed tows. Filtration pressure across the mesh varies with the square of the approach velocity; thus, 3.5-knot tows will exert a pressure approximately 5.4 times higher than the 1.5-knot tows (Tranter and Smith, 1968). Because this study was conducted at or near the height of the spring phytoplankton bloom in the region, sample biomass in the slower tow was likely elevated by the retention of larger diatom species that dominate the spring bloom on Georges Bank (O'Reilly and Zetlin, 1998). The results indicate that sample displacement volumes for the 3.5-knot tows conducted during early spring should be increased by 40% before comparison to levels for the 1.5-knot tows. Owing to the widespread seasonal and spatial variability of plankton populations, caution should be exercised in applying this conversion factor to other data sets. Colton et al. (1980) also reported that displacement volumes for replicate 3.5-knot tows were lower than those for 1.5-knot tows, but they found the difference was only 20.8%. Their study was conducted in the same region as ours, but samples were collected at one location in early November over a five-day period. Further comparative studies in other

seasons and regions would be needed to precisely convert the displacement volumes measured for the two tow speeds.

For projects focusing on zooplankton studies, there may be a need to consider the higher tow speed as the preferred sampling procedure. The escape reaction of the dominant species to the approaching net or loss of dominant species by extrusion through the net does not appear to change substantially between 1.5 and 3.5 knots. At higher tow speeds cleaner samples are collected—samples that are easier to process because more phytoplankton and detritus are extruded from the nets. Although the slower speed has been found to be less damaging to ichthyoplankton specimens (Colton et al., 1980), the condition of the zooplankton specimens captured at the two tow speeds in this study was similar.

This study demonstrates that mean and median counts of common zooplankton taxa collected during 3.5-knot bongo tows are not significantly different from those collected during 1.5-knot tows. On the basis of these findings, we feel that zooplankton data collected at these two tow speeds can be used to compare or extend time series data at the regional level.

Acknowledgments

The authors are grateful to the Narragansett laboratory facility support staff that restored the vfin depressor to its original specifications.

Literature cited

- Anderson, J. T., and W. G. Warren.
1991. Comparison of catch rates among small and large bongo samplers for *Calanus finmarchicus* copepodite stages. *Can. J. Fish. Aquat. Sci.* 48:303–308.
- Beaugrand, G., P. C. Reid, F. Ibanez, J. A. Lindley, and M. Edwards.
2002. Reorganization of North Atlantic marine copepod biodiversity and climate. *Science* 296:1692–1694.
- Bray, J. R., and J. T. Curtis.
1957. An ordination of the upland forest communities of southern Wisconsin. *Ecol. Mono.* 27:325–349.
- Colton, J. B., J. R. Green, R. R. Byron, and J. L. Frisella.
1980. Bongo net retention rates as effected by towing speed and mesh size. *Can. J. Fish. Aquat. Sci.* 37: 606–623.
- Frank, K. T., B. Petrie, J. S. Choi, and W. C. Leggett.
2005. Trophic cascades in a formerly cod-dominated ecosystem. *Science* 308:1621–1623.
- Kane, J.
1993. Variability of zooplankton biomass and dominant species abundance on Georges Bank, 1977–1986. *Fish. Bull.* 91: 464–474.
- Licandro, P., F. Ibanez, and T. S. Zunini.
2001. Long term variations of zooplankton in the Ligurian Sea (Western Mediterranean). *Archo. Oceanogr. Limnol.* 22:159–166.
- Lough, R. G., G. R. Bolz, M. Pennington, and M. D. Grosslein.
1985. Larval abundance and mortality of Atlantic Herring (*Clupea harengus* L) spawned in the Georges Bank and Nantucket Shoals areas, 1971–78 seasons, in relation to spawning stock size. *J. Northw. Atl. Fish. Sci.* 6:21–35.
- O'Reilly, J. E., and C. Zetlin.
1998. Seasonal, horizontal, and vertical distribution of phytoplankton chlorophyll *a* in the Northeast U.S. continental shelf ecosystem. *NOAA Tech. Rep. NMFS* 139, 120 p.
- Pershing, A. J., C. H. Greene, J. W. Jossi, L. O'Brien, J. Brodziak, and B. Bailey.
2005. Interdecadal variability in the Gulf of Maine zooplankton community, with potential impacts on fish recruitment. *ICES J. Mar. Sci.* 62:1511–1523.
- Posgay, J. A., and R. R. Marak.
1980. The MARMAP bongo zooplankton samplers. *J. Northw. Atl. Fish. Sci.* 1:91–99.
- Tranter, D. J., and P. E. Smith.
1968. Filtration performance. *In* *Reviews on zooplankton sampling methods, Part I* (D. J. Tranter, ed.), p. 27–56. *Monogr. Oceanogr. Methodol.* 2, Zooplankton Sampling. UNESCO (United Nations Educational, Scientific, and Cultural Organization) Press, Paris.
- Wiebe, P. H., and W. R. Holland.
1968. Plankton patchiness: effects of repeated net tows. *Limnol. Oceanogr.* 13: 315–321.

Fishery Bulletin

Guidelines for authors

Content of manuscripts

Contributions published in *Fishery Bulletin* describe original research in marine fishery science, fishery engineering and economics, as well as the areas of marine environmental and ecological sciences (including modeling). Although all contributions are subject to peer review, responsibility for the contents of papers rests upon the authors and not upon the editor or publisher. *Submission of an article implies that the article is original and is not being considered for publication elsewhere.* Manuscripts must be written in English. Authors whose native language is not English are strongly advised to have their manuscripts checked by English-speaking colleagues prior to submission. **Articles** may range from relatively short contributions (10–15 typed, double-spaced pages, tables and figures not included) to extensive contributions (20–30 typed pages). **Notes** are reports of 5 to 10 pages without an abstract and describe methods or results not supported by a large body of data.

Manuscript preparation

Title page should include authors' full names and mailing addresses and the senior author's telephone, fax number, and e-mail address, and a list of key words to describe the contents of the manuscript. **Abstract** should be limited to 150 words (one-half typed page), state the main scope of the research, and emphasize the author's conclusions and relevant findings. Do not review the methods of the study or list the contents of the paper. Because abstracts are circulated by abstracting agencies, it is important that they represent the research clearly and concisely. **Text** must be typed in 12 point Times New Roman font throughout. A brief introduction should convey the broad significance of the paper; the remainder of the paper should be divided into the following sections: **Materials and methods**, **Results**, **Discussion (or Conclusions)**, and **Acknowledgments**. Headings within each section must be short, reflect a logical sequence, and follow the rules of multiple subdivision (i.e., there can be no subdivision without at least two items). The entire text should be intelligible to interdisciplinary readers; therefore, all acronyms, abbreviations, and technical terms should be written out in full the first time they are used. Include FAO common names for species in the list of keywords and in the introduction. Regional common names may be used throughout the rest of the text if they are different from FAO common names which can be found at <http://www.fishbase.org/search.html>. Follow the U.S. Government Printing Office Style Manual (1984 ed.) and the CBE Style Manual (6th ed.) for editorial style; for fish nomenclature follow the most current issue of the American Fisheries Society's Common

and Scientific Names of Fishes from the United States and Canada. Dates should be written as follows: 11 November 2000. Measurements should be expressed in metric units, e.g., 58 metric tons (t); if other units of measurement are used, please make this fact explicit to the reader. Write out the numbers zero through nine unless they form part of measurement units (e.g., nine fish but 9 mm).

Literature cited comprises published works and those accepted for publication in peer-reviewed literature (in press). Follow the name and year system for citation format in the "Literature cited" section. If there is a sequence of citations in the text, list chronologically: (Smith, 1932; Green, 1947; Smith and Jones, 1985). Abbreviations of serials should conform to abbreviations given in the Serial Sources for the BIOSIS Previews Database. Authors are responsible for the accuracy and completeness of all citations. Literature citation format: Author (last name, followed by first-name initials). Year. Title of report or manuscript. Abbreviated title of the series to which it belongs. Always include number of pages. Cite all software and special equipment or chemical solutions used in the study, not in a footnote but within parentheses in the text (e.g., SAS, vers. 6.03, SAS Inst., Inc., Cary, NC).

Tables and figures—general format

- Zeros should precede all decimal points for values less than one.
- Sample size, *n*, should be italicized.
- Capitalize the first letter of the first word in all labels within figures.
- Do not use overly large font sizes in maps and for units of measurements along axes in figures.
- Do not use bold fonts or bold lines in figures.
- Do not place outline rules around graphs.
- Do not use horizontal lines in graphs to indicate measurement units on axes.
- Use a comma in numbers of five digits or more (e.g. 13,000 but 3000).
- Maps should have a North arrow (or compass sign) and degrees latitude-longitude (e.g., 170°E)

Tables are often overused in scientific papers; it is seldom necessary or even desirable to present all the data associated with a study. Tables should not be excessive in size and must be cited in numerical order in the text. Headings should be short but ample enough to allow the table to be intelligible on its own. All unusual symbols must be explained in the table legend. Other incidental comments may be footnoted with italic footnote markers. Use asterisks to indicate probability in statistical data. Do not type table legends on a separate page; place them on the same page as the table data. *Do not submit tables in photo mode.*

Figures include line illustrations, photographs (or slides), and computer-generated graphs and must be cited in numerical order in the text. Graphics will aid in the comprehension of the text, but they should be limited to presenting patterns rather than raw data. Figures are costly to print and should be limited to six. Figures

must be labeled with author's name and number of figure. Avoid placing labels vertically (except on y-axis). Figure legends should explain all symbols and abbreviations and should be double-spaced on a separate page at the end of the manuscript. Please note that we do not print graphs in color.

**Failure to follow these guidelines and
to correspond with editors
in a timely manner will delay
publication of a manuscript.**

Copyright law does not apply to *Fishery Bulletin*, which falls within the public domain. However, if an author reproduces any part of an article from *Fishery Bulletin* in his or her work, reference to source is considered correct form (e.g., Source: Fish. Bull 97:105).

Reprints are available free of charge to the senior author (50 copies) and to his or her laboratory (50 copies).

Submission

The Scientific Editorial Office encourages authors to submit their manuscripts as a *single* PDF (preferred),

or Word (zipped) document by e-mail to Fishery.Bulletin@noaa.gov. Please use the subject heading "Fishery Bulletin manuscript submission." *Do not* send encrypted files. For further details on electronic submission, please contact the Scientific Editorial Office directly (see address below). Or you may send your manuscript on compact disc in one of the above formats along with four printed copies (one original plus three copies [stapled]) to the Scientific Editor, at the address shown below.

Dr. Adam Moles
Scientific Editor, *Fishery Bulletin*
Auke Bay Laboratories,
Alaska Fisheries Science Center
17109 Pt. Lena Loop Rd.
Juneau, AK 99801

Once the manuscript has been accepted for publication, you will be asked to submit a final software copy of your manuscript. When requested, the text and tables should be submitted in Word or Word Rich Text Format. Figures should be sent as PDF files, Windows metafiles, tiff files, or as EPS files. Send a copy of figures in original software if conversion to any of these formats yields a degraded version.





U.S. Department
of Commerce

Volume 105
Number 4
October 2007

Fishery Bulletin



**U.S. Department
of Commerce**

Carlos M. Gutierrez
Secretary

**National Oceanic
and Atmospheric
Administration**

Vice Admiral
Conrad C. Lautenbacher Jr.,
USN (ret.)

Under Secretary for
Oceans and Atmosphere

**National Marine
Fisheries Service**

William T. Hogarth
Assistant Administrator
for Fisheries



The *Fishery Bulletin* (ISSN 0090-0656) is published quarterly by the Scientific Publications Office, National Marine Fisheries Service, NOAA, 7600 Sand Point Way NE, BIN C15700, Seattle, WA 98115-0070. Periodicals postage is paid at Seattle, WA. POSTMASTER: Send address changes for subscriptions to *Fishery Bulletin*, Superintendent of Documents, Attn.: Chief, Mail List Branch, Mail Stop SSOM, Washington, DC 20402-9373.

Although the contents of this publication have not been copyrighted and may be reprinted entirely, reference to source is appreciated.

The Secretary of Commerce has determined that the publication of this periodical is necessary according to law for the transaction of public business of this Department. Use of funds for printing of this periodical has been approved by the Director of the Office of Management and Budget.

For sale by the Superintendent of Documents, U.S. Government Printing Office, Washington, DC 20402. Subscription price per year: \$36.00 domestic and \$50.40 foreign. Cost per single issue: \$21.00 domestic and \$29.40 foreign. See back for order form.

Fishery Bulletin

Scientific Editor

Adam Moles, Ph.D.

Associate Editor

Elizabeth Siddon

Ted Stevens Marine Research Institute
Auke Bay Laboratories
Alaska Fisheries Science Center
17109 Pt. Lena Loop Road
Juneau, Alaska 99801

Managing Editor

Sharyn Matriotti

National Marine Fisheries Service
Scientific Publications Office
7600 Sand Point Way NE, BIN C15700
Seattle, Washington 98115-0070

Editorial Committee

Jeffrey M. Leis	Australian Museum, Sydney, Australia
Thomas Shirley	Texas A&M University
David Somerton	National Marine Fisheries Service
Mark Terceiro	National Marine Fisheries Service

***Fishery Bulletin* web site: www.fishbull.noaa.gov**

The *Fishery Bulletin* carries original research reports and technical notes on investigations in fishery science, engineering, and economics. It began as the Bulletin of the United States Fish Commission in 1881; it became the Bulletin of the Bureau of Fisheries in 1904 and the *Fishery Bulletin* of the Fish and Wildlife Service in 1941. Separates were issued as documents through volume 46; the last document was No. 1103. Beginning with volume 47 in 1931 and continuing through volume 62 in 1963, each separate appeared as a numbered bulletin. A new system began in 1963 with volume 63 in which papers are bound together in a single issue of the bulletin. Beginning with volume 70, number 1, January 1972, the *Fishery Bulletin* became a periodical, issued quarterly. In this form, it is available by subscription from the Superintendent of Documents, U.S. Government Printing Office, Washington, DC 20402. It is also available free in limited numbers to libraries, research institutions, State and Federal agencies, and in exchange for other scientific publications.

U.S. Department
of Commerce
Seattle, Washington

Volume 105
Number 4
October 2007

Fishery Bulletin

Contents

Articles

- 447–456 Katakura, Seiji, Hisatoshi Ikeda, Akira Nishimura, Tsuneo Nishiyama, and Yasunori Sakurai
An allometric smoothing function to describe the relation between otolith and somatic growth over the lifespan of walleye pollock (*Theragra chalcogramma*)
- 457–469 Able, Kenneth W., Peter J. Clarke, R. Christopher Chambers, and David A. Witting
Transitions in the morphological features, habitat use, and diet of young-of-the-year goosefish (*Lophius americanus*)
- 470–484 Stewart, Ian J.
Defining plausible migration rates based on historical tagging data: a Bayesian mark-recapture model applied to English sole (*Parophrys vetulus*)
- 485–492 Magel, Christopher, Kirstin Wakefield, Nancy Targett, and Richard Brill
Activity in the pallial nerve of knobbed (*Busycan carica*) and channeled (*Busycotypus canaliculatum*) whelks recorded during exposure of the osphradium to odorant solutions
- 493–508 Eveson, J. Paige, Tom Polacheck, and Geoff M. Laslett
Incorporating fishery observer data into an integrated catch-at-age and multiyear tagging model for estimating mortality rates and abundance
- 509–526 Barlow, Jay, and Karin A. Forney
Abundance and population density of cetaceans in the California Current ecosystem

The conclusions and opinions expressed in *Fishery Bulletin* are solely those of the authors and do not represent the official position of the National Marine Fisheries Service (NOAA) or any other agency or institution.

The National Marine Fisheries Service (NMFS) does not approve, recommend, or endorse any proprietary product or proprietary material mentioned in this publication. No reference shall be made to NMFS, or to this publication furnished by NMFS, in any advertising or sales promotion which would indicate or imply that NMFS approves, recommends, or endorses any proprietary product or proprietary material mentioned herein, or which has as its purpose an intent to cause directly or indirectly the advertised product to be used or purchased because of this NMFS publication.

MBLWHOI Library
DEC 20 2007
WOODS HOLE
Massachusetts 02543

- 527–537 Tupper, Mark H.
Spillover of commercially valuable reef fishes from marine protected areas in Guam, Micronesia
- 538–547 Kilbansky, Nikolai, and Francis Juanes
Species-specific effects of four preservative treatments on oocytes and ovarian material of Atlantic cod (*Gadus morhua*), haddock (*Melanogrammus aeglefinus*), and American plaice (*Hippoglossoides platessoides*)
- 548–559 Miller, Todd W., and Richard D. Brodeur
Diets of and trophic relationships among dominant marine nekton within the northern California Current ecosystem

Companion article and note

- 560–570 Lauth, Robert R, Jared Guthridge, Dan Nichol, Scott W. McEntire, and Nicola Hillgruber
Timing and duration of mating and brooding periods of Atka mackerel (*Pleurogrammus monoptyerygius*) in the North Pacific Ocean
- 571–576 Lauth, Robert R. and Deborah M. Blood
Description of embryonic development of Atka mackerel (*Pleurogrammus monoptyerygius*)

Notes

- 577–581 Daniel K. Kimura
Using the empirical Bayes method to estimate and evaluate bycatch rates of seabirds from individual fishing vessels
- 582–587 DeVries, Douglas A.
No evidence of bias from fish behavior in the selectivity of size and sex of the protogynous red porgy (*Pagrus pagrus*, Sparidae) by hook-and-line gear
- 588 Acknowledgment of reviewers
- 590 List of titles
- 593 List of authors
- 595 Subject index
- 598 Guidelines for authors

Abstract—We propose a new equation to describe the relation between otolith length (OL) and somatic length (fork length [FL]) of fish for the entire lifespan of the fish. The equation was developed by applying a mathematical smoothing method based on an allometric equation with a constant term for walleye pollock (*Theragra chalcogramma*)—a species that shows an extended longevity (>20 years). The most appropriate equation for defining the relation between OL and FL was a four-phase allometric smoothing function with three inflection points. The inflection points correspond to the timing of settlement of walleye pollock, changes in sexual maturity, and direction of otolith growth. Allometric smoothing functions describing the relation between short otolith radius and FL, long otolith radius and FL, and FL and body weight were also developed. The proposed allometric smoothing functions cover the entire lifespan of walleye pollock. We term these equations “allometric smoothing functions for otolith and somatic growth over the lifespan of walleye pollock.”

An allometric smoothing function to describe the relation between otolith and somatic growth over the lifespan of walleye pollock (*Theragra chalcogramma*)

Seiji Katakura (contact author)¹

Hisatoshi Ikeda²

Akira Nishimura¹

Tsuneo Nishiyama³

Yasunori Sakurai²

Email address for S. Katakura: seijika@fra.affrc.go.jp

¹ Hokkaido National Fisheries Research Institute
116, Katsurakoi, Kushiro
Hokkaido 085-0802, Japan

² Graduate School of Fisheries Sciences
Hokkaido University, 3-1-1, Minato-cho, Hakodate
Hokkaido 041-8611, Japan

³ Department of Marine Sciences and Technology
Hokkaido Tokai University, 5-1-1-1, Minamisawa, Minami-ku
Sapporo, Hokkaido 005-8601, Japan

The power function $y = ax^b$, used as an allometric equation (Huxley, 1924), is a useful tool for growth analysis of organisms. Equations that describe the relation between fish otolith length (OL: distance between the tip of rostrum and tip of postrostrum) and somatic length (e.g., fork length; FL: distance between the tip of head and fork of tail fin) have been widely used in fishery biology and ecological studies to estimate somatic length at younger ages with back-calculation methods. These methods are based on linear equations, log-transformed allometric equations, and quadratic equations (reviewed by Francis, 1990). However, these previous equations do not adequately reflect the complex changes in growth over the lifetime of a fish, especially for long-lived species.

Walleye pollock (*Theragra chalcogramma* (Pallas)) is the most abundant fish in the Bering Sea, constitutes the majority of the commercial catches from this area (Wespestad, 1993), and is a long-lived species. The oldest recorded age for this species is 28 years (McFarlane and Beamish, 1990). Juvenile walleye pollock serve

as a substantial prey source for older walleye pollock, other fish species, marine mammals, and sea birds. Thus, the year-class strength and population dynamics of walleye pollock have a significant influence on the entire ecosystem (Springer, 1992; Hunt et al., 2002). Estimations of somatic length and growth analyses at particular ages or life stages are imperative for fishery biology and ecological studies of walleye pollock.

In studies of the growth of walleye pollock, the equation that describes the relation between OL and somatic length (i.e., fork length) (referred to as the “OL-FL equation” in this article) is required in order to reconstruct the size of walleye pollock from otoliths collected from the stomachs of predators. Frost and Lowry (1981) applied two linear equations, with an inflection point at 10 mm OL, corresponding to 220 mm FL, in a total size range of 60–570 mm FL. Nishimura and Yamada (1988) applied the log-transformed allometric equation of the three linear equations with log-transformed OL and total length (TL: distance between the tip of head and tip of tail fin; 4.6–

680 mm) to data for three stages: larval stage (4.6–14.0 mm TL), juvenile stage (11–96 mm TL), and young-adult stage (88–680 mm TL). Zeppelin et al. (2004) adapted a quadratic equation for a fish size range of 49–530 mm FL. These previous equations allowed researchers to characterize the growth patterns of walleye pollock by regression analysis (the least-squares method), but they have several shortcomings because somatic length is not estimated across the whole life span of the fish. First, the equations, each of which represents a different life stage, do not facilitate comprehension of the continuity of each life stage. The equations are fitted to each segment of the data separately by inflection points that are derived from empirical data or visually from the scatter plots. Second, the quadratic equation has limitation in the shape of its curve which does not show the inflection point. The complex growth patterns are not adequately reflected in the equation. Third, the least-squares method does not allow for the incorporation of increasing variance with increasing fish length. When the sample distribution is biased, the calculated equation is largely influenced by the range of fish lengths from the largest number of samples. Fourth, previous OL-FL equations were not considered objectively in the selection of an adequate equation. No attempt has been made to apply information criteria such as Akaike’s information criterion (AIC: Akaike, 1974), which is an operational way of trading off the complexity of an estimated equation against how well the equation fits the data.

To overcome these problems, we developed a new OL-FL equation for the whole lifespan of walleye pollock using a proposed allometric smoothing function to describe the relation between OL and FL. We also derived three distinctive allometric smoothing functions to establish the relationships between the short otolith radius (SOR: from core to the tip of rostrum) and FL, between the long otolith radius (LOR: from core to the tip of postrostrum) and FL, and between the FL and body weight (BW: wet body weight).

Materials and methods

General equations

The general equations in this analysis are linear equations (Eqs. 1 and 2), an allometric equation (Eq. 3), and an allometric equation with a constant term (Eq. 4):

$$y = ax \tag{1}$$

$$y = ax + c \tag{2}$$

$$y = ax^b \tag{3}$$

$$y = ax^b + c \tag{4}$$

where x = the independent variable;
 y = the dependent variable; and
 a , b , and c = parameters.

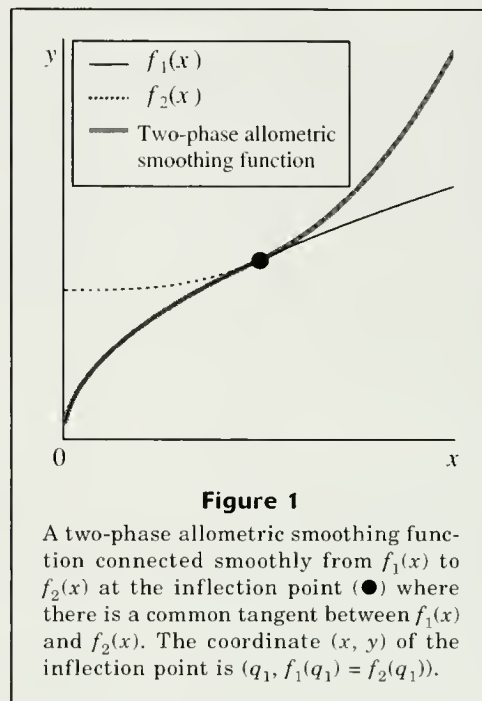


Figure 1
 A two-phase allometric smoothing function connected smoothly from $f_1(x)$ to $f_2(x)$ at the inflection point (●) where there is a common tangent between $f_1(x)$ and $f_2(x)$. The coordinate (x, y) of the inflection point is $(q_1, f_1(q_1) = f_2(q_1))$.

Allometric smoothing function

A new OL-FL equation was developed by using a mathematical smoothing method based on an allometric equation with a constant term. The assumption of the allometric smoothing function was to have a common tangent at the inflection point to reflect the variable allometric growth smoothly. A composite of two or more allometric smoothing functions was defined as follows:

$$\delta_i(x) = \begin{cases} 1 & (q_{i-1} \leq x \leq q_i) \\ 0 & (x < q_{i-1}, q_i < x) \end{cases} \tag{5}$$

$$f_i(x) = \delta_i(x)(a_i x^{b_i} + c_i),$$

where $\delta_i(x)$ = switch function;
 q_i = a value of x on the inflection point, here $q_0 = 0$;
 $f_i(x)$ = a number i of function; and
 a_i , b_i , and c_i = parameters for the function of i .

$f_i(x)$ is validated between the inflection points $(q_{i-1} \leq x \leq q_i)$ which depend on the $\delta_i(x)$.

We assumed that for the smooth integration of $f_i(x)$ and $f_{i+1}(x)$ (the function on the next order of i), both functions must pass through the inflection point $(x, y) = (q_i, f_i(q_i) = f_{i+1}(q_i))$ and have a common tangent at this point (Fig. 1). To satisfy the above conditions, the following two equations must be equal.

$$f_i(q_i) = f_{i+1}(q_i) \tag{6}$$

Table 1

The size ranges (in terms of length and weight) of walleye pollock (*Theragra chalcogramma*) examined in the Bering Sea during 1983–2002 to describe the relation between x (the independent variable) and y (the dependent variable). OL = otolith length; FL = fork length; SOR = short otolith radius; LOR = long otolith radius; and BW = body weight.

The variables (x [left below] and y [right below])	Range of x		Range of y		Number of samples (n)
	Minimum	Maximum	Minimum	Maximum	
OL (mm) and FL (mm)	2.27×10^{-2}	25.98	4.56	803	2354
SOR (mm) and FL (mm)	9.22×10^{-3}	11.80	4.56	803	1752
LOR (mm) and FL (mm)	1.22×10^{-2}	14.50	4.56	803	1704
FL (mm) and BW (g)	35.88	803	0.24	3014	2891

$$f'_i(q_i) = f'_{i+1}(q_i). \tag{7}$$

When Equation 5 is substituted for Equations 6 and 7, the following equations are obtained:

$$a_i q_i^{b_i} + c_i = a_{i+1} q_i^{b_{i+1}} + c_{i+1} \tag{8}$$

$$a_i b_i q_i^{b_i-1} = a_{i+1} b_{i+1} q_i^{b_{i+1}-1}. \tag{9}$$

Solving Equations 8 and 9 simultaneously yields

$$a_{i+1} = \frac{a_i b_i}{b_{i+1}} q_i^{b_i-b_{i+1}} \tag{10}$$

$$c_{i+1} = a_i q_i^{b_i} \left(1 - \frac{b_i}{b_{i+1}} \right) + c_i. \tag{11}$$

The functions of $f_i(x)$ and $f_{i+1}(x)$ can be smoothly connected at the inflection point if Equations 10 and 11 are equal. The formula of the allometric smoothing function y is shown as follows:

$$y = \sum_{i=1}^n f_i(x) = \sum_{i=1}^n \delta_i(x) (a_i x^{b_i} + c_i). \tag{12}$$

Fitting the OL-FL equations

The allometric smoothing function (Eq. 12) is fitted by using the maximum likelihood method. In the fitting, the sample distribution around the dependent variable was assumed to have a normal distribution. The estimated standard deviation (SD) for the dependent variable was used to calculate the weighted likelihood. The fitting procedure is shown as follows (see Appendix Table):

$$\hat{FL} = f_i(OL_j) = a_i OL_j^{b_i} + c_i + \varepsilon_j \quad (q_{i-1} \leq OL_j \leq q_i), \tag{13}$$

where \hat{FL}_j = the calculated FL for individual j ;
 OL_j = the measured OL of individual j ; and
 ε_j = the error for individual j .

Equation 13 is validated between the inflection points ($q_{i-1} \leq OL_j \leq q_i$).

The distribution of ε_j is assumed to have a normal distribution N (mean, variance) = $N(0, \hat{\sigma}_{FL_j}^2)$:

$$\hat{\sigma}_{FL_j} = dOL_j^e + f, \tag{14}$$

where $\hat{\sigma}_{FL_j}$ = the estimated SD of the FL of individual j ; and
 d , e , and f = parameters.

The variable $\hat{\sigma}_{FL_j}$ is assumed to fit the general equations (Eqs. 3 or 4).

To fit \hat{FL}_j to the general equations (Eqs. 1–3), the following procedures are used. For Equation 1, the parameters in Equation 13 are fixed as $b_i = 1$ and $c_i = 0$; for Equation 2, the parameter is fixed as $b_i = 1$; and for Equation 3, the parameter is fixed as $c_i = 0$.

A likelihood of measured FL is calculated by the following equations:

$$L_j = \frac{1}{\sqrt{2\pi\hat{\sigma}_{FL_j}}} \exp \left\{ -\frac{(FL_j - \hat{FL}_j)^2}{2\hat{\sigma}_{FL_j}^2} \right\} \tag{15}$$

and

$$LL = \sum_{j=1}^n \ln L_j, \tag{16}$$

where L_j = likelihood (the probability density) of FL_j ;
 FL_j = the measured FL of individual j ; and
 LL = a log-likelihood.

LL is maximized by changing the parameters.

Determination of the OL-FL equations

The equation with the minimum AIC was selected:

$$AIC = -2MLL + 2p \tag{17}$$

where MLL = the maximum LL and
 p = the number of parameters.

In the composite of two or more functions, a_i and c_i of $i \geq 2$ are calculated by Equations 10 and 11. Therefore, these parameters are not included in the number of parameters needed to calculate the AIC (see Appendix Table).

The upper and lower 95% confidence intervals (CI_j) of \hat{FL}_j were determined as follows:

$$CI_j = \hat{FL}_j \pm 1.96\hat{\sigma}_{FL_j}. \quad (18)$$

The equations for describing the relation between SOR and FL, LOR and FL, and FL and BW were calculated in the same way.

Application of equations to walleye pollock

Walleye pollock were collected and used as a model for long-lived species. The relevant biological data were collected, processed, and compiled from various cruise data conducted by Japanese and U.S. agencies at a total of 97 sampling stations in the Bering Sea (95 stations) and Chukchi Sea (northeastward extension of the Bering Sea; 2 stations) during 1983–2002 (Fig. 2).

In the central Bering Sea (Aleutian Basin), adult walleye pollock vary in age from 5 to >20 years (McFarlane and Beamish, 1990; Traynor et al., 1990). Young fish (0 to 4) are distributed on the continental shelf and slope and then migrate into the basin area beginning at age 5 (Traynor et al., 1990). In the present study, the samples of walleye pollock in the Bering Sea are presumed to have been collected from the same population of fish. Samples of juvenile walleye pollock at two discrete positions in the Chukchi Sea were also treated as originating from the Bering Sea. Larvae were sampled with a MOCNESS net, and juveniles and adults were captured with mid-water or bottom trawl nets. We measured the somatic length and BW of each fish and removed its otoliths (sagittae). For walleye pollock larger than 15 mm in somatic length, we measured FL, and for those smaller than 15 mm (with undeveloped fin rays), we measured TL. Difference in FL and TL was negligible in fish <15 mm; therefore TL is referred to as FL in the present analysis.

Specimens examined in the present study ranged from 4.56 mm to 803 mm FL. The number of samples used in the analysis of OL-FL equations is given in Table 1, as well as the size range of otolith measures and fish sizes. The approximate length of newly hatched larvae is 4.6 mm FL (=TL), 0.02 mm OL, and 0.01 mm SOR and LOR.

The relation between OL and FL was fitted to the general equations (Eqs. 1–4) and the allometric smoothing function (Eq. 12). The equations for describing the relation between SOR and FL, LOR and FL, and FL and BW were calculated in the same way.

Otolith processing

For measurement of SOR and LOR, the left or right otolith was selected and processed as a frontal section

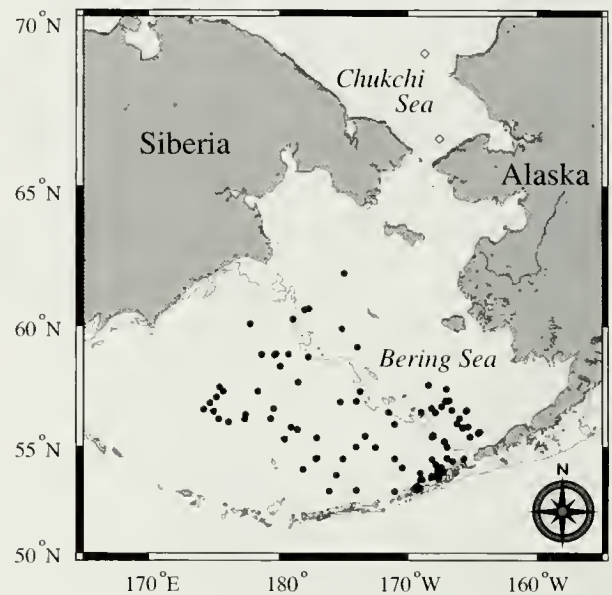


Figure 2

Map showing the sampling locations for walleye pollock (*Theragra chalcogramma*) in the present study. There were 97 total sampling stations: Bering Sea (●: 95 stations) and Chukchi Sea (○: 2 stations) in 1983–2002.

to reveal the perpendicular structure of the proximal surface, including the tips of rostrum and postrostrum, and core (Fig. 3A). The procedure for otolith processing followed that of Secor et al. (1992).

Larval and juvenile otoliths were embedded in epoxy resin adhesive (Epoxy bond quick 5; Konishi Co., Ltd., Osaka, Japan) on a glass slide, and OL was measured under a microscope (SMZ-U or Labophot-2A; Nikon Co., Tokyo, Japan) by using an image analysis system (ARGUS-10; Hamamatsu Photonics K. K. Co., Shizuoka, Japan). The otolith was then carefully polished with wet sandpaper (no. 1200) and lapping paper (12–0.3 μ) as preparation for making the frontal section (Fig. 3B).

For the frontal section of large otoliths of postjuvenile and adult fish, the otolith proximal surface was placed facing up, and OL was measured. Then, the otolith proximal surface was marked at three points: the tip of the rostrum, the tip of the postrostrum, and the core region on the central concave area. The otolith was embedded in epoxy resin (Epoxicure; Buehler Ltd., Lake Bluff, IL) on a hardened epoxy bed about 3 mm deep in a plastic mold. The hardened epoxy block containing the otolith was cut and trimmed by a micro cutter (MC-201; Maruto Instrument Co., Ltd., Tokyo, Japan) to a 3-mm-wide section that included the three marks. The trimmed sample was fixed on a slide glass with hot wax (Stick wax; Maruto Instrument Co., Ltd., Tokyo, Japan) and polished with wet sandpaper (no. 400–800) on a polishing machine (ML-101; Maruto Instrument Co., Ltd., Tokyo, Japan and SBT900; South Bay Technology Inc., San Clemente, CA). Polishing was continued until the core and tips of the rostrum and postrostrum appeared. The polishing was also made on the opposite side of the

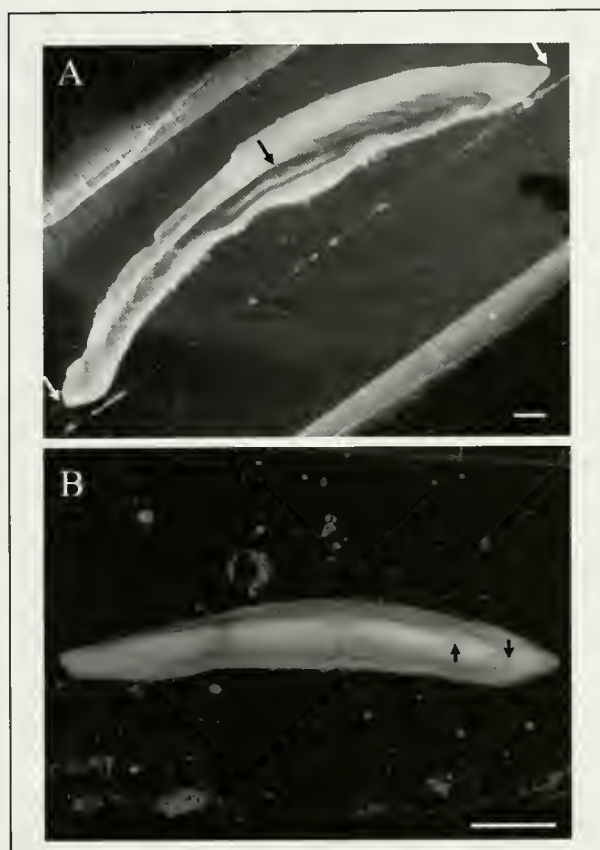


Figure 3

The frontal sections of an otolith from an adult walleye pollock (*Theragra chalcogramma*) (567 mm FL) viewed under transmitted light (A) and from a juvenile (138.8 mm FL) under reflected light (B). (A) The short otolith radius (SOR) was measured from the core (middle black arrow) to the tip of rostrum (right white arrow), and the long otolith radius (LOR) was measured from the core to the tip of postrostrum (left white arrow). The older annual rings are seen in the proximal surface region (the upper left side of the otolith, the clear white region). (B) The check-mark (left arrow) was observed inside of the first annual ring (right arrow). Scale bars = 1 mm

section. The section was finally polished by hand with wet sandpaper (no. 1200). The thickness of the polished frontal section (including the thickness of the wax) was 0.28 ± 0.07 mm (mean \pm SD, $n=50$). The OL in the frontal section shrank ($98.7 \pm 2.5\%$, $n=1775$) after the polishing; however the decrease was not analyzed in this study.

Results

Relation between otolith length (OL) and fork length (FL)

The most suitable equation to describe the OL (mm) and FL (mm) relationship chosen with the minimum AIC was

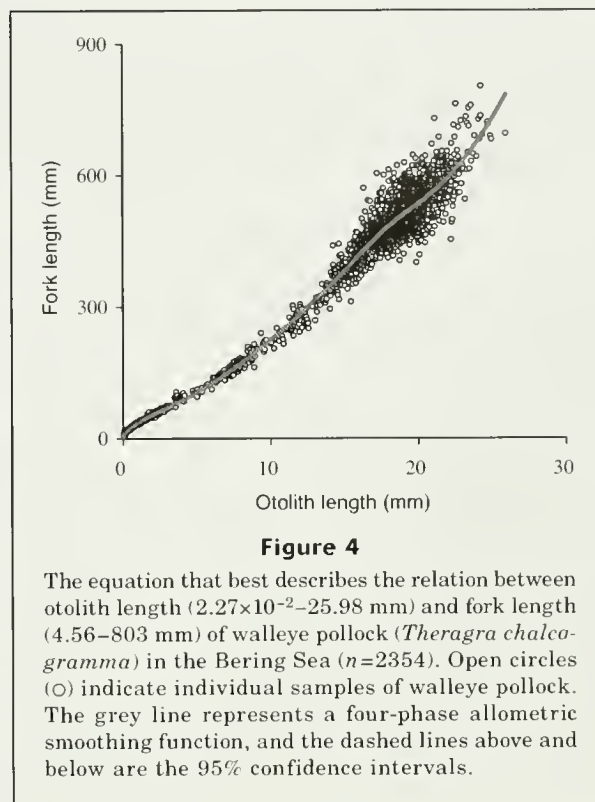


Figure 4

The equation that best describes the relation between otolith length (2.27×10^{-2} –25.98 mm) and fork length (4.56–803 mm) of walleye pollock (*Theragra chalcogramma*) in the Bering Sea ($n=2354$). Open circles (○) indicate individual samples of walleye pollock. The grey line represents a four-phase allometric smoothing function, and the dashed lines above and below are the 95% confidence intervals.

the four-phase allometric smoothing function (Fig. 4). The minimum AIC in the general equations was an allometric equation with a constant term (Eq. 4). In the AIC, all allometric smoothing functions produced lower estimates than all of the general equations. In the allometric smoothing functions, the AIC decreased with the number of allometric smoothing functions, which increased from two to four. However, the AIC in the five-allometric smoothing function was higher than that in the four-phase allometric smoothing function (Table 2). The relation between OL (mm) and $\hat{\sigma}_{FL}$ (mm) is given as follows:

$$FL = 31.55 OL^{0.67} + 4.05 \quad (0.00 < OL < 2.92) \quad (19.1)$$

$$FL = 5.64 OL^{1.51} + 40.11 \quad (2.92 \leq OL < 16.48) \quad (19.2)$$

$$FL = -26083.56 OL^{-1.49} + 831.85 \quad (16.48 \leq OL < 19.65) \quad (19.3)$$

$$FL = 1.28 \times 10^{-4} OL^{4.56} + 424.57 \quad (19.65 \leq OL) \quad (19.4)$$

$$\hat{\sigma}_{FL} = 0.41 OL^{1.52} + 1.80. \quad (20)$$

The coordinates (OL, FL) of the three inflection points were found at (2.92, 68.7), (16.48, 433.0), and (19.65, 525.0).

Relation between short otolith radius (SOR) and fork length (FL)

For the relation between SOR (mm) and FL (mm), we fitted the general equations (Eqs. 1–4) and the allometric

Table 2

Types of equations, range of otolith length (OL), inflection points, parameters, and Akaike's information criterion (AIC) for the equations used to describe the relation between OL (2.27×10^{-2} –25.98 mm) and fork length (FL: 4.56–803 mm) of walleye pollock (*Theragra chalcogramma*) in the Bering Sea ($n = 2354$). The minimum AIC was the four-phase allometric smoothing function. Estimated standard deviation of FL ($\hat{\sigma}_{FL} = d OL^e + f$).

Relational equation types	Range of OL		Inflection points		Parameter for equations			Parameter for $\hat{\sigma}_{FL}$			AIC
	Minimum	Maximum	OL	FL	a	b	c	d	e	f	
General equations											
$FL = a OL$	—	—	—	—	26.42	—	—	3.16	0.81	6.77	22,820
$FL = a OL + c$	—	—	—	—	25.94	—	7.02	5.66	0.68	1.27	22,573
$FL = a OL^b$	—	—	—	—	21.37	1.07	—	1.28	1.07	9.73	22,706
$FL = a OL^b + c$	—	—	—	—	15.18	1.18	15.14	0.74	1.31	4.61	22,016
Allometric smoothing functions											
$FL = a_1 OL^{b_1} + c_1$	0.00	2.25	—	—	32.41	0.64	3.34	0.41	1.54	1.76	21,194
$FL = a_2 OL^{b_2} + c_2$	2.25	—	2.25	57.7	8.33	1.37	32.40	—	—	—	—
$FL = a_1 OL^{b_1} + c_1$	0.00	2.87	—	—	31.59	0.67	4.02	0.40	1.53	1.80	21,089
$FL = a_2 OL^{b_2} + c_2$	2.87	15.58	2.87	68.0	5.81	1.50	39.56	—	—	—	—
$FL = a_3 OL^{b_3} + c_3$	15.58	—	15.58	400.7	3853.78	0.11	-4748.09	—	—	—	—
$FL = a_1 OL^{b_1} + c_1$	0.00	2.92	—	—	31.55	0.67	4.05	0.41	1.52	1.80	21,066
$FL = a_2 OL^{b_2} + c_2$	2.92	16.48	2.92	68.7	5.64	1.51	40.11	—	—	—	—
$FL = a_3 OL^{b_3} + c_3$	16.48	19.65	16.48	433.0	-26083.56	-1.49	831.85	—	—	—	—
$FL = a_4 OL^{b_4} + c_4$	19.65	—	19.65	525.0	1.28×10^{-4}	4.56	424.57	—	—	—	—
$FL = a_1 OL^{b_1} + c_1$	0.00	2.92	—	—	31.54	0.67	4.06	0.41	1.52	1.80	21,069
$FL = a_2 OL^{b_2} + c_2$	2.92	16.53	2.92	68.7	5.64	1.51	40.12	—	—	—	—
$FL = a_3 OL^{b_3} + c_3$	16.53	19.97	16.53	434.8	-35709.22	-1.63	800.80	—	—	—	—
$FL = a_4 OL^{b_4} + c_4$	19.97	20.42	19.97	532.0	9.28×10^{-17}	13.49	499.52	—	—	—	—
$FL = a_5 OL^{b_5} + c_5$	20.42	—	20.42	543.3	2.40×10^{-3}	3.68	382.98	—	—	—	—

smoothing function (Eq. 12). The minimum AIC was the four-phase allometric smoothing function. The relation between SOR (mm) and $\hat{\sigma}_{FL}$ (mm) was also shown as follows:

$$FL = 55.18 SOR^{0.61} + 2.51 \quad (0.00 < SOR < 1.00) \quad (21.1)$$

$$FL = 24.22 SOR^{1.39} + 33.47 \quad (1.00 \leq SOR < 7.55) \quad (21.2)$$

$$FL = -55349.12 SOR^{-2.78} + 639.86 \quad (7.55 \leq SOR < 8.96) \quad (21.3)$$

$$FL = 6.68 \times 10^{-4} SOR^{5.25} + 447.65 \quad (8.96 \leq SOR) \quad (21.4)$$

$$\hat{\sigma}_{FL} = 2.19 SOR^{1.37} + 1.91. \quad (22)$$

The coordinates (SOR, FL) of the three inflection points were found at (1.00, 57.8), (7.55, 437.3), and (8.96, 514.1).

Relation between long otolith radius (LOR) and fork length (FL)

In a similar way, the relationship between LOR (mm) and FL (mm) was derived, and the minimum AIC was a four-phase allometric smoothing function. The rela-

tion between LOR (mm) and $\hat{\sigma}_{FL}$ (mm) is also shown as follows:

$$FL = 48.98 LOR^{0.65} + 3.26 \quad (0.00 < LOR < 1.54) \quad (23.1)$$

$$FL = 14.84 LOR^{1.48} + 39.86 \quad (1.54 \leq LOR < 9.03) \quad (23.2)$$

$$FL = -16116.83 LOR^{-1.77} + 754.41 \quad (9.03 \leq LOR < 11.30) \quad (23.3)$$

$$FL = 1.34 \times 10^{-4} LOR^{5.44} + 464.28 \quad (11.30 \leq LOR) \quad (23.4)$$

$$\hat{\sigma}_{FL} = 1.77 LOR^{1.32} + 1.85. \quad (24)$$

The coordinates (LOR, FL) of the three inflection points were found at (1.54, 68.1), (9.03, 428.8), and (11.30, 535.6).

Relation between fork length (FL) and body weight (BW) (g)

The relation between FL (mm) and BW (g) was fitted to the general equations (Eqs. 3 and 4), the allometric

smoothing function (Eq. 12), and an allometric smoothing function without a constant term in the first function ($c_1=0$). The minimum AIC was the three-phase allometric smoothing function without c_1 . The relation between FL (mm) and $\hat{\sigma}_{BW}$ (g) is shown as follows:

$$BW = 2.01 \times 10^{-5} FL^{2.77} \quad (0.00 < FL < 70.0) \quad (25.1)$$

$$BW = 6.61 \times 10^{-6} FL^{3.02} + 0.21 \quad (70.0 \leq FL < 431.2) \quad (25.2)$$

$$BW = 4.17 \times 10^{-6} FL^{3.09} + 13.89 \quad (431.2 \leq FL) \quad (25.3)$$

$$\hat{\sigma}_{BW} = 1.06 \times 10^{-5} FL^{2.63} \quad (26)$$

The coordinates (FL, BW) of the two inflection points were seen at (70.0, 2.6) and (431.2, 586.2).

Discussion

The allometric smoothing function

The best equation to describe the relation between OL and FL in walleye pollock throughout the entire lifespan of the fish was depicted by a four-phase allometric smoothing function with three inflection points. In our preliminary analysis, a quadratic equation was applied for the OL and FL relationship, and the resulting AIC was 21,743. This value was smaller than that derived from general equations, but was higher than the value derived from any of our allometric smoothing functions (see Table 2). The general equations and the quadratic equation do not adequately reflect the variable otolith and somatic allometric growth during the whole lifespan of the species.

Equations relating OL to somatic length have been developed to represent complex growth curves. Bervian et al. (2006) used an allometric equation transformed from the logistic function for the OL-TL relationship in whitemouth croaker (*Micropogonias furnieri*). Imai et al. (2002) applied a Gompertz model to the relation between otolith height and standard length in cyprinid fish "Ukekuchi-ugui" (*Tribolodon nakamurai*). However, these two models have limitations in both the shape of the curve and the number of inflection points. If the species in the model, such as walleye pollock in this study, has more than two inflection points in the derived curve, these models cannot represent the allometric growth patterns adequately. Our present allometric smoothing function has no such limitation in the number of inflection points or the shape of curve between inflection points and responds appropriately to the growth pattern of the fish.

Our allometric smoothing function has the ability to satisfy both the needs for mathematical continuity (see Fig. 1) and objectivity in the selection of an equation (see Table 2) while allowing for biological events. The allometric smoothing function was developed by using a mathematical smoothing method based on an

allometric equation with a constant term. Among the smoothing methods available, the moving average, autoregression, and spline curve proved to be useful for fitting scatter sample plots, a type of plot that cannot be properly fitted in a single function. Nevertheless, the moving average requires that the modeler be subjective in determining the number of data points used to calculate the average. In contrast, the autoregression allows a measure of objectivity in selecting the equation; however steady growth conditions are assumed with this method. Finally, the spline curve is based on a multidimensional function developed by mathematical procedure where biological events were not taken into consideration.

Until recently, back-calculation models for individual fish growth have been developed to estimate past fish length and growth, under the assumption that fish growth is proportional to otolith growth (Francis, 1990). However, many studies have recognized that fish growth and otolith growth are uncoupled. "Growth rate effect" and "age effect" are two of the most important factors affecting uncoupling. The growth rate effect occurs when otoliths from slow growing fish are larger than those of fast growing fish, when these fish are compared at the same somatic length (Reznick, 1989; Campana, 1990; Secor and Dean, 1992). Adapting Campana's (1990) biological intercept method can reduce the error inherent in back-calculated somatic length from this growth-rate effect. Additionally, with the back-calculation model developed by Morita and Matsuishi (2001), the fact that age effect on otolith size increases continuously during nongrowth periods (Mugiya, 1990; Secor and Dean, 1992) can be taken into account. The inclusion of these growth and age effects of individual fish to our allometric smoothing function provides a more accurate analysis of growth at the individual level in the back-calculation model.

Application of the allometric smoothing function for walleye pollock

Our best equation to describe the relation between OL and FL was derived as a four-phase allometric smoothing function with three inflection points (Fig. 4). In Huxley's (1924) allometric equation ($y=ax^b$), relative growth rate was expressed by the relative growth coefficient (allometric coefficient, b). Our allometric smoothing function is based on the allometric equation with an added constant term ($y=ax^b + c$). The superscript b in our equation is not an allometric coefficient; it indicates the relative growth between x and y on the slope of the curve between inflection points.

The explicit changes in the shape of the curves and the appearance of inflection points in our equation imply that ecological and physiological changes are associated with unique aspects of life history of walleye pollock. In the first function (Eq. 19.1), somatic growth is slower than otolith growth, whereas in the second function (Eq. 19.2), somatic growth is faster than otolith growth. Concerning these contrasting

outcomes, previous findings indicate that possible ecological changes may have occurred at a particular size range, as evidenced by otolith characters such as the check-mark. Nishimura (1993) reported that 32% of age-1 walleye pollock caught in the Bering Sea revealed check-marks inside the first annual ring of the otolith and he concluded that the check-mark would have been formed at 40–80 mm FL (mode: 70 mm) at an age of 4 months. This check-mark was frequently detected in our samples (Fig. 3B). Similarly, in Funka Bay, Japan, 58% of age-1 walleye pollock had check-marks inside the first annual ring (Katakura et al., 2003). The settlement of juvenile walleye pollock from pelagic to benthic habitat began from 70 mm TL and was completed when the fish reached >85 mm TL in Funka Bay (Nakatani and Maeda, 1987). Our calculated FL at the first inflection point was 68.7 mm, which is approximately the same size as that when settlement begins. The check-mark on the otoliths of walleye pollock appears to occur, irrespective of differences in geographic features of inhabited waters. Victor (1982) suggested that the check-mark occurs as a settlement mark and indicates the occurrence of physiological changes or biological processes associated with settlement. Thus, we conclude that the first inflection point at a particular size in our allometric growth curve shows the adaptive response of walleye pollock to physiological and environmental changes at the time of settlement.

The state of $b < 0$ but $a < 0$ in the third function (Eq. 19.3) also implies that somatic growth is slower than otolith growth. The allometric coefficient between OL and somatic length drastically changes in association with sexual maturity (Bervian et al., 2006). The Bogoslof area in the Aleutian Basin is known as one of the main spawning grounds of walleye pollock in winter. In this area, fish length at maturity was 360–570 mm FL (mean 464 mm) in males and 370–610 mm FL (482 mm) in females (Traynor et al., 1990). The second inflection point that appeared at 433.0 mm FL in our study is situated within the size range of maturing fish. We assume that the fish length around the second inflection point corresponds to the timing of an energy shift from somatic growth to gonad development, and to corresponding changes that occur in the shifts of the allometric growth curve.

Both the third inflection point at 525.0 mm FL and the fourth function (Eq. 19.4) indicate faster somatic growth than otolith growth. Otolith growth persists despite the cessation of body growth (Mugiya, 1990; Secor and Dean, 1992); therefore, the otolith is also assumed to grow throughout the lifetime of walleye pollock (McFarlane and Beamish, 1990). Older annual rings appear on the ventral proximal surface region, as evidenced in the transverse section (McFarlane and Beamish, 1990), similar to those seen in the proximal surface region of the frontal section (Fig. 3A). The shape of the large otolith is an arched curve connecting the tip of the rostrum, core, and tip of the postrostrum. Thus, the third inflection point is con-

sidered to be closely related to the slow growth phase of otoliths, accompanying the change in the direction of growth in otoliths from length (between the tips of rostrum and postrostrum) to width (proximal surface region increasing), and an increase in the slope of the curve.

The best equations that describe the relation of SOR to FL, and LOR to FL were also represented by the four-phase allometric smoothing function with three inflection points (Eqs. 21.1–21.4 and 23.1–23.4). The characteristics of the allometric otolith and somatic growth patterns are similar, as found in the OL and FL relation. These relationships can be useful for the analysis of growth of juvenile walleye pollock from the back-calculation of adult otoliths. The measurements of the SOR or LOR of fish at young ages allow one to convert these measurements to FL values. Similarly, our equations allow the conversion of FL from any otolith measurement (OL, SOR, and LOR) into BW.

The resultant coordinates of the two inflection points at FL of 70.0 mm and 431.2 mm derived from our FL and BW relationship (Eqs. 25.1–25.3) were very close to the first (68.7 mm FL) and second (433.0 mm FL) inflection points that emerged in the OL and FL relationship (Eqs. 19.1–19.4). Because settlement and sexual maturity are distinct biological events in the life history of this fish, the timing of these events will be clearly demonstrated in allometric growth.

The condition factor (CF) of fish is generally calculated by a formula ($CF = 10^3 \times BW / FL^3$). However, our results indicate that the relation between FL and BW is not constant over the lifetime of walleye pollock, and probably for other fish species. In our equations, b increased as fish grew in association with life stages from $b_1 = 2.77$ to $b_2 = 3.02$ and $b_3 = 3.09$, and this inflation has potential implications for studies of fish growth.

The present equations can be applied to the reconstruction of size composition of fish from the remnant otoliths found in the digestive organs of predators. We expect that these reliable equations, with transformation of otolith measurement data into FL or BW values, are useful not only for fish growth analysis, but also for food habit and energetic studies (e.g., food conversion efficiency studies) because these studies rely substantially on the back-calculation method.

The samples of walleye pollock used in this study provided a range of fish lengths from 4.56 mm FL (=TL in larvae) to 803 mm FL. Newly hatched walleye pollock measure about 4.6 mm TL (Nishimura and Yamada, 1988), and the oldest fish reported from the Bering Sea was 28 years old and measured 530 mm FL (McFarlane and Beamish, 1990). Thus, the present data set can be regarded as including almost the entire size range of walleye pollock over the whole life span. Because the proposed allometric smoothing functions can be extensively applicable to all life stages of walleye pollock, we term these equations “allometric smoothing functions for otolith and somatic growth over the lifespan of walleye pollock.”

Acknowledgments

We thank J. R. Bower, K. Morita, N. J. Williamson, and the anonymous referees for invaluable advice on the manuscript, T. Yanagimoto, K. Mito, T. Honkalehto, S. de Blois, N. Tanimata, R. Nanbu, and O. Sakai for assistance with the sampling and measurements of fish samples. We also thank the scientists of the following agencies for the offer of biological data and otolith samples: National Research Institute of Far Seas Fisheries, Fisheries Research Agency, Japan; Hokkaido National Fisheries Research Institute, Fisheries Research Agency, Japan; Graduate School of Fisheries Sciences, Hokkaido University, Japan; and Alaska Fisheries Science Center, National Marine Fisheries Service, National Oceanic and Atmospheric Administration, USA. We also thank the crews of the RV *Kaiyo Maru*, TS *Oshoro Maru*, RV *Miller Freeman*, and chartered fishing vessels.

Literature cited

- Akaike, H.
1974. A new look at statistical model identification. IEEE (Institute of Electrical and Electronics Engineers, Inc.) Transactions on Automatic Control 19:716–723.
- Bervian, G., N. F. Fontoura, and M. Haimovici.
2006. Statistical model of variable allometric growth: otolith growth in *Micropogonias furnieri* (Actinopterygii, Sciaenidae). J. Fish Biol. 68:196–208.
- Campana, S. E.
1990. How reliable are growth back-calculations based on otoliths? Can. J. Fish. Aquat. Sci. 47:2219–2227.
- Francis, R. I. C. C.
1990. Back-calculation of fish length: a critical review. J. Fish Biol. 36:883–902.
- Frost, K. J., and L. F. Lowry.
1981. Trophic importance of some marine gadids in northern Alaska and their body-otolith size relationships. Fish. Bull. 79:187–192.
- Hunt, G. L., P. Stabeno, G. Walters, E. Sinclair, R. D. Brodeur, J. M. Napp, and N. A. Bond.
2002. Climate change and control of the southeastern Bering Sea pelagic ecosystem. Deep-Sea Res. II 49:5821–5853.
- Huxley, J. S.
1924. Constant differential growth-ratios and their significance. Nature 14:895–896.
- Imai, C., H. Sakai, K. Katsura, W. Honto, Y. Hida, and T. Takazawa.
2002. Growth model for the endangered cyprinid fish *Tribolodon nakamurai* based on otolith analyses. Fish. Sci. 68:843–848.
- Katakura, S., M. Ohta, M. Jin, and Y. Sakurai.
2003. Otolith-marking experiments of juvenile walleye pollock *Theragra chalcogramma* using oxytetracycline, alizarin complexone, and alizarin red S. Suisanzoshoku 51:327–335. [In Japanese with English summary.]
- McFarlane, G. A., and R. J. Beamish.
1990. An examination of age determination structures of walleye pollock (*Theragra chalcogramma*) from five stocks in the northeast Pacific Ocean. Int. North Pac. Fish. Comm. Bull. 50:37–56.
- Morita, K., and T. Matsuishi.
2001. A new model of growth back-calculation incorporating age effect based on otoliths. Can. J. Fish. Aquat. Sci. 58:1805–1811.
- Mugiya, Y.
1990. Long-term effects of hypophysectomy on the growth and calcification of otoliths and scales in the goldfish *Carassius auratus*. Zool. Sci. 7:273–279.
- Nakatani, T., and T. Maeda.
1987. Distribution and movement of walleye pollock larvae *Theragra chalcogramma* in Funka Bay and the adjacent waters, Hokkaido. Nippon Suisan Gakkaishi 53:1585–1591. [In Japanese with English summary.]
- Nishimura, A.
1993. Age determination of walleye pollock based on the otoliths (Review). In Present status and prospects of research on the biology and fisheries resources of walleye pollock and other gadid species in the waters around Hokkaido—special edition of the “Hokkaido Suketoudara Kenkyu Group” (Hokkaido Walleye Pollock Research Group) for the 25th anniversary (H. Yoshida, ed.), p.37–49. Sci. Rep. Hokkaido Fish. Exp. Stn. 42. Hokkaido Central Fisheries Experimental Station, Yoichi, Hokkaido, Japan. [In Japanese with English summary.]
- Nishimura, A., and J. Yamada.
1988. Geographical differences in early growth of walleye pollock *Theragra chalcogramma*, estimated by back-calculation of otolith daily growth increments. Mar. Biol. 97:459–465.
- Reznick, D.
1989. Slower growth results in larger otoliths: an experimental test with guppies (*Poecilia reticulata*). Can. J. Fish. Aquat. Sci. 46:108–112.
- Secor D. H., and J. M. Dean.
1992. Comparison of otolith-based back-calculation methods to determine individual growth histories of larval striped bass, *Morone saxatilis*. Can. J. Fish. Aquat. Sci. 49:1439–1454.
- Secor D. H., J. M. Dean, and E. H. Laban.
1992. Otolith removal and preparation for microstructural examination. In Otolith microstructure examination and analysis (D. K. Stevenson, and S. E. Campana, eds.), p. 19–57. Can. Spec. Publ. Fish. Aquat. Sci. 117.
- Springer, A. M.
1992. A review: walleye pollock in the North Pacific—how much difference do they really make? Fish. Oceanogr. 1:80–96.
- Traynor, J. J., W. A. Karp, T. M. Sample, M. Furusawa, T. Sasaki, K. Teshima, N. J. Williamson, and T. Yoshimura.
1990. Methodology and biological results from surveys of walleye pollock (*Theragra chalcogramma*) in the eastern Bering Sea and Aleutian Basin in 1988. Int. North Pac. Fish. Comm. Bull. 50:69–100.
- Victor, B. C.
1982. Daily otolith increments and recruitment in two coral-reef wrasses, *Thalassoma bifasciatum* and *Haliichoeres bivittatus*. Mar. Biol. 71:203–208.
- Wespestad, V. G.
1993. The status of Bering Sea pollock and effect of the “Donut Hole” fishery. Fisheries 18:18–25.
- Zeppelin, T. K., D. J. Tollit, K. A. Call, T. J. Orchard, and C. J. Gudmundson.
2004. Sizes of walleye pollock (*Theragra chalcogramma*) and Atka mackerel (*Pleurogrammus monopterygius*) consumed by the western stock of sea lions (*Eumetopias jubatus*) in Alaska from 1998 to 2000. Fish. Bull. 102: 509–521.

Abstract—This study was designed to improve our understanding of transitions in the early life history and the distribution, habitat use, and diets for young-of-the-year (YOY) goosefish (*Lophius americanus*) and, as a result, their role in northeastern U.S. continental shelf ecosystems. Pelagic juveniles (>12 to ca. 50 mm total length [TL]) were distributed over most portions of the continental shelf in the Middle Atlantic Bight, Georges Bank, and into the Gulf of Maine. Most individuals settled by 50–85 mm TL and reached approximately 60–120 mm TL by one year of age. Pelagic YOY fed on chaetognaths, hyperiid amphipods, calanoid copepods, and ostracods, and benthic YOY had a varied diet of fishes and benthic crustaceans. Goosefish are widely scattered on the continental shelf in the Middle Atlantic Bight during their early life history and once settled, are habitat generalists, and thus play a role in many continental shelf habitats.

Transitions in the morphological features, habitat use, and diet of young-of-the-year goosefish (*Lophius americanus*)

Kenneth W. Able (contact author)¹

Peter J. Clarke¹

R. Christopher Chambers²

David A. Witting³

Email address for K. W. Able: able@marine.rutgers.edu

¹ Rutgers University, Institute of Marine and Coastal Sciences
Marine Field Station
800 c/o 132 Great Bay Boulevard
Tuckerton, New Jersey 08087-2004

² National Oceanic and Atmospheric Administration (NOAA)
National Marine Fisheries Service
Northeast Fisheries Science Center (NEFSC)
James J. Howard Marine Science Laboratory
74 Magruder Road, Highlands, New Jersey 07732

³ NOAA/Montrose Settlements Restoration Program (MSRP)
501 West Ocean Blvd, Suite 4470
Long Beach, California 90802-4213

Our understanding of the life history and ecology of the goosefish (*Lophius americanus*) is incomplete. Much of what we believe to be true is drawn by analogy from European congeners (Caruso, 2002). This lack of knowledge is especially relevant given the development of an important fishery for goosefish since the 1980s (Caruso, 2002) and given the evidence that goosefish were overexploited in the 1990s (Almeida et al., 1995). Goosefish are found in the western North Atlantic from the Grand Banks off Newfoundland to the east coast of Florida (Wood, 1982; Caruso, 1983). Larval development, from hatching to completion of fin rays (up to 12 mm total length [TL]) has been described in detail (Everly, 2002). Little is known about pelagic and settled young-of-the-year (YOY) life stages and thus their role in continental shelf ecosystems. The smallest benthic individuals reported by Caruso (2002) were 76–114 mm TL ($n=3$).

Information on ages of YOY goosefish appears to be contradictory, but does indicate that sizes attained by the end of age 1 can be quite variable. Size of YOY goosefish by their

first fall has been variously reported as 64–76 mm TL (Steimle et al., 1999) and as 59 mm TL (Scott and Scott, 1988). However, larger sizes have been reported by Armstrong et al. (1992) for goosefish from southern New England–Mid-Atlantic Bight (average of 123–126 mm TL at age 1 for females and males) and by Hartley (1995) for goosefish from the Gulf of Maine (120–139 mm TL). Scott and Scott (1988) reported fish of 100–114 mm TL to be 2 years of age.

A portion of the National Marine Fisheries Service (NMFS) groundfish survey data and associated collections along the northeast coast of North America have been examined to determine some aspects of the life history and food habits for large juveniles and adult goosefish (Armstrong et al., 1992, 1996; Almeida et al., 1995; Hartley, 1995; Martinez, 1999). These studies focused on reproduction, age, and growth over short time periods and relied on data collected from geographically disparate sources. Recently, goosefish distribution and abundance in relation to depth and temperature were summarized from a large portion of the NMFS

database for groundfish surveys in the Gulf of Maine and the Middle Atlantic Bight (Steimle et al. 1999). Steimle et al. (1999) grouped all fish <43 cm TL into the juvenile category. As a result, several age classes were combined and there was no resolution for habitat of YOY goosefish. Prior descriptions of other aspects of the life history and ecology of YOY goosefish include associations of fish with depth and substrate type for Canadian waters (Jean, 1965; Scott, 1982), and with food habits for juveniles and adults (Sedberry, 1983; Armstrong et al., 1996).

The gaps in our knowledge about YOY goosefish, as articulated by Steimle et al. (1999), motivated the efforts reported here. Our objectives were 1) to describe more fully the morphological development of goosefish during the transition from pelagic larvae to benthic juveniles, 2) to estimate the timing, sizes, and ages of early life history events, and the growth rates of YOY goosefish, 3) to determine the distribution of pelagic and benthic juveniles in time and space, and 4) to identify the food habits and habitats of settled YOY goosefish.

Materials and methods

Two species of *Lophius* are found in the waters of the northwestern Atlantic, goosefish (*L. americanus* Valenciennes) and blackfin goosefish (*L. gastrophysus* Miranda-Ribeiro) (Caruso, 2002), and thus correct taxonomic identification is essential. Previously, *L. gastrophysus* was considered to be distributed from Brazil to Florida, and *L. americanus* was considered to range from Nova Scotia to Cape Hatteras (Bigelow and Schroeder, 1953; Scott and Scott, 1988) and to overlap occasionally between Florida and Cape Hatteras (Caruso, 1983). Preliminary data from the NMFS Commercial Cooperative Research goosefish survey indicate that *L. gastrophysus* has a much broader range, which is believed to extend into the Gulf of Maine (Richards¹). To ensure proper identification of our specimens, we used the diagnostic characters reported for these congeners (Caruso, 1983).

Morphological development

For some species of fish, ontogenetic state of an individual has proven to be a better metric of early life history events than has age (Policansky, 1983; Fuiman et al., 1998). For this reason, we used morphological and meristic data from pelagic and benthic individuals of *L. americanus* as a basis for describing early life history stages and for estimating size and age at settlement. We define planktonic juveniles as those individuals that have completed fin ray formation (>12 mm TL; Everly, 2002), but have not yet settled. Benthic juveniles include

all postsettlement YOY and juveniles of older age classes. A total of 88 fish (9.8–188 mm TL) were collected and examined (three fish per 5-mm size class) from a variety of sources (Table 1). These specimens were either collected and frozen, preserved in a solution of 70–95% ethanol or 5% formalin onboard the sampling vessel, or were obtained from museum collections. Shrinkage was determined by measuring fish upon capture and after preservation in ethanol or formalin. In total, 28 morphometric and meristic characters were examined (Table 2). These characters were based largely on those general character definitions provided by Hubbs and Lagler (1958). Modifications to these definitions in our study were due to the unique features possessed by *L. americanus*. Head length was measured from the anterior tip of the premaxillary bone to the gill opening. The length of the first dorsal spine, or illicium, was measured from its base to the base of the esca, the fleshy distal pendant of the illicium. The length of the esca was measured from its base to its distal end. An ocular micrometer was used for lengths ≤10 mm and a dial caliper was used for lengths >10 mm; all measurements were taken to 0.1-mm resolution.

Changes in body proportions that occurred during the pelagic-benthic transition were determined by examining the relation between each morphological character and total length. Such changes in allometry were detected by alteration in the slope of the line relating a focal character and total length (or any other reference character) on a log-log scale. When a fish is growing but not changing shape (i.e., exhibits isometric growth), the slope of this relationship is unity. When an individual or, as used here, an ontogenetic series of individuals, exhibits changes in shape with increasing total length, this means that the character(s) defining shape have changed in relation to total length. This transition in the degree of allometry will be reflected by a systematic deviation of the slope in the bivariate character plot. The magnitude of the slope before and after the transition, as well as the total length at which the transition occurred, were estimated by using piecewise regression (Toms and Lesperance, 2003).

Unlike measures of body proportions, other characters that change during the larval–juvenile–adult states are difficult to quantify. For example, the degree of pigmentation and the development of tubercles (Wiley and Collette, 1970) and cirri (fleshy flaps or tags, see Caruso, 2002) change gradually and in multiple dimensions during the progression from larval to juvenile phenotypes. These types of characters were scored as 0 or 1 for the larval state and juvenile–adult state, respectively. The juvenile–adult state was assumed to be represented by the largest size class that we examined (185–190 mm TL). For each of these characters, the median and standard error (SE) of size at transition to the juvenile/adult state were identified by fitting a cumulative normal distribution to the 0–1 scores by using a probit regression model. Because these estimates are based on data at the population level, our estimate of the mean size at transition was actually the size

¹ Richards, A. 2004. Personal commun. National Oceanic and Atmospheric Administration, National Marine Fisheries Service, Northeast Fisheries Science Center, 166 Water Street, Woods Hole, MA 02543-1026.

at which 50% of individuals expressed the juvenile-adult state of the character. The standard error of the median was converted to a 95% confidence interval, which indicates the sizes at which 5% to 95% of individuals express the adult state of the character.

Size and age at early life history events

Events during the early life history of goosfish were assessed by examination of sizes of fish at capture and by determination of ages and past events in the life of the fish as reflected in its otolith microstructure. Pelagic and benthic specimens (51–128 mm TL) used for daily otolith increment analysis were collected from a variety of sources (Table 1). An additional set of larvae hatched in the laboratory from egg veils collected in coastal waters off Long Beach Island, New Jersey, were examined for evidence of otolith microstructure that reflected hatching and the absorption of yolk. Preliminary examination of all three otoliths indicated that the lapilli were the easiest to interpret because of the clarity of increments and the lack of secondary growth structures. Hislop et al. (2001) came to a similar conclusion for *L. piscatorius*. Before otolith removal, individual fish were measured to the nearest 1 mm TL. Lapilli were removed, cleaned in bleach, and dried in 95% ethanol before they were mounted on glass slides by using a thermoplastic adhesive (Crystal Bond, Electron Microscopy Sciences, Hatfield, PA). Lapilli from fish >70 mm TL were ground and polished to the primordia on both surfaces with 1500 grit wet-dry sand paper with water as a lubricant, then finely polished with a 0.3-micron micropolish on a Buehler micropolishing cloth. Lapilli from fish <70 mm TL were polished to the primordia with the same materials but on the surface of the sulcus. Lapilli were cleaned with distilled water before they were immersed in oil for viewing. An analysis of

Table 1

Sources of data and specimens from field surveys used to determine aspects of the life history transitions, distribution, and diet of young-of-the-year goosfish (*Lophius americanus*). MAB = Middle Atlantic Bight (Cape Hatteras to Cape Cod); GB = Georges Bank; GOM = Gulf of Maine. NMFS = National Marine Fisheries Service; Mass DEP = Massachusetts Department of Environmental Protection; NJDEP = New Jersey Department of Environmental Protection; ACE = Army Corps of Engineers; VIMS = Virginia Institute of Marine Science.

Source	MAB	GB	GOM	Sampling gear	Sampling period	Sampling frequency	Range of sample depths (m)	Number of specimens (n)	Size range of specimens (mm total length)
NMFS	X	X	X	Bongo plankton net (1 m)	1977–87	6–8 cruises per year	11–1400	827	2.9–54.6
NMFS	X	X	X	Otter trawl (24 m)	1982–present	One cruise during fall, winter, and spring	9–365	3551	50–300
Michaels (2001)			X	Frame net	2000–2001	One cruise/year, generally in fall	35.5–818	66	20–210
NMFS	X	X	X	Commercial otter trawl	2001	Two simultaneous cruises	20–600	1093	25–300
NMFS	X	X	X	Scallop dredge	1982–2001	One cruise per year	21–144	9541	20–300
Mass DEP	X	X	X	Otter trawl (15 m)	1978–2001	Semi-annual sampling; spring and fall	6–82	490	40–300
NJDEP	X			Otter trawl (30 m)	1989–2000	Winter, spring, summer, fall	5–30	118	30–290
ACE	X			Bongo plankton net (1m)	1995–99	Bimonthly during summer	0–7	787	3.6–15.61
VIMS	X			Otter trawl (13.5 m)	1973–76	One cruise per year	35–818	587	53.37–299.37
NMFS	X			Otter trawl	2000	One cruise	20–330	98	180–300
Steves et al. (1999)	X			Beam trawl (2 m)	1996–97	Monthly cruises summer and fall; bimonthly winter and spring	20–90	19	72–233

Table 2

Summary of changes for 18 morphological characters in relation to total length of young-of-the-year goosefish (*Lophius americanus*). All estimates are derived from a linear piecewise regression. "Slope" refers to the estimate of the slope in the allometric equations applied to characters before and after the shift from juvenile to adult state. "Size" refers to the estimated size at which the shift occurs. Back-calculated lower and upper 95% confidence limits (L95 and U95, respectively) pertain to the estimated size at shift. R^2 (coefficient of what?) values and significance levels are for the entire piecewise regression model. (* $P < 0.05$, ** $P < 0.001$, *** $P < 0.0001$, ns not significant.)

Character	Slope		Size (mm)	L95	U95	R^2	
	Pre-shift	Post-shift					
Second dorsal ray (Illicium)	2.98	1.06	27.39	24.51	30.75	0.97	***
Esca length	1.61	0.8	84.10	50.91	138.38	0.80	*
Dorsal base length	1.41	0.95	20.11	14.44	28.50	0.98	**
Pectoral fin length	1.24	0.82	46.99	36.23	60.34	0.97	***
Snout length	1.2	0.95	42.56	24.05	75.19	0.97	**
Caudal peduncle depth	1.06	0.59	39.41	26.31	58.56	0.91	***
Head width	1	1.39	39.25	26.58	58.56	0.98	***
Pelvic fin length	0.93	0.24	48.42	41.26	57.40	0.92	***
Standard length	0.84	1.05	26.05	20.49	33.12	0.99	***
Orbit diameter	0.72	0.96	61.19	38.09	98.49	0.95	**
Head depth	0.49	1.1	60.95	34.81	107.77	0.79	***
Second dorsal ray length	0.45	1.06	84.10	67.36	104.58	0.86	***
Predorsal length	0.12	0.79	53.52	40.85	70.11	0.73	***
Caudal peduncle length	0.10	0.90	27.66	20.70	37.34	0.88	***
Head length	1.44	0.45	12.94	2.94	56.26	0.99	ns
Upper jaw length	1.23	1.33	39.25	7.88	197.16	0.98	ns
Third dorsal ray length	0.53	0.36	38.09	3.22	454.86	0.56	ns
Otolith size	0.33	0.71	17.97	10.5	30.91	0.97	**

evidence of allometric shifts in otolith dimensions for pelagic and settled YOY goosefish (8.6–285 mm TL, $n=60$) was conducted in the same manner as described above for body proportions.

Lapilli were viewed by transmitted light with an Olympus BH-2 compound microscope and Optimus 6.2 video imaging software (OPTIMUS Corp., Fort Collins, CO) at a magnification of 1250 \times . Distances from the primordium to each of multiple distinct marks (checks) on the otolith (e.g., at hatching, yolksac absorption, settlement, annulus formation) were taken along an axis to the dorsal edge. Increments (which are believed to be formed daily) were counted along the axis that exhibited the least ambiguous sequence of increments and greatest distance from the primordium to the outer edge. Increment counts and location of checks were determined twice on each otolith by a single observer.

Although we were reasonably confident of the age estimates derived with the above approach, we attempted to evaluate the precision and accuracy of our daily increment counts. A subset of otoliths ($n=20$) from fish (11–251 mm TL) were compared between the primary reader (PJC) and a second reader (K. Lang, NMFS, Woods Hole). The differences between readers in increment counts were small but increased with the size of

the otolith from 6.5% (the interval from the hatching check) to 8.8% (focus to yolk absorption), to 10.6% (focus to otolith edge).

Distribution and abundance

Pelagic and benthic goosefish were collected on the continental shelf in waters from the Gulf of Maine, Georges Bank, and the Middle Atlantic Bight (Table 1, Fig. 1A). Major sources of data for pelagic juveniles were the NMFS Hydroacoustic Survey 2000 to 2001, collections from the Harvard Museum of Comparative Zoology (MCZ), and the NMFS Marine Resources Monitoring, Assessment and Prediction Program (MARMAP) Survey spanning from 1977 to 1987 (Morse et al., 1987), as well as miscellaneous collections from throughout the study area. The primary source for recently settled benthic individuals ($n=6731$; 20–200 mm TL) was the historical scallop survey conducted by NMFS (Serchuk and Wigley, 1986).

Food habits and habitat

Fish used for analysis of food habitats in relation to settlement were collected from a variety of sources (Table 1). Immediately after capture, whole fish were either flash

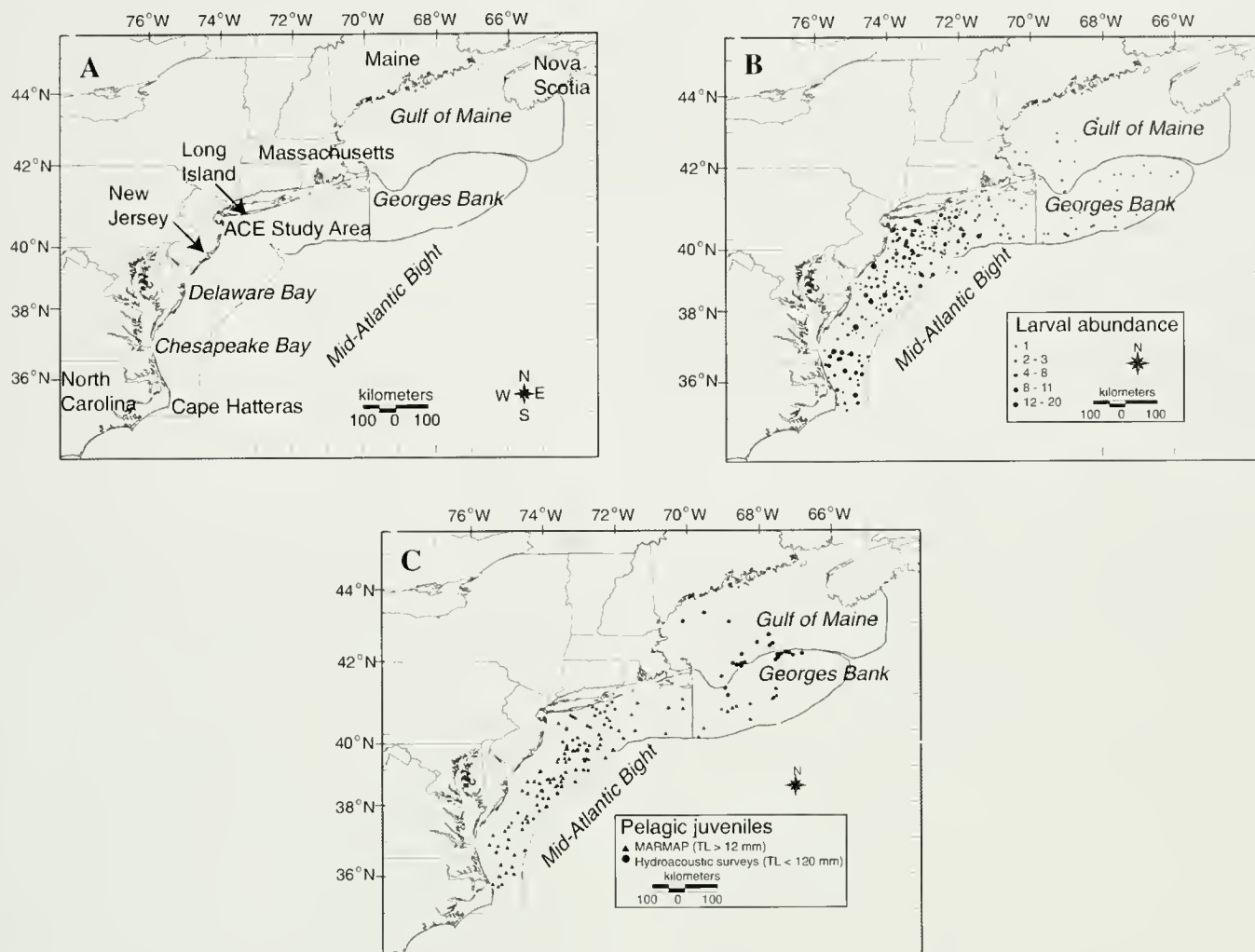


Figure 1

(A) Study area, including the Middle Atlantic Bight, Georges Bank, and Gulf of Maine. Study area boundaries are indicated by the light gray lines, which in most instances approximate the 200-m isobath. ACE = Army Corps of Engineers. (B) Distribution of larval (≤ 12 mm total length [TL]) goosefish (*Lophius americanus*) in the study area based on National Marine Fisheries Service and Marine Resources Monitoring, Assessment and Prediction sampling programs during the period from 1977 to 1987. Size of the symbol at each location is in proportion to the composite abundance (number of fish per location). (C) The distribution and abundance of pelagic juvenile (>12 to 130 mm TL) goosefish in the study area based on composite collections (Table 1).

frozen or preserved in ethanol to preserve stomach contents. In the laboratory, frozen fish were thawed, fish lengths (TL mm) were recorded, and stomachs were extracted and placed in 95% ethanol. A solution of rose bengal was later added to the stomach contents to aid in the identification of the contents. Upon examination, the proportion (by weight) of each prey category was determined according to the sieve-fractionation method of Carr and Adams (1972), by using sieves of three sizes (2000, 850, and 75 μ). All prey were identified to the lowest taxonomic level practical.

General inferences about the habitats of YOY goosefish were based on the location and depth of collection and the known habitat of items found in the stomach con-

tents of goosefish specimens. Special attention was given to whether the prey was of pelagic or benthic origin, if known, to help us identify presettlement (pelagic) and postsettlement (benthic) goosefish. This method was effective in identifying size at settlement in haddock (*Melanogrammus aeglefinus*) for Mahon and Neilson (1987).

Results and discussion

Morphological development

Goosefish undergo changes in morphological features and pigmentation during the transition from pelagic

Table 3

Summary of changes in seven qualitative characters of goosefish (*Lophius americanus*). Size at shift represents the total length (TL) at which 50% of the individuals in the sample achieved an adult state in the character. SE = standard error. Back-calculated lower (CL [lower]) and upper (CL [upper]) 95% confidence limits are shown.

Character	Size at shift (TL, mm, mean \pm SE)	CL (lower)	CL (upper)
Body pigmentation	68.64 \pm 11.46	46.18	91.10
Fin pigmentation	129.97 \pm 57.95	16.38	243.56
Tubercle development	78.77 \pm 20.11	39.35	118.20
Esca pigmentation	64.74 \pm 18.97	27.55	101.92
Illicium pigmentation	64.74 \pm 9.76	45.60	83.87
Lateral line pigmentation	71.67 \pm 16.13	40.06	103.28
Cirri	70.55 \pm 17.27	36.72	104.39

larvae to settled juveniles. The size range examined here (10–188 mm TL) brackets the interval from late larvae to juveniles. All but four of the 18 morphological characters displayed significant shifts in their relations to total length during the transition from pelagic juveniles (Table 2). These shifts occurred between 20.1 mm TL (dorsal base length) and 84.1 mm TL (esca length) resulting in a transformation from a laterally compressed, pelagic shape to a dorso-ventrally compressed, benthic shape. Eleven of the 14 morphological characters shifted from an allometric (body proportions changing) to isometric (body proportions not changing) growth pattern. Many of the allometric changes in characters that occurred during the pelagic phase were related to the flattening of the head and the reorganization of the dorsal fin, particularly the illicium. Five characters exhibited rapid growth (in relation to total length) during the pelagic phase. These characters were lengths of the dorsal fin base, the second dorsal ray (resulting in the development of the illicium and the esca), the snout (to accommodate the illicium), the esca, and the pectoral fin. Six characters exhibited slow growth (in relation to total length) during the pelagic phase to near isometric growth. These included a decrease in head depth, in orbit diameter, in caudal peduncle length, and in the length of the second dorsal ray. A dramatic reduction also occurred in the predorsal length as the anterior dorsal rays migrate towards the snout.

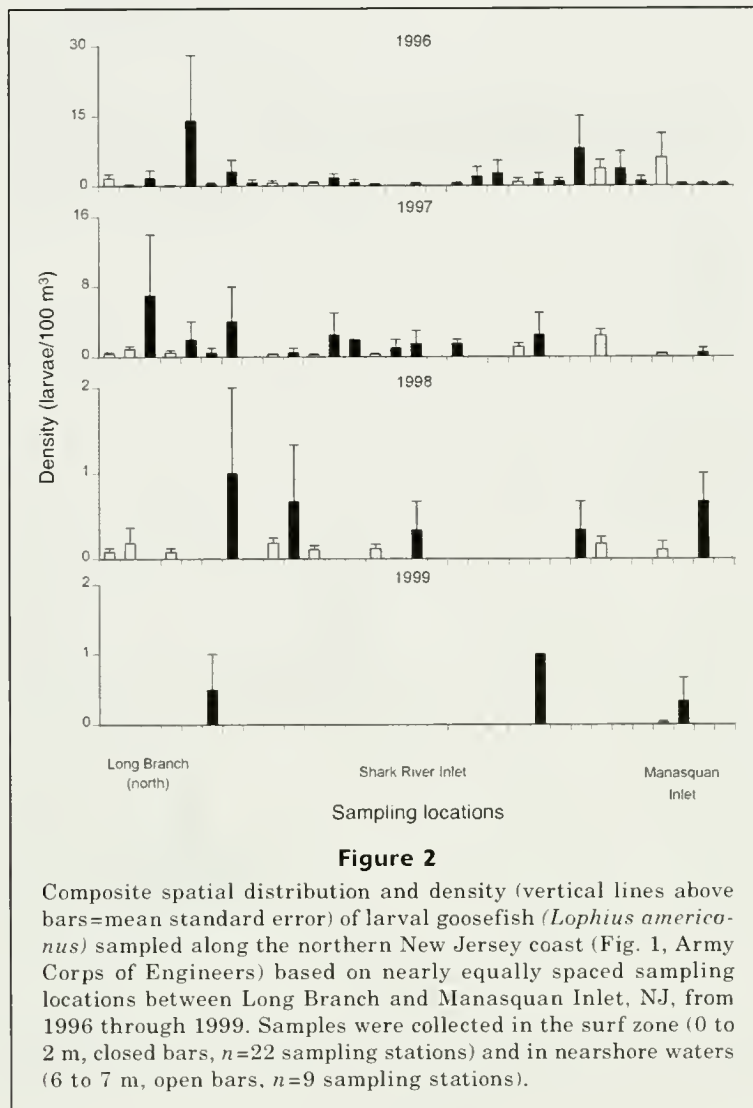
For the characters changes, better described as qualitative transitions (i.e., for changes in pigment, in the development of tubercle and cirri) and scored either as representing a larval (0) or juvenile-adult (1) state (Table 3), the start of such changes began at about 30 mm TL and ended at about 120 mm TL. The most dramatic changes occurred between 60 and 80 mm TL. The size range over which changes in fin pigmentation occurred was broader (16–243 mm TL). Although the timing of fin pigmentation may be intrinsically more variable than the other qualitative characters that were scored, the variability in fin pigmentation can also be an artifact of preservation technique.

As a result of these procedures, the changes in morphometric and character state traits (i.e., the changes in the shape from a lateral compressed pelagic larvae with long trailing pelvic fins to a dorsoventrally compressed head and body with much shorter pelvic fins as represented in some published illustrations) were quantified (Fahay, 1983; Caruso, 2002). These general changes in body proportions were found to be similar to those of *L. piscatorius* (Tåning, 1923; Dahlgreen, 1928) and *L. budegassa* (Stiasny, 1911; Bowman, 1919).

Several of the specimens evaluated for size-specific character transitions appeared to be at the pelagic juvenile stage (i.e., they were 21.6, 30.7, and 32.3 mm TL), although they were reportedly collected with benthic sampling gear. We suspect that these individuals were inadvertently collected in the water column because 1) they shared the same morphological and pigmentation characters as other pelagic individuals, 2) they were collected with gear that lacked opening and closing capability and thus the specimens could have been collected anywhere in the water column, and 3) the collection data indicated that in each instance the sampling gear spent more time in the water column than it did on the bottom. We therefore treated these individuals, in subsequent analyses, as pelagic juveniles.

Size and age at early life history events

The distribution of YOY goosefish was affected to a large degree by the timing and location of reproduction. Along much of the northeast coast of the United States, spawning occurs from spring through early fall (Wood, 1982; Hartley, 1995; Caruso, 2002), although exact details of spawning locations are lacking (Steimle et al., 1999). Collections during May through July 1996–99 in the surf zone (0–2 m, mean=0.66 individuals/100 m³) and nearshore (6–7 m, mean=0.68 individuals/100 m³) off northern New Jersey between Long Branch and Manasquan Inlet (Army Corps of Engineers [ACE] study area, Fig. 1A) showed densities of larval (3.6–15.6 mm TL, mean 7.6 mm) goosefish to be large in June (peak

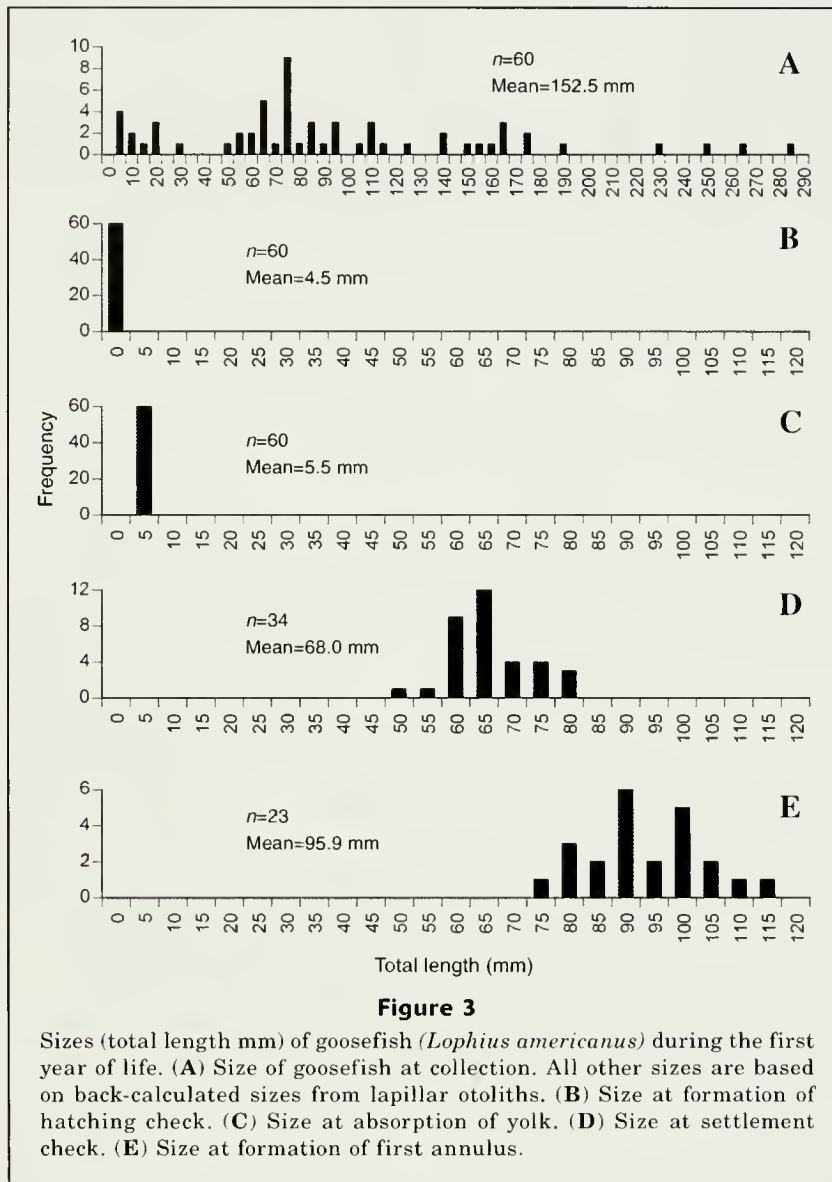


and July (Fig. 2). These collections of goosefish larvae were consistent with a May–June reproductive period estimated from gonadal condition of specimens collected in the area from Cape Hatteras to southern New England (Armstrong et al., 1992).

Our examination of lapillar otoliths provided estimates of the timing of several early life history events. There was good correspondence between the release of just-hatched larvae from the veil and the formation of a hatching check on the lapilli of laboratory-reared individuals. There were multiple microincrements before hatching (mean=5, range: 0–8). The variable number of microincrements prior to a “hatching check” on the lapillar otoliths may reflect the completion of hatching from the chorion and subsequent release of larvae from the egg veil. The completion of the yolk absorption appeared to correspond with a second check. The hatching and yolk absorption checks corresponded to similar checks in the otoliths of *L. piscatorius* (Hislop et al., 2001). Further, examination of otoliths from juvenile

goosefish caught in the Middle Atlantic Bight indicated good correspondence between the hatching check and back-calculated mean size at hatching (4.5 mm TL, Fig. 3) and hatching sizes (2.5–4.5 mm TL) (Caruso, 2002). Back-calculations to a hatching check in lapilli (see below) indicated that hatching in specimens collected in the Middle Atlantic Bight occurred from June to October and peaked around July. This prolonged period of spawning and hatching was in agreement with several other spawning and hatching estimates for goosefish in the area (Caruso, 2002). The check on lapillar otoliths corresponding to yolk absorption occurred after 9–26 (mean=18) increments (days) at reported sizes of 6–8 mm TL (Caruso, 2002; Everly, 2002).

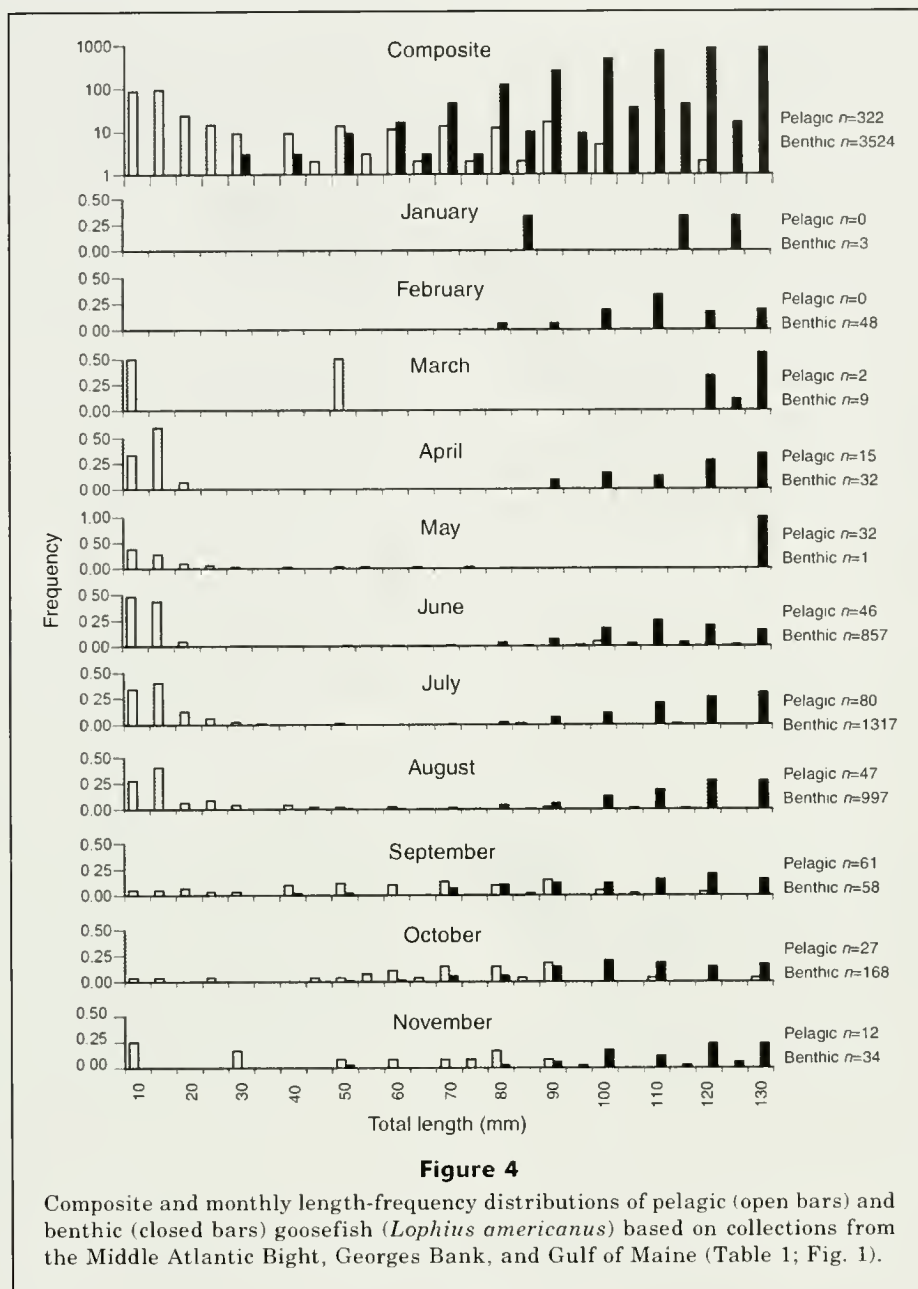
A third check (Fig. 3), which we believe corresponded with settlement, occurred in 57% of the lapilli examined. Back-calculated lengths at this check resulted in estimates of sizes at settlement from 52–83 (mean=68) mm TL and at ages 34–71 days after hatching. Individuals at these sizes were undergoing rapid changes in



relative body proportions as they approached or equaled the juvenile-adult condition (Table 2). Most of these changes occurred between 30 and 120 mm TL and were especially prominent in individuals of 60–80 mm TL. Settlement, as indicated by the length frequency of pelagic and benthic individuals, occurred over a relatively large range of sizes (Figs. 3 and 4). This interpretation may have been influenced by gear biases, the seasonal nature of the collections, and the ability of *Lophius* spp. to re-enter the water column, as occurs for *L. americanus* (Bigelow and Schroeder, 1953) and *L. piscatorius* (Hislop et al., 2000). The overlap in the magnitude of the size range of pelagic and benthic specimens was approximately 30–120 mm depending on the sampling technique (Figs. 3 and 4). Most of the individuals larger than 60 mm TL collected from May to November in the pelagic zone were collected with a mid-water trawl. The smallest benthic individuals (<60 mm TL) were collected

in June, July, and August as incidental captures in scallop dredges. Benthic individuals were also collected, at low levels, from September to November. Together, these observations suggest that settlement occurs at sizes of 30–83 mm TL and extends from June into November. The two smallest settled individuals previously reported were 64 and 76 mm (Connolly, 1921). Similarly small-size settled individuals were reported for individuals of *L. piscatorius* (Bowman, 1919).

The growth of YOY goosefish appears to be fast compared to that of other north temperate marine fishes. Using size at capture, as well as estimates of age, size, and life history event checks deduced from otoliths, we estimated growth rates of 1.4 and 1.3 mm/day for the pelagic and benthic YOY life stages, respectively. A marginal increment analysis of lapilli indicated that the first annulus forms at sizes of 70–119 (mean=95.8) mm TL (Fig. 2). This estimate of size at first annulus forma-



tion was consistent with estimates from whole goosefish otoliths made by resource scientists (Lang²).

Distribution and abundance

Spawning of goosefish, as inferred from the distribution of larvae (≤ 12 mm TL) is centered in the Middle Atlantic Bight (Fig. 1B). Far fewer larvae have been

collected on Georges Bank and in the Gulf of Maine relative to the Middle Atlantic Bight, although sampling effort was comparable between regions (Steimle et al., 1999). Local collections of goosefish larvae (range: 1.7–10.8 mm notochord length [NL]) along the northern New Jersey coast from 1996 to 1999 reveal their densities to be similar between the surf (mean=0.68 [± 0.19] individuals/100 m³) and nearshore (mean=0.66 [± 0.11] individuals/100 m³) habitats (Fig. 2). The abundance of larvae along the northern New Jersey coast was variable and there were no consistent patterns between years (Fig. 2). These local, inshore data show that the larvae inhabit waters shallower than those surveyed in the NMFS MARMAP program.

² Lang, K. 2004. Personal commun. National Oceanic and Atmospheric Administration, National Marine Fisheries Service, Northeast Fisheries Science Center, 166 Water Street, Woods Hole, MA 02543-1026.

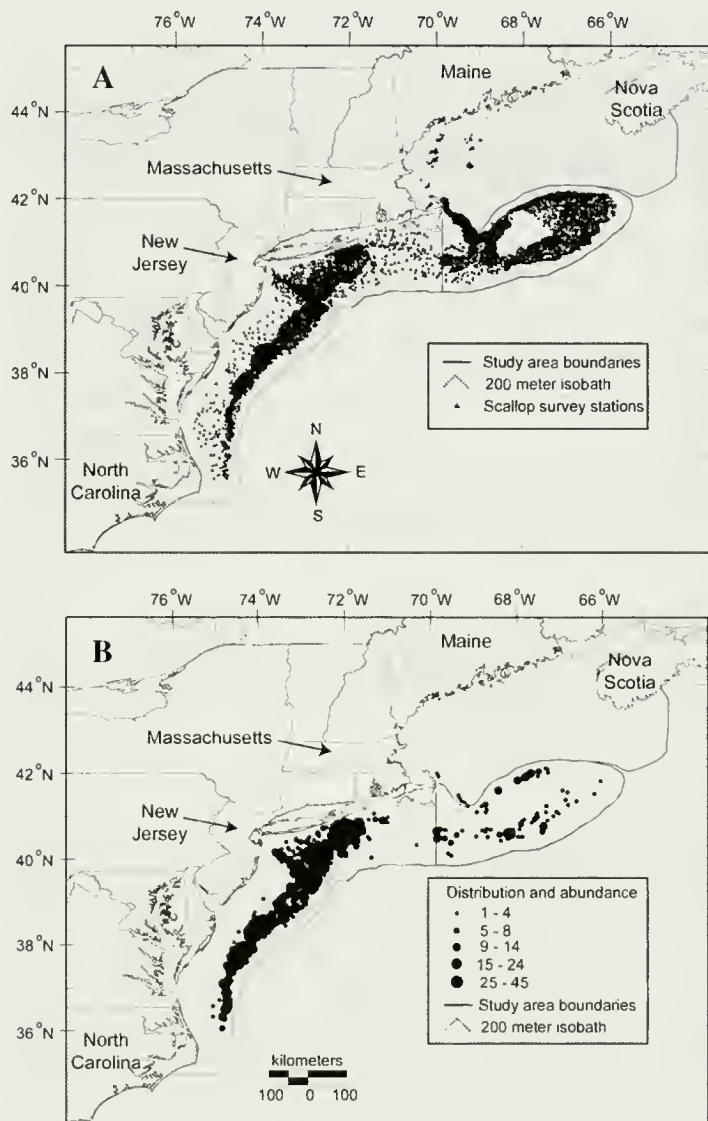


Figure 5

Distribution of (A) scallop dredge survey stations in the study area during 1982–2001 and (B) collections of benthic young-of-the-year (20–130 mm total length) goosefish (*Lophius americanus*) from these same surveys during the same period.

In the Middle Atlantic Bight, settlement may occur in a smaller area than that over which larvae are distributed. Even though the larvae (≤ 12 mm TL) were generally evenly distributed over the continental shelf up to and including the surf zone (Fig. 1B), pelagic juveniles (>12 –120 mm TL) were concentrated in the middle and outer portion of the shelf (Fig. 1C). An exception to this pattern was the collection of some pelagic juveniles in waters close to the coast of Long Island, NY. Although goosefish larvae were not abundant on Georges Bank and in the Gulf of Maine (Fig. 1B), pelagic juveniles were captured there in relatively large numbers along the northern edge of Georges Bank and the adjacent portion of the Gulf of Maine (Fig. 1C). In these latter

collections during NMFS hydroacoustic cruises from September through October 2000 and 2001, frame trawls were used to verify fish species. This sampling gear captured pelagic juveniles (50–130 mm TL) at depths ranging from the surface to 95 m within water depths of 65–191 m.

Most of the data and the majority (76%) of the benthic YOY (20–120 mm TL) goosefish specimens were collected from the NMFS scallop assessment surveys in the Middle Atlantic Bight and on Georges Bank during 1982 to 2001 (Fig. 5). The distribution of YOY goosefish reflects the boundaries of this survey. In the Middle Atlantic Bight, benthic YOY goosefish were collected on the central portion of the continental shelf from

approximately the Virginia–North Carolina state line north to eastern Long Island, NY, where they were found in shallow nearshore waters. The benthic YOY goosefish also were present up the Hudson Canyon shelf valley. Few benthic YOY goosefish were collected in waters off Rhode Island and southern Massachusetts—likely the result of lower sampling effort (Fig. 5). On Georges Bank, the benthic YOY goosefish were distributed around the perimeter of the bank but were not collected as frequently on the eastern end of the bank, even though these areas were well sampled. YOY goosefish were occasionally collected off the “elbow” of Cape Cod, but were found infrequently in the Gulf of Maine.

Benthic juveniles are probably more widely distributed over the continental shelf and on the upper slope than indicated by the sea scallop survey. The best evidence for their distribution in deeper waters has been from four seasonal cruises centered on the continental shelf and slope off Virginia covering depths to 3080 m (Wenner, 1978; Wenner³). Many juveniles were collected at depths from 75–900 m and the greatest density was found at 200–399 m depths. A large number of these individuals (30%) were <120 mm TL and the smallest specimen was 53.4 mm TL.

Food habits and habitats

The stomach contents of YOY goosefish in the Middle Atlantic Bight were diverse (Table 4). The dominant prey group in the stomach contents comprised fish (45.1% frequency of occurrence [FO]) and crustaceans (17.6% FO). The most numerous prey fish were gadids, *Ammodytes*, and bothid and pleuronectid flatfishes. Invertebrates were also consumed, including mollusks, chaetognaths, nematodes, nemerteans, trematodes, polychaetes, and crustaceans. This diversity of prey has been frequently reported for juveniles and adults of *L. americanus* (Sedberry, 1983; Armstrong et al., 1996; Bowman et al., 2000; Caruso, 2002) and other congeners, including *L. piscatorius* (Tsimenidis, 1980; Crozier, 1985; Laurenson and Priede, 2005) and *L. budegassa* (Tsimenidis, 1980). The greater occurrence of invertebrates in the stomachs of *L. americanus* in our study (67.2% FO, Table 4) than in prior studies (Sedberry, 1983; Armstrong et al., 1996) was probably due to our emphasis on examining smaller YOY fish.

The food habits of YOY goosefish varied with fish size; a shift to a larger proportion of fish in the diet occurred at larger sizes (Fig. 6, A and B). Although invertebrates were common in the diet of all YOY examined, they occurred in 100% of the stomach contents at sizes smaller than approximately 50 mm TL and to a variable extent in most larger YOY fish. The vast majority of stomach contents, on the basis of weight (Table 4), were composed of fish in larger goosefish. Prior studies

Table 4

Prey items of young-of-the-year and small juvenile (age 1+) goosefish (*Lophius americanus*). Gut contents were expressed by percentage frequency of occurrence (% FO) across all specimens examined and average percent total weight in individual stomachs. Determination of prey habitat (P=pelagic, B=benthic, I=indeterminate, potentially both benthic and pelagic habitat) was based on knowledge of the life history of prey.

Prey	Habitat	% FO	% Total weight
Osteichthyes	B, I	79.4	86
Invertebrates		67.2	8.8
Molluska	I, B	1.6	7.2
Chaetognatha	P	3.1	<0.1
Nematoda			
(free-living)	B	3.1	<0.1
(unspecified)	I	1.5	<0.1
Nemertea	B	4.6	<0.1
Trematoda	I	7.6	<0.1
Polychaeta	B	3.8	<0.1
Hirudinea	I	0.8	<0.1
Crustacea	B, P	17.6	0.3
Other	I	58	5.2

are equivocal on ontogenetic change in diet. Armstrong et al. (1996) reported smaller (<200 mm TL) individuals to have a higher proportion of invertebrates in their diet than we observed. Sedberry (1983) found the diets of all size classes of goosefish, including the two smallest (<100 and 101–200 mm), were dominated by fishes. Our results clarify the sizes at which this change to piscivory occurs (i.e., >50 mm TL).

The food habits also changed as a result of the transition from presettlement (pelagic) to postsettlement (benthic) habitats (Fig. 6, C and D). Individuals that were captured in the water column (<50 mm TL) had pelagic taxa such as chaetognaths, hyperiid amphipods, calanoid copepods, and ostracods in their stomachs. The dominance of pelagic prey was apparent whether prey were quantified as percent weight or percent frequency of occurrence. The stomach contents of larger individuals (60–280 mm TL, YOY, and small juveniles) were dominated by benthic prey when expressed as percent frequency of occurrence. The shift to benthic prey was not as obvious, however, when prey were expressed as percent weight. This was due to a large percentage of prey items that could not be assigned unequivocally to either benthic or pelagic habitats. The benthic prey comprised a variety of fishes and crustaceans including amphipods, cumaceans, mysids, shrimps, nematodes, nemerteans, and polychaetes (Table 4). The location of capture of some prey, such as that of small gadids and squid, was considered indeterminate because these prey could have been consumed by goosefish in either pelagic or benthic habitats.

³ Wenner, C. 2004. Personal commun. Marine Resources Research Institute South Carolina Department of Natural Resources, P.O. Box 12559, Charleston, SC 29422.

Conclusions

It appears that goosfish in the Middle Atlantic Bight spend ~5–10 weeks in the plankton as larvae and pelagic juveniles. As they change from pelagic larvae and juveniles to benthic juveniles (ca. 30–85 mm TL from June to November), they undergo major changes in body

shape, pigmentation, and diet. Some of these life history changes are reflected in the microstructure of lapillar otoliths. Overall, changes in these suites of characteristics are most evident before and during settlement. Most of the events in the early life history of goosfish appear to occur without dependency on water depth or location across the continental shelf. Larvae, pelagic juveniles, and benthic juveniles tend to be most abundant on the mid to outer continental shelf, but they are also widely distributed inshore, indicating that they are habitat generalists.

Acknowledgments

L. Despres, A. Richards, M. Jech, V. Nordhal, P. Berrien, and V. Guida provided access to distribution and abundance data. K. Lang assisted with otolith interpretation. Others who provided access to data include J. Musick, B. Cowen, M. Sullivan, B. Steves, L. Van Guelpen, C. Wenner, K. Hartel, D. Clarke, and M. Burlas. This research was supported in part by the National Marine Fisheries Service (NMFS)—Rutgers University Cooperative Marine Education and Research (CMER) program, by NMFS Northeast Fisheries Science Center, and by the Institute for Marine and Coastal Sciences (IMCS), Rutgers University. This is Institute of Marine and Coastal Sciences contribution number 2007-2.

Literature cited

- Almeida, F. P., D. L. Hartley, and J. Burnett.
1995. Length-weight relationships and sexual maturity of goosfish off the northeast coast of the United States. *N. Am. J. Fish. Manag.* 15:14–25.
- Armstrong, M. P., J. A. Musick, and J. A. Colvocoresses.
1992. Age, growth, and reproduction of the goosfish *Lophius americanus* (Pisces: Lophiiformes). *Fish. Bull.* 90:217–230.
1996. Food and ontogenetic shifts in feeding of the goosfish, *Lophius americanus*. *J. Northwest Atl. Fish. Sci.* 18:99–103.
- Bigelow, H. B., and W. C. Schroeder.
1953. *Fishes of the Gulf of Maine*. U.S. Fish Wildl. Serv., Fish. Bull. 53, 577 p.
- Bowman, A.
1919. The eggs and larvae of the angler (*Lophius piscatorius*) in Scottish waters. *Fish Board Scotland Rep. Sci. Invest.* 1919:(2):21–23.
- Bowman, R. E., C. E. Stillwell, W. L. Michaels, and M. D. Grosslein.
2000. Food of Northwest Atlantic fishes and two common species of squid. U.S. Dep. Commer., NOAA Tech. Memo. NMFS-F/NE-155, 138 p.
- Carr, W. E., and C. A. Adams.
1972. Food habits of juvenile marine fishes: evidence of the cleaning habit in the leath-

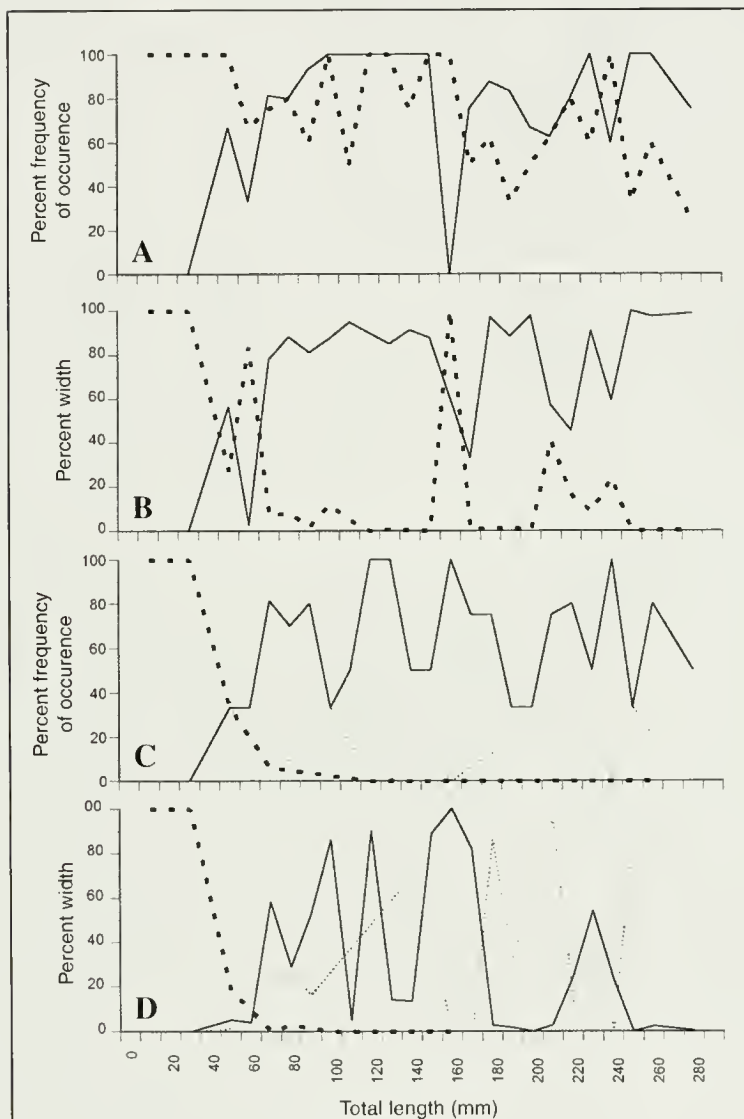


Figure 6

Change in diet (A, B) and habitat (C, D) of young-of-the-year goosfish (*Lophius americanus*) with increasing total length (TL). Diet changed from mostly invertebrates (dotted line) to mostly fish (solid line), whether expressed as percent frequency of occurrence (A) or percent weight in stomach contents (B). Habitat, determined from stomach contents, changed as a function of goosfish sizes (TL). Prey in stomach was expressed as frequency of occurrence (C) and percent weight (D). Prey habitats, based on knowledge of prey life history, were classified as either benthic (solid line), pelagic (large dotted line), or indeterminate (small dotted line).

- erjacket, *Oligoplites saurus*, and the spottail pinfish, *Diplodus holbrooki*. Fish. Bull. 70:1111–1120.
- Caruso, J. H.
1983. The systematics and distribution of the lophiid anglerfishes: II. Revisions of the genera *Lophiomus* and *Lophius*. Copeia 1983:11–30.
2002. The goosefishes or monkfishes. Family Lophidae. In Bigelow and Schroeder's Fishes of the Gulf of Maine (B. B. Collette, and G. Klein-MacPhee, eds.), 561 p. Smithsonian Institution Press, Washington, D.C.
- Connolly, C. J.
1921. On the development of the angler (*Lophius piscatorius* L.). Contrib. Can. Biol. 7:115–124.
- Crozier, W. W.
1985. Observations on the food and feeding of the angler-fish, *Lophius piscatorius* L., in the northern Irish Sea. J. Fish Biol. 27:655–665.
- Dahlgreen, U.
1928. The habits and life history of *Lophius*, the angler fish. Nat. Hist. 28:18–32.
- Everly, A. W.
2002. Stages of development of the goosfish, *Lophius americanus*, and comments on the phylogenetic significance of the development of the luring apparatus in Lophiiformes. Environ. Biol. Fishes 64:393–417.
- Fahay, M. P.
1983. Guide to the early stages of marine fishes occurring in the western North Atlantic Ocean, Cape Hatteras to the southern Scotian Shelf. J. Northwest Atl. Fish. Sci. 4:1–423.
- Fuiman L., K. R. Poling, and D. M. Higgs.
1998. Quantifying developmental progress for comparative studies of larval fishes. Copeia 3:602–611.
- Hartley, D. L.
1995. The population biology of the goosfish, *Lophius americanus*, in the Gulf of Maine. M.S. thesis, 142 p. Univ. of Mass., Amherst, MA.
- Hislop, J. R., A. Gallego, M. R. Heath, F. M. Kennedy, S. A. Reeves, and P. J. Wright.
2001. A synthesis of the early life history of the anglerfish, *Lophius piscatorius* (Linnaeus, 1758) in northern British waters. ICES J. Mar. Sci. 58:70–86.
- Hislop, J. R. G., J. C. Holst, and D. Skagen.
2000. Near-surface captures of post-juvenile anglerfish in the North-east Atlantic—an unsolved mystery. J. Fish Biol. 57:1083–1087.
- Hubbs, C. L., and K. F. Lagler.
1958. Fishes of the Great Lakes region, 332 p. Univ. Michigan Press, Ann Arbor, MI.
- Jean, Y.
1965. Seasonal distribution of monkfish along the Canadian Atlantic mainland. J. Fish. Res. Board Can. 22:621–624.
- Laurenson, C. H., and I. G. Priede.
2005. The diet and trophic ecology of anglerfish *Lophius piscatorius* at the Shetland Islands, U.K. J. Mar. Biol. Assn. U.K. 85:419–424.
- Mahon, R., and J. D. Neilson.
1987. Diet changes in Scotian Shelf haddock during the pelagic and demersal phases of the first year of life. Mar. Ecol. Prog. Ser. 37:123–130.
- Martinez, C. M.
1999. The reproductive biology of goosfish, *Lophius americanus*. M.S. thesis, 78 p. Univ. Rhode Island, Naragansett, RI.
- Michaels, W. L. (ed.)
2001. Report on the third Northwest Atlantic herring acoustic workshop, Univ. Maine, Darling Marine Center, Walpole, ME, March 13–14, 2001. U.S. Dep. Commer., NOAA Tech. Memo. NMFS-NE-166, 18 p.
- Morse, W. W., M. P. Fahay, and W. G. Smith.
1987. MARMAP surveys of the continental shelf from Cape Hatteras, North Carolina to Cape Sable, Nova Scotia (1977–1984). Atlas no. 2: Annual distribution patterns of fish larvae. U.S. Dep. Commer., NOAA Tech. Memo. NMFS-NEFSC, 215 p.
- Policansky, D.
1983. Size, age and demography of metamorphosis and sexual maturation in fishes. Amer. Zool. 23:57.63.
- Scott, J. S.
1982. Selection of bottom type by groundfishes of the Scotian Shelf. Can. J. Fish. Aquat. Sci. 39:943–947.
- Scott, W. B., and M. G. Scott.
1988. Atlantic fishes of Canada. Can. Bull. Fish. Aquat. Sci. 219, 731 p.
- Sedberry, G. R.
1983. Food habits and trophic relationships of a community of fishes on the outer continental shelf. NOAA Tech. Rep. NMFS-SSRF-773, 56 p.
- Serchuk, F. M., and S. E. Wigley.
1986. Evaluation of USA and Canadian research vessel surveys for sea scallops (*Placopecten magellanicus*) on Georges Bank. J. Northwest Atl. Fish. Sci. 7:1–13.
- Steimle, F. W., W. W. Morse, and D. L. Johnson.
1999. Essential fish habitat source document: Goosfish, *Lophius americanus*, life history and habitat characteristics. NOAA Tech. Memo. NMFS-NE-127, 31 p.
- Steves, B. P., R. K. Cowen, and M. H. Malchoff.
1999. Settlement and nursery habits for demersal fishes on the continental shelf of the New York Bight. Fish. Bull. 98: 167–188.
- Stiasny, G.
1911. Regarding certain postlarval development stages of *Lophius piscatorius* L. Arbeit. Zool. Inst. Vienna 19:54–74. [In German.]
- Täning, Å. V.
1923. *Lophius*. Danish Oceanogr. Exped., 1908–10, Rep. no. 7, vol. 2 (Biol.), A 10, 30 p.
- Toms, J. D., and M. L. Lesperance
2003. Piecewise regression: a tool for identifying ecological thresholds. Ecology 84:2034–2041.
- Tsimenidis, N. H.
1980. Contribution to the study of the angler-fishes *Lophius budegassa* Spinola, 1807 and *L. piscatorius* L. 1758 in Greek seas. Spec. Publ. Inst. Oceanogr. Fish. Res. Athens 4, 190 p. [In Greek.]
- Wenner, C. A.
1978. Making a living on the continental slope and in the deep-sea: life history of some dominant fishes of the Norfolk Canyon area. Ph.D. diss., 294 p. College of William and Mary, Williamsburg, VA.
- Wiley, M. L., and B. B. Collette.
1970. Breeding tubercles and contact organs in fishes: their occurrence, structure, and significance. Bull. Am. Mus. Nat. Hist. 143(3):145–216.
- Wood, P. W., Jr.
1982. Goosfish, *Lophius americanus*. In Fish distribution (M. D. Grosslein, and T. R. Azarovitz, eds.), p. 67–70. MESA New York Bight Atlas Monograph 15. N.Y. Sea Grant Institute, Albany, NY.

Abstract—A generalized Bayesian population dynamics model was developed for analysis of historical mark-recapture studies. The Bayesian approach builds upon existing maximum likelihood methods and is useful when substantial uncertainties exist in the data or little information is available about auxiliary parameters such as tag loss and reporting rates. Movement rates are obtained through Markov-chain Monte-Carlo (MCMC) simulation, which are suitable for use as input in subsequent stock assessment analysis. The mark-recapture model was applied to English sole (*Parophrys vetulus*) off the west coast of the United States and Canada and migration rates were estimated to be 2% per month to the north and 4% per month to the south. These posterior parameter distributions and the Bayesian framework for comparing hypotheses can guide fishery scientists in structuring the spatial and temporal complexity of future analyses of this kind. This approach could be easily generalized for application to other species and more data-rich fishery analyses.

Defining plausible migration rates based on historical tagging data: a Bayesian mark-recapture model applied to English sole (*Parophrys vetulus*)

Ian J. Stewart

Email address: Ian.Stewart@noaa.gov

National Oceanic & Atmospheric Administration
National Marine Fisheries Service
Northwest Fisheries Science Center
2725 Montlake Boulevard East (F/NWC4)
Seattle, Washington 98112-2097

Mark-recapture data are used to estimate growth parameters, mortality rates, and population size (Hilborn and Walters, 1992; Quinn and Deriso, 1999). However, researchers are often interested in home range, site-fidelity, or migration rates which are important quantities for management and the design or evaluation of marine protected areas. The standard approach with mark-recapture data is to use an integrated model linking the underlying dynamics of the tagged population with an observation model describing the predicted recoveries and a likelihood function relating observations with model predictions (Hilborn, 1990). This integrated method has been applied to many fisheries, ranging from those for sablefish (*Anoplopoma fimbria*; Heifetz and Fujioka, 1991) to those for yellowfin tuna (*Thunnus albacares*; Hampton and Fournier, 2001).

Requirements of the integrated method include extensive tag recovery, data on fishing effort, auxiliary information on tag loss, as well as reporting rates in order to adequately estimate movement rates and other parameters (Punt et al., 2000). Analysis often benefits from fixing some model parameters at reasonable values based on external analysis or expert opinion. However, the values selected for these parameters can represent a substantial source of uncertainty in the estimates of movement rates because these parameters are poorly known for many historical tagging projects.

Bayesian methods start with prior distributions for the parameters of interest (information available before the analysis), and integrate over the joint posterior distribution of all model parameters, capturing parameter uncertainty as well as the correlation structure among these parameters. The Bayesian approach provides a logical alternative to likelihood methods when the researcher is faced with substantial uncertainty in the data and input parameters and has a desire for a probabilistic interpretation of the results (Punt and Hilborn, 1997).

One way in which uncertainty and auxiliary information about migration rates could be included in stock assessments is through the use of informative priors based on Bayesian analysis of mark-recapture data. Priors specifically applicable to west coast groundfish stock assessments have been derived for survey catchability (Millar and Methot, 2002), the steepness of the stock-recruit function (Dorn, 2002), the relationship between catch per unit of effort (CPUE) and abundance (Harley et al., 2001), and for other studies currently underway. Researchers in other regions have aggregated historical tagging information for commercially important species, such as north Atlantic cod (*Gadus morhua*; Robichaud and Rose, 2004). However, in the northeast Pacific there are many groundfish tagging studies that have never been analyzed simultaneously or used in stock assessments.

Stock assessments of west coast flatfish (and other groundfish species) have been based on one of two assumptions about latitudinal movement: no movement at all (multiple isolated stocks) or complete mixing (single stock models). In a Bayesian context, these two opposite assumptions fix the magnitude of movement rates before analysis and therefore can be considered highly informative priors. The goal of this study was to provide a generalized method with which to develop informative priors on movement rates based on quantitative analysis of historical tagging data, thereby adding a third choice of prior for use in stock assessments.

Materials and methods

Model development

A model very similar to those used in other mark-recapture studies (e.g., Hilborn, 1990; Hampton and Fournier, 2001) was developed to predict the number of tags returned from multiple tag-release events (tags released in one spatial area over a short period of time; hereafter referred to as a data set) by projecting each population forward in time. Predicted returns are tracked by month and for each spatial area. The predicted number of tags present (\hat{N}) in each data set (d), month (t), and area (i) are given by

$$\hat{N}_{d,t,i} = \sum_j \left(\hat{N}_{d,t-1,j} P_{t,j \rightarrow i} \right) e^{-\frac{(F_d + M + \Omega)}{12}}, \quad (1)$$

where F_d = the average fishing mortality rate for each data set;

M = the average natural mortality rate; and

Ω = the instantaneous rate of tag loss (ongoing "attrition" due to fouling or mechanical failure; often referred to as "type-2 tag loss" in traditional terms; Beverton and Holt, 1957).

The subscript j denotes all possible source areas, and the proportion of individuals moving from each area to another in any month is given by the matrix P_t . The P_t matrix (area \times area for month t) includes nonzero values in only the first off-diagonals, and a variable number of parameters within each diagonal depending on the movement hypothesis to be explored. Instantaneous rates are divided by 12 because they are applied on a monthly basis. Predicted numbers in the first month are the reported tag releases (alternately, type-1 tag loss, those tags that are shed immediately after tagging, could be included by multiplying the initial releases by $1 - \text{type-1 tag-loss rate}$). The predicted recoveries (\hat{R}) by data set, month, and area are then

$$\hat{R}_{d,t,i} = \phi \hat{N}_{d,t,i} \left(\frac{F_d}{F_d + M + \Omega} \right) \left(1 - e^{-\frac{(F_d + M + \Omega)}{12}} \right), \quad (2)$$

where ϕ = the reporting rate of captured tags during the time period over which tag recoveries occurred. Given these dynamics, the tagged population and predicted recoveries for all data sets available may be projected forward simultaneously.

The major departure from previous models is the use of a single average fishing mortality rate for each data set (an approach that reflects a lack of direct effort or of fishing mortality information). If only a single data set is analyzed in this manner, it is clear that any heterogeneity in fishing mortality over time or space could result in substantially biased estimates of movement rates. However, if multiple tagging events are analyzed simultaneously, and there is no consistent relationship between location of tag releases and areas of increased fishing mortality, this potential source of bias may be reduced. Were information on the spatial and temporal variability in fishing mortality available, it would be simple (and recommended) to extend the notation further to either input mortality rates directly into the analysis or to estimate them from relative effort.

Variability in observed recoveries is caused by many factors, including schooling behavior, heterogeneous distribution of fishing effort, tag loss or tag reporting over time and space, and by the stochastic nature of very low recovery rates. Because of the many potential sources of extra-model error, a likelihood function that allows for substantial variation among observations is desired. The negative binomial likelihood is the logical choice for this type of tagging data (e.g., Cormack and Skalski, 1992; Hampton and Fournier, 2001). If each tag-release group is assumed to be independent, the full likelihood (L) of the observed recoveries (R) is given by

$$L(R_{d,t,i} | \hat{R}_{d,t,i}, k) = \prod_d \prod_t \prod_i \frac{(k + R_{d,t,i} - 1)!}{(R_{d,t,i})!(k-1)!} \left(1 + \frac{k}{\hat{R}_{d,t,i}} \right)^{-R_{d,t,i}} \left(\frac{\hat{R}_{d,t,i}}{k} + 1 \right)^{-k}, \quad (3)$$

where \hat{R} = the predicted recoveries in a data set, month, and area; and

k = the overdispersion (variance) parameter.

The negative binomial asymptotically approaches the Poisson distribution as the value of the overdispersion parameter moves to infinity (Bishop et al., 1988).

A common problem with historical data is that only summarized reports are available for analysis. Where tag recoveries have been aggregated across time or space, the model predictions and the original observations are no longer on an equivalent scale. This problem is easily dealt with by aggregating the predicted recoveries to match the observed recoveries, while still maintaining the same predictive model structure. However, this method creates different types of comparisons within the likelihood (monthly recoveries compared to

monthly recoveries vs. annual recoveries compared to annual recoveries). The method and notation above is therefore extended to estimate a separate overdispersion parameter (k) for each type of data aggregation included in the analysis. The likelihood equation (Eq. 3) becomes

$$L(R_{c,d,l} | \hat{R}_{c,d,l}, k_c) = \prod_c \prod_d \prod_l \frac{(k_c + R_{c,d,l} - 1)!}{(R_{c,d,l})! (k_c - 1)!} \left(1 + \frac{k_c}{\hat{R}_{c,d,l}}\right)^{-R_{c,d,l}} \left(\frac{\hat{R}_{c,d,l}}{k_c} + 1\right)^{-k_c} \quad (4)$$

where the likelihood component notation remains the same, but the subscripts are revised to include the following: data aggregation type (c), data set (d), and time-space combination (l , identical within each c ; e.g., month-area or year-area depending on the level of data aggregation).

Data sources

English sole (*Parophrys vetulus*) was selected for analysis because of the large amount of tagging data available and the commercial importance of the species. English sole are widely distributed from southern California to Alaska (Hart, 1973) and are frequently captured by the bottom-trawl fisheries of both the United States and Canada. Many English sole tagging programs have been conducted by both U.S. and Canadian scientists since the 1930s. These have included

releases off the coast of British Columbia (Ketchen, 1956; Forrester, 1969), Washington (Pattie, 1969), Oregon (Harry, 1956), and California (Jow, 1969). Additional tagging within Puget Sound (Menasveta, 1958; Day, 1976) and the Strait of Georgia have focused specifically on population dynamics within these waters. Most tagging data reported between 1946 and 1979 were available only through unpublished reports from the Research Board of Canada, Oregon Department of Fish and Wildlife, and the Washington Department of Fisheries. In total, 44 tagging events (defined as tags released in one area during a one-month period) resulted in the release of 57,839 tags of which 9988 (17.3 %) were recovered. The primary objective of most of these studies was to determine the amount of migration (as a percentage of the total population) that occurred among areas with the highest abundance of English sole (e.g., Harry, 1956).

Tag recoveries have been most frequently reported for the historical Pacific Marine Fisheries Commission (PMFC) areas; these areas were therefore the logical (and only) spatial context in which to analyze the results. To reduce the latitudinal range of the largest PMFC areas, PMFC area 1A was divided into two sub-areas (north and south of Point Conception) and PMFC area 1B was divided into three sub-areas (north of Point Arena, between Point Arena and Pigeon Point, and south of Pigeon Point). This division of areas resulted in 17 PMFC-like areas (area 5E is shown for reference only; for simplicity, all data from 5E were treated as if they were collected from 5C or 5D (i.e., 5E data were integrated into similar 5C and 5D areas to make the areas linear) with an average latitudinal span of 138 km (range=83–204 km, Fig. 1). Reporting of tag releases and recoveries was sufficiently detailed to allow an analysis that included these additional boundaries and that did not exclude any studies.

Only studies reporting the area, month, and year for each tagging event were included in this analysis. Additionally, tag recoveries must have been reported at one of four levels of resolution: type-1 resolution, where data were available for year, month, and area for each individual tag recovery; type-2 resolution, where data were available for month and area only; type-3 resolution, where data were available for area only; and type-4 resolution, where data were only available to indicate recovery inside or outside the area of tagging. After this screening (removing 16,375 releases), there were 25 English sole tagging events from the open coast remaining in the analysis, including 17,056 releases and 3464 recoveries; these projects, summarized in Jow (1969), Forrester (1969), and Pattie (1969) ranged from southern California to northern British Columbia and from 1936 to 1965 (Table 1).

There were many differences among individual studies that had to be reconciled or ac-

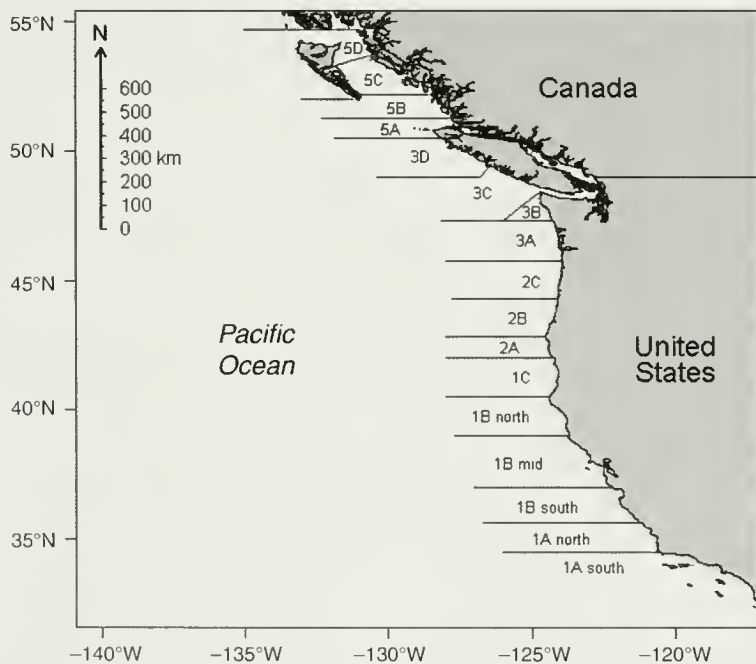


Figure 1

Map of areas based on historical Pacific Marine Fisheries Commission (PMFC) boundaries used in this analysis. The largest PMFC areas, 1A and 2B, were subdivided to make the latitudinal ranges more consistent across all areas.

Table 1

Summary of English sole (*Parophrys vetulus*) tagging events off the coast of the United States and Canada modeled in this article. Years listed include the year of initial tagging through the final tag return. "Number released" represent total numbers tagged in a one Pacific Marine Fisheries Commission (PMFC) area (Fig. 1) in a single month. "Number recovered" and "Percent recovered" represent only those tags with complete recovery information; tags recovered within one month of tagging were excluded. Data quality categories were the following: 1, where data were available for year, month, and PMFC area for each individual tag recovery, 2, where data were available for only month and area, 3, where data were available for area only, and 4, where data were only available to indicate recovery inside or outside the area of tagging. NA = not available.

Years	PMFC area	Number released	Number recovered	Percent recovered	Number excluded	Data quality	Reference
1936-37	1B-south	16	1	6.25	0	1	Jow (1969)
1936-37	1B-south	45	9	20.00	NA	3	Jow (1969)
1938-40	1C	400	25	6.33	5	1	Jow (1969)
1939	1B-south	38	1	2.63	0	1	Jow (1969)
1939-41	1B-mid.	30	4	13.33	0	1	Jow (1969)
1940-42	1B-mid.	746	21	2.82	2	1	Jow (1969)
1940-43	1C	852	61	7.21	6	2	Jow (1969)
1940-46	1B-north	1103	27	3.35	0	1	Jow (1969)
1945-47	3C	24	1	4.35	1	1	Forrester (1969)
1945-51	5D/5E	1505	316	21.21	15	4	Forrester (1969)
1945-51	3C	132	29	21.97	NA	3	Forrester (1969)
1949-51	1B-mid.	926	32	3.47	3	1	Jow (1969)
1949-51	1C	415	69	17.16	13	2	Jow (1969)
1950-51	1C	9	1	11.11	0	1	Jow (1969)
1950-52	1B-south	19	1	5.26	0	1	Jow (1969)
1950-53	1B-mid.	200	5	2.50	0	1	Jow (1969)
1950-56	5D/5E	3039	1405	46.55	21	4	Forrester (1969)
1952-58	5D/5E	2235	737	33.21	16	4	Forrester (1969)
1956-61	3B	871	76	8.82	9	2	Pattie (1969)
1958-59	1C	6	3	50.00	0	3	Jow (1969)
1958-61	1B-mid.	97	6	6.19	0	1	Jow (1969)
1958-63	1C	4130	623	15.84	196	2	Jow (1969)
1959	1B-mid.	103	2	1.94	0	1	Jow (1969)
1963-64	1A-north	2	1	50.00	0	1	Jow (1969)
1963-65	1A-nouth	113	8	7.08	0	3	Jow (1969)
	Total	17,056	3464	20.37	287		

counted for to perform a simultaneous analysis. Where possible, recoveries in the same month as the tagging program were excluded (and subtracted from tag releases, $n=287$) to avoid potentially skewed estimates of movement and fishing mortality rates before any movement could reasonably have occurred. Exclusion of immediate recoveries is common practice when analyzing tag-recovery data (McGarvey and Feenstra, 2002; Robichaud and Rose, 2004). This decision also obviated having to scale the fishing mortality rate during the first month by the number of days after tagging, which is problematic when tagging has occurred over a number of days or is reported only by the month in which it took place. Many different methods of tagging were used in these studies, but all tags were assumed to have the same rate of tag loss. Comparison of tag loss rates for disk and spaghetti tags, although limited, has not identified substantial differences (Meehan and

Milburn¹), although variation certainly exists given the advances in tagging methods over the four decades spanned by these studies. The reporting rates for tags captured by different fisherman were another source of variability; all recoveries were assumed to have been reported at the same rate in all time periods because there was no information with which to address this issue. Researchers conducting all studies primarily tagged adult fish of both sexes, and recoveries were obtained with commercial or similar fishing gear; however little detail regarding the age or length structure of the fish tagged was available. No accounting was made for

¹ Meehan, J. M., and G. S. Milburn. 1965. Comparison of returns from dart and Peterson disc tags on Dover sole. Fish Commission of Oregon Research Briefs. 13:127. Oregon Department of Fish and Wildlife, 3406 Cherry Avenue NE, Salem, OR 97303.

Table 2

General structure of the monthly movement parameter matrices (P) for all models explored in this analysis; p_n = proportion of population moving north, p_s = proportion of population moving south. Movement rates assumed to be zero in all models are indicated in the off-diagonals. The table is compressed over the central 11 areas (denoted by "..."), where the structure of the matrix did not vary from those cells shown.

From	To						
	1A south	1A north	1B south	...	5B	5C	5D
1A south	$1-p_n$	p_n	0	...	0	0	0
1A north	p_s	$1-p_n-p_s$	p_n	...	0	0	0
1B south	0	p_s	$1-p_n-p_s$...	0	0	0
...
5B	0	0	0	...	$1-p_n-p_s$	p_n	0
5C	0	0	0	...	p_s	$1-p_n-p_s$	p_n
5D	0	0	0	...	0	p_s	$1-p_s$

fish size or age in this analysis. Relative fishing effort at the spatial scale of PMFC areas was not available for these years.

Initial examination of the data (for a qualitative assessment) was performed for tagging projects conducted in Puget Sound and the Strait of Georgia (24,408 tags released and 5756 recovered). Many of these experiments were conducted with varied goals (other than that of estimating movement rates) and an attempt to recover tags from distant areas was not undertaken. Therefore, these data were excluded from the mark-recapture model but were used to structure the spatial extent of the analysis.

Movement hypotheses

Many researchers have noted seasonal changes in catch rates in specific areas, and the temporally transient appearance of aggregations of flatfish. For English sole, these aggregations seem to be associated with the winter spawning season (Alverson, 1960). Spawning of English sole occurs from early fall through late spring, and most growth occurs during the rest of the year. December and April appear to be the first and last months of strong spawning activity across all latitudes for English sole (Castillo, 1995); migration associated with movement to and from the spawning grounds could therefore reasonably be expected to take place in the fall and spring just before and following this spawning activity.

For all modeled tag recoveries, movement was restricted to adjacent areas (north or south), and the same rates of movement were applied to all areas along the coast (Puget Sound and the Strait of Georgia were excluded). This simplification restricted the P matrices (area/area for each month) to nonzero values in only the first off-diagonals, and repeated the same parameters within each diagonal (Table 2). The time-increments considered reflect the trade-off between biologically realistic hypotheses and the likely constraints on complexity in future stock assessments. English sole move-

ment over large distances has been observed to occur at a rate of three to eight kilometers per day (Forrester, 1969). With an average latitudinal span of 138 kilometers per area, it could therefore take 17 to 46 days for at least some English sole to cross a single area; this rate of movement indicated that a one-month time-step would be appropriate to accommodate interarea migration. In the simplest hypotheses, movement was considered to take place only at one time per year, and all P matrices contained only zeros except for the month in which movement occurred but allowed northerly and southerly movement to differ. These models included movement occurring in January (the standard break for assessment years), October, November, May, and June. An additional four hypotheses were considered that included movement in the fall and spring and that resulted in two different P matrices—one movement applied in a spring month and one in the fall with two unique parameters (a north and south movement) in each. Five hypotheses included movement during more than two months of the calendar year (Table 3).

Bayesian implementation

Prior distributions are required for each of the model parameters (Table 4). Priors were selected to be non-informative, allowing the likelihood function to dominate the posterior probability distribution. However, the choice of appropriate noninformative priors is difficult and case specific, requiring estimation on the appropriate scale for each parameter, often either diffuse (near uniform) or uniform over log-space (Gelman et al., 1995). In some cases, additional information was available with which to constrain the priors. All movement parameters were bounded between zero and one, and had uniform prior density. The maximum possible reporting rate was estimated by calculating one minus the proportion of recovered tags with incomplete information (no area, date, or both, and were not included in the analysis); this value was 0.92 per tag lifetime. If tag loss rate was

Table 3

Specific structure of the movement parameter matrices (P) for the 14 models explored in this analysis. One-season models (1–5) allowed movement to occur only once per year in the month shown, two-season models (6–9) allowed movement in two months per year, and monthly movement models (10–14) allowed movement in >2 months per year, as specified.

Model	Movement parameter matrices
One-season: two movement parameters (north and south in the month indicated)	
1	October
2	November
3	January
4	May
5	June
Two-seasons: four movement parameters (north and south in the months indicated)	
6	October, May
7	October, June
8	November, May
9	November, June
Monthly movement	
10	One parameter, all months, north=south
11	Two parameters, all months, north and south
12	One parameter, movement from May through November only
13	Two parameters, movement from May through November only, north and south
14	Four parameters, movement from May through October, north and south, and movement in November, north and south

Table 4

Prior distributions applied to parameters in all models. NA = not applicable.

Parameter	Name (number)	Distribution (parameters describing the prior distribution)	Prior distribution parameter values	Parameter bounds: low, high
F_d	Fishing mortality rate/year for each data set ($n=25$)	Lognormal (median, coefficient of variation)	F_{med} , 0.25	-5, 5
F_{med}	Median fishing mortality rate/year	Scaled beta ($shape1$, $shape2$)	1.02, 1.02	0.01, 0.80
M	Natural mortality rate/year	Fixed	0.26	NA
Ω	Tag loss rate/year	Scaled beta ($shape1$, $shape2$)	1.02, 1.02	0.01, 1.52
ϕ	Reporting rate	Scaled beta ($shape1$, $shape2$)	1.02, 1.02	0.21, 0.92
p_n, p_s	Proportion moving ($n=1-4$, depending on the hypothesis)	Uniform (bounds)	NA	0.00, 1.00
K_c	Overdispersion ($n=4$)	Gamma (shape, rate)	1.001, 0.01	0.001, 1000

zero and all tags were recaptured immediately, then the minimum possible reporting rate would be the ratio of tags returned to total releases; this value, 0.21, is therefore a logical lower bound on reporting rate. These bounds are comparable to the range of reporting rates observed for other species (Gaertner and Hallier, 2004). Long-term tag-induced mortality (included in tag loss in this model) may be twice that of natural mortality (Manzer, 1952). Tag loss was also reported to be high

because of corrosion of the tag pins for English sole tagged in a similar fashion over roughly the same period (Forrester and Ketchen, 1955). The proportion of tags lost could not have been greater than 0.78 because 0.22 of the tags were recovered; this value (0.22) is greater than that used to calculate the minimum bound for reporting rate because it includes those tags recovered without full reporting of location information. The value of 0.78 for the proportion of tags lost corresponds to a

maximum instantaneous rate of tag loss of 1.52, which was used as the upper bound for this parameter. The tag loss rate was given a lower bound of 0.01 in the absence of other information. The median rate of fishing mortality across data sets (F_{med}) was bounded to lie between 0.01 and 0.8. Reporting rate, tag loss rate, and median fishing mortality rate were all assigned a scaled-beta distributed prior with both shape parameters equal to 1.02. This prior has the desirable properties of a nearly uniform density over most of the parameter space, except immediately adjacent to the bounds, which have zero density. Data set-specific fishing rates (F_d) were assumed to be related in a common hierarchy; the values of these parameters were constrained with a lognormal prior (F_{med} , 0.25). The overdispersion parameters (one for each category of data) were given a gamma-distributed prior (shape=1.001, rate=0.01) and bounded to lie between 0.001 and 1000. This choice reflected the desire for a generally uninformative prior, but one that favored a substantially larger variance than that in a simple Poisson likelihood. Exploration of the sensitivity of the model inference to the choice of priors was conducted by changing the values, rerunning the analysis, and comparing the results. The effect of six key prior distributions were explored through sensitivity analysis by modifying the shape of these distributions: doubling the coefficient of variation of the prior on deviations from F_{med} , using a uniform prior on the log scale for the overdispersion parameter (k), reducing the upper bound on movement parameters to 0.25, extending the prior bounds on reporting rate (0.01 to 1.0), and sequentially setting the priors on tag loss and F_{med} to be uniform.

This model was programmed in AD Model Builder© (Otter Research Ltd., Sidney, B.C., Canada), which uses a Metropolis-Hastings algorithm to sample from the joint posterior distribution of all model quantities. Markov-chain Monte-Carlo (MCMC) sampling was performed for five to fifteen million iterations for each hypothesis. Each chain was thinned by taking every 1000th (or fewer) draws to achieve low autocorrelations (<0.3) within chains and by taking nearly equal actual and effective (modified to account for autocorrelation) sample sizes. Convergence was assumed to have occurred for each chain when the criteria above were met, visual inspection of trace plots and cumulative quantiles (0.05, 0.5, 0.95) indicated stationarity in all model parameters, and most parameters had a Geweke statistic (Geweke, 1992) less than 1.96 (this statistic can be interpreted as a z -score and will produce some significant values due to random chance).

Bayes factors are frequently used in Bayesian analyses to compare the weight of evidence among various model hypotheses, accounting for differences in the number of estimated parameters (Gelman et al., 1995; Burnham and Anderson, 2002). In the present analysis, harmonic mean posterior likelihood for each model was used to calculate approximate Bayes factors (Kass and Raftery, 1995). Model support (among those compared) is based on twice the log of the ratio of mean likelihoods (hereafter referred to as the Transformed Bayes

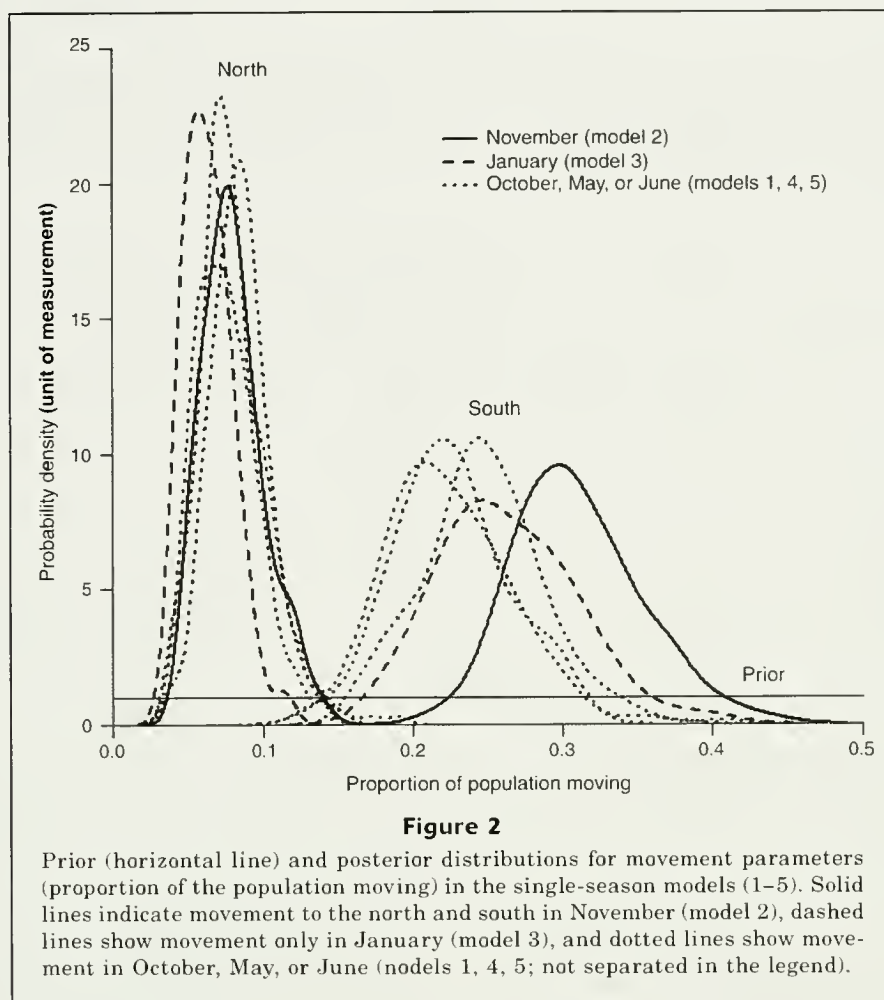
Factor, TBF), judged on the following scale: 0–2, not worth more than a bare mention; 2–6, positive; 6–10, strong; and >10, very strong support for one model over another (Kass and Raftery, 1995). For this application, the TBF metric appeared quite stable and robust to sampling effects arising from the posterior distributions in preliminary testing.

Results

Most of the recoveries of tagged fish across all data sets occurred in the area that initial tagging took place, indicating relatively low rates of movement over all areas and time periods. Of the 3464 tagged English sole recovered off the open coast, only 130 (3.8%) of these had moved from the area of tagging and only 55 (1.6%) had moved more than one area. Low levels of exchange were particularly pronounced for those fish released in Puget Sound and the Strait of Georgia. Of 24,408 tagged English sole released in Puget Sound and the Strait of Georgia, only 12 (0.002%) of the 5756 recoveries were captured off the open coast. Conversely, only 3 (0.001%) of 4232 tagged fish recovered from 32,431 released fish (including some that could not be included in the quantitative analysis) on the open coast were recaptured within Puget Sound or the Strait of Georgia. A single release of 282 English sole in the Strait of Juan de Fuca (Forrester, 1969) resulted in 59 recoveries, 34 of which were from the open coast, mostly off Washington, but recoveries ranged as far south as Oregon. In aggregate, these results indicate that Puget Sound and the Strait of Georgia are substantially isolated from the open coast, but that mixing of adults does occur in the Strait of Juan de Fuca (and possibly at the north end of the Strait of Georgia). Therefore, in all model hypotheses considered in this analysis, Puget Sound and the Strait of Georgia were not included as part of the coastal population.

All five single time-step models resulted in English sole movement estimates that were three to four times more southerly than northerly, although the posterior distributions for the movement parameters were not identical (Fig. 2). TBFs of 49–152 indicated strong support for the model, allowing movement only in November over all other single time-step models (Table 5). In this model, the posterior median proportion of English sole expected to move to the north each year was 0.08, and the 90% posterior interval ranged from 0.05 to 0.12, and 0.31 (0.25–0.39) to the south. The model including movement in January was second best (TBF=49) and qualitatively similar with 0.06 (0.04–0.09) moving to the north, and 0.26 (0.19–0.34) moving to the south each year.

The two-season models also showed some consistency in parameter estimates regardless of the months in which movement was allowed to occur (Fig. 3). TBFs of 16–26 indicated strong support for the model allowing movement in November and May (Table 5). Results from this two-season model showed that the proportion of English sole moving in the spring and to the



north to be 0.10 (0.04–0.18) and to be 0.09 (0.04–0.17) to the south. In the fall, parameter medians were 0.05 (0.02–0.09) to the north and 0.27 (0.17–0.38) to the south. This model was strongly supported over the best single-season model (TBF=49). The next best two-season model (TBF=16) allowed movement in October and May. Movement rates estimated from two-season models showed a similar pattern to those estimated from the single time-step models. Net movement to the south was identified in both cases, primarily in the fall, and although movement rates from two-season models were somewhat reduced, they were applied twice per year. The cumulative expected value for movement in the best two-season model was 0.11 to the north and 0.30 to the south, very close to the values from the best single-season model.

When movement was allowed in each month of the year, parameter estimates were much smaller per month (implying a similar magnitude of annual movement), but greater movement was still predicted to the south than to the north (Fig. 4). The best monthly model (no. 11) included separate proportions moving north (0.02 [0.02–0.03]), and south (0.04 [0.03–0.04]). This model received strong support over the best two-season model

(TBF=101), but only slightly more support from the data (TBF=3) than constant and equal movement all year (model 10). The cumulative expected value of this movement was 0.21 to the north and 0.29 to the south, similar to the best two-season model, but with more net movement to the north. With only a single movement parameter, the median proportion moving in model 10 was 0.03 (0.02–0.04). Although more complex models including movement in only some months were explored, none were supported by the data (TBFs 16–34) over models 10 or 11 (Table 5).

Model parameters other than movement rates showed no obvious restriction by their priors, although posterior distributions included much of the marginal parameter space within the prior bounds. For all models, the overdispersion parameters (k_c) for each data type had substantial density below 1.0, indicating variability far in excess of that expected from a Poisson distribution (Fig. 4). Reporting rate was generally less than 0.75 and was highly correlated with the median fishing mortality rates. Tag loss rates were predicted to be high (often greater than 0.5), but quite uncertain. Sensitivity analysis to the shape of key prior distributions did not result in any substantial changes for the posterior

Table 5

Transformed Bayes Factors (TBFs) used for comparison of models allowing movement in only one month (one-season), in two months (two-seasons), or in >2 months of each year (monthly). Support for one model over another was based on the following TBF scale: 0–2, not worth more than a bare mention; 2–6, positive; 6–10, strong; and >10, very strong (Kass and Raftery, 1995).

Comparison	Model	Number of estimated parameters	TBFs: $2 \times \log(\text{likelihood of the best model} / \text{likelihood of model on row})$
Among one-season models:	1	34	97
	2	34	Best one-season model
	3	34	49
	4	34	134
	5	34	152
Among two-season models:	6	36	16
	7	36	26
	8	36	Best two-season model
	9	36	20
Among monthly models:	10	33	3
	11	34	Best monthly model
	12	33	16
	13	34	14
	14	36	34
Among time-steps:			
Best one-season model	2	34	151
Best two-season model	8	36	101
Best monthly model	11	34	Best model

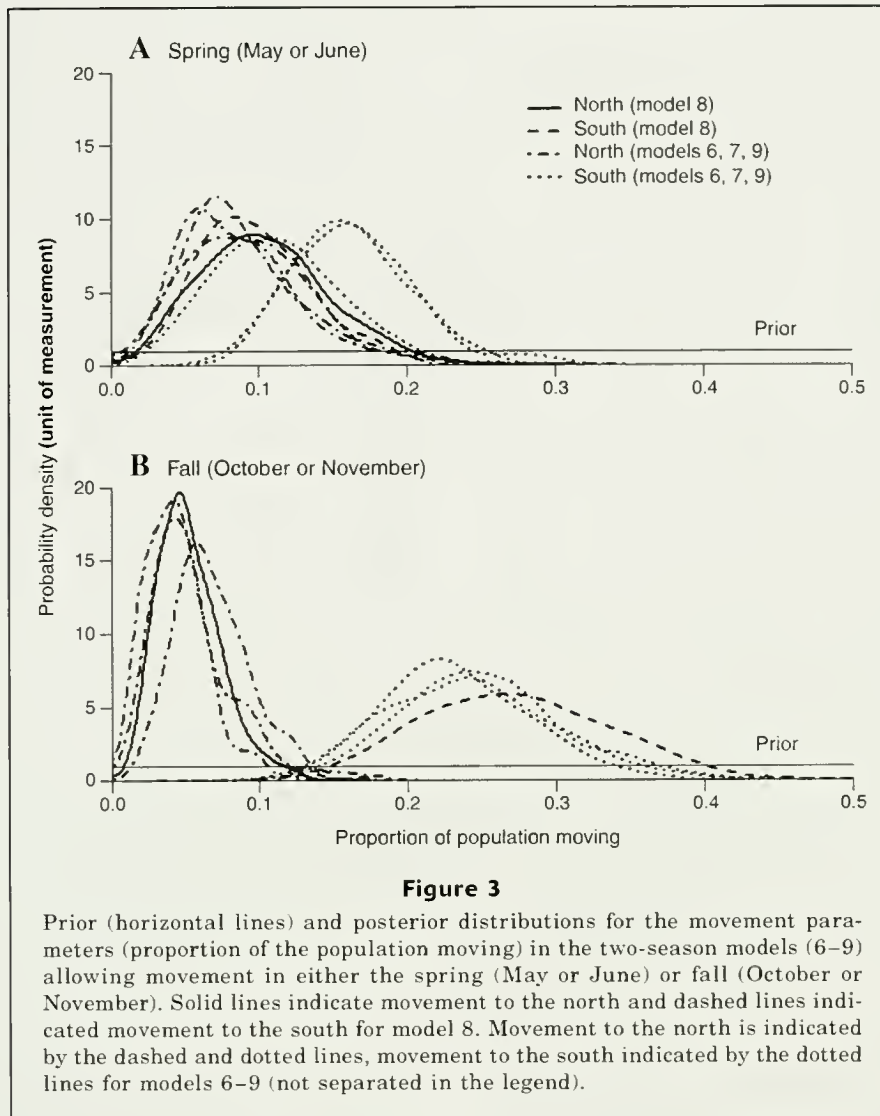
distributions of the movement parameters for any of the six alternate sets of parameter values considered (Fig. 5). A further check was made by rerunning the model assuming high (75%) initial tag loss; again no appreciable change in posterior distributions was observed, and median parameter values changed by less than 0.001.

The ability to quantify the plausibility of the observed data given the fitted model, Bayesian goodness-of-fit, was examined by checking the posterior predictive distribution (the probability distribution for an unobserved data point), which can indicate the degree to which the model structure, priors, and likelihoods assumed in the model are appropriate (Gelman et al., 1995). The posterior predictive distribution for expected recoveries corresponding to each of the observed recoveries was generated during MCMC sampling. The posterior predictive check compares the observed data to a distribution of predictions and summarizes the information across data types. The mean standardized residuals were calculated by dividing the raw residual (between the observed value and the x^{th} percentile of the posterior predictive distribution) by the expected standard deviation (based on the negative binomial likelihood), and by taking the mean of these values for each number of observed recoveries. Figure 6 shows the mean standardized residual for the 95th, 50th, and 25th percentiles of the posterior distribution of expected recoveries for

each of the four types of data. There are a few observations well in excess of the range expected for standardized residuals, primarily for the type-1 data sets. In addition, some trend was observed in the residuals for the type-4 data sets with larger residuals occurring at the largest observed values. Further, although the zero-line for the 5th percentile of the predictions does lie below more than 95% of the residuals, there appears to be an excess of residuals above the zero-line for the 95th percentile of the posterior predictions. This excess of residuals indicates that model predictions generally resulted in fewer recoveries (for some time and space combinations) than were observed.

Discussion

Bayesian analyses are ideal for fisheries applications because uncertainty is explicitly and transparently incorporated into them, they allow for the use of several data sources (Hilborn and Mangel, 1997), provide easily interpretable probability inference (Wade, 2000), and yield results suitable for formal decision analysis (McAllister et al., 1994). The Bayesian framework developed here allows calculation of probability distributions for key parameters governing English sole movement rates. The results from this analysis qualitatively support what can be directly inferred from the original



published analyses of these data sets: English sole are not highly mixed across the entire coast but are also not sedentary at the scale of hundreds of kilometers. The approach of modeling the open coast separately is supported by the observation that only rarely are tagged English sole observed to move between the open coast and Puget Sound or the Strait of Georgia. This result may be specific to the biological and ecological habits of the species but it is commonly assumed to be the result for other species as well.

Also in concordance with historical observations about the seasonal and latitudinal movements of flatfish, the current analysis supports models that include more than just one movement per year. Movement appears to be of greater magnitude in the fall, just before the spawning season, but this pattern is not supported when monthly hypotheses are explored. This lack of a consistent pattern could be due to interannual variability in spawning activity. Research shows that spawning,

in the case of English sole, is related to temperature (Kruse and Tyler, 1983; Peterman et al., 1987), as well as latitude (Castillo, 1995). Because this analysis lacked temperature as a covariate, there may not be adequate data support for specific spring and fall movement rates with the potential variation in timing of spawning activity (when compared to uniform monthly movement). If specific environmental information were available for each year of the analysis, covariates could be developed to improve assignment of the correct month for pre-spawning migration to the south and post-spawning migration to the north.

Of potential importance to stock assessment is the net movement to the south predicted by nearly all of the models. Although this pattern does not fit the data substantially better than simple diffusion (equal movement north and south) throughout the year, increased movement to the south estimated in simpler models may be worth further investigation. The effect of net

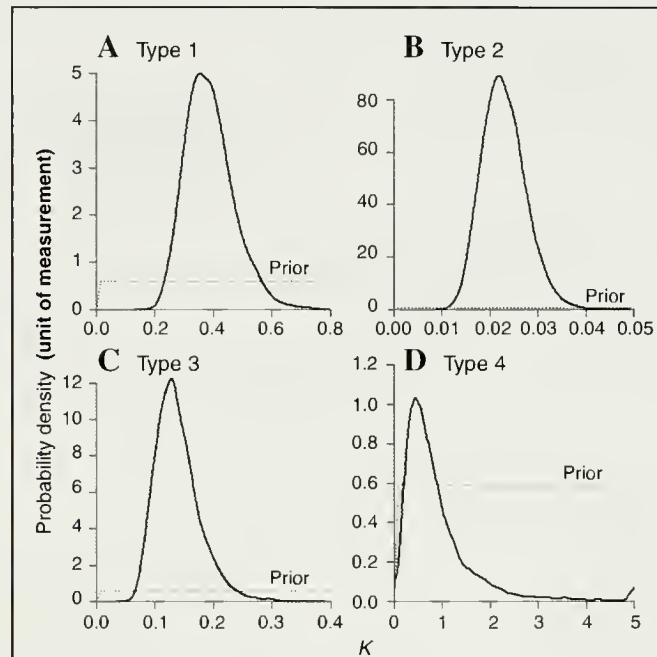


Figure 4

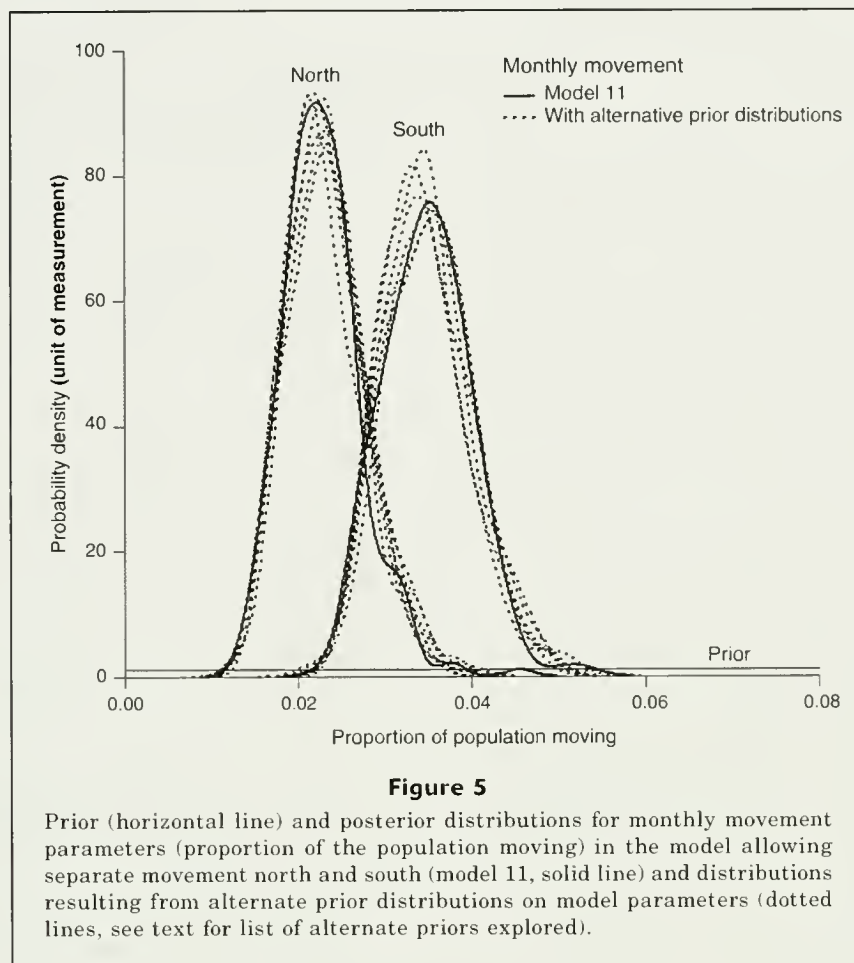
Prior (dotted lines) and posterior distributions for over-dispersion parameters (K) by data type (type 1, where data were available for year, month, and PFMC area for each individual tag recovery; type 2, where data were available for only month and area; type 3, where data were available for area only; and type 4, where data were only available to indicate recovery inside or outside the area of tagging for model 11. Priors are scaled to be more visible on the plot.

southerly movement on equilibrium harvests of adult English sole should be explored because this movement would have implications for current and future management strategies.

Given the presence of significant outliers, the degree of support among models based on the posterior probability should be interpreted with caution. There are many potential reasons for the outliers in observed recoveries present in the data. Although an attempt was made to retain a structure commensurate with what might be possible to replicate in a stock assessment, the analysis may simply not be complex enough. Many parameters, such as fishing mortality, reporting rate, and tag loss rate, are assumed to be temporally and spatially invariant because of a lack of available data. Spatial differences in the location of the initial tagging within the larger PMFC area were not accounted for and reporting rates could be variable due to a mixture of Canadian and U.S. fishing vessels with varied incentives for returning tags. During much of the time period over which tags were recovered, there was a substantial fishery for mink food; this fishery may have had very different handling and tag-recovery practices than those of the concurrent fishery targeting fish for human con-

sumption. The relative effects of violating these various assumptions could be addressed in the future through simulation testing.

Spatially and temporally local increases in fishing-induced mortality rates, resulting in additional recaptured tags, could have generated many of the positive residuals from a model that does not allow fishing mortality to vary within a single data set. Exploration of how model parameters are influenced by localized increases in fishing mortality should be explored through future simulation analysis. Another potential use of this method is to extend the hierarchical model of fishing mortality rates, allowing them to vary over space, time (or both) within a data set. Estimation of the coefficient of variation of this distribution could also be explored. The coefficient of variation of total U.S. catch over the years in which tagging projects were conducted for English sole is on the order of 0.5, indicating that interannual variation in fishing mortality rate may be an important factor absent from the analysis. Similarly, a hierarchical approach could be taken with regard to movement parameters between specific areas. Geographic regions could be defined on the basis of likely bathymetric features such as submarine canyons or rocky headlands



that might serve to disrupt movement along the coast. Although conceptually appealing, these extensions may cause technical problems for MCMC because of the low information content of the aggregated historical tagging data.

Movement rates are notoriously difficult to estimate (Xiao, 1996). However, the general approach to integrated tag analysis based on maximum likelihood has been found to be reliable through simulation testing (Maunder, 2001). In this application, the error structure, although intended to accommodate clustered recoveries and the inclusion of zero recoveries in many space-time combinations, may be inadequate for the observed level of variability in recoveries. Specifically, there were many cases of observed recoveries in areas where no recoveries could have been predicted under simple models, given the structure imposed by the population dynamics that were assumed. Future extension and simulation testing to evaluate other error structures, such as zero-inflated Poisson or negative binomial models, should be undertaken. Further, there may be interactive effects of the prior distributions used, despite lack of observed response to one-dimensional sensitivity testing. Some important elements of uncertainty may not have been included in the

present analysis; however, uncertainty is a problem faced by most modeling applications in fisheries.

It is unlikely that future stock assessments will be structured around areas as small as PMFC areas. Conversion of the movement rates reported here for use as priors in stock assessments will require assumptions regarding the distribution of biomass within areas modeled and the correspondence of the areas modeled to PMFC areas. Research survey data may provide a fishery-independent source on which to base these assumptions. The estimation of fishing mortality in this analysis should also be considered if it is to be applied within a stock assessment framework. These issues would appear to be no more daunting than currently accepted assumptions of thorough mixing across the coast or of completely isolated stock groups.

Tagging programs for groundfish species off the U.S. west coast have generally decreased over the last 75 years, and there are no plans for large-scale tagging programs in the future. An analysis of all available tagging data may therefore provide the only quantitative source of guidance and an important avenue to allow for uncertainty in movement rates without new data with which to estimate these rates. This type of method

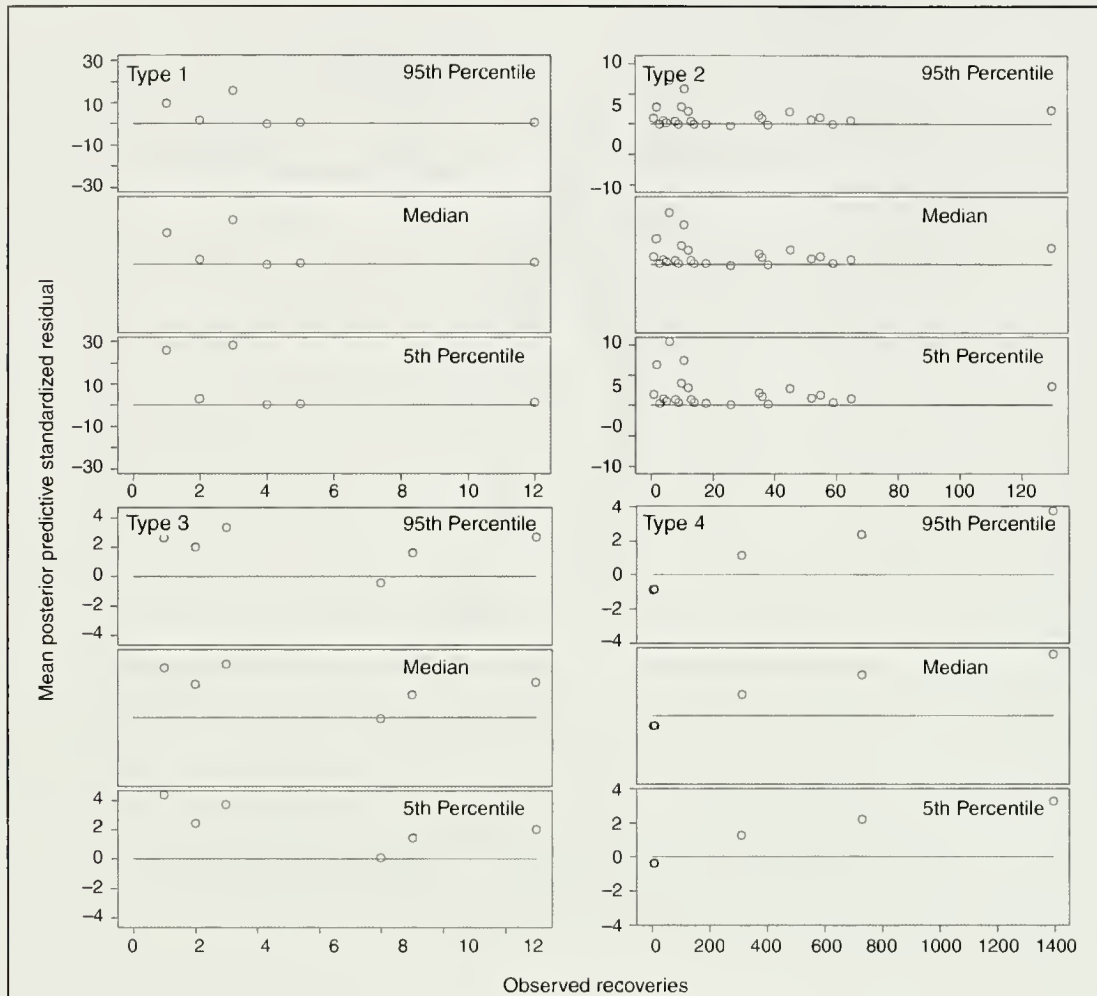


Figure 6

Distribution of mean posterior predictive standardized residuals showing plausibility of observed data, given the model and error structure. Residuals were calculated by dividing the raw residual between the observed value and the X^{th} percentile of the posterior predictive distribution by the expected standard deviation and by taking the mean of these values for each data type (type 1, where data were available for year, month, and PFMC area for each individual tag recovery; type 2, where data were only available for only month and area; type 3, where data were available for area only; and type 4, where data were only available to indicate recovery inside or outside the area of tagging) and percentile of the posterior predictive distribution.

has been demonstrated for English sole but could be extended to other species that have also been the subject of multiple tagging projects. When compared with the status quo assumptions invoked with single (unit) or multiple independent stocks, these results may provide a more realistic integration of spatial movement off the west coast of North America into assessment models. Use of these results could lead to a better representation of the uncertainty associated with estimates of biomass and in the case of stock assessments, they could lead to predictions of exploitation rates that allow a sustainable resource.

Acknowledgments

T. Branch, D. Gunderson, A. Magnusson, C. Minte-Vera, and A. Silva all generously assisted with data sources or analysis. This article was significantly improved by comments on preliminary drafts from T. Branch, R. Hilborn, R. Methot, A. Punt, and I. Taylor. Three anonymous reviewers and A. Moles made many suggestions improving the clarity and content of the manuscript. The author was supported by a National Marine Fisheries Service/National Sea Grant fellowship in population dynamics.

Literature cited

- Alverson, D. L.
1960. A study of annual and seasonal bathymetric catch patterns for commercially important groundfishes of the Pacific Northwest coast of North America. *Pac. Mar. Fish. Comm. Bull.* 4:1-99.
- Beverton, R. J. H., and S. J. Holt.
1957. On the dynamics of exploited fish populations, 533 p. Chapman and Hall, London.
- Bishop, Y. M. M., S. E. Feinberg, and P. W. Holland.
1988. Discrete multivariate analysis: theory and practice, 9th ed., 557 p. Massachusetts Inst. Technology Press, Cambridge, MA.
- Burnham, K. P., and D. R. Anderson.
2002. Model selection and multimodel inference: a practical information-theoretic approach, 2nd ed., 488 p. Springer-Verlag, New York, NY.
- Castillo, G. C.
1995. Latitudinal patterns in reproductive life history traits of northeast Pacific flatfish. *In* Proceedings of the international symposium on north Pacific flatfish, p. 51-72. Alaska Sea Grant College Program, Univ. Alaska, Fairbanks, AK.
- Cormack, R. M., and J. R. Skalski.
1992. Analysis of coded wire tag returns from commercial catches. *Can. J. Fish. Aquat. Sci.* 49:1816-1825.
- Day, D. E.
1976. Homing behavior and population stratification in central Puget Sound English sole (*Parophrys vetulus*). *J. Fish. Res. Board Can.* 33:278-282.
- Dorn, M. W.
2002. Advice on West Coast rockfish harvest rates from Bayesian meta-analysis of stock-recruit relationships. *N. Am. J. Fish. Manage.* 22:280-300.
- Forrester, C. R.
1969. Results of English sole tagging in British Columbia waters. *Pac. Mar. Fish. Comm. Bull.* 7:1-10.
- Forrester, C. R., and K. S. Ketchen.
1955. The resistance to salt water corrosion of various types of metal wire used in the tagging of flatfish. *J. Fish. Res. Board Can.* 12:134-142.
- Gaertner, D., and J.-P. Hallier.
2004. Combining Bayesian and simulation approaches to compare the efficiency of two types of tags used in tropical tuna fisheries. *Aquat. Living Res.* 17:175-183.
- Gelman, A., J. B. Carlin, and D. B. Stern.
1995. Bayesian data analysis, 526 p. Chapman and Hall/CRC, Boca Raton, FL.
- Geweke, J.
1992. Evaluating the accuracy of sampling-based approaches to the calculation of posterior moments. *In* Bayesian statistics 4 (J. M. Bernardo, J. Berger, A. P. Dawid, and A. F. M. Smith, eds.), p. 169-193. Oxford Univ. Press, Oxford.
- Hampton, J., and D. A. Fournier.
2001. A spatially disaggregated, length-based, age-structured population model of yellowfin tuna (*Thunnus albacares*) in the western and central Pacific Ocean. *Mar. Freshw. Res.* 52:937-963.
- Harley, S. J., R. A. Myers, and A. Dunn.
2001. Is catch-per-unit-effort proportional to abundance? *Can. J. Fish. Aquat. Sci.* 58:1760-1772.
- Harry, G. Y., Jr.
1956. Analysis and history of the Oregon otter-trawl fishery. Ph. D. diss., 329 p. Univ. Washington, Seattle, WA.
- Hart, J. L.
1973. Pacific fishes of Canada, 740 p. Fish. Res. Board Canada, St. Andrews, New Brunswick, Canada.
- Heifetz, J., and J. T. Fujioka.
1991. Movement dynamics of tagged sablefish in the northeastern Pacific. *Fish. Res.* 11:355-374.
- Hilborn, R.
1990. Determination of fish movement patterns from tag recoveries using maximum likelihood estimators. *Can. J. Fish. Aquat. Sci.* 47:635-643.
- Hilborn, R., and M. Mangel.
1997. The ecological detective: confronting models with data, 315 p. Princeton Univ. Press, Princeton, N.J.
- Hilborn, R., and C. J. Walters.
1992. Quantitative fisheries stock assessment: choice, dynamics and uncertainty, 570 p. Chapman and Hall, London.
- Jow, T.
1969. Results of English sole tagging off California. *Pac. Mar. Fish. Comm. Bull.* 7:15-33.
- Kass, R. E., and A. E. Raftery.
1995. Bayes factors. *J. Am. Stat. Assoc.* 90:773-795.
- Ketchen, K. S.
1956. Factors influencing the survival of the lemon sole (*Parophrys vetulus*) in Hecate Strait, British Columbia. *J. Fish. Res. Board Can.* 13:647-694.
- Kruse, G. H., and A. V. Tyler.
1983. Simulation of temperature and upwelling effects on the English sole (*Parophrys vetulus*) spawning season. *Can. J. Fish. Aquat. Sci.* 40:230-237.
- Manzer, J. I.
1952. The effects of tagging upon a Pacific coast flounder, *Parophrys vetulus*. *J. Fish. Res. Board Can.* 8:479-485.
- Maunder, M. N.
2001. Integrated tagging and catch-at-age analysis (ITCAAN): model development and simulation testing. *In* Spatial processes and management of marine populations (G. H. Kruse, N. Bez, A. Booth, M. W. Dorn, S. Hills, R. N. Lipcius, D. Pelletier, C. Roy, S. J. Smith, and D. Witherell, eds.), p. 123-146. Alaska Sea Grant College Program, Univ. Alaska, Fairbanks, AK.
- McAllister, M. K., E. K. Pikitch, A. E. Punt, and R. Hilborn.
1994. A Bayesian approach to stock assessment and harvest decisions using the sampling/importance resampling algorithm. *Can. J. Fish. Aquat. Sci.* 51:2673-2687.
- McGarvey, R., and J. E. Feenstra.
2002. Estimating rates of fish movement from tag recoveries: conditioning by recapture. *Can. J. Fish. Aquat. Sci.* 59:1054-1064.
- Menasveta, D.
1958. Migration and fishing mortality of English sole (*Parophrys vetulus*) in Saratoga Passage, and adjacent waters. M.S. thesis, 84 p. Univ. Washington, Seattle, WA.
- Millar, R. B., and R. D. Methot.
2002. Age-structured meta-analysis of the U.S. West Coast rockfish (Scorpaenidae) populations and hierarchical modeling of trawl survey catchabilities. *Can. J. Fish. Aquat. Sci.* 59:383-392.
- Pattie, B. H.
1969. Dispersal of English sole, *Parophrys vetulus* tagged off the Washington coast in 1956. *Pac. Mar. Fish. Comm. Bull.* 7:11-14.

- Peterman, R. M., M. J. Bradford, and G. H. Kruse.
1987. Simulation model of English sole (*Parophrys vetulus*) population dynamics in Washington and Oregon coastal waters. *Can. J. Fish. Aquat. Sci.* 44:1870-1878.
- Punt, A. E. and R. Hilborn.
1997. Fisheries stock assessment and decision analysis: the Bayesian approach. *Rev. Fish Biol. Fish.* 7:35-63.
- Punt, A. E., F. Pribac, T. I. Walker, B. L. Taylor and J. D. Prince.
2000. Stock assessment of school shark, *Galeorhinus galeus*, based on a spatially explicit population dynamics model. *Mar. Freshw. Res.* 51:205-220.
- Quinn, T. J. II., and R. B. Deriso.
1999. Quantitative fish dynamics, 542 p. Oxford Univ. Press, New York., NY.
- Robichaud, D., and G. A. Rose.
2004. Migratory behaviour and range in Atlantic cod: inference from a century of tagging. *Fish Fish.* 5:185-214.
- Wade, P. R.
2000. Bayesian methods in conservation biology. *Cons. Biol.* 14:1308-1316.
- Xiao, Y.
1996. A framework for evaluating experimental designs for estimating rates of fish movement from tag recoveries. *Can. J. Fish. Aquat. Sci.* 53:1272-1280.

Abstract—Adult horseshoe crabs (*Limulus polyphemus*) are the preferred bait in the U.S. east coast whelk pot fishery, but their harvest is being restricted because of severe population declines in the Chesapeake and Delaware bays. To identify other baits, the activity in the pallial nerve of whelks was determined during exposure of the osphradium to odorant solutions prepared from horseshoe crab eggs, horseshoe crab hemolymph, and hard clam (*Merccenaria mercenaria*) tissue. All three elicited significant responses; bait based on them may provide an alternative to the use of adult horseshoe crabs, although extensive behavioral testing remains to be done. Channeled whelk did not respond to molecular weight fractions (>3 kDa and <3 kDa) prepared from horseshoe crab egg odorant solutions but did respond when the molecular weight fractions were recombined. Whelks appear to have broadly tuned chemoreceptors and manufactured baits may need to mimic the complex mixture of odorants derived from natural sources.

Activity in the pallial nerve of knobbed (*Busycon carica*) and channeled (*Busycotypus canaliculatum*) whelks recorded during exposure of the osphradium to odorant solutions

Christopher Magel

Virginia Institute of Marine Science
P.O. Box 1346
Gloucester Point, Virginia 23062

Kirstin Wakefield

Nancy Targett

College of Marine and Earth Studies
University of Delaware
Lewes, Delaware 19958

Richard Brill (contact author)

Email address for R. Brill: rbrill@vims.edu

National Marine Fisheries Service
National Oceanic and Atmospheric Administration
Northeast Fisheries Science Center

Present address: Virginia Institute of Marine Science
P.O. Box 1346
Gloucester Point, Virginia 23062

Knobbed and channeled whelks (*Busycon carica* and *Busycotypus canaliculatum*, respectively) are common in inshore areas of the east coast of the United States from Georgia to Massachusetts (Walker, 1988) and form the basis of a substantial commercial fishery. The currently preferred bait in the pot fishery is adult horseshoe crabs (*Limulus polyphemus*) (Ferrari and Targett, 2003). The directed harvesting for bait has contributed to severe population declines of horseshoe crabs in the Chesapeake and Delaware bays (Berkson and Shuster, 1999) and increasingly stringent catch restrictions are being implemented. These restrictions include a moratorium on horseshoe crab harvest from Delaware Bay (issued by the Delaware Department of Natural Resources and Environmental Control and the New Jersey Department of Environmental Protection in 2006). These restrictions are being promulgated in large

measure because horseshoe crab eggs are a primary food source for migratory shorebirds, such as the red knot (*Calidris canutus*), during their northward spring migrations (Tsipoura and Burger, 1999; Weidensaul, 2006). Because of a continuing decline in the breeding population of the red knot (Morrison et al., 2004), the species has been proposed for inclusion on the Endangered Species List (Weidensaul, 2006).

Work is underway to create alternative bait for the whelk pot fishery (Ferrari and Targett, 2003). As part of these efforts, the sensitivities of knobbed and channeled whelks to odorant solutions prepared from horseshoe crab eggs, horseshoe crab hemolymph, and hard clam (*Merccenaria mercenaria*) tissue were examined. Odorant solutions prepared from horseshoe crab eggs, and molecular weight fractions of these, were tested because they have been reported to

be attractive to mud snails (*Ilyanassa obsoleta*), and because horseshoe crab eggs have been proposed as a source of compounds for inclusion in manufactured bait (Ferrari and Targett, 2003). Horseshoe crab hemolymph was tested as a potential source of attractant for inclusion in replacement bait because it is a readily available natural product. It is a waste product produced during the preparation of *Limulus* amoebocyte lysate (LAL), a clotting agent used worldwide to test for bacterial contamination of pharmaceuticals and implantable medical devices. More importantly, when handled properly, horseshoe crabs used for hemolymph collection show low rates of postrelease mortality (Walls and Berkson, 2000). A patent has been issued for hemolymph-based bait for whelks (U.S. Patent 6391295), but we are unaware of any published studies documenting its efficacy in the whelk pot fishery. Odorant solutions prepared from hard clam tissue were tested because bivalve mollusks are a common prey item for whelks (Walker, 1988).

Electrophysiological techniques were used to test each proposed bait, rather than behavioral methods, because the former allows precise control of stimulus parameters and the rapid assay of various compounds and concentrations on individual animals. Electrophysiological techniques, moreover, have been used for many years to investigate successfully chemosensory questions in both aquatic invertebrates (e.g., Borroni et al., 1986; Kamio et al., 2005) and vertebrates (e.g., Hara, 1975; Wilson, 2004). Behavioral methods, such as flume choice (Y-maze) experiments, can also be difficult with whelks. A large cross-sectional area within a flume is necessary to accommodate adult whelks. This large cross-sectional area requires a high-volume flow rate and concomitantly large volumes of odorant solution to achieve a detectable concentration over the long time periods necessary for whelk to respond behaviorally (Ferner and Weissburg, 2005); large volumes of odorant solutions can be difficult and costly to produce (Ferrari and Targett, 2003; Ferner and Weissburg, 2005). Electrophysiological techniques, however, cannot differentiate between attractive and repulsive odors and must subsequently be paired with behavioral studies.

Activity in the pallial nerve was recorded while odorant solutions were applied directly to the osphradium. The pallial nerve connects the osphradium to the supraesophageal ganglia, which is part of the central nervous system (Alexander, 1970). The osphradium is considered to be the primary chemosensory organ of prosobranch mollusks because its leaf-like structure bears a strong resemblance to the nasal rosettes of aquatic vertebrates (Hansen and Reutter, 2004), and because its location at the base of the incurrent siphon maximizes exposure to odorants (Bailey and Laverack, 1966; Emory, 1992). It should be noted, however, that the osphradium is not the only chemosensory organ in gastropod mollusks. The rhinophores may also provide sensory information allowing gastropod mollusks to track odor plumes (Levy et al., 1997; Rahman et al., 2000; Ferner and Weissburg, 2005). Indeed, the rhino-

phores are considered a primary chemosensory organ in nudibranch mollusks (Alexander, 1970; Wedemeyer and Schild, 1995). A record of activity in the pallial nerve during exposure of the osphradium to odorant solutions derived from various sources therefore provides a robust method to determine whether a specific odorant solution is detectable by whelks and is a candidate for subsequent behavioral testing.

Materials and methods

Knobbed and channeled whelks were obtained from local processing plants or collected from estuaries behind the barrier islands on the eastern shore of Virginia. They were maintained at the Virginia Institute of Marine Science (VIMS) (Gloucester Point, VA) and also at the VIMS Eastern Shore Laboratory (Wachapreague, VA) in tanks supplied with running water drawn directly from the mouth of the York River or the Virginia eastern shore estuaries, respectively.

Horseshoe crab eggs were obtained from beaches bordering the Chesapeake and Delaware Bays, sealed in sterile 50-mL plastic tubes, and stored frozen. Hard clams were obtained from stocks maintained by the VIMS Eastern Shore Laboratory and only fresh tissue was used. Stock odorant solutions were prepared according to methods described by Ferrari and Targett (2003). In brief, horseshoe crab eggs were mixed (1:2 egg to liquid volume) with aerated, filtered, and ultraviolet sterilized water (FSW) drawn from the same sources supplying the holding tanks. The tissue was then crushed with a clean mortar and pestle and the mixture was allowed to sit overnight at 4°C. It was then centrifuged to remove cellular debris and sand. Clam tissue was treated likewise. In addition, horseshoe crab extract solution was prepared as described above, with the exception that 50 mM Tris buffer solution (pH 7.5, a mixture of Trizma HCl and Trizma Base, Sigma Chemical Co, St. Louis, MO) was used instead of FSW. Two molecular weight fractions (>3 kDa and <3 kDa) were then generated by using stirred cell ultra-filtration with YM-3 membranes (Millipore Inc., Billerica, MA). The molecular weight fractions were tested individually on channeled whelk, and after they were recombined. The stock odorant solutions were diluted with FSW 1:10³, 1:10⁴, 1:10⁵, and 1:10⁶ (volume to volume) immediately before experiments. Horseshoe crab hemolymph (free of any anticoagulants or preservatives) was obtained from Wako Chemicals (Cape Charles, VA) and stored at 4°C. It was likewise diluted (1:100, 1:133, 1:200, and 1:400) with FSW immediately before use.

During experiments, an individual whelk was presented with at least four concentrations of an individual odorant solution, plus controls consisting of FSW or a 50 mM Tris buffer solution in random order. The limited funding available for this project precluded the testing of all odorants on both species of whelks. The specific odorants presented to each whelk species are summarized in Table 1.

Table 1

Summary of odorant solutions derived from various sources tested on knobbed (*Busycon carica*) and channeled (*Busycotypus canaliculatum*) whelks. The odorant solutions that were tested on a species are indicated by an "X". FSW = aerated, filtered, and ultraviolet sterilized water.

	Knobbed whelk	Channeled whelk
Horseshoe crab (<i>Limulus polyphemus</i>) eggs extracted with FSW	X	X
Hard clam (<i>Mercenaria mercenaria</i>) tissue	X	
Horseshoe crab hemolymph	X	X
Horseshoe crab eggs extracted with 50 mM Tris buffer solution, <30 kDa and >30 kDa molecular weight fractions of horseshoe crab eggs produced by ultrafiltration, and the molecular weight fractions recombined		X

Quantifying activity in the pallial nerve in response to odorant solutions required that the whelk be removed from its shell, the pallial nerves exposed, and the osphradium isolated. To remove the animal from its shell, the apex of the shell was cut away at the spire, the columella muscle detached from the central column, and the animal gently pulled through the opercular opening. The individual was then immediately submerged in a large dish of aerated FSW. The viscera and the majority of the foot were removed and the mantle cavity opened with a dorsal incision starting medially between the cephalic eye stalks. The preparation was pinned to a Sylgard® (Dow Corning Corp., Midland, MI) lined Petri dish such that the body cavity was open and the buccal mass held out of the way. The overlying connective tissue was carefully dissected to expose the circumesophageal ganglia, specifically the supraesophageal ganglion, and the Petri dish holding the preparation was moved to a second plastic chamber (filled with FSW) mounted under a dissecting microscope. A modified 10-mL plastic syringe barrel with a small amount of quick-setting silicon elastomer (Kwik-Cast®, World Precision Instruments, Sarasota, FL) around the base was placed over the osphradium to isolate it from the fluid in the chamber containing the animal (Fig. 1A).

The odorant delivery system consisted of a glass reservoir (filled with FSW) and polyethylene and stainless steel tubing (Fig. 1A). FSW was continuously delivered to the osphradium chamber by gravity at approximately 6 ml/min. Odorant solutions were switched into the delivery system without a change in flow rate by using a three-way stopcock. The 10-mL volume odorant solution was therefore delivered to the osphradium chamber within approximately 90 seconds, and then flushed out of the osphradium chamber by switching the flow back to FSW. Because the volume of liquid in the osphradium chamber was maintained as close to 2 mL as possible, peak stimulus concentration in the osphradium chamber reached approximately 60% of the original stimulus concentration (Fig. 1B) (Steffensen, 1989).

To record activity in the pallial nerve associated with the exposure of the osphradium to odorant solutions, the nerve was cut and the afferent end was drawn into

a suction electrode (Fig. 1B). The resulting signal was amplified (80 dB gain) and filtered (10 Hz high pass and 1 k Hz low pass) by using a DAM-50 amplifier (World Precision Instruments, Sarasota, FL). The signal was further conditioned to remove 60 Hz noise with the use of a Humbug® active electronic filter (Quest Scientific, North Vancouver, B.C., Canada), and then displayed on a digital storage oscilloscope. The signal was digitized (at 1 kHz sampling rate) with a USB analog to digital I/O interface (model 1208LS, Measurement Computing, Middleboro, MA). The digital data were filtered (5 Hz high pass and 75 Hz low pass filters), processed, recorded, and displayed on a computer screen by using a custom designed computer program developed within DasyLab (version 7.0, National Instruments Corp., Austin, TX).

It was not practical to quantify responses by discrimination and by counting single nerve spikes because the recordings contained a broad amplitude signal due to activity in multiple nerve fibers, and because of the long intervals of activity in response to odorant solutions (Fig. 2). Instead, the differentiation and integration module within DasyLab was used to generate an output value proportional to the integral of the filtered nerve signal (Fig. 2B). The module was programmed to integrate over 10.2-second intervals (i.e., 20 data blocks, as defined within the DasyLab program) to reset the output to zero, and then resume integrating. The digital system was thus functionally equivalent to an analog electronic "leaky RC integrator" circuit commonly used to measure the magnitude of nerve activity (e.g., Hara, 1975; Kamio et al., 2005).

For each trial, data were recorded for 12 minutes: 6 minutes before the introduction of an odorant solution into the osphradium chamber, and 6 minutes after. This recording interval was chosen on the basis of long integration times reported for the chemosensory abilities of whelks (Ferner and Weissburg, 2005) and other mollusks (Murphy and Hadfield, 1997). An additional 3 minutes were allowed between odor trials to ensure that the odorant solution was flushed from the osphradium chamber and that the activity in the pallial nerve had returned to prestimulus levels (Fig. 2). Only data

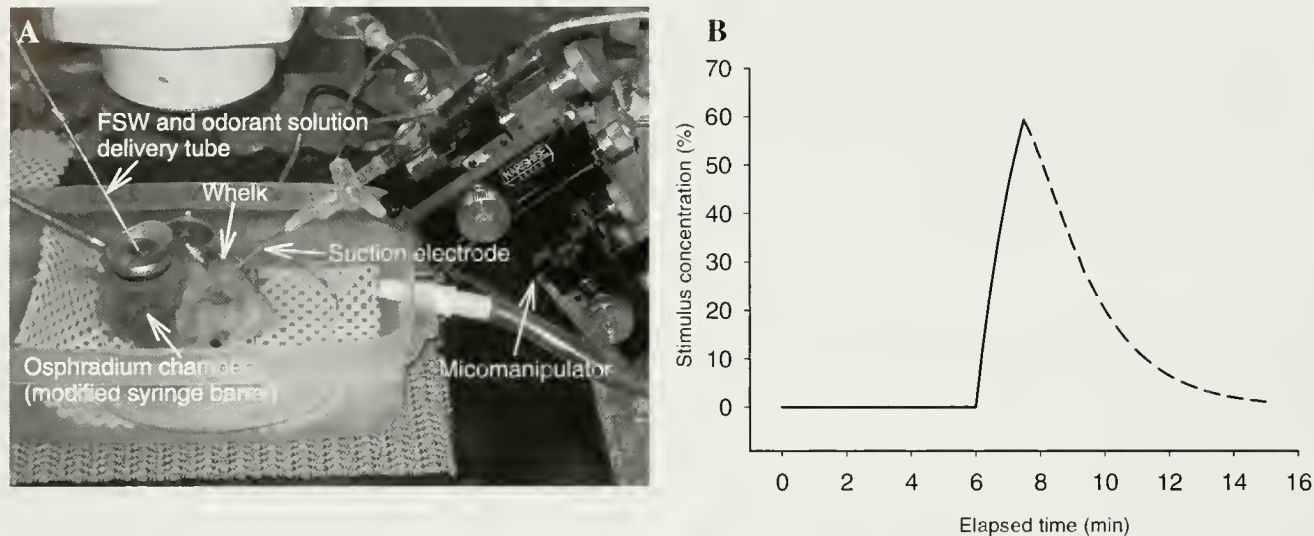


Figure 1

(A) Experimental setup showing a whelk, the osphradium chamber (modified syringe barrel), the aerated, filtered, and ultraviolet sterilized water (FSW) and odorant solution delivery tube, and the micromanipulator holding the suction electrode. (B) The predicted growth (solid line) and decay (dashed line) of the concentration of stimulus within the osphradium chamber over the course of a 15-minute trial, expressed as a percentage of the original odorant solution concentration.

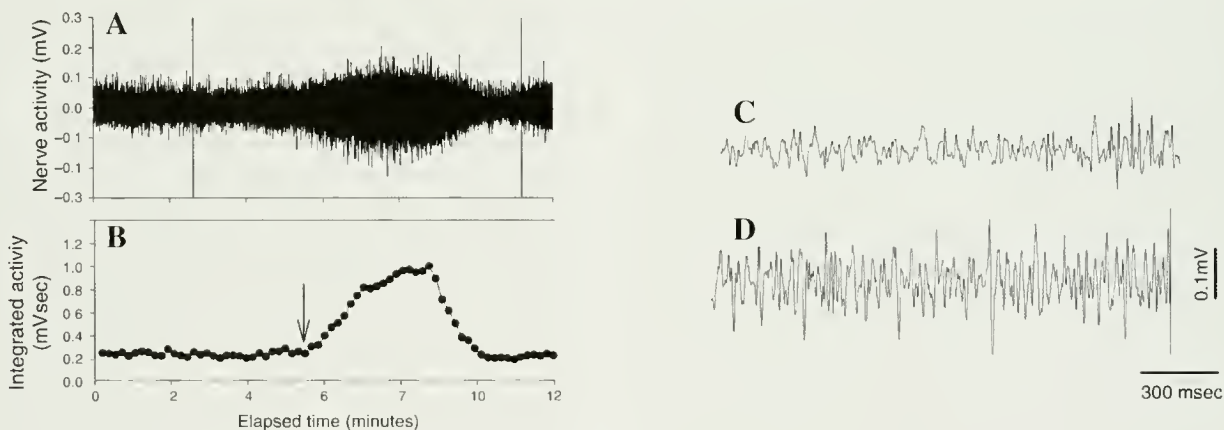


Figure 2

(A) Activity in the pallial nerve in a channeled whelk (*Busycotypus canaliculatum*) before and during exposure of the osphradium to an odorant solution prepared from horseshoe crab (*Limulus polyphemus*) eggs. The arrow in panel B indicates the approximate initial entry of the odorant solution into the osphradium chamber. The two brief large increases in activity (occurring at approximately 2 and 11 minutes after the start of the record) were associated with slight movements of the animal. (B) Nerve activity integrated over 10.2-second intervals was documented with DasyLab 7.0 software (National Instruments Corp., Austin, TX). (C) Nerve activity recorded before initial entry of the odorant solution into the osphradium chamber (3 minutes after the beginning of the record shown in Panel A). (D) Nerve activity at the apex of the response to the odorant solution (8 minutes after the beginning of the record shown in Panel A).

recorded 5 minutes immediately before and 5 minutes immediately after the initial introduction of an odorant solution were analyzed. This procedure resulted in approximately thirty equally spaced data points (i.e., one data point recorded every 10.2 seconds for five minutes),

representing integrated nerve activity in each time period (Fig. 2B). The area under the curves representing integrated nerve activity (Fig. 2) was calculated by summing the points from each 5-minute period (i.e., the data recorded before and during presentation of an

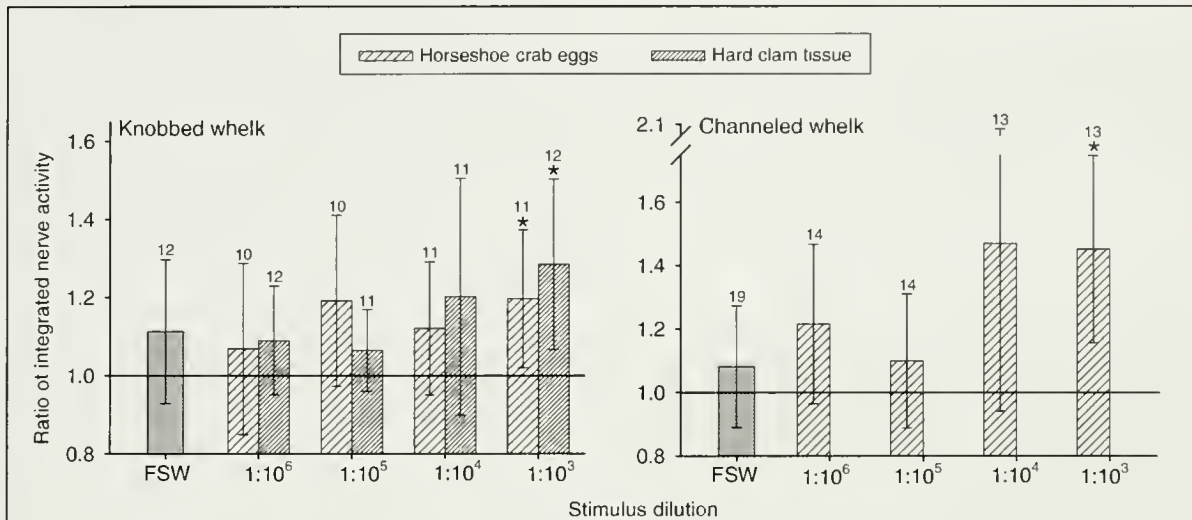


Figure 3

Mean responses ($\pm 95\%$ CI) of knobbed (*Busycon carica*) and channeled (*Busycotypus canaliculatum*) whelks to odorant solutions prepared from horseshoe crab (*Limulus polyphemus*) eggs and hard clam (*Mercenaria mercenaria*) tissue. FSW refers the use of filtered sterilized water in place of an odorant solution. The data are the ratio of integrated activity in the pallial nerve recorded *during* exposure of the osphradium to integrated activity in the pallial nerve recorded *before* exposure to the odorant solutions. The numbers of individuals used in each trial (n) are shown above each bar. A significant response (indicated by “*”) was determined to have occurred when the mean ratio of integrated nerve activity was significantly different from 1.0 (based on the 95% confidence interval). The solid line indicates a ratio of integrated activity value = 1.0.

odorant solution). The ratios of nerve activities during application of the odorant solutions to that recorded immediately before application were calculated to test for the presence of responses. This technique reduces the influence of interanimal variability, as well as the inherent variability associated with the use of suction electrodes (Stys et al., 1991).

Data sets were screened for normal distributions with the Anderson-Darling test (Minitab version 14.20.2, Minitab Inc., State College, PA) and all passed. Data were averaged across individuals for each species of whelk, and the standard errors (SE) and 95% confidence intervals (CIs) were calculated. A significant response to an odorant solution was deemed to have occurred if the 95% CI of the mean ratio of integrated nerve activity did not overlap 1.0. This was equivalent to using a two-tailed t -test with $P < 0.05$ taken as the level of significance.

Results

The pallial nerve typically showed spontaneous activity, although nerve activity clearly increased as the concentration of a detectable odorant solution in the osphradium chamber reached maximal concentration (Fig. 2). Once the flow of FSW was resumed (90 seconds after stimulus onset), the concentration of odorant solution in the osphradium chamber decreased (Fig. 1B) and nerve

activity diminished (Fig. 2). Nerve activity generally returned to near prestimulus levels within the recording period (Fig. 2).

Neither species responded to FSW alone (Fig. 3). Odorant solutions extracted from horseshoe crab eggs with FSW elicited a significant increase in pallial nerve activity in both knobbed and channeled whelks at a dilution of $10^3:1$, but not at any of the higher dilution ratios (i.e., lower concentrations) (Fig. 3). Odorant solutions extracted from hard clam tissue also elicited a significant increase in pallial nerve activity of knobbed whelk at the $10^3:1$ dilution ratio, but not at higher dilutions (Fig. 3). This solution was not tested on channeled whelk. In contrast to odorant solutions prepared from horseshoe crab eggs by using FSW, odorant solutions containing horseshoe crab hemolymph generated a species-specific pattern of responses. These elicited significant increases in pallial nerve activity in knobbed whelk at both 100:1 and 133:1 dilutions, whereas channeled whelk did not respond to any of the four concentrations tested (Fig. 4).

Odorant solutions prepared from horseshoe crab eggs by using 50 mM Tris buffer solution were tested only on channeled whelk (Table 1). This stimulus elicited a significant increase in pallial nerve activity at a dilution of $10^3:1$, but not at higher dilutions (Fig. 5)—a result identical to that recorded in channeled whelk with the use of horseshoe crab eggs odorant solutions prepared with FSW (Fig. 3). Channeled whelk did not respond

to the Tris buffer solution alone (Fig. 5). Nor did they respond to either of the molecular weight fractions (>3 kDa nor <3 kDa) prepared from the horseshoe crab egg odorant solutions by ultrafiltration at any concentration tested (Fig. 5). When recombined, the molecular weight fractions again induced a response at $10^3:1$ dilution (Fig 5).

Discussion

Electrophysiological techniques appear suitable for determining odorant solutions that stimulate the pallial nerve in both knobbed and channeled whelks. The sustained increases in nerve activity of the pallial nerves of these two species (exemplified by the results shown in Fig. 2) are similar to those recorded by Bailey and Laverack (1963, 1966) upon exposure of the osphradium of the common whelk (*Buccinum undatum*) to extracts prepared from the blue mussel (*Mytilus edulis*). Bailey and Laverack (1966) also observed extended periods of increased nerve activity, which they termed "the *Mytilus* response." Wedemeyer and Schild (1995) demonstrated similar increases in activity of the pallial nerves of the pond snail (*Lymnaea stagnalis*) in response to exposure of the osphradium to mixtures of amino acids, to hypercapnia, and to hypoxia. The sustained activity in

the pallial nerve during odor stimulation observed in knobbed and channeled whelks (exemplified in Fig. 2) is also consistent with Ferner and Weissburg's (2005) findings that slow moving gastropod mollusks locate odor sources in turbulent flow conditions by temporally averaging odor concentrations across a plume. In contrast, the more rapid onset and offset of olfactory responses (i.e., shorter temporal resolution) of the crustacean olfactory system (Gomez and Atema, 1996) appears to hinder their olfactory navigation in turbulent environments (Weissburg and Zimmer-Faust, 1993, 1994).

It is possible that increases in nerve activity in response to odorant solutions also include increases in proprioceptor activity resulting from odor-induced muscular contractions. The pallial nerve appears to be a sensory nerve that conveys a suite of information to the circumesophageal ganglion (Laverack and Bailey, 1963). The pallial nerves of whelks show a low level of almost constant spontaneous activity (Fig. 2C), and rapid onset and offset increases in activity associated with slight spontaneous movements of the head, proboscis, or siphon (Fig. 2A). The origin of the spontaneous activity is unknown, but the latter (the rapid onset and offset increases in activity) are most likely due to activity of axons within the pallial nerve originating from proprioceptors (Laverack and Bailey, 1963). It is possible, therefore, that the ultimate origin for nerve activity seen during application of odorant solutions to the osphradium are proprioceptors, and that these are being stimulated by increased movements in response to application of odorant solutions to the osphradium. This does not, however, invalidate the results. Responses to odorant solutions are still being recorded, albeit not directly in the manner assumed.

One of the objectives of the present project was to determine whether odorant solutions prepared from horseshoe crab eggs stimulated chemosensory receptors in the whelk species targeted by the pot fishery. Ferrari and Targett (2003) suggested the potential use of olfactory attractants from horseshoe crab egg extracts as an alternative to horseshoe crab bait. Their conclusion was based on the behavioral responses of the common mud snail to heat-stable proteinaceous compounds extracted from horseshoe crab eggs. Because both knobbed and channeled whelks respond to horseshoe crab egg odorant solutions prepared with FSW at a $10^3:1$ dilution (Fig. 3), our results support their findings. Horseshoe crab eggs clearly contain a compound (or compounds) detectable by whelks even at low concentrations; therefore odorant solutions prepared from horseshoe crab eggs need to be examined further.

Defining chemical cues from a specific molecular weight class that elicit a response in whelks may prove to be difficult. Channeled whelk responded to odorant solutions prepared from horseshoe crab eggs with Tris buffer solution, as well as the recombined molecular weight fractions (i.e., >3 kDa and <3 kDa). They did not respond to either molecular weight fraction independently (Fig. 5). These results imply that neither the initial extraction (FSW vs. Tris buffer solution) nor ul-

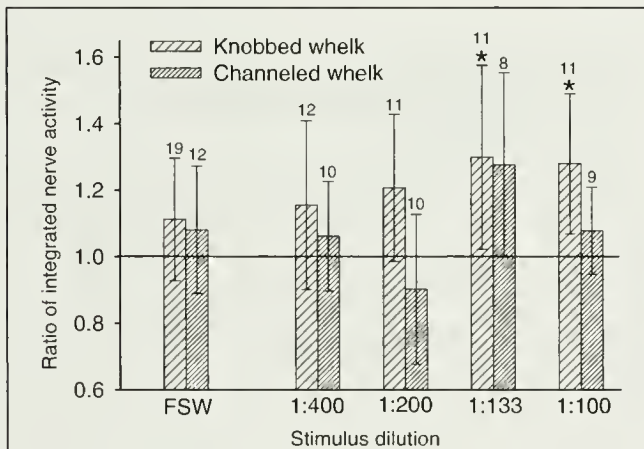


Figure 4

Mean responses ($\pm 95\%$ confidence interval) of knobbed (*Busycyon carica*) and channeled (*Busycotypus canaliculatum*) whelks to horseshoe crab (*Limulus polyphemus*) hemolymph diluted with filtered sterilized water. The data are the ratio of integrated activity in the pallial nerve recorded during exposure of the osphradium to odorant solutions to integrated activity recorded before exposure to odorant solution. The numbers of individuals used in each trial are shown above each bar (n). A significant response (indicated by “*”) was determined to have occurred when the mean ratio of integrated nerve activity was significantly different from 1.0 (based on the 95% CI). The solid line indicates a ratio of integrated activity value = 1.0.

trafiltration procedures destroy the stimulatory components present within the horseshoe crab egg extract. These results also imply that channeled whelk have broadly tuned chemoreceptors requiring a range of low and high molecular weight constituents to elicit a response. Channeled whelk thus appear to differ from other aquatic animals that generally respond to a narrow spectrum of chemical stimulants (e.g., fishes, Carr et al., 1996; Zielinski and Hara, 2007, and crustaceans, Borroni et al., 1986; Kozłowski et al., 2001). Our results from whelk also differ from behavioral experiments on mud snails, in that mud snails are apparently capable of detecting the low molecular weight fractions (<10 kDa) of horseshoe crab egg extracts prepared by ultrafiltration (Ferrari and Targett, 2003).

Knobbed whelk responded to an odorant solution prepared from hard clam tissue (Fig. 3). Because hard clams are a common prey item of whelks (Magalhaes, 1948; Walker, 1988), we surmise that channeled whelk would respond similarly. Bait based on hard clam tissue, or some extract thereof, could potentially serve as replacement for horseshoe crabs in the whelk pot fishery. The cost of raw material may be prohibitive, however, because hard clams are also harvested for human consumption. Likewise, knobbed whelk responded to horseshoe crab hemolymph even when diluted 133:1 (Fig. 4). Surprisingly, hemolymph did not induce a response in channeled whelk at even the highest concentration tested. There is no apparent explanation for this difference in response by the two species. Horseshoe crab hemolymph may offer some promise as the basis for manufactured bait for the whelk pot fishery primarily because it can be obtained in large quantities from an ecofriendly source (i.e., from the pharmaceutical companies producing LAL), and probably at a reasonable cost. It should be noted that horseshoe crab blood is generally treated with proprietary chemical mixtures during LAL production to prevent clotting and to prepare the amoebocyte cells for further processing. If the chemicals are toxic, this could prevent the use of waste hemolymph directly in manufactured baits and preclude their eventual release into the environment.

In summary, electrophysiological techniques recording afferent activity in the pallial nerves of whelks can be used to identify effective odorant solutions, as well as approximate detectable odor concentration limits. Knobbed and channeled whelks responded to extracts prepared from horseshoe crab eggs, and the former responded to horseshoe crab hemolymph diluted up to 133 times, as well as to extracts prepared from hard clam tissue. Channeled whelk do not respond to individual molecular weight fractions of horseshoe crab

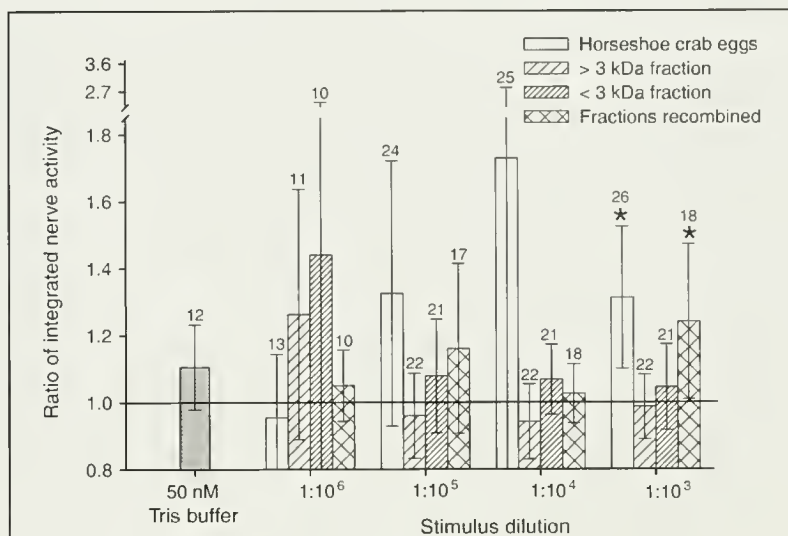


Figure 5

Mean responses ($\pm 95\%$ confidence interval) of channeled whelk (*Busycotypus canaliculatum*) expressed as the ratio of integrated activity in the pallial nerve before the introduction odorant solutions or 50 mM Tris buffer solution. The odorant solutions were prepared from horseshoe crab (*Limulus polyphemus*) eggs extracted with 50 mM Tris buffer solution, two molecular fractions (>3 kDa and <3 kDa) of this odorant solution prepared by ultrafiltration, and the two molecular weight fractions recombined. The numbers of individuals exposed to various odorant solutions are shown above each bar (n). A significant response (indicated by “*”) was determined to have occurred when the mean ratio of integrated nerve activity was significantly different from 1.0 (based on the 95% CI). The solid line indicates a ratio of integrated activity value = 1.0.

egg extracts, and this result implies that whelks have broadly tuned chemoreceptors and that manufactured baits may need to mimic the complex mixture of odors derived from natural sources.

Acknowledgments

This project was supported by grants from the National Oceanic and Atmospheric Administration Chesapeake Bay Office (PO no. DG133F04SE1208), the National Marine Fisheries Service (Northeast Fisheries Science Center), Delaware Sea Grant (RF-9 05/07), Delaware Department of Natural Resources and Environmental Control, and the National Fish and Wildlife Foundation. We acknowledge R. Fisher (Virginia Institute of Marine Science Sea Grant Program) for his support throughout the project; R. Robins Jr. and M. Pegg for donations of live whelk and horseshoe crab hemolymph; J. Harding, R. Mann, and J. Shields (VIMS) for their help in getting us started; the VIMS Eastern Shore Laboratory for providing live whelk, hard clams, animal holding space, and laboratory facilities. This is contribution no. 2828 from the Virginia Institute of Marine Science.

Literature cited

- Alexander, C. G.
1970. The osphradium of *Conus flovidus*. *Mar. Biol.* 6:236–240.
- Bailey, D. F., and M. S. Laverack.
1963. Central nervous responses to chemical stimulation of a gastropod osphradium. *Nature* 200:1122–23.
1966. Aspects of the neurophysiology of *Buccinum undatum* L.—central responses to stimulation of the osphradium. *J. Exp. Biol.* 44:131–148.
- Berkson, J., and C. N. Shuster.
1999. The horseshoe crab: the battle for a true multiple-use resource. *Fisheries* 24:6–11.
- Borroni, P. F., L. S. Handrich, and J. Atema.
1986. The role of narrowly tuned taste cell populations in lobster (*Homarus omericanus*) feeding behavior. *Behav. Neurosci.* 100:206–212.
- Carr, W. E. S., J. C. Netherton, R. A. Gleeson, and C. D. Derby.
1996. Stimulants of feeding behavior in fish: analyses of tissues of diverse marine organisms. *Biol. Bull.* 190:149–160.
- Emory, D. G.
1992. Fine structure of olfactory epithelia of gastropod mollusks. *Microsc. Res. Techniq.* 22:307–324.
- Ferner, M. C., and M. J. Weissburg.
2005. Slow-moving predatory gastropods track prey odors in fast and turbulent flow. *J. Exp. Biol.* 208:809–819.
- Ferrari, K., and N. M. Targett.
2003. Chemical attractants in horseshoe crab, *Limulus polyphemus*, eggs: the potential for an artificial bait. *J. Chem. Ecol.* 29:477–496.
- Gomez, G., and J. Atema.
1996. Temporal resolution in olfaction: Stimulus integration time of lobster chemoreceptor cells. *J. Exp. Biol.* 199:1771–1770.
- Hansen, A., and K. Ruetter.
2004. Chemosensory systems in fish: structural, functional and ecological aspects. *In* The senses of fish (G. von der Emde, J. Mogdans, and B. G. Kapoor, eds.), p. 55–89. Kluwer Academic Publs., Boston, MA.
- Hara, T. J.
1975. Olfaction in fish. *Prog. Neuro. Biol.* 5:271–335.
- Kamio, M., A. Makota, T. Nagayama, S. Matsunaga, and N. Fusetani.
2005. Behavioral and electrophysiological experiments suggest that the antennular outer flagellum is the site of pheromone reception in the male helmet crab *Telmessus cheiragonus*. *Biol. Bull.* 208:12–19.
- Kozlowski, C., K. Yopak, R. Voigt, and J. Atema
2001. An initial study on the effects of signal intermittency on the odor plume tracking behavior of the American lobster, *Homarus americanus*. *Biol. Bull.* 201: 274–276.
- Laverack, M. S., and D. F. Bailey.
1963. Movement receptors in *Buccinum undatum*. *Comp. Biochem. Physiol.* 8:289–98.
- Levy, M., S. Blumberg, and A. J. Susswein.
1997. The rhinophores sense pheromones regulating multiple behaviors in *Aplysia fasciata*. *Neurosci. Lett.* 225:133–16.
- Magalhaes, H.
1948. An ecological study of snails of the genus *Busycon* at Beaufort, North Carolina. *Ecol. Monogr.* 18:377–409.
- Morrison, R. I. G., R. K. Ross, and L. J. Niles.
2004. Declines in wintering populations of red knots in southern South America. *Condor* 106:60–70.
- Murphy, B. F., and M. G. Hadfield.
1997. Chemoreception in the nudibranch gastropod *Phestilla sibogae*. *Comp. Biochem. Physiol. A.* 118:727–35.
- Rahman, Y. J., R. B. Forward, and D. Rittschof.
2000. Responses of mud snails and periwinkles to environmental odors and disaccharide mimics of fish odor. *J. Chem. Ecol.* 26:679–696.
- Steffensen, J. F.
1989. Some errors in respirometry of aquatic breathers: how to avoid and correct them. *Fish. Physiol. Biochem.* 6:49–59.
- Stys, P. K., B. R. Ransom, and S. G. Waxman.
1991. Compound action potential of nerve recorded by suction electrode: a theoretical and experimental analysis. *Brain Res.* 546:18–32.
- Tsipoura, N., and J. Burger.
1999. Shorebird diet during spring migration stopover on Delaware Bay. *Condor* 101:635–644.
- Walker, R. L.
1988. Observations of intertidal whelk (*Busycon* and *Busycotypus*) populations in Wassaw Sound, Georgia. *J. Shellfish Res.* 7:473–478.
- Walls, E. A., and J. Berkson.
2000. Effects of blood extraction on the mortality of the horseshoe crab, *Limulus polyphemus*. *Va. J. Sci.* 51: 195–198.
- Wedemeyer, H., and D. Schild.
1995. Chemosensitivity of the osphradium of the pond snail *Lymnaea stagnalis*. *J. Exp. Biol.* 198:1743–1754.
- Weidensaul, S.
2006. Red knots in a bind; conservationists race to save these wandering shorebirds from extinction. *Defenders* 81:13–19.
- Weissburg, M. J., and R. K. Zimmer-Faust.
1993. Life and death in moving fluids: hydrodynamic effects on chemosensory mediated predation. *Ecology* 74:1428–1443.
1994. Odor plumes and how blue crabs use them to find prey. *J. Exp. Biol.* 197:349–375
- Wilson, D. A.
2004. Fish smell. Focus on “odorant specificity of single olfactory bulb neurons to amino acids in the channel catfish”. *J. Neurophysiol.* 92:38–39.
- Zielinski, B. S., and T. J. Hara.
2007. Olfaction. *In* Sensory systems neuroscience (T. J. Hara, and B. S. Zielinski, eds.), p. 1–44. Fish physiology, vol. 25. Academic Press, San Diego, CA.

Abstract—Tagging experiments are a useful tool in fisheries for estimating mortality rates and abundance of fish. Unfortunately, nonreporting of recovered tags is a common problem in commercial fisheries which, if unaccounted for, can render these estimates meaningless. Observers are often employed to monitor a portion of the catches as a means of estimating reporting rates. In our study, observer data were incorporated into an integrated model for multiyear tagging and catch data to provide joint estimates of mortality rates (natural and fishing), abundance, and reporting rates. Simulations were used to explore model performance under a range of scenarios (e.g., different parameter values, parameter constraints, and numbers of release and recapture years). Overall, results indicated that all parameters can be estimated with reasonable accuracy, but that fishing mortality, reporting rates, and abundance can be estimated with much higher precision than natural mortality. An example of how the model can be applied to provide guidance on experimental design for a large-scale tagging study is presented. Such guidance can contribute to the successful and cost-effective management of tagging programs for commercial fisheries.

Incorporating fishery observer data into an integrated catch-at-age and multiyear tagging model for estimating mortality rates and abundance

J. Paige Eveson (contact author)¹

Tom Polacheck¹

Geoff M. Laslett²

Email for J. Paige Eveson: paige.eveson@csiro.au

¹ Commonwealth Scientific and Industrial Research Organization (CSIRO)

Marine and Atmospheric Research

Castray Esplanade

Hobart, Tasmania 7000, Australia

Postal address: GPO Box 1538

Hobart, Tasmania 7001, Australia

² CSIRO Mathematical and Information Sciences

Private Bag 33

Clayton South, Victoria 3169, Australia

Tagging experiments are becoming increasingly important in large pelagic fisheries as a means of providing estimates of stock abundance and fishing mortality rates that are independent of catch-rate data (Polacheck and Hearn, 2003). In Polacheck et al. (2006), we developed a maximum likelihood model that combines two traditional, but fundamentally different, approaches for analyzing tagging data with a single, terminal recapture (note that we refer to this as “tag-recapture” data, but the term “tag-recovery” data is often used in the literature). The first approach, generally referred to as a Brownie model (Brownie et al., 1985), uses tag-recapture data from multiple years of tagging to provide annual estimates of mortality rates by comparing return rates over time from the releases in consecutive years. Only the numbers of tag releases and returns by year are required, not the number of animals examined for tags. The standard Brownie model is formulated in terms of rates of survival and tag recovery, but can also be expressed in terms of instantaneous rates of natural mortality and exploitation (Pollock et al., 1991; Hoenig et al., 1998a). This latter formulation is particularly useful in fishery applications (e.g., Hampton,

2000; Frusher and Hoenig, 2001; Polacheck et al., 2006). The second approach, known as a Petersen model (e.g., Seber, 1982), uses data from a single release event to provide an estimate of population size at the time of tagging based on the ratio of the number of tags returned from a sample of the population to the total number of tags in the population. In fishery applications, commercial catch data usually constitute the sample from which tags are returned.

The model developed by Polacheck et al. (2006) integrates catch data with data from a multiyear tagging experiment and, in essence, incorporates a Petersen estimator into a Brownie model; we will refer to it as the Brownie-Petersen (BP) model. The BP model involves a likelihood for the tag-recapture data and a likelihood for the catch data, which can be jointly maximized to provide estimates of natural mortality rates, fishing mortality rates, and abundance. The addition of catch data to the traditional Brownie model not only allows for the population size at the time of first tagging to be estimated but also improves the precision of the mortality-rate estimates (Polacheck et al., 2006). For readers familiar with multiple-recapture tagging models,

the BP model has similarities with an age-structured Jolly-Seber (JS) model (Jolly, 1965; Seber, 1965; Pollock, 1981). Both the BP and JS models have a likelihood component for the recapture data, from which survival rates can be estimated. For the BP model, this component equates to a Brownie model, and for the JS model, it equates to a Cormack-Jolly-Seber (CJS) model (Cormack, 1964). Additionally, they both have a likelihood component involving the total number of animals sampled, from which abundance can be estimated (i.e., the Petersen component). However, for the JS model there is an unresolved problem with the Petersen component regarding how the information from unmarked animals should be integrated into the likelihood, and a variety of approaches have been developed to address this problem (see section 4.3 of Schwarz and Seber, 1999, and references therein). The Petersen component of the BP model (i.e., the catch component) is more general and integration into the likelihood is more straightforward.

A recognized problem with applying tagging experiments in fishery situations is that of nonreporting. When recapture information comes from commercial fisheries, it is unlikely that all recaptured tags will be reported, or that the rate of reporting will be known. Although Brownie models can provide estimates of total mortality rates when reporting rates are unknown (Brownie et al., 1985), the separation of natural mortality from fishing mortality generally requires that reporting rates are either known or estimable (Pollock et al., 1991; Hoenig et al., 1998a). Petersen models also require reporting rates to determine abundance estimates.

A number of methods exist for estimating reporting rates (see Pollock et al., 2001). For some methods, such as planted (also called "seeded") tag experiments, the data are independent of the tag-recapture and related catch data from the primary tagging study. In developing the BP model, we assumed that independent reporting rate data were available; therefore a likelihood could be constructed for these data and simply multiplied to the likelihoods for the tag-recapture and catch data. Another common method for estimating reporting rates is to have observers monitor a portion of the catches. Under the assumption that 100% of tags will be returned (i.e., reported) from the observed catches, the reporting rate for the unobserved catches can be estimated by using the relative return rate of tags from the unobserved versus observed catches (Hearn et al., 1999). In the case of longline fisheries, where fish are not brought into port for processing, the use of observers to estimate reporting rates is probably the most viable approach. Unlike data from a planted tag experiment, observer data cannot be considered independent of the tagging or related catch data and therefore incorporating the estimation of reporting rates into the BP model is more complicated.

Pollock et al. (2002) showed how a standard Brownie model can be modified to include the estimation of reporting rates when one component of a multicomponent fishery has 100% reporting rates (e.g., one component

has observers). This modification required that supplementary catch data be brought into the model to assist in the estimation of reporting rates. Pollock et al. (2002) acknowledged that uncertainty in the catch data was not accounted for in their model, and also that it would be resourceful to take advantage of the extra information provided by the catch data to estimate population size. As a topic of future research, they advocated the development of an integrated analysis that estimates all parameters (fishing mortality, natural mortality, population size, and reporting rates) within a single likelihood.

In this article, the BP model is extended to include the estimation of reporting rates by using observer data. We will refer to this extended model as the BPO model, short for the Brownie-Petersen model with observers. The BPO model fulfills the goal of Pollock et al. (2002) for an integrated likelihood that can provide joint estimates of mortality rates, abundance, and reporting rates, and it also directly incorporates uncertainty in the catch data. Results from applying the model to simulated data are presented which demonstrate the accuracy and precision that can be achieved in the parameter estimates under various scenarios (e.g., different parameter values, different numbers of release and recapture years, different parameter constraints). Tag-recapture data and catch data from most field studies will exhibit more variability than the model predicts (i.e., will be overdispersed). Thus, extra variability was included in the simulated data sets to investigate the consequences of applying the model to overdispersed data. Finally, a practical illustration is given of how the model can be used to evaluate the trade-off between releasing more tags and increasing the level of observer coverage in terms of the accuracy and precision of the parameter estimates. Polacheck and Hearn (2003) investigated this issue using a much simpler model (e.g., only one release event; only fishing mortality rates estimated) and making many simplifying assumptions (e.g., natural mortality known; no uncertainty in the catch data; no overdispersion in the data). The BPO model provides a much more comprehensive framework for evaluating such trade-offs and can thereby make an important contribution to the successful and cost-effective management of tagging programs for commercial fisheries.

Materials and methods

Model description

Consider a multiyear tagging study in which a single cohort of fish is tagged in A consecutive years starting at age 1 (i.e., at age 1 in year 1, age 2 in year 2, up to age A in year A). Fish from this cohort are subsequently caught in a fishery over years, or ages, 1 to I ($I \geq A$), and a percentage of the tags that are recaptured each year are reported. Observers monitor a portion of the catches, and 100% of recaptured tags are reported from the observed component of the fishery. Furthermore, all fish caught

in the observed component of the fishery are sampled for length or age, but no fish from the unobserved component are sampled. The catch monitored by observers is assumed to be representative of the total catch (i.e., catches from the observed and unobserved components have the same expected age distribution). If the expected catch-at-age distribution differed between the two components, then separate age information would need to be available for each component and the catch likelihood presented below would need to be modified.

The basic assumptions common to all multiyear tagging models, as summarized in Pollock et al. (1991), are also required for the BPO model. The most important of these are: 1) tagged and untagged fish are thoroughly mixed throughout the population of interest, 2) the fate of each fish is independent of the fate of other fish, 3) all fish of a given age class have the same survival and capture probabilities, and 4) there is no tag shedding or tag-induced mortality. If tag shedding or tag-induced mortality, or both, exist at non-trivial levels (i.e., assumption 4 is not met), then additional parameters and potentially additional data need to be introduced to account for them. Failing to do so will lead to biased parameter estimates and overly optimistic estimates of their precision. If any of assumptions 1 to 3 is violated, then the variance of the tag return counts will be underestimated by the model. Similarly, if assumption 2 or 3 is violated, the variance of the catch numbers will be underestimated. Extra variability, or overdispersion, in the tag return and catch data is discussed in the next section.

Assumption 1 implies that newly tagged fish are mixed throughout the population immediately after tagging. This mixing can be difficult to achieve in practice, especially when the population has a widespread geographical distribution or tagging occurs in a limited area of its distribution. Hoenig et al. (1998b) showed how delayed mixing of newly tagged fish can be incorporated into a Brownie model by allowing these fish to have a different fishing mortality rate in the year of tagging than that of previously tagged fish. In our application of the BP model to southern bluefin tuna (SBT, *Thunnus maccoyii*) data in Polacheck et al. (2006), we allowed for initial nonmixing with this approach. Only the tag-recapture component of the model needed to be modified. It would be straightforward to modify the tag-recapture component of the BPO model in an analogous manner in situations where modification was considered necessary.

Before proceeding, we introduce the notation that will be used throughout this study. The data required by the model are

N_a = the number of tag releases of age a fish from a particular cohort;

$R_{a,i}^o$ = the number of tag returns from fish that were tagged at age a and recaptured at age i in the observed (o) component of the fishery;

$R_{a,i}^u$ = the number of tag returns from fish that were tagged at age a and recaptured at age i in the unobserved (u) component of the fishery; and

C_i^o = the estimated number of age i fish from the cohort of interest caught in the observed (o) component of the fishery.

The model parameters assumed to be known are

δ_i = the proportion of fish from the cohort of interest caught in the observed component of the fishery in year i ;

η_i^2 = the variance of the aging error for C_i^o .

The model parameters to be estimated from the data are

M_i = the instantaneous natural mortality rate for age i fish;

F_i = the instantaneous fishing mortality rate for age i fish;

P_1 = the population size of the tagged cohort at the age of first tagging (assumed to be age 1 for convenience); and

λ_i = the tag reporting rate for fish captured at age i in the unobserved component of the fishery.

In addition, the annual survival rate (S_i) and exploitation rate (u_i), respectively, of an age i fish, are defined to be

$$S_i = \exp(-(F_i + M_i));$$

$$u_i = \frac{F_i}{F_i + M_i} (1 - S_i).$$

Note that because only a single cohort of fish is being considered, age and year can be used interchangeably in the above definitions. If more cohorts were added to the model, it would then be important to distinguish whether the parameters vary by year, by age, or both. For example, λ may vary by year, M by age, and F by both. Because the age distribution of the catch is assumed to be the same for the observed and unobserved components, δ would vary with year, not age, when there is more than one cohort (i.e., the probability of a fish being caught in the observed component of the fishery in year i would be the same for all ages within the year). If the age distribution of the catch was allowed to differ between the observed and unobserved components, then δ would need to vary with both year and age, but it would not be estimable unless information was available about the age distribution of the unobserved catches.

First consider the tag-recapture component of the model. The probability of a fish, tagged at age a , being caught in the observed component of the fishery at age i , and having its tag returned, is

$$p_{a,i}^o = \begin{cases} \delta_i u_i & i = a \\ \delta_i S_a \cdots S_{i-1} u_i & i > a \end{cases} \quad (1)$$

Similarly, the probability of a fish, tagged at age a , being caught in the unobserved component of the fishery at age i , and having its tag returned, is

$$p_{a,i}^u = \begin{cases} (1-\delta_i)u_i\lambda_i & i=a \\ (1-\delta_i)S_a \cdots S_{i-1}u_i\lambda_i & i>a \end{cases} \quad (2)$$

Thus, the probability of a fish, tagged at age a , not being recaptured by age I from either component is $p_a' = 1 - p_{a,i}^o - p_{a,i}^u$. Here, and below, a dot in the subscript denotes summation over the index it replaces.

For tags released at age a , the numbers of returns at ages a to I from the observed component ($R_{a,i}^o, i=a, \dots, I$) and unobserved component ($R_{a,i}^u, i=a, \dots, I$), plus the number not returned by age I from either component ($R_a' = N_a - R_{a,i}^o - R_{a,i}^u$), are multinomial with probabilities given by Equations 1, 2 and p_a' , respectively. Thus, the likelihood equation for the returns from tags released at all ages is the product of multinomials, given by

$$L_R = \gamma \prod_{a=1}^A \left\{ (p_a')^{R_a'} \prod_{i \geq a} (p_{a,i}^o)^{R_{a,i}^o} (p_{a,i}^u)^{R_{a,i}^u} \right\}, \quad (3)$$

where

$$\gamma = \prod_{a=1}^A \frac{N_a!}{R_a! \prod_{i \geq a} (R_{a,i}^o! R_{a,i}^u!)}.$$

Note that γ is a constant that can be left out when maximizing the likelihood.

Next, consider the catch component of the model. Recall that no age information is obtained for the unobserved catches; therefore only catch-at-age data from the observed component are available for inclusion in the model. The probability of an age-1 fish from the cohort of interest subsequently being caught at age i in the observed component of the fishery is

$$\pi_i^o = \begin{cases} \delta_i u_i & i=1 \\ \delta_i S_1 \cdots S_{i-1} u_i & i>1 \end{cases} \quad (4)$$

If the numbers of fish from the cohort of interest that are caught at ages 1 to I in the observed component of the fishery ($C_i^o, i=1, \dots, I$) are known accurately, then these numbers, along with the number of fish from the cohort not caught by age I , are multinomial and have probabilities given by Equation 4. Usually, however, the numbers of fish caught at each age are not known precisely because the ages are estimated either from lengths or from annuli in hard parts (the estimates will be more accurate in the latter case, but will still contain uncertainty). We assume the aging error of the age i catch has a Gaussian distribution with mean 0 (i.e., no bias) and a variance η_i^2 .

Rather than modeling the catch data with both multinomial process error and Gaussian aging error, which

would require a fairly complex approach, we approximated the distribution of the catch of age i fish in the observed component, C_i^o , as Gaussian with overall variance $\sigma_i^2 = \eta_i^2 + \tau_i^2$, where $\tau_i^2 = P_1 \pi_i^o (1 - \pi_i^o)$, is the multinomial variance component. The aging error, unless negligible, will tend to dominate the process error when the cohort size is reasonably large ($\geq 100,000$ individuals), as would be expected in most commercial fishery situations. For example, if the coefficient of variation (CV) of the aging error is 0.10, the cohort size is 100,000 and the probability of catching an age i fish (in either the observed or unobserved component of the fishery) is 0.10, then the ratio of the aging error variance to the process error variance is ~ 10 when the proportion of the catch in the observer component is 0.10, and it is ~ 50 when the proportion of the catch in the observer component is 0.50.

Thus, assuming that the C_i^o 's are independent between ages, the likelihood for the observer catch data is

$$L_C = \prod_{i=1}^I \frac{1}{\sqrt{2\pi\sigma_i^2}} \exp\left(-\frac{1}{2\sigma_i^2} (C_i^o - E(C_i^o))^2\right), \quad (5)$$

where $E(C_i^o) = P_1 \pi_i^o$.

When only a single cohort of fish is being modeled, the assumption that the catch data are independent between ages (i.e., years) should be reasonable in most situations. First, the correlation in the multinomial errors will be close to zero when the size of the cohort is much larger than the size of the catch (as would be expected in most fisheries). Second, the aging errors should be uncorrelated between years provided sampling and aging data are collected each year. However, in some situations, particularly where age is being estimated from a growth curve, covariance in the estimates between years may exist and should be accounted for. Furthermore, if more than one cohort is being modeled, then catch data from multiple ages within the same year will enter the model, and aging errors within a year will be correlated across ages. The level of correlation, and thus the degree to which the independence assumption is violated, will depend on the specifics of the situation, such as how many age classes are present in the year's catch. When the correlation is strong, a more sophisticated approach for modeling the catch data may be required.

The overall likelihood for the combined recapture and catch data can be obtained by multiplying likelihoods (Eqs. 3 and 5) together:

$$L = L_R \times L_C. \quad (6)$$

In a tagging experiment with A consecutive release years, estimates can be obtained, at most, for $A-1$ natural mortality-rate parameters (regardless of the number of recapture years) because information for estimating M_i comes from the differential between the expected returns at age $i+1$ of fish released at age i and those released at age $i+1$. One option is to assume that $M_i = M_{A-1}$ for $i \geq A$,

but other options, such as assuming M is constant or linear with age, are also possible. Furthermore, there is not enough information in the current formulation to estimate the proportion of fish caught each year in the observed component of the fishery (i.e., the δ_i 's). To estimate this proportion would require knowing the total observer catch in each year, as well as the total overall catch in each year. Rather than bringing these data into the model, we assumed that the total catches are known well enough that the δ_i 's can be treated as known without error. Lastly, the aging error variance parameters for the observer catches (i.e., the η_i^2 's) cannot be estimated reliably and therefore they are assumed to be known without error. In Polacheck et al. (2006), we gave a detailed explanation of why the catch variance cannot be estimated reliably in the BP model, and the same argument applies here. We found, however, that the model results were fairly insensitive to the value used for the catch variance so long as it was in the right ballpark (e.g., within ~40% of the true value). The parameters that can be estimated by maximizing Equation 6 are F_i and λ_i for $i = 1$ to I , M_i for $i = 1$ to $A-1$, and P_1 .

As is true when combining any sources of information, it is important to check that the tag-recapture data and the catch data are consistent. This can be done by maximizing the tag-recapture likelihood (Eq. 3) alone and comparing the mortality-rate estimates with those obtained from the joint likelihood (Eq. 6) (note that the catch likelihood alone is insufficient to yield parameter estimates). If the estimates are significantly different, this result would indicate that the tag-recapture and catch data are inconsistent and should not be combined; doing so would yield average values with little biological meaning. Instead, the source of the inconsistency should be investigated (i.e., does it stem from problems with the data or with the applicability of the assumptions in the model?).

Overdispersion in the recapture and catch data

In the model a multinomial distribution is assumed for the tag-recapture data. If one (or more) of model assumptions 1 to 3 is violated, then the observed return counts are expected to be more variable than predicted by a multinomial distribution; i.e., to be overdispersed in relation to multinomial data. Polacheck et al. (2006) provided a thorough discussion of possible sources of overdispersion and ways in which it can be accounted for. When overdispersion exists in the return counts, the parameter estimates obtained by using a multinomial likelihood should still be unbiased, but their standard errors, as estimated from traditional likelihood methods (i.e., from the inverse Hessian matrix), would be too small. A number of possible methods for obtaining more realistic standard errors are discussed in Polacheck et al. (2006) and Pollock et al. (2001), one of which is to use bootstrap procedures.

If overdispersion exists in the recapture data as a result of model assumptions 2 or 3 being violated, then it will also exist in the catch data. That is, the compo-

nent of the variance in the catch-at-age numbers due to process error will be underestimated by a multinomial distribution. As asserted previously, aging error will generally dominate the multinomial process error in the catch data. This will often still be true when the process error is overdispersed. For example, assume that the process error variance is φ times that of multinomial variance; i.e., $\tau_i^2 = \varphi P_1 \pi_i^{\varphi} (1 - \pi_i^{\varphi})$. Then, in the example that was given above for multinomial process error, if $\varphi = 3$, the ratio of the aging error variance to the process error variance would still be 3.3 ($=10/3$) and 17 ($=50/3$) when the proportion of catch in the observer component is 0.10 and 0.50, respectively. In situations where the aging error dominates, not accounting for overdispersion in the catch data should have little effect on the standard error estimates of the parameter estimates.

The degree to which the likelihood-based estimates of the standard errors are underestimated by not accounting for overdispersion in the tag-recapture data and catch data was investigated through simulations, as described below.

Simulation methods

Model performance To evaluate how the model performs in terms of the accuracy and precision of the parameter estimates, a series of Monte-Carlo simulations were conducted. The first scenario considered, which we will refer to as scenario 1, involved a single cohort of fish being tagged in five consecutive years starting at age 1 (i.e., at age i in year i for $i=1, \dots, 5$), and recaptured over the same five years. The number of tag releases was set to be 1000 at each age. Corresponding to the releases at each age, tag returns were generated from the observed and unobserved fishery components by using a Dirichlet-multinomial (D-M) distribution (Mosimann, 1962). The D-M distribution allows for overdispersion in the return counts by modeling the return probabilities as random Dirichlet variables (see Appendix A of Polacheck et al., 2006). It can be parameterized in terms of the return probabilities and an overdispersion factor, φ , that specifies the amount of extra variation in relation to multinomial data. For scenario 1, φ was set to be 3 (i.e., three times greater variance than a multinomial distribution). Other parameters were set as follows: $F_i = 0.15$, $M_i = 0.2$, $\lambda_i = 0.75$, and $\delta_i = 0.10$, for $i=1, \dots, 5$. Catch-at-age numbers (ages 1 to 5) for the observer component of the fishery were generated by using, first, a D-M distribution with $P_1 = 100,000$ and the same φ , δ_i , M_i , and F_i values as for the tag-recapture data. To these catch-at-age numbers, additional Gaussian aging error was added by using a constant CV of $v = 0.10$ for all ages (i.e., $\eta_i = vE(C_i^{\varphi})$).

The BPO model was fitted to the simulated tag-recapture and catch data by maximizing Equation 6. For this process, φ and v were assumed to be known without error, and natural mortality was constrained to be the same at ages 4 and above (i.e., $M_4 = M_5$; recall that only four natural mortality parameters can

Table 1

Description of simulation scenarios. In all scenarios, data were generated for a single cohort of fish tagged at ages 1 to A and recaptured at ages 1 to I , by using an age 1 cohort size of P_1 , a constant natural mortality rate of M , a constant fishing mortality rate of F , a constant reporting rate in the unobserved fishery component of λ , a constant coefficient of variation for the catch aging error of v , and an overdispersion factor of φ (values specified in table). Unless otherwise stated, data were generated by using $N=1000$ releases per year and a constant proportion of observer coverage of $\delta=0.20$. In fitting the model, φ and v were assumed to be known, and natural mortality was constrained to be the same for ages $A-1$ to I . Additional parameter constraints for each scenario are specified in the table. Bold text for a given scenario indicates a difference from scenario 1.

Scenario	Parameter values used to generate data								Parameter constraints imposed for model fitting
	A	I	P_1	M	F	λ	v	φ	
1	5	5	100,000	0.20	0.15	0.75	0.10	3	λ constant
2	5	5	100,000	0.40	0.15	0.75	0.10	3	λ constant
3	5	5	100,000	0.20	0.30	0.75	0.10	3	λ constant
4	5	5	100,000	0.20	0.15	0.50	0.10	3	λ constant
5	5	5	100,000	0.20	0.15	0.90	0.10	3	λ constant
6	5	5	100,000	0.20	0.15	0.75	0.10	1	λ constant
7	5	5	100,000	0.20	0.15	0.75	0.10	9	λ constant
8	5	5	100,000	0.20	0.15	0.75	0.10	3	λ constant; M constant
9	5	5	100,000	0.20	0.15	0.75	0.10	3	λ constant; F linear¹
10	5	5	100,000	0.20	0.15	0.75	0.10	3	none
11	3	3	100,000	0.20	0.15	0.75	0.10	3	λ constant
12	3	5	100,000	0.20	0.15	0.75	0.10	3	λ constant

¹ The line is parameterized in terms of F_1 and F_5 ; i.e., $F_i = F_1 + (i-1) \times (F_5 - F_1) / 4$ for $i = 1, \dots, 5$.

be estimated with five release years). The unobserved tag reporting rate was also constrained to be constant over all recapture years (i.e., $\lambda_i = \lambda$ for $i=1, \dots, 5$). It seems reasonable that the tag reporting rate would be constant, or at least similar, over the course of the experiment. Exceptions would occur if there was a significant change in the fishery or in tag-return promotional activities during this time, or if the fishery involves multiple fleets with different reporting rates so that the overall reporting rate would change if the distribution of catches among fleets changed. To account for such situations, year-specific reporting rates were allowed for in a later scenario (see next paragraph). The only other constraints imposed were simple bound constraints to keep all parameters positive and to keep the reporting rate from exceeding one. Thus, the parameters estimated were F_i ($i=1, \dots, 5$), M_i ($i=1, \dots, 4$), P_1 , and λ .

Model performance will be affected by a large number of factors, including the following: 1) the parameter values used for the mortality rates, cohort size, reporting rates, catch aging error, and overdispersion factor; 2) model parameterization (i.e., whether parameters are assumed to vary with age, year, or both, or to have a particular functional form); and 3) the design of the tagging experiment (e.g., number of release and recapture years; number of releases per year; level of observer coverage). There are endless possibilities with regard to these factors; therefore we have chosen a number of scenarios that we feel are most illustrative for which to present results (Table 1). All of these scenarios use

scenario 1 as a base but include a variation on one of the factors.

Scenarios 2 through 7 investigate changes to the parameter values (factor 1). In particular, scenario 2 increases the natural mortality rate, scenario 3 increases the fishing mortality rate, scenarios 4 and 5 decrease and increase the reporting rate, respectively, and scenarios 6 and 7 decrease and increase the overdispersion factor, respectively. Changes to the cohort size and variance of the catch aging error had less impact on the results and are therefore not included here.

Model parameterization (factor 2) can have a large effect on how well parameters can be estimated. For example, if natural mortality can be assumed to be constant across ages (this is a fairly common assumption in fishery models, at least over a limited range of age classes), then the precision and accuracy of the natural mortality-rate estimate should improve, which in turn may lead to improvements in other parameter estimates. Scenario 8 explores the benefits of having a constant natural mortality rate. Another standard way of reducing the number of parameters in fishery models is to model fishing mortality as a function of age by using an appropriate selectivity curve. Scenario 9 considers the situation where fishing mortality is constrained to be a linear function of age. Note that we parameterized the line in terms of F_1 and F_5 (i.e., $F_i = F_1 + (i-1) \times (F_5 - F_1) / 4$), because this made it easy to constrain the fishing mortality rates to be positive. Instead of imposing additional constraints, scenario 10 relaxes the assumption of a con-

stant reporting rate and allows reporting rates to differ across years. This scenario has the maximum number of parameters that can be estimated by the model (i.e., the model is saturated).

In terms of experimental design (factor 3), the effect of varying the number of tag releases and the proportion of observer coverage is investigated in detail in the next section; therefore only variations to the numbers of release and recapture years are considered here. In particular, scenario 11 reduces the number of release and recapture years from five to three, whereas scenario 12 still has five recapture years but only three release years. For both scenarios, natural mortality was constrained to be equal at ages 2 and above, because only two natural mortality parameters can be estimated with three release years. For scenario 12, this meant constraining natural mortality to be equal at ages 2 to 5. In such a case, alternative constraints may be preferable, such as assuming natural mortality is a linear function of age. This was the approach taken in our application of the BP model to SBT data in Polacheck et al. (2006).

For each scenario in Table 1, 1000 sets of data were generated, as described above for scenario 1, and fitted by using the BPO model. For each parameter estimated, the percent median bias and the CV of the 1000 estimates were calculated, where percent median bias is defined as $(\text{median} - \text{true}) / \text{true} \times 100\%$ and CV is defined as SD / true (where SD denotes standard deviation). The median was used instead of the mean in calculating the bias because many of the parameter estimates had a skewed distribution, making the median a better measure of centrality (see “Results” section). The SDs of the parameter estimates obtained from the 1000 simulation runs (which approximate the true standard errors of the estimates) were compared with the standard error estimates obtained from the inverse Hessian matrix (these are obtained for every run; therefore we averaged the standard errors over the 1000 runs). The purpose was to see how much the Hessian-based standard errors were underestimated by applying a model that does not account for overdispersion in the data.

Trade-off between number of releases and observer coverage Of the factors that affect model performance, only the experimental design can be directly controlled by the researcher in a real application. Although model parameterization is superficially in the researcher’s control, it is the true parameter values that will determine whether any parameter constraints are advantageous (i.e., imposing constraints on parameters that do not represent the true situation will lead to poorer model performance, not improved performance). Thus, in designing a tagging experiment and deciding how best to distribute resources, it would be very useful for the researcher to know the level of performance that can be achieved under different designs, as well as which design elements have the most influence on the results. Here, we illustrate how the BPO model can be used to provide such information. In particular, simulations are

used to evaluate how well the parameters are estimated with different numbers of tag releases and different proportions of observer coverage, and to evaluate the trade-off between releasing more tags versus increasing observer coverage (i.e., to evaluate which leads to larger improvements in accuracy and precision of the parameter estimates).

Initially, simulations were carried out under scenario 1. For simplicity, the number of releases was kept the same for all release ages (i.e., $N_a = N$ for all a) and the proportion of observer coverage was the same over all recapture years (i.e., $\delta_i = \delta$ for all i). N was varied from 250 to 2500, and δ from 0.05 to 0.50. For each combination of N and δ , 1000 tag-recapture and corresponding catch data sets were generated, as described in the previous section, and fitted by using the BPO model. The results were used to evaluate how the percent median bias and CV of the parameter estimates changed as the number of releases and level of observer coverage changed.

For a true field study, the researcher would need to carry out such simulations using parameter values and model constraints that roughly represent the population and fishery dynamics for their situation. Our purpose was not to provide guidance on appropriate numbers of releases and observer coverage for any specific situation, but to illustrate how the model could be used to this end. Nevertheless, it is of interest to know whether the general findings using scenario 1 are likely to remain similar under other scenarios. The absolute levels of accuracy and precision that can be achieved will clearly depend on the scenario, but it is less clear whether the relative changes in these measures from increasing tag releases or increasing observer coverage will be highly scenario dependent. To investigate, we repeated the trade-off simulations using a subset of the other scenarios (4, 6, 8, 10, 11, and 12).

Results

Model performance

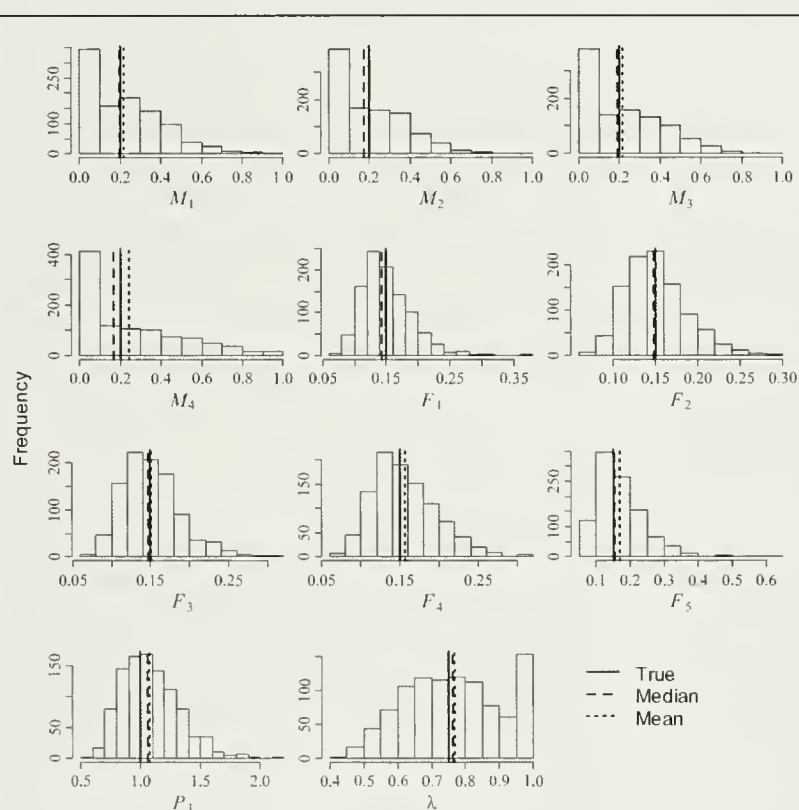
The biases in the medians of the parameter estimates were small for almost all parameters and scenarios (Table 2). A few of the natural mortality estimates had negative biases of greater than 5%, but this result more likely reflects the large variability and non-normality of these estimates (see next paragraph) than true biases.

Histograms of the parameter estimates revealed features that are important for evaluating biases. In particular, the natural mortality estimates often hit the lower bound of zero, and the proportion that did so was highest when the variability was largest (e.g., scenario 7, which has a high amount of overdispersion; Fig. 1). This feature makes it difficult to assess bias for these parameters and explains why the median biases seen in some of the natural mortality-rate estimates, such as scenario 7, are not likely to be meaningful. In scenarios 5, 7, and 10, the reporting-rate estimates often hit their

Table 2

Percent median bias (i.e., $(\text{median}-\text{true})/\text{true} \times 100\%$) of the parameter estimates for each scenario listed in Table 1. Results were based on 1000 simulation runs per scenario. M_i = natural mortality rate for age i fish; F_i = fishing mortality rate for age i fish; P_1 = population size of tagged cohort at age 1; λ_i = tag reporting rate for fish captured at age i in the unobserved component of the fishery.

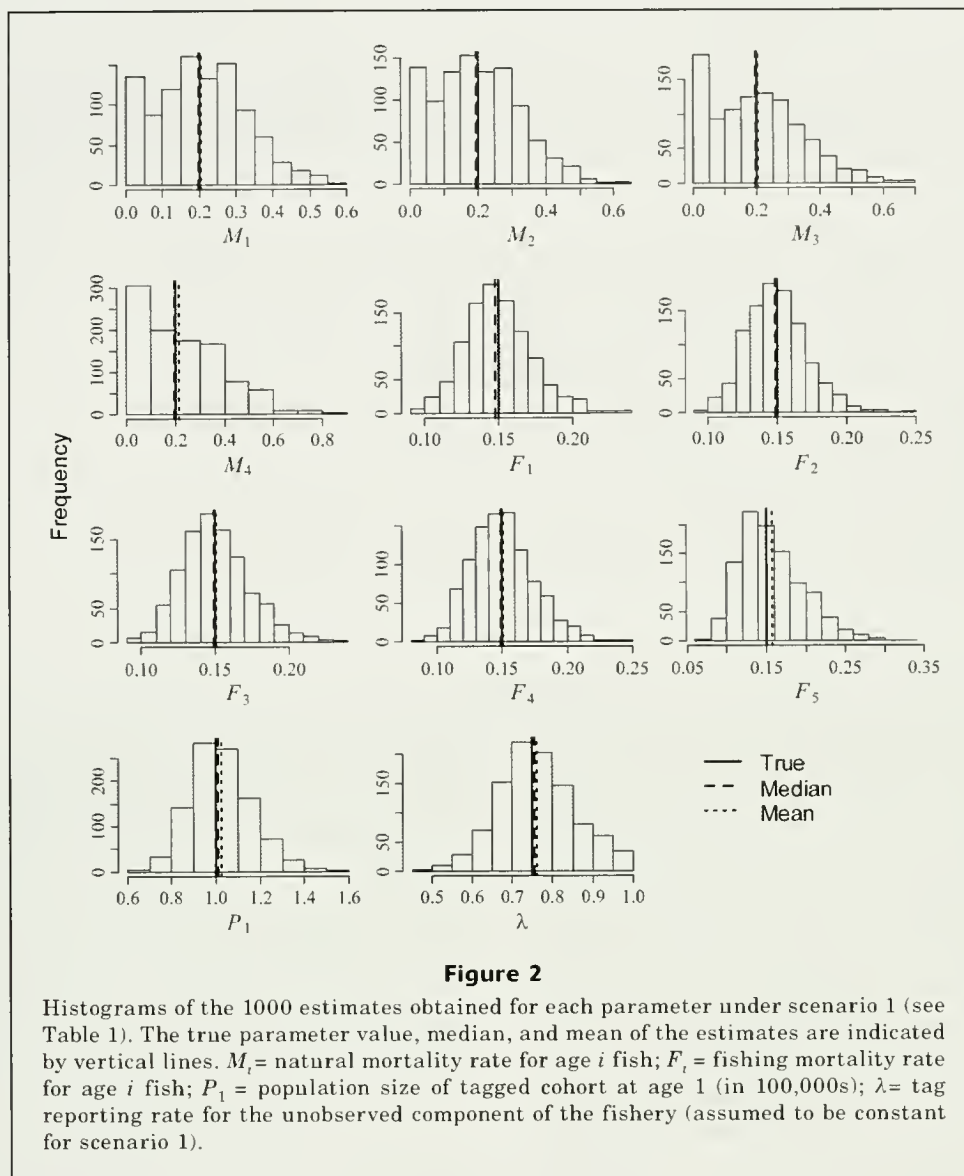
Scenario	M_1	M_2	M_3	M_4	F_1	F_2	F_3	F_4	F_5	P_1	λ_1	λ_2	λ_3	λ_4	λ_5
1	-1.0	-3.0	-1.5	-2.0	-1.3	-1.3	-0.7	-0.7	0.7	1.0	0.5	—	—	—	—
2	0.3	-1.3	-1.8	0.0	-0.7	-1.3	-0.7	0.0	0.7	1.0	0.0	—	—	—	—
3	0.0	-2.0	-1.5	0.5	-0.7	0.0	-0.7	-1.0	0.3	0.0	-0.1	—	—	—	—
4	1.5	-9.5	-4.0	-3.0	0.0	0.0	-0.7	1.3	1.3	0.0	-0.8	—	—	—	—
5	-2.0	-5.5	1.5	-0.5	0.0	-0.7	0.0	0.7	0.0	0.0	0.6	—	—	—	—
6	3.5	-1.5	-2.0	1.5	0.0	0.0	-1.3	-0.7	0.0	-1.0	0.4	—	—	—	—
7	-0.5	-13.0	-5.0	-16.0	-4.0	-2.0	-2.0	0.0	2.7	6.0	1.7	—	—	—	—
8	0.5	—	—	—	-2.0	-0.7	-0.7	-1.3	-0.7	1.0	0.4	—	—	—	—
9	1.5	-0.5	3.5	-0.5	-1.3	—	—	—	-0.7	1.0	0.5	—	—	—	—
10	-2.5	-3.0	-2.5	1.0	0.0	-1.3	-0.7	-0.7	1.3	0.0	-2.3	1.2	0.1	0.3	0.4
11	-5.5	-6.5	—	—	-0.7	-1.3	-3.3	—	—	1.0	1.6	—	—	—	—
12	1.5	-3.0	—	—	-0.7	-1.3	-0.7	-2.0	-2.0	1.0	0.4	—	—	—	—

**Figure 1**

Histograms of the 1000 estimates obtained for each parameter under scenario 7 (see Table 1). The true parameter value, median, and mean of the estimates are indicated by vertical lines. M_i = natural mortality rate for age i fish; F_i = fishing mortality rate for age i fish; P_1 = population size of tagged cohort at age 1 (in 100,000s); λ = tag reporting rate for the unobserved component of the fishery (assumed to be constant for scenario 7).

upper bound of 1.0, and the frequency was greatest in scenario 5 where the true value was 0.90. Nevertheless, the median biases were still small. The fishing mortality estimates generally had distributions that were right skewed, and the degree of skewness became more pronounced at older ages. The skewness was usually small enough that the mean and median were still similar (e.g., scenario 1; Fig. 2). However, this was not always true. For example, in scenario 7 (Fig. 1), the median bias for F_5 was 2.7%, whereas the mean bias was 13.3%.

In Polacheck et al. (2006), we used mean bias to summarize simulation results obtained with the BP model. This meant that positive biases in the fishing mortality estimates that increased with age were reported, as well as positive biases in the natural mortality estimates. Had median bias been used instead, the bias results would have been similar to those presented here (i.e., negative biases in the natural mortality estimates, and only small biases in any of the fishing mortality estimates). In retrospect, we believe that the median provides a more reliable measure of bias. This is especially true in cases where the estimates have a skewed distribution, but should also be true in cases where a large proportion of the estimates fall on a bound.



In regard to precision, we estimated fishing mortality rates, cohort size, and reporting rates with much greater precision (CVs generally in the range of 0.10 to 0.20) than that for the natural mortality estimates (CVs often exceeding 0.50) across all scenarios (Table 3). Only when natural mortality was constrained to be constant across ages (scenario 8) was reasonable precision achieved for this parameter (CV of 0.22). Of the fishing mortality parameters, the estimates for the oldest age of recapture (i.e., F_3 in scenario 11, F_5 in all other scenarios) always had the highest CV, and usually notably so.

Comparing the CVs for a specific scenario with those for scenario 1, we found that the results were generally predictable, at least in terms of direction (Table 3). For example, increasing the value used for the fishing mortality rate (scenario 3) or for the reporting rate (scenario 5) resulted in greater precision (i.e., lower

CVs) for all parameters, because these changes lead to more tag returns. The results for scenario 2 were not instantly as intuitive. We would expect increasing natural mortality to give higher CVs because more fish would die naturally, leaving fewer tagged fish to be caught. Although small increases were observed in the CVs for the other parameters, large decreases were observed for the natural mortality estimates. This serves as a reminder that the CV is calculated in relation to the true parameter value, and therefore direct comparisons for parameters whose true values have been changed are more complicated. When the SDs of the natural mortality estimates from scenario 2 were compared with those from scenario 1 instead of the CVs, they did in fact increase (although this may in part be due to the fact that fewer estimates are truncated at their lower bound of zero when the value used for natural mortality is higher).

Table 3

Coefficient of variation (CV) of the parameter estimates for each scenario listed in Table 1. Results were based on 1000 simulation runs per scenario. M_i = natural mortality rate for age i fish; F_i = fishing mortality rate for age i fish; P_1 = population size of the tagged cohort at age 1; λ_i = tag reporting rate for fish captured at age i in the unobserved component of the fishery.

Scenario	M_1	M_2	M_3	M_4	F_1	F_2	F_3	F_4	F_5	P_1	λ_1	λ_2	λ_3	λ_4	λ_5
1	0.62	0.62	0.72	0.87	0.15	0.14	0.15	0.16	0.27	0.14	0.13	—	—	—	—
2	0.40	0.43	0.47	0.55	0.17	0.17	0.17	0.19	0.30	0.16	0.14	—	—	—	—
3	0.46	0.51	0.55	0.69	0.12	0.11	0.12	0.12	0.21	0.11	0.10	—	—	—	—
4	0.72	0.74	0.79	0.98	0.15	0.15	0.15	0.17	0.32	0.15	0.13	—	—	—	—
5	0.56	0.59	0.66	0.82	0.14	0.13	0.13	0.15	0.25	0.12	0.10	—	—	—	—
6	0.39	0.42	0.46	0.58	0.09	0.09	0.09	0.10	0.15	0.09	0.07	—	—	—	—
7	0.94	0.90	0.99	1.28	0.25	0.24	0.25	0.27	0.47	0.23	0.19	—	—	—	—
8	0.22	—	—	—	0.15	0.14	0.15	0.15	0.17	0.13	0.13	—	—	—	—
9	0.62	0.59	0.64	0.56	0.13	—	—	—	0.19	0.14	0.13	—	—	—	—
10	0.66	0.64	0.73	0.88	0.15	0.15	0.16	0.17	0.29	0.13	0.22	0.20	0.18	0.18	0.18
11	0.72	0.85	—	—	0.18	0.19	0.27	—	—	0.18	0.17	—	—	—	—
12	0.61	0.63	—	—	0.16	0.16	0.21	0.37	0.75	0.15	0.14	—	—	—	—

Several other points are worth noting. Changing the level of overdispersion in the data (scenarios 6 and 7) had the greatest influence on the CVs across all parameters. The only exception was that constraining natural mortality to be constant (scenario 8) had a greater effect on the CV of the natural mortality-rate estimation. Constraining natural mortality to be constant (scenario 8) not only reduced the CV of the M estimate substantially, but also the CV of the F_5 estimate. Similarly, constraining fishing mortality to be linear (scenario 9) substantially reduced the CV of the F_5 estimate, but also the M_4 estimate, and to a lesser degree the M_3 estimate. Interestingly, however, neither of these constraints affected the CVs of the P_1 and λ estimates. Also of interest is that allowing reporting rates to vary across years (scenario 10) had only a small effect on the precision of the mortality rate and abundance estimates. The reporting-rate estimates themselves were less precise and had a high tendency to hit the upper bound of one, but usually these parameters are not the ones of primary interest. Lastly, we note that having five recapture years but only three release years (scenario 12) resulted in much higher CVs for the F_3 , F_4 , and F_5 estimates, and increasingly so with age (with a CV of 0.75 for F_5). Thus, having more recapture years allows for more years of fishing mortality rates to be estimated, but these estimates quickly become uninformative unless the number of release years is also increased.

High correlations were present between many of the parameter estimates (Table 4; results are shown for scenario 1, but the patterns are very similar for all scenarios). Given the nature of the model, high correlations were expected, and have already been documented and discussed for the BP model in Polacheck et al. (2006). For example, to yield the same number of tag returns in a particular year, a higher

estimate of fishing mortality for that year could be compensated by a higher estimate of natural mortality for the previous year, so that estimates of F_i and M_{i-1} tend to be positively correlated. Alternatively, it could be compensated by a higher estimate of the reporting rate; hence estimates of F_i and λ tend to be negatively correlated. When two parameters have highly correlated estimates, a large CV for one of these parameters will tend to mean a large CV for the other parameter. This may explain some of the results observed above. For example, in scenarios 1–7, 9, and 10, estimates of F_5 and M_4 were highly correlated; therefore the high uncertainty in F_5 is likely due to the very high uncertainty in M_4 . An analogous statement can be made about F_3 and M_2 in scenario 11. The high correlation between estimates of F_5 and M_4 also explains why, in scenarios 8 and 9, constraints that improved the precision of one of these parameters also improved the precision of the other.

The Hessian-based standard error estimates in relation to the standard errors derived from the simulations are presented in Table 5. In all of the scenarios with $q=3$, the Hessian-based standard errors were underestimated by a factor close to $\sqrt{3} = 1.73$, and had a mean across all parameters and scenarios of 1.67 (ranging from 1.45 to 1.91). In the scenario with $q=1$ (i.e., multinomial data), the Hessian-based and simulation-based standard errors were very similar, as expected. In the scenario with $q=9$, the Hessian-based estimates were underestimated by a factor reasonably close to $\sqrt{9}=3.0$ —the largest exception being a factor of 2.49 for P_1 . Nevertheless, these results indicate that if q can be estimated after fitting the model (e.g., from the residuals), then multiplying the Hessian-based standard error estimates by \sqrt{q} can provide improved, and perhaps adequate, estimates of the true standard errors. Further investigation of additional scenarios

Table 4

Correlation matrix for the parameter estimates obtained using scenario 1 (see Table 1). Results were based on 1000 simulation runs. M_i = natural mortality rate for age i fish; F_i = fishing mortality rate for age i fish; P_1 = population size of tagged cohort at age 1; λ = tag reporting rate for the unobserved component of the fishery (assumed to be constant for scenario 1).

	M_1	M_2	M_3	M_4	F_1	F_2	F_3	F_4	F_5	P_1	λ
M_1	1.00	-0.40	0.00	0.01	0.01	0.10	-0.07	-0.06	-0.03	0.55	0.14
M_2		1.00	-0.38	-0.06	-0.27	0.03	0.14	-0.06	-0.07	0.12	0.11
M_3			1.00	-0.35	-0.10	-0.25	0.08	0.26	-0.12	0.12	0.06
M_4				1.00	0.00	-0.04	-0.19	0.19	0.77	-0.01	0.06
F_1					1.00	0.47	0.40	0.37	0.27	-0.56	-0.61
F_2						1.00	0.49	0.38	0.27	-0.41	-0.63
F_3							1.00	0.52	0.25	-0.39	-0.63
F_4								1.00	0.59	-0.37	-0.59
F_5									1.00	-0.27	-0.39
P_1										1.00	0.67
λ											1.00

Table 5

Simulation-based standard error divided by Hessian-based standard error of the parameter estimates for each scenario listed in Table 1. Results were based on 1000 simulation runs per scenario. Recall that an overdispersion factor of $\varphi = 3$ was used in all scenarios except scenario 6, for which $\varphi = 1$, and scenario 7, for which $\varphi = 9$. M_i = natural mortality rate for age i fish; F_i = fishing mortality rate for age i fish; P_1 = population size of tagged cohort at age 1; λ_i = tag reporting rate for fish captured at age i in the unobserved component of the fishery.

Scenario	M_1	M_2	M_3	M_4	F_1	F_2	F_3	F_4	F_5	P_1	λ_1	λ_2	λ_3	λ_4	λ_5
1	1.71	1.64	1.76	1.75	1.60	1.60	1.69	1.70	1.73	1.54	1.76	—	—	—	—
2	1.65	1.74	1.74	1.70	1.62	1.66	1.67	1.74	1.75	1.54	1.69	—	—	—	—
3	1.68	1.74	1.71	1.78	1.61	1.64	1.73	1.65	1.77	1.47	1.68	—	—	—	—
4	1.73	1.77	1.72	1.74	1.56	1.59	1.62	1.66	1.78	1.55	1.75	—	—	—	—
5	1.65	1.68	1.69	1.70	1.54	1.61	1.64	1.66	1.73	1.48	1.82	—	—	—	—
6	1.01	1.02	0.99	0.99	0.99	0.99	0.97	1.03	0.98	1.00	0.97	—	—	—	—
7	3.07	2.97	3.00	3.20	2.67	2.73	2.86	2.86	3.05	2.49	3.08	—	—	—	—
8	1.72	—	—	—	1.62	1.63	1.73	1.71	1.76	1.53	1.76	—	—	—	—
9	1.70	1.64	1.72	1.58	1.62	—	—	—	1.71	1.53	1.76	—	—	—	—
10	1.74	1.66	1.77	1.76	1.45	1.47	1.57	1.58	1.68	1.50	1.62	1.65	1.59	1.62	1.68
11	1.69	1.70	—	—	1.64	1.64	1.70	—	—	1.56	1.70	—	—	—	—
12	1.69	1.65	—	—	1.61	1.66	1.70	1.73	1.91	1.56	1.73	—	—	—	—

may allow for more accurate correction factors to be developed.

Trade-off between number of tag releases and observer coverage

We first concentrated on the results for scenario 1, and how changes in N and δ affected the accuracy of the parameter estimates. For all parameters, biases in the median of the estimates decreased rapidly as N increased, especially between 250 and 1000 releases (Fig. 3). Biases also tended to decrease as δ increased, especially for P_1 , λ , and F_1 to F_3 . In any case, only the biases in natural mortality estimates at the lowest

release numbers ($N \leq 500$) were large enough to be of concern, and further investigation showed they were the result of a large proportion of the estimates falling on the lower bound of zero.

As seen in the previous section, evaluating biases could be complicated in some scenarios because of natural mortality estimates hitting a lower bound of zero, reporting-rate estimates hitting an upper bound of one, and fishing mortality estimates having right-skewed distributions, especially at older ages. These problems became more pronounced as N and δ decreased, such that with $N=250$ and $\delta=0.05$ the median and mean differed significantly for many parameters (e.g., M_4 had a median bias of -23% but a mean bias of +23%;

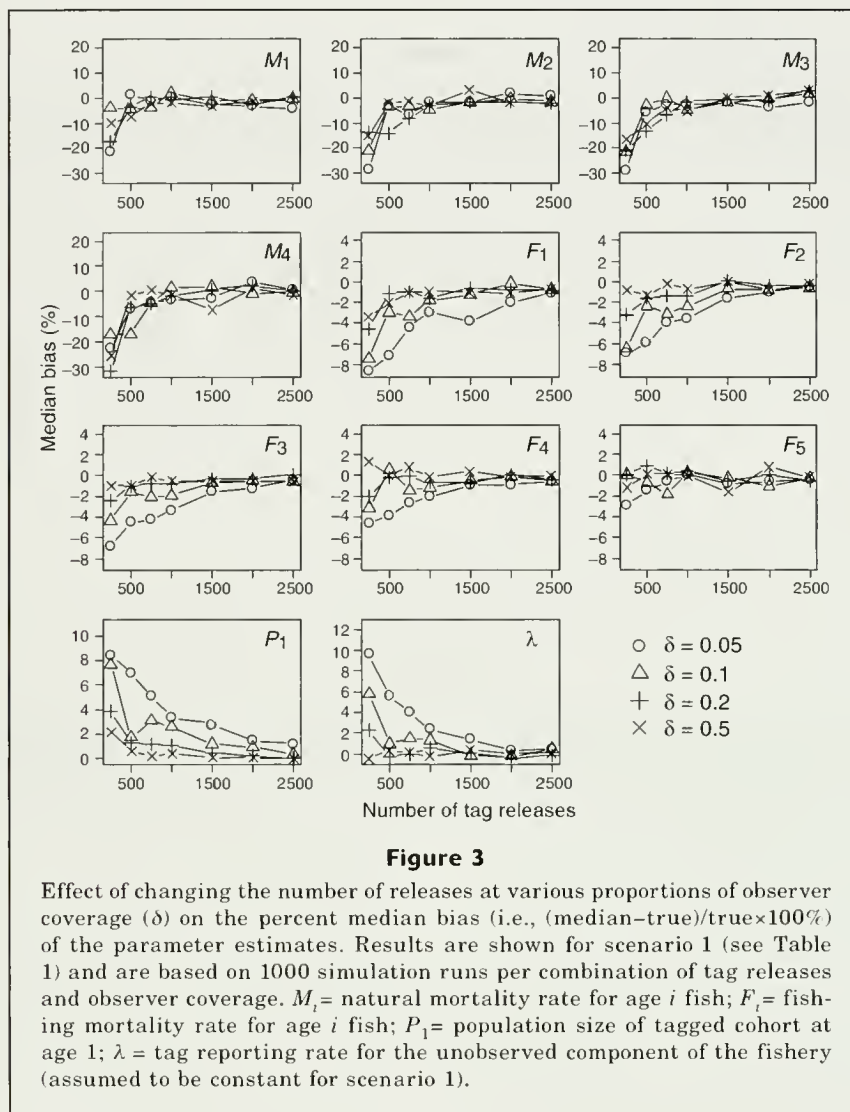


Figure 3

Effect of changing the number of releases at various proportions of observer coverage (δ) on the percent median bias (i.e., $(\text{median} - \text{true})/\text{true} \times 100\%$) of the parameter estimates. Results are shown for scenario 1 (see Table 1) and are based on 1000 simulation runs per combination of tag releases and observer coverage. M_i = natural mortality rate for age i fish; F_i = fishing mortality rate for age i fish; P_1 = population size of tagged cohort at age 1; λ = tag reporting rate for the unobserved component of the fishery (assumed to be constant for scenario 1).

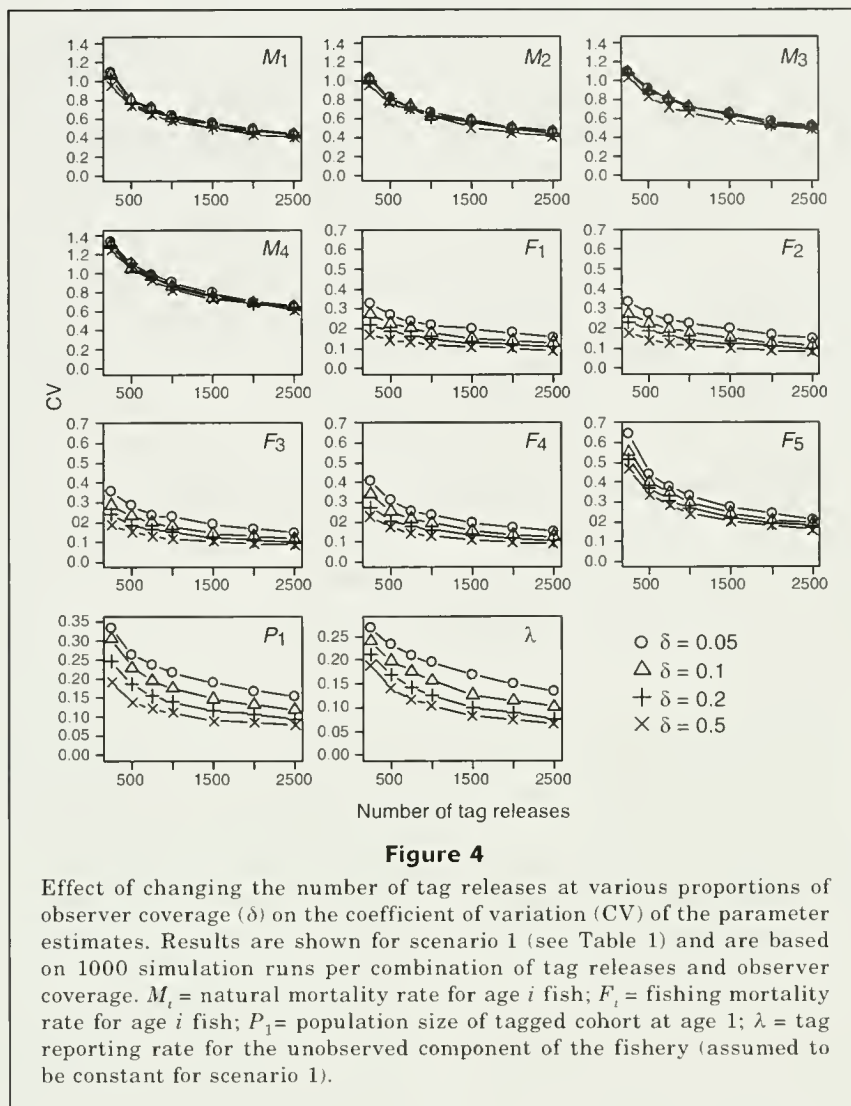
F_5 had a median bias of only -3% but a mean bias of $+16\%$). Thus, with small N and δ , the real issue was not with biases, but with the non-normality and very high variability (as seen next) of the estimates.

We now consider how changes in N and δ affected the precision of parameter estimates. For a given value of δ , increasing N reduced the CVs of all estimates in an exponential fashion (Fig. 4). For the fishing mortality estimates, the rate of decline became greater with age, and was particularly notable for F_5 . The CVs of the fishing mortality, abundance, and reporting rate estimates all decreased as δ increased; however, the natural mortality estimates did not change much. Overall, larger gains were achieved in the precision of the fishing mortality, abundance, and reporting rate estimates by increasing δ from 0.05 to 0.50 than by increasing N from 500 to 2500 (note that going from 250 to 500 releases led to significant decreases in the CVs of most parameter estimates). On the contrary, much larger gains were achieved in the precision of

the natural mortality estimates by increasing N than by increasing δ .

As a specific example of using such simulation results to aid in the design of a tagging study, suppose a researcher's goal was to achieve a CV of 0.20 or lower in the estimate of abundance. This could be accomplished under scenario 1 with the following: $N=250$ and $\delta=0.50$; $N=500$ and $\delta=0.20$; $N=1000$ and $\delta=0.10$; or, $N=2000$ and $\delta=0.05$. If, in addition, the researcher's goal was to achieve a CV of 0.30 or lower in all of the fishing mortality estimates, then only the latter two of these options would still be acceptable.

Although the magnitude of the CVs varied significantly between scenarios (as seen in Table 3), the relative changes that resulted from increasing N or δ were very similar to those seen for scenario 1. The most significant difference came from constraining natural mortality to be constant (scenario 8), in which case the precision of the natural mortality parameter became influenced by changes in δ (Fig. 5).



Discussion

The current article extends the integrated BP model for tag-recapture and catch data developed in Polacheck et al. (2006) to incorporate the estimation of reporting rates through observer data, which we refer to as the BPO model. This is an important and practical extension because nonreporting of tags is a serious problem in many commercial fisheries that needs to be accounted for in the model to obtain meaningful results, and observer data often provide the most viable means of doing so.

In the way the BPO model was formulated, increasing the level of observer coverage improves the parameter estimates not only by improving the reporting rate estimates, but also by improving the precision of the catch-at-age data. If all fish caught in the observer component were not sampled, then the improvements would not be expected to be as great. As an extreme case, the precision of the catch-at-age data could be assumed to be independent of the level of observer cov-

erage, in which case increasing the level of observer coverage would only improve the parameter estimates through the reporting-rate estimates. However, it is difficult to envisage a situation where observers would not take age or length samples from at least a portion of the catches.

In the study by Pollock et al. (2002), where a standard Brownie model was modified to include the estimation of reporting rates when one component of a multicomponent fishery has observers (i.e., 100% reporting rates), the authors show how the overall likelihood for their model can be partitioned into two conditionally independent components. They argue that the reporting rates can be estimated by maximizing the second likelihood component, and then plugged into the first component to estimate the mortality rates, and that doing so provides the maximum likelihood estimates of the reporting rates and mortality rates for the joint likelihood. Although a similar partitioning could be done for the BPO model, the estimates obtained from

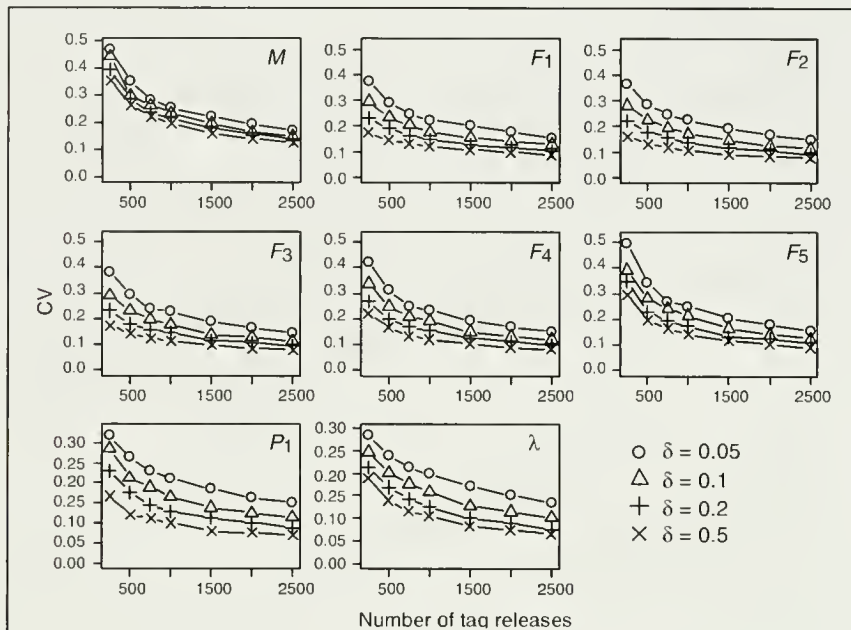


Figure 5

Effect of changing the number of tag releases at various proportions of observer coverage (δ) on the coefficient of variation (CV) of the parameter estimates. Results are shown for scenario 8 (see Table 1) and are based on 1000 simulation runs per combination of tag releases and observer coverage. M = natural mortality rate (assumed to be constant for scenario 8); F_i = fishing mortality rate for age i fish; P_1 = population size of tagged cohort at age 1; λ = tag reporting rate for the unobserved component of the fishery (assumed to be constant for scenario 8).

maximizing the separate components would not be the overall maximum likelihood estimates because there is information in the catch data about the mortality rates. Furthermore, we assert that even in the model by Pollock et al. (2002), the estimates obtained from the two-step likelihood procedure are only the maximum likelihood estimates of the overall likelihood when the reporting rates are allowed to vary by year and age, and not, as the study would indicate, when there are any constraints on these parameters.

The BPO model allows for simultaneous estimation of age-specific fishing mortality rates, natural mortality rates, and reporting rates, as well as cohort size at first tagging, for a cohort tagged in consecutive years. All parameters appear to be estimated with reasonable accuracy, but the level of precision that can be achieved varies greatly, depending on the specifics of the population, the fishery, and the experimental design, and also on the parameter. Nevertheless, some general observations can be made based on our simulations. Cohort size appears to be estimated well in all situations (with a CV between 0.10 and 0.20 in the majority of scenarios considered). With the exception of the oldest age of fish at recapture, the fishing mortality rates also tend to be estimated with good precision (CVs of less than 0.20 achievable in many situations).

In general, natural mortality is estimated poorly in comparison to the other parameters, with CVs above 0.60 in many cases. If, however, natural mortality can be assumed constant over enough release years (or otherwise constrained), then it too can be estimated with reasonable precision (e.g., CV on the order of 0.20 for our scenario 8 with 1000 releases per year).

Reducing the number of parameters that need to be estimated through imposing parameter constraints can greatly improve the accuracy and precision of the estimates. However, this is only true if the constraints imposed approximate reality; for example, modeling natural mortality as a constant will not lead to better parameter estimates if in fact natural mortality changes significantly with age. In practice, standard model selection techniques, such as Akaike's information criterion (AIC; Akaike, 1974) and its many variations (e.g., AIC_c for small sample sizes, QAIC for overdispersed data; see Burnham and Anderson, 1998, and references therein), can be used to determine which parameter constraints are most supported by the data.

For ease of presentation, the model was developed for, and applied to, one cohort of tagged fish. In practice, it is likely that several cohorts (i.e., age classes) would be tagged in each year of tagging. If all parameters being estimated are both year- and age-dependent, then

modeling multiple cohorts simultaneously will give very similar results to modeling each cohort individually. The results would be identical if the catch-at-age data for all cohorts were modeled as independent, but there is likely to be correlation between catch estimates for different cohorts in the same year that should be accounted for. If some constraints can be put on the parameters, such as natural mortality varying only with age or fishing mortality following an age selectivity curve, then precision in the parameter estimates should improve. For example, we re-ran the simulations for scenario 1 as described in the model performance section, but with data generated for three cohorts instead of one. In fitting the model, both natural mortality and fishing mortality were allowed to vary only with age. In comparison to the CVs obtained for scenario 1 with one cohort (Table 3), the CVs obtained with three cohorts were roughly 35–40% less for all parameters. Again, to determine which parameter constraints are most appropriate in a real situation, standard model selection procedures such as AIC can be used.

As was illustrated, the BPO model can be used to evaluate the effect of releasing more tags versus increasing observer coverage on the precision and bias of the parameter estimates. Because these programs can be costly to run and resources are usually limited, it is useful to have a statistical framework for comparing how alternate allocations of resources affect the results that can be achieved. Our results confirm the general conclusion of Polacheck and Hearn (2003) that it is important to ensure both adequate numbers of tag releases and adequate observer coverage (the latter for robust estimation of reporting rates, as well as for improved estimation of catch-at-age numbers in our model). However, while Polacheck and Hearn (2003) found a relatively direct trade-off between the level of observer coverage and number of tag releases with their approximate model, we found with our more comprehensive model that the trade-off depends on the parameters of interest. In particular, greater improvements could generally be achieved in the precision of the fishing mortality and cohort size estimates by increasing the proportion of observer coverage than by increasing the number of releases. On the contrary, much larger gains were achieved in the precision of the natural mortality-rate estimates by increasing the number of tag releases than by increasing the proportion of observer coverage. Although the results will be highly case-specific, these general observations were true in all of the scenarios we considered, and we expect they will hold true in a fairly wide range of scenarios. That being said, the purpose of the simulations was not to draw any specific conclusions, but to illustrate how the model can be used to provide practical guidance about the experimental design of a tagging study.

A version of the BPO model has been used to provide advice to the Commission for the Conservation of Southern Bluefin Tuna (CCSBT) on the levels of observer coverage and tag releases necessary to achieve their objectives for a long-term tagging program

conducted on SBT. To make the model more closely resemble the situation for SBT it was necessary to extend the model to a two-fishery situation with a purse-seine fishery and a longline fishery, where tag reporting rates were estimated from planted tags in the purse-seine fishery and from observer data in the longline fishery. Simulations, similar to those presented here, were conducted with input parameter values that best simulate the situation for SBT. The results showed that the numbers of tags that were being released each year were adequate, but that an increase in the CCSBT's target level of observer coverage from 10% to about 30% was required to meet the objectives of the program regarding precision of the mortality-rate estimates.

In summary, the model presented here provides a robust statistical framework for obtaining joint estimates of mortality rates and abundance from tagging data in situations where observers are present in the fishery. The model can be used to provide insight into design issues for those starting up new, or modifying current, tagging and observer programs for the purposes of estimating mortality rates and abundance.

Acknowledgments

We thank K. Pollock, D. Peel, and three anonymous reviewers for constructive comments and suggestions on drafts of this manuscript. The Australian Fisheries Research and Development Corporation (FRDC) provided funding support for this research.

Literature cited

- Akaike, H.
1974. A new look at the statistical model identification. IEEE (Inst. Electrical and Electronics Engineers) Transactions on Automatic Control 19:716–723.
- Brownie, C., D. R. Anderson, K. P. Burnham, and D. S. Robson.
1985. Statistical inference from band recovery data: a handbook, 2nd ed., 305 p. U.S. Fish Wildl. Serv. Resour. Publ. 156.
- Burnham, K. P. and D. R. Anderson.
1998. Model selection and inference: a practical information-theoretic approach, 353 p. Springer-Verlag, New York, NY.
- Cormack, R. M.
1964. Estimates of survival from the sighting of marked animals. Biometrika 51:429–438.
- Frusher, S. D., and J. M. Hoenig.
2001. Estimating natural and fishing mortality and tag reporting rate of southern rock lobster *Jasus edwardsii* from a multiyear tagging model. Can. J. Fish. Aquat. Sci. 58:2490–2501.
- Hampton, J.
2000. Natural mortality rates in tropical tunas: size really does matter. Can. J. Fish. Aquat. Sci. 57:1002–1010.
- Hearn, W. S., T. Polacheck, K. H. Pollock, and W. Whitelaw.
1999. Estimation of tag reporting rates in age-struct-

- tured multicomponent fisheries where one component has observers. *Can. J. Fish. Aquat. Sci.* 56:1255-1265.
- Hoenig, J. M., N. J. Barrowman, W. S. Hearn, and K. H. Pollock.
1998a. Multiyear tagging studies incorporating fishing effort data. *Can. J. Fish. Aquat. Sci.* 55:1466-1476.
- Hoenig, J. M., N. J. Barrowman, K. H. Pollock, E. N. Brooks, W. S. Hearn, and T. Polacheck.
1998b. Models for tagging data that allow for incomplete mixing of newly tagged animals. *Can. J. Fish. Aquat. Sci.* 55:1477-1483.
- Jolly, G. M.
1965. Explicit estimates from capture-recapture data with both death and immigration—stochastic model. *Biometrika* 52:225-247.
- Mosimann, J. E.
1962. On the compound multinomial distribution, the multivariate β -distribution, and correlations among proportions. *Biometrika* 49:65-82.
- Polacheck, T., J. P. Eveson, G. M. Laslett, K. H. Pollock, and W. S. Hearn.
2006. Integrating catch-at-age and multi-year tagging data: a combined Brownie and Petersen estimation approach in a fishery context. *Can. J. Fish. Aquat. Sci.* 63:534-538.
- Polacheck, T., and W. Hearn.
2003. Designing tagging programs for pelagic longline fisheries: trade-offs between the number of releases and observer coverage. *N. Am. J. Fish. Manage.* 23:810-821.
- Pollock, K. H.
1981. Capture-recapture models allowing for age-dependent survival and capture rates. *Biometrics* 37:521-529.
- Pollock, K. H., W. S. Hearn, and T. Polacheck.
2002. A general model for tagging on multiple component fisheries: an integration of age-dependent reporting rates and mortality estimation. *Environ. Ecol. Stat.* 9:57-69.
- Pollock, K. H., J. M. Hoenig, W. S. Hearn, and B. Calingaert.
2001. Tag reporting rate estimation: 1. An evaluation of the high-reward tagging method. *N. Am. J. Fish. Manage.* 21:521-532.
- Pollock, K. H., J. M. Hoenig, and C. M. Jones.
1991. Estimation of fishing and natural mortality when a tagging study is combined with a creel survey or port sampling. *Am. Fish. Soc. Symp.* 12:423-434.
- Schwarz, C. J., and G. A. F. Seber.
1999. Estimating animal abundance: review III. *Statist. Sci.* 14:427-456.
- Seber, G. A. F.
1965. A note on the multiple recapture census. *Biometrika* 52:249-259.
1982. The estimation of animal abundance and related parameters, 2nd ed., 654 p. Macmillan Publ. Co., New York, NY.

Abstract—The abundance and population density of cetaceans along the U.S. west coast were estimated from ship surveys conducted in the summer and fall of 1991, 1993, 1996, 2001, and 2005 by using multiple-covariate, line-transect analyses. Overall, approximately 556,000 cetaceans of 21 species were estimated to be in the 1,141,800-km² study area. Delphinoids (Delphinidae and Phocoenidae), the most abundant group, numbered ~540,000 individuals. Abundance in other taxonomic groups included ~5800 baleen whales (Mysticeti), ~7000 beaked whales (Ziphiidae), and ~3200 sperm whales (Physeteridae). This study provides the longest time series of abundance estimates that includes all the cetacean species in any marine ecosystem. These estimates will be used to interpret the impacts of human-caused mortality (such as that documented in fishery bycatch and that caused by ship strikes and other means) and to evaluate the ecological role of cetaceans in the California Current ecosystem.

Abundance and population density of cetaceans in the California Current ecosystem

Jay Barlow (contact author)¹

Karin A. Forney²

Email address for J. Barlow: Jay.Barlow@noaa.gov

¹ National Ocean and Atmospheric Administration
Southwest Fisheries Science Center
8604 La Jolla Shores Drive
La Jolla, California 92037

² NOAA Southwest Fisheries Science Center
110 Shaffer Road
Santa Cruz, California 95060

Estimates of cetacean abundance, biomass, and population density are key to assessing the potential effects of anthropogenic perturbations on cetacean populations (Carretta et al., 2006) and in understanding the ecological role of cetaceans in marine ecosystems (Trites et al., 1997). Along the U.S. west coast, most cetacean species are vulnerable as bycatch in gillnet fisheries (Julian and Beeson, 1998; Carretta et al., 2005), and fisheries catch many of the same species that cetaceans consume (Trites et al., 1997). Large whales also die from ship strikes (Carretta et al., 2006). West coast cetaceans may be affected by anthropogenic sound (e.g., sonar, ship noise, and seismic surveys) and climate change. There is little published information on current abundance to evaluate direct anthropogenic impacts on cetacean species and to estimate their resource needs.

The abundance of cetaceans along the U.S. west coast was previously estimated for some species in some areas, but most available estimates are based on surveys that were conducted 16 to 30 years ago (Dohl et al., 1986; Barlow, 1995). In addition, most estimates are based only on surveys that were conducted within 185 km of the coast. There was only one survey (in 1991) in waters greater than 185 km offshore of California, and there are no published estimates of cetacean abundance for far offshore waters of Oregon or Washington. The lack of recent estimates and the lack of es-

timates for offshore waters represent clear gaps in our knowledge of west coast cetaceans.

In this study, new estimates of abundance were determined in order to fill our gaps in knowledge about cetaceans in the California Current ecosystem. Line-transect methods were used to analyze data collected from Southwest Fisheries Science Center (SWFSC) ship surveys in 1991, 1993, 1996, 2001, and 2005 off the U.S. west coast. A new multiple-covariate, line-transect approach (Marques and Buckland, 2003) was used to account for multiple factors that affect the distance at which cetaceans can be seen in different conditions. Because cetaceans dive and can be missed by visual observers, the probability of detecting a group of cetaceans directly on the transect line was estimated from observations made by independent observers on those 1991–2005 surveys and from other sources. Observer-specific corrections were applied to remove a bias in estimating group sizes. These results represent one of the most comprehensive analyses of cetacean abundance and density for any large marine ecosystem.

Materials and methods

Survey

Surveys in 1991, 1993, 1996, 2001, and 2005 were conducted in summer

and fall with the same line-transect survey methods from two National Oceanographic and Atmospheric Administration (NOAA) research vessels: the 53-m RV *McArthur* and the 52 m RV *David Starr Jordan*. A third ship, the 62-m RV *McArthur II*, was also used for a very short time in 2005. Transect lines followed a grid that was established before each survey to uniformly cover waters between the coast and approximately 556 km (300 nmi) offshore. Surveys were designed with a uniform grid of transect lines anchored by a randomly chosen start point. Ships traveled at 16.7–18.5 km/h (9–10 kt) through the water. The 1991 and 1993 surveys only covered waters off California, but the subsequent surveys also included waters off Oregon and Washington (Fig. 1).

Experienced field biologists (henceforth referred to as “observers”) searched for cetaceans from the flying bridge deck of the ships (observation height ~10.5 m for the two primary vessels, 15.2 m for the RV *McArthur II*). Typically, six observers rotated among three observation stations (left station, where 25× binoculars were used; forward station where the data recorder was positioned; and right station, where 25× binoculars were used). Each observer and recorder watched for 2 hours and then rested for 2 hours. The recorder searched with unaided eyes (and occasionally 7× binoculars) and entered effort and sighting data using a data entry program on a laptop computer. The observers were selected on the basis of previous experience searching for and identifying marine mammals at sea; at least four observers on each ship had previous line-transect experience with cetaceans and at least two were experts in marine mammal identification at sea. Before each survey, observers were given a refresher course in marine mammal identification and group size estimation. Group size and the percentage of each species in a group were estimated and recorded independently and confidentially by each on-duty observer. Generally, after a group of cetaceans was seen, observers took as much time as necessary to estimate group size and species composition. Starting in 1996, at least one hour was allocated to group size estimation for sperm whales to provide reasonable confidence that all members of the group surfaced at least once. Species determinations were recorded only if observers were certain of their species identification; otherwise, animals were identified to the lowest taxonomic level or general category (e.g., large whale or baleen whale) that an observer could determine with certainty. Observers were also encouraged to record separately the most probable species if the actual species could not be determined with certainty. In this article, we used probable species identifications if certain identifications were missing, rather than prorating the unidentified sightings into species categories, as done in other studies (Gerrodette and Forcada, 2005). If probable species identifications were not available, species were classified as unidentified delphinoids, small whales, beaked whales, rorqual whales, or large whales. Common and scientific names for all species are given in Table 1.

Most surveys were conducted in closing mode during which the ship diverted from the trackline as necessary to allow closer estimation of group size and species composition. The ship was not diverted if observers felt that group size and species could be determined from the transect line, as was frequently the case of nearby sightings of Dall’s porpoise or large baleen whales. To investigate potential biases associated with the use of closing mode surveys, every third day of effort in 1996 was conducted in passing mode during which the ship did not divert from the trackline except for species of particular interest (sperm whales, short-finned pilot whales, and Baird’s beaked whales). No consistent biases were found between the two survey modes; however, group size estimation and species determination suffered in passing mode, and therefore the latter (passing mode) was not undertaken during subsequent surveys.

Frequently, a fourth observer searched for cetacean groups that were missed by the primary team of three observers. Sightings made by this fourth observer were recorded after the group had passed abeam and had been clearly missed by the primary team. The data from the fourth observer were considered conditionally independent of the primary team (conditioned on the animals not being seen by the primary team) and were used to estimate the proportion of sightings missed by the primary team.

Calibration of group size

Individual observers may tend to over- or under-estimate group sizes, and their estimates can be improved by calibration based on a subset of groups with known size (Gerrodette and Forcada, 2005) or based on comparison to data from an unbiased observer (Barlow, 1995). Calibration factors were used to correct estimates made by observers who were previously calibrated by using aerial photographic estimates of group size taken from a helicopter on dolphin surveys in the eastern tropical Pacific (Gerrodette and Forcada, 2005). These calibrations were not applied to groups whose size was outside the range of sizes used in the calibration study. A direct helicopter calibration could not be used on these west coast surveys because the weather was too rough and the water is too turbid. Therefore, we used an indirect calibration method (Barlow, 1995) to calibrate these remaining observers in relation to the directly calibrated observers. The indirect calibration coefficient, β_0 , for a given observer was estimated by comparison to calibrated estimates of directly calibrated observers by using log-transformed, least-squares regression through the origin:

$$\ln S^* = \beta_0 \cdot \ln \bar{S}, \quad (1)$$

where S^* = the observer’s best estimate of group size; and

\bar{S} = the mean of calibrated, bias-corrected estimates for all other calibrated observers.

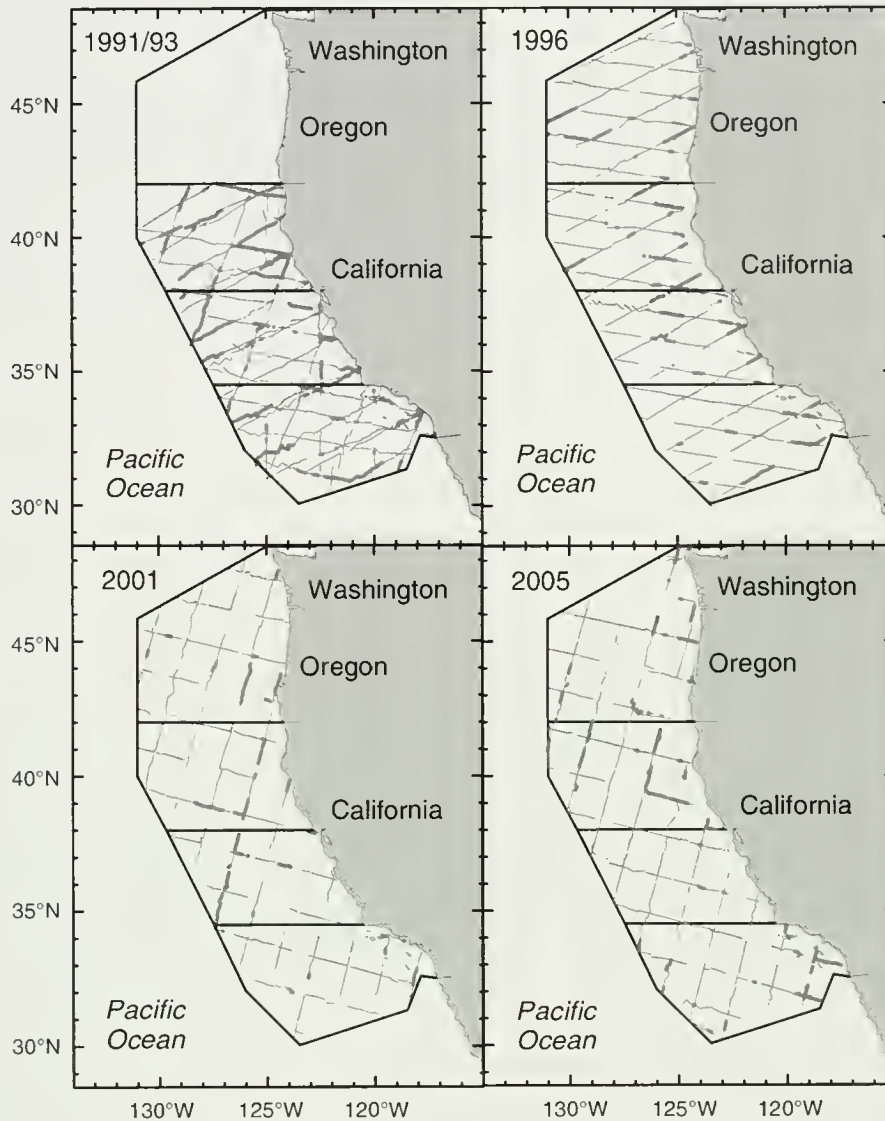


Figure 1

Transect lines (gray) surveyed during 1991 and 1993, 1996, 2001, and 2005 surveys. Thick transect lines were surveyed in Beaufort sea states of 0–2 and thin lines in Beaufort sea states 3–5. Black lines on all maps indicate the boundaries of the four geographic regions.

Logarithms were used in Equation 1 because standard errors were found to be proportional to the mean. Sightings were included in calculating indirect calibration coefficients if group size estimates were made by at least two other directly calibrated observers. We use a weighted geometric mean of the individual, calibrated group-size estimates (weighted by the inverse of the mean squared estimation error) as the best estimate of overall group size in all of the analyses presented here.

Estimation of abundance from line-transect data

Cetacean abundance was estimated by using line-transect methods (Buckland et al., 2001) with multiple covari-

ates (Marques and Buckland, 2003). The entire study area (1,141,800 km²) was divided into four geographic strata (Fig. 1): 1) waters off Oregon and Washington (322,200 km² north of 42°N); 2) northern California (258,100 km² south of 42°N and north of Point Reyes at 38°N); 3) central California (243,000 km² between Point Conception at 34.5°N and Point Reyes); and 4) southern California (318,500 km² south of Point Conception). The OR-WA region was not surveyed in 1991 or 1993 and thus received less survey effort. The density, D_i , for a given species within geographic region i was estimated as

$$D_i = \frac{1}{2L_i} \sum_{j=1}^{n_i} \frac{f(0|z_j) \cdot s_j}{g_j(0)}, \quad (2)$$

Table 1

Species groups that were pooled and the range of Beaufort sea states used in estimating line-transect detection probabilities as functions of perpendicular sighting distance and other covariates. Within a group, the indicated subgroups were identified and tested as covariates in the line-transect parameter estimation. When sample size and patterns of species co-occurrence permitted, groups and subgroups comprised only one species. Mean effective strip widths (ESWs) are the product of the truncation distance (W) and the mean probability of detection within that distance for each group.

Species group Subgroup Common name	Scientific name(s)	Beaufort sea state	Mean ESW (km)	Truncation distance, W (km)
Delphinids				
Small delphinids				
Short-beaked common dolphin	<i>Delphinus delphis</i>	0–5	2.22	4.0
Long-beaked common dolphin	<i>Delphinus capensis</i>	0–5	2.85	4.0
Unclassified common dolphin	<i>Delphinus</i> spp.	0–5	2.28	4.0
Striped dolphin	<i>Stenella coeruleoalba</i>	0–5	2.41	4.0
Pacific white-sided dolphin	<i>Lagenorhynchus obliquidens</i>	0–5	2.24	4.0
Northern right whale dolphin	<i>Lissodelphis borealis</i>	0–5	2.05	4.0
Unidentified delphinoid		0–5	1.71	4.0
Large delphinids				
Bottlenose dolphin	<i>Tursiops truncatus</i>	0–5	2.54	4.0
Risso's dolphin	<i>Grampus griseus</i>	0–5	2.37	4.0
Short-finned pilot whale	<i>Globicephalus macrorhynchus</i>	0–5	2.70	4.0
Dall's porpoise	<i>Phocoenoides dalli</i>	0–2	1.09	2.0
Small whales				
Small beaked whales				
<i>Mesoplodon</i> spp.	<i>Mesoplodon</i> spp.	0–2	2.85	4.0
Cuvier's beaked whale	<i>Ziphius cavirostris</i>	0–2	2.68	4.0
Unidentified ziphiid whale	<i>Mesoplodon</i> spp. or <i>Z. cavirostris</i>	0–2	2.95	4.0
<i>Kogia</i> spp.	<i>Kogia breviceps</i> or <i>Kogia sima</i>	0–2	1.01	4.0
Minke whale	<i>Balaenoptera acutorostrata</i>	0–2	2.16	4.0
Unidentified small whale		0–2	2.71	4.0
Medium-size whales				
Baird's beaked whale	<i>Berardius bairdii</i>	0–5	1.94	4.0
Bryde's whale	<i>Balaenoptera edeni</i>	0–5	3.54	4.0
Sei whale	<i>Balaenoptera borealis</i>	0–5	1.59	4.0
Sei or Bryde's whale	<i>B. edeni</i> or <i>B. borealis</i>	0–5	2.89	4.0
Fin, blue, and killer whales				
Fin whale	<i>Balaenoptera physalus</i>	0–5	2.61	4.0
Blue whale	<i>Balaenoptera musculus</i>	0–5	2.58	4.0
Killer whale	<i>Orcinus orca</i>	0–5	2.65	4.0
Humpback whale	<i>Megaptera novaeangliae</i>	0–5	3.20	4.0
Sperm whale	<i>Physeter macrocephalus</i>	0–5	2.97	4.0
Unidentified rorqual		0–5	2.70	4.0
Unidentified large whale		0–5	2.78	4.0

where L_i = the length of on-effort transect lines in region i ;

$f(0|z_j)$ = the probability density function evaluated at zero perpendicular distance for group j with associated covariates z ;

s_j = the number of individuals of that species in group j ;

$g_j(0)$ = the trackline detection probability of group j ; and

n_i = the number of groups of that species sighted in region i .

Annual abundances for each species in California (1991–2005) and in Oregon–Washington (1996–2005) were estimated from Equation 2 based on the sightings and search effort for the given year. The California total was the sum of the three California region. Because transects covered only 35 km in calm conditions in the central California region in 2005, that region was pooled in 2005 with the northern California region to estimate abundance for Dall's porpoises and small whales (whose abundance was based only on surveys in calm sea states—see below). Only half-normal detection

models were considered for estimating $f(0|z_j)$ because hazard-rate models have been shown to give highly variable estimates (Gerrodette and Forcada, 2005) and because hazard-rate models often did not converge on best-fit solutions. In estimating $f(0|z_j)$, data from all years and geographic strata were pooled, and species were pooled into groups with similar sighting characteristics (Barlow et al., 2001): delphinids (excluding killer whales); Dall's porpoise; small whales; medium whales; blue, fin, and killer whales; humpback whales; and sperm whales (Table 1). To improve the ability to fit the probability density function, $f(0|z_j)$, sightings were excluded if they were farther from the trackline than an established truncation distance (Buckland et al., 2001): 2 km for Dall's porpoises and 4 km for all other species. This procedure eliminated approximately 15% of sightings. The covariates for the $f(0)$ function were chosen by forward step-wise model building by using the corrected Akaike information criterion (AIC_c). Potential covariates included the total group size or its natural logarithm ($TotGS$ or $LnTotGS$), Beaufort sea state ($Beauf$), survey year ($Year$: 1991, 1993, 1996, 2001, or 2006), survey vessel ($Ship$: *McArthur* or *Jordan*), geographic region ($Region$), the presence of rain or fog within 5 km of the ship ($RainFog$), the presence of glare on the trackline ($Glare$), the estimated visibility in nautical miles (Vis), the method used to first detect the group ($Bino$: 25× binoculars or other tool), and the cue that first drew an observer's attention to the presence of a group (Cue : splash, blow, or other). As covariates, $TotGS$, $LnTotGS$, $Beauf$, and Vis were treated as continuous variables and the others as categorical. Categorical covariates were used only if all factor levels had at least ten observations. See Barlow et al. (2001) for a more complete description of these covariates and their influence on the distance at which various species can be seen. When sample size permitted, another covariate ($SppGroup$, a coded value for the most abundant species within a group) was added to sub-stratify a species group, allowing for differences in detection distances between members of the *a priori* species groupings (Table 1). Because very few cryptic species, such as small whales and Dall's porpoise, are seen in rough conditions and sample sizes were too small to estimate $g(0)$ for those conditions, the abundance of these species was estimated by using search effort conducted only in calm seas (Beaufort sea state 0 to 2); abundance of other species was based on search effort in Beaufort sea states 0 to 5.

Some animals sighted could not be identified to species or probable species, and, for completeness, we also estimated the abundance of the cetaceans represented by these sightings. Sample sizes were small; therefore these unidentified categories were pooled with other similar species for estimating $f(0|z_j)$. Unidentified delphinoids were pooled with all delphinids; unidentified small whales were pooled with *Ziphius*, *Mesoplodon* and *Kogia* spp.; unidentified rorquals were pooled with all rorqual species; and unidentified large whales were pooled with rorquals and sperm whales.

In traditional (noncovariate) line-transect analyses, effective strip width (ESW) gives a measure of the distance from the trackline at which species were seen (with an upper limit defined by a chosen truncation distance). For the covariate line-transect method, ESW varies with the covariates for each sighting. The mean ESW was calculated as the truncation distance multiplied by the mean probability of detecting a group within that distance for all sightings of a species.

The total abundance, N , for a species was estimated as the sum over the four geographic regions of the densities, D_i , in each stratum multiplied by the size of the stratum, A_i :

$$N = \sum_{i=1}^4 D_i \cdot A_i. \quad (3)$$

Abundance and density were not estimated for harbor porpoises (*Phocoena phocoena*), gray whales (*Eschrichtius robustus*), or the coastal stock of bottlenose dolphins (*Tursiops truncatus*) because their inshore habitats were inadequately covered in our study and because good abundance estimates are available for these species from specialized studies (Carretta et al., 1998; Rugh et al., 2005; Carretta et al., 2006).

The areas, A_i , within each stratum were limited to waters deeper than 20 m (the safe operating limit of the vessels). The total areas between the coast and the offshore boundaries were estimated with the program GeoArea (available from Gerrodette¹). The stratum areas were estimated by subtracting the area between 0 and 20 m depth (and the areas of the Channel Islands in the southern California stratum) from these total areas. The area between the 0- and 20-m depth contours in the southern California stratum (including the Channel Islands) was estimated with the ArcGIS 9.1 software package. The 20-m contour was derived from a bathymetry data set with grids providing 200 m horizontal resolution, 0.1 m vertical resolution) from the California Department of Fish and Game, Marine Region. Coastline data from the NOAA National Ocean Service Medium Resolution Digital Vector Shoreline (1:70,000 scale) was used for the 0-m contour.

The coefficients of variation (CV) for abundance were estimated by using mixed parametric and nonparametric bootstrap methods (Efron and Gong, 1983). Variance attributed to sampling and model fitting were estimated with the nonparametric bootstrap method by using 150-km segments of survey effort as the sampling unit (roughly the distance surveyed in one day). Adjacent survey segments, sometimes from different days, were appended together to make bootstrap segments. A new bootstrap segment was begun for each survey and whenever a ship crossed into a new region. Within each geographic region, effort segments were

¹ Gerrodette, T. 2007. National Oceanic and Atmospheric Administration, Southwest Fisheries Science Center, 8604 La Jolla Shores Dr., La Jolla CA 92037. Website: <http://swfsc.noaa.gov/prd.aspx> (accessed 26 June 2007).

sampled randomly with replacement from all survey years, and the sightings associated with those segments were used with step-wise model building to fit the multiple-covariate model of $f(0|z_j)$. For each of 1000 bootstrap iterations, a parametric bootstrap was used to choose the values of $g(0)$ by drawing randomly from a logit-transformed normal distribution with a mean and variance selected to give the values of $g(0)$ and $CV(g(0))$ used for abundance estimation.

Probability of detection of a cetacean group along the trackline

The line-transect parameter $g(0)$ represents the probability of detecting a group that is located directly on the transect line. This value is often assumed to be 1.0 in estimating abundance for dolphins that are found in large groups (Gerrodette and Forcada, 2005); therefore, in these analyses it was implicit that 100% of the groups located on the trackline were detected. In our study, for dolphins, porpoises, and large baleen whales, data from the conditionally independent observer were used to estimate the trackline detection probability for the primary observer team, $g_1(0)$, with the method developed by Barlow (1995):

$$g_1(0) = 1.0 - \frac{n_{w2} \cdot f_2(0)}{n_{w1} \cdot f_1(0)}, \quad (4)$$

where the subscript 1 refers to parameters for the primary observers, subscript 2 refers to parameters for the conditionally independent observer, and n_w = the number of sightings within the truncation distance w used for estimating the line-transect parameter $f(0)$.

Sightings by the primary team were included in estimating n_1 and $f_1(0)$ only if a conditionally independent observer was also on duty. This estimator (Eq. 4) is positively biased (Barlow, 1995), which results in an overestimation of $g(0)$ for the primary observers. Fully independent observer methods (Buckland et al., 2004) are generally superior to this conditionally independent method (referred to as the "removal method" by Buckland et al. [2004]); however, such methods could not be used because of the need to approach groups to determine species and estimate group sizes. The line-transect parameter $f(0)$ was estimated independently for the primary and independent observers with the software program Distance 5.0 (available from Thomas²); half-normal models were fitted with cosine adjustments (Buckland et al., 2001), and the best-fit model was selected by AIC_c . Because of sample size limitations, species were pooled into three categories for estimating $g(0)$: 1) delphinids (excluding killer whales),

2) large whales (most baleen whales and killer whales), and 3) Dall's porpoises. Killer whales were included with large baleen whales because they are very conspicuous and are seen at greater distances than are other delphinids (Barlow et al., 2001). Because trackline detection probabilities may vary with the size of the group (Barlow, 1995) or observation conditions, the numbers of sightings made by primary and independent observers were tested with Fisher's exact test to determine if the proportion varied with group size or Beaufort sea state. Delphinids and large whales were stratified into large and small groups with cut-points at 20 and 3 individuals, respectively. Because of sample size limitations, a single detection function was fitted to large and small groups of delphinids seen by the independent observer. Estimates of $g(0)$ were stratified if this test was significant for either factor. Data for estimating $g(0)$ included transects covered on the preplanned survey grid and during more opportunistic survey periods, such as transits from a port to the starting point on the survey grid. Coefficients of variation for $g(0)$ estimates from the conditionally independent method were based on Equation 9 in Barlow (1995).

The above conditionally independent observer method for estimating $g(0)$ requires that all animals be available to be seen by the primary observer team. This approach does not work with long-diving species that may be submerged for the entire time that the ship is within visual range. Values of $g(0)$ for sperm whales, dwarf sperm whales, pygmy sperm whales, and all beaked whales were taken from a model of their diving behavior, detection distances, and the searching behavior of observers (Barlow, 1999).

Trackline detection probabilities for minke whales posed a special problem. Insufficient sightings were made to estimate $g(0)$ from the conditionally independent observer method (only one conditionally independent sighting was made) and insufficient information exists on their diving behavior to use the modeling approach. Here we assumed that $g(0)$ for minke whales was similar to that for small groups of delphinids (but see "Discussion" section).

Results

Surveys

Survey effort in Beaufort sea states from 0 to 5 covered the study areas fairly uniformly (Fig. 1). Although not all the planned transects were surveyed (because of inclement weather and mechanical breakdowns), the holes in the survey grid were small in relation to the entire study area, and all areas appeared to be well represented. Survey effort in calm sea conditions (Beaufort states 0–2) was not as uniformly distributed (Fig. 1) and was particularly poor in the Oregon-Washington region. Survey effort varied among years because of the availability of ship time.

² Thomas, L. 2005. Research Unit for Wildlife Population Assessment, University of St. Andrews, Scotland, UK. Website: <http://www.ruwpa.st-and.ac.uk/distance/> (accessed 26 June 2007).

Table 2

Numbers of sightings (n) and mean group sizes for all species in the four geographic regions. For each group, size was estimated as the geometric mean of the observers' individual estimates and therefore is not necessarily an integer. The mean for each region is an arithmetic mean over all groups used in the abundance estimation. The overall mean group size is an average of all regions weighted by the number of sightings in each region.

Species	Southern California		Central California		Northern California		Oregon-Washington		All regions
	n	Mean group size	n	Mean group size	n	Mean group size	n	Mean group size	Mean group size
Short-beaked common dolphin	239	168.0	165	142.7	52	210.2	3	238.3	164.1
Long-beaked common dolphin	16	286.6	3	465.8	0	—	0	—	314.9
Unclassified common dolphin	17	67.6	11	19.8	1	8.0	0	—	47.4
Striped dolphin	37	67.2	22	28.6	13	33.8	1	2.2	48.7
Pacific white-sided dolphin	15	33.7	19	153.8	18	59.0	19	57.0	78.5
Northern right whale dolphin	12	13.9	13	45.0	17	20.9	18	35.4	29.1
Bottlenose dolphin	31	13.4	4	4.0	3	10.0	0	—	12.2
Risso's dolphin	50	15.1	25	32.1	13	16.4	22	29.7	22.0
Short-finned pilot whale	1	31.6	1	9.6	3	16.3	0	—	18.0
Killer whale	2	4.1	6	4.9	5	8.1	10	7.5	6.6
Dall's porpoise	5	2.5	27	3.8	115	3.6	67	3.7	3.6
<i>Mesoplodon</i> spp.	1	2.3	4	1.3	4	2.4	2	2.2	2.0
Cuvier's beaked whale	3	2.7	10	2.5	4	2.8	0	—	2.6
Baird's beaked whale	1	7.0	3	14.5	3	13.8	8	5.9	9.3
<i>Kogia</i> spp.	0	—	3	1.5	1	1.0	1	1.0	1.3
Sperm whale	19	8.1	5	7.2	22	8.5	9	7.6	8.1
Minke whale	4	1.6	7	1.1	4	1.1	3	1.0	1.2
Bryde's whale	0	—	1	2.1	0	—	0	—	2.1
Sei whale	0	—	2	1.0	3	1.8	2	1.3	1.4
Sei or Bryde's whale	2	1.0	2	1.0	0	—	0	—	1.0
Fin whale	35	2.4	100	2.4	51	2.1	28	1.3	2.2
Blue whale	106	1.8	67	1.8	18	1.5	7	1.0	1.8
Humpback whale	5	2.1	83	2.0	16	1.7	25	1.7	1.9
Unidentified delphinoid	14	44.9	18	13.6	10	5.4	4	4.8	20.6
Unidentified ziphiid whale	2	1.7	1	1.0	3	1.3	0	—	1.4
Unidentified small whale	7	1.5	1	1.1	3	1.4	1	1.0	1.4
Unidentified roqual whale	4	2.4	26	1.4	7	1.0	7	1.0	1.4
Unidentified large whale	12	1.5	8	1.7	7	1.4	3	1.4	1.5

The number of sightings of most species varied among geographic regions (Table 2). Short- and long-beaked common dolphins and striped dolphins were seen much more frequently in central and southern California. Dall's porpoises were seen much more commonly in the northern California and Oregon-Washington regions. The number of sightings of other dolphin species (including Risso's dolphins, Pacific white-sided dolphins, northern right whale dolphins, and killer whales) showed no clear pattern with geographic region. Dolphin group sizes were generally largest for the two species of common dolphin, but Pacific white-sided dolphins were consistently found in large groups in the central California region (Table 2). Blue whales were the most commonly seen baleen

whale in the southern region, but were replaced by fin whales and humpback whales as the most common baleen whale in the northern regions (Table 2). The sighting locations are illustrated in Figure 2 for some common species. Locations of sightings of all species have been provided in the reports for each survey (Hill and Barlow, 1992; Mangels and Gerrodette, 1994; Von Sauner and Barlow, 1999; Appler et al., 2004; Forney, 2007).

Cetaceans were often found in mixed species assemblages. In some cases, species were obviously traveling together in close association; in other cases, the individual species may have been in the same area because they were feeding on the same resource or were there by coincidence. Some species (striped dolphins, bottle-

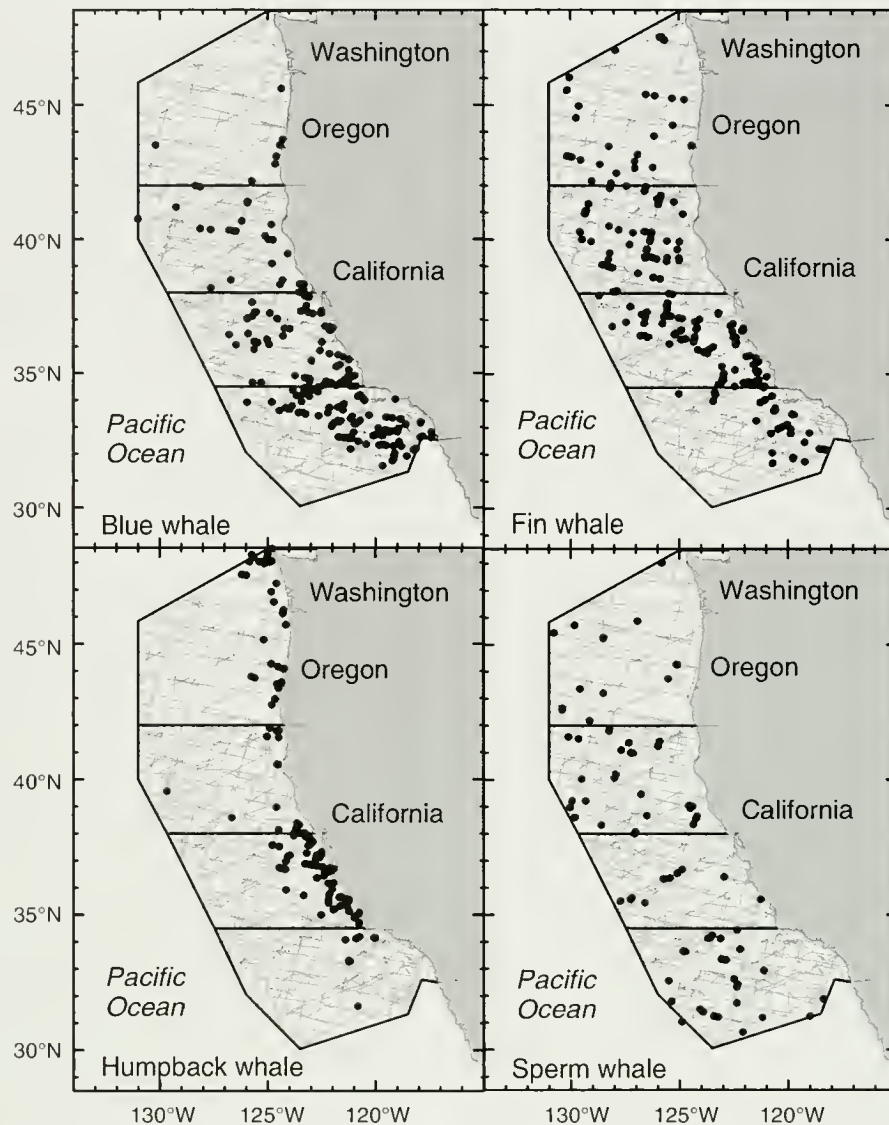


Figure 2

Sighting locations (•) for the species most commonly seen on the 1991–2005 surveys. Light gray lines indicate transects surveyed, and black lines indicate the four geographic regions.

nose dolphins, and Pacific white-sided dolphins) were found with other species more often than they were found alone, indicating that these associations were not coincidental.

Calibration of group size

Most regression coefficients for the indirect method of group-size calibration were less than one, indicating that observers were more likely to underestimate group size. For all groups and all species in this study, the ratio of the sum of all uncalibrated group sizes divided by the sum of all calibrated group sizes was 0.79. The mean ratio of calibrated to uncalibrated group size estimates was 0.92. This difference implies that proportionately larger corrections were applied to larger groups.

Probability of detection along the trackline

New trackline detection probabilities, $g(0)$, were estimated from sightings that were made by the independent observers but missed by the primary observers (Table 3). Beaufort sea state was not a significant factor in the numbers of delphinids or large whales seen by the independent observers (Fisher's exact test, $P=0.60$ and 0.87 , respectively). Group size was a significant factor for delphinids ($P<0.0001$), but not for large whales ($P=0.79$). Consequently, estimates of $g(0)$ for delphinids were stratified by group size. The number of Dall's porpoise sightings by independent observers ($n=12$) was insufficient to stratify estimates of $g(0)$ for this species. Values of $g(0)$ from the literature that were used for other long-diving species are given in Table 4.

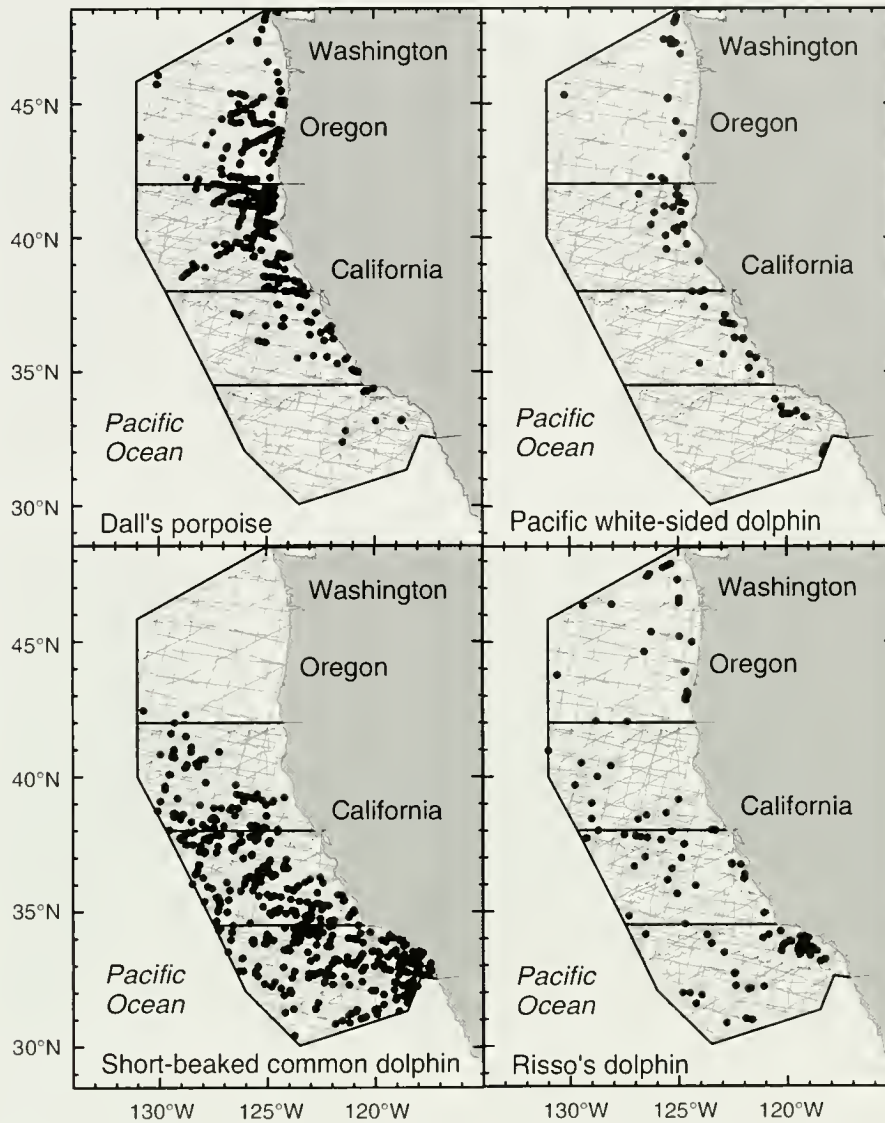


Figure 2 (continued)

Estimation of abundance from line-transect data

Short-beaked common dolphins dominated the abundance estimates for all regions except Oregon-Washington (Table 5), both because of the large number of sightings and the large group sizes for this species. Dall's porpoise was, by far, the most abundant small cetacean in the Oregon-Washington region (Table 5). Short-beaked common dolphins and Dall's porpoises together represented approximately 81% of all delphinoids and 79% of all cetaceans, and baleen whales (mysticetes) represented only about 1% of the total estimated cetacean individuals along the U.S. west coast (Table 6).

The estimated abundance of most species varied considerably among years (Tables 7 and 8). In large part, the year-to-year variation in abundance for most species could be attributed to low sample size and sampling variation; however, the distributions of all spe-

cies extended beyond the boundaries of the study area and some of the annual variation was likely due to a different portion of a larger population being in the study area within a given year (Forney and Barlow, 1998). Because all years and all regions were pooled for estimating the line-transect parameters, the abundance estimates for different regions (Table 5) and for different years (Tables 7 and 8) were correlated and these estimates cannot be used in standard statistical tests of difference among regions or among years.

The most important covariates, z , for estimating line-transect function $f(0|z)$ varied among species and species groups (Table 4). Covariates appearing in more than one model were *Bino*, *Beauf*, *LnTotGS*, *Ship*, and *RainFog*. In addition to these, a covariate that coded for difference among species within a group (*SppGrp*) was chosen in the model for delphinids (large vs. small delphinids) and for small whales (beaked whales vs. *Kogia* spp. vs. minke whales). The mean ESWs for most

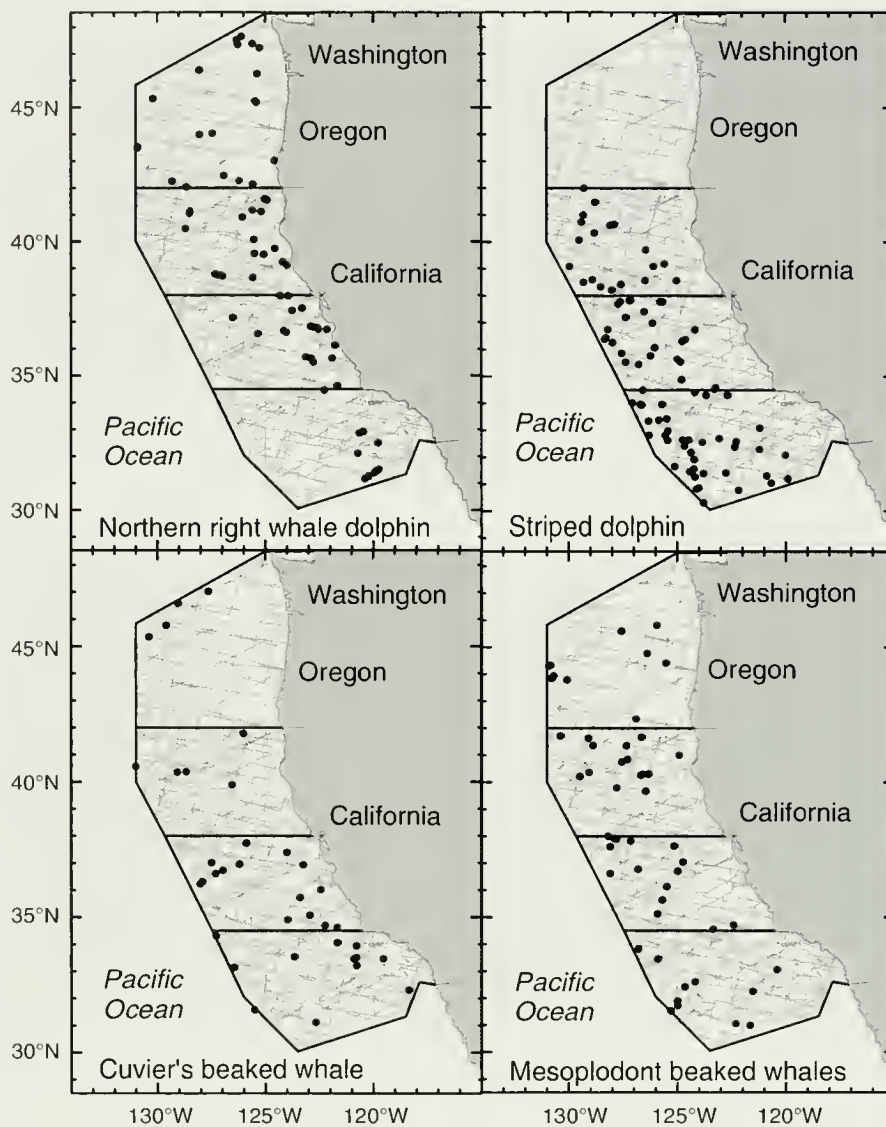


Figure 2 (continued)

species were between 2 and 3 km (Table 1). Dall's porpoise and *Kogia* species had the narrowest effective strip widths (~1 km), and humpback whales had the greatest values (~3.2 km).

Discussion

Abundance and density of cetaceans

Delphinidae Delphinids off the U.S. west coast can be classified as warm-temperate (short- and long-beaked common dolphins, striped dolphins, and short-finned pilot whales), cold-temperate (Pacific white-sided dolphins and northern right whale dolphins), or cosmopolitan (Risso's dolphin, bottlenose dolphins, and killer whales). The warm temperate species are generally more common in southern and central California,

and the cold-temperate species are more common in the northern California and Oregon-Washington regions. In 1996, when waters were relatively cool off California, the abundance of striped dolphins (the most tropical species) was lower than average and the abundance of the two cold-temperate species was higher. Four of the five sightings of short-finned pilot whales were in 1993, a warm year. All four species have distributions that extend outside our study area. These changes in abundance are consistent with shifts in the distribution of these species into and out of our study area with changes in water temperature. The tendency for these species to change distribution with water temperature is also seen in seasonal distribution changes (Forney and Barlow, 1998). The abundance of common dolphins and the cosmopolitan species did not vary consistently with warm and cold years (Table 7).

Table 3

Trackline detection probabilities, $g(0)$, estimated with the conditionally independent observer method for delphinids, large whales, and Dall's porpoises. Values of $g(0)$ were derived from the estimated probability density functions evaluated at zero distance, $f(0)$, for sightings made by primary observers (n_1) and independent observers (n_2) (Eq. 4). Coefficients of variation (CV) are given for $f(0)$ and $g(0)$ values. Delphinids include all species except killer whales and are stratified into small (≤ 20) and large (>20) groups. Large whales include killer whales and all baleen whales, except minke whales.

Species groups and group size strata	Primary observers			Independent observers				
	n_1	$f(0)$	CV $f(0)$	n_2	$f(0)$	CV $f(0)$	$g(0)$	CV $g(0)$
Delphinids (truncation distance=1 km)								
Group size ≤ 20	141	2.74	0.13	25	2.23	0.21	0.856	0.056
Group size >20	188	1.60	0.11	4	2.23	0.21	0.970	0.017
Large whales (truncation distance=2.5 km)								
All group sizes	296	0.58	0.05	32	0.42	0.19	0.921	0.023
Dall's porpoises (truncation distance=1 km)								
All group sizes	115	1.34	0.09	12	2.30	0.34	0.822	0.101

Table 4

The covariates selected for the best-fit line-transect models and the trackline detection probabilities ($g(0)$ and its coefficient of variation, CV, in parentheses) for each of the species and species groups used for abundance estimates. Covariates in parentheses were not included in all of the models that were averaged. The species group (*SppGrp*) covariate allowed variation in the scale factor of the detection function for different subgroups within a species group for delphinids (small delphinids vs. large delphinids—see Table 1) and small whales (small ziphiids vs. *Kogia* spp. vs. minke whales). Other selected covariates included binocular type (*Bino*), total group size (*TotGS*), the logarithm of total group size (*LnTotGS*), Beaufort sea state (*Beauf*), survey vessel (*Ship*), initial sighting event (*Cue*), the presence of rain or fog (*RainFog*), visibility (*Vis*), and geographic region (*Region*). Values of $g(0)$ are from Table 3, Barlow (1999), and Barlow and Taylor (2005).

Species Species group	Best-fit line-transect model	Small groups		Large groups	
		$g(0)$	CV $g(0)$	$g(0)$	CV $g(0)$
Delphinids	<i>Bino+Beauf+LnTotGS+Cue+SppGrp+Ship</i>	0.856	(0.056)	0.970	(0.017)
Dall's porpoise	<i>Bino+Ship (+LnTotGS+RainFog)</i>	0.822	(0.101)	0.822	(0.101)
Small whales	<i>SppGrp (+LnTotGS+TotGS+Ship+Beauf)</i>				
<i>Mesoplodon</i> spp.		0.450	(0.230)	0.450	(0.230)
Cuvier's beaked whale		0.230	(0.350)	0.230	(0.350)
Unidentified ziphiid whale		0.340	(0.290)	0.340	(0.290)
<i>Kogia</i> spp.		0.350	(0.290)	0.350	(0.290)
Minke whale		0.856	(0.056)	0.856	(0.056)
Unidentified small whale		0.856	(0.056)	0.856	(0.056)
Medium-size whales	<i>Vis+Beauf (+LnTotGS+TotGS+Ship)</i>				
Baird's beaked whales		0.960	(0.230)	0.960	(0.230)
Bryde's and sei whales		0.921	(0.023)	0.921	(0.023)
Fin, blue, and killer whales	<i>Bino+RainFog+Region (+Ship)</i>	0.921	(0.023)	0.921	(0.023)
Humpback whale	<i>Null model</i>	0.921	(0.023)	0.921	(0.023)
Sperm whale	<i>Null model (+LnTotGS+Ship+Vis)</i>	0.870	(0.090)	0.870	(0.090)
Unidentified rorqual	<i>Bino+RainFog+LnTotGS</i>	0.921	(0.023)	0.921	(0.023)
Unidentified large whale	<i>Bino+RainFog+LnTotGS (+Ship)</i>	0.921	(0.023)	0.921	(0.023)

Table 5

Estimated abundances (N) and coefficients of variation (CV) for each species in each of the four geographic regions. Data from 1991 to 2005 were pooled. CVs were not available (NA) if no sightings were made. Variances were assumed to be additive in estimating the CVs of the column totals. Unidentified large whales and small whales were not sufficiently specified to be included in the subtotals.

Species	Southern California		Central California		Northern California		Oregon–Washington	
	Abundance N	CV(N)	Abundance N	CV(N)	Abundance N	CV(N)	Abundance N	CV(N)
Short-beaked common dolphin	165,400	0.19	115,200	0.21	66,940	0.42	4555	0.77
Long-beaked common dolphin	17,530	0.57	4375	1.03	0	NA	0	NA
Unclassified common dolphin	4281	0.85	1313	0.49	35	1.00	0	NA
Striped dolphin	12,529	0.28	2389	0.42	4040	0.76	16	1.07
Pacific white-sided dolphin	2196	0.71	9486	0.74	4137	0.54	7998	0.37
Northern right whale dolphin	1172	0.52	2032	0.55	1652	0.46	6242	0.42
Bottlenose dolphin (offshore)	1831	0.47	61	0.77	133	0.68	0	NA
Risso's dolphin	3418	0.31	3197	0.30	1036	0.41	4260	0.52
Short-finned pilot whale	118	1.04	48	1.02	184	0.60	0	NA
Killer whale	30	0.73	116	0.47	142	0.47	521	0.37
Dall's porpoise	727	0.99	8870	0.64	27,410	0.26	48,950	0.71
Mesoplodon spp.	132	0.96	269	0.53	341	0.78	435	0.70
Cuvier's beaked whale	911	0.68	2647	0.74	784	1.18	0	NA
Baird's beaked whale	127	1.14	159	1.02	200	0.74	520	0.54
Kogia spp.	0	NA	710	0.58	130	1.25	397	1.25
Sperm whale	607	0.57	143	0.66	736	0.40	448	0.63
Minke whale	226	1.02	284	0.74	102	1.56	211	0.84
Bryde's whale	0	NA	7	1.01	0	NA	0	NA
Sei whale	0	NA	14	0.78	47	0.68	37	1.14
Sei or Bryde's whale	7	1.07	11	0.79	0	NA	0	NA
Fin whale	359	0.40	992	0.27	448	0.43	299	0.33
Blue whale	842	0.20	528	0.27	115	0.37	63	0.51
Humpback whale	36	0.51	586	0.38	90	0.47	231	0.36
Unidentified delphinoid	2845	0.53	1609	0.54	299	0.47	214	0.58
Unidentified ziphiid whale	226	0.86	65	1.11	172	0.65	0	NA
Unidentified small whale	357	0.66	27	1.44	73	0.60	72	1.14
Unidentified roqual whale	34	0.53	147	0.31	30	0.42	59	0.37
Unidentified large whale	72	0.33	54	0.61	35	0.44	28	0.82
Subtotal: Delphinoids	212,077	0.16	148,695	0.18	106,007	0.27	72,756	0.49
Subtotal: Ziphiidae	1396	0.49	3140	0.63	1497	0.66	955	0.43
Subtotal: Physeteridae	607	0.57	853	0.49	866	0.39	845	0.68
Subtotal: Balaenopteridae	1504	0.21	2568	0.17	831	0.31	900	0.25
Total	216,014	0.15	155,336	0.17	109,309	0.27	75,556	0.47

Dall's porpoise Abundance estimation for Dall's porpoise is difficult because of their attraction to vessels (Turnock and Quinn, 1991). To obtain unbiased estimates, these animals must be detected before they react to the survey vessel. Our data indicate that the behavior of the vast majority of Dall's porpoise seen at low sea states is "slow rolling." This contrasts with the "rooster-tailing" or fast swimming behavior seen by animals that are approaching the ship. However, when effort is limited to calm conditions (Beaufort states 0–2), the amount of

search effort is greatly reduced (Fig. 1). As a result, the coefficients of variation for Dall's porpoise abundance are greater than would be expected for such a common species. Off California, the temporal pattern shows higher Dall's porpoise abundance in 1996 (Table 7), mirroring the higher abundance that year of cold-temperate delphinids. Forney (2000) found that sea surface temperature was a very good predictor of Dall's porpoise distribution. In their 12 year time series of surveys off central California, Keiper et al. (2005) also found that

Table 6

Total numbers of sightings (n), estimated cetacean abundance (N), and density per 1000 km² within the entire study area. Data from 1991 to 2005 were pooled within geographic regions, and estimates of abundance for each region were summed to give total abundance. Coefficients of variation (CV) apply to both abundance and density estimates. CVs and 95% confidence intervals (CI) were based on a bootstrap calculation. Variances were assumed to be additive in estimating the CVs of the subtotals and totals. Unidentified large whales and small whales were not sufficiently specified to be included in the subtotals.

Species	n	Abundance N	CV(N)	Lower 95% CI	Upper 95% CI	Density per 1000 km ²
Short-beaked common dolphin	459	352,069	0.18	234,430	489,826	309.35
Long-beaked common dolphin	19	21,902	0.50	4833	43,765	19.24
Unclassified common dolphin	29	5629	0.64	1127	14,231	4.95
Striped dolphin	73	18,976	0.28	9286	29,038	16.67
Pacific white-sided dolphin	71	23,817	0.36	9991	40,760	20.93
Northern right whale dolphin	60	11,097	0.26	5654	16,712	9.75
Bottlenose dolphin (offshore)	38	2026	0.44	743	4443	1.78
Risso's dolphin	110	11,910	0.24	7501	19,255	10.46
Short-finned pilot whale	5	350	0.48	68	708	0.31
Killer whale	23	810	0.27	408	1157	0.71
Dall's porpoise	214	85,955	0.45	42,318	211,118	75.53
<i>Mesoplodon</i> spp.	11	1177	0.40	311	1648	1.03
Cuvier's beaked whale	17	4342	0.58	1636	11,555	3.82
Baird's beaked whale	15	1005	0.37	382	1821	0.88
<i>Kogia</i> spp.	5	1237	0.45	0	4981	1.09
Sperm whale	55	1934	0.31	991	3163	1.70
Minke whale	18	823	0.56	403	2874	0.72
Bryde's whale	1	7	1.01	0	21	0.01
Sei whale	7	98	0.57	15	227	0.09
Sei or Bryde's whale	4	18	0.65	0	46	0.02
Fin whale	214	2099	0.18	1448	2934	1.84
Blue whale	198	1548	0.16	1138	2087	1.36
Humpback whale	129	942	0.26	584	1411	0.83
Unidentified delphinoid	46	4968	0.36	2044	8585	4.37
Unidentified ziphiid whale	6	463	0.50	115	986	0.41
Unidentified small whale	12	528	0.50	209	1370	0.46
Unidentified roqual whale	44	270	0.20	170	373	0.24
Unidentified large whale	30	189	0.25	107	292	0.17
Subtotal: Delphinoids	1147	539,509	0.14			474.05
Subtotal: Ziphiidae	49	6987	0.37			6.14
Subtotal: Physeteridae	60	3171	0.26			2.79
Subtotal: Balaenopteridae	615	5805	0.12			5.10
Total	1913	556,189	0.14			488.71

Dall's porpoise abundance was inversely related to sea surface temperature.

Balaenopteridae The common baleen whales in California waters were blue, fin, and humpback whales. The abundance of these species was consistently high during the summer and fall study period. Our estimates of humpback whale abundance increased from 1991 to 1996 and decreased slightly in 2001 and 2005; however, humpback whales were observed to be highly concentrated in

productive nearshore waters off California and northern Washington during 2005 that were not well sampled during our surveys. A more comprehensive and precise abundance estimate of 1769 humpback whales (CV=0.16) was obtained when additional survey effort was included within these areas (Forney, 2007). More precise estimates from mark-recapture studies also indicate an increase in abundance from 1991 to 1997 (Calambokidis and Barlow, 2004), a decrease in 1999–2000 and in 2000–2001, and a subsequent increase to about 1400

Table 7

Number of sightings (n) and estimated abundance (N) for each species in the three California regions for the years 1991, 1993, 1996, 2001, and 2005. The total lengths of transects surveyed were 9893, 6287, 10,251, 6438, and 7779 km for these years, respectively, in Beaufort sea states of 5 or less and were 2160, 1521, 1556, 852, and 1055 km, respectively, in Beaufort sea states of 2 or less. Unidentified large whales and small whales were not sufficiently specified to be included in the subtotals.

Species	1991		1993		1996		2001		2005	
	n	Abundance N								
Short-beaked common dolphin	119	249,044	94	397,813	103	313,994	64	335,365	76	483,353
Long-beaked common dolphin	5	16,714	0	0	6	49,431	2	20,076	6	11,191
Unclassified common dolphin	8	4568	3	1454	10	2768	1	383	7	18,968
Striped dolphin	21	32,370	14	14,622	13	4796	6	12,570	18	29,037
Pacific white-sided dolphin	11	4843	10	4222	19	37,762	9	9209	3	13,677
Northern right whale dolphin	14	4554	6	2554	9	7950	12	6337	1	897
Bottlenose dolphin (offshore)	14	2165	2	1058	7	382	9	5375	6	2066
Risso's dolphin	28	10,746	15	7510	15	5083	17	8521	13	7036
Short-finned pilot whale	0	0	4	1506	0	0	0	0	1	639
Killer whale	3	193	2	385	4	380	2	270	2	203
Dall's porpoise	57	59,112	1	206	50	54,501	23	18,125	16	45,373
<i>Mesoplodon</i> spp.	3	697	5	2116	1	202	0	0	0	0
Cuvier's beaked whale	9	9546	4	5137	2	1152	1	3217	1	2615
Baird's beaked whale	2	99	3	1591	2	913	0	0	0	0
<i>Kogia</i> spp.	2	1970	2	1345	0	0	0	0	0	0
Sperm whale	11	837	7	1335	6	593	9	2495	13	2795
Minke whale	4	502	0	0	4	522	2	486	5	236
Bryde's whale	1	28	0	0	0	0	0	0	0	0
Sei whale	0	0	2	117	1	114	1	29	1	47
Sei or Bryde's whale	2	27	2	75	0	0	0	0	0	0
Fin whale	23	892	29	1514	55	1832	19	1784	60	3082
Blue whale	53	1908	39	1965	74	1927	9	516	16	665
Humpback whale	6	196	15	570	49	1282	14	765	20	662
Unidentified delphinoid	11	1237	5	7697	14	4890	3	587	9	9768
Unidentified ziphiid whale	0	0	2	652	2	615	0	0	2	1104
Unidentified small whale	6	582	0	0	2	482	2	825	1	483
Unidentified roqual whale	3	63	2	93	18	423	2	70	12	296
Unidentified large whale	9	221	1	23	9	246	3	75	5	143
Subtotal: Delphinoids	291	385,546	156	439,027	250	481,937	148	416,818	158	622,208
Subtotal: Ziphiidae	14	10,342	14	9496	7	2881	1	3217	3	3719
Subtotal: Physeteridae	13	2807	9	2680	6	593	9	2495	13	2795
Subtotal: Balaenopteridae	92	3616	89	4334	201	6100	47	3650	114	4988
Total	425	403,114	269	455,561	475	492,238	210	427,080	294	634,335

in 2002–2003 (Calambokidis³). Our estimates of blue whale abundance decreased markedly in 2001 and 2005 compared to previous estimates, and they were more widespread in offshore and northern waters than during the 1990s. The lower abundance estimates, rather than reflecting a true population decline, appear to be caused by a redistribution of animals outside of the study

area. Mark-recapture estimates of blue whale abundance remained high (1781) in the period of 2000–2003, but blue whales have recently been seen off British Columbia (Calambokidis³) and in the Gulf of Alaska (J. Barlow, unpubl. data). The recruitment of krill off central and northern California was poor during 2005 (Peterson et al., 2006), and given that this is the sole food for blue whales, the redistribution may be a result of decreased food supplies. Fin whales appeared to be monotonically increasing in abundance during the three

³ Calambokidis, J. 2005. Personal commun. Cascadia Research, 218½ W. 4th Avenue, Olympia, WA 98501.

Table 8

Number of sightings (n) and estimated abundance (N) for each species in the Oregon-Washington region for the years 1996, 2001, and 2005. The total lengths of transects surveyed were 4336, 3100, and 2525 km for these years, respectively, in Beaufort sea state of 5 or less and were 532, 380, and 292 km, respectively, for Beaufort sea state of 2 or less. Unidentified large whales and small whales were not sufficiently specified to be included in the subtotals.

Species	1996		2001		2005	
	n	Abundance N	n	Abundance N	n	Abundance N
Short-beaked common dolphin	1	3749	1	219	1	11,286
Long-beaked common dolphin	0	0	0	0	0	0
Unclassified common dolphin	0	0	0	0	0	0
Striped dolphin	1	37	0	0	0	0
Pacific white-sided dolphin	7	5812	7	8884	5	10,708
Northern right whale dolphin	5	3397	10	8600	3	8265
Bottlenose dolphin (offshore)	0	0	0	0	0	0
Risso's dolphin	11	5248	9	5584	1	549
Short-finned pilot whale	0	0	0	0	0	0
Killer whale	3	250	4	881	3	548
Dall's porpoise	46	79,479	12	17,315	8	28,806
<i>Mesoplodon</i> spp.	1	479	0	0	1	926
Cuvier's beaked whale	0	0	0	0	0	0
Baird's beaked whale	3	179	2	348	3	1319
<i>Kogia</i> spp.	1	899	0	0	0	0
Sperm whale	3	318	2	98	4	1103
Minke whale	2	340	1	194	0	0
Bryde's whale	0	0	0	0	0	0
Sei whale	0	0	0	0	2	147
Sei or Bryde's whale	0	0	0	0	0	0
Fin whale	8	210	10	334	10	409
Blue whale	0	0	3	87	4	141
Humpback whale	1	13	7	331	17	483
Unidentified delphinoid	2	292	1	126	1	189
Unidentified ziphiid whale	0	0	0	0	0	0
Unidentified small whale	1	162	0	0	0	0
Unidentified roqual whale	1	20	2	60	4	127
Unidentified large whale	1	14	0	0	2	85
Subtotal: Delphinoids	76	98,264	44	41,609	22	60,351
Subtotal: Ziphiidae	4	658	2	348	4	2245
Subtotal: Physeteridae	4	1217	2	98	4	1103
Subtotal: Balaenopteridae	12	583	23	1006	37	1307
Total	98	100,897	71	43,061	69	65,091

survey periods, and a more detailed study of trends in fin whale abundance is warranted.

Bryde's and sei whales are very rare off the U.S. west coast, and minke whales are not common, particularly in offshore waters. Bryde's whales are commonly viewed as tropical baleen whales and therefore their low abundance is expected. However, sei whales were previously harvested commercially along the west coast by coastal whaling stations, and their near absence is more of a mystery. Minke whales are known

to be common in some nearshore areas (Stern, 1992), which were not well sampled during our broad-scale cruises, but overall densities were low. Minke whale densities may have been underestimated in the study area because trackline detection probabilities were not directly estimated. There are no previous estimates of $g(0)$ for minke whales based on observers searching with 25 \times binoculars. Skaug et al. (2004) used observers searching with naked eyes and estimated $g(0)$ values between approximately 0.7 in Beaufort 1 and

0.5 in Beaufort 2. We assumed that $g(0)$ for minke whales in Beaufort 0 to 2 would be the same as for small groups of delphinids (0.846), but minke whales are very difficult to detect and an overestimate of this parameter would lead to an underestimate of minke whale abundance.

Physeteridae The estimated abundance of sperm whales is temporally variable off California (Table 7), but the two most recent estimates (2001 and 2005) were markedly higher than the estimates for 1991–96. Following the 1997–98 Niño, giant squid (*Dosidicus gigas*) have been more frequently observed off northern California and Oregon, in particular beginning in 2002 (Percy, 2002; Field et al., in press). Sperm whales are known to forage on giant squid, and their increased abundance within our study area may have been related to the increased availability of this prey species in recent years. Compared to baleen whales, sperm whales are found in larger groups, and fewer groups were seen on each survey, both of which contribute to more variable estimates. Also, the sperm whale population is likely to extend outside the study area, at least during certain times of the year. Of 176 tags that were implanted in sperm whales off southern California in winter, only three were later recovered by whalers (Rice, 1974); of these three, one was recovered outside the study area (far west of British Columbia). It is likely that at least some fraction of the population is absent during part of the year, and that fraction may vary with oceanographic conditions. This pattern of distribution differs from the situation with humpback whales; the majority of the humpback population appeared to be feeding in U.S. west coast waters during the time of the surveys. The density of sperm whales estimated in our study for the California Current (1.7 per 1000 km²) is similar to the worldwide global average for this species (1.4 per 1000 km²; Whitehead, 2002) but is less than recent estimates for waters in the eastern temperate Pacific (3–5 per 1000 km²; Barlow and Taylor, 2005) and around Hawaii (2.8 per 1000 km²; Barlow, 2006).

Dwarf and pygmy sperm whales are seldom seen by people because of their offshore distribution and cryptic behavior. Nonetheless, the estimated number of individuals found off the U.S. west coast exceeds the number of some much more commonly seen species, such as killer whales.

Ziphiidae Although they are rarely seen, approximately 7000 beaked whales were found in west coast waters—a number that exceeds that documented for baleen whales. The absence of California sightings for two beaked whale genera (*Mesoplodon* and *Berardius*, Table 7) since 1996 is disconcerting, especially in light of recent discoveries about the susceptibility of this group to loud anthropogenic sounds (Simmonds and Lopez-Jurado, 1991; Cox et al., 2006); however, weather conditions were less favorable for the detection of beaked whales during the more recent surveys (Fig. 1) and it is unclear whether this may have played a role in their apparent decrease. The

distributions of all beaked whale species extend outside the study area, and it is likely that some individuals move in to and out of the study area as habitat changes. An analysis of trends in beaked whale abundance should include consideration of these effects.

Previous abundance estimates

Estimates presented in this study differ, typically by a small amount, from previous estimates from the 1991 survey (Barlow, 1995) and preliminary estimates from the 1993 (Barlow and Gerrodette, 1996), 1996 and 2001 (Carretta et al., 2006), and 2005 (Forney, 2007) surveys. The differences are primarily due to differences in the stratification and in the use of multiple covariates in the line-transect modeling. Both modifications should result in more precise estimates of cetacean abundance. In addition, some of these previous estimates did not include group-size calibration for individual observers, and therefore our estimates corrected a small negative bias present in those earlier estimates. The principle weakness of the current analysis is the small sample size for several rare species. However, we believe it is better to include all species for completeness and to properly quantify uncertainty in the estimates for rare species.

Acknowledgments

We thank the marine mammal observers (W. Armstrong, L. Baraff, S. Benson, J. Cotton, A. Douglas, D. Everhardt, H. Fearnbach, G. Friedrichsen, J. Gilpatrick, J. Hall, N. Hedrick, K. Hough, D. Kinzey, E. LaBrecque, J. Larese, H. Lira, M. Lycan, S. Lyday, R. Mellon, S. Miller, L. Mitchell, L. Morse, S. Noren, S. Norman, C. Oedekoven, P. Olson, T. O'Toole, S. Perry, J. Peterson, B. Phillips, R. Pitman, T. Pusser, M. Richlen, J. Quan, C. Speck, K. Raum-Suryan, S. Rankin, J. Rivers, R. Rowlett, M. Rosales, J. C. Salinas, G. Serra-Valente, B. Smith, C. Stinchcomb, N. Spear, S. Tezak, L. Torres, B. Troutman, and E. Vasquez), cruise leaders (E. Archer, L. Ballance, E. Bowly, J. Carretta, S. Chivers, T. Gerrodette, P. S. Hill, M. Lowry, K. Mangels, S. Mesnick, R. Pitman, J. Redfern, B. Taylor, and P. Wade), survey coordinators (J. Appler, A. Henry, P. S. Hill, A. Lynch, K. Mangels, and A. VonSaunders), and officers and crew who dedicated many months of hard work collecting these data. T. Gerrodette was the chief scientist for the 1993 survey. J. Cabbage and R. Holland wrote the data entry software. Data were edited and archived by A. Jackson. Areas within the 20-m depth contour were calculated by R. Cosgrove. J. Laake provided his R-language code for fitting the multiple-covariate line-transect models. This article benefited from the reviews and comments by M. Ferguson, L. Thomas, and the Pacific Scientific Review Group. Funding was provided by National Oceanic and Atmospheric Administration and the Strategic Environmental Research and Development Program (SERDP). This work was supported in part by the Monterey Bay Sanctuary Foundation.

Literature cited

- Appler, J., J. Barlow, and S. Rankin.
2004. Marine mammal data collected during the Oregon, California and Washington line-transect expeditions (ORCAWALE) conducted aboard the NOAA ships McArthur and David Starr Jordan, July–Dec 2001. NOAA Tech. Memo. NMFS-SWFSC-359, 28 p.
- Barlow, J.
1995. The abundance of cetaceans in California waters. Part I: Ship surveys in summer and fall of 1991. *Fish. Bull.* 93:1–14.
1999. Trackline detection probability for long-diving whales. In *Marine mammal survey and assessment methods* (G. W. Garner, S. C. Amstrup, J. L. Laake, B. F. J. Manly, L. L. McDonald, and D. G. Robertson, eds.), p. 209–221. Balkema Press, Rotterdam, The Netherlands.
2006. Cetacean abundance in Hawaiian waters estimated from a summer/fall survey in 2002. *Mar. Mamm. Sci.* 22(2):446–464.
- Barlow, J., and T. Gerrodette.
1996. Abundance of cetaceans in California waters based on 1991 and 1993 ship surveys. NOAA Tech. Memo. NMFS-SWFSC-233, 15 p.
- Barlow, J., T. Gerrodette, and J. Forcada.
2001. Factors affecting perpendicular sighting distances on shipboard line-transect surveys for cetaceans. *J. Cetacean Res. Manage.* 3(2):201–212.
- Barlow, J., and B. L. Taylor.
2005. Estimates of sperm whale abundance in the north-eastern temperate Pacific from a combined acoustic and visual survey. *Mar. Mamm. Sci.* 21(3):429–445.
- Buckland, S. T., D. R. Anderson, K. P. Burnham, J. L. Laake, D. L. Borchers, and L. Thomas.
2001. *Introduction to Distance Sampling: Estimating abundance of biological populations*, 432 p. Oxford Univ. Press, Oxford, England.
2004. *Advanced Distance Sampling: Estimating abundance of biological populations*, 416 p. Oxford Univ. Press, Oxford, England.
- Calambokidis, J., and J. Barlow.
2004. Abundance of blue and humpback whales in the eastern North Pacific estimated by capture-recapture and line-transect methods. *Mar. Mamm. Sci.* 21(1):63–85.
- Carretta, J. V., K. A. Forney, and J. L. Laake.
1998. Abundance of southern California coastal bottlenose dolphins estimated from tandem aerial surveys. *Mar. Mamm. Sci.* 14(4):655–675.
- Carretta, J. V., K. A. Forney, M. M. Muto, J. Barlow, J. Baker, B. Hanson, and M. S. Lowry.
2006. U.S. Pacific Marine Mammal Stock Assessments: 2005. NOAA Tech. Memo. NMFS-SWFSC-388, 317 p.
- Carretta, J. V., T. Price, D. Petersen, and R. Read.
2005. Estimates of marine mammal, sea turtle, and seabird mortality in the California drift gillnet fishery for swordfish and thresher shark, 1996–2002. *Mar. Fish. Rev.* 66(2):21–30.
- Cox, T. M., T. J. Ragen, A. J. Read, E. Vos, R. W. Baird, K. Balcomb, J. Barlow, J. Caldwell, T. Cranford, L. Crum, A. D'Amico, G. D'Spain, A. Fernandez, J. Finneran, R. Gentry, W. Gerth, F. Gulland, J. Hildebrand, D. Houser, T. Hullar, P. D. Jepson, D. Ketten, C. D. MacLeod, P. Miller, S. Moore, D. C. Moun-
tain, D. Palka, P. Ponganis, S. Rommel, T. Rowles, B. Taylor, P. Tyack, D. Wartzok, R. Gisiner, J. Mead, and L. Benner.
2006. Understanding the impacts of anthropogenic sound on beaked whales. *J. Cetacean Res. Manage.* 7(3):177–187.
- Dohl, T. P., M. L. Bonnell, and R. G. Ford.
1986. Distribution and abundance of common dolphin, *Delphinus delphis*, in the Southern California Bight: A quantitative assessment based on aerial transect data. *Fish. Bull.* 84:333–343.
- Efron, B., and G. Gong.
1983. A leisurely look at the bootstrap, the jackknife, and cross-validation. *Am. Stat.* 37(1):36–48.
- Field, J. C., K. Baltz, A. J. Phillips, and W. A. Walker.
In press. Range expansion and trophic interactions of the jumbo squid, *Dosidicus gigas* in the California Current. *Calif. Coop. Fish. Invest. Rep.*
- Forney, K. A.
2000. Environmental models of cetacean abundance: reducing uncertainty in population trends. *Conserv. Biol.* 14(5):1271–1286.
2007. Preliminary estimates of cetacean abundance along the U.S. West Coast and within four National Marine Sanctuaries during 2005. NOAA Tech. Memo. NMFS-SWFSC-TM-406, 27 p.
- Forney, K. A., and J. Barlow.
1998. Seasonal patterns in the abundance and distribution of California cetaceans, 1991–92. *Mar. Mamm. Sci.* 14(3):460–489.
- Gerrodette, T., and J. Forcada.
2005. Non-recovery of two spotted and spinner dolphin populations in the eastern tropical Pacific Ocean. *Mar. Ecol. Prog. Ser.* 291:1–21.
- Hill, P. S., and J. Barlow.
1992. Report of a marine mammal survey of the California coast aboard the research vessel McARTHUR July 28–November 5, 1991. NOAA Tech. Memo. NMFS-SWFSC-169, 103 p.
- Julian, F., and M. Beeson.
1998. Estimates of marine mammal, turtle, and seabird mortality for two California gillnet fisheries: 1990–95. *Fish. Bull.* 96:271–284.
- Keiper, C. A., D. G. Ainley, S. G. Allen, and J. T. Harvey.
2005. Marine mammal occurrence and ocean climate off central California, 1986 to 1994 and 1997 to 1999. *Mar. Ecol. Prog. Ser.* 289:285–306.
- Mangels, K. F., and T. Gerrodette.
1994. Report of cetacean sightings during a marine mammal survey in the eastern Pacific Ocean and the Gulf of California aboard the NOAA ships *McArthur* and *David Starr Jordan* July 28–November 6, 1993. NOAA Tech. Memo. NMFS-SWFSC-211, 86 p.
- Marques, F. C., and S. T. Buckland.
2003. Incorporating covariates into standard line transect analysis. *Biometrics* 59:924–935.
- Pearcy, W. G.
2002. Marine nekton off Oregon and the 1997–98 El Niño. *Prog. Oceanogr.* 54: 399–403.
- Peterson, W. T., R. Emmett, R. Goericke, E. Venrick, A. Mantyla, S. J. Bograd, F. B. Schwing, R. Hewitt, N. Lo, W. Watson, J. Barlow, M. Lowry, S. Ralston, K. A. Forney, B. E. Lavaniegos, W. J. Sydeman, D. Hyrenbach, R. W. Bradley, P. Warzybok, F. Chavez, K. Hunter, S. Benson, M. Weise, J. Harvey, G. Gaxiola-Castro, and R. Durazo.
2006. The state of the California Current, 2005–2006:

- warm in the north, cool in the south. Calif. Coop. Fish. Invest. Rep. 47:30-74.
- Rice, D. W.
1974. Whales and whale research in the eastern North Pacific. In *The whale problem: a status report* (W. E. Schevill, ed.), p. 170-195. Harvard Press, Cambridge, MA.
- Rugh, D. J., R. C. Hobbs, J. A. Lerczak, and J. M. Breiwick.
2005. Estimates of abundance of the eastern North Pacific stock of gray whales 1997 to 2002. *J. Cetacean Res. Manage.* 7(1):1-12.
- Simmonds, M. P., and L. F. Lopez-Jurado.
1991. Whales and the military. *Nature* 51:448.
- Skaug, H. J., N. Øien, T. Schweder, and G. Bøthun.
2004. Abundance of minke whales (*Balaenoptera acutorostrata*) in the Northeast Atlantic: variability in time and space. *Can. J. Fish. Aquat. Sci.* 61:870-886.
- Stern, J. S.
1992. Surfacing rates and surfacing patterns of minke whales (*Balaenoptera acutorostrata*) off central California, and the probability of a whale surfacing within visual range. Reports of the International Whaling Commission 42:379-385.
- Trites, A. W., V. Christensen, and D. Pauly.
1997. Competition between fisheries and marine mammals for prey and primary production in the Pacific Ocean. *J. Northwest Atl. Fish. Sci.* 22:173-187.
- Turnock, B. J., and T. J. Quinn, II.
1991. The effect of responsive movement on abundance estimation using line transect sampling. *Biometrics* 47: 701-715.
- Von Saunder, A., and J. Barlow.
1999. A report of the Oregon, California and Washington Line-transect Experiment (ORCAWALE) conducted in west coast waters during summer/fall 1996. NOAA Tech. Memo. NMFS-SWFSC-264, 40 p.
- Whitehead, H.
2002. Estimates of the current global population size and historical trajectory for sperm whales. *Mar. Ecol. Prog. Ser.* 242:295-304.

Abstract—Does adult spillover (movement out of marine protected areas [MPAs]) of fish create a net export of fish biomass from MPAs to adjacent fished reefs? Biomass of five commercial reef fish species was estimated by visual census within and outside three MPAs in Guam, Micronesia. For most species and sites, biomass was significantly higher within the MPAs than in adjacent fished sites. Movement of fishes into and out of the MPAs was determined by mark-recapture experiments, in which fishes were tagged both inside and outside of MPAs. Four out of five species studied showed little or no net movement out of MPAs. However, the orangespine surgeonfish (*Naso lituratus*) showed a net spillover of biomass from all three MPAs; 21.5% of tagged individuals and 29% of the tagged biomass emigrated from MPAs. Patterns of spillover were strongly influenced by physical habitat barriers, such as channels, headlands, or other topographic features. MPAs that are physically connected by contiguous reef structures will likely provide more spillover to adjacent fished sites than those that are separated by habitat barriers. This study demonstrates that MPAs can enhance export of fish biomass to fished areas, but spillover is species-specific and depends on factors such as species size and mobility.

Spillover of commercially valuable reef fishes from marine protected areas in Guam, Micronesia

Mark H. Tupper

Email address: m.tupper@cgiar.org

The WorldFish Center (address for correspondence)

Jalan Batu Maung, Batu Maung

11960 Bayan Lepas

Penang, Malaysia

and

Marine Laboratory

University of Guam, UOG Station

Mangilao, Guam 96923

Over the past two decades, marine protected areas (MPAs) have been increasingly adopted as an important fisheries management tool. The primary goals for MPAs are to protect critical habitat and biodiversity, to sustain or enhance fisheries by preventing spawning stock collapse, and to provide recruitment to fished areas (Gell and Roberts, 2003; Halpern, 2003). Enhancement of fished areas may occur through transport of larvae from spawning stock within the MPA (Gerber et al., 2005) or by a net emigration of adult fish to adjacent fished areas—a movement that is commonly known as “spillover” (e.g., Alcalá et al., 2005; Abesamis et al., 2006; Goni et al., 2006).

The role of spillover in determining MPA effectiveness has been addressed in both theoretical modeling studies (e.g., DeMartini, 1993; Kramer and Chapman, 1999; Gerber et al., 2005) and in empirical studies. The latter involve indirect documentation of spillover inferred from increases in fish biomass or catch per unit of effort (CPUE) in adjacent fished areas (e.g., Russ and Alcalá, 1996; Roberts et al., 2001; Tupper and Rudd, 2002; Alcalá et al., 2005), and direct documentation of fish movement through mark-recapture or sonic tracking experiments (e.g., Chapman and Kramer, 2000; Meyer et al., 2000; Kaunda-Arara and Rose, 2004; Meyer and Holland, 2005). There are a number of ways in which movement across MPA boundaries may occur; these

include random movements of fish during their routine activities (sometimes referred to as diffusion), emigration in response to density dependence (e.g., Tupper and Juanes, 1999; Abesamis and Russ, 2005), directed dispersal due to migration, and ontogenetic habitat shifts (Gerber et al., 2005). In order for spillover to effectively enhance adjacent fisheries, the net direction of these movements, and the number and size of fishes moving, must result in a net flow of biomass out of the MPA. Measuring the movement of biomass into the MPA should therefore be equally important to measuring outward movements. However, few studies have measured immigration, and therefore net spillover, and those that do address bidirectional movements have reported conflicting results, depending on the species or life history stage, the habitat, and the size and placement of the MPA (e.g., Kelly and MacDiarmid, 2003; Zeller et al., 2003; Tremain et al., 2004; Goni et al., 2006).

The degree of spillover from MPAs depends on the rate of fish migration across MPA boundaries (DeMartini, 1993; Gerber et al., 2005). Larger or more mobile species with large home ranges may spend too much time outside of the MPAs to be effectively protected, whereas smaller, more sedentary species with small home ranges may not cross MPA boundaries in sufficient numbers to enhance adjacent fisheries by spillover (DeMartini, 1993; Tupper and Rudd, 2002). If the

goal of a MPA is to enhance local fisheries by spillover in addition to conserving spawning biomass, then it must be designed and situated so that net movement of fishes from the MPA to fished areas can take place. In most tropical island nations, enhancement of local fisheries by adult spillover may be critical for continued support of the preserve system by the local fishing community (Russ and Alcala, 1999; Galal et al., 2002). In general, arguments for larval spillover carry little weight with fishermen because dispersal may not occur on spatiotemporal or "visual" scales that are meaningful to them (Russ and Alcala, 1996; Russ, 2002; Abesamis et al., 2006). This situation is doubtless the case in Guam, where little is known about the movement of fishes on coral reefs.

One characteristic of heavily exploited reefs is the very low abundance (in some cases virtual absence) of large carnivorous fishes, particularly groupers (Serranidae) and snappers (Lutjanidae) (Russ, 1991, 2002; Medley et al., 1993). In Guam, grouper biomass is noticeably lower than at the less heavily populated islands in Micronesia (e.g., Palau). Much research has therefore been directed at determining the effects of implementing MPAs on populations of large predatory fishes (e.g., Russ and Alcala, 1996, 2004). In Micronesia, however, herbivorous fishes, particularly surgeonfishes and unicornfishes (Acanthuridae) and parrotfishes (Scaridae) are equally important to local fisheries, and in many areas they have dominated the catch (Amesbury et al., 1986). Thus, it is important to understand the effects of MPAs on herbivorous and carnivorous fishes.

To address whether MPAs in Guam can increase fish biomass and provide spillover to adjacent reef areas, biomass of five important reef fish species inside three MPAs in Guam and on adjacent exploited reefs was determined by using underwater visual census. Net movements of both herbivorous and carnivorous reef fish across MPA boundaries were determined by using mark-recapture experiments.

Materials and methods

Study sites

In May of 1997, the Guam Department of Aquatic and Wildlife Resources (DAWR) established a network of five MPAs, termed "marine preserves," around the island, which accounted for 11.8% of Guam's shoreline and 15.3% of Guam's reef area. Fishing within these MPAs is restricted to shore-based cast netting and hook-and-line fishing for select reef species, except for the Piti Bomb Holes Marine Preserve, where no reef fishing (i.e., fishing from the shore to the reef margin) is allowed. Trolling seaward of the reef margin for pelagic fish is allowed in all preserves. Despite being implemented in 1997, the marine preserves did not become enforced until October 1999. Even then, only warnings were issued until January 2001, at which time the regulations became fully enforced, and all violators were subject to

any or all penalties applicable under the law. This study was conducted in 2003–04 at three MPA sites (Achang Reef Flat Marine Preserve, Piti Bomb Holes Marine Preserve, and Tumon Bay Marine Preserve—hereafter referred to as Achang, Piti, and Tumon, respectively) on the western and southern coasts of Guam, Micronesia (Fig. 1). All three sites consist of shallow reef flats that lead seaward to a reef crest and then drop off to a reef slope. The two remaining marine preserves, Sasa Bay and Pati Point, were not surveyed. Sasa Bay is a mangrove swamp with no coral reefs within its boundaries, and Pati Point is located within a restricted military area (Anderson Air Force Base).

The Achang preserve is the largest of the three preserves (4.8 km²). It includes a wide variety of habitats: mangroves, seagrass, sand, coral, and three channels that cut through the fringing reef from the outer reef slope to the reef flat. The largest of these, Manell Channel, separates Achang reef flat from Cocos Lagoon, to the west of Achang Reef Flat. To the west, the reef flat narrows and is interrupted by a rocky headland. Reference fished sites for the Achang Preserve were located in Cocos Lagoon. Seasonal traditional fishing is permitted in the Achang Preserve for juvenile streamlined spinefoot (*Siganus argenteus*), juvenile fusiliers (*Ptercaesio tile*), and big eye scad (*Selar crumenophthalmus*) under special permit.

The Piti preserve covers 3.6 km² and consists of a broad reef flat (1.4 km²) in Piti Bay bordered by Tepungan Channel to the west. The fringing reef is continuous from Piti Bay eastward to the fished sites at Asan Bay. The reef flat includes unique features known as "bomb holes," which provide sheltered areas of deeper water. The deepest of these sinkholes were 9–10 m deep and were densely populated by a variety of hard and soft coral species. They host rich soft coral communities and fish and invertebrate assemblages not often found within the reef margin. The main sinkhole is occupied by an 11-m in diameter underwater observatory that was completed in 1996. It is also frequented by commercial scuba divers during diving tours (up to 200 divers a day). Fish feeding is a common practice around the observatory; therefore, our survey sites were located away from the sinkholes in order to minimize possible confounding effects of fish feeding and diver presence.

The Tumon preserve lies adjacent to the central tourist district on Guam. It is 4.5 km² in total area and consists of extensive reef flats (2.7 km²), a gently sloping fore reef slope, and a broad shelf habitat. The reef flat is dominated by coral patch reefs. The Tumon MPA is bordered by headlands to the east and west, which interrupt the reef flat, although there is contiguous fringing reef which links Tumon with Tanguisson to the east. However, there is a sewage outfall at Tanguisson which may reduce movement of fish to the east. Because of the distance from the reef flat at the western boundary of the Tumon MPA to the reef flat at East Agana Bay (approximately 3 km), Tanguisson was the location chosen for the fished sites. Limited traditional fishing with hook-and-line or cast net from shore is allowed in

the Tumon Bay preserve for four types of fish: convict surgeonfish (*Acanthurus triostegus*), spinefeet (*Siganus* spp., known regionally as rabbitfish), juvenile jacks and trevallies (*Caranx* spp.), and juvenile goatfishes (Mullidae). Cast nets are sometimes used for convict surgeonfish and spinefeet along the reef margin.

At each site, visual census and tagging were performed as near to the geometric center of the MPA as possible. The closest distance to the MPA boundary was measured, and census sites on adjacent fished reefs were chosen at this same distance outside the MPA. All transects were surveyed and tagging was conducted in habitats as similar as possible, generally on the seaward edge of the reef flat at a 2–3 m depth, where the substrate typically consisted of sand, rubble, and scattered patch reefs (mainly *Porites* spp.), and where seagrass beds are nearer to shore (except in Tumon, where seagrass is scarce). This experimental design served to minimize bias due to among-site variation in distance from the reserve boundary and habitat type.

Estimation of biomass in MPAs and adjacent fished areas

Underwater visual census was used to estimate biomass of five exploited reef fishes at three MPAs and adjacent fished sites. These included three herbivores: convict surgeonfish (*Acanthurus triostegus*), orangespine unicornfish (*Naso lituratus*), and little spinefoot (*Siganus spinus*), and two carnivores: yellowstripe goatfish (*Mulloidichthys flavolineatus*), and honeycomb grouper (*Epinephelus merra*). These five species were chosen because of their great abundance and prevalence in the Guam nearshore reef fishery and because they are relatively easy to capture and tag. At each study site, four 50 m × 5 m transects were laid haphazardly. Divers swam each transect slowly, counting all commercially important species and estimating their lengths to the nearest cm. All divers were trained in fish size estimation for one month before this study. Biomass estimates were conducted biweekly from May through August 2003. In total, 32 transects were completed at each MPA and adjacent reference sites (8 census days × 4 transects at each site). Biomass was estimated by substituting the length of each fish on the transect into length-weight regressions for that species. The total weight of all fish by species was then used as an estimate of biomass.

Mark-recapture study

The five study species were collected from three preserves and from surrounding areas of reference sites. Within each preserve, six permanent quadrats, each



Figure 1

Map of Guam showing the locations of the three marine protected areas (MPAs) and three reference sites. MPAs (hatched areas) are Achang Reef Flat Marine Preserve, Piti Bomb Holes Marine Preserve, and Tumon Bay Marine Preserve. Reference sites are Cocos Lagoon, Asan Bay, and Tanguisson. Inset shows the location of Guam within the Western Pacific region.

20 × 20 m in planar area, were located at a distance of 800 m from the boundary of the MPA and reference site. The perimeter of each study site was marked at 1-m intervals by tying flagging tape to a dead coral. Another six quadrats were marked on fished reefs at the reference site, also at a distance of 800 m from the MPA boundary. This distance was chosen because it allowed the location of the study sites to fall into appropriate and similar habitats at all MPAs and fish sites. This distance also ensured that all tagged fish had an equal distance to move in order to enter or leave the MPA. It also represented sufficient distance from the MPAs to encompass a large area of fished reef. A square area was chosen for the mark-recapture study because it was easier to deploy surround nets

and to quantify fishing effort in a large square than in a typical narrow rectangle used for belt transects. Within each permanent quadrat, fish were captured by squirting an anesthetic (10% solution of Quinaldine sulfate in seawater) into the water where the fish were hiding and by casting a surround net (for smaller and more sedentary fishes) around corals heads or small patch reefs. For each species, an attempt was made to tag the same number of individuals at each MPA and reference site. Because target species density was generally lower at the fished sites (see "Results" section), fish were captured and tagged first at the fished sites by exhaustively fishing each 20×20 m quadrat. The same numbers of fish were then tagged in quadrats within the MPAs. This procedure ensured that tagging effort was equal across all sites, although fishing effort was often lower in the MPAs because sufficient fish could be captured in a shorter time. For recaptures of tagged fish, all permanent quadrats were fished exhaustively and all tagged individuals were recorded.

Tagging took place biweekly from May through July 2003 and from January through March 2004. Recaptured fish were collected weekly from May through August 2003 and January through April 2004 ($n=32$ total recapture attempts per site), allowing 1 week to 6 months between tagging and recapture. Captured fish were identified, measured, and tagged with visible implant elastomer (VIE) tags (Northwest Marine Technologies, Inc., Shaw Island, WA), and immediately released at the site of capture. The VIE tag was implanted under a fish's skin and thus would not become entangled, scraped off, or fouled with algae. Tag loss can lead to underestimates of recapture rates if a fish is recaptured after losing its tag. Past studies with several reef fish families (Labridae, Scaridae, Acanthuridae, and Serranidae) showed high (>90%) retention of elastomer implants, particularly for individuals greater than 150 mm standard length (Tupper, 2007). The effective life of the VIE tag in most reef fish is about 6 months, after which the tissue surrounding the tag generally has overgrown and obscured the tag (Tupper, 2007). The use of surround nets allowed for capture of resighted tagged fish. This approach enabled much higher recapture rates than those in more conventional studies where external tags and nonselective gears (such as traps) are solely used.

Analysis of data

To calculate spillover (S) for a given species, the numbers and biomass of tagged fish emigrating or immigrating across an MPA boundary were estimated. Spillover was calculated as the number (or biomass) of emigrants minus the number (or biomass) of immigrants. Percent spillover was calculated as the proportion of tagged fish (numbers and biomass) exported to adjacent fished areas minus the proportion of tagged biomass imported to the MPA:

$$S = (B_e/B_p - B_i/B_R) \times 100,$$

where S = percent spillover;

B_e = biomass emigrating from the preserve;

B_p = biomass remaining in the preserve;

B_i = biomass immigrating into the preserve;

and

B_R = biomass remaining in the reference site.

A positive value would indicate net spillover; a negative value would indicate net influx of biomass to the MPA. Thus, a positive value indicates that the MPA is a source of biomass for adjacent fished areas, where a negative value indicates that the MPA is a biomass sink and perhaps better suited to conserving biomass of a given species than to enhancing local fisheries.

Before analysis, all raw data were tested for normality by using the Shapiro-Wilk W test and for homogeneity of variance by using Levene's test (Sokal and Rohlf, 1995). Because raw density and raw spillover data did not initially meet these assumptions, they were square-root transformed. Percent spillover data were arc-sin transformed. All transformed data met the assumptions of parametric analysis of variance (ANOVA). Variation in mean fish biomass between locations and between MPAs and fish sites was determined with 2-way ANOVA. For this analysis, each MPA was paired with its adjacent fished site and this grouping resulted in three pairs: North (Tumon and Tanguisson), central (Piti and Asan Bay), and south (Achang and Cocos Lagoon). The ANOVA design was crossed, with location (north vs. central vs. south) as one factor and protection status (MPA vs. fished site) as a second factor. Variation in mean spillover between locations and between species was also analyzed by using 2-way ANOVA. Tukey's honestly significant difference (HSD) was used as a *post hoc* comparison test to determine pairwise differences in mean biomass and mean spillover in MPAs and reference sites. Linear regression was used to explore the relationship between density (expressed as biomass) of fish within the MPAs and the spillover rate from the MPAs.

Results

Biomass estimates

Mean biomass of the three herbivorous species was higher in MPAs than in the fished sites (Fig. 2). Mean biomass of convict surgeonfish did not differ between locations (i.e., between south, central, and north, 2-way ANOVA, $F=0.79$, $P=0.46$) but was significantly higher in MPAs than in fished sites at all locations ($F=13.47$, $P<0.001$; Tukey's HSD, $P<0.05$ for all paired comparisons). There was no significant interaction between location and protective status. Mean biomass of orange-spine unicornfish also did not differ between locations (2-way ANOVA, $F=0.90$, $P=0.42$) but was significantly higher in MPAs than in fished sites ($F=12.02$, $P<0.0001$). There was a significant interaction ($F=9.4$, $P<0.01$) between location and protective status because biomass

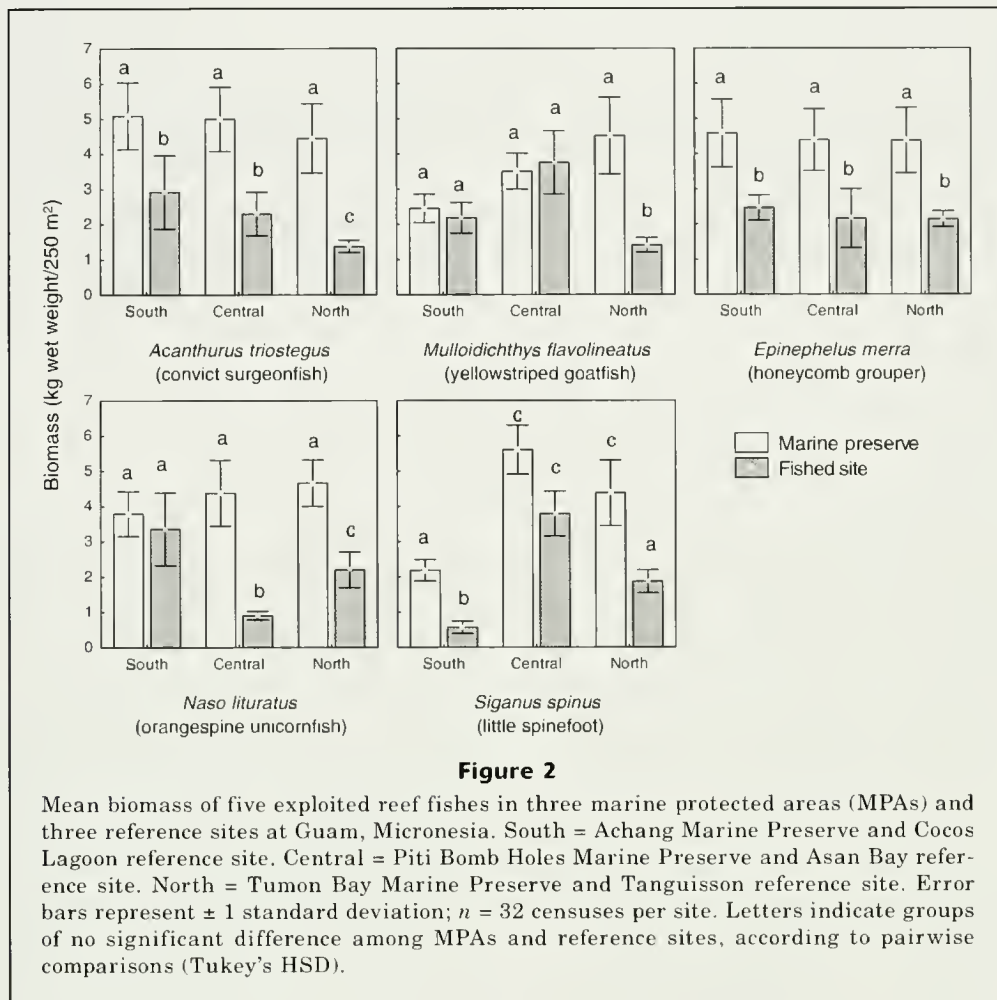


Figure 2

Mean biomass of five exploited reef fishes in three marine protected areas (MPAs) and three reference sites at Guam, Micronesia. South = Achang Marine Preserve and Cocos Lagoon reference site. Central = Piti Bomb Holes Marine Preserve and Asan Bay reference site. North = Tumon Bay Marine Preserve and Tanguisson reference site. Error bars represent ± 1 standard deviation; $n = 32$ censuses per site. Letters indicate groups of no significant difference among MPAs and reference sites, according to pairwise comparisons (Tukey's HSD).

of orangespine unicornfish was significantly higher in the Piti and Tumon MPAs than in adjacent fished sites (Tukey's HSD, $P < 0.05$), but there was no significant difference in biomass between Achang and Cocos Lagoon (Tukey's HSD, $P < 0.05$). Mean biomass of little spinefoot differed significantly between locations (2-way ANOVA, $F = 15.02$, $P < 0.0001$) and was significantly higher in the north and central locations than in the south (Tukey's HSD, $P < 0.05$). Mean biomass of little spinefoot was also significantly higher on protected reefs ($F = 16.01$, $P < 0.0001$) at all locations (Tukey's HSD, $P < 0.05$ for all paired comparisons).

For carnivorous species, mean biomass of yellowstripe goatfish (Fig. 2) did not differ between locations (2-way ANOVA, $F = 1.76$, $P = 0.18$). There was a nonsignificant higher abundance in MPAs than in reference sites ($F = 3.30$, $P = 0.076$). There was a significant interaction between location and protective status ($F = 3.32$, $P < 0.05$), which occurred because biomass of yellowstripe goatfish was higher in the Tumon MPA than at Tanguisson, but did not differ between MPAs and reference sites at the central and south locations. Mean biomass of honeycomb grouper (Fig. 2) did not differ between locations (2-way ANOVA, $F = 0.07$, $P = 0.93$) but was significantly higher

in MPAs than at fished sites ($F = 11.33$, $P = 0.002$) at all locations.

Spillover

A total of 2674 fishes were tagged; of these 935 (35%) were recaptured (Table 1). The species with the highest recapture rate (78%) was the honeycomb grouper; a solitary, benthic predator. Mobile, schooling species such as yellowstripe goatfish and little spinefoot had lower recapture rates (25–35%) but were abundant enough to allow relatively large numbers of returns.

Most recaptured fish did not cross the MPA boundaries. The overall grand mean spillover (i.e., over all species at all sites) was 5.9% of individuals and 8.0% of biomass from the MPAs. Table 2 shows biomass and mean number of tagged fish remaining within each MPA and fished site, immigrating to each MPA, and emigrating to each fished site. The difference between emigration and immigration is shown in Table 2 as the net flux in biomass and as the net flux in numbers. Spillover (the proportion of tagged fish exported to adjacent fished areas minus the proportion of tagged fish imported to the MPA) is also presented as spillover in

Table 1

Number of fish tagged and recaptured at three marine protected areas (MPAs) and three fished sites in Guam, Micronesia. Study species were convict surgeonfish (*Acanthurus triostegus*), honeycomb grouper (*Epinephelus merra*), yellowstripe goatfish (*Mulloidichthys flavolineatus*), orangespine unicornfish (*Naso lituratus*), and little spinefoot (*Siganus spinus*).

Species	Achang MPA	Cocos Lagoon	Piti MPA	Asan Bay	Tumon MPA	Tanguisson	Total	Recaptures	% Recaptured
Convict surgeonfish	135	134	135	130	132	130	796	247	31.0
Orangespine unicornfish	50	47	48	45	50	44	284	112	39.4
Yellowstrip goatfish	65	62	65	65	70	63	390	137	35.1
Honeycomb grouper	40	40	41	40	40	39	240	188	78.3
Little spinefoot	162	157	165	158	164	158	964	251	26.0
Total	452	440	454	438	456	434	2674	935	35.0

biomass and in numbers. For both net flux and spillover, a positive value indicates net movement out of the MPA; a negative value indicates net movement into the MPA. For the combination of all species, overall spillover was lowest at the Tumon MPA, where only 1.7% of all tagged biomass was exported (two-way ANOVA, $F=17.12$, $P<0.01$, Tukey's HSD, $P<0.05$). Spillover did not differ between the other two MPAs (20.3% at Piti and 16.7% at Achang, Tukey's HSD, $P<0.05$).

A significant interaction between species and location (two-way ANOVA, $F=7.73$, $P<0.0001$) warranted a closer inspection of fish movements at each location. Orangespine unicornfish was the only species exported from all three MPAs. The overall mean spillover for orangespine unicornfish was 29.4% of biomass (Table 2) and 21.5% of individuals (Table 2). This was significantly higher than the other four species (2-way ANOVA, $F=6.27$, $P<0.0001$). There was no significant difference in spillover of orangespine unicornfish between MPAs (2-way ANOVA, $F=2.71$, $P=0.34$). Although yellowstripe goatfish showed low overall mean spillover (1.1% of individuals imported to MPAs but 16.4% of biomass exported), it was actually very mobile; 34% of its tagged biomass moved into the Achang MPA, and 31% of its tagged biomass moved out of the Piti MPA. These net inward and outward movements at different locations cancelled each other in the calculation of overall mean spillover for this species. No movement of this species occurred across the Tumon MPA boundaries. In contrast, net export of convict surgeonfish occurred at Achang and Piti MPAs, but there was a net import of surgeonfish biomass to the Tumon MPA (Table 2). Spillover of convict surgeonfish did not differ between the Achang and Piti MPAs (Tukey's HSD, $P>0.05$). Honeycomb grouper showed an overall mean outward movement of 3.3% of tagged biomass (Table 2). However, there was no net movement of individuals across MPA boundaries at all sites (Table 2); this result indicated that primarily larger individuals moved out of the MPAs.

In general, for most species, the percentage of biomass exported from the MPAs was greater than the percentage of individuals exported. The exception was

that of yellowstripe goatfish at the Achang MPA, which showed a net outward movement of 15.6% of individuals (Table 2) but a net inward movement that was 34.2% of biomass (Table 2), indicating that the fish moving into Achang MPA were much larger than the fish moving out. In contrast, at Piti there was a net outward movement of 15.6% of individuals and 30.8% of the biomass for yellowstripe goatfish, indicating that larger fish were primarily exported. The effect of resident biomass on spillover of each species was examined by plotting spillover (in biomass) against the biomass ratio of each species at each MPA, measured as biomass inside the MPA divided by the biomass at the fished site. The variation in density between censuses rendered it impossible to create separate regressions for each species or MPA. Thus, the overall mean biomass ratio and mean spillover were pooled for all species and MPAs into a single regression. No relationship was found between the biomass ratio and mean spillover ($r^2=0.1$, $P=0.34$; Fig. 3).

Discussion

One of the primary effects of protection from fishing is an increase in size and abundance of fishes, and therefore in biomass, in MPAs (Russ, 2002; Halpern, 2003). Biomass of reef fish was greater in marine reserve areas than in fished areas after about six years of effective no-take protection at Sumilon and Apo Islands in the Philippines (Alcala et al., 2005). Moreover, these differences became larger with increased duration of protection up to 19 years. Russ and Alcala (2004) concluded that the time required for full recovery of reef fish populations at the Sumilon and Apo Island MPAs would be 15 and 40 years, respectively. Biomass of leopard coral grouper (*Plectropomus leopardus*) and spotted coral grouper (*P. maculatus*), two large roving grouper species, was five times higher in no-fishing zones than in fished zones of the Great Barrier Reef Marine Park, after 14 years of protection (Evans and Russ, 2004). Numerous other studies had found no difference in biomass of *Plectro-*

Table 2

Summary of mean numbers and biomass of recaptured fish that remained resident in the marine protected areas (MPAs) and fished sites, or that moved into or out of the MPAs. Spillover is the difference between emigration from and immigration to the MPAs. Percent spillover is the proportion of tagged fish emigrating from the MPAs minus the proportion of tagged fish immigrating to the MPAs. Data are presented as biomass of fish and number of fish. All data are means ± 1 standard deviation; $n = 32$ recapture events for each site. Superscripts (^{a,b}) indicate significant differences among MPAs according to pairwise comparisons (Tukey's honestly significant difference [HSD] test). Fished sites for Achang, Piti, and Tumon were Cocos Lagoon, Asan Bay, and Tanguisson, respectively (see Fig. 1). Study species were convict surgeonfish (*Acanthurus triostegus*), honeycomb grouper (*Epinephelus merra*), yellowstripe goatfish (*Mulloidichthys flavolineatus*), orangespine unicornfish (*Naso lituratus*), and little spinefoot (*Siganus spinus*).

Biomass of fish							
Species	Location	Fish biomass (MPA) 250 m ²	Fish biomass (fished site) g wet wt/ 250 m ²	Biomass immigrants g wet wt/ 250 m ²	Biomass emigrants g wet wt/ 250 m ²	Spillover (biomass) g wet wt/ 250 m ²	Spillover (%)
Convict surgeonfish	Achang	2207 \pm 408	2742 \pm 777	407 \pm 316	1232 \pm 658	825 \pm 742	22.1 \pm 19.8 ^a
	Piti	4051 \pm 1684	4806 \pm 1376	1137 \pm 666	1848 \pm 791	711 \pm 1055	14.1 \pm 15.9 ^a
	Tumon	2720 \pm 1757	2969 \pm 1841	2018 \pm 682	1109 \pm 326	-910 \pm 564	-19.8 \pm 18.0 ^b
Honeycomb grouper	Achang	3206 \pm 863	3206 \pm 862	141 \pm 283	184 \pm 367	42 \pm 85	1.4 \pm 2.7
	Piti	1886 \pm 304	1716 \pm 463	530 \pm 398	749 \pm 59	220 \pm 358	7.5 \pm 12.4
	Tumon	2494 \pm 362	2588 \pm 285	141 \pm 283	168 \pm 336	27 \pm 53	0.9 \pm 1.9
Yellowstripe goatfish	Achang	2514 \pm 759	2524 \pm 791	1647 \pm 551	523 \pm 1045	-1125 \pm 561	-34.2 \pm 19.7 ^a
	Piti	2005 \pm 986	2752 \pm 1517	209 \pm 246	1227 \pm 472	1016 \pm 720	30.8 \pm 31.4 ^b
	Tumon	2267 \pm 396	2267 \pm 396	0	0	0	0 ^b
Orangespine unicornfish	Achang	1872 \pm 1248	2932 \pm 1682	291 \pm 346	1351 \pm 379	1060 \pm 450	33.6 \pm 5.2
	Piti	4546 \pm 689	6459 \pm 592	1321 \pm 995	3234 \pm 1139	1914 \pm 630	25.4 \pm 9.3
	Tumon	2563 \pm 1353	4046 \pm 2543	341 \pm 404	1824 \pm 1437	1483 \pm 1614	29.2 \pm 35.5
Little spinefoot	Achang	4097 \pm 1434	3824 \pm 1599	1476 \pm 334	1203 \pm 417	-272 \pm 311	-6.2 \pm 5.6 ^a
	Piti	2629 \pm 994	4357 \pm 1624	547 \pm 271	2275 \pm 405	1728 \pm 639	23.7 \pm 6.3 ^b
	Tumon	3524 \pm 1530	3169 \pm 1526	806 \pm 678	451 \pm 302	-644 \pm 228	-8.6 \pm 19.5 ^a

Number of fish							
Species	Location	Number of fish (MPA)	Number of fish (reference site)	Number of immigrants	Number of emigrants	Spillover (numbers)	Spillover (%)
Convict surgeonfish	Achang	6.5 \pm 0.58	7.8 \pm 0.96	1.0 \pm 0.82	2.3 \pm 0.96	1.3 \pm 0.96	13.9 \pm 10.6 ^a
	Piti	9.3 \pm 3.30	9.8 \pm 1.71	2.8 \pm 1.50	3.3 \pm 1.50	0.5 \pm 1.73	6.0 \pm 13.1 ^a
	Tumon	7.8 \pm 1.89	6.8 \pm 3.20	3.3 \pm 0.96	1.5 \pm 0.58	-1.8 \pm 0.96	-20.0 \pm 20.2 ^b
Honeycomb grouper	Achang	5.0 \pm 1.41	5.0 \pm 1.41	0.3 \pm 0.50	0.3 \pm 0.50	0	0
	Piti	3.0 \pm 0.82	3.0 \pm 0.82	1.0 \pm 0.82	1.0 \pm 0.00	0.0 \pm 0.82	0.0 \pm 16.3
	Tumon	4.5 \pm 0.58	4.5 \pm 0.58	0.3 \pm 0.50	0.3 \pm 0.50	0	0
Yellowstripe goatfish	Achang	4.8 \pm 1.50	4.8 \pm 2.06	3.0 \pm 0.82	1.3 \pm 2.50	-1.8 \pm 1.89	1.5 \pm 5.8
	Piti	4.5 \pm 1.73	5.0 \pm 2.71	0.5 \pm 0.58	1.5 \pm 0.58	1.0 \pm 1.15	15.6 \pm 19.4
	Tumon	4.5 \pm 0.58	4.5 \pm 0.58	0	0	0	0
Orangespine unicornfish	Achang	3.5 \pm 1.73	4.8 \pm 2.22	0.5 \pm 0.58	1.8 \pm 0.50	1.3 \pm 0.50	23.8 \pm 2.5
	Piti	9.0 \pm 4.08	9.5 \pm 1.73	1.8 \pm 1.26	3.8 \pm 1.71	2.0 \pm 0.82	17.2 \pm 6.5
	Tumon	4.0 \pm 1.63	5.8 \pm 3.10	0.5 \pm 0.58	2.3 \pm 1.71	1.8 \pm 2.06	23.4 \pm 33.4
Little spinefoot	Achang	9.8 \pm 2.22	9.3 \pm 2.99	2.8 \pm 0.50	2.3 \pm 1.26	-0.5 \pm 1.00	-5.8 \pm 8.3 ^a
	Piti	6.8 \pm 2.22	9.5 \pm 3.32	1.3 \pm 0.50	4.0 \pm 0.82	2.8 \pm 1.26	24.5 \pm 7.7 ^b
	Tumon	7.8 \pm 1.50	7.0 \pm 2.58	1.8 \pm 1.71	0.8 \pm 0.50	-1.0 \pm 1.63	-11.6 \pm 20.5 ^a

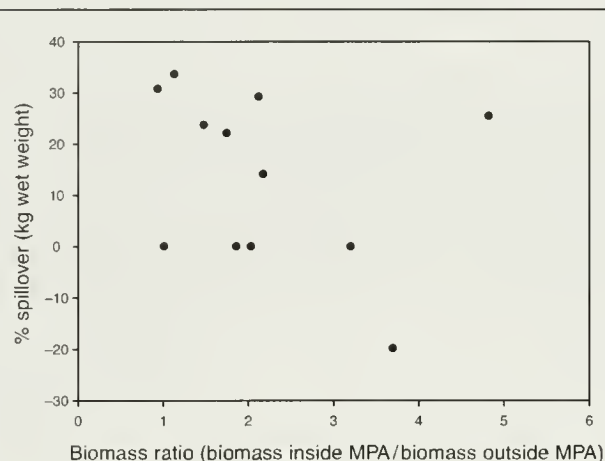


Figure 3

Effect of biomass ratio (biomass in marine protected area/ biomass in reference site) on spillover of reef fishes from marine protected areas in Guam, Micronesia. Points represent the level of spillover for a given biomass ratio. Data are pooled for five species and three MPAs. Study species are convict surgeonfish (*Acanthurus triostegus*), honeycomb grouper (*Epinephelus merra*), yellowstripe goatfish (*Mulloidichthys flavolineatus*), orangespine unicornfish (*Naso lituratus*), and little spinefoot (*Siganus spinus*).

pomus spp. after <10 years of protection (reviewed in Evans and Russ, 2004). In Kenyan MPAs, complete recovery of fish populations was estimated to take 22 years (McClanahan and Graham, 2005). Other studies have reported more rapid buildup of biomass. Biomass of five commercially exploited fish families tripled within three years of implementation of the Soufriere Marine Management Area in St. Lucia (Roberts et al., 2001). Biomass of reef fish in another MPA in St. Lucia, Anse Chastanet Reserve, doubled within two years of effective protection (Roberts and Hawkins, 1997) and a similar, rapid buildup of biomass was observed in a small MPA in Saba (Roberts, 1995). Rates of biomass buildup inside MPAs should generally be consistent with life history characteristics of the fish (Russ and Alcala, 1996; Mosquera et al., 2000; Alcala et al., 2005). Large predators (e.g., epinepheline serranids [large groupers], Lutjanidae, Lethrinidae, and Carangidae) and many Acanthuridae (surgeonfish) are long-lived, often with low rates of natural mortality and recruitment. Such characteristics would indicate that recovery rates would be gradual, as observed by Evans and Russ (2004) and Alcala et al. (2005).

In this study, it was not possible to determine the rate of biomass buildup because data were not collected at the initial implementation of the MPAs or at the initiation of full enforcement. After approximately 2.5 years of protection, biomass of all five study species of reef fish was higher within the MPAs than in fished sites, although the difference was not statistically sig-

nificant at the 95% confidence level for yellowstripe goatfish. A longer period of protection may result in greater biomass differentials between the marine preserves and fished sites. Biomass of all three species of herbivores was significantly higher within the MPAs, indicating that fishing pressure on herbivores in Guam is sufficient to show a biomass increase within no-fishing zones. Thus, increasing herbivore biomass on exploited reefs through spillover from MPAs may have the potential to reduce algal overgrowth, at least within a limited area adjacent to the MPA.

Given rapid population turnover, coupled with high fishing effort in the reference areas, significantly higher biomass in the MPAs may be evident after only 2–3 years of protection. All the species in this study are small to medium-size fishes with rapid growth and maturation rates (Choat and Robertson, 2002). What is somewhat surprising is that the densities of convict surgeonfish, yellowstripe goatfish, and little spinefoot were all significantly higher in the Tumon MPA than at the adjacent fished site, given that these species were legally targeted by subsistence fishermen within the MPA. However, the regulations stipulate that fishing with hook-and-line or cast net only and from shore or the exposed reef margin only. Moreover, fishermen in Tumon would have to contend with large numbers of tourists in the immediate vicinity, and fishing effort appeared low throughout the course of this study.

Several studies indicate that MPAs connected to fished areas by continuous reef will have higher rates of spillover (e.g., Kaunda-Arara and Rose, 2004). In this study, the highest overall spillover to surrounding fished reefs occurred from Piti, where the MPA and fished site are connected by a continuous reef flat. This was the only site at which no net inward movement of any species occurred. Fishermen were often seen along the boundary of the marine preserve, no doubt “fishing the line” in hopes of catching larger fish emigrating from the Piti MPA. When species were combined, the lowest rate of net flux occurred at Tumon. The fished site to the east of Tumon was at Tanguisson. These two bays are divided by a high, rocky headland (Punta Dos Amantes) with no reef flat. A sewage outfall just north of Punta Dos Amantes also separates the MPA and fished site. However, three of the five study species appeared to move freely between Tumon and Tanguisson—only yellowstripe goatfish and honeycomb grouper did not. Thus, the low overall rate of net flux was caused by the net import of convict surgeonfish and little spinefoot that balanced the net export of orangespine unicornfish. The overall spillover from Achang to Cocos Lagoon was also low, perhaps partly because these areas are separated by a wide tidal channel to the west of the Achang reef flat. However, the low mean spillover from Achang occurred because of the large number of adult yellowstripe goatfish moving into the MPA. These results demonstrate the importance of determining spillover at the species level. Because different species can vary in their market value, the mean spillover of all fishes from an MPA may not be

indicative of the net value of fish moving from MPAs to fished reefs.

The results of this study demonstrate that large, mobile herbivores like orangespine unicornfish may be exported from MPAs. The high rates of spillover for this species may result in part from its larger size in relation to the other species. In general larger fish have larger home ranges (Kramer and Chapman, 1999). In this study, the percentage of biomass exported from a given MPA tended to be higher than the percentage of individuals exported, indicating that spillover was primarily accomplished by larger fish. However, some acanthurids are known to be very site attached (e.g. Bell and Kramer, 2000; Meyer and Holland, 2005). For example, the larger congener (*N. unicornis*) is very site attached, and Meyer and Holland (2005) found little evidence for spillover of this species from a small (0.34 km²) no-take marine reserve in Waikiki, Hawaii. Movements of adult *N. vlamingii* across the boundaries of Apo Island marine reserve are rare, but density-dependent interactions within the reserve are sufficient to displace smaller fish from the reserve (Abesamis and Russ, 2005). In a separate study, no cross-boundary migration was found for three other acanthurids: *Acanthurus nigricans*, *Ctenochaetus striatus*, and *N. unicornis* (M. Tupper, unpubl. data). Convict surgeonfish showed notable spillover (14–22% of tagged biomass) at Achang and Piti, but showed a net import of 20% of tagged biomass into Tumon. Similarly, yellowstripe goatfish showed net import to Achang and net spillover from Piti. These species tended to form large, mobile foraging schools at all locations. The spatial variation in movement of these two species may be a function of foraging or spawning movements constrained or modified by natural physical barriers (channels or headlands) and possibly anthropogenic barriers (e.g., the sewer outfall south of Tanguisson). For example, net inward movement of yellowstripe goatfish to Achang may be related to a spawning aggregation of this species located in Asgadao Channel, in the center of the Achang MPA (M. Tupper, unpubl. data). Alternatively, the disparity in direction of net movement at different sites may be simply explained by large ranging schools that happened to be tagged inside but recaptured outside the MPA at one location and vice versa at another. As might be expected, the honeycomb grouper, a small, sedentary, ambush predator, showed very low rates of spillover; no net movement in either direction was found at any of the study sites.

Movement across MPA boundaries may occur as a result of random dispersal of fish during their routine activities, directed dispersal due to migration or ontogenetic habitat shifts (Gerber et al., 2005), or emigration in response to density dependence. High densities of conspecifics in MPAs may lead to increased juvenile mortality (Goeden, 1979; Tupper and Juanes, 1999), decreased growth (Béné and Tewfik, 2003; Tewfik and Béné, 2003), or increased emigration, or to a combination of all three (Tupper and Juanes, 1999; Abesamis and Russ, 2005). In this study, there was no relation

between density and spillover of reef fish. This may have been due to fact that the density of fish in Guam's MPAs has not yet reached carrying capacity, i.e., the biomass within the MPAs is not yet representative of virgin, unfished stocks. It should be noted that pooled species and locations were used in the regression analysis. More data on individual species and locations would result in a more powerful test.

In conclusion, rates of adult import or export from MPAs appear to result from a combination of foraging behavior, potential spawning movements, and random daily movements across MPA boundaries. These movements were influenced by reef topography. Spillover was highest in areas joined by continuous fringing reef systems and lowest where reefs were separated by a headland barrier. Knowledge of fish movement patterns with respect to reef topography may be useful for choosing MPA boundaries in order to maximize the spillover of target species. The herbivorous orangespine unicornfish showed the highest rate of spillover from MPAs, which indicates that MPAs have the potential to provide herbivore biomass to adjacent fished areas which may be suffering from algal overgrowth due to fishing of herbivores and from nutrient input due to agricultural activities. However, given the declines in density of exploited fishes at the fished sites since the implementation of the MPAs (Gutierrez¹), it is evident that overall spillover has not yet been sufficient to increase fish biomass on adjacent reefs. This is not surprising, given the relatively short time since the implementation of these MPAs and the displacement of fishing effort from the MPAs to adjacent fished areas. Although spillover rates of four out of five study species were quite low, adult migration is only one process that may benefit fisheries. Further research is needed to determine the role of MPAs in enhancing larval supply and the transport of recruits from Guam's MPAs to adjacent fished areas.

Acknowledgments

I am grateful to J. Castro and J. Cruz for their invaluable assistance in collecting and tagging fishes. I thank G. Davis, C. Leberer, and J. Gutierrez of the Guam Division of Aquatic and Wildlife Resources for permitting me to collect fishes at the marine preserves. I am also grateful to D. Burdick and S. J. Teoh for assistance with the map shown as Figure 1. Funding for data collection was provided by grants to the University of Guam from the National Oceanic and Atmospheric Administration's Coral Reef Ecosystems Studies Program, the National Oceanic and Atmospheric Administration State and Territorial Coral Reef Management program and from the U.S. Department of Fish and Wildlife. Funding for data analysis and for manuscript writing was provided by the WorldFish Center.

¹ Gutierrez, J. 2004. Personal commun. Division of Aquatic and Wildlife Resources, 163 Dairy Road, Mangilao, Guam 96910.

Literature cited

- Abesamis, R. A., and G. R. Russ.
2005. Density-dependent spillover from a marine reserve: long-term evidence. *Ecol. Appl.* 15(5):1798–1812.
- Abesamis, R. A., A. C. Alcalá, and G. R. Russ.
2006. How much does the fishery at Apo Island benefit from spillover of adult fish from the adjacent marine reserve? *Fish. Bull.* 104:360–375.
- Alcalá, A. C., G. R. Russ, A. E. Maypa, and H. P. Calumpong.
2005. A long-term, spatially replicated experimental test of the effects of marine reserves on local fish yields. *Can. J. Fish. Aquat. Sci.* 62:98–108.
- Amesbury, S. S., F. A. Cushing, and R. K. Sakamoto.
1986. *Fishing on Guam*, 110 p. Univ. Guam Press, Mangilao, Guam.
- Bell, T., and D. L. Kramer.
2000. Territoriality and habitat use by juvenile blue tangs, *Acanthurus coeruleus*. *Environ. Biol. Fishes* 58:401–409.
- Béné, C., and A. Tewfik.
2003. Biological evaluation of a Marine Protected Area: evidence of crowding effect on a protected population of queen conch in the Caribbean. *Mar. Ecol.* 24(1) 45–58.
- Chapman, M. R., and D. L. Kramer.
2000. Movements of fishes within and among fringing coral reefs in Barbados. *Environ. Biol. Fishes* 57:11–24.
- Choat, J. H., and D. R. Robertson.
2002. Age-based studies. In *Coral reef fishes: dynamics and diversity in a complex ecosystem* (P. F. Sale, ed.), p. 57–80. Academic Press, San Diego, CA.
- DeMartini, E. E.
1993. Modelling the potential of fishery reserves for managing Pacific coral reef fishes. *Fish. Bull.* 91: 414–427.
- Evans, R. D., and G. R. Russ.
2004. Larger biomass of targeted reef fish in no-take marine reserves on the Great Barrier Reef, Australia. *Aquatic Conserv. Mar. Freshw. Ecosyst.* 14: 505–519.
- Galal, N., R. F. G. Ormond, and O. Hassan.
2002. Effect of a network of no-take reserves in increasing catch per unit effort and stocks of exploited reef fish at Nabq, South Sinai, Egypt. *Mar. Freshw. Res.* 53:199–205.
- Gell, F., and C. M. Roberts.
2003. Benefits beyond boundaries: the fishery effects of marine reserves. *Trends Ecol. Evol.* 18: 448–455.
- Gerber, L. R., S. S. Heppell, F. Ballantyne, and E. Sala.
2005. The role of dispersal and demography in determining the efficacy of marine reserves. *Can. J. Fish. Aquat. Sci.* 62:863–871.
- Goeden, G. B.
1979. Is the Great Barrier Reef being overfished? *Aust. Fish.* 1979:18–20.
- Goni, R., A. Quetglas, and O. Reñones.
2006. Spillover of spiny lobsters *Palinurus elephas* from a marine reserve to an adjoining fishery. *Mar. Ecol. Prog. Ser.* 308:207–219.
- Halpern, B. S.
2003. The impact of marine reserves: do reserves work and does reserve size matter? *Ecol. Appl.* 13(1):S117–S137.
- Kaunda-Arara, B., and G. A. Rose.
2004. Out-migration of tagged fishes from marine reef National Parks to fisheries in coastal Kenya. *Environ. Biol. Fishes* 70:363–372.
- Kelly, S., and A. B. MacDiarmid.
2003. Movement patterns of mature spiny lobsters, *Jasus edwardsii*, from a marine reserve. *N. Z. J. Mar. Freshw. Res.* 37:149–158.
- Kramer, D. L., and M. R. Chapman.
1999. Implications of fish home range size and relocation for marine reserve function. *Environ. Biol. Fishes* 55:65–79.
- McClanahan, T. R., and N. A. J. Graham.
2005. Recovery trajectories of coral reef fish assemblages within Kenyan marine protected areas. *Mar. Ecol. Prog. Ser.* 294:241–248.
- Medley, P. A., G. Guadian, and S. Wells.
1993. Coral reef fisheries stock assessment. *Rev. Fish Biol. Fish.* 3:242–285.
- Meyer, C. G., and K. N. Holland.
2005. Movement patterns, home range size and habitat utilization of the bluespine unicornfish, *Naso unicornis* (Acanthuridae) in a Hawaiian marine reserve. *Environ. Biol. Fishes* 73:201–210.
- Meyer, C. G., K. N. Holland, B. M. Wetherbee, and C. G. Lowe.
2000. Movement patterns, habitat utilization, home range size and site fidelity of whitesaddle goatfish, *Parupeneus porphyreus*, in a marine reserve. *Environ. Biol. Fishes* 59:235–242.
- Mosquera, I., I. M. Côté, S. Jennings, and J. D. Reynolds.
2000. Conservation benefits of marine reserves for fish populations. *Anim. Conserv.* 4:321–332.
- Roberts, C. M.
1995. Rapid buildup of fish biomass in a Caribbean marine reserve. *Conserv. Biol.* 9: 815–826.
- Roberts, C. M., J. A. Bohnsack, F. Gell, J. P. Hawkins, and R. Goodridge.
2001. Effects of marine reserves on adjacent fisheries. *Science* 294:1920–1923.
- Roberts, C. M., and J. Hawkins
1997. How small can a marine reserve be and still be effective? *Coral Reefs* 16:150.
- Russ, G. R.
1991. Coral reef fisheries: effects and yields. In *The ecology of fishes on coral reefs* (P. F. Sale, ed.), p. 601–635. Academic Press, San Diego, CA.
2002. Yet another review of marine reserves as reef fisheries management tools. In *Coral reef fishes: dynamics and diversity in a complex ecosystem* (P. F. Sale, ed.), p. 421–443. Academic Press, San Diego, CA.
- Russ, G. R., and A. C. Alcalá.
1996. Do marine reserves export adult fish biomass? Evidence from Apo Island, central Philippines. *Mar. Ecol. Prog. Ser.* 132:1–9.
1999. Management histories of Sumilon and Apo Marine Reserves, Philippines, and their influence on national marine resource policy. *Coral Reefs* 18:307–319.
2004. Marine reserves: long-term protection is required for full recovery of predatory fish populations. *Oecologia* 138:622–627.
- Sokal, R. R., and F. J. Rohlf.
1995. *Biometry: the principles and practice of statistics in biological research*, 3rd ed., 887 p. W. H. Freeman and Co., New York, NY.
- Tewfik, A., and C. Béné.
2003. Effects of natural barriers on the spillover of

- a marine mollusk: implications for fisheries reserves. *Aquatic Conserv: Mar. Freshw. Ecosyst.* 13:473-488.
- Tremain, D. M., C. W. Harnden, and D. H. Adams.
2004. Multidirectional movements of sportfish species between an estuarine no-take zone and surrounding waters of the Indian River Lagoon, Florida. *Fish. Bull.* 102:533-544
- Tupper, M.
2007. Identification of nursery habitats for commercially valuable humphead wrasse (*Cheilinus undulatus*) and large groupers (Pisces: Serranidae) in Palau. *Mar. Ecol. Prog. Ser.* 332:189-199.
- Tupper, M., and F. Juanes.
1999. Effects of a marine reserve on recruitment of grunts (Pisces: Haemulidae) at Barbados, West Indies. *Environ. Biol. Fishes* 55:53-63.
- Tupper, M., and M. A. Rudd.
2002. Species-specific impacts of a small marine reserve on reef fish production and fishing productivity in the Turks and Caicos Islands. *Environ. Cons.* 29(4):484-492.
- Zeller, D. C., S. L. Stoute, and G. R. Russ.
2003. Movements of reef fishes across marine reserve boundaries: effects of manipulating a density gradient. *Mar. Ecol. Prog. Ser.* 254:269-280.

Abstract—The lack of information concerning the preservation of ovarian material of fish species inhibits standardization of methods for determining fecundity and measuring oocytes. The effects of four preservatives (10% phosphate-buffered formalin, modified Gilson's solution, 70% ethanol, and freezing) on ovarian material weight and oocyte size were quantified for prespawning Atlantic cod (*Gadus morhua*), haddock (*Melanogrammus aeglefinus*), and American plaice (*Hippoglossoides platessoides*). Effects of preservation were similar between Atlantic cod and haddock but different between Atlantic cod and American plaice for nearly all comparisons. Although all treatments affected the weight of ovarian material, freezing caused the most change and formalin caused the least. Such significant species-specific effects should be quantified in the calculation of life history characteristics, such as fecundity, to minimize error. This is one of few studies dedicated to evaluating the effects of preservation on oocytes and ovarian material and is the first to evaluate multiple preservatives on species.

Species-specific effects of four preservative treatments on oocytes and ovarian material of Atlantic cod (*Gadus morhua*), haddock (*Melanogrammus aeglefinus*), and American plaice (*Hippoglossoides platessoides*)

Nikolai Klibansky

Francis Juanes (contact author)

Email address for F. Juanes: juanes@forwild.umass.edu

Department of Natural Resources Conservation
University of Massachusetts
160 Holdsworth Way
Amherst, Massachusetts 01003

Because of the weak relationship between spawning stock biomass and stock reproductive potential (Marshall et al., 1998, 2003), stock assessment scientists recommend incorporating basic reproductive biology (such as fecundity) into estimates of stock reproductive potential. Estimating fecundity and other reproductive biological parameters often requires oocytes or ovarian material, preserved chemically or by freezing. Ovaries can sometimes be weighed fresh, but often, as when they are collected aboard ships where special marine scales are not available, they must be preserved until they are weighed in the laboratory.

Common preservatives can affect the size and weight of oocytes differently among species. Formalin can increase the mean diameter of catfish eggs by 4–11% (Tan-Fermin, 1991), and the mean diameter of cod eggs by 3.5% (Svaasand et al., 1996), but does not affect the weight of salmon eggs (Fleming and Ng, 1987). Common preservatives have also been shown to affect oocyte size of the same species differently in different studies. Schaefer and Orange (1956) found that standard Gilson's solution and formalin had the same effect on oocyte diameter of yellowfin (*Neot-hunnus macropterus*) and skipjack (*Katsuwonus pelamis*). In contrast, Joseph (1963) found the mean diameter of oocytes of these same tuna

species preserved in standard Gilson's solution to be 24% smaller than the mean diameter of oocytes preserved in formalin.

To enable accurate comparisons of fecundity information among populations and years, data should be collected and analyzed by a standard method and a standard preservative should be used for storing oocytes and ovarian material. But because little research has been conducted on the effects of preservatives on oocyte size, the selection of a preservative is usually based more on popular use than empirical knowledge—a process that may perpetuate the use of inferior preservatives and unnecessary toxins. Preservatives that have been used in past fecundity research may be adequate for determining fecundity but may not preserve ovarian material well enough for related analyses, particularly histology.

The three most commonly employed chemical treatments for ovarian material are 10% buffered formalin (3.7% formaldehyde), standard Gilson's solution, and freezing. Formalin and freezing are best used for short-term preservation (up to two years) of ovarian material; however, formalin is ideally employed as a fixative. Standard Gilson's solution also preserves ovarian material but was developed to dissolve the interstitial material that holds oocytes together

Table 1

Summary information for all Atlantic cod (*Gadus morhua*), haddock (*Melanogrammus aeglefinus*), and American plaice (*Hippoglossoides platessoides*) sampled on Georges Bank (GB) and in the Gulf of Maine (GOM). Maturity stage is based on Tomkiewicz et al. (2003a). Month = month of sampling; Jan = January, Feb = February, Mar = March, etc. *n* = number of individuals sampled.

Species	Month	Region	Spawning season (peak)	Maturity stage	<i>n</i>
Atlantic cod	Feb 04	GB	Nov–May (Feb–Mar)	Ripening, stage IV	19
Haddock	Feb 04	GB	Jan–May (Mar–Apr)	Ripening, stage IV	16
Atlantic cod	May 04	GOM	Nov–May (Mar–May)	Ripening, stage IV	23
American plaice	May 04	GOM	Feb–Jun (Apr–May)	Ripening, stage IV	16

so they could then be counted and measured more easily (Simpson, 1951).

In this analysis, the effects of four preservatives on ovarian material weight and oocyte diameter of three species of commercially important Northwest Atlantic groundfish are evaluated. The preservatives are formalin (0.037 formaldehyde, 0.015 methyl alcohol, <0.01 sodium phosphate dibasic, <0.01 sodium phosphate monobasic, 0.93 deionized water), modified Gilson's solution (0.10 60% ethanol, 0.015 nitric acid, 0.008 glacial acetic acid, 0.88 distilled water), 70% ethanol, and freezing and are hereafter referred to simply as formalin, Gilson's, ethanol, and freezing. The three species used in this project included two gadids, Atlantic cod (*Gadus morhua*) and haddock (*Melanogrammus aeglefinus*), and one pleuronectid, American plaice (*Hippoglossoides platessoides*). These species are hereafter referred to as cod, haddock, and plaice. All are historically important groundfish species in the Northwest Atlantic that have been reduced to low numbers over the past century (Boreman et al., 1997) and are now managed together in the Northeast multispecies fishery. Reproductive biology and ecology are similar among these species: they are all iteroparous, determinate, batch spawners exhibiting group-synchronous ovarian organization (Murua and Saborido-Rey, 2003). Although data are abundant for these species on many characteristics used to predict stock reproductive potential, such as maturity and sex-ratio, data on fecundity and oocyte size remain very limited (Tomkiewicz et al., 2003b).

Materials and methods

Ovary collection

All ovarian specimens were taken from fish caught in bottom trawls in the Northwest Atlantic during peak spawning (Table 1). In February 2004 the ovaries of 19 ripening (classified as stage IV by the maturity key developed by Tomkiewicz et al. [2003a]) cod and 16 haddock were collected by bottom trawling in the western portion of Georges Bank (GB). In May 2004 the ovaries of 23 ripening cod and 16 ripening plaice were collected

by bottom trawling in the inshore waters of the Gulf of Maine (GOM).

Preservation and measurement

For all specimens collected on GB (cod and haddock), fresh weight of the left ovary was measured at sea, to the nearest 1.0 g, with a Marel marine balance (Marel Food Systems, Gardabaer, Iceland). These ovaries were then preserved in formalin. Specimens collected in the GOM (cod and plaice) could not be weighed at sea and therefore were packed in ice until they could be weighed to the nearest 0.001 g in the laboratory 24 hours later. The left ovarian lobes of 17 cod caught in the GOM were reweighed after 48 hours on ice to determine if time on ice affected ovary weight.

Within minutes of weighing, the entire left lobe of most specimens was placed in a 1-L jar containing a volume of formalin approximately equal to four times the volume of the ovary. When the left lobe was too large (>250 g) to fit through the opening of the jar, a large portion weighing 250 g or less was cut off and weighed and preserved as above. These whole lobes and lobe portions of ovarian material remained in formalin for 158–175 (mean=169) days and were then reweighed to the nearest 0.001 g. These are hereafter referred to as lobe-formalin samples.

From the center of the right ovary of each fish, four 1.5-mL subsamples of ovarian material (i.e., one subsample per fish for each of four treatments: formalin, Gilson's, ethanol, and freezing) almost entirely comprising vitellogenic oocytes, were removed with a 3-mL plastic syringe tube, the end of which was cut off at the zero mark. The collection of subsamples from fresh ovaries in this way was very easy, gave no evidence of damaged oocytes, and repeatedly produced subsamples with a mean of 1.54 g (*n*=155, coefficient of variation [CV]=3.70). Across fish species, differences in oocyte size and density within and between left and right ovarian lobes are uncommon (West, 1990), and oocyte size tends not to vary among different locations in cod ovaries (Kjesbu and Holm, 1994). Still, in this study ovarian material was always taken from the same part of each ovary in order to ensure that subsamples of

oocytes removed from the same localized population of oocytes all had the same mean size and density. Each of these subsamples was then preserved in one of four ways, such that one subsample from each fish was placed in each treatment (i.e., one replicate per fish within a treatment). Only subsamples from specimens collected in May in the GOM (i.e., 23 cod and all 16 plaice) were weighed to the nearest 0.001 g before preservation.

In the formalin treatment (termed the sub-formalin treatment in weight comparisons to distinguish it from the lobe-formalin treatment), a subsample of ovarian material was placed in a vial (10-mL plastic vial with screw cap) containing 5 mL of formalin. Similarly in the Gilson's treatment, a subsample of ovarian material was placed in a vial containing 5 mL of modified Gilson's solution. This modified form of Gilson's solution was employed because it does not contain mercuric chloride, and is thus not toxic, but still effectively preserves and separates oocytes (Friedland et al., 2005). These samples were capped and shaken to ensure oocytes were all thoroughly immersed in the preservative, and were then stored upright in a rack at room temperature. In the ethanol treatment, a subsample of ovarian material was placed in a vial and immersed in 4 mL of 95% ethanol for approximately 15 seconds, before 1.5 mL of distilled water was added to the sample through a graduated pipette, before the solution was diluted to 70% ethanol. Samples in this treatment were also shaken and stored at room temperature. Briefly submerging the material in 95% ethanol is meant to act as a fixative, whereas 70% ethanol is better for long-term preservation (Black and Dodson, 2003). In the freezing treatment a subsample of ovarian material was immersed in a vial of distilled water. Because of our concern that the expansion with freezing too much water might crack the vials, 3 mL of water was used rather than 5 mL as in the other treatments. These samples were also shaken, but then placed (upright) in the freezer so that the ovarian material would be frozen solid in ice. The samples were frozen in this way to preserve the shape of the oocytes and to stop them from drying out or becoming freezer damaged.

Subsamples that were weighed fresh (i.e., those collected in May) were reweighed after 97–111 (mean=102) days of preservation and then returned to their preservative vials. To weigh a preserved subsample, the entire content of a vial was poured into a 40- μ mesh, nylon cell-strainer fitted atop a hand operated vacuum pump. Excess fluid was then removed from each sample by repeatedly squeezing the handle of the hand pump until preserved ovarian material was all that remained in the strainer. The strainer and its contents were then weighed to the nearest 0.001 g, and the known weight of the strainer was subtracted to find the preserved subsample weight.

In addition to the four treatments mentioned above, a fifth split-formalin treatment (so termed because preservation was split into two phases described below) was used for the left ovarian lobes. After 91–131 (mean=111) days of preservation in formalin, each left lobe was

removed from its jar and a 1.5-mL subsample was removed from its center and placed in a vial containing 5 mL of formalin. Because they were not preweighed, these subsamples were used only for examining preservative effects on oocyte size. These subsamples remained in vials for another 33–92 (mean=63) days before they were analyzed. Including the total time that split-formalin samples were preserved, the time that samples from all treatments were preserved was 117–164 (mean=145) days before the mean oocyte diameter of each sample was estimated.

The method used here for measuring oocytes is largely based on the work of Thorsen and Kjesbu (2001) but is described here because of differences in details. To start, a vial was shaken vigorously for 30–60 seconds to break apart any oocytes still connected. Samples in modified Gilson's solution did not require shaking because the oocytes were already chemically separated. Most other samples broke apart very well from this shaking, especially those with larger oocytes. Samples in ethanol and samples containing the smallest oocytes were more difficult to break apart and required more shaking. After the vial was shaken, a transfer pipette was used to agitate the oocytes by the action of drawing in and expelling the solution rapidly, so that all oocytes were effectively mixed randomly in suspension and would not settle out by size. While the suspension was being agitated, a portion of the vial's contents was drawn and quickly emptied into a Petri dish containing \approx 2 mm of the respective preservative and a drop of 5% Palmolive soap solution which helped the oocytes spread out in the dish and kept them from floating. Oocytes were then added to the Petri dish until the bottom of the dish was filled but so that the oocytes could still be spread out without clumping. A black lid was then placed on the dish to serve as a contrasting background, and an image of the sample was captured with a flatbed scanner. Each sample was scanned at 1200 dpi in 16-bit gray scale and a contrast setting of 18 with the use of an Epson Perfection 1670 scanner (Epson, Long Beach, CA). The same selection marquis was used for each sample so that all images were exactly the same size: 3688 \times 3671 pixels, within a 12.9 MB uncompressed TIFF file.

Because samples in most treatments were stored at room temperature, no temperature adjustment was needed before they were scanned. For samples in the freezing treatment, however, care was taken to be sure that vials were thawed one hour before they were scanned out of concern that oocyte diameter may be affected by how much time thawed samples were left in water.

Once scanned, each image was analyzed in the free-ware program Scion Image (Scion Image, version beta 4.0.2, Scion Corporation, Frederick, MD) by first setting the scale of each image to 1200 pixels per inch (472 pixels per cm), and the measurements to micrometers. The lower limit of the density slice tool was then set to 40 and the upper limit ranged from 180 to 205, and was typically 195. The upper limit varied because the grey value of the oocyte margins varied between samples depending on how dark the oocytes were. The Scion

Image software used those grey values to determine the perimeter of the particles; therefore standardizing the upper limit of the density slice among samples would result in less accurate measurements. Then the “analyze particles” command was run on particles from 150 to 1500 pixels in area. The process was also set to include interior holes and to ignore particles touching the perimeter as the oocytes were measured.

The output of this process produced four columns of data: area, perimeter, major axis length, and minor axis length for each particle. These data were then transferred to a Microsoft Excel spreadsheet (Microsoft® Office Excel 2003, Microsoft Corporation, Redmond, WA), where a macro was run to filter out measurements of non-oocytes by accepting only particles within a narrow range of roundness values. The macro then calculated the mean oocyte diameter of each sample, as well as other descriptive statistics, and produced a percent frequency histogram for the sample of roundness-filtered particles.

Ideally all samples would have been analyzed after the same amount of time that they had been preserved, although it was not practical to do so. Thus time (days) preserved was recorded for each sample and the average time that the sample was preserved was compared between groups where appropriate.

Statistical analyses

The preserved weight of a lobe or subsample of ovarian material was compared to its fresh weight. Percent change in weight was calculated with Equation 1:

$$\% \Delta_{W_t} = ((Wt_{Preserved} - Wt_{Fresh}) / Wt_{Fresh}) \times 100, \quad (1)$$

where $\% \Delta_{W_t}$ = the percent change between $Wt_{Preserved}$ and Wt_{Fresh} ;

$Wt_{Preserved}$ = preserved weight of a sample of ovarian material; and

Wt_{Fresh} = fresh weight of that sample.

A positive $\% \Delta_{W_t}$ indicated an increase in weight due to preservation.

It was not logistically possible to measure the diameters of fresh oocytes; therefore it was necessary to use one of the preservative treatments as a control treatment. The formalin treatment was chosen for this purpose, because it is a standard preservation method and thus was expected to have the most consistent effect on oocyte size. In this experiment, the other four treatments (Gilson's, ethanol, freezing, and split-formalin) were considered experimental treatments. Change in mean oocyte diameter due to preservation in the experimental treatments was quantified by using Equation 2:

$$\% \Delta_{OD} = ((OD_{Experimental} - OD_{Control}) / OD_{Control}) \times 100, \quad (2)$$

where $\% \Delta_{OD}$ = the percent difference in mean oocyte diameter between $OD_{Experimental}$ and $OD_{Control}$;

$OD_{Experimental}$ = the mean oocyte diameter of a subsample of an ovary preserved in one of the four experimental treatments; and

$OD_{Control}$ = the mean oocyte diameter of a subsample of the same ovary preserved in the formalin treatment.

A positive $\% \Delta_{OD}$ indicates that the mean oocyte diameter of a subsample in the experimental treatment is larger than in the formalin treatment.

For examining $\% \Delta_{W_t}$ and $\% \Delta_{OD}$, samples were grouped by experimental treatment within species, and then in the case of cod where samples were collected from two regions, the samples were further grouped by region. *T*-tests were conducted within these groups to test the null hypothesis (H_0) that $\% \Delta = 0$ for each experimental treatment. Assessment of normality of each group by examining boxplots and histograms indicated that data did not require transformation. Statistical analyses were performed with SAS (version 9.1, SAS Institute Inc., Cary, NC). Each test had $n_1 + n_2 - 2$ degrees of freedom (Tables 2 and 3) where n_1 and n_2 were the total numbers of observations from each group. Where *t*-tests were conducted in groups, significance (α) levels were adjusted by the sequential Bonferroni procedure (Quinn and Keough, 2002), to minimize family-wise type-I error rate.

When a significant difference in $\% \Delta_{OD}$ was found between two groups, time preserved was investigated as a confounding factor, although any major change in oocyte size due to preservation typically happens within one day (Kjesbu et al., 1990). A *t*-test of time preserved between the groups was conducted in which the ratio of time preserved in experimental treatment to time preserved in control treatment was used as a metric of time preserved, because the calculation for $\% \Delta_{OD}$ includes $OD_{Control}$ in the denominator (see Eq. 2). If no significant difference was found, we concluded that the difference in $\% \Delta_{OD}$ was not due to time preserved. If a significant difference was found, a one-tailed *t*-test of $\% \Delta_{OD}$ between these groups was conducted. Assuming that the sign of the slope of the relationship between time preserved and oocyte diameter is constant after the initial changes that occur within days of preservation, the group with a higher time preserved value should have exhibited a greater $|\% \Delta_{OD}|$. Thus the H_0 for each one-tailed *t*-test was: $|\text{mean } \% \Delta_{OD}|$ of group preserved for more time $\leq |\text{mean } \% \Delta_{OD}|$ of group preserved for less time. If this analysis implicated time preserved as a likely cause of a significant difference in $\% \Delta_{OD}$, then the effect of the experimental treatment would be considered confounded.

In situations where there was a significant difference in $\% \Delta_{OD}$ and time preserved, but the sign of $\% \Delta_{OD}$ was different between the groups, no such test was performed. Instead it was concluded that the difference in $\% \Delta_{OD}$ was not due to time preserved, based on the assumption that the sign of the slope of the relationship between time preserved and oocyte diameter is constant.

Table 2

The effects of method and treatment on ovary weight among the species Atlantic cod (*Gadus morhua*), haddock (*Melanogrammus aeglefinus*), and American plaice (*Hippoglossoides platessoides*), within the region Georges Bank (GB), the Gulf of Maine (GOM) or within both regions combined (Combined), and between regions for Atlantic cod. *T*-tests compare percent change in fresh weight among species within each treatment group. The methods column designates whether ovaries were used as 1.5-mL subsamples (Sub) or as entire lobes (Lobe). *df* = degrees of freedom, *t* = *t*-statistic, * = statistically significant at the appropriate Bonferroni adjusted α -value.

Species	Method	Region	Treatment	<i>t</i>	<i>df</i>	<i>P</i> -value	α -value ¹
Atlantic cod	Sub	GOM	Formalin	-0.24	38	0.81	0.05
American plaice	Sub	GOM	Gilson's	3.05	37	0.0042*	0.025
			Ethanol	-9.61	37	<0.001*	0.013
			Freezing	7.47	32	<0.001*	0.017
Atlantic cod	Lobe	GB	Formalin	-3.73	40	<0.001*	0.05
Atlantic cod	Lobe	GOM					
Atlantic cod	Sub	GOM	Formalin	6.06	44	<0.001*	0.05
Atlantic cod	Lobe	GOM					
Atlantic cod	Lobe	GB	Formalin	-1.19	36	0.24	0.05
Haddock	Lobe	GB					
Atlantic cod	Lobe	Combined	Formalin	1.33	59	0.19	0.05
Haddock	Lobe	GB					

¹ α -values lower than 0.05 were adjusted by the sequential Bonferroni procedure for multiple comparisons (Quinn and Keough, 2002).

Similar analyses were conducted when a significant difference in $\% \Delta_{W_t}$ was identified between two groups. For these comparisons, however, days preserved was used as the metric of time preserved, since fresh weights were taken for all these samples.

Results

Effect of preservation on weight of ovarian material

All four experimental treatments had significant effects on subsample weight for cod and plaice (Fig. 1), except for plaice samples in the freezing treatment ($P=0.12$), which also had the highest standard error (SE) of $\% \Delta_{W_t}$ (SE=4.93). For cod, standard error of $\% \Delta_{W_t}$ was also highest in the freezing treatment (SE=3.37) along with mean $\% \Delta_{W_t}$ (mean=51.32). Mean $\% \Delta_{W_t}$ was lowest for cod in the ethanol treatment (mean=-4.21) but highest for plaice (mean=25.3). In the lobe-formalin treatment there was a significant difference in $\% \Delta_{W_t}$ for GB cod ($P=0.036$), GOM cod ($P<0.001$), all cod combined ($P<0.001$), and haddock ($P=0.002$). These data were not available for plaice.

Mean $\% \Delta_{W_t}$ was not significantly different between cod and haddock in the lobe-formalin treatment regardless of whether haddock was compared with cod samples restricted to GB ($P=0.24$, $\alpha=0.03$) or when all cod were combined ($P=0.28$, $\alpha=0.05$). Mean $\% \Delta_{W_t}$ of subsamples was significantly different between cod and plaice for the ethanol ($P<0.001$), freezing ($P<0.001$), and Gilson's ($P=0.0042$) treatments (Table 2). There was

no difference in $\% \Delta_{W_t}$ between cod and plaice in the subformalin treatment ($P=0.81$). This test marks the only comparison between cod and plaice where no difference was found. There was a significant difference in mean $\% \Delta_{W_t}$ ($P<0.001$) for cod between GB (mean=1.41) and the GOM (mean=6.79) in the lobe-formalin treatment. For cod from the GOM, there was a significant ($P<0.001$) and nearly threefold difference in mean $\% \Delta_{W_t}$ between lobe-formalin (mean=6.79) and sub-formalin (mean=19.32) treatments.

For the 17 ovaries collected from cod caught in the GOM, all of which were weighed after 24 and then 48 hours on ice (fresh weights were not available), mean percent change in weight during this interval was significantly different from zero ($P=0.02$). However this change was very slight (mean=-0.32, SE=0.11).

Effect of preservation on oocyte diameter

Oocyte diameter in the experimental treatment was significantly different from that of the control treatment (Fig. 2), in all but three comparisons. Significant differences were not detected for plaice ($P=0.22$) in the ethanol treatment or for GB cod ($P=0.59$) or haddock ($P=0.37$) in the split-formalin treatment. Of the four experimental treatments, the freezing treatment produced the highest mean $\% \Delta_{OD}$ for GB cod (mean=18.81), GOM cod (mean=26.99), GB and GOM cod combined (mean=23.29), and haddock (mean=28.88). Plaice samples in the freezing treatment also exhibited a significant positive change ($P<0.001$, mean=9.90), but a larger change was exhibited in the Gilson's treatment

Table 3

The effects of experimental treatment (Gilson's, ethanol, freezing, and split-formalin) on oocyte diameter among the species Atlantic cod (*Godus morhua*), haddock (*Melanogrammus aeglefinus*), and American plaice (*Hippoglossoides platessoides*) within the regions of Georges Bank (GB), the Gulf of Maine (GOM), or within both regions combined (Combined), and between regions for Atlantic cod. *T*-tests were used to compare mean percent difference¹ in oocyte diameter between experimental and control (formalin) treatments among species. *t* = *t*-statistic, *df* = degrees of freedom, * = statistically significant at the appropriate Bonferroni adjusted α -value.

Species	Region	Treatment	<i>t</i>	<i>df</i>	<i>P</i> -value	α -value ²
Atlantic cod	GB	Gilson's	5.19	40	<0.001*	0.013
Atlantic cod	GOM	Ethanol	-1.79	40	0.082	0.05
		Freezing	-3.91	37	<0.001*	0.025
		Split-Formalin	-4.21	39	0.001*	0.017
Atlantic cod	GB	Gilson's	2.49	33	0.018	0.017
Haddock	GB	Ethanol	-2.09	33	0.045	0.025
		Freezing	-2.62	33	0.013	0.013
		Split-Formalin	-1.11	32	0.28	0.05
Atlantic cod	Combined	Gilson's	0.36	56	0.72	0.05
Haddock	GB	Ethanol	-1.75	56	0.085	0.017
		Freezing	-1.92	53	0.06	0.013
		Split-Formalin	0.72	54	0.48	0.025
Atlantic cod	GOM	Gilson's	2.84	37	0.0073*	0.05
American plaice	GOM	Ethanol	-5.39	37	<0.001*	0.017
		Freezing	11.40	32	<0.001*	0.013
		Split-Formalin	3.41	36	0.002*	0.025
Atlantic cod	Combined	Gilson's	4.33	56	<0.001*	0.013
American plaice	GOM	Ethanol	-5.74	56	<0.001*	0.025
		Freezing	6.18	51	<0.001*	0.017
		Split-Formalin	2.98	55	0.0043*	0.05

¹ Defined by the following: $(TreatmentDiameter - FormalinDiameter) \times 100$, where *TreatmentDiameter* = the mean oocyte diameter of a subsample of an ovary preserved in one of the experimental treatments and *FormalinDiameter* = the mean oocyte diameter of a subsample of the same ovary preserved in the formalin treatment.

² α -values lower than 0.05 were adjusted by the sequential Bonferroni procedure for multiple comparisons (Quinn and Keough, 2002).

(mean=-18.43). Of the four experimental treatments, the split-formalin treatment produced the smallest mean % Δ_{OD} for GB cod (mean=-0.31), GOM cod (mean=2.90), GB and GOM cod combined (mean=1.41), and haddock (mean=0.77). Plaice samples in the split-formalin treatment also exhibited only a small change (mean=-2.59), but the smallest change (mean=0.94) was in the ethanol treatment.

Mean % Δ_{OD} was not significantly different between cod and haddock for any treatment (Table 3), regardless of whether haddock samples were compared with cod samples restricted to GB or when cod from GB and GOM were combined. Mean % Δ_{OD} was significantly different between cod and plaice for all treatments, also regardless of whether cod samples were restricted to GB or when all cod were combined. There was a significant difference in mean % Δ_{OD} for cod from GB and cod from the GOM in the Gilson's ($P < 0.001$, $\alpha = 0.013$), freezing ($P < 0.001$, $\alpha = 0.025$), and split-formalin ($P = 0.001$,

$\alpha = 0.017$) treatments, but not the ethanol treatment ($P = 0.08$, $\alpha = 0.05$).

In the comparison between lobe-formalin and subformalin samples, analyses showed time preserved could not have caused the difference in preserved weight between these groups. Although significant differences in % Δ_{Wt} of subsamples were detected between cod and plaice in the Gilson's, ethanol, and freezing treatments, time preserved between species was consistent for all treatments.

There were only five comparisons where it was appropriate to investigate time preserved as a possible cause for differences in % Δ_{OD} between two groups. These comparisons were the following: cod from GB and GOM in the Gilson's, freezing, and split-formalin treatments, and cod (GB and GOM combined) and plaice, in the Gilson's and freezing treatments. The H_0 that mean % Δ_{OD} of group preserved longer \leq mean % Δ_{OD} of group preserved shorter was only rejected in the comparison

between cod (GM and GOM combined) and plaice in the freezing treatment ($P < 0.001$).

For four haddock samples in the freezing treatment, mean oocyte diameter was measured immediately after the sample was freshly thawed, and then again after 48 hours of refrigeration. Mean oocyte diameter of the samples decreased by 3–10% after refrigeration, although the average decrease of 4.4% was not significantly different from zero ($P = 0.11$), perhaps because of the small sample size.

Discussion

Of the preservatives tested in this study, the results with formalin were most similar among individuals and species, and the results from freezing were the least

consistent among individuals within and among species. In terms of image quality, samples preserved in formalin were clearest and contained the least debris. In weight comparisons between cod and plaice, the subformalin treatment was the only one where no significant difference between the two species was found. Of the tested preservatives, the best option for a standard preservative was formalin, especially when samples might be used for histology, where postovulatory follicles and fine cellular structures must be preserved.

When realized fecundity is estimated from total potential fecundity, estimates may be biased if samples are collected too late in the season and spawning has already begun, or if atresia is likely to occur between sampling and the time of spawning. Both of these biases are quantified through histological analysis. In species or stocks where the developing stage is difficult to identify or where high rates of atresia are expected, histological analysis is necessary to assure that estimates of realized fecundity are accurate. Although Gilson's solution and ethanol may be used for fecundity research and may be superior in certain situations for particular species, they do not preserve tissue well enough for histological analysis, and thus they are undesirable in many situations.

Formalin is a common preservative for ovarian material and is widely used to fix and preserve animal tissue. Although our results show differences between formalin samples and Gilson's and frozen samples that contrast with results of studies on other species, the effects of formalin preservation were very consistent among the species we studied. Formalin preservation resulted in an increase in sample weight in all species, and when compared between species these changes were similar.

The differences between the formalin and split-formalin treatments for all species (Fig. 2), although significant for GB and GOM cod combined, GOM cod, and plaice, were quite small and therefore indicated that formalin preserves oocyte size similarly whether ovarian material is in large membrane-bound lobes or in 1.5-mL subsamples. However, the large and significant difference in $\% \Delta_{W_t}$ of samples of GOM cod ovarian material between the lobe-formalin and subformalin treatments indicates a conflict because oocyte diameter and ovarian material weight are inherently related. If ovarian material weight increases much more in one treatment than another, oocyte size should as well. The reason for this disagreement may lie in the fact that after subsamples in the split-formalin treatment were removed from whole preserved lobes, they were preserved as subsamples for several weeks before the

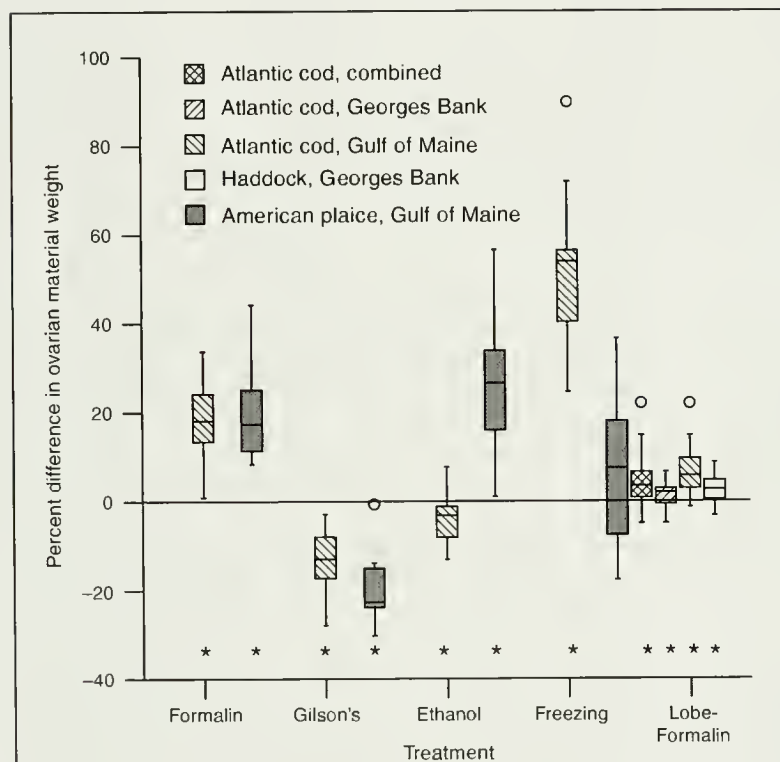


Figure 1

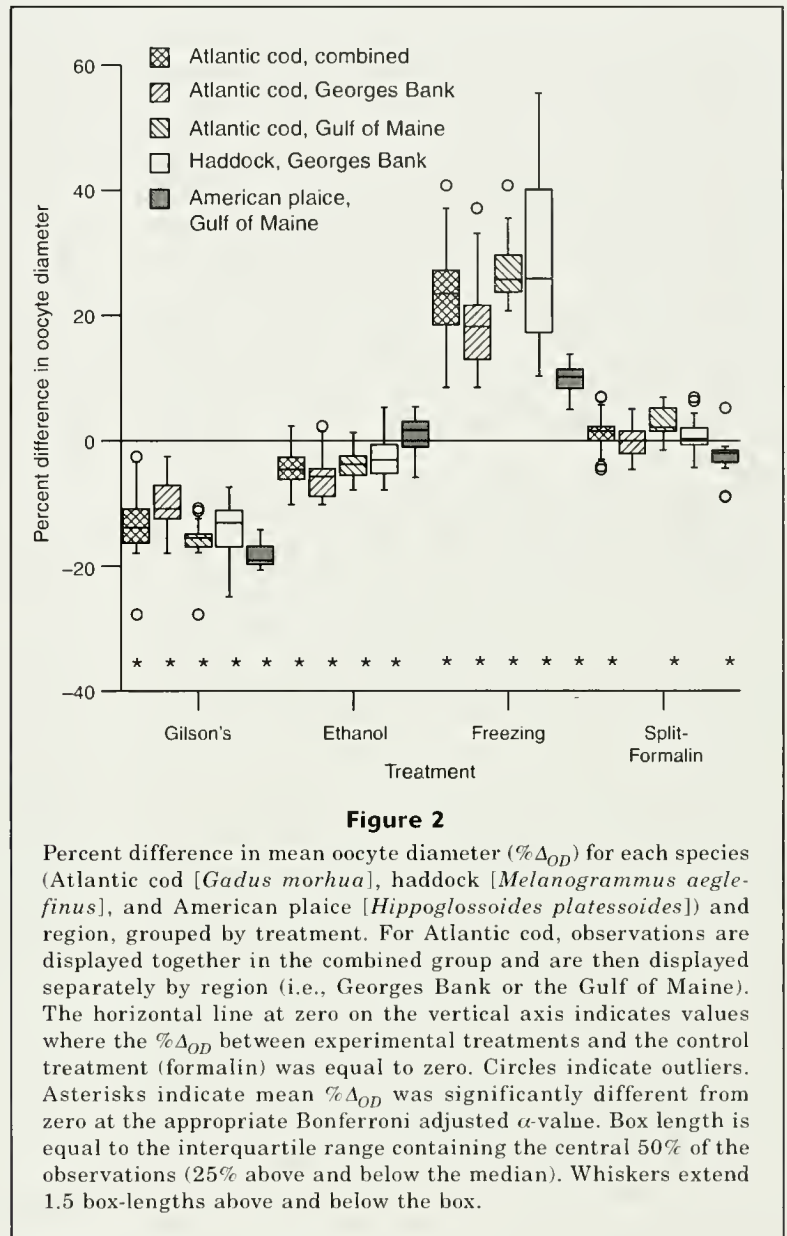
Percent difference in ovarian material weight ($\% \Delta_{W_t}$) for each species (Atlantic cod [*Godus morhua*]), haddock [*Melanogrammus aeglefinus*], and American plaice [*Hippoglossoides platessoides*]) and region, grouped by treatment. For Atlantic cod, observations are displayed together in the combined group and are then displayed separately by region (i.e., Georges Bank or the Gulf of Maine). The horizontal line at zero on the vertical axis indicates values where the percent difference in weight between preserved and fresh ovarian material was equal to zero. Circles indicate outliers. Asterisks indicate that mean $\% \Delta_{W_t}$ was significantly different from zero at the appropriate Bonferroni adjusted α -value. Box length is equal to the interquartile range which contains the central 50% of the observations (25% above and below the median). Whiskers extend 1.5 box-lengths above and below the limits of the box.

oocytes were measured. During that time, swelling that was inhibited by the dense packing of oocytes in the ovarian lobe may have occurred; therefore by the time they were measured, oocytes were very similar in size to those preserved in the sub-formalin treatment.

Standard Gilson's solution has been a common oocyte preservative since it was developed. Joseph (1963) found that tuna oocytes preserved in standard Gilson's solution were 24% smaller than those preserved in 4% formalin. In contrast Schaefer and Orange (1956) concluded that mean diameters of oocytes from the same tuna species, preserved in standard Gilson's solution and formalin (concentration not specified) were similar, although they did not present statistical evidence to support this conclusion. Cod, haddock, and plaice oocytes preserved in modified Gilson's solution were 13.28%, 13.77%, and 18.43% smaller, respectively, than those preserved in 10% formalin. These results were all significant, and are similar to Joseph's (1963) results. The discrepancy between our results and those of Joseph (1963) could be attributed to interspecies variation. Although differences were identified, we consider the effects of modified Gilson's solution to be fairly consistent among species.

Ethanol is rarely used to preserve ovarian material used in fecundity studies, but because Black and Dodson (2003) used ethanol to successfully fix and preserve water fleas (*Daphnia pulex*) and their eggs, and ethanol caused less distortion and change in body size than a solution of sucrose and 4% formalin, it was evaluated in this study. Oocytes preserved in this treatment were of sufficient quality for use in digital image analysis. Ethanol also had a bleaching effect on oocytes, which resulted in greater contrast between oocytes and the black background. The ethanol treatment tended to cause smaller changes to oocyte size and ovarian material weight than other treatments, except for the large increase in subsample weight in plaice. In ethanol, $\% \Delta_{Wt}$ was negative for cod, $\% \Delta_{OD}$ was negative for cod and haddock, and both were positive for plaice. Such results make it difficult to generalize about the effects of ethanol on ovarian material across taxa and may make this treatment less desirable than others.

Freezing is one of the most common methods of ovary preservation, but this treatment has not been used to preserve oocytes for digital image analysis. Although freezing was expected to result in many ruptured oocytes, oocytes in the frozen treatment maintained a very round shape and rarely broke even after vigorous shaking and agitation. Freezing the oocytes solid in distilled water may have improved the ultimate quality



of the samples by limiting the exposure of oocytes to the oxidizing and desiccating effects of air. Although the quality of the images obtained from these samples was high enough for measurement and counting, percent change in ovarian material weight and oocyte diameter of frozen specimens proved to be very variable and often very high (Figs. 1 and 2).

Although the mean diameter of cod, haddock, and plaice oocytes preserved in the freezing treatment was 23.29%, 28.88%, and 9.90% larger, respectively, than the mean diameter of oocytes in the formalin treatment, Ramon and Bartoo (1997) found that the mean diameter of tuna eggs in 10% buffered formalin was generally 5–10% larger than the mean diameter of oocytes from frozen ovaries. It may not be surprising to find a difference between the species we studied and the tunas, but

such a substantial difference showing an opposite trend is somewhat surprising and is probably largely due to the difference in freezing methods. Although freezing ovarian material in water may improve the quality of the preserved oocytes, it is probably responsible for the large and variable changes that we observed. Because ovarian material is placed in hypotonic distilled water, it will absorb the water, thus increasing the size and weight of the oocytes. If it takes a long time for ovarian material in water to become isotonic, the material may not be osmotically stable by the time it is frozen and even by the time the oocytes are measured, which could cause the observed changes and variation in size and weight. In future research ovarian material should be frozen in an isotonic solution to prevent oocytes from swelling.

The initial reason ovary samples were preserved in a variety of treatments was to determine if oocytes preserved by these methods could be used in digital image analysis. The only studies we are aware of that employ digital image analysis to count and measure fish oocytes preserve them in either formalin (Thorsen and Kjesbu, 2001; Yoneda and Wright, 2004) or modified Gilson's solution (Friedland et al., 2005). All treatments in our study preserved ovarian material of cod, haddock, and plaice well enough to permit easy identification and measurements of oocytes. Clumping was a factor for many samples in all but the Gilson's treatment, but most clumps could be broken up well by shaking the vial for 30–60 seconds. Very tight clumps could be broken apart by rapidly drawing in and expelling oocytes and solution for 30–120 seconds with a 10-mL glass pipette with an \approx 1 mm diameter and a plastic, thumb-wheel pipette pump. A glass pipette worked better than a plastic transfer pipette, probably because its rigidity allows more suction to be created as fluid is quickly drawn into it. With simple, albeit occasionally time-consuming (up to five minutes) mechanical separation, all clumps could be sufficiently broken up so that the oocytes could be measured and counted.

Considering all comparisons for all three species, cod and haddock oocytes and ovarian material are affected similarly by a given type of preservative, whereas effect on plaice tends to differ with different preservatives. This is not unexpected because cod and haddock are in the same family, Gadidae, whereas the narrowest taxonomic group common to cod and plaice is the subdivision Euteleostei. One would expect tissues of closely related species would have similar chemical properties, and should thus be affected similarly by preservatives. Although it could be inferred from results among studies that differences in preservation exist among fish species, specific differences have not been reported before the present study.

A difference in the effect of preservation between cod samples from GB and those from GOM is also reported. This difference is unexpected but is supported by the results of comparisons of oocyte size in the Gilson's, freezing, and split-formalin treatments, and by the comparison of ovarian material weight in the lobe-formalin

treatment. Samples from GB were collected in February, whereas samples from the GOM were collected in May, which may somehow contribute to this difference. Still, it is unclear why time of year or region of sample collection would affect preservation and we suggest this as an area worthy of future research.

We successfully evaluated and quantified the effects of several preservatives on the ovarian material of several fish species, but perhaps more importantly we demonstrated how preservation can add variation to seemingly simple measurements like ovary weight and oocyte size, and can have different effects between species. Thus we stress the importance of consistent experimental methods and suggest that in studies of preserved ovarian material it should not be assumed that the effects of different preservatives and preservation treatments are consistent.

Acknowledgments

We thank R. Brown, J. Ford, R. Sherman, B. Hoffman, M. Russo and T. Ligenza for providing us with access to ovary samples. We also thank K. Friedland, E. Garcia-Vazquez, O. S. Kjesbu, two anonymous reviewers, A. Moles, and E. Calvert for their suggestions and comments. Funding for this study was provided through the Cooperative Marine Education and Research Program (CMER) at the University of Massachusetts, Amherst and a Hatch grant. Writing was completed while F. Juanes was a Center Fellow at the National Center for Ecological Analysis and Synthesis, funded by NSF (Grant #DEB-0553768), the University of California, Santa Barbara, and the State of California.

Literature cited

- Black, R., and S. I. Dodson.
2003. Ethanol: a better preservation technique for *Daphnia*. *Limnol. Oceanogr. Methods*. 1:45–50.
- Boreman, J. L., B. S. Nakashima, J. A. Wilson, and R. L. Kendall.
1997. Northwest Atlantic groundfish: perspectives on a fishery collapse, 242 p. *Am. Fish. Soc.*, Bethesda, MD.
- Fleming, I. A., and S. Ng.
1987. Evaluation of techniques for fixing, preserving and measuring salmon eggs. *Can. J. Fish. Aquat. Sci.* 44:1957–1962.
- Friedland, K. D., D. Ama-Abasi, M. Manning, L. Clarke, G. Kligys, and R. C. Chambers.
2005. Automated egg counting and sizing from scanned images: Rapid sample processing and large data volumes for fecundity estimates. *J. Sea Res.* 54:307–316.
- Joseph, J.
1963. Fecundity of yellowfin tuna (*Thunnus albacares*) and skipjack (*Katsuwonus pelamis*) from the eastern Pacific Ocean. *Inter-Am. Trop. Tuna Comm. Bull.* 7:255–292.
- Kjesbu, O. S., and J. C. Holm.
1994. Oocyte recruitment in first-time spawning Atlantic

- cod (*Gadus morhua*) in relation to feeding regime. *Can. J. Fish. Aquat. Sci.* 51:1893–1898.
- Kjesbu, O. S., P. R. Witthames, P. Solemdal, and M. Greer Walker.
1990. Ovulatory rhythm and a method to determine the stage of spawning in Atlantic cod (*Gadus morhua*). *Can. J. Fish. Aquat. Sci.* 47:1185–1193.
- Marshall, C. T., O. S. Kjesbu, N. A. Yaragina, P. Solemdal, and O. Ulltang.
1998. Is spawner biomass a sensitive measure of the reproductive and recruitment potential of Northeast Arctic cod? *Can. J. Fish. Aquat. Sci.* 55:1766–1783.
- Marshall, C. T., L. O'Brien, J. Tomkiewicz, F. W. Koster, G. Kraus, G. Marteinsdottir, M. J. Morgan, F. Saborido-Rey, J. L. Blanchard, D. H. Secor, P. J. Wright, N. V. Mukhima, and H. Bjornsson.
2003. Developing alternative indices of reproductive potential for use in fisheries management: case studies for stocks spanning an information gradient. *J. Northw. Atl. Fish. Sci.* 33:161–190.
- Murna, H., and F. Saborido-Rey.
2003. Female reproductive strategies of marine fish species of the North Atlantic. *J. Northw. Atl. Fish. Sci.* 33:23–31.
- Quinn, G. P., and M. J. Keough.
2002. *Experimental design and data analysis for biologists*, 520 p. Cambridge Univ. Press, Cambridge, UK; New York, NY.
- Ramon, D., and N. Bartoo.
1997. The effects of formalin and freezing on ovaries of albacore, *Thunnus alalunga*. *Fish. Bull.* 95:869–872.
- Schaefer, M. B., and C. J. Orange.
1956. Studies of the sexual development and spawning of yellowfin tuna (*Neothunnus macropterus*) and skipjack (*Katsuwonus pelamis*) in three areas of the eastern Pacific Ocean, by examination of gonads. *Inter-Am. Trop. Tuna Comm. Bull.* 1:283–320.
- Simpson, A. C.
1951. The fecundity of the plaice. *Fish. Invest.* 11: 17:1–27.
- Svaasand, T., K. E. Jorstad, H. Otteraa, and O. S. Kjesbu.
1996. Differences in growth performance between Arcto-Norwegian and Norwegian coastal cod reared under identical conditions. *J. Fish Biol.* 49:108–119.
- Tan-Fermin, J. D.
1991. Suitability of different formalin-containing fixatives for the eggs of freshwater Asian catfish *Clarias macrocephalus* (Gunther). *Isr. J. Aquacult.-Bamid.* 43:57–61.
- Thorsen, A., and O. S. Kjesbu.
2001. A rapid method for estimation of oocyte size and potential fecundity in Atlantic cod using a computer-aided particle analysis system. *J. Sea Res.* 46:295–308.
- Tomkiewicz, J., M. J. Morgan, J. Burnett, and F. Saborido-Rey.
2003b. Available information for estimating reproductive potential of Northwest Atlantic groundfish stocks. *J. Northw. Atl. Fish. Sci.* 33:1–21.
- Tomkiewicz, J., L. Tybjerg, and A. Jespersen.
2003a. Micro- and macroscopic characteristics to stage gonadal maturation of female Baltic cod. *J. Fish Biol.* 62:253–275.
- West, G.
1990. Methods of assessing ovarian development in fishes: a review. *Aust. J. Mar. Freshw. Res.* 41:199–222.
- Yoneda, M., and P. J. Wright.
2004. Temporal and spatial variation in reproductive investment of Atlantic cod *Gadus morhua* in the northern North Sea and Scottish west coast. *Mar. Ecol. Prog. Ser.* 276:237–248.

Abstract—In this study we analyzed the diets of 26 nekton species collected from two years (2000 and 2002) off Oregon and northern California to describe dominant nekton trophic groups of the northern California Current (NCC) pelagic ecosystem. We also examined interannual variation in the diets of three nekton species. Cluster analysis of predator diets resulted in nekton trophic groups based on the consumption of copepods, euphausiids, brachyuran larvae, larval-juvenile fishes, and adult nekton. However, many fish within trophic groups consumed prey from multiple trophic levels—euphausiids being the most widely consumed. Comparison of diets between years showed that most variation occurred with changes in the contribution of euphausiids and brachyuran larvae to nekton diets. The importance of euphausiids and other crustacean prey to nekton indicates that omnivory is an important characteristic of the NCC food web; however it may change during periods of lower or higher upwelling and ecosystem production.

Diets of and trophic relationships among dominant marine nekton within the northern California Current ecosystem

Todd W. Miller (contact author)¹

Richard D. Brodeur²

Email address for T. W. Miller: millertw@dpc.ehime-u.ac.jp

¹ Cooperative Institute for Marine Resources Studies
Oregon State University
Newport, Oregon 97365

Present address: Center for Marine Environmental Studies (CMES)
Ehime University, 2-5 Bunkyo-cho, Matsuyama
Ehime, 790-8577, Japan

² National Oceanic and Atmospheric Administration
National Marine Fisheries Service, Northwest Fisheries Science Center
Hatfield Marine Science Center
Newport, Oregon 97365

Eastern Pacific boundary upwelling zones, such as the California Current, are generally highly productive and support major fisheries, yet these ecosystems also exhibit substantial temporal fluctuations in primary and higher-level production (Francis and Hare, 1994; Carr, 2002; Chavez et al., 2003). This variation has been attributed to variability in abiotic forcing through relatively short-term (inter-annual) El Niño and La Niña events (Percy and Schoener, 1987), as well as long-term (decadal) environmental forcing (Francis and Hare, 1994; Mantua et al., 1997). This apparent link between abiotic forcing and the ecosystem has led to considerable discussion regarding energy flow through large marine ecosystems (Jackson et al., 2001). However, few studies have comprehensively examined multispecies trophic patterns within a system. Understanding trophic patterns and temporal changes between species across multiple trophic groups is essential in understanding energy transfer within a system and mechanisms behind ecosystem stability (Worm and Duffy, 2003).

The northern California Current (NCC) system encompasses the northern region of the California Current production zone (approximately 41–49° N) along the continental shelf and shelf break between northern

California and Washington. This system is a major upwelling region, where Pacific sardine (*Sardinops sagax*), northern anchovy (*Engraulis mordax*), jack mackerel (*Trachurus symmetricus*), market squid (*Loligo opalescens*), and Pacific hake (*Merluccius productus*) are the dominant nektonic species (Brodeur and Percy, 1986; Brodeur et al., 2005). Between April and September, strong but episodic coastal upwelling is the dominant hydrographic feature of the NCC. This upwelling provides cool nutrient-rich water to the euphotic zone across the shelf (Huyer, 1983), allowing for high levels of primary production (Hood et al., 1991). Inter-annual variation in coastal upwelling, particularly between El Niño and La Niña events, greatly influences primary production (Corwith and Wheeler, 2002) and higher trophic levels (Ainley et al., 1996). On an interdecadal scale, the California Current also experiences production regimes of 30 years or more, which have been linked to salmon survival (Mantua et al., 1997) and variation in NCC zooplankton biomass (McGowan et al., 1998).

The diets of multiple species within the NCC pelagic ecosystem have been examined in only a few studies, and these studies were mostly performed on single or a few closely related spe-

cies (e.g., Brodeur and Pearcy, 1990; Robinson, 2000). During the 1980s, Brodeur et al. (1987) analyzed the diets from a diverse assemblage of pelagic nekton from the NCC, but since that time, the NCC system has exhibited major shifts in the abiotic environment and in community composition (Peterson and Schwing, 2003) and a concomitant change in nekton species composition (Emmett and Brodeur, 2000). Observed environmental shifts and changes in the NCC pelagic community are undoubtedly conveyed in-part through trophic interactions. Description of the NCC in the context of the current ocean environment and nekton community is therefore important in determining the mechanisms linking climate change and pelagic ecosystem response. In this study we analyzed the diets of 26 nekton species collected during two separate years (2000 and 2002) from coastal northern California to central Oregon, applied cluster analysis to diet data to delineate trophic groups based on dominant prey taxa, and compared the importance of these prey between the two years for several species.

Materials and methods

Field collections

Nekton were collected for diet analyses from Northeast Pacific Global Ocean Ecosystems Dynamics (GLOBEC) cruises during 29 May–18 June and 29 July–12 August 2000, and 29 May–18 June and 31 July–19 August 2002. Sampling occurred along nine transects across the shelf between Crescent City, CA (41°54'N), and Newport, OR (44°39'N) (for station locations see Brodeur et al. [2004] and Reese and Brodeur [2006]), during daylight hours. At each station, nekton were collected with a Nordic-264 (Nor'Eastern Trawl Systems, Bainbridge Island, WA) rope trawl (30 m wide × 18 m deep) that was towed for 30 minutes. Up to 30 individuals per species were collected per tow for diet analysis. Nekton were immediately frozen on ship (−20°C) after removal from the net and then processed at a later date in the laboratory.

Laboratory analysis

Laboratory processing of nekton involved measurement of individuals and extraction of stomachs for diet analysis. Lengths of fish and squid were measured (± 1.0 mm) for either fork length, standard length, or dorsal mantle length. Stomachs were extracted and immediately placed in 10% buffered formalin for 10 days, rinsed with tap water, and transferred to 70% ethanol. Diet analyses were performed by assessing fullness, digestive condition, and identification and quantification of prey taxa in each stomach. Fullness was assessed on a scale of 0–5, with 0 being empty and 5 being distended. Condition of individual digested prey was assessed by using a 0–4 scale, with 0 being unrecognizable and 4 being fresh. Prey taxa were identified to the lowest possible taxon, enumerated, and wet weighed (± 0.1 mg) after excess

water was removed with blotting paper. When individual prey items were too numerous to enumerate, individual weights were estimated by obtaining the damp weight of a known number of animals and regressing this number on the total weight of the prey. For Pacific sardine, diets comprised large amounts of phytoplankton mixed with small zooplankton and euphausiid eggs that required a subsampling method for diet analysis (Emmett et al., 2005). Chinook salmon (*Oncorhynchus tshawytscha*) were divided into subyearlings, yearlings, and adults, and coho salmon (*O. kisutch*) were separated into yearlings and adults (Brodeur et al., 2004).

Data analysis

Trophic relationships of nekton were examined by using agglomerative hierarchical cluster analysis (AHCA) to form cluster dendrograms. The percent wet weight contribution of prey to predator diets were arranged in a simple predator (row) × prey (column) matrix. For AHCA we used the Sørensen (Bray-Curtis) distance measure and Ward's linkage method. Trophic groups from cluster analysis were established by choosing a cutoff level with biological meaning while maintaining a reasonable level (at least 40%) of information explained in the cluster dendrogram. The significance of trophic groups was examined using a multiresponse permutation procedure (MRPP), which tests for the null hypothesis of no difference between groups. MRPP gauges within and between group differences using an A-statistic that ranges between 0 and 1, with 0 being no agreement within a group and 1 being complete agreement. All AHCA and MRPP analyses were performed with PC-ORD software (version 4, MjM Software, Gleneden Beach, OR).

Before nonparametric analyses of diets, certain modifications to the data were performed. Nekton species that were found in <5% of the tows within a cruise were excluded from analyses, although these species were retained in the general description of diets. This level of exclusion was somewhat arbitrary; however exclusion of nekton species that were found in 5–10% of tows would have removed many predator species from analyses. Prey taxa modifications involved removal of rare species and aggregation of certain groups. Larval-juvenile fishes, hyperiid amphipods, brachyuran and decapod larvae, and adult fish prey were combined into higher taxonomic categories and life history stages. This arrangement was required to retain important species groups for multivariate analyses. Adjustments for all data involved the removal of rare prey that were only present in $\leq 10\%$ of the nekton diets (rows) in the main matrix. Removal of rarer species reduced noise in the data and allowed for comparisons of important prey between nekton predators.

Trophic relationships were also analyzed by calculating the degree of diet similarity between nekton species pairs by using Schoener's similarity index (Schoener, 1974), modified as a percent similarity index (PSI) of the diets of paired nekton:

$$PSI = \left[1 - 0.5 \sum_{i=1}^n |p_{ik} - p_{jk}| \right] \times 100, \quad (1)$$

where p = the proportion of biomass (wet weight) of the k th prey species consumed by predator species i and j .

Diet overlap values $\geq 60\%$ were considered biologically significant (Wallace and Ramsay, 1983). As in the AHCA, prey items of unidentified material, and fish and crustacean tissue, were eliminated from the calculation of PSI.

Diets (percent wet weight of major prey taxa) from selected species were compared with respect to interannual differences. Comparisons between 2000 and 2002 were limited to species and life history stages of nekton that were found in $\geq 5\%$ of the total number of hauls within a cruise, which left only yearling and adult chinook and coho salmon, and juvenile steelhead trout (*O. mykiss*). Comparisons between years were undertaken by visual inspection of plotted diet data.

Results

Trophic groups

A total of 3161 stomachs from 26 species of marine nekton were analyzed for diet composition from the June and August 2000 and 2002 cruises. A species-specific summary of number of stomachs analyzed, nekton percent frequency of occurrence, nekton size (mean and standard deviation), and mean stomach fullness and condition are presented in Table 1. A more detailed description of specific prey species consumed by nonsalmonids can be found in Miller (2006). Results from cluster analysis and MRPP showed major trophic groups for both years based on nekton diet (percent wet weight) of the following general prey groups: adult fish, larval-juvenile fish, euphausiids (*Thysanoessa spinifera* and *Euphausia pacifica*), decapod larvae, copepods, and other mixed zooplankton groups (predominantly hyperiid amphipods, gelatinous zooplankton, and phytoplankton). For 2000 and 2002, five significant trophic groups (2000 MRPP, A statistic=0.37, $P < 0.001$; 2002 MRPP, A statistic=0.31, $P < 0.001$) were observed at the cutoff level of 60% and 52% information remaining, respectively (Fig. 1).

From AHCA of nekton diets for the year 2000, trophic group A (blue shark [*Prionace glauca*] and adult coho salmon, Figs. 1 and 2) had diets that consisted (62% and 80%, respectively) of adult Osteichthyes (Clupeidae and unidentifiable fish tissue), and to a lesser extent of larval-juvenile Osteichthyes (for adult coho salmon) and euphausiids (for blue shark). Trophic group B (juvenile and adult salmon) had diets comprising $>90\%$ larval-juvenile fish and adult euphausiids for each age class. Of the euphausiids consumed, *T. spinifera* contributed the highest proportion by wet weight to salmonid diets. Trophic group C (jack mackerel, Pacific saury [*Cololabis saira*], and Pacific sardine) had diets of 86%, 93%, and

90% euphausiids, respectively; most euphausiids consumed by this group were identified as *E. pacifica*. Trophic group D (market squid and surf smelt [*Hypomesus pretiosus*]) had the most diverse diet of all nekton: mixed species of crustacean zooplankton (brachyuran larvae, euphausiids, hyperiid amphipods) accounted for most of the diet by wet weight. Trophic group E (Pacific herring [*Clupea pallasii*], whitebait smelt [*Allosmerus elongates*], and juvenile sablefish [*Anoplopoma fimbria*]), consumed euphausiids that contributed 77%, 96%, and 97% to the wet weight of their diets, respectively. Except for *E. pacifica*, which was consumed most by juvenile steelhead trout, *T. spinifera* was the dominant euphausiid species consumed by nekton within this group. The remaining nekton not included in the cluster analysis generally consumed a mix of crustacean zooplankton or crustacean zooplankton and larval-juvenile Osteichthyes (Fig. 2).

There was a similar trend in 2002 nekton diets based on the consumption of adult and larval-juvenile Osteichthyes, euphausiids, and brachyuran larvae (Figs. 1 and 3). As in 2000, blue shark and adult coho salmon (trophic group A, Figs. 1 and 3) diets consisted mainly of adult Osteichthyes (81% and 30%, respectively); blue shark diets consisted secondarily of osteichthyan tissue (16%), and adult coho salmon diet consisted secondarily of brachyuran larvae (69% of which were Dungeness crab [*Cancer magister*] megalopae). Pacific hake and adult chinook salmon, also in this group, consumed adult Osteichthyes (predominantly Clupeidae), larval-juvenile Osteichthyes (chinook salmon only), euphausiids (Pacific hake only), and brachyuran larvae (adult chinook and coho salmon). Trophic group B (Fig. 1) consisted of jack mackerel, northern anchovy, Pacific herring, juvenile sablefish, and whitebait smelt, whose diets consisted mostly of euphausiids (predominantly *T. spinifera*) and various other zooplankton and larval-juvenile Osteichthyes (Fig. 3). Juvenile chinook, coho, and chum salmon (*O. keta*), and juvenile steelhead trout formed a trophic group (C, Fig. 1), where larval-juvenile Osteichthyes represented $>50\%$ of wet weight of diet for all species (Fig. 3). Euphausiids were important in only juvenile steelhead trout (35%). Trophic group D (Fig. 1) consisted of market squid, surf smelt, spiny dogfish (*Squalus acanthias*), and Pacific sand lance (*Ammodytes hexapterus*) which consumed a mix of crustacean zooplankton (euphausiids, brachyuran larvae, hyperiids) and in the case of spiny dogfish, gelatinous zooplankton. Pacific sardine, juvenile widow rockfish (*Sebastes entomelas*), and Pacific saury clustered into a group (trophic group E, Fig. 1) that had mixed zooplankton diets of copepods, euphausiid eggs, and euphausiids. The remaining nekton not included in the cluster analysis were juvenile rockfish (*Sebastes* spp.) species and juvenile lingcod (*Ophiodon elongatus*). Juvenile lingcod diets consisted mostly of large copepods (68%, *Calanus* spp.), and larval-juvenile Osteichthyes (30%). Juvenile rockfish consumed a combination of euphausiids, copepods, hyperiid amphipods, and gelatinous zooplankton or material (Fig. 3).

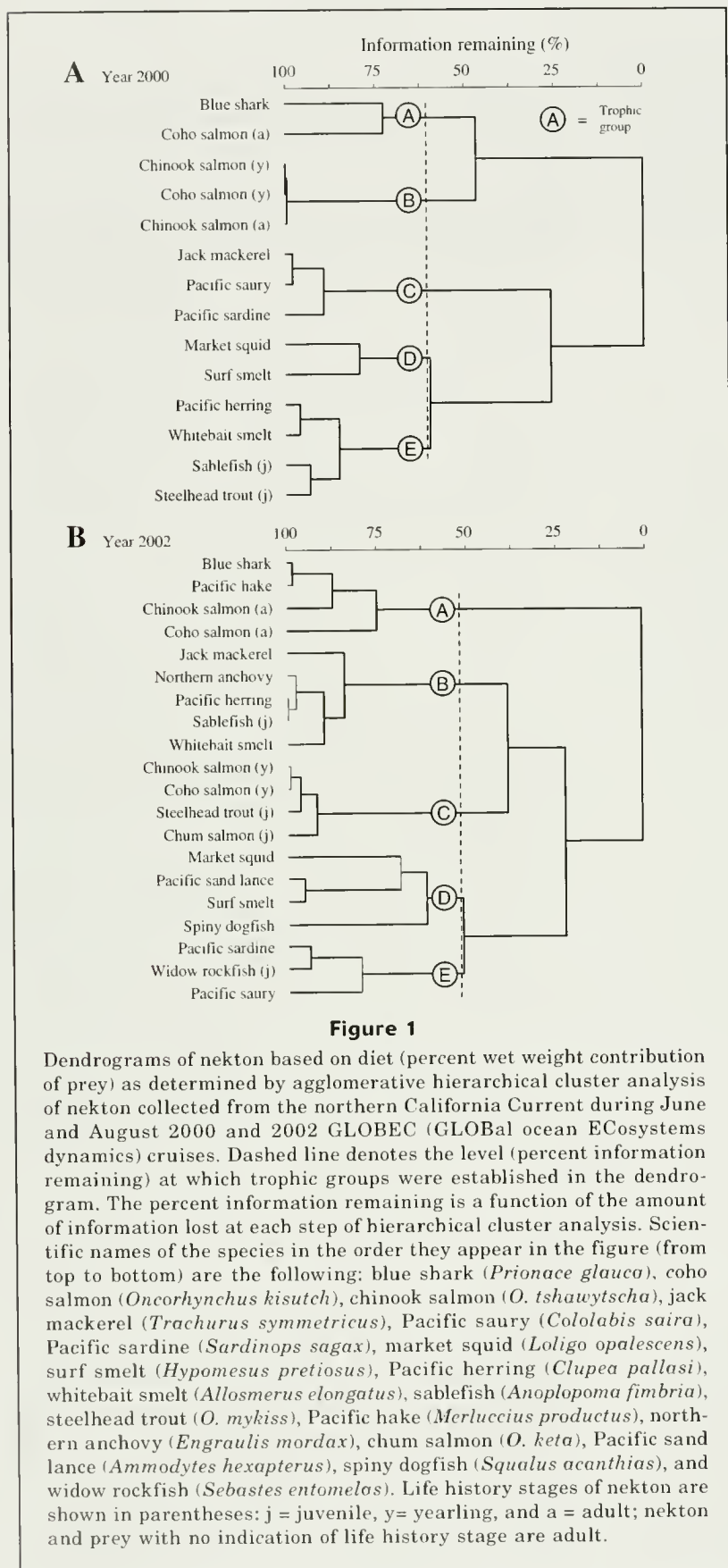
Table 1

Summary of nekton species analyzed for stomach contents from June and August 2000 and 2002 GLOBEC cruises in the northern California Current ecosystem. Percent frequency of occurrence (FO) of individual species is the occurrence of a species from 163 and 212 net tows in 2000 and 2002, respectively. Length denotes fork length with the exception of *Loligo opalescens*, which was measured in dorsal mantle length, and *Prionace glauca*, *Merluccius productus*, and *Squalus acanthias* measured in total length. Standard deviation of length is denoted as SD.

Nekton taxa	2000				2002			
	n	FO (%)	Length (mm)		n	FO (%)	Length (mm)	
			Mean	SD			Mean	SD
Market squid (<i>Loligo opalescens</i>)	38	4.8	72	17	178	5.8	84	25
Blue shark (<i>Prionace glauca</i>)	9	6.3	1331	136	13	3.3	1607	234
Spiny dogfish (<i>Squalus acanthias</i>)				128	6.3	263	34	
Northern anchovy (<i>Engraulis mordax</i>)	4	2.5	152	6	177	12.7	157	16
Pacific herring (<i>Clupea pallasii</i>)	134	8.3	146	11	152	5.8	192	24
Pacific sardine (<i>Sardinops sagax</i>)	160	13.4	221	27	108	4.1	198	24
Surf smelt (<i>Hypomesus pretiosus</i>)				87	2.5	137	11	
Whitebait smelt (<i>Allosmerus elongatus</i>)	89	4.2	100	9	69	2.0	109	7
Chinook salmon (subyearling)								
(<i>Oncorhynchus tshawytscha</i>)	56	3.8	137	14	29	15.3	283	29
(yearling)	100	18.1	225	30	100	22.4	281	33
(adult)	32	12.6	378	43	100	24.3	378	108
Coho salmon (yearling) (<i>O. kisutch</i>)	84	19.7	261	48	38	25.0	25	182
(juvenile)				148	10.6	114	11	
(adult)	13	7.1	594	71	56	8.7	9	514
Chum salmon (juvenile) (<i>O. keta</i>)	147	10.6	113	11				
Cutthroat trout (adult) (<i>O. clarki</i>)	4	2.2	297	19	7	5.9	321	28
Steelhead trout (juvenile) (<i>O. mykiss</i>)	55	13.4	284	29	15	5.5	268	30
(adult)	1	1	430					
Pacific hake (<i>Merluccius productus</i>)				72	1.9	252	51	
Pacific saury (<i>Cololabis saira</i>)	40	5.1	157	22	140	5.8	214	38
Bank rockfish (juvenile) (<i>Sebastes rufus</i>)				9	1.0	84	25	
Canary rockfish (juvenile) (<i>S. pinniger</i>)				16	2.9	27	3	
Darkblotched rockfish (juvenile) (<i>S. crameri</i>)	7	1.2	47	4	11	2.9	29	2
Yellowtail rockfish (juvenile) (<i>S. flavidus</i>)	26	2.4	49	4				
Rockfish (juvenile) (<i>Sebastes</i> spp.)	4	1.2	48	2	19	2.9	37	7
Widow rockfish (juvenile) (<i>Sebastes entomelas</i>)				41	4.8	53	4	
Lingcod (juvenile) (<i>Ophiodon elongatus</i>)	10	4.8	74	4	1	1.0	64	
Sablefish (<i>Anoplopoma fimbria</i>)	6	2.5	157	22	15	5.0	181	9
Jack mackerel (<i>Trachurus symmetricus</i>)	74	11.4	497	75	242	13.1	505	54
Pacific mackerel (<i>Scomber japonicus</i>)	24	1.3	325	19				
Pacific sand lance (juvenile)								
(<i>Ammodytes hexapterus</i>)				73	5.8	57	5	
Total	1117				2044			

Percent similarity of diets between nekton species varied by year (Tables 2 and 3). During 2000 (Table 2), highest similarity values were found between yearling chinook and yearling coho salmon (94%), yearling and adult chinook salmon (88%), and yearling coho salmon and adult chinook salmon (88%). Trophic groups B (yearling and adult chinook salmon and yearling coho salmon) and C (jack mackerel, Pacific saury, and Pacific sardine) had the highest similarities in diet (mean 90% and 58%, respectively). For trophic group B, larval-

juvenile Osteichthyes and adult euphausiids together accounted for over 80% of the total percent similarity in diets among the three nekton, and larval-juvenile Osteichthyes accounted for 60% of the overlap. Other nekton that had significant (>60%) percent similarity in diets (Table 2) were 1) jack mackerel and juvenile steelhead trout and 2) juvenile steelhead trout and Pacific herring; and the similarities were primarily due to euphausiids, or to species that fed on euphausiids and other mixed zooplankton, or in the case of adult coho



salmon and blue shark, to adult Osteichthyes (Fig. 2).

In 2002, trophic group C containing yearling chinook and coho salmon, juvenile chum salmon, and steelhead trout had the highest overall mean percent similarity (63%); and the highest similarity (78%) was between yearling chinook and yearling coho salmon (Table 3). Most of the similarity in diet within this trophic group was due to larval-juvenile Osteichthyes (70% of total similarity). Trophic groups B and A had the next highest similarities in diet (mean 61% and 46%, respectively). Similarities in diet within these two groups were primarily attributed to euphausiids (that represented 68% of total similarity) for trophic group B, and adult Osteichthyes (that represented 58% of total similarity) for trophic group A. The remaining trophic groups D and E had percent similarities <30%.

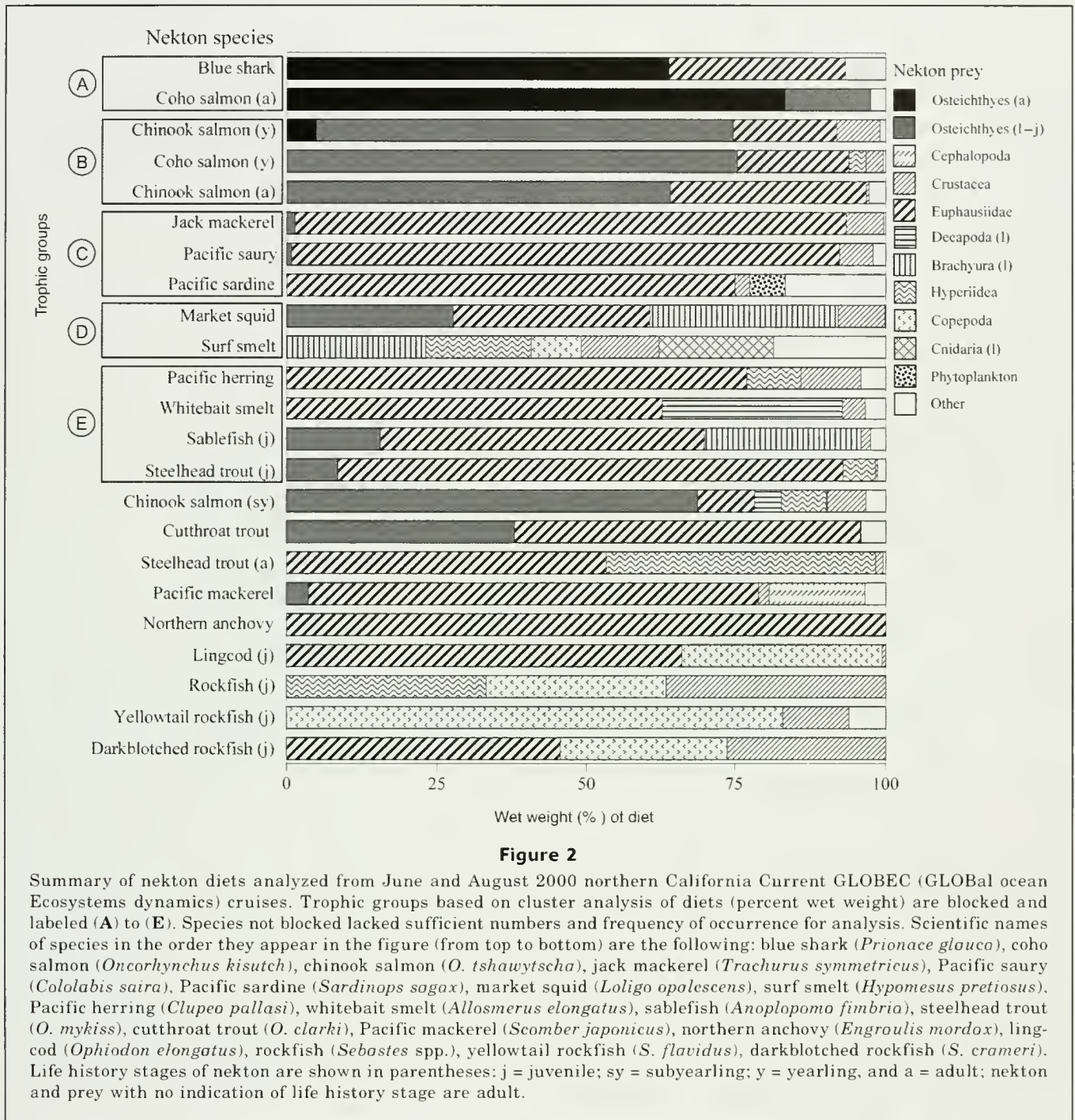
Interannual variation

Adult coho salmon and juvenile steelhead trout displayed the largest contrast in diet between 2000 and 2002. For adult coho salmon, adult and larval-juvenile Osteichthyes contributed >95% of the diet in 2000, and brachyuran larvae contributed approximately 50% of the diet in 2002 (Fig. 4). Steelhead trout had a greater proportion of its diet from euphausiids (84%) in 2000, whereas larval-juvenile Osteichthyes were more important in 2002 (57%). The remaining nekton displayed relatively similar diets between years, although differences were observed in the contribution of euphausiids and brachyuran larvae. Yearling coho and chinook salmon showed that larval-juvenile fishes contributed >70% of their diet for both years. Euphausiids contributed more to diets of both species during 2000 ($\geq 18\%$) compared to 2002 ($>5\%$), whereas in 2002 brachyuran larvae were more prominent in the diets (Fig. 4). The trend of higher proportions of euphausiids in diets in 2000 and of brachyuran larvae in 2002 was also observed in adult coho and chinook salmon.

Discussion

Trophic groups

Diet analysis of 26 nekton species of the northern California Current ecosystem



revealed general trophic groups that primarily consumed adult Osteichthyes, larval-juvenile Osteichthyes, euphausiids, mixed zooplankton, and copepods; however, in each trophic group omnivory was expressed and actually predominated in some nekton trophic groups. The importance of omnivory in the higher trophic group of blue shark and adult coho salmon indicated that the typical mid-trophic level taxa, such as anchovy and Pacific sardine, were sometimes bypassed for direct feeding on

large zooplankton, in particular adult euphausiids. Previous studies from the NCC system have also shown that blue shark (Brodeur et al., 1987; Harvey, 1989), adult coho (Brodeur et al., 1987), and adult chinook (Hunt et al., 1999) salmon feed on adult nekton and euphausiids. With the exception of Pacific hake, top-down trophic pressure from fish may be less influential in the NCC because top nekton predators are not as abundant in this system as nekton prey such as euphausiids (Ressler

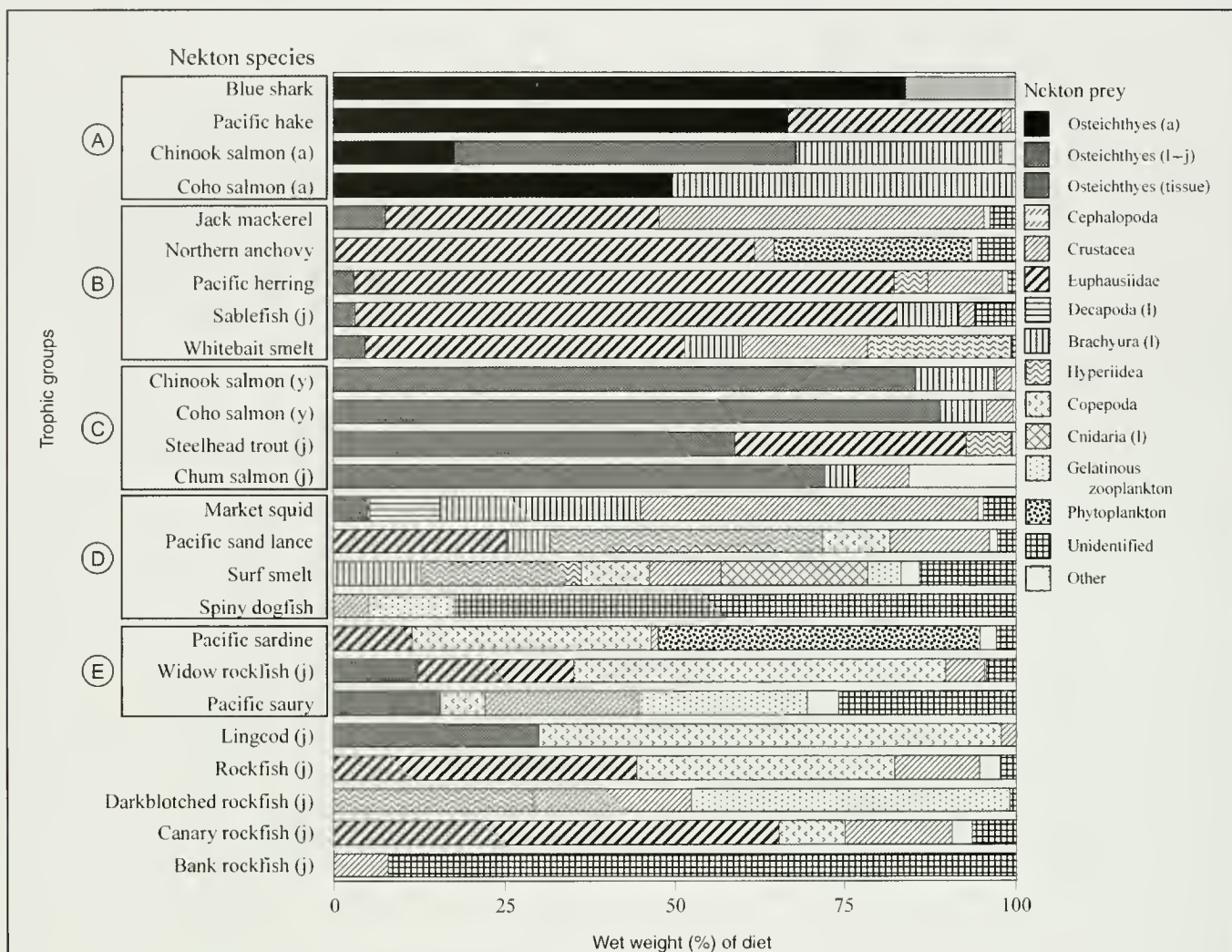


Figure 3

Summary of nekton diets analyzed from June and August 2002 northern California Current GLOBEC (GLOBAL ocean ECosystems dynamics) cruises. Trophic groups based on cluster analysis of diets (percent wet weight) are blocked and labeled (A) to (E). Species not blocked lacked sufficient numbers and frequency of occurrence for analysis. Scientific names of species in the order they appear in the figure are the following: blue shark (*Prionace glauca*), Pacific hake (*Merluccius productus*), chinook salmon (*Oncorhynchus tshawytscha*), coho salmon (*O. kisutch*), jack mackerel (*Trachurus symmetricus*), northern anchovy (*Engraulis mordax*), Pacific herring (*Clupea pallasii*), sablefish (*Anoplopoma fimbria*), whitebait smelt (*Allosmerus elongatus*), steelhead trout (*O. mykiss*), chum salmon (*O. keta*), market squid (*Loligo opalescens*), Pacific sand lance (*Ammodytes hexapterus*), surf smelt (*Hypomesus pretiosus*), spiny dogfish (*Squalus acanthias*), Pacific sardine (*Sardinops sagax*), widow rockfish (*Sebastes entomelas*), Pacific saury (*Cololabis saira*), lingcod (*Ophiodon elongatus*), rockfish (*Sebastes* sp.), darkblotched rockfish (*S. crameri*), canary rockfish (*S. pinniger*), and bank rockfish (*S. rufus*). Life history stages of nekton are shown in parentheses: j = juvenile, y = yearling, and a = adult; nekton and prey with no indication of life history stage are adult.

et al., 2005). Pacific hake likely represent the largest predatory biomass off the west coast of North America (Methot and Dorn, 1995). They feed on adult nekton (Brodeur et al., 1987; Emmett and Krutzikowsky, in press) but also extensively on euphausiids (Brodeur et al., 1987; Tanasichuk, 2002) and give evidence that as omnivores they may not impose direct and intensive trophic pressures upon adjacent trophic species in this

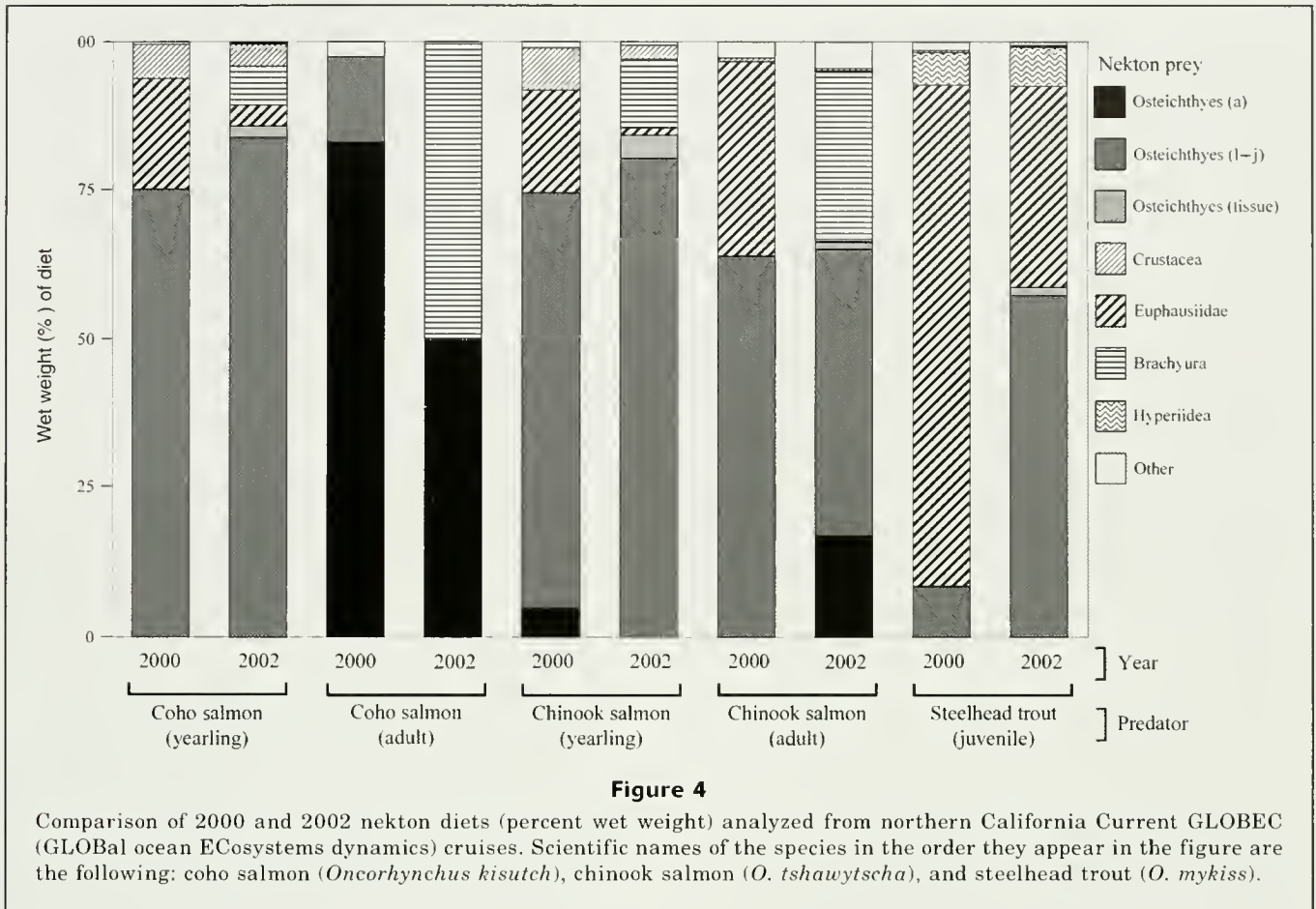
upwelling ecosystem, as would be implied by the classical theory of top-down control.

Euphausiids were also observed as important prey of many middle-trophic-level nekton species. Three trophic groups were evident at this trophic level: 1) a group of species that consumed predominantly larval-juvenile fish and to a lesser degree euphausiids, 2) a group of species that consumed mostly euphausiids, and 3) a group of

Table 3

Percent similarity index (PSI) of diets of nekton species collected from the northern California Current during June and August 2002 GLOBEC cruises. Trophic groups were derived from agglomerative hierarchical cluster analysis (AHCA) of percent wet weight of diet. Blocked PSI values denote within-trophic group comparisons. PSI values >60% are shown in bold. Life history stages of nekton are shown in parentheses and represent juvenile (j), yearling (y), and adult (a); nekton with no indication of life history stage are adult.

Trophic group	Nekton species	<i>Prionace glauca</i>	<i>Merluccius productus</i>	<i>Oncorhynchus tshawytscha</i> (a)	<i>O. kisutch</i> (a)	<i>Trachurus symmetricus</i>	<i>Engraulis mordax</i>	<i>Clupea pallasi</i>	<i>Anoplapoma fimbria</i> (j)	<i>Allosmerus elongatus</i>	<i>O. tshawytscha</i> (y)	<i>O. kisutch</i> (y)	<i>O. mykiss</i> (y)	<i>O. keta</i> (j)	<i>Laligo opalescens</i>	<i>Ammodytes hexapterus</i>	<i>Hypomesus pretiosus</i>	<i>Squalus acanthias</i>	<i>Sardinops sagax</i>	<i>Sebastes entomelas</i> (j)	<i>Cololabis saira</i>	
A	<i>Prionace glauca</i>	X																				
	<i>Merluccius productus</i>	67	X																			
	<i>Oncorhynchus tshawytscha</i> (a)	41	62	X																		
	<i>O. kisutch</i> (a)	30	33	41	X																	
	<i>Trachurus symmetricus</i>	1	26	27	8	X																
B	<i>Engraulis mordax</i>	0	30	31	2	33	X															
	<i>Clupea pallasi</i>	1	33	34	6	49	63	X														
	<i>Anaplapoma fimbria</i> (j)	0	32	34	10	39	61	76	X													
	<i>Allosmerus elongatus</i>	0	26	33	6	28	43	62	58	X												
	<i>O. tshawytscha</i> (y)	0	41	35	5	38	24	40	28	34	X											
C	<i>O. kisutch</i> (y)	1	27	78	27	37	34	44	38	28	78	X										
	<i>O. mykiss</i> (j)	0	31	53	5	39	38	49	40	36	54	74	X									
	<i>O. keta</i> (j)	0	4	34	4	15	9	19	9	19	71	57	45	X								
	<i>Laligo opalescens</i>	1	5	7	2	7	4	8	4	13	8	7	3	9	X							
	<i>Ammodytes hexapterus</i>	0	14	19	5	12	33	44	30	38	19	27	21	10	6	X						
D	<i>Hypomesus pretiosus</i>	0	7	14	6	13	13	29	10	24	15	19	11	21	15	50	X					
	<i>Squalus acanthias</i>	0	4	8	1	8	7	9	6	8	7	11	6	7	3	3	8	X				
	<i>Sardinops sagax</i>	0	10	16	4	14	51	26	12	16	16	17	15	14	5	26	21	8	X			
	<i>Sebastes entomelas</i> (j)	0	3	19	2	13	11	17	9	13	19	18	18	21	3	17	18	4	49	X		
	<i>Cololabis saira</i>	0	3	16	6	16	11	17	10	15	13	19	16	18	3	15	18	5	17	23	X	



Feeding by many nekton directly on phytophagous euphausiids results in more direct food webs and fewer trophic levels, and concomitant increases in food-web efficiency. Observations by Brodeur and Pearcy (1992) and by the authors of the present study thus indicate that trophic characteristics of the NCC system may have periods of high production when euphausiids are consumed across many trophic levels. Additional research of trophic relationships between dominant nekton and zooplankton within the NCC at varying levels of production would further clarify whether this pattern is an important characteristic of this ecosystem.

Interannual variation

Limited interannual variation in diets was observed; only juvenile steelhead trout and adult coho salmon expressed major differences between 2000 and 2002. Other nekton, particularly yearling coho and chinook salmon, showed relatively little variation in diet; only euphausiids and brachyuran larvae (which represent a small portion of nekton diet in general) varied most between the two years. Whether this variability was an artifact of sampling is uncertain; however, it is interesting to note that the higher prevalence of euphausiids in the 2000 diets and the higher prevalence of brachyuran

larvae in 2002 diets indicated that variation between the two years may have been a result of the relative abundance of these prey. Other studies from the NCC have also indicated high temporal variation in zooplankton (Mackas et al., 2001, 2004) and in the diets of Pacific hake (Emmett and Krutzikowsky, in press) and juvenile salmonids (Brodeur and Pearcy, 1990). Although both 2000 and 2002 were years of high upwelling and high production, substantial interannual variability in the hydrographic environment was observed. During the summer of 2002, an intrusion of cold, nutrient-rich, subarctic bottom water resided on the Oregon shelf, resulting in high phytoplankton production in surface waters and in hypoxic conditions near the bottom (Thomas et al., 2003; Wheeler et al., 2003). Although it is possible that this nutrient-rich water may have influenced the prey field available to the different predators, no discernible effect on their diet was observed in our study.

The temporal variability in nekton diets reveals an important characteristic of the NCC system in that this variability reflects the duration of trophic interactions between predator and prey in relation to population-scale parameters. If variability in the time scale of trophic links is short compared to nekton population dynamics, then more short-lived species (such as market squid) or those exhibiting a critical ontogenetic

shift (such as juvenile salmonids) will be more influenced by interannual variability in the availability and quality of prey. Species exhibiting extensive feeding migrations through the NCC system, such as Pacific hake and Pacific sardine, may be less influenced by localized prey limitation because critical feeding for recruitment success can occur in other regions with different physical and biological parameters.

Interannual and interdecadal comparisons of species distribution and community structure of pelagic nekton have demonstrated that the northern California Current ecosystem can vary between months and years (Brodeur et al., 2005). As fishery management shifts away from single-species towards multispecies or ecosystem-based fishery management (Pikitch et al., 2004), detailed information on the trophic interactions within this pelagic ecosystem as presented here will become indispensable for development of management plans and ecosystem models. Further analysis of the relationships between major nekton and their prey is warranted to elucidate differences in trophic relationships between major upwelling regions, especially those that are influenced by strong climatic variability.

Acknowledgments

We thank R. Emmett, J. Fisher, C. Bucher, P. Bentley, R. Baldwin, and S. Pool for field and laboratory support and the captains and crew of the FV Sea Eagle and FV Frosti for help with sampling. H. Li, B. Pearcy (both at Oregon State University), Ed Casillas (Northwest Fisheries Science Center, Seattle), and three anonymous reviewers provided valuable comments on earlier drafts of the manuscript. This work was funded in part by a Mamie Markham Fellowship, the U.S. GLOBEC Northeast Pacific Program, and the Bonneville Power Administration. This article is contribution number 540 of the U.S. GLOBEC Program.

Literature cited

- Ainley, D. G., L. B. Spear, and S. G. Allen.
1996. Variation in the diet of Cassin's auklet reveals spatial, seasonal, and decadal occurrence patterns of euphausiids off California, USA. *Mar. Ecol. Prog. Ser.* 137:1-10.
- Brodeur, R. D., J. P. Fisher, R. L. Emmett, C. A. Morgan, and E. Casillas.
2005. Species composition and community structure of pelagic nekton off Oregon and Washington under variable oceanographic conditions. *Mar. Ecol. Prog. Ser.* 298:41-57.
- Brodeur, R. D., J. P. Fisher, D. J. Teel, R. L. Emmett, E. Casillas, and T. W. Miller.
2004. Juvenile salmonid distribution, growth, condition, origin, and environmental and species associations in the northern California Current. *Fish. Bull.* 102:25-46.
- Brodeur, R. D., H. V. Lorz, and W. G. Pearcy.
1987. Food habits and dietary variability of pelagic nekton off Oregon and Washington, 1979-1984. NOAA Tech. Rep. NMFS 57:1-32.
- Brodeur, R. D., and W. G. Pearcy.
1986. Distribution and relative abundance of pelagic nonsalmonid nekton off Oregon and Washington, 1979-84. NOAA Tech. Rep. NMFS 46, 85 p.
1990. Trophic relations of juvenile Pacific salmon off the Oregon and Washington coast. *Fish. Bull.* 88:617-636.
1992. Effects of environmental variability on trophic interactions and food web structure in a pelagic upwelling ecosystem. *Mar. Ecol. Prog. Ser.* 84:101-119.
- Carr, M. E.
2002. Estimation of potential productivity in eastern boundary currents using remote sensing. *Deep-Sea Res.* 11 49:59-80.
- Chavez, F. P., J. Ryan, S. E. Lluch-Cota, and M. C. Niquen.
2003. From anchovies to sardines and back: multidecadal change in the Pacific Ocean. *Science* 299:217-221.
- Corwith, H. L., and P. A. Wheeler.
2002. El Niño related variations in nutrient and chlorophyll distributions off Oregon. *Prog. Oceanogr.* 54:361-380.
- Emmett, R. L., and R. D. Brodeur.
2000. Recent changes in the pelagic nekton community off Oregon and Washington in relation to some physical oceanographic conditions. *Bull. North Pac. Anadrom. Fish. Comm.* 2:11-20.
- Emmett, R. L., R. D. Brodeur, T. M. Miller, S. S. Pool, P. J. Bentley, G. K. Krutzikowsky, and J. McCrae.
2005. Pacific sardine (*Sardinops sagax*) abundance, distribution and ecological relationships in the Pacific Northwest. Calif. Coop. Oceanic Fish. Invest. Rep. 46:122-143.
- Emmett, R. L., and G. R. Krutzikowsky.
In press. Nocturnal feeding by Pacific hake (*Merluccius productus*) and jack mackerel (*Trachurus symmetricus*) off the mouth of the Columbia River, 1999-2004: implications for juvenile salmon predation. *Trans. Am. Fish. Soc.*
- Feinberg, L. R., and W. T. Peterson.
2003. Variability in duration and intensity of euphausiid spawning off central Oregon, 1996-2001. *Prog. Oceanogr.* 57:363-379.
- Francis, R. C., and S. R. Hare.
1994. Decadal-scale regime shifts in the large marine ecosystems of the North-east Pacific: a case for historical science. *Fish. Oceanogr.* 3:279-291.
- Hand, C. H., and L. Berner.
1959. Food of the Pacific sardine (*Sardinops caerulea*). *Fish. Bull.* 164:175-184.
- Harvey, J. T.
1989. Food habits, seasonal abundance, size, and sex of the blue shark, *Prionace glauca*, in Monterey Bay, California. *Cal. Fish Game.* 75:33-44.
- Hood, R. R., M. R. Abbott, and A. Huyer.
1991. Phytoplankton and photosynthetic light response in the coastal transition zone off northern California in June 1987. *J. Geophys. Res.* 96(C8):14769-14780.
- Hunt, S. L., T. J. Mulligan, and K. Komori.
1999. Oceanic feeding habits of chinook salmon, *Oncorhynchus tshawytscha*, in the northern California Current. *Fish. Bull.* 97:101-119.

- corhynchus tshawytscha*, off northern California. *Fish. Bull.* 97:717–721.
- Huyer, A.
1983. Coastal upwelling in the California Current system. *Prog. Oceanogr.* 12:259–284.
- Jackson, J. B., M. X. Kirby, W. H. Berger, K. A. Bjorndal, L. W. Botsford, B. J. Bourque, R. H. Bradbury, R. Cooke, J. Erlandson, J. A. Estes, T. P. Hughes, S. Kidwell, C. B. Lange, H. S. Lenihan, J. M. Pandolfi, C. H. Peterson, R. S. Steneck, M. J. Tegner, and R. R. Warner.
2001. Historical overfishing and the recent collapse of coastal ecosystems. *Science* 293:629–637.
- Mackas, D. L., W. T. Peterson, and J. E. Zamon.
2004. Comparisons of interannual biomass anomalies of zooplankton communities along the continental margins of British Columbia and Oregon. *Deep Sea Res. II* 51:875–896.
- Mackas, D. L., R. E. Thomson, and M. Galbraith.
2001. Changes in the zooplankton community of the British Columbia continental margin, 1985–1999, and their covariation with oceanographic conditions. *Can. J. Fish. Aquat. Sci.* 58:685–702.
- Mantua, N. J., S. R. Hare, Y. Zhang, J. M. Wallace, and R. C. Francis.
1997. A Pacific decadal climate oscillation with impacts on salmon. *Bull. Am. Meteorol. Soc.* 78:1069–1079.
- McGowan, J. A., D. R. Cayan, and L. M. Dorman.
1998. Climate-ocean variability and ecosystem response in the northeast Pacific. *Science* 281:210–217.
- Methot, R. D., and M. W. Dorn.
1995. Biology and fisheries of North Pacific hake (*M. productus*). In *Hake: biology, fisheries and markets* (J. Alheit, and T. J. Pitcher, eds.), p. 389–414. Chapman and Hall, London.
- Miller, T. W.
2006. Trophic dynamics of marine nekton and zooplankton in the northern California Current pelagic ecosystem. Ph. D. diss., 212 p. Oregon State Univ., Corvallis, OR.
- Pearcy, W. G., and A. Schoener.
1987. Changes in the marine biota coincident with the 1982–1983 El Niño in the northeastern subarctic Pacific Ocean. *J. Geophys. Res.* 92(C13):14,417–14,428.
- Peterson, W. T., and F. B. Schwing.
2003. A new climate regime in northeast Pacific ecosystems. *Geophys. Res. Lett.* 30(17):1896.
- Pikitch, E. K., C. Santora, E. A. Babcock, A. Bakun, R. Bonfil, D. O. Conover, P. Dayton, P. Doukakis, D. Fluharty, B. Heneman, E. D. Houde, J. Link, P. A. Livingston, M. Mangel, M. K. McAllister, J. Pope, and K. J. Sainsbury.
2004. Ecosystem-based fishery management. *Science* 305:346–347.
- Reese, D. C., and R. D. Brodeur.
2006. Identifying and characterizing biological hot spots in the Northern California Current. *Deep Sea Res. II* 53:291–314.
- Reilly, C. A., T. W. Echeverria, and S. Ralston.
1992. Interannual variation and overlap in the diets of pelagic juvenile rockfish (Genus: *Sebastes*) off central California. *Fish. Bull.* 90:505–515.
- Ressler, P. H., R. D. Brodeur, W. T. Peterson, S. K. Pierce, P. M. Vance, A. R. Røstad, and J. A. Barth.
2005. The spatial distribution of euphausiid aggregations in the northern California Current during August 2000. *Deep Sea Res. II* 52:89–108.
- Robinson, C. L. K.
2000. The consumption of euphausiids by the pelagic fish community off southwestern Vancouver Island, British Columbia. *J. Plankton Res.* 22(9):1649–1662.
- Schoener, T. W.
1974. Resource partitioning in ecological communities. *Science* 185:27–39.
- Tanasichuk, R. W.
2002. Implications of interannual variability in euphausiid population biology for fish production along the southwest coast of Vancouver Island: a synthesis. *Fish. Oceanogr.* 11:18–30.
- Thomas, A. C., P. T. Strub, and P. Brickley.
2003. Anomalous satellite-measured chlorophyll concentrations in the northern California Current in 2001–2002 spring 2005 in the California Current. *Geophys. Res. Lett.* 30(15), 8022.
- Wallace, H., and J. S. Ramsay.
1983. Reliability in measuring diet overlap. *Can. J. Fish. Aquat. Sci.* 40:347–351.
- Wheeler, P. A., A. Huyer, and J. Fleischbein.
2003. Cold halocline, increased nutrients and higher chlorophyll off Oregon in 2002. *Geophys. Res. Lett.* 30(15), 8021.
- Worm, B., and J. E. Duffy.
2003. Biodiversity, productivity and stability in real food webs. *Trends Ecol. Evol.* 18:628–632.

Abstract—The timing and duration of the reproductive cycle of Atka mackerel (*Pleurogrammus monopterygius*) was validated by using observations from time-lapse video and data from archival tags, and the start, peak, and end of spawning and hatching were determined from an incubation model with aged egg samples and empirical incubation times ranging from 44 days at a water temperature of 9.85°C to 100 days at 3.89°C. From June to July, males ceased diel vertical movements, aggregated in nesting colonies, and established territories. Spawning began in late July, ended in mid-October, and peaked in early September. The male egg-brooding period that followed continued from late November to mid-January and duration was highly dependent on embryonic development as affected by ambient water temperature. Males exhibited brooding behavior for protracted periods at water depths from 23 to 117 m where average daily water temperatures ranged from 4.0° to 6.2°C. Knowledge about the timing of the reproductive cycle provides a framework for conserving Atka mackerel populations and investigating the physical and biological processes influencing recruitment.

Timing and duration of mating and brooding periods of Atka mackerel (*Pleurogrammus monopterygius*) in the North Pacific Ocean

Robert R. Lauth¹ (contact author)

Jared Guthridge^{2,3}

Dan Nichol¹

Scott W. McEntire¹

Nicola Hillgruber³

Email address for R. R. Lauth: Bob.Lauth@noaa.gov

¹ National Oceanic and Atmospheric Administration
National Marine Fisheries Service
Alaska Fisheries Science Center
Resource Assessment and Conservation Engineering Division
7600 Sand Point Way NE
Seattle, Washington 98115

² Alaska SeaLife Center
301 Railway Avenue
Seward, Alaska 99664

³ School of Fisheries and Ocean Sciences
University of Alaska Fairbanks
11120 Glacier Highway
Juneau, Alaska 99801

Atka mackerel (*Pleurogrammus monopterygius*) is distributed along the edges of the North Pacific Ocean and adjoining basins in rocky shelf regions near landmasses and archipelagos, and in rocky reefs atop prominent bathymetric features rising from the sea floor (Rutenberg, 1962; Allen and Smith, 1988). Atka mackerel is one of the most abundant groundfish in the central and western North Pacific Ocean (Zenger, 2004) where it is a key prey item for marine fishes, birds, and mammals (Murie, 1959; Kenyon, 1965; Sinclair and Zeppelin, 2002). Modern large-scale commercial trawling by U.S. and foreign fishing vessels began during the latter half of the twentieth century, and since the end of the joint venture fishing in 1989, total landings of U.S. fishing vessels have averaged 54,000 metric tons annually (Lowe et al., 2006).

Knowledge about the timing of the reproductive cycle and temporal use of nesting habitat is essential for understanding processes affecting the recruitment and population dynamics of Atka mackerel, and for making management decisions regarding

commercial fishing activity. Despite Atka mackerel's relatively high abundance and value to the ecosystem, surprisingly little is known about its life history and ecology. Access to Atka mackerel is difficult and costly because the species inhabits a vast and remote region that is notorious for inclement weather and rough seas. Studies on the reproductive biology of Atka mackerel are further limited by a general lack of knowledge about the location of spawning and nesting sites in these remote areas. In the eastern North Pacific Ocean off the coast of Kamchatka Peninsula, there are only a handful of known spawning and nesting sites (Zolotov, 1993), and in the central and eastern North Pacific Ocean, the geographic and bathymetric distribution of spawning and nesting sites was completely unknown until recently (Lauth et al., in press).

Previously published studies have used ovarian condition to determine the start and end of the spawning period (Gorbunova, 1962; Zolotov, 1993; McDermott and Lowe, 1997), but very little has been done to investigate the time spent by males in

either establishing nesting territories before spawning or in brooding eggs afterwards. Only from the western North Pacific Ocean is there published information on the nesting period from beginning to end, but methods and results have been vague and have relied on catch data from various nonstandardized fishing gears and methods (Gorbunova, 1962; Zolotov, 1993). Egg incubation times are useful for approximating the end of the male nest brooding period (Gorbunova, 1962; Lauth and Blood, 2007), however, controlled rearing experiments at a wider range of water temperatures are needed to accurately determine how the rate of embryonic development is affected (Lauth and Blood, 2007).

The objective of this study was to clarify Atka mackerel's temporal use of breeding habitat by investigating the timing and duration of nesting, spawning, and brooding phases in the North Pacific Ocean. This study makes use of *in situ* visual and behavioral observations of male Atka mackerel and an incubation model that synthesizes data from laboratory incubation experiments, egg mass collections from three different nesting sites, and descriptions of embryonic development from a companion manuscript (Lauth and Blood, 2007).

Materials and methods

Direct observation of nesting behavior

Visual and behavioral observations from time-lapse video and data from archival tags were used for determining the beginning and end of the nesting period (i.e., the duration of male territoriality), and to document nesting behaviors before the onset of spawning. Sexual dichromatism (Medveditsyna, 1962; Rutenberg, 1962) and behavioral changes in males (Nichol and Somerton, 2002; Lauth et al., in press) are primary indications of nesting activity. Nest guarding males are distinguished by their bright yellow or orange color and dark black vertical stripes. When males are breeding, they defend a nesting territory for long periods and refrain from vertical migrations. Sexually mature females or non-spawning Atka mackerel of both sexes are bluish-green or gray and typically undergo diel vertical migrations year round (Nichol and Somerton, 2002).

Time-lapse camera Diving operations to deploy and retrieve underwater camera equipment were conducted from the National Atmospheric and Oceanic Administration (NOAA) National Marine Fisheries Service (NMFS) charter vessels FV *Morning Star* (May 2002), FV *Sea Storm* (July 2002), and the United States Fish and Wildlife Service RV *Tigllax* (August 2002). A Sony Hi8 (Sony Electronics, Inc., San Diego, CA) video camera was placed inside a Plexiglas housing and secured to a mooring on the seafloor at 23 m by a diver at a known nesting site at Seguam Island, Alaska (52 22.10°N, 172 20.26°W) on 31 May 2002. The video camera had a time-lapse controller that could be set by the user to record video images at periodic intervals. The camera was attached

to a tripod frame made of welded steel. On the initial deployment, the time-lapse controller was set to record 1 minute of video each day. It was recovered on 28 July 2002 (60 days later) and reset at the same location to record 1 minute of video every hour until 7 August 2002 (a 10-day period). The camera was recovered and reset a final time to record 15 sec/h until 31 August 2002 (a 24-day period) when the camera was recovered.

Archival tags Archival tag data from a previously published study on Atka mackerel diel behavior (Nichol and Somerton, 2002) were used to infer nest-guarding behavior and to corroborate nesting periods. In July 2000, 117 Atka mackerel were captured by trawl, tagged, and released in Seguam Pass with archival tags that recorded the time, depth, and temperature once each minute (Nichol and Somerton, 2002). Commercial trawlers recovered 14 Atka mackerel with tags. Data from four of the tags were from males that showed no vertical movement for extended periods, which is consistent with nesting. Data from two of the four tags were also reported in Nichol and Somerton (2002).

Laboratory incubation experiments

Results from laboratory rearing experiments were used to develop parameters for an incubation model to determine how Atka mackerel incubation time varies between nesting sites. Laboratory experiments were conducted at the Alaska Sealife Center (ASLC) with egg masses spawned by captive Atka mackerel. In October 2002, a commercial fishing vessel with a bottom trawl collected 20 live Atka mackerel from Seguam and Tanaga Passes. The fish were kept live in tanks on board the fishing vessel and transported to the ASLC. After acclimation, antibiotic treatment, and a one-month quarantine at the ASLC, 14 Atka mackerel were transferred to ASLC exhibit tanks equipped with a submersible video camera for documenting spawning and nesting behavior. Each time an egg mass was discovered, the videotape was reviewed to determine the time of egg mass deposition. Fertilized egg masses were transferred to one of four closed-system incubation tanks consisting of a 150-L tank, recirculation pump, and a 1/3 hp inline chiller controlled by an electronic thermostat. The configuration of the system provided stable temperatures with very little fluctuation. Temperatures for the incubation chambers were chosen on the basis of *in situ* observations at nesting sites in the Aleutian Islands (Lauth et al., in press). Ten incubation experiments were conducted at four different water temperatures: three each at 4°, 5°, and 7°C, and two at 10°C. The light cycle in the aquaria was regulated with an electronic timer set at 12 h light and 12 h dark.

For all incubation experiments, hatching day for an egg mass was defined as the first day larvae hatched from the egg mass. A scatter plot of incubation temperature versus total days to first hatching was constructed for all incubation temperature trial data, and regression analysis (Zar, 1999) was used to determine how total days to hatching varied as a function of temperature.

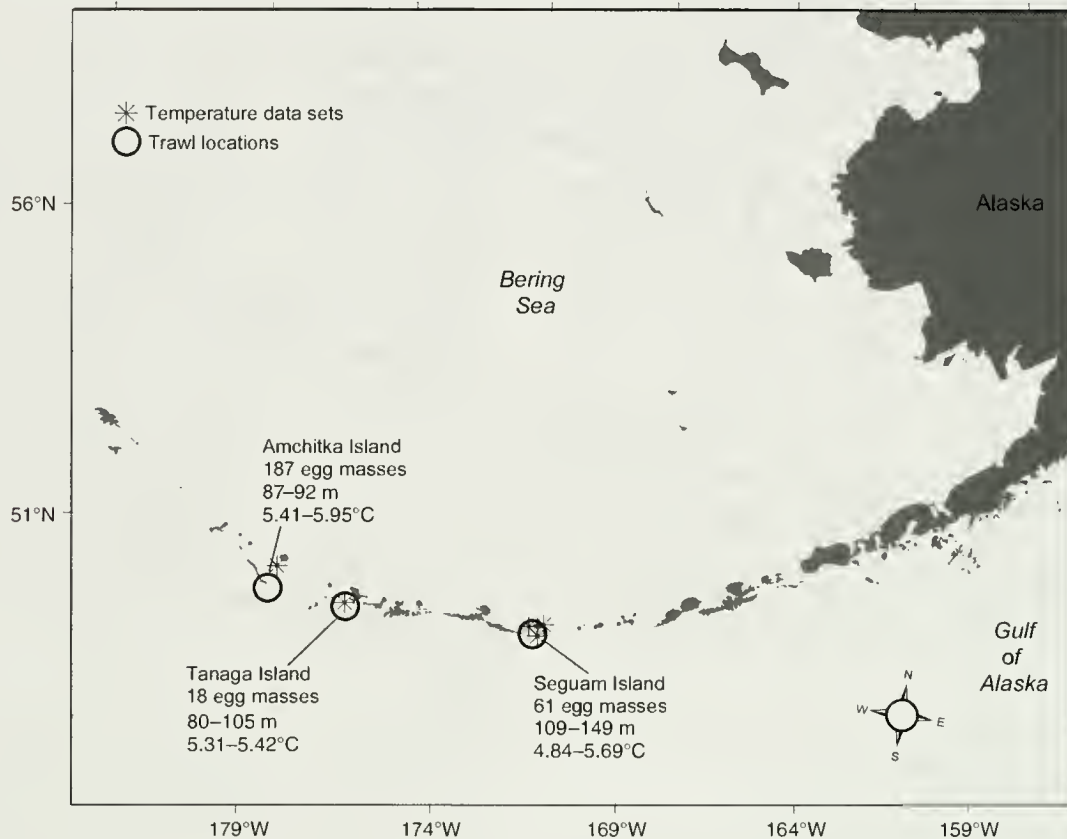


Figure 1

Map showing collection sites for water temperature data sets (asterisks; also see Table 1) and trawl locations where Atka mackerel (*Pleurogrammus monopterygius*) egg masses were collected (open circles). The number of egg masses collected and the range of water depth and temperature are listed beneath each trawling location.

Incubation model

An incubation model was used for extrapolating spawning and hatching dates for egg mass samples collected from three different Atka mackerel nesting sites. During the period 7–23 October 2004, egg masses were collected from trawl hauls aboard the commercial stern-trawler FV *Seafisher* and samples were preserved in 10% phosphate-buffered formalin. The October collection period was chosen because histological studies have indicated it is the month when spawning ends in Alaska (McDermott and Lowe, 1997). A total of 266 egg masses were collected: 187 from the Amchitka Island area, 18 from near Tanaga Island, and 61 from the waters surrounding Seguam Island (Fig. 1). In the laboratory, egg mass samples were placed underneath a stereo dissecting microscope and aged to the nearest day by using the descriptions of embryonic development from the incubation experiment described by Lauth and Blood (2007).

The calculation of spawning and hatching dates was based on the assumption that the effect of temperature on incubation rate for any given development stage was

nearly a constant linear relationship for the entire incubation period. The constant relationship is generally true for temperatures normally encountered by eggs in their habitat (Ahlstrom, 1943; Riley, 1974; Hempel, 1979). Spawning and hatching dates were estimated by using the following relationship:

$$d_t = \frac{D_t s_{6^\circ C}}{S_{6^\circ C}}$$

where d_t = age of the egg mass (days) at temperature t ;
 D_t = total incubation time (days) at temperature t ;

$s_{6^\circ C}$ = estimated age of the collected egg mass (days) using the descriptions of embryonic development from Lauth and Blood (2007);

$S_{6^\circ C}$ = total number of days for first egg to first hatching;

Spawning date = Egg mass collection date - d_t , and
 Hatching date = (Egg mass collection date - d_t) + D_t .

Table 1

Source, latitude, longitude, depth, and time periods for water temperature data sets from sites surrounding Amchitka/Tanaga and Seguam Islands (also see Fig. 1). PMEL EPIC = Pacific Marine Environmental Laboratory Eastern Pacific Investigation of Climate Processes.

Source	Latitude (N)	Longitude (W)	Depth (m)	Time period
Amchitka and Tanaga sslands				
PMEL EPIC buoy data	51°46.12'	179°30.70'	39	08 June 1987 to 18 June 1988
PMEL EPIC buoy data	51°35.40'	178°12.60'	142	03 May 2002 to 11 May 2003
Seguam Island				
PMEL EPIC buoy data	52°08.08'	172°25.57'	109	03 May 2002 to 01 Oct 2002
PMEL EPIC buoy data	52°08.08'	172°25.57'	109	01 Oct 2002 to 03 Nov 2002
PMEL EPIC buoy data	52°16.00'	172°45.10'	147	02 May 2002 to 10 May 2003
PMEL EPIC buoy data	52°16.00'	172°45.10'	147	19 May 2001 to 13 Oct 2001
PMEL EPIC buoy data	52°16.00'	172°45.10'	139	13 Oct 2001 to 13 Feb 2001
Atka mackerel archival tag	Exact location unknown		92	23 July 2000 to 21 Jan 2001
Nearshore current meter ¹	52°22.09'	172°20.26'	22	01 June 2002 to 01 Sept 2002

¹ The current meter was anchored to substrate within an Atka mackerel nesting site.

Values for the total incubation time of a collected egg mass (D_t) were calculated with a best-fit regression equation derived from the laboratory incubation experiments.

Temperature data sets used for determining a low and high range of D_t were obtained from buoys operated by the Eastern Pacific Investigation of Climate Processes (EPIC) program of the NOAA Pacific Marine Environmental Laboratory (PMEL; Table 1; Fig. 1). There were two EPIC temperature data sets available for the Amchitka and Tanaga Island area and five for the Seguam Island area (Table 1). The depths for the EPIC buoy data ranged from 39 to 147 m, which are close to the depth limits where Atka mackerel nesting sites were observed (Lauth et al., in press). In addition to the EPIC data sets for the Seguam Island area, two more temperature data sets were available from a shallow (22 m) and deep (92 m) Atka mackerel nesting site (Table 1). The temperature data from the shallow nesting site were collected from the data logger attached to the time-lapse camera and the data from the deep nesting site were collected from an archival tag on a male that exhibited nesting behavior. Daily water temperatures were pooled by area for calculating an average daily water temperature and standard deviation. The minimum and maximum average daily water temperatures from each area for the period 1 July to 15 January were used in the incubation model for the low and high D_t .

Egg mass spawning and hatching dates were pooled by week and ogives of the pooled data were made for a low and high range of D_t for each egg collection area. To estimate the timing of spawning and nesting periods across the entire geographical region, pooled data for both low and high temperatures from all three areas were proportioned equally, combined, and plotted by relative frequency over time.

Results

Direct observation of nesting behavior

Time-lapse camera The time-lapse camera was used for documenting the arrival of male Atka mackerel at a nesting site near Seguam Island in 2002 (Fig. 1). Divers at the site observed no males or Atka mackerel egg masses when the camera was deployed on 31 May, nor were males observed in the camera footage for the first five days. On 5 June, a bright yellow male with black vertical stripes (male nesting coloration) swam across the screen during a 10-second period. There was a similar observation on 6 June. Neither of these males exhibited territorial behavior toward a specific patch of rocky substrate. On 9 June, two males hovered close to the bottom at mid-screen in the background for the entire minute, and on 10 June, one male pursued another Atka mackerel of unknown sex, followed it (off screen), and then returned to mid-screen and hovered for the remainder of the minute. Atka mackerel were not observed with the time-lapse camera for the next two days. On 13 June, a group of three males swam across the screen in the distance. On 14, 15, and 17 June, males were observed hovering in the distance or swimming across the screen. On 18 June, a bright yellow male with dark black vertical bands was positioned in front of the camera. The same male was observed in the same area in front of the camera every day after that through 31 August (74 days). Between 18 June and 31 August, other males were periodically observed in the background exhibiting nesting behavior. During all three recoveries of the time-lapse camera, divers observed two egg masses within a 1 m radius of the camera mooring.

Archival tags Two archival tags were retrieved from Seguam Pass in September 2000, and one each in September 2001 and January 2001. It was evident from the depth data of two tags that Atka mackerel males made

regular diel vertical movements during the nonbreeding season from mid-December through May (Fig. 2, A and B). During the breeding season from June to December, the behavior of all four tagged males was characterized by an extended period of time on the bottom and very limited or no vertical movement (Fig. 2). It was assumed that these periods corresponded with nesting behavior. The earliest date within a year that such nesting behavior was observed was 4 June (Fig. 2A) and the latest was 12 December (Fig. 2B). The male in Fig. 2A was at liberty for 406 days and exhibited 89 days of limited vertical movement before being captured. The male in Fig. 2B displayed nesting behavior for 141 consecutive days,—the longest uninterrupted time period for all tagged males. Also unique to the male in Figure 2B was a depth shift from 125 to 92 m on 14 September followed by a continuation of nesting behavior until 14 December (89 days). Three of the four males displayed nesting behavior shortly after being released (Fig. 2, B–D), but two of these males (Fig. 2, C and D) abandoned the behavior after only 33 days, whereas the other male (Fig. 2B) shifted depth and continued nesting behavior. Males in Figures 2B and 2D also showed unexplained and periodic ascents and descents during periods of presumed nesting behavior.

The average depths where male nesting behavior was displayed ranged from 92 to 117 m and the water temperatures at those locations ranged from 4.5° to 4.9°C. Water temperatures varied by a maximum of 2.6°C during these periods.

Laboratory incubation experiments

In 2004, ten egg masses were fertilized and all were incubated successfully at the ASLC. The first spawning event for the captive Atka mackerel was recorded on 27 July, and the last was on 13 October. For 2005, the first and last spawning dates were 13 July and 12 October. The average temperature for each of the four treatments was 3.89°, 5.04°, 7.03°, and 9.85°C. The incubation time of 74 days at 6.15°C from Lauth and Blood (2007) was also used in the analysis. The best fit of the data was a logarithmic function with a negative slope (Fig. 3). Total incubation time (D_t) was a function of the natural logarithm of incubation temperature (t) with days to first hatching ranging from 44 days at 9.85°C to 100 days at 3.89°C (Fig. 3).

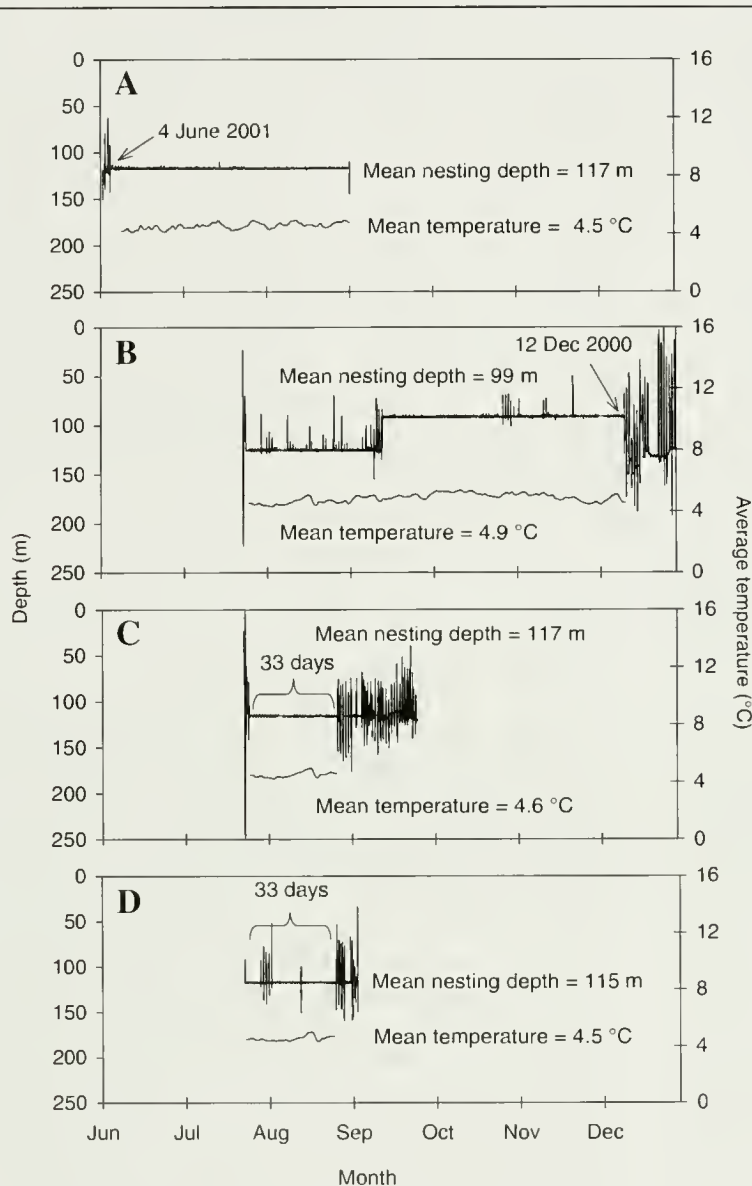
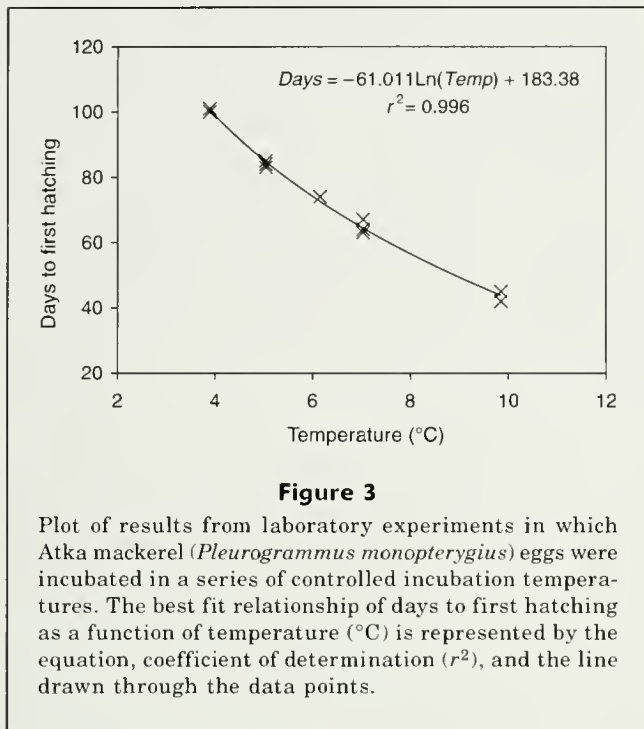


Figure 2

Plots A–D show the depth and temperature data of archival tags from four captured male Atka mackerel (*Pleurogrammus monopterygius*) that were originally tagged and released in July 2000. The calendar year for plot A is 2001, and for plots B–D is 2000. All four males exhibited periods of limited vertical movement consistent with nesting behavior. An arrow points to the start of nesting behavior in plot A and the end of nesting behavior in plot B, and plots C and D have brackets delineating the nesting periods and the length of nesting behavior (days) is indicated above the brackets. Mean water depth and temperature of nesting behavior periods are also presented along with average daily water temperature represented by the lower black line in each plot. Periods with frequent and repeated diel vertical migrations outside the arrows and brackets are consistent with non-nesting behavior.

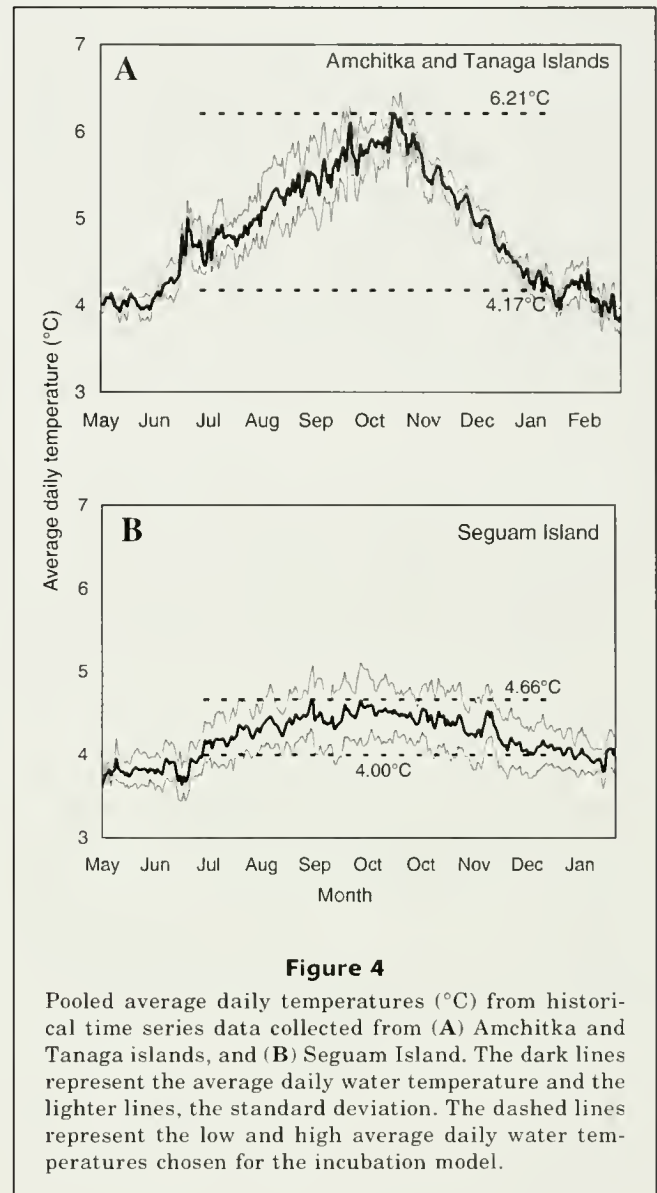


Incubation model

Water temperatures varied by area and time of year; daily averages were generally highest during the spawning and hatching periods from late summer to early winter, and higher near Amchitka and Tanaga Islands compared to Seguam Island (Fig. 4). During the period 1 July to 15 January, average daily water temperatures from Amchitka and Tanaga Islands reached a maximum of 6.21°C during October and a minimum of 4.17°C in January (Fig. 4A). Average daily water temperatures were generally lower and more variable for the same period at Seguam Island, ranging from 4.00°C in June and January to 4.66°C in August (Fig. 4B). The mean and standard deviation for all daily average water temperatures for the period 1 July to 15 January was $5.22 \pm 0.16^\circ\text{C}$ for Amchitka Island and $4.34 \pm 0.50^\circ\text{C}$ for Seguam Island.

Amchitka Island Spawning started from late-July to early August, peaked from mid-August to early September, and ended in late September (Fig. 5). Some of the egg masses collected at Amchitka Island were at an advanced stage of development; therefore hatching began about the same time that egg masses were collected in mid-October and was completed by early to mid-December.

Tanaga Island Assuming the same incubation temperatures as Amchitka Island, calculated spawning and hatching dates for Tanaga Island were about a half-month later than Amchitka Island (Fig. 5). Spawning



commenced from early to mid-August and ended in late September or early October. Hatching began in early November and ended by late December or early January.

Seguam Island Spawning and hatching dates for Seguam Island were the latest among the three areas sampled (Fig. 5). Spawning began in mid-August, peaked in mid-September, and ended in early-October. Hatching commenced in mid-November and ended from early to mid-January.

All areas and temperatures combined For all areas combined, spawning began in mid-July, peaked in early September, and ended mid-October (Fig. 6). Hatching immediately followed the end of spawning, peaked in early December, and continued until late January.

Discussion

The mating and brooding cycle (i.e., reproductive cycle) of Atka mackerel lasts from June to January. The mating phase begins with males aggregating in nesting colonies where they establish individual nesting territories. Time-lapse camera footage and archival tag data show that male Atka mackerel begin aggregating and establishing nesting territories in early June, 1.5 months before spawning commences. The reason for the lengthy nest-establishment period is unknown, but fishes that provide male parental care of eggs typically put considerable effort into choosing and preparing an

optimal nesting territory because it can be an important determinant for maximizing reproductive success (e.g., Sargent, 1982; Sikkil, 1988; Bisazza et al., 1989; Östlund-Nilsson, 2000).

The second phase of mating consists of courtship and spawning, during which time a territorial male can mate with multiple females. Spawning begins mid-July and ends in mid-October. A July to October spawning period has been corroborated by a histological study of 978 Atka mackerel ovaries from collections made across the entire North American geographical range (McDermott and Lowe, 1997), and from observations of captive spawning Atka mackerel used in the incubation experiments from the present study. Because such a high proportion of egg masses were found in later stages of development at Amchitka, it is possible that some hatching occurred before the egg mass collections. This would have the effect of shifting the onset of the spawning and hatching period at Amchitka to an earlier time. Because egg masses collected from Tanaga and Seguam Islands were much younger at the time they were collected, it is not likely that some earlier hatching took place, especially given the low water temperatures characteristic of each nesting site.

Detailed analysis of spawning times by area, with the use of aged egg masses, indicated a later onset of and peak in spawning as spawning activity moved from west to east. Female Atka mackerel spawn an average of 4.6 separate batches of eggs during the 12-week spawning period (McDermott et al., 2007), but uncertainty about precise ambient temperatures precludes conclusions regarding the periodicity of separate spawning events and whether these events were continuous or episodic.

During the brooding phase, spawning has ended and males guard the incubating egg masses within their territory until all the eggs hatch. The duration of the male brooding phase is highly dependent on water temperature. The average water temperature of 106 nesting sites covering a broad temporal, bathymetric, and geographic range in the Aleutian archipelago was 5.4°C (Lauth et al., in press). If this water temperature represented a true mean for the entire range of Atka mackerel, the average male brooding period would be 11.5 weeks. Using a video drop camera on 30 November 2005, the principal author verified that males were still aggregated and exhibiting nesting behavior at a nesting site near Dutch Harbor, AK. Considering that egg masses are spawned until late October and that *in situ* water temperatures as low as 3.99°C are observed at nesting sites, it is plausible

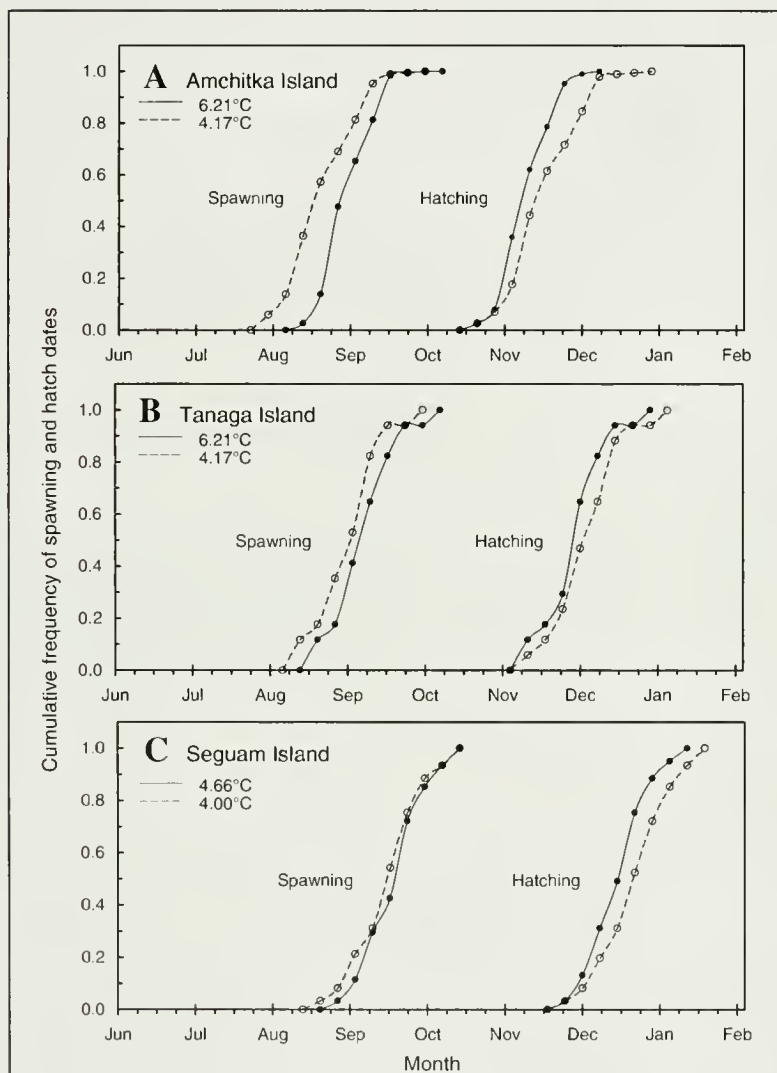


Figure 5

Ogive plots of incubation model results for Atka mackerel (*Pleurogrammus monopterygius*) egg masses collected from (A) Amchitka Island, (B) Tanaga Island, and (C) Seguam Island. The y-axis is the cumulative frequency of egg mass spawning and hatching dates by week for low (dashed line) and high (solid line) average daily water temperatures for each area (see Fig. 4).

that some males brood eggs at nesting sites until January.

There may be several reasons for the 2-month difference in the duration of the reproductive cycle between Alaska (7+ months) and the western Pacific Ocean (5+ months; Gorbunova, 1962; Zolotov, 1993). First, all the western Pacific Ocean nesting sites were located in coastal areas in water depths <32 m where water temperatures were likely higher and the length of the brooding period shorter than those in Alaskan waters. Second, no distinction was made between the onset of the nesting and spawning periods; that is, Gorbunova (1962) and Zolotov (1993) assumed both periods commenced in June. In Alaska, males aggregate and prepare nesting territories 1–2 months before spawning. Without a direct means for observing males at a nesting site with such tools as archival tags and time-lapse cameras, it is difficult to determine when males first arrive. Assuming a 1-month nest establishment period during May and longer incubation times for the western Pacific Ocean population, the duration of the reproductive cycle for Atka mackerel is similar to the duration of the cycle for other parts of the North Pacific Ocean.

The timing of the Atka mackerel reproductive cycle is unusual because fishes in temperate and subarctic waters typically synchronize the hatching time of larvae with periods of high zooplankton abundance in the spring or early summer (Cushing, 1990; Halderson et al., 1993). The possible adaptive significance of hatching during the late fall and early winter may be predator avoidance, dispersal, or availability of specific prey. Atka mackerel larvae are neustonic after hatching (Kendall and Dunn, 1985) and have large mouths (Gorbunova, 1962) capable of feeding on larger planktonic prey.

The temporal, geographic, and bathymetric distribution of sampling for this study was relatively limited given the temporally and spatially complex marine environment that Atka mackerel inhabit (Ladd et al., 2005; Ohshima et al., 2005). Large-scale climate changes to the ecosystem (Rodionov et al., 2005) can cause alterations in recruitment dynamics that may affect population structure (Bailey, 2000; Ciannelli et al., 2005) and ultimately change the timing of the reproductive cycle (Hutchings and Myers, 1994; Wieland et al., 2000; Ojaveer and Kalejs, 2005). We did not investigate how water temperature or other environmental factors vary over larger scales, or how such variability influences the timing of the Atka mackerel's reproductive cycle. This study does, however, provide a framework for process-oriented investigations of stock dynamics, recruitment, and distribution of Atka mackerel populations. Time of

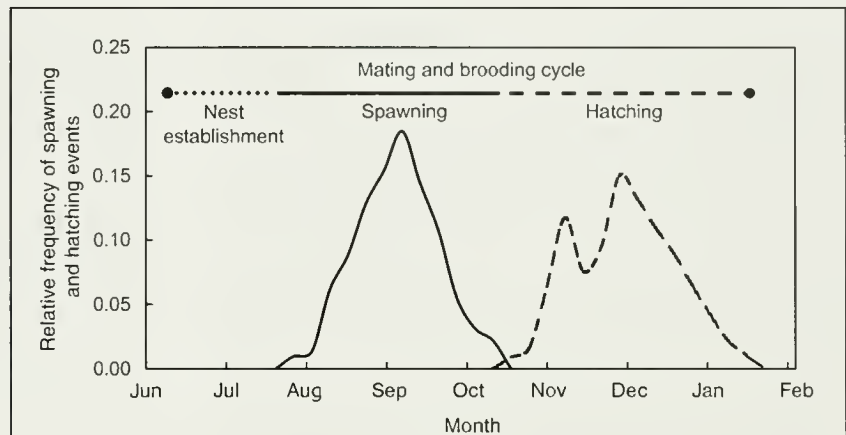


Figure 6

Plot of incubation model results for Atka mackerel (*Pleurogrammus monopterygius*) egg masses collected from Amchitka, Tanaga, and Seguam islands combined. The y-axis is the relative frequency of egg mass spawning (solid line) and hatching events (dashed line) by week for pooled low and high average daily water temperatures. The horizontal line at top represents the duration of the mating and brooding cycle and identifies the periods of nest establishment (dotted line), spawning (solid black line), and hatching (dashed line).

hatching, geographic location, and hydrographic features can all affect the dispersal of larvae and play a significant role, along with biological processes, in determining recruitment success and population structure (Napp et al., 2000).

For unknown reasons, nest fidelity varied among the tagged male Atka mackerel. Given a late July onset of spawning and relatively low ambient water temperatures at nesting sites, it is unlikely that males are able to successfully tend, from start to end, more than one brood of egg masses per season. Nests are commonly composed of eggs from multiple females (Lauth et al., in press) deposited over the 3-month spawning period and by the time the first batch of eggs hatches, the spawning period is nearing completion or has ended.

It appears that none of the four archival tags contained data from a nesting male for the duration of one complete mating and brooding cycle. All four males were captured, tagged, and released while the breeding season was underway in late July. The first male (Fig. 2A) did not exhibit nesting behavior until June of the following year. The other three males (Fig. 2, B–D) resumed nesting behavior shortly after being released; and their behavior may indicate that they were defending nesting territories before they were captured and tagged. Two of the males ended nesting behavior after one month, and the third appeared to abandon one nesting territory and establish a second when it abruptly started exhibiting nesting behavior at a shallower depth on 14 September 2000 (Fig. 2B). It appears that the male that changed depths may have established a new nest, spawned, and successfully brooded

eggs because nesting behavior ended 89 days later, which is a few days longer than the period needed for eggs to incubate and hatch at the water temperatures recorded by the archival tag (mean=4.9°C). If one considers that this male may have already spent 2 months establishing a nest before being captured and tagged, the total nesting period would be 6.5 months. Given the ambient water temperature and late July start of spawning, there was insufficient time for the other three male Atka mackerel to brood a new or existing batch of eggs. Being displaced from an original nesting territory or failing to attract a female to spawn may be reasons for changing a nesting site or for abandoning it altogether. Nesting colonies can have a broad depth range, cover areas over many square kilometers, and be physically and biologically diverse (Lauth et al., in press); therefore the quality of some territories within a nesting colony may be more suitable for attracting females to spawn.

In addition to males changing the depth and location of their nesting territory, there is evidence to suggest that some male Atka mackerel adopt already existing nesting territories containing eggs. In the exhibit tank at the ASLC, a non-nesting male displaced a territorial nest-guarding male and adopted the egg masses already present on the nest. Adoptive nest behavior is also thought to be a characteristic of another hexagrammid, lingcod (*Ophiodon elongates*) (Withler et al., 2004). Abandoning nests or allowing another fish to assume nest-guarding responsibilities is a common behavior in males that provide parental care of eggs (Gozlan et al., 2003). Male fish that guard territories containing eggs are more reproductively successful because females prefer to mate with males that already have eggs (e.g., Marconato and Bisazza, 1986; DeMartini, 1987; Pruett-Jones, 1992).

There is a high energetic cost to male parental care (Marconato et al., 1993; Gillooly and Baylis, 1999; Steinhart et al., 2005), and protracted nest-guarding severely restricts feeding opportunities for males. Egg cannibalism by males is common in Atka mackerel (Zolotov, 1993; Yang, 1999) and may serve as a means for nest-guarding males to sustain themselves during the protracted nesting season (Zolotov, 1993). Cannibalism of eggs within a male's own nesting territory (filial cannibalism) is considered an adaptive behavior in marine fishes that provide paternal care of eggs and it is especially common in species with protracted breeding cycles (Rowher, 1978; Kondoh and Okuda, 2002).

Commercial trawling on nesting habitat during the spawning and breeding periods would probably result in high mortality of both nest-guarding males and developing embryos. Atka mackerel aggregate for spawning and nesting (Lauth et al., in press), and aggregating behavior is generally predictable and makes a population easier to target and more vulnerable to fishing (Colin et al., 2003). The reproductive success of a fish species is also negatively impacted by alterations to the structural habitat and the benthic

community—alternations that are caused by fishing gears (Auster and Langton, 1999). There is some spatial and temporal overlap of commercial trawling and nesting sites in the Aleutian archipelago (Fritz and Lowe, 1998; Lauth et al., in press), but it is difficult to assess the impacts of the fishery on the reproductive success of Atka mackerel without knowing the total distribution of nesting habitat. Knowledge of the temporal use of breeding habitat can be used as a management tool for minimizing negative impacts of the commercial fishery during crucial periods of Atka mackerel life history.

Conclusions

This study provides detailed information about the timing and duration of three specific phases of the Atka mackerel's reproductive cycle: 1) establishment of a nest, 2) spawning, and 3) egg brooding. An accurate incubation rate from controlled laboratory experiments, egg mass collections from nesting sites, and water temperatures characteristic of those observed at nesting sites were used in an incubation model that showed that nest-guarding males use nesting habitat for more protracted periods than previously known. Model results for the start and end of the reproductive cycle were validated with observations from a time-lapse video camera and archival tags. The duration of the reproductive cycle appears to be affected most by the length of the male brooding phase, which can double in duration within the range of ambient water temperatures observed in our laboratory incubation experiments. Knowledge about the timing and duration of the reproductive cycle is essential for conserving Atka mackerel populations and for providing a solid framework for investigations into the physical and biological processes influencing recruitment and population dynamics.

Acknowledgments

This project was funded by grants from the North Pacific Research Board (# F0417) and the National Marine Fisheries Service (NMFS) Essential Fish Habitat (EFH) fund. Rearing experiments at the Alaska Sealife Center (ASLC) by J. Guthridge were part of the requirements for his Master of Science thesis at the University of Alaska, Fairbanks. R. Lauth thanks the skippers and crew from the FV *Morning Star*, FV *Sea Storm*, FV *Sea-fisher*, and RV *Tiglâx*, especially K. Bell, S. Branstiter, P. Deng, T. Meintz, and S. Clark for field support of this research. Many thanks to S. Atkinson from ASLC for assisting with the proposal and those who helped with field support, scuba diving, or reviewing this manuscript including D. Cooper, G. Duker, G. Hoff, J. Lee, L. Logerwell, S. Lowe, S. McDermott, R. Nelson, K. Rand, C. Rilling, D. Somerton, G. Stauffer, S. VanSant, and two anonymous reviewers.

Literature cited

- Ahlstrom, E. H.
1943. Studies on the Pacific pilchard or sardine (*Sardinops caerulea*). 4. Influence of temperature on the rate of development of pilchard eggs in nature. U.S. Fish Wildl. Serv. Spec. Sci. Rep. No. 23:1-26.
- Allen, M. J., and G. B. Smith.
1988. Atlas and zoogeography of common fishes in the Bering Sea and Northeastern Pacific. NOAA Tech. Rep. NMFS 66, 151 p.
- Auster, P. J., and R. W. Langton.
1999. The effects of fishing on fish habitat. In Fish habitat: essential fish habitat and rehabilitation (L. Benaka, ed.), p. 150-187. Am. Fish. Soc., Symposium 22, Bethesda, MD.
- Bailey, K. M.
2000. Shifting control of recruitment of walleye pollock *Theragra chalcogramma* after a major climatic and ecosystem change. Mar. Ecol. Prog. Ser. 198:215-244.
- Bisazza, A., A. Marconato, and G. Marin.
1989. Male competition and female choice in *Padogobius martensi* (Pisces, Gobiidae). Anim. Behav. 38:406-413.
- Ciannelli, L., K. M. Bailey, K.-S. Chan, A. Belgrano, and N. C. Stenseth.
2005. Climate change causing phase transitions of walleye pollock (*Theragra chalcogramma*) recruitment dynamics. Proc. R. Soc. B 272:1735-1743.
- Colin, P. L., Y. J. Sadovy, and M. L. Domeier.
2003. Manual for the study and conservation of reef fish spawning aggregations, 98 p. Society for the Conservation of Reef Fish Aggregations Special Publication no. 1 (version 1.0), Oceanside, CA.
- Cushing, D. H.
1990. Plankton production and year-class strength in fish populations: an update of the match/mismatch hypothesis. Adv. Mar. Biol. 26:249-293.
- DeMartini, E. E.
1987. Paternal defense, cannibalism and polygamy: factors influencing the reproductive success of painted greenling (Pisces, Hexagrammidae). Anim. Behav. 35:1145-1158.
- Fritz, L. W., and S. A. Lowe.
1998. Seasonal distributions of Atka mackerel (*Pleurogrammus monoptyerygius*) in commercially-fished areas of the Aleutian Islands and Gulf of Alaska. U. S. Dep. Commer., NOAA Tech. Memo. NMFS-AFSC-92, 29 p.
- Gillooly, J. F., and J. R. Baylis.
1999. Reproductive success and the energetic cost of parental care in male smallmouth bass. J. Fish Biol. 54:573-584.
- Gorbunova, N. N.
1962. Spawning and development of greenlings (family Hexagrammidae). In Greenlings: taxonomy, biology, interoceanic transplantation (T. S. Rass, ed.), p. 121-185. Tr. Inst. Okeanol., Akad. Nauk. SSSR 59:118-182. [In Russian.] (translated by Isr. Program. Sci. Trans., 1970). [Available from Natl. Tech. Inf. Serv., Springfield, VA, as TT 69-55097 S.]
- Gozlan, R. E., C. J. Flower, and A. C. Pinder.
2003. Reproductive success in male sunbleak, a recent invasive fish species in the U.K. J. Fish Biol. 63:131-143.
- Haldorson, L., M. Pritchett, D. Sterritt, and J. Watts.
1993. Abundance patterns of marine fish larvae during spring in a southeastern Alaskan bay. Fish. Bull. 91:36-44.
- Hempel, G.
1979. Early life history of marine fish: the egg stage, 70 p. Washington Sea Grant, Seattle, WA.
- Hutchings, J. A., and R. A. Myers.
1994. Timing of cod reproduction: interannual variability and the influence of temperature. Mar. Ecol. Prog. Ser., 108:21-31.
- Kendall, A. W., and J. R. Dunn.
1985. Ichthyoplankton of the continental shelf near Kodiak Island, Alaska. U.S. Dep. Commer., NOAA Tech. Memo. NMFS-20, 89 p.
- Kenyon, K. W.
1965. Food of harbor seals at Amchitka. J. Mamm. 46:103-104.
- Kondoh, M., and N. Okuda.
2002. Mate availability influences filial cannibalism in fish with paternal care. Anim. Behav. 63:227-233.
- Ladd, C., G. L. Hunt, Jr., C. W. Mordy, S. Salo, and P. Stabeno.
2005. Marine environment of the eastern and central Aleutian Islands. Fish. Oceanogr., 14(Suppl. 1): 22-38.
- Lauth, R. R., S. W. McEntire, and H. H. Zenger.
In press. Geographic distribution, depth range, and description of Atka mackerel (*Pleurogrammus monoptyerygius*) nesting habitat in Alaska. Alaska Fish. Res. Bull.
- Lauth, R. R., and D. M. Blood.
2007. Description of embryonic development of Atka mackerel (*Pleurogrammus monoptyerygius*). Fish. Bull. 105:571-576.
- Lowe, S., J. Ianneli, M. Wilkins, K. Aydin, R. Lauth, and I. Spies.
2006. Stock assessment of Aleutian Islands Atka mackerel. In Stock assessment and fishery evaluation report for the groundfish resources of the Bering Sea/Aleutian Islands regions, p. 949-1016. North Pacific Fishery Management Council, Anchorage, AK.
- Marconato, A., and A. Bisazza.
1986. Males whose nests contain eggs are preferred by female *Cottus gobio* L. (Pisces: Cottidae). Anim. Behav. 34:1580-1582.
- Marconato, A., A. Bisazza, and M. Fabris.
1993. The cost of parental care and egg cannibalism in the river bullhead, *Cottus gobio* L. (Pisces: Cottidae). Behav. Ecol. Sociobiol. 32:229-237.
- McDermott, S. F., and S. A. Lowe.
1997. The reproductive cycle of Atka mackerel, *Pleurogrammus monoptyerygius*, in Alaska waters. Fish. Bull. 95:321-333.
- McDermott, S. F., K. Pearson, and D. Gunderson.
2007. Annual fecundity, batch fecundity, and oocyte atresia of Atka mackerel (*Pleurogrammus monoptyerygius*) in Alaska waters. Fish. Bull. 105:19-29.
- Medveditsyna, A. V.
1962. Data on the Atka mackerel (*Pleurogrammus monoptyerygius* (Pallas)). In Greenlings: taxonomy, biology, interoceanic transplantation (T. S. Rass, ed.), p.104-106. Tr. Inst. Okeanol., Akad. Nauk. SSSR 59:101-103. In Russian (translated by Isr. Program. Sci. Trans., 1970). [Available from Natl. Tech. Inf. Serv., Springfield,VA, as TT 69-55097 S.]
- Murie, O. J.
1959. Fauna of the Aleutian Islands and Alaska Pen-

- insula. U.S. Fish Wildl. Serv., North American Fauna 61:395-406
- Napp, J. M., A. W. Kendall Jr., and J. D. Schumacher.
2000. A synthesis of biological and physical processes affecting the feeding environment of larval walleye pollock (*Theragra chalcogramma*) in the eastern Bering Sea. *Fish. Oceanogr.* 9:147-162
- Nichol, D. G., and D. A. Somerton.
2002. Diurnal vertical migration of the Atka mackerel *Pleurogrammus monopterygius* as shown by archival tags. *Mar. Ecol. Prog. Ser.* 239:193-207.
- Ohshima, K. I., Y. Fukamachi, T. Mutoh, and M. Wakatsuchi.
2005. A generation mechanism for mesoscale eddies in the Kuril Basin of the Okhotsk Sea: baroclinic instability caused by enhanced tidal mixing. *J. Oceanogr.* 61:247-260.
- Ojaveer, E., and M. Kalejs.
2005. The impact of climate change on the adaptation of marine fish in the Baltic Sea. *ICES J. Mar. Sci.* 62:1492-1500.
- Östlund-Nilsson, S.
2000. Are nest characters of importance when choosing a male in the fifteen-spined stickleback (*Spinachia spinachia*)? *Behav. Ecol. Sociobiol.* 48(3):229-235.
- Pruett-Jones, S.
1992. Independent versus nonindependent mate choice: do females copy each other? *Am. Nat.* 140:1000-1009.
- Riley, J. D.
1974. The distribution and mortality of sole eggs (*Solea solea* L.) in inshore areas. In *The early life history of fish* (J. H. S. Blaxter, ed.) p. 39-52. Springer, Heidelberg, Germany.
- Rodionov, S. N., J. E. Overland, and N. A. Bond.
2005. Spatial and temporal variability of the Aleutian climate. *Fish. Oceanogr.* 14 (suppl.) 1:3-21.
- Rohwer, S.
1978. Parent cannibalism of offspring and egg raiding as a courtship strategy. *Am. Nat.* 112:429-440.
- Rutenberg, E. P.
1962. Survey of the fishes family Hexagrammidae. In *Greenlings: taxonomy, biology, interoceanic transplantation* (T. S. Rass, ed.), p.1-103. Tr. Inst. Okeanol., Akad. Nauk. SSSR 59:3-100. In Russian (translated by Isr. Program. Sci. Trans., 1970). [Available from Natl. Tech. Inf. Serv., Springfield, VA, as TT 69-55097 S.]
- Sargent, R. C.
1982. Territory quality, male quality, courtship intrusion and female nest-choice in the three-spined stickleback, *Gasterosteus aculeatus*. *Anim. Behav.* 30:364-374.
- Sikkel, P. C.
1988. Factors influencing spawning site choice by female garibaldi, *Hypsypops rubicundus* (Pisces: Pomacentridae). *Copeia* 1988:710-718.
- Sinclair E. H., and T. K. Zeppelin.
2002. Seasonal and spatial differences in diet in the western stock of Steller sea lions (*Eumetopias jubatus*). *J. Mamm.* 83:973-990.
- Steinhart, G. B., M. E. Sandreneh, S. Weavera, R. A. Steina, and E. A. Marschalla.
2005. Increased parental care cost for nest-guarding fish in a lake with hyperabundant nest predators. *Behav. Ecol.* 2005 16(2):427-434.
- Wieland, K., A. Jarre-Teichmann, and K. Horbowa.
2000. Changes in the timing of spawning Baltic cod: possible causes and implications for recruitment. *ICES J. Mar. Sci.* 57:452-464.
- Withler R. E., J. R. King, and J. B. Marliave.
2004. Polygamous mating and high levels of genetic variation in lingcod (*Ophiodon elongatus*) of the Strait of Georgia, British Columbia. *Environ. Biol. Fishes* (69):345-357.
- Yang, M-S.
1999. The trophic role of Atka mackerel, *Pleurogrammus monopterygius*, in the Aleutian Islands area. *Fish. Bull.* 97(4):1047-1057.
- Zar, J. H.
1999. *Biostatistical analysis*, 4th ed., 663 p. Prentice-Hall, Inc., Englewood Cliffs, NJ.
- Zenger, H. H., Jr.
2004. Data report: 2002 Aleutian Islands bottom trawl survey. U.S. Dep. Commer., NOAA Tech. Memo. NMFS-AFSC-143, 247 p.
- Zolotov, O. G.
1993. Notes on the reproductive biology of *Pleurogrammus monopterygius* in Kamchatkan waters. *J. Ichthyol.* 4:25-37.

Description of embryonic development of Atka mackerel (*Pleurogrammus monopterygius*)

Robert R. Lauth (contact author)

Deborah M. Blood

Email address for R.R. Lauth: Bob.Lauth@noaa.gov

National Oceanic and Atmospheric Administration
National Marine Fisheries Service
Alaska Fisheries Science Center
Resource Assessment and Conservation Engineering Division
7600 Sand Point Way NE
Seattle, Washington 98115

Atka mackerel (*Pleurogrammus monopterygius*) is a hexagrammid fish that inhabits the temperate and subarctic North Pacific Ocean and neighboring seas (Fig. 1). This highly abundant fish is a critically important prey species (Sinclair and Zeppelin, 2002; Zenger, 2004) that supports a directed commercial trawl fishery (Lowe et al., 2006). Atka mackerel is a demersal spawner and males provide parental care to eggs (Zolotov, 1993). During breeding periods, sexually mature males aggregate on the bottom at nesting sites where they establish territories (Lauth et al., in press). Sexually mature females periodically visit male nesting territories from July to October to spawn batches of demersal egg masses (McDermott and Lowe, 1997; McDermott et al., 2007). Individual nests may consist of multiple egg masses deposited by different females, and males defend nesting territories for a protracted period lasting from the time territories are being established until all eggs within the territory are completely hatched (Lauth et al., 2007). Knowledge about the timing of the reproductive cycle and the use of spawning habitat are important for understanding population structure and the dynamics of stock recruitment, which in turn are important factors in the management of Atka mackerel populations.

The male brooding phase of the reproductive cycle has not been a focus of studies despite its critical importance in the propagation and survival

of Atka mackerel. The incubation period from fertilization to hatching is a good proxy for determining the time that nest-guarding males stay at nesting sites once spawning has ended. There is one published study describing embryonic development of Atka mackerel at 11°C (Gorbunova, 1962); however the results are incomplete and provide only a partial description of embryonic development. An accurate and complete timetable of embryonic development is essential for determining how temperature affects the incubation period and the timing of the reproductive cycle in the North Pacific Ocean (Lauth et al., 2007). The objective of this study was to determine the incubation period of Atka mackerel embryos by using a controlled water temperature, and to construct a complete embryonic development series, from fertilization to first hatching, with particular reference to morphological features and pigmentation for categorizing preserved egg specimens.

Materials and methods

Eggs used to construct the embryonic development series were obtained by scuba divers from a nearshore Atka mackerel nesting site at Seguam Island in the Aleutian archipelago (Fig. 1) on 7 August 2002. The *in situ* egg mass was deposited and fertilized on a nest at an unknown time between two scuba dives at 1115 and 1720 Alaska Daylight Time (ADT).

For the purpose of this experiment, the time of egg fertilization was assumed to be 6 hours before egg mass collection. The bottom water temperature at the time of the collection dive was 4.1°C

The egg mass was brought to the surface, separated into two halves, and each half was placed in a four-liter glass jar with seawater and an air stone. The jars with incubating egg masses were secured in a refrigerator set at 6.0°C and water temperature was monitored with a Tidbit Datalogger (Onset Computers, Bourne, MA) that recorded temperature once every minute. On 16 August 2004, eggs were transported inside thermoses and coolers with ice by air to the Alaska Fisheries Science Center (AFSC) in Seattle, WA. Upon arrival, the egg masses were placed in two 38-L aquaria housed in a temperature-controlled room maintained at 6.0°C. Each aquarium was equipped with air pumps, air stones, and a water circulation pump and water flow directed at the eggs. Seawater for the aquaria was pumped from Puget Sound, WA, run through 1- μ m filters, sterilized with ultraviolet light, and stored in 200-L plastic barrels. The seawater in the barrels was adjusted to 32–33 ppt by using aquarium salt, and the barrels were kept inside the temperature-controlled room at the AFSC to maintain the same water temperature as that of the aquaria. Half the water volume in the aquaria was changed on a daily basis and incandescent lights were set on automatic timers to simulate daylight from 0600 to 1800 Pacific Daylight Time (PDT). Five to ten eggs were sampled every 1–3 days from 16 August to hatching and preserved in phosphate-buffered 5% formalin solution. Chorions were removed from eggs to facilitate examination of development with a stereo dissecting microscope. Descriptions of obvious morphological features or pigmentation were recorded for each

Manuscript submitted 31 May 2007
to the Scientific Editor's Office.

Manuscript approved for publication
29 July 2007 by the Scientific Editor.
Fish. Bull. 105:571–576 (2007).

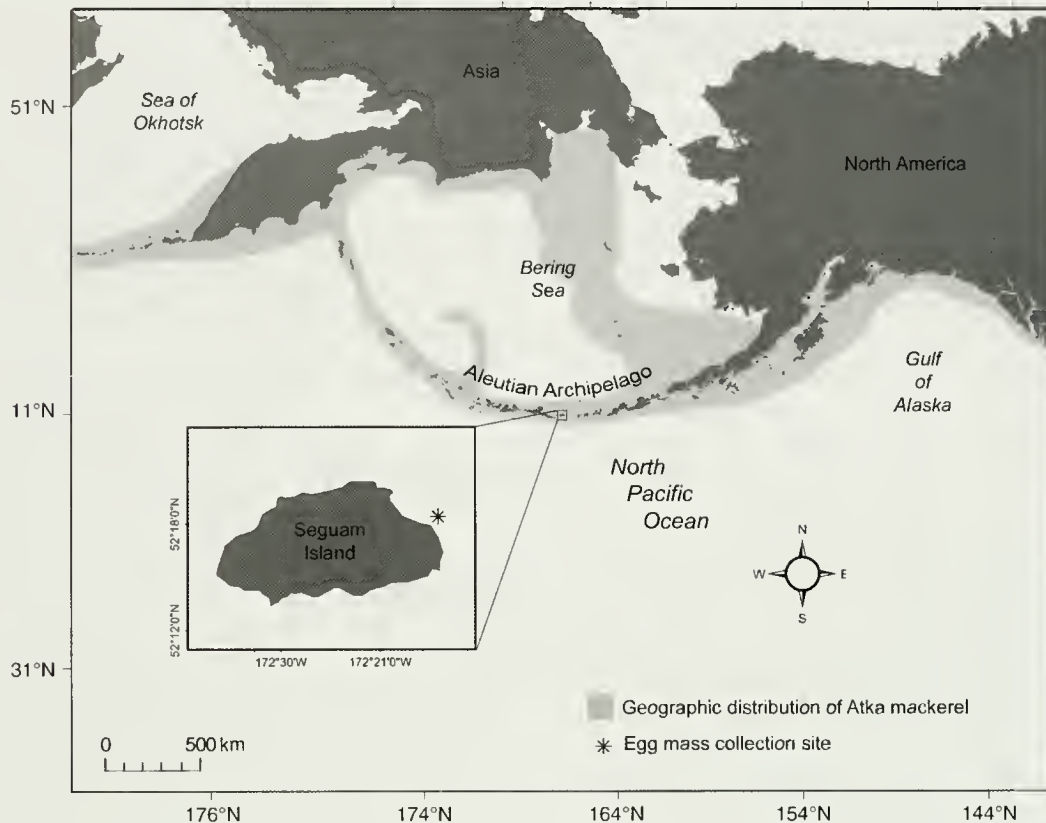


Figure 1

Map showing the geographic distribution of Atka mackerel (*Pleurogrammus monopterygius*; light gray shading) in the North Pacific Ocean and adjoining seas. Also shown is the location (*) near Seguam Island where a newly fertilized Atka mackerel egg mass was obtained for an incubation experiment.

preserved embryo and the observations from the entire progression were used to construct a chronological series describing embryonic development at 6.0°C.

Results

The newly fertilized eggs were collected from a nest containing several separate egg masses. The eggs were light green and were relatively soft and loosely clumped, in contrast to their character in the following days when they became more firm, rubbery, and tightly attached to one another. As the eggs aged, their color turned reddish brown. The original egg mass had approximately 1500 eggs that ranged in diameter from 2.5 to 2.8 mm. The average daily water temperature during the incubation ranged from 5.42° to 6.57°C and the mean and standard deviation were 6.2° and $\pm 0.3^\circ\text{C}$, respectively. Incubated eggs began hatching on day 74 and preserved length of yolk sac larvae was 9.4–10.9 mm SL.

Embryonic development

The description of embryonic development was divided into two sections: the first section is a description of the

development of morphological features, and the second is a description of the development of pigmentation. For brevity, each paragraph in the pigmentation section describes one or more pigment type from the time they first appear until they are fully developed. Table 1 provides descriptive summaries for the progression of both morphological features and pigmentation.

Morphological features

Preserved eggs from the day of collection (fertilization) had a single blastomere sitting on a yolk containing a group of >50 oil globules varying in size (0.08–0.20 mm). After 72 hours of meroblastic cleavage, a blastodermal cap formed on top of the yolk. Over the next four days, the blastodermal cap flattened and increased in diameter as the edge began folding under (gastrulation) to form a germ ring that started moving downward over the yolk (epiboly; Table 1). The embryonic shield formed as the germ ring advanced over the yolk. The blastopore closed on day 15 when the germ ring completely enveloped the yolk. During days 17–21, the optic capsule and eye lenses formed, the head and anterior body became thick and more defined, and the notochord, myomeres, and Kupffer's vesicle became visible (Table 1).

One week after blastopore closure (day 22), the tail region began lifting away from the yolk, and within two days, the length of the embryo was 50% of the circumference of the yolk. As the tail grew longer, it curved further away from its longitudinal axis, causing the embryo to curl around the top quarter of the yolk rather than at the equator. The tail was 75% of its way around the yolk by day 29 and touched the snout by day 36. Lengthening further, the tail extended past the anterior edge of the eye (day 40) and past the posterior edge of the head (day 48); the maximum length was reached on day 64 when it was 1.75 times the circumference of the yolk.

Pigmentation

Embryo pigmentation first appeared on day 31. Sparse melanophores appeared in the eye surrounding the lens and along the dorsal midline, nape, and gut (Table 1; Fig. 2). The eye became completely pigmented and much darker by day 38. The beginning of the dorsal midline series was observed as scattered melanophores in the area between 20% body length (BL) and 50% BL. By day 44 the dorsal midline series extended as a double row anterior to the nape and posterior to 50% BL where it joined to form a single row of irregularly spaced melanophores that continued to 70% BL. On day 49, the single row of dorsal midline pigment extended to 5–6 myomeres anterior to the caudal peduncle. At hatching, the dorsal midline series was a double row of continuous pigment extending from the nape to three myomeres anterior of the caudal peduncle (Fig. 3). Dorsal gut pigment first appeared halfway along the gut where the pigment progressively spread posteriorly toward the anus, and then anteriorly toward the head. On day 42, the dorsal gut pigment extended the full length of the gut, excluding the anus. During subsequent development, a few melanophores migrated ventrally onto the lateral gut wall and others moved close to the newly developed pectoral fin buds. By the last week of development (day 71), there was heavy dorsal gut pigment, moderate pigment on the lateral gut, and no pigment on the ventral gut or anus (Fig. 3).

The head remained unpigmented until day 36 when melanophores appeared on the snout, forebrain, midbrain, and nape (Fig. 2). Initially, head pigment was scattered lightly across the dorsal surface except where it outlined the posterior edge of both lobes of the nape. The nape pigment converged toward the double row of melanophores extending anteriorly from the dorsal midline series. During days 37–61, the dorsal midbrain and nape pigment increased, leaving an unpigmented area along the midline (Fig. 2) and several melanophores also became visible on the opercle between the eye and pectoral-fin base. By day 61, opercular pigment concentrated into one dark spot and a second smaller spot appeared on the opercle below the right lower quadrant of the eye (Fig. 3). Head pigmentation was complete by day 64; stellate melanophores coalesced on the midbrain and nape and heavy pigment covered the nape and mid-

Table 1

Description of embryonic development by day for Atka mackerel (*Pleurogrammus monoptyerygius*) eggs incubated at 6.2°C.

Day	Description
0	Single blastomere; yolk contains group of >50 oil globules; meroblastic cleavage begins
1	4 blastomeres
2	32 blastomeres
3	64–28 blastomeres
4	Blastodermal cap; individual cells indistinguishable and begin to flatten
7	Gastrulation, epiboly, and formation of embryonic shield begin
9	25% epiboly
11	50% epiboly
12	75% epiboly
15	Blastopore closed
17	Optic vesicles begin to form
18	Myomeres visible on anterior body behind nape
19	Kupffer's vesicle visible; optic vesicles formed; myomeres visible on central 60% of body
21	Posterior 50% of body thick and raised from surface of yolk; eye lenses are formed
22	Midbrain enlarges to form bump; tail region lifts away from yolk
23	Midbrain differentiates and forms a bump behind eyes
24	Embryo arches over 50% of the yolk
25	Tail curves away from longitudinal axis
26–27	Otic capsules formed
28	Dorsal finfold on posterior 1/3 of body extends anteriorly to 60% BL
29	Dorsal finfold extends anteriorly to nape; embryo 75% of the way around yolk
31	Pigmentation first appears in eye and along dorsal midline, posterior dorsolateral nape, and dorsal gut
35	Pectoral fin buds formed
36	Head pigment on snout, midbrain and nape; embryo tail touches snout
40	Nares visible; embryo tail extends past anterior edge of eye
41	Nares formed
42	Lower jaw beginning to form
48	Embryo tail extends past posterior edge of head
51	Postanal ventral midline pigment appears
55	Nape enlarges to form hump
58	Opercular pigment; lower jaw fully formed
62	Internal notochord pigment visible
64	Embryo tail length is 1.75× circumference of yolk
65	External lateral pigment visible
71	Pigmentation indistinguishable between embryos and hatched larvae
74	First hatching

brain except for an unpigmented midline through the midbrain and anterior half of the nape. Internal pigment was also visible at the base of the midbrain near the nape and external pigment increased slightly on the forebrain and disappeared on the snout (Fig. 2).

Postanal ventral melanophores (pvm) became visible late during the embryonic development (day 51) along the ventral midline at 80% BL. By day 65, the pvm

series extended anteriorly to 50% BL. At time of hatching, the completed series consisted of a light irregular line of melanophores at 50% BL, larger and more closely spaced melanophores at 60–80% BL, and ended 1–2 myomeres anterior to the terminus of the dorsal midline series (Fig. 3).

The internal and external lateral pigment series were the last two pigments to appear. On day 62, internal

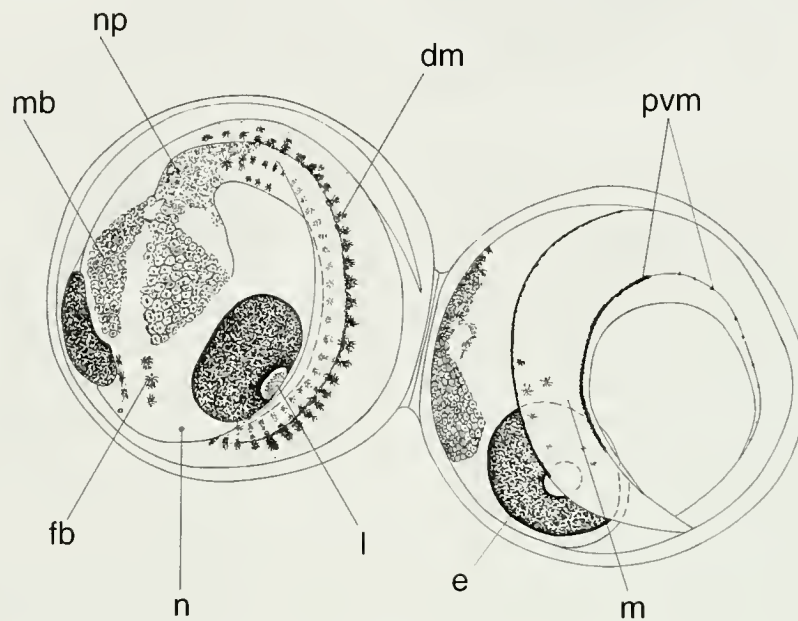


Figure 2

Drawing of two Atka mackerel (*Pleurogrammus monopterygius*) embryos with egg diameters of 2.5–2.8 mm after 11 weeks of development at 6.15°C (areas of pigment: fb = forebrain, mb = midbrain, np = nape, dm = dorsal midline, and pvm = postanal ventral melanophores; morphological features: n = nares, l = lens, e = eye, and m = myomere).

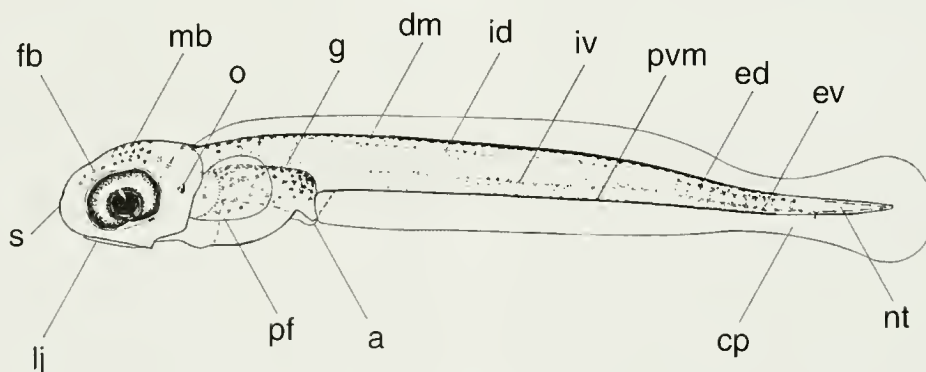


Figure 3

Drawing of a 10.9 mm Atka mackerel (*Pleurogrammus monopterygius*) larva one day after hatching (areas of pigment: fb = forebrain, mb = midbrain, o = opercular, g = gut, dm = dorsal midline, id = internal dorsal, iv = internal ventrolateral, pvm = postanal ventral melanophores, ed = external dorsolateral, and ev = external ventrolateral; morphological features: s = snout, lj = lower jaw, pf = pectoral fin, a = anus, cp = caudal peduncle, and nt = notochord).

pigment was observed above and below the notochord, posterior to the anus, and extending toward the tail; the ventrolateral series began 2–5 myomeres posterior to the start of the dorsolateral series. On day 65, the external lateral pigment appeared on the posterior 20% of the body above and below the notochord and on the ventrolateral caudal body. From day 71 to 74, there were no appreciable differences between hatched and unhatched embryos (Fig. 3). The internal dorsolateral series began just anterior to the anus and was spaced regularly with about one melanophore per myomere until termination at a point even with the dorsal midline series. The internal ventrolateral series began 10–12 myomeres posterior to the anus with similar spacing until 80% BL, where it became irregular until terminating three myomeres before the end of the pvm (postanal ventral melanophore) series. The external dorsolateral and ventrolateral pigment covered the posterior 25% of the body; dorsolateral pigment ended even with the dorsal midline series and the ventrolateral series extended halfway onto the caudal peduncle. Some larvae had one melanophore on the caudal peduncle midway between the last myomere and notochord tip.

Discussion and conclusions

This study provides a complete description of embryonic development that details the progression of morphological features and pigmentation in Atka mackerel embryos from fertilization to first hatching. Daily egg development did not deviate from known fish embryology, and the incubation period was 74 days at an average daily water temperature of 6.2°C. The formerly published incubation period of 40–45 days at an average water temperature of 11°C was based on a 19-day rearing experiment supplemented with data from *in situ* egg samples collected from nesting sites (Gorbunova, 1962). Additional imprecision may have been introduced by unregulated and widely varying water temperatures used during the incubation experiment (8–15°C; Gorbunova, 1962). Comparing our study with that of Gorbunova (1962), we found that incubation time was inversely related to temperature, which is commonly known to be true for fishes (Hempel, 1979).

A review of the scientific literature on near-bottom water temperatures at North Pacific Ocean nesting sites shows that temperatures are generally within several degrees of the incubation temperature used in our study (6.2°C). At western North Pacific Ocean nesting sites, water temperatures ranged from 2.5° to 8.2°C in 1958 (Gorbunova, 1962), and from 4.84° to 8.30°C in 1985 and 1992 (Zolotov, 1993). Similarly, across the central and eastern North Pacific Ocean, the mean and standard deviation of water temperature at 106 nesting sites was 5.4±1.2°C and was as low as 3.9°C (Lauth et al., in press). It is apparent from our study that the use of nesting substrate by males increases substantially with the longer incubation periods caused by lower water temperatures. In such cases where males are guarding

multiple egg masses at varying developmental stages, the brooding phase will be more protracted than that where there is only a single egg mass.

Additional controlled rearing experiments at a wider range of water temperatures are needed to determine more accurately how the rate of embryonic development, and hence male brooding period, is affected. The complete embryonic development series from this study and an empirically derived incubation rate can be used for modeling the relative spawning and hatching dates of egg masses collected from different nesting sites (Lauth et al., 2007). Such an incubation model would be useful for investigating the variability in timing of the reproductive cycle across the broad longitudinal range of Atka mackerel, which is important for conserving and managing Atka mackerel populations and nesting habitat.

Acknowledgments

This project was funded by a grant from the National Marine Fisheries Service (NMFS) Essential Fish Habitat (EFH) fund. This work would not have been possible without the help of S. Porter and A. Dougherty who taught R. Lauth incubation techniques and let him use their wet lab. B. Vinter drew the illustrations of the Atka mackerel egg and larva. R. Lauth thanks S. Branstitter and the crew from the *FV Sea Storm* for field support of this research. Many thanks to those who helped with field support, scuba diving, or reviewing this manuscript: B. Dixon, G. Duker, J. Lee, L. Logerwell, S. Lowe, S. McDermott, R. Nelson, C. Rilling, D. Somerton, G. Stauffer, J. Watson, and two anonymous reviewers.

Literature cited

- Gorbunova, N. N.
1962. Spawning and development of greenlings (family Hexagrammidae). In *Greenlings: taxonomy, biology, interoceanic transplantation* (T. S. Rass, ed.), p.121–185. Tr. Inst. Okeanol., Akad. Nauk. SSSR 59:118–182. In Russian (translated by Isr. Program. Sci. Trans., 1970). [Available from Natl. Tech. Inf. Serv., Springfield, VA, as TT 69-55097 S.]
- Hempel, G.
1979. Early life history of marine fish: the egg stage, 70 p. Washington Sea Grant, Seattle, WA.
- Lauth, R. R., J. Guthridge, D. Nichol, S. W. McEntire, and N. Hillgruber.
2007. Timing of mating and brooding periods of Atka mackerel (*Pleurogrammus monopterygius*) in the North Pacific Ocean. *Fish. Bull.* 105:560–571.
- Lauth, R. R., S. W. McEntire, and H. H. Zenger.
In press. Geographic distribution, depth range, and description of Atka mackerel (*Pleurogrammus monopterygius*) nesting habitat in Alaska. *Alaska Fish. Res. Bull.*
- Lowe, S., J. Ianelli, M. Wilkins, K. Aydin, R. Lauth, and I. Spies.
2006. Stock assessment of Aleutian Islands Atka

- mackerel. In Stock assessment and fishery evaluation report for the groundfish resources of the Bering Sea/Aleutian Islands regions, p. 949-1016. North Pacific Fishery Management Council, Anchorage, AK.
- McDermott, S. F., and S. A. Lowe.
1997. The reproductive cycle of Atka mackerel, *Pleurogrammus monopterygius*, in Alaska waters. Fish. Bull. 95:321-333.
- McDermott, S. F., K. Pearson, and D. Gunderson.
2007. Batch spawning, atresia, and fecundity of Atka mackerel (*Pleurogrammus monopterygius*) in Alaska waters. Fish. Bull. 105:19-29.
- Sinclair E. H., and T. K. Zeppelin.
2002. Seasonal and spatial differences in diet in the western stock of Steller sea lions (*Eumetopias jubatus*). J. Mamm. 83:973-990.
- Zenger, H. H., Jr.
2004. Data report: 2002 Aleutian Islands bottom trawl survey. U.S. Dep. Commer., NOAA Tech. Memo. NMFS-AFSC-143, 247 p.
- Zolotov, O. G.
1993. Notes on the reproductive biology of *Pleurogrammus monopterygius* in Kamchatkan waters. J. Ichthyol. 4:25-37.

Using the empirical Bayes method to estimate and evaluate bycatch rates of seabirds from individual fishing vessels

Daniel K. Kimura

E-mail address: dan.kimura@noaa.gov

Alaska Fisheries Science Center
National Marine Fisheries Service
National Oceanic and Atmospheric Administration
7600 Sand Point Way NE
Seattle, Washington 98115-6349

Minimizing bycatch of seabirds is a major goal of the U.S. National Marine Fisheries Service. In Alaska waters, the bycatch (i.e., inadvertent catches) of seabirds has been an incidental result of demersal groundfish longline fishery operations. Notably, the endangered short-tailed albatross (*Phoebastria albatrus*) has been taken in this groundfish fishery. Bycatch rates of seabirds from individual vessels may be of particular interest because vessels with high bycatch rates may not be functioning effectively with seabird avoidance gears, and there may be a need for suggestions on how to use these avoidance gears more effectively. Therefore, bycatch estimates are usually made on an individual vessel basis and then summed to obtain the total estimate for the entire fleet.

The empirical Bayes (EB) (Efron and Morris, 1975; Casella, 1985) method offers the possibility of improving within-vessel bycatch estimates, with the assumption that the individual vessel bycatch rate of seabirds has a gamma prior distribution. With the resulting Poisson-gamma EB model, it is assumed that each vessel's bycatch of seabirds has a Poisson distribution conditioned on the realized "true" bycatch rate. The basic principle of the EB method comes from the realization that the parameters for the gamma distribution can be estimated from individual vessel bycatches, and that the resulting EB estimators of indi-

vidual vessel bycatch rates should provide estimates of individual bycatch rates that have smaller total mean squared error (TMSE) than the individual vessel bycatch rates estimated independently. The independently estimated individual vessel bycatch rate is simply the bycatch per thousand hooks fished for each vessel. A more complete introduction to the empirical Bayes method as it has been applied to different types of problems is provided by Ver Hoef (1996).

The goal of this note is to clearly describe empirical Bayes estimation and provide a detailed example of its application to the problem of estimating seabird bycatch. It is to be hoped that a better understanding of the theory underlying empirical Bayes methods will lead to more applications in the area of fisheries management.

Materials and methods

General theory

Mathematically, the empirical Bayes (EB) method can be described as a statistical procedure that has clearly defined steps (Carlin and Louis, 2000). Let the prior distribution of a parameter θ (the parameter of greatest interest) be $g(\theta|\eta)$, where the η are unknown parameters, and the sampling distribution for each stratum observation y is $f(y|\theta)$.

From the joint distribution defined by $h(y, \theta|\eta) = f(y|\theta)g(\theta|\eta)$, the marginal distribution of the observed y can be derived by integrating out θ : $m(y|\eta) = \int h(y, \theta|\eta) d\theta$. The empirical Bayes method arises from the recognition that η can be estimated from $m(y|\eta)$ by using the marginal maximum likelihood (MML) estimators or related methods. Once $\hat{\eta}$ is estimated, the posterior distribution of θ can be obtained by using the Bayes rule, $p(\theta|y, \hat{\eta}) = f(y|\theta)g(\theta|\hat{\eta})/m(y|\hat{\eta})$, and an EB estimate of θ can be made from this posterior distribution.

The Poisson-gamma empirical Bayes model

The Poisson-gamma model is ideal for illustrating how to calculate EB estimators from the general theory because the all the required integrals result in a gamma function. For this model, denote the gamma prior for the seabird bycatch rate of vessel i as $g(\lambda_i|\alpha, \beta)$, and the Poisson sampling distribution as $f(y_i|\lambda_i, \tau_i)$, where y_i is the number of seabirds observed, and τ_i are the number of hooks observed. The joint distribution of y_i and λ_i is then

$$h(y_i, \lambda_i | \alpha, \beta, \tau_i) = \frac{\exp(-\lambda_i \tau_i) (\lambda_i \tau_i)^{y_i}}{y_i!} \times \frac{\lambda_i^{\alpha-1} \exp(-\lambda_i / \beta)}{\Gamma(\alpha) \beta^\alpha}$$

$$\text{for } \alpha, \beta, \lambda_i > 0, y_i \geq 0.$$

The marginal distribution is calculated by integrating out λ_i :

$$m(y_i | \alpha, \beta, \tau_i) = \frac{\tau_i^{y_i}}{y_i! \Gamma(\alpha) \beta^\alpha} \frac{\Gamma(y_i + \alpha)}{(\tau_i + 1 / \beta)^{y_i + \alpha}}$$

Manuscript submitted 2 April 2007 to the Scientific Editor's Office.

Manuscript approved for publication 16 May 2007 by the Scientific Editor.

Fish. Bull. 105:577-581 (2007).

The probability for all vessels (i.e., strata) can then be written as

$$P\{X_1 = y_1, \dots, X_n = y_n \mid \tau_1, \dots, \tau_n\} = \prod_{i=1}^n \frac{\tau_i^{y_i}}{y_i! \Gamma(\alpha) \beta^\alpha} \frac{\Gamma(y_i + \alpha)}{(\tau_i + 1/\beta)^{y_i + \alpha}}$$

The parameters of the gamma prior, $g(\lambda_i \mid \alpha, \beta)$, can then be estimated by maximizing the marginal likelihood given above and arriving at MML estimates $(\hat{\alpha}, \hat{\beta})$. Initial estimates for the gamma distribution can be provided by moment estimators (Carlin and Louis, 2000) where: $r_i = m_i / \tau_i$, and \bar{r} and s_r^2 and the sample mean and variance of the $\{r_i\}$, and

$$\hat{\alpha}_0 = \bar{r}^2 / (s_r^2 - \bar{r}) \sum_{i=1}^n (1/\tau_i) / n \text{ and } \hat{\beta}_0 = \bar{r} / \hat{\alpha}$$

The gamma prior is the conjugate distribution (Patrick, 1972; Carlin and Louis, 2000) for the Poisson sampling distribution, which means that the posterior distribution is in the same family as the prior distribution for each stratum. The posterior distribution is $p(\lambda_i \mid y_i, \hat{\alpha}, \hat{\beta}, \tau_i) = f(y_i, \lambda_i \mid \hat{\alpha}, \hat{\beta}, \tau_i) / g(y_i \mid \hat{\alpha}, \hat{\beta}, \tau_i)$, which can be verified to have the gamma distribution $g(\lambda_i \mid \alpha = y_i + \alpha, \beta = 1/(\tau_i + 1/\beta))$. The mean of this posterior distribution, providing estimators for the λ_i , can be calculated from

$$\begin{aligned} \tilde{\lambda}_i &= E(\lambda_i) \\ &= \int_0^\infty \lambda_i p(\lambda_i \mid y_i, \hat{\alpha}, \hat{\beta}, \tau_i) d\lambda_i \\ &= (y_i + \hat{\alpha}) / (\tau_i + 1/\hat{\beta}) \end{aligned}$$

or more simply can be recognized as the product of the parameters of the posterior distribution.

The conventional maximum likelihood (ML) estimator of λ_i for the Poisson strata is $\hat{\lambda}_i = y_i / \tau_i$. The EB estimator of λ_i based on the mean of the posterior distribution can be seen as the weighted average of the ML stratum estimator and the mean of the gamma prior $\hat{\alpha}\hat{\beta}$ and will lie between these two values.

Simulation methods

Simulation was performed on the Poisson-gamma EB model described above. Each replication simulated the seabird bycatch of 50 vessels, and was repeated 1000 times. Each replication assumed that the “true” bycatch rate for each vessel (λ_i) was distributed as an observation from the gamma distribution $g(\lambda_i \mid \alpha = 0.603, \beta = 0.030)$; whose parameters were estimated in the EB analysis which follows. The number of hooks that were “observed,”

in thousands, was distributed uniformly as $U(0, \tau_{\max})$, with $\tau_{\max} = \{200, 500, 1000, 2000, 5000\}$. For each of these simulations then, $\tau_{\text{ave}} = \{100, 250, 500, 1000, 2500\}$. Finally, the number of “observed” seabirds (y_i) was simulated using the Poisson distribution with $\lambda'_i = \lambda_i \tau_i$, where λ_i and τ_i were previously randomly generated as described.

For each replication, the simulated (y_i, τ_i) were analyzed by using the empirical Bayes method, by first estimating $(\hat{\alpha}, \hat{\beta})$ using the MML, and then using these parameters to calculate the EB estimate $\hat{\lambda}_i = (y_i + \hat{\alpha}) / (\tau_i + 1/\hat{\beta})$. The ML estimator for each stratum was $\hat{\lambda}_i = y_i / \tau_i$, and the global unstratified (GU) estimator was $\hat{\lambda} = \Sigma y_i / \Sigma \tau_i$. The performance of these estimators was measured by using

$$TMSE = \sum_{i=1}^{50} (X_i - \lambda_i)^2 / 50,$$

where X_i could be any of $\hat{\lambda}_i, \tilde{\lambda}_i$, or $\hat{\lambda}$. The simulation was repeated 1000 times, and the *TMSE* values were averaged to measure the overall performance of these estimators.

Analysis of bycatch data

In 2002, The North Pacific Longline Association, which has many longline vessel operators as members, voluntarily followed proposed regulations that required the use of effective seabird avoidance gear during fishing operations. These voluntary guidelines were implemented into formal regulations in February 2004.

EB analysis was performed on the bycatch of seabirds from individual longline vessels fishing in the eastern Bering Sea. The data were the annual observed bycatches of seabirds (y_i) and the total number of observed hooks in thousands (τ_i) of individual fishing vessels for 2002 and 2003. The 2002 data were used to fit the EB model, and resulting λ_i estimates were used to predict the λ_i for 2003. As a comparison, a similar analysis was performed on data collected from 1997 and 1998, a time when many vessels did not use bird-avoidance gear and when the bycatch rate of seabirds was much higher than in 2002 and 2003.

Results

Simulation results

All simulations consisted of 1000 replications as described above. When measured by *TMSE*, the EB estimator was clearly superior to both the maximum likelihood (ML) and global unstratified (GU) estimators (Table 1). This was true regardless of whatever value of τ_{\max} was used in the simulations. The ratio $R = TMSE(\hat{\lambda}_i) / TMSE(\tilde{\lambda}_i)$ increased as τ_{\max} increased, but the values of *TMSE* for GU remained constant. Note that the $(\hat{\alpha}, \hat{\beta})$ appeared biased when $\tau_{\max} = 5000$ (Table 1).

Table 1

Simulation results from the Poisson-gamma empirical Bayes (EB) model with the assumption of 50 vessels (strata), and with random sample sizes (observed number of 1000 hooks) distributed as $U(0, \tau_{\max})$ and replicated 1000 times. The gamma distribution prior was assumed to have parameters $\alpha=0.603$, $\beta=0.030$, as were estimated from the seabird bycatch analysis, and the average $\hat{\alpha}$ and $\hat{\beta}$ were calculated from the 1000 replications. The seabird bycatch rate for vessel i , λ_i , was estimated by the maximum likelihood (ML) estimator $\hat{\lambda}_i$, the empirical Bayes (EB) estimator $\tilde{\lambda}_i$, and the global unstratified (GU) estimator $\hat{\lambda}$. Performance of these estimators was measured by the total mean squared error (*TMSE*) averaged over the 1000 replications, and R was defined as the ratio of *TMSE* values calculated for ML and EB estimates.

Sample size τ_{\max}	$TMSE(\hat{\lambda}_i)$ ML	$TMSE(\tilde{\lambda}_i)$ EB	$TMSE(\hat{\lambda}_i)$ GU	$R = \frac{TMSE(\hat{\lambda}_i)}{TMSE(\tilde{\lambda}_i)}$	Average $\hat{\alpha}$	Average $\hat{\beta}$
200	0.001390	0.000189	0.000542	7.4	0.712	0.029
500	0.001440	0.000103	0.000531	14.0	0.655	0.029
1000	0.001000	0.000063	0.000541	15.9	0.638	0.030
2000	0.000935	0.000038	0.000532	24.6	0.621	0.031
5000	0.000906	0.000018	0.000537	50.3	0.473	0.041

Results from fitting the Poisson-gamma model

The bycatch per thousand hooks in 1997–98, when bird avoidance gear was not as common, was 0.085 birds, compared with 0.013 birds in 2002–03 when seabird avoidance gear was voluntarily employed. Thus, the bycatch rate for all seabirds was reduced in 2002–03 to 15% of the 1997–98 value.

For the 2002 bycatch data, initial parameter estimates for the gamma distribution were made with the moment estimators described earlier. These initial estimates were refined by using the maximum of the marginal likelihood also described earlier. The final MML estimates were $\hat{\alpha}=0.603$ and $\hat{\beta}=0.030$.

For 2002, the resulting EB bycatch rate estimates per vessel, $\tilde{\lambda}_i$ (Table 2), differed little from conventional ML estimates per vessel. A similar result occurred in the 1997–98 analysis. However, vessel 28 (Table 2), showed a large adjustment between the ML and EB estimates. It is apparent from Table 2 that this vessel had unusually low effort ($\tau_{28}=34$) and a relatively large seabird bycatch ($y_{28}=8$). This adjustment towards the aggregate mean is a predictable EB adjustment for situations where individual stratum data are weak. For vessel 28, the predicted EB estimate of seabird bycatch rate per thousand hooks was 4.4, whereas the actual observed bycatch rate was 8 (Table 2).

When the 2002 seabird bycatch rates were used to predict the 2003 seabird bycatch rates for individual vessels, neither the ML or EB estimates provided a significant correlation ($\rho=0.036$, $n=38$). In contrast, when the 1997 bycatch rates were used to predict the 1998 bycatch rates, there was a significant correlation for the one-tailed test $\rho=0.324$, $n=33$, $P=0.033$.

Discussion and conclusion

Empirical Bayes estimators are superior to Bayes estimators in the sense that prior distributions can be estimated rather than assumed. If one prefers the Bayes

method, one would counter that noninformative priors make the assumption of priors relatively benign, whereas for the empirical Bayes model, the assumption of the family of priors may be quite critical.

The empirical Bayes method can be applied even when the marginal distribution is analytically intractable, by substituting numerical integration for analytical integrals. However, the computational intensity required by using numerical integration can appear daunting even with the current speed of desktop computers (Laslett et al., 2002).

Nevertheless, if the prior family is properly selected, the empirical Bayes method can provide very precise estimates. For our Poisson-gamma simulation, the empirical Bayes method provided uniformly superior estimates of the Poisson λ_i for a wide range of τ_{\max} values. Although the ratio values in Table 1 indicate that the EB estimator is most useful when τ_{\max} is large, the greatest benefit of the EB method is probably on the opposite end of the scale when individual stratum sampling is relatively weak. Note that the bias in $(\hat{\alpha}, \hat{\beta})$ when $\tau_{\max} = 5000$ (Table 1) may be simply bias in marginal maximum likelihood estimates because maximum likelihood estimators are not generally unbiased. Another possibility is that bias was caused by computational error in calculating the marginal likelihood when the τ_i 's were large, even though the marginal likelihood was calculated on the log-scale.

In the seabird bycatch analysis, results show that in almost all cases estimates of bycatch rates at the individual vessel level were not significantly affected by using the EB method. These results may indicate that individual vessel sampling levels (i.e., τ_i) are at a sufficiently high level that ML estimates are already precise estimates of seabird bycatch rates. For the prediction of the 2003 bycatch rate of seabirds from the 2002 analysis, the *TMSE* of the ML estimator of λ_i was reduced a minor amount from 0.0007904 to 0.0007339 by using the EB estimator of λ_i . However, the important issue is that neither the ML nor EB estimates for 2002 significantly correlated with the observed 2003 bycatch

rates of seabirds. From the point of view of the EB method, this lack of correlation indicates that the Poisson catch rate, λ_i , was not a characteristic of individual fishing vessels, but is largely due to chance in any one year. Vessels 28 and 36 did not fish in 2003 and were excluded in the comparison. More detailed studies with current data should be carried out to determine if this is a valid conclusion.

As in 2002, the EB estimates for 1997 did not improve on stratum ML estimates for estimating seabird bycatch rates per vessel. However, ML and EB estimates of individual vessel bycatch rates in 1997 were found to be significantly positively correlated with observed bycatch rates for 1998. In this era of high bycatch rates of seabirds, bycatch rates were found to be more dependent on the practices of individual vessels.

Table 2

Bycatch of seabirds from the 2002 longline groundfish fishery in the eastern Bering Sea, where τ_i refers to the number of hooks observed, y_i is the observed number of birds caught, $\hat{\lambda}_i$ is the maximum likelihood (ML) estimate of the seabird bycatch rate, $\tilde{\lambda}_i$ is the empirical Bayes (EB) estimate of the seabird bycatch rate, and $\tilde{\lambda}_i \tau_i$ is the EB estimate of the expected observed number of birds caught.

Vessel number	Hooks (1000's) τ_i	Birds caught (numbers) y_i	ML vessel estimate $\hat{\lambda}_i$	EB estimate $\tilde{\lambda}_i$	EB estimate of birds caught $\tilde{\lambda}_i \tau_i$
1	1042	11	0.0106	0.0108	11.2
2	3895	22	0.0057	0.0058	22.4
3	917	16	0.0175	0.0175	16.0
4	1487	5	0.0034	0.0037	5.5
5	1272	12	0.0094	0.0097	12.3
6	2446	93	0.0380	0.0378	92.3
7	1477	0	0.0000	0.0004	0.6
8	1016	4	0.0039	0.0044	4.5
9	1758	6	0.0034	0.0037	6.5
10	253	0	0.0000	0.0021	0.5
11	1380	39	0.0283	0.0280	38.7
12	199	0	0.0000	0.0026	0.5
13	233	0	0.0000	0.0023	0.5
14	1212	13	0.0107	0.0109	13.2
15	2304	162	0.0703	0.0696	160.3
16	1408	30	0.0213	0.0212	29.9
17	2292	5	0.0022	0.0024	5.5
18	559	2	0.0036	0.0044	2.5
19	1332	26	0.0195	0.0195	26.0
20	753	17	0.0226	0.0224	16.9
21	2255	37	0.0164	0.0164	37.1
22	699	0	0.0000	0.0008	0.6
23	2907	5	0.0017	0.0019	5.5
24	3308	8	0.0024	0.0026	8.5
25	2221	10	0.0045	0.0047	10.4
26	1797	15	0.0084	0.0085	15.3
27	1413	13	0.0092	0.0094	13.3
28	34	8	0.2334	0.1271	4.4
29	659	101	0.1533	0.1468	96.7
30	1738	16	0.0092	0.0094	16.3
31	1527	4	0.0026	0.0030	4.5
32	2278	49	0.0215	0.0215	48.9
33	1332	19	0.0143	0.0144	19.1
34	2059	17	0.0083	0.0084	17.3
35	3089	2	0.0007	0.0008	2.6
36	1435	7	0.0049	0.0052	7.4
37	625	11	0.0176	0.0176	11.0
38	5447	14	0.0026	0.0027	14.5
39	1598	8	0.0050	0.0053	8.4
40	757	29	0.0383	0.0375	28.4

The empirical Bayes method indicates that sampling levels aboard individual vessels are sufficient to support individual vessel estimates of seabird bycatch rates. This seabird bycatch study was more an observational rather than a controlled study. It was not known which vessels used bird avoidance gear, or how this gear was deployed, or what other relevant onboard practices were taking place. Nevertheless, this seabird bycatch study illustrates how EB methods can provide alternative estimators and evaluation methods for a variety of sampling problems.

Acknowledgments

I thank S. Fitzgerald, J. Breiwick, P. Livingston, and three anonymous reviewers for comments that helped to improve the manuscript.

Literature cited

- Carlin, B. P., and T. A. Louis.
2000. *Bayes and Empirical Bayes Methods for Data Analysis*, 419 p. Chapman and Hall/CRC, New York, NY.
- Casella, G.
1985. An introduction to empirical Bayes data analysis. *Am. Stat.* 39(2):83–87.
- Efron, B., and C. Morris.
1975. Data analysis using Stein's estimator and its generalizations. *J. Am. Stat. Assoc.* 70(350):311–319.
- Laslett, G. M., J. P. Eveson, and T. Polacheck.
2002. A flexible maximum likelihood approach for fitting growth curves to tag-recapture data. *Can. J. Fish. Aquat. Sci.* 59:976–986.
- Patrick, E. A.
1972. *Fundamentals of pattern recognition*, 504 p. Prentice-Hall, Englewood Cliffs, NJ.
- Ver Hoef, J. M.
1996. Parametric empirical Bayes methods for ecological applications. *Ecol. Appl* 6(4):1047–1055.

No evidence of bias from fish behavior in the selectivity of size and sex of the protogynous red porgy (*Pagrus pagrus*, Sparidae) by hook-and-line gear

Douglas A. DeVries

Email address: doug.devries@noaa.gov

National Oceanic and Atmospheric Administration
National Marine Fisheries Service
Southeast Fisheries Science Center
Panama City Laboratory
3500 Delwood Beach Road
Panama City, Florida 32408

Most fisheries select the size of fish to be caught (are size selective), and many factors, including gear, market demands, species distributions, fishery laws, and the behavior of both fishermen and fish, can contribute to that selectivity. Most fishing gear is size-selective and some, such as gill nets, are more so than others. The targeting behavior of fishermen is another key reason commercial and recreational fisheries tend to be size-selective. The more successful fishermen constantly seek areas and methods that yield larger or more profitable sizes of fish. Fishery regulations, especially size limits, produce size-selective harvests. Another factor with the potential to cause selectivity in a hook-and-line fishery is the different behavioral responses of fish to the bait or lure, whether the different responses arise among different fish sizes or between the sexes.

There is reason for concern over the effect of size-selective fishing on protogynous species, i.e., sequential hermaphrodites, which begin life as females and later change sex to males. In one way, size-selective fishing affects gonochoristic (sexes separate) and protogynous species similarly: it not only reduces numbers, but also truncates size distributions. These effects can result in earlier maturation at smaller sizes and hence, at the very least, a reduction in individual fecundity (Jørgensen, 1990). Size-selective fishing can, however, uniquely affect protogynous species in at least two other ways. Because there is essentially a second maturation when sex change occurs, barring some compensatory response, size-selective fishing is sex-selective fishing. As exploitation removes the larger and primarily male members of the population, sperm limitation and decreased fertilization rates can occur. These effects could be caused by a reduction in the number of males or because rapidly skewed sex ratios disrupt the social cues for mating (Bannerot et al., 1987; Huntsman and Schaaf, 1994; Coleman et al., 1996). Naturally low sex ratios can decline precipitously in some heavily fished protogynous species, especially those that form large, temporally and spatially, predictable spawning aggregations (Coleman et al., 1996). The second potential effect of size-selective fishing that is unique to protogynous species is a decrease in population fecundity (Vincent and Sadovy, 1998), which could accompany a compensatory drop in size at sex change, because this drop in size would essentially equate to increased mortality on the largest, most fecund females (Shepard and Idoine, 1993). Such an effect, however, would only occur if at least some females were initially included in the exploited portion of the population.

The documented responses of protogynous species to fishing have varied. Significantly, fewer male daggerhead seabream (*Chrysolephus cristiceps*) and Roman seabream (*C. laticeps*), both sparids, were found in areas open than in areas closed to fishing—a finding attributed to selective removal of larger size classes (Buxton, 1993). In contrast, the average size and age of male leopard coral grouper (*Plectropomus leopardus*), a serranid, were not consistently smaller, nor was the sex ratio consistently more female-biased in areas open to fishing than in closed areas (Adams et al., 2000).

Recent significant declines in the modal sizes and proportions of males of gag (*Mycteroperca microlepis*) and scamp (*M. phenax*)—both serranids and protogynous species—in the Gulf of Mexico (GOM) were likely due to size-selective or sex-selective harvesting, or both, that was affected by fish behavior (Coleman et al., 1996). Among gag, the proportion of males fell from 17% during 1977–80 (Hood and Schlieder, 1992) to 1.3–2.7% during 1991–93 (Coleman et al., 1996) in the GOM, and from 19.6% during 1976–82 to 5.5% in 1995 in catches from U.S. Atlantic waters (McGovern et al., 1998). Coleman et al. (1996) cited Gilmore and Jones (1992) for their conclusions about behavior-related selectivity in scamp and personal observations by Gilmore for similar conclusions regarding gag. Gilmore and Jones (1992) speculated that the bias towards large males that they noted in hook-and-line collections of gag and scamp was related to the more aggressive behavior and greater movement of males, and the higher position of males in the water column. Even though these are the only protogynous species in which behavior-related size or sex selectivity has been documented (and only by observations, not experiments), the shift in size and sex ratio in gag has often been cited as an example of how a species with this kind of mating system responds to exploitation (Vincent and Sadovy, 1998).

The objective of the present study was to determine if there was any

Manuscript submitted 9 June 2006 to the Scientific Editor's office.
Manuscript approved for publication 15 July 2007 by the Scientific Editor.
Fish. Bull. 105:582–587.

evidence that the behavior-related (as opposed to gear- or fishery-related) size or sex selectivity reported for gag and scamp also occurred in fishery-independent hook-and-line catches of the similarly protogynous, co-occurring red porgy (*Pagrus pagrus*) (Sparidae). In other words, at a given location, were males or larger individuals (more likely to be males in a protogynous species) more aggressive and more likely to bite a baited hook and be caught before females or smaller (more likely to be female) individuals? Such selectivity has never been experimentally demonstrated in any protogynous species.

The red porgy is found in warm temperate to subtropical waters on both sides of the N. Atlantic, including the northern GOM and Mediterranean Sea, and in the S.W. Atlantic from Venezuela to Argentina (Manooch and Hassler, 1978). This sparid is one of the most abundant, potentially exploitable reef fishes in the northeastern GOM but is only lightly fished there, entirely by hook-and-line gear. Red porgy are, however, often taken as bycatch by fishermen targeting other reef species. In contrast, the population(s) of red porgy in the Atlantic waters off the southeastern United States declined so steeply during the 1980s and 1990s (89% drop in spawning stock biomass and a two-orders-of-magnitude drop in recruitment to age 1), presumably because of overexploitation, that a one-year moratorium on their harvest and possession was enacted in 1999 (Vaughan and Prager, 2002).

It is important to establish whether behavior-related size or sex selectivity occurs in hook-and-line catches of red porgy. From a sampling (whether fishery-dependent or fishery-independent) and assessment standpoint, such selectivity could lead to very biased conclusions about population demographics and dynamics, life history traits, and stock status. In addition, the potential for this sort of selectivity to rapidly skew sex ratios, especially if it occurs in conjunction with size-selective harvesting caused by the gear and the targeting behavior of fishermen, could partly explain the apparent crash of the Atlantic population(s) of red porgy off the southeastern United States. Also, given the large number of exploited protogynous species among sparids and many other families, and the need to predict the effects of fishing, it is important to determine whether such behavior-related selectivity characterizes most fishes with this mating system or whether it is restricted to certain serranids. If demonstrated to occur in red porgy, this would be the first experimental evidence of selectivity caused by the behavior of a protogynous species other than a serranid.

Materials and methods

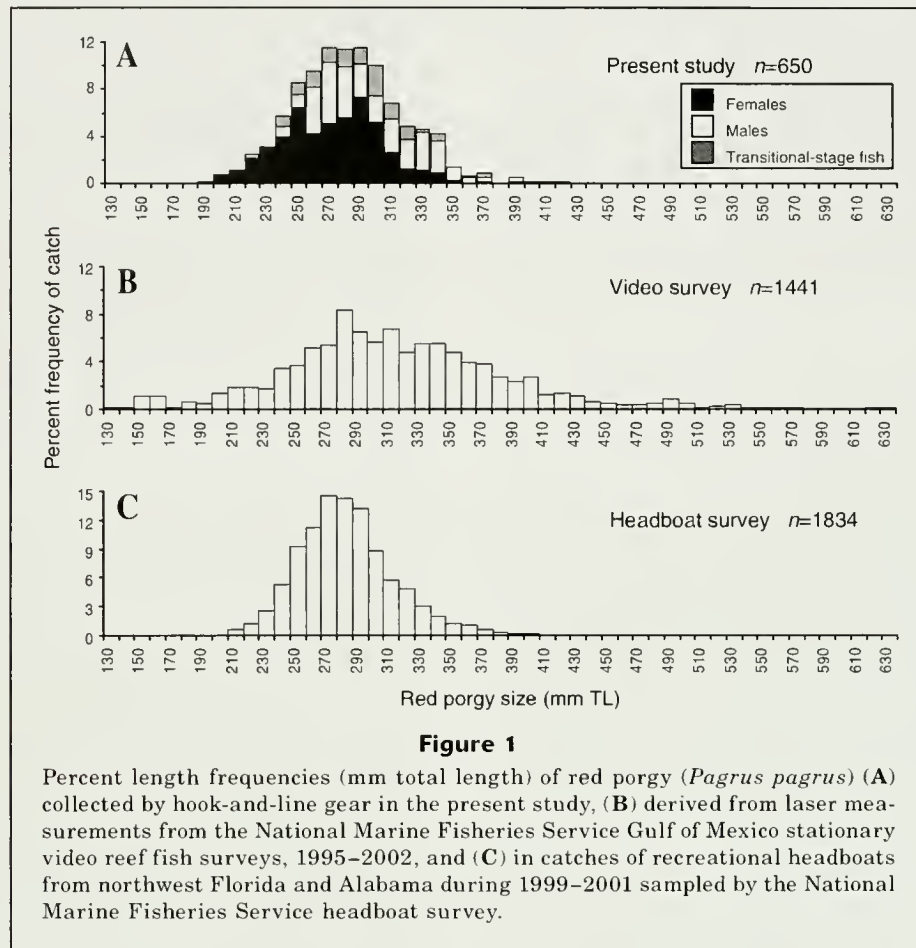
Red porgy were collected with standardized hook-and-line gear during February–November 2000 at seven low-relief (less than 0.5 m) hard (live) bottom sites at 41–67 m depths in the northeastern GOM, off Panama City, FL. The sites were a subset, and the deepest, of

nine sites that had been regularly sampled for a larger study of small-scale spatial variation in population traits of red porgy (Fig. 3.1 in DeVries, 2006). Site selection was driven primarily by logistic constraints. Locations with the most consistently high catch rates were chosen to maximize the amount of information collected and to enable among-collection comparisons. Gear consisted of one or two size-1 Mustad j-style hooks (O. Mustad and Son (USA) Inc., Auburn, NY) attached to 5–10 cm droppers on a 27 kg test monofilament leader with a terminal lead sinker of varying (depending on current and wind conditions) weight. Bait consisted of squid and occasionally cut fish. All fishing was undertaken by two to four anglers (with varying levels of experience) during daytime hours and from an anchored boat.

Target sample size each time a site was fished was 25–30 red porgy, although for logistic reasons (primarily variable catch rates) that goal was not always met. For each collection, each fish was tagged with a unique sequential identification number indicating the order in which it was captured, and then placed on ice. The next day fish were measured to the nearest mm total length (TL) and sex was determined macroscopically, after which histological samples were taken from the gonads of any fish identified as female or transitional (DeVries, 2006). Final determination of sex was based on histological findings.

Nonparametric runs tests “above and below the median” and “up and down” (Sokal and Rohlf, 1981a; Zar, 1999) were used to look for evidence of behavior-related size selectivity in individual collections. Critical values for determining acceptance or rejection of the hypothesis that the order was random were obtained from statistical tables (Sokal and Rohlf, 1981b; Zar, 1999). Total length was the variable used in both tests. In general, runs tests are used to determine whether the order of a sequence of observations is random or whether each observation is independent of its predecessor. A run is defined as a sequence of one or more like elements preceded and followed by unlike elements (Sokal and Rohlf, 1981a). In the “above and below the median” test, observations above the median are labeled pluses and those below as minuses. The order of those pluses and minuses is then tested for randomness. If fish caught at the beginning of the collection tended to be larger, as would occur if larger individuals (more likely to be males) were more aggressive and tended to bite the hook before smaller ones (more likely females), there would be fewer runs than expected. The “up and down” test, particularly designed for trend data, examines the sequence of the signs of the difference from the previous value (Sokal and Rohlf, 1981a). Again, if larger fish tended to be caught before the smaller ones, the signs would be mostly negative and therefore there would be fewer changes in sign than if the sequence of lengths was random.

A runs test for dichotomized data (Sokal and Rohlf, 1981a; Zar, 1999) was used to determine if the order in which sexes were captured in a given collection was random. Because it was not known if transitional-stage



fish behave more like males or females, this test was run two ways: one in which transitional-stage fish were considered males and another in which they were considered females. Transitional gag and scamp may be as susceptible to behavior-related sex selectivity as fully transformed males if they adopt male behaviors before completing sex change (Coleman et al., 1996). The lyretail anthias (*Pseudanthias squamipinnis*) exhibits such a shift to male behavior before any visible morphological changes (Shapiro, 1979).

Results

A total of 27 collections of red porgy were made, both during and outside the spawning season, which runs November–March but peaks December–February (DeVries, 2006). Sample sizes were >20 in 21 of 27 instances (range: 10–31). Mean sizes and 95% confidence intervals (CI) of males, females, and transitional-stage fish were 296 ± 4 mm, 270 ± 3 mm, and 291 ± 7 mm TL, respectively. The overall size distribution is shown in Figure 1. Mean proportion and 95% CI of males in 19 collections from five of the seven sites was 0.39 ± 0.07 , assuming transitional-stage fish were males, and 0.24 ± 0.05 ,

assuming transitional-stage fish were females. The two remaining sites were persistently and significantly more male-biased than the other sites (DeVries, 2006). Mean proportions of males at the eight collections from the two remaining sites were 0.66 ± 0.10 (transitional fish as males) and 0.53 ± 0.08 (transitional fish as females). For further details on the temporal and spatial distribution of the collections, see DeVries (2006).

The order in which red porgy were caught in each of 27 collections was random with respect to both size and sex, i.e., there was no evidence that larger fish or males were more likely to be caught before smaller individuals or females (Fig. 2). In both the “above and below the median” and “up and down” runs tests, the hypothesis that the sequence of lengths was random could not be rejected at $\alpha=0.05$ for any of the collections (Table 1.1 in DeVries, 2006). Whether transitional-stage fish were considered males or females, the hypothesis that the order in which sexes were caught was random could not be rejected at $\alpha=0.05$ for all but four of the collections (Table 1.2 in DeVries, 2006). In each of those four collections only one male was caught. The statistical table used for determining critical values (Table 28; Sokal and Rohlf, 1981b) required a minimum sample size of two for both of the dichotomous variables used (number

of males and number of females); therefore these four collections could not be tested.

Discussion

The absence of any evidence of behavior-related size or sex selectivity indicates that hook-and-line sampling can provide reasonably unbiased information on the population biology and stock status of red porgy. As hook size approaches the extremes, vulnerability will decrease and bias will increase, and therefore choice of hook size is critical. There is evidence in some reef fishes that, across at least a moderate range of hook sizes, selectivity can be relatively constant (Ralston, 1982; Dalzell, 1996). Size-1 Mustad j-style hooks were chosen for this study on the basis of considerable experience of the author in catching many species of reef fishes in the study area—experience that indicated that such hooks would readily catch all sizes of red porgy typically observed in both recreational and commercial catches in the GOM. During the study, red grouper (*Epinephelus morio*) that were much larger than the largest red porgy collected and that had considerably larger gapes were caught on the same hooks, as were many tomtates (*Haemulon aurolineatum*) which were similar in size and had similar gapes as the smallest red porgies caught.

A critical assumption of this study was that all sizes of red porgy present at a location when a given sample was collected were equally vulnerable to the gear. If, because of gear selectivity, smaller individuals were considerably less vulnerable than larger ones, and significant numbers of small fish were present at a site being sampled, then it would be possible for behavior-related selectivity for larger fish to occur undetected, or at least its magnitude would be underestimated.

Several lines of evidence indicate that the aforementioned scenario is very unlikely. Size data from the eastern GOM, collected during recent annual National Marine Fisheries Service (NMFS) reef fish surveys with the use of stationary video cameras equipped with laser measuring devices, showed no evidence of noticeably greater proportions of small fish than those seen in the hook-and-line samples of the present study (Fig. 1). Although the size distributions were statistically different (Kolmogorov-Smirnov 2-sample test, $P < 0.001$)—not surprising given the very large sample sizes—the primary difference appeared to be that the distribution of red porgy sizes shown in the video data, which should have had little or at least much less bias, was shifted towards larger, not smaller fish. Although a few (3.6%) individuals in the video data were smaller than the smallest (193 mm TL) in the hook-and-line samples, it is important to note that the proportion of large fish (>360 mm) was almost 10-fold greater than in the hook-and-line samples, i.e., 21.6% versus 2.5%. Thus, if anything, the size distribution in the

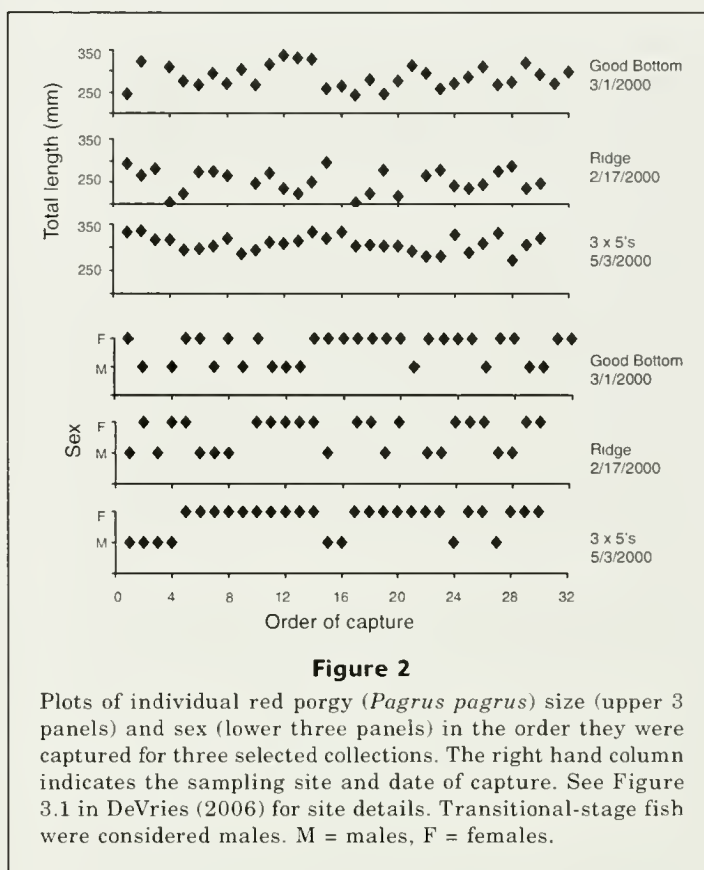


Figure 2

Plots of individual red porgy (*Pagrus pagrus*) size (upper 3 panels) and sex (lower three panels) in the order they were captured for three selected collections. The right hand column indicates the sampling site and date of capture. See Figure 3.1 in DeVries (2006) for site details. Transitional-stage fish were considered males. M = males, F = females.

hook-and-line data is biased downwards, not upwards. The higher proportion of larger fish in the video data probably reflects spatial and bathymetric differences in the sampling more than different gear selectivities. The video survey focused on the hard bottom, high-relief habitat along the 73-m (40-fathom) isobath and inshore of that isobath in the Florida Middle Grounds. In contrast, all fish in the present study were caught between 41 and 67 m and on low-relief habitat. Larger red porgy have been found in deeper water and in the Florida Middle Grounds (Harris and McGovern, 1997; Hood and Johnson, 2000).

Red porgy size-structure data from the NMFS recreational headboat survey collected during 1999–2001 in northwest Florida and Alabama almost mirrored the data from this study (Fig. 1). The headboats regularly catch red snapper (*Lutjanus campechanus*) as large as or larger than the largest red porgy taken in this study, and their fishing grounds completely overlap the area, depths, and habitats sampled in the present study. If significant numbers of red porgy larger than those collected in the present study inhabited the area sampled in this study, it seems very unlikely they would not show up in the NMFS survey samples of headboat catches from the same region. Larger red porgy are in fact caught regularly by headboats fishing the Florida Middle Grounds off the central west coast of Florida (Hood and Johnson, 2000).

On many occasions over several years while scuba diving on hard-bottom habitat in the study area in depths from 25 to 30 m, I have observed red porgy of the size that dominated the distribution of those collected in the present study, but virtually none of the size in the left-hand tail (smaller fish) of the distribution from the NMFS video survey (Fig. 1). Similarly, individuals smaller than that typically seen in hook-and-line samples have rarely, if ever, been observed by personnel from the Panama City NMFS Laboratory, either from ROVs or stationary camera arrays at many sites in the N.E. Gulf of Mexico.

Lastly, juvenile red porgy have been found primarily on sandy bottom and typically in shallower waters than those inhabited by adults (Manooch and Hassler, 1978; Labropoulou et al., 1999). These findings, together with the scuba and video observations, support the validity of the assumption that the range of sizes of red porgy in a given collection in this study were the same or at least very similar to those actually present at the site at the time the sample was taken.

If the size structure of the hook-and-line samples in this study accurately reflect the true size distribution at the site at the time of the collection, then the sex ratios of those samples should also accurately reflect true values, and hence the finding of no evidence of sex selectivity is also valid. The absence of behavior-related size or sex selectivity in hook-and-line samples means that any evidence of truncation in size structure or skewing of sex ratios in exploited red porgy populations should not be attributed to greater aggression or "hook attraction" in males. Instead, such size truncation or skewing of sex ratios can be easily explained as the result of simple size-selective harvesting caused by the targeting behavior of fishermen, not by the behavior of the fish, and is a common phenomenon not unique to protogynous fishes.

Although there is historic evidence of such size-selective harvesting in red porgy fisheries off the southeastern United States, there is none indicating that behavior-related selectivity contributed to the crash of those fisheries in the 1980s. From the late 1970s through the mid 1990s, annual mean weights of red porgy in the southeastern United States were roughly 20–30% less in the recreational headboat fishery than in the commercial hook-and-line fishery (Fig. 2 in Vaughan and Prager, 2002). Such size-selective harvesting (taking larger individuals more likely to be male) may have skewed sex ratios temporarily, but there was no evidence of a long-term effect, i.e., an increasingly female-biased sex ratio. Males composed 15.8%, 13.3%, and 20.4% of red porgy taken in a fishery-independent survey in U.S. Atlantic waters during 1979–81, 1988–90, and 1991–94, respectively (Harris and McGovern, 1997). The increasingly female-biased sex ratios observed in gag catches in the 1980s and 1990s have been attributed to behavior-related selectivity (Coleman et al., 1996; McGovern et al., 1998). An increasing trend in the proportion of males in smaller size classes off the southeastern United States indicates that red porgy

compensated for the effects of fishery-driven selectivity for size by changing sex at smaller sizes (Harris and McGovern, 1997).

The targeting behavior of fishermen has produced selectivity in red porgy fisheries in the GOM, as well. Mean lengths of recreationally and commercially caught red porgy from the Florida Middle Grounds and off west central Florida have differed significantly (321 vs. 350 mm TL) (Hood and Johnson, 2000), in a manner similar to the pattern in weight differences in the Atlantic fisheries noted by Vaughan and Prager (2002). It is unlikely these length differences are related to fish behavior. More likely they reflect gear selectivity as well as spatial differences in areas fished. DeVries (2006) found persistent, significant, small-scale (<10 km) spatial differences in size structure and many other demographics and life history traits of red porgy in the N.E. GOM—differences that indicate that the species has a complex subpopulation or metapopulation structure. Further analysis of data from Hood and Johnson's (2000) study indicated that sex ratios also differed between the two fisheries: males composed 40.5% of the recreational and 49% of the commercial samples, although the sex of 78 of the 274 fish collected from the latter samples was not determined and these 78 fish were not included in the calculations. These differences in sex ratios likely reflect, and are consistent with, the differences in size structure. Additionally, as in the Atlantic, there was no evidence that sex ratios have become increasingly female biased. In 1978 and 1979 males composed 30% and 38%, respectively, of red porgy sampled from charter boat and headboat catches in northwest Florida (Salomon and Fable, 1981). Two decades later Hood and Johnson (2000) found that males composed 40.5% of recreational and 49% of the commercial samples, and in the present study the percentage of males averaged 39% from five of the sites and 66% at the remaining two sites.

Size or sex selectivity resulting from fish behavior does not appear to characterize the hook-and-line fisheries of all exploited protogynous species. Besides the apparent absence, in the case of red porgy, of selection for males with the use of hook-and-line gear, there is also no indication of such selection in the hook-and-line fishery for the red hind (*Epinephelus guttatus*), a seranid (Shapiro et al., 1993; Coleman et al., 1996). It may be that rapid skewing of sex ratios in protogynous fishes caused by behavior-related size or sex selectivity is the exception rather than the rule. The evidence that aggressive behavior in large, primarily male scamp and gag can lead to sex selection in their fisheries and rapidly skew sex ratios (Gilmore and Jones, 1992; Coleman et al., 1996) is primarily circumstantial or observational and there have been no controls or statistical tests. Although the case for behaviorally caused sex selectivity in gag is fairly convincing, more statistically rigorous and direct testing of the hypothesis would strengthen these conclusions. Until more studies, like the present one, are conducted on other species, the prevalence of

this phenomenon and whether it is unique to serranids will remain unknown.

Acknowledgments

Thanks to C. Palmer and B. Walling for invaluable help in the field and lab. J. Brusher, J. Mikulas, C. Mangum, D. Harris, and many other coworkers, interns, and volunteers also helped collect and process samples. C. Gledhill provided size data from the National Marine Fisheries Service (NMFS) reef fish video survey. R. Dixon provided data from the NMFS headboat survey. P. Hood provided raw data from his Marine Fisheries Initiative study on red porgy. J. Travis, C. Grimes, C. Koenig, and D. Levitan provided helpful review and comments.

Literature cited

- Adams, S., B. D. Mapstone, G. R. Russ, and C. R. Davies.
2000. Geographic variation in the sex ratio, sex specific size, and age structure of *Plectropomus leopardus* (Serranidae) between reefs open and closed to fishing on the Great Barrier Reef. *Can. J. Fish. Aquat. Sci.* 57:1448–1458.
- Bannerot, S. W., W. Fox Jr., and J. E. Powers.
1987. Reproductive strategies and the management of snappers and groupers in the Gulf of Mexico and Caribbean. In *Tropical snappers and groupers: biology and fisheries management* (J. J. Polovina, and S. Ralston, eds.), p. 561–603. Westview Press, Boulder, CO.
- Buxton, C. D.
1993. Life-history changes in exploited reef fishes on the east coast of South Africa. *Environ. Biol. Fish.* 36:47–63.
- Coleman, F. C., C. C. Koenig, and L. A. Collins.
1996. Reproductive styles of shallow-water groupers (Pisces: Serranidae) in the eastern Gulf of Mexico and the consequences of fishing spawning aggregations. *Environ. Biol. Fish.* 47:129–141.
- Dalzell, P.
1996. Catch rates, selectivity and yields of reef fishing. In *Reef fisheries* (N. V. C. Polunin, and C. M. Roberts, eds.), p. 161–192. Chapman and Hall, London.
- DeVries, D. A.
2006. The life history, reproductive ecology, and demography of the red porgy, *Pagrus pagrus*, in the northeastern Gulf of Mexico. Ph.D. diss, 160 p. Florida State Univ., Tallahassee, FL.
- Gilmore, R. G., and R. J. Jones.
1992. Color variation and associated behavior in the epinepheline groupers, *Mycteroperca microlepis* (Goode and Bean) and *M. phenax* Jordan and Swain. *Bull. Mar. Sci.* 51:83–103.
- Harris, P. J., and J. C. McGovern.
1997. Changes in the life history of red porgy, *Pagrus pagrus*, from the southeastern United States, 1972–1994. *Fish. Bull.* 95:732–747.
- Hood, P. B., and A. K. Johnson.
2000. Age, growth, mortality, and reproduction of red porgy, *Pagrus pagrus*, from the eastern Gulf of Mexico. *Fish. Bull.* 98:723–735.
- Hood, P. B., and R. A. Schlieder.
1992. Age, growth, and reproduction of gag *Mycteroperca microlepis*, (Pisces: Serranidae), in the eastern Gulf of Mexico. *Bull. Mar. Sci.* 51:337–352.
- Huntsman, G. R., and W. E. Schaaf.
1994. Simulation of the impact of fishing on reproduction of a protogynous grouper, the graysby. *N. Am. J. Fish. Manage.* 14:41–52.
- Jørgensen, T.
1990. Long-term changes in age at sexual maturity of Northeast Arctic cod (*Gadus morhua* L.). *J. Cons. Int. Explor. Mer* 46(3):235–248.
- Labropoulou, M., A. Machias, and N. Tsimenides.
1999. Habitat selection and diet of juvenile red porgy, *Pagrus pagrus* (Linnaeus, 1758). *Fish. Bull.* 97:495–507.
- Manooch, C. S., and W. W. Hassler.
1978. Synopsis of biological data on the red porgy, *Pagrus pagrus* (Linnaeus). NOAA Tech. Rep. NMFS Circ. 412, 19 p.
- McGovern, J. C., D. M. Wyanski, O. Pashuk, C. S. Manooch II, and G. R. Sedberry.
1998. Changes in the sex ratio and size at maturity of gag, *Mycteroperca microlepis*, from the Atlantic coast of the southeastern United States during 1976–1995. *Fish. Bull.* 96:797–807.
- Ralston, S.
1982. Influence of hook size in the Hawaiian deep-sea handline fishery. *Can. J. Fish. Aquat. Sci.* 39:1297–1302.
- Saloman, C. H., and W. A. Fable Jr.
1981. Length-frequency distributions of recreationally caught reef fishes from Panama City, Florida in 1978 and 1979. NOAA Tech. Memo. NMFS-SEFC-61, 22 p.
- Shapiro, D. Y.
1979. Social behavior, group structure, and the control of sex reversal in hermaphroditic fish. *Adv. Study Behav.* 10:43–102.
- Shapiro, D. Y., Y. Sadovy, and M. A. McGehee.
1993. Size, composition, and spatial structure of the annual spawning aggregation of the red hind, *Epinephelus guttatus*, (Pisces: Serranidae). *Copeia* 1993:399–406.
- Shepard, G. R., and J. S. Idoine.
1993. Length-based analyses of yield and spawning biomass per recruit for black sea bass, *Centropristis striata*, a protogynous hermaphrodite. *Fish. Bull.* 91:328–337.
- Sokal, R. R., and F. J. Rohlf.
1981a. *Biometry*, 2nd ed., 776 p. W. H. Freeman and Company, New York, NY.
1981b. *Statistical tables*, 2nd ed., 219 p. W. H. Freeman and Company, New York, NY.
- Vaughan, D. S., and M. H. Prager.
2002. Severe decline in abundance of the red porgy (*Pagrus pagrus*) population off the southeastern United States. *Fish. Bull.* 100:351–375.
- Vincent, A., and Y. Sadovy.
1998. Reproductive ecology in the conservation and management of fishes. In *Behavioral ecology and conservation biology* (T. Caro, ed.), p. 209–245. Oxford Univ. Press, New York, NY.
- Zar, J. H.
1999. *Biostatistical analysis*, 4th ed., 663 p. Prentice Hall, Upper Saddle River, NJ.

Acknowledgment of reviewers

The editorial staff of Fishery Bulletin would like to acknowledge the scientists who reviewed articles published in 2006–2007. Their contributions have helped ensure the publication of quality science.

-
- | | | |
|-----------------------------|-------------------------------|---------------------------|
| Dr. M. Shiham Adam | Dr. Daniel J. Gaughan | Dr. Takayuki Matsumoto |
| Dr. Robyn P. Angliss | Dr. Stephen R. Goldberg | Dr. Tim McClanahan |
| Dr. Alexander I. Arkhipkin | Dr. Churchill B. Grimes | Dr. Duncan E. McGehee |
| Dr. Michael P. Armstrong | | Dr. Richard D. Methot |
| Dr. Peter J. Auster | Dr. Steven L. Haeseker | Dr. David A. Milton |
| | Dr. Dana Haggarty | Dr. Sally A. Mizroch |
| Ms. Julia K. Baum | Dr. Richard G. Hartnoll | Dr. William Montevecchi |
| Dr. Richard J. Beamish | Dr. Euan Sinclair Harvey | Dr. Beatriz Morales-Nin |
| Dr. David A. Bengston | Dr. James T. Harvey | Dr. Cheryl Morgan |
| Dr. Paul Bentzen | Dr. Dan Hennen | Dr. Franz-Josef Mueter |
| Dr. Steve A. Berkeley | Dr. Alexander Hesp | Ms. Kristen Munk |
| Dr. Jim Berkson | Dr. John Hess | Dr. John A. Musick |
| Dr. Barbara Block | Dr. Joseph E. Hightower | |
| Dr. James A. Bohnsack | Dr. Nicola Hillgruber | Dr. John D. Neilson |
| Dr. John Boreman | Dr. Michael H. Hoff | Dr. David L. Nieland |
| Dr. Brian W. Bowen | Dr. Kim N. Holland | Dr. Paul Nitschke |
| Dr. Richard W. Brill | Dr. Simon Hoyle | |
| Mr. Michael Burton | Dr. Michelle Huepel | Mr. Ranier Oeberst |
| | Dr. John R. Hunter | Dr. Jeff Olsen |
| | | |
| Dr. John Calambokidis | Dr. Kym Jacobson | Dr. Debra Palka |
| Dr. John Caprio | Ms. Pamela C. Jensen | Dr. Steve Parker |
| Dr. James Carretta | Dr. Donna L. Johnson | Dr. Frank A. Parrish |
| Dr. Jennifer Caselle | Dr. Francis Juanes | Dr. George R. Parsons |
| Dr. Michael Castellini | | Mr. Grey Pendleton |
| Dr. R. Christopher Chambers | Dr. Constantina Karlou-Riga | Dr. Michael Pennington |
| Dr. Edward J. Chesney, Jr. | Dr. Arthur W. Kendall | Dr. Theodore W. Pietsch |
| Dr. Bruce B. Collette | Dr. William Kiene | Dr. Graham Pilling |
| Mr. L. Alan Collins | Dr. Michael C. S. Kingsley | Dr. Kenneth H. Pollock |
| | Dr. Olav S. Kjesbu | Ms. Jennifer C. Potts |
| Dr. Gary E. Davis | Ms. Chris Kondzela | |
| Ms. Michelle L. Davis | | Dr. Terrance J. Quinn II |
| Dr. Joseph T. DeAlteris | Dr. Han-Lin Lai | |
| Dr. Edward E. DeMartini | Dr. Craig Landry | Dr. Carol Reeb |
| Dr. Douglas DeMaster | Dr. Ralph J. Larson | Dr. Vincent Ridoux |
| Dr. Charles Derby | Dr. Robert J. Latour | Dr. Christopher N. Rooper |
| Mr. Edward J. Dick | Dr. Mark A. Lazzari | Dr. Garry R. Russ |
| Dr. Marlis Douglas | Dr. Cheng-Shen Lee | |
| Dr. Miriam J. Doyle | Dr. James B. Lindholm | Dr. Marlowe Sabater |
| Dr. Edward G. Durbin | Dr. Jason S. Link | Dr. Fran Saborido-Rey |
| | Dr. Phillip S. Lobel | Dr. Yvonne Sadovy |
| Dr. Scott Eckert | Dr. Thomas Loughlin | Dr. Keith M. Sakuma |
| Dr. Lisa Eisner | Dr. Susan K. Lowerre-Barbieri | Dr. Robert Schroeder |
| Dr. Karim Erzini | Mr. Chris Lunsford | Ms. Rebecca Schroepfer |
| | Dr. Joanne Lyczkowski-Shultz | Dr. Carl James Schwarz |
| Dr. John Field | | Dr. David H. Secor |
| Dr. Alan M. Friedlander | Dr. Gavin Macaulay | Mr. Jun Shoji |
| Dr. Jean-Marc Fromentin | Ms. Beverly J. Macewicz | Dr. Michael F. Sigler |
| Dr. Kathryn J. Frost | Dr. Ken MacKenzie | Dr. Michael A. Simpkins |
| | Dr. Jeffrey B. Marliave | Dr. Elizabeth H. Sinclair |
| Dr. Daniel Gaertner | Dr. Takashi Matsuishi | Mr. Joseph W. Smith |
| Dr. Lance P. Garrison | | |

Dr. Paul Spencer
Dr. Alan M. Springer
Dr. Kostas I. Stergiou
Dr. Colette St. Mary
Dr. Jan Straley
Dr. Chi-Lu Sun

Dr. David Tallmon
Dr. Clyde Tamaru
Dr. Len Thomas
Dr. Bruce A. Thompson
Dr. Juan Timi

Dr. James Tolan
Dr. Michael Tringali
Dr. Juan Guillermo Vaca-Rodriguez
Dr. Douglas S. Vaughan
Dr. Laurent Vigliola

Dr. Susan L. Waddy
Dr. John R. Waldman
Dr. Robert (Trey) Walker
Dr. Eric Ward
Dr. Robert D. Ward

Dr. Joseph D. Warren
Dr. John C. Whitehead
Dr. Terrie M. Williams
Dr. Peter R. Witthames
Dr. Mark Wuenschel

Dr. Yongshun Xiao

Dr. Orio Yamamura
Dr. Richard E. Young

Ms. Tonya K. Zeppelin

Fishery Bulletin Index

Volume 105(1–4), 2007

List of titles

105(1)

- 1 Temporal variation in growth of yellowfin tuna (*Thunnus albacares*) larvae in the Panama Bight, 1990-97, by Jeanne B. Wexler, Seinen Chow, Toshie Wakabayashi, Kenji Nohara, and Daniel Margulies
- 19 Annual fecundity, batch fecundity, and oocyte atresia of Atka mackerel (*Pleurogrammus monopterygius*) in Alaskan waters, by Susanne F. McDermott, Katherine P. Maslenikov, and Donald R. Gunderson
- 30 Modification of the biological intercept model to account for ontogenetic effects in laboratory-reared delta smelt (*Hypomesus transpacificus*), by James A. Hobbs, William A. Bennett, Jessica E. Burton, and Bradd Baskerville-Bridges
- 39 Relationship between abundance of juvenile rockfishes (*Sebastes* spp.) and environmental variables documented off northern California and potential mechanisms for the covariation, by Thomas E. Laidig, James R. Chess, and Daniel F. Howard
- 49 The potential use of time-area closures to reduce catches of bigeye tuna (*Thunnus obesus*) in the purse-seine fishery of the eastern Pacific Ocean, by Shelton J. Harley and Jenny M. Suter
- 62 Oceanic migration rates of Upper Chesapeake Bay striped bass (*Morone saxatilis*), determined by otolith microchemical analysis, by David H. Secor and Philip M. Piccoli
- 74 Ecotypic variation and predatory behavior among killer whales (*Orcinus orca*) off the eastern Aleutian Islands, Alaska, by Craig O. Matkin, Lance G. Barrett-Lennard, Harald Yurk, David Ellifrit, and Andrew W. Trites
- 88 Removing observational noise from fisheries-independent time series data using ARIMA models, by William T. Stockhausen and Michael Fogarty
- 102 Abundance and distribution of the eastern North Pacific Steller sea lion (*Eumetopias jubatus*) population, by Kenneth W. Pitcher, Peter F. Olesiuk, Robin F. Brown, Mark S. Lowry, Steven J. Jeffries, John L. Sease, Wayne L. Perryman, Charles E. Stinchcomb, and Lloyd F. Lowry
- 116 Precision estimates and suggested sample sizes for length-frequency data, by Hans D. Gerritsen and David McGrath
- 121 Early marine growth in relation to marine-stage survival rates for Alaska sockeye salmon (*Oncorhynchus nerka*), by Edward V. Farley Jr., James M. Murphy, Milo D. Adkison, Lisa B. Eisner, John H. Helle, Jamal H. Moss, and Jennifer Nielsen
- 131 Degeneration of postovulatory follicles in the Iberian sardine *Sardina pilchardus*: structural changes and factors affecting resorption, by Konstantinos Ganiyas, Cristina Nunes, and Yorgos Stratoudakis
- 140 Use of genetic data to assess the uncertainty in stock assessments due to the assumed stock structure: the case of albacore (*Thunnus alalunga*) from the Atlantic Ocean, by Haritz Arrizabalaga, Victoria López-Rodas, Eduardo Costas, and Alberto González-Garcés
- 147 New information from fish diets on the importance of glassy flying squid (*Hyaloteuthis pelagica*) (Teuthoidea: Ommastrephidae) in the epipelagic cephalopod community of the tropical Atlantic Ocean, by Yves Cherel, Richard Sabatié, Michel Potier, Francis Marsac, and Frédéric Ménard
- 153 Measurements of total scattering spectra from bocaccio (*Sebastes paucispinis*), by Stéphane G. Conti, Benjamin D. Maurer, Mark A. Drawbridge, and David A. Demer

105(2)

- 161 Sensitivity of angler benefit estimates from a model of recreational demand to the definition of the substitute sites considered by the angler, by Brad Gentner
- 168 Multiscale habitat associations of deepwater demersal fishes off central California, by Tara J. Anderson and Mary M. Yoklavich
- 180 Use of endoparasitic helminths as tags in delineating stocks of American plaice (*Hippoglossoides platessoides*) from the southern Gulf of St. Lawrence and Cape Breton Shelf, by Gary McClelland and Jason Melendy
- 189 Implications of substrate complexity and kelp diversity for south-central Alaskan nearshore fish communities, by Judy Hamilton and Brenda Konar
- 197 Genetic variability in spotted seatrout (*Cynoscion nebulosus*), determined with microsatellite DNA markers, by Rocky Ward, Kevin Bowers, Rebecca Hensley, Brandon Mobley, and Ed Belouski

- 207** Review of the crevalle jacks, *Caranx hippos* complex (Teleostei: Carangidae), with a description of a new species from West Africa, by William F. Smith-Vaniz and Kent E. Carpenter
- 234** Diets of Steller sea lions (*Eumetopias jubatus*) in Southeast Alaska, 1993–1999, by Andrew W. Trites, Donald G. Calkins, and Arliss J. Winship
- 249** Spawning and early development of captive yellowfin tuna (*Thunnus albacares*), by Daniel Margulies, Jenny M. Suter, Sharon L. Hunt, Robert J. Olson, Vernon P. Scholey, Jeanne B. Wexler, and Akio Nakazawa
- 266** Re-estimation of small-scale fishery catches for U.S. flag-associated island areas in the western Pacific: the last 50 years, by Dirk Zeller, Shawn Booth, Gerald Davis, and Daniel Pauly
- 278** Whole-gear efficiency of a benthic survey trawl for flatfish, by David A. Somerton, Peter T. Munro, and Kenneth L. Weinberg
- 292** Yellow (*Perca flavescens*) and Eurasian (*P. fluviatilis*) perch distinguished in fried fish samples by DNA analysis, by Rex M. Strange and Carol A. Stepien
- 296** Natural mortality rate, annual fecundity, and maturity at length for Greenland halibut (*Reinhardtius hippoglossoides*) from the northeastern Pacific Ocean, by Daniel W. Cooper, Katherine P. Maslenikov, and Donald R. Gunderson
- 305** Validation of back-calculation equations for juvenile bluefish (*Pomatomus saltatrix*) with the use of tetracycline-marked otoliths, by Marja E. Roemer and Kenneth Oliveira
- 105(3)**
- 313** Diel variation in vertical distribution of an offshore ichthyoplankton community off the Oregon coast, by Toby D. Auth, Richard D. Brodeur, and Kathleen M. Fisher
- 327** Validation of a method for estimating realized annual fecundity in a multiple spawner, the long-snouted seahorse (*Hippocampus guttulatus*), using underwater visual census, by Janelle M. R. Curtis
- 337** Abundance, distribution, and habitat of leatherback turtles (*Dermochelys coriacea*) off California, 1990–2003, by Scott R. Benson, Karin A. Forney, James T. Harvey, James V. Carretta, and Peter H. Dutton
- 348** Comparison of survey methods for estimating abundance of harbor seals (*Phoca vitulina*) in glacial fjords, by John L. Bengtson, Alana V. Phillips, Elizabeth A. Mathews, and Michael A. Simpkins
- 356** Age and growth of swordfish (*Xiphias gladius*) caught by the Hawaii-based pelagic longline fishery, by Edward E. DeMartini, James H. Uchiyama, Robert L. Humphreys Jr., Jeffrey D. Sampaga, and Happy A. Williams
- 368** Systematics of the North American menhadens: molecular evolutionary reconstructions in the genus *Brevoortia* (Clupeiformes: Clupeidae), by Joel D. Anderson
- 379** Vertical movement patterns of skipjack tuna (*Katsuwonus pelamis*) in the eastern equatorial Pacific Ocean, as revealed with archival tags, by Kurt M. Schaefer and Daniel W. Fuller
- 390** Decline in condition of northern bluefin tuna (*Thunnus thynnus*) in the Gulf of Maine, by Walter J. Golet, Andrew B. Cooper, Robert Campbell, and Molly Lutcavage
- 396** Geographic and seasonal variations in maturation and growth of female Pacific cod (*Gadus macrocephalus*) in the Gulf of Alaska and Bering Sea, by James W. Stark
- 408** Interactions between marine mammals and pelagic longline fishing gear in the U.S. Atlantic Ocean between 1992 and 2004, by Lance P. Garrison
- 418** Changes in egg production of the western rock lobster (*Panulirus cygnus*) associated with appendage damage, by Roy Melville-Smith and Simon de Lestang
- 426** Diversity of estuarine movements of striped bass (*Morone saxatilis*): a synoptic examination of an estuarine system in southern New Jersey, by Kenneth W. Able and Thomas M. Grothues
- 436** Microsatellite multiplex panels for genetic studies of gray snapper (*Lutjanus griseus*) and lane snapper (*Lutjanus synagris*), by Mark A. Renshaw, Eric Saillant, Siya Lem, Philip Berry, and John R. Gold
- 440** Effect of towing speed on retention of zooplankton in bongo nets, by Joseph Kane and Jacquelyn L. Anderson
- 105(4)**
- 447** An allometric smoothing function to describe the relation between otolith and somatic growth over the lifespan of walleye pollock (*Theragra chalcogramma*), by Seiji Katakura, Hisatoshi Ikeda, Akira Nishimura, Tsuneo Nishiyama, and Yasunori Sakurai

- 457 Transitions in the morphological features, habitat use, and diet of young-of-the-year goosefish (*Lophius americanus*), by Kenneth W. Able, Peter J. Clarke, R. Christopher Chambers, and David A. Witting
- 470 Defining plausible migration rates based on historical tagging data: a Bayesian mark-recapture model applied to English sole (*Parophrys vetulus*), by Ian J. Stewart
- 485 Activity in the pallial nerve of knobbed (*Busycon carica*) and channeled (*Busycotypus canaliculatum*) whelks recorded during exposure of the osphradium to odorant solutions, by Christopher Magel, Kirstin Wakefield, Nancy Targett, and Richard Brill
- 509 Abundance and population density of cetaceans in the California Current ecosystem, by Jay Barlow, and Karin A. Forney
- 527 Spillover of commercially valuable reef fishes from marine protected areas in Guam, Micronesia, by Mark H. Tupper
- 538 Species-specific effects of four preservative treatments on oocytes and ovarian material of Atlantic cod (*Gadus morhua*), haddock (*Melanogrammus aeglefinus*), and American plaice (*Hippoglossoides platessoides*), by Nikolai Klibansky and Francis Juanes
- 548 Diets of and trophic relationships among dominant marine nekton within the northern California Current ecosystem, by Todd W. Miller and Richard D. Brodeur
- 560 Timing and duration of mating and brooding periods of Atka mackerel (*Pleurogrammus monopterygius*) in the North Pacific Ocean, by Robert R. Lauth, Jared Guthridge, Dan Nichol, Scott W. McEntire, and Nicola Hillgruber
- 571 Description of embryonic development of Atka mackerel (*Pleurogrammus monopterygius*), by Robert R. Lauth and Deborah M. Blood
- 577 Using the empirical Bayes method to estimate and evaluate bycatch rates of seabirds from individual fishing vessels, by Daniel K. Kimura
- 582 No evidence of bias from fish behavior in the selectivity of size and sex of the protogynous red porgy (*Pagrus pagrus*, Sparidae) by hook-and-line gear, by Douglas A. DeVries

Fishery Bulletin Index

Volume 105(1–4), 2007

List of authors

- Able, Kenneth W. 426, 457
 Adkison, Milo D. 121
 Anderson, Jacquelyn L. 440
 Anderson, Joel D. 368
 Anderson, Tara J. 168
 Arrizabalaga, Haritz 140
 Auth, Toby D. 313
- Barlow, Jay 509
 Barrett-Lennard, Lance G. 74
 Baskerville-Bridges, Bradd 30
 Belouski, Ed 197
 Bengtson, John L. 348
 Bennett, William A. 30
 Benson, Scott R. 337
 Berry, Philip 436
 Blood, Deborah 571
 Booth, Shawn 266
 Bowers, Kevin 197
 Brill, Richard 485
 Brodeur, Richard D. 313, 548
 Brown, Robin F. 102
 Burton, Jessica E. 30
- Calkins, Donald G. 234
 Campbell, Robert 390
 Carpenter, Kent E. 207
 Carretta, James V. 337
 Chambers, Christopher 457
 Cherel, Yves 147
 Chess, James R. 39
 Chow, Seinen 1
 Clarke, Peter J. 457
 Conti, Stéphane G. 153
 Cooper, Andrew B. 390
 Cooper, Daniel W. 296
 Costas, Eduardo 140
 Curtis Janelle M. R. 327
- Davis, Gerald 266
 de Lestang, Simon 418
 DeMartini, Edward E. 356
 Demer, David A. 153
 DeVries, Douglas A. 582
 Drawbridge, Mark A. 153
 Dutton, Peter H. 337
- Eisner, Lisa B. 121
 Ellifrit, David 74
 Eveson, J. Paige 493
- Farley, Edward V., Jr. 121
 Fisher, Kathleen M. 313
 Fogarty, Michael 88
 Forney, Karin A. 337, 509
 Fuller, Daniel W. 379
- Ganias, Konstantinos 131
 Garrison, Lance P. 408
 Gentner, Brad 161
 Gerritsen, Hans D. 116
 Gold, John R. 436
 Golet, Walter J. 390
 González-Garcés, Alberto 140
 Grothues, Thomas M. 426
 Gunderson, Donald R. 19, 296
 Guthridge, Jared 560
- Hamilton, Judy 189
 Harley, Shelton J. 49
 Harvey, James T. 337
 Helle, John H. 121
 Hensley, Rebecca 197
 Hillgruber, Nicola 560
 Hobbs, James A. 30
 Howard, Daniel F. 39
 Humphreys, Robert L., Jr. 356
 Hunt, Sharon L. 249
- Ikeda, Hisatoshi 447
- Jeffries, Steven J. 102
 Juanes, Francis 538
- Kane, Joseph 440
 Katakura, Seiji 447
 Klibansky, Nikolai 538
 Kimura, Daniel K. 577
 Konar, Brenda 189
- Laidig, Thomas E. 39
 Laslett, Geoff M. 493
 Lauth, Robert R. 560, 571
 Lem, Siya 436
 López-Rodas, Victoria 140
 Lowry, Lloyd F. 102
 Lowry, Mark S. 102
 Lutcavage, Molly 390
- Magel, Christopher 485
 Margulies, Daniel 1, 249
- Marsac, Francis 147
 Maslenikov, Katherine P. 19, 296
 Mathews, Elizabeth A. 348
 Matkin, Craig O. 74
 Maurer, Benjamin D. 153
 McClelland, Gary 180
 McDermott, Susanne F. 19
 McEntire, Scott 560
 McGrath, David 116
 Melendy, Jason 180
 Melville-Smith, Roy 418
 Ménard, Frédéric 147
 Miller, Todd W. 548
 Mobley, Brandon 197
 Moss, Jamal H. 121
 Munro, Peter T. 278
 Murphy, James M. 121
- Nakazawa, Akio 249
 Nichol, Dan 560
 Nielsen, Jennifer 121
 Nishimura, Akira 447
 Nishiyama, Tsuneo 447
 Nohara, Kenji 1
 Nunes, Cristina 131
- Olesiuk, Peter F. 102
 Oliveira, Kenneth 305
 Olson, Robert J. 249
- Pauly, Daniel 266
 Perryman, Wayne L. 102
 Phillips, Alana V. 348
 Piccoli, Philip M. 62
 Pitcher, Kenneth W. 102
 Polocheck, Tom 493
 Potier, Michel 147
- Renshaw, Mark A. 436
 Roemer, Marja E. 305
- Sabatié, Richard 147
 Saillant, Eric 436
 Sakurai, Yasunori 447
 Sampaga, Jeffrey D. 356
 Schaefer, Kurt M. 379
 Scholey, Vernon P. 249
 Sease, John L. 102
 Secor, David H. 62
 Simpkins, Michael A. 348
 Smith-Vaniz, William F. 207
 Somerton, David A. 278
 Stark, James W. 396
 Stepien, Carol A. 292
 Stewart, Ian J. 470
 Stinchcomb, Charles E. 102

-
- Stockhausen, William T. 88
Strange, Rex M. 292
Stratoudakis, Yorgos 131
Suter, Jenny M. 49, 249
- Targett, Nancy 485
Tupper, Mark H. 527
Trites, Andrew W. 74, 234
- Uchiyama, James H. 356
- Wakabayashi, Toshie 1
Wakefield,, Kirstin 485
Ward, Rocky 197
Weinberg, Kenneth L. 278
Wexler, Jeanne B. 1, 249
Williams, Happy A. 356
- Winship, Arliss J. 234
Witting, David A. 457
- Yoklavich, Mary M. 168
Yurk, Harald 74
- Zeller, Dirk 266

Fishery Bulletin Index

Volume 105(1–4), 2007

List of subjects

- Abundance
 estimation 509
 rockfish 39
 sea lion, Steller 102
 turtles, leatherback 337
 zooplankton 440
- Acoustics 74
- Age
 -at-maturity (cod, Pacific) 396
 validation (smelt, delta) 30
- Alaska 577
- Albacore, Atlantic 140
- Aleutian Islands 19
 eastern 74
- Allometric
 equation 447
 smoothing function 447
- Appendage damage 418
- Atlantic Ocean, Northeast 131
- Atresia
 halibut, Greenland 296
 mackerel, Atka 19
- Bandwidth (acoustic) 153
- Bass, striped 62, 426
- Batch fecundity
 mackerel, Atka 19
 seahorse, long-snouted 327
- Behavior
 courtship 249
 predatory 74
- Bering Sea 447
- Billfishes 147
- Bluefish 305
- Bongo net 440
- Brevoortia* – see menhaden
- Bristol Bay 121
- Brooding (Atka mackerel) 560
- Bycatch
 estimates (of seabirds) 577
 incidental 408
- California Current ecosystem 509,
 548
- Carangidae 207
- Caranx hippos* – see jack, crevalle
- Catch re-estimation 266
- Catchability 278
- Census
 methods 348
 shore-based m348
- Cetaceans 509
- Clam, hard 485
- Cod 189
 Atlantic 538
 Pacific 396
- Condition (northern bluefin tuna)
 390
- Crab, horseshoe 485
- Cynoscion nebulosus* – see seatrout,
 spotted
- Cytochrome *b* 292
- Daily egg production method 131
- Depredation 408
- Dermochelys coriacea* – see turtle,
 leatherback
- Development, embryonic
 (Atka mackerel) 571
- Diet
 goosefish 457
 marine nekton 548
 sea lion, Steller 234
- Distribution
 depth (ichthyoplankton) 313
 diel (ichthyoplankton) 313
 sea lion, Steller 102
- Dolphin 509
 Risso's 408
- Ecotype variation 74
- Egg production (western rock lobster)
 418
- Ekman transport 39
- Estuaries 426
 San Francisco 30
- Estuarine movements 426
- Eumetopias jubatus* – see sea lion,
 Steller
- Experimental design 493
- Fecundity
 halibut, Greenland 296
 mackerel, Atka 19
- Fish
 assemblages (temperate) 168
 eggs 313
 -habitat associations 168
 herding 278
- Fishery
 artisanal 266
 longline 577
 reef 266, 527
 subsistence 266
- Floating objects 379
- Food web 548
- Gadidae 189
- Gadus*
macrocephalus – see cod, Pacific
morhua – see cod, Atlantic
- Gear selectivity 278
- Genetics
 albacore, Atlantic 140
 menhaden 368
 whale, killer 74
- Glacial fjords 348
- Globicephala* spp. – see whale, pilot
- Goosefish 457
- Grampus griseus* – see dolphin, Risso's
- Great Lakes 292
- Greenlings 189
- Growth
 bluefish 305
 tuna, yellowfin 1
 validation (swordfish) 356
- GSI (gonadosomatic index) 296
- Gulf of Maine 390, 538
- Habitat
 Fish associations 168
 foraging (leatherback turtles) 337
 utilization 379
 goosefish 457
 microhabitat 168
- Haddock 538
- Halibut, Greenland 296
- Hawaiian Islands 356
- Hemolymph 485
- Hexagrammos* spp. – see greenlings
- Hippocampus guttulatus* – see
 seahorse, long-snouted
- Hippoglossoides platessoides* – see
 plaice, American
- Hyaloteuthis pelagica* – see squid,
 glassy flying
- Hyperostosis 207
- Hypomesus transpacificus* – see smelt,
 delta
- Ichthyoplankton 1, 313
- Identification (perch) 292
- Incubation period (Atka mackerel)
 571
- Jack, crevalle 207
- Katsuwonus pelamis* – see tuna,
 skipjack
- Kelp 189
 canopy 189
- Lancetfishes 147
- Larval fish 313
 tuna, yellowfin 1, 249

- Length
 -at-maturity (Pacific cod) 396
 frequency 116
 precision estimates 116
Limulus polyphemus – see crab, horseshoe
 Lobster, western rock 418
 Longline, pelagic 408
Lophius americanus – see goosefish
Lutjanus
griseus – see snapper, gray
synagris – see snapper, lane
- Mackerel, Atka 19, 560, 571
 Marine protected areas 527
 Mark-recapture 527
 sole, English 470
 Maturity (Greenland halibut) 296
Melanogrammus aeglefinus – see haddock
 Menhaden 368
Mercenaria mercenaria – see clam, hard
 Microsatellite
 menhaden 368
 seatrout, spotted 197
 snapper 436
 Migration
 albacore, Atlantic 140
 bass, striped 62, 426
 Mitochondrial DNA
 menhaden 368
 perch 292
 tuna, yellowfin 1
 Modeling
 ARIMA 88
 Bayesian 470
 biological intercept 30
 Brownie 493
 choice sets 161
 empirical Bayes 577
 modified Fry 30
 Petersen estimator 493
 Poisson-gamma 577
 posterior distribution 470
 prior 470
 random utility 161
 site choice 161
 spawning fraction method 327
 time-varying growth 30
Morone saxatilis – see bass, striped
 Morphology (goosefish) 457
 Mortality, natural (Greenland halibut) 296
- Nesting (Atka mackerel) 560
 New species 207
 Northern oscillation index 337
- Omnivory (marine nekton) 548
Oncorhynchus nerka – see salmon, sockeye
Orcinus orca – see whale, killer
 Oregon 313
 Otolith
 age determination of 1
 bluefish 305
 microchemistry 62
 smelt, delta 30
- Pacific Ocean
 eastern 49
 North 313
Pagrus pagrus – see porgy, red
 Panama Bight 1
Panulirus cygnus – see lobster, western rock
 Parasites, helminthes 180
Parophrys vetulus – see sole, English
 Perca
flavescens – see perch, yellow
fluviatilis – see perch, Eurasian
 Perch
 Eurasian 292
 yellow 292
Phoca vitulina – see seal, harbor
 Pilchard, European – see sardine, Iberian
 Plaice, American 180, 538
Pleurogrammus monopterygius – see mackerel, Atka
 POF (postovulatory follicle) 131
 Pollock, walleye 447
Pomatomus saltatrix – see bluefish
 Population
 dynamics 470
 estimation 348
 genetics 197
 sea lion, Steller 102
 Porgy, red 582
 Porpoises 509
 Preservatives (on oocytes) 538
 Purse-seine 49
- Recreational demand 161
 Recruitment (juvenile rockfish) 39
Reinhardtius hippoglossoides – see halibut, Greenland
 Reporting rate 493
 Reproduction (seahorse, long-snouted) 327
 Reproductive
 biology (Atka mackerel) 19
 cycle (Atka mackerel) 560
 Rockfish 39, 168, 189
 bocaccio 153
 year-class strength 39
- Salmon, sockeye 121
 Sampling design 116
Sardina pilchardus – see sardine, Iberian
 Sardine, Iberian 131
 Scattering spectra, total 153
 Sea level anomaly 39
 Sea lion, Steller 102, 234
 Seahorse, long-snouted 327
 Seal, harbor 348
 Seatrout, spotted 197
Sebastes spp. 39, 168, 189
paucispinis – see rockfish, bocaccio
 Sex ratio, skewing of 582
 Size structure 582
 Smelt, delta 30
 Snapper
 gray 436
 lane 436
 Sole, English 470
 Spawning
 fraction 131
 frequency 62
 seahorse, long-snouted 327
 mackerel, Atka 560
 tuna, yellowfin 249
 Species group 207
 Sperm limitation (red porgy) 582
 Spillover, of fish from MPAs (marine protected areas) 527
 Squid, glassy flying 147
 Statistical methods
 Back-calculation 447
 Maximum likelihood 493
 Stock
 assessment 140
 structure 140, 180
 Survey
 aerial 337
 photography 348
 line transect 509
 submersible 168
 trawl 88, 278
 efficiency 278
 Survival (sockeye salmon) 121
 Swordfish 356
- Tag
 archival 379
 biological 180
 -recapture 493
 -recovery 493
 Target strength, total 153
 Telemetry, ultrasonic 426
 Temperature, water 249
Theragra chalcogramma – see pollock, walleye

-
- Thunnus*
 alalunga – see albacore, Atlantic
 albacares – see tuna, yellowfin
 obesus – see tuna, bigeye
 thynnus – see tuna, northern bluefin
- Time
 and area closures 49
 -depth recorder 337
 series analysis 88
- Tow speed 440
Trophic relationships 147
Tuna 147
 bigeye 49
 northern bluefin 390
 skipjack 49, 379
 yellowfin 1, 249
Turtle, leatherback 337
- Vertical movement (skipjack tuna)
 379
- Whales 509
 killer 74
 pilot 408
- Xiphias gladius* – see swordfish

Fishery Bulletin

Guidelines for authors

Content of manuscripts

Contributions published in *Fishery Bulletin* describe original research in marine fishery science, fishery engineering and economics, as well as the areas of marine environmental and ecological sciences (including modeling). Preference will be given to manuscripts that examine processes and underlying patterns. Descriptive reports, surveys, and observational papers may occasionally be published but should appeal to an audience outside the locale in which the study was conducted. Although all contributions are subject to peer review, responsibility for the contents of papers rests upon the authors and not on the editor or publisher. *Submission of an article implies that the article is original and is not being considered for publication elsewhere.* **Articles** may range from relatively short contributions (10–15 typed, double-spaced pages, tables and figures not included) to extensive contributions (20–30 typed pages). **Notes** are reports of 5 to 10 pages without an abstract and describe methods or results not supported by a large body of data. Manuscripts must be written in English; authors whose native language is not English are strongly advised to have their manuscripts checked by English-speaking colleagues before submission.

Manuscript Preparation

Title page should include authors' full names and mailing addresses and the senior author's telephone, fax number, and e-mail address, and a list of key words to describe the contents of the manuscript. **Abstract** should be limited to 200 words (one-half typed page), state the main scope of the research, and emphasize the author's conclusions and relevant findings. Do not review the methods of the study or list the contents of the paper. Because abstracts are circulated by abstracting agencies, it is important that they represent the research clearly and concisely. **Text** must be typed in 12 point Times New Roman font throughout. A brief introduction should convey the broad significance of the paper; the remainder of the paper should be divided into the following sections: **Materials and methods**, **Results**, **Discussion** (or **Conclusions**), and **Acknowledgments**. Headings within each section must be short, reflect a logical sequence, and follow the rules of multiple subdivision (i.e., there can be no subdivision without at least two items). The entire text should be intelligible to interdisciplinary readers; therefore, all acronyms, abbreviations, and technical terms should be written out in full the first time they are mentioned. Include

FAO common names for species in the list of keywords and in the introduction. Regional common names may be used throughout the rest of the text if they are different from FAO common names which can be found at <http://www.fishbase.org/search.html>. Follow the U.S. Government Printing Office Style Manual (1984 ed.) and the CBE Style Manual (6th ed.) for editorial style; for fish nomenclature follow the most current issue of the American Fisheries Society's Common and Scientific Names of Fishes from the United States and Canada. Dates should be written as follows: 11 November 2000. Measurements should be expressed in metric units, e.g., 58 metric tons (t); if other units of measurement are used, please make this fact explicit to the reader. Write out the numbers zero through nine unless they form part of measurement units (e.g., nine fish but 9 mm). Refrain from using the shorthand slash (/), an ambiguous symbol, in the general text

Literature cited comprises published works and those accepted for publication in peer-reviewed literature (in press). Follow the name and year system for citation format in the "Literature cited" section (that is say, citations should be listed alphabetically by the authors' last names, and then by year if there is more than one citation with the same authorship). If there is a sequence of citations in the text, list chronologically: (Smith, 1932; Green, 1947; Smith and Jones, 1985). Abbreviations of serials should conform to abbreviations given in the Serial Sources for the BIOSIS Previews Database. Authors are responsible for the accuracy and completeness of all citations. Literature citation format: Author (last name, followed by first-name initials). Year. Title of report or manuscript. Abbreviated title of the series to which it belongs. Always include number of pages. Cite all software and special equipment or chemical solutions used in the study, not in a footnote but within parentheses in the text (e.g., SAS, vers. 6.03, SAS Inst., Inc., Cary, NC).

Tables and figures—general format

- Zeros should precede all decimal points for values less than one.
- Sample size, *n*, should be italicized.
- Capitalize the first letter of the first word in all labels within figures.
- Do not use overly large font sizes in maps and for units of measurements along axes in figures.
- Do not use bold fonts or bold lines in figures.
- Do not place outline rules around graphs.
- Do not use horizontal lines through graphs to indicate measurement units.
- Use a comma in numbers of five digits or more (e.g. 13,000 but 3000).
- Maps require a North arrow and degrees latitude-longitude (e.g., 170°E).

Tables are often overused in scientific papers; it is seldom necessary or even desirable to present all the data associated with a study. Tables should not be excessive in size and must be cited in numerical order in the text. Headings should be short but ample enough to allow the table to be intelligible on its own. All unusual symbols must be explained in the table legend. Other incidental comments may be footnoted with italic numeral footnote markers. Use asterisks to indicate probability in statistical data. Do not type table legends on a separate page; place them above the table data. *Do not submit tables in photo mode.*

Figures include line illustrations, photographs (or slides), and computer-generated graphs and must be cited in numerical order in the text. Graphics should aid in the comprehension of the text, but they should be limited to presenting patterns rather than raw data. Figures should not exceed one figure for every four pages of text. Figures must be labeled with author's name and number of the figure. Avoid placing labels vertically (except of y axis). Figure legends should explain all symbols and abbreviations and should be double-spaced on a separate page at the end of the manuscript. Please note that we do not print graphs in color.

**Failure to follow these guidelines
and failure to correspond with editors
in a timely manner will delay
publication of a manuscript.**

Copyright law does not apply to *Fishery Bulletin*, which falls within the public domain. However, if an author reproduces any part of an article from *Fishery Bulletin* in his or her work, reference to source is considered correct form (e.g., Source: Fish. Bull 97:105).

Submission

The Scientific Editorial Office encourages authors to submit their manuscripts as a *single* PDF (preferred) or Word (zipped) document by e-mail to Fishery.Bulletin@noaa.gov. Please use the subject heading, "Fishery Bulletin manuscript submission". *Do not* send encrypted files. For further details on electronic submission, please contact the Scientific Editorial Office directly (see address below). Or you may send your manuscript on a compact disc in one of the above formats along with four printed copies (one original plus three copies [stapled]) to the Scientific Editor, at the address shown below.

Dr. Adam Moles
Scientific Editor, *Fishery Bulletin*
NOAA/NMFS/AFSC
17109 Point Lena Loop Road
Juneau, AK 99801-8626

Once the manuscript has been accepted for publication, you will be asked to submit a final electronic copy of your manuscript. When requested, the text and tables should be submitted in Word or Word Rich Text Format. Figures should be sent as PDF files, Windows metafiles, tiff files, or EPS files. Send a copy of figures in the original software if conversion to any of these formats yields a degraded version.

Questions? If you have questions regarding these guidelines, please contact the Managing Editor, Sharyn Matriotti, at

Sharyn.Matriotti@noaa.gov

Questions regarding manuscripts under review should be addressed to Adam Moles, Scientific Editor, at Adam.Moles@noaa.gov

